REPORT DOCUMENTATION PAGE

Form Approved OMB NO. 0704-0188

The public reporting burden for this collection of information is estimated to average 1 hour per response, including the time for reviewing instructions, searching existing data sources, gathering and maintaining the data needed, and completing and reviewing the collection of information. Send comments regarding this burden estimate or any other aspect of this collection of information, including suggesstions for reducing this burden, to Washington Headquarters Services, Directorate for Information Operations and Reports, 1215 Jefferson Davis Highway, Suite 1204, Arlington VA, 22202-4302. Respondents should be aware that notwithstanding any other provision of law, no person shall be subject to any oenalty for failing to comply with a collection of information if it does not display a currently valid OMB control number.
PLEASE DO NOT RETURN YOUR FORM TO THE ABOVE ADDRESS.

1. REPORT DATE (DD-MM-YYYY)	2. REPORT TYPE	3. DATES COVERED (From - To)
19-12-2022	Final Report	1-Mar-2018 - 28-Feb-2019

4. TITLE AND SUBTITLE
Final Report: Support for the 26th International Conference on Atomic Physics, ICAP 2018

5a. CONTRACT NUMBER
W911NF-18-1-0104

5b. GRANT NUMBER

5c. PROGRAM ELEMENT NUMBER
611102

6. AUTHORS

5d. PROJECT NUMBER

5e. TASK NUMBER

5f. WORK UNIT NUMBER

7. PERFORMING ORGANIZATION NAMES AND ADDRESSES
ICFO-The Institute of Photonic Sciences
ICFO-The Institute of Photonic Sciences
Av. Carl Friedrich Gauss, num.3

8. PERFORMING ORGANIZATION REPORT NUMBER

9. SPONSORING/MONITORING AGENCY NAME(S) AND ADDRESS (ES)
U.S. Army Research Office
P.O. Box 12211
Research Triangle Park, NC 27709-2211

10. SPONSOR/MONITOR'S ACRONYM(S)
ARO

11. SPONSOR/MONITOR'S REPORT NUMBER(S)
73044-PE-CF.1

12. DISTRIBUTION AVAILIBILITY STATEMENT
Approved for public release; distribution is unlimited.

13. SUPPLEMENTARY NOTES
The views, opinions and/or findings contained in this report are those of the author(s) and should not contrued as an official Department of the Army position, policy or decision, unless so designated by other documentation.

14. ABSTRACT

15. SUBJECT TERMS

16. SECURITY CLASSIFICATION OF:			17. LIMITATION OF ABSTRACT	15. NUMBER OF PAGES	19a. NAME OF RESPONSIBLE PERSON
a. REPORT	b. ABSTRACT	c. THIS PAGE			Maciej Lewenstein
UU	UU	UU	UU		19b. TELEPHONE NUMBER +34-935-5340

RPPR Final Report
as of 19-Dec-2022

Agency Code: 21XD

Proposal Number: 73044PECF **Agreement Number: W911NF-18-1-0104**
INVESTIGATOR(S):

Name: Maciej Lewenstein
Email: maciej.lewenstein@icfo.eu
Phone Number: +34935534072
Principal: Y

Organization: **ICFO-The Institute of Photonic Sciences**
Address: ICFO-The Institute of Photonic Sciences, Castelldefels, 08860
Country: ESP

DUNS Number: 512781907 EIN:
Report Date: 31-May-2019 Date Received: 19-Dec-2022
Final Report for Period Beginning 01-Mar-2018 and Ending 28-Feb-2019
Title: Support for the 26th International Conference on Atomic Physics, ICAP 2018
Begin Performance Period: 01-Mar-2018 **End Performance Period:** 28-Feb-2019
Report Term: 0-Other

Submitted By: Noelia Cuesta Ronda Email: noelia.cuesta@icfo.eu
Phone: (000) 000-0000

Distribution Statement: 1-Approved for public release; distribution is unlimited.

STEM Degrees: **STEM Participants:**

Major Goals: Support the 26th International Conference on Atomic Physics, ICAP 2018

Accomplishments: 26th International Conference on Atomic Physics, ICAP 2018 was conducted.

Training Opportunities: Nothing to Report

Results Dissemination: Nothing to Report

Honors and Awards: Nothing to Report

Protocol Activity Status:

Technology Transfer: Nothing to Report

RPPR Final Report
as of 19-Dec-2022

Partners

,

I certify that the information in the report is complete and accurate:
Signature: Marciej Lewenstein
Signature Date: 12/19/22 10:26AM

ICAP2018

The 26th International Conference on Atomic Physics

26th INTERNATIONAL CONFERENCE ON ATOMIC PHYSICS

22 - 27 JULY

Barcelona, Spain

Book of Abstracts



ICFO

UNIVERSITAT DE BARCELONA

UAB Universitat Autònoma de Barcelona

UNIVERSITAT POLITÈCNICA DE CATALUNYA BARCELONATECH



WELCOME TO ICAP 2018

Dear Colleagues, Dear Friends,

It is with great pleasure that we welcome you to our beautiful city of Barcelona for the 26th edition of the International Conference on Atomic Physics, ICAP 2018.

First, we would like to thank all of you for your participation at the conference. We are aware that many of you have had difficulties in obtaining funding, visas, travel tickets, and many have travelled a long way to reach us. Thank you!

In the current edition of the ICAP we are proud to have an outstanding scientific program, reporting the main developments in the field in the last two years in the form of 33 invited talks, a selection of 8 hot topic presentations with recent relevant advances and the presentation of the IUPAP Young Scientist Prize. In addition, the conference will host three poster sessions where all the attendees will be able to present their recent research. This, together with a very nice social program with excursions and a Gala Dinner at the Maritime Museum of Barcelona with a Jazz concert, and the well-known attractions of the city of Barcelona, will certainly make your participation at the conference an unforgettable one.

On top of that, in this edition we will host two open-to-the-public scientific events. The first one will be a Nobel Panel session on the "Past, Present and Future of Atomic Physics" which will count with the participation of 6 Nobel Prize Awardees in the field. The second outreach activity will be a lecture on the New International System of Units, given by Prof. Vanderlei Bagnato and Prof. William D. Phillips where the new standards will be presented.

All this has been possible thanks to your participation, to our sponsors support and to our helpers involvement.

We do hope that you enjoy your attendance at the ICAP 2018!

Maciej Lewenstein — Chairman ICAP 2018
Verònica Ahufinger — Vice-Chairman ICAP 2018
Bruno Juliá Díaz — Vice-Chairman ICAP 2018

COMMITTEES

International Program Committee

Verònica Ahufinger, *Spain*
Vanderlei Bagnato, *Brasil*
Rainer Blatt, *Austria*
Antoine Browaeys, *France*
Dmitry Budker, *Germany*
Simon L. Cornish, *UK*
David DeMille, *USA*
Francesca Ferlaino, *Austria*
Selim Jochim, *Germany*
Bruno Juliá-Díaz, *Spain*
Gediminas Juzeliunas, *Lithuania*
Hidetoshi Katori, *Japan*
Reinhard Kienberger, *Germany*
Yoon-Ho Kim, *South Korea*
Stefan Kuhr, *UK*
Anne L'Huillier, *Sweden*
Wu-Ming Liu, *China*
Maciej Lewenstein, *Spain*
Mikhail Lukin, *USA*
Robert Moszynski, *Poland*
Christoph Naegerl, *Austria*
Chang-Hee Nam, *South Korea*
Elena Ostrovskaya, *Australia*
Jian-Wei Pan, *China*
Tilman Pfau, *Germany*
Anatoli Polkovnikov, *USA*
Cindy Regal, *USA*
Jakob Reichel, *France*
Ana Maria Rey, *USA*
Giacomo Roati, *Italy*
Mariana Safronova, *USA*
Christophe Salomon, *France*
Anna Sanpera, *Spain*
Robert Schoelkopf, *USA*
Aditi Sen De, *India*
Georgy Shlyapnikov, *France*
Michael Tarbutt, *UK*
Jun Ye, *USA*
Martin Zwierlein, *USA*

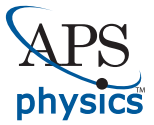
Local Organizing Committee

Maciej Lewenstein (Chair), *ICFO*
Verònica Ahufinger (Vice-chair), *UAB*
Bruno Juliá-Díaz (Vice-chair), *UB*
Jens Biegert, *ICFO*
Hugues de Riedmatten, *ICFO*
Jose Ignacio Latorre, *UB*
Ferran Mazzanti, *UPC*
Morgan Mitchell, *ICFO*
Artur Polls, *UB*
Anna Sanpera, *UAB*
Leticia Tarruell, *ICFO*

International Advisory Committee

Ennio Arimondo, *Italy*
Hans Bachor, *Australia*
Vanderlei Bagnato, *Brazil*
Viktor Balykin, *Russia*
Rainer Blatt, *Austria*
Immanuel Bloch, *Germany*
Gretchen Campbell, *USA*
Donghyun Cho, *South Korea*
Claude Cohen-Tannoudji, *France*
Robin Côté, *USA*
Gordon Drake, *Canada*
Norval Fortson, *USA*
Philippe Grangier, *France*
Theodor Hänsch, *Germany*
Peter Hannaford, *Australia*
Serge Haroche, *France*
Ed Hinds, *UK*
Massimo Inguscio, *Italy*
Wonho Jhe, *South Korea*
Wolfgang Ketterle, *USA*
Daniel Kleppner, *USA*
Michèle Leduc, *France*
Hélène Perrin, *France*
William D. Phillips, *USA*
Lev Pitaevskii, *Russia*
Trey Porto, *USA*
Fujio Shimizu, *Japan*
Winthrop Smith, *USA*
Jook Walraven, *The Netherlands*
David Wineland, *USA*
Tsutomu Yabuzaki, *Japan*
Mingsheng Zhan, *China*

SPONSORS























































SUPPORTED BY













SCHEDULE

	22nd July	23rd July	24th July	25th July	26th July	27th July
8:45-9:00		**Opening**				
9:00-9:30		Jean Dalibard	Antoine Browaeys	Paul Corkum	Jacqueline Bloch	Karsten Danzmann
9:30-10:00		Ed Hinds	Francesca Calegari	Michel Devoret	Piet Schmidt	Yoshiro Takahashi
10:00-10:30		Ping Koy Lam	Mark Kasevich	Yong-il Shin	Ian Spielman	Antonio Acín
10:30-11:00			10:30-10:45 Group photo	**Coffee break**		
11:00-11:30		Peter Zoller	John M. Doyle	Holger Mueller	Andreas Becker	Darrick Chang
11:30-12:00		Thomas Udem	Zoran Hadzibabic	Gerhard Rempe	Tilman Esslinger	Jörg Schmiedmayer
12:00-12:30		Tanya Zelevinsky	Immanuel Bloch	Xinhua Peng	Doerte Blume	Christian Gross
12:30-14:30		**Lunch break**			**Lunch break**	
14:30-15:00		**Poster Session I** Coffee break during Poster session from 16:00 to 16:30	**Poster Session II** Coffee break during Poster session from 16:00 to 16:30	**Free Afternoon**	**Poster Session III** Coffee break during Poster session from 16:00 to 16:30	**Hot Topics Sessions V to VIII** 14:30 – 14:55 Waseem Bakr 14:55 – 15:20 Ben P. Lanyon 15:20 – 15:45 Kang-Kuen Ni 15:45 – 16:10 Charles Adams
15:00-15:30						
15:30-16:00						
16:00-16:30						**16:15-16:45 Poster Awards**
16:30-17:00		IUPAP Prize Session Alexey Gorshkov			Dietrich Leibfried	**Closing**
17:00-17:30		**Hot Topics Sessions I to IV** 17:00 – 17:25 Ana Maria Rey 17:25 – 17:50 Mikhail Lukin 17:50 – 18:15 Francesca Ferlaino 18:15 – 18:40 Susanne Yelin			Arno Rauschenbeutel	
17:30-18:00					André Eckardt	
18:00-18:30			Nobel Prize Panel			
18:30-19:00						
19:00-19:30	**Welcome Reception at Universitat de Barcelona**					
19:30-20:00				**Gala Dinner**	IUPAP Public Lecture: The New SI	
20:00-20:30						
20:30-21:00						
21:00-21:30						

PROGRAM

Sunday 22nd July

19:00 - 21:00 Welcome Reception at Universitat de Barcelona

Monday 23rd July

8:45 - 9:00 Opening

Session I Chair: D. Kleppner, *Massachusetts Institute of Technology*

9:00 - 9:30 **Revisiting the two-fluid model with atomic gases**
Jean Dalibard, *Laboratoire Kastler Brossel* 51

9:30 - 10:00 **Experiments with ultracold CaF and YbF molecules**
Ed Hinds, *Imperial College of London* 52

10:00 - 10:30 **Multiparameter Optimisation of a Magneto-Optical Trap Using Deep Learning Artificial Neural Networks**
Ping Koy Lam, *The Australian National University* 53

10:30 - 11:00 Coffee break

Session II Chair: L. Leblanc, *University of Alberta*

11:00 - 11:30 **Quantum Simulations in the Innsbruck Quantum Cloud**
Peter Zoller, *University of Innsbruck* 54

11:30 - 12:00 **Challenging QED with atomic Hydrogen**
Thomas Udem, *Max Planck Institute of Quantum Optics* 55

12:00 - 12:30 **Lattice clocks and quantum-state-controlled chemistry with ultracold molecules**
Tanya Zelevinsky, *Columbia University* 56

12:30 - 14:30 Lunch break

14:30 - 16:30 **Poster Session I** Coffee break during Poster Session from 16:00 to 16:30

16:30 - 17:00 **IUPAP Prize Session**
Chair: R. Rivarola, *Instituto de Física Rosario*

Information propagation and entanglement generation with long-range interactions
Alexey Gorshkov, *JQI, QuICS, NIST and University of Maryland* 57

17:00 - 18:40 **Hot Topics Sessions I to IV**
Chair: S. Cornish, *Durham University*

17:00 – 17:25 **Entanglement dynamics in a trapped ion quantum magnet**
Ana Maria Rey, *JILA, NIST and University of Colorado* **58**

17:25 – 17:50 **Probing quantum many-body dynamics in Rydberg atom arrays**
Mikhail Lukin, *Harvard University* **59**

17:50 – 18:15 **Probing the Roton Excitation Spectrum in an Erbium Dipolar Quantum Gas**
Francesca Ferlaino, *Innsbruck University and IQOQI* **60**

18:15 – 18:40 **Quantum optics with two-dimensional atomic arrays**
Susanne Yelin, *Harvard University and University of Connecticut* **61**

PROGRAM

Tuesday 24nd July

Session I Chair: C. Salomon, *École Normal Supérieure, Paris*

9:00 - 9:30 **Experimental many-body physics using arrays of individual atoms**
Antoine Browaeys, *Institut d'Optique, CNRS* 62

9:30 - 10:00 **Probing electron dynamics in bio-relevant molecules**
Francesca Calegari, *DESY, Hamburg Universität and CNR-IFN* 63

10:00 - 10:30 **Phase estimation for quantum sensors**
Mark Kasevich, *Standford University* 64

10:30 - 10:45 Group photo

10:45 - 11:00 Coffee break

Session II Chair: R. González-Férez, *Universidad de Granada*

11:00 - 11:30 **Laser cooled molecules for quantum information and particle physics - recent progress and future prospects**
John M. Doyle, *Harvard - MIT CUA and Harvard University* 65

11:30 - 12:00 **Bose gases quenched to unitarity**
Zoran Hadzibabic, *University of Cambridge* 67

12:00 - 12:30 **Probing Topological Order and Hidden Magnetism using Quantum Gas Microscopy**
Immanuel Bloch, *Ludwig Maximilians Universität and Max Planck Institut für Quantenoptik* 68

12:30 - 14:30 Lunch break

14:30 - 16:30 **Poster Session II** Coffee break during Poster Session from 16:00 to 16:30

18:00 - 19:30 **Nobel Prize Panel**
Atomic Physics: past, present and future
Chairs: Verònica Ahufinger, *Universitat Autònoma de Barcelona*
Bruno Juliá-Díaz, *Universitat de Barcelona*

Claude Cohen-Tannoudji *(NP 1997)*
William D. Phillips *(NP 1997)*
Wolfgang Ketterle *(NP 2001)*
Roy J. Glauber *(NP 2005)*
Theodor W. Hänsch *(NP 2005)*
Serge Haroche *(NP 2012)*

PROGRAM

Wednesday 25th July

Session I Chair: A. Sanpera, *Universitat Autònoma Barcelona*

9:00 - 9:30 **Attosecond pulses generated in gases and solids**
Paul Corkum, *University of Otawa and National Research Council Canada* 69

9:30 - 10:00 **Catching and reversing a quantum jump mid-flight**
Michel Devoret, *Yale Quantum Institute, Yale University* 70

10:00 - 10:30 **Quantum vortex shedding in atomic superfluid gases**
Yong-il Shin, *Seoul National University* 71

10:30 - 11:00 Coffee break

Session II Chair: D. Stamper-Kurn, *University of California, Berkeley*

11:00 - 11:30 **Measurement of the fine-structure constant as a test of the Standard Model**
Holger Mueller, *University of California, Berkeley* 72

11:30 - 12:00 **Cavity QED: Quantum Bits and Quantum Fields**
Gerhard Rempe, *Max Planck Institute of Quantum Optics* 73

12:00 - 12:30 **Towards quantum simulation of exotic quantum many-body physics with nuclear spins**
Xinhua Peng, *University of Science and Technology of China, Hefei* 74

12:30 - 18:00 Free Afternoon

19:30 - 21:30 Gala Dinner at Drassanes Maritim Museum*
Av. de les Drassanes, s/n, 08001 Barcelona
*only for participants with dinner voucher

PROGRAM

Thursday 26th July

Session I Chair: J. Arlt, *Aarhus Universitet*

9:00 - 9:30 **Cavity polariton in semiconductor lattices : a non-linear photonic emulator**
Jacqueline Bloch, *CNRS, Université Paris-Sud and Université Paris-Saclay* 75

9:30 - 10:00 **Quantum Logic Spectroscopy of a Single Molecular Ion**
Piet Schmidt, *Physikalisch-Technische Bundesanstalt and Leibniz Universität Hannover* 76

10:00 - 10:30 **Thin Hofstadter ribbons: topology and a Diophantine equation**
Ian Spielman, *JQI, NIST and University of Maryland* 77

10:30 - 11:00 Coffee break

Session II Chair: M. Zhan , *Wuhan Institute of Physics and Mathematics*

11:00 - 11:30 **Generation and application of attosecond laser pulses**
Andreas Becker, *JILA and University of Colorado* 78

11:30 - 12:00 **Composing many-body systems with quantum gases**
Tilman Esslinger, *ETH Zurich* 79

12:00 - 12:30 **Few-body aspects of spin-orbit coupled cold atom systems**
Doerte Blume, *The University of Oklahoma* 80

12:30 - 14:30 Lunch break

14:30 - 16:30 **Poster Session III** Coffee break during Poster Session from 16:00 to 16:30

Session III Chair: P. Treutlein, *University of Basel*

16:30 - 17:00 **Quantum Control of Atomic and Molecular Ions**
Dietrich Leibfried, *National Institute of Standards and Technology* 81

17:00 - 17:30 **Seeing A Single Atom Where It Is Not**
Arno Rauschenbeutel, *TU of Wien and Humboldt-Universität zu Berlin* 82

17:30 - 18:00 **Dynamically probing many-body states of matter in optical lattices**
André Eckardt, *Max-Planck-Institut für Physik komplexer Systeme* 83

19:30 - 21:00 IUPAP Public Lecture: The New SI
Vanderlei Bagnato *Universidade de Sao Paulo*
William D. Phillips *(NP 1997) National Institute of Standards and Technology*

PROGRAM

Friday 27th July

Session I Chair: M. Modugno, *Ikerbasque & UPV/EHU*

9:00 - 9:30 **Gravitational wave astronomy: We can hear the universe!**
Karsten Danzmann, *Max Planck Institute for Gravitational Physics and Leibniz Universität Hannover* 84

9:30 - 10:00 **Quantum Simulation with Ytterbium Fermi Gases**
Yoshiro Takahashi, *Kyoto University* 85

10:00 - 10:30 **Certification of many-body quantum states**
Antonio Acín, *ICFO and ICREA* 86

10:30 - 11:00 Coffee break

Session II Chair: M. Weitz, *University of Bonn*

11:00 - 11:30 **Quantum optics using ordered atomic arrays**
Darrick Chang, *ICFO and ICREA* 87

11:30 - 12:00 **Higher-order correlations and what we can learn about the solution for many body problems from experiments**
Jörg Schmiedmayer, *Vienna Center for Quantum Science and Technology* 88

12:00 - 12:30 **Microscopy of ultracold Rydberg macrodimers**
Christian Gross, *Max-Planck-Institut für Quantenoptik* 89

12:30 - 14:30 Lunch break

14:30 - 16:10 **Hot Topics Sessions V to VIII**
Chair: G. Ferrari, *INO–CNR BEC Center, Università di Trento and INFN*

14:30 – 14:55 **Bad Metallic Transport in a Cold Atom Fermi-Hubbard System**
Waseem Bakr, *Princeton University* **90**

14:55 – 15:20 **Entangling and verifying a 20 qubit register**
Ben P. Lanyon, *Osterreichische Akademie der Wissenschaften and IQOQI* **91**

15:20 – 15:45 **Building single molecules**
Kang-Kuen Ni, *Harvard - MIT CUA and Harvard University* **92**

15:45 – 16:10 **Engineering collective light-matter interactions**
Charles Adams, *Durham University* **93**

16:15 - 16:45 **Poster Awards**
Chair: F. Haake, *Universität Duisburg-Essen*

16:45 - 17:00 Closing

POSTER LIST

Page

Monday 23rd July

TOPIC: ATOMIC CLOCKS AND QUANTUM METROLOGY

Sensing beyond the Heisenberg limit
Tarun Dutta *CQT, National University of Singapore* 95

A master oscillator based on 48.5 cm long optical cavity as a reference for a universal synthesizer
Marco Schioppo *National Physical Laboratory* 96

E2 transitions between hyperfine structure components of the D^+_2 molecular ion
Petar Danev *INRNE, BAS* 97

Measurement of the Infrared Magic Wavelengths for the $^{40}Ca^+$ Ion Clock Transition
Kelin Gao *Wuhan Institute of Physics and Mathematics (WIPM) of Chinese Academy of Sciences* 98

Progress towards deployable primary pressure sensors based on lithium magneto-optical traps
Daniel Barker *National Institute of Standards and Technology* 99

Onsite calibration of time and length standards for atom gravimeters
Duan Xiaochun *Huazhong University of Science & Technology* 100

Quantum Logic Spectroscopy with a $^{40}Ca^+/^{27}Al^+$ mixed ion crystal
Milena Guevara-Bertsch *Institut for quantum optics and quantum information* 101

Comparing Optical Clocks at 10^{-18} level
Holly Leopardi *NIST/ University of Colorado* 102

Transortable optical lattice clock-measurement campaigns and characterisation
Silvio Koller *PTB* 103

Spin squeezing of an atomic ensemble with 10^{11} atoms
Han Bao *Fudan University* 104

Micro-integrated extended cavity diode laser with integrated optical amplifier for precision spectroscopy in space
Christian Kürbis *Ferdinand-Braun-Institut* 105

Quantum metrology of displacements with diffusion: single photon recoil spectroscopy
Marius Schulte *Leibniz University Hannover* 106

Progress on a compact Yb^+ optical clock
Marion Delehaye *Femto-ST* 107

Explore cesium nuclear magnetic octupole moment with electronic $6S_{1/2} \rightarrow 6D_{3/2}$ hyperfine transitions
Wang-Yau Cheng *Department of Physics, National Central University* 108

Remote and local comparisons of optical atomic clocks for geodesy and metrology
Filippo Bregolin *INRIM Istituto Nazionale di Ricerca Metrologica* 109

The system of intra-object transmission of the strontium optical clock frequency to the primary standard of units of time, frequency and the national time scale
Denis Sutyrin *FSUE 'VNIIFTRI'* 110

POSTER LIST

Page

Development of optical clock modules for the creation of a portable optical frequency clock on ytterbium atoms
Gleb Belotelov *FSUE 'VNIIFTRI'* 111

Cryogenic multi-path cavity made of monocrystalline silicon
Piotr Morzyński *National Institute of Information and Communications Technology* 112

An optical frequency comb stabilized to an optical lattice clock laser through optical fiber networks
Eunmi Chae *The University of Tokyo* 113

Weak measurement correlation spectroscopy for magnetic field sensing
Qu Weizhi *Fudan University* 114

Theory of the high-quality magneto-optical resonances observed in a buffer-gas-filled vapour cell
Aleksey Novokreshchenov *Institute of Laser Physics SB RAS* 115

High-sensitive all-optical magnetometer for nuclear magnetic resonance gyroscope
Xinye Xu *East China Normal University* 116

A mercury optical lattice clock
Valentin Cambier *CNRS SYRTE OP SU LNE* 117

Sideband cooling and transport of cold ytterbium atoms in a one-dimensional optical lattice
Xinye Xu *East China Normal University* 118

TOPIC: COLD MOLECULES

Ultracold Triplet Ground State $^{23}Na^{6}Li$ Molecules
Hyungmok Son *Harvard University/MIT* 119

Two interacting molecules in a one-dimensional harmonic trap
Anna Dawid-Łękowska *University of Warsaw* 120

Fermi degeneracy and evaporation in a gas of reactive polar molecules
Giacomo Valtolina *JILA - CU Boulder* 121

Direct measurement of branching ratios, and progress towards laser cooling of barium monohydride
Rees McNally *Columbia University* 122

Interactions of benzene, naphthalene, and azulene with alkali-metal and alkaline-earth-metal atoms for ultracold studies
Pawel Wójcik *University of Warsaw* 123

Isotopic shift of atom-dimer Efimov resonances in K-Rb mixtures
Kohei Kato *Osaka city university* 124

Two-photon spectroscopy of ultracold dipolar ^{6}Li - ^{40}K molecules
Sofia Botsi *Centre for Quantum Technologies, National University of Singapore* 125

Testing the parity symmetry in chiral molecules using vibrational spectroscopy
Mathieu Manceau *Laboratoire de physique des Lasers* 126

Towards laser cooling of AlF molecules
Stefan Truppe *Fritz Haber Institute of the Max Planck Society* 127

POSTER LIST

Page

Ultracold Lithium for Sympathetically Cooling Polar Molecules
Sidney Wright *Imperial College London* 128

Collision studies of slow, cold polyatomic molecules
Isabel Rabey *Max-Planck-Institut für Quantenoptik* 129

Long Coherence Times in Trapped RbCs
Jacob Blackmore *Durham University* 130

Magic-Wavelength Molecular Clock and Ultracold Chemistry With Lattice-Trapped Molecules
Christian Liedl *Columbia University* 131

Photoassociation and photoionization in a two-species Rb-Hg MOT
Marcin Witkowski *Institute of Physics University of Opole* 132

Towards quantum simulations with ultracold KCs molecules
Apichayaporn Ratkata *Joint Qauntum Centre* 133

Towards ground state CsYb molecules
Kali Wilson *Durham University* 134

The DESIREE storage ring
Dag Hanstorp *University of Gothenburg* 135

Atom-molecule coherence in heteronuclear Yb-Li
Alaina Green *University of Washington* 136

Towards trapping of a single molecule in an optical tweezer
Sarunas Jurgilas *Imperial College London* 137

Ultracold YbF molecules for measuring the electron's electric dipole moment
Michael Trigatzis *Imperial College London* 138

Control of atom-ion reactions at low temperatures
Michael Mills *University of California, Los Angeles* 139

Optical transport of ultracold atoms for the production of groundstate RbYb
Axel Görlitz *University of Düsseldorf* 140

Theoretical description of photodissociation of ultracold diatomic molecules
Iwona Majewska *University of Warsaw* 141

Towards Magneto-Optical Trapping of Polyatomic Molecules
Louis Baum *Harvard University* 142

Laser Cooling of Optically Trapped Molecules
Loic Anderegg *Harvard University* 143

Order of Magnitude increased sensitivity to the electron electric dipole moment
Zack Lasner *Yale University* 144

Is laser cooling without spontaneous emission possible?
Daniel Comparat *Laboratoire Aimé Cotton (CNRS)* 145

Coherent control of ultracold ground-state $^{87}Rb^{133}Cs$ molecules in an optical trap
Simon Cornish *Durham University* 146

POSTER LIST

Page

Prospects for formation of ultracold RbSr molecules : Novel implementation of an optical Feshbach resonance
Adrien Devolder *Laboratoire Aimé Cotton,CNRS* 147

State selection, magnetic trapping and coherent control of laser-cooled molecules
Luke Caldwell *Imperial College London* 148

Electronic excitation-exchange and spin-orbit coupling in ultracold ion-atom collisions
Ruti Ben Shlomi *Weizmann institute* 149

Optical clock spectroscopy in weakly bound molecules
Mateusz Borkowski *Nicolaus Copernicus University* 150

Menagerie of MOTs
Kyle Jarvis *Imperial College London* 151

Towards Direct Laser Cooling of Barium Monofluoride
Tim Langen *University of Stuttgart* 152

TOPIC: FUNDAMENTAL TESTS ANS QUANTUM MEASUREMENTS

Quantitative optical spectroscopy of alkali-metal vapour in DC magnetic fields up to 0.4 T
Francisco Sebastian Ponciano-Ojeda *Durham University* 153

Laser Induced Fluorescence and Optogalvanic Spectroscopy applied to find the magnetic splitting of energy levels of La I
Lukasz Sobolewski *University of Gdansk* 154

Towards a high-density squeezed-light magnetometer
Charikleia Troullinou *ICFO* 155

Continuum contributions to the atomic electric dipole moments
Pawel Syty *Gdansk University of Technology* 156

Progress towards parity violation measurements in dysprosium
Arijit Sharma *Helmholtz-Institut Mainz* 157

In-beam hyperfine spectroscopy of hydrogen and antihydrogen
Eberhard Widmann *Stefan Meyer Institute* 158

Towards Ramsey-Comb Spectroscopy of the 1S-2S Transition in Helium Ions
Julian Krauth *Vrije Universiteit Amsterdam* 159

A 10-nT level magnetic shielding for the 10-m long-baseline atom interferometer
Chuan He *Wuhan Institute of Physics and Mathematics, Chinese Academy of Sciences* 160

Experimental upgrades to measure the electron's electric dipole moment using YbF molecules
Christopher Ho *Imperial College London* 161

Towards precision spectroscopy of the 2S-6P transition in atomic hydrogen
Vitaly Andreev *Max-Planck-Institute of Quantum Optics / Ludwig-Maximilians-University of Munich* 162

POSTER LIST

Page

High contrast EIT spectra in a hot atomic medium
Yi-Hsin Chen *Department of Physics, National Sun Yat-Sen University, Taiwan* 163

Search for a violation of the Pauli Exclusion Principle with electrons in the LNGS underground laboratory
Andreas Pichler *Stefan Meyer Institute for subatomic physics* 164

Measurement of the ^{4}He 2 ^{3}S - 2 ^{1}S transition in a magic wavelength optical dipole trap
Wim Vassen *LaserLaB Vrije Universiteit Amsterdam* 165

Isotope shift, non-linearity of King plots and the search for new particles
Amy Geddes *UNSW Sydney* 166

Quantum State Transportation of Rubidium Atoms inside a Photonic Waveguide
Mingjie Xin *Nanyang Technological University* 167

Sub-Doppler Molecular Spectroscopy, Frequency Metrology, and PNC induced Optical Rotation Measurement based on NICE-OHMS Scheme with a High Finesse Cavity
Tzu-Ling Chen *National Tsing Hua University* 168

Continuous motional sensing with highly dispersive medium
Wui Seng Leong *Nanyang Technological University* 169

Enhanced nuclear spin dependent parity violation effects using the 199HgH molecule
Amy Geddes *UNSW Sydney* 170

Spatial entanglement patterns and Einstein-Podolsky-Rosen steering in Bose-Einstein condensates
Matteo Fadel *University of Basel* 171

Precision spectroscopy of the 1S-2S transition in antihydrogen
Graham Stutter *Aarhus University* 172

Theory of large-momentum-transfer Bose-Einstein condensate interferometers
Jan-Niclas Siemß *Institute for Theoretical Physics, Leibniz University Hannover* 173

Coherence in a cold quantum matrix
Yuki Miyamoto *Okayama University* 174

Measurement-induced nonlocal entanglement in a hot, strongly-interacting atomic system
Jia Kong *ICFO-The Institute of Photonic sciences* 175

Coherent two-photon emission from hydrogen molecules towards neutrino mass spectroscopy
Hideaki Hara *Okayama University* 176

Magneto-optical trapping in glass cell evacuated by Non-Evaporable Getters
Takumi Oda *Tokyo Institute of Technology* 177

A strict experimental test of macroscopic realism in a light-matter interfaced system
Xiao Liu *University of Science and Technology of China* 178

Measurement of the Fine Structure Constant as a Test of the Standard Model
Richard Parker *UC Berkeley* 179

RF microplasmas with energies suited to selective cleaning of surface adsorbates in ion microtraps
Mariam Akhtar *NPL / Strathclyde University* 180

POSTER LIST

Page

Current Status of the JILA eEDM Experiment
Kia Boon Ng *JILA, University of Colorado, Boulder* 181

Initial progress of high precision measurement of time-reversal symmetry violation in Thallium nucleus
Konrad Wenz *Columbia University* 182

Comparative study of mechanical and structure properties of geopolymer matrices incorporated by nano-silica, nano-alumina and nano-zinc
Zidi Zeineb *Faculty of science of gabes* 183

TOPIC: OTHERS

International Union of Pure and Applied Physics
IUPAP 184

Quantum sensing with laser-cooled atoms: from an experiment to a product
Jean Lautier Gaud *Muquans* 185

The non-exactness of SWKB for additive SI potentials
Constantin Rasinariu *Loyola University Chicago* 186

Shortcuts to Adiabaticity Assisted by Counterdiabatic Born-Oppenheimer Dynamics
Callum Duncan *Heriot-Watt University* 187

Quenching interatomic Coulombic decay width by screening effect
Petra Votavova *Institute of Theoretical Physics, Charles University* 188

High coherence superconducting artificial atom
Long Bao Nguyen *University of Maryland* 189

High-efficiency cold-atom transport into a waveguide trap
Ashby Hilton *University of Adelaide* 190

Optical pumping of ^{87}Rb atoms with Xe and high-pressure buffer gas in a cubic cell
Hoon Yu *Hanwha Denfense R&D center* 191

Local rectification of heat flux
Marisa Pons *Universidad País Vasco / Euskal Herriko Unibertsitatea* 192

Absorption Spectroscopy of Thallium forbidden transition with Amplitude- and Phase- Modulation
Wei-Ling Chen *National Tsing Hua University* 193

Phase Locked Atomic Interferometers for Gravity Gradiometry
Chester Camm *University of Southampton* 194

Monitoring Ultra Cold Gases in Situ and in Real Time by Ionization Sampling
Max Eisele *Physikalisches Institut Uni Tübingen* 195

Strong Optical Forces on Atoms Using Adiabatic Rapid Passage
Harold Metcalf *Stony Brook University* 196

Detecting universal properties of lattice models with entanglement Hamiltonians
Tiago Mendes Santos *ICTP* 197

POSTER LIST

Page

Ultracold atom-ion collisions in a laser-cooled ^{6}Li-$^{40}Ca^{+}$ hybrid systmes
Takumi Kojima *Osaka University* 198

All-optical metastable excitation techniques for precision noble-gas radio-isotope ratiometry using atom-trap trace analysis
Philip Light *University of Adelaide* 199

The Electron Anity of Thallium by Laser Photodetachment Threshold Spectroscopy
Dan Gibson *Denison Univ* 200

Entanglement preserving local thermalization
Chung-Yun Hsieh *ICFO The Institute of Photonic Sciences* 201

The $5P_{3/2} \rightarrow 6P_{3/2}$ electric quadrupole transition in atomic rubidium as a probe of the Autler-Townes effect
Jose Jimenez Mier *UNAM* 202

Novel quantum technologies based on atomic vapour cells
Robert Loew *University of Stuttgart* 203

Loss-rate measurement in a magneto-optical trap for metastable europium
Yuki Miyazawa *Tokyo Institute of Technology* 204

Production and study of new neutron rich isotopes of heavy atoms
Segey Zemlyanoy *Joint Institute for Nuclear Research* 205

Spectroscopy of the $5p_{3/2} \rightarrow 6p_{1/2}$ electric dipole forbidden transition in atomic rubidium
Fernando Ramirez-Martinez *Instituto de Ciencias Nucleares, UNAM* 206

Sub-Doppler saturated fluorescence spectroscopy of the $5_{s1/2} \rightarrow 6_{p3/2}$ transition in room temperature rubidium atoms
Lina Marieth Hoyos *Universidad Nacional Autónoma de México* 207

Mirrorless optical parametric oscillator inside an all-optical waveguide
Sushree Subhadarshinee Sahoo *National Institute of Science Education and Research, Bhubaneswar* 208

Plasma environment effects on the decay properties of atomic K-vacancy states belonging to the oxygen and iron isonuclear sequences of astrophysical interest
Patrick Palmeri *Université de Mons - UMONS* 210

HFR+CPOL and MCDHF oscillator strengths of strong electric dipole (E1) lines of U^{+} of interest in cosmochronology
Patrick Palmeri *Université de Mons - UMONS* 211

The Roentgen-term and related gems in atom-light interaction
Matthias Sonnleitner *University of Innsbruck* 212

Holographically controlled 3D atomic population structures
Adam Selyem *University of Glasgow* 213

Phonons dispersion curves of dielectric materials
Said Talbaoui *University sultane moulay slimane, Faculty of sciences and techniques, benimellal Morocco* 214

POSTER LIST

Page

TOPIC: QUANTUM COMPUTATION AND COMMUNICATION

Realization of a T^3 Matter-Wave Interferometer on an Atom Chip
Omer Amit *Ben-Gurion University* 215

TOPIC: QUANTUM GASES

Interacting bosonic atoms in triangular lattices with varying geometry
Dan Stamper-Kurn *University of California* 216

Realization of a fractional period adiabatic superlattice
Dimitris Trypogeorgos *JQI* 217

Optical visibility and core structure of vortex filaments in a three-dimensional bosonic superfluid
Franco Dalfovo *INO-CNR BEC Center and University of Trento* 218

Non-classical spin states with ultracold dysprosium atoms
Thomas Chalopin *Laboratoire Kastler Brossel, CNRS* 219

High Sensitivity Rf Spectroscopy of a Strongly-Interacting Fermi Gas
Constantine Shkedrov *Technion - Israel Institute of Technology* 220

Experiment of Newton Cradle in One Dimensional Bose Gas
Xuzong Chen *Peking University* 221

Atom loading into a modulated optical dipole trap under Λ-enhanced gray molasses cooling
Ming-Shien Chang *Institute of Atomic and Molecular Sciences, Academia Sinica* 222

Quantum reflection of ultracold atoms by a spherical surface
Rina Kanamoto *Meiji University* 223

Roton in a many-body dipolar system
Rafał Ołdziejewski *Center for Theoretical Physics of the Polish Academy of Sciences* 224

Particle-Hole Character of Higgs and Goldstone Modes in Strongly Interacting Lattice Bosons
Marco Fedele Di Liberto *Université Libre de Bruxelles* 225

Fast rotating Bose gases in RF adiabatic potentials
Mathieu De Goër de Herve *Laboratoire de Physique des Lasers (LPL), Université Paris 13 and CNRS* 226

Resummation of diagrammatic series with zero convergence radius for the unitary Fermi gas
Takahiro Ohgoe *University of Tokyo* 227

Tunneling dynamics of a superfluid Bose-Fermi mixture in the Bose-Einstein-condensate-unitarity crossover
Zhenxia Niu *Renmin University of China* 228

Laser Cooling at Resonance
Yaakov Yudkin *Bar-Ilan University* 229

Quantum dark solitons in 1D quantum gases
Joachim Brand *Massey University* 230

POSTER LIST

Page

Excitation dynamics and dispersive shocks in spin-orbit-coupled Bose-Einstein condensates
Peter Engels *Washington State University* 231

Staggered fluxes for Bose-Hubbard model in two leg ladder configuration
Friederike Metz *Okinawa Institute of Science and Technology Graduate University* 232

Light scattering by cold interacting two-level atoms
Ludovic Brossard *IOGS* 233

Droplet Phases in Dipolar and Rabi-Coupled Condensates
Alberto Cappellaro *University of Padova* 234

Observation of the Higgs mode in a strongly interacting fermionic superfluid
Martin Link *Universität Bonn* 235

Local control of transport in an atomic quantum wire
Philipp Fabritius *ETH Zurich* 236

Evolution of Few-Body Correlations in Bose Gases Quenched to Unitarity
Silvia Musolino *Eindhoven University of Technology* 237

Multi-second magnetic coherence in a single domain spinor Bose-Einstein condensate
Silvana Palacios *ICFO* 238

Fermionic properties of two interacting bosons in a two-dimensional harmonic trap
Pere Mujal *Universitat de Barcelona* 239

Non-linear resonnances in ^{23}Na spinor condensates
An Qu *Laboratoire Kastler Brossel* 240

Extended Bose-Hubbard Model with dipolar and contact interactions
Jakub Zakrzewski *Jagiellonian University* 241

Low-momentum Bragg Spectroscopy of a Unitary Fermi Gas
Carlos Claiton Noschang Kuhn *Swinburne University of Technology* 242

Observation of a dynamical sliding phase superfluid with P-band bosons
Shengjie Jin *Peking University* 243

Quantum Bose-Fermi droplets
Debraj Rakshit *Instytutu Fizyki PAN* 244

Physics of ultracold Yb-^{6}Li and Yb-^{7}Li mixtures
Florian Schaefer *Kyoto University* 245

Single-particle properties and effective range corrections in a strongly interacting Fermi gas
Hiroyuki Tajima *RIKEN Nishina Center* 246

Effect of a magnetic field on molecule-solvent angular momentum transfer
Wojciech Rzadkowski *Institute of Science and Technology Austria (IST Austria)* 247

Portable and flexible cold atom experiments
Philip Ireland *University of St Andrews* 248

Temperature dependence of the Bose polaron in a Bose-Einstein condensate
Magnus Graf Skou *Aarhus University, Department of Physics and Astronomy* 249

POSTER LIST

Page

Superfluid flow of an annular Bose gas
Hélène Perrin *LPL/CNRS - Université Paris 13 - IFRAF* 250

Real and imaginary part of conductivity of strongly interacting bosons in optical lattices
Barbara Grygiel *Institute of Low Temperature and Structure Research, Polish Academy of Sciences in Wroclaw* 251

Pinning Transition of Bose-Einstein Condensates in Optical Ring Resonators
Simon Schuster *Physikalisches Institut Tübingen* 252

Radiofrequency-Dressed Adiabatic Potentials to Observe Thermalisation of Two-Dimensional Quantum Gases
Kathrin Luksch *University of Oxford* 253

2D fermionic dipoles at T = 0
Raúl Bombín *Universidad Politécnica de Cataluña (UPC)* 254

Variable potentials for thermalized light and coupled condensates
Martin Weitz *University of Bonn, Institute for Applied Physics* 255

Induced transitions in the attractive Bose-Hubbard model
Lev Khaykovich *Bar Ilan University* 256

Measurements with cold thulium atoms in optical dipole trap.
Vladimir Khlebnikov *Russian Quantum Center* 257

Quantum scale anomaly and spatial coherence in a 2D Fermi superfluid
Marvin Holten *University of Heidelberg* 258

Spinor gases of fermionic erbium atoms
Gabriele Natale *University of Innsbruck* 259

Progress on the research on prototype of Cold Atom Physics Rack for the Chinese Space Station
Jingxin Sun *Peking University* 260

Pair condensation theory for systems of trapped cold fermionic atoms
Junichi Takahashi *Waseda University* 261

Bose-Einstein Condensates with Rotating Dipole Moments
Srivatsa Badariprasad *University of Melbourne* 262

Further Cooling of Alkali Atomic Gas in ``micro-gravity'' on earth
Wei Xiong *Peking University* 263

Grassmann Phase Space Theory for Fermions
Bryan Dalton *Swinburne University of Technology* 264

Flat-band ferromagnetism of SU(N) Hubbard model on Tasaki lattice
Ruijin Liu *Renmin University of China* 265

Entanglement and squeezing for two Bose Polarons
Miguel Angel Garcia-March *ICFO* 266

Design of an ultra-cold atom setup in microgravity
Bin Wang *Shanghai Institute of Optics and Fine Mechanics, Chinese Academy of Sciences* 267

POSTER LIST

Page

Prospects of reaching the quantum regime in Li/Yb^+
Henning Fürst *Universiteit van Amsterdam - Institute of Physics* 268

Quantum Criticality and Tomonaga-Luttinger Liquid in One-dimensional Bose Gases
Bing Yang *Physikalische institut* 269

Collisional cooling of trapped ions with ultracold atoms
Sadiqali Abbas Rangwala *Raman Research Institute* 270

Frequency comb cooling of atoms
Ticijana Ban *Institute of Physics* 271

Correlations of few-body quantum systems in position and momentum space
Ralf Klemt *Heidelberg University* 272

Dysprosium dipolar Bose-Einstein condensate with broad Feshbach resonances
Luca Tanzi *LENS* 273

Topological edge states and Aharanov-Bohm caging with ultracold atoms carrying orbital angular momentum
Gerard Pelegrí *Universitat Autònoma de Barcelona* 274

Dynamical formation of the Bose polaron through impurity-bath decoherence
Kristian Knakkergaard Nielsen *Department of Physics and Astronomy, Aarhus University* 275

Quantum probe spectroscopy for cold atomic systems
Jordi Mur-Petit *University of Oxford* 276

Ultracold atoms in an optical kagome lattice
Tiffany Harte *University of Cambridge* 277

Observation of Roton Mode Population in a Dipolar Quantum Gas
Daniel Petter *Institute for Experimental Physics* 278

Controlling Spin Exchange of Single Impurities in a Bose-Einstein Condensate
Artur Widera *Technische Universität Kaiserslautern* 279

Experimental realization of driven interacting many-body systems
Michael Messer *ETH Zurich* 280

Full-Contrast Fermionic Hanbury Brown-Twiss Interference
Philipp Preiss *Heidelberg University* 281

One-dimensional ultradilute quantum liquids
Grigory Astrakharchik *UPC* 282

Selective inter-band transition by pulse sequences in 1D bichromatic Bose lattices
Tomotake Yamakoshi *Univ. Electro-Communications* 283

Spin current in spin-orbit coupling Bose-Fermi mixture
Ryohei Sakamoto *Tokyo Metropolitan University* 284

POSTER LIST

Page

TOPIC: QUANTUM OPTICS ANS QUANTUM NANOPHOTONICS

Ultralow mechanical dissipation for quantum optomechanics
Nils Johan Engelsen *École Polytechnique Fédérale de Lausanne* 285

Monochromatic thermal radiation from a sub-micron dielectric particle
Maki Tachikawa *Meiji University* 287

Storage of Single Photons Generated from Cavity-enhanced Spontaneous Parametric Down Conversion in Cold Atomic Ensembles
Ying-Cheng Chen *Institute of Atomic and Molecular Sciences, Academia Sinica* 288

Atom-chip interferometry with Bose-Einstein condensates
Matthias Gersemann *Institut für Quantenoptik, Leibniz Universität Hannover* 289

Phase Sensitive Amplification Enabled by Coherent Population Trapping
Pascal Neveu *Laboratoire Aimé Cotton* 290

Repulsive photons in a quantum nonlinear medium
Wenchao Xu *Harvard University* 291

Two-photon interferences with paired photons generation in a two-level atomic ensemble
Shuyu Zhou *Shanghai Institute of Optics and Fine Mechanics, Chinese Academy of Sciences* 292

Active temporal mode purification of quantum dots emission by quantum memory
Shaobo Gao *University of Oxford* 293

Quantum nondemolition measurement of mechanical motion quanta
Luca Dellantonio *University of Copenhagen* 294

Exploring Two Photon Processes Mediated by an Atom
Vindhiya Prakash *ICFO-The Institute of Photonic Sciences* 295

1D Atomic Lattices For Atom-Photon Physics
Lucas Peng *California Institute of Technology* 296

Deterministic quantum entanglement among three distant atomic ensembles
Zhihui Yan *Shanxi University* 297

Four-wave-mixing and entanglement of spatially separated light
Wanxia Cao *Fudan University* 298

Statistics of Atom Pair Production by Four Wave Mixing
Christoph Westbrook *Institut d'Optique Graduate School* 299

Photons in the presence of parabolic mirrors
Rocio Jauregui *Instituto de Física, Universidad Nacional Autónoma de México* 300

Optical nanoantennas for light - matter coupling through parallel multipolar mechanisms
Piotr Gładysz *Institute of Physics, Faculty of Physics, Astronomy and Informatics, Nicolaus Copernicus University* 301

Interaction of an asymmetric two-level quantum system with light
Piotr Gładysz *Institute of Physics, Faculty of Physics, Astronomy and Informatics, Nicolaus Copernicus University* 302

Fast, noise-free memory for photon synchronization at room temperature
Ran Finkelstein *Weizmann Institute of Science* 303

POSTER LIST

Page

Interfacing single trapped atoms to a pair of indistinguishable photons
Natalia Bruno *ICFO* 304

Atom-phonon interaction in fiber-based optical traps
Daniel Hümmer *IQOQI Innsbruck* 305

Quantum optics in the hyperfine Paschen-Back regime
Renju Mathew *Renju Mathew* 306

A Fabry-Perot microcavity for enhancing entangling rate in a diamond-based quantum network
Suzanne Van Dam *QuTech, Delft University of Technology* 307

Coherent control of the spins of NV centers in levitating diamonds
Gabriel Hétet *ENS* 308

Quantum and nonlinear effects in transmission of light through planar arrays of atoms
Robert Bettles *Durham University* 309

Preparation and reconstruction of an entangled state of two microwave cavities
Valentin Métillon *Collège de France* 310

Controlling ultra-cold atomic ensembles with simultaneous radio-frequency and microwave dressing
German Sinuco *University of Sussex* 311

Fano resonance via 7F state in rubidium atom
Masashi Abe *Chuo University* 312

Tuesday 24th July

TOPIC: ATOMIC CLOCKS AND QUANTUM METROLOGY

High Precision Phase and Frequency Measurements in Rare Earth Doped Crystals for Probing Nanoresonator Behavior
Nicolas Galland *CNRS SYRTE UGA Institut Neel* 313

Towards a quantum-enhanced trapped-atom clock on a chip
Mengzi Huang *Laboratoire Kastler Brossel* 314

Measurement of magic wavelength for 1140 μm clock transition in Tm atoms
Dmitry Tregubov *Lebedev Physical Institute of RAS* 315

Cross-correlation measurement between two Ti:Sapphire optical frequency combs referencing a clock laser transferred via an optical fiber link
Kota Nakashima *The University of Tokyo* 316

Towards a second generation for the brazilian atomic fountain frequency standard: Tests with the new MOT chamber
Daniel Magalhães *University of São Paulo* 317

Coherence properties of NV ensembles in HPHT diamond plates
Vadim Vorobyov *P.N. Lebedev Physical Institute of the Russian Academy of Sciences* 318

POSTER LIST

Page

Rotation Sensing with an Atomic Clock
Jamie Johnson *University of Nottingham* 319

Spin-Squeezing for Entanglement-Enhanced Matterwave Interferometers
Graham Greve *JILA/CU-Boulder* 320

Steady-state ultracold Sr with unity phase-space density
Chunchia Chen *University of Amsterdam, Institute of Physics* 321

Ultra-stable laser based on a compact Fabry-Perot cavity
Séverine Denis *Femto-st* 322

Measurement of ultracold atom velocity distributions by matterwave interferometry
Tim Freegarde *University of Southampton* 323

Developing a Transportable Ultra-cold Atomic Rotation Sensor
David Elcock *University of Southampton* 324

Near-Unitary Spin-Squeezing for Optical Clocks
Simone Colombo *Massachusetts Institute of Technology* 325

Nondestructive measurement of trapped cold atoms
Xian Zhang *Zhejiang University* 326

Development of a planar ion trap aimed at ion spacing control by anharmonic potential
Hironori Sasaki *Osaka University* 327

Pumped-Up SU(1,1) Interferometry
Stuart Szigeti *The Australian National University* 328

Simultaneous precision magnetic and inertial sensor based on spatial fringes using Bragg transitions
Paul Wigley *The Australian National University* 329

AMBiT: A program for high-precision relativistic atomic structure calculations
Julian Berengut *University of New South Wales* 330

Sensitivity limists of an Atomic gravimeter using Raman atom interferometer
Sang-Bum Lee *Korea Research Institute of Standard and Science* 331

Development of NPL's 2nd Generation Strontium Lattice Clock
William Bowden *Oxford University* 332

A search for the low-energy ^{229}Th nuclear isometric transition using an "optical" pumping technique at 29-keV
Satoshi Uetake *Okayama University* 333

A compact inertial sensor using atom interferometry: pushing towards high-dynamic range
Indranil Dutta *Imperial College London* 334

Atomic structure calculations and study the parameters of hyperfine constants, Lande g-factors and isotope shifts of Xe LIII
Dhia Elhak Salhi *National Center for Nuclear Sciences and Technologies* 335

POSTER LIST

Page

TOPIC: INTENSE FIELDS AND ULTRAFAST SCIENCE

Ultracold and ultrafast: Strong-field ionization of trapped alkali atoms
Philipp Wessels *The Hamburg Centre for Ultrafast Imaging* 336

Extracting spectroscopic molecular parameters from short pulse photo-electron angular distributions
Mourad Telmini *University of Tunis El Manar* 337

Wave packet motion analysis on the role of excited states in the multiphoton ionization
Shih-Da Jheng *National Chiao Tung University Institute of Physics* 338

Strong field approximation model for frustrated tunneling ionization and subsequent free induction decay
Je Hoi Mun *Institute for basic science (IBS)* 339

Angle resolved photodetachment time delay
Soumyajit Saha *Indian Institute of Technology Madras* 340

Interferences in photoelectron spectra - Holographic structures
Sebastián David López *Instituto de Astronomía y Física del Espacio - (UBA - CONICET)* 341

Time delays in (ω, 2ω) above threshold ionization
Sebastián David López *Instituto de Astronomía y Física del Espacio - (UBA - CONICET)* 342

Theoretical modeling of the high-harmonic generation and ionization processes with a discrete representation of the continuum
Piotr Gniewek *University of Warsaw* 343

Multi-photon spectroscopy of the many-electron atoms and ions in a laser eld with accounting for the Debye plasma effects
Eugeny Ternovsky *Odessa State University - OSENU* 344

Strong field three electron ionization - ab initio time-dependent study
Jakub Zakrzewski *Jagiellonian University* 345

Laser Electron-Gamma-Nuclear Spectroscopy of Atmos and Multicharged Ions: Shake-Up and NEET Effects
Olga Khetselius *Odessa State University - OSENU* 346

The effect of intermediate continuum states on two-photon ionization cross section
Andrej Mihelic *Jozef Stefan Institute* 347

Instantaneous ionization rate as a functional derivative
Igor Ivanov *Institute for Basic Science* 348

Creating and multiplying knots in the polarization state of light
Emilio Pisanty *ICFO - The Institute of Photonic Sciences* 349

Fast transport and spin control of atoms in moving traps
Qi Zhang *Shanghai University* 350

POSTER LIST

Page

TOPIC: OTHER

Turbulent cascades in out-of-equilibrium Bose gas
Vanderlei S Bagnato *Universidade de Sao Paulo* 351

TOPIC: OUT OF EQUILIBRIUM QUANTUM SYSTEMS

Creating a superfluid by kinetically driving a Mott insulator
Charles Creffield *Universidad Complutense de Madrid* 352

Revealing missing charges with generalised quantum fluctuation relations
Jordi Mur-Petit *University of Oxford* 353

Weakly interacting Bose gases far from thermal equilibrium - Engineering condensation with a hot needle
Alexander Schnell *Max-Planck-Institut für Physik kompexer Systeme* 354

Quench dynamics in a two-particle system with a combination of synthetic spin-orbit coupling and Raman coupling
Ayaka Usui *OIST Graduate university* 355

Impact of geometry on many-body localization
Dariusz Wiater *Institute of Physics Polish Academy of Sciences* 356

Collective modes and quantum thermalisation with tilted dipoles
Lucas Gabardos *Laboratoire de Physique des Lasers UMR 7538 CNRS UP13.IG* 357

Monitoring squeezed collective modes of a 1D Bose gas after an interaction quench using density ripples analysis
Max Schemmer *Laboratoire Charles Fabry, Institut d'Optique* 358

Probing many-body localization in the presence of a quantum bath
Antonio Rubio Abadal *Max Planck Institute of Quantum Optics* 359

Dynamical Phase Transition in the Collective Heisenberg Model
Kenneth Jackson *University of Toronto* 360

Quantum master equation in paired degenerate subspace of finite-size dissipative Dicke model
Ryosuke Imai *Waseda university* 361

Nontrivial Bloch oscillations in an optical lattice due to spin-orbit coupling
Lu Zhou *East China Normal University* 362

Turning-off two-body and generating three-body interactions between ultracold neutral bosonic atoms
Philip Johnson *American University* 363

Scale-dependent anomalous diffusion in spatially disordered environments
Gorka Muñoz *ICFO* 364

Quantum noise in a transversely pumped cavity Bose-Hubbard model
Gergely Szirmai *Wigner Research Centre* 365

POSTER LIST

Page

Out-of-equilibrium many-body systems: a numerical approach based on non-equilibrium Green's functions
Natale Walter Talarico *University of Turku* 366

A many-ion quantum simulator of the Dicke model for probing entanglement, chaos and information scrambling
Robert Lewis-Swan *JILA, NIST, University of Colorado* 367

Relaxation dynamics of non-equilibrium quantum gas in a uniform box potential
Jinyi Zhang *The Cavendish Laboratory, University of Cambridge* 368

Nonlinear damping of quantum gas at ultra–low temperature in a cylindrical box potential
Jinyi Zhang *The Cavendish Laboratory, University of Cambridge* 369

Floquet-Gibbs state for dissipative quantum systems
Tatsuhiko Shirai *University of Tokyo* 370

Formulation of quantum field theory for driven-dissipative Bose-Einstein condensation
Takahiro Oyama *Waseda University* 371

Non-equilibrium phase structure and dynamics of driven-dissipative Rydberg spin systems
Stephan Helmrich *Heidelberg University* 372

Exploring extreme nonequilibrium dynamics with ultracold atoms
Toshihiko Shimasaki *University of California Santa Barbara* 373

Universal phase fluctuations in low dimensional quantum systems
Ryan Plestid *McMaster University* 374

Dynamics in an isolated disordered Heisenberg spin system
Gerhard Zuern *University of Heidelberg* 375

A model for strong-coupling, finite-time and finite-size interactions: the Gaussian Otto cycle
Alejandro Pozas-Kerstjens *ICFO* 376

Kapitza stabilization of a repulsive Bose-Einstein condensate in an oscillating optical lattice
John Martin *University of Liège* 377

Direct measurement of localization and logarithmically-slow correlation dynamics in the many-body-localized phase
Robert Schittko *Harvard University* 378

Probing microscopic models for system-bath interactions via parametric driving
Anastasia Dietrich *University of Oxford* 379

Optical conductivity of a quantum gas
Peihang Xu *University of Toronto* 380

POSTER LIST

Page

TOPIC: QUANTUM COMPUTATION AND COMMUNICATION

Two-electron atoms: The Greens function approach to the Fock expansion calculations
Evgeny Liverts *The Hebrew University* 381

A fibre-tip Fabry-Pérot cavity for deterministic, strong atom-photon interactions
Marwan Mohammed *University of Oxford* 382

Polarised Single-Photons from a Cavity-Enhanced Atom-Light Interface in Photonic Quantum Networks
Thomas Barrett *University of Oxford* 383

From Reservoir Engineering with Trapped Ions to GKP Coding State and Phonon Lasing
Thanh Long Nguyen *ETH Zurich* 384

Demonstration of a passive photon-atom swap gate
Adrien Borne *Weizmann Institute of Science* 385

Hight-fidelity Single-Qubit Gates of a Neutral-Atom Qubit in a Magic-Intensity Optical Dipole Trap
Cheng Sheng *WIPM* 386

Using and reusing coherence to realize quantum processes
María García Díaz *Universitat Autònoma de Barcelona* 387

Photonic quantum state engineering using single-photon Raman interaction
Ziv Aqua *Weizmann Institute of Science* 388

Sub-Megahertz Single Photon Source Suitable for Quantum Memories
W. Y. Sarah Lau *University of Queensland* 389

Repeated multi-qubit readout and feedback with a mixed-species trapped-ion register
Matteo Marinelli *ETH Zurich* 391

Spatially dependent Electromagnetically Induced Transparency
Francesco Castellucci *University of Glasgow* 392

Photonic quantum state transfer between a cold atomic gas and a crystal
Nicolas Maring *ICFO* 393

Energy-time entanglement between a single photon and a spin wave in a solid state quantum memory
Margherita Mazzera *ICFO* 394

Multiplexed storage and real-time manipulation based on a multiple-degree-of-freedom quantum memory
Tianshu Yang *University of Science and Technology of China* 395

Speeding Up Reinforcement Learning on a Trapped Ion Quantum Computer
Ivan Boldin *University of Siegen* 396

Scaling of electric field noise in surface ion traps
Clemens Matthiesen *University of California, Berkeley* 397

Progress towards entanglement of atomic ensemble qubits via Rydberg blockade
Minho Kwon *Department of Physics, University of Wisconsin-Madison* 398

Independent gate operations on two adjacent atomic qubits in a 532-nm 1D optical lattice
Donghyun Cho *Korea University* 399

POSTER LIST

Page

Modular segmented ion trap with an integrated optical cavity
Simon Ragg *ETH Zurich* 400

Towards a temporally multiplexed quantum repeater node based on laser-cooled atoms
Lukas Heller *ICFO* 401

Quasi-continuous variable quantum computation with collective spins in multi-path interferometers
Tomas Opatrny *Palacky University* 402

Eliminating Noise from a Broadband and Single-Mode Quantum Memory
Thomas Hird *University of Oxford* 403

High-Dimensional Temporal Mode Manipulation using Quantum Memories
Sarah Thomas *University of Oxford* 404

Microfabricated optical elements towards a photonic interface for ion microtrap arrays
Matthew Day *University of Bristol* 405

Electron and Nuclear spin dynamics of Kramers ion at Subkelvin Temperatures
Peiyun Li *University of Science and Technology of China* 406

Highly-Efficient Quantum Memory for Polarization Qubits in a Spatially-Multiplexed Cold Atomic Ensemble
Mingtao Cao *LKB* 408

Electron and Nuclear spin dynamics of Kramers ion at Subkelvin temperatures
Chao Liu *University of Science and Technology of China* 409

Spiral bandwidth of four-wave mixing in rubidium vapour
Aidan Arnold *University of Strathclyde* 411

Superconducting qubit-qutrit circuit: A toolbox for efficient quantum gates
Thomas Bækkegaard *Aarhus University* 412

Optimal condition for a cavity QED-based quantum gate
Rui Asaoka *Meiji University* 413

RF-induced evaporative cooling in an optical trap
Meungho Seo *Korea University* 414

A novel integrated platform for quantum storage of heralded single photons
Alessandro Seri *ICFO* 415

Efficient single-photon collection for long-distance entanglement of atoms
Robert Garthoff *LMU Munich* 416

Towards quantum interfaces based on trapped $^{25}Mg^{+}$ ions
Aleksandr Borisenko *Russian Quantum Center (RQC)* 417

Tomography of a Raman Quantum Memory for Temporal Modes
Sarah Thomas *University of Oxford* 418

Towards heralded entanglement of single atoms over long distances
Tim Van Leent *LMU Fakultät für Physik* 419

POSTER LIST

Page

Optimized Entangled State Retrieval from Quantum Memories for Networking
Siddhartha Santra *US Army Research Laboratory* 420

Engineering the components of a quantum cryptographic network enhanced by quantum memories
Sonali Gera *Stony Brook University* 421

Cubic Hamiltonian in few steps
Šimon Bräuer *Palacký University* 422

Modal Properties of the Off-resonant Cascaded Absorption Memory
Oscar Gerardo Lazo Arjona *University of Oxford* 423

Broadband Light-Matter Interactions with an Atomic Frequency Comb in a Rare-Earth-Ion-Doped Crystal
Patrick Ledingham *University of Oxford* 424

Storing single photons emitted by a quantum memory on a highly excited Rydberg state
María Auxiliadora Padrón Brito *ICFO* 425

Quantum compilation optimized for experiments with multi-qubit gates
Liangyu Ding *Renmin University of China* 426

A novel quantum memory protocol for coherent storage and manipulation of broadband photons via dynamically controlled Autler-Townes absorption
Anindya Rastogi *University of Alberta* 427

Strong upper bounds for the classical capacity on Gaussian quantum channels
Kabgyun Jeong *Seoul National University* 428

Investigation of the Hyperfine Structure of the Electronically Excited State through Raman Heterodyne Detection
Yu Ma *University of Science and Technology of China* 429

Genuinely entangled symmetric states with no N-partite correlations
John Martin *University of Liège* 431

Observing the quantum interference and entanglement of electron-nuclear system on Bloch sphere by Wigner distribution
Heng Shen *University of Oxford* 432

Verifying high-fidelity multi-particle processes in an ion-trap quantum computer
Alexander Erhard *University of Innsbruck* 433

Half-Deterministic Atom-Photon Entanglement for Quantum Repeaters
Jun Li *University of Science and Technology of China* 434

Quantum memory for light: beyond the three-level Λ-scheme approximation
Alexandra Sheremet *Sorbonne Université* 435

TOPIC: QUANTUM GASES

Negative-mass effects in spin-orbit coupled Bose-Einstein condensates
David Colas *The University of Queensland* 436

POSTER LIST

Page

Quantum Phases and Excitations in Bose-Fermi Mixtures in a Three-Dimentional Optical Lattice
Hatsuda Rei *Tokyo Metropolitan University* 437

Magnetic phases of spin-1 lattice gases with random interactions
Simone Paganelli *University of L'aquila* 438

Laser cooling of ^{87}Rb to quantum degeneracy
Alban Urvoy *Massachusetts Institute of Technology* 439

Measurement of interorbital spin-exchange interaction of ytterbium atoms
Koki Ono *Kyoto university* 440

Shear viscosity of a strongly-interacting Fermi gas
Daichi Kagamihara *Keio University* 441

Sound Propagation excited by Density Perturbation in a Bose-Fermi Mixture Superfluid at Finite Temperatures
Yosuke Ono *Tokyo Metropolitan University* 442

Observation of Atom Number Fluctuations in a Bose-Einstein Condensate
Jan Arlt *Aarhus Universitet* 443

Isothermal Compresibility and Strong Coupling Effects in an Ultracold Fermi Gas
Ryohei Sato *Keio University* 444

Photoemission Spectrum in an Ultracold Bose-Fermi Mixture with Hetero-Pairing Interaction
Koki Manabe *Keio University* 445

Phase-separated state in a repulsive Bose-Fermi mixture: Interface structure and breathing mode
Bo Huang *IQOQI Innsbruck, ÖAW* 446

An experiment for the study of small Hubbard models with rapid repetition rate
Martin Schlederer *Institute for Laser Physics, University of Hamburg* 447

Temperature-dependent break-down of disorder-induced localization for interacting fermions coupled to a thermal bath
Lingna Wu *Max Planck Institute for the Physics of Complex Systems* 448

Collisional Properties of Fermionic Potassium in the Vicinity of a D-Wave Feshbach Resonance
Markus Bohlen *Laboratoire Kastler Brossel, ENS* 449

Long-range interactions and symmetry-breaking in quantum gases through optical feedback
Yongchang Zhang *Aarhus University* 450

Dynamical control of phases in a Driven-Dissipative Bose-Einstein Condensate in an Optical Cavity
Jayson Cosme *University of Hamburg* 451

2D and 3D Grating Magneto-Optical Traps as Cold Atom Sources
Oliver Burrow *University of Strathclyde* 452

Doppler-sensitive holographic Microscopy of cold atoms
Wang Yuzhuo *Fudan University* 453

POSTER LIST

Page

Superfluid weight and Berezinskii-Kosterlitz-Thouless temperature of spin-imbalanced and spin-orbit-coupled Fulde-Ferrell phases in lattice systems
Aleksi Julku *Department of Applied Physics, Aalto University* 454

Out-of-time-ordered correlator of quenched state in many-body localization
Juhee Lee *Gwangju Institute of Science and Technology* 455

Collisionless sound in a uniform Bose gas
Miki Ota *University of Trento* 456

Fast manipulation of Bose-Einstein condensates with an atom chip
Robin Corgier *Institut für Quantenoptik, Leibniz Universität Hannover* 457

Spatially distributed genuine multipartite entanglement enables EPR steering of Bose-Einstein Condesates
Philipp Kunkel *Universität Heidelberg, Kirchhoff-Institut für Physik* 458

Coherent splitting and recombination of bright solitary matter waves
Ana Rakonjac *Durham University* 459

Bilayer system of dipolar bosons: few-body bound state
Grecia Guijarro *Universitat Politècnica de Catalunya* 460

A new apparatus for the study of Sodium spinor BECs in highly stable magnetic field environment
Arturo Farolfi *Università degli Studi di Trento* 461

A Spinor BEC co-magnetometer for phase resolving spin amplification
Pau Gómez Kabelka *ICFO* 462

Anomalous momentum diffusion in a Bose-Hubbard gas
Raphael Bouganne *Laboratoire Kastler-Brossel* 463

Quantized circular dichroism in ultracold atoms
Duc-Thanh Tran *Université Libre de Bruxelles* 464

Speed of sound in a superfluid 2D Bose gas
Raphaël Saint-Jalm *Laboratoire Kastler Brossel* 465

Non-demolition quantum thermometry of BECs in the sub-nK domain
Mohammad Mehboudi *ICFO* 466

Two-dimensional Condensation of Polar Molecules in a Synthetic Gauge Field
I-Kang Liu *Department of Physics and Graduate Institute of Photonics, National Changhua University of Education* 467

Non-linear relaxation of interacting bosons coherently driven on a narrow optical transition
Manel Bosch *Laboratoire Kastler Brossel* 468

Observation of Spin Superfluidity in a Bose Gas Mixture
Carmelo Mordini *University of Trento* 469

Synthetic dimensions in ultracold polar molecules: From topology to quantum strings
Bhuvanesh Sundar *Rice University* 470

Universality of liquid Bose-Bose mixture of ultracold atoms
Leandra Vranjes Markic *University of Split* 471

POSTER LIST

Page

Modeling atom diffraction beyond the weakly-diffracting limit
Benjamin Beswick *Durham University* 472

Quantum Monte Carlo simulations of spin-orbit coupled systems
Andrii Gudyma *University of Split, Faculty of Science* 473

Raise and fall of a bright soliton in an optical lattice
Piero Naldesi *LPMMC Grenoble* 474

Towards ultracold erbium-potassium quantum gas mixtures
Jackson Ang'ong'a *University of Illinois at Urbana-Champaign* 475

Quantum liquid droplets in a mixture of Bose-Einstein condensates
Cesar Cabrera Cordova *ICFO* 476

Many-body effects in synthetic lattices
Fangzhao An *University of Illinois at Urbana-Champaign* 477

Dynamics and Thermodynamics of Strongly Interacting Homogeneous Bose Gases
Timon Hilker *University of Cambridge* 478

Supersolid Phase with Ultracold Bose Gases in an Optical Lieb Lattice
Hisashi Kawaguchi *Aoyama-Gakuin University* 479

Squeezed field description of second sound in Bose-Einstein condensates
Ludwig Mathey *University of Hamburg* 480

Universal few-body correlations in a Bose polaron
Shimpei Endo *Tohoku University* 481

Spin-dependent artificial magnetic fields and superfluidity in Bose-Einstein condensates
Lindsay Leblanc *University of Alberta* 482

Collective oscillations of a strongly interacting 2D Fermi gas
Paul Dyke *Swinburen University of Technology* 483

Bistability and Non-equilibrium Condensation in a Driven-Dissipative Atomic Superfluid
Matthew Reeves *University of Queensland* 484

Synthetic Frustrated Antiferromagnets with Coherently-Coupled Binary Fermi Gases in a Triangular Optical Lattice
Daisuke Yamamoto *Aoyama Gakuin University* 485

Self-bound Bose mixtures
Robert Zillich *Johannes Kepler University* 486

Superfluidity of Light in an atomic vapor
Quentin Glorieux *LKB - ENS - Sorbonne Université* 488

Interaction control and interorbital molecules exploiting clock transition in two electron atoms
Jacopo Catani *LENS & INO-CNR National Institute of Optics CNR* 490

Strong-coupling effects on p-wave contacts in an ultracold Fermi gas with a p-wave interaction
Daisuke Inotani *Department of Physics, Keio University* 491

POSTER LIST

Page

Precision imaging of cold atoms with high resolution holographic microscopy
Jian Zhao *Fudan University* 492

Drag force and superfluidity in the supersolid stripe phase of a spin-orbit-coupled Bose-Einstein condensate
Giovanni Italo Martone *CNRS LPTMS* 493

Towards weakly-destructive, real-time transport measurements of interacting Fermi Gas
Barbara Cilenti *EPFL* 494

Feshbach resonances and Feshbach molecules in an ultracold ^{6}Li-^{133}Cs mixture
Bing Zhu *Heidelberg University* 495

Long range interactions in time lattices
Krzysztof Giergiel *Jagiellonian University in Krakow* 496

Quantum phase transition of a frustrated Bose-Hubbard model on triangular lattice: Density matrix renormalization group study
Yutaka Saiki *Aoyama-Gakuin University. Department of Physics and Mathematics* 497

Observation of semimetal phase for ultracold fermions with 2D spin-orbit coupling in an optical lattice
Chengdong He *Hong Kong University of Science and Technology* 498

Two-photon spectroscopy of ultracold rubidium atoms in magnetic field
Ryo Yasuda *Chuo University* 499

Observation of Superradiant Decay of Cold Atoms via the 350 Hz Intercombination Line of Calcium
Hannes Winter *Universität Hamburg* 500

Blue light emission from ultracold rubidium atoms via optical double resonance
Sakura Seta *Chuo University* 501

Coupled order parameters with ultracold atoms in two crossed cavities
Philip Zupancic *ETH Zurich* 502

Two photon spectroscopy of ultracold rubidium atoms near dielectric surface
Taro Mashimo *Chuo university* 503

Observation of the $5^{2}P_{3/2}$ - $6^{2}P_{3/2}$ forbidden transition in laser-cooled rubidium atoms
Miki Fukui *Chuo University* 504

A two-dimensional box trap for ultracold ^{39}K atoms with tuneable interactions
Panagiotis Christodoulou *University of Cambridge* 505

Lifetime of a chiral superfluid in an orbital optical lattice
Raphael Eichberger *Universität Hamburg* 506

One-dimensional spinor Bose gases: Spin-domain formation and giant spin-dipole polarizability
Bertrand Evrard *CNRS Laboratoire Kastler Brossel* 507

POSTER LIST

Page

TOPIC: QUANTUM OPTICS ANS QUANTUM NANOPHOTONICS

Nanosecond geometric control of electric dipole
Saijun Wu *Fudan University* 508

Optical switching in Doppler broadened multilevel atomic systems
Kavita Yadav *Indian Institute of Technology Roorkee* 509

Highly bright polarization-entangled photon-pairs from a Doppler-broadened ladder-type atomic ensemble
Han Seb Moon *Pusan National University* 510

Bidirectional lasing with cold atoms in a ring cavity
Jon Goldwin *University of Birmingham* 511

A simple approach to quantum dispersive light through single-particle quantum mechanics
Nicla Westerberg *Institute of Photonics and Quantum Sciences, Heriot-Watt University* 512

Direct frequency-comb-driven Raman transitions in the terahertz range
Cyrille Solaro *Aarhus University* 513

Excitation enhancement in optical forbidden transitions near nano structure
Satoshi Tojo *Chuo University* 514

A versatile neutral-atom microtrap using high NA optics to study light-matter interaction
Lorena C. Bianchet *ICFO* 515

Microscale atom-photon junction
Elisa Da Ros *University Nottingham* 516

Tuning dipole-dipole interactions in atomic vapours via cavities
Helge Dobbertin *Universität Rostock, Institut für Physik* 517

Towards a quantum interface between cold atoms and a nano membrane
Chun Tat Ngai *University of Basel* 518

Two-mode intensity squeezing using OAM-carrying pump and probe beams
Nikunjkumar Prajapati *William &Mary* 519

Quantum Mechanics in Technicolor; Analytic Expressions for a Spin-Half Particle Driven by Polychromatic Light
Ben Yuen *University of Oxford* 520

Spatially-multiplexed coherent beamsplitter for squeezed light
Jian Sun *Fudan University* 521

Narrowband four photon entanglement swapping
Li Zongfeng *CAS Key Laboratory of Quantum Infomation, USTC* 522

Towards a BEC-ONF Interface
Alexandros Chantif Alampounti *Swansea University* 523

Transverse and Upstream Motion of Photons in Moving Atomic Media
Akbar Safari *University of Ottawa* 524

POSTER LIST

Page

Multi-mode state retrodiction from optodynamical measurements of collective atomic dynamics
Jonathan Kohler *UC Berkeley* 525

Heralded entanglement in a spinor gas in an optical cavity
Stuart Masson *University of Auckland* 526

What filter do you need for your heralded single photon source?
Daniel Blay *Macquarie University* 527

Atom-light interaction in thermal Rubidium vapours confined to a volume less than λ^3
William Hamlyn *Durham University* 528

Electromagnetically induced transparency (EIT), absorption (EIA) and Autler Townes (AT) splitting in N-type system
Bankim Chandra Das *Saha Institute of Nuclear Physics* 529

Pulse delay and group velocity dispersion measurement in V-type electromagnetically induced transparency of hot ^{85}Rb atom
Bankim Chandra Das *Saha Institute of Nuclear Physics* 530

Angular momentum spacial symmetry transformation in rubidium ground-state
Arturs Mozers *University of Latvia* 531

Designing regular atomic arrays as `free-space' photonic quantum link
Pierre-Olivier Guimond *IQOQI Innsbruck* 532

Heralding of a single collective excitation in a 1D atomic array coupled to an optical nanofiber
Jeremy Raskop *LKB (Laboratoire Kastler Brossel)* 533

Thursday 26th July

TOPIC: ATOMIC CLOCKS AND QUANTUM METROLOGY

Measurement of the hyperfine structure of the 5s5d $^3D_3$ state in ^{87}Sr using a hollow cathode lamp
Takumi Sato *The University of Tokyo* 534

Progress in the stability and frequency uncertainty of strontium optical lattice clocks at NPL
Richard Hobson *National Physical Laboratory* 535

Search for biomagnetism in venus-flytrap plants
Anne Fabricant *Helmholtz Institute Mainz* 536

A geometrically asymmetric optical cavity for a spin squeezed ^{171}Yb optical atomic clock
Edwin Pedrozo *Massachusetts Institute of Technology* 537

Quantum metrology with Rydberg atoms
Sebastien Gleyzes *Laboratoire Kastler Brossel* 538

Tunable phase-locked laser system for quantum sensing applications
Joseph Thom *M Squared Lasers Ltd* 539

POSTER LIST

Page

Development of Yb optical lattice clocks at KRISS
Dai-Hyuk Yu *Korea Research Institute of Standards and Science* 540

A compact grating magneto-optical trap for ultracold Yb
Robert Fasano *National Institute of Standards and Technology* 541

Towards a spin-squeezed atomic gradiometer with multipass cells
Vito Giovanni Lucivero *Princeton University* 542

MEMS fabrication and operation of 3D ion microtraps
Alastair Sinclair *National Physical Laboratory* 543

Crossover from quantum cats to classical mixtures in ultra-cold atom interferometers
Shane Kelly *UCR* 544

Novel atom interferometers with ultra-cold alkaline-earth atoms
Nicola Poli *Università Degli Studi di Firenze* 545

Ramsey Spectroscopy with Frequency Displaced Jumps
Moshe Shuker *NIST* 546

Spin self-rephasing in the system of several atoms
Konrad Szymanski *Marian Smoluchowski Institute of Physics, Jagiellonian University* 548

Ytterbium optical lattice clocks supporting 1×10^{-18} frequency comparisons
William McGrew *NIST* 549

Entanglement, interferometric sensitivity, and macroscopic superposition states by scanning through quantum phase transitions in spinor Bose-Einstein condensates
Polina Feldmann *Leibniz Universität Hannover, Institut für Theoretische Physik* 550

Towards Quantum Logic Spectroscopy of Highly Charged Ions
Piet Schmidt *PTB Braunschweig/LUH Hannover* 551

Dynamics of a Strontium Cold Atom Laser
Mikkel Tang *Niels Bohr Institute* 552

Route to a Portable Optical Clock
Yogeshwar Kale *Birmingham University* 553

Precision Measurements with Trapped-Ion Optical Clocks at NIST
David Hume *National Institute of Standards and Technology* 554

Two clock transitions in neutral Yb for the highest sensitivity to variations of the fine-structure constant
Sergey Porsev *University of Delaware* 555

TOPIC: FUNDAMENTAL TESTS ANS QUANTUM MEASUREMENTS

Fringe Visibility, Which-Way Information and Weak Value
Sang Wook Kim *Kyung Hee University* 556

Sympathetic cooling of trapped ions for high resolution spectroscopy
Thomas Louvradoux *Laboratoire Kastler Brossel* 557

POSTER LIST

Page

Anderson Localisation Experiments with Ultracold Atoms in a 2D Programmable Potential
Maarten Hoogerland *University of Auckland* 558

Atomic diffraction through nano grating for a novel Casimir-Polder potential measurement
Gabriel Dutier *IG / University Paris13 / CNRS UMR 7538* 559

EDM ^{3} : a new search for the electron electric dipole moment using molecules in a matrix
Eric Hessels *York University* 560

Development of a hybrid atom chip.
Julien Alibert *Laboratoire Collisions Agrégats Réactivité* 561

Precision microwave measurement of the n = 2 triplet P_1 to P_2 fine structure interval of atomic helium
Eric Hessels *York University* 562

Parity-nonconserving interaction-induced light shifts in the $7S_{1/2}$ - $6D_{3/2}$ transition of the ultracold ^{210}Fr atoms to probe new physics beyond the standard model
Takatoshi Aoki *The University of Tokyo* 563

Optical dipole force trapping of rubidium atoms for a dual-isotope co-magnetomter toward the electron electric dipole moment
Aiko Uchiyama *Tohoku University* 564

Diffraction Phases in Large Momentum Separation Contrast Interferometry with Yb Bose-Einstein condensates
Katherine McAlpine *University of Washington* 565

Dephasing due to Gravitational Interaction in Atomic Interferometer
Sohitri Ghosh *University of Maryland,College Park* 566

Directional detection of dark matter using spectroscopy of crystal defects
Ronald Walsworth *Harvard-Smithsonian* 567

Towards deployable atomic gravimeters for geophysics
Zachary Pagel *University of California, Berkeley* 568

Reflecting on an alternative (parity-time-symmetric) quantum theory, and its analog in optics
Ray-Kuang Lee *National Tsing Hua University* 569

Development of Multi-shell Magnetic Shields for Atomic Spin Gyroscope
Zaeill Kim *Agency for Defense Development* 571

Investigating Particle Indistinguishability with a Freely Rotating Coulomb Crystal
Erik Urban *University of California, Berkeley* 572

Experimental probe of the tunneling time for ultra-cold atoms
Jesus Ramon Ramos Benitez *University of Toronto* 573

Precision Search for CP Violation with Polyatomic Molecules
Nicholas Hutzler *California Institute Technology* 574

Realization of a 12 m atom fountain and suppression of wave-front-aberration phase noise in atom interferometers
Jin Wang *Wuhan Institute of Physics and Mathematics, Chinese Academy of Sciences* 575

POSTER LIST

Page

Generation of Atomic Beams of Highly Refractory Elements for Laser Spectroscopy
Alonso Castro *Los Alamos National Laboratory* 576

High Sensitivity Ring Laser Gyroscopes for Geodesy and Fundamental Physics
Nicolo' Beverini *INFN- Sezione di Pisa* 577

Towards high-precision spectroscopy of the 1S-2S transition in He^+
Fabian Schmid *Max Planck Institute of Quantum Optics* 578

Tune-out wavelength for the 1s2s ^3S state of helium
Gordon Drake *University of Windsor* 579

Contribution to resolution of the proton radius puzzle via measurement of the n=2 Lamb shift in atomic hydrogen
Eric Hessels *York University* 580

TOPIC: QUANTUM GASES

Repulsive self-generated lattice from a BEC in an optical resonator
Davide Dreon *ETHZ* 581

Vortex Lattice Formation in a Stirred Bose-Einstein Condensate
Emmanuel Mercado Gutierrez *Instituto de Fisica de Sao Carlos - Universidade de Sao Paulo* 582

A versatile apparatus for quantum simulation with ultracold dipolar Erbium atoms
Bojeong Seo *The Hong Kong University of Science and Technology* 583

Few-mode Treatment of Interacting Bose Gases with Spin-Orbit Coupling
Josep Cabedo Bru *Universitat Autònoma de Barcelona* 584

Progress toward single atom microscopy for ultracold Yb atoms in optical lattice
Jongchul Mun *Korea Research Institute of Standards and Science* 585

Towards ultracold potassium-cesium mixture.
Mariusz Semczuk *University of Warsaw* 586

Dynamics in the dissipative Fermi-Hubbard Model
Lukas Freystatzky *University of Hamburg* 587

Global thermodynamic susceptibilities for harmonic trapped gases
Freddy Jackson Poveda Cuevas *Universidad Nacional Autónoma de México* 588

Coherent inflation in Bose Einstein condensate.
Sicong Ji *Atominstitut, Technische Universität Wien* 589

Time resolved study of competing instabilities on a Fermi gas quenched to strong repulsion
Andrea Amico *University of Florence, LENS, CNR-INO* 590

Matter wave speckle observed in an out-of-equilibrium quantum fluid
Pedro Ernesto Schiavinatti Tavares *Instituto de Física de São Carlos - USP* 591

A two species superfluid system to study quantum phases transitions in an atomic vortex lattice
Pedro Ernesto Schiavinatti Tavares *Instituto de Física de São Carlos - USP* 592

POSTER LIST

Page

Large arrays of bosonic atoms in optical tweezers
Mark Brown *CU Boulder / JILA* 593

Complex Networks on Quantum States: From Quantum Phase Transitions to Emergent Dynamics of Quantum Cellular Automata
Lincoln Carr *Colorado School of Mines* 594

Mixtures in radiofrequency-dressed potentials
Elliot Bentine *Department of Physics, Oxford University* 595

Magnetically tunable Feshbach resonances in ultracold gases of europium atoms and mixtures of europium and alkali-metal atoms
Klaudia Zaremba-Kopczyk *University of Warsaw* 596

Studying Quantum Turbulence in Two Species Superfluid: The State of the Art of NaK System
Kilvia Mayre Farias *Instituto de Física de São Carlos - Universidade de São Paulo* 597

Bright Soliton to Quantum Droplet Transition in a Mixture of Bose-Einstein Condensates
Julio Sanz *ICFO* 598

Anomalous expansion of turbulent Bose-Einstein condensates
Gustavo Telles *University of Sao Paulo* 599

Thermodynamic measurement of the sound velocity of a Bose gas across the Bose-Einstein condensation
Gustavo Telles *University of Sao Paulo* 600

Few-Photon-Level Atom-Mediated Cross-Phase Modulation at Room Temperature
Steven Sagona-Stophel *Stony Brook University* 601

Dark State Optical Lattice with a Subwavelength Spatial Structure
Sarthak Subhankar *University of Maryland at College Park* 602

Quantum Monte Carlo description of dipolar droplets
Ferran Mazzanti *Universitat Politècnica de Catalunya* 603

Dynamical transfer of vortex states between two coupled Bose-Hubbard rings
Muntsa Guilleumas Morell *Universitat de Barcelona* 604

Matter Wave Subradiance with Bose-Einstein Condensates in an Optical Ring Resonator
Philip Wolf *Physikalisches Institut Tübingen* 605

Non-linear spin dynamics in atomic magnetometers
Rafal Gartman *National Physical Laboratory* 606

Studying Quantum Turbulence in Two Species Superfluid: Cooling Process for Potassium Specie
Humberto Duque *Institute of Physics of São Carlos - USP* 607

Vortex lattices in binary Bose-Einstein condensates with dipole-dipole interactions
Kishor Kumar Ramavarmaraja *Departamento de Fisica Experimental Instituto de Fisica, Universidade de Sao Paulo* 608

Ultracold collisional magnetic gradiometer
Krzysztof Jachymski *University of Stuttgart* 609

A three-mode treatment of spin-1 ultra-cold quantum gases with spin-orbit coupling
Josep Cabedo Bru *Universitat Autònoma de Barcelona* 610

POSTER LIST

Page

Tomography of Correlation Functions in Sodium Bose-Einstein Condensates
Haiyu Liang *Institute for Interdisciplinary Information Sciences, Tsinghua University* 611

Spin-orbit coupling in quantum systems: a quantum Monte Carlo approach
Juan Sánchez-Baena *Universitat Politècnica de Catalunya* 612

Experimental determination of the equation of state of an interacting one-dimensional Bose gas.
Francisco Salces-Carcoba *Joint Quantum Institute - University of Maryland & NIST* 613

Towards Quantum Many-Body Physics with Strontium in Optical Lattices
Sebastian Blatt *Max-Planck-Institut für Quantenoptik* 614

Effective two-mode description of the dynamics of interacting bosons confined in a double-well trap
Jacek Dobrzyniecki *Institute of Physics of the Polish Academy of Sciences* 615

Confinement-Induced Resonance of Alkaline-Earth-Metal Atoms in Anisotropic Quasi-one Dimensional Geometry
Qing Ji *Renmin University of China* 616

Entanglement and dynamical phase transition in a spin-orbit-coupled Bose-Einstein condensate
Fengxiao Sun *Peking University* 617

Finite-range Efimov physics in strongly-interacting Bose gases
Paul Mestrom *Eindhoven University of Technology* 618

Josephson oscillation and self-trapping in momentum space
Shijie Yang *Beijing normal University* 619

Efimov physics in the dynamical formation of unitary Bose gases
Victor Colussi *Eindhoven University of Technology* 620

Generation of Bose-Einstein Condensates' Ground State Through
Yongsheng Zhang *University of Science and Technology of China* 621

Self-bound quantum droplets of atomic mixtures in free space
Giovanni Ferioli *LENS - European Laboratory for Non-Linear Spectroscopy* 622

Atoms, or Electrons and Nuclei? ISRE Nuclear and Electron Spin Waves in Spin-Polarized Atomic Hydrogen
Lauri Lehtonen *University of Turku* 623

Singular loops and their non-Abelian geometric phases in ultracold spin-1 atoms
Bharath Hebbe Madhusudhana *Georgia Institute of Technology* 624

Bosonic Mixture of Sodium and Potassium
Alessandro Zenesini *University of Hannover/ IQO* 625

Effective interactions in a quantum Bose-Bose mixture
Vitaly Andreev *Max-Planck-Institute of Quantum Optics / Ludwig-Maximilians-University of Munich* 626

Second sound in the BEC-BCS crossover
Vijay Singh *ZOQ/ILP, University of Hamburg* 627

How does a binary mixture separate in a three-well potential?
Andrea Richaud *Politecnico di Torino* 628

POSTER LIST

Page

Andreev-reflection and Aharonov-Bohm dynamics in atomtronic circuits
Tobias Haug *Centre for Quantum Technologies* 629

Chaotic and regular spin-orbit entanglement of ultracold atoms
Wenhua Hai *Hunan Normal University* 630

Uncover Topology by Quantum Quench Dynamics
Wei Sun *University of Science and Technology of China* 631

Highly controllable and Robust 2D Spin-Orbit Coupled Topological Bose Gas
Wei Sun *University of Science and Technology of China* 632

Ramsey interferometry with trapped motional quantum states
Linxiao Niu *Peiking University* 633

Stability and excitations of droplet phases in dipolar and two-component condensates
Tommaso Macrì *Federal University of Rio Grande do Norte* 634

Strongly interacting homogeneous Fermi gases
Biswaroop Mukherjee *Massachusetts Inst of Tech-MIT* 635

Continuum of classical-field ensembles from canonical to grand canonical and the onset of their equivalence
Joanna Pietraszewicz *Insitute of Physics Polish Academy of Science* 636

Experimental realization of a supersolid-like stripe-phase in a spin-orbit-coupled Bose-Einstein condensate enabled by momentum-space hopping
Sean Mossman *Washington State University* 637

Matter-wave optics with thermal and quantum degenerate atoms
Ioannis Drougkakis *Foundation for Research and Technology Hellas* 638

An experiment for dipolar quantum mixtures of erbium and dysprosium atoms
Claudia Politi *Institute for Quantum Optics and Quantum Information* 639

Experiments with dipolar Bose-Einstein condensates: quantum droplets, self-organization and superfluidity
Tim Langen *University of Stuttgart* 640

Ultradilute quantum liquid drops
Viktor Cikojević *Faculty of Science Split, Croatia* 641

TOPIC: QUANTUM OPTICS ANS QUANTUM NANOPHOTONICS

Non-Linear Two-Dimensional Atomic Arrays
Maria Moreno-Cardoner *ICFO* 642

Quantum Batteries: Fundamental bounds and spin-system architecture
Tymoteusz Salamon *ICFO* 643

Energy exchange between atoms and a Quartz Crystal μ-balance
Oscar-Andrey Herera *University of Costa Rica* 644

POSTER LIST

Page

Nanophotonic cavity QED with individually trapped atoms
Tamara Dordevic *Harvard University* 645

Subradiance and radiation trapping in cold atoms
Patrizia Weiss *Institute de Physique de Nice* 646

Atomic memory using higher-order nonlinear processes
Gabriel Da Cruz Borba de Andrade *UFPE* 647

Atom-Light Interactions in Photonic Crystal Waveguides
Alex Burgers *California Institute of Technology* 648

Enhancing optical nonlinearities in atomic ensembles to single-photon levels with photonic crystals
Michal Bajcsy *Institute for Quantum Computing, University of Waterloo* 649

Towards a quantum communication platform using rare-earth chelates
Tal Ohana *Weizmann Institute of Science* 650

High-efficiency backward four-wave mixing by quantum interfernce
Yong-Fan Chen *Physics Department, National Cheng Kung University* 651

Single-Photon Interferometry with Frequency Comb States
Tai Hyun Yoon *Korea University, Dept. of Physics* 652

Lasing from Cold Ytterbium Atoms
Dmitriy Sholokhov *University of Saarland* 653

Coherent population trapping (CPT) versus electromagnetically induced transparency (EIT)
Sumanta Khan *Indian Institute of Science* 654

Experimental demonstration of composite stimulated Raman adiabatic passage
Alexander Bruns *Technische Universität Darmstadt* 655

Raman Gray Molasses Cooling of Cesium Atoms on the D2 Line
Ya-Fen Hsiao *Institute of Atomic and Molecular Sciences, Academia Sinica* 656

Ultrabright, narrow-band photon-pair source for atomic quantum memories
Pin Ju Tsai *Institute of Atomic and Molecular Sciences, Academia Sinica* 657

Random singlet phase of cold atoms coupled to one-dimensional photonic crystals
David Li *ICFO* 658

Exchange of optical vortices using an electromagnetically induced transparency based four-wave mixing setup
Hamid Reza Hamedi *Institute of Theoretical Physics and Astronomy, Vilnius University* 659

Coupled-cavities quantum electrodynamics with a cavity array in a single optical fiber
Shinya Kato *Waseda University* 660

Stopped light pulses at the single-photon level in a laser-cooled ensemble loaded into a hollow-core fiber
Thorsten Peters *Technical University of Darmstadt* 661

Collective scattering in nanofiber-trapped atomic ensembles
Adarsh Shankar Prasad *Technische Universität Wien* 662

POSTER LIST

Page

Atomic frequency comb quantum memory via piecewise adiabatic passage
Daniel Viscor *UAB* 663

Phase-coherent light scattering from long trapped ion strings
Lukas Slodicka *Department of Optics, Palacky University* 664

Exploring string patterns in the doped Hubbard with a Fermi gas microscope
Daniel Greif *Harvard University* 665

Experimental implementation of a degenerate optical resonator supporting more than 46 Laguerre-Gaussian modes
Cheng Zedi *USTC* 666

Experimental Quantum Simulation of a Coherence-Enhanced Microscopic Heat Engine in Diamond
Jonas Nils Becker *University of Oxford* 667

Ultrafast many-body electron dynamics in a strongly correlated ultracold Rydberg gas and its application to ordered systems
Akira Tanaka *Institute for Molecular Science* 668

Atomic quantum simulator of generalized lattice Wilson-Dirac fermions in (1+1) dimensions
Yoshihito Kuno *Kyoto University* 669

Trapping ultracold atoms in sub-micron-period triangular and square magnetic lattices
Peter Hannaford *Swinburne University of Technology* 670

Towards a register of single-atoms in a ber cavity for multi-particle entanglement
Baghdad Mohamed *Laboratoire Kastler Brossel-ENS* 671

Phase transition kinetics for a Boes Einstein condensate in a periodically driven band system
Eric Michon *Laboratory Collisions Agrégats Réactivité, Université Paul Sabatier* 672

Evaluation of polariton-number variances in the Jaynes-Cummings-Hubbard model with trapped ions
Kyoichi Takayama *Osaka University* 673

Dissipative Bose-Hubbard system with metastable $^3P_2$ state of ytterbium atoms
Takafumi Tomita *Kyoto University* 674

Antiferromagnetic spin correlation of SU(N) Fermi gas in an optical dimerized lattice
Hideki Ozawa *Institute of Physical and Chemical Research* 675

Site-resolved imaging of a fermionic Mott insulator using ^{173}Yb
Masato Takagi *Tokyo Institute of Technology* 676

Preparation of two-dimensional fermionic spin mixtures in a quantum-gas microscope apparatus
Bruno Peaudecerf *University of Strathclyde* 677

Direct observation of incommensurate magnetism in Hubbard chains
Guillaume Salomon *Max-Planck Institute for Quantum Optics* 678

Trapping ions in an optical lattice for quantum simulation
Christoph Fischer *ETH Zurich* 679

Probing many-body dynamics on a Rydberg quantum simulator
Alexander Keesling *Harvard University* 680

POSTER LIST

Page

Strongly-correlated bosons on a dynamical lattice
Przemyslaw Grzybowski *ICFO* 681

Synthetic atomic quantum systems with two electron fermions
Lorenzo Francesco Livi *Università degli studi di Firenze* 682

Atomic interactions via diffractive light coupling for magnetic ordering and supersolids
Thorsten Ackemann *University of Strathclyde* 683

Time-Dependent Solution of the Generalized Fano Model
Hedvika Gedeonova *Institute of Theoretical Physics, Charles University* 684

Ultracold atoms in a two-dimensional optical quasicrystal
Konrad Viebahn *University of Cambridge* 685

Simulation of Quantum Chemistry problems using cold atoms
Javier Argüello-Luengo *Max Planck Institute of Quantum Optics* 686

Motional quantum state engineering of two heteronuclear atoms with spin-selective optical tweezers
Kunpeng Wang Wuhan *Institute of physics and mathematics, Chinese academy of sciences* 687

Taking pictures of black holes: spatially-resolved imaging of cavity-mediated nonlocal interactions
Gregory Bentsen *Stanford University* 688

Ba-Li: towards a quantum mixture of Barium ions and ultracold Lithium gases
Amelia Detti *University of Florence* 689

TOPIC: RYDBERG AND ARTIFICIAL ATOMS AND MOLECULES

A room temperature single-photon source based on strongly interacting Rydberg atoms
Tilman Pfau *University of Stuttgart, 5th Institute of Physics* 690

Femtosecond multiphoton π-pulse control of Rydberg states in Rubidium atoms
Iduabo John Afa *Universitat Politecnica de Catalunya* 691

An enhanced optical non-linearity based on Rydberg electromagnetically induced transparency for pulses from 1 to 100s of photons
Josiah Sinclair *University of Toronto* 692

Ionic Impurity in a Bose-Einstein Condensate at Submicrokelvin Temperatures
Kathrin Kleinbach *Physikalisches Institut, Universität Stuttgart* 693

Single-shot Non-destructive Detection of Ensembles of Rydberg Atoms with Microwave Cavity Transmission Measurements
Sébastien Garcia *ETH* 694

Searching for magnetic micro-defects by magnetic field imaging that employs nitrogen vacancy centers in diamond crystal
Andris Berzins *University of Latvia* 695

Resonant enhancement of optical nonlinearities in a Rydberg gas
Clément Hainaut *Physikalisches Institut* 696

POSTER LIST

Page

Rydberg optical Feshbach resonances in cold gases
Rosario González-Férez *Universidad de Granada* 697

Electronic Structure of the Rydberg Triatomic Molecule: K(nl-KRb(vN)
Rosario González-Férez *Universidad de Granada* 698

Coherent Control of Addressable Rydberg Atoms for Hybrid Quantum Information Processing
Jonathan Pritchard *University of Strathclyde* 699

Light-matter interface using cold-atoms coupled to hollow-core fiber
Mohammad Noaman *Johannes Gutenberg University, Mainz* 700

Van der Waals interactions of Rydberg particles near surfaces
Johannes Block *Institut fuer Physik, Uni Rostock* 701

Rydberg-Dressed Magneto-optical Trap
Niamh Jackson *Durham University* 702

Rydberg-mediated long-range interactions between stored optical photons
Teodora Ilieva *Durham University* 703

Rydberg excitation of a Bose-Einstein condensate and Mott insulator with a picosecond laser pulse
Michiteru Mizoguchi *Institute for Molecular Science* 704

Study of light storage with Rydberg-state electromagnetically-induced-transparency in cold rubidium atoms
Bongjune Kim *National Tsing Hua University* 705

Quantum Simulation of Energy Transport with Rydberg Atoms
Sayali Ganesh Shevate *University of Strasbourg* 706

Stability study of the two-photon detuning using the Rydberg-EIT spectrum of laser-cooled atoms
Ko-Tang Chen *National Tsing Hua University* 707

Single shot non destructive photon counting of microwave photons using slow Rydberg atoms
Frédéric Assémat *Laboratoire Kastler Brossel* 708

Interacting Rydberg ions
Chi Zhang *Stockholm University* 709

Coherent control of a trapped Rydberg ion
Markus Hennrich *Stockholm University* 710

Circular Rydberg Atoms as a Tool for Quantum Simulation
Rodrigo Cortiñas *LKB* 711

Towards continuous-wave terahertz laser via optically pumped Rydberg states
Sambit Bikas Pal *National University of Singapore* 712

Rydberg Excitation of Lattice-trapped Ultra-cold Atoms on a Chip
Klaasjan Van Druten *University of Amsterdam* 713

Rydberg interactions on an atom chip
Julius De Hond *University of Amsterdam* 714

POSTER LIST

Page

Nonequilibrium many-body spin dynamics in strongly interacting Rydberg systems
Nithiwadee Thaicharoen *Heidelberg University* 715

Microscopic observation of Rydberg macrodimers at the single-atom limit
Jun Rui *Max Planck Institute of Quantum Optics* 716

Circular Rydberg states in helium and λ/4 co-planar microwave waveguide resonators for hybrid cavity QED
Alexandre Morgan *University College London* 717

Generation and detection of Rubidium 20s Rydberg atoms with coherent 420 and 1050 nm radiation
Fernando Ramírez-Martínez *Instituto de Ciencias Nucleares, UNAM* 718

Advanced relativistic energy approach and many-body perturbation theory too computing radiation transition energies, probabilities and hyperne structure constants for heavy ions
Eugeny Ternovsky *Odessa State University - OSENU* 719

Relativistic theory of excitation and ionization of the heavy Rydberg atoms in a black-body radiation eld
Olga Khetselius *Odessa State University - OSENU* 720

Comprehensive calculations of photoabsorption and lifetimes of high-n states of Li
Constantine Theodosiou *Manhattan College* 721

High resolution cold atom source of single ions using correlations and Rydberg blockade
Robert Scholten *The University of Melbourne* 722

A Photon-Photon Quantum Gate Based on Rydberg Polaritons
Stephan Dürr *Max-Planck Institute of Quantum Optics* 723

TOPIC: TOPOLOGY IN ATOMIC SYSTEMS

Quenched dynamics and spin-charge separation in an interacting topological lattice
Luca Barbiero *Universitè Libre de Bruxelles* 724

Signatures of quantum spin liquids in small lattices
Abel Yuste *UAB, GIQ* 725

Topological states in the Kronig-Penney model with arbitrary barriers
Irina Reshodko *Okinawa Institute of Science and Technology* 726

Hall conductivity of strongly interacting bosons in optical lattice
Konrad Patucha *Institute of Low Temperature and Structure Research, Polish Academy of Sciences in Wroclaw* 727

Anyons from Hard-Core Three-Body Interactions in One-Dimension
Nathan Harshman *American University* 728

Topological characterization of chiral models through their long time dynamics
Maria Maffei *ICFO* 729

Majorana Quasi-Particles Protected by Z_2 Angular Momentum Conservation
Fernando Iemini *The Abdus Salam International Centre for Theoretical Physics* 730

POSTER LIST

Page

Floquet engineering of optical solenoids and quantized charge pumping along tailored paths in two-dimensional Chern insulators
Botao Wang *Max Planck Institute for the Physics of Complex Systems* 731

Artificial Gauge Fields with Atom-Chip Based Quantum Simulator
Emine Altuntas *Joint Quantum Institute, National Institute of Standards and Technology and University of Maryland* 732

Quench dynamics of a synthetic three-leg Hall ladder with ultracold neutral fermions in an optical lattice
Jeong Ho Han *Seoul National University* 733

Stability of Floquet topological phases against disorder
Oles Shtanko *Massachusetts Institute of Technology* 734

Evidence for the topological Anderson insulator
Eric Meier *University of Illinois at Urbana-Champaign* 735

Probing topology in out of equilibrium cold atomic systems
Nur Ünal *Max Planck Institute PKS* 736

A Continuously Tunable Topological Pump in High-dimensional Cold Atomic Gases
Yanbin Yang *Tsinghua University* 737

Geometry, Topology and Control of Spin-1 Atoms
Maryrose Barrios *Georgia Institute of Technology* 738

Correspondence between a shaken honeycomb lattice and the Haldane model
Michele Modugno *Ikerbasque & UPV/EHU* 739

Transport in optical lattices with flux
Ana Hudomal *Institute of Physics Belgrade* 740

Invited Talks

Revisiting the two-fluid model with atomic gases

Jean Dalibard
Laboratoire Kastler Brossel, Collège de France, Paris, France
e-mail: *jean.dalibard@college-de-france.fr*

The two-fluid model was proposed in the 1940s by Tisza and Landau to describe the low temperature behavior of liquid helium [1, 2, 3]. It is based on the concept of a superfluid component characterized by a density ρ_s and a velocity $\vec{v}_s$, which comes in addition to the normal fraction of the fluid. For a weakly interacting 3D gas, the superfluid and Bose-condensed components essentially coincide, and the two-fluid model is usually of little use. In more exotic situations however, the two notions may strongly differ, either because of strong interactions or in reduced dimensionality. In this presentation we will explore the case of a uniform 2D gas for which no condensation is expected in the thermodynamic limit, but where a superfluid transition may still take place. The two-fluid model is then relevant to address specific properties of the system, such as sound propagation. As an illustration I will present a recent investigation of the so-called *second sound* in this system [4, 5], as well as a new probing of its coherence properties.

References

[1] L. Tisza, Nature **141**, 913 (1938), Comptes Rendus Acad. Sc. **207**, 1035; 1186 (1938).

[2] L. D. Landau, Phys. Rev. **60**, 356 (1941); J. Phys. USSR **5**, 71 (1941).

[3] S. Balibar, Journal of Low Temperature Physics **146**, 441 (2007).

[4] J.L. Ville, R. Saint-Jalm, E. Le Cerf, M. Aidelsburger, S. Nascimbene, J. Dalibard, J. Beugnon, arXiv:1804.04037.

[5] T. Ozawa and S. Stringari, Phys. Rev. Lett. **112**, 025302 (2014). M. Ota, F. Larcher, F. Dalfovo, L. Pitaevskii, N.P. Proukakis, S. Stringari, arXiv:1804.04032.

Experiments with ultracold CaF and YbF molecules

E. A. Hinds, L. Caldwell, H. J. Williams, S. Jurgilas, M. A. Trigatzis, S. Truppe, J. Rodewald, J. R Almond, N. J. Fitch, J. Lim, T. Wall, M. Hambach,
J. A. Devlin, B. E. Sauer and M. R. Tarbutt
Centre for Cold Matter, Physics Department, Imperial College London, Prince Consort Road, London SW7 2AZ, United Kingdom
e-mail: *ed.hinds@imperial.ac.uk*

The production of ultracold atoms by laser cooling has been the key to preparing quantum degenerate gases, optical lattices, atomic fountains and many other applications. A broad set of new applications [1] has been awaiting the extension of laser cooling to produce ultracold molecules by magneto-optical trapping and sub-Doppler cooling. That has now begun, with the realisation of magneto-optical traps of SrF [2, 3, 4] and CaF [5, 6]. Recently we have shown that CaF [7] and YbF [8] can be cooled far below the Doppler temperature, by making use of their dark states to give strong cooling in a blue-detuned molasses. Further, we have loaded ultracold CaF molecules into a magnetic trap and have demonstrated coherent control of the rotational states while the molecules are trapped [9].

I will summarise the current state of laser cooling molecules and will comment on some of the imminent applications to a wide range of problems.

[1] L. D. Carr, D. DeMille, R. V. Krems and J. Ye, New J. Phys. **11**, 055049 (2009).

[2] J. F. Barry, D. J. McCarron, E. B. Norrgard, M. H. Steinecker, and D. DeMille, Nature **512**, 286 (2014).

[3] D. J. McCarron, E. B. Norrgard, M. H. Steinecker, and D. DeMille, New J. Phys. **17**, 035014 (2015).

[4] M. H. Steinecker, D. J. McCarron, Y. Zhu, and D. DeMille, ChemPhysChem **17**, 3664 (2016).

[5] H. J. Williams, S. Truppe, M. Hambach, L. Caldwell, N. J. Fitch, E. A. Hinds, B. E. Sauer, and M. R. Tarbutt, New J. Phys. **19**, 113035 (2017).

[6] L. Anderegg, B. L. Augenbraun, E. Chae, B. Hemmerling, N. R. Hutzler, A. Ravi, A. Collopy, J. Ye, W. Ketterle, and J. M. Doyle, Phys. Rev. Lett. **119**, 103201 (2017).

[7] S. Truppe, H. J. Williams, M. Hambach, L. Caldwell, N. J. Fitch, E. A. Hinds, B. E. Sauer, and M. R. Tarbutt, Nat. Phys. **13**, 1173 (2017).

[8] J. Lim, J. R. Almond, M. A. Trigatzis, J. A. Devlin, N. J. Fitch, B. E. Sauer, M. R. Tarbutt, and E. A. Hinds, Phys. Rev. Lett. **120**, 123201 (2018).

[9] H. J. Williams, L. Caldwell, N. J. Fitch, S. Truppe, J. Rodewald, E. A. Hinds, B. E. Sauer, and M. R. Tarbutt, Phys. Rev. Lett. **120**,163201 (2018).

Multiparameter Optimisation of a Magneto-Optical Trap Using Deep Learning Artificial Neural Networks

A. D. Tranter, H. Slatyer, M. Hush, A. Leung, K. Paul, G. T. Campbell, B. C. Buchler and P. K. Lam
ARC of Excellence for Quantum Computation and Communication Technology,
Research School of Physics and Engineering, The Australian National University,
Canberra ACT2601, AUSTRALIA
e-mail: *ping.lam@anu.edu.au*

Many important physical processes have dynamics that are too complex to completely model analytically. Optimisation of such processes often relies on intuition, trial-and-error, or the construction of empirical models. Machine learning based on artificial neural networks has emerged as an efficient means to develop empirical models of complex systems. We implement a deep learning artificial neural network to optimise the magneto-optic cooling and trapping of neutral Rb atomic ensembles. When the optical density of an atomic ensemble is high, many-body interactions start to give rise to complex dynamics that preclude precise analytic optimisation of the cooling and trapping process. The solution identified by our neural networks produces higher optical densities and is radically different to the smoothly varying adiabatic solutions commonly used. Machine learning may provide a pathway to a new understanding of the dynamics of the cooling and trapping processes in cold atomic ensembles

Cold atomic systems have been a fundamental tool for studying atom-light interactions providing a technically simpler interface than cavity quantum electrodynamics. Recently interest has been generated around the possibility of machine learning to optimise and control atomic systems [1]. Such systems provide an ideal case for online optimisation techniques possessing complex dynamics that are often difficult or intractable to simulate fully and short timescales providing quick duty cycles and thus, plentiful training data.

One signifcant application of cold atomic ensembles is the realisation of quantum memories which are integral to quantum information networks. A promising scheme is gradient echo memory (GEM) using cold atomic ensembles which has demonstrated efficiencies of up to 87% [2]. In this scheme a probe pulse is mapped onto the atomic spinwave of the ensemble, facilitating the storage of the incident probe light as an atomic excitation. Here we report the first application of a deep learning algorithm to optimise such a cold atomic ensemble.

To improve the efficiency and storage time of the GEM protocol it is advantageous to address the main limitations of the system; the dynamics of the cold atomic ensemble. The optical depth (OD) of the ensemble is intrinsically linked to the temperature and density of the atomic cloud and as such can be modified by changing the characteristics of the cold atom trap.

We prepare a dense cloud of Rb87 atoms in an elongated magneto-optical trap (MOT). Dynamical control over the trapping frequency, repump frequency and magnetic field allows for the use of online optimisation techniques to modify the trap characteristics. We use an artificial neural network as a function approximater to provide a mapping from a set of experimental parameters to a cost landscape, for which the minimum cost corresponds to a high optical depth. To this end a multilayer perceptron model is trained using a set of training data gathered experimentally after sampling from the parameter space. A minimisation search is then performed across this landscape identifying regions of interest which are then explored experimentally to find a global minimum while continuing to train the model. The trapping frequency, repump frequency and magnetic fields are divided into 21 time bins each over a 20ms period providing a total of 63 optimisation parameters. The transmission of an off resonant probe pulse, scaled to a reference intensity, is calculated as the cost function which is then minimised, resulting in an increasing optical depth.

Using these techniques we report an improvement in optical depth from 530 ± 8 to 970 ± 20 with convergence demonstrated after 703 optimisation runs. We find a physical change corresponding to the spatial distribution of the atomic ensemble, acquired using off resonant side imaging collimated onto a CCD. We also apply the optimisation to the GEM protocol to optimise memory efficiency.

[1] Wigley, P. et al. Fast machine-learning online optimiza- tion of ultra-cold-atom experiments. Scientific Reports 6, (2016).

[2] Cho, Y. et al. Highly efficient optical quantum memory with long coherence time in cold atoms. Optica 3, 100 (2016).

Quantum Simulations in the Innsbruck Quantum Cloud

Peter Zoller[1,2]

[1] *Institute for Theoretical Physics, University of Innsbruck, Austria*

[2] *Institute for Quantum Optics and Quantum Information, Austrian Academy of Sciences, Innsbruck, Austria*

e-mail: *peter.zoller@uibk.ac.at*

We report results from a theory [1] - experiment [2] collaboration on variational quantum simulations of the ground state of the Schwinger Model, as a Lattice Gauge Theory of 1D Quantum Electrodynamics.

The idea is to establish a feedback loop between a classical computer and a programmable quantum simulator, as familiar from quantum approximate optimization algorithms, and quantum chemistry. The quantum simulator is represented by a string of (up to twenty) ions realizing a long-range Ising spin model with transverse magnetic field. In combination with single particle rotations this provides us with quantum resources to build highly entangled states on the quantum machine depending on a set of variational parameters. The feedback loop then allows us to minimize the expectation value of the Schwinger Hamiltonian to obtain an approximation to the ground state wave function stored in quantum memory. The two key elements for an efficient implementation are: (i) the symmetries of the Schwinger problem are matched by corresponding symmetries in quantum resources generating the variational quantum state; and (ii) a classical search algorithm, which for a given number of maximum calls to the quantum simulator, carefully allocates resources between a search for the global minimum in the energy landscape of parameters, and number of measurements for given parameters to reduce projection noise (c.f. Fig. 1). Remarkably, we can quantify energy error bars, and thus *self-verify* our quantum results experimentally by calculating the variance of the Hamiltonian for the approximate quantum variational state (c.f. Fig. 2). Furthermore, we discuss computation of excited states, convergence as scaling with system size, and crossing a quantum phase transition. Our techniques should be useful in establishing quantum simulations for condensed matter and high-energy physics problems.

We conclude with brief remarks on several related topics, in particular a protocol to measure Renyi entanglement entropies, extracted from statistical correlations in random measurements, and variational entangled state preparation for optimal quantum parameter estimation in quantum sensing.

[1] Theory collaborators: C. Kokail, R.M.W van Bijnen, P. Silvi, C. Muschik, A. Elben and B. Vermersch

[2] Experimental collaborators: P. Jurcevic, C. Maier, T. Brydges, P. Schindler, R. Stricker, E. Martinez, T. Monz, B. P. Lanyon, C. Roos and R. Blatt.

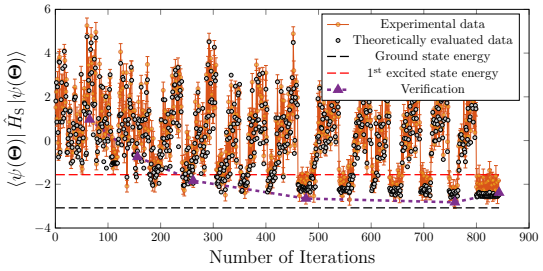


Figure 1: Convergence of the energy expectation value towards the ground state of the Schwinger model $\hat{H}_S$, as a function of the number of iterations. We use a total budget of $3 \cdot 10^4$ projective measurements for the whole optimisation. Orange connected points indicate experimental data, whereas grey dots represent theoretically calculated expectation values. The triangles indicate points for which we verify our quantum simulation by measuring the Hamiltonian variance (see Figure 2)

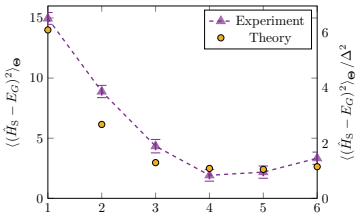


Figure 2: Ab-initio (self-) verification of energy for the variational ground state preparation of the Schwinger model. For parameter vectors $\mathbf{\Theta}$, corresponding to the triangles indicated in Figure 1, we measure the Hamiltonian variance $\langle(\hat{H}_S - E_G)^2\rangle$, where E_G denotes the final ground state energy obtained from the experimental optimization. Dots indicate the Hamiltonian variance obtained by numerically evaluating the variance in the variational state.

Challenging QED with atomic Hydrogen

Lothar Maisenbacher, Axel Beyer, Vitaly Andreev, Alexey Grinin, Arthur Matveev, Ksenia Khabarova, Nikolai Kolachevsky, Randolf Pohl, Dylan Yost, Theodor Hänsch and Thomas Udem

Max-Planck Institute of Quantum Optics, 85748 Garching, Germany

e-mail: *thu@mpq.mpg.de*

Finding discrepancies between the predictions of fundamental theories and experimental observations is the main driver to develop physics further – the route to more advanced theories ("new physics") that fix the discrepancies. In that sense, quantum electrodynamics (QED) is currently seen as the most advanced fundamental theory, serving as the blueprint for any other quantum field theory. Progress is expected to come from ever more precise testing through comparison of theoretical predictions and experimental data. A good test compares values that can be both computed and measured with high accuracy. Some QED predictions excel in that respect, such as for the transition frequencies of atomic hydrogen [1] and the gyromagnetic ratio of the electron [2].

Most theories, including QED, depend on parameters that have to be adjusted to the experimental data. This means that the number of measurements must exceed the number of parameters, otherwise the theory can always be made correct. The test is passed if the various values for the parameters agree within their respective uncertainties. Precision-spectroscopy determinations and computations of transition frequencies of atomic hydrogen provide the best test for QED. The QED expression for the hydrogen energy levels effectively comes with two parameters: the Rydberg constant R_∞ and the rms proton charge radius r_p. Other parameters, such as the fine structure constant and the electron-to-proton mass ratio, appear as well, but can be better determined from other experiments.

Until 2010, the 15 distinct measurements of transition frequencies in atomic hydrogen as used by CODATA [3] gave 13 value pairs for R_∞ and r_p that were consistent with QED. This situation changed, however, when the frequency of a particular transition (the 2s-2p transition) in muonic hydrogen was measured [4]. Muonic hydrogen is just like regular hydrogen but with the electron replaced by its big brother, the muon. With this replacement the proton-radius term in the theoretical description and thus the sensitivity to this parameter – is seven orders of magnitude larger than for regular hydrogen. The result was a much more precise but also significantly smaller value of r_p. This meant the QED test failed. The discrepancy between the "small" and "large" charge radius amounts to four combined standard deviations.

In addition to the hydrogen data the CODATA team uses data for the proton charge radius obtained from electron-proton scattering. This increases the discrepancy to 5.6σ and triggered intense discussions in the community whether or not this should be seen as a hint of new physics. It should be mentioned though that electron-proton scattering experiments are notoriously difficult to evaluate and values for r_p from different groups disagree. The cleaner way to test QED is to compare only quantities that should obey the same physics, namely various transitions in regular and muonic hydrogen. After publication of the muonic hydrogen results, our group remeasured one of the broader hydrogen lines with better accuracy. Our motivation was that the discrepancy with the muonic value only shows up when all available hydrogen data is averaged. Our latest result for the 2s-4p transition frequency is as accurate as the previous "world data" and supports the "muonic" proton radius.

Meanwhile Héelène Fleurbaey and her team at the Laboratoire Kastler Brossel, Paris have re-measured the 1s-3s transition frequency with a significantly improved accuracy and again find the "large" charge radius [5]. At our lab we have also been working on this transition with a different method. We hope to be ready to report some preliminary results. This would provide a unique opportunity to compare two highly accurate measurements obtained at different labs. In case of disagreement this would be a strong hint for a measurement problem causing the "proton radius puzzle".

[1] A. Beyer *et al.* Science 358, 79 (2017).

[2] G. Gabrielse *et al.* PRL 97, 030802 (2006).

[3] P.J. Mohr *et al.* RMP 88, 035009 (2014).

[4] R.Pohl *et al.* Nature 466, 213 (2010).

[5] H. Fleurbaey *et al.* PRL 120, 183001 (2018).

Lattice clocks and quantum-state-controlled chemistry with ultracold molecules

T. Zelevinsky[1]

[1] *Department of Physics, Columbia University, 538 West 120th Street, New York, NY 10027-5255, USA*

e-mail: *tanya.zelevinsky@columbia.edu*

Ultracold molecules can be synthesized from laser-cooled atoms and trapped in optical lattices such that their internal and motional quantum states are completely controlled. This allows lattice-clock style manipulation of the molecules with very long coherence times of the clock state superpositions. An important ingredient in extending the coherence times is the "magic" trapping technique where the presence of the trap does not perturb the superpositions. Magic trapping can be achieved for narrow optical molecular transitions that utilize two-body subradiance, as well as for terahertz vibrational transitions with no atomic analogs. The coherence times of vibrational state superpositions are extended by several orders of magnitude. This is directly applicable to quantum information storage and to high-precision spectroscopy for testing molecular QED and ultrashort-range Newton's law.

The precise control of molecular quantum states also enables studies of ultracold chemistry via state-selected photodissociation, a basic process that uses light to break molecular bonds. In this implementation, photodissociation exhibits the hallmarks of ultracold chemistry such as matter wave interference, barrier tunneling, and reaction control with weak applied fields. The tunability of the reaction energy by several orders of magnitude allows direct observations of the crossover from the ultracold to the classical chemistry regime.

Information propagation and entanglement generation with long-range interactions

Alexey V. Gorshkov
Joint Quantum Institute and Joint Center for Quantum Information and Computer Science, NIST/University of Maryland, College Park, MD 20742, USA
e-mail: *gorshkov@jqi.umd.edu*

Atomic, molecular, and optical systems often exhibit long-range interactions, which decay with distance r as a power law $1 = r^{\alpha}$. In this talk, we will derive bounds on how quickly information can propagate and entanglement can be generated in such quantum systems. We will also present protocols that attempt to saturate these bounds. Finally, we will touch on numerous applications of these bounds and protocols, ranging from bounding and enhancing the speed of quantum computers to illuminating the properties of quantum phases and phase transitions in and out of equilibrium.

Entanglement dynamics in a trapped ion quantum magnet

Ana Maria Rey[1,2]

[1] *JILA, NIST, and Dept. of Physics, University of Colorado, 440 UCB, Boulder, CO 80309, USA*
[2] *Center for Theory of Quantum Matter, University of Colorado, Boulder, CO 80309, USA*
e-mail: *arey@jilau1.colorado.edu*

One of the most important goals of modern quantum sciences is to learn how to control and entangle many-body systems and use them to make powerful and improved quantum devices, materials and technologies. In this talk I will report on our current effort to develop protocols that can quantify the build-up of quantum correlations and storage of quantum information in a planar crystal of trapped ions. Using a pair of lasers, we couple the spins to the vibrational modes (phonons) of the crystal. The phonons mediate tunable-range interactions between the spins which we use to generate entanglement starting from easily prepared uncorrelated states. We can operate in two different regimes. In one regime, phonons do not play an active role in the many-body dynamics and instead are used to mediate spin-spin coupling between ions [1]. In the other regime, phonons actively participate [2] and we use them to simulate the Dicke model an iconic model in quantum optics which describes the coupling of a (large) spin to an oscillator. The Dicke model is known to exhibit rich and interesting phenomena. For instance, it features a quantum critical point, and displays classical chaotic behavior. I will also discuss a new measurement scheme, implemented by using a many-body echo sequence that reverses the Hamiltonian dynamics, which can give experimental access to a type of out-of-time-order correlations (OTOCs) [3, 4] which have caught great deal of interest in the recent years. The reason is that those correlations can measure the scrambling of quantum information across the systems many-body degrees of freedom. Measuring OTOCs in controllable atomic laboratories can not only have a great impact on quantum information processing and quantum enhanced metrology, but also opens a path for future tests of the holographic duality between quantum and gravitational systems.

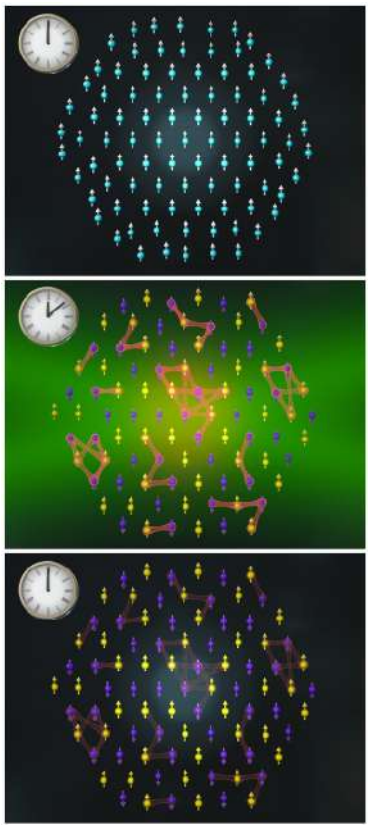


Figure 1: We study 2D planar arrays of ions in a Penning trap and encode a spin 1/2 degree of freedom in their lowest hyperfine states. Laser beams are used to excite the center of mass phonon mode which mediate long range spin interactions. By controlling the laser parameters we can reverse the sign of the Hamiltonian and measure OTOCs to diagnostic scrambling.

[1] J. G. Bohnet*et al* Quantum spin dynamics and entanglement generation with hundreds of trapped ions, Science **352**, 1297 (2016).

[2] A. Safavi-Naini *et al*, *Exploring adiabatic quantum dynamics of the Dicke model in a trapped ion quantum simulator*, arXiv:1711.07392v2 (2017).

[3] M. Gärttner *et al*,*Measuring out-of-time-order correlations and multiple quantum spectra in a trapped ion quantum magnet* Nat. Phys., **13**, 781 (2017)

[4] M. Gärttner, P. Hauke, and A. M. Rey,*Relating out-of-time-order correlations to entanglement via multiple-quantum coherences* Phys. Rev. Lett. **120**, 040402 (2018).

Probing quantum many-body dynamics in Rydberg atom arrays

Mikhail Lukin
Physics Department, Harvard University
Cambridge, MA 02138 USA
e-mail: *lukin@physics.harvard.edu*

We demonstrate a method for the creation of controlled many-body quantum matter that combines deterministically prepared, reconfigurable arrays of individually trapped cold atoms with strong, coherent interactions enabled by excitation to Rydberg states. Using this approach we demonstrate high fidelity manipulation of individual atoms and entangled atomic states and realize a programmable Ising-type quantum spin model with tunable interactions and system sizes up to 51 qubits. Within this model, we observe transitions into ordered states that break various discrete symmetries, verify their high-fidelity preparation, and investigate dynamics across the phase transition in large atom arrays. In particular, we probe critical dynamics in the vicinity of the quantum phase transitions and observe novel, robust many-body dynamics corresponding to persistent oscillations of the order after a sudden quantum quench. These observations enable new approaches for exploring many-body phenomena and open the door for realizations of novel quantum algorithms.

Probing the Roton Excitation Spectrum in an Erbium Dipolar Quantum Gas

Francesca Ferlaino[1,2]
[1] *Institut für Experimentalphysik, Universität Innsbruck, 6020 Innsbruck, Austria*
[2] IQOQI- *Institute for Quantum Optics and Quantum Information, Österreichische Akademie der Wissenschaften, 6020 Innsbruck, Austria*
e-mail: *Francesca.Ferlaino@uibk.ac.at*
www.erbium.at

In the early 40's, Lev Landau predicted a very special, yet fascinating, collective excitation in He superfluid, namely the roton quasi-particle. He found that such elementary excitation carries minimal energy at large momentum and its existence was essential to understand the mysterious thermodynamics properties of He II. It was then related by Richard Feynman to the strong correlations, resulting from the strong interactions occurring in the quantum liquid. About 15 years ago, a similar phenomena has been predicted in dipolar quantum gases, despite their weakly interacting character. Such a counter-intuitive finding roots in the long-range (momentum-dependent) and anisotropic nature of the dipole-dipole interaction, from which strong correlations can emerge. Despite the great attention dipolar rotons has attracted, its observation was remained an elusive goal. With the advent of quantum gases of strongly magnetic lantanide species novel possibilities of investigation opened up. We here report on the first observations of roton mode in a dipolar Bose-Einstein condensate of Erbium atoms. By driving the system out of equilibrium via an interaction quench, we populate the roton mode and study their dynamics. A careful study of the scaling of the roton momentum and its imaginary energy reveals the universal properties of the phenomena. Finally, we will report on the creation of the first dipolar Bose-Bose and Bose-Fermi quantum mixtures of Erbium and Dysprosium atoms.

References

[1] L. D. Landau, *The theory of superfuidity of helium II*, J. Phys. (Moscow) **5**, 71 (1941).

[2] L. Santos, G. V. Shlyapnikov, and M. Lewenstein, *Roton-maxon spectrum and stability of trapped dipolar Bose-Einstein condensates*, Phys. Rev. Lett. **90**, 250403 (2003).

[3] L. Chomaz, R. M. W. van Bijnen, D. Petter, G. Faraoni, S. Baier, J. H. Becher, M. J. Mark, F. Wachtler, L. Santos, and F. Ferlaino, *Observation of roton mode population in a dipolar quantum gas*, Nature Phys., **14**, 442 (2018).

Quantum optics with two-dimensional atomic arrays

Susanne Yelin[1,2]
[1] *Department of Physics, Harvard University, Cambridge, MA 02138, USA*
[2] *Department of Physics, University of Connecticut, Storrs, CT 06269, USA*
e-mail: *syelin@physics.harvard.edu*

We consider quantum optical phenomena in two-dimensional (2D) dipolar arrays with sub-wavelength spacing. We show that cooperative resonances of the surface modes in such arrays allow for implementation of a nearly perfect atomically thin mirror, shaping of the emission patterns from individual quantum emitters, and realization of topological quantum optical systems. Experimental implementation using ultracold arrays of trapped atoms and excitons in atomically thin semiconductor materials will be discussed. Potential applications ranging from atomically thin metasurfaces to quantum optomechanics and quantum photon nonlinear optics will be described.

Experimental many-body physics using arrays of individual atoms

A. Browaeys
Laboratoire Charles Fabry, Institut dOptique, CNRS
2 avenue A. Fresnel, 91127 Palaiseau, France
e-mail: *antoine.browaeys@institutoptique.fr*

This talk will present our effort to control and use the dipole-dipole interactions between cold Rydberg atoms in order to implement spin Hamiltonians useful for quantum simulation of condensed matter situations. In our experiment, we trap individual atoms in two-dimensional arrays of optical tweezers [1] separated by few micrometers and excite them to Rydberg states using lasers. The arrays are produced by a spatial light modulator, which shapes the dipole trap beam. We can create almost arbitrary geometries of the arrays with near unit filling in two and three dimensions up to 70 atoms [2, 3]. We have demonstrated the coherent energy exchange in chains of Rydberg atoms resulting from their resonant dipole-dipole interaction [4] and its control by addressable lasers [5]. This interaction realizes the XY spin model. We use this control to study elementary excitations in dimerized spin chains featuring topological properties, thus implementing the Su-Schrieffer-Heeger model [6]. We have also implemented the quantum Ising model [7] in one-dimensional chains of atoms with periodic boundary conditions and two-dimensional arrays containing up to about 50 atoms. We measure the dynamics of the excitation for various strengths of the interactions and compare the data to numerical simulations of this many-body system. This control of an ensemble of interacting Rydberg atoms demonstrates an interesting platform for quantum simulation using neutral atoms, complementary to the other platforms based on ions, magnetic atoms or dipolar molecules.

References

[1] F. Nogrette, H. Labuhn, S. Ravets *et al.*, Phys. Rev. X **4**, 021034 (2014).

[2] D. Barredo, S. de Léséleuc, V. Lienhard *et al.*, Science **354**, 1021 (2016).

[3] D. Barredo, V. Lienhard, S. de Léséleuc *et al.*, arXiv:1712.02727.

[4] D. Barredo, H. Labuhn, S. Ravets *et al.*, Phys. Rev. Lett. **114**, 113002 (2015).

[5] S. de Léséleuc, D. Barredo, V. Lienhard *et al.*, Phys. Rev. Lett. **119**, 053202 (2017).

[6] W.P. Su, J.R. Schrieffer and A.J. Heeger, Phys. Rev. Lett. **42**, 1698 (1979).

[7] H. Labuhn, D. Barredo, S. Ravets *et al.*, Nature **534**, 667 (2016).

Probing electron dynamics in bio-relevant molecules

F. Calegari[1,2,3]

[1] *Center for Free-Electron Laser Science, DESY, Notkestr. 85, 22607, Hamburg, Germany*
[2] *Institut fr Experimentalphysik, Hamburg Universitt, Luruper Chaussee 149, 22761 Hamburg, Germany*
[3] *Institute of Photonics and Nanotechnologies, CNR-IFN, Piazza Leonardo da Vinci 32, 20133, Milano, Italy*
e-mail: *francesca.calegari@desy.de*

Ionizing radiation causes mutations and irreparable damage to DNA. However, nucleobases also exhibit relatively high inherent photo-stability. The complexity of these molecules makes it a challenging task to elucidate in detail all the physical mechanisms activated by ionization including fragmentation, internal energy dissipation and electronic correlation effects. As recently shown, access to the time scale immediately following ionization of a bio-chemically relevant molecule can be gained using an extreme ultraviolet (XUV) attosecond pump in combination with a near-infrared (NIR) few-femtosecond probe [1, 2]. Moreover, attosecond pulses can be produced in the 20-40 eV energy range, which is highly relevant for the biological context. This is indeed the typical energy range of secondary electrons that - by impacting DNA - represent the main source of indirect damage following tissue irradiation [3]. Ionization with 20-40 eV energies is often accompanied by the transition of an outer shell electron to an unoccupied state by a shake-up mechanism. It has been demonstrated that the population of such shake-up states can be probed with attosecond time resolution [4]. So far this investigation has been only limited to atoms and small molecules.

Here we present a time-resolved study of photo-fragmentation of the nucleobase adenine, one of the key building blocks of DNA, following ionization by an XUV attosecond pulse. Our most intriguing observation is that a stable dication of the parent molecule can be produced if (and only if) the probing NIR pulse is very briefly delayed from the XUV pulse. Our experimental and theoretical findings indicate that this short delay corresponds to the time required for a shake-up process to occur.

In our experiment, ionization of adenine was initiated by isolated sub-300-as pulses with photon energies between 17 eV and 40 eV, and subsequently probed by sub-4-fs, waveform-controlled NIR pulses. Adenine was evaporated and carried to the laser interaction region by a buffer gas. The produced ions were then collected using a VMI spectrometer operated in the ion time-of-flight mode as a function of the XUV-pump NIR-probe delay. The time dependent yield of many fragments displays a clear step-like increase, in some cases followed by a rapid decay. In the mass spectrum we identified the presence of the parent molecule dication (67.5 u/e). By fitting the time-dependent signal we find that the formation of this dication is delayed compared to the other cationic fragments by about 2.3 fs. It is worth noting that no stable dication of the parent is observed in the XUV-only signal, or in the combined XUV+NIR signal when the XUV energy is below 17 eV.

Theoretical calculations based on the Time-Dependent Density Functional Theory (TDDFT) indicate that direct single (or double) ionization of adenine by XUV pulses inevitably leads to dissociation. This implies that the sub-sequent creation of a stable parent dication requires relaxation of the system. Here we propose that the energy dissipation occurs via ionization of a shake-up state by the NIR probe pulse. Using the GW quasiparticle approximation and the time dependent perturbation theory based on DFT molecular orbitals, we calculated the characteristic time of shake-up and found a good agreement with the measured time delay of 2.3 fs.

References

[1] F. Calegari, D. Ayuso, A. Trabattoni, L. Belshaw, S. De Camillis, S. Anumula, F. Frassetto, L. Poletto, A. Palacios, P. Decleva, J. B. Greenwood, F. Martn and M. Nisoli, Science **346**, 336 (2014)

[2] E. P. Mansson, S. De Camillis, M. C. Castrovilli, M. Galli, M. Nisoli, F. Calegari and J. B. Greenwood, Phys. Chem. Chem. Phys. **19**, 19815 (2017)

[3] C. Caleman et al, Europhys. Lett. **85**, 18005 (2009)

[4] M. Uiberacker et al., Nature **446**, 627 (2007)

Phase estimation for quantum sensors

M. A. Kasevich
Department of Physics, Stanford University, Stanford, California 94305
e-mail: *kasevich@standford.edu*

Phase estimation is central to the operation of interferometric sensors. This talk will discuss quantum limits of phase estimation for precision atomic sensors and for phase contrast microscopy. In particular we will describe experiments that have demonstrated nearly 20 dB metrological improvement for atomic sensors using spin-squeezed atomic ensembles and recent application of these methods to free-space configurations relevant to high performance clocks and atom interferometers. We will present a multi-pass electron microscopy method which is capable of yielding at 10-fold reduction in sample damage for phase-contrast images of nm-scale biological proteins, and describe progress toward the design and operation of such a microscope.

Laser cooled molecules for quantum information and particle physics - recent progress and future prospects

John M. Doyle[1,2]
[1] *The Harvard/MIT Center for Ultracold Atoms, Cambridge MA, USA*
[2] *Department of Physics, Harvard University, Cambridge MA, USA*
e-mail: *doyle@physics.harvard.edu*

Wide-ranging scientific applications have created growing interest in ultracold molecules. Heteronuclear bialkali molecules, assembled from ultracold atoms, enabled the study of long-range dipolar interactions and quantum-state-controlled chemistry [1, 2], and recently have been brought to quantum degeneracy [3]. Assembling such molecules one-by-one in tweezers for quantum information applications is one exciting avenue of this work [4]. Beyond bialkalis, there are a range of molecules with advantageous properties for applications in quantum simulation [5, 6, 7] and quantum information [8, 9]. For example, polar molecules that feature unpaired electron spins are sought after because they can possess both non-zero electric and magnetic moments providing an additional degree of freedom. They can be used to simulate a large variety of lattice spin models [10], some of which host topological phases, opening up the possibility of topologically protected quantum memories and gates [11].

Molecules also have a special place in pushing forward precision searches for new particle physics beyond the Standard Model (BSM) [12, 13, 14, 15]. For example, current searches for the electron electric dipole moment probe T-violating physics due to particles with masses up to 30 TeV, which is a mass scale already well beyond the reach of particle colliders. Several experiments currently use heavy molecules (e.g. YbF [16], HaF^+ [17], ThO [18]) to probe BSM physics [19, 20, 21]. Importantly, complementary nuclear EDM experiments probe similar new particle mass ranges, with the most stringent limit produced using atomic mercury [22]. Searches for T-violation in the hadronic sector could greatly benefit from the use of molecules [23]. Currently, diatomic molecules are being used in several next-generation and new experiments searching for BSM physics [16, 17, 18, 24, 25].

Polyatomic molecules may be powerful tools in both of the above-mentioned areas of research, quantum information and particle physics. Polyatomics share key features with diatomics and have significant additional useful properties (and added complications). For example, states of non-zero projection of orbital angular momentum, electronic or nuclear, along the molecular axis are generically present in low-lying modes of all polyatomics. This allows for full polarization of molecules using very low electric fields and thus the creation of pairs of closely spaced molecular orientation states in the lab frame. More generally, polyatomics have the right combination of features and complexity that could improve the applicability of molecules to quantum information processing, as well as increase the discovery power of experimental probes into BSM physics. Examples include the use of symmetric top molecules for quantum simulation and computation systems [26, 27], and ultracold, heavy triatomic or symmetric top molecules could push BSM sensitivity to beyond the 1000 TeV level [28].

There are currently several approaches to producing ultracold molecules: atom association (e.g. bialkalis, see above), magnetic [29, 30], electric [31, 32], centrifugal [33], off-resonant optical [34] deceleration, and laser cooling. Optical cycling is needed for laser cooling and is a challenging task in molecules, even for those with diagonal Franck-Condon (FC) factors. There is, however, a generic class molecules, metal-oxide-radicals, that can have reasonably diagonal FC factors [35, 36]. With the metal atom being an alkaline earth (AE), the (remaining) valence electron is pushed away from the oxygen and is located nearly completely around the AE atom in both the ground and first electronically excited state. In particular, AE atoms bonded to fluorides or pseudofluorides are a generic class of molecules that have good cycling with the transition significantly decoupled from molecular excitations. These optical cycling center molecules (OCCM) allow for technologically feasible cycling of thousands of photons [35], which is above the threshold for laser slowing, magneto-optical trapping, and more advanced optical cooling methods well into ultracold regime, and also allow for high-fidelity quantum state detection. One might describe ultracold OCCMs as "atoms with powerful extra features."

Recently, laser cooling and magneto-optical trapping of diatomic OCCMs, first with SrF [37] and then with CaF [38, 39], were reported. Building on this, magnetic and optical confinement of these OCCMs has also been accomplished [40, 41, 42]. This is an important step as the confinement of molecules in a conservative trap is needed for many envisioned future works in precision spectroscopy, EDM and dark matter searches, molecular degenerate quantum gases, quantum information, and fundamental studies of ul-

tracold collisions and chemistry.

We will describe in this talk our recent results on optical trapping and Λ-enhanced laser cooling and imaging of CaF molecules [43], the laser cooling of SrOH molecules [44], and the prospects for laser cooling of larger polyatomic molecules [35], such as $CaOCH_3$, $YbOCH_3$, CaCCCa, $SrOCF_2CF_2OCa$, and $CaO(CH_2)_nOR$, where R is a radical termination ligand. We also will briefly present recent progress in the field of electric dipole moment searches using heavy diatomic molecules and future prospects, including the use of polyatomic molecules [28].

References

[1] B. Yan et al. Nature **501**, 521 (2013).

[2] S. Ospelkaus et al. Science **327**, 853 (2010).

[3] J. Ye. DAMOP, Session J02 (2018).

[4] L. R. Liu et al. Science **360**, 6391 (2018).

[5] L. D. Carr et al. New J. Phys. **11**, 055049 (2009).

[6] G. Pupillo et al. PRL. **100**, 050402 (2008).

[7] H. P. Büchler et al. PRL **98**, 060404 (2007).

[8] D. DeMille. PRL **88**, 067901 (2002).

[9] S. F. Yelin et al. PRA **74**, 050301 (2006).

[10] A. Micheli et al. Nat. Phys. **2**, 341 (2006).

[11] N. Y. Yao et al. Nat. Comm. **4**, 1585 (2013).

[12] Y. Nakai et al. J. High Energ. Phys. **08**, (2017).

[13] J. L. Feng Annu. Rev. Nucl. Part. S. **63**, 351 (2013).

[14] J. Engel et al. Prog. Part. Nucl. Phys. **71**, 21 (2013).

[15] M. Pospelov et al. Ann. Phys. **318**, 119 (2005).

[16] J.J Hudson et al. Nature **473**. 493 (2011).

[17] W. B. Cairncross et al. PRL **119**, 153001 (2017).

[18] ACME Collaboration. Science **343**, 269 (2014).

[19] P. G. H. Sandars. PRL **19**, 1396 (1967).

[20] O. P. Sushkov. JETP **48**, 608 (1978).

[21] M.G. Kozlov et al. J. Phys. B **28**, 1933 (1995).

[22] B. Graner et al. PRL **116**, 161601 (2016).

[23] V. V. Flambaum et al. Phys. Rev. Lett. **113**, 103003 (2014).

[24] E. B. Norrgard et al. Phys. Rev. A **95** 062506 (2017).

[25] NL-eEDM Collaboration arxiv:1804.10012v1. (2018).

[26] M. L. Wall et al. New J. Phys.**17**, 025001 (2015).

[27] P. Yu et al. Manuscript in preparation.

[28] I. Kozyryev et al. PRL **119**, 133002 (2017).

[29] Y. Liu et al. PRL **118**, 093201 (2017).

[30] N. Akerman et al. PRL **119**, 073204 (2017).

[31] H. L. Bethlem et al. Nature **406**, 491 (2000).

[32] A. Prehn et al. PRL **116**, 063005 (2016)

[33] X. Wu et al. Science **358**, 645 (2017).

[34] R. Fulton et al. PRL **93**, 243004 (2004).

[35] I. Kozyryev et al. Chem. Phys. Chem. **17**, 3641 (2016).

[36] T. A. Isaev et al. PRL **116**, 063006 (2016).

[37] J. F. Barry et al. Nature **512**, 286 (2014).

[38] S. Truppe et al. Nat. Phys. **13**, 1173 (2017).

[39] L. Anderegg et al. PRL **119**, 103201 (2017).

[40] H. Williams et al. PRL **120** (2018).

[41] D. J. McCarron et al. arXiv:1712.01462 (2017).

[42] L. Anderegg et al. arXiv:1712.01462 accepted Nat. Phys. (2018).

[43] L. Anderegg et al. Manuscript submitted for publication.

[44] I. Kozyryev et al. PRL **118**, 173201 (2017).

Bose gases quenched to unitarity

Zoran Hadzibabic
Cavendish Laboratory, University of Cambridge,
J.J. Thomson Avenue, Cambridge CB3 0HE, United Kingdom
e-mail: *zh10001@cam.ac.uk*

In ultracold atomic gases, Feshbach resonances give us access to the so-called unitary regime, where the s-wave scattering length diverges and two-body interactions are as strong as allowed by the laws of quantum mechanics. Following more than a decade of exciting experiments on the unitary Fermi gases, in particular on the BEC-BCS crossover in those systems, the unitary Bose gases have more recently emerged as a new experimental frontier. An additional challenge in understanding these gases is that due to rapid three-body recombination they are intrinsically non-equilibrium systems, which are in practice studied using rapid interaction quenches. I will give an overview of recent experiments trying to understand the dynamics and thermodynamics following a quench of a Bose gas to unitarity. These include measurements of the universal decay dynamics, energy and condensed fraction of degenerate unitary Bose gases, as well as observations of non-universal three-body Efimov physics in these systems.

Probing Topological Order and Hidden Magnetism using Quantum Gas Microscopy

Immanuel Bloch[1,2]
[1] *Fakultät für Physik, Ludwig Maximilians Universität, 80799 Munich, Germany*
[2] *Max Planck Institut für Quantenoptik, 85748 Garching, Germany*
e-mail: *immanuel.bloch@mpq.mpg.de*

Recent experiments with quantum gas microscopes allow for an unprecedented view and control of quantum matter in new parameter regimes and with new probes. In our fermionic quantum gas microscope, we can detect both charge and spin degrees of freedom simultaneously, thereby gaining maximum information on the intricate interplay between the two in the paradigmatic Hubbard model. The doped 1D systems are characterised by a hidden non-local antiferromagnetic (AFM) order that can be revealed using non-local string correlators, very similar to the non-local topological order in Spin-1 Haldane chains. This hidden AFM order probed in our experiments is the foundation of spin-charge separation in one-dimensional fermionic systems. Instead of probing such effects via dynamical probes and spectroscopy, one can now reveal such hidden correlations underlying many-body topological order directly in experiments.

In my talk, I will also outline how charge or magnetization doping of such systems gives rise to unconcentional incommensurate antiferromagnetic order in one dimension. Finally, I will present latest data on how the magentic environment is modified around a single density impurity in two dimensions, providing evidence for the formation of a polaron in the Fermi-Hubbard model. Our measurements consitute the first direct spatially resolved imaging of such polarons, which are believed to play a crucial role for the formation of high-T_c superconductors.

Attosecond pulses generated in gases and solids

P. B. Corkum
Joint Attosecond Science Lab
University of Ottawa and National Research Council of Canada
Room 464, Advanced Research Complex, Ottawa, ON, Canada K1N 5N6
e-mail: *pcorkum@uOttawa.ca*

Attosecond pulses are generated by electrons that are extracted from a quantum system by an intense light pulse and travel through the continuum under the influence of the electric field of the light. Portions of each electron wave packet are forced to re-collide with its parent ion after the field reverses direction. Upon re-collision, the electron and ion can recombine, emitting soft X-ray radiation that can be in the form of attosecond pulses. This highly nonlinear process occurs in atoms, molecules and solids and offers unique opportunities for measurement and control for measuring the attosecond pulse itself; the orbital(s) from which it emerged; the band structure of material in which the wave packets moves; and controlling soft X-ray radiation so that it naturally focusses.

Catching and reversing a quantum jump mid-flight

Michel Devoret[1,2]
[1] *Departments of Physics and Applied Physics, Yale University, New Haven, Connecticut 06520, USA*
[2] *Yale Quantum Institute, Yale University, New Haven, Connecticut 06511, USA*
e-mail: *michel.devoret@yale.edu*

The basic phenomenon of quantum jumps between two states of a system driven by a deterministic force while undergoing continuous monitoring is exploited in precision quantum measurements and plays a key role in our fundamental understanding of open quantum systems. Quantum jumps are emblematic of the special nature of randomness in quantum theory. Although it had been argued in the past that their nature is discontinuous, modern measurement theory stipulates that the state of the system evolves continuously during a jump. Even more remarkable, in the case of a system possessing at least 3 states, it was shown theoretically that it is possible i) to obtain an advance warning that the jump is about to occur, and consequently ii) to reverse it if it was initiated by a coherent drive. We have successfully implemented the indirect QND measurement of a superconducting artificial atom transition from its ground state G to a dark state D by monitoring the occupancy of an auxiliary bright level B coupled to G by a Rabi drive. By conditioning the tomography and manipulation of the G-D manifold on the non-occupancy of the B level for a deterministic duration, we catch and even reverse the jump [1]. Our experimental results, in agreement with the predictions of quantum trajectories theory with essentially no adjustable parameters, provide new ground for the exploration of real-time intervention techniques in the control of quantum systems, such as early detection of error syndromes.

References

[1] Z. Minev, S.O. Mundhada, S. Shankar, P. Reinhold, R. Guttierez, R.J. Schoelkopf, M. Mirrahimi, H. Carmichael, M.H. Devoret arXiv:1803.00545.

Quantum vortex shedding in atomic superfluid gases

Y. Shin

Department of Physics and Astronomy, Seoul National University, Seoul 08826, Korea

e-mail: *yishin@snu.ac.kr*

The wake behind a moving obstacle is a classic problem in fluid dynamics and it is well known that a transition from laminar to turbulent flow universally occurs in a viscous classical fluid as the Reynolds number increases. A superfluid gives an interesting situation where zero viscosity does not allow the Reynolds number and vorticity is restriced with quantized circulation. When a superfluid flows past a large obstacle, the nucleation of quantized vortices occurs above a certain critical velocity v_c, giving rise to drag and dissipation in the superfluid. The details of the vortex nucleation process and its relation to the microscopic modes of excitation remain as open questions in the study of dissipative superfluid dynamics. In this talk, I will present our recent vortex-shedding experiments with weakly interacting atomic Bose-Einstein condensates [1, 2] and strongly interacting fermionic superfluid gases [3]. Highly oblate large atomic samples were prepared and perturbed by translating a repulsive optical obstacle formed by a focused laser beam, and their responses in terms of vortex nucleation were investigated for various sweeping conditions. We observed a regular-to-turbulent transition of vortex shedding pattern as the obstacle velocity increases, resembling the universal behavior of classical fluids [1], and development of spatial pair correlations of vortices and antivortices in the turbulent superfluid containing many vortices [2]. In the experiments with strongly interacting atomic Fermi gases, we investigated the critical vortex shedding across the BEC-BCS crossover and observed a qualitative change of the dependence of v_c on the sweeping distance, which is attributed to the participation of pair breaking in the vortex shedding dynamics [3]. Finally, I will discuss the extension of the vortex-shedding experiment to a spinor superfluid which has mass and spin superfluidities simultanesouly [4].

References

[1] W. J. Kwon, J. H. Kim, S. W. Seo, and Y. Shin, Phys. Rev. Lett. **117**, 245301 (2016).

[2] S. W. Seo, B. Ko, J. H. Kim, and Y. Shin, Sci. Rep. **7**, 4587 (2017).

[3] J. W. Park, B. Ko, and Y. Shin, arXiv:1805.08950.

[4] J. H. Kim, S. W. Seo, and Y. Shin, Phys. Rev. Lett. **119**, 185302 (2017).

Measurement of the fine-structure constant as a test of the Standard Model

Holger Mueller
Department of Physics, University of California, Berkeley, California 94720, USA
e-mail: *hmberkeley@gmail.com*

Measurements of the fine-structure constant require methods from across subfields and are thus powerful tests of the consistency of theory and experiment in physics. Using the recoil frequency of cesium-133 atoms in a matter-wave interferometer, we recorded the most accurate measurement of the fine-structure constant to date: $\alpha = 1/137.035999046(27)$ at 2.0×10^{-10} accuracy. Using multiphoton interactions (Bragg diffraction and Bloch oscillations), we demonstrate the largest phase (12 million radians) of any Ramsey-Bord interferometer and control systematic effects at a level of 0.12 part per billion. Comparison with Penning trap measurements of the electron gyromagnetic anomaly $g_e - 2$ via the Standard Model of particle physics is now limited by the uncertainty in $g_e - 2$; a 2.5σ tension has implications for physics beyond the Standard Model that warrants further investigation, such as dark photons and electron substructure.

Cavity QED: Quantum Bits and Quantum Fields

Gerhard Rempe
Max Planck Institute of Quantum Optics, Hans-Kopfermann-Str. 1, 85748 Garching, Germany
e-mail: *gerhard.rempe@mpq.mpg.de*

Quantum electrodynamics (QED) deals with phenomena that are not possible within classical electrodynamics. In contrast to what founders of QED expected, the theory stands and guides experimental investigations. QED in a cavity is at the forefront of this research, mainly because it provides the effectively strongest possible optical nonlinearity at the single-photon level. This nonlinearity lies at the heart of a plethora of quantum non-demolition, entanglement, teleportation, quantum-logic and quantum-memory experiments that established cavity QED as the prime toolbox for hybrid quantum networking. More recently, a double cavity QED system has shown that it can directly and strongly couple two distinguishable photons, thereby opening up new possibilities for all-optical quantum sensing. While these experiments demonstrate the versatility of cavity QED for probabilistic quantum-superposition bits, it now seems timely to extend the experimental possibilities towards deterministic quantum-superposition fields. The talk will present the new achievements and put them into perspective.

Towards quantum simulation of exotic quantum many-body physics with nuclear spins

Zhihuang Luo[1], Jun Li[1], Zhaokai Li[1], Ling-Yan Hung[3], Yidun Wan[3], **Xinhua Peng**[1], & Jiangfeng Du[1]

[1] *Department of Modern Physics, University of Science and Technology of China, Hefei, Anhui 230026, China*

[2] *Beijing Computational Science Research Center, Beijing 100094, China*

[3] *State Key Laboratory of Surface Physics and Department of Physics, Fudan University, 220 Handan Road, 200433 Shanghai, China*

e-mail: *xhpeng@ustc.edu.cn*

The modern conception of phases of matter has undergone tremendous developments since the first observation of topologically ordered states in fractional quantum Hall systems in the 1980s. Topological phase not only plays a significant role in the basic scientific research of condensed matter physics, but also provides a natural medium for fault-tolerant quantum computation. However, the experiments for the exotic matter face the great challenges although they have been intensively and theoretically studied in recent years.

Recently, a new approach called quantum simulation [1] may provide an ideal intermediate between in situ experiment and numerical simulation in many ways [2, 3]. Here we report our recent progress on experimental quantum simulation to investigate exotic many-body physics using nuclear spins [4]. We explore the question: How much details of the physics of topological orders can in principle be observed by scalable quantum simulation experiments with little theoretical data? We find that using surprisingly little data, namely the toric code Hamiltonian in the presence of generic disorders and detuning from its exactly solvable point, the modular matrices – characterizing anyonic statistics that are some of the most fundamental finger prints of topological orders – can be reconstructed with very good accuracy solely by experimental means. Using a kind of nuclear magnetic resonance simulator, we realize a first experimental demonstraton of these fundamental signatures of a topological order, a test of their robustness against perturbations, and a proof of principle – that current technologies have attained the precision to identify phases of matter and, as such, probe an extended region of phase space around the soluble point before its breakdown. Given the special role of anyonic statistics in quantum computation, our work promises myriad applications both in probing and realistically harnessing these exotic phases of matter.

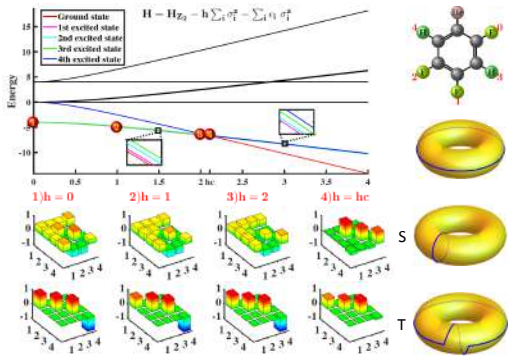


Figure 1: Energy-level diagram of the studied model and experimental results of standard modular S and T matrices.

[1] R. P. Feynman, *Int. J. Theor. Phys.* **21**, 467 (1982).

[2] X. Peng and D. Suter. Front. Phys. China, 5,1, 2010.

[3] X. Peng, Z. Luo, W. Zheng, S. Kou, D. Suter, & J. Du, *Phys. Rev. Lett.* **113**, 080404 (2014).

[4] Z. Luo, J. Li, Z. Li, L. Hung, Y. Wan, X. Peng, J. Du, *Nat. Phys.* **14**, 160165 (2018).

Cavity polariton in semiconductor lattices : a non-linear photonic emulator

Jacqueline Bloch[1]

[1] *Centre de Nanoscience et de Nanotechnologies, CNRS / Universits Paris Saclay et Paris Sud*
e-mail: *jacqueline.bloch@c2n.upsaclay.fr*

Semiconductor microcavities appear today as a promising photonic platform for the study of manybody physics with ligh. They enable confining both light and electronic excitations (excitons) in very small volumes. The resulting strong light-matter coupling gives rise to hybrid light-matter quasi-particles named cavity polaritons. Polaritons propagate like photons but strongly interact with their environment via their matter part: they are fluids of light and have been shown to exhibit fascinating properties such as superfluidity or nucleation of quantized vortices [1]. Sculpting microcavities at the micron scale, it is possible to engineer lattices of various geometries and use this photonic platform for the emulation of different Hamiltonians [2].

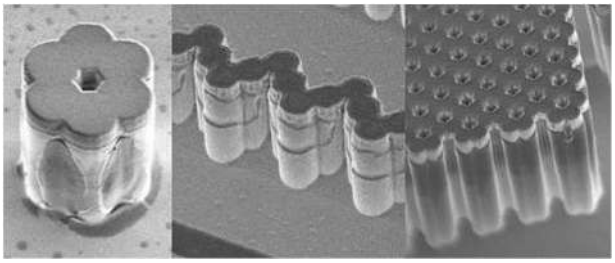


Figure 1: Scanning electron microscopy image of microstructures in which cavity polaritons can be generated: (left) A benzene photonic molecule, (center) a 1D lattice and (right) a 2D honeycomb lattice of coupled resonators.

After a general introduction, I will illustrate with some recent experiments, the potential of this photonic plateform both for fundamental and more applied perspectives.
I will first describe how a photonic benzene molecule, the elementary building block of honeycomb lattices, allows fabricating a microlaser with controlled Orbital Angular Momentum of the lasing mode [3]. Thanks to a strong spin orbit coupling, lasing with finite orbital angular momentum can be triggered. The helicity of this novel microlaser is simply controlled by the circular polarization of the optical excitation.

The second part of the talk will be devoted to the exploration of 2D honeycomb lattices of coupled micropillars [4]. Dirac cones and edge states can be directly visualized both in real and reciprocal space. Deforming the lattices to mimic the effect of strain in real graphene, we evidence several types of topological transitions linked to the merging of Dirac cones. This work opens many perspectives with respect to transport properties of new quasi-particles and to the development of photonic topological insulators.

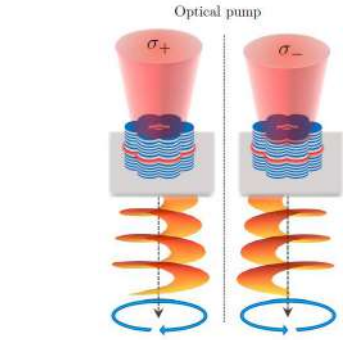


Figure 2: Schematics of the experiment where changing the polarization of the excitation beam, a microlaser made of six coupled semiconductor resonators (photonic benzene molecule) emits a mode with controlled Orbital Angular Momentum

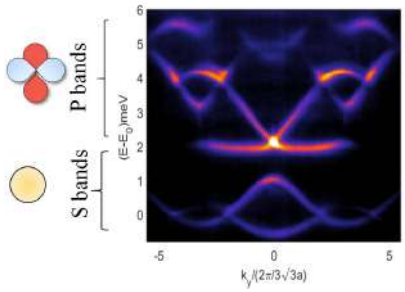


Figure 3: Angularly resolved emission of a honeycomb lattice showing a band structure emulating the physics of graphene.

[1] C. Ciuti and I. Carusotto, Rev. of Modern Physics **85**, 299 (2013).

[2] A. Amo and J. Bloch, Comptes Rendus Physique **17**,934 (2016)

[3] N. Carlon Zambon, P. St-Jean et al., arXiv:1806.04590

[4] M. Milicevic et al., Phys. Rev Lett. **118**, 107403 (2017).

Quantum Logic Spectroscopy of a Single Molecular Ion

P.O. Schmidt[1,2]

[1] *Physikalisch-Technische Bundesanstalt, Bundesallee 100, 38116, Braunschweig, Germany*

[2] *Institut für Quantenoptik, Leibniz Universität Hannover, Welfengarten 1, 30167 Hannover, Germany*

e-mail: *Piet.Schmidt@quantummetrology.de*

Precision spectroscopy is a driving force for the development of our physical understanding. In particular laser cooling and manipulation has led to an advancement in precision spectroscopy. However, only few atomic and molecular species offer suitable transitions for laser cooling, limiting the variety of accessible species. This restriction can be overcome in trapped ion systems through quantum logic spectroscopy. Coherent laser manipulation, originally developed in the context of quantum information processing, allows to combine the special spectroscopic properties of one ion species (spectroscopy ion) with the excellent control over another species (logic or cooling ion) [1].

We experimentally demonstrate how the internal state of a single $^{24}MgH^+$ molecular ion can be detected through coupling to a $^{25}Mg^+$ atomic ion (see Fig. 1(a)). Starting from the ground state of motion of a joint motional mode, a molecular state-selective optical dipole force changes the motional state only if the molecule is in a specific rovibrational state. The change of the motional state is efficiently detected on the atomic ion. This way, we observe black body radiation-driven quantum jumps between rotational states in the molecule (see Fig. 1(b)). The detuning-dependence of the coupling strength of the optical dipole force allows us to perform spectroscopy on a specific electronic transition in the molecule [2]. This non-destructive detection technique represents a first step towards extending the exquisite control achieved over selected atomic species to much more complex species, such as molecular ions. Possible applications are model-independent probes for a possible variation of the electron-to-proton mass ratio [3], tests of parity violation using chiral molecules [4], or measurements of the electric dipole moment of the electron [5].

Residual off-resonant excitation followed by rovibrational diffusion in the molecular ion limits the efficiency of internal state detection. We show how excited motional Fock states enhance the detection sensitivity of such small forces beyond the classical limit and thus can in principle reduce the required interaction between the optical dipole force and the molecule (see Fig. 1(c)). In contrast to schemes that rely on e.g. squeezing, Fock state metrology requires no phase coherence between the interaction creating the state and the signal to be measured. We demonstrate this phase independence by performing measurements of displacement and trapping frequency of a single ion with sensitivities below the classical limits in separate experiments, but using the same quantum state.

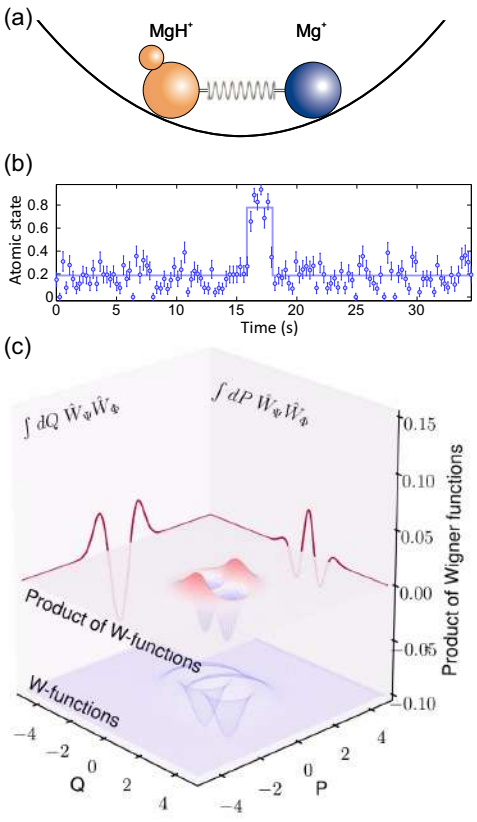


Figure 1: Quantum jumps in a molecular ion. (a) A molecular ion is strongly coupled to an atomic ion via the Coulomb interaction. (b) A quantum jump into and out of the $J = 1$ rotational state of the molecular ground state, detected in real time via the atomic ion. (c) Interference in phase space results to a higher displacement sensitivity for Fock states.

[1] P. O. Schmidt *et al.*, Science **309**, 749–752 (2005).

[2] F. Wolf *et al.*, Nature **530**, 457–460 (2016).

[3] M. Kajita, Phys. Rev. A **95**, 023418 (2017).

[4] C. Daussy *et al.*, Phys. Rev. Lett. **83**, 1554–1557 (1999).

[5] W. B. Cairncross *et al.*, Phys. Rev. Lett. **119**, 153001 (2017).

Thin Hofstadter ribbons: topology and a Diophantine equation

I. B. Spielman[1], **D. Genkina**[1], **and L. M. Aycock**[1,2], **H.-I Lu**[1], **M. Lu**[1], **and A. M. Pineiro**[1]
[1] *Joint Quantum Institute, National Institute of Standards and Technology, and University of Maryland, Gaithersburg, Maryland, 20899, USA*
[2] *Department of Physics, Cornell University, Ithaca, NY 14850*
e-mail: *ian.spielman@nist.gov*

Physical systems with non-trivial topological order find direct applications in metrology[1] and promise future applications in quantum computing[2, 3]. The quantum Hall effect derives from transverse conductance, quantized to unprecedented precision in accordance with the system's topology[4]. At magnetic fields beyond the reach of current condensed matter experiment, around 10^4 Tesla, this conductance remains precisely quantized but takes on different values[5]. Hitherto, quantized conductance has only been measured in extended 2-D systems. Here, we engineered and experimentally studied narrow 2-D ribbons, just 3 or 5 sites wide along one direction, using ultracold neutral atoms where such large magnetic fields can be engineered[6, 7, 8, 9, 10, 11]. We microscopically imaged the transverse spatial motion underlying the quantized Hall effect. Our measurements identify the topological Chern numbers with typical uncertainty of 5%, and show that although band topology is only properly defined in infinite systems, its signatures are striking even in nearly vanishingly thin systems.

[1] Klitzing, K. v., Dorda, G. & Pepper, M. New method for high-accuracy determination of the fine-structure constant based on quantized hall resistance. *Phys. Rev. Lett.* **45**, 494–497 (1980).

[2] Freedman, M. H. Quantum computation and the localization of modular functors. *Foundations of Computational Mathematics* **1**, 183–204 (2001).

[3] Kitaev, A. Fault-tolerant quantum computation by anyons. *Annals of Physics* **303**, 2 – 30 (2003).

[4] Laughlin, R. B. Quantized hall conductivity in two dimensions. *Phys. Rev. B* **23**, 5632–5633 (1981).

[5] Thouless, D. J., Kohmoto, M., Nightingale, M. P. & den Nijs, M. Quantized hall conductance in a two-dimensional periodic potential. *Phys. Rev. Lett.* **49**, 405–408 (1982).

[6] D. Jaksch, P. Z. Creation of effective magnetic fields in optical lattices: the hofstadter butterfly for cold neutral atoms. *New Journal of Physics* **5**, 56 (2003).

[7] Miyake, H., Siviloglou, G. A., Kennedy, C. J., Burton, W. C. & Ketterle, W. Realizing the harper hamiltonian with laser-assisted tunneling in optical lattices. *Phys. Rev. Lett.* **111**, 185302 (2013).

[8] Aidelsburger, M. *et al.* Realization of the hofstadter hamiltonian with ultracold atoms in optical lattices. *Phys. Rev. Lett.* **111**, 185301– (2013).

[9] Celi, A. *et al.* Synthetic gauge fields in synthetic dimensions. *Phys. Rev. Lett.* **112**, 043001– (2014).

[10] Stuhl, B. K., Lu, H.-I., Aycock, L. M., Genkina, D. & Spielman, I. B. Visualizing edge states with an atomic bose gas in the quantum hall regime. *Science* **349**, 1514– (2015).

[11] Mancini, M. *et al.* Observation of chiral edge states with neutral fermions in synthetic hall ribbons. *Science* **349**, 1510– (2015).

Generation and application of attosecond laser pulses

A. Becker[1], C. Hernández-Garcia[2], C. Goldsmith[1], J. Venzke[1], J. Su[1], C.G. Durfee[3], D.D. Hickstein[1], I.J. Sola[2], L. Plaja[2], M.-C. Chen[4], M.M. Murnane[1], H.C. Kapteyn[1], and A. Jaroń-Becker[1]

[1] *JILA and Department of Physics, University of Colorado, Boulder, CO 80309, USA*

[2] *Grupo de Investigacíon en Aplicaciones del Láser y Fotónica, University of Salamanca, E-37008 Salamanca, Spain*

[3] *Department of Physics, Colorado School of Mines, Golden, CO 80401, USA*

[4] *Institute of Photonics Technologies and Department of Physics, National Tsing Hua University, Hsinchu, Taiwan*

e-mail: *andreas.becker@colorado.edu*

Capture of ultrafast physical processes involving electron dynamics require the development of sources and measurement techniques operating on time scales of attoseconds (1 as = 10^{-18} s) to femtoseconds (1 fs = 10^{-15} s). High-order harmonics generation (HHG) is a technique to produce coherent radiation in a train of bursts as short as a few tens of attoseconds. For many years research in HHG focused on the generation and application of linearly polarized attosecond pulses.

Recently, physical principles and techniques have been proposed and developed to control the polarization of the harmonics. For example, using two noncollinear beams with counter-rotating circular polarization [1], spatially separated circularly polarized high harmonics of different energy and helicity have been generated. Based on this technique different schemes for the generation of isolated attosecond pulses of pure circular polarization have been proposed [2]. Using results of numerical simulations it is shown that the reduction of the driver pulse duration can limit the number of pulses in the attosecond pulse train, similarly to results previously observed in the case of linear polarization. Furthermore, it has been found that a temporal delay between the two crossed driver pulses forms an effective polarization gate which provides an alternative route to the generation of isolated circularly polarized pulses. Based on the application and extension of these schemes a robust polarization control of isolated extreme-ultraviolet pulses has recently been demonstrated [3].

One of the key applications of attosecond pulses for time-resolved measurements is the attosecond streaking method [4], in which the momentum of the photoelectron, ionized by an isolated attosecond pulse is changed by a superimposed infrared streaking pulse. Observation of the energy of the photoelectron as a function of the phase of the streaking pulse, at which the center of the ionizing XUV pulse is applied, provides the streaking trace. By comparing the streaking trace to the oscillation of the vector potential a temporal shift, called streaking time delay, occurs. It has been shown that this time delay can be interpreted as due to the dynamics of the photoelectron determined by the Coulomb interaction with the parent ion and the electric field of the streaking pulse [5, 6, 7]. Furthermore, this understanding of the streaking time delay opens the perspective to retrieve time-resolved information during the transition of the electron in the continuum if the technique is extended to resonant two-photon ionization [8].

[1] D.D. Hickstein et al., Nat. Photon. **9**, 743 (2015).

[2] C. Hernandez-Garcia et al., Phys. Rev. A **93**, 043855 (2016).

[3] P.-C. Huang et al., Nat. Photon. **12**, 349 (2018).

[4] J. Itatani, F. Quéré, G.L. Yudin, M.Y. Ivanov, F. Krausz, and P.B. Corkum, Phys. Rev. Lett. **88**, 173903 (2002).

[5] J. Su, H. Ni, A. Becker, and A. Jaron-Becker, Phys. Rev. A **89**, 013404 (2014).

[6] C. Goldsmith, J. Su, A. Becker, and A. Jaron-Becker, Phys. Rev. A **96**, 053410 (2017).

[7] C. Goldsmith, A. Jaron-Becker, and A. Becker, J. Phys. B **51**, 025601 (2018).

[8] J. Su, H. Ni, A. Jaron-Becker, and A. Becker, Phys. Rev. Lett. **113**, 263002 (2014).

Composing many-body systems with quantum gases

Tilman Esslinger
Department of Physics, ETH Zurich, 8093 Zürich, Switzerland
e-mail: *esslinger@phys.ethz.ch*

Cooling and manipulating atomic gases have opened up new avenues to explore fundamental concepts in quantum many-body physics. Synthetically created potentials and control of atom-atom interactions have made it possible to tailor the properties of experimental systems at a microscopic level. This led to the concept of quantum simulation – here a system capable of reproducing the physics of many-body Hamiltonians. One of the goals of this approach is to provide answers to open questions in the context of condensed matter physics. An equally important frontier is the construction of novel systems, which may at present not be realizable in solid-state or other systems. This path leads to new questions and surprises.

Few-body aspects of spin-orbit coupled cold atom systems

Doerte Blume

[1] *Homer L. Dodge Department of Physics and Astronomy, The University of Oklahoma, 440 W. Brooks Street, Norman, Oklahoma 73019, USA*

e-mail: *doerte9999@gmail.com*

Spin-orbit coupled cold atom systems, governed by Hamiltonians that contain quadratic kinetic energy terms typical for a particles motion in the usual Schrdinger equation and linear kinetic energy terms typical for a particles motion in the usual Dirac equation, have attracted a great deal of attention recently since they provide an alternative route for realizing fractional quantum Hall physics, topological insulators, and spintronics physics. This talk will discuss selected few-body aspects of spin-orbit coupled cold atom systems. Two topics will be discussed. 1) It will be shown that spin-orbit coupling terms can notably modify the two-body scattering properties [1, 2]. 2) It will be discussed what happens to Efimovs famous radial scaling law if single-particle spin-orbit coupling terms are added to the three-boson Hamiltonian with two-body short-range interactions [3].

References

[1] Q. Guan and D. Blume, Scattering framework for two particles with isotropic spin-orbit cou- pling applicable to all energies. Physical Review A **94**, 022706 (2016).

[2] Q. Guan and D. Blume, Analytical coupled- channel treatment of two-body scattering in the presence of three-dimensional isotropic spin- orbit coupling. Physical Review A **95**, 020702(R) (2017).

[3] Q. Guan and Blume, Three-boson spectrum in the presence of 1D spin-orbit coupling: Efimovs generalized radial scaling law. To appear in Physical Review X (2018).

Quantum Control of Atomic and Molecular Ions

Dietrich Leibfried[1],
[1] *Ion Storage Group, National Institute of Standards and Technology, Boulder, CO 80305, USA*
e-mail: *dietrich.leibfried@nist.gov*

This talk will give an overview of recent work on quantum control, quantum information processing and quantum logic optical clocks realized with trapped ions at NIST[1].

Miniaturized surface-electrode traps offer a number of advantages for quantum control of trapped ions. For example, it becomes possible to generate sufficient magnetic fields and gradients at microwave and radio-frequencies to efficiently drive single-qubit and multi-qubit operations on hyperfine qubits. This approach has potential advantages over laser-based operations, including the absence of spontaneous emission, precise phase and amplitude control as well as the relative maturity of miniaturized microwave electronics. Comparisons of different mechanisms for entangling operations with microwave and radio-frequency magnetic fields will be discussed.

In a proof-of principle experiment, we integrate superconducting meander-wire detectors into a linear surface-electrode trap (see Fig. 1) with the goal of directly detecting state dependent fluorescence from an ion without any imaging optics and in a manner that is scalable to a large number of detection zones in larger trap devices. We will give an update on the current status of this experiment.

The close proximity of the ions to electrodes in miniaturized surface traps (30-50 μm) also amplifies challenges that any precise quantum control of trapped ions will face, such as stray electric fields at the position of the ions and increased anomalous heating.

We demonstrate techniques that are applicable to any harmonic oscillator in the quantum regime, irrespective of the type of experiment and physical implementation. By utilizing non-classical states, such as squeezed states and superpositions of number states, we characterize ion motional frequency noise over a wide range of time-scales, with a quantum advantage over more traditional approaches. To this end, we demonstrate the preparation of approximately pure number states of ion motion up to $n = 100$, coherent superpositions of the ground state with number states up to $n = 16$ and squeezing to more than 20 dB over a motional ground state.

Two $^{9}Be^{+}$ clock qubits and two $^{25}Mg^{+}$ qubits have been used in a two-dimensional trap array to implement and characterize a teleported controlled-NOT gate in a dual species experiment featuring the majority of elements required for scalable quantum information processing, including multi-species transport and separation of ions within the array and gates between like and different species of ions. We characterize the teleported gate operation by informationally complete quantum process tomography.

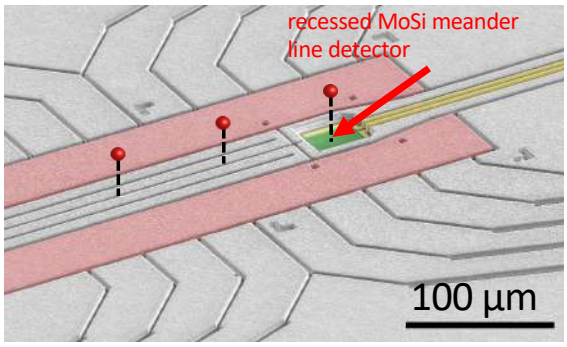


Figure 1: Electron microscope picture of linear surface electrode trap with integrated meander line detector. The rf-electrodes are in red false color and the detector meander area is in green. The bias and read-out lines of the detector are in yellow. The red balls symbolize the ion positions for different potentials applied to the electrodes off to side of the rf-electrodes.

By combining techniques from quantum logic ion clocks with far-detuned Raman-transitions driven by a continuous laser or a frequency comb, we implement a methods set to initialize and coherently manipulate pure quantum states that is generally applicable to a wide range of molecular ions using the same experimental setup. We demonstrate the salient features of this approach by performing kHz-precision spectroscopy and coherent manipulation of pure rotational quantum states of CaH^{+} [1].

Results from a recent accuracy evaluation for the Al^{+} quantum-logic optical clock will also be presented (see poster #21 on 7/26 by D. Hume). Frequency ratio measurements between this clock and two optical-lattice clocks at NIST are ongoing.

References

[1] C. W. Chou, C. Kurz, D. B. Hume, P. N. Plessow, D. R. Leibrandt, and D. Leibfried, Nature **545**, 203 (2017).

[1]This work was supported by IARPA, ARO, ONR, DARPA and the NIST quantum information program.

Seeing A Single Atom Where It Is Not

G. Araneda[1], S. Walser[2], Y. Colombe[1], D. B. Higginbottom[1,3], J. Volz [2], R. Blatt [1], and A. Rauschenbeutel[2,4]

[1] *Institut für Experimentalphysik, Universität Innsbruck, Technikerstraße 25, 6020 Innsbruck, Austria*

[2] *Atominstitut, TU Wien, Stadionallee 2, 1020 Wien, Austria*

[3] *Centre for Quantum Computation and Communication Technology, Research School of Physics and Engineering, The Australian National University, Canberra ACT 2601, Australia*

[4] *Institut für Physik, Humboldt-Universität zu Berlin, Newtonstraße 15, 12489 Berlin, Germany*

e-mail: *arno.rauschenbeutel@hu-berlin.de*

The precise determination of the position of subwavelength scale emitters and scatterers using far-field optical imaging techniques is of utmost importance for a wide range of applications in medicine, biology, astronomy, and physics. In this talk, I theoretically and experimentally show that, for a standard optical imaging system like an optical microscope, the image of an elliptically polarized point-like emitter does not coincide with the emitter's real position. Instead, even for perfect, aberration-free imaging with high numerical aperture, the image will in general be shifted. This can lead to a systematic error in the optical localization of emitters which exceeds the typical precision of super-localization microscopes by far. Moreover, for the case of small numerical aperture, the shift can in principle reach arbitrarily large values. Imaging a single trapped atom as well as a single gold nanoparticle, we experimentally demonstrate this effect and observe wavelength-scale shifts. Beyond its relevance for optical imaging, the demonstrated phenomenon may also occur for sources of other types of waves. Consequently it can, e.g., impede the precision of the localization of remote objects with imaging radar and sonar as well as the future localization of stellar objects in gravitational wave

Dynamically probing many-body states of matter in optical lattices

André Eckardt

Max-Planck Institut für Physik komplexer Systeme, Nöthnitzer Str. 38, 01187 Dresden, Germany

e-mail: *eckardt@pks.mpg.de*

I will talk about our recent theoretical work on probing many-body states of matter in optical lattices and present different schemes that exploit the high resolution with respect to time (and space) available in these systems both for imaging and control.

This includes measurement protocols that are based on monitoring the dynamics of a system following sudden changes in the Hamiltonian (quenches). Here I will describe a proposal for measuring the winding numbers characterizing two-dimensional Floquet topological lattice systems and their anomalous edge modes [1]. Also a scheme for reconstructing the off-diagonal elements of the single-particle density matrix with respect to pairs of distant lattice sites will be discussed [2]. I will, furthermore, report on a collaboration with the experimental group of David Weld, where a double quench protocol is employed to measure the localization of the ground state of a static optical lattice in the basis of the Floquet states of the strongly driven lattice [3]. While for an integrable non-interacting system it is localized and reaches a state consistent with a generalized Gibbs ensemble, delocalization (ergodicity) is observed when integrability is broken by interactions.

If time permits, I will briefly mention also a recent proposal for engineering local artificial magnetic fields piercing a single plaquette [4] (Fig. 1). Such "optical solenoids" would not only allow for probing the elementary excitations of integer and fractional Chern insualtors [5], but can also be employed for quantized charge pumping along tailored paths in these two-dimensional systems [4].

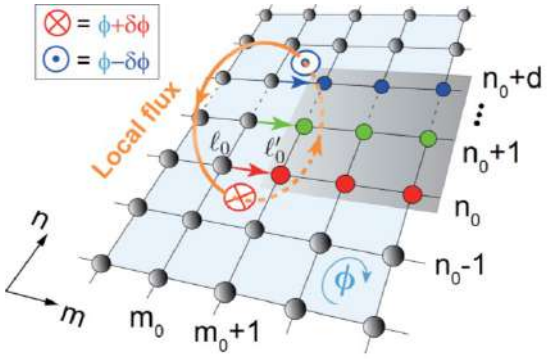


Figure 1: Engineering solenoid-type local magnetix fluxes in an optical lattice. Taken from [4].

[1] F.N. Ünal, B. Seradjeh, and A. Eckardt, in preparation.

[2] L. A. Peña Ardila, M. Heyl, and A. Eckardt, Measuring the single-particle density matrix for fermions and hard-core bosons in an optical lattice, *arXiv:1806.08171*

[3] K. Singh et al., in preparation.

[4] B. Wang, F.N. Ünal, and A. Eckardt, Floquet engineering of optical solenoids and quantized charge pumping along tailored paths in two-dimensional Chern insulators, *Phys. Rev. Lett.* **120**, 243602 (2018),

[5] M. Raciunas, F.N. Ünal, E. Anisimovas, and A. Eckardt, Creating, probing, and manipulating fractionally charged excitations of fractional Chern insulators in optical lattices, *arXiv:1804.02002*

Gravitational wave astronomy: We can hear the universe!

K. Danzmann[1]

[1] *Max Planck Institute for Gravitational Physics and Leibniz Universität Hannover, 30167 Hannover, Germany*

e-mail: *karsten.danzmann@aei.mpg.de*

For thousands of years we have observed the universe using light. Since September of 2015 everything is different. Gravitational waves were discovered and we can finally hear the universe. The first objects detected were unexpectedly heavy black holes. By now black hole merger observations are almost routine even though the design sensitivity of the large gravitational wave detectors has not even been reached. But just before going offline for another round of upgrading, the large detectors have observed another source type, the merger of two neutron stars. Ground-based gravitational wave astronomy is now on the way to a bright future. But in June 2017 the European Space Agency ESA has approved LISA as L3 mission in its future science program after the technology precursor LISA Pathfinder has delivered beautiful results showing that LISA technology works. LISA will launch in the early 2030s and open the low-frequency gravitational wave window at frequencies from a fraction of a mHz to 1 Hz, to observe supermassive black holes and maybe even the early universe.

Quantum Simulation with Ytterbium Fermi Gases

Y. Takahashi[1], **Y. Takasu**[1], **S. Taie**[1], **H. Ozawa**[1,2], **K. Ono**[1], **Y. Amano**[1], **K. Sato**[1], **and J. Kobayashi**[1,3]

[1] *Department of Physics, Graduate School of Science, Kyoto University, 606-8502 Kyoto, Japan*
[2] *RIKEN Center for Emergent Matter of Science, Japan*
[3] *PRESTO, Japan Science and Technology Agency, Japan*
e-mail: *yitk@scphys.kyoto-u.ac.jp*

Ultracold atoms in an optical lattice offers an intriguing possibility of simulating a strongly correlated quantum many-body system with high controllability [1]. An illustrative example is the successful observation of a superfluid-Mott insulator transition for Bose gases loaded in an optical lattice. While a great deal of progress in many-body physics has been also made recently for Fermi gases of alkali atoms in an optical lattice, there has been increasing interest for Fermi gases of two-electron atoms due to the unique possibilities they can provide. In this talk, I will report our recent experiments using ultracold Fermi gases of ytterbium (Yb) atoms in an optical lattice.

One of the unique properties of Fermi gases of two-electron atoms is a high spin symmetry of SU($\mathcal{N}$=2$\mathcal{I}$+1) of nuclear spin $\mathcal{I}$, which will show novel quantum magnetism[2]. Previously we demonstrated a formation of SU(6) Mott insulator owing to the Pomerachuk cooling effect enhanced for large spin degrees of freedom[3]. In our recent study, we investigate the short-range quantum magnetism of the SU($\mathcal{N}$ >2) system loaded in an optical dimerized lattice[4], by extending the pioneering work for SU(2) short-range magnetism[5]. In our experiment, we develop a technique for optically inducing a nuclear spin singlet-triplet oscillation with a spin-dependent potential gradient, and combine it with a photo-association technique, enabling us to confirm the formation of nearest-neighbor anti-ferromagnetic spin correlations of a ^{173}Yb Fermi gas with SU($\mathcal{N}$) symmetry. In particular, the control of the spin degrees of freedom by an optical pumping technique enables us a straightforward comparison between the cases of SU(2) and SU(4), revealing that the anti-ferromagnetic correlation is enhanced for the SU(4) spin system compared with SU(2) as a consequence of an enhanced Pomeranchuk cooling effect. This work is an important step towards the realization of novel SU($\mathcal{N}$) quantum magnetism.

The existence of the long-lived metastable states of ^{3}P$_2$ and ^{3}P$_0$ is also one of unique properties of two-electron atoms. In particular, the two-orbital system of the ^{3}P$_0$ and the ground ^{1}S$_0$ states is a candidate for the quantum simulation of a Kondo effect [6, 7]. Towards this possibility, we recently investigate a Fermi gas of ^{171}Yb atoms, different from the previously studied atomic species which show ferro-magnetic spin-exchange interaction [8, 9]. After cooling the ^{171}Yb atoms down to a Fermi degenerate regime by sympathetic cooling with ^{173}Yb atoms, we successfully measure the resonances associated with the ^{1}S$_0$↔^{3}P$_0$ clock transition for the atoms loaded into a 3D optical lattice. A systematic clock transition spectroscopy at various magnetic fields will enable us to obtain the information on the spin-exchange interaction which is important in the study of a Kondo effect.

[1] I. Bloch, J. Dalibard, andW. Zwerger, Rev. Mod. Phys. **80**, 885 (2008).

[2] M. A. Cazalilla and A. M. Rey, Rep. Prog. Phys. **77**, 124401 (2014).

[3] S. Taie, R. Yamazaki, S. Sugawa, and Y. Takahashi, Nat. Phys. **8**, 825 (2012).

[4] H. Ozawa, S. Taie, Y. Takasu, and Y. Takahashi, arXiv:1801.05962 (2018).

[5] D. Greif, T. Uehlinger, G. Jotzu, L. Tarruell, and T. Esslinger, Science **340**, 1307 (2013).

[6] A. V. Gorshkov *et al.*, Nat. Phys. **6**, 289 (2010).

[7] M. Foss-Feig *et al.* Phys. Rev. A. **81**, 051603(**R**)(2010).

[8] F. Scazza *et al.*, Nat. Phys. **10**, 779 (2014).

[9] X. Zhang *et al.*, Science **345**, 1467 (2014).

Certification of many-body quantum states

A. Acín[1,2]

[1] *ICFO-Institut de Ciencies Fotoniques, The Barcelona Institute of Science and Technology, 08860 Castelldefels (Barcelona), Spain*

[2] *ICREA–Institució Catalana de Recerca i Estudis Avançats, Lluis Companys 23, 08010 Barcelona, Spain*

e-mail: *antonio.acin@icfo.eu*

Understanding the properties of many-body systems represents one of the most fundamental questions in physics. Moreover, it is crucial for the development of quantum technologies. An ubiquitous question is to certify that a given many-body quantum system satisfies an operational property: is this given system in an entangled state? Does it display non-classical correlations? Does it provide a good approximation to the ground state of a relevant Hamiltonian? Does it contain the solution to a classical optimisation problem? In all these cases, the certification problem is challenging due to the well-known fact that the number of parameters needed to describe a many-body system increases exponentially with the number of particles.

In the talk, we first review methods for polynomial optimisation based on hierarchies of semi-definite programming (SDP). Then, we show two applications of these methods in a many-body context. First, we provide a technique for device-independent entanglement detection that involves a polynomial number of correlation functions [1]. We apply this technique to several physically relevant situations allowing us to detect entangled states for systems up to few tens of qubits. Second, we move to the computation of ground states of classical spin systems. These systems are relevant because they can encode the solution to classical optimisation problems and are often used to benchmark quantum annealers. We combine SDP methods with two other techniques, known as branch and bound and chordal extension, to design a method for the computation of ground-state spin configurations [2]. An advantage of the resulting method is that it provides upper and lower bounds to the ground-state energy, so that the error in the approximation is under control. We apply it to 2D square ferromagnetic Ising models with random magnetic fields, solving systems of size 35×35. We also test it against the D-wave machine in 2D triangular ferromagnetic Ising systems with random magnetic fields for systems of size 13×24. Our method yields the exact ground state and ground state energy for the largest system size simulatable on the D-Wave machine, which sometimes coincides and sometimes outperforms the upper bound obtainable from the quantum annealer. Our method may thus become an important tool for the benchmark of quantum annealers.

[1] F. Baccari, D. Cavalcanti, P. Wittek and A. Acín, Phys. Rev. X **7**, 021042 (2017).

[2] F. Baccari, C. Gogolin, P. Wittek and A. Acín, in preparation.

Quantum optics using ordered atomic arrays

D. E. Chang[1,2]

[1] *ICFO-Institut de Ciencies Fotoniques, The Barcelona Institute of Science and Technology, 08860 Castelldefels (Barcelona), Spain*

[2] *ICREA-Institució Catalana de Recerca i Estudis Avançats, 08015 Barcelona, Spain*

e-mail: *darrick.chang@icfo.eu*

Ensembles of atoms or other quantum emitters are envisioned to be an important component of quantum technologies ranging from magnetometers to quantum memories for light. It has historically been an outstanding challenge to exactly solve for the quantum dynamics of an optical field as it propagates through and interacts with an ensemble. The standard axiomatic approach is to use the one-dimensional Maxwell-Bloch equations, which treats the interaction between the ensemble and a quasi-1D optical mode of interest, while the interaction with the remaining 3D continuum of modes is assumed to result in independent spontaneous emission of excited atoms. Strictly speaking, this assumption can not be correct, as the emission of light is a wave phenomenon, and thus the emitted intensity must depend on interference and correlations between the atoms. Here, we discuss an alternative theoretical approach, which accounts for interference and the precise atomic positions. In this formalism, an interacting quantum spin model describes the dynamics of the atomic internal degrees of freedom under multiple photon scattering, while the field properties can subsequently be re-constructed from the spin correlations. Using this model, we then show how interference can be exploited as an extremely powerful resource to suppress the unwanted emission of light and the subsequent loss of information into undesirable directions. The effects of interference are particularly prominent in ordered arrays of emitters. As a specific example, we construct a new protocol for a quantum memory for light based upon an ordered array, whose error rate as a function of system resources scales exponentially better than previously known bounds. This raises the intriguing question of whether interference and arrays can be used to enhance all other applications involving atomic light-matter interfaces.

Higher-order correlations and what we can learn about the solution for many body problems from experiments

J. Schmiedmayer[1]

[1] *Vienna Center for Quantum Science and Technology, Atominstitut, TU-Wien, Vienna, Austria*
e-mail: *schmiedmayer@atomchip.org*

The knowledge of all correlation functions of a system is equivalent to solving the corresponding quantum many-body problem [1]. If one can identify the relevant degrees of freedom, the knowledge of a finite set of correlation functions is in many cases enough to determine a sufficiently accurate solution of the corresponding field theory.

A correlation function $G^{(N)}$ of order N can be decomposed into [2]

$$G^{(N)}(\mathbf{z}) = G^{(N)}_{\text{dis}}(\mathbf{z}) + G^{(N)}_{\text{con}}(\mathbf{z}) \ .$$

The first term, the *disconnected* part $G^{(N)}_{\text{dis}}$, is fully determined by the lower-order correlation functions and therefore does not contain new information at order N. The second term, the *connected* part $G^{(N)}_{\text{con}}$, contains genuine new information about the system at order N. In a diagrammatic expansion, $G^{(N)}_{\text{con}}$ is given by a sum of fully connected diagrams with N external lines.

If $G^{(N)}_{\text{con}}$ is zero for all $N > 2$, the correlation functions factorise and the quantum many-body states are Gaussian. Finding the degrees of freedom that lead to complete factorisation corresponds to solving the quantum many-body problem.

Determining up to which order N the connected correlation function can be estimated with statistical significance gives a direct handle on how much of the complexity of the underlying quantum many-body system is accessible in a given experiment.

In my talk I will shows how this powerful theoretical concept can be applied to analyse many body systems in experiment.

In our Experiments we study a pair of tunnel-coupled one-dimensional atomic super-fluids. From the measured phase profiles $\varphi(z)$ we extract the N^{th}-order correlation functions of the phase:

$$G^{(N)}(\mathbf{z}, \mathbf{z}') = \langle [\varphi(z_1) - \varphi(z'_1)] \dots [\varphi(z_N) - \varphi(z'_N)] \rangle \ ,$$

with coordinates $\mathbf{z} = (z_1, \dots, z_N)$ and $\mathbf{z}' = (z'_1, \dots, z'_N)$ along the length of the system.

A detailed analysis of the interference reveals under which conditions the phase correlation functions factorise. This allows us to characterise the essential features of the model solely from our experimental measurements: We detect the relevant quasi-particles, their interactions and the different topologically distinct vacuum-states [3]. This demonstrates, that a pair of tunnel-coupled one-dimensional atomic super-fluids is a quantum simulator of the quantum sine Gordon model.

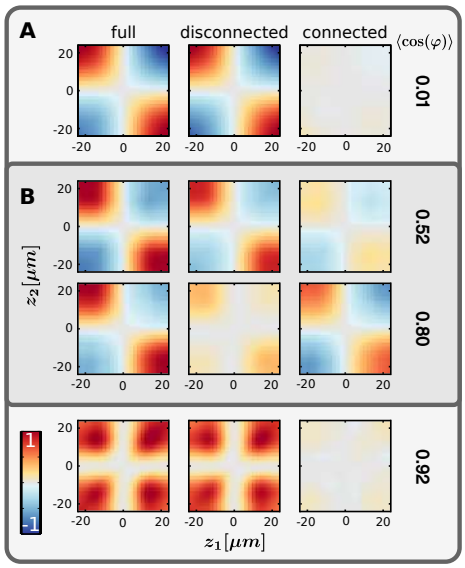


Figure 1: (**A**) for uncoupled ($\langle\cos(\varphi)\rangle \simeq 0$) and strongly phase-locked ($\langle\cos(\varphi)\rangle \simeq 1$) the 4^{th}-order correlation function $G^{(4)}(\mathbf{z}, \mathbf{z}')$ factorises; (**B**) In the intermediate regime a significant $G^{(4)}_{\text{con}}$ remains. (adapted from [3])

Starting from this analysis I will discuss how one can extract details about the scattering processes and the intrinsic parameters of the model from the 'bare' correlators.

We further more study Gaussification when quenching into a free theory (J=0), and the dynamics of phase locking when quenching from a free system (J=0) into the sine Gordon model (finite J).

Our examples establish a general method to analyse quantum systems through experiments. It thus represents a crucial ingredient towards the implementation and verification of quantum simulators.

Work performed in collaboration with J. Berges and T. Gasenzer at the Univ. Heidelberg, and supported by the ERC advanced grant *QuantumRelax*, and by the Austrian Science Fund (FWF) through the SFB: *FoQuS* and the SFB 1225 *ISOQUANT* financed by the German Research Foundation (DFG) and the FWF.

[1] J. Schwinger, Proc. Natl. Acad. Sci. **37**, 452 (1951).

[2] J. Zinn-Justin, *Quantum Field Theory and Critical Phenomena* (Oxford Univ. Press, Oxford, 2002).

[3] T. Schweigler, et al., Nature **545**, 323 (2017).

Microscopy of ultracold Rydberg macrodimers

C. Gross

Max-Planck-Institut für Quantenoptik Hans-Kopfermann-Straße 1, 85748 Garching, Germany

e-mail: *christian.gross@mpq.mpg.de*

Pairs of Rydberg atoms feature complex interaction potentials even at micrometer distance. In particular, attractive and repulsive pair potentials of the same symmetry may come close in energy, forming an avoided crossing at a distance much larger than the electronic wave function extend of the individual Rydberg atoms. The avoided crossing leads to a deep potential well, which supports multiple vibrational bound states. Here we report on the microscopic observation of such exotic Rydberg-Rydberg macrodimers using single site resolved imaging of an ultracold quantum gas in an optical lattice. We directly image the macrodimers as pairs of missing atoms and laser spectroscopy reveals the vibrational spectrum with high precision. We observe a strong dependence of the relative strength of the odd and even lines on the laser polarization and our local measurement reveals a clear spatial anisotropy of the excitation probability. Combining narrow line excitation to such Rydberg macrodimers with atomic motion in the lattice might be used to engineer many-body states stabilized through dissipation.

Bad Metallic Transport in a Cold Atom Fermi-Hubbard System

P. Brown[1], D. Mitra[1], E. Guardado-Sanchez[1], R. Nourafkan[2], A. Reymbaut[2], C.-D. Hébert[2], S. Bergeron[2], A.-M. Tremblay[2,3], J. Kokalj[4,5], D. Huse[1], P. Schauss[1], and W. Bakr[1]

[1] *Department of Physics, Princeton University, Princeton, New Jersey 08544 USA*

[2] *Département de Physique, Institut Quantique, and Regroupement Québécois sur les Matériaux de Pointe, Université de Sherbrooke, Sherbrooke, Québec, Canada J1K 2R1*

[3] *Canadian Institute for Advanced Research, Toronto, Ontario, Canada M5G 1Z8*

[4] *Faculty of Civil and Geodetic Engineering, University of Ljubljana, SI-1000 Ljubljana, Slovenia*

[5] *Jožef Stefan Institute, Jamova 39, SI-1000 Ljubljana, Slovenia*

e-mail: *wbakr@princeton.edu*

Transport measurements are a revealing probe of the quantum properties of materials. They uncover the exotic microscopic properties of diverse systems, including superconductors, superfluid helium, and spintronic devices. Historical attempts to understand the results of these measurements have led to the development of the band theory of metals, Fermi liquid theory and BCS superconductivity. Despite these successes with weakly interacting systems, a general framework for transport in strongly interacting quantum systems is lacking. A unifying theme for these systems is that the distinct particle-like nature of the charge carriers is blurred by interactions or temperature, resulting in a "quantum soup". In this talk, I will present our study of the charge conductivity of the Fermi-Hubbard model, a natural testing ground for strong interaction physics, in a clean quantum system - ultracold ^{6}Li in a 2D optical lattice. We use a quantum gas microscope to observe time-resolved microscopic charge transport. We measure the diffusion constant and current relaxation rate of our Fermi-Hubbard system over a range of temperatures by imposing a density modulation and modelling its decay hydrodynamically. The diffusion constant is converted to a resistivity, which we find scales linearly with temperature and exceeds the Mott-Ioffe-Regel limit with no sign of saturation. Our results demonstrate that Fermi-Hubbard systems can exhibit similar anomalous resistivity phenomenology to what is seen in real bad metals and suggest non-quasiparticle transport at high temperatures.

Entangling and verifying a 20 qubit register

B. P. Lanyon[1], T Brydges[1,2], A. Elben[1,4], N. Friis[5], O. Marty[6], C. Maier[1,2], Milan Holzäpfel[6], P. Jurcevic[1,2], B. Vermersch[1,4], C Hempel[3], M. Joshi[1], M Huber[5], M. Plenio[6], P. Zoller[1,4], R. Blatt[1,2], C. F. Roos[1]

[1] *Institut für Quantenoptik und Quanteninformation, Osterreichische Akademie der Wissenschaften, Technikerstr. 21A, 6020 Innsbruck, Austria*

[2] *Institut für Experimentalphysik, Universität Innsbruck, Technikerstr. 25, 6020 Innsbruck, Austria*

[3] *ARC Centre for Engineered Quantum Systems, School of Physics, The University of Sydney, Sydney, New South Wales 2006, Australia.*

[4] *Institut für Theoreticalphysik, Universität Innsbruck, Technikerstr. 25, 6020 Innsbruck, Austria*

[5] *Institute for Quantum Optics and Quantum Information - IQOQI Vienna, Austrian Academy of Sciences, Boltzmanngasse 3, 1090 Vienna, Austria*

[6] *Institut für Theoretische Physik and IQST, Albert-Einstein-Allee 11, Universität Ulm, 89069 Ulm, Germany*

e-mail: *ben.lanyon@uibk.ac.at*

Engineered quantum systems, consisting of tens of individually-controllable interacting quantum particles, are currently being developed using different physical platforms; including atoms in optical arrays, ions in radio-frequency traps and superconducting circuits. These systems offer the possibility of generating and probing complex quantum states and dynamics particle by particle, finding application in the near-term as quantum simulators, and in the longer-term as quantum computers. As these systems are developed, new protocols are required to characterize them; to verify that they are performing as desired and to measure quantum phenomena of interest.

In this talk I'll present two recent works in this context, carried out using an engineered quantum system of cold trapped atomic ions. In the first [1], using custom-built entanglement witnesses, we observe the generation of multipartite entanglement in a fully-controlled 20 qubit register. In the second [2], we demonstrate a new method to measure entropy (and therefore the entanglement structure) of engineered quantum systems, using randomised measurements. This method, applicable to any physical platform with single qubit control, enables the overall coherence and entanglement to be verified for arbitrary states of up to around 20-qubit partitions. Finally, if there is time, I'll briefly explain how it should soon be practical to distribute long-lived entanglement between trapped-ion systems that are separated by hundreds of kilometres.

[1] N. Friis, O. Marty, C. Maier, C. Hempel, M. Holzapfel, P. Jurcevic, M. Plenio, M. Huber, C. Roos, R. Blatt, B. Lanyon, Phys Rev X. **8** 021012 (2018)

[2] T. Brydges, A. Elben, P. Jurcevic, B. Vermersch, C. Maier, B. P. Lanyon, P. Zoller, R. Blatt and C. F. Roos, arXiv:1806.05747 (2018)

Building single molecules

Kang-Kuen Ni[1,2]
[1] *Harvard-MIT Center for Ultracold Atoms*
[2] *Department of Chemistry and Chemical Biology, Harvard University, Cambridge, MA 02138, USA*
e-mail: *ni@chemistry.harvard.edu*

Control and imaging of individually trapped ions and neutral atoms have been crucial to developing them as powerful quantum building blocks for qubits, logic gates, and clocks. Bringing these capabilities to molecules promises additional quantum applications, enabled by the rich internal degrees of freedom and inter-molecular coupling. I will present our experimental work to achieve single-particle control of molecules. Our approach begins by trapping individual cesium and sodium atoms and transporting them into a single optical tweezer. Two atoms in a tweezer allow clean studies of collisions and reactions in the ultracold regime. To build a molecule out of two atoms as a proof-of-principle, we utilize photoassociation [1]. The individual atoms have been brought under full quantum control [2, 3]. Currently, we are learning to create individual molecules coherently for quantum simulation, quantum information processing [4], and ultracold chemistry with precise initial reactant preparation.

References

[1] L. R. Liu, J. D. Hood, Y. Yu, J. T. Zhang, N. R. Hutzler, T. Rosenband, and K.-K. Ni, Building one molecule from a reservoir of two atoms, Science, **360** (6391):900903, 2018.

[2] L. R. Liu, J. T. Zhang, Y. Yu, N. R. Hutzler, Y. Liu, T. Rosenband, and K.-K. Ni. Ultracold Molecular Assembly. ArXiv:1701.03121, January 2017.

[3] Y. Yu, N. R. Hutzler, J. T. Zhang, L. R. Liu, T. Rosenband, and K.-K. Ni. Motional Ground State Cooling Outside the Lamb-Dicke Regime, ArXiv:1708.03296, August 2017.

[4] K.-K. Ni, T. Rosenband, and D. D. Grimes. Dipolar Exchange Quantum Logic Gate with Polar Molecules. ArXiv:1805.10930, May 2018.

Engineering collective light-matter interactions

R. J. Bettles, T. Ilieva, N. L. R. Spong, H. Busche and C. S. Adams
Joint Quantum Centre (JQC) Durham-Newcastle, Department of Physics, Durham University, Durham DH1 3LE, UK
e-mail: *c.s.adams@durham.ac.uk*

Strong light-matter coupling—without cavities—requires a high optical depth such that any incident photon has a high probability of interacting. For a single dipole, optical depth (extinction) optimization is achieved by frequency matching and spatial mode matching of the incident light, $\mathcal{E}_\mathrm{i}$ to the dipolar emission pattern $\mathcal{E}_\mathrm{d}$, see Fig. 1. For many dipoles, optical depth maximisation becomes a complex many-body problem, where one may need to include the effects of the interactions between dipoles and the vector nature of the electromagnetic field.

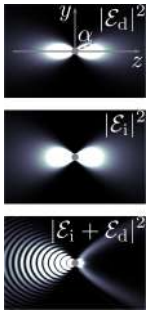


Figure 1: Intensity in the yz plane. Top: dipolar radiation pattern. Middle: Focused laser beam. Bottom: Interference between the laser beam and dipolar field. [1]

In general, for many dipoles, the light interacts with a collective mode, and in a strongly-interacting medium the optical response of these collective modes is a non-linear function of the number of emitters, N, i.e., $\chi \neq N\chi_1$, where χ_1 is the simple emitter response. In this sense, the non-linearity in collective response is analogous to quantum non-linear optics, where the optical response is a non-linear function of the photon number. In strongly-interacting media, such as Rydberg ensembles [2], both collective and quantum non-linear optical effects are present. An open question is whether one can re-engineer the collective response in order to optimize the non-linear optical response. For example, using sub-wavelength arrays it is possible to engineer subradiant modes where the effective cross section of each emitter is enhanced [3].

In order to engineer the collective modes, a better understanding of collective light-matter interactions in the laboratory setting is required. Surprisingly, we find that collective modes dynamics are far more subtle that might be expected. For example, in violation of naive intuition, it is possible to observe faster than superradiant light emission, and decay rates that are much larger than the resonance line width. To see why, it is helpful to start from the collective eigenmodes of N interacting dipoles. In Fig. 2 we show the eigenfrequencies, Δ_ℓ, (measured relative to the unperturbed resonance) and modified decay rates, Γ_ℓ of collective modes. Figure 2e is calculated for a pair of dipoles with different values of their separation. The light couples more strongly to the symmetric modes as indicated by the dark blue dots. Figure 2f shows the case of a random ensemble of 400 dipoles. Here, the field couples more strongly to the superradiant states with $\Gamma_\ell > \Gamma_0$. From this plot we might expect to observe a resonance line width and emission decay rate of between 0.7 and 1.7 Γ_0, however, both experimentally and theoretically, we find that the decay rate is around 3 Γ.

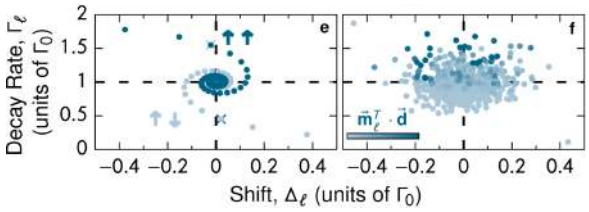


Figure 2: The frequencies, Δ_ℓ, and free space vacuum couplings, Γ_ℓ, for (**e**) atom pairs with different spacing, and (**f**) a random ensemble of $N = 400$ dipoles.

The explanation of this faster than superradiant decay is that it is the interference between modes with different frequencies rather than the individual decay rates that dominates the dynamical response. This result has important implications for understanding light-matter interactions in both atomic and solid-state systems [4], and for engineering materials for quantum non-linear optics.

[1] C. S. Adams and I. G. Hughes, *Optics f2f*, OUP (2018).

[2] O. Firstenberg, C. S. Adams and S. Hofferberth, J. Phys. B **49**, 152003 (2016).

[3] R. J. Bettles, S. A. Gardiner, and C. S. Adams, Phys. Rev. Lett. **116**, 103602 (2016).

[4] G. Scuri *et al.* Phys. Rev. Lett. **120**, 037402 (2018).

Posters

Sensing beyond the Heisenberg limit

T. Dutta[1], **and M. Mukherjee**[1,2]

[1] *Centre for Quantum Technologies, National University Singapore, Singapore 117543*

[2] *Department of Physics, National University Singapore, Singapore 117551.*

In the recent years trapped and laser cooled ions have evolved as the forerunner in quantum computation as well as precision measurement. In particular, quantum metrology has enhanced the sensitivity of parameter estimation. Here the optimality of quantum metrology for frequency measurement has been used to surpass the Heisenberg scaling of the measurement uncertainty with the observation time(T). In a single ion experiment, we show that the uncertainty in the frequency measurement scales as the square of the observation time (*i.e*, $1/T^2$) instead of linear dependence for over 100 μs time scale limited by the de-phasing time of the probe state [1]. The scheme is based on the recent theoretical proposal [2] implemented on a laser-cooled single ion probe which has been coupled to an external time-dependent field. This method, when applied to the electron spin interacting with an external time-dependent field leads to the test of detectability of axion-like dark matter particle. Even though the limit on the coupling strength is a weak limit, we provide a feasible experimental proposal by which the limit can be strengthened to complement the other dark matter search experiments. The dark matter search is one of the key questions to our understanding of Physics beyond the Standard Model of particle physics.

References

[1] T. Dutta and M. Mukherjee, arXiv:1803.01724v2

[2] S. Pang and A. N. Jordan, Nat. Commun. **8**, 14695 (2017).

A master oscillator based on 48.5 cm long optical cavity as a reference for a universal synthesizer

M. Schioppo[1], A. Silva[1], M. Dovale[1,2], R. A. Williams[1], R. Hobson[1], W. Bowden[1], I. R. Hill[1], C. F. A. Baynham[1], B. I. Robertson[1], P. Gill[1] and H. S. Margolis[1]

[1] *National Physical Laboratory, Teddington, TW11 0LW, United Kingdom*
[2] *University of Birmingham, Birmingham, B15 2TT, United Kingdom*

e-mail: *marco.schioppo@npl.co.uk*

The rapid development of optical frequency metrology has led to a variety of optical standards that need to be systematically compared to evaluate their performance. At the National Physical Laboratory (UK) we have developed a universal synthesizer scheme to transfer frequency stability from a master optical oscillator to multiple microwave and optical clocks, namely the Cs fountain, Yb^+ ion, Sr^+ ion, and Sr lattice clocks. The universal synthesizer is based on a self-referenced optical frequency comb working in a transfer oscillator scheme [1, 2].

Here we present the details of a new master oscillator, based on a monolithic Nd:YAG laser stabilized to an optical cavity. This laser has been chosen for its narrow free-running linewidth of 1 kHz, which simplifies the design of the servo loop system for frequency stabilization. Additionally, the high output power of 500 mW at 1064 nm allows for a reliably high signal-to-noise ratio on the optical beat notes necessary for phase noise cancellation of the different fibre delivered outputs.

The optical cavity consists of a 48.5 cm long cylindrical ULE spacer, mounted horizontally, and operated at room temperature. Two fused silica mirrors (1 m radius of curvature and flat) are optically contacted to the spacer, with ULE annuli on the back of each mirror to increase the temperature at which the effective coefficient of thermal expansion is zero. The cavity is surrounded by three layers of nested passive radiative shields made of polished aluminium (see Fig. 1), separated by fused silica spheres to minimize the thermal contact, with the whole assembly kept in vacuum at a pressure of 3×10^{-7} mbar. The exterior of the vacuum system is temperature stabilized at a few degrees above room temperature with ~ 1 mK stability. The dielectric high-reflectivity mirror coating sets the estimated thermal noise floor at $\sim 7 \times 10^{-17}$ fractional frequency instability.

We have measured a cavity finesse of 155 000, with an excess of 5 ppm losses per mirror with respect to the design specification. Residual amplitude modulation is actively stabilized to keep its contribution to the frequency instability below the thermal noise floor. The vibration sensitivity was measured by subjecting the cavity to controlled shaking, and comparing the resultant frequency modulation against an independent stable reference. Measured sensitivities for the vertical, transverse, and longitudinal directions are $5.9 \times 10^{-10}\,g^{-1}$, $2.4 \times 10^{-10}\,g^{-1}$, and $1.8 \times 10^{-10}\,g^{-1}$, respectively.

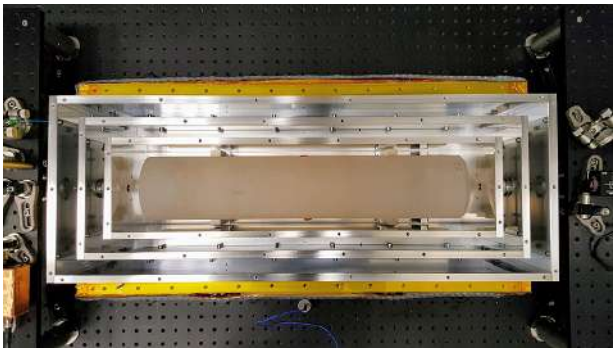


Figure 1: Top view of the open vacuum chamber, hosting the optical cavity and the surrounding low emissivity aluminium thermal shields.

The residual non-linear uncompensated drift of the cavity, measured with respect to the ^{87}Sr lattice clock transition, is a few $mHz\,s^{-1}$. Using this upgraded universal synthesizer we have been able to extend the operational interrogation time of the ^{87}Sr optical atomic transition to 300 ms [3, 4]. The master oscillator has been compared against two other local oscillators in a three-cornered-hat scheme with a resulting measured fractional frequency instability below 1.5×10^{-16} from 1 s to 100 s integration time, likely limited by sensitivity to vibrations [5].

A second system with improved optical performance and reduced vibration sensitivity is under construction to allow direct frequency comparison of optical cavities with similar performance.

[1] H. Telle, B. Lipphardt, and J. Stenger., Applied Physics B **74**, 1-6 (2002).

[2] D. Nicolodi, *et al.*, Nature Photonics **8**, 219-223 (2014).

[3] R. Hobson, *et al.*, ICAP (2018).

[4] W. Bowden, *et al.*, ICAP (2018).

[5] S. Häfner, *et al.*, Optics Letters **40**, 2112-2115 (2015).

E2 transitions between hyperfine structure components of the D_2^+ molecular ion

P. Danev[1], **V.I. Korobov**[2], **and D. Bakalov**[1]

[1] *Institute for Nuclear Research and Nuclear Energy, Bulgarian Academy of Sciences, blvd. Tsarigradsko ch. 72, Sofia 1142, Bulgaria*

[2] *Joint Institute for Nuclear Research, 141980, Dubna, Russia*

e-mail: *petar_danev@abv.bg*

Due to the possibility of precise theoretical evaluation of their spectrum, transitions, and external effect shifts, it is shown that the hydrogen molecular ions are of metrological relevance [1], [2]. In [3], the intensity of laser-induced electric quadrupole transitions between arbitrary Zeeman split components of the hydrogen molecular ion H_2^+ hyperfine structure has been calculated. In the present work, we continue studying hydrogen molecular ions by computing the ro-vibrational electric quadrupole transition rates of the deuterium molecular ion D_2^+. The matrix elements of the electric quadrupole operator are calculated with nonrelativistic wavefunctions obtained in the variational approach used in [4]. In comparison with earlier results of Pilon [5] our work includes higher vibrational states and takes into account all the details of D_2^+ hyperfine and Zeeman structure of the E2 transition spectrum.

The authors (P.D. and D.B.) gratefully acknowledge the support of the Bulgarian National Science Fund under Grant No. FNI 08-17, and of the Bulgarian Academy of Sciences under Grant No. DFNP-17-166.

[1] S. Schiller, D. Bakalov, and V.I. Korobov, *Simplest molecules as Candidates for Precise Optical Clocks*, Phys. Rev. Lett. **113**, 023004 (2014).

[2] D. Bakalov, S. Schiller, *The electric quadrupole moment of molecular hydrogen ions and their potential for a molecular ion clock*. Appl. Phys. B (2014) **114**, pp.213-230. Erratum: Volume **116**, Issue 3, pp 777-778.

[3] V.I. Korobov, P. Danev, D. Bakalov, and S. Schiller, *Laser-stimulated electric quadrupole transitions in the molecular hydrogen ion* H_2^+, Phys. Rev. A **97**, 032505 (2018).

[4] V. I. Korobov, D. Bakalov, and H. J. Monkhorst, Phys. Rev. A 59, R919(R) (1999).

[5] H.O. Pilon, *Quadrupole transitions in the bound rotationalvibrational spectrum of the deuterium molecular ion*, J. Phys. B: At. Mol. Opt. Phys. 46 245101 (2013).

Measurement of the Infrared Magic Wavelengths for the $^{40}Ca^{+}$ Ion Clock Transition

Kelin Gao[1], **Yao Huang**[1], **and Hua Guan**[1]

[1] *Wuhan Institute of Physics and Mathematics, Chinese Academy of Sciences, Wuhan 430071 China*

e-mail: *klgao@wipm.ac.cn*

One of the infrared magic wavelengths for Ca^{+} ion is measured with high precision. Lambrecht et al shows that the ions can be all-optical trapped for longer time with infrared lasers because of the lower heating rates[1]. Promisingly, the measurement of these magic wavelengths paves the way to building all-optical trapped ion clocks. Furthermore, the measured wavelength agrees well with the theoretical calculations but has higher accuracy. The related oscillator strengths can be determined with higher accuracy by using the measured magic wavelength.

In our previous publication [2], optical clocks with all-optical trapping scheme is proposed: by all-optical trapping of the ions during the clock interrogation, the Doppler shift and uncertainty caused by ion micromotion can be eliminated. We calculated and found that it is possible to trap Ca^{+} ions with the laser at our measured wavelength, which gives us confidence to build an optical clock with all-optical ion trapping technique. It was found that the ion lifetime in dipole trap would be a few ms with a few hundreds of GHz red detuning lasers, yet the lifetime can be extended to a few second with a few hundred THz far-off-resonance lasers [1]. To realize the ion optical clocks with all-optical trapping scheme, lifetime of at least 100 ms is required and one need to make the heating rate as low as possible to lower the Doppler and dc Stark shifts caused by the kinetic motion. Building a clock with infrared lasers hundreds THz of red detuning looks like a better choice comparing to with the 395 nm laser. Besides, one can easily obtain a fiber laser with higher power at the Ca^{+} infrared magic wavelength of about 1050 nm). To date, there are a few theoretical calculation results, calculation difference of tens of nm still exists between different groups, some results have uncertainty of a few tens of nm [3-5]. As a result, it is important to precise measure the wavelength experimentally.

The basic idea about how the light shift is measured is the same as in Ref. [2]. Briefly speaking, the differential light shift can be measured directly and accurately by experiments; therefore, the magic wavelength λ_m could be derived with high precision. A single ion is trapped in the miniature ring Paul trap, and the temperature of the ion is laser cooled to be a few mK. To measure the magic wavelength, the clock laser was locked to the Zeeman components and the light shift on the clock transition can be observed by switching on/off the laser with wavelength

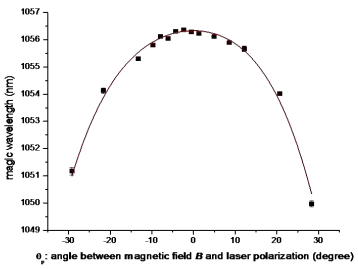


Figure 1: the measured magic wavelength as a function of the angle between the magnetic field and the laser polarization

1050 nm (named L_m laser for short in the following sections). To keep the L_m laser linear polarized during the measurement, we use a polarizer (Glan-Tyler Prism) is placed in the light path before ion-light interaction. The wavelength of the L_m laser used in the experiment is measured with precision of 100 MHz by a wavemeter. To precisely measure the magic wavelength, shift and uncertainty due to the uncertainty of the angle between the magnetic field and the laser k-vector or the laser polarization is studied and evaluated. Figure 1 shows an example of the measured magic wavelength as a function of the angle between the magnetic field and the laser polarization.

After taking into amount of the systematic and the statistical uncertainties, the infrared magic wavelegnth is measured as 1056.37(9)nm, which is in good agreement with Ref. [3-5] but with much higher precision.

[1] A. Lambrecht et al, Nat. Photon. **11**, 704(2017).

[2] P. Liu et al, n Phys. Rev. Lett. **114**, 223001 (2015).

[3] J. Kaur et al, Phys. Rev. A **92**,031402 (2015).

[4] Y. Tang et al, Phys. Rev. A **87**, 042517(2013).

[5] J. Jiang et al, Phys. Rev. A **96**, 042503(2017)).

Progress towards deployable primary pressure sensors based on lithium magneto-optical traps

D. S. Barker[1], **E. B. Norrgard**[2], **J. Scherschligt**[1], **N. N. Klimov**[1], **J. A. Fedchak**[1], **and S. Eckel**[1]
[1] *Sensor Science Division, National Institute of Standards and Technology, Gaithersburg, MD 20899, USA*
[2] *Quantum Measurement Division, National Institute of Standards and Technology, Gaithersburg, MD 20899, USA*
e-mail: *daniel.barker@nist.gov*

Preparation and control of extreme-high-vacuum (XHV) environments, necessary for emerging technologies, has been hindered by the lack of primary pressure gauges. We present preliminary studies of pressure sensing with a lithium magneto-optical trap (MOT). The loss rate from the MOT is compared to semi-classical collision theory to extract the vacuum pressure. We discuss our efforts to miniaturize Li MOTs and vapor sources for deployable vacuum sensors. We have investigated two low-outgassing lithium vapor sources: a 3D-printed titanium dispenser and light-induced atomic desorption. Both vapor sources allow us to load MOTs with sufficient population for vacuum sensing while minimally increasing the background gas pressure. We also demonstrate a nanofabricated grating MOT with an integrated Zeeman slower. The grating MOT is capable of loading $> 10^6$ ^{7}Li atoms at a temperature $\approx$ 1 mK in less than 2 seconds. Our grating MOT design is easily adaptable to other elements that cannot be trapped from background vapor (*e.g.* strontium), allowing for a variety of devices and sensors based on laser-cooled atoms.

Onsite calibration of time and length standards for atom gravimeters

Xiao-Chun Duan[1], **Yao-Yao Xu**[1], **Jia-Feng Cui**[1], **Kun Qi**[1], **Min-Kang Zhou**[1], **and Zhong-Kun Hu**[1]

[1] *School of Physics, Huazhong University of Science and Technology, Wuhan 430074, China*
e-mail: *Email: zkhu@hust.edu.cn*

Time and length are two fundamental quantities for atom gravimeters, the combination of which makes up the unit of gravity, m/s^2. In atom gravimeters, the ruler for length measurement is defined by laser wavelength, and the time base for time measurements usually resorts to 10 MHz frequency standards. Here we present an onsite calibration of both laser absolute frequency and time base only relying on an atom gravimeter itself. The calibration utilizes transition lines of ^{87}Rb atoms as references, and takes advantage of cold atom free fall as well as developed techniques of evaluating hyperfine level shift within atom gravimeters.

Quantum logic spectroscopy with a $^{40}Ca^+$ / $^{27}Al^+$ mixed ion crystal

M. Guevara-Bertsch[1,2], M. Guggemos[1,2], D. Heinrich[1,2], O.A. Herrera-Sancho [3,4], R. Blatt [1,2] and C. Roos[1,2]

[1] Institut für Quantenoptik und Quanteninformation, Österreichische Akademie der Wissenschaften, Technikerstr. 21a, 6020 Innsbruck, Austria

[2] Institut für Experimentalphysik, Universität Innsbruck, Technikerstr. 25, 6020 Innsbruck, Austria

[3] Escuela de Física, Facultad de Ciencias, Universidad de Costa Rica, 2060 San Pedro, San José, Costa Rica

[4]Centro de Investigación en Ciencia e Ingeniería de Materiales, Universidad de Costa Rica, 2060 San Pedro, San José, Costa Rica

e-mail: *milena.guevara-bertsch@uibk.ac.at*

The search for more precise and accurate frequency standards has played a key role in the development of basic science, precision measurements and technical applications [1, 2]. Recently, with the inclusion of essential ingredients from quantum information science, by means of Quantum Logic Spectroscopy (QLS) [3], it is possible to perform high precision spectroscopy to atoms that lack suitable transitions for efficient laser cooling, internal state preparation, and detection. QLS consists of the combined implementation of an auxiliary "logic" ion, which is stored in a miniature linear radio-frequency trap, together with a "spectroscopy" ion. The "logic" ion is then used to cool down the initially hot "spectroscopy" ion via the Coulomb interaction and additionally allows the preparation and detection of the internal state of the "spectroscopy" ion.

Our research is focused on the implementation of QLS to perform optical spectroscopy of the Al^+ ion. A single $^{40}Ca^+$ ion ("logic" ion) and a single $^{27}Al^+$ ion ("spectroscopy" ion) are loaded by means of laser-ablation and trapped in a linear Paul trap. Due to the observation of long sympathetic cooling times before crystallization, we developed a new technique that allows us to detect the loading and cooling of an initially hot ion ("spectroscopy" ion)[4]. Through the monitoring of the motional state of the Doppler-cooled ion ("logic" ion) we are able to detect the presence of the hot ion ("spectroscopy" ion) in the trap and then to observe when the two-ion crystal of Ca^+ and Al^+ is finally cooled. Once the crystal is in its motional ground state by laser cooling the Ca^+ ion, we interrogate the "spectroscopy" ion and map its internal state onto the Ca^+ ion via the common vibrational state. Through the implementation of QLS, we have measured the $^{27}Al^+$ ($^1S_0$, F = 5/2) ($^3P_1$, F = 7/2) transition frequency with a preliminary value of 1 122 842 857 335(1) kHz [5].

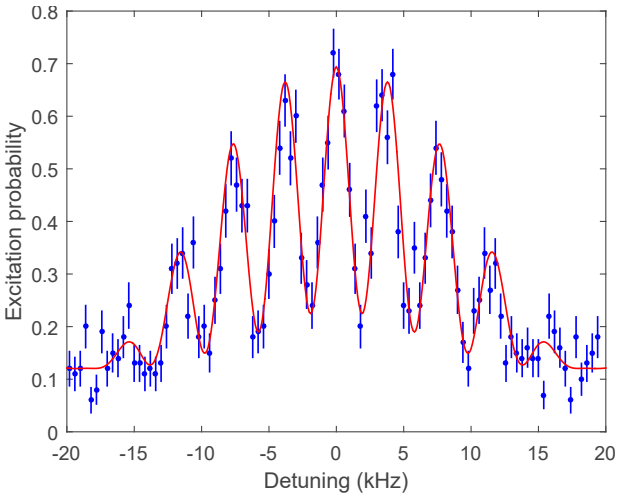


Figure 1: Ramsey experiment on the $^{27}Al^+$ $(3s^2)\,^1S_0, m_F = -5/2 \leftrightarrow (3s3p)\,^3P_1, F = 7/2, m_{F'} = -7/2$ carrier transition: measured excitation as a function of the laser detuning (blue points) for Ramsey pulses of 50 μs duration and waiting time of 200 μs. The data is fitted (solid line) by a numerical integration of the master equation describing the Ramsey experiment including spontaneous decay of the $^3P_1$ level, adjusted for a frequency offset, an excitation baseline and a reduction in contrast.

[1] C.W. Chou, D.B. Hume, J.C.J. Koelemeij, D.J. Wineland , and T. Rosenband ,Phys.Rev.Lett 104, 070802 (2010).

[2] C.W. Chou, D.B. Hume, T. Rosenband, and D.J. Wineland, Science 329, 1630 (2010).

[3] P.O. Schmidt, T. Rosenband, C. Langer, W.M. Itano, J.C. Bergquist and D.J. Wineland Science 309, 749 (2005).

[4] M. Guggemos, D. Heinrich, O.A. Herrera-Sancho, R. Blatt and C.F. Roos, New J. Phys. 17, 103001 (2015).

[5] M. Guggemos, M.Guevara-Bertsch, D. Heinrich, O.A. Herrera-Sancho, R. Blatt and C.F. Roos, to be published (2018).

Comparing Optical Clocks at 10^{-18} level

H. Leopardi[1,2], **J. Davila-Rodriguez**[2], **J. A. Sherman**[2], **F. Quinlan**[2], **S. Diddams**[1,2] **and T. Fortier**[2]

[1] *University of Colorado Boulder, Boulder, Colorado, USA*

[2] *National Institute of Standards and Technology, Boulder, Colorado, USA*

e-mail: *holly.leopardi@colorado.edu*

Optical transition frequencies are among the most precisely measured quantities in physics, providing up to 18-digits of precision and accuracy. Comparison of these state-of-the-art optical atomic clocks can enable fundamental tests of physics at tabletop scales and provides confirmation of the predicted accuracy and stability of the systems. Here we describe the results of current and ongoing atomic clock intercomparisons at NIST and JILA, involving the ^{171}Yb lattice clock [1], ^{87}Sr lattice clock [2] and ^{27}Al^{+} ion logic clock [3]. Because the comparison of these systems below the 10^{-17} level is non-trivial, we present results of the characterization of the measurement system, including the role and performance of the optical frequency comb (OFC) within the comparison.

To evaluate the performance of optical synthesis in our measurement campaign, we use two OFCs, an octave-spanning Ti:S laser [5] and a single-branch Er:fiber laser [6], and compare the agreement in the measurement of optical frequencies between the OFCs. From measurements performed over the course of six months we observe agreement of the Al^{+}/Yb ratio measured by the two OFCs at the mid 10^{-19} level. From the same measurements we observe a total instability at the mid 10^{-18} for the Al^{+}/Yb ratio.

Because ion clocks exhibit higher short term instability due to low atom number, statistical measurements at the 10^{-18} level require much greater than 100,000 seconds of averaging. To decrease this averaging time, we intend to use the technique of coherent spectroscopy to compare optical clocks [4]. By coherently distributing a single high-stability clock laser via an OFC amongst multiple clocks, the noise contribution from the clock lasers should be eliminated, allowing for extended probe times and enabling clock comparisons at the quantum projection noise limit [1, 4]. With this in mind, we evaluate the limitations imposed by the OFC by comparing the residual phase between the OFCs in the measurement setup shown in Figure 1. The results of this measurement, shown in Figure 2 as the blue curve, give a modified Allan deviation of 1x10^{-17} at 1 second. From this result we demonstrate that the OFCs can support phase transfer at the levels required by a coherent clock probe protocol. The results of this investigation will be included along with the results of OFC agreement for the current clock comparison campaign.

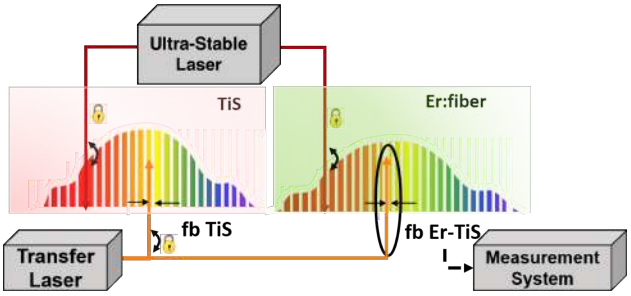


Figure 1: Residual phase measurement setup between Er:fiber and Ti:S optical frequency combs. Both combs are locked to the same optical reference cavity. A transfer laser is stabilized to one comb and the phase between the transfer laser and the second comb is measured.

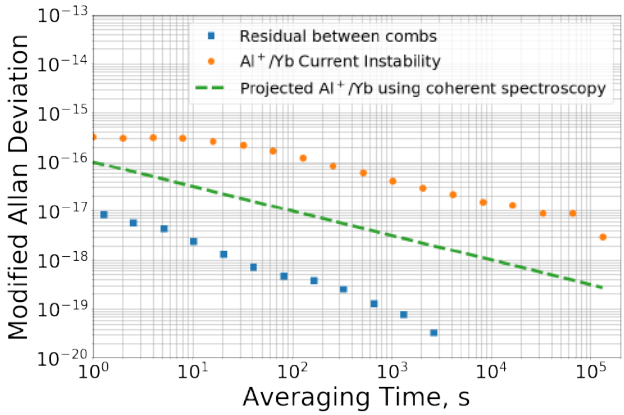


Figure 2: Stability of Al^{+}/Yb ratio for total measurement campaign at NIST is shown in orange circles. The green dashed curve shows the projected improvement in stability enabled by coherent spectroscopy [4]. The blue squares represent the residual stability between the two optical frequency combs from the residual phase measurement shown in Figure 1.

[1] M. Schioppo, et. al., Nature Photonics 11.1 (2017).

[2] B. J. Bloom, et. al., Nature 506, 7486 (2014).

[3] T. Rosenband, et. al., Science 319, 5871 (2008).

[4] D. B. Hume, et. al., Phys. Rev. A, 93, 032138 (2016)

[5] T. M. Fortier, et al, Optics Letters 31.7 (2006).

[6] H. Leopardi, et al, Optica, 4.8, (2017).

Transportable optical lattice clock – measurement campaigns and characterisation

J. Grotti[1], S. B. Koller[1], St. Vogt[1], S. Herbers[1], S. Häfner[1], U. Sterr[1], A. Al-Masoudi[1], S. Dörscher[1], R. Schwarz[1], Ch. Lisdat[1], A. Kuhl[1], S. Koke[1], T. Waterholter[1], G. Grosche[1], E. Benkler[1], M. Pizzocaro[2], P. Thoumany[2], B. Rauf[2], F. Bregolin[2], A. Tampellini[2,3], P. Barbieri[2,3], M. Zucco[2], G. A. Constanzo[2,3], C. Clivati[2], F. Levi[2], A. Mura[2], D. Calonico[2], F. Baynes[3], A. Rolland[3], H. S. Margolis[3], M. Zampaolo[4], R. Le Targat[5], H. Álvares Martínez[6,7], J. Lodewyck[6], A. Amy-Klein[7], O. Lopez[7], E. Cantin[6,7], P.-E. Pottie[6], Ch. Voigt[9,10], L. Timmen[9], H. Denker[9]

[1] *Abteilung 4.3, PTB, 38116 Braunschweig, Germany*; [2] *Tempo e Frequenza, INRiM, 10135 Torino, Italy*; [3] *Dipartimento di Elettronica e Telecomunicazioni, Politecnico di Torino, 10129 Torino, Italy*; [4] *Time & Frequency, NPL, Teddington, TW110 LW Middlesex, UK*; [5] *LSM, 73500 Modane France*; [6] *LNE-SYRTE, Observatoire de Paris, Université PSL, CNRS, Paris, France*; [7] *Sección de Hora, ROA, San Fernando, Spain*; [8] *LPL, Université de Paris 13, CNRS, Villetaneuse, France*; [9] *IfE, 20167 Hannover, Germany*; [10] *GFZ, 14473 Potsdam, Germany*

e-mail: *silvio.koller@ptb.de*

The superior accuracy [1, 2, 3] and stability of optical clocks [4], and the technological capability to make them transportable [5, 6, 7] allows for several applications: By exploiting the gravitational redshift the comparison of two clocks connected via fiber link can measure the potential difference over a few 1000 km distance. This is advantageous over satellite measurements which average over several 10^4 km^2 and over spirit leveling, which is a quasi-differential technique based on horizontal lines of sight with target distances of 30 m to 50 m per setup. In addition to laboratory clocks, a transportable optical clock (TOC) allows to eliminate potentially undetected systematic errors of laboratory clocks with a local comparison and to choose arbitrary locations.

Since time and frequency are the most accurate physical units realized, a transportable optical lattice clock makes them available to any laboratory for precision measurements e.g. in fundamental physics.

The comparison of clocks is an important step towards a redefinition of the second. With telecom fibres and suitable amplifier techniques the accuracy and stability can be disseminated over a few 1000 km [8, 9, 10]. However, they are not able to bridge intercontinental distances and comparisons via satellites are not stable enough. A TOC solves this problem.

We present two campaigns with the PTB TOC. In a first proof-of-principle test for relativistic geodesy and frequency metrology with a TOC [11] we show the feasibility of such measurements at a remote site, LSM in the Fréjus tunnel in the French alps, that is connected with an optical fiber link [12] to the Cs fountain and the Yb clock at INRiM in Torino, Italy. We then moved the TOC to INRiM to compare directly with the Cs-fountain and the Yb clock. The potential difference of 10038(174) m^{2}s^{-2} derived from the clock comparison and using the gravitational redshift formula confirmed the potential difference measured with classical geodetic means. The uncertainty corresponds to about 20 m in height difference, limited by statistics due to the limited up times of the TOC at the time and the usage of a Cs-fountain.
Via the Paris-Braunschweig fibre link [9, 10] connecting the TOC and the stationary clock at PTB we confirmed the height difference between the two cites to 35 cm accuracy in 8000 s averaging time due to the much longer up times and a TOC characterized at 2×10^{-17} during this campaign by reducing the uncertainties of the lattice light and density shift.

[1] N. Huntemann et al., Phys. Rev. Lett. **116**, 063001 (2016).

[2] I. Ushijiama et al., Nat. Phot. **9**, 185–189 (2015).

[3] T. Nicholson et al., Nat. Comm. **6**, 6869 (2015).

[4] M. Schioppo et al., Nat. Phot. **11**, 48–52 (2017).

[5] S. B. Koller et al., Phys. Rev. Lett. **118**, 073601 (2017).

[6] J. Cao et al., Appl. Phys. B **123**,112 (2017).

[7] K. Bongs et al., C. R. Phys. **16**, 553-564 (2015).

[8] K. Predehl et al., Science **336**, 6080 (2012).

[9] S. Raupach et al., Phys. Rev. A **92** 021801(R) (2015)

[10] Ch. Lisdat et al., Nat. Com. **7**, 12443 (2016).

[11] J. Grotti et al., Nat. Phys. **14**, 437-441 (2018).

[12] D. Calonico et al., Appl. Phys. B **117**, 979 (2014).

Spin Squeezing of an Atomic Ensemble with 10^{11} Atoms

Han Bao[1], **Xingda Lu**[1], **Heng Shen**[2], **and Yanhong Xiao**[1]

[1] *Department of Physics, State Key Laboratory of Surface Physics, Key Laboratory of Micro and Nano Photonic Structures(Ministry of Education),Fudan University, 200433 Shanghai, China*

[2] *Clarendon Laboratory, University of Oxford, Parks Road, Oxford, OX1 3PU, UK*

e-mail: *13110190055@fudan.edu.cn*

Atomic ensembles with large atom number N are desirable in precision measurement, since the minimal measurable quantity is proportional to $1/\sqrt{N}$ at the standard quantum limit given by atom projection noise. Surpassing this limit through spin squeezing is an important goal in metrology. However, spin squeezing for larger N is challenging mainly because of the more demanding requirement on the signal to noise ratio of the measurement. So far, most spin squeezing experiments have been performed in cold atom systems where N ranges from 10^3 to 10^6 [1], and the only experiment with warm atoms has 10^8 atoms confined in a room temperature microcell[2] within an optical cavity to enhance the atom-light coupling. Here we report experimental realization of spin squeezing in a ^{87}Rb vapor cell containing 10^{11} atoms in free space. 1.07 ± 0.14 dB conditional spin squeezing has been observed in a 25 mm $\times$ 7 mm $\times$ 7 mm cubic vapor cell at 60°C, representing the largest spin squeezed state so far.

The atoms are first pumped to a coherent spin state (CSS) $|5S, F = 2, m_F = 2\rangle$ by circularly polarized on-resonant D1 pump laser and D2 repump laser propagating along the x-direction, along which a magnetic field is applied to retain the classical spin under residual ambient magnetic field inside the magnetic shield. The degree of atomic polarization was measured to be about 97% by a quadratic Zeeman effect[2]. A linearly x-polarized far off-resonant D2 probe laser was sent along the z-direction to measure and squeeze the z-component of the collective atomic spin J_z. This far off-resonance interaction Hamiltonian is

$$H = \alpha \widehat{J}_z \widehat{S}_z. \tag{1}$$

Here $\widehat{S}_z$ is the z-component of the optical Stokes operator, corresponding to the photon number difference in σ_+ and σ_- polarization of the probe light, and α describes the interaction strength. Since $\widehat{J}_z$ commutes with the Hamiltonian, it remains unchanged during the interaction, forming a quantum non-demolition (QND) measurement.

The magnetic field causes the spin to rotate around x, hence we need to detect $\widehat{J}_z$ stroboscopically to avoid back-action by using a pulsed probe beam at twice the Larmor frequency and with a small occupation ratio of 15%. For our atomic system of a relatively large physical size, achieving a spatially uniform spin state and coupling strength across the entire cell volume is the key of the experiment, even though motional averaging of atoms in the paraffin coated cell can reduce the inhomogeneity. Residual inhomogeneity, such as the imperfect parallelism of the wave vector of the pump laser and the magnetic field can give rise to a finite classical spin component along z, which can easily dominate over atom projection noise especially for large N since the former is proportional to N and the latter to $\sqrt{N}$. To facilitate the alignment, we modulated the pump laser at Larmor frequency to amplify the signal from this classical spin by more than 1000 times, which has greatly improved parallelism and made it possible to observe the atom projection noise. Currently, the limiting factors for the degree of squeezing are mainly the small optical depth and the spontaneous decay process due to the probe. We found that the atomic spin relaxation rate increases with the laser power of the probe beam, which accounts for the trend shown in Fig. 1. Ways to effectively enhance the optical depth will be studied, and unconditional spin squeezing mechanisms will also be explored.

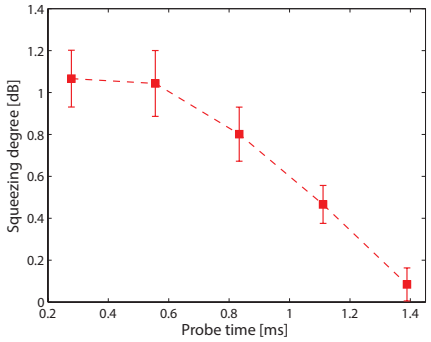


Figure 1: Squeezing coefficient for different probe time. Error bar is acquired from 10 identical measurements.

[1] L. Pezzé, A. Smerzi, M. K. Oberthaler, R. Schmied, P. Treutlein, arXiv:1609.01609.

[2] G. Vasilakis, H. Shen, K. Jensen, M. Balabas, D. Salart, B. Chen, and E. S. Polzik, Nat. Phys. **11**, 389 (2015).

Micro-integrated extended cavity diode laser with integrated optical amplifier for precision spectroscopy in space

Christian Kürbis[1], **Ahmad Bawamia**[1], **Robert Smol**[1], **Andreas Wicht**[1], **Achim Peters**[1,2], and **Günther Tränkle**[1]

[1] *Ferdinand-Braun-Institut, Leibniz-Institut für Höchstfrequenztechnik, Gustav-Kirchhoff-Str. 4, 12489 Berlin, Germany*

[2] *Institut für Physik, Humboldt-Universität zu Berlin, Newtonstr. 15, 12489 Berlin, Germany*

e-mail: *Christian.Kuerbis@fbh-berlin.de*

GaAs diode laser-based hybrid micro-integration technology meets the demand for precision spectroscopy applications in space for compact, robust, and energy-efficient laser modules. It supports applications at wavelengths ranging from 630 nm to 1200 nm and is already used for quantum optics experiments in space [1],[2].

Here, we present a narrow linewidth, high power extended cavity diode laser (ECDL) master oscillator power amplifier (MOPA) laser module (see figure 1) for operation as local oscillator of an iodine-based frequency reference on board a sounding rocket. The laser module is based on a versatile technology platform which facilitates integration of any two chips, either active (e.g. laser, amplifier) or passive (e.g. phase modulator) in a single laser module. The module utilizes a micro-optical bench (MioB) consisting of structured aluminium nitride substrates which are encapsulated into a hermetically sealed Kovar housing. The MioB accommodates an ECDL, a tilted ridge-waveguide PA chip, electronics, and fiber coupling assembly to couple light into a single mode, polarization maintaining optical fiber. The footprint of the MioB is $80 \times 30\,\mathrm{mm}^2$. The cavity of the ECDL is formed by a volume holographic Bragg grating (VHBG) and the front facet of a ridge-waveguide laser chip. The main output of the ECDL is collimated by micro-optical lenses, passed through a micro-optical isolator, and injected into the PA chip by micro-optical lenses. The output of the PA chip is collimated by an aspheric lens, passed through a thin film polarizer and coupled into a single mode, polarization maintaining optical fiber. The laser module features a mass of 750 g, and its form factor corresponds to $125 \times 75 \times 22.5\,\mathrm{mm}^2$. The ECDL-MOPA emits 570 mW of optical power ex fiber at a frequency of 281,630 GHz at a MioB temperature of 27.7 °C, a VHBG temperature of 25.0 °C, a MO injection current of 97.0 mA and a PA injection current of 1500 mA. The ECDL can be continuously frequency-tuned by sweeping of the injection current with a sensitivity of 74 MHz/mA. The continuous tuning range is limited by the free spectral range of the laser. Coarse tuning is provided by thermal tuning of the VHBG at 2.8 GHz/K. The spectral stability of the laser was determined by creating a beat note spectrum through a self-delayed heterodyne interferometer. To derive the frequency noise spectrum the beat note signal was analyzed according to [4]. At the working point specified above the linewidth was estimated to 26 kHz (FWHM, 1 ms) via the beta-separation line method [3]. The Lorentzian FWHM linewidth derived from the white noise floor of the frequency noise power spectrum was determined to be as small as 584 Hz. The side mode suppression ratio (SMSR) exceeds 45 dB.

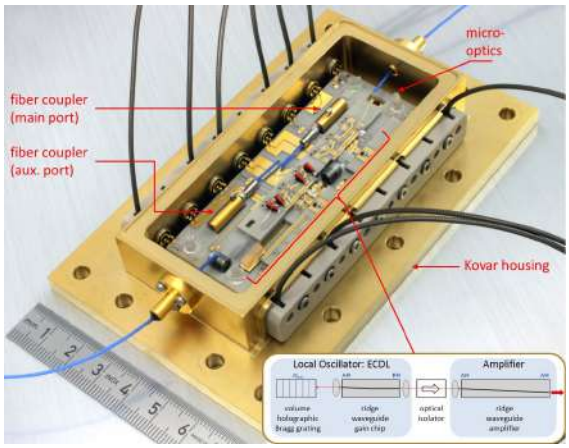


Figure 1: Photograph of the micro-integrated ECDL-MOPA

[1] Aline N. Dinkelacker *et al.*, "Autonomous frequency stabilization of two extended cavity diode lasers at the potassium wavelength on a sounding rocket," Appl. Opt **56**, 1388-1396 (2017)

[2] V. Schkolnik *et al.*, "A compact and robust diode laser system for atom interferometry on a sounding rocket," Appl. Phys. **122**:217 (2016)

[3] Gianni Di Domenico *et al.*, "Simple approach to the relation between laser frequency noise and laser line shape," Appl. Opt. **49**, 4801-4807 (2010).

[4] M. Schiemangk *et al.*, "Accurate frequency noise measurement of free-running lasers," Appl. Opt. **53**, 7138-7143 (2014).

Quantum metrology of displacements with diffusion: single photon recoil spectroscopy

M. Schulte[1], N. Lörch[2], P.O. Schmidt[3,4] and K. Hammerer[1]

[1] *Institute for Theoretical Physics and Institute for Gravitational Physics (Albert-Einstein-Institute), Leibniz University Hannover, Appelstrasse 2, 30167 Hannover, Germany*

[2] *Department of Physics, University of Basel, Klingelbergstrasse 82, CH-4056 Basel, Switzerland*

[3] *QUEST Institut, Physikalisch-Technische Bundesanstalt, 38116 Braunschweig, Germany*

[4] *Institute for Quantum Optics, Leibniz University Hannover, Welfengarten 1, 30167 Hannover, Germany*

e-mail: *marius.schulte@itp.uni-hannover.de*

This work studies quantum metrology in a continuous variable system when the relevant dynamics can be described by drift and diffusion in phase space. In our setup [1] we investigate the estimation of a parameter which is contained in the rate at which a state is displaced in position or momentum, i. e. the drift rate in phase space. Including effects which lead to a diffusion of the phase space distribution serves as a more general case compared to an ideal unitary dynamic. Such an additional diffusive noise process leads to decreased precision with which the parameter can be estimated and a main result of our work evaluates this loss of sensitivity in force measurements for different initial states. More specifically, we study how this transition away from unitary displacements affects squeezed states and Schrödinger cat states which were identified theoretically to enhance the sensitivity in the case without diffusion [2, 3]. This quantum enhancement has been explored experimentally for instance with single trapped ions using Schrödinger cat states [5] or Fock states, i. e. phonon number states [6]. The latter demonstrated an enhancement in both amplitude and phase measurements with the same state but with nearly unitary dynamics.

Recoil spectroscopy in ion traps [4] on the other hand is discussed as an example application where the contribution of the diffusion may not be negligible. For this, a theoretical model describing the dynamics of the ion's motional state under laser spectroscopy gives rise to a Fokker-Planck equation for phase space distributions where the relevant drift and diffusion coefficients can be evaluated based on the spectroscopy parameters. The initial quantum metrology study is then used in order to examine the enhancement possibilities in recoil sensitivity for spectroscopy with squeezed states, Schrödinger cat states and Fock states under drift and diffusion. Furthermore, limitations to the sensitivity based on imperfect state preparation or measurements are discussed and compared to the maximally attainable sensitivity based on quantum Fisher information. A further result for photon recoil spectroscopy predicts Doppler effects that lead to systematic shifts in the observed resonance frequency.

References

[1] M. Schulte, et al., *Quantum metrology of displacements with diffusion: single photon recoil spectroscopy*, in preparation

[2] M. D. Lang and C. M. Caves, *Optimal Quantum-Enhanced Interferometry Using a Laser Power Source*, Phys. Rev. Lett. **111**, 173601 (2013).

[3] F. Toscano, et al., *Sub-Planck phase-space structures and Heisenberg-limited measurements*, Phys. Rev. A **73**, 023803 (2006).

[4] Y. Wan, et al., *Precision spectroscopy by photon-recoil signal amplification*, Nat. Commun. 5:3096 (2014)

[5] C. Hempel, et al., *Entanglement-enhanced detection of single-photon scattering events*, Nature Photonics, 7:630633, (2013)

[6] F. Wolf, et al., *Fock state interferometry with trapped ions for quantum- enhanced amplitude and phase measurements*, in preparation

Progress on a compact Yb^+ optical clock

M. Delehaye, L. Groult, B. Achi, M. Souidi, J. Millo, P.-Y. Bourgeois, Y. Kersalé, and C. Lacroûte

FEMTO-ST Institute - CNRS - ENSMM - UBFC, 25030 Besançon, France

e-mail: *clement.lacroute@femto-st.fr*

We report on the ongoing realization of a compact optical $^{171}Yb^+$ clock on a chip. The targeted fractional frequency stability is $10^{-14}\tau^{-1/2}$ for a total volume of less than 500 L, including vacuum cell, optics and electronics. It will be part of the growing European optical clock network, that already triggers new applications in a large variety of domains, ranging from relativistic geodesy to fundamental science [1, 2].

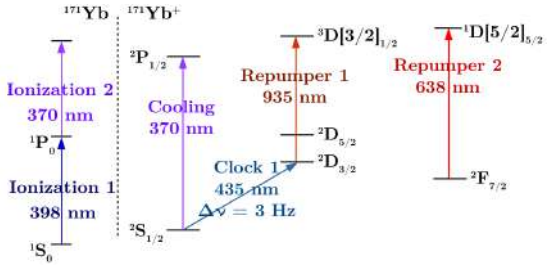


Figure 1: Relevant atomic levels of ^{171}Yb and $^{171}Yb^+$.

Four lasers at 370, 398, 638 and 935 nm are needed for ionization, cooling and repumping, see Fig. 1. They are frequency controlled using a commercial wavelength meter with an accuracy of 60 MHz and a frequency drift of 20 MHz/day [3]. The quadrupole clock transition of $^{171}Yb^+$ at 435.5 nm will be excited using a frequency-doubled laser diode at 871 nm. We have characterized the phase noise induced by the second harmonic generation modules with a Mach-Zehnder interferometer and observed a relative phase noise as low as $40\,\mathrm{dBrad^2/Hz}$ at 1 Hz, which makes them compatible with the best up-to-date optical clocks and ultra-stable cavities [4]. The compact reference cavity at 871 nm will be based on an existing design.

Experiment control is essentially made with compact home-built digital electronics.

The ion trap is based on a surface-electrode linear Paul trap. It follows the "five wires" design and microfabrication techniques that have been primarily developed and used by the quantum information community [5]. It relies on two planar RF electrodes driven at 5.8 MHz and 190 V that generate a linear Paul trap of 300 meV depth and harmonic trapping frequencies of 360 kHz radially and 100 kHz axially. The ions are trapped 500 µm from the surface. The current chip is $30 \times 60\,\mathrm{mm^2}$ large and has a mini-SD connector in order to allow fast plug-and-play replacements, see Fig. 2. It is now a PCB board,

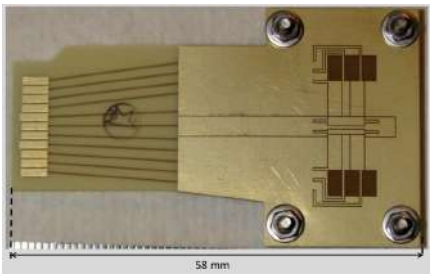


Figure 2: Photograph of the chip. It is driven at 5.8 MHz and 190 V to generate a linear Paul trap with 300 meV depth.

but the next version will take advantage of standard cleanroom microfabrication techniques.

We will present the first characterization of our trap, including including ion temperature, lifetime and heating rate measurements.

[1] C. Lisdat et al., Nat. Comm. **7**, 12443 (2016)

[2] F. Riehle, Nat. Phot. **11**, 1 (2017)

[3] K. Saleh et al., App. Opt **54**, 32 (2015)

[4] M. Delehaye et al., IEEE PTL **29**, 19 (2017)

[5] S. Seidelin et al., Phys. Rev. Lett. **96**, 25 (2006)

Explore cesium nuclear magnetic octupole moment with electronic $6S_{1/2} \rightarrow 6D_{3/2}$ hyperfine transitions

W.-Y. Cheng, T. –J. Chen, J. –E. Chen and H. –H. Yu

Department of Physics, National Central University, 32001, Taiwan

e-mail: *wycheng@ncu.edu.tw*

Cesium hyperfine structure was once resolved with a record resolution to the influence of nuclear magnetic octupole moment via $6P_{3/2}$ hyperfine spectrum [1] and by using an atomic beam. However, the deduced hyperfine constant contributed by the nuclear magnetic octupole interaction did not agree with what was calculated by nuclear shell model [1], that is, differ by a fact of 40. Therefore, it would be very interesting to verify whether the shell model is valid for cesium. We present in this conference the second determination [2] of the hyperfine constant of the magnetic octupole interaction by totally different approach from reference [1]. We compared the unperturbed, $6S_{1/2} \rightarrow 6D_{3/2}$ Doppler-free two-photon spectra simultaneously with two laser systems. Our optical layout efficiently moves out the residual Doppler background since a new scheme of the "crossover" in two-photon interfered spectrum was employed [3], as shown in Fig. 1. An update of the related hyperfine constants is listed in Table 1.

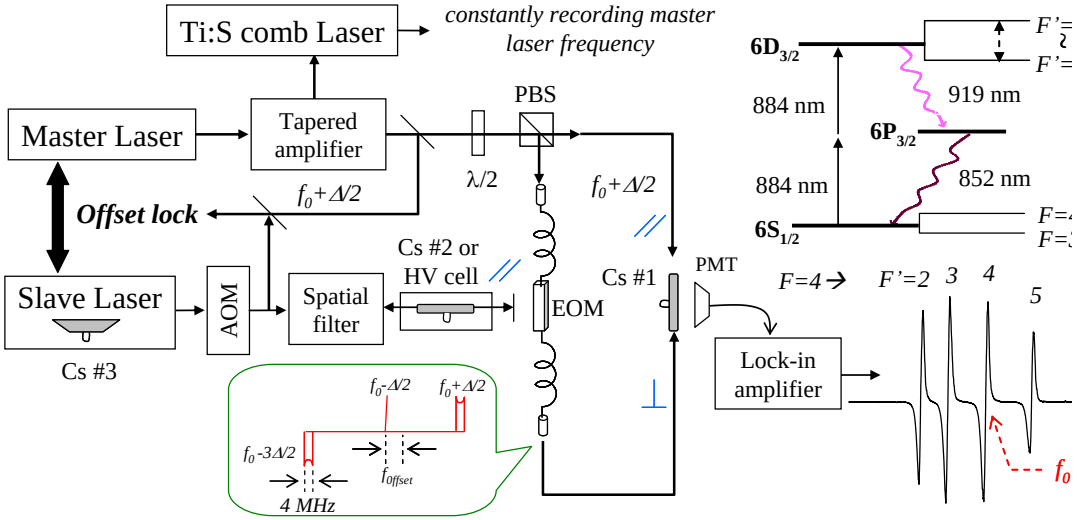


Table 1: hyperfine intervals and constants at Cs $6D_{3/2}$ level*

	$(f_{45}-f_{44})*2$	$(f_{44}-f_{43})*2$	$(f_{43}-f_{42})*2$	A (MHz)	B (MHz)	C (kHz)
This work	81.615 (30)	65.335 (14)	49.164 (24)	16.338 (3)	-0.136 (24)	4.3 (10)
A. Kortyna	81.8 (1)	65.1 (2)	49.0 (1)	16.34 (3)	-0.1 (2)	0.11 (127)
T. Ohtsuka	81.15 (84)	64.18 (51)	48.76 (64)	16.17 (17)		

*obtained via Cs #3 system, see Fig. 1.

[1] V. Gerginov, A. Derevianko and C. E. Tanner, "Observation of the nuclear magnetic octupole moment of ^{133}Cs", Phys. Rev. Lett. **91**, 072501 (2003)

[2] T. -Ju Chen, J. –E. Chen, H. –H. Yu, T. –W. Liu, Y. –F. Hsiao, Y. –C. Chen, M. –S. Chang and W. –Y. Cheng, "Absolute frequency of cesium $6S_{1/2}$-$6D_{3/2}$ hyperfine transition with resolution to nuclear magnetic octupole interaction", Opt. Lett **28**, 1954 (2018)

[3] C. -M. Wu, T. –W. Liu and W. –Y. Cheng, "Quantum interference in two-photon spectroscopy for laser stabilization and cesium cell comparisons", Phys. Rev. A **92**,042504 (2015).

Remote and local comparisons of optical atomic clocks for geodesy and metrology

F. Bregolin[6,7], J. Grotti[1], S. Koller[1], S. Vogt[1], S. Häfner[1], U. Sterr[1], C. Lisdat[1], H. Denker[2], C. Voigt[2,3], L. Timmen[2], A. Rolland[4], F. N. Baynes[4], H. S. Margolis[4], M. Zampaolo[5], P. Thoumany[6], M. Pizzocaro[6], B. Rauf[6,7], A. Tampellini[6,7], P. Barbieri[6,7], M. Zucco[6], G. A. Costanzo[6,7], C. Clivati[6], F. Levi[6] and D. Calonico[6],

[1] *Physikalisch-Technische Bundesanstalt, 38116 Braunschweig, Germany*

[2] *Institut für Erdmessung, Leibniz Universität Hannover, 20167 Hannover, Germany*

[3] *GFZ German Research Centre for Geosciences, 14473 Potsdam, Germany*

[4] *National Physical Laboratory, Teddington, Middlesex, TW11 0LW, UK*

[5] *Laboratoire Souterrain de Modane, Carré Sciences, 70500 Modane, France*

[6] *Istituto Nazionale di Ricerca Metrologica (INRIM), 10135 Torino, Italy*

[7] *Politecnico di Torino, 10129 Torino, Italy*

e-mail: *f.bregolin@inrim.it*

Optical lattice clocks have demonstrated accuracies of a few parts in 10^{18} [1, 2] and instabilities at the $10^{-16}\sqrt{\tau/\mathrm{s}}$ level [3]. These results, together with the demonstration of low noise fibre link networks [4], enable local and remote clock comparisons in the 10^{-18} fractional uncertainty regime. Frequency measurements at these levels of accuracy foster the interest towards the redefinition of the SI second on an optical transition, and opened the way for a novel approach to tackle physical and technological challenges. For example, geodetic measurements and tests of relativity can now be performed using optical clocks exploiting the relativistic redshift effect in gravitational fields with a resolution able to challenge traditional methods.

Within the European project ITOC [5] we performed a local frequency comparison between the PTB Sr transportable lattice clock [6] and the stationary INRIM Yb lattice clock [7]. The frequency ratio was evaluated with an accuracy of 3.4×10^{-16} [8], limited by the clock accuracies evaluated during the campaign to be 1.8×10^{-16} and 1.6×10^{-16} respectively. The Yb/Sr ratio is to our knowledge the only direct optical frequency ratio measured by three independent research groups. This result thus provides a significant contribution to the generation of an internationally consistent clock frequency value to be considered as a candidate for the redefinition of the unit of time.

Optical clocks at the mentioned levels of accuracies are already able to be exploited in geodetic experiments, as they can resolve an elevation difference of few metres. As a proof of principle we performed a remote frequency comparison between the Sr transportable clock located at the LSM laboratory in Modane (France) and the INRIM Cs primary standard, used as reference, in Torino (Italy). The two sites are connected by a 150 km multiplexed fibre link for optical frequency transfer with a residual instability of 3×10^{-19} in a few hours of measurement, well below the Sr and Cs clock accuracies. The comparison was possible thanks to the NPL transportable frequency comb, which measured the Sr optical clock frequency against the link transfer laser. Taking a second local measurement of the Sr absolute frequency in INRIM we could evaluate the difference in gravity potential between the two sites with an uncertainty not limited by the prior knowledge of the Sr absolute frequency [8]. Our chronometric levelling agrees with measurements we performed using traditional geodetic means.

Improvements in the Yb and Sr clock performances are underway, and recent results already show a better accuracy and reliability towards more accurate metrological and geodetic measurements.

[1] T. Nicholson et al., Nat. Commun. **6**, 6896 (2015).

[2] I. Ushijima, M. Takamoto, M. Das, T. Ohkubo, and H. Katori, Nat. Photonics **9**, 185 (2015).

[3] M. Schioppo et al., Nat. Photonics **11**, 48 (2017).

[4] D. Calonico et al., Appl. Phys. B **117**, 979 (2014).

[5] *International Timescales with Optical Clocks*, projects.npl.co.uk/itoc.

[6] S. Koller et al., Phys. Rev. Lett. **118**, 073601 (2017).

[7] M. Pizzocaro et al., Metrologia **54**, 102 (2017).

[8] J. Grotti et al., Nat. Phys. **14**, 437 (2018).

The system of intra-object transmission of the strontium optical clock frequency to the primary standard of units of time, frequency and the national time scale

D. V. Sutyrin[1], **A. Yu. Gribov**[1,2], **O. I. Berdasov**[1,2], **S. A. Strelkin**[1,2], **R.I. Balaev**[1], **G.S. Belotelov**[1], **A.S. Kostin**[1], **D. M. Fedorova**[1,2], **A. N. Malimon**[1], **and S.N. Slyusarev**[1]

[1] *FSUE "VNIIFTRI", Mendeleevo, 141570 Moscow region, Solnechnogorskii district, Russian Federation*

[2] *National Nuclear Research University 'MEPhI', Kashirskoe sh. 31, 123182 Moscow, Russian Federation*

e-mail: *sutyrin@vniiftri.ru*

An accurate realization of time scales plays an important role in many modern technologies such as global navigations and telecommunications network synchronization. The current determination of a SI second is based on the frequency between the two hyperfine levels of the ground state in the ^{133}Cs atom. Optical frequency standards (OFS) have superb frequency instability and accuracy comparing to microwave primary frequency standards, so that it is an attractive option to integrate them into International Atomic Time (TAI) and to Coordinated Universal Time (UTC) [1].

As a start step in this direction, developing of "optically steered" time scales in national metrology institutes is performing [2]. We are developing a system to use ^{87}Sr OFS for the Russian National Time Scale UTC(SU) at FSUE "VNIIFTRI". In substance, there are two parts of work. The first part is focused on the increasing autonomic continues work operation of OFS [3], which is now compatible with other groups [4]. The second part, which we describe here, is a system for 1.5 km intra-object transferring the frequency of the VNIIFTRI strontium OFS to the primary time and frequency standard and the national time scale. It is necessary for long-term comparisons between optical clock, rubidium and cesium fountains and an ensemble of clocks based on hydrogen masers. The developed system, on the one hand, allows to determine the absolute frequency of the optical clock, and on the other - to determine the drift of the hydrogen timekeepers, which allows more accurately reproduce the size of the units of time and frequency and more accurately realize the national time scale.

References

[1] P. Gill, "When should we change the redefinition of the second?" Phil.Trans. Roy. Soc. London, vol. A369, pp. 4109–4130, October 2011.

[2] H. Hachisu, F. Nakagawa, Y. Hanado and T. Ido. (2018). Months-long real-time generation of a time scale based on an optical clock. Scientific reports, 8(1), 4243.

[3] O.I. Berdasov, D.V. Sutyrin, S.A. Strelkin, A. Yu. Gribov, G.S. Belotelov, A.S. Kostin, N.N. Kolachevsky, S.N. Slyusarev, "On the duration of continuous operation of the optical frequency standard on strontium atoms", QUANTUM ELECTRON, 2018, 48 (5), 431–437.

[4] J. Lodewyck et al. Optical to microwave clock frequency ratios with a nearly continuous strontium optical lattice clock, Metrologia .-2016.-T.53.-N.4.-C.1123.

Development of optical clock modules for the creation of a portable optical frequency clock on ytterbium atoms

G.S. Belotelov[1], **D.V. Sutyrin**[1], **and S.N. Slyusarev**[1]

[1] *FSUE "VNIIFTRI", Mendeleevo, 141570 Moscow region, Solnechnogorskii district, Russian Federation*

e-mail: *gleb.belotelov@gmail.com*

The achieved level of optical frequency standards accuracy and stability lead to provide more stringent test of fundamental physical principles and high accuracy measurements of gravitational potential. However, it requires high performance of optical frequency standards with precision calibration (for example, a fractional frequency accuracy of 10^{-17} corresponds to a resolution of about 10 cm in height), which were demonstrated in few labs. Development of transportable optical frequency standards not only increases the flexibility in measurement but reduce the risk of undetected errors through local calibrations [1], [2].

Here we present the transportable and portable ytterbium lattice optical frequency clocks modules, which are developing at FSUE "VNIIFTRI". The work goal is to improve properties of optical clocks such as compactness, mass, power efficiency with preservation of typical for stationary optical clocks high relative frequency stability and accuracy level [3] and long-term continuous operation [4]. We discuss physical principles and design solutions for the implementation of systems with the required characteristics. In particular, we present our step on way of the portable distribution breadboard for first and second stage magneto-optical trap (MOT), compact vacuum chamber and new ceramics atomic oven development. For the portable optical clock version, we use FEM methods to test the idea of mini MOT with 1 cooling beam instead of 6 beam from the classical MOT [5]. The compactness coefficient is calculated for transportable and portable optical clocks with respect to the stationary system. For example, volume of system changed in 10 times in transportable variant and in 20 times in portable. Power consumption changed in two times and size of laser cooling systems in 2000 times for the transportable version.

The results of the developments will serve as a basis for transportable optical frequency standards and for on-board precision navigation systems based on optical frequency standard.

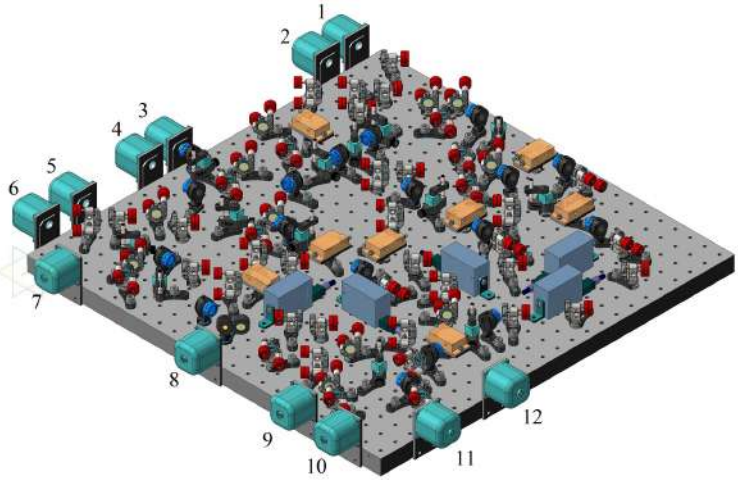


Figure 1: Portable distribution breadboard for first and second stage cooling. Size 60 x 60 cm. Colimators: 1 – frequency stabilisation output 556 nm , 2 – frequency stabilisation output 399 nm, 3 – input 556 nm, 4 – input 399 nm, 5, 6, 7 – output MOT 556+399 nm, 8 – output MOT 1 beam 556+399 nm, 9, 11 – output 2-D MOT 399 nm, 10 – detection output 399 nm, 12 – output Zeeman slower 399 nm.

[1] J. Grotti, et al., Geodesy and metrology with a transportable optical clock. arXiv preprint arXiv:1705.04089. (2017).

[2] N. Poli, et al., A transportable strontium optical lattice clock, arXiv:1409.4572v2 physics.atom-ph (17 Sep 2014).

[3] B. J. Bloom, et al.,An optical lattice clock with accuracy and stability at the 1e-18 level. Nature, 506(7486), 71. (2014).

[4] O.I. Berdasov, et al., "On the duration of continuous operation of the optical frequency standard on strontium atoms", QUANTUM ELECTRON, 48 (5), 431–437, (2018).

[5] Wei He, Towards Miniaturized Strontium Optical Lattice Clock, PhD Thesis, The University of Birmingham.

Cryogenic multi-path cavity made of monocrystalline silicon

P. Morzyński[1,2], H. Hachisu[1], H. Ishijima[1] and T. Ido[1]

[1] *Space-Time Standards Laboratory, National Institute of Information and Communications Technology, 4-2-1 Nukui-kitamachi, Koganei, Tokyo, 184-8795, Japan*

[2] *International Research Fellow of Japan Society for the Promotion of Science*

e-mail: *pmorzynski@nict.go.jp*

We report on the construction of the cryogenic multi-path cavity made of monocrystalline silicon operating at a temperature of 17 K. The football shape spacer made of monocrystalline silicon supports four Fabry-Perot resonators with a length of 10 cm and longitudinal axes oriented in vertical position. To investigate aging properites of mirros coating we apply both Ta_2O_5/SiO_2 in three cavities and TiO_2/SiO_2 in another one cavity as a material of high-reflectivity dielectric multilayers. The fiber laser at 1.5 μm wavelength splited to four beams will be independently locked to each cavities. The main feature of this device is extremely high short-term stability of the laser frequency. However, also long-term stability in the near future may become competitive to hydrogen masers commonly used as an stable oscillator in microwave domain. In combination with atomic reference it serves as an local oscillator to generate time scale [1] and may be also used in experiments in fundamental physics, such as searching for transient variations of physical constant[2] since the sensitivities of atoms and cavity to this constants are different.

Operating the cavity in cryogenic environment is one of the possibilities to reduce thermal noise. Indeed, the most stable optical cavities are operating at 124 K [3] and it seems that the natural way to achieve better results is further cooling to lower possible temperatures [4, 5]. In case of monocrystalline silicon willingly used as a spacer material because of good rigidity no aging effect and high thermal conductivity, the next temperature below 124 K of zero thermal expansion coefficient is close to 17 K [6].

A system operating at so low temperature requires more inventive design to prevent mechanical noise coming from a cryocooler. In our design the cryostat is stiffly connected to the pulse tube refrigerator while the cavity is supported by three pillars located at the active vibration cancellation platform. Heat transfer between the spacer and the cryostat takes place through radiation and conductivity in thin, elastic wires. In this approach the cavity is mechanically decoupled from the cooling system. We also expect that differences of laser frequencies stabilized to different cavities spatially distributed in horizontal direction on the spacer may serve as an precise accelerometer and be exploited to cancel frequency noise coming from horizontal mechanical perturbations.

This work was partly supported by JSPS KAKENHI JP17F17018.

[1] H. Hachisu, F. Nakagawa, Y. Hanado, and T. Ido, Sci. Rep. **8**, 4243 (2018).

[2] P. Wcisło, P. Morzyński , M. Bober, A. Cygan, D. Lisak, R. Ciuryło, and M. Zawada, Nat. Astron. **1**, 0009 (2016).

[3] G. Matei *et al*, Phys. Rev. Lett. **118**, 263202 (2017).

[4] W. Zhang *et al*, Phys. Rev. Lett. **119**, 243601 (2017).

[5] E. Wiens, A. Yu. Nevsky, and S. Schiller, Phys. Rev. Lett. **117**, 271102 (2016).

[6] E. Wiens, Q. Chen, I. Ernsting, H. Luckmann, U. Rosowski, A. Nevsky, and S. Schiller, Opt. Lett. **39**, 3242 (2014).

An optical frequency comb stabilized to an optical lattice clock laser through optical fiber networks

E. Chae[1], T. Ikeda[2], K. Nakashima[2], K. Sugiyama[2], T. Takano[2], I. Ushijima[2,3], N. Ohmae[3,4], T. Akatsuka[3,5], H. Katori[2,3,4], M. Kuwata-Gonokami[6,7], and K. Yoshioka[1]

[1] *Photon Science Center, the University of Tokyo, Bunkyo-ku, Tokyo, Japan*

[2] *Department of Applied Physics, School of Engineering, the University of Tokyo, Bunkyo-ku, Tokyo, Japan*

[3] *Quantum Metrology Laboratory, RIKEN, Wako-shi, Saitama, Japan*

[4] *Center for Advanced Photonics, RIKEN, Wako-shi, Saitama, Japan*

[5] *NTT Basic Research Laboratories, Atsugi-shi, Kanagawa, Japan*

[6] *Institute for Photon Science and Technology, Graduate School of Science, The University of Tokyo, Bunkyo-ku, Tokyo, Japan*

[7] *Department of Physics, Graduate School of Science, The University of Tokyo, Bunkyo-ku, Tokyo, Japan*

e-mail: *chae@fs.t.u-tokyo.ac.jp*

Optical frequency combs have been used as an absolute optical frequency measure with its broadband spectrum that consists of discrete, equally spaced sharp lines [1]. When two degrees of freedom of the spectrum, a carrier-envelope offset frequency (f_{CEO}) and a repetition frequency (f_{rep}), are stabilized, all optical frequencies of the individual comb teeth are determined precisely. To achieve a better precision, one tooth of the comb can be stabilized to a stable, narrow-linewidth optical reference such as optical atomic clocks. By directly phase-locking optical frequency combs to the optical standard, the unprecedented accuracy and uncertainty of the optical atomic clocks would be transferred to the whole spectrum of the optical frequency comb [2, 3]. Here, we demonstrate stabilization of an optical frequency comb to ^{87}Sr optical lattice clock laser that is sent through telecom-wavelength fiber networks [4]. This work would be a cornerstone to fully utilize the next-generation time-frequency standard of optical atomic clocks by distributing the accuracy and the precision over the entire visible to near infrared frequencies beyond the spatial constraint.

The overall experimental setup is depicted in figure 1. An optical frequency standard used in this experiment is a ^{87}Sr optical lattice clock laser (Clock laser) at 698 nm. Optical fiber networks of the University of Tokyo (UTNET) is used to send the optical standard to a remote site where an optical frequency comb locates. Two external cavity diode lasers (ECDLs) are employed to convert the visible light to infrared and to compensate the optical power loss through UTNET. By phase-locking the two ECDLs to Clock laser in succession, a coherent copy of Clock laser is delivered through 2.9 km long optical fiber networks.

A home-built Ti:Sapphire optical frequency comb is used to convert the frequency of the optical standard to broad range of optical spectra. Using a self-reference technique, f_{CEO} is phase-stabilized to a radio-frequency source referenced to a GPS-disciplined Rb frequency standard. The output of the frequency comb is combined with the copy of Clock laser for stabilization of the remaining degree of freedom of the frequency comb. A heterodyne beat between the optical standard and one tooth of the frequency comb is detected and phase-locked by sending feedbacks to the length of the Ti:Sapphire oscillator cavity.

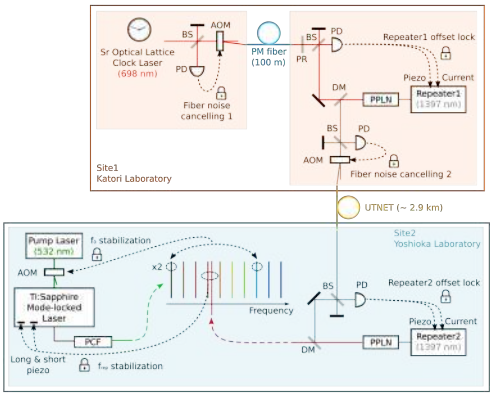


Figure 1: The overall experimental setup.

As the two degrees of freedom stabilized, this completes optical frequency standards spanning throughout visible and near infrared wavelengths with the precision of the optical atomic clocks transmitted through an optical fiber network. Currently, the achieved total relative instability of the optical frequency comb with respect to Clock laser is 8.1×10^{-18} at 1 s and 1.5×10^{-19} in 1000 seconds, which are better than the current limit of optical atomic clocks. This allows the next-generation time-frequency standard to be utilized throughout the frequency regime, from radio frequency to visible, beyond the spatial constraints for precision measurements and metrologies.

This work is supported by Photon Frontier Network Program of MEXT, Japan and JSPS KAKENHI Grant Number JP17H06205.

[1] S. T. Cundiff and J. Ye, Rev. Mod. Phys., **75**, 325 (2003).

[2] H. Leopardi et al., Optica **4**, 879 (2017).

[3] N. Ohmae et al., Appl. Phys. Exp. **10**, 062503 (2017).

[4] E. Chae et al., in preparation.

Weak measurement correlation spectroscopy for magnetic field sensing

Weizhi Qu[1], **Jian Sun**[1], **Shencao Jin**[1], **Eugeniy Mikhailov**[2], **Liang Jiang**[3], **Jianming Wen**[4], and **Yanhong Xiao**[1]

[1] *Department of Physics, State Key Laboratory of Surface Physics, and Key Laboratory of Micro and Nano Photonic Structures (Ministry of Education), Fudan University, Shanghai 200433, China*

[2] *Department of Physics, College of William and Mary, Williamsburg, Virginia 23185, USA*

[3] *Department of Applied Physics, Yale University, New Haven, Connecticut 06511, USA*

[4] *Department of Physics, Kennesaw state University, Kennesaw, Georgia 30144, USA*

e-mail: *08300190033@fudan.edu.cn*

Weak measurement (WM) can amplify an otherwise invisible small signal and holds great potential for precision measurements [1, 2]. Among physical quantities, frequency measurement has the highest precision thanks to stable narrow atomic transitions, and developing new schemes to improve on such measurements is of long standing interest. However, the application of weak measurement in precise measurement of atomic resonance has rarely been explored. Here, we propose a weak measurement resonance spectroscopy method to achieve narrow linewidth near 0.1 Hz. By tuning the overlap between the output optical state and the nearly perpendicular input state, the resonance linewidth, as well as the signal to noise can be optimized. Utilizing this narrow resonance, we experimentally demonstrated a magnetic field sensitivity of 8 fT/Hz$^{1/2}$ (near DC), in a room-temperature Rb vapor cell and using only one laser beam with power as low as 5 μW. Our results extend the theoretical framework of weak measurement to classical regime (frequency post-selection), and provides new insights in precision measurement techniques.

The atom-light interaction system can be simplified as a three-level Λ-type configuration, with two Zeeman ground states coupled to a common excited state by the two orthogonal circular components of a linearly polarized laser beam, forming Electromagnetically Induced Transparency (EIT). We describe the system by the density-matrix formalism and use the rotating frame of the input laser field with frequency modulation (FM) at ω_m. Under certain approximations, the following weak measurement Hamiltonian for the light can be obtained:

$$\mathcal{H} = -i\xi\sigma_z \otimes (|-\omega_m\rangle\langle 0| + |\omega_m\rangle\langle 0|)\,. \qquad (1)$$

where the grouped constant ξ represents the effective coupling strength between the system and the pointer, the frequency and the polarization of the light respectively. The pointer operator $\sigma_z = \begin{pmatrix} 1 & 0 \\ 0 & -1 \end{pmatrix}$ acts on the Jones vectors of light in circular basis, and characterizes the change in the polarization of light due to differential absorption between the left and right circularly polarized components. Owing to the absorption nature of the weak light-matter interaction, the effective Hamiltonian is purely imaginary and non-Hermitian. The system operator $|-\omega_m\rangle\langle 0| + |\omega_m\rangle\langle 0|$ represents the electric-field conversion process from the center-frequency component to the first sidebands. In the experiment, the initially x-polarized continuous wave (CW) laser field takes the full initial state as $|\Psi_i\rangle = |\Phi_{pi}\rangle \otimes |\Psi_{si}\rangle = \frac{1}{\sqrt{2}}\binom{1}{1} \otimes |0\rangle$. The post-selection on frequency results in the post-selected system state as $|\Psi_{sf}\rangle = \frac{1}{\sqrt{(1-D)^2+2}}[(1-D)|0\rangle + |\omega_m\rangle + |-\omega_m\rangle]$, where the parameter D (close to unity) characterizes the effective DC intensity filtering in the measurement. The weak value amplifies the expectation value of $\langle\sigma_z\rangle$, resulting in a sub-coherence-lifetime-limited linewidth (depending on D) of the measured $g^{(2)}(0)$ spectrum [3] with respective to the magnetic field (i.e., the two-photon detuning). Here, $g^{(2)}(0)$ is the second order intensity correlation of the two EIT fields at zero time delay, but with fields after frequency post-selection. Then, we measure the magnetic field sensitivity on the slope of the $g^{(2)}(0)$ spectrum, and by optimizing the post-selection parameter D, the sensitivity can be maximized given certain technical noise sources. The WM method reduces advent effects of technical noises such as residual amplitude modulation, a typical noise source in FM spectroscopy. The current sensitivity of 8 fT/Hz$^{1/2}$ is limited by the laser intensity noise, photo-detector noise and the fluctuation of the applied magnetic field itself, which are under investigation. This result is among the best magnetometer sensitivity obtainable near DC and with room temperature vapor cells.

[1] Y. Aharonov, D. Z. Albert and L. Vaidman, Phys. Rev. Lett. 60, 1351 (1988).

[2] J. Dressel, M. Malik, F. M. Miatto, A. N. Jordan and R. W. Boyd, Rev. Mod. Phys. 86, 307 (2014).

[3] L. Feng, P. Li, L. Jiang, J. Wen and Y. Xiao, Phys. Rev. Lett. 109, 233006 (2012).

Theory of the high-quality magneto-optical resonances observed in a buffer-gas-filled vapour cell

A.S. Novokreshchenov[1], **D.V. Brazhnikov**[1,2], **Ch. Andreeva**[3], **and S. Gateva**[3]

[1] *Institute of Laser Physics SB RAS, 630090 Novosibirsk, Russia*

[2] *Novosibirsk State University, 630090 Novosibirsk, Russia*

[3] *Institute of Electronics BAS, 1784 Sofia, Bulgaria*

e-mail: *aleksey-box@mail.ru*

The electromagnetically induced absorption (EIA) resonance usually manifests itself as a steep increase in the absorption of a medium. This subnatural-linewidth resonance was first observed under a bichromatic laser field composed of two beams with opposite circular polarizations [1]. Then the effect was also studied under a single-frequency light wave accompanied by a static magnetic field (magneto-optical or so-called Hanle configuration) [2]. The main reason that seriously limits EIA use consists of the problem for obtaining the high-contrast and sufficiently narrow resonance. Therefore, getting high-quality EIA resonances will promote their application in many directions of quantum technologies.

A new scheme for observing the high-contrast magneto-optical EIA resonances was proposed in [3]. The idea consisted of exploiting two counter-propagating laser beams with mutually orthogonal linear polarizations to excite an open optical transition in the ^{87}Rb D_1 line. The proposed scheme of excitation and the optical transition chosen allows one using a buffer-gas-filled vapor cell to greatly improve the properties of the nonlinear signals. Recently we have used such the cell to check that idea [4]. In particular, the EIA signals registered in a probe-wave transmission reach an unprecedented contrast of about 135% with respect to the wide ("Doppler") absorption pedestal and 29% with respect to the residual level of background transmission. These contrast values correspond to a relatively small FWHM of about 7.2 mG (5.3 kHz). The width of the narrowest EIA resonance observed is about 2.1 mG (1.5 kHz). To our knowledge, such a large relative contrast at the kHz-width is the record result for EIA.

In spite of the success reached, any explicit and consistent theory of the high-quality EIA-resonances effect that would quantitatively predict the experimental data has yet been presented. Our current work is aimed to develop such the theory based on the standard quantum-mechanical density matrix approach. First, the results obtained agree well with the experimental data. Second, the theory helps us to understand potential abilities of the new observation scheme. For instance, we studied influence of a stray magnetic field on the properties of high-contrast EIA resonances. In particular, it is seen from Fig. 1 that

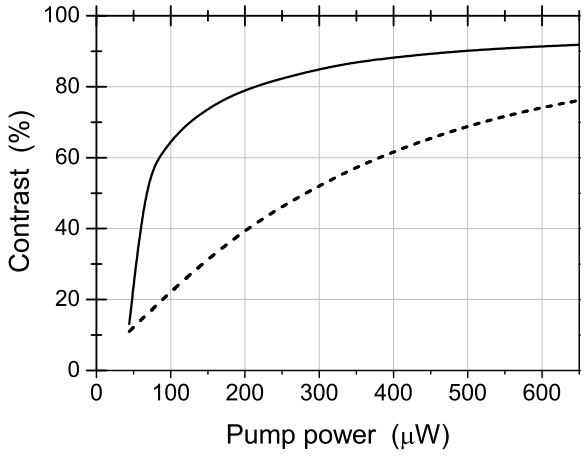


Figure 1: The resonance contrast vs. pump wave power. It is defined with respect to the total absorption level. The transverse stray magnetic field is absent for the solid line and it equals to 10 mG for the dashed one.

the contrast of EIA with respect to magnitude of total absorption at the center of the resonance curve can be very high, but stray magnetic field can significantly limit its value.

An explicit analytical expression for the spectroscopic signal has been derived for the optical transition $F_g = 1 \rightarrow F_e = 1$ in the ^{87}Rb D_1 line. A new feature of the magneto-optical resonances has been revealed that consists of observation of a shift of the resonance center. An analytical expression for the shift has been also derived. It appears that the shift itself can serve as a basis for the new method of magnetic-field vector measurements.

The authors thank Russian Foundation for Basic Research (grant nos. 18-32-00707, 18-52-18003).

[1] A. Akulshin, S. Barreiro and A. Lezama, Phys. Rev. A **57**, 2996 (1998).

[2] Y. Dancheva et al., Opt. Commun. **178**, 103 (2000).

[3] D. Brazhnikov et al., Laser Phys. Lett. **11**, 125702 (2014).

[4] D. Brazhnikov et al., Laser Phys. Lett. **15**, 025701 (2018).

High-sensitive all-optical magnetometer for nuclear magnetic resonance gyroscope

Xinxin Peng, Zhengyi Xu, Lianhua Li, Yinmin Zhou, Min Zhou and Xinye Xu*

State Key Laboratory of Precision Spectroscopy, East China Normal University, Shanghai 200062, China

e-mail: *51162099020@stu.ecnu.edu.cn; xyxu@phy.ecnu.edu.cn*

We describe a high-sensitive all-optical magnetometer for nuclear magnetic resonance gyroscope [1] (NMRG) signal detection [2]. In our experiment, a vapor cell contains nuclear magnetic resonance (NMR) isotopes such as ^{129}Xe, ^{131}Xe, alkali atom ^{133}Cs, and some buffer gas. Two crossed light beams, probe light and pumping light beam, are involved in this experiment. The circularly polarized light orients the spin of ^{133}Cs along B_0 parallel to z axis and nuclear spin of Xe polarizes by spin exchange collisions with ^{133}Cs. In presence of transverse static or oscillating magnetic field, the orientation experiences a nonzero torque and precess about magnetic field total B. The net transverse projection of spin is detected by linearly polarized light based on nonlinear magneto-optical rotation (NMOR) depending on transverse magnetic field and the detuning of probe light, as shown in Fig. 1. The average polarization rotation angle sensitivity of the magnetometer at f = 5 Hz point reaches $F = 7.7 \times 10^{-8} rad/Hz^{1/2}$, as shown in Fig. 2. When the frequency of oscillating magnetic field matches the Lamor frequency of nuclear spin of Xe, the coherent spin precession is generated with applied continuous oscillating magnetic fields perpendicular to B_0. The signal of coherent spin precession of Xe is detected by all-optical magnetometer. When oscillating magnetic field turns off, free induction decay (FID) occurs with transverse relaxation time 11.3 s, as shown in Fig. 3(a). Fig. 3(b) preliminarily give NMRG signal by altering the frequency of applied oscillating magnetic fields instead of rotating the NMRG system.

[1] D. W. Zhang, Z. Y. Xu, M Zhou, and X.Y. Xu, Chin. Phys. B, Vol.**26**, No.**2**, 023201 (2017).

[2] E A Donley. Sensors. IEEE, 17-22 (2010).

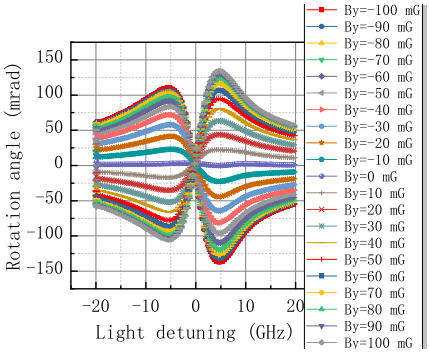


Figure 1: NMOR angle as a function of probe light detuning with a series of transverse magnetic fields.

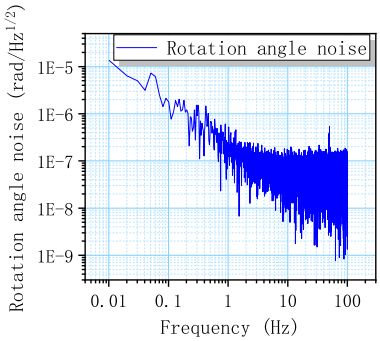


Figure 2: FFT spectrum of the rotation angle noise signal from Lock-in Amplifier.

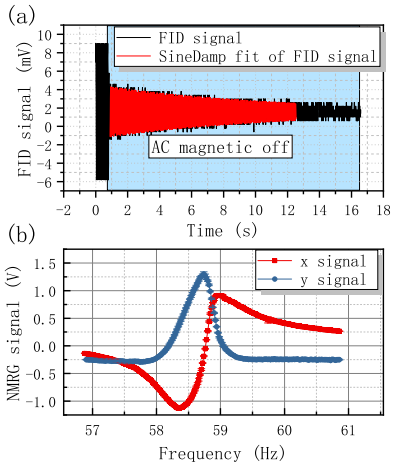


Figure 3: (a) FID of nuclear magnetic resonance signal of ^{129}Xe; (b) NMRG signal by altering the frequency of applied oscillating magnetic field.

A mercury optical lattice clock

V. Cambier[1], **J. Calvert**[1], **C. Guo**[1], **M. Favier**[1], **L. De Sarlo**[1] **and S. Bize**[1]
[1] *SYRTE, Observatoire de Paris, Université PSL, CNRS, Sorbonne Universités, LNE, Paris, France*
e-mail : *valentin.cambier@obspm.fr*

Tremendous progress performed over the past half-century both in atomic physics - in particular in the cooling and trapping of atoms - and in laser stabilisation have lead in the early 2000's to the realisation of optical lattice clocks [1]. The best microwave atomic clocks have been surpassed by these optical lattice clocks in which cold atoms are confined in a dipole-trap. These developments allowed to reach unprecedent stability levels and accuracy in the 10^{-18} range. These accuracy levels are very promising for tests in fundamental physics such as testing the variation of fundamental constants and for new applications like chronometric geodesy [2].

Neutral mercury (^{199}Hg) is a promising candidate to build an extremely reproducible optical lattice clock at room temperature. It has a reduced sensitivity to blackbody radiation shift (BBR) and a high vapour pressure at room temperature, suppressing the need of an oven an thus reducing temperature gradients on the experimental setup. Furthermore the 1/2 spin of the (^{199}Hg) gives a null-tensor component of differential polarisability. As an alkaline-earth-like atom, mercury has different metastable states but especially the strongly forbidden $^1S_0 \rightarrow {}^3P_0$ transition ($\approx$ 100 mHz wide), interesting as a clock transition. Finally, mercury has many naturally occurring isotopes, both bosons and fermions, opening the door to study of isotopic shifts.

In spite of these advantages, a big challenge lies in the need for suitable (narrow-linewidth, tunable, reliable) CW laser sources in the UV region of the spectrum at 254, 362 and 266 nm respectively for cooling, trapping and probing the mercury atoms

I will present the mercury optical lattice clock at SYRTE [3] and the recent improvements to the experimental setup. These improvement enabled us to characterise with better uncertainty many of the systematic effects affecting the clock. In my presentation I will focus in particular on the linear lattice light-shift (AC-Stark shift) and the quadratic Zeeman shift.

In order to evaluate the linear component of lattice-induced light-shift, we need to control the lattice wavelength and accurateky determine the so-called magic wavelength [4]. With these objectives, we developed an original scheme to reference the lattice wavelength to an accurate optical frequency comb.

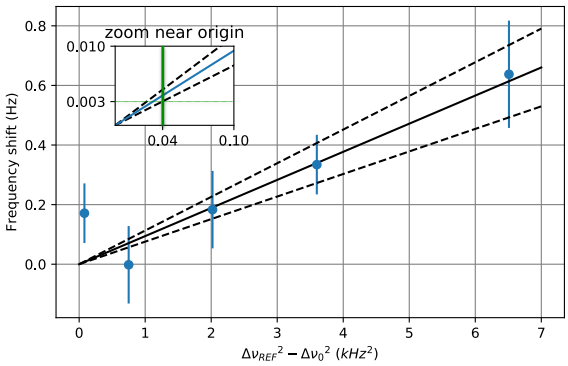


FIGURE 1 – Quadratic Zeeman shift as a function of the square of the splitting between the two π components. The black line is a linear fit to the data, the dotted black line represent the 1-σ confidence interval on the fit. The green line is our nominal operating point corresponding to a 60 μT bias field .

Concerning the quadratic Zeeman shift, we improved the statistical uncertainty over this effect by increasing the maximum exploitable field. The uncertainty over this effect is now 0.7×10^{-18} at the operating magnetic field of the clock of 60 μT (see figure 1). I will also present a few preliminary results about the operation of a mercury 2D-MOT.

Finally, I will discuss the perspectives of the mercury optical lattice clock and how we took part to a European measurement campaign between different optical lattice clocks thanks to coherent optical fibre links.

[1] A. D. Ludlow et al 2015 Optical atomic clocks Rev. Mod. Phys. 87637–701

[2] C. Lisdat et al. A clock network for geodesy and fundamental science. Nature Communications, 7 :12443–, August 2016.

[3] R. Tyumenev et al. Comparing a mercury optical lattice clock with microwave and optical frequency standards. New J. Phys. 18 113002 (2016).

[4] H.Katori et al. Ultrastable Cptical Clock with Neutral Atoms in an Engineered light Shift Trap Phys. Rev. Lett. 91173005 (2003).

Sideband cooling and transport of cold ytterbium atoms in a one-dimensional optical lattice

Hao Qiao, Chengyin Han, Shuang Zhang, Di Ai, Ge Lou, Mengya Zhang, Limeng Luo, Changyue Sun, Sheng Zhang, Min Zhou and Xinye Xu*

State Key Laboratory of Precision Spectroscopy, East China Normal University, Shanghai 200062, China

e-mail: *haoqiao1955@163.com; xyxu@phy.ecnu.edu.cn*

For an optical clock towards realizing below the 10^{-17} uncertainty, the blackbody radiation shift is one of the major concerns in the systematic effects. Transport of cold atoms into the cryogenic environment can essentially reduce the blackbody radiation shift [1]. In the ^{171}Yb optical clock, two counter-propagating lasers at 759 nm with the same polarization are used to form the one-dimensional optical lattice. Through chirping the frequency of one of the lasers, the optical lattice can be movable and the atomic transport distance is proportional to both the frequency difference between lasers and the chirp time. Using an ICCD (intensified CCD), we get a series of images of the moving atom cloud, as shown in Fig. 1(a), which shows a distance of over one centimeter can be obtained. The transfer distances of different chirp frequencies are plotted in Fig. 1(b). Furthermore, by adjusting the chirp frequency with opposite detuning, the lattice can be controlled to move in opposite direction and return to the original position.

In order to reduce the atom loss during transport, a lower atomic temperature is necessary. When atoms are confined in the optical lattice, the resolved-sideband cooling is an efficient method to cool atoms to the vibrational ground state. We obtain the resolved sideband region with narrow linewidth clock translation at 578 nm. Based on the clock laser and two repumping laser at 649 nm and 770 nm, sideband cooling is realized by preparing most of the atoms to vibrational ground state, showing that the atoms have a lower temperature. The temperature of atoms, which has been reduced to 3 μ K, is calculated by the area ratio between the red and blue sideband of the clock transition spectrum [2, 3], as shown in Fig. 2.

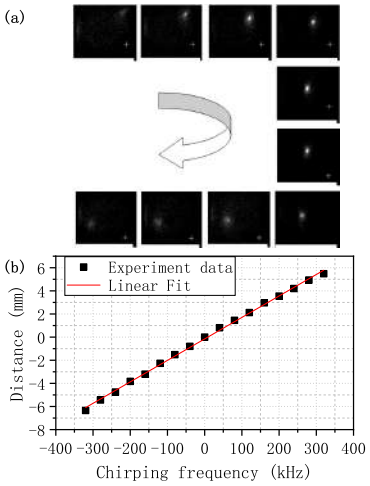


Figure 1: (a)The pictures of atoms for different chirp frequencies after transmission; (b)The transfer distances of different chirp frequencies.

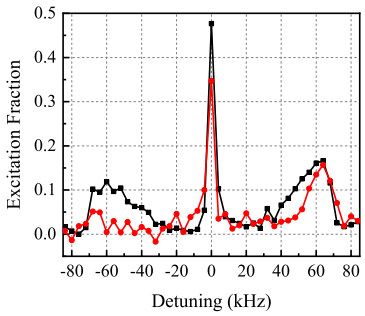


Figure 2: Clock-transition spectra (red) with and (black) without sideband cooling.

[1] I. Ushijima, M. Takamoto, M. Das, T. Ohkubo, and H. Katori, Nat. Photon. **9**, 185 (2015).

[2] C. Y. Han, M. Zhou, X. H. Zhang, Q. Gao, Y. L. Xu, S. Y. Li, S. Zhang, and X. Y. Xu, Sci. Rep.**8**, 7927 (2018).

[3] Q. Gao, M. Zhou, C. Y. Han, S. Y. Li, S. Zhang, Y. Yao, B. Li, H. Qiao, D. Ai, G. Lou, M. Y. Zhang, Y. Y. Jiang, Z. Y. Bi, L. S. Ma, and X. Y. Xu, Sci. Rep.**8**, 8022 (2018).

Ultracold Triplet Ground State ^{23}Na^{6}Li Molecules

Hyungmok Son[1,2], **Timur M. Rvachov**[1], **Juliana J. Park**[1], **Martin W. Zwierlein**[1], **Alan O. Jamison**[1] **and Wolfgang Ketterle**[1]

[1] *MIT-Harvard Center for Ultracold Atoms, Research Laboratory for Electronics, and Department of Physics, Massachusetts Institute of Technology, Cambridge, MA 02139, USA*

[2] *Department of Physics, Harvard University, Cambridge, MA 02138, USA*

e-mail: *hson@g.harvard.edu*

Ultracold molecules with permanent electric dipole moments offer a unique platform for the study of quantum many-body physics, quantum information processing, and quantum chemistry [1]. For this purpose, diatomic molecules in the absolute, singlet ground state (i.e., without electronic magnetic moments) have been created with various combinations of alkali atoms [2, 3]. Heteronuclear molecules with additional magnetic dipole moments provide an extra knob for the control of collision rates and chemical reactions [1] and for the realization of spin-lattice Hamiltonians [4]. For this reason, direct laser cooling of diatomic molecules with both electric and magnetic dipole moments have been demonstrated, but these molecules are far from quantum degeneracy (temperature $\gtrsim 50\mu$K, density $< 10^7 cm^{-3}$) [5].

As a different route, magnetoassociation of the ultracold atoms into the loosely bound state followed by a coherent two-photon transfer to the ground state has reached closer to the quantum degenerate regime [2, 6]. By employing this scheme, we have recently created ultracold, fermionic NaLi molecules in the triplet ground state (temperature $\sim 3\mu K$, density $\sim 5\times10^{10} cm^{-3}$) [7]. Unlike other biakali molecules [2], the triplet ground state NaLi molecules have a long lifetime of 4.6 seconds due to weak singlet-triplet mixing and slow two-body scattering rates. This is close to the p-wave universal loss rate limit [7].

In this conference, I will report the results of our recent experiments with triplet ground state NaLi molecules, including the rf electron spin resonance (ESR) spectrosocpy of the ground state hyperfine structures [7] and optical spectroscopy of the triplet excited and ground molecular potentials [8].

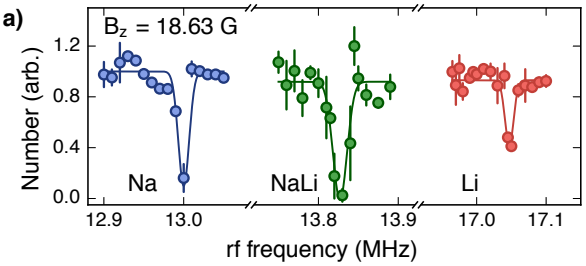


Fig. 1: Sample ESR spectra showing distinct loss features for transitions in Na $|F, m_F\rangle = |1, 1\rangle \rightarrow |1, 0\rangle$, NaLi $|7/2, 7/2\rangle \rightarrow |7/2, 5/2\rangle$, and Li $|1/2, 1/2\rangle \rightarrow |1/2, -1/2\rangle$. For NaLi, F=F_1+I_{Li}, where F_1=S+I_{Na} and S=s_{Li}+s_{Na} (s is the electronic spin and I is the nuclear spin) [7].

[1] R. V. Krems, Phys. Chem. Chem. Phys. **10**, 4079 (2008).

[2] K.-K. Ni, S. Ospelkaus, M. H. G. de Miranda, A. Peer, B. Neyenhuis, J. J. Zirbel, S. Kotochigova, P. S. Julienne, D. S. Jin, and J. Ye, Science **322**, 231 (2008).

[3] T. Takekoshi, L. Reichsllner, A. Schindewolf, J. M. Hutson, C. R. Le Sueur, O. Dulieu, F. Ferlaino, R. Grimm, and H.-C. Ngerl, Phys. Rev. Lett. **113**, 205301 (2014); P. K. Molony, P. D. Gregory, Z. Ji, B. Lu, M. P. Kppinger, C. R. Le Sueur, C. L. Blackley, J. M. Hutson, and S. L. Cornish, Phys. Rev. Lett. **113**, 255301 (2014); J. W. Park, S. A. Will, and M. W. Zwierlein, Phys. Rev. Lett. **114**, 205302 (2015); M. Guo, B. Zhu, B. Lu, X. Ye, F. Wang, R. Vexiau, N. Bouloufa-Maafa, G. Qumner, O. Dulieu, and D. Wang, Phys. Rev. Lett. **116**, 205303 (2016).

[4] A. Micheli, G. K. Brennen, and P. Zoller, Nat. Phys. **2**, 341 (2006).

[5] J. F. Barry, D. J. McCarron, E. B. Norrgard, M. H. Steinecker, and D. DeMille, Nature (London) **512**, 286 (2014); L. Anderegg, B. Augenbraun, E. Chae, B. Hemmerling, N. R. Hutzler, A. Ravi, A. Collopy, J. Ye, W. Ketterle, and J. Doyle, Phys. Rev. Lett. **119**, 103201 (2017).

[6] J. G. Danzl, E. Haller, M. Gustavsson, M. J. Mark, R. Hart, N. Bouloufa, O. Dulieu, H. Ritsch, and H.-C. Ngerl, Science **321**, 1062 (2008)

[7] T. M. Rvachov, H. Son, A. T. Sommer, S. Ebadi, J. J. Park, M. W. Zwierlein, W. Ketterle and A. O. Jamison, Phys. Rev. Lett. **119**, 143001 (2017)

[8] T. M. Rvachov, H. Son, J. J. Park, P. M. Notz, T. T. Wang, M. W. Zwierlein, W. Ketterle and A. O. Jamison, Phys. Chem. Chem. Phys. **20**, 4746-4751 (2018); T. M. Rvachov, H. Son, J. J. Park, S. Ebadi, M. W. Zwierlein, W. Ketterle and A. O. Jamison, Phys. Chem. Chem. Phys. **20**, 4739-4745 (2018)

Two interacting molecules in a one-dimensional harmonic trap

A. Dawid[1], **M. Lewenstein**[2,3], **and M. Tomza**[1]

[1] *Faculty of Physics, University of Warsaw, Pasteura 5, 02-093 Warsaw, Poland*

[2] *ICFO - Institut de Ciències Fotòniques, The Barcelona Institute of Science and Technology, 08860 Castelldefels, Spain*

[3] *ICREA - Instituciò Catalana de Recerca i Estudis Avançats, 08010 Barcelona, Spain*

e-mail: *Anna.Dawid@fuw.edu.pl*

In last 15 years ultracold atoms in traps and optical lattices have become a well-established platform to test models of many-body physics in new regimes [1]. They are used to build systems governed by the Hamiltonian that reproduce models relevant to condensed matter physics. However, for most atomic gases the interactions are exceedingly simple: they are spatially isotropic and sufficiently short-range to be well approximated by contact interactions. Replacing atoms with molecules opens new possibilities stemming from their rich internal structure, more abundant short-range interactions as well as their dipolar interactions being both long-range and anisotropic [2]. A wider range of many-body physics phenomena could be explored with these more complicated systems e.g. the interaction of magnetic spins in condensed matter systems as it is long-range and spatially anisotropic, much like the electric dipole-dipole interaction. Ultracold trapped molecules were proposed among others as simulators of extended Hubbard model, polarons transitions and many more. Over the past decade, a signicant progress has been made in preparing isolated ultracold few-atom systems experimentally. Moreover, a variety of tools for manipulating and probing such systems has been developed. Using few-body quantum systems with complete control over its quantum state [3] allowed among others for experimental observation of fermionisation phenomenon, research on crossover between few- and many-body physics, and realisation of antiferromagnetic Heisenberg spin chain. Motivated by all these possible applications, this work takes first steps towards a bottom-up molecule-by-molecule assembled molecular quantum simulator by analysing in detail the system of two rotating molecules in a one-dimensional harmonic trap.

We investigate the properties of two interacting ultracold polar molecules described as distinguishable quantum rigid rotors effectively trapped in a one-dimensional harmonic potential. The molecules interact via a multichannel two-body contact potential incorporating the short-range anisotropy of intermolecular interactions including dipole-dipole interaction. The impact of external electric and magnetic fields resulting in Stark and Zeeman shifts of molecular rovibrational states is also included. Energy spectra and eigenstates are calculated by means of the exact diagonalisation. The importance and interplay of the molecular rotational structure, anisotropic interactions, spin-rotation coupling, electric and magnetic fields, and harmonic trapping potential are examined in detail and compared to the system of two harmonically trapped distinguishable atoms. Presented model and results may provide microscopic parameters for molecular many-body Hamiltonians and may be useful for the development of bottom-up molecule-by-molecule assembled molecular quantum simulators.

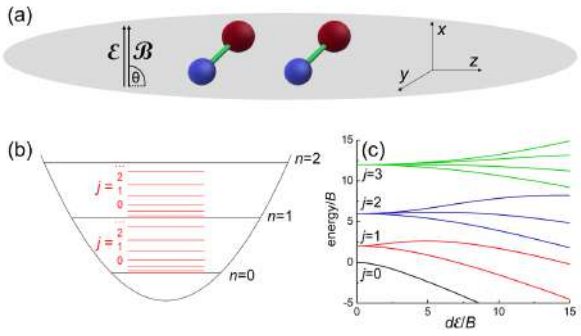


Figure 1: Schematic representation of the investigated system and its features. (a) Illustration of two diatomic polar molecules in a 1D trap in external electric E and magnetic B fields. (b) The energy spectrum of a rotating molecule in a 1D harmonic trap. (c) The energy of a polar molecule in an electric field (Starks effect).

[1] M. Lewenstein, A. Sanpera, and V. Ahufinger, *Ultracold Atoms in Optical Lattices: Simulating quantum many-body systems*. Oxford University Press, 2012.

[2] R. V. Krems., W. C. Stwalley, and B. Friedrich, *Cold Molecules: Theory, Experiment, Applications*. CRC Press, 2009.

[3] F. Serwane, G. Zürn, T. Lompe, T. B. Ottenstein, A. N. Wenz, and S. Jochim, Science, **332**, 336 (2011).

Fermi degeneracy and evaporation in a gas of reactive polar molecules

G. Valtolina[1], **L. De Marco**[1], **K. Y. Matsuda**[1], **W. G. Tobias**[1], **and J. Ye**[1]
[1] *JILA, National Institute of Standards and Technology and University of Colorado, and Department of Physics, University of Colorado, Boulder, CO 80309, USA*
e-mail: *giva4289@colorado.edu*

Ultracold polar molecules interact via long-range, anisotropic dipole-dipole potentials, allowing the realization of novel many-body quantum phases [1, 2]. Proposed areas of study for polar molecule lattice systems include topological matter and exotic superfluidity [3, 4]. For these, the achievement of quantum degeneracy in molecular gases is a fundamental requirement. Here we report on the realization on a redesigned apparatus of the first bulk degenerate Fermi gas of molecules, by producing a cloud with up to 100000 molecules and T/T_F below 0.5.
To manipulate molecular rotational states and control interactions, the apparatus contains in-vacuum electrodes for generating microwave fields and large (30 kV/cm) homogeneous DC electric fields, including adjustable field gradients. In combination with a one-dimensional optical lattice, these bias and gradient E-fields can be used to increase the ratio of elastic collisions over inelastic ones and further evaporatively cool down the molecules[5, 6]. We present a first investigation about how the interplay of interactions, dimensionality and chemical reactivity affects the evaporation efficiency and how this can be exploited to further increase the phase-space density of our molecular system.

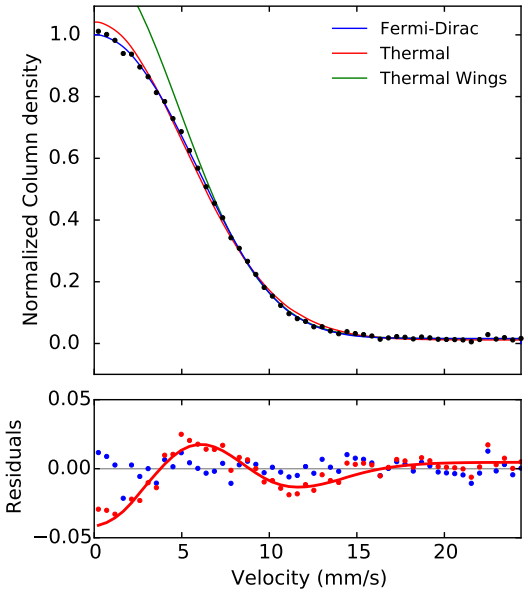


Figure 1: Top: Momentum distribution in time-of-flight of a Fermi gas of molecules at $T/T_F = 0.35(8)$. Bottom: Residuals of the Fermi-Dirac (blue) and Gaussian (red) fits.

[1] K.K. Ni et al., Science **322** (5899), 231-235 (2008).

[2] B. Yan et al., Nature **501**, 521-525 (2013).

[3] M.A. Baranov et al., Chemical Reviews **112** (9), 5012-5061 (2012).

[4] A.V. Gorshkov et al., Phys. Rev. Lett. **107**, 115301 (2011).

[5] M.H.G. de Miranda et al., Nature Physics **7**, 502-507 (2011).

[6] G. Quemener, P.S. Julienne, Chemical Reviews **112** (9), 4949-5011 (2012).

Direct measurement of branching ratios, and progress towards laser cooling of barium monohydride

R. L. McNally[1], **G. Z. Iwata**[1†], **S. F. Vazquez**[1], **M. P. Aitken**[1], **and T. Zelevinsky**[1]

[1] *Department of Physics, Columbia University, 538 West 120th Street, New York, NY 10027 USA*

[†] *Present address: Johannes Gutenberg Universitt, 55128 Mainz, Germany*

e-mail: *reeslmcnally@gmail.com*

We report progress on the laser cooling of diatomic BaH, based on a buffer gas beam source. This progress includes direct measurements of the branching ratios critical to efficient re-pumping of the molecule, identification of re-pump transitions necessary to scatter $\approx$ 50,000 photons[1], and initial measurements of the scattering rate. With this understanding of optical cycling in our molecule, and previous experiments understanding the relevant energy structure[2], we have begun experiments towards optical pushing, and eventually slowing of our molecular beam.Looking forward, plans for molecule slowing followed by magneto-optical trapping will be presented. Finally, we discuss the feasibility of photodissociation of ultracold BaH as a source of dilute ultracold hydrogen suitable for precision spectroscopy, a unique application for the monohydrides[3].

[1] Keith Moore, and Ian C. Lane, arXiv:1803.04849 (2018).

[2] G. Z. Iwata, R. L. McNally, and T. Zelevinsky, Phys. Rev. A **96**, 022509 (2017).

[3] Ian C. Lane, Phys. Rev. A **92**, 0022511 (2015).

Interactions of benzene, naphthalene, and azulene with alkali-metal and alkaline-earth-metal atoms for ultracold studies

P. Wójcik[1], **T. Korona**[2], **and M. Tomza**[1]

[1] *Faculty of Physics, University of Warsaw, Pasteura 5, 02-093 Warsaw, Poland*

[2] *Faculty of Chemistry, University of Warsaw, Pasteura 1, 02-093 Warsaw, Poland*

e-mail: *p.wojcik3@student.uw.edu.pl*

Intermolecular interactions are essential in many areas of natural sciences because they govern properties and dynamics of molecular systems at the microscopic level. At ultracold conditions even a tiny change in the interaction energy can be larger than the collision energy and thus can modify the rates of elastic, inelastic and chemical reactive scattering by many orders of magnitude. Therefore, a combination of experimental and theoretical efforts applied to study molecules at ultralow temperatures can be very instructive and shed new light on intermolecular interactions [1, 2].

Recently, helium buffer-gas cooling of benzonitrile (C_6H_6CN) to low temperatures was demonstrated [3] and opened the way for slowing down and trapping of polyatomic aromatic molecules at ultralow temperatures. Here, we consider collisional studies of benzene, naphthalene, and azulene immersed into ultracold atomic gases and investigate intermolecular interactions of these polyatomic aromatic molecules with alkali-metal (Li, Na, K, Rb, Cs) and alkaline-earth-metal (Mg, Ca, Sr, Ba) atoms. This is the first step towards the evaluation of prospects for sympathetic cooling of polyatomic aromatic molecules with ultracold atoms. We have selected above aromatic molecules because they can be well described within the rigid rotor approximation simplifying future scatting calculations.

We apply the state-of-the-art *ab initio* techniques to compute the potential energy surfaces (PESs). We use the coupled cluster method restricted to single, double, and noniterative triple excitations, CCSD(T), with extensive atomic orbital bases sets to reproduce the correlation energy and the small-core energy-consistent pseudopotentials to model the scalar relativistic effects in heavier metal atoms. The PESs are characterized in detail and the nature of intermolecular interactions is analyzed and benchmarked using symmetry adapted perturbation theory (in HF-SAPT and DFT-SAPT variants). We also report the leading long-range isotropic and anisotropic dispersion and induction interaction coefficients. The full three-dimensional potential energy surfaces are provided for selected systems within atom-bond pairwise additive representation and can be employed in scattering calculations.

Finally, we suggest azulene, an isomer of naphthalene which posses a significant permanent electric dipole moment and optical transitions in the visible range, as a promising candidate for electric field manipulation and buffer-gas or sympathetic cooling.

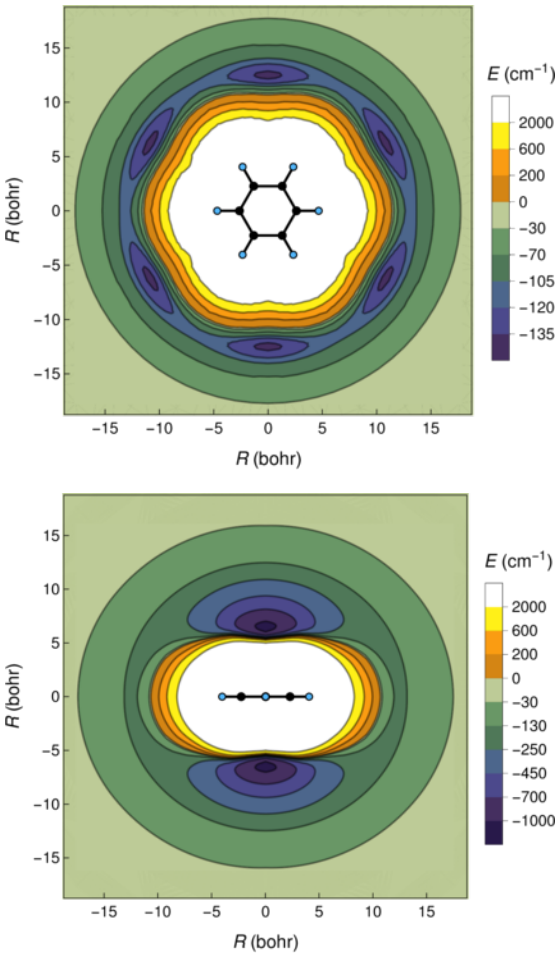


Figure 1: Two dimensional cuts through an interaction energy potential of Rb atom - benzene molecule system. Note different energy scales.

[1] O. Dulieu, R. Krems, M. Weidemuller, and S. Willitsch, Phys. Chem. Chem. Phys., **13**, 18703 (2011).

[2] L. D. Carr, D. DeMille, R. V. Krems, and J. Ye, New J. Phys. **11**, 055049 (2009).

[3] D. Patterson and J. M. Doyle, Phys. Chem. Chem. Phys., **17**, 5372 (2015).

Isotopic shift of atom-dimer Efimov resonances in K-Rb mixtures

K. Kato[1], Yujun Wang[2], J. Kobayashi[3], Paul S. Julienne[4] and S. Inouye[1]

[1] *Graduate School of Science, Osaka City University, Sumiyoshi-ku, Osaka 558-8585, Japan*

[2] *American Physical Society, 1 Research Road, Ridge, New York 11961, USA*

[3] *PRESTO, Japan Science and Technology Agency, Kyoto 606-8502, Japan*

[4] *Joint Quantum Institute, University of Maryland and NIST, College Park, Maryland 20742, USA*

e-mail: *k_kato@sci.osaka-cu.ac.jp*

Universality has played an essential role in understanding fundamental quantum physics. Efimov states, an infinite series of three-body bound states with discrete scale invariance when a two-body scattering length diverges, provided us a unique opportunity to investigate universality in few-body phenomena. For a long time, it has been believed that binding energy of Efimov states depends on the details of short-range interaction, that is represented by a three-body parameter [1]. Recent experiments and theories, however, have revealed that three-body parameters are determined by only long-range van der Waals interactions in some limiting cases [2]. This achievement suggests that the necessity of including precise few-body short-range chemical forces in studies of universal few-body phenomena may be removed.

We investigated Efimov physics in ultracold heteronuclear admixtures of K and Rb atoms. We measured three-body recombination coefficients and atom-dimer loss coefficients in ^{41}K-^{87}Rb systems and the resonant feature is clearly observed in the atom-dimer loss coefficients. We observed a shift in the scattering length where the first atom-dimer resonance appears in the ^{41}K-^{87}Rb system relative to the position of the previously observed atom-dimer resonance in the ^{40}K-^{87}Rb system [3]. These isotopes have almost the same van der Waals interactions and atomic masses, therefore, the shift in the atom-dimer resonance positions can be cleanly ascribed to the difference of the properties of Feshbach resonances. We calculated loss coefficients by using multi-channel spinor model, and this calculation successfully reproduced the experimental results. Our study demonstrates the role of multichannel Feshbach physics in determining Efimov resonances in heteronuclear three-body systems.

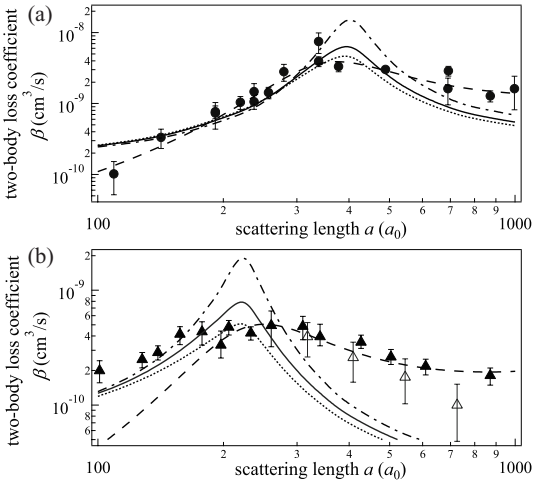


Figure 1: Comparisons of numerically calculated and experimentally measured loss coefficients for (a) Rb-^{41}KRb and (b) Rb-^{40}KRb (experimental data obtained from Ref.[3]) collisions[4].

[1] E. Braaten and H. -W. Hammer, Phys. Rep. **428**, 259 (2006).

[2] Pascal Naidon and Shimpei Endo, Rep. Prog. Phys. **80** 056001 (2017).

[3] R. S. Bloom, M. -G. Hu, T. D. Cumby, and D. S. Jin, Phys. Rev. Lett. **111**, 105301 (2013).

[4] K. Kato, Yujun Wang, J. Kobayashi, Paul S. Julienne, and S. Inouye, Phys. Rev. Lett. **118** 163401 (2017).

Two-photon spectroscopy of ultracold dipolar ^{6}Li -^{40}K molecules

A. Yang[1], S. Botsi[*1], S. Kumar[1], A. Laugharn[1], S. B. Pal[1], M. Lam[1], and K. Dieckmann[1,2]

[1] *Centre for Quantum Technologies (CQT), 3 Science Drive 2, 117543 Singapore*
[2] *Department of Physics, National University of Singapore, 2 Science Drive 3, 117542 Singapore*
e-mail: *e0242929@u.nus.edu*

With the creation of dipolar molecules in their ro-vibrational ground state, a long-standing scientific goal has been achieved [1, 7]. Ultracold dipolar molecules at high phase-space density are a promising tool for the quantum simulation of a large class of many body effects [8] and for quantum bit manipulation based on the dipole-dipole interaction [9]. In our experiment, we use bosonic heteronuclear dimers of ^{6}Li and ^{40}K in their deeply-bound ro-vibronic states, which possess a large electric dipole moment of 3.6 Debye and a long lifetime ($\geq$ 200 ms). This makes them a suitable candidate for investigating long-range anisotropic dipole-dipole interactions.

Starting from a sympathetically cooled, quantum-degenerate Fermi-Fermi mixture, we create weakly-bound ^{6}Li-^{40}K molecules via magnetic Feshbach association at 215.6 G in an optical dipole trap. The initial closed-channel Feshbach state is a superposition of the highest vibrational $X^1\Sigma$ and $a^3\Sigma$ states just below the dissociation threshold of the electronic ground state. In our approach, we select a Feshbach molecular state with a sole singlet admixture. On the basis of the Asymptotic Bound-state Model (ABM) [10], we calculate this singlet admixture to be 52% for the case of fully alligned nuclear spins. This choice allows us to address a single hyperfine state of the excited states manifold and hence avoid coupling to several intermediate states during Stimulated Raman Adiabatic Passage (STIRAP) to the molecular ground state. In particular, we were able to address very deeply bound states of the $A^1\Sigma$ potential that offer a large overlap with the ground state at this inner turning point. We present data from our one-photon spectroscopic survey of the $B^1\Pi$ and $A^1\Sigma$ electronically excited states showing a variety of new lines complementing existing data of the weakest bound states. We then present two-photon spectroscopy to investigate the deeply-bound ro-vibrational levels of the electronic ground state of ^{6}Li and ^{40}K molecules. We first were able to identify the $v = 3$ state by Autler-Townes spectroscopy, as this state is favored by the overlap factor and accessibility of the laser wavelength. More recently, the implementation of a new dye laser setup provided the necessary output power and wavelength tuning range for the discovery of the lower vibrational states $v = 2$ and $v = 1$ and eventually the absolute electronic and ro-vibronic ground state $v = 0$ (Fig.1). Next, the ground state will be populated via STIRAP and strong, homogeneous and rotatable electric fields will be applied to enable the determination of the dipole moment of the ground state ^{6}Li -^{40}K molecules.

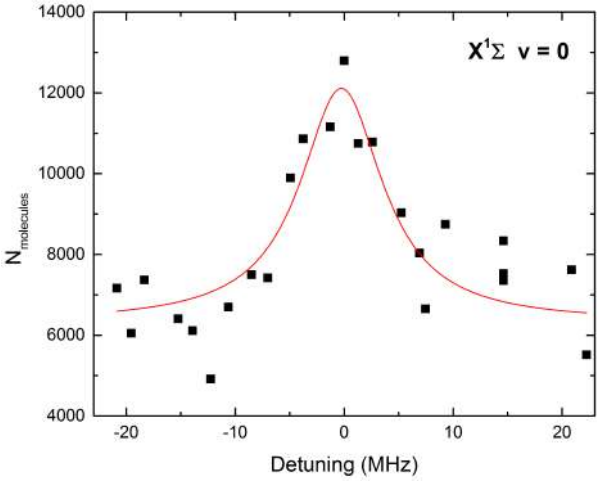


Figure 1: Two-photon resonance addressing the absolute ro-vibronic ground state of the $X^1\Sigma$ potential at the 215.6 G Feshbach resonance.

[1] K. - K. Ni., et al., Science, **322**, 231-235 (2008).

[2] M. Debatin, Ph.D. Thesis (2013). T. Takakoshi, et al., Phys. Rev. Lett. **113**, 205301 (2014).

[3] Peter K. Molony, et al., Phys. Rev. Lett. **113**, 255301 (2014).

[4] J. W. Park, S. Will, M.W. Zwierlein, Phys. Rev. Lett. **114**, 205302 (2015).

[5] J. W. Park, S. Will, M.W. Zwierlein, New Journ. Phys. **17**, 075016 (2015).

[6] M. Y. Guo, et al., Phys. Rev. Lett. **116**, 205303 (2016).

[7] Timur M. Rvachov, et al., Phys. Rev. Lett. **119**, 143001 (2017).

[8] M. A. Baranov, et al., Chem. Rev. **112** (9), 5012-5061 (2012).

[9] A. Micheli, G. K. Brennen & P. Zoller, Nature Physics **2**, 341-347 (2006)

[10] T. G. Tiecke, et al., Phys. Rev. A, **82**, 042712 (2010).

Testing the parity symmetry in chiral molecules using vibrational spectroscopy

M. Manceau[1], M. Pierens[1], L. Lecordier[1], A. Cournol[1], D.B.A Tran[1], R. Santagata[1], B. Argence[1], A. Shelkovnikov[1], O. Lopez[1], C. Daussy[1], C. Chardonnet[1], M. Abgrall[2], Y. Le Coq[2], R. Le Targat[2], W. K. Lee[2], D. Xu[2], P-E Pottie[2], R. J. Hendricks[3], T. E. Wall[4], J. Bieniewska[4], B. E. Sauer[4], M. R. Tarbutt[4], A. Amy-Klein[1], S. K. Tokunaga[1], B. Darquié[1]

[1] *Laboratoire de Physique des Lasers, CNRS, Université Paris 13, Villetaneuse, France*

[2] *LNE-SYRTE, Observatoire de Paris, PSL Research University, CNRS, Sorbonne Universits, UPMC Univ. Paris 06, Paris, France*

[3] *National Physical Laboratory, NPL, Teddington, United Kingdom*

[4] *Centre for Cold Matter, Imperial College London, London, United Kingdom*

e-mail: *mathieu.manceau@univ-paris13.fr*

Unlike the other fundamental interactions, the weak interaction is known to violate the parity symmetry, i.e the symmetry under spatial inversion. It was experimentally demonstrated using nuclear and atomic systems and in high energy physics. However, despite being theoretically predicted, parity-violation (PV) was never measured in molecules. In particular for a chiral molecule, i.e. a molecule non-superimposable to its mirror image, it is expected to lead to energy differences between the left- and right-handed enantiomers, and in turn to frequency differences in their rovibrational spectra potentially measurable using precise mid-infrared spectroscopy. Those PV frequency shifts are however predicted to be extremely small, in the mHz to Hz range [1] depending on the species considered for vibrational transitions at ~ 30 THz. Measuring this allows several fundamental questions to be addressed, from the limit of the standard model in the low-energy regime to the still unexplained origin of biomolecular homochirality, while it can also serve as a benchmark in relativistic quantum chemistry calculations.

Attempting a measurement of PV in chiral molecules starts with the choice of the molecular species to be probed. As the PV effects scale with the fifth power of the nuclear charge Z, large molecules with heavy atoms are considered [1, 2]. Chiral species with a rhenium atom are currently under study. The transitions of interest for measuring PV are vibrational transitions of modes involving the heavy atom, typically in the mid-infrared (MIR) region of the electromagnetic spectrum (~ 10 μm). We are constructing a Ramsey interferometry experiment which comprises three parts: the preparation of molecules in cold, slow and intense beams, an interrogation zone using an ultra-stable and tuneable MIR laser system and finally a part for the detection of internal molecular state populations. First, the molecules will be prepared in high flux, low velocity buffer-gas-cooled beams, one of the latest molecular beam technology. After exiting the cryogenic buffer gas cell, the molecular beam will be probed by a Ramsey interferometer based on frequency stabilized quantum cascade lasers (QCLs) calibrated against primary standards. QCLs offer broad and continuous tuning and cover the entire mid-infrared thus providing considerable flexibility on the chosen rovibrational transitions that can be studied. Finally, after the MIR Ramsey interrogation, the population needs to be measured. We are currently investigating new measurement procedures in the microwave domain to enhance the detection sensitivity compared to direct detection schemes in the MIR region and to enable enantiomer specific measurements [3].

In this context, I will report our latest results on buffer-gas-cooling in the gas phase of complex polyatomic molecules solid at room temperature such as methyltrioxorhenium [4, 5] (MTO, closely related to chiral rhenium complexes for which the parity-violating energy differences between enantiomers is measurable [2]) and trioxane. I will present precise Doppler-broadened and sub-Doppler spectroscopic measurements of the cooled molecules around 10 μm. I will also present ultra-high resolution spectroscopic measurements using a QCL stabilized at the sub-Hz level, via an optical frequency comb, on an ultra-stable near infrared reference signal provided by the French metrology institute (LNE-SYRTE) [6]. This allows rovibrational frequencies to be determined at record uncertainties, with traceability to primary frequency standards.

[1] S. K. Tokunaga, et al. , Mol. Phys. **111**, (2013).

[2] N Saleh, et al., Chirality **30**, (2018).

[3] S. Eibenberger, et al. , Physical review letters, **118(12)**, (2017)

[4] S. K. Tokunaga, et al., New Journal of Physics, **19(5)**, (2017).

[5] P. Asselin, et al., Phys. Chem. Chem. Phys. **19**, (2017).

[6] B. Argence, et al., Nature Photonics **9.7** (2015).

Towards laser cooling of AlF molecules

S. Truppe[1], **S. Marx**[1], **S. Kray**[1], **M. Doppelbauer**[1], **H.-C. Schewe**[1], **B. G. Sartakov**[2], **G. Meijer**[1]

[1] *Fritz-Haber-Institut der Max-Planck-Gesellschaft, Faradayweg 4-6, 14195 Berlin, Germany*
[2] *General Physics Institute, Russian Academy of Sciences, Vavilovstreet 38, 119991 Moscow, Russia*
e-mail: *truppe@fhi-berlin.mpg.de*

Direct laser cooling has been demonstrated for four diatomic molecules (SrF [1], YO [2], CaF [3, 4] and YbF [5]) and one polyatomic molecule (SrOH [6]) so far. For all these molecules, the laser cooling transition is between a $^2\Sigma^+$ ground state and an electronically excited $^2\Pi_{1/2}$ state. For laser cooling to be feasible, the molecule must have a short-lived excited state that decays with very high probability to just one or a few vibrational levels of the ground state. Molecules with a $^1\Sigma^+$ ground state and a $^1\Pi$ excited state, such as AlF are particularly attractive candidates for laser cooling, though none have yet been cooled [7]. The excited $A^1\Pi$ state of the AlF molecule has a lifetime of 2 ns permitting rapid photon scattering and a large capture velocity for a magneto-optical trap [8, 9, 10]. The hyperfine structure in the ground state is smaller than the linewidth of the laser cooling transition, so that all hyperfine components are addressed with a single laser frequency. The vibrational branching is expected to be exceedingly small, allowing 10^4 photons to be scattered with a single laser. To slow a molecule from a speed of 140 m/s to standstill it needs to scatter about 3500 photons which corresponds to a stopping distance of less than 5 mm. The AlF molecule also possesses a spin-forbidden $a^3\Pi \leftarrow X^1\Sigma^+$ transition which can be used to laser cool the molecules close to the recoil temperature of 3 μK. We present first results on high resolution optical, radio-frequency and microwave spectroscopy of the ground $X^1\Sigma^+$ and first excited $A^1\Pi$ states and the metastable $a^3\Pi$ state in AlF to determine their rotational, hyperfine and Zeeman levels and derive new spectroscopic constants with unprecedented accuracy. We also determine the electric dipole moment of AlF in $X^1\Sigma^+$ and $a^3\Pi$.

References

[1] E. S. Shuman, J. F Barry, D. R. Glenn, D. DeMille, PRL **103**, 223001 (2009).

[2] M. T. Hummon, M. Yeo, B. K. Stuhl, A. L. Collopy, Y. Xia, J. Ye, PRL **110**, 143001 (2013).

[3] V. Zhelyazkova, A. Cournol, T. E. Wall, A. Matsushima, J. J. Hudson, E. A. Hinds, M. R. Tarbutt, B. E. Sauer, PRA **89**, 053416 (2014).

[4] B. Hemmerling, E. Chae, A. Ravi, L. Anderegg, G. K. Drayna, N. R. Hutzler, A. L. Collopy, J. Ye, W. Ketterle, J. M. Doyle, J. Phys. B **49**, 174001 (2016).

[5] J. Lim, J. R. Almond, M. A. Trigatzis, J. A. Devlin, N. J. Fitch, B. E. Sauer, M. R. Tarbutt, E. A. Hinds, PRL **120**, 123201 (2018).

[6] I. Kozyryev, L. Baum, K. Matsuda, B. L. Augenbraun, L. Anderegg, A. P. Sedlack, J. M. Doyle, PRL **118**, 173201 (2017).

[7] R. J. Hendricks, D. A. Holland, S. Truppe, B. E. Sauer, M. R. Tarbutt, Frontiers in Physics **2**, 51 (2014).

[8] J. F. Barry, D. J. McCarron, E. B. Norrgard, M. H. Steinecker, D. DeMille, Nature **512**, 286-289 (2014).

[9] S. Truppe, H. J. Williams, M. Hambach, L. Caldwell, N. J. Fitch, E. A. Hinds, B. E. Sauer, M. R. Tarbutt, Nat. Phys **13**, 1173 (2017).

[10] L. Anderegg, B. L. Augenbraun, E. Chae, B. Hemmerling, N. R. Hutzler, R. Aakash, A. Collopy, J. Ye, W. Ketterle, J. M. Doyle, PRL **119**, 103201 (2017).

Ultracold Lithium for Sympathetically Cooling Polar Molecules

S. C. Wright, T. E. Wall, and M. R. Tarbutt
Centre for Cold Matter, Blackett Laboratory, Imperial College London, United Kingdom
e-mail: *s.wright15@imperial.ac.uk*

The ability to produce large ensembles ($N \sim 10^6$) of ultracold dipolar molecules would be beneficial for many precise tests of fundamental physics, and presents exciting opportunities for quantum simulation and cold chemistry. A number of molecule traps suitable for cold molecules have been realized, most recently magneto-optical trapping of the monofluoride radicals SrF [1] and CaF [2]. A viable option for further cooling of molecules is sympathetic cooling with an ultracold atomic gas. Importantly, one could take advantage of the high densities currently attainable with atomic gases to indirectly evaporatively cool the molecules using the atoms.

We have implemented Raman Grey Molasses (RGM) in ^{7}Li to cool it below the Doppler Limit, and have studied the cooling process using both the D_1 and D_2 transitions. We find that the cooling can be effective in a number of laser detuning configurations which are hitherto unreported. Our lithium gas is now sufficiently cold to load a microwave trap, in which we aim to implement sympathetic cooling with CaF molecules.

[1] J. F. Barry, D. J. McCarron, E. B. Norrgard, M. H. Steinecker, and D. DeMille, Magneto-optical trapping of a diatomic molecule. Nature **512** (2014)

[2] S. Truppe, H. J. Williams, M. Hambach, L. Caldwell, N. J. Fitch, E. A. Hinds, B. E. Sauer, M. R. Tarbutt, Nature Physics **13** (2017)

Collision studies of slow, cold polyatomic molecules

I. M. Rabey[1], **T. Gantner**[1], **M. Koller**[1], **X. Wu**[1,2], **S. Chervenkov, M. Zeppenfeld**[1] **and G. Rempe**[1]

[1] *Max-Planck-Institut für Quantenoptik, Hans-Kopfermann-Str. 1, 85748 Garching, Germany*
[2] *Present address: Department of Physics, Yale University, New Haven, CT 06511, USA*
e-mail: *isabel.rabey@mpq.mpg.de*

Cold molecules represent a fascinating research frontier in physics and chemistry. Techniques in the field are advancing at a rapid pace, motivated by a broad range of possible applications — precision measurement of fundamental physics, quantum information and simulation, studies of collision dynamics and ultracold chemistry. These applications typically require large numbers of molecules to be slowed, cooled and trapped, ideally at high densities. In addition, control over the internal states of the system is also necessary. We present a novel solution to this goal. Using a sequence of buffer gas cooling and centrifuge deceleration we remove 99% of the initial kinetic energy to produce slow, cold polar molecules with energies below 1 K $\times\, k_B$ [1] [2]. Together, this setup is known as the *cryofuge*. The cryofuge delivers a flux exceeding 10^{10} molecules per second which have velocities below 20 m/s and a single state purity of up to 92% [3]. As neither step is dependent on the specific internal structure of the molecule, the technique is generic and has been extended to several polyatomic species including fluoromethane (CH_3F) and ammonia (ND_3).



Figure 1: A photo of the centrifuge decelerator. The electrodes used to guide the molecules are highlighted in red and blue.

An electrostatic quadrupole guide at the output of the cryofuge contains densities exceeding 10^9 cm^{-3}. With interaction times in the guide of longer than 25 ms, we have observed dipolar collisions between these molecules at a measured rate of $\sim$ 10 Hz [3]. To enable a more detailed study of these collisions, a microstructured electric trap [4] has been added to the end of the setup. With a storage time of several seconds in the present system, this offers a route towards observation of rethermalisation inside the trap, allowing us to test the feasibility of evaporative cooling across a variety of molecule species.

[1] S. Chervenkov, X. Wu, J. Bayerl, A. Rohlfes, T. Gantner, M. Zeppenfeld and G. Rempe, Phys. Rev. Lett. **112**, 013001 (2014).

[2] X. Wu, T. Gantner, M. Zeppenfeld, S. Chervenkov and G. Rempe, ChemPhysChem **17**, 22 (2016).

[3] X. Wu, T. Gantner, M. Koller, M. Zeppenfeld, S. Chervenkov and G. Rempe, Science **358**, 645 (2017).

[4] B. G. U. Englert, M. Mielenz, C. Sommer, J. Bayerl, M. Motsch, P. W. H. Pinkse, G. Rempe and M. Zeppenfeld, Phys. Rev. Lett. **107**, 263003 (2011).

Long Coherence Times in Trapped $^{87}Rb^{133}Cs$

J. A. Blackmore[1], **P. D. Gregory**[1], **E. M. Bridge**[1], **R. Sawant**[1] **and S. L. Cornish**[1]
[1] *Joint Quantum Centre (JQC) Durham-Newcastle, Department of Physics, Durham University, South Road, Durham, DH1 3LE, UK*
e-mail: *j.a.blackmore@durham.ac.uk*

We are able to produce a sample of up to 4000 $^{87}Rb^{133}Cs$ molecules in the hyperfine and rovibronic ground state at 181.5 G by following a two step process. An initial mixture of ^{87}Rb and ^{133}Cs gas is converted to weakly-bound molecules by magnetoassociation at an interspecies Feshbach resonance. These weakly bound molecules are then transferred into the ground state via stimulated Raman adiabatic passage (STIRAP)[1] with a one-way efficiency in excess of 90%. This work builds upon our previous successes transferring the $^{87}Rb^{133}Cs$ molecules between rotational hyperfine states in free-space [2] and studying the AC Stark effect within a $\lambda =$ 1550 nm dipole trap [3].

The Ramsey sequence allows for high precision measurement in molecules by separating the spectroscopic interactions into two separate pulses, separated by a fixed interaction time T. Performing these measurements in free-space is limited by the time it takes for the molecular cloud to expand and fall out of our detection region - limited by the size of our STIRAP beams. By applying an optical dipole trap we are able to extend this time, however due to the AC Stark shift of the rotational levels the contrast of Ramsey fringes is destroyed as the molecular sample dephases.

By utilising our knowledge of the AC Stark shift [2] we are able to identify regions where the variations in intensity across the cloud (typically ∼3% of the peak intensity) translates to a narrower distribution of frequencies. In one such region on the transition to the $|N = 1, M_F = +4\rangle$ from the ground state we are able to measure a peak coherence time of 0.75(6) ms. We compare this time to superpositions on the transition to $|N = 1, M_F = +5\rangle$ which dephases in < 100 μs.

References

[1] P. K. Molony, P. D. Gregory, Z. Ji, B. Lu, M. P. Köppinger, C. R. Le Sueur, C. L. Blackley, J. M. Hutson, and S. L. Cornish, Phys. Rev. Lett. **113**, 255301 (2014).

[2] P. D. Gregory, J. A. Blackmore, J. Aldegunde, J. M. Hutson, and S. L. Cornish, Phys. Rev. A **96**, 021402(R) (2017).

[3] P. D. Gregory, J. Aldegunde, J. M. Hutson, and S. L. Cornish, Phys. Rev. A **94**, 041403(R) (2016).

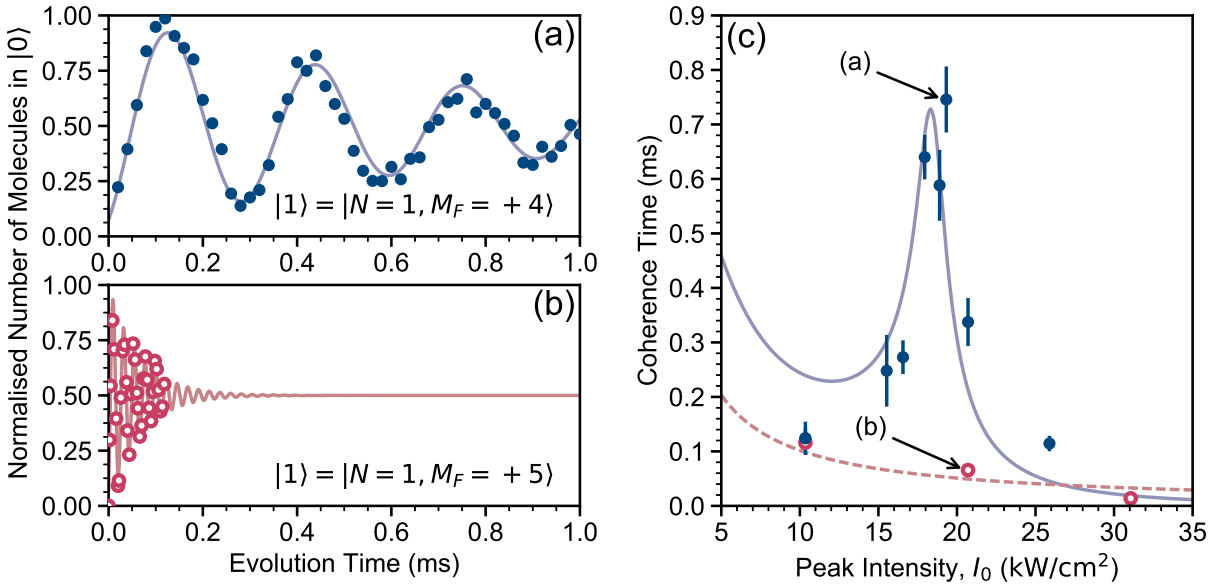


Figure 1: The coherence of a rotational superposition in RbCs molecules. (a) A comparison between a rotational superposition around an avoided crossing and in a linear AC Stark shifted state. (b) Ramsey fringes with contrast existing over 800 μs (c) The Ramsey fringes for an equivilant superposition of a linear Stark shifted state where coherence lasts only 100 μs.

Magic-Wavelength Molecular Clock and Ultracold Chemistry With Lattice-Trapped Molecules

S.S. Kondov [1], **C. Liedl**[1], **C.-H. Lee**[1], **K.H. Leung**[1], **T. Zelevinsky**[1]
[1] *Department of Physics, Columbia University, 10027 New York, USA*
e-mail: *ssk2224@columbia.edu*

Quantum control and precision spectroscopy of ultracold molecules offer new possibilities for tests of fundamental physics such as searches for drift in fundamental constants, modifications of gravity at the nano-scale, and probing the regime of ultracold chemistry.

We extend techniques commonly used in optical atomic clocks to perform precise metrology and coherent control of deeply bound $^{88}Sr_2$ molecules in a 1D optical lattice. Clock transitions between two vibrational levels in the electronic ground state potential are driven via a two-photon Raman process. We achieve Rabi oscillations across the ground state potential and employ a magic wavelength technique to eliminate the differential light shift using narrow polarizability resonances. This allows us to increase coherence by three orders of magnitude to obtain a preliminary linewidth of ≈150 Hz for a 26 THz transition.

Starting with molecules in a single quantum state, we demonstrate dissociation into the scattering continuum at a narrow energy range. The angular distribution of photofragments in this basic chemical reaction reveals remarkable complexity. We study the competition between dissociation channels and their interaction with a magnetic field. Additionally, we identify a crossover from complex quantum mechanical behavior to certain quasiclassical limits at higher dissociation energies. The experiment is informed by state-of-the-art multichannel quantum chemistry theory which faithfully reproduces our observations.

Photoassociation and photoionization in a two-species Rb-Hg MOT

M. Witkowski[1,2], **R. Muñoz-Rodriguez**[1], **M. Borkowski**[1], **P. S. Żuchowski**[1], **R. Ciuryło**[1], **M. Zawada**[1]

[1] *Institute of Physics, Faculty of Physics, Astronomy and Informatics, Nicolaus Copernicus University in Toruń, Grudziadzka 5, 87-100 Toruń, Poland*

[2] *Institute of Physics, University of Opole, Oleska 48, PL-45-052 Opole, Poland*

e-mail: *mwitkowski@uni.opole.pl*

We present the detection of near-threshold bound states of excited heteronuclear Rb*Hg molecules through photoassociation spectroscopy [1] near the 795 nm Rb D1 line. The necessary ultracold mixture of Rb and Hg atomic gases was produced using a two-species magneto-optical trap (MOT) [2]. The interaction properties of the RbHg system as well as the prospects for photoassociation near Rb resonance lines and the production of RbHg molecules in their rovibrational ground state were recently analysed *ab initio* [3]. These theoretical predictions helped find and identify the photoassociation resonances.

Ground state molecules composed of an alkali-metal and a closed-shell atom, like RbYb[4] or RbHg, offer both permanent magnetic-dipole and electric-dipole moments thanks to their unpaired valence electron. Recently, magnetic Feshbach resonances were observed in such systems [5] providing a valuable tool for efficient control of atomic collisions. On the other hand, Hg is applicable in fundamental research with optical atomic clocks [6]. Dimers containing Hg were also proposed as good candidate species in the search for the electron electric dipole moment [7].

We also measure photoionization cross sections of the $5S_{1/2}$ and $5P_{3/2}$ states of ^{87}Rb in the Rb-Hg MOT using the Hg cooling laser operating at 254 nm. Since the 254 nm laser ionizes both the $5S_{1/2}$ and $5P_{3/2}$ states, we calibrate the latter state fraction by measuring the photoionization rate induced by an additional 401.5 nm laser. The photoionization cross section for the Rb $5P_{3/2}$ state at 401.5 nm agrees quantitatively with previous determinations[8].

[1] K. M. Jones, E. Tiesinga, P. D. Lett, and P. S. Julienne, Rev. Mod. Phys. **78**483 (2006).

[2] M. Witkowski, B. Nagrny, R. Muñoz-Rodriguez, R. Ciuryo, P. S. uchowski, S.Bilicki, M. Piotrowski, P. Morzyski, and M. Zawada, Opt. Express **91**879 (2017).

[3] M. Borkowski, R. Muñoz-Rodriguez, M. B. Kosicki, R. Ciuryo, and P. S. uchowski, Phys. Rev. A **96**063411 (2017).

[4] N. Nemitz, F. Baumer, F. Mnchow, S. Tassy, and A. Grlitz, Phys. Rev. A **79** 061403(R) (2009).

[5] V. Barbe, A. Ciamei, B. Pasquiou, L. Reichsollner, F. Schreck, P. S. uchowski, and J.M.Hutson, Nat. Phys. (2017) (in press) arXiv:1710.03093.

[6] K. Yamanaka, N. Ohmae, I. Ushijima, M. Takamoto, and H. Katori, Phys. Rev. Lett. **114** 230801 (2015).

[7] E. R. Meyer, J. L. Bohn Phys. Rev. A **80** 042508 (2009).

[8] T. P. Dinneen, C. D. Wallace, K.-Y. N. Tan, and P. L. Gould Opt. Lett. **17** 1706 (1992).

Towards quantum simulations with ultracold KCs molecules

A. Ratkata[1], **E. M. Bridge**[1], **D. Boddy**[1], **Z. Fu**[1], **J. Aldegunde**[2], **J. M. Hutson**[2] and **S. L. Cornish**[1]

[1] *Joint Quantum Centre (JQC) Durham-Newcastle, Department of Physics, Durham University, South Road, Durham DH1 3LE, U.K.*

[2] *Joint Quantum Centre (JQC) Durham-Newcastle, Department of Chemistry, Durham University, South Road, Durham DH1 3LE, U.K.*

e-mail: *apichayaporn.ratkata@durham.ac.uk*

Ultracold polar molecules, such as KCs, offer a wide range of exciting research areas thanks to their long-range anisotropic dipole-dipole interactions. Example applications include quantum simulation [1], precision measurement [2], and quantum chemistry [3]. In particular, ultracold heteronuclear molecules confined in optical lattices have been proposed as an ideal platform for simulating few-body phenomena in condensed-matter physics, specific applications include the study of electron interactions in the crystalized structure of solid-state materials, quantum magnetism [3] and bilayer superfluidity (Fig. 1) [4].

Our project aims to realize a molecular gas of ultracold KCs molecules in their rovibrational ground state. The recipe of molecule formation consists of three steps. First we will cool atomic samples of K and Cs to reach quantum degeneracy. Then, control of the magnetic fields will allow us to sweep across a Feshbach resonance to magnetoassociate the atoms to form highly excited KCs molecules. We will then use stimulated Raman adiabatic passage (STIRAP) to coherently transfer the molecules to their rotational, vibrational and hyperfine ground state. Previous experiments [5] followed by advances in theoretical calculations [6] have shown some heteronuclear molecular samples to undergo reactive collisions of the form $2AB \rightarrow A_2+B_2$ and $2AB \rightarrow A_2B+B$, considerably shortening their lifetime. Ground state KCs molecules have been shown to be non-reactive for all possible reaction paths [6]. KCs also has the advantage over other bi-alkali molecules in that we are able to produce both bosonic and fermionic molecules, which is important for simulating fermionic systems.

Our intermediate goal is to build an apparatus capable of cooling and trapping an ultracold mixtures of K and Cs atoms in order to precisely measure the interspecies Feshbach resonances of all K isotopes, building on the work done by M. Gröbner et al. [7]. To prepare trapped samples of ultracold Cs and K atoms, we aim to first make a Cs BEC as a benchmark of our system performance. We start off by pre-cooling Cs atoms in a 3D magneto-optical trap (MOT) loaded from a pyramid MOT and then compress the 3D MOT to increase the density. Degenerate Raman sideband cooling (DRSC) [8] will be implemented to further cool the atomic cloud before we load it into a reservoir dipole trap. To achieve Cs BEC, we will increase the phase-space density by loading into a dimple trap followed by evaporative cooling. Subsequently, we plan to use the ultracold Cs to sympathetically cool K atoms to achieve a quantum-degenerate mixture containing the K isotope of our choice. We present our recent results towards ultracold mixtures of Cs and K atoms.

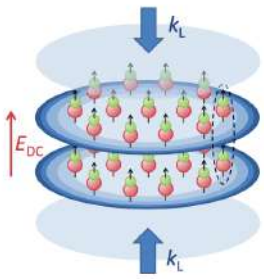


Figure 1: Ultracold fermionic $^{40}K^{133}Cs$ molecules confined in a one-dimensional optical lattice of two-dimensional pancake traps. The green spheres represent ^{40}K and the red spheres represent ^{133}Cs. The trap is constructed by interfering two counter-propagating laser beam having identical wavevector k_L. The dipole moments of the molecules are aligned by applying an external electric field E_{DC}. Such a system may be used to explore a bilayer superfluidity[4] which the dashed line represents an interlayer Cooper pair.

[1] I. M. Georgescu, S. Ashhab, and F. Nori, Rev. Mod. Phys. **86**(1), 153-185 (2014).

[2] L. D. Carr, D. DeMille, R. V. Krems, and J. Ye, New J. Phys. **11**, 055049 (2009).

[3] Bohn et al., Science **357**, 1002-1010 (2017).

[4] M.A. Baranov et al., Phys. Rev. A 83, 043602 (2011).

[5] S. Ospelkaus et al., Science 327, 853-857 (2010).

[6] P. S. Żuchowski and J. M. Hutson, Phys. Rev. A, **81**(6), 060703 (2010).

[7] M. Gröbner et al., Phys. Rev. A, **95**(2), 022715, (2017).

[8] A. J. Kerman, V. Vuleti, C. Chin, and S. Chu, Phys. Rev. Lett., **81**, 439 (2000).

Towards ground state CsYb molecules

K. E. Wilson[1], **A. Guttridge**[1], **J. Segal**[1], **M. D. Frye**[2], **J. M. Hutson**[2], **and S. L. Cornish**[1]

[1] *Joint Quantum Centre (JQC) Durham-Newcastle, Department of Physics, Durham University, South Road, Durham DH1 3LE, United Kingdom.*

[2] *Joint Quantum Centre (JQC) Durham-Newcastle, Department of Chemistry, Durham University, South Road, Durham DH1 3LE, United Kingdom.*

e-mail: *kali.e.wilson@durham.ac.uk*

Ultracold dipolar molecules provide a promising experimental platform for atomic and molecular physics with applications for studies of quantum matter, many-body physics, and ultracold chemistry. Heteronuclear $^2\Sigma$ molecules such as CsYb have both an electric and a magnetic dipole moment in the electronic ground state. In addition to the long-range dipole-dipole interactions, the additional degree of freedom afforded by the magnetic dipole moment makes CsYb a promising environment for quantum simulations of lattice spin models [1]. Such studies will require high phase-space densities of molecules confined in optical traps or lattices.

We present progress towards a dual-degenerate gas of Cs and Yb atoms in a bichromatic optical dipole trap, a critical step for producing ground state CsYb molecules. Recent interspecies thermalization [2] and two-photon photoassociation [3] measurements allow more accurate calculation of the interspecies scattering lengths shown in Fig. 1, and identification of experimentally-feasible Feshbach resonances for magnetoassociation of Cs and Yb, as recently observed in SrRb [4]. We will discuss the prospects for producing miscible degenerate mixtures and will outline our plans to produce CsYb molecules by magnetoassociation.

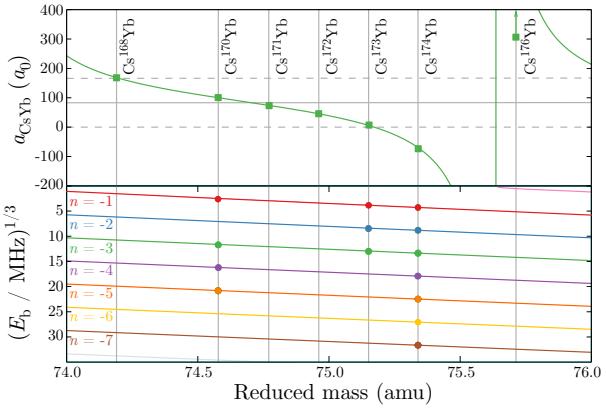


Figure 1: CsYb scattering length for all isotopologs. The CsYb interaction potential is fitted to two-photon photoassociation measurements of the binding energy (E_b) of the $X^2\Sigma^+_{1/2}$ potential for different CsYb isotpologs. The upper panel shows the CsYb scattering length as a function of reduced mass, with the masses of stable CsYb isotpologs shown by vertical gray lines. The horizontal solid gray line shows the value of the mean scattering length, $\bar{a}$. The lower panel shows the binding energy of vibrational levels versus reduced mass. The solid colored circles are experimentally measured binding energies and the solid colored lines are a fit of the molecular potential to the binding energy measurements.

[1] A. Micheli, G. K. Brennen and P. Zoller, Nat. Phys. **2**, 341 (2006).

[2] A. Guttridge, S. A. Hopkins, S. L. Kemp, M. D. Frye, J. M. Hutson, and S. L. Cornish, Phys. Rev. A **96**, 012704 (2017).

[3] A. Guttridge, M. D. Frye, B. C. Yang, J. M. Hutson, and S. L. Cornish, (in preparation).

[4] V. Barbé, A. Ciamei, B. Pasquiou, L. Reichsöllner, F.Schreck, P. S. Zuchowski, and J. M. Hutson, arXiv:1710.03093 (2017).

The DESIREE storage ring

D. Hanstorp[1], J. Sundberg [1], M. K. Kristiansson[2], O. M. Hole[2], G. Eklund[2], E. K. Anderson[2], K. Chartkunchand[2], P. Löfgren[2], A. Simonsson[2], A. Källberg[2], P. Reinhed[2], N. de Ruette[2], S. Rosén[2], R. D. Thomas[2], J. D. Alexander[2], M. Blom[2], M. Björkhage[2], M. Gatchell[2], M. H. Stockett[2], H. Hartman[3], H. Zettergren[2], H. Cederquist[2] and H. T. Schmidt[2]

[1] *Department of Physics, University of Gothenburg, SE 412 96 Gothenburg, Sweden*
[2] *Department of Physics, Stockholm University, SE 10691 Stockholm, Sweden*
[3] *Materials Science and Applied Mathematics, Malmö University, SE 20506 Malmö, Sweden*
e-mail: *dag.hanstorp@gu.se*

DESIREE (Double ElectroStatic Ion Ring ExpEriment), shown in Fig. 1, is a world-unique facility for studies of individual reactions with ions in well-defined quantum states [1, 2]. It is one of only three cryogenic ion-beam storage rings in operation worldwide and the only one where ion-ion interactions, important for e.g. interstellar processes, can be investigated. The facility has two 8.6 m circumference storage rings in a 13-Kelvin chamber where ion beams of atoms, molecules or clusters are stored and merged. This allows for unique studies of quantum-state resolved interactions of individual anion-cation pairs.

Since January 2018 a consortium consisting of Stockholm University, the University of Gothenburg and Malmö University operates DESIREE as a Swedish national infrastructure financed by the Swedish Research Council. The facility is open for beam-time for international users. Details about the facility and how to apply for beam-time can be found on the link https://www.desiree-infrastructure.com/.

This poster will present an overview of the experimental facility, and short descriptions of different types of experiments that have been conducted so far. The main feature of DESIREE is that the double ring system facilitates investigations of collisions between positive and negative ions at very low collision energies. Results of the first such test experiments will be presented. Second, investigations of lifetimes of excited states in atomic [3] and molecular [4] ions and the stability of negatively charged molecules and clusters, which can be investigated by using one of the two rings, will be discussed. Finally, an overview of how the quantum states of stored ions can be manipulated using pulsed or CW lasers interacting either in a crossed or collinear geometry will be presented [4].



Figure 1: The DESIREE storage rings in their cryogenic enclosure.

[1] R. D. Thomas *et al*, Rev. Sci. Instrum. **82**, 065112 (2011).

[2] H. T. Schmidt *et al*, Rev. Sci. Instrum. **84**, 055115 (2013).

[3] E. Bäckström *et al*, Phys. Rev. Lett. **114**, 143003 (2015).

[4] H. T. Schmidt *et al*, Phys. Rev. Lett. **119**, 073001 (20177).

Atom-molecule coherence in heteronuclear Yb-Li

A. Green[1], **J.H. See Toh**[1], **K. Ton**[1], **and S. Gupta**[1]
[1]*Department of Physics, University of Washington, Seattle, Washington, 98195 USA*
e-mail: *agreen13@uw.edu*

We have demonstrated coherent coupling between Yb+Li free atom pairs and YbLi molecules in the electronic ground state via two-photon free-bound Raman processes. Coherent control is manifest in the creation of a dark atom-molecule superposition state. Evidence for this dark state is observed in a crossed optical dipole trap containing a mixture of ultracold ^{6}Li and ^{174}Yb, as the suppression of photoassociative loss within a narrow (sub-natural) frequency range. We intend to utilize this dark state to perform Stimulated Raman Adiabatic Passage (StiRAP) to create ultracold samples of YbLi in the electronic ground state. The non-bialkali YbLi molecule possesses both electric and magnetic dipole moments, and the unpaired electron degree of freedom could be utilized towards magnetic trapping of ultracold molecules as well as tuning of molecular collisions and reactions.

Towards trapping of a single molecule in an optical tweezer

S. Jurgilas[1], **J.Rodewald**[1],**N. Fitch**[1], **B.E. Sauer**[1], **E.A. Hinds**[1], **and M.R. Tarbutt**[1]

[1] *Centre for Cold Matter, Blackett Laboratory, Imperial College London, Prince Consort Road, London SW7 2AZ, UK*

e-mail: *s.jurgilas16@imperial.ac.uk*

Recent advances in the production of ultracold dipolar molecules [1] make it feasible to build versatile quantum simulators with single molecules as the fundamental entities. Such simulators may be used to investigate problems intractable to even the most powerful conventional computers. To demonstrate the fundamental building block of a quantum simulator we are designing an experiment to trap a single CaF molecule in an optical tweezer, cool it to its motional ground state and demonstrate full quantum state control. The large electric dipole moment of CaF may in principle be tuned on demand and various arbitrary interaction potentials created to mimic a wide range of quantum many body systems [2].

The experimental sequence for trapping a single molecule will begin by capturing CaF in a MOT after an initial stage of 1-D slowing and cooling. The molecules can then be cooled to below 50 μK in an optical molasses. The molecules will then be transferred to a moving magnetic trap and transported to a science chamber where the tweezer experiment will take place. Here, an optical molasses will provide a dissipative mechanism for the molecule to cool into the optical trap and will make the molecule bright to our imaging system.

To create the optical tweezer itself we will employ techniques developed for trapping single atoms [3]. A high numerical aperture aspheric lens inside the vacuum chamber will be used to both focus the far off-resonant trapping light and collect the fluorescence of the trapped molecule. An imaging system capable of registering small numbers of photons will be used to detect the presence of a trapped molecule and trigger the single particle experiments.

We will present our progress in developing this new apparatus for studying many-body quantum physics.

References

[1] Truppe, S., et al. "Molecules cooled below the Doppler limit." Nature Physics 13.12 (2017): 1173.

[2] Micheli, Andrea, G. K. Brennen, and Peter Zoller. "A toolbox for lattice-spin models with polar molecules." Nature Physics 2.5 (2006): 341.

[3] Nogrette, Florence, et al. "Single-atom trapping in holographic 2D arrays of microtraps with arbitrary geometries." Physical Review X 4.2 (2014): 021034.

Ultracold YbF molecules for measuring the electron's electric dipole moment

J. Lim, M. A. Trigatzis, J. R. Almond, J. A. Devlin, N. J. Fitch, B. E. Sauer, M. R. Tarbutt and E. A. Hinds

Centre for Cold Matter, Blackett Laboratory, Imperial College London, Prince Consort Road, London SW7 2AZ, United Kingdom

e-mail: *m.trigatzis15@imperial.ac.uk*

The electron's electric dipole moment (eEDM) may be measured by observing electric field-induced spin precession in YbF molecules [1]. Theories that extend the Standard Model generally contain additional sources of charge conjugation and parity (CP) symmetry violation and predict an eEDM that is large enough to be measured by today's experiments. Recent measurements [1, 2, 3] already strongly constrain some of these theories.

Laser cooling of a beam of diatomic molecules was first demonstrated in 2010 [4], and this new field promises a number of applications including cold chemistry, quantum simulations and quantum information, and precision measurements. A laser-cooled beam of YbF could increase the eEDM experiment's sensitivity by two orders of magnitude [5]. We recently demonstrated one-dimensional sub-Doppler transverse laser cooling of our YbF cryogenic buffer gas beam to below 100 μK [6], investigated the magnetically assisted and polarisation gradient Sisyphus cooling mechanisms, and successfully modelled our experiment.

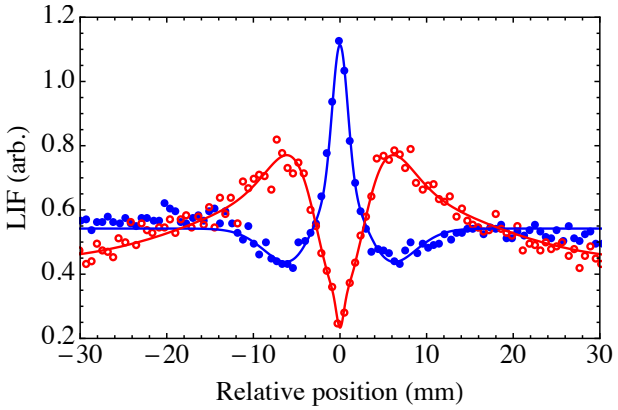


Figure 1: One-dimensional position distributions of YbF beams, measured by imaging laser-induced fluorescence (LIF). The figure shows evidence of laser cooling for blue detuning (blue, filled circles) and heating for red detuning (red, unfilled circles). The curves are a four-Gaussian fit used to place an upper limit on the 1D temperature of the molecular beam, as described in ref. [6].

[1] J. J. Hudson, D. M. Kara, I. J. Smallman, B. E. Sauer, M. R. Tarbutt, and E. A. Hinds, Nature **473**, 493 (2011).

[2] J. Baron, W. C. Campbell, D. DeMille, J. M. Doyle, G. Gabrielse, Y. V. Gurevich, P. W. Hess, N. R. Hutzler, E. Kirilov, I. Kozyryev, B. R. O'Leary, C. D. Panda, M. F. Parsons, E. S. Petrik, B. Spaun, A. C. Vutha, and A. D. West, Science **343**, 269 (2014).

[3] W. B. Cairncross, D. N. Gresh, M. Grau, K. C. Cossel, T. S. Roussy, Y. Ni, Y. Zhou, J. Ye, E. A. Cornell, Phys. Rev. Lett. **119**, 153001 (2017).

[4] E. S. Shuman, J. F. Barry, and D. DeMille, Nature **467**, 820 (2010).

[5] M. R. Tarbutt, B. E. Sauer, J. J. Hudson, and E. A. Hinds, New J. Phys. **15**, 053034 (2013).

[6] J. Lim, J. R. Almond, M. A. Trigatzis, J. A. Devlin, N. J. Fitch, B. E. Sauer, M. R. Tarbutt and E. A. Hinds, Phys. Rev. Lett. **20**, 123201 (2018).

Control of atom-ion reactions at low temperatures

Michael Mills[1], **Prateek Puri**[1], **Elizabeth West**[1], **Christian Schneider**[1], **Eric Hudson**[1]
[1] *Department of Physics and Astronomy, University of California – Los Angeles, Los Angeles, California, 90095, USA*
e-mail: *mcmills@ucla.edu*

We discuss experiments performed in the MOTion trap, a hybrid atom-ion trap comprised of a linear quadrupole trap and a co-located magneto-optical trap. We first present the synthesis of $BaOCa^+$, the first molecule of its type to be observed. With the tools of the MOTion trap, we identify and investigate the mechanism of its formation via the barrierless reaction of Ca (^3P_J) with $BaOCH_3^+$. Next, we describe our studies of excited-state atom-ion reactions at low temperatures. We observe a suppression of the reaction rate at low temperature due to the electric field of the ion shifting the transition energies of the neutral, and we propose a general method to eliminate this suppression, enabling control of low-temperature atom-ion reactions. Finally, we introduce a new method of controlling collision energy. By varying the axial confinement voltages of our ion trap, we shuttle the ions through the cloud of neutral atoms, providing a general technique with energy resolutions improved over current methods by an order of magnitude for collision temperatures ranging from a few mK to 10s of K.

Optical transport of ultracold atoms for the production of groundstate RbYb

T. Franzen[1], **B. Pollklesener**[1], **F. Türck**[1], **A. Görlitz**[1]
[1] *Institut für Experimentalphysik, Heinrich-Heine-Universität Düsseldorf, Germany*
e-mail: *axel.goerlitz@hhu.de*

Ultracold dipolar molecules constitute a promising system for the investigation of topics like ultracold chemistry, novel interactions in quantum gases, precision measurements and quantum information.

Here we report on a versatile transport apparatus for the production of ultracold RbYb molecules. This setup constitutes an improvement of our old apparatus, where the interactions in RbYb and possible routes to molecule production have already been studied extensively [1,2]. In the new setup a major goal is the efficient production of ground state RbYb molecules.

We employ optical tweezers to transport individually cooled samples of ultracold Rb and Yb from their separate production chambers to a dedicated science chamber. Here we transfer the atoms to a crossed dipole trap, where further evaporative cooling creates a starting point for the exploration of interspecies interactions and pathways towards ground state molecules.

[1] M. Borkowski et al., PRA 88, 052708 (2013)
[2] C. Bruni et al., PRA 94, 022503 (2016)

Theoretical description of photodissociation of ultracold diatomic molecules

I. Majewska[1] **and R. Moszyński**[1]

[1] *Faculty of Chemistry, University of Warsaw, Pasteura 1, 02-093 Warsaw, Poland*

e-mail: *iwona.ewa.majewska@gmail.com*

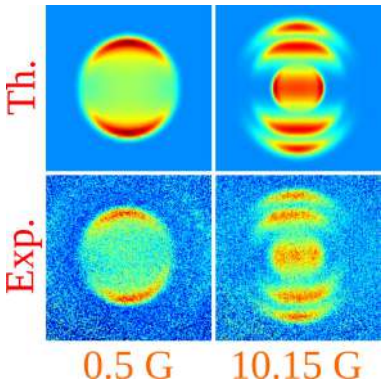


Figure 1: Experimental image compared with the quantum prediction for different magnetic fields.

Chemistry and physics of ultracold (below 1 mK) molecules is a fast growing field with wide possibilities for future applications. One of them is the control of the chemical reactions dynamics. The reaction investigated experimentally by the group of Tanya Zelevinsky at the Columbia University in New York was a light-induced photodissociation of the diatomic strontium molecule $Sr_2 \rightarrow Sr + Sr$. The experiment was performed with the full control over the initial quantum states of the molecule and final states of the fragments. After a controlled decay, the fragments were recorded, creating 2D patterns (Fig. 1).

The theoretical description of the experimental results is based on the formula for the photodissociation cross section

$$\sigma(\theta,\phi) = \sum_{l=0}^{\infty}\sum_{m=0}^{l} \beta_{lm} P_l^m(\cos\theta)\cos(l\phi), \qquad (1)$$

where (θ,ϕ) are the scattering angles and β_{lm} are anisotropy parameters. In the full quantum model, the formulas for the anisotropy parameters were derived using Fermi golden rule with the appropriate transition operator and the wave functions of the initial molecule and final photodissociated fragments [2].

The theoretical results fully explained unexpected experimental findings. It was proven that the well-known quasiclassical model of the photodissociation [3] is not sufficient to describe the experiment with full quantum state control.

The photodissociation model was extended to the case where the total angular momentum is not conserved. The violation of the $\Delta J = 0, \pm 1$ selection rule for E1 transition in the magnetic field due to the Zeeman interaction was observed experimentally and supported by the quantum mechanical calculations [1]. The Sr_2 molecules were prepared in the specific rovibrational level of the electronic ground state and photodissociated to the first excited continuum. Since the ground state of strontium is nearly non-magnetic, the magnetic field effect was introduced via the continuum wave function of the fragments. The theoretical model fully explained surprisingly complicated experimental patterns by including higher angular momenta and predicting strong mixing of partial waves in the photofragment continuum.

The crossover between the quantum and classical regime was studied both experimentally [4] and theoretically [5]. For higher energies above the continuum, the photodissociation patterns converge to its axial recoil limit. In some cases it is well described by the widely used quasiclassical approximation [3], but sometimes the bosonic or fermionic quantum statistics of the identical nuclei causes the quasiclassical approximation to fail.

The authors would like to thank ZLAB: the experimental group of Tanya Zelevinsky from the Columbia University in New York for a very fruitful collaboration.

[1] M. McDonald, I. Majewska, C.-H. Lee, S. S. Kondov, B. H. McGuyer, R. Moszynski, and T. Zelevinsky, *Phys. Rev. Lett*, **120**, 033201 (2018).

[2] M. McDonald, B. H. McGuyer, F. Apfelbeck, C.-H. Lee, I. Majewska, R. Moszynski, and T. Zelevinsky, *Nature*, **535**, 122 (2016).

[3] R. Zare, *Mol. Photochem.*, **4**, 1 (1972).

[4] S. S. Kondov, C.-H. Lee, M. McDonald, B. H. McGuyer, I. Majewska, R. Moszynski, and T. Zelevinsky, arXiv:1805.08850 (2018).

[5] I. Majewska, S. S. Kondov, C.-H. Lee, M. McDonald, B. H. McGuyer, R. Moszynski, and T. Zelevinsky, arXiv:1805.09482 (2018).

Towards Magneto-Optical Trapping of Polyatomic Molecules

L. Baum[1,2], **I. Kozyryev**[1,2], **P. Yu**[1,2], **and J. M. Doyle**[1,2]
[1] *Department of Physics, Harvard University, Cambridge, MA, USA*
[2] *Harvard-MIT Center for Ultracold Atoms*
e-mail: *louis@cua.harvard.edu*

The scientific promise of ultracold molecules in fields ranging from quantum computation to particle physics lies in these features: vibrations, rotations, and body-frame properties such as electric dipole moment and angular momentum projection. The properties of these additional (compared to atoms) quantum states make this scientific frontier worth exploring. For example, a non-zero projection of Orbital angular momentum (electronic or nuclear) along the molecular axis results in a linear stark shift at very low applied electric fields, along with pairs of fully polarized, narrowly split molecular orientation states. These states are found generically in polyatomic molecules as they can arise from vibrations (in all polyatomics, including linear triatomics) and certain rotations (e.g. in symmetric tops). Such states could enable novel quantum information platforms and particle physics applications with polyatomic molecules in the ultracold regime [1, 2].

Molecular complexity, on the other hand, presents technical challenges to laser cooling. In diatomic molecules these challenges were recently overcome to produce magneto optical traps (MOTs) [3, 4, 5], sub-Doppler cooling, and trapping using both magnetic(CaF and SrF [6, 7]) and optical (CaF [8]) fields. We are now working to extend the full arsenal of laser cooling and trapping methods to polyatomic molecules. We recently demonstrated laser cooling of one of the simplest types of polyatomic molecules, triatomics, with SrOH [9] and are continuing this work by developing a MOT for CaOH. We are further building on experimental and theoretical results [10, 11] to implement laser cooling of hexatomic symmetric top molecules, e.g. $CaOCH_3$,and even larger molecules, including diastereomic and enantiomeric species.

[1] M. L. Wall et al. New J. Phys.**17** 025001 (2015).

[2] I. Kozyryev et al. PRL **119** 133022 (2017).

[3] E. B. Norrgard et al. PRL **116** 063004 (2016).

[4] S. Truppe et al. Nat. Phys. **13** 1173 (2017).

[5] L. Anderegg et al. PRL **119** 103201 (2017).

[6] H. Williams et al. PRL **120** (2018).

[7] D. J. McCarron et al. arXiv:1712.01462 (2017).

[8] L. Anderegg et al. arXiv:1712.01462 accepted Nat. Phys. (2018).

[9] I. Kozyryev et al. PRL **118** 173201 (2017).

[10] I. Kozyryev et al.Chem. Phys. Chem. **17** (2016).

[11] T. A. Isaev and R. Berger. PRL **116** 063006 (2016).

We demonstrate laser cooling and non-destructive imaging of optically trapped CaF molecules. $\Lambda-$enhanced grey molasses cools the CaF molecules 5 μK allowing us to load the molecules into an optical dipole trap. Optical trapping lays the groundwork for many research directions, including ultracold collisions and chemistry, quantum simulations, and new precision measurements. A particularly promising avenue is constructing optical tweezer arrays of molecules, where one can realize full quantum control in a scalable platform. In addition, the ability to cool optically trapped molecules opens up new paths towards quantum degeneracy.

Order of magnitude increased sensitivity to the electron electric dipole moment

Z. D. Lasner[1], **V. Andreev**[2], **D. G. Ang**[3], **D. DeMille**[1], **J. Doyle**[3], **G. Gabrielse**[4], **J. Haefner**[3], **N. R. Hutzler**[5], **C. Meisenhelder**[3], **B. R. O'Leary**[1], **C. D. Panda**[3], **A. D. West**[6], **E. P. West**[6], **X. Wu**[1,3]

[1] *Department of Physics, Yale University, New Haven, CT, USA*
[1] *Max Planck Institute of Quantum Optics, Garching, Germany*
[3] *Department of Physics, Harvard University, Cambridge, MA, USA*
[4] *Department of Physics, Northwestern University, Evanston, IL, USA*
[5] *Department of Physics, California Institute of Technology, Pasadena, CA, USA*
[6] *Department of Physics, University of California, Los Angeles, CA, USA*
e-mail: *zack.lasner@yale.edu*

Measurement of the electron electric dipole moment (eEDM) provides a powerful probe of physics beyond the Standard Model. We report on our recent measurement, which improves upon the sensitivity of the 2014 result, $|d_e| < 9 \times 10^{-29}\, e \cdot \mathrm{cm}$ [1], by an order of magnitude. More efficient state preparation, improved fluorescence signal detection, and larger molecular beam solid angle subtended by the science region collectively increase the detected molecule number by a factor of 400 and hence reduce the statistical shot-noise uncertainty by over an order of magnitude. Imperfections in laboratory fields and laser parameters such as power and polarization can lead to systematic errors, i.e., eEDM-mimicking effects. By exaggerating dozens of experimental parameters, we investigate possible systematic errors and limit their total contribution to a level below the statistical sensitivity. We describe in detail the improved apparatus as well as mechanisms for systematic errors that were observed, characterized, and suppressed.

[1] ACME Collaboration, Science **343** 269-272 (2014).

Is laser cooling without spontaneous emission possible?

Thierry Chanelière, Daniel Comparat and Hans Lignier
Laboratoire Aimé Cotton, CNRS, Univ. Paris-Sud, ENS Paris Saclay, Université Paris-Saclay, Bât. 505, 91405 Orsay, France
e-mail: *daniel.comparat@u-psud.fr*

It is usually believed that the phase-space density (PSD) of non interacting particles cannot be increased by using only pure Hamiltonian evolution and any PSD increase would require some dissipation mechanism [1]. In the context of laser cooling, this dissipation is usually ensured by spontaneous emission. In recent years, several papers claimed to have experimentally demonstrated an optical cooling where spontaneous emission is supposed to play no role. This counter intuitive results was also supported by theoretical arguments and semi-classical simulations using classical laser fields. This of course triggered a debate [2, 3, 4, 5].

We study the possibility to enhance the phase space density of non interacting particles submitted to a classical laser field without spontaneous emission. We clearly state that, when no spontaneous emission is present, a quantum description of the atomic motion is more reliable than semi-classical description which can lead to large errors especially if no care is taken to smooth structures smaller than the Heisenberg uncertainty principle. Whatever the definition of position - momentum phase space density used, its gain is severely bounded especially when started from a thermal sample. More precisely, the maximum phase space density, can only be improved by a factor M for a M levels atoms. This simply comes from a transfer between external and internal degree of freedoms. Ways to circumvent this theorem is by using non coherent field states, informational feedback cooling schemes, or by allowing a single spontaneous emission event or collectives states between fields and atoms.

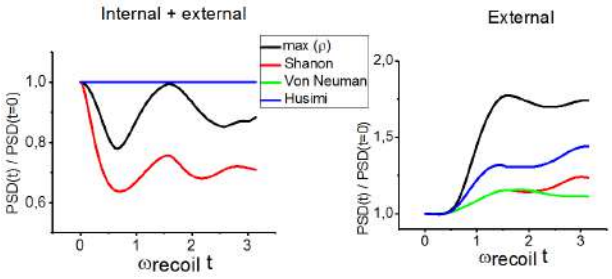


Figure 1: Evolution of several phase space density measurement: Husimi, maximum density matrix, Von-Neuman and Shanon entropies under 4 pi pulses Left: evolution for the total (external + internal degree of freedom). Right: only external degree of freedom, where we clearly see that the phase space density can increase but only by a factor 2 for this 2 level system.

References

[1] W. Ketterle and D. E. Pritchard. Atom cooling by time-dependent potentials. *Phys. Rev. A*, 46:4051–4054, October 1992.

[2] C. Corder, B. Arnold, and H. Metcalf. Laser Cooling without Spontaneous Emission. *Physical Review Letters*, 114(4):043002, January 2015.

[3] Harold Metcalf. Colloquium: Strong optical forces on atoms in multifrequency light. *Rev. Mod. Phys.*, 89:041001, Oct 2017.

[4] M. A. Norcia, J. R. K. Cline, J. P. Bartolotta, M. J. Holland, and J. K. Thompson. Narrow-line laser cooling by adiabatic transfer. *New Journal of Physics*, 20(2):023021, February 2018.

[5] G. P. Greve, B. Wu, and J. K. Thompson. Laser Cooling with Adiabatic Transfer on a Raman Transition. *ArXiv e-prints*, May 2018.

Coherent control of ultracold ground-state $^{87}Rb^{133}Cs$ molecules in an optical trap

Phil Gregory[1], Jacob Blackmore[1], Rahul Sawant[1], Jesus Aldegunde[2], Jeremy M. Hutson[3], and Simon L. Cornish[1]

[1] *Joint Quantum Centre (JQC) Durham-Newcastle, Department of Physics, Durham University, South Road, Durham DH1 3LE, UK*

[2] *Departamento de Quimica Fisica, Universidad de Salamanca, 37008 Salamanca, Spain*

[3] *Joint Quantum Centre (JQC) Durham-Newcastle, Department of Chemistry, Durham University, South Road, Durham DH1 3LE, UK*

e-mail: *s.l.cornish@durham.ac.uk*

The formation of ultracold heteronuclear molecules possessing long-range dipole-dipole interactions opens up many exciting areas of research spanning precision measurement, quantum computation, quantum simulation, ultracold chemistry and fundamental studies of quantum matter. Long-lived, trapped samples of molecules with full quantum control of the molecular internal state are crucial to many of these applications.

Here we demonstrate coherent microwave control of the rotational and hyperfine state of ultracold, chemically stable $^{87}Rb^{133}Cs$ molecules. We create up to 4000 molecules in the rovibrational and hyperfine ground state at a temperature of $\simeq 1.2\mu$K and a peak density of $\simeq 10^{11}\,\mathrm{cm}^{-3}$ using magnetoassociation on a Feshbach resonance [1] followed by optical transfer using stimulated Raman adiabatic passage [2]. We then use precision microwave spectroscopy of the rotational transition to probe the rich hyperfine structure of the molecule and exploit coherent Rabi oscillations to transfer the total population of molecules between hyperfine levels [3]. We subsequently investigate the AC Stark effect due to the trapping light in low-lying rotational levels and reveal a rich energy structure with many avoided crossings (see Fig. 1) between hyperfine states [4].

Understanding the AC Stark shift allows us to trap the molecules in a range of internal states. We study the collisional lifetimes of the molecules in such traps for various rotational and hyperfine states, shedding light on the 'sticky collision' issue [5]. Finally, we describe our future plans for imaging and addressing of single molecules in ordered arrays as a basis for quantum simulation of models relevant to quantum magnetism.

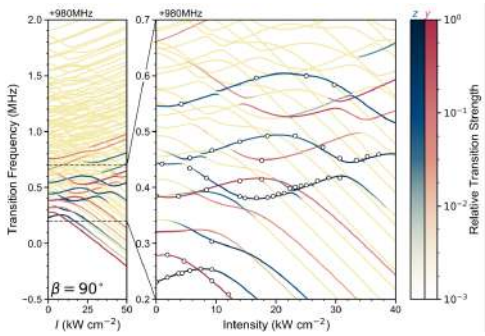


Figure 1: AC Stark shift of the microwave transition between $N = 0, M_F = +5$ and $N = 1$ in $^{87}Rb^{133}Cs$ molecules for the trapping laser polarised orthogonal to the magnetic field [4].

[1] M. P. Köppinger, D. J. McCarron, D. L. Jenkin, P. K. Molony, H.-W. Cho, C. R. Le Sueur, C. L. Blackley, J. M. Hutson and S. L. Cornish, Phys. Rev. A **89**, 033604 (2014).

[2] P. K. Molony, P. D. Gregory, Z. Ji, B. Lu, M. P. Köppinger, C. R. Le Sueur, C. L. Blackley, J. M. Hutson, and S. L. Cornish, Phys. Rev. Lett. **113**, 255301 (2014).

[3] P. D. Gregory, J. Aldegunde, J. M. Hutson, and S. L. Cornish, Phys. Rev. A **94**, 041403(R) (2016).

[4] P. D. Gregory, J. A. Blackmore, J. Aldegunde, J. M. Hutson, and S. L. Cornish, Phys. Rev. A **96**, 021402(R) (2017).

[5] M. Mayle, G. Quéméner, B. P. Ruzic, and J. L. Bohn, Phys. Rev. A **87**, 012709 (2013).

Prospects for formation of ultracold RbSr molecules : Novel implementation of an optical Feshbach resonance

A.Devolder[1], **E. Luc-Koenig**[1], **M. Desouter-Lecomte**[2], **O. Atabek**[3] **and O. Dulieu** [1]

[1] *Laboratoire Aimé Cotton, CNRS, Univ. Paris-Sud, ENS Cachan, Univ. Paris-Saclay 91405 Orsay, France*

[2] *Laboratoire de Chimie Physique, CNRS, Univ. Paris-Sud, Univ. Paris-Saclay, 91405 Orsay, France*

[3] *Institut des Sciences Moléculaires d'Orsay, CNRS, Univ. Paris-Sud, Univ. Paris-Saclay 91405 Orsay, France*

e-mail: *adrien.devolder@u-psud.fr*

Compared to ultracold atoms, ultracold polar molecules have a rich internal structure and strong anisotropic interactions that make them promising for high-precision measurements, for discovering new types of quantum matter, or for quantum simulation. Open-shell polar molecules composed of an alkali-metal atom and an akaline-earth atom (like RbSr) are particularly suited for such applications [1]. The pioneering method to create ground-state ultracold molecules is photoassociation (PA), namely the resonant excitation of the scattering state of an atom pair into a bound level of an excited molecular state (Fig. 1), followed by spontaneous emission (SE). In ongoing PA experiments on RbSr [2], a PA laser is slightly red-detuned from the Sr intercombination transition $5s^2\,{}^1S \rightarrow 5s5p\,{}^3P_1$. The observed PA rates are very weak. Using the methodology of Ref. [3] and our potential energy curves [4], we show that these low PA rates originate from the forbidden nature of the atomic transition. We have also modeled PA toward the molecular states correlated to the Rb allowed transition $5s\,{}^2S \rightarrow 5p\,{}^2P$. The computed PA rates are found higher by about 5 orders of magnitude than in the previous case. However SE mainly populates weakly-bound levels of the electronic ground state.

Assuming that the atoms are initially confined in a tight optical trap, the initial scattering state can be represented as a discrete motional level of the trap. A coherent population transfer like STIRAP (Stimulated Raman Adiabatic Passage) could then be applied. Our simulation of a STIRAP process from the lowest trap level to the absolute ground state leads to unrealistic laser intensities. However, the creation of molecules in a well-defined weakly-bound level is found efficient. A second STIRAP sequence could be implemented for populating the absolute ground state. Our calculations lead to quite tedious experimental conditions, while feasible in principle. Note that a STIRAP process implemented starting from the recently discovered magnetic Feshbach resonances in RbSr [5] would lead to a similar conclusion.

To circumvent these difficulties, we propose a novel implementation of an optical Feshbach resonance based on the dressing of the molecular ground state by infrared photons. We show that the PA rate can be enhanced by 6 orders of magnitude as in the case of Feshbach-Optimized PA [6], and that the PA levels preferentially relax down to the absolute ground state. In this context, we will discuss further the creation of ground-state molecules using an adiabatic frequency ramp (chirp).

[1] A. Micheli, G. et al. , Nature Physics **2**,341-347 (2006)

[2] F.Schreck , private communication (2017)

[3] A. Fioretti et al. , Eur. Phys. J. D **15**,189-198 (2001)

[4] P. Zuchowski et al. , Phys. Rev. A **90**,012507 (2014)

[5] V.Barb et al.; `https://arxiv.org/abs/1710.03093` (2017)

[6] P. Pellegrini, Phys. Rev. Lett **101**, 053201 (2008)

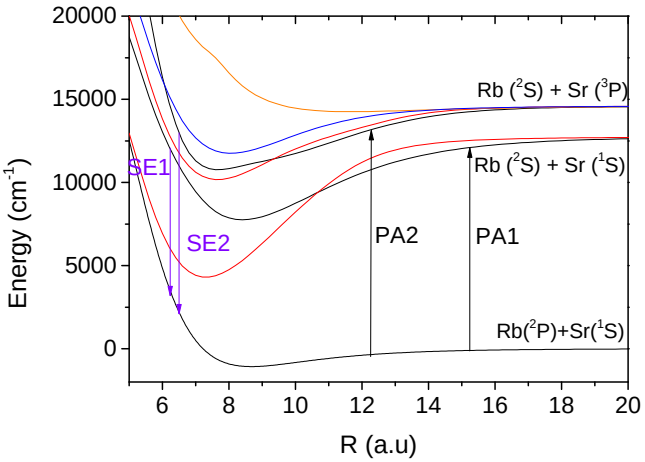


Figure 1: Computed RbSr potential energy curves: PA1 and SE1 (resp. PA2 and SE2) involve the molecular states correlated to the allowed (resp. forbidden) atomic transition in Rb (resp. Sr)

State selection, magnetic trapping and coherent control of laser-cooled molecules

L. Caldwell, H. J. Willams, N. J. Fitch, S. Truppe, J. Rodewald, E. A. Hinds, B. E. Sauer, M. R. Tarbutt

Centre for Cold Matter, Blackett Laboratory, Imperial College London, Prince Consort Road, London, SW7 2AZ UK

e-mail: *l.caldwell@imperial.ac.uk*

In the last few years, magneto-optical traps (MOTs) for simple diatomic molecules have been realised for the first time [1, 2, 3]. Further cooling in an optical molasses has proven an effective method to produce samples of molecules in the ultracold regime [2]. Most of the proposed applications for ultracold molecules, including simulation of strongly interacting quantum many-body Hamiltonians, precision tests of fundamental physics and utilisation in quantum information processing, require coherent control over the internal state of the molecular sample.

We present optical pumping of a sample of ultracold CaF molecules into a single internal state, transfer to a conservative magnetic trap and coherent microwave control over their rotational, hyperfine and Zeeman sub levels [4]. As prototypes of future experiments possible with laser-cooled molecules, we demonstrate state dependent measurements of magnetic trap loss rates and explore rotational coherence times in and out of the trap using Ramsey interferometry (shown in Fig. 1).

[1] J. F. Barry, D. J. McCarron, E. B. Norrgard, M. H. Steinecker and D. DeMille, Nature **512**, 286 (2014).

[2] S. Truppe, H. J. Williams, M. Hambach, L. Caldwell, N. J. Fitch, E. A. Hinds, B. E. Sauer and M. R. Tarbutt, Nat. Phys. **13**, 1173-1176 (2017).

[3] L. Anderegg, B. L. Augenbraun, E. Chae, B. Hemmerling, N. R. Hutzler, A. Ravi, A. Collopy, J. Ye, W. Ketterle and J. M. Doyle, Phys. Rev. Lett. **119**, 103201 (2017).

[4] H. J. Williams, L. Caldwell, N. J. Fitch, S. Truppe, J. Rodewald, E. A. Hinds, B. E. Sauer and M. R. Tarbutt, Phys. Rev. Lett. forthcoming.

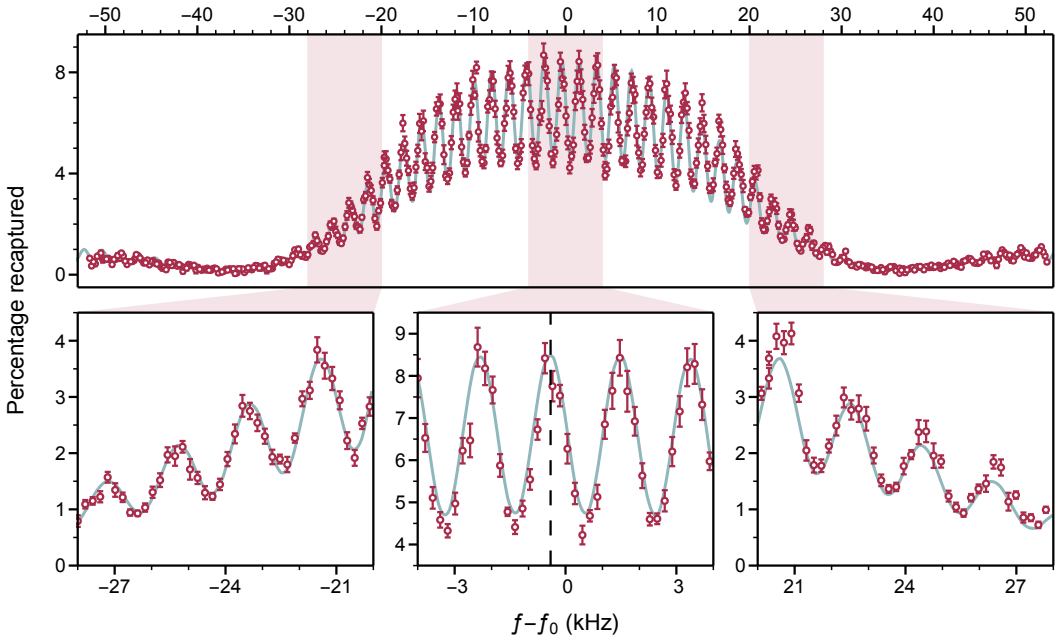


Figure 1: Ramsey spectroscopy for CaF molecules confined in a magnetic quadrupole trap and prepared in a coherent superposition of $|N=0, F=1, M_F=1\rangle$ and $|N=1, F=2, M_F=2\rangle$ states. Two 27 μs microwave $\pi/2$ pulses are separated by a free evolution time of 493 μs. Plots show the percentage recaptured into the MOT, proportional to the number in $N=1$, as a function of microwave frequency, f, relative to the transition frequency measured in free space, f_0. The vertical dashed line in the central lower plot indicates the position of the central fringe; the transition frequency in the magnetic trap is shifted by -404(1) Hz from f_0.

Electronic excitation-exchange and spin-orbit coupling in ultracold ion-atom collisions

R. Ben Shlomi[1], **Z. Meir**[1], **T. Sikorsky**[1], **M. Pinkas**[1], **N. Akerman**[1], **and R. Ozeri**[1]
[1] *Department of Physics of Complex Systems, Weizmann Institute of Science, 7610001 Rehovot, Israel*
e-mail: *ruti.ben-shlomi@weizmann.ac.il*

We experimentally study the dynamics of single and many inelastic collisions between ultracold ^{87}Rb atoms and a single $^{88}Sr^{+}$ ion. A single spin-polarized ion is trapped in a linear Paul trap, laser cooled to 1 mK, and then immersed in a ultracold (μK), spin-polarized Rb cloud (20,000 atoms). We studied relaxation rates of the ion from the metastable D-state due to collisions with atoms. We measured relaxation to the S-state after two Langevin collisions on average, followed by an energy release of 1500 K. This can be explained by a non-adiabatic excitation-exchange process: $Sr^{+}(D) + Rb(S) \rightarrow Sr^{+}(S) + Rb(P)$. This observation is supported by preliminary ab-initio calculations [1]. We also measured an energy release of 200 K when initializing the ion in $D_{5/2}$-state. This process is explained by a non-adiabatic crossing between the different spin-orbit levels: $Sr^{+}(D_{5/2}) + Rb(S) \rightarrow Sr^{+}(D_{3/2}) + Rb(S)$. We further investigate the dependence of these processes on the mutual spin orientation of the ion and atoms. We found that the relaxation rates is insensitive to the spin state and fine structure of the ion.

References

[1] O. Delieu, private communication.

Optical clock spectroscopy in weakly bound molecules

Mateusz Borkowski[1]

[1] *Institute of Physics, Faculty of Physics, Astronomy and Informatics, Nicolaus Copernicus University, Grudziadzka 5, 87-100 Torun, Poland*

e-mail: *mateusz@fizyka.umk.pl*

Molecular optical clocks promise unparalleled sensitivity to proton-to-electron mass ratio and also could find use as simple prototype systems in searches for physics beyond the Standard Model. We propose to observe clock $^1S_0 \rightarrow {}^3P_0$ transitions in weakly bound bosonic $^{174}Yb_2$ molecules [1]. As in bosonic atomic clocks, a small transition dipole moment could be induced by means of a weak external magnetic field [2]. The positions of $^1S_0+{}^3P_0$ vibrational states can be predicted to high accuracy using the recently measured ^{174}Yb $^1S_0+{}^3P_0$ scattering length [3]. Simulations show that while direct photoassociation would likely be impractical, one could instead perform clock spectroscopy using ground state Yb_2 molecules which could be efficiently produced by STIRAP. Thanks to favorable Franck-Condon factors the magnetically induced molecular Rabi frequencies can be comparable, or even exceed the atomic Rabi frequencies under same laser intensities and magnetic fields. A successful observation of these transitions could pave the way towards Hz-level molecular spectroscopy.

The positions of ground state near-threshold energy levels of Yb_2 have been determined by two-color photoassociation spectroscopy [4]. The positions of vibrational levels of the $^{174}Yb_2$ molecule near the $^1S_0$-$^3P_0$ dissociation limit are determined by solving the radial Schrödinger equation for a model potential where the long range van der Waals coefficients are based on *ab initio* calculations [5], while the quantum defect is tuned so that the scattering length of this potential matches the experimental $a_{ge} = 94.84(0.14)\,a_0$ [3, 4]. Some of the possible molecular clock transitions are shown in Fig. 1a.

Optical atomic clocks utilizing bosonic species rely on external magnetic fields to create an artificial $^1S_0$-$^3P_0$ transition dipole moment by Zeeman mixing of atomic $^3P_0$ and $^3P_1$ states. Applying a clock laser then induces Rabi flipping between ground $^1S_0$ and $^3P_0$ states at a frequency Ω_{at} proportional to the square root of laser intensity $\sqrt{I}$ and to the magnetic field $|\mathbf{B}|$ [2]. It can be shown that in a weakly bound molecule, clock spectroscopy can also be magnetically induced and the *molecular* Rabi frequency

$$\Omega_{mol} \approx \sqrt{2}\sqrt{f_{FC}}\,\Omega_{at}, \qquad (1)$$

where $f_{FC} = \left|\int_0^\infty \Psi_g(R)\Psi_e(R)dR\right|^2$ is the usual Franck-Condon factor between ground- and excited-state wavefunctions $\Psi_g(R)$ and $\Psi_e(R)$ shown in Fig. 1b. The $^{174}Yb_2$ dimer has similar vibrational wavefunctions in ground and excited states which makes the Franck-Condon factors extremely favorable, of up to 0.95 for the strongest transition. As a result, the magnetically induced Rabi frequencies, shown as a function of light intensity in Fig. 1c, can be of the same order as atomic, reaching several Hz at reasonable magnetic and optical fields of $|\mathbf{B}| = 1$ mT and $I = 1$ W/cm^2, respectively.

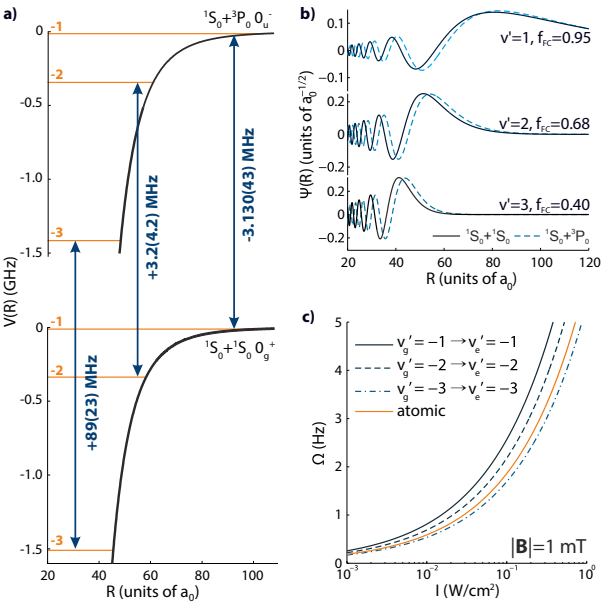


Figure 1: Molecular clock spectroscopy of $^{174}Yb_2$. a) Ground $^1S_0+{}^1S_0$ and excited $^1S_0+{}^3P_0$ 0_u^- long range potentials, near-threshold vibrational states and molecular transition energies with respect to atomic clock line. b) Radial wavefunctions of near-threshold bound states in ground and excited electronic states. c) Magnetically induced molecular Rabi frequencies calculated using Eq. (1). Thanks to favorable Franck-Condon factors the molecular Rabi frequencies are as large as atomic.

[1] M. Borkowski, Phys. Rev. Lett. **120**, 083202 (2018)

[2] A.V. Taichenachev, V. I. Yudin, C.W. Oates, C.W. Hoyt, Z.W. Barber, and L. Hollberg, Phys. Rev. Lett. **96**, 083001 (2006)

[3] L. Franchi, L. F. Livi, G. Cappellini, G. Binella, M. Inguscio, J. Catani, and L. Fallani, New J. Phys. **19**, 103037 (2017)

[4] M. Borkowski, A. A. Buchachenko, R. CiuryÅo, P. S. Julienne, H. Yamada, Y. Kikuchi, K. Takahashi, Y. Takasu, and Y. Takahashi, Phys. Rev. A **96**, 063405 (2017).

[5] S. G. Porsev, M. S. Safronova, A. Derevianko, and C.W. Clark, Phys. Rev. A **89**, 012711 (2014).

Menagerie of MOTs

K. N. Jarvis[1], **B. E. Sauer**[2], **and M. R. Tarbutt**[3]
[1] *Centre for Cold Matter, Blackett Laboratory, Imperial College London, Prince Consort Road, London SW7 2AZ, United Kingdom*
e-mail: *k.jarvis14@imperial.ac.uk*

Ever since the first demonstration of the magneto-optical trap (MOT), made over three decades ago, examples have existed of 'type-II' MOTs [1]. In contrast to a normal atomic MOT, where the hyperfine quantum number of the excited state F' is related to that of the ground state F by $F' = F + 1$, type-II MOTs have $F' \leq F$. The presence of dark ground-state sublevels in type-II systems leads to the unfavorable characteristics of high temperature and poor confinement, and so these MOTs have not been studied much. In recent years, however, the diatomic molecules SrF [2] and CaF [3, 4] have been successfully laser cooled and trapped in a MOT using type-II transitions. Despite this impressive progress, the inherently low phase-space densities are likely to hamper some of the most exciting proposed applications of laser-cooled molecules from being realized. Using ^{87}Rb we demonstrate that the properties of type-II MOTs can be dramatically improved by using a novel approach where the light is blue-detuned from the transition [5], and present a detailed characterization of the blue-detuned MOT. The phase-space density is increased by almost a factor of one million over comparable red-detuned MOTs. Additionally, we demonstrate the existence of at least eight stable magneto-optical trapping configurations, in addition to the type-I MOT, and present an overview of the properties of these new MOTs. Our findings could be used in the study of cold and ultracold collisions between atoms.

[1] E. L. Raab, M. Prentiss, A. Cable, S. Chu, and D. E. Pritchard, Phys. Rev. Lett. **59**, 2631 (1987).

[2] J. F. Barry, D. J. McCarron, E. B. Norrgard, M. H. Steinecker, and D. DeMille, Nature (London) **512**, 286 (2014).

[3] S. Truppe, H. J. Williams, M. Hambach, L. Caldwell, N. J. Fitch, E. A. Hinds, B. E. Sauer, and M. R. Tarbutt, Nat. Phys. **13**, 1173 (2017).

[4] L. Anderegg, B. L. Augenbraun, E. Chae, B. Hemmerling, N. R. Hutzler, A. Ravi, A. Collopy, J. Ye, W. Ketterle, and J. Doyle, Phys. Rev. Lett. **119**, 103201 (2017).

[5] K. N. Jarvis, J. A. Devlin, T. E. Wall, B. E. Sauer, and M. R. Tarbutt, Phys. Rev. Lett. **120**, 083201 (2018).

Towards Direct Laser Cooling of Barium Monofluoride

R. Albrecht, T. Sixt, L. Hofer, R. Schaber, T. Reinsch, and T. Langen
5. Physikalisches Institut and Center for Integrated Quantum Science and Technology IQST, Universität Stuttgart, Pfaffenwaldring 57, 70550 Stuttgart, Germany
e-mail: *t.langen@physik.uni-stuttgart.de*

We present a new experimental setup for the laser cooling and trapping of barium monofluoride molecules. Laser cooling of molecules had long been considered impossible due to their complex vibrational and rotational level structure. However, beneficial Franck-Condon factors and selection rules allow for optical cycling in many molecular species [1, 2, 3, 4, 5], including barium monofluoride [6]. The molecules are generated through laser ablation in a 4K cryostat and precooled by collisions with a helium buffer gas. This results in a cold and intense beam that provides ideal starting conditions for transversal laser cooling, slowing and subsequent loading of a 3D magneto-optical trap. The resulting cold gas of heavy diatomic molecules will pave the way for a large number of novel and interdisciplinary applications ranging from few- and many-body physics to cold chemistry and tests of fundamental symmetries.

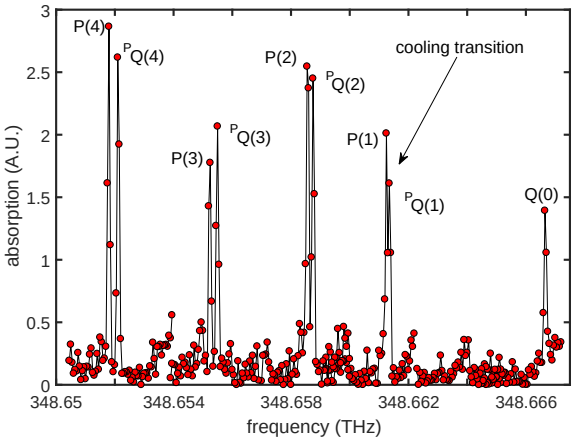


Figure 1: Absorption spectroscopy of buffer-gas-cooled $^{138}B^{19}F$ molecules around the main cooling transition.

[1] J. F. Barry *et al.*, Nature **512**, 286 (2014).

[2] M. Yeo *et al.*, Phys. Rev. Lett. **114**, 223003 (2015).

[3] S. Truppe *et al.*, Nature Phys. **13**, 1173 (2017).

[4] L. Anderegg *et al.*, Phys. Rev. Lett. **119**, 103201 (2017).

[5] I. Kozyryev *et al.*, Phys. Rev. Lett. **118**, 173201 (2017).

[6] T. Chen *et al.*, Phys. Rev. A **96**, 053401 (2017).

Quantitative optical spectroscopy of alkali-metal vapour in DC magnetic fields up to 0.4 T

Francisco S. Ponciano-Ojeda,[1,*] **James Keaveney**,[1] **Stefan M. Rieche**,[1] **Mark J. Raine**,[2] **Damian P. Hampshire**,[2] and **Ifan G. Hughes**[1]

[1] *Joint Quantum Centre (JQC) Durham-Newcastle, Department of Physics, Durham University, South Road, Durham, DH1 3LE, United Kingdom*

[2] *Superconductivity Group, Centre for Materials Physics, Department of Physics, Durham University, South Road, Durham, DH1 3LE, United Kingdom*

We present a spectroscopic investigation of a thermal Rb atomic vapour in the presence of an externally applied magnetic field. Our experimental setup allows us to obtain measurements of atomic spectra over a range of magnetic field strengths up to 0.4 T in the Voigt geometry (see Fig. 1) as well as the behaviour of the spectra as a function of the angle ϕ. By fitting the experimental spectra with a theoretical model [1, 2], we extract the magnetic field strength and the angle of the field, up to reflections in two cartesian axes, relative to the direction of propagation of the light. This work serves as a complement to research previously done in the Faraday geometry [3–7], thus providing a more complete panorama of the interactions between atomic systems and external magnetic fields. Finally, we present an investigation of the relative spectral sensitivity of this technique to variations in the field strength and angle.

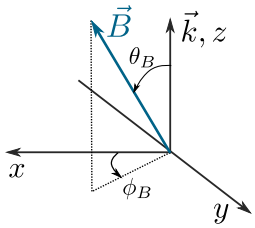


FIG. 1: Geometry of the experimental system used. $\vec{k}$ is the wave vector of the light, $\vec{B}$ is the direction of the magnetic field, ϕ_B is the angle between the x axis and the projection of $\vec{B}$ on the xy-plane and θ_B is the angle between $\vec{B}$ and the z-axis. For the Voigt geometry, $\theta_B = \pi/2$, while $\theta_B = 0$ gives the Faraday geometry.

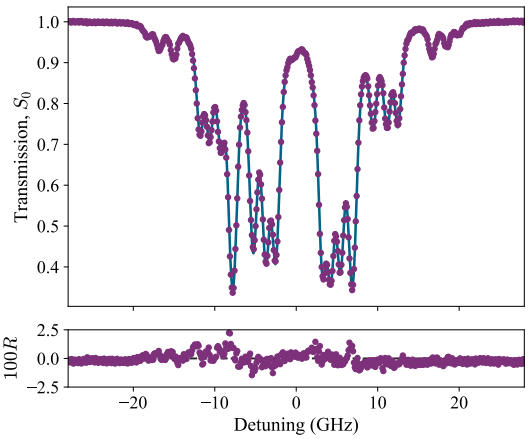


FIG. 2: Experimental data and fit to the *ElecSus* model for a measured magnetic field strength of (390±1) mT and polarisation angle of $\phi \approx \pi/2$ in the Voigt geometry. From this fit we extract a magnetic field strength of (396±1) mT. The residuals, plotted below, have been multiplied by a factor of 100 and show very good agreement between our model and the experiment.

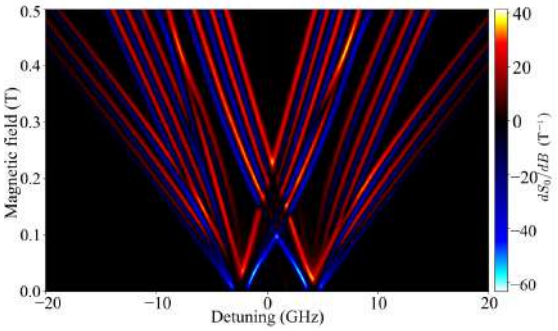


FIG. 3: Calculated sensitivity of the spectra to changes in the magnetic field strength, shown as the gradient dS_0/dB as a function of detuning and magnetic field. Hot spots, shown as bright/white spots indicate points at which the gradient takes an extreme value and the system has higher sensitivity.

* francisco.s.ponciano-ojeda@durham.ac.uk

[1] M. A. Zentile, J. Keaveney, L. Weller, D. J. Whiting, C. S. Adams, and I. G. Hughes, Comput. Phys. Commun. **189**, 162 (2015).

[2] J. Keaveney, C. S. Adams, and I. G. Hughes, Comput. Phys. Commun. **224**, 311 (2018), arXiv:1708.05305.

[3] M. A. Zentile, *Applications of the Faraday Effect in Hot Atomic Vapours*, Ph.D. thesis (2015).

[4] S. L. Kemp, I. G. Hughes, and S. L. Cornish, J. Phys. B **44**, 235004 (2011).

[5] M. A. Zentile, J. Keaveney, R. S. Mathew, D. J. Whiting, C. S. Adams, and I. G. Hughes, J. Phys. B **48**, 185001 (2015).

[6] M. A. Zentile, D. J. Whiting, J. Keaveney, C. S. Adams, and I. G. Hughes, Opt. Lett. **40**, 2000 (2015), arXiv:1502.07187.

[7] J. Keaveney, W. J. Hamlyn, C. S. Adams, and I. G. Hughes, Rev. Sci. Instrum. **87**, 095111 (2016), arXiv:1607.01969.

Laser Induced Fluorescence and Optogalvanic Spectroscopy applied to find the magnetic splitting of energy levels of La I

Ł. M. Sobolewski[1,2], **L. Windholz**[2], **and J. Kwela**[1]

[1] *Institute of Experimental Physics, Faculty of Mathematics, Physics and Informatics, University of Gdanńsk, 80-308, Poland*

[2] *Institute of Experimental Physics, Graz University of Technology, Petersgasse 16, A-8010 Graz, Austria*

e-mail: *info@icap2018.eu*

After the excitation of the La- Ar plasma in a hollow cathode lamp, a large number of atomic lines that could not be interpreted as transitions between already known La energy levels were observed by the use of optogalvanic spectroscopy.

Using the laser induced fluorescence (LIF) method and computer simulations of the hyperfine and Zeeman structures of the observed lines, we derived parameters such as energy levels, J numbers, A hyperfine constants and Lande g_J- factors of the energy levels involved in the transition. The existence of unknown weak lines was confirmed by a large number of excitations from lower energy levels.

The Zeeman spectra were recorded in the presence of a magnetic field of about 800G produced by a permanent magnet for two linear polarizations of the exciting laser light.

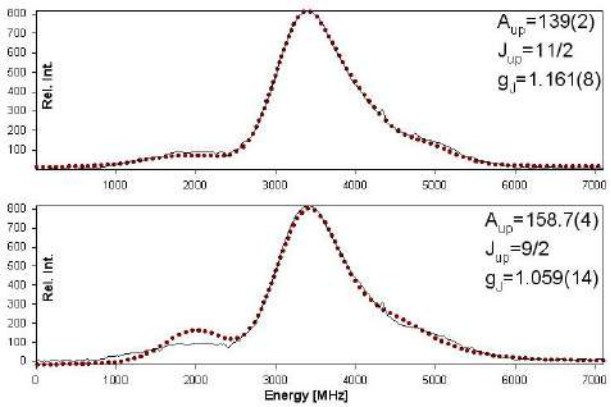


Figure 1: Experimental and simulated Zeeman structures of 582.2874 nm line for σ- view. The presented simulation show that the earlier published set of data A^{up}= 158.7 MHz, J=9/2, and $g_J{}^{up}$=1.059 is not correct.

Our measurements provided a lot of new experimental results for previously unknown La I levels which should help in their designation. We also received results for earlier studied lines. For a number of levels we corrected earlier published sets of data for: J number, A and B hfs constants and g_J- factors. One of these examples is presented in Figure 1.

We used two experimental methods for the Zeeman structure measurements: LIF technique and optogalvanic spectroscopy. Our experiment proved that OG spectroscopy can be succesfully used for such measurements. A very strong point of this method is the ability to observe the Zeeman effect of very weak atomic lines inaccessible for other spectroscopic methods. However, in the case of close-lying lines, the optogalvanic spectra contain overlapping structures, which may cause problems in the analysis. The LIF technique is free from this problem, but can be used only for relatively strong lines.

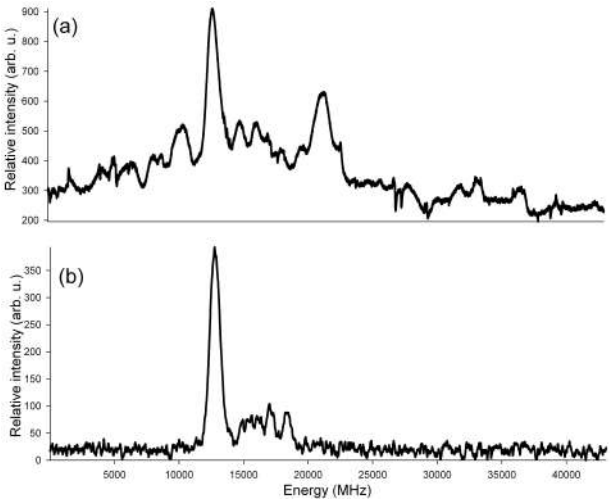


Figure 2: Optogalvanic spectrum around 596.1 nm. The spectrum can be explained as overlapping structures of several lines. These lines can be separated by the use of LIF technique. The bottom figure shows the structure of 596.0933 nm line observed by the LIF technique.

[1] Ł. M. Sobolewski, L. Windholz, J. Kwela, J. Quant. Spectrosc. Radiat. Transfer 189 221-227 (2017).

[2] Ł. M. Sobolewski, T. Binder, C. Güney, B. Gamper, J. Kwela, L. Windholz, J. Quant. Spectrosc. Radiat. Transfer 200 108-112 (2017).

[3] Ł. M. Sobolewski, L. Windholz, J. Kwela, J. Quant. Spectrosc. Radiat. Transfer 201 30-34 (2017).

[4] Ł. M. Sobolewski, L. Windholz, J. Kwela, J. Quant. Spectrosc. Radiat. Transfer 201 180-183 (2017).

Towards a high-density squeezed-light magnetometer

C. Troullinou[1], **R. Jiménez-Martínez**[1], **J. Kong**[1] **and M.W. Mitchell**[1],[2]

[1] *ICFO-Institut de Ciencies Fotoniques, The Barcelona Institute of Science and Technology, 08860 Castelldefels (Barcelona), Spain*

[2] *ICREA Institucio Catalana de Recerca i Estudis Avancats, 08015 Barcelona, Spain*

e-mail: *charikleia.troullinou@icfo.es*

Increasing the sensitivity of alkali-based magnetometers is an active area of interest [1-3], with potential applications ranging from space science to medical diagnosis. Quantum-non-demolition (QND) measurements to generate spin squeezing [4,5] and squeezed light techniques [6-8] have both enabled magnetic sensitivities beyond their respective standard quantum limits in such instruments. In theory these techniques are synergistic, although they are yet to be combined in a single instrument. At the same time, they have not been applied to high-atomic-density sensors [7], which are used in microfabricated [9] and SERF magnetometers [10], and in which spin noise is more prominent.

Squeezed-light-enhanced vapor-cell magnetometers reached nT/(Hz) sensitivity in 2010 [**?**] and 2 pT/(Hz) in 2011 [7]. Here we report a high-density magnetometer with sensitivity below 100 fT/(Hz) in an instrument that is simultaneously limited by optical shot noise and spin projection noise. This makes the instrument an attractive candidate, not just for the highest-sensitivity quantum-enhanced magnetometer, but also as a test bed for combining optical and atomic squeezing.

In contrast to previous squeezed-light magnetometers, based on spin-alignment [6-8], we use a magnetometer architecture based on spin-orientation of the atoms and use phase-sensitive detection to extract the magnetometer signal. This approach allows us to implement features not found in previous squeezed light magnetometers: We probe the spin orientation of the atomic ensemble via the optical Faraday effect, which is an efficient technique for QND measurements, and employ Bell-Bloom excitation, which allows us to work at frequencies of 10s of kHz, where detectors and squeezed-light sources can easily be shot-noise limited. This magnetometer architecture is simple and it is amenable for squeezed light probing. In fact, the same setup used for spin noise spectroscopy our group achieved squeezing of 3.2dB in unpolarized Rb vapor [11].

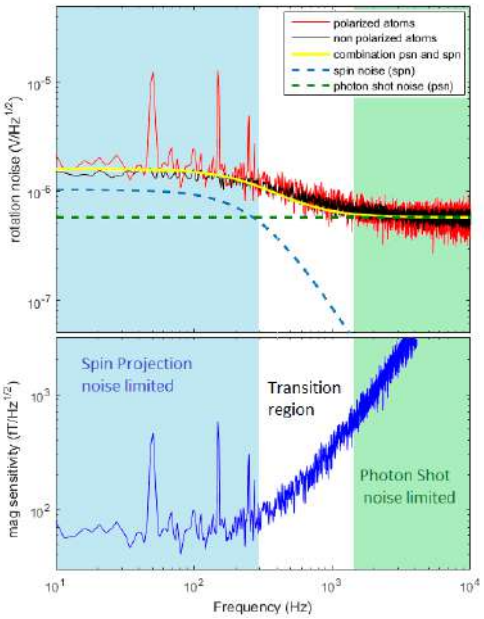


Figure 1: Power spectral density of the phase sensitive signal corresponding to photon shot noise limited performance of the magnetometer. The use of squeezed light probing is predicted to have beneficial effects in each frequency region: directly lowering the magnetic noise floor for high frequency signals, for which photon shot-noise dominates, giving stronger QND measurements for low-frequency signals, for which atomic projection noise dominates, and increasing the effective bandwidth of the sensor in the transition region

References

[1] Sheng et al, Phys. Rev. Lett. **110**, 160802 (2013).

[2] Grujic et al, Eur. Phys. J. D, 69: **135** (2015).

[3] Lucivero et al, Rev. Sc. Instr. **85**, 113108 (2014).

[4] Wasilewski et al, Phys. Rev. Lett. **104**, 133601 (2010).

[5] Sewell et al, Phys. Rev. Lett. **109**, 253605 (2012).

[6] Wolfgramm et al, Phys. Rev. Lett. **105**, 053601, (2010).

[7] Horrom et al, Phys. Rev. A **86**, 023803, (2012).

[8] Otterstrom et al, Opt. Lett. **39**, 6533 (2014).

[9] Sander et al, Bio. Opt. Exp. **3**, 981 (2012).

[10] Kominis et al, Nature **422**, 596, (2003).

[11] Lucivero et al, Phys. Rev. A **95**, 041803(R) (2017).

Continuum contributions to the atomic electric dipole moments

P. Syty[1], **J.E. Sienkiewicz**[1], **G. Gaigalas**[2], **L. Radžiūtė**[2] **and J. Bieroń**[3]

[1] *Department of Theoretical Physics and Quantum Information, Gdańsk University of Technology, Narutowicza 11/12, 80-233 Gdańsk, Poland*

[2] *Institute of Theoretical Physics and Astronomy, Vilnius University, Saulėtekio Al. 3, 10257 Vilnius, Lithuania*

[3] *Department of Atomic Optics, Jagiellonian University, Stanisława Łojasiewicza 11 , 30-348 Kraków, Poland*

e-mail: *pawel.syty@pg.edu.pl*

In last years the electric dipole moments (EDM) of elementary particles, nuclei, atoms and molecules have been subject of intensive experimental and theoretical studies. The importance of these studies relies in fact that if the EDM does not exist than the prediction of T, P and CP violations by unification theory is not correct. In other words eventual existence of EDM violates the CP invariants due to the CPT invariance. Significant enhancement of the electron EDM makes hopes for decisive measurements. Nevertheless, the current experimental limits significantly constrain the validity of unification theory.

The main purpose of present work was to estimate contribution of the continuum states to the atomic EDM. Nowadays, the focus is on EDM of diamagnetic atoms like Xe, Y or No, and as the example system the ^{129}Xe was chosen. The measurements of the EDM of Xe have significant potential for improvements in the experimental limit by using a nuclear spin maser technique [1], [2]. Very recent experimental studies in newly designed EDM cell indicate the possibility of improving the EDM upper limit by at least of one order in magnitude to achieve the accuracy as low as 10^{-28} $e$cm [4], while the most precise measurement of the EDM [3] gives the value of $\mathrm{d}(^{129}\mathrm{Xe}) = (0.7 \pm 3.3 \pm 0.1) \times 10^{-27} e\mathrm{cm}$.

Discrete states of ^{129}Xe were calculated with the relativistic atomic structure package GRASP2K [5], based on multiconfiguration Dirac-Hartree-Fock (MCDHF) approach. Continuum states were calculated using the COWF code, prepared in frames of the RATIP package [6], adapted to the GRASP2K. Let us stress, that the contribution to EDM coming from continuum electrons is calculated for the first time in a variational approach. To ensure correctness of our approach we get detailed insight into behavior of electron wave function while passing through the ionization energy.

In the next step, EDM arising from (P;T)-odd e-N tensor-pseudotensor and pseudoscalar-scalar interactions, nuclear Schiff moment, interaction of electron electric dipole moment with nuclear magnetic moments, and atomic electric dipole matrix elements, were calculated for both discrete and continuum states (see Fig. 1).

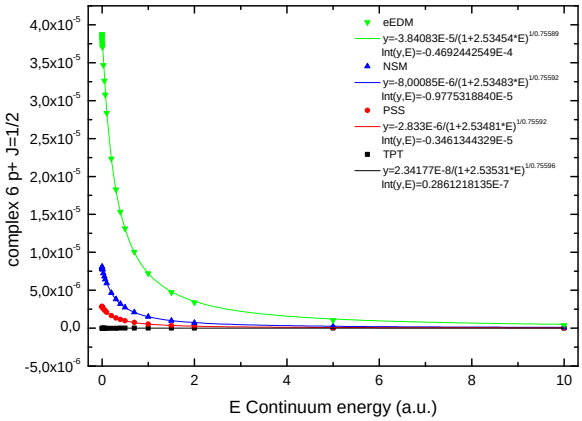


Figure 1: Dependence of EDM values for all interaction from continuum energy (in a.u.), for p+ orbital in DF approximation, state of ground configuration for Xe^+ is $J = 1/2$ with fitted equations and values of integrals.

The results show small contribution of continuum state electron to the final EDM value.

[1] T. Inouea *et al.*, Phys, Proc. **17**, 100 (2011)

[2] T. Furukawa *et al.*, J. Phys.: Conf. Ser. **312**, 102005 (2011)

[3] M.A. Rosenberry, T. E. Chupp, Phys. Rev. Lett. **86**, 22 (2001)

[4] F. Kuchler *et al.*, Hyperfine Interact. **237**, 95 (2016)

[5] P. Jönsson, G. Gaigalas, J. Bieroń, C. Froese Fischer, I.P. Grant, Comp. Phys. Comm. **184**, 2197 (2013)

[6] S. Fritzsche, Comp. Phys. Comm. **183**, 1525 (2012)

Progress towards parity violation measurements in dysprosium

A. Sharma[2], **M. Leyser**[2], **L. Bougas**[1], **D. Antypas**[1] **and D. Budker**[1,2]
[1] *Helmholtz Institut Mainz (HIM), Staudingerweg 18, Mainz 55128, Germany*
[2] *Institut für Physik, Johannes Gutenberg Universität, Mainz 55128, Germany*
e-mail: *sharijit@uni-mainz.de*

The observation of weak interactions in atomic systems can provide a sensitive test of the Standard Model (SM). Atomic parity violation (APV) is the only route to investigate weak interactions at low momentum transfer. APV is caused by the exchange of Z^0 bosons between the electrons and the quarks in the nucleus and it causes the atomic states to acquire a small admixture of opposite-parity states. The parity mixing effect is tiny, but it has been shown [1] that it scales as Z^3, where Z is the nuclear charge, and hence the effect is larger for heavier atoms. In addition to this Z^3 scaling, the Bouchiats' also proposed a technique where parity violating interactions are amplified through interference with an electric-field-induced mixing of opposite-parity states. This method has since been known as the Stark-interference technique [2].

So far several experiments [3, 4, 5, 6, 7] have succeeded in observing parity violating signals in atoms like bismuth (Bi), lead (Pb), thallium (Tl), and cesium (Cs). In more recent years, our group has reported on two parity violation experiments in more heavy and complex atomic systems, ytterbium (Yb) [8] and dysprosium (Dy) [9]. Both systems were predicted to gain enhancements both from their high nuclear charge and the existence of closely spaced opposite parity levels that enhances weak mixing effects. Atomic dysprosium is remarkable for containing two nearly degenerate electronic states of opposite parity, labeled A (even) and B (odd), with an electric-dipole transition between them as shown in Fig. 1. Both states have total electronic angular momentum J = 10 and are found at an energy of 19798 cm^{-1} above the ground state. The energy splitting between these states varies as a function of isotope, with stable isotopes at atomic masses of A = 156, 158 and A = 160→164. The sensitivity to PNC (parity non-conservation) mixing is enhanced in this system by the small energy separation between these levels, which can be crossed by applying an external magnetic field.

We have exploited this system as a productive laboratory for fundamental physics measurements and searches for physics beyond the standard model in a series of experiments carried out at Berkeley, with the experimental installation recently moved to Mainz. Since the work of Budker et al. [10], the apparatus and measurements techniques for the Dy microwave transitions have been continuously refined. We have

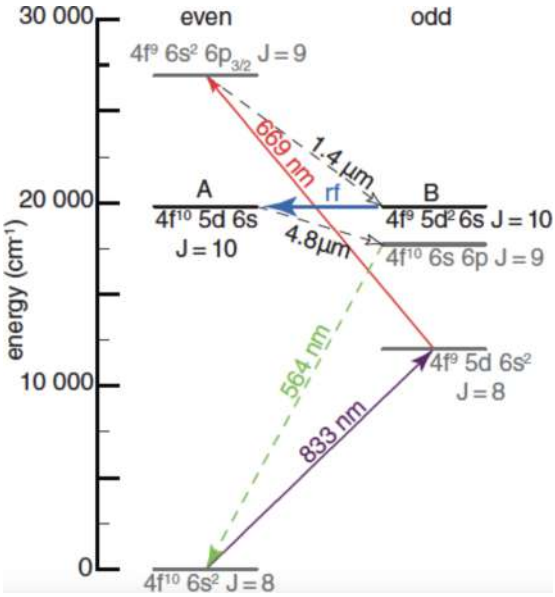


Figure 1: Relevant energy level diagram in dysprosium.

initiated spectroscopy of the 833 nm and 669 nm transition as part of our initial activities towards measurement of the parity violating signal in Dy. We also report here measurements on Zeeman crossing spectroscopy in Dy atoms and the effects of optical pumping on the Zeeman spectrum using light at 421 nm.

[1] M. A. Bouchiat et al., Phys. Lett. B **48** 111-114 (1974).

[2] M. A. Bouchiat et al., J. Phys. II (France) **36**, 493 (1975).

[3] L. M. Barkov et al., JETP Letters **27**, 357 (1998).

[4] M. D. Macpherson, et al., Phys. Rev. Lett., **67** 2784 (1991).

[5] D. M. Meekhof, Phys. Rev. A **71**, 3442 (1993).

[6] P. Vetter et al., Phys. Rev. Lett. **74**, (1995). 2658

[7] C. S. Wood et al., Science **275**, 1759-1763 (1997).

[8] D. Antypas et al., arXiv:1804.05747

[9] N. Leefer et al., arXiv:1412.1245

[10] D. Budker et al., Phys. Rev. A **50**, 132 (1994).

In-beam hyperfine spectroscopy of hydrogen and antihydrogen

E. Widmann[1], C. Amsler[1], S. Arguedas Cuendis[1], H. Breuker[2], M. Diermaier[1], P. Dupré[2], C. Evans[6], M. Fleck[1], A. Gligorova[1], H. Higaki[3], Y. Kanai[4], T. Kobayashi[5], B. Kolbinger[1], N. Kuroda[5], M. Leali[6], A.M.M. Leite[1], V. Mäckel[1], C. Malbrunot[7,1], V. Mascagna[6], O. Massiczek[1], Y. Matsuda[5], D.J. Murtagh[1], Y. Nagata[8], A. Nanda[1], D. Phan[1], C. Sauerzopf[1], M.C. Simon[1], M. Tajima[4], H. Spitzer[1], M. Strube[1], S. Ulmer[2], L. Venturelli[6], M. Wiesinger[1], Y. Yamazaki[2], and J. Zmeskal[1]

[1] *Stefan Meyer Institute, Austrian Academy of Sciences, 1090 Vienna, Austria*
[2] *Ulmer Fundamental Symmetry Laboratory, RIKEN, Saitama 351-0198, Japan*
[3] *Graduate School of Advanced Science of Matter, Hiroshima University, Kagamiyama, Higashi-Hiroshima, 739-8530 Hiroshima, Japan*
[4] *Nishina Center for Accelerator-Based Science, RIKEN Saitama 351-0198, Japan*
[5] *Institute of Physics, University of Tokyo, 153-8902, Japan*
[6] *Dipartimento di Ingegneria dell'Informazione, Università degli Studi di Brescia, I-25133 Brescia, Italy and Istituto Nazionale di Fisica Nucleare, Sez. di Pavia, I-27100 Pavia, Italy*
[7] *CERN 1211, Geneva 23, Switzerland*
[8] *Department of Physics, Tokyo University of Science, Shinjuku, Tokyo 162-8601, Japan*
e-mail: *eberhard.widmann@oeaw.ac.at*

The ground-state hyperfine structure (GS-HFS) of hydrogen is known from the hydrogen maser to a relative precision of 10^{-12}. It is of great interest to measure the same quantity for its antimatter counterpart, antihydrogen, to test the fundamental CPT symmetry, which states that all particles and antiparticles have opposite electric charges and magnetic moments but otherwise exactly equal properties. Since CPT is strictly conserved in the Standard Model of particle physics, a violation, if found, would point directly to theories beyond this framework. The application of the maser technique requires the confinement of the atoms in a field-free matter box for 1000 seconds and is currently not applicable to antihydrogen. Therefore, the ASACUSA collaboration at the Antiproton Decelerator of CERN has built a Rabi-type beam spectroscopy setup [1] for a measurement of GS-HFS. Using three-body recombination of antiprotons and positrons stored in a nested Penning trap, the first beam of antihydrogen atoms has been observed 2.7 m downstream of the formation region [2] where magnetic stray fields are negligible. Recently the principal quantum number distribution of this beam has been measured [3] showing that the rate of atoms in states that are short-lived enough to reach the ground-state before entering the microwave cavity is still too low. Efforts are under way to improve the positron plasma temperature and density which are essential parameters to increase both rate and ground-state fraction of the formed antihydrogen atoms [4].

With the initial aim of characterizing the setup devised to measure the GS-HFS and to evaluate its potential, a beam of cold, polarized, monoatomic hydrogen was built and used together with the microwave cavity and sextupole magnet designed for the antihydrogen experiment [1]. The $(F, M) = (1, 0) \rightarrow (0, 0)$ transition was measured to a precision of 2.7 ppb [5], more than a factor 10 better than in the previous measurement using a hydrogen beam. This result shows that the apparatus developed is capable of making a precise measurement of the GS-HFS of antihydrogen, providing that a beam of similar characteristics (velocity, polarization, quantum state) becomes available.

In a recent publication on the non-minimal Standard Model Extension (SME), describing possible violations of Lorentz and CPT invariance, Kostelecky and Vargas [6] conclude that the in-beam hyperfine measurements of *hydrogen* alone can be used to constrain certain coefficients of their model, which have never been measured before.

The status and prospects of in-beam measurements of hydrogen and antihydrogen will be presented.

[1] E. Widmann *et al.*, Hyperfine Interact. **215** (2013), 1.

[2] N. Kuroda *et al.*, Nat. Commun. **5** (2014), 3089.

[3] C. Malbrunot *et al.*, Phil. Trans. Roy. Soc. Lond. A **376** (2018), 20170273.

[4] B. Radics, D. J. Murtagh, Y. Yamazaki and F. Robicheaux, Phys. Rev. A **90** (2014), 032704.

[5] M. Diermaier et al., Nat. Commun. 8 (2017), 15749.

[6] V.A. Kostelecky and A.J. Vargas, Phys. Rev. D **92** (2015), 056002.

Towards Ramsey-Comb Spectroscopy of the 1S-2S Transition in Helium Ions

J.J. Krauth[1], **L.S. Dreissen**[1], **C. Roth**[1], **E.L. Gründeman**[1], **M. Favier**[1], **and K.S.E. Eikema**[1]
[1] *LaserLaB, Department of Physics and Astronomy, Vrije Universiteit Amsterdam, De Boelelaan 1081, 1081 HV Amsterdam, The Netherlands*
e-mail: *j.krauth@vu.nl*

In recent years an increasing number of high-precision atomic physics experiments have been started in order to test bound-state quantum electrodynamics (QED) and contribute to solving the so-called proton radius puzzle (PRP). PRP is the popular term for the discrepancy between different measurements of the root-mean-square (rms) charge radius of the proton: Laser spectroscopy in muonic hydrogen [1] yields values of the proton radius which are 4% and 5.6 standard deviations smaller than the CODATA value [2], which combines results from laser spectroscopy in atomic hydrogen as well as from electron-proton scattering. The very precise measurement of the 1S-2S transition in atomic hydrogen causes a close to 100% correlation between the proton charge radius and the Rydberg constant. The PRP can therefore also be seen as a Rydberg puzzle. Note, that the two most recent results from atomic hydrogen measurements [3, 4] disagree with each other and do not allow further conclusions.

An appealing idea to approach the PRP is therefore to go to different kinds of atomic or even molecular systems in order to independently measure the proton radius or the Rydberg constant and help solve the PRP.

Our goal is to measure the 1S-2S transition of the helium ion, which requires extreme ultra-violet (XUV). In combination with the helium charge radius from the muonic helium experiments [5] (results not published yet), we will be able to determine the Rydberg constant, or we can use the Rydberg constant from atomic hydrogen and perform an improved bound-state QED test.

In order to measure the 30 nm He^+ 1S-2S transition, we developed a method called Ramsey-Comb spectroscopy (RCS) [6, 7]. RCS uses two amplified and upconverted pulses from the pulse train of a frequency comb (FC) to perform a Ramsey-like excitation. The pulse pairs are amplified to the mJ-level which drastically increases the efficiency of the high-harmonic generation (HHG). The coarse inter-pulse delay is changed in multiples of the repetition time, and allows a maximum Ramsey free evolution on the order of μs. Recording of the Ramsey fringes requires to fine-tune the relative phase of the two pulses on an attosecond scale, which is realized by changing the repetition rate or the carrier-envelope offset phase (CEO) of the comb laser. Systematics which are constant between different pulse pairs, such as the AC Stark shift, cancel. In order to drastically increase the excitation probability we use an unequal photon-scheme, where instead of the typical 2×60 nm, we use a 790 nm fundamental photon together with its 25th harmonic at 32 nm. This scheme takes advantage of the much higher power of the 790 nm beam and the virtual intermediate state comes much closer to a real state; both facts lead to a substantial enhancement of the transition probability.

The helium ion is trapped in a linear Paul trap and sympathetically cooled with a beryllium ion. Any frequency shift due to the motion of the helium ion is significantly reduced by synchronizing the repetition rate of the laser with the secular frequency of the trap.

Our goal is to reach a precision below 1 kHz which allows a valuable insight into the PRP and provides a stringent test of bound-state QED.

As intermediate steps we are now working on measurements in xenon and neutral helium which will give us the opportunity to test the HHG and the unequal photon scheme, respectively, and pave the way for the measurement of the 1S-2S transition in He^+.

[1] R. Pohl, A. Antognini, F. Nez et al., Nature **466**, 213-216 (2010). A. Antognini, F. Nez, K. Schuhmann et al., Science **339**, 417-420 (2013).

[2] P.J. Mohr, D.B. Newell, B.N. Taylor, Review of Modern Physics **88**, 035009 (2016).

[3] A. Beyer, L. Maisenbacher, A. Matveev et al., Science **358**, 79-85 (2017).

[4] H. Fleurbaey, S. Galtier, S. Thomas et al., Physical Review Letters **120**, 183001 (2018).

[5] A. Antognini, F. Biraben, J.M.R. Cardos et al., Canadian Journal of Physics **89**, 47-57 (2011).

[6] J. Morgenweg, I. Barmes, K.S.E. Eikema, Nature Physics **10**, 30-33 (2013).

[7] R.K. Altmann, L.S. Dreissen, E.J. Salumbides et al., Physical Review Letters **120**, 043204 (2018).

A 10-nT level magnetic shielding for the 10-m long-baseline atom interferometer

C. He[1,2,3], **S. T. Yan**[1,2,3], **Y. H. Ji**[1,2], **C. Zhou**[1,2], **S. Barthwal**[1,2], **W. T. Duan**[1,2,3], **B. Tang**[1,2], **L. Zhou**[1,2], **J. Wang**[1,2], **M. S. Zhan**[1,2]

[1] *State Key Laboratory of Magnetic Resonance and Atomic and Molecular Physics, Wuhan Institute of Physics and Mathematics, Chinese Academy of Sciences, Wuhan 430071, China*

[2] *Center for Cold Atom Physics, Chinese Academy of Sciences, Wuhan 430071, China*

[3] *School of Physics, University of Chinese Academy of Sciences, Beijing 100049, China*

e-mail: *hechuan@wipm.ac.cn*

Weak equivalence principle test with microscopic particles based on atom interferometer has made new progress in recent years [1–8]. We designed and completed a 10-meter atom interferometer [9], and test the weak equivalence principle using ^{85}Rb-^{87}Rb double-diffraction Raman atom interferometer at a level of 10^{-8} [5]. The precision of weak equivalence principle test is still limited by many factors, such as vibration noise, Coriolis effect, ac Stark shift, background magnetic field noise, etc.. To reduce the background magnetic field noise, the improvement of magnetic field shielding system is necessary. After years of hard work, multiple rounds of overall welding, annealing and tests, the technical bottleneck of the long-baseline magnetic shielding is overcome, and the active compensation technologies inside and outside magnetic shielding layer are developed. As a result, the fluctuation of the magnetic field of interference area is compressed to 10 nT level.

[1] S. Fray, C. A. Diez, T. W. Hänsch, M. Weitz, Phys. Rev. Lett., **93**, 240404(2004).

[2] A. Bonnin, N. Zahzam, Y. Bidel, A. Bresson, Phys. Rev. A, **88**, 043615(2013).

[3] D. Schlippert, J. Hartwig, H. Albers, et al., Phys. Rev. Lett., **112**, 203002(2014).

[4] M. G. Tarallo, T. Mazzoni, N. Poli, D. V. Sutyrin, X. Zhang, G. M. Tino, Phys. Rev. Lett., **113**, 023005(2013).

[5] L. Zhou, S. T. Long, B. Tang, et al., Phys. Rev. Lett., **115**, 013004(2015).

[6] B. Barrett, L. Antoni-Micollier, L. Chichet, et al., Nat. Commun., **7**, 13786(2016).

[7] X. C. Duan, M. K. Zhou, X. B. Deng, et al., Phys. Rev. Lett., **117**, 023001(2016).

[8] G. Rosi, G. D'Amico, L. Cacciapuoti, et al., Nat. Commun., **8**, 15529(2017).

[9] L. Zhou, Z. Xiong, W. Yang, et al., Gen. Relativ. Gravit., **43**, 1931(2011).

Experimental upgrades to measure the electron's electric dipole moment using YbF molecules

C. J. Ho[1], **J. A. Devlin**[1], **I. M. Rabey**[1], **M. R. Tarbutt**[1], **B. E. Sauer**[1] **and E. A. Hinds**[1]
[1] *Centre for Cold Matter, The Blackett Laboratory, Imperial College London, London SW7 2BW*
e-mail: *christopher.ho15@imperial.ac.uk*

The existence of a permanent electric dipole moment (EDM) of the electron is intimately related to the violation of time-reversal symmetry in nature, and to the observed matter-antimatter asymmetry in the universe. The Standard Model of particle physics predicts an upper limit to the electron EDM that is far below current experimental sensitivities ($|d_e| < 10^{-38} e$.cm) [1]. However, modern extensions to the Standard Model predict electron EDM values in the range $|d_e| \sim 10^{-27}$–$10^{-30} e$.cm [2]. The current generation of experiments that utilize cold molecules [3, 4] and molecular ions [5] are precise enough to measure this. The current upper limit to the electron EDM is $|d_e| < 9.4 \times 10^{-29} e$.cm [4].

We report improvements made to increase the sensitivity of an interferometry experiment to measure the electron EDM using ytterbium fluoride (YbF) molecules [3]. We have increased the initial population of YbF molecules in the ground state by a factor of six through a combination of repump lasers, microwaves and rf fields (Fig. 1). We have also improved our detection efficiency by a factor of 40. This is due to better collection optics, and a better detection scheme which can scatter many more photons per molecule [6]. This also allows us to detect both quadratures on the interferometer (Fig. 2), giving us another gain in sensitivity of $\sqrt{2}$.

Spurious magnetic fields are a major source of random and systematic error in our experiment, and therefore we have improved our control and measurement of magnetic fields. This was done by redesigning the electric field plates for lower magnetic Johnson noise [7], and by installing several low-noise magnetometers inside the machine.

Together, these factors will allow us to measure d_e at the $10^{-29} e$.cm level.

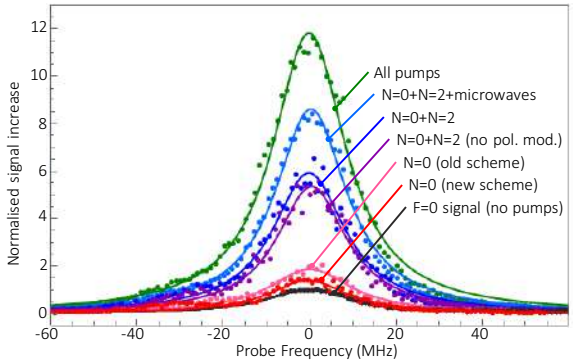


Figure 1: Increased population in the ground hyperfine, rovibrational and electronic state of YbF due to better state preparation.

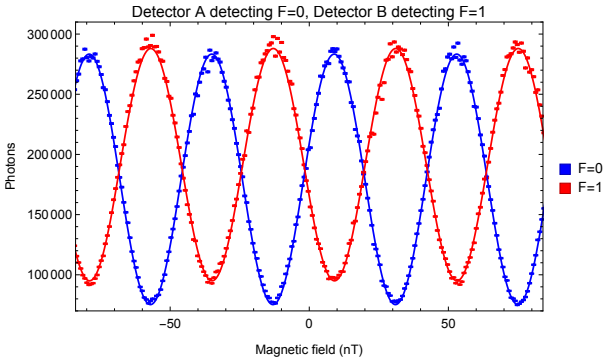


Figure 2: Detection scheme that allows us to detect both quadratures of the interferometer.

[1] B.L. Roberts and W. J. Marciano, *Lepton Dipole Moments* (World Scientific Publications, Singapore, 2010).

[2] I. B. Khriplovich and S. K. Lamoreaux, *CP Violation Without Strangeness* (Springer, New York, 1997).

[3] J. J. Hudson, D. M. Kara, I. J. Smallman, B. E. Sauer, M. R. Tarbutt, and E. A. Hinds, Nature **473**, 493 (2011).

[4] J. Baron, W. C. Campbell, D. DeMille, J. M. Doyle, G. Gabrielse, Y. V. Gurevich, P. W. Hess, N. R. Hutzler, E. Kirilov, I. Kozyryev, B. R. O'Leary, C. D. Panda, M. F. Parsons, E. S. Petrik, B. N. Spaun, A. C. Vutha, and A. D. West, Science **343**, 269 (2014).

[5] W. B. Cairncross, D. N. Gresh, M. Grau, K. C. Cossel, T. S. Roussy, Y. Ni, Y. Zhou, J. Ye, and E. A. Cornell, Phys. Rev. Lett. **119**, 153001 (2017).

[6] I. M. Rabey, Ph.D. Thesis, Imperial College London, 2017.

[7] I. M. Rabey, J. A. Devlin, E. A. Hinds, and B. E. Sauer, Rev. Sci. Instrum. **87**, 115110 (2016).

Towards precision spectroscopy of the 2S-6P transition in atomic hydrogen

V. Andreev[1], **L. Maisenbacher**[1], **A. Matveev**[1], **A. Grinin**[1], **R. Pohl**[1,2], **K. Khabarova**[1,3], **N. Kolachevsky**[1,3], **T. W. Hänsch**[1,4] **and Th. Udem**[1]

[1] *Max-Planck-Institut für Quantenoptik, Garching, Germany.*
[2] *Johannes Gutenberg-Universität Mainz, Mainz, Germany.*
[3] *On leave from: Lebedev Physical Institute, Moscow, Russia.*
[4] *Ludwig-Maximilians-Universität, Munich, Germany.*
e-mail: *v.andreev@mpq.mpg.de*

The fundamental description of nature is rooted in an extraordinarily accurate understanding of simple systems. In our research, we focus on the most basic stable atomic system of all, the hydrogen atom. Understanding this bound system of an electron and a proton was crucial for the history of quantum mechanics and ever since provides an excellent framework to test our knowledge of the laws of nature.

The 1S-2S two-photon transition frequency in hydrogen is measured most accurately compared to other transitions in hydrogen due to its narrow natural line width, and serves as a corner stone for fundamental constants [1]. However, only a combination of the 1S-2S transition with additional measurements allows to extract specific constants such as the proton root mean square charge radius r_p as well as the Rydberg constant R_∞, and to test the consistency of Quantum Electrodynamics. More precise measurements of the 2S-nP transition frequencies (e.g. with $n = 4, 6$) can be used to overcome current limitations in the framework of determining fundamental constants. Compared to the 1S-2S transition with the natural linewidth of only 1.3 Hz, the natural line widths of the 2S-nP transitions lies in the MHz region. To achieve a high-precision measurement of these transitions, it is therefore crucial to precisely study the line distortions, for instance caused by quantum interference.

The proton radius has become particularly interesting since the measurement of muonic hydrogen revealed a value of r_p much more precise than, but discrepant with the value derived from hydrogen spectroscopy [2]. Important steps towards the solution of this so-called proton radius puzzle are more precise measurements of other transitions in hydrogen. Recently, the 2S-4P transition has been measured in our group with a relative uncertainty of 4 parts in 10^{12} [3]. Combining this result with the 1S-2S transition frequency leads to a r_p value which is 3.3 combined standard deviations smaller than the value deduced from previous hydrogen world data, but in good agreement with the value from muonic hydrogen. Since the origin of this discrepancy is currently unknown, more measurements with even higher precision are needed.

Using the same apparatus as for the 2S-4P data, we aim to measure the 2S-6P transition. With a natural line width of 3.8 MHz, the 2S-6P transition has the potential to be measured more precisely than the 2S-4P transition, which has a line width of 12.9 MHz. In addition to the known challenges from the previous experiment, the new transition requires to rebuild the system for 410 nm (2S-6P) as opposed to 486 nm (2S-4P) laser light. The shorter wavelength leads to difficulties such as a complete re-design of our collimator used for the active fiber-based retroreflector [4], and increased Rayleigh scattering in the optical fiber resulting in etalon-like effects. This poster reports on the current status of the 2S-6P hydrogen experiment, with a particular focus on the upgrade for the shorter wavelength.

[1] C. G. Parthey *et al.*, Physical Review Letters **107** (2011), 203001.

[2] A. Antognini *et al.*, Science **339** (2013), 417.

[3] A. Beyer, L. Maisenbacher, A. Matveev *et al.*, Science **358** (2017), 79.

[4] A. Beyer, L. Maisenbacher, A. Matveev *et al.*, Opt. Express **24** (2016), 17470.

High contrast EIT spectra in a hot atomic medium

Gang Wang[1,2], Yu-Sheng Wang[1], Emily Kay Huang[1], Weilun Hung[1], Kai-Lin Chao[1], Ping-Yeh Wu[1], Yi-Hsin Chen[1,3], and Ite A. Yu[1]

[1] *Department of Physics, National Tsing Hua University, Hsinchu 30013, Taiwan*

[2] *College of Physics, Jilin University, Changchun 130012, China*

[3] *Department of Physics, National Sun Yat-Sen University, Kaohsiung, 80424, Taiwan*

e-mail: *yhchen920@gmail.com*

We report high-contrast electromagnetically-induced-transparency (EIT) spectra in a heated vapor cell. The EIT spectrum has high resonant transmission of up to 67%, subnatural linewidth of 1.1 MHz, and low baseline transmission of 3% [1]. We consider the possible amplification resulted from the effects of amplification without population inversion and four-wave mixing. The gain from these effects is negligible, and therefore, the high EIT peak transmission is not artificial. We further provide a theoretical model to simulate EIT spectra. The prediction fits the data well and the experimental parameters can be reasonably derived from the model. Hence, the theoretical model advances our knowledge in the EIT study in thermal systems. In addition, such excellent EIT characteristics lead to the realization of optical memory using slow light and the generation of photon sources with subnatural linewidth. In practical applications, the narrow and high-contrast spectral profile can be employed as a high precision bandpass filter. The central frequency tuning range of the filter is larger than 100 MHz with out-of-band blocking $\geq$ 15 dB. Our study paves the avenue for the realization of quantum devices in Doppler-broadening media.

[1] G. Wang, Y. S. Wang, E. K. Huang, W. Hung, K. L. Chao, P. Y. Wu, Y. H. Chen*, and I. A. Yu, Ultranarrow-bandwidth filter based on a thermal EIT medium, Sci. Rep. **8**, 7959 (2018).

Search for a violation of the Pauli Exclusion Principle with electrons in the LNGS underground laboratory

A. Pichler[1] **and J. Marton**[1] **on behalf of the VIP2 collaboration**
[1] *Stefan Meyer Institute for subatomic physics, Boltzmanngasse 3, 1090 Vienna, Austria*
e-mail: *andreas.pichler@oeaw.ac.at*

In quantum physics, the Pauli Exclusion Principle (PEP) is the foundation for our understanding where systems of fermions are concerned. In the light of its utmost importance, it is crucial to test possible limitations of the PEP. In a pioneering experiment, Ramberg and Snow supplied an electric current to a Cu target, and searched for PEP violating atomic transitions of the "fresh" electrons from the current. The non-existence of the anomalous X-rays from such transitions then set the upper limit for a PEP violation.

The VIP2 (VIolation of Pauli Exclusion Principle) experiment improves this method, by searching for Pauli-forbidden atomic transitions from the 2p to the 1s shell in copper at about 8 keV. The core part of the setup are Silicon Drift Detectors, which detect the possible X-rays from Pauli-forbidden transitions. The experimental setup and the results from the first data taking period in the underground laboratory of Gran Sasso will be presented. The experiment was for example described in [1]. First results of the experiment were published in [2].

References

[1] C.Curceanu, J. Marton et al. Putting the Pauli exclusion principle on trial. *Cern Courier*, March 2018.

[2] H. Shi, J. Marton, A. Pichler, et al. Experimental search for the violation of Pauli exclusion principle. *The European Physical Journal C*, 78(4):319, 2018.

Measurement of the ^{4}He 2 ^{3}S - 2 ^{1}S transition in a magic wavelength optical dipole trap

Bob Rengelink[1], Yuri van der Werf[1], Remy Notermans[1], Raphael Jannin[1], Kjeld Eikema[1], Maarten Hoogerland[2], and Wim Vassen[1]

[1] *LaserLaB Vrije Universiteit, Amsterdam, The Netherlands*

[2] *Department of Physics, University of Auckland, Auckland, New Zealand*

e-mail: *w.vassen@vu.nl*

We have measured the transition frequency between the two metastable states of ^{4}He, 2 $^3S_1$ (lifetime 8 ks) and 2 $^1S_0$ (lifetime 20 ms), with 0.20 kHz accuracy (1.0×10^{-12} relative accuracy) [1]. Our result is almost a factor of ten more accurate than the previous result [2] and agrees within 2σ. The result connects orthohelium and parahelium tightly and constitutes the most accurate optical frequency measurement in the helium atom to date.

Our measurement is performed on a Bose-Einstein Condensate (BEC) of ^{4}He atoms in the 2 $^3S_1$ state, confined at a temperature of 0.2 μK in a crossed optical dipole trap (ODT). We have used an ODT near the 319.8 nm magic wavelength, minimizing ac Stark shifts in the transition frequency. We measured this magic wavelength with 0.00015 nm accuracy and found very good agreement with calculations based on tabulated level energies and dipole matrix elements [3] as well as more accurate relativistic full-configuration-interaction techniques [4].

In the experiment we excite the 1557-nm transition with a telecom fiber laser, offset-locked to an ultrastable (∼1 Hz) laser via a femtosecond frequency comb laser, realizing a 5 kHz laser linewidth over our 0.1 s interrogation time of the trapped atoms. We observe the transition (linewidth typically 10 kHz, see Fig. 1) counting the ions produced by Penning ionization of 2 ^{1}S atoms with 2 ^{3}S atoms in the trap. The excitation inside a BEC also causes a mean-field shift of the transition frequency, similar to the 1S - 2S experiments in an atomic hydrogen BEC [5]. Varying the chemical potential we extract the s-wave singlet-triplet scattering length with 5% accuracy. It strongly disagrees with a quantum chemistry calculation based on a complex potential of the 2 ^{1}S - 2 ^{3}S helium dimer.

Our new value of the transition frequency agrees very well with the most recent QED calculations, which have an accuracy of 0.8 MHz [7]. Strong cancellation of QED terms in the isotope shift lead to a theoretical accuracy in the point-nucleus isotope shift of 0.19 kHz [7]. When we combine our new ^{4}He measurement with our earlier result on the same transition for ^{3}He, which has a 1.5 kHz accuracy [2], the difference in the squared nuclear charge radii δr^2 of the alpha-particle and the helion is determined with 0.007 fm^2 accuracy (6×10^{-3} relative accuracy). We hope to significantly improve on this accuracy in the near future by measuring the ^{3}He transition in a magic-wavelength trap as well. Our present value for δr^2 still disagrees with δr^2 measurements from the isotope shift in the 2 ^{3}S - 2 ^{3}P transition, that also disagree among each other [8]. Comparison with δr^2 from μ-^{3,4}He$^+$ Lamb shift measurements at the muon facility of the Paul Scherrer Institute [9] will reveal if there is also a helium nuclear size puzzle.

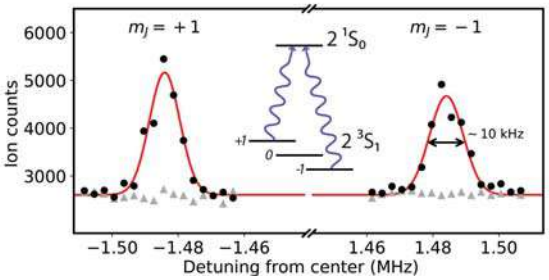


Figure 1: Observation of the 2 ^{3}S - 2 ^{1}S transition in a BEC. The grey triangles are background calibration points. The atoms are alternately excited from the m_J = +1 and m_J = -1 states to account for the Zeeman shift. The red line is a fit of two Gaussians showing typical widths of about 10 kHz.

[1] R.J. Rengelink et al., arXiv:1804.06693 (2018).

[2] R. van Rooij et al., Science **333**, 196 (2011).

[3] R.P.M.J.W. Notermans et al., Phys. Rev. A **90**, 052508 (2014).

[4] F.-F. Wu et al., arXiv:1804.01218 (2018).

[5] T. Killian et al., Phys. Rev. Lett. **81**, 3807 (1998).

[6] R.P.M.J.W. Notermans et al., Phys. Rev. Lett. **117**, 213001 (2016).

[7] K. Pachucki et al., Phys. Rev. A **95**, 012508 (2017).

[8] X. Zheng et al., Phys. Rev. Lett. **119**, 263002 (2017).

[9] M. Diepold et al., arXiv:1606.05231v2 (2017).

Isotope shift, non-linearity of King plots and the search for new particles

A. J. Geddes[1], **A. V. Viatkina**[2], **and V. V. Flambaum**[1,2]
[1] *School of Physics, University of New South Wales, Sydney 2052, Australia*
[2] *Helmholtz Institute Mainz, Johannes Gutenberg University, 55099 Mainz, Germany*
e-mail: *a.geddes@unsw.edu.au*

It has been recently suggested to use the measurements of the King plot non-linearity in a search for hypothetical new light bosons [1]. However, in order to extract and put limits on the effect on new bosons, one must find the non-linear corrections to the King-plot already arising in the Standard Model framework. A King plot is constructed from the isotope shifts between four isotopes of a given atom for two different transitions; the points are conventionally fitted with a line in order to extract nuclear parameters and electronic isotope shift terms.

We investigate the notion of a non-linear King plot and focus on contributions to the non-linearity arising from relativistic effects in the isotope field-shift, the nuclear polarizability and many-body effects [2]. It is found that the nuclear polarizability contribution can lead to the significant deviation of the King plot from linearity. Therefore, the measurements of the non-linearity of King plots may be applied to obtain the nuclear polarizability change between individual isotopes. We then proceed to provide a rough analytical estimate of the non-linearity arising solely from the effect of a hypothetical scalar boson. Our predictions give theoretical limitations on the sensitivity of the search for new interactions and should help to identify the most suitable atoms for corresponding experiments.

In addition, we derive a mean-field relativistic formula for the isotope shift of an electronic energy level for arbitrary angular momentum; we then use it to predict the spectra of superheavy metastable neutron-rich isotopes belonging to the hypothetical island of stability [2]. Our results may be applied to the search for superheavy atoms in astrophysical spectra using the known values of the transition frequencies for the neutron deficient isotopes produced in the laboratory [3]. An example of a relevant astrophysical system may be the spectra of the Przybylski's star where superheavy elements up to $Z = 99$ have been possibly identified [4].

[1] , J. C. Berengut, D. Budker, C. Delaunay, V. V. Flambaum, C. Frugiuele, E. Fuchs, C. Grojean, R. Harnik, R. Ozeri, G. Perez, and Y. Soreq, Phys. Rev. Lett. **120**, 9 091801 (2018)

[2] V. V. Flambaum, A. J. Geddes and A. V. Viatkina, Phys. Rev. A **97**, 3 032510 (2018)

[3] V. A. Dzuba, V. V. Flambaum, and J. K. Webb, Phys. Rev. A **95**, 062515 (2017)

[4] V. F. Gopka, A. V. Yushchenko, V. A. Yushchenko, I. V. Panov and C. Kim, Kinematics and Physics of Celestial Bodies **24**, 89 (2008)

Quantum State Transportation of Rubidium Atoms inside a Photonic Waveguide

M. Xin, W. S. Leong, Z. Chen and S.-Y. Lan
School of Physical and Mathematical Sciences, Nanyang Technological University, 637371, Singapore
e-mail: *XINM0002@e.ntu.edu,sg*

Coherent interactions between electromagnetic and matter waves lie at the heart of quantum science and technology. We optically trap cold 85Rb atoms in a hollow-core photonic crystal fiber and use the waveguide fields as matter-wave beam splitter and mirror pulses to demonstrate a Mach-Zehnder interferometer. The results suggest that the coherence of a quantum superposition state of atoms can be coherently interrogated by the optical guided mode inside the hollow core fiber.

We also experimentally study the ground state coherence properties of 85Rb atoms inside the hollow-core fiber. We find that, the dephasing of atomic ground states is mainly due to the inhomogeneous broadening of differential ac stark shift between the ground states introduced by the optical dipole beams. In order to cancel the differential ac stark shift, we introduce vector light shift by applying an external magnetic field and adjusting polarization of the dipole beams. After the cancellation, we achive a long coherence time of T=250 ms, and able to maintain the coherence of a quantum superposition state over one centimeter distance of transportation along the optical fiber. The integration of phase coherent photonic and quantum systems here shows great promise to the advance capability of atom interferometers, compact atomic clock, quantum memory and optical fiber quantum network.

[1] M. Xin, W. S. Leong, Z. Chen, S.-Y. Lan, An atom interferometer inside a hollow-core photonic crystal fiber. Sci. Adv. **4**, e1701723 (2018).

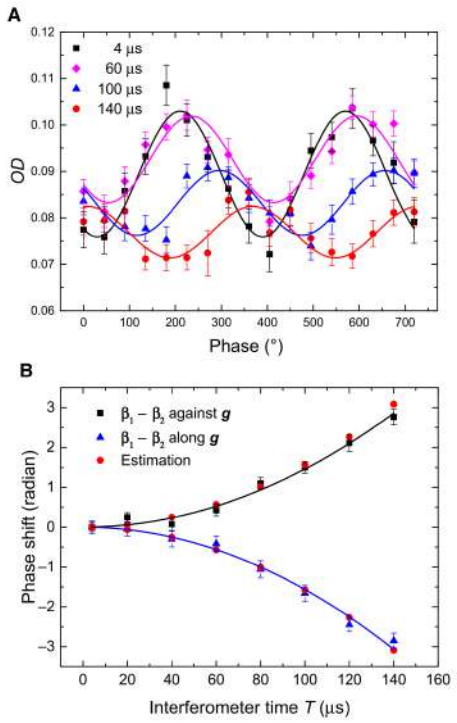


Figure 1: Mach-Zehnder interferometer. (A) OD versus phase with different interferometer times T. (B) Phase shift versus time T. Each data point is extracted from the fitting of a sinusoidal function as in (A) with the Raman beam direction along and opposite to the gravity.

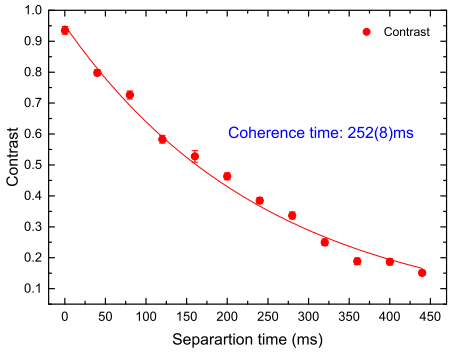


Figure 2: Contrast as a function of seperation time for spin echo using microwave. The red line represents exponential fit with dacay time of 252(8) ms.

Sub-Doppler Molecular Spectroscopy, Frequency Metrology, and PNC induced Optical Rotation Measurement based on NICE-OHMS Scheme with a High Finesse Cavity

Tzu-Ling Chen[1], **Wei-Ling Chen**[1], **and Yi-Wei Liu**[1]

[1] *Department of Physics, National Tsing Hua University, Hsinchu 30013, Taiwan*

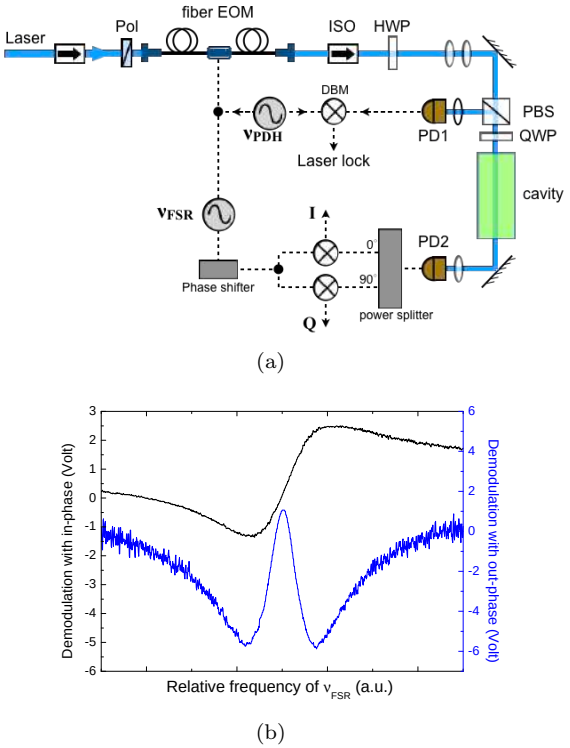
e-mail: *tlchen@mx.nthu.edu.tw*

Noise-immune cavity-enhanced optical heterodyne molecular spectroscopy (NICE-OHMS) [1], taking advantage of combining the cavity enhancement and frequency modulation techniques, provides an excellent method enable for ultra sensitive detection. The advantage of noise immunity benefit from the combination enables for shot-noise limit detection, which is strengthened particular in the employment of a high finesse cavity. Here, we report some applications taking advantage of NICE-OHMS using an optical cavity with a high finesse >100,000.

First, we present our work on the quantum-dot (QD) laser stabilization at 1.28 μm nitrous oxide (N_2O) overtone transitions. For overtone transitions or symmetrical molecules with ultra-small dipole moments, NICE-OHMS provides a superior strategy to achieve sub-Doppler saturation spectroscopy [2]. We demonstrate the potential of the N_2O as a marker because of its particularly rich spectrum at the vicinity of 1.28 μm where there are several important forbidden transitions of atomic parity violation measurements. At a pressure of several mTorr, the saturation dip is observed with a full width at half-maximum of about 2 MHz. The QD laser is then locked to this dispersion signal with a stability of 15 kHz at 1 s integration time.

Second, the dual-frequency modulation light used in NICE-OHMS also enable for the precise measurement of cavity FSR. Instead of using widely used method invented by DeVoe and Brewer, here we propose and demonstrate a new method for FSR locking and real-time measurements processing with more simplifier RF electronics. By using phase modulation light locked in the off-resonance of the cavity modes, a dispersion signal with an accurate indicator enabling for FSR locking can be generated as shown in Fig. 1. In our result, the measured cavity FSR is with a precision of 10^{-9}.

Finally, we propose a novel cavity based polarimeter on the basis of modified NICE-OHMS. The refraction unbalance between left- and right- circulated light results in optical rotation enable for parity nonconservation (PNC) measurements. It is challenging, for its weak signal, which urge the developments in high finesse cavity based polarimetry. However, the intrinsically reciprocal feature of the optical rotation make two-mirrors cavity can't be realized without the help of other intra-cavity elements. This limit



(a)

(b)

Figure 1: (a) Simplified experimental setup for precise measurements of cavity FSR, (b) The demodulation signal with in- and out- phase for the error signal generation and the central of the cavity FSR indicator respectively.

the achievable enhancement and ultimate sensitivity performed by two-mirrors cavity based polarimeter. Here, a novel cavity based polarimeter capable of robust enhancement is proposed with a non-orthogonal beam system, where the Doppler shift can break the reciprocal property and thus allow a continued increase of optical rotation in a pure two-mirrors cavity without experiencing extra loss.

[1] J. Ye, L. S. Ma, and J. L. Hall, J Opt Soc Am B **15**, 6 (1998).

[2] F.M.J. Cozijn, P. Dupr, E.J. Salumbides, K.S.E. Eikema, and W. Ubachs, Phys. Rev. Lett. **120**, 153002 (2018).

[3] T.-L. Chen and Y.-W. Liu, Optics Letters **42**, 2447 (2017).

Continuous motional sensing with highly dispersive medium

W. S. Leong, P.-C. Kuan, C. Huang and S.-Y. Lan
Division of Physics and Applied Physics, School of Physical and Mathematical Sciences, Nanyang Technological University, Singapore
e-mail: *wleong016@e.ntu.edu,sg*

Current state-of-the-art atoms-based motional sensors rely on measuring the first-order Doppler shift of the atomic transition of single-particles. By using Doppler-sensitive detection methods to map out the Doppler distribution of an atomic ensemble, the center-of-mass velocity of the atom ensemble can be measured precisely. On the contrary, here, we demonstrate a novel method of measuring the center-of-mass motion of an atomic ensemble directly using the collective interference of light passing through the ensemble under the condition of electromagnetically-induced-transparency (EIT). With the large enhancement of the dispersion in the EIT medium, we realize an atom-based velocimeter that has a sensitivity two orders of magnitude higher than the velocity width of the atomic medium used. This method has the advantages of high data rate and convenient detection of the interference phase of light over the conventional method of detecting the florescence of atoms and could lead to a new design of compact atoms-based motional sensors.

[1] P.-C. Kuan, C. Huang, W. S. Chan, S. Kosen, S.-Y. Lan, Large Fizeaus light-dragging effect in a moving electromagnetically induced transparent medium. Nat. Com. **7**, 13030 (2016).

Enhanced nuclear spin dependent parity violation effects using the ^{199}HgH molecule

A. J. Geddes[1], **L. V. Skripnikov**[2,3], **A. Borschevsky**[4], **J. C. Berengut**[1], **V. V. Flambaum**[1], **T. P. Rakitzis**[5,6]

[1] *School of Physics, University of New South Wales, Sydney, New South Wales 2052, Australia*
[2] *National Research Centre Kurchatov Institute B.P. Konstantinov Petersburg Nuclear Physics Institute, Gatchina, Leningrad district 188300, Russia*
[3] *Department of Physics, Saint Petersburg State University, Saint Petersburg, Petrodvoretz 198904, Russia*
[4] *Van Swinderen Institute, University of Groningen, Nijenborgh 4, 9747 AG Groningen, The Netherlands*
[5] *Department of Physics, University of Crete, 71003 Heraklion-Crete, Greece*
[6] *Institute of Electronic Structure and Laser, Foundation for Research and Technology-Hellas, 71110 Heraklion-Crete, Greece*
e-mail: *a.geddes@unsw.edu.au*

The violation of symmetry under a parity operation is known as parity non-conservation (PNC) which, in atoms and molecules, can be classified as nuclear spin dependent (NSD) or nuclear spin independent (NSI) PNC. The nuclear anapole moment is one example of a manifestation of NSD PNC in atoms and molecules [1, 2] and has been detected only once within the ^{133}Cs atom [3], where NSD PNC is sub-dominant. This is because experimental techniques have lacked the sensitivity to detect NSD PNC effects with certainty.

NSD PNC calculations in molecules provide a new window of opportunity to study the parity violating nuclear forces that create the nuclear anapole moment. Importantly, PNC effects are enhanced within diatomic molecules due to closely spaced rotational levels of opposite parity [4, 5]. Mercury hydride (HgH) in particular is a promising choice for the study of PNC effects, not only because it gives an enhanced, pure NSD PNC signal but also because it is easy to make at room temperature.

A low-energy optical rotation experiment is being proposed with the aim of observing NSD PNC interactions in HgH. Using the relativistic coupled cluster method, we present a complete calculation of the circular polarization parameter $P = 2\,\mathrm{Im}(E1_{PNC})/M1 \approx 3 \times 10^{-6}\ \kappa$ for the $^2\Sigma_{1/2} \rightarrow ^2\Pi_{1/2}$ optical transition of HgH, where κ is a dimensionless constant determined by the nuclear anapole moment [6]. This provides an improvement in sensitivity to NSD PNC by 2 – 3 orders of magnitude over the leading atomic Xe, Hg, Tl, Pb and Bi optical rotation experiments, and shows that the proposed measurement will be sensitive enough to extract the ^{199}Hg anapole moment and shed light on the underlying theory of hadronic parity violation.

[1] V.V. Flambaum, I.B. Khriplovich. ZhETF **79**, 1656, 1980. [JETP **52**, 835, (1980)].

[2] V.V. Flambaum, I.B. Khriplovich, O.P. Sushkov. Phys. Lett. B. **146**, 367, 1984.

[3] C. S. Wood, S. C. Bennett, D. Cho, B. P. Masterson, J. L. Roberts, C. E. Tanner, and C. E. Wieman, Science **275**, 1759 (1997)

[4] O. P. Sushkov and V. V. Flambaum, Sov. Phys. JETP **48**, 608 (1978).

[5] L. N. Labzowsky, Sov. Phys. JETP **48**, 434 (1978).

[6] A. J. Geddes, L. V. Skripnikov, A. Borschevsky, J. C. Berengut, V. V. Flambaum, T. P. Rakitzis, (2018) arXiv:1804.05475 [physics.atom-ph]

Spatial entanglement patterns and Einstein-Podolsky-Rosen steering in Bose-Einstein condensates

Matteo Fadel, Tilman Zibold, Boris Décamps, Philipp Treutlein
Department of Physics, University of Basel, Klingelbergstrasse 82, Basel CH-5046, Switzerland
e-mail: *matteo.fadel@unibas.ch*

Entanglement is an essential resource for quantum technologies such as quantum metrology with atomic clocks and interferometers [1]. At the same time, it is a fundamental concept of quantum physics that still presents conceptual challenges, in particular when applied to many-body systems of indistinguishable particles. For example, spin-squeezed and other non-classical states of atomic ensembles were used to enhance measurement precision in quantum metrology, but the notion of entanglement in these systems was debated because the correlations between the indistinguishable atoms were witnessed by collective measurements only [2].

In this work [3], we experimentally prepare two-component Rubidium-87 BECs, consisting of a few hundred atoms, on an atom-chip [4]. Using state-selective potentials to tune the collisional interactions (one-axis twisting dynamics), we prepare many-particle non-classical states [5]. After a time-of-flight expansion, high-resolution imaging allows us to access sub-regions of the atomic density distribution of various shapes and measure the spin correlations between them, see Fig. 1.

We observe that bi-partitions violate a separability criterion, showing the presence of entanglement between different spatial regions of our many-body system. In some of such partitions, entanglement is strong enough for Einstein-Podolsky-Rosen steering: measurement outcomes for non-commuting observables in one spatial region can be predicted based on corresponding measurements in the other region with an inferred uncertainty product below the Heisenberg relation [6]. This feature could be exploited for imaging of electromagnetic and other field distributions with an uncertainty beyond the standard quantum limit.

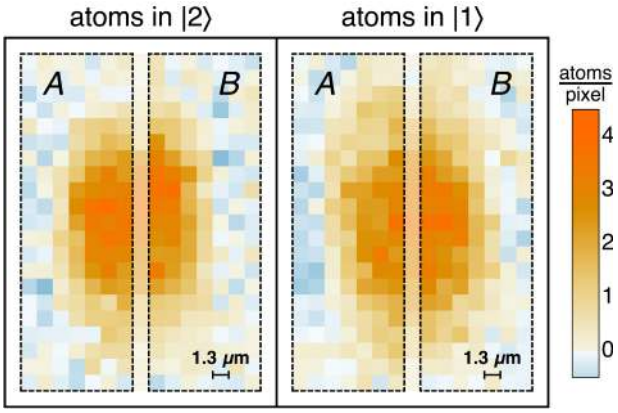


Figure 1: Single-shot absorption images of the atomic densities in $|2\rangle$ and $|1\rangle$, showing example regions A and B used to define the (local) collective spins $\hat{S}^A$ and $\hat{S}^B$ entering in the entanglement and EPR steering criteria.

[1] L. Pezzè, A. Smerzi, M. K. Oberthaler, R. Schmied, and P. Treutlein, to appear in Rev. Mod. Phys., preprint at arXiv:1609.01609 (2017).

[2] N. Killoran, M. Cramer, and M. B. Plenio, Phys. Rev. Lett. **112** 150501 (2014).

[3] M. Fadel, T. Zibold, B. C. Decámps, and P. Treutlein, Science **360**, 409 (2018)

[4] P. Böhi, et al., Nature Physics **5**, 592 (2009).

[5] M. F. Riedel, et al., Nature **464**, 1170 (2010).

[6] M. D. Reid, et al., Rev. Mod. Phys. **81**, 1727 (2009).

Precision spectroscopy of the 1S–2S transition in antihydrogen

G. Stutter[1] **for the ALPHA collaboration**
[1] *Aarhus University, DK-8000 Aarhus C, Denmark*
e-mail: *graham.stutter@cern.ch*

Performing precision spectroscopy on the 1S–2S transition in antihydrogen is a long-standing goal of the antimatter community and is a common goal of many of the experiments based in the Antiproton Decelerator (AD) facility at CERN. We present a spectroscopic measurement of the lineshape of 1S–2S transition in antihydrogen, shown in Figure 1 [1]. Comparing this result to the measured transition in hydrogen, which has been recorded with a precision of 10^{-15} [2], provides a direct test of the CPT theorem which dictates that the spectra of hydrogen and antihydrogen must be identical. This new measurement of the resonance frequency is an improvement of nearly two orders of magnitude on our 2016 measurement [3] and agrees with the predicted value for hydrogen to within 5 kHz, or 2 parts in 10^{-12}.

In the ALPHA experiment we produce antihydrogen by mixing plasmas of positrons with antiprotons from the AD in a nested well Penning trap. Atoms with kinetic energy of less that 0.54 K are trapped in a magnetic multipole neutral atom trap. Our silicon vertex detector is able to detect loss of antihydrogen from the trap due to laser ionisation or spin flip with single atom resolution during the laser exposure ('appearance' mode), and is also to used to count how many atoms remain at the end of the experiment ('disappearance' mode).

Over 15000 antihydrogen atoms were trapped during the spectroscopy trials presented in Figure 1, and a total of 72000 during the 2017 run as a whole. These numbers represent a significant advance to the field of antimatter physics, with the prospects for improving measurements of the ground state hyperfine splitting [4], gravitational mass [5] and fine structure of antihydrogen also greatly improved.

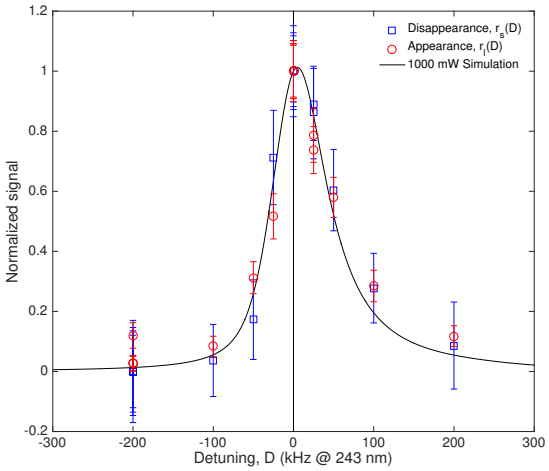


Figure 1: The measured 1S–2S antihydrogen spectrum, recorded during the 2017 run, showing both the appearance and disappearance signals. The solid line shows a numerical simulation for 1 W of circulating laser power at 243 nm [1].

[1] M. Ahmadi et al., Nature **557**, 71–75 (2018)

[2] C. G. Parthey et al., Physical Review Letters, **107**, 203001 (2011)

[3] M. Ahmadi et al., Nature **451**, 506–510 (2017)

[4] M. Ahmadi et al., Nature **548**, 66–69 (2017)

[5] C. Amole et al., Nature Communications **4**, 1785 (2013)

Theory of large-momentum-transfer Bose-Einstein condensate interferometers

J.-N. Siemß[1,2], **E. M. Rasel**[2], **K. Hammerer**[1] **and N. Gaaloul**[2]
[1] *Inst. für Theoretische Physik, Leibniz Uni. Hannover, Appelstrasse 2, 30167 Hannover, Germany*
[2] *Inst. für Quantenoptik, Leibniz Uni. Hannover, Welfengarten 1, 30167 Hannover, Germany*
e-mail: *siemss@iqo.uni-hannover.de*

Light-based large-momentum-transfer (LMT) beam splitters and mirrors for matter waves are likely to become integral parts of next generation atom interferometers measuring inertial forces. LMT schemes aim at increasing the spatial separation of the two interferometer arms, thereby enhancing the sensitivity of such atomic detectors. Alternatively, one would employ large interrogation times in microgravity [1] and fountains [2].

A promising method to realize novel high fidelity LMT schemes is to combine Bragg pulses and Bloch oscillations in optical lattices to coherently split and recombine the atomic wave packets. This technique already allows for state-of-the-art momentum separation in an atom interferometer with up to 208 photon recoils ($\hbar k$) as well as for beam splitters with up to 1008 $\hbar k$ momentum separation [3].

The fidelity of such LMT sequences, however, is constrained by damping of Bloch oscillations caused by tunneling and the finite momentum width of the atomic ensemble. This motivates the use of Bose-Einstein condensates as highly coherent atomic sources with inherent small momentum dispersion for sensitive LMT-based atomic sensors.

During my doctoral research, I simulate interferometric sequences involving Bose-Einstein condensates driven by symmetric optical lattices to interpret and optimize pioneering experiments performed in the QUANTUS collaboration. To this end, analytical methods together with a time-dependent Gross-Pitaevskii model are developed and adapted to typical experimental environments. Our analysis allows us to assess these LMT schemes and to identify the dominant loss mechanisms leading to a reduction of the interferometric contrast with increasing momentum acceleration.

Having understood the current limitations we aim at analyzing the scalability of LMT schemes using Bloch lattices on a fundamental level. Considering realistic experimental parameters we want to quantify the maximally achievable momentum separation of the atomic superposition states with this technique while still maintaining coherence between them.

In close collaboration with the experimental team, our efforts are enabling us to propose novel LMT schemes for highly sensitive atom interferometers featuring separations of thousands of $\hbar k$.

[1] H. Müntinga et al. Phys. Rev. Lett. **110**, 093602 (2013).

[2] S. M. Dickerson et al. Phys. Rev. Lett. **111**, 083001 (2013).

[3] S. Abend, *Atom-chip gravimeter with Bose-Einstein condensates* (PhD thesis), Leibniz University Hannover, 2017.

[4] S. Chiow et al. Phys. Rev. Lett. **107**, 130403 (2011).

Coherence in a cold quantum matrix

Y. Miyamoto[1], **for the SPAN collaboration**

[1] *Research Institute for Interdisciplinary Science, Okayama University, Okayama 700-8530, Japan*
e-mail: *miyamo-y@okayama-u.ac.jp*

The physics beyond the standard model of particle physics is one of the most important scientific problems today. Recent technical developments in atomic, molecular, and optical sciences make it possible to try the problems even in small laboratories. The search for the electric dipole moment of the electron using cold atoms and molecules is a typical and successful example [1]. In general, the signals suggesting signs of the physics beyond the standard model is very weak so that it is essential to amplify the signal intensity. A simple answer to obtain large signals is to increase the number of targets. From such a point of view, solid-state targets are advantageous because their target density can be orders of the magnitude larger than that achievable in the gas phase. The strong interaction in solids, however, would veil faint signals and significant information on physics. The ideal targets should satisfy the two conflicting requirements simultaneously: high density and isolated environment.

Cold matrices, which are usually solids of rare gases or hydrogen molecules, would provide a solution. It is known that atoms and molecules trapped in the matrices are "nearly" isolated because of their weak intermolecular interactions. The atoms or molecules of the matrices themselves can also be targets. There are several proposals to investigate fundamental physics using cold matrices: a search for electron electric dipole moment [2], neutrino mass spectroscopy [3], and a dark matter (axion) search [4].

A further amplification mechanism is necessary for the neutrino mass spectroscopy because the expected signal rate is extremely small. We, SPAN (SPectroscopy of Atomic Neutrinos) collaboration, have planned to amplify the rate by coherence between targets. Process in the coherently excited targets is enhanced by the quantum interference. We have conducted proof-of-principle experiments using rare QED processes, such as multi photon processes, towards the neutrino mass spectroscopy [5]. The enhancement factor of the coherence amplification is proportional to the square of the number of targets so that the effect is huge when the target density is high, as in solid states. The coherence amplification would be helpful for studies on other problems in fundamental physics.

We previously observed coherence amplification of the two photon emission between the vibrational levels of solid hydrogen [6], which is called as quantum solid. The quantum solid has many attractive properties due to its light mass and weak intermolecular interactions. The long coherence time of the vibrational states is a key feature here among these properties. The vibrational coherence of solid hydrogen was generated by the stimulated Raman process. The observed temporal dependence of the intensity of the two photon emission showed that the prepared coherence develops even after the Raman driving pulses pass through the target. The origin of this surprising development still remains a mystery. It is important to deepen our understanding about the coherence in solids to take full advantage of the coherence amplification.

Recently, we observed the coherence amplification of the phase-conjugate two photon emission in solid hydrogen. In the present experiment, the vibrational coherence is prepared by absorption of two photons which propagate in the opposite direction. This counter-propagating ladder excitation and phase-conjugate two photon emission is not only interesting as a coherent transient phenomenon but also important for the neutrino mass spectroscopy because massive neutrinos can be emitted only when the target is excited by this scheme. It is found that the coherence prepared by this scheme does not develop after the driving pulses. On the contrary, the coherence prepared by one-directional two photon absorption, which is monitored simultaneously by the third harmonic generation, develops after the driving pulses as is the case with the previous Raman experiment. This difference due to the excitation geometry may open the way for understanding the origin of the mysterious development. We will present the current experimental setup and results in detail.

[1] J. J. Hudson *et al.*, Nature **473**, 493 (2011).

[2] K. G. Kozlov and A. Derevianko, Phys. Rev. Lett. **97**, 063001 (2006).

[3] A. Fukumi *et al.*, Prog. Theor. Exp. Phys. **2012**, 04D002 (2012).

[4] M. Yoshimura and N. Sasao, arXiv:1710.11262 [hep-ph] (2017).

[5] Y. Miyamoto, *et al.*, Prog. Theor. Exp. Phys. **2015**, 081C01 (2015).

[6] Y. Miyamoto, *et al.*, J. Phys. Chem. A **121**, 3943 (2017).

Measurement-induced nonlocal entanglement in a hot, strongly-interacting atomic system

Jia Kong[1], **R. Jiménez-Martínez**[1], **C. Troullinou**[1], **V. G. Lucivero**[2], **M. W. Mitchell**[1,3]

[1] *Institut de Ciències Fotòniques, The Barcelona Institute of Science and Technology, 08860 Castelldefels, Spain*

[2] *Department of Physics, Princeton University, Princeton, New Jersey 08544, USA*

[3] *ICREA – Institució Catalana de Recerca i Estudis Avançats, 08010 Barcelona, Spain*

e-mail: *jia.kong@icfo.eu*

Quantum entanglement is one of the most non-classical feature of quantum theory, however it's notoriously sensitive to decohering processes. For this reason, many implementations take elaborate measures to remove entropy from their environments, e.g. cryogenics or optical cooling. Here we demonstrate that the opposite strategy, actively promoting strong interactions and thermalization, can excel in generating and preserving entanglement.

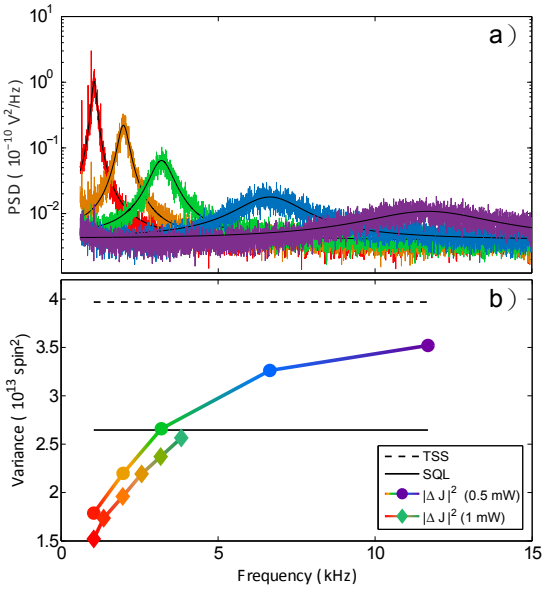


Figure 1: QND detection of collective spin in the strongly-interacting regime. a) Spin noise spectra with atomic spin signal driven by thermal fluctuations and precessing at the Larmor frequency ($\nu_L = \omega_L/2\pi$) rising above shot noise of the Faraday rotation probe. Different spectra correspond to different bias field strengths. Black lines are single Lorentz fits for the spectra. b) Spin variance versus Larmor frequency. Black dashed line shows the noise level of thermal spin state (TSS $= 3N_A/4$), the black solid-line shows standard quantum limit (SQL $= N_A/2$) where N_A is effective atomic number. Round symbols show the total spin variance $|\Delta\mathbf{J}|^2$ measured with 0.5 mW of probe light, corresponding to the spectra in a), and diamonds show $|\Delta\mathbf{J}|^2$ measured with 1 mW.

We work with a vapour of ^{87}Rb heated to 450 K and a number density of 3.6×10^{14} atoms/cm^3. Under these conditions random spin-exchange collisions dominate the spin physics, promoting both coherence time and optical depth via the so-called spin-exchange-relaxation-free (SERF) effect[1], which are critical parameters for optically-probed atomic ensembles technology. For example, it has been translated into orders-of-magnitude improvements in sensitivity of optical magnetometry [2]. However, no experimental evidence showed that the SERF-regime could also help for quantum optics. Here we describe experiments to harness this physics for entanglement generation through quantum non-demolition (QND) measurements. To generate and quantify entanglement in this system, we push the atoms working into SERF-regime and use Kalman filtering techniques to reconstruct the spin dynamics in real-time [3]. We observe extremely efficient entanglement generation, including projection of at least 2.3×10^{13} atoms into non-local singlet states. In addition to breaking all records for entanglement generation[4, 5], and synthesising for the first time a many-body state resembling a spin liquid, this shows that the unique properties of SERF-regime ensembles are extremely attractive for QND-based quantum technologies, with potential applications in quantum memories, quantum sensing and quantum simulation.

References

[1] W. Happer and H. Tang. Spin-exchange shift and narrowing of magnetic resonance lines in optically pumped alkali vapors. *Phys. Rev. Lett.*, 31(5):273–276, July 1973.

[2] IK Kominis, TW Kornack, JC Allred, and MV Romalis. A subfemtotesla multichannel atomic magnetometer. *Nature*, 422(6932):596–599, 2003.

[3] Ricardo Jiménez-Martínez, Jan Kołodyński, Charikleia Troullinou, Vito Giovanni Lucivero, Jia Kong, and Morgan W. Mitchell. Signal tracking beyond the time resolution of an atomic sensor by kalman filtering. *Phys Rev Lett*, 120(4):040503, January 2018.

[4] N. Behbood, F. Martin Ciurana, G. Colangelo, M. Napolitano, Géza Tóth, R. J. Sewell, and M. W. Mitchell. Generation of macroscopic singlet states in a cold atomic ensemble. *Phys. Rev. Lett.*, 113:093601, Aug 2014.

[5] P. Zarkeshian, C. Deshmukh, N. Sinclair, S. K. Goyal, G. H. Aguilar, P. Lefebvre, M. Grimau Puigibert, V. B. Verma, F. Marsili, M. D. Shaw, S. W. Nam, K. Heshami, D. Oblak, W. Tittel, and C. Simon. Entanglement between more than two hundred macroscopic atomic ensembles in a solid. *Nature Communications*, 8(1):906, 2017.

Coherent two-photon emission from hydrogen molecules towards neutrino mass spectroscopy

H. Hara[1], **for the SPAN collaboration**

[1] *Research Institute for Interdisciplinary Science, Okayama University, Okayama 700-8530, Japan*

e-mail: *hhara@okayama-u.ac.jp*

We (SPAN project: SPectroscopy of Atomic Neutrino) propose to study extremely weak processes which emit plural particles involving neutrinos (RENP: Radiative Emission of Neutrino Pair) [1]. Our ultimate goal is to investigate unknown neutrino properties such as their absolute masses, mass type (Dirac or Majorana), and CP-violating phases [2] from spectra of RENP.

For this study, enhancement of the rare process emitting plural particles is crucial. We propose a rate amplification mechanism by using material coherence like superradiance. The requirement for the rate amplification corresponds to phase matching in nonlinear optics. We confirmed this mechanism by coherent amplification of a two-photon emission process from the first vibrationally excited state of parahydrogen molecules (p-H_2). This process is easier to observe than RENP because it is a QED process without any weak interaction. We generated coherence among these vibrational levels by stimulated Raman transition, and observed coherently amplified two-photon emission triggered by midinfrared laser pulses [3]. By applying this mechanism to RENP process, it becomes possible to solve the remaining problems on neutrino.

However, the process of emission of neutrinos, which have finite masses, cannot be amplified by Raman transition. To realize successful RENP experiment, it is essential to excite atoms or molecules without giving them any momentum. Coherence generation using ladder excitation by counter-propagating photons is the most basic configuration for our purpose. As a demonstration of the amplification mechanism, we generate coherence between the vibrational levels of p-H_2 by using ladder excitation and observe coherently amplified two-photon emission.

Coherence between the vibrational levels is prepared by two-photon absorptions. Figure 1 (a) and (b) show the energy diagram of p-H_2 and the experimental setup, respectively. The two absorbed photons, which are referred as pump1 and pump2 pulses, have the identical wavelengths of 4806 nm. To generate high coherence, lasers with high intensity and narrow linewidth are required. We developed the mid-infrared laser pulses by using nonlinear optical processes. The counter-propagating pump pulses are injected into the p-H_2 target cell. If coherence is prepared, the trigger pulses induce the coherently amplified two-photon emission process, which generates pairs of another trigger photon and a two-photon emission signal photon. The wavelength of the trigger pulses is also 4806 nm. It can be shifted from those of the pump pulses. The signal photons, whose wavelength is also 4806 nm, propagate in the direction opposite to the trigger photons due to the requirement for the amplification. We succeeded in excitation of p-H_2 by the counter-propagating photons and observation of the coherently amplified two-photon emission signal. Furthermore, we investigated the dependences of the signal energy on the various parameters, such as the frequency detuning of the pump pulses, the target gas pressure, the input pulse energies, and the frequency and the timing of the trigger pulses. It is helpful for understandings of coherent amplification to compare the measured parameter dependences to the the approximate model or the numerical simulation. In our poster, we introduce our plan of neutrino mass spectroscopy and the current status of the demonstration of the coherent amplification of the two-photon emission.

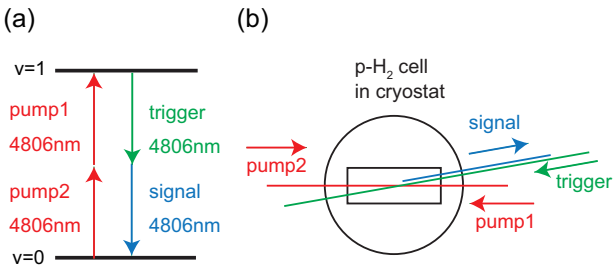


Figure 1: (a) Energy diagram of p-H_2. (b) Experimental setup.

[1] A. Fukumi *et al.* , Prog. Theor. Exp. Phys. **2012**, 04D002 (2012).

[2] S. M. Bilenky and S. T. Petcov, Rev. Mod. Phys. **59**, 671 (1987).

[3] Y. Miyamoto *et al.* , Prog. Theor. Exp. Phys. **2015**, 081C01 (2015).

Magneto-optical trapping in glass cell evacuated by Non-Evaporable Getters

T. Oda, R. Inoue, T. Hosoya, and M. Kozuma

Department of Physics, Tokyo Institute of Technology, 2-12-1 O-okayama, Meguro-ku, Toyko 152-8550, Japan

e-mail: *oda.t.ad@m.titech.ac.jp*

Magneto-optical trapping (MOT) of atoms is a promising tool for developing advanced devices which enable high-precision measurements for applications such as time synchronization, metrology, and navigation [1, 2]. While the physics for the applications are well-known, towards the long-term goal, further investigations on a cold-atom system with reduced size and power are required. A non-evaporable getter (NEG) enables us to maintain an ultra-high vacuum level (UHV) without an electric power supply. The vacuum system with NEG demonstrates high pumping speed comparable with an ion pump for most gases in the vacuum environment, but not for noble gases including helium. The partial pressure of helium in the atmosphere ($\sim$ 0.5 Pa) might be the most significant limiting factor in achieving UHV since the permeated helium through glass walls cannot be pumped by NEG.

To investigate the feasibility of the miniaturization using the NEG, we have prepared a prototype which consists of a glass cell, a temperature controlled rubidium source, a NEG pump, and an ion pump. The inflow of helium owing to the permeation through the glass walls can be measured by turning off the ion pump and monitoring loading time of the MOT in the glass cell. Additionally, the prototype chamber enables us to control the ambient gas of the glass cell. Figure 1 shows the inflow when the ambient gas of the glass cell is an air ($\sim$100 Pa), pure N_2 ($\sim 10^5$ Pa), and an air ($\sim 10^5$ Pa). The two white region of Figure 1 shows inflow when the ambient gas of the glass cell is an air ($\sim$100 Pa). The first shading region of Figure 1 shows inflow when the ambient gas of the glass cell is pure N_2 ($\sim 10^5$ Pa). The second shading region of Figure 1 shows inflow when the ambient gas of the glass cell is the air ($\sim 10^5$ Pa). The experimental results indicate that the observed inflow is mainly caused by the permeated helium.

In this poster, we will also show the experimental results of the relation between the inflow and ambient helium pressure.

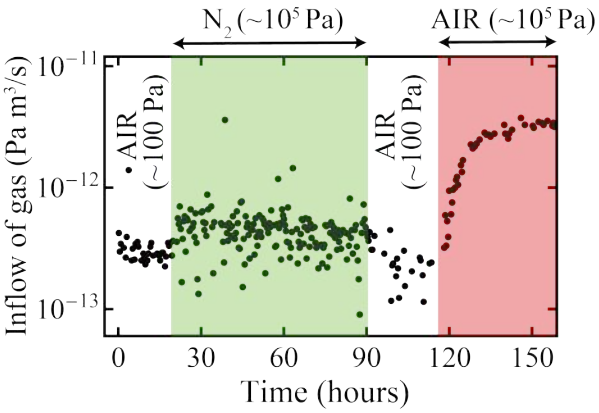


Figure 1: Inflow of gases into the vacuum system through glass wall. We controlled ambient gas of the glass cell to examine the limiting factor of the vacuum level.

[1] S. M. Dickerson, J. M. Hogan, A. Sugarbaker, D. M. S. Johnson, and M. A. Kasevich, Phys. Rev. Lett. **111**, 083001 (2013).

[2] I. Ushijima, M. Takamoto, M. Das, T. Ohkubo, and H. Katori, Nat. Photon. **9**, 185-189 (2015).

[3] T. Arpornthip, C. A. Sackett, and K. J. Hughes, Phys. Rev. A **85**, 033420 (2012).

A strict experimental test of macroscopic realism in a light-matter interfaced system

Xiao Liu[1,2], **Zong-Quan Zhou**[1,2], **and Chuan-Feng Li**[1,2]

[1] *CAS Key Laboratory of Quantum Information, University of Science and Technology of China, Hefei, 230026, China*

[2] *Synergetic Innovation Center of Quantum Information and Quantum Physics, University of Science and Technology of China, Hefei, 230026, China*

e-mail: *xiaoliu1@mail.ustc.edu.cn*

Macroscopic realism is a classical worldview that a macroscopic system is always determinately in one or other of the macroscopically distinguishable states available to it, and so is never in a superposition of these states. The question that whether there is a fundamental limitation on the possibility to observe quantum phenomena at the macroscopic scale remains unclear. Here we implement an experimentally simplified protocol to test macroscopic realism in a light-matter interfaced system. By determining classical disturbance with control experiments, we address the clumsiness loophole. Specifically, we create a micro-macro entanglement with two macroscopically distinguishable solid-state components and rule out non-disturbance condition (NDC) [1] for up to 76 atomic excitations in two solids. These results provide a general method to enhance "quantumness" by utilizing quantum memory techniques, which could be used in other systems to expand the size of quantum superpositions in matter and test macroscopic realism in a larger scale.

Our implementation starts with a single-photon micro-micro entanglement, which is subsequently displaced to the micro-macro entanglement using local displacement operation ($\hat{D}(\alpha)$) in optical phase space. The displaced photon is then mapped to an atomic ensemble, creating the light-matter micro-macro entangled state. Through a back-displacement operation [2], the micro-micro entanglement is retrieved and sent for analysis. The whole NDC test needs two sets of analogous experiments, one control experiment used to determine the worst case disturbance when classical states are prepared and one main experiment to measure the disturbance not explainable merely by appealing to the clumsiness revealed in the control experiments.

The experiment setup is illustrated in Fig. 1. One photon of a photon pair is used for trigger and the other photon is sent for NDC test. After absorption by the quantum memory, the atomic state can be written as

$$|\Phi_{12}\rangle = |\Omega_1\rangle_L|g\rangle_R + |\Omega_2\rangle_L|e\rangle_R, \qquad (1)$$

where $|g\rangle_R$ and $|e\rangle_R$ denote states for the R crystal with and without one photon excitation, while $|\Omega_1\rangle_L$ and $|\Omega_2\rangle_L$ represent the atomic excitation states of

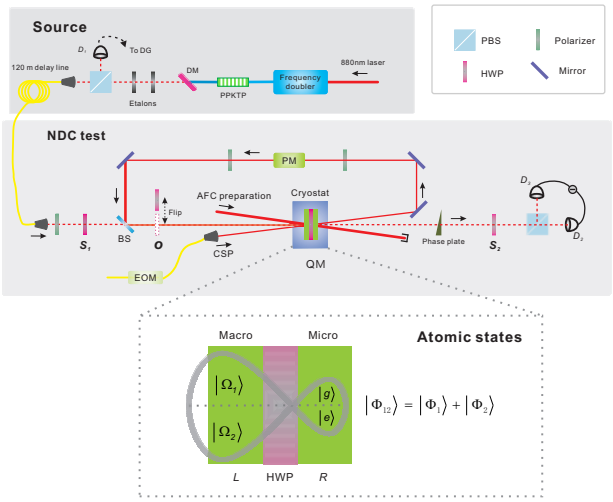


Figure 1: The experimental setup for violation of NDC with a light-matter interfaced system.

$\hat{D}(\alpha)|1\rangle$ and $|\alpha\rangle$ in the L crystal. The state (1) can be considered as a micro-macro entangled state with the atoms involving in L crystal playing the role of the 'macro' component and the atoms involving in R crystal of 'micro' component

we define a precise and operational notion of macrorealism that is tested in our experiment. Using conditional probabilities, disturbance parameter can be defined as [1]

$$\begin{aligned} d(\Phi) =& [P(Q_3 = +1|\Phi, O) - P(Q_3 = -1|\Phi, O)] \\ & - [P(Q_3 = +1|\Phi) - P(Q_3 = -1|\Phi)], \end{aligned} \qquad (2)$$

According to NDC, the fact that $d(\Phi_1) = d(\Phi_2) = 0$ but $d(\Phi_{12}) \neq 0$ could be thought of as an violation of the macrorealist view. In our experiment, we find violations $d(\Phi_{12}) - d(\Phi_1) = 0.80079$ and $d(\Phi_{12}) - d(\Phi_2) = 0.81553$, which are both 21 s.d. away from zero, respectively, for up to 76 excitations. We further calculate the disconnectivity of the state to be $\mathcal{D} \approx 5$.

[1] G. C. Knee, K. Kakuyanagi, M.-C. Yeh, *et al.*, Nat. Commun. **7**, 13253 (2016).

[2] A. Tiranov, J. Lavoie, P. C. Strassmann, *et al.*, Phys. Rev. Lett. **7**, 116, 190502 (2016).

Measurements of the fine structure constant α, using methods from atomic, condensed-matter, and particle physics, are powerful tests of the overall consistency of theory and experiment across physics. We have measured α= 1/137.035999046(27), at 2.0 x 10^-10 accuracy, via the recoil frequency of cesium-133 atoms in a matter-wave interferometer. We used multiphoton interactions such as Bragg diffraction and Bloch oscillations to increase the phase difference for the interferometer to over 12 million radians, which reduced the statistical uncertainty and enabled control of systematic effects at the 0.12 part-per-billion level. This is an unprecedented test of the standard model of particle physics, being the first direct measurement of α with an error below the 5th order quantum electrodynamics contribution in the electron's gyromagnetic anomaly. It also has implications for the unexplained anomaly of the muon's magnetic moment, and strongly constrains multiple dark sector candidates as well as substructure of the electron.

RF microplasmas with energies suited to selective cleaning of surface adsorbates in ion microtraps

M. Akhtar[1,2], **G. Wilpers**[1], **K. Choonee**[1], **E. Riis**[2], **and A. G. Sinclair**[1]
[1] *National Physical Laboratory, Teddington, TW11 0LW, UK*
[2] *Department of Physics, University of Strathclyde, Glasgow, G4 0NG, UK*
e-mail: *mariam.akhtar@npl.co.uk*

Ion traps have a number of applications in optical atomic clocks, quantum metrology and quantum information processing. However motional heating rates in ion microtraps remain a significant limitation to the quantum coherence time. Experiments with surface microtraps showed that carbon-based surface contaminants, thought to be sources of electric field noise, can be treated with ion beam sputtering to enable a significant reduction in heating rate [1, 2]. This method is not suited to microtraps with a 3D electrode geometry and therefore we present an alternative approach.

We have demonstrated a capacitively-coupled, RF microplasma inside the 3D segmented electrode structure of a microtrap [3], towards selective processing of surface contaminants. For this work, devices with an inter-electrode distance of 350 μm and array lengths of 2.6 mm (type A) and 6.4 mm (type B) were used. The microplasmas were operated at $\Omega_{RF}/2\pi =$ 23 MHz, in both He and He:N_2 gas mixtures, over a range of RF amplitudes (140 V to 200 V) and pressures (250 mbar to 910 mbar). Analysis of the He I 667 nm and Hα 656 nm spectral emission lines enabled the gas temperature and electron density to be measured. In turn, these quantities permitted calculation of the mean ion bombardment energy. For the range of operating parameters studied, we calculated mean He^+ energies to be between 0.8 eV and 5.1 eV. While these energies are less than the threshold for He sputtering of hydrocarbon adsorbates on Au, we calculate that the high energy tail of the distribution should remove adsorbate monolayers within 1 minute of processing (see Fig. 1). We also calculate that the distribution is insufficiently energetic to have any significant effect on the Au electrode surface within that duration. Our results suggest that the microplasma technique is suited to *in situ* selective removal of surface adsorbates from ion microtrap electrodes.

[1] N. Daniilidis, et. al., Phys. Rev. B **89**, 245435 (2014).

[2] D. A. Hite, et. al., Phys. Rev. Lett. **109**, 1 (2012).

[3] G. Wilpers, et. al., Nat. Nanotechnol. **7**, 572 (2012).

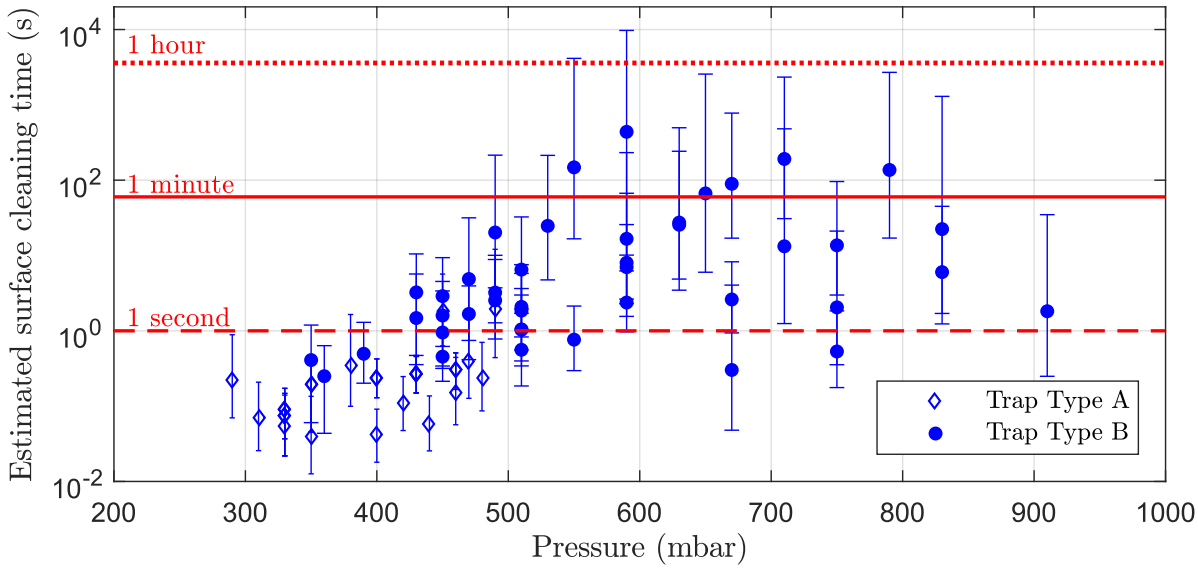


Figure 1: Estimated cleaning time to reduce 2 monolayers of carbon contamination to 1 atom/mm^2 for two different trap aperture lengths (type A in diamonds and type B in dots). The thresholds for a second, a minute and an hour cleaning time are indicated with a dashed, solid and dotted line respectively.

Current Status of the JILA eEDM Experiment

Kia Boon Ng[1], William B. Cairncross[1], Tanya S. Roussy[1], Yan Zhou[1], Yuval Shagam[1], Daniel N. Gresh[1], Kevin Boyce[1], Madeline Pettine[1], Antonio Vigil[1], Lan Cheng[2], Jun Ye[1], and Eric A. Cornell[1]

[1] *JILA, NIST and University of Colorado, and Department of Physics, University of Colorado, Boulder CO 80309-0440, USA*

[2] *Department of Chemistry, Johns Hopkins University, Baltimore, MD 21218, USA*

e-mail: *ngkiaboon@gmail.com*

A measurement of the electric dipole moment of the electron (eEDM, d_e) provides a direct test of theories beyond the Standard Model to provide insight into new physics like baryonic asymmetry and dark matter. Molecular ions like HfF^+ and ThF^+ are sensitive to the eEDM, and allow for excellent rejection of systematics through the $^3\Delta_1$ science state. The JILA eEDM experiment takes advantage of the large effective electric field and long coherence times of these trapped ions for the probe of the eEDM.

In the first generation JILA eEDM experiment, we obtained an upper bound of $|d_e| < 1.3 \times 10^{-28} e\,\mathrm{cm}$ (90% confidence) with trapped HfF^+[1]. Herein, I present an overview of the ongoing improvements to the experiment. In the current experiment, we are working on improving our statistics. Some of the improvements involved are (i) rotational cooling of the science state through optical pumping and microwave coupling to increase the number of useful ions in the trap; (ii) redesigning the trap for a larger trap volume and field homogeneity; and (iii) an improved ion counting scheme for a more efficient state readout. In parallel, we are also exploring the possibility of using ThF^+ for the eEDM experiment to take advantage of the longer coherence time and larger effective electric field as compared to HfF^+ to push the limit down even further[2, 3].

[1] W. B. Cairncross, et. al., Physical Review Letters, **119**, 153001 (2017).

[2] D. Gresh, et. al., Journal of Molecular Spectroscopy, **319**, 1-9 (2016).

[3] L. V. Skripnikov, and A. V. Titov, Physical Review A, **91**, 042504 (2015).

Initial progress of high precision measurement of time-reversal symmetry violation in Thallium nucleus

K. Wenz[1], **O. Grasdijk**[2], **J. Kastelic**[2], **O. Timgren**[2], **D. DeMille**[2], **D. Kawall**[3], **S. Lamoreaux**[2], **T. Zelevinsky**[1]

[1] *Department of Physics, Columbia University in the City of New York, 538 West 120th Street, New York, NY 10027, USA*

[2] *Department of Physics, Yale University, New Haven, CT 06520, USA*

[3] *Department of Physics, University of Massachusetts Amherst, Amherst, MA 01003, USA*

e-mail: *kw2577@columbia.edu*

We discuss the plans and initial progress of an experimental search for time-reversal symmetry violation in a thallium nucleus by exploiting its Schiff moment (SM). We expect a 30-fold improvement of the sensitivity to the QCD θ parameter, with respect to previous measurements, in the first generation of the experiment. The experiment will require us to interrogate a cold molecular beam and manipulate quantum-states of the molecule using optical and microwave transitions. To acquire a cold beam of thallium fluoride, our CENTReX collaboration is designing a cryogenic source providing an intense beam. The SM measurement will utilize the molecular ground state, enabling us to take advantage of a long interaction region, where an applied electric field will strongly polarize the molecules and cause precession of the SM.

Recent progress includes construction and testing of frequency-stabilized ultraviolet light sources for optical manipulations of TlF, designing the detection region with applied microwaves, detection light, and a high collection efficiency of cycling optical photons, as well as testing the molecule source, and a previously modeled molecule lens that is supposed to focus the molecular beam in the detection region using a quadrupole electric field and the J=2 rotational state of the molecules. We also numerically solve optical Bloch equations to obtain insight into rotational cooling of TlF.

Comparative study of mechanical and structure properties of geopolymer matrices incorporated by nano-silica, nano-alumina and nano-zinc

Z. Zidi[a], M. Ltifi[b,c], Z.Ben Ayadi[a] and L.El Mir[a,d]

a. Laboratory of Physics of Materials and Nanomaterials Applied at Environment, College of Sciences in Gabes, Tunisia
b. Al-Imam Mohammad Ibn Saud Islamic University, College of Engineering, Department of Civil engineering, Riyadh, Saudi Arabia
c. Al Manar University, National Engineering School of Gabes, Department of Civil engineering, Gabes, Tunisia
d. Al-Imam Mohammad Ibn Saud IslamicUniversity, College of Sciences, Department of Physics, Riyadh, SaudiArabia

---

Abstract:

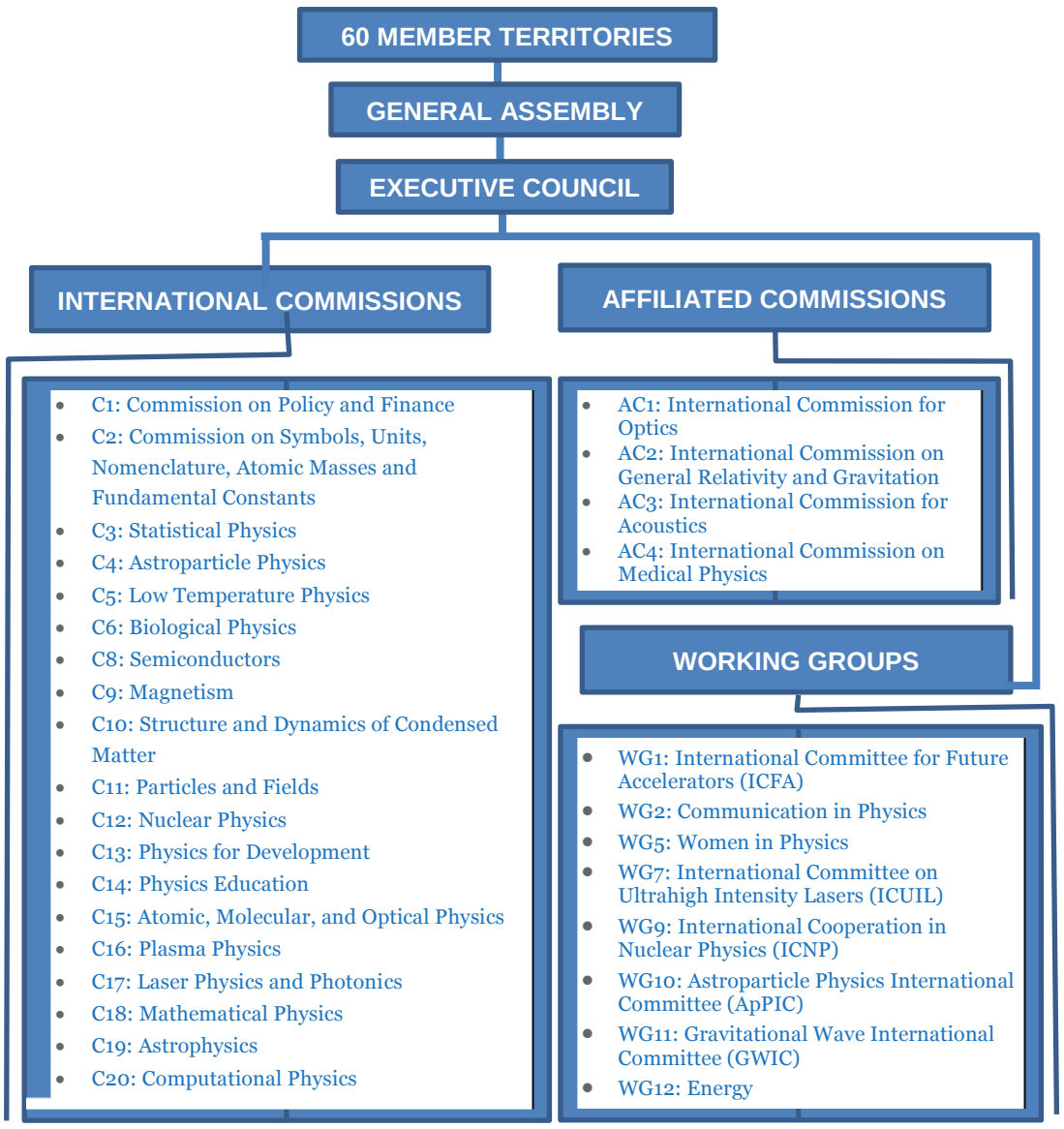
This work aims to study the effect of nano-silica, nano-alumina and nano-zinc on structural and mechanical properties of geopolymer matrix. The composite is produced by metakaolin, alkaline solution constant L/S ratio 0.55. The products is investigated by XRD, XRF,FTIR, SEM, UV/VIS and compressive strength test .The result show that nano-alumina increased more the mechanical and structural properties of geopolymer than nano-silica and nano-zinc. From FTIR spectra, we find that amorphous structure and geopolymer gel content are increased for the all nanoparticles but nano-alumina is more effective than other oxides. Dense structure as also observed in SEM investigation. Same results are also seen on physicals properties.

Key words: geopolymer, nano-silica, nano-alumina, nano-zinc, mechanical properties, structure properties

* Corresponding author. Tel.: 0021620647158.
E-mail address: Zidizoo18@gmail.com

INTERNATIONAL UNION OF PURE AND APPLIED PHYSICS

"To assist in the worldwide development of physics, to foster international cooperation in physics, and to help in the application of physics toward solving problems of concern to humanity"



Aims:

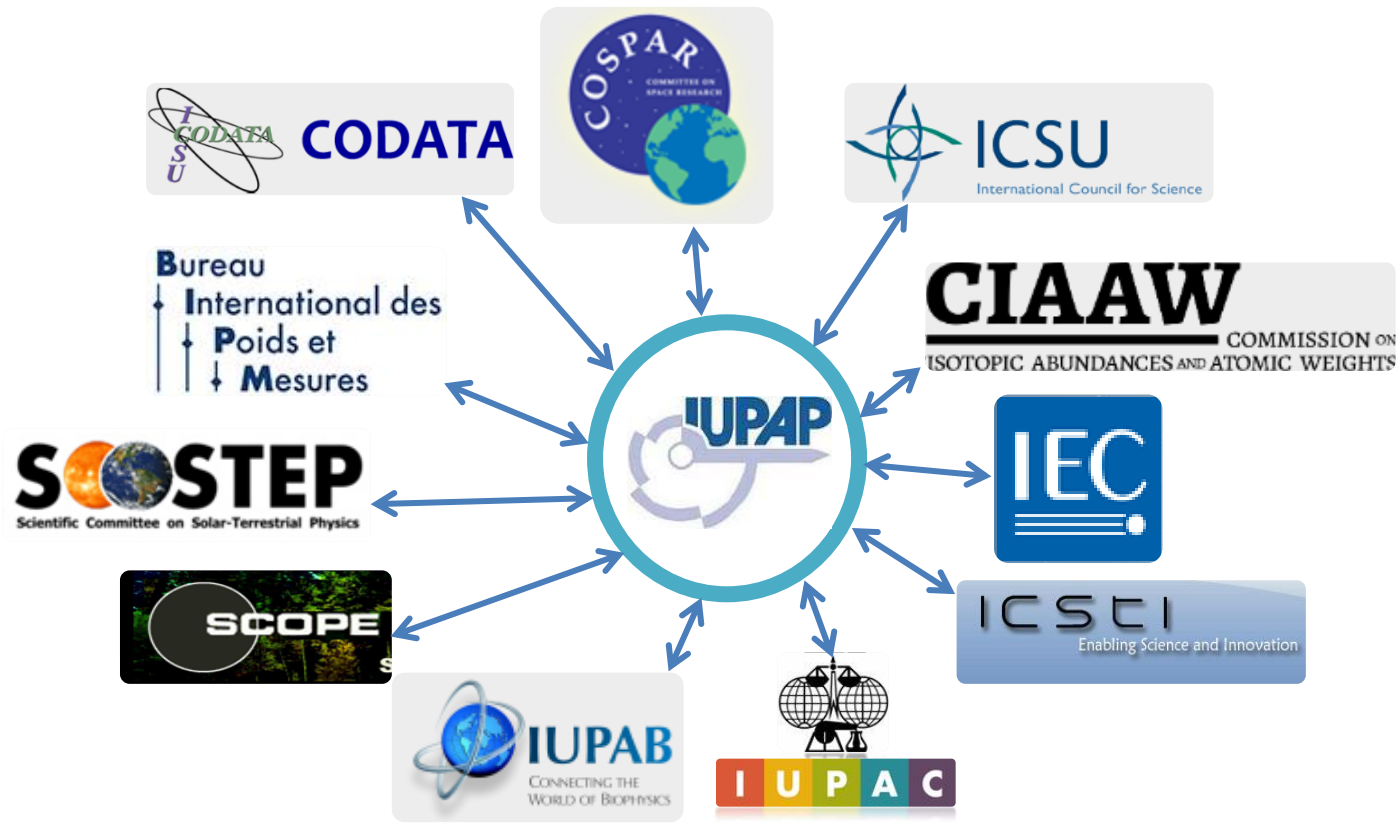
- to stimulate and promote international cooperation in physics;
- to sponsor suitable international meetings and to assist organizing committees;
- to promote international agreements on other use of symbols, units, nomenclature and standards;
- to foster free circulation of scientists; to encourage research and education.

Conference Sponsorship

Each year, IUPAP sponsors from 20 to 30 international conferences and awards grants to some of them. The financial support given to these International Conferences is derived from funds collected as membership dues from the members of IUPAP.

Inter Union Relations

As one of the basic sciences, physics relates to all branches of natural science. Many of the most exciting developments take place in the border areas between different disciplines. To cover interdisciplinary activities IUPAP maintains close liaison with several other Unions, ICSU Global Programs and ISCU Interdisciplinary Bodies. These collaborations take many forms, other organisations may have associate members on IUPAP Commissions, IUPAP may have representatives in their governing structures, or IUPAP may appoint people as official liaisons with them.





Young Scientist Awards
Commission Awards

Publications

IUPAP General Report: published after each General Assembly.

Newsletter: published three times a year, contains Union news.

SUNAMCO Document: IUPAP's authoritative guide to correct usage of symbols, units, and nomenclature. Translated into several languages.

Contact Us

IUPAP Singapore
Institute of Advanced Studies,
Nanyang Technological University,
Nanyang Executive Centre #02-18,
60 Nanyang View,
Singapore 639673
Tel: +65 6790 6491
Fax: +65 6794 4941
Email: IUPAP.Admin@ntu.edu.sg
Website: www.iupap.org

Quantum sensing with laser-cooled atoms: from an experiment to a product

P. Vermeulen[1], V. Ménoret[1], B. Pelle[1], R. Szmuk[1], C. Busquet[1], A. Landragin[2], P. Bouyer[3], and B. Desruelle[1]

[1] *MUQUANS, Institut d'Optique d'Aquitaine, Rue François Mitterrand, 33400, Talence, France*

[2] *LNE–SYRTE, Observatoire de Paris, Universit PSL, CNRS, Sorbonne Université, 61 avenue de l'Observatoire, F–75014 Paris, France*

[3] *LP2N, Laboratoire de Photonique Numérique et Nanosciences, Institut d'Optique Graduate School, Rue François Mitterrand, 33400 Talence, France*

e-mail: *bruno.desruelle@muquans.com*

This paper reports on recent achievements of cold-atom technologies and related operational devices in the area of Quantum Sensing and Metrology.

First, we will describe the status of the Absolute Quantum Gravimeter (AQG) that has left the laboratory for geophysical studies (Fig. 1). The AQG is an industry-grade commercial gravity sensor which today meets the objective to provide a gravimeter based on atom interferometry with laser-cooled ^{87}Rb atoms as a mobile turn-key device. We report on an operational stability of the absolute measurements of the acceleration of the Earth gravity g at the level of 1×10^{-9} and will show that such high precision measurement can be sustained over a month. Over the past years, several measurement campaigns have validated the ease of use and the robustness of such technology.



Figure 1: The Absolute Quantum Gravimeter developed by Muquans. The AQG relies on atom interferometry with laser-cooled Rb atoms.

Second, we will also report on the performances of the Muclock, a micro-wave frequency standard based on the Ramsey interrogation of laser-cooled ^{87}Rb atoms (Fig. 2). In particular, a frequency stability of 3×10^{-13} at 1 s averaging time and a frequency stability of 1×10^{-15} at 1 day averaging time have been demonstrated.

This paper will also be the occasion to describe in more details the high degree of maturity of several key



Figure 2: Muclock developed by Muquans. The Muclock is an atomic clock using laser-cooled Rb atoms.

enabling technologies such as intelligent integrated laser systems that can help Quantum Technologies with cold atoms taking-off for a wider range of applications in Quantum Computing, Quantum Simulation and Quantum Communication.

The non-exactness of SWKB for additive SI potentials

J. Bougie[1], **A. Gangopadhyaya**[1], **and C. Rasinariu**[1]
[1] *Department of Physics, Loyola University Chicago, Chicago, U.S.A.*
e-mail: *crasinariu@luc.edu*

Comtet, Bandrauk and Campbell [1] showed that SWKB is exact for the conventional additive shape invariant potentials (SIP); it was widely believed that SWKB yields exact results for all additive SIP. Here we report [2] an example of an additive SIP for which the SWKB method fails to produce exact results.

• SUSYQM: factorizes the Hamiltonian [3] with the help of $\mathcal{A}^{\pm} = \mp\hbar\frac{d}{dx} + W(x,a)$, where a is a parameter, and $2m = 1$. $W(x,a)$ is the superpotential. Then, the Hamiltonian can be written as

$$H_- = \mathcal{A}^+ \cdot \mathcal{A}^- = -\hbar^2\frac{d^2}{dx^2} + W^2(x,a) - \hbar\frac{dW}{dx}$$

where $V_-(x,a) = W^2(x,a) - \hbar\,\frac{dW}{dx}$ is the potential. The Hamiltonian $H_+ = \mathcal{A}^- \cdot \mathcal{A}^+$ is isospectral with H_-. Its potential is $V_+(x,a) = W^2(x,a) + \hbar\,\frac{dW}{dx}$.

• Shape Invariance (SI): Let a_i be a set of parameters and let $a_0 = a,\ a_{i+1} = f(a_i)$. $W(x,a_i)$ is SI if

$$W^2(x,a_i) + \hbar\frac{d\,W(x,a_i)}{dx} + g(a_i) =$$
$$W^2(x,a_{i+1}) - \hbar\frac{d\,W(x,a_{i+1})}{dx} + g(a_{i+1})\ .$$

SIP eigenenergies are $E_n^{(-)}(a_0) = g(a_n) - g(a_0)$.

• SWKB:

$$\int_{x_L}^{x_R}\sqrt{E_n - W^2(x)}\,\mathrm{d}x = n\pi\hbar\ ,\quad n = 0,1,2,\cdots.$$

• Additive parameter change: $a_{i+1} \equiv f(a_i) = a_i + \hbar$. "Conventional" additive SI potentials (HO, 3D-HO, Morse, Coulomb, Scarf, Eckart, Pösch-Teller, Rosen-Morse, etc.) all yield exact spectra under SWKB.

• Extended ($\hbar$ -dependent) additive SI superpotentials: $W(x,a,\hbar) = \sum_{j=0}^{\infty}\hbar^j W_j(x,a)$. Substituting this power series into the SI condition, we get [4]:

$$2\frac{\partial W_0}{\partial x} - \frac{\partial}{\partial a}\left(W_0^2 + g\right) = 0\ ;\ \text{for } j = 1,$$
$$\frac{\partial W_1}{\partial x} - \frac{\partial}{\partial a}\left(W_0\,W_1\right) = 0\ ;\ \text{for } j = 2,$$

and for $j \geq 3$

$$2\,\frac{\partial W_{j-1}}{\partial x} - \sum_{s=1}^{j-1}\sum_{k=0}^{s}\frac{1}{(j-s)!}\frac{\partial^{j-s}}{\partial a^{j-s}}W_k\,W_{s-k} +$$
$$\sum_{k=2}^{j-1}\frac{1}{(k-1)!}\frac{\partial^k\,W_{j-k}}{\partial a^{k-1}\,\partial x} + \left(\frac{j-2}{j!}\right)\frac{\partial^j W_0}{\partial a^{j-1}\partial x} = 0\ .$$

• Start from the 3-D oscillator, $W_0 = \frac{1}{2}\omega x - \frac{\ell}{x}$, and set $W_1 = 0$. From the above equations we obtain

$$W(x,\ell) = \frac{\omega x}{2} - \frac{\ell}{x} + \left(\frac{2\omega x\hbar}{\omega x^2 + 2\ell - \hbar} - \frac{2\omega x\hbar}{\omega x^2 + 2\ell + \hbar}\right)\ ,$$

which is an $\hbar$-dependent additively SI superpotential first obtained in [5].

• Define the residual quantity

$$R = 1 - \frac{I(n,\ell)}{n\pi}\ ;\ \ I(n,\ell) = \int_{x_L}^{x_R}\sqrt{E_n - W^2(x,\ell)}\,\mathrm{d}x.$$

Note that $R = 0$ when the approximation is exact; in general, smaller R will correspond to a more precise approximation. In Fig. 1 we plot R as a function of n and various ℓ. We see that, as expected, R does

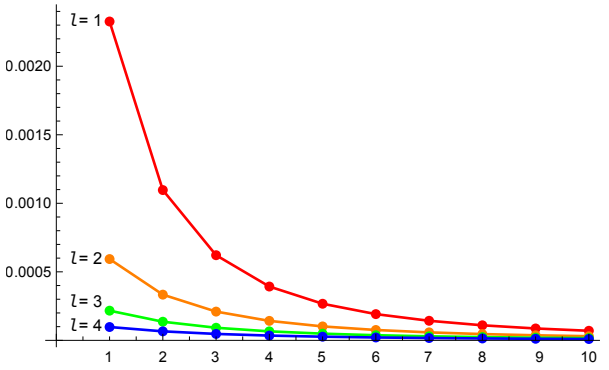


Figure 1: R as a function of n for the following cases: $\ell = 1$ (red), $\ell = 2$ (orange), and $\ell = 3$ (blue).

indeed decrease with increasing n and ℓ.

• Conventional SIP have exactly solvable spectra. They also share the property of making the SWKB quantization condition exact.

• Extended SIP are exactly solvable due to additive SI. However, additive SI does not guarantee SWKB exactness as shown for the extended radial oscillator.

• This result suggests that the exactness of the conventional superpotentials may be connected to their $\hbar$-independence. Further investigation of the role of $\hbar$-dependence of the SWKB approximation could play a role in better understanding the properties of these extensions.

[1] A. Comtet, A. D. Bandrauk, and D. K. Campbell, Phys. Lett. **150B**, 159 (1985).

[2] J. Bougie, A. Gangopadhyaya, and C. Rasinariu, `https://arxiv.org/abs/1802.00068`

[3] E. Witten, Nucl. Phys. **B 185**, 513 (1981); L. E. Gendenshtein, JETP Lett. **38**, 356 (1983).

[4] J. Bougie, A. Gangopadhyaya, J. V. Mallow, C. Rasinariu, Symmetry 4 (3), 452 (2012).

[5] C. Quesne, J. Phys. **A 41**, 392001:1 (2008).

Shortcuts to Adiabaticity Assisted by Counterdiabatic Born-Oppenheimer Dynamics

C. W. Duncan[1,2] **and A. del Campo**[2,3]

[1] *SUPA, Institute of Photonics and Quantum Sciences, Heriot-Watt University, Edinburgh EH14 4AS, United Kingdom*

[2] *Department of Physics, University of Massachusetts, Boston, MA 02125, USA*

[3] *Theory Division, Los Alamos National Laboratory, MS-B213, Los Alamos, NM 87545, USA*

e-mail: *cd130@hw.ac.uk*

Shortcuts to adiabaticity provide control protocols to guide the dynamics of a quantum system through an adiabatic reference trajectory in an arbitrary prescheduled time. Designing STA proves challenging in complex quantum systems when the dynamics of the degrees of freedom span different time scales. We introduce Counterdiabatic Born-Oppenheimer Dynamics (CBOD) as a framework to design STA in systems with a large separation of energy scales. CBOD exploits the Born-Oppenheimer approximation to separate the Hamiltonian into effective fast and slow degrees of freedom and calculate the corresponding counterdiabatic drivings for each subsystem. We show the validity of the CBOD technique via an example of coupled harmonic oscillators, which can be solved exactly for comparison.

Tailoring the nonadiabatic dynamics of quantum matter is an open problem at the frontiers of physics with important applications in emergent quantum technologies. Control protocols relying on adiabatic dynamics are natural to prescribe the evolution of a system along a reference adiabatic trajectory. While they are robust against uncontrolled errors in the experimental implementation, they are susceptible to decoherence. Driving protocols known as shortcuts to adiabaticity provide an alternative, by speeding up an adiabatic reference trajectory of a quantum system in a prescheduled amount of time [1].

Designing shortcuts to adiabaticity requires the ability to control and describe the time-evolution of a system, an ubiquitous challenge across a variety of fields when dealing with complex quantum systems. Among them, a prominent instance occurs in quantum chemistry, in the study of quantum systems with degrees of freedom spanning different time and energy scales. When the separation of scales is sufficiently large, it is possible to decouple the dynamics via the Born-Oppenheimer approximation [2].

In this work [3], we introduce Counterdiabatic Born-Oppenheimer Dynamics (CBOD) as an efficient technique for the fast control of complex systems that are well described by the Born-Oppenheimer approximation. We consider an example of two interacting harmonic oscillators of differing mass, which is an exactly solvable problem, as a test bed for the CBOD method.

References

[1] X. Chen, A. Ruschhaupt, S. Schmidt, A. del Campo, D. Gury-Odelin, and J. G. Muga, Phys. Rev. Lett. 104, 063002 (2010).

[2] M. Born and R. Oppenheimer, Annalen Der Physik 74, 1 (1924).

[3] C. W. Duncan and A. del Campo, arXiv:1804.00434 (2018).

Quenching interatomic Coulombic decay width by screening effect

P. Votavová[1], T. Miteva[2], N. Sisourat[2] and P. Kolorenč[1]

[1] *Charles University, Faculty of Mathematics and Physics, Institute of Theoretical Physics, V Holesovickach 2, 180 00, Praha 8, Czech Republic*

[2] *Université Pierre et Marie Curie, Laboratoire de Chimie Physique Matière et Rayonnement, 4 Place Jussieu, 75005 Paris, France*

e-mail: *petra.votavovp@gmail.com*

Interatomic Coulombic decay (ICD) is non-radiative relaxation process in which an inner-valence vacancy is filled by an outer-valence electron and the excess energy is transferred to a neighboring atom, causing its ionization. ICD mechanism shortens the lifetime of the inner-valence ionized state of an atom or molecule, which is surrounded by other atoms or molecules. The lifetime decreases even more if a recently discovered mechanism, the superexchange ICD [1], is operative. In superexchange ICD, the energy transfer between the inner-valence ionized atom and a neighboring atom is enhanced by a coupling between the ionized state and intermediate virtual states of another (bridge) atom.

In the present work, we study different possible effect of environment which, in contrast to superexchange ICD, results in prolongation of the lifetime of the ionized state. We show that NeMg or NeBe dimer lives longer in the presence of a bridge He atom. Or equivalently, that the ICD width of NeMg or NeBe decreases. The decrease in the ICD width of the $^2\Sigma_g$ state of $Ne^+(2s^{-1})$Mg dimer in the presence of the He atom is plotted in the upper panel of Fig. 1. In the equilibrium distance of 4.4 Å [2] between the Ne and Mg atom the ICD width decreases from 3.6 meV to 1.5 meV (2.4 times). The decrease in the ICD width of the $^2\Sigma_g$ state of $Ne^+(2s^{-1})$Be dimer in the presence of the He atom is not so significant as in the case of the Mg system and it also takes place only at small distances below 3.6 Å. At larger distances, the superexchange ICD mechanism becomes dominant and thus it cancels the decrease in the decay width.

We demonstrate that the quenching of the decay width is due to a screening effect between Ne and Mg (or Be) atom caused by the He atom. The presence of the He atom lowers the overlap between Ne and Mg (or Be) orbitals and thus it suppresses the electron transfer.

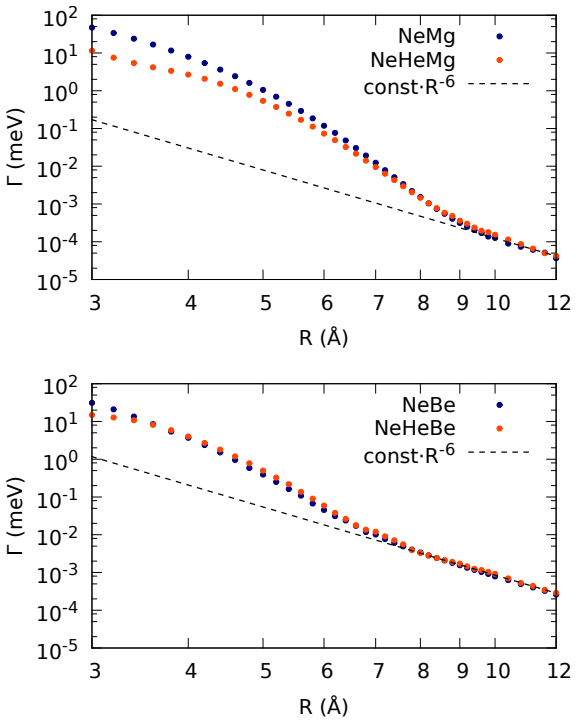


Figure 1: Quenching of the ICD width Γ of NeMg and NeBe dimer in the presence of a bridge He atom. Upper panel: Γ of the $^2\Sigma_g$ state of $Ne^+(2s^{-1})$HeMg (orange) and $Ne^+(2s^{-1})$Mg (blue). Lower panel: Γ of the $^2\Sigma_g$ state of $Ne^+(2s^{-1})$HeBe (orange) and $Ne^+(2s^{-1})$Be (blue). R is the distance between Ne and Mg (or Be).

[1] T. Miteva, *et al.*, Phys. Rev. Lett. **119**, 083403 (2017).

[2] P. Kolorenč *et al.*, J. Chem. Phys. **129**, 244102 (2008).

High coherence superconducting artificial atom

L. B. Nguyen[1], **YH. Lin**[1], **R. Mencia**[1], **A. Somoroff**[1], **N. Cottet**[2] **and V. Manucharyan**[1]
[1] *University of Maryland, College Park, MD 20742, USA*
[2] *École Normale Supérieure de Lyon, 69007 Lyon, France*
e-mail: *longbnguyen47@gmail.com*

Fluxonium [1] is a versatile multilevel superconducting artificial atom. It consists of a capacitor, a superinductor [2], and a Josephson junction in parallel (Fig. 1). The three elements can be tuned to reach different regimes with interesting physical properties, for example the metastable regime with milliseconds energy relaxation time [3, 4]. The circuit can be further controlled via an external magnetic flux: at integer and half-integer flux quantum, its spectrum is similar to those of transmon and flux qubit, respectively (Fig. 2).

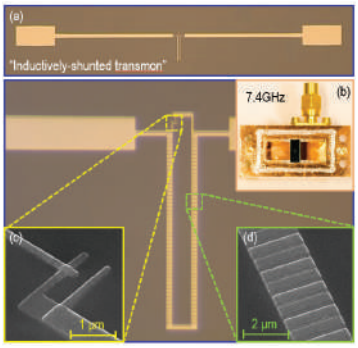


Figure 1: Fluxonium device. The long antenna (a) provides coupling to a 3D copper cavity (b). The tunnel Josephson junction (c) is shunted by an array of junctions (d), which behaves as a large inductor.

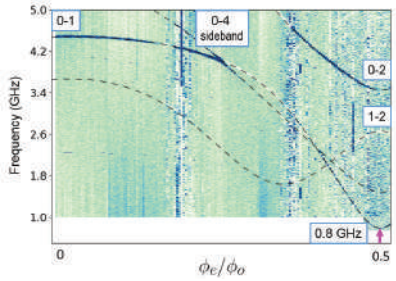


Figure 2: Fluxonium spectrum showing 0-1, 0-2, 1-2, and a sideband 0-4 transitions

Here we report coherence measurement of 0-1 transition in a 3D fluxonium circuit capacitively coupled to a box resonator. The circuit was fabricated by Al evaporation on an untreated silicon substrate. Energy relaxation time (T_1) varies from a few microseconds at integer flux to over 100 microseconds at half-integer flux sweet spot, and coherence time (T_2) approaches $2T_1$ (Fig. 3). Interestingly, T_1 is limited at the sweet spot by dielectric loss with an effective loss tangent an order of magnitude higher than a recently reported value in transmon devices [5, 6]. Therefore, we expect that our fluxonium design has the potential to reach millisecond coherence once state-of-the-art fabrication techniques are employed.

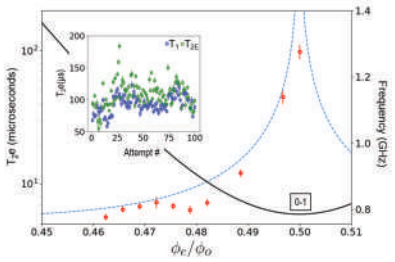


Figure 3: Coherence data of 0-1 transition near half-integer flux. Away from the sweet spot, T_2 is limited by flux noise with corresponding amplitude equals to $(1.8 \times 10^{-6}\Phi_o)^2$ (blue dashed line). Inset: Variation of T_1 and T_2^{Echo} at the sweet spot over time.

We also briefly report fluorescence "shelving" readout scheme that couples 0-3 transition smoothly to a 50 Ohm transmission line and at the same time protects 0-1 qubit transition via a 3D waveguide. Information from the computational space is efficiently mapped onto the propagating photons at 0-3 frequency.

[1] V. Manucharyan, J. Koch, L. Glazman, M. Devoret, Science 326, (2009).

[2] V. Manucharyan, PhD thesis, (2012)

[3] YH Lin, L. B. Nguyen, N. Grabon, J. San Miguel, N. Pankratova, and V. E. Manucharyan, Physical Review Letters 120, (2018)

[4] N. Earnest, S. Chakram, Y. Lu, N. Irons, R.K. Naik, N. Leung, L. Ocola, D.A. Czaplewski, B. Baker, Jay Lawrence, Jens Koch, and D.I. Schuster, Physical Review Letters 120, (2018)

[5] Y. Chu, C. Axline, C. Wang, T. Brecht, Y. Gao, L. Frunzio and R. Schoelkopf, Applied Physics Letters 109, (2016)

[6] C. Wang, C. Axline, Y. Gao, T. Brecht, Y. Chu, L. Frunzio, M. Devoret and R. Schoelkopf, Applied Physics Letters 107, (2015)

High-efficiency cold-atom transport into a waveguide trap

A. P. Hilton[1], **C. Perrella**[1], **F. Benabid**[2], **B. M. Sparkes**[1], **A. N. Luiten**[1], **and P. S. Light**[1]

[1] *Institute for Photonics and Advanced Sensing (IPAS), School of Physical Sciences, University of Adelaide, Adelaide, SA, Australia*

[2] *GPPMM group, Xlim Research Institute, UMR CNRS 7252, Université de Limoges, France*

e-mail: *Ashby.Hilton@Adelaide.edu.au*

Guided by robust simulation we have developed an atom-guiding technique that efficiently loads 3×10^6 cold rubidium atoms into hollow-core optical fibre [1], an order-of-magnitude improvement over literature, delivering a powerful technology for atom-optics and quantum-information processing.

Ultra-strong atom-light interaction is a key resource for numerous applications in quantum information processing, sensing and measurement [2, 3, 4, 5]. To maximize the strength of the interaction, one must maximize the atom-light coherent interaction time while simultaneously ensuring that there is a good match between the optical mode size and the atomic cross-section. For ensemble experiments, one wants to do this with the largest possible number of atoms at the same time. Here we report on a highly successful approach to generate these optimal conditions by creating a method to efficiently load a large number of laser-cooled atoms into a hollow-core optical fibre, producing optical depths of 600(10), shown in 1(a).

Our fibre-loading system is based on a Magneto-Optical Trap (MOT) of 1×10^8 atoms formed above a 10 cm length of 45 µm core kagome lattice hollow-core photonic-crystal fibre. A red-detuned Gaussian beam coupled through the fibre intercepts the MOT, generating a strong dipole trap that guides atoms from the MOT into the fibre, shown in 1(b). With appropriate choices of detuning and power of the guide beam we have achieved a peak atom loading efficiency limited only by the geometric overlap of the guide and MOT.

A detailed Monte-Carlo simulation of the atom loading process was developed to aid in optimising the dipole trap parameters and support our understanding of the complex behaviour of the system, shown in 1(c). We find a high degree of quantitative agreement between the simulation and experiment which provides confidence in the models predictions on the achievable atom coupling, the guide scattering rate, atomic lifetime, and atom temperature.

This state of the art experimental performance, together with the powerful predictive power of the Monte Carlo simulation, delivers a new platform technology for the field.

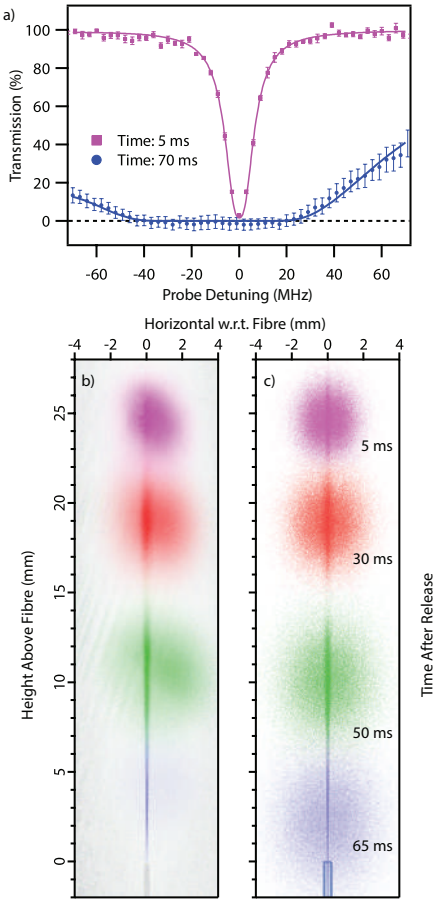


Figure 1: Transmission measurements of the ensemble before and after loading into the fibre, b) optical depth map imaged from the side a sequence of times showing atom loading, and c) simulated optical depth map at matching time steps.

[1] A. P. Hilton et al, `arXiv:1802.05396` (2018)

[2] B. M. Sparkes et al, New Journal of Physics **15**, 085027 (2013).

[3] Z. Y. Liu et al, Physical Review Letters **117**, 203601 (2016).

[4] Y.-W. Cho et al, Optica **3**, 100-107 (2016).

[5] C. C. N. Kuhn et al, New Journal of Physics **16**, 073035 (2016).

Optical pumping of ^{87}Rb atoms with Xe and high-pressure buffer gas in a cubic cell

Hoon Yu and Jai Seung Yoo

Department of navigation system development, Hanwha corporation/defense, Daejeon, Rep. of Korea

e-mail: *hoonyu99@hanwha.com*

We simulated the optical pumping rate of ^{87}Rb atoms with Xe and high-pressure buffer gas in a cubic cell. We numerically found the optimal beam waist and linewidth of a pumping laser for the maximal optical pumping rate as the temperature and the size of a cell. We calculated absorption cross-section as a frequency of the pumping laser by considering pressure and Doppler broadening. The spin polarization of ^{87}Rb gas in a cubic cell was obtained as a result of the optical pumping and the atomic population in each ground state for the steady state. We found that the optimal beam waist is 0.3 times of a cubic cell with 250 torr of dinitrogen and 50 torr of xenon gas. The optimal beam linewidth was parabolically increasing as the cell temperature and the increasing rate was exponentially decaying as the cell size. This numerical result shows appropriate experimental parameter as a cell temperature and a size for the spin polarization.

In this work, we numerically calculated the absorption cross-section of a pumping laser in rubidium and xenon gas mixture with high-pressure dinitrogen gas. We consider an attenuation of a pumping laser through the gas mixture to calculate spin polarization in a cubic cell. As a result of light absorption, atomic population probability, ρ_k, in each k-th state at the steady state is given by

$$0 = -\lambda_k \rho_k(t,\vec{r}) + \frac{1}{8}\sum_{i=1}^{8} \lambda_i \rho_i(t,\vec{r}) + (\frac{1}{8} - \rho(t,\vec{r}))R_{SD} \quad (1)$$

where k and i are the indices for the ground Zeeman state of rubidium atoms and we considered D1 transition [1]. Time,t, indicates interaction time between atom and light, $\lambda_k = \int_{-\infty}^{\infty} \sigma_k(\nu)\Phi(\nu,\vec{r})d\nu$ is a pumping rate of the k-th state and R_{SD} is the spin destruction rate as a result of collisions. $\sigma_k(\nu)$ is the absorption cross-section of medium from k-th ground state. $\Phi(\nu,\vec{r})$ is the photon flux of a pumping laser. The attenuation of the photon flux is following Beer's law, $\Phi(\vec{r}) = \Phi_0(x,y)e^{-\sigma n z}$ where $\Phi_0(x,y)$ describes a Gaussian distribution in our calculation. Spin destruction rate of ^{87}Rb atoms is described by $R_{SD} = R_{SD}^{BC} + R_{wall} + R_{van}$ [2-3]. Spin polarization probability was calculated from the each population probability.

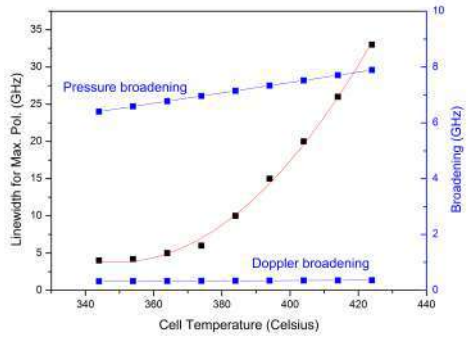


Figure 1: Sample figure, ICAP 2018 logo.

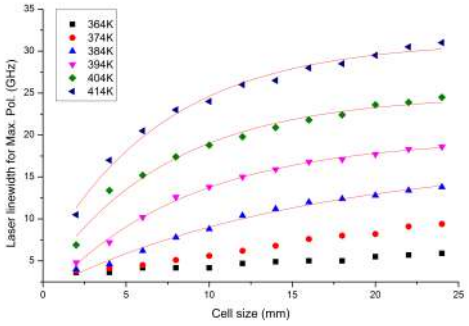


Figure 2: Sample figure, ICAP 2018 logo.

Fig.1 and 2 show the optimal linewidth of the pumping laser for the maximum spin polarization as a cell temperature and a size. The efficiency of a spin polarization is the result of how much light has been absorbed through the cell. Too narrow line width, the laser is not able to reach the end of a cell due to the high absorption rate. Too wide line width, laser is not fully absorbed. This research is funded by Agency for Defense Development of Korea.

[1] W. Franzen and A. G. Smslie, Phys. Rev. **108**(6), 1453-1458 (1957).

[2] Z. G. Wang, et. Al., AIP Advances **6**, 085110 (2016).

[3] Linlin Chen, et. Al., AIP Advances **7**, 115101 (2017).

Local rectification of heat flux

M. Pons[1], **M.A. Simón**[2], **and J.G. Muga**[2]
[1] *Departmento de Física Aplicada I, Universidad del País Vasco, UPV-EHU, Bilbao, Spain*
[2] *Departmento de Química-Física, Universidad del País Vasco, UPV-EHU, Leioa, Spain*
e-mail: *marisa.pons@ehu.es*

In spite of much work on thermal rectification after the first model proposal in 2002 [1] (for a broad perspective on heat rectification see [2, 3]), the manipulation of phononic heat fluxes is still far from being completely controlled as no efficient and feasible thermal diodes have been found. The thermal rectifier, a device where the heat current changes when the temperature bias of the thermal baths at the boundaries is reversed, is one of the key tools needed to manipulate heat currents and build thermal circuits. A wealth of research is underway to meet the challenge posed by a near standstill of the field [4, 5], combined with the prospects of widespread and impactful practical applications. Together with experimental progress, at this stage work exploring new models is important to test possibilities that may become feasible as control capabilities improve [2].

In this poster we present a new proposal as a rectifying scheme based on the effect of a local defect, or impurity, in an otherwise homogeneous system. In this chain-of-atoms model the heat is rectified, with different fluxes from the hot to the cold baths located at the chain boundaries when the temperature bias is reversed. The chain is homogeneous except for boundary effects and a local modification of the interactions at one site, the "impurity". The rectification mechanism is due here to this localized impurity, the only asymmetrical element of the structure, apart from the externally imposed temperature bias, and does not rely on putting in contact different materials or other known mechanisms such as grading or long-range interactions. The effect survives if all interaction forces are linear except the ones for the impurity.

References

[1] M. Terraneo, M. Peyrard and G. Casati, Phys. Rev. Lett. **88**, 094302 (2002).

[2] N. A. Roberts and D. G. Walker, Int. J. Therm. Sci. **50**, 648 (2001).

[3] N. Li, J. Ren, L. Wang, G. Zhang, P. Ha nggi and B. Li, Rev. Mod. Phys. **48**, 1045 (2012).

[4] S. Chen, E. Pereira and G. Casati, EPL **111**,30004 (2015).

[5] E. Pereira, Phys. Rev. E, **96**, 012114 (2017).

Absorption Spectroscopy of Thallium forbidden transition with Amplitude- and Phase-Modulation

Wei-Ling Chen[1], **Tzu-Ling Chen**[1], **and Yi-Wei Liu**[1]

[1] *Department of Physics, National Tsing Hua University, Hsinchu, Taiwan, R.O.C*

e-mail: *ywliu@phys.nthu.edu.tw*

We report on a method to enhance spectral sensitivity on laser-absorption spectrometry in thallium atom. Thallium is one attractive proving ground for PNC tests because it has one valence p electron and relatively high atomic weight, and it is simpler than most elements. In our experiment, we measured the $6P_{1/2}$ to $6P_{3/2}$ forbidden transition because selection rule is allowed by parity conservation. If the phenomenon of parity non-conversation exist, the thallium p state will mix with s state. Therefore, the spectral sensitivity of this transition is important.

In Figure 1 we used 1283 nm laser to interact with thallium at $6P_{1/2}$ to $6P_{3/2}$ mixed magnetic dipole and electric quadrupole transition. However, this transition is 10^7 lower than other thallium allowed transition. Therefore, utilizing a method to enhance the sensitivity is necessary. we applied chopped radio frequency to the fiber-EOM as amplitude modulation instead of conventional modulation on light intensity. Fiber-EOM produced two sidebands which were far from the carrier and only one frequency was within the Doppler profile, this approach could increase the signal to noise ratio and eliminate the background noise from laser light intensity fluctuation.

We used a cylindrical cell with the thallium vapor pressure is 10 Pa at 930 Kelvin as our target. The absorption length is only 10 cm in our experiment. However, even if the interaction area is limited, in Figure 2 the signal to noise ratio can still up to 250. Therefore, this method can help to clarify the influence on a weak transition.

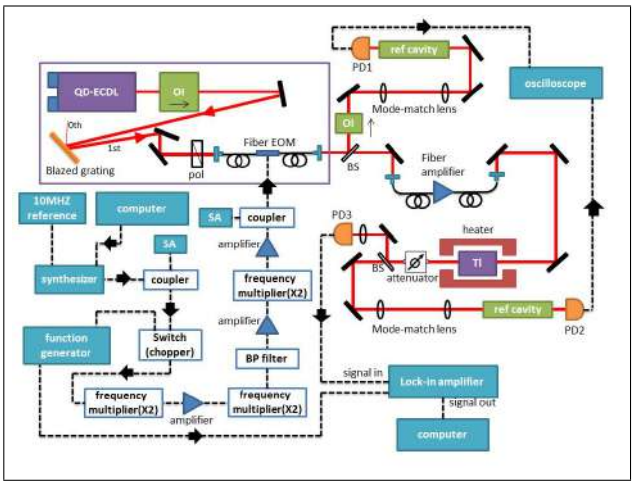


Figure 1: we used a quantum dot external cavity diode laser (ECDL) to produce 1283 nm laser. With approximately 10.5 GHz radio frequency (RF) signal importing into fiber EOM, it generated two sideband frequencies. The frequency difference between these two sidebands is 21 GHz, which is equal to the hyperfine splitting of thalliums ground state. Also, we used RF switch and lock-in amplifier to perform amplitude modulation on the sidebands. It can cancel out a lot of intensity noise that caused by light and improve the signal to noise ratio.

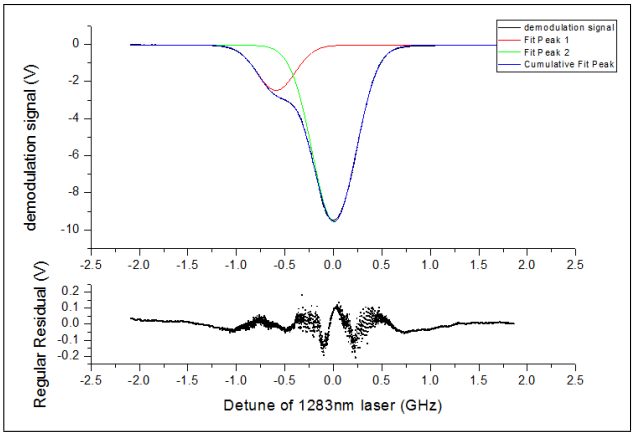


Figure 2: The forbidden transition from $6P_{1/2}$,F=1 to $6P_{3/2}$,F=1 (green part) and $6P_{1/2}$,F=1 to $6P_{3/2}$,F=2 (red part) with r-square (COD) is 0.99981 and signal-to-noise ratio (SNR) is 250.

[1] DV Neuffer and ED Commins, Phys. Rev. A **16**, 844 (1977).

[2] PA Vetter, DM Meekhof, PK Majumder, SK Lamoreaux and EN Fortson, Phys. Rev. Lett. **74**, 2658 (1995).

[3] AD Cronin, RB Warrington, SK Lamoreaux and EN Fortson, Phys. Rev. Lett. **80**, 3719 (1998).

[4] TL Chen and and YW Liu, Phys. Rev. A **86**, 052524 (2012).

[5] NH Edwards, SJ Phipp, PEG Baird and S Nakayama, Phys. Rev. Lett. **74**, 2654 (1995).

Phase Locked Atomic INterferometers for Gravity Gradiometry (PLAIN-GG)

C. H. Camm[1], **A. Dragomir**[1], **and M. D. Himsworth**[1]

[1] *Integrated Atom Chip group, Faculty of Physical Sciences and Engineering, University of Southampton, University Road, Southampton, SO17 1BJ, UK*

e-mail: *C.Camm@soton.ac.uk*

From mapping the geoid of the earth to detecting subterranean structures; accurate measurements of gravity can reveal intriguing and important details about the world beneath us. Developments in using atoms as inertial sensors have increased the precision and sensitivity of these measurements [1]. Such devices work by dropping ultra-cold atoms and measuring the change in their Doppler shift to obtain a value of their acceleration.

Measurements of gravity need not always be the absolute value. We focus on a gravity gradiometer; a device which measures the difference of gravity in space. Gradiometers benefit from the elimination of common-mode noise signals, found in relative and absolute detectors, as the measurements in both locations are subject to the same inertial noise and addressed with the same light field. Current atomic gravity gradiometers employ a single Raman beam passing through both atom clouds [2] in order to eliminate common-mode noise sources. This limits the geometry and portability of such devices as the atom clouds must be in-line with each other, and usually within the same bulky vacuum chamber.

This project aims to address the atom clouds in two separate vacuum chambers connected by a stabilised optical fibre interferometer. The optical interferometer will be used to phase lock separate Raman beams, reducing the limitations of conventional gradiometers whilst still eliminating the common-mode noise - creating two correlated atomic interferometers. This technique follows a method used to extend the optical phase stability over 100's of kilometres of optical fibre for distributing atomic clock time [3].

Separating the two chambers can make this device ideal for practical applications due to a decrease in size and greater flexibility of geometry. This allows the angle between the chambers to be changed freely and enables probing of the gravity tensor or multiple phase locked accelerometers.

References

[1] A. Peters, K. Y. Chung and S. Chu, Metrologia, **38**, 1 (2001).

[2] J. M. McGuirk, G. T. Foster, J. B. Fixler, M. J. Snadden, and M. A. Kasevich, Phys. Rev. A **65**, 3 (2002)

[3] S. M. Foreman, A. D. Ludlow, M. H. G. de Miranda, J. E. Stalnaker, S. A. Diddams, and J. Ye Phys. Rev. Lett. **99**, 15 (2007)

Monitoring Ultra Cold Gases in Situ and in Real Time by Ionization Sampling

M. Eisele[1] **and C. Zimmermann**[1]

[1] *Physikalisches Institut, Eberhard Karls Universität Tübingen, Auf der Morgenstelle 14, D-72076 Tübingen, Germany*

e-mail: *max-albert.eisele@uni-tuebingen.de*

Single atom detection by means of photo-ionization and efficient ion counting [1, 2] allows for taking small samples of a quantum gas without significantly perturbing the gas. In contrast to standard absorption imaging, real time and in situ observations of cold atoms is possible this way. In particular, complete decay curves can be recorded within a single experimental cycle. Inelastic loss spectroscopy as used for investigating Feshbach resonances [3] and Efimov states [4, 5] becomes far more efficient.

The detection system implemented in our experimental setup is designed for ^{87}Rb and can operate in magnetic fields up to 1200G. The atoms are ionized by multi-photon absorption: ground state rubidium atoms are excited via a two-photon absorption into the $5D_{5/2}$ state. This transition is hyperfine selective for the initial and the final state. For magnetic fields above a few G Zeeman splitting can be resolved as well. The excited atoms are ionized by a third photon at a wavelength near 1070nm. This light is provided by the crossed dipole trap in which the atoms are confined. The ions are extracted from the trapping region by an electric field of about 2 kV/cm and detected with a channel electron multiplier. It is possible to record complete Zeeman-spectra at magnetic fields up to 400G by ionizing only 0.02% of the atomic ensemble. The experimentally determined single atom detection efficiency amounts to about 60%.

We test the detector with well known s- and p-wave Feshbach resonances in the magnetic field range between 4 and 18G [6]. Decay curves for the spin mixture in the hyperfine states $5S_{1/2}|F = 1, m_F = 1\rangle$ and $5S_{1/2}|F = 2, m_F = 0\rangle$ are recorded at a temperature of 5μK. The ionization loss rate is less than 0.2Hz and can be neglected compared to the much faster decay due to two body collisions. From the measured decay curves we can extract the two-body loss coefficients with a short term magnetic field resolution of 2mG. For the future we plan to apply this novel technique to investigate Efimov states in rubidium-lithium mixtures as continuation of our recent work [7].

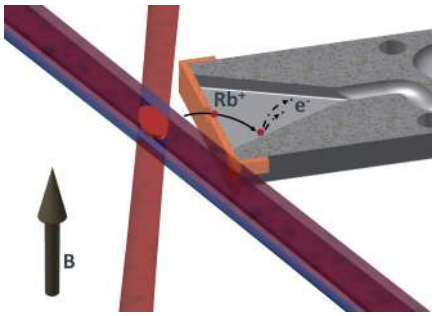


Figure 1: Schematic representation of the ionization sampling process of ^{87}Rb atoms in the crossed dipole trap with 1070nm wavelength (red beams) prepared at a homogeneous magnetic field B. The excitation laser of the $5D_{5/2}$ state at a wavelength of 778nm (blue beam) in conjunction with the overlapped 1070nm light ionize a small sample of the ^{87}Rb atoms. These ions then are efficiently detected by a channel electron multiplier.

[1] Stibor, A., et al. New Journal of Physics 12.6 (2010): 065034.

[2] Henkel, Florian, et al. Phys. Rev. Lett. 105.25 (2010): 253001.

[3] Chin, Cheng, et al. Reviews of Modern Physics 82.2 (2010): 1225.

[4] Ferlaino, Francesca, and Rudolf Grimm. Physics 3 (2010): 9.

[5] Ulmanis, Juris, et al. National Science Review 3.2 (2016): 174-188.

[6] Sawyer, Bianca J., et al. Phys. Rev. A 96.2 (2017): 022705.

[7] Maier, R. A. W., et al. Phys. Rev. Lett. 115.4 (2015): 043201.

Strong Optical Forces on Atoms Using Adiabatic Rapid Passage*

Harold Metcalf
Physics and Astronomy, Stony Brook University, Stony Brook NY 11794-3800 USA
e-mail: *harold.metcalf@stonybrook.edu*

Optical forces on two-level atoms from a single frequency of light have been extensively studied and exploited for many years. The results have been beam slowing, optical molasses, optical lattices, optical traps, band structure effects, and many others [1]. Within a few years after the early experiments, it became clear that this simple view was inadequate, and that the multiple level structure of real atoms was necessary to explain some experiments.

This more complete description was motivated by the discovery of cooling below the Doppler temperature $T_D \equiv \hbar\gamma/2k_B$ [2]. This could be explained only by polarization gradient cooling in atoms with multiple ground state levels, and was labeled "Sisyphus cooling" in Ref. [3]. In addition to this Sisyphus cooling, many more phenomena could be described. These include the magneto-optic trap (multiple excited state levels) and velocity selective coherent population trapping (multiple ground state levels).

Thus the extension from two-level to multi-level atoms gave an unexpected richness to the topic of atomic motion in optical fields. One might expect a comparable multitude of new phenomena to be found for the motion of atoms in multi-frequency fields [4], but this topic has not received as much attention.

We have explored the forces from both bichromatic and swept frequency light [5], and the consequences are impressively larger forces with comparably larger velocity capture ranges. This poster will address the huge forces resulting from such polychromatic light, with particular focus on swept frequency light implemented by adiabatic rapid passage (ARP). It uses only stimulated transition processes, and the absence of spontaneous emission (SpE) allows adiabatic exchange of momentum between atoms and light.

The dressed atom picture of a two-level atom provides a useful description of ARP. The eigenenergies are $E_{\pm}=(\hbar/2)\left[\delta(t)\pm\sqrt{\delta(t)^2+|\Omega(t)|^2}\right]$ and are plotted in Fig. 1. The indicated path is a possible trajectory for ARP, and shows how one state evolves into the other coherently as the detuning $\delta(t)$ and Rabi frequency $\Omega(t)$ are varied. Multiple such cycles with different $\vec{k}$-vectors results in a rapid, coherent exchange of momentum between atoms and light.

In laser cooling, only the outgoing light can remove the thermal energy and entropy from the atomic sample. In Doppler molasses or atomic beam slowing, energy exchange is enabled because the incident light is at a frequency ω_ℓ below the SpE frequency $\omega_f \geq \omega_\ell$ for all emission directions in the lab frame. That

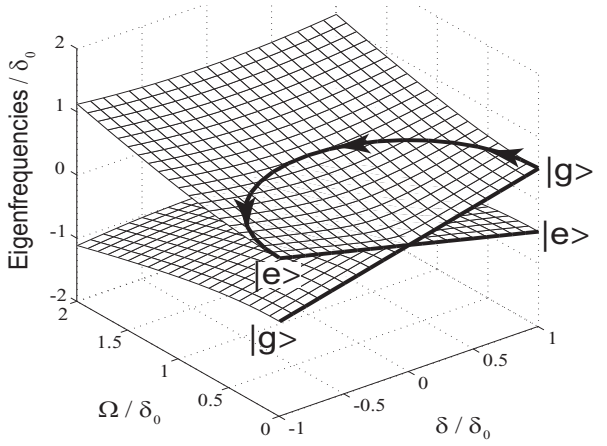


Figure 1: The dressed states eigenenergies.

is, the angular distribution and concomitant Doppler shifts of SpE mediate a net energy transfer from the atoms to the light field. Even in more elaborate cooling techniques such as polarization gradient cooling, $\omega_f \geq \omega_\ell$ by approximately the light shift difference between different ground state sublevels. By contrast, in multi-frequency light, energy can be removed by purely stimulated processes if absorption of the lower frequency light (*i.e.* red) is followed by stimulated emission into the higher frequency field (blue).

In the familiar case of single-frequency light, the 4π solid angle of the SpE provides so very many states accessible to the system of [atoms+light] that it seems natural to assume that the entropy loss of the cooled atoms is also mediated by this fluorescent light. But extending this notion to the claim that SpE is therefore **required** for entropy dissipation is not necessarily correct, and some examples have been explored in Ref's. [5, 7]. Thus multi-frequency light fields can enable both energy and entropy exchange, as well as cooling, with stimulated processes only.

* Supported by the U.S. Office of Naval Research.

[1] H. Metcalf and P. van der Straten, *Laser Cooling and Trapping* (Springer Verlag, NY, 1999).
[2] P. Lett, R. Watts, C. Westbrook, W. Philips, P. Gould, and H. Metcalf, Phys. Rev. Lett. **61**, 169 (1988).
[3] J. Dalibard and C. Cohen-Tannoudji, J. Opt. Soc. Am. B **6**, 2023 (1989).
[4] J. Söding, R. Grimm, Y. Ovchinnikov, P. Bouyer, and C. Salomon, Phys. Rev. Lett. **78**, 1420 (1997).
[5] H. Metcalf, Rev. Mod. Phys **89**, 041001 (2017).
[6] C. Corder, B. Arnold, and H. Metcalf, Phys. Rev. Lett. **114**, 043002 (2015).
[7] H. Metcalf, Phys. Rev. A **77**, R 061401 (2008).

DETECTING UNIVERSAL PROPERTIES OF LATTICE MODELS WITH ENTANGLEMENT HAMILTONIANS

T. MENDES-SANTOS[1], G. GIUDICI[1 2], M. DALMONTE[1]
INTERNATIONAL CENTER FOR THEORETICAL PHYSICS, ICTP[1]
SCUOLA INTERNAZIONALE SUPERIORE DI STUDI AVANZATI, SISSA[2]

The modular (or entanglement) Hamiltonian (EH) of a quantum system provides an alternative way to uniquely characterize its entanglement properties. In particular, an appealing fact, which can be explored in both numerical and real experiments, is that the ground state entanglement entropy is directly related to the thermodynamic entropy of the EH. However, in the context of lattice models, the explicit form of the EH is analytically known just for the quantum Ising model. On the other hand, a closed form of the modular EH is provided by the Bisognano-Wichmann (BW) for quantum field theory. Here we explore the lattice version of this theorem to construct the entanglement Hamiltonian for a variety of lattice models, supporting diverse quantum phases and critical points, and scanning several universality classes, including Ising, Potts, and Luttinger liquids. Extensive numerical simulations based on density matrix renormalization group, exact diagonalization, and quantum Monte Carlo, are then used to provide a comparison between exact results and the lattice version of BW theorem. Our results provide evidence that the lattice EH is close to the BW one. In particular, we show that the entanglement entropy obtained via the BW theorem properly decribes universal properties in both one- and two-dimensional lattice models.

Ultracold atom-ion collisions in a laser-cooled ^{6}Li-^{40}Ca^{+} hybrid systmes

T. Kojima[1], **R. Saito**[1], **S. Haze**[2], **M. Raoult**[3], **H. Da Silva Jr.**[3], **O. Dulieu**[3], **T. Mukaiyama**[1]

[1] *Graduate School of Engineering Science, Osaka University, Machikaneyamamachi1-3, Toyonaka, Osaka 560-8531, Japan*

[2] *Institut für Quantenmaterie and Center for Integrated Quantum Science and Technology (IQST), Universität Ulm, 89069 Ulm, German*

[3] *Laboratoire Aimé Cotten, CNRS, Univerité Paris-sud, ENS Cachan, Université Paris-Saclay, 91405 Orsay Cedex, Franc*

e-mail: *u603234h@ecs.osaka-u.ac.jp*

Atom-ion hybrid systems have attracted interest from researchers in the field of quantum collisions and chemistry because of the capability to control the internal and external states of the reactant atoms and ions precisely at a single quantum level using optical means [1]. Since ultracold temperature regime can be reached in the laser-cooled atoms and ions, the atom-ion hybrid system is one of the most promising candidates to investigate the quantum statistical nature in chemical reactions. To study quantum statistical features in chemical reactions, we need to reach and stably keep the low temperature conditions in the atom-ion hybrid system. This is currently a big challenge since the dynamical nature of the ion trap easily heats up the ions particularly when they are co-trapped with atoms [2]. In our experiment we choose ^{6}Li-^{4}0Ca^{+} combination to minimize the excess heating arising from the atom-ion interactions.

The first half of the presentation will be devoted to the characterization of inelastic collisions in the ^{6}Li-^{4}0Ca^{+} system at the temperature down to 1mK. When we prepare the ^{4}0Ca^{+} ions at the metastable D states and overlap them with ^{6}Li atoms, we frequently observe the loss of ion fluorescence. The process has been identified as charge exchange collisions from the mass spectrometry [3, 4]. We further investigate the internal-state dependence of the charge-exchange collisions and find out the fact that the energy dependence of the charge-exchange collision cross-section is consistent with the Langevin collision model down to the collision energy of 1mK. The charge-exchange collision channel has been identified in the calculated potential energy curves of ^{6}Li-^{4}0Ca^{+} combination [4].

The second half of the presentation will be devoted to the observation of the atom-ion thermalization through the elastic collisions [5]. We have been able to observe the cooling effect of the ions when they are immersed in an ultracold gas of neutral atoms using the Doppler recooling method (Figure 1). From the time evolution of the ion energy, we quantify the energy reduction ratio per single atom-ion elastic collision. Since the heating due to excess micromotion is expected to be the obstacle to study quantum chemistry in the atom-ion hybrid system, understanding the elastic collisional properties between atoms and ions is an important step for the realization of the sympathetic cooling of the ions using atoms.

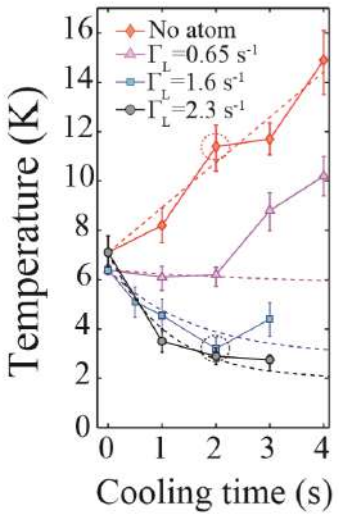


Figure 1: Cooling dynamics in the Li-Ca^{+} system. The vertical axis shows the ion temperature and the horizontal axis shows the holding time of the ions mixed with neutral atoms. Γ_L indicates the Langevin collision rate. The dashed curves show the best fit result with our simple collision model.

[1] M. Tomza et al. arXiv:1708.07832

[2] Z. Meir et al. Phys. Rev. Lett. **117**, 243401 (2016).

[3] S. Haze et al., Phys. Rev. A **91**, 032709 (2015).

[4] R. Saito, et al., Phys. Rev. A **95**, 032709 (2017).

[5] S. Haze et al., Phys. Rev. Lett. **120**, 043401 (2018).

All-optical metastable excitation techniques for precision noble-gas radio-isotope ratiometry using atom-trap trace analysis

P. S. Light[1], **R. D. Glover**[2], **M. A. Dakka**[1], **G Tsiminis**[1], **R. T. Sang**[2] **and A. N. Luiten**[1]

[1] *Institute for Photonics and Advanced Sensing (IPAS)* and *School of Physical Sciences, University of Adelaide, Adelaide, SA 5005, Australia*

[2] *Centre for Quantum Dynamics* and *School of Natural Sciences, Griffith University, Brisbane, QLD 4111, Australia*

e-mail: *philip.light@adelaide.edu.au*

Atom-trap trace analysis (ATTA) is a laser-based technique for measuring noble-gas radio-nuclide ratios (specifically 81Kr, 85Kr and 39Ar) for the dating of ground-water and ocean-water samples [1]. It allows determination of water ages ranging from less than a year, through to millions of years, by comparing the abundance of a specific radio-nuclide in the sample with the abundance in 'new' water, which is known to be in equilibrium with the atmospheric abundance. The rare radio-isotopes, which have an abundance as low as 1×10^{-17} compared to the stable isotope, present a great measurement problem. The recent development of ATTA made such measurements feasible, as it uses magneto-optical trapping to count individual atoms of the radio-isotopes, rather than counting radioactive decay as used in conventional techniques.

Laser cooling of the noble-gas sample first requires excitation of the atoms into the metastable state, from which laser-cooling is readily achievable using a cyling transition at ≈810 nm. Current ATTA systems use RF discharge techniques to excite atoms into the metastable state. As well being inefficient ($\approx 1 \times 10^{-4}$), contamination problems arise in the vacuum system due to high kinetic energy ions produced in the process. More efficient and cleaner metastable excitation methods would allow reduced measurement time, reduced flushing time, and measurement of smaller samples. While optical lamp-based excitation techniques have been considered before [2], laser-based schemes remain largely unexplored. Here we explore how two laser-based techniques could benefit an ATTA measurement system.

Multi-photon Excitation: We have modelled and experimentally measured two-photon transitions for optical excitation of the metastable level. A two-photon excitation into krypton $2p^6$ state decays directly into the $1s^5$ metastable state with favourable 75 % branching ratio. We have demonstrated efficiencies of 2 % per pulse, using a broad-bandwidth excitation source. Our model suggests that efficiencies up to 30 % are possible through the two-photon excitation scheme under optimal conditions [3]. Fig. 1 shows EMCCD images of the fluorecence observed in a Kr gas cell excited by a 215 nm laser focussed through the cell, as a result of the decay from $2p^6$ to $1s^5$ metastable state.

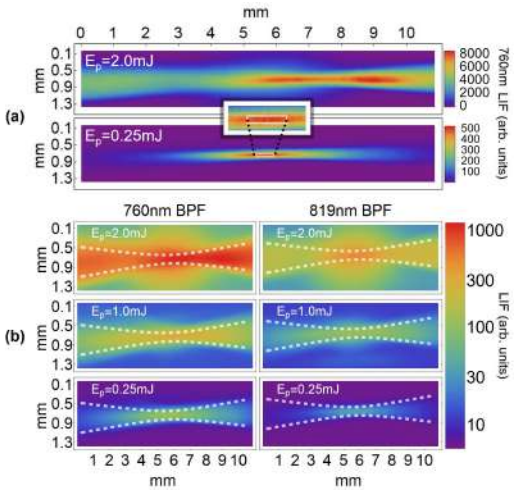


Figure 1: (a) LIF images at 760nm showing evidence of filamentation at higher energies. (b) Representative log scale images at 760nm (left) and 819nm (right).

Frustrated Tunnel Ionization: A second metastable excitation method we are considering is the strong-field excitation technique of frustrated tunnel ionization [4, 5], which takes advantage of a neutral exit channel available in the tunneling regime of strong-field ionization. By application of static electric fields, we are currently attempting to optimize excitation into the desired metastable state, rather that the Rydberg states that have previously been targeted for other applications. We will present our measured metastable efficiencies obtained using frustrated tunnel ionization, and compare this technique with both the direct laser excitation discussed above, and with the conventional RF discharge technique currently used in ATTA systems.

[1] Z. T. Lu et al., Earth-Science Rev., **138** 192-214 (2014)

[2] H. Daerr et al., Rev. Sci. Instrum. **82** 073106 (2011)

[3] M. A. Dakka et al., arXiv:1805.05669 [physics.atom-ph]

[4] T. Nubbemeyer et al., Phys. Rev. Lett. **101** 233001 (2008)

[5] H. Zimmermann et al., Phys. Rev. Lett. **114** 123003 (2015)

The Electron Affinity of Thallium by Laser Photodetachment Threshold Spectroscopy*

N.D. Gibson[1], **C.W. Walter**[1], **G.R. Drumm**[1], **Y. Li**[1], **and S.M. Miller**[1]
[1] *Denison University, Granville, Ohio, 43023 USA*
e-mail: *gibson@denison.edu*

The electron affinity of thallium has been experimentally measured using tunable laser photodetachment threshold spectroscopy. The relative cross section for neutral atom production following photodetachment from Tl^- was measured with a crossed laser–ion beam apparatus over the photon energy range 0.30 – 0.50 eV. An *s*-wave threshold was observed due to the opening of the Tl^- ($6p^2\ ^3P_0$) to Tl ($6p\ ^2P_{1/2}$) ground-state to ground-state transition, yielding a preliminary value for the Tl electron affinity. The electron affinity measured in the present work is compared with both previous experimental [1] and theoretical [2] results.

* This material is based on work supported by the National Science Foundation under Grant Nos. 1404109 and 1707743.

[1] D. L. Carpenter, A. M. Covington, and J. S. Thompson, *Phys. Rev. A* **61**, 042501 (2000).

[2] see for example J. Li, Z. Zhao, M. Andersson, X. Zhang, and C. Chen, *J. Phys. B-At. Mol. Opt. Phys.* **45**, 165004 (2012) and D. Figgen, A. Wedig, H. Stoll, M. Dolg, E. Eliav, U. Kaldor, *J. Chem. Phys.* **128**, 024106 (2008),

Entanglement preserving local thermalization

Chung-Yun Hsieh[1], **Matteo Lostaglio**[1], **and Antonio Acín**[1,2]

[1] *ICFO - Institut de Ciències Fotòniques, The Barcelona Institute of Science and Technology, 08860 Castelldefels, Spain*

[2] *ICREA-Institució Catalana de Recerca i Estudis Avancats, Lluis Companys 23, 08010 Barcelona, Spain*

e-mail: *chung-yun.hsieh@icfo.eu*

Can entanglement survive the thermalization of subsystems? While the answer is no in the absence of any shared resource, our findings show that entanglement can be preserved by locally performed thermalization processes in the presence of shared randomness.

Main Results – Being a core feature of quantum theory, entanglement is one of the most representative resources in quantum information science. While being a powerful resource, entanglement may not always survive common dynamical evolutions. In particular, from the thermodynamics point of view, it is interesting to ask *whether entanglement can survive a locally performed subsystem thermalization.* To be formal, consider the following bipartite setting. Suppose two agents at first share an unknown input state and then separate. We assume that they neither share additional quantum resources, such as another known entangled state, nor can they communicate with each other. What they can do are local operations, and they may exploit classical randomness shared before they separated. The channels so defined are *Local Operations plus Shared Randomness* (LOSR), which of course cannot create entanglement. After their disconnection, each party thermalizes its half of the (unknown) input state. From this scenario, we define a *local thermalization* to be a LOSR channel that on each subsystem thermalizes arbitrary states to a predefined thermal state. The map $(\cdot) \mapsto \gamma_{\mathrm{A}} \otimes \gamma_{\mathrm{B}}$, where γ_{A} (γ_{B}) is the predefined thermal state on A (B), is a trivial local thermalization, but destroys entanglement. The central question of this paper can be summarized as: *Do Entanglement Preserving Local Thermalizations (EPLT) exist?* Ultimately this is a fundamental question about the relation between entanglement and thermalization. Answering it also suggests that shared randomness may be a useful resource to sustain entanglement during thermalization.

As a natural first step one may ask whether it is truly necessary to use shared randomness. The natural setting for the thermalization of two non-interacting systems is one in which only local operations are allowed. However, no correlations (even classical ones), can be preserved in this scenario. More precisely, we show that local thermalizations with no randomness reduce to the channel $(\cdot) \mapsto \gamma_{\mathrm{A}} \otimes \gamma_{\mathrm{B}}$ described above.

From the above observation, one learns that EPLT must exploit randomness. Formally, we prove the following result. We define the normalized temperature of a thermal state $\gamma_{\mathrm{X}} = e^{\frac{-H_{\mathrm{X}}}{kT_{\mathrm{X}}}}/\mathrm{tr}(e^{\frac{-H_{\mathrm{X}}}{kT_{\mathrm{X}}}})$ as $\tau_{\mathrm{X}} = \frac{kT}{E_{\mathrm{X}}}$, where k is the Boltzmann constant, T is the temperature, and E_{X} is the highest eigenenergy of H_{X}. Also denote by $\mathcal{B}$ the set of channels on AB that do not preserve entanglement for any input and $\mathcal{B}_{\mathrm{free}}$ those that can only preserve bound entangled states [1] (i.e., every output is separable or bound entangled). Then [Let $\mathcal{D}(\mathcal{E}\,;\,\mathcal{B}) = \inf_{\Lambda\in\mathcal{B}} \|\mathcal{E}-\Lambda\|_1$]

Theorem 1. *For every $\delta > 0$, there exists a $\tau_\delta > 0$ such that for every pair $(\gamma_{\mathrm{A}}, \gamma_{\mathrm{B}})$ with $\min_{\mathrm{X}} \tau_{\mathrm{X}} > \tau_\delta$, there exist two EPLTs denoted by $\mathcal{E}_+$ and $\mathcal{E}_- \notin \mathcal{B}_{\mathrm{free}}$ such that*

$$\mathcal{D}(\mathcal{E}_+\,;\,\mathcal{B}) > (1-\delta)\left(1-\frac{1}{d}\right) \quad \& \quad \mathcal{D}(\mathcal{E}_-\,;\,\mathcal{B}) < \delta. \quad (1)$$

The above theorem tells us that EPLTs exist, provided that the *normalized* temperatures on both parties are high enough (we remark that this does not require high temperatures T in general). Furthermore, the above theorem illustrates more properties of EPLTs; namely, we find EPLTs "far" from $\mathcal{B}$, as well as EPLTs arbitrarily close to $\mathcal{B}$ but still able to preserve *free* entanglement [1]. This feature also shows an interesting relation between $\mathcal{B}$ and $\mathcal{B}_{\mathrm{free}}$: they share some common boundary points.

As a special case, our result can be improved in two-qubit systems by the positive partial transpose criterion [1]. As an application of the formalism, one can construct a witness of the nonlocal correlations of arbitrarily given states via the thermal properties of a corresponding locally thermal state. This method can also witness nonlocal correlations that cannot be witnessed using mutual information.

As a final remark, generalizations to multipartite systems are also presented. More precisely, the proof of the existence of EPLTs can be generalized to arbitrarily (finitely) many parties. In particular, genuinely multipartite entanglement such as that of the Greenberger-Horne-Zeilinger state [1] can also be preserved by local thermalizations in some cases.

References

[1] R. Horodecki, P. Horodecki, M. Horodecki, and K. Horodecki, Rev. Mod. Phys. **81**, 865 (2009).

The $5P_{3/2} \rightarrow 6P_{3/2}$ electric quadrupole transition in atomic rubidium as a probe of the Autler-Townes (AT) effect

F. Ponciano-Ojeda[1], S. Hernández-Gómez[1], C. Mojica-Casique[1], L. M. Hoyos-Campo[1], J. Flores-Mijangos[1], F. Ramírez-Martínez[1], D. Sahagún[2], R. Jáuregui[2], and J. Jiménez-Mier[1]

[1] *Instituto de Ciencias Nucleares, Universidad Nacional Autónoma de México , Ciudad Universitaria, 04510 Coyoacán, Ciudad de México, México*

[2] *Instituto de Física, Universidad Nacional Autónoma de México, Ciudad Universitaria, 04510 Coyoacán, Ciudad de México, México*

e-mail: *ferama@nucleares.unam.mx; jimenez@nucleares.unam.mx*

In the Autler-Townes effect a weak transition line is split when one of the two levels involved is coupled to a third state by a strong resonant electromagnetic field [1]. In this work we show that the $5S_{1/2} \rightarrow 5P_{3/2} \rightarrow 6P_{3/2}$ excitation sequence in atomic rubidium is ideal to observe the Autler-Townes splitting. Here the first step is the D2 resonant line in rubidium, and provides a strong coupling between the $5S_{1/2}$ and $5P_{3/2}$ states. The second step is forbidden by the electric dipole approximation, and it naturally constitutes a weak probe. The first observation of this optical double with an electric quadrupole transition was reported recently [2].

In the experiment presented here a 780 nm diode laser is locked to the $5S\ F = 2 \rightarrow 5P_{3/2}F = 3$ cyclic transition for zero velocity ^{87}Rb atoms. The frequency of a 911 nm probe laser is scanned across the forbidden transition, and the 420 nm fluorescence from the $6P_{3/2} \rightarrow 5S_{1/2}$ direct decay is detected with a photomultiplier tube (Hamamatsu, 1P28) and a lock-in amplifier (Princeton Applied Research, 5209). The use of collinear beams results in fluorescence spectra in which the hyperfine structure of the $6P_{3/2}$ state is resolved. The Autler-Townes effect is observed when the fluorescence peaks are broaden and then split as the intensity of the 780 nm laser is increased. A three-level master equation system is used to calculate the line profiles of the Autler-Townes doublets. In particular, it was found that the spontaneous decay fluorescence directly follows the behavior of the population of the $6P_{3/2}$ hyperfine states.

A comparison between experimental fluorescence spectra and the results of the calculation is made in Fig. 1. The laser linewidths and relative hyperfine intensities were used as overall parameters in this comparison, with the only change among the spectra produced by the Rabi frequency associated to the first excitation step. The calculation also indicates that in our system the two-step excitation produces a dipole allowed coherence between the $5S_{1/2}$ and $6P_{3/2}$ states that should result in coherent blue emission, with a line profile significantly different from that of the spontaneous decay.

We thank J. Rangel for his help in the construction of the diode laser. This work was supported by DGAPA-UNAM, México, under projects PAPIIT Nos. IN112516, IN107317, by National Laboratory project 293471. L. M. Hoyos-Campo thanks UNAM-DGAPA for the postdoctoral fellowship and IUPAP for the travel grant.

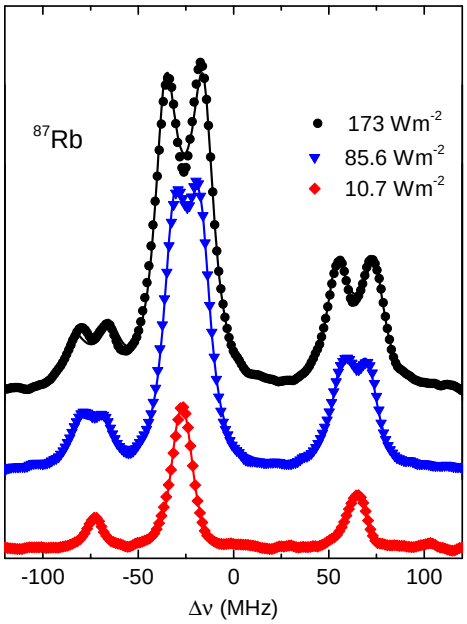


Figure 1: Fluorescence spectra showing the Autler-Townes effect. The intensity of the 780 nm used for each spectrum is indicated.

[1] C. Cohen-Tannoudji, B. Diu and F. Laloë, *Quantum Mechanics*, Vol. 2, Wiley, 1977.

[2] F. Ponciano-Ojeda, *et al.*, Phys. Rev. A **92**, 042511 (2015); C Mojica-Casique *et al.*, J. Phys. B **50** 025003 (2017); F. Ponciano-Ojeda *et al.*, Am. J. Phys. **86**, 7 (2018).

Novel quantum technologies based on atomic vapour cells

R. Löw, H. Kübler, H. Alaeian, R. Ritter, F. Ripka, D. Weller, H. Zhang, J. Schmidt and T. Pfau

5th Institute of Physics, University of Stuttgart, 70569 Stuttgart, Germany

e-mail: *r.loew@physik.uni-stuttgart.de*

Photonic quantum devices based on atomic vapours at room temperature combine the advantages of atomic vapours being intrinsically reproducible with various options for scalability and integrability. We show how we integrate photonic and electronic components into vapour cells and we will focus among a variety of applications on two topics.

First we will present optical chips immersed in an atomic vapour providing several waveguide geometries for spectroscopy applications. This includes integrated ring resonators, Mach Zehnder interferometers, slot waveguides and counter propagating coupling schemes. This work demonstrates a next step towards miniaturization and integration of alkali atom spectroscopy and provides a platform for further fundamental studies of strong atom light coupling where cooperativities on the order of 1 are within reach [1].

The second project is a proof of principle experiment for a new type of a gas sensor. Here we make use of multi-photon excitations to Rydberg states which subsequently get ionized by collisions with a background gas. The resulting charges can directly read out with integrated trans-impedance amplifiers. First tests with Rb and NO have been performed. This method has the potential to reach ppb-sensitivities in micro-liter volumes [2].

References

[1] R. Ritter et. al., PRX **8**, 021032 (2018).

[2] J. Schmidt, et. al. arXiv:1801.09453

Loss-rate measurement in a magneto-optical trap for metastable europium

Y. Miyazawa, R. Inoue, and M. Kozuma
Department of physics, Tokyo Institute of Technology, 2-12-1 O-okayama, Meguro-ku, Tokyo 152-8550 Japan
e-mail: *miyazawa.y.ab@m.titech.ac.jp*

Europium (Eu) is one of good candidates for investigating strongly dipolar phenomena, because it has a large magnetic dipole moment $7\,\mu_B$, as with Cr ($6\,\mu_B$), Er ($7\,\mu_B$) and Dy ($10\,\mu_B$). Stable bosonic isotopes of Eu (^{151}Eu and ^{153}Eu) have hyperfine structure, which enables us to control an s-wave scattering length using RF fields even under zero DC magnetic field [1, 2]. These features are of interest for exploring ground state phases of dipolar BEC with spin degrees of freedom, such as spin textures and vortices [3], where the magnetic dipole-dipole interaction couples spin and orbital angular momenta. In our previous work, we measured a lower limit of the leakage probability from a $|g\rangle \leftrightarrow |e1\rangle$ transition (see Fig. 1) as $1.05(2) \times 10^{-3}$ [4]. To avoid this leak, we operated Zeeman slowing and magneto-optical trapping (MOT) by using a $|m3\rangle \leftrightarrow |e3\rangle$ cyclic transition [5]. We optically pumped atoms in the ground state $|g\rangle$ to the metastable state $|m3\rangle$ by driving three transitions, whose wavelength is 460 nm, 507 nm and 513 nm.

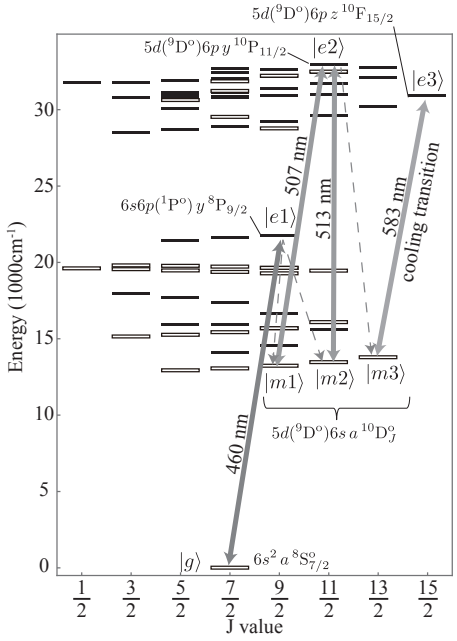


Figure 1: The energy levels of Eu up to 32948.41 cm^{-1}, which corresponds to the uppermost level $|e2\rangle$ in our experiment. It also shows the pumping and laser-cooling transitions. Odd parity states are indicated by open box.

In order to observe dipolar phenomena, we have to prepare degenerated Eu atoms in the ground state $|g\rangle$. Investigating the loss mechanism in a MOT is important for this goal. We measure loss rate by monitoring fluorescence decay of a MOT. A two-body loss rate is estimated as 10^{-10}cm^3/s from a non-exponential loss of atoms at high densities. In addition, we find that one-body loss rate γ depends strongly on the existence of pumping laser beams, particularly at the wavelength of 513 nm and on the power of the cooling-laser beams, as shown in Fig. 2. This could be explained by the assumption of fractional leakage from upper cooling level $|e3\rangle$ to $|m2\rangle$ as one of the main loss mechanism, since the 513-nm repumper can return the atoms from metastable state $|m2\rangle$ to the quasi-cyclic transition $|m3\rangle \leftrightarrow |e3\rangle$.

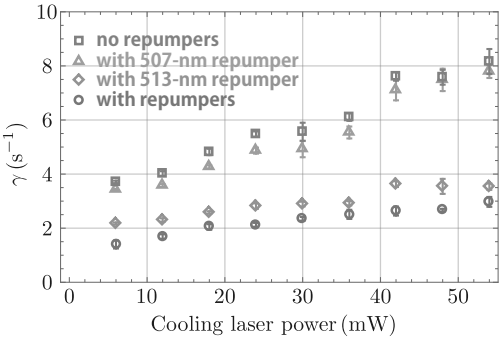


Figure 2: Dependence of the one-body loss rate γ on the existence of repumpers and the total power of the cooling light.

[1] D. J. Papoular, G. V. Shlyapnikov, and J. Dalibard, Phys. Rev. A **81**, 041603 (2010).

[2] T. M. Hanna, E. Tiesinga, and P. S. Julienne, New J. Phys. **12**, 083031 (2010).

[3] Y. Kawaguchi, H. Saito, and M. Ueda, Phys. Rev. Lett. **97**, 130404 (2006).

[4] Y. Miyazawa, R. Inoue, K. Nishida, T. Hosoya, and M. Kozuma, Opt. Commun. **329**, 171 (2017).

[5] R. Inoue, Y. Miyazawa, and M. Kozuma, arXiv: 1803.06475.

Production and study of new neutron rich isotopes of heavy atoms

S. Zemlyanoy[1], **V. Zagrebaev**[1], **K. Avvakumov**[1], **Yu. Kudryavtsev**[2], **V. Fedosseev**[3], **R. Bark**[4], **Z. Janas**[5]

[1] *Joint Institute for Nuclear Research, Dubna 141980, Russia*
[2] *Instituut voor Kern- en Stralingsfysica, Leuven, Belgium*
[3] *CERN, Switzerland*
[4] *iThemba LABS, Nat. Research Foundation, South Africa*
[5] *Faculty of Physics, University of Warsaw, Warsaw, Poland*

e-mail: *zemlya@jinr.ru*

A new setup, based on stopping nuclei in the gas cell and subsequent resonance laser ionization and separation by magnetic field is under stage of realization at Flerov lab. JINR. This setup is intended for synthesis and study of new neutron rich isotopes of heavy atomic nuclei formed in low energy multinucleon transfer reactions.

The heavy isotopes of neutron rich atomic nuclei are very important for atomic and nuclear physics investigations, for the understanding of astrophysical nucleosynthesis and r-process. In this region is located the closed neutron shell N=126 which is the last so-called "waiting point".

Study of the structural properties of nuclei along the neutron shell N = 126 could also contribute to the present discussion of the quenching of shell gaps in nuclei with large neutron excess.

A creation and launch of this facility will open a new field of research in low-energy heavy-ion physics, and new horizons in the study of unexplored "north-east" area of the nuclear map. It could be helpful also for finding a new way for production of heavy and superheavy atomic nuclei.

The current status of this setup will be discussed.

Spectroscopy of the $5p_{3/2} \rightarrow 6p_{1/2}$ electric dipole forbidden transition in atomic rubidium.

F. Ponciano-Ojeda[1], S. Hernández-Gómez[1], C. Mojica-Casique[1], L. M. Hoyos-Campo[1], J. Flores-Mijangos[1], F. Ramírez-Martínez[1], D. Sahagún[2], R. Jáuregui[2], and J. Jiménez-Mier[1]

[1] *Instituto de Ciencias Nucleares, Universidad Nacional Autónoma de México , Ciudad Universitaria, 04510 Coyoacán, Ciudad de México, México*

[2] *Instituto de Física, Universidad Nacional Autónoma de México, Ciudad Universitaria, 04510 Coyoacán, Ciudad de México, México*

e-mail: *ferama@nucleares.unam.mx; jimenez@nucleares.unam.mx*

We present the first observation of the $5p_{3/2} \rightarrow 6p_{1/2}$ electric quadrupole transition in atomic rubidium. In a similar scheme to the one reported in [1] for the measurement of the $5p_{3/2} \rightarrow 6p_{3/2}$ excitation, the experiment presented in this work has been done in a room temperature rubidium vapor cell using Doppler-free optical-optical double-resonance spectroscopy with counter-propagating beams.

The $5s_{1/2} \rightarrow 5p_{3/2}$ electric dipole excitation is produced with an external cavity diode laser locked to the $F = 3(2) \rightarrow 4(3)$ cyclic transition of the D_2 line in ^{85}Rb (^{87}Rb). This prepares the atoms in the first excited state and the $5p_{3/2} \rightarrow 6p_{1/2}$ dipole-forbidden excitation establishes a two-photon ladder excitation scheme. The 917 nm radiation required for this quadrupole excitation is generated by a commercial Ti:Sapphire laser. The two laser components are sent through the Rb cell in a co-linear configuration; both are prepared in linearly polarized states; and their relative direction of polarization can be controlled by means of a half-wave-plate placed in the path of the 917 nm component.

Production of atoms in the $6p_{1/2}$ excited state is determined by detection of the 421 nm fluorescence that results from the direct decay $6p_{1/2} \rightsquigarrow 5s_{1/2}$ into the ground state. A band-pass filter centered at 420 ± 2 nm (FWHM 10 ± 2 nm) and a two-lens system for the collection of this fluorescence are located next to and at the middle along the length of the Rb spectroscopy cell. The lens system faces the interaction region at a right angle with respect to the direction of propagation of the excitation beams and focuses the fluorescence onto the cathode of a photomultiplier tube (PMT).

The polarization dependence of the relative intensities of the lines of the decay fluorescence is investigated in detail. For instance, representative spectra for parallel and perpendicular polarizations are shown in figure 1. Experimental data for different polarization configurations of the light beams are compared with the results of calculations that consider a strong atom-field coupling in the preparation step, followed by a weak electric quadrupole excitation and the blue fluorescence decay emission. Good agreement between experiment and this three-step model

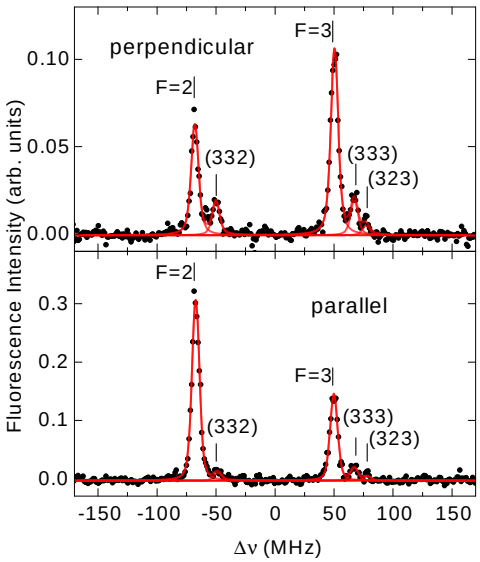


Figure 1: Representative spectra for the perpendicular and parallel polarization configurations in ^{85}Rb. The two main components in each spectra correspond respectively to the bare atomic transitions $5s_{1/2}, F = 3 \rightarrow 5p_{3/2}, F = 4 \rightarrow 6p_{1/2}, F = 2$, 3. Adjacent peaks due to velocity selective resonances are identified with their corresponding excitation path ($FF'F''$).

is found, particularly in the case of linear-linear polarizations in both isotopes. This agreement confirms that it is possible to use the relative direction of polarization of the two laser excitation components to exploit quadrupole selection rules for the preparation of hyperfine atomic states in the $6p_{1/2}$ manifold.

We thank J. Rangel for his help in the construction of the diode laser. This work was supported by DGAPA-UNAM, México, under projects PAPIIT Nos. IN112516, IN107317, by National Laboratory project 293471. LMHC thanks UNAM-DGAPA for the postdoctoral fellowship and IUPAP for the travel grant. JFM, FRM, and JJM thank the "Programa de Movilidad Académica Internacional, CIC-UNAM".

[1] F. Ponciano-Ojeda, *et al.*, Phys. Rev. A **92**, 042511 (2015); C Mojica-Casique *et al.*, J. Phys. B **50** 025003 (2017); F. Ponciano-Ojeda *et al.*, Am. J. Phys. **86**, 7 (2018).

Sub-Doppler saturated fluorescence spectroscopy of the $5s_{1/2} \rightarrow 6p_{3/2}$ transition in room temperature rubidium atoms

J. E. Navarro-Navarrete, A. E. Díaz-Calderón, L. M. Hoyos-Campo, F. Ponciano-Ojeda, J. Flores-Mijangos, F. Ramírez-Martínez and J. Jiménez-Mier

Instituto de Ciencias Nucleares, Universidad Nacional Autónoma de México, Circuito Exterior S/N, Ciudad Universitaria, 04510 Coyoacán, México

e-mail: *ferama@nucleares.unam.mx, jimenez@nucleares.unam.mx*

We present a novel and simple experimental scheme for the sub-Doppler spectroscopy of the $5s_{1/2} \rightarrow 6p_{3/2}$ transition with a 420 nm laser in thermal rubidium atoms. With a simple experimental arrangement, the major advantage exploited by this scheme is the highly simple and efficient detection of infrared fluorescence at 780 nm and 795 nm conveying information of the hyperfine structure of the $6p_{3/2}$ energy level (see Fig. 1). There are multiple decay paths for the $6p_{3/2}$ level; one of these, the one with the lowest probability, is a direct decay into the ground energy level emitting 420 nm radiation. The other decay channels transit necessarily through the intermediate levels $5p_j$ $(j = 1/2, 3/2)$ and finally decay back down to the ground state with the emission of either 780 nm or 795 nm fluorescence.

Radiation from a 420 nm *cat-eye* external cavity diode laser is sent through and retroreflected back into the room temperature spectroscopy cell to create a two counter-propagating beam configuration. A lens, an IR bandpass filter and a photo-multiplier tube (PMT) located next to, at the middle along the length of the cell, and directed at a right angle with respect to the direction of propagation of the excitation beams are used respectively to collect, select and register the infrared fluorescence.

Saturation effects are revealed for the velocity groups of atoms that simultaneously interact with both laser beams [1]. This, therefore, leads to the appearance of Lamb dips [2] in the Doppler-broadened fluorescence signal as a result of an effective decrease in the population of the intermediate states $5p_j$ and the corresponding decrease in the amount of fluorescence generated by these velocity groups of atoms.

As exemplified in Fig. 1, this simple system allows to resolve the hyperfine structure of the $6p_{3/2}$ energy level within the fluorescence well. This also leads to a novel scheme for locking the frequency of the 420 nm laser to most of the observed $6p_{3/2}$ hyperfine levels or crossovers of either of the two most abundant rubidium isotopes.

In addition, a third beam from the same 420 nm laser modulated with an acousto-optic modulator (AOM) in a double pass configuration has also been included in the spectroscopy system. This provides a basis for an absolute measurement of the hyperfine energy splitting of the $6p_{3/2}$ state with a resolution of the order of 1 MHz, mainly limited at the present stage of this investigation by broadening effects caused by the 420 nm laser intensity and nonlinearities on the scanning of the laser piezo-electric.

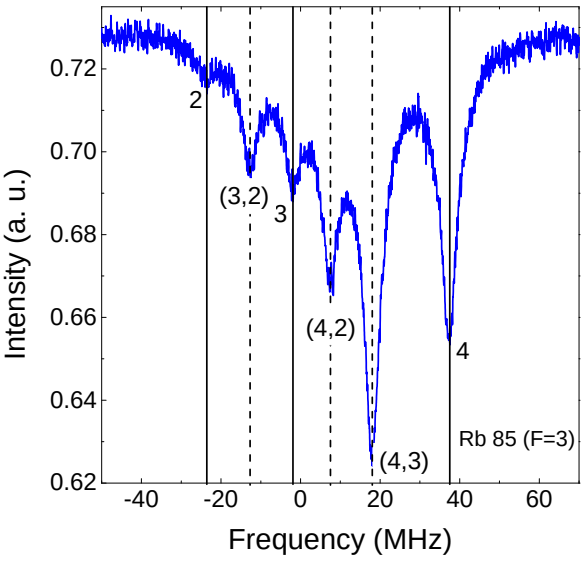


Figure 1: Hyperfine structure of the $6p_{3/2}$ level for the ^{85}Rb isotope. The peaks labeled as 2, 3 and 4 correspond respectively to the transitions $(F = 3 \rightarrow F' = 2, 3, 4)$ and the labels $(3, 2)$, $(4, 2)$ and $(4, 3)$ show the corresponding crossovers. The solid and dashed vertical lines provide, respectively, an indication of the relative positions of the atomic transitions and crossovers given the energy splitting of the $6p_{3/2}$ level as calculated with the hyperfine constants reported in [3].

We thank J. Rangel for his help in the construction of the diode laser. This work was supported by DGAPA-UNAM, México, under projects PAPIIT Nos. IN112516, IN107317, by National Laboratory project 293471. LMHC thanks UNAM-DGAPA for the postdoctoral fellowship and IUPAP for the travel grant. JFM, FRM, and JJM thank the "Programa de Movilidad Académica Internacional, CIC-UNAM".

[1] E. Döpel, D. Kühlke, W. Dietel, Opt. Commun. A **25**, 62-64 (1978).

[2] Helen K. Holt, Phys. Rev. A **30**, 2495 (1984).

[3] J. E. Sansonetti, J. Phys. Chem. Ref. Data **45**, No. 1, pp. 301-421 (2006).

Mirrorless optical parametric oscillator inside an all optical waveguide

Sushree S. Sahoo[1], **Snigdha S. Pati, and Ashok K. Mohapatra**[2]
National Institute of Science Education and Research, Bhubaneswar, India
e-mail: [1]*sushree.ss@niser.ac.in*, [2]*a.mohaptra@niser.ac.in*

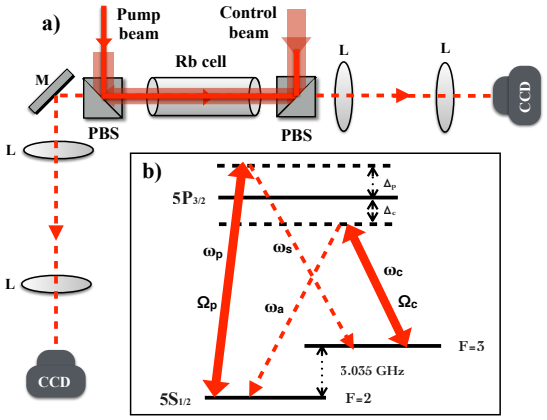


Figure 1: a) Experimental setup for MOPO in thermal rubidium vapor, PBS: polarising beam splitter, M: mirror, L: Lens. b) Energy level diagram of ^{85}Rb showing the coupling of pump and control laser fields (solid lines) and the generated Stokes and anti-Stokes fields (dashed lines).

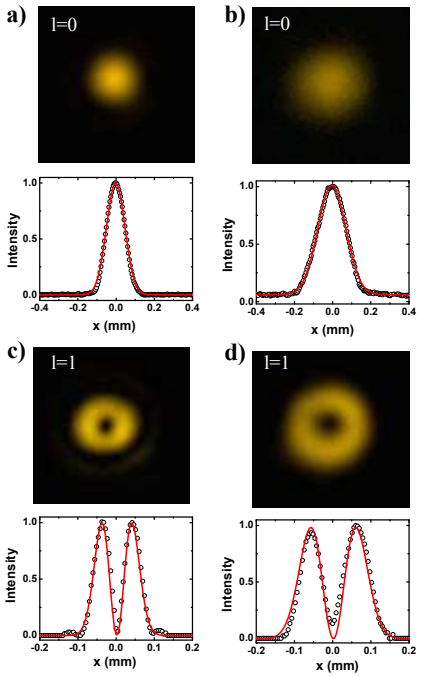


Figure 2: The symmetric gaussian mode and the corresponding transverse intensity patterns in the generated a) Stokes and b) anti-Stokes fields. The first-order Laguerre-Gaussian (LG01) mode and the corresponding transverse intensity patterns in the generated c) Stokes and d) anti-Stokes fields.

Mirrorless optical parametric oscillator (MOPO) is a consequence of intrinsic feedback provided by the nonlinearity in a medium due to the interaction of a pair of strong counter-propagating fields. As the name suggests, the device doesn't require a cavity for lasing other than the nonlinear medium. It has attracted a lot of attention ever since the phenomenon was first theoretically predicted by S.E. Harris [1]. Here, we report the demonstration of MOPO under the effect of an all-optical waveguide. The efficient four-wave mixing process due to counter-propagating pump and control fields interacting with a multilevel atomic system facilitates the generation of mirrorless Stokes and anti-Stokes fields counter-propagating to each other [2, 3, 4]. The maximum generated laser power could rise up to mW with pump conversion efficiency more than 30%. Furthermore, the cross-phase modulation due to the pump field creates an all-optical waveguide [5, 6, 7] for the generated fields and hence induces different spatial modes in the Stokes as well as the anti-Stokes fields. With suitable experimental parameters, we could generate correlated Gaussian mode or Laguerre-Gaussian mode for both the generated fields.

The schematic of the experimental setup and the relevant energy level diagram for the system are shown in Fig. 1. A pump laser field with Rabi frequency Ω_p and optical frequency ω_p and control field with Rabi frequency Ω_c and optical frequency $\omega_c$counter-propagate with each other through a 5 cm long rubidium vapor cell housed inside two layers of magnetic shields. The temperature of the vapor cell is kept between $110^0 - 120^0$C using a controlled heater which corresponds to a number density of approximately $10^{13}/\text{cm}^3$. The spatial modes of the generated fields under the effect of the all-optical waveguides can be studied using their propagation equations through the nonlinear medium given as,

$$i\frac{\partial A_s}{\partial z} = \beta_s A_s$$

where, $\beta_s = -\frac{\nabla_T^2}{2k_s} + V(r)$. $V(r) = -\frac{3}{2n_s} Re(\chi_{\text{XPM}}^{(eff)}(r))$ is the near-Gaussian potential experienced by the Stokes field with $\chi_{\text{XPM}}^{(eff)}$ being the value of the effective susceptibility at the peak of the potential.

The 4-f imaging technique is used to image the generated beams at the respective exit-faces of the vapor cell. In Fig. 2 (a) and (b), we show the CCD images of

the Gaussian mode and in Fig. 2 (c) and (d), we show the Laguerre-Gaussian mode with the corresponding intensity profiles along the transverse co-ordinate x for Stokes and anti-Stokes beams respectively.

References

[1] S. E. Harris, *Appl. Phys. Letts.* **9**, 114, 1966.

[2] S. Du, J. Wen, and M. H. Rubin, *J. Opt. Soc. Am. B* **25**, C98–C108, 2008.

[3] S. Du, P. Kolchin, C. Belthangady, G. Y. Yin, and S. E. Harris. *Phy. Rev. Lett* **100**, 183603, 2008.

[4] Y. Mei, X. Guo, L. Zhao, and S. Du, *Phy. Rev. Lett* **119**, 150406, 2017.

[5] J. A. Andersen, M. E. J. Friese, A. G. Truscott, Z. Ficek, P. D. Drummond, N. R. Heckenberg, and H. Rubinsztein-Dunlop, *Phy. Rev. A* **63**, 023820, 2001.

[6] A. G. Truscott, M. E. J. Friese, N. R. Heckenberg, and H. Rubinsztein-Dunlop, *Phy. Rev. Lett.* **82**, 063902, 1999.

[7] P. K. Vudyasetu, D. J. Starling, and J. C. Howell, *Phy. Rev. Lett.* **102**, 123602, 2009.

Plasma environment effects on the decay properties of atomic K-vacancy states belonging to the oxygen and iron isonuclear sequences of astrophysical interest

J. Deprince[1], M. A. Bautista[2], S. Fritzsche[3,4], J. Garcia[5], T. R. Kallman[6], C. Mendoza[2], P. Palmeri[1] and P. Quinet[1,7]

[1] *Physique Atomique et Astrophysique, Université de Mons – UMONS, B-7000 Mons, Belgium*
[2] *Department of Physics, Western Michigan University, Kalamazoo, MI 49008, USA*
[3] *Helmholtz Institut Jena, 07743 Jena, Germany*
[4] *Theoretisch Physikalisches Institut, Friedrich Schiller University at Jena, 07743 Jena, Germany*
[5] *Department of Astronomy, California Institute of Technology, Pasadena, CA 91125, USA*
[6] *NASA Goddard Space Flight Center, Code 662, Greenbelt, MD 20771, USA*
[7] *IPNAS, Université de Liège, B-4000 Liège, Belgium*
e-mail: *patrick.palmeri@umons.ac.be*

The emission lines in the X-ray spectral region from accreting black holes, most notably those involving K-vacancy states of cosmically abundant elements, have observed widths and shifts which imply an origin very close to the compact object [1]. The intensity of these lines can provide insight into the effects of special and general relativity in the emitting region as well as insight into some properties of the compact object itself. Magnetohydrodynamics simulations of accreting black holes with 10 solar masses, computed by Schnittman *et al.* [2], seem to reveal that the plasma conditions in such an environment should be characterized by an electronic temperature ranging from 10^5 to 10^7 K and an electronic density ranging from 10^{18} to 10^{21} cm^{-3}. Such physical conditions may affect the atomic structure and processes corresponding to the ionic species present in the plasma. However, atomic data used in the standard programs to model astrophysical X-ray spectra arise from isolated ion approximation calculations. This shortcoming is thought to be the major reason of inconsistencies observed in the results [3].

The main goal of the present work is to estimate the effects of high-density plasma environment on the atomic parameters, such as the ionization potentials, the radiative decay and Auger rates, associated with the K-vacancy states along the oxygen and iron isonuclear sequences within the astrophysical context of accretion disks around black holes. In this purpose, relativistic atomic structure calculations have been carried out using the multiconfiguration Dirac-Fock (MCDF) method, in which a time averaged Debye-Hückel potential has been considered for both the electron-nucleus and electron-electron interactions in order to model the plasma environment, using a combination of the GRASP92 [4] and of the RATIP [5] codes. A comparison with the results obtained by another independent computational method, namely the multiconfiguration Breit-Pauli (MCBP) pseudo-relativistic method as implemented in the AUTOSTRUCTURE code [6, 7], has also been carried out, showing that both approaches are in very good agreement as far as the influence of plasma environment on the different atomic parameters is concerned.

[1] C. S. Reynolds and M. A. Nowak, Phys. Rep. **377**, 389 (2003).

[2] J. D. Schnittman, J. H. Krolik and S. C. Noble, Astrophys. J. **769**, 156 (2013).

[3] J. Garcia *et al.*, Mon. Not. Roy. Astron. Soc. **462**, 751 (2016).

[4] F. A. Parpia, C. Froese Fischer and I. P. Grant, Comput. Phys. Commun. **94**, 249 (1996).

[5] S. Fritzsche, Comput. Phys. Commun. **183**, 1523 (2012).

[6] N. R. Badnell, J. Phys. B : At. Mol. Opt. Phys. **30**, 1 (1997).

[7] N. R. Badnell, Comput. Phys. Commun. **182**, 1528 (2011).

HFR+CPOL and MCDHF oscillator strengths of strong electric dipole (E1) lines of U^+ of interest in cosmochronology

S. Gamrath[1], P. Palmeri[1] and P. Quinet[1,2]

[1] *Physique Atomique et Astrophysique, Université de Mons – UMONS, B-7000 Mons, Belgium*

[2] *IPNAS, Université de Liège, B-4000 Liège, Belgium*

e-mail: *patrick.palmeri@umons.ac.be*

To our knowledge, there have been very few available calculations of oscillator strengths for singly ionized uranium (U^+) [1]. The main reason is that the complexity of the electron configurations involved in the excited states and the fragmentory knowledge of the experimental spectrum of this ion make theoretical computations extremely difficult. However, transition probabilities and oscillator strengths for U^+ radiative transitions are expected to be important in astrophysics, in particular in cosmochronology where the age of a star can be determined by the use of a radiaoactive isotope of a sufficiently long lifetime. Up until a few years ago, the radioisotope ^{232}Th, with a half-life of 14 Gyr, was used to date galactic stars [2, 3, 4] but it decays only by a factor of two over the lifetime of the Universe. It was indeed pointed out by Goriely and Clerbaux [5] that new accurate observations of heavy radioactive elements could improve the accuracy of cosmochronometry analyses. More particularly, ^{238}U, with a half-life of 4.5 Gyr, represents a much more precise age indicator. In 2001, Cayrel *et al.* [6] reported the first detection of a spectral line at a wavelength of 385.957 nm, from singly ionized uranium, in the very metal-poor star BPS CS31082-001. The derived uranium abundance yielded an age of 12.5 ± 3 Gyr, which led to the best estimate of the age of the Galaxy and consequently provided a lower limit to the age of the Universe.

However, as mentioned in [6], the accuracy of this uranium dating technique is still limited by the lack of available radiative parameters for U^+ electric dipole (E1) transitions. Some reliable oscillator strengths were obtained experimentally by combining branching fraction measurements with laboratory lifetimes determined using laser spectroscopy [7, 8] but these data concern only a small number of strong lines. In order to partly fill this gap, we carried out extensive calculations of oscillator strengths for the strongest U^+ lines of potential cosmochronological interest using two independent theoretical approches, i.e. the pseudo-relativistic Hartree- Fock [9] with core-polarization corrections (HFR+CPOL) [10] and the fully relativistic multiconfiguration Dirac-Hartree-Fock (MCDHF) [11] methods. Some preliminary results will be presented at the conference.

[1] A. Meftah *et al.*, Atoms **5**, 24 (2017).

[2] H. R. Butcher, Nature **328**, 127 (1987).

[3] P. François, M. Spite and F. Spite, Astron. Astrophys. **274**, 821 (1993).

[4] J. J. Cowan *et al.*, Astrophys. J. **521**, 194 (1999).

[5] S. Goriely and B. Clerbaux, Astron. Astrophys. **346**, 798 (1999).

[6] R. Cayrel *et al.*, Nature **409**, 691 (2001).

[7] H. Lundberg *et al.*, Astron. Astrophys. **372**, L50 (2001).

[8] H. Nilsson *et al.*, Astron. Astrophys. **381**, 1090 (2002).

[9] R. D. Cowan, *The Theory of Atomic Structure and Spectra*, University of California Press, Berkeley (1981).

[10] P. Quinet *et al.*, Mon. Not. Roy. Astron. Soc. **307**, 934 (1999).

[11] I. P. Grant, *Relativistic Quantum Theory of Atoms and Molecules*, Springer-Verlag, New York (2007).

The Roentgen-term and related gems in atom-light interaction

M. Sonnleitner[1], **H. Ritsch**[1], **and S. M. Barnett**[2]
[1] *Institut für Theoretische Physik, Universität Innsbruck, Austria*
[2] *School of Physics and Astronomy, Universiy of Glasgow, United Kingdom*
e-mail: *matthias.sonnleitner@uibk.ac.at*

The Roentgen term is a usually neglected contribution to the atom-light Hamiltonian in the electric dipole approximation. Despite being small, this term is often necessary to understand properly the interaction between light and matter, especially if the particle is moving or the radiation field is modulated in time. We show how this overlooked term opens the way to surprising radiation forces and discuss how $E = mc^2$ enters non-relativistic quantum optics.

In these exciting times where lasers control atoms with ever increasing precision it becomes necessary to remember small effects and interactions which could previously be safely neglected, but may soon become measurable.

One of these effects is the Roentgen term which describes the interaction between an atom and the magnetic component of a radiation field. It changes the (multipolar) atom-light coupling to

$$H_{\mathrm{AL}} = -\mathbf{d}\cdot\mathbf{E} + \tfrac{1}{2M}\left[\mathbf{P}\cdot(\mathbf{d}\times\mathbf{B}) + \mathrm{H.C.}\right] ,$$

where $\mathbf{d}$ is the electric dipole moment of the atom with momentum $\mathbf{P}$ and mass M while $\mathbf{E}$ and $\mathbf{B}$ are the electric and magnetic components of the external radiation field. Its physical interpretation is that a moving electric dipole (the atom) appears to have a magnetic dipole moment in the laboratory frame such that it can interact with magnetic fields as well.

Although this Roentgen interaction is very weak it has been shown, for example, that it must be included in the calculation of emission patterns of moving atoms [1]. A simple extension of these calculations leads to the surprising result, that an excited two-level atom moving through vacuum appears to experience a spurious friction force in first order v/c. At first this seems to be in obvious contradiction to other calculations showing that the interaction with the vacuum does not change the velocity of an atom. Even worse, it appears to be in contradiction to the principle of relativity. It can be shown, however, that this is a side effect of the surprising appearance of mass-energy in non-relativistic atomic physics [2].

More generally however, the Roentgen term leads to a difference between the atom's canonical momentum $\mathbf{P}$ and its kinetic momentum $M\dot{\mathbf{R}}$ [3, 4]. This leads to additional forces between the atom and the radiation field, even if the atom is initially at rest. These forces appear whenever there is some time-modulation in the atom-light coupling, for example, if the light intensity or phase is modified or if the laser frequency is detuned from the atomic transition. We will discuss the characteristics of these Roentgen forces, explore their magnitudes and several peculiar results, such as forces acting perpendicular to the propagation axis of circularly polarized laser beams as shown in figure 1.

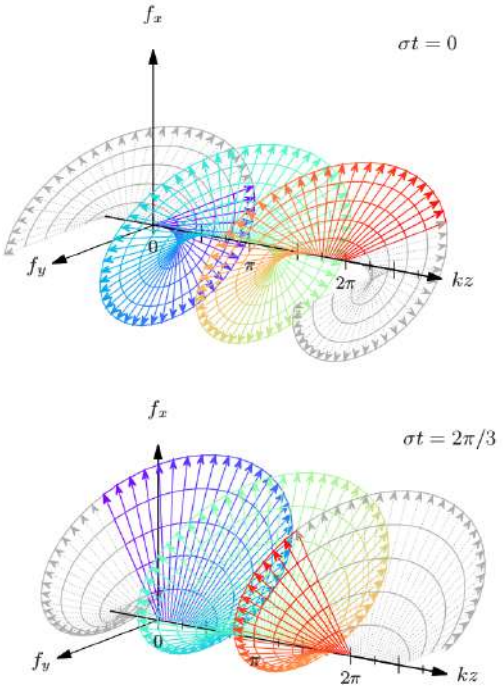


Figure 1: The Roentgen forces on a 4-level atom interacting with two plane waves of orthogonal circular polarization are acting perpendicular to the beam-propagation axis z. They change on a time-scale σ (here $\propto$ atom-laser detuning) [4].

[1] M. Wilkens, Phys. Rev. A **49**, 570 (1994).

[2] M. Sonnleitner, N. Trautmann, S.M. Barnett, Phys. Rev. Lett. **118**, 053601 (2017).

[3] V.E. Lembessis, M. Babiker, C. Baxter, R. Loudon, Phys. Rev. A **48**, 1594 (1993).

[4] M. Sonnleitner, S.M. Barnett, EPJD **71**, 336 (2017).

Holographically controlled 3D atomic population structures

A. Selyem[1], **S. Fayard**[2], **T.W. Clark**[1,3], **A.S. Arnold**[4], **N. Radwell**[1] **and S. Franke-Arnold**[1]
[1]*School of Physics and Astronomy, SUPA, University of Glasgow, G12 8QQ, Glasgow, United Kingdom*
[2]*Institut d'Optique Graduate School, 91127 Palaiseau, France*
[3]*Institute for Solid State Physics and Optics, Wigner Research Centre for Physics, Budapest, Hungary*
[4]*Department of Physics, SUPA, University of Strathclyde, G4 0NG, Glasgow, United Kingdom*
e-mail: *a.selyem.1@research.gla.ac.uk*

We demonstrate the use of 3D light structures to shape the local atomic population distributions and a technique to visualise these distributions in a hot vapour. Structured light is often analysed in terms of its 2D beam profile, but on propagation interesting 3D structures can be realised, including optical vortex knots, bottle beams and 3D lattices. We have developed a method to reconstruct the full 3D structure by measuring light scattered from an atomic vapour [1].

The structured light in [1], however, also affects the electronic levels of the atoms in the vapour. Atoms are pumped between electronic levels at rates dependent on the local light intensity, generating 3D population structures. We use a structured control beam shaped by a spatial light modulator to deplete an upper hyperfine ground state ($5^2S_{1/2}$ F=3, $|1\rangle$) of rubidium 85 via excitation of a short-lived excited state ($5^2P_{1/2}$ F=3, $|C\rangle$) and subsequent spontaneous decay into the lower ground state ($5^2S_{1/2}$ F=2, $|0\rangle$), see figure 1a). In dark regions of the beam, atoms remain in $|1\rangle$ and we can probe this remaining population with an unshaped laser at a different frequency, analogous to electron shelving. We then tomographically reconstruct the 3D population pattern from the fluorescence of this probe laser. Bright regions of the control beam coincide with suppressed fluorescence from the probe laser, as $|1\rangle$ is depleted. The retrieved 3D fluorescence patterns are therefore complementary to each other as shown in figure 1b) and c).

We establish a link between fluorescence rates and populations using a spatially resolved rate equation model. We expect this work to have implications for 2D and 3D atomic memories.

[1] N. Radwell, M. A. Boukhet and S. Franke-Arnold, Opt. Express **21**, 22215-22220 (2013).

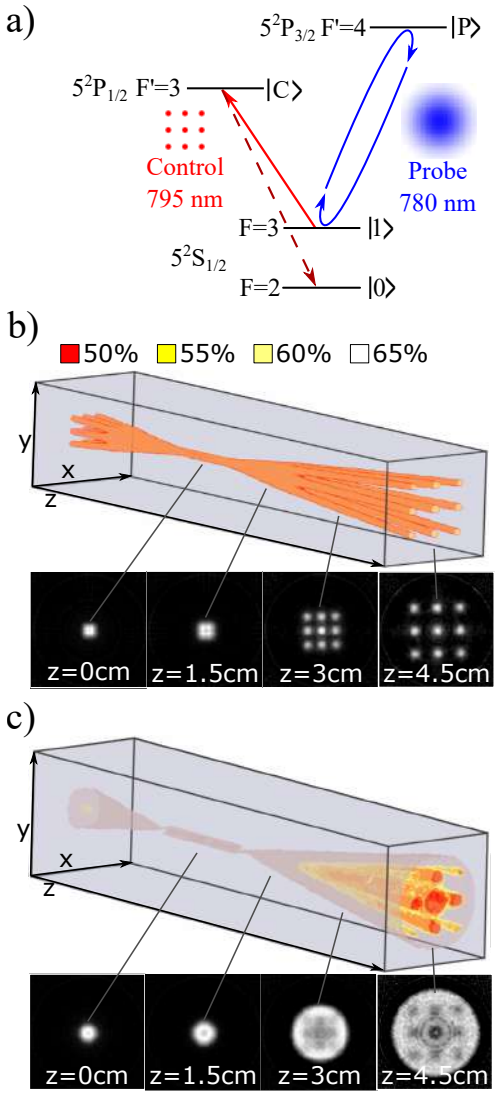


Figure 1: a) Level scheme used in the experiments showing spectroscopic notation, and b) sample reconstructed control beam and c) probe fluorescence visualised as isosurfaces drawn at the indicated fractions of peak intensity. Insets show sample cross-sections.

Phonons dispersion curves of dielectric materials.

S. Talbaoui, E. Baqloul, A. Laassouli, H. Grimech

Laboratory of Materials Physics, Faculty of Sciences and Technologies, Sultan Moulay Slimane University, Beni Mellal, Morocco

Abstract

In this paper we present a theoretical study based on the vibrational properties of crystal lattices; such as diamond, silicon and germanium. A detailed calculation has been made to determine the dynamic matrices of these lattices. The phonon dispersion curves presented in this work concern the acoustic and optical modes propagating in the ΓX, ΓK and ΓL directions of the Brillouin zone (3D). In order to determine these dispersion curves we used the Born-von Karman model with the approximation of the central forces between the first and second neighbors. The radial and angular force constants were determined by fitting on experimental data using the generalised least squares method. This approach allows to determine the interaction parameters and the vibrational properties for each of the materials studied.

Keywords : ***phonons, force constants, dispersion curves, vibrational properties***

Courbes de dispersion des phonons de matériaux diélectriques

Résumé

On présente une étude théorique sur les propriétés vibrationnelles des réseaux cristallins de diamant, de silicium et de germanium. Un calcul détaillé a été effectué pour déterminer les matrices dynamiques de ces réseaux. Les courbes de dispersion des phonons présentées dans ce travail concernent les modes acoustiques et optiques se propageant dans les directions ΓX, ΓK et ΓL de la zone de Brillouin (3D). Pour déterminer ces relations de dispersion, on a utilisé le modèle Born-von Karman avec l'approximation des forces centrales entre les atomes premiers et seconds voisins. Les constantes de force radiales et angulaires ont été déterminées par ajustement sur des données expérimentales en utilisant la méthode des moindres carrées. Cette démarche permet de déterminer les paramètres d'interaction et les propriétés vibrationnelles pour chacun des matériaux étudiés.

Mots clés : *phonons, constantes de force, courbes de dispersion, propriétés vibrationnelles*

Realization of a T^3 Matter-Wave Interferometer on an Atom Chip

O. Amit[1], Y. Margalit[1], O. Dobkowski[1], Z. Zhou[1], Y. Japha[1], M. Zimmermann[2], M. A. Efremov[2], F. A. Narducci[3], E. M. Rasel[4], W. P. Schleich[2] and R. Folman[1]

[1] *Department of Physics, Ben-Gurion University, Be'er Sheva, Israel*

[2] *Institut für Quantenphysik and Center for Integrated Quantum Science and Technology (IQST), Universität Ulm, Ulm, Germany*

[3] *Department of Physics, Naval Postgraduate School, Monterey, USA*

[4] *Institut für Quantenoptik, Leibniz Universität Hannover, Hannover, Germany*

e-mail: *oamitt@gmail.com*

Already in the early years of quantum mechanics, Kennard [1, 2] showed that the wave function of a particle of mass m exposed for a time T to a constant linear potential with the force F accumulates a phase scaling as F^2T^3/m. Being position-independent, this phase does not contribute to the phase shift (proportional to FT^2/m) of a conventional matter-wave interferometer used to measure a constant acceleration. More recently, several theoretical and experimental works [3, 4, 5] have discussed this cubic phase in the context of an interferometer.

We present here our own unique realization of a T^3 matter-wave interferometer based on a Bose-Einstein Condensate (BEC) near an atom chip and utilizing the Stern-Gerlach effect in order to create a state-dependent force.

[1] E. H. Kennard, Zeitschrift für Physik **44**, 326 (1927).

[2] E. H. Kennard, Jour. Frank. Inst. **207**, 47 (1929).

[3] F. Fratini and L. Safari, Physica Scripta **89**, 085004 (2014).

[4] G. D. McDonald, C. C. N. Kuhn, S. Bennetts, J. E. Debs, K. S. Hardman, J. D. Close, and N. P. Robins, EPL **105**, 63001 (2014).

[5] M. Zimmermann, M. A. Efremov, A. Roura, W. P. Schleich, S. A. DeSavage, J. P. Davis, A. Srinivasan, F. A. Narducci, S. A. Werner, and E. M. Rasel, Appl. Phys. B **123**, 102 (2017).

Interacting bosonic atoms in triangular lattices with varying geometry

Dan M. Stamper-Kurn[1,2], **Thomas Barter**[1], **Tsz-Him (Zephy) Leung**[1], **Masayuki Okano**[1], **and Claire Thomas**[1]

[1] *Department of Physics, University of California, Berkeley, CA 94720, USA*

[2] *Materials Sciences Division, Lawrence Berkeley National Laboratory, Berkeley, CA 94720, USA*

e-mail: *dmsk@berkeley.edu*

Interacting ultracold atoms in optical lattice potentials offer a means to study fundamental ideas emerging from condensed-matter physics in an idealized experimental form. To realize this scientific potential, we have developed means to characterize precisely and to drastically vary the geometry of optical lattice potentials.

This poster presents four main results. First, we present our method for producing two-dimensional non-bravais triangular lattices by overlaying lattices formed with light of two commensurate wavelengths [1]. By controlling the relative position of the two lattices, and also the polarization of the lattice light, we realize a number of interesting lattice geometries. Three particular lattice geometries are highlighted: the kagome lattice, the trimerized kagome lattice and the hexamerized honeycomb lattice.

Second, we demonstrate how the diffraction of matter waves exposed to an optical lattice potential can be regarded as a form of crystallography that provides detailed information on the lattice structure. In particular, we illustrate how slight departures from spatial inversion symmetry can yield robust signatures in the matter-wave diffraction pattern [3].

Third, we present a quantitative test of the predictions of the Bose-Hubbard model by quantum simulation with ultracold atoms. While Bose-Hubbard systems have been studied experimentally with cold atoms for more than a decade, one finds that quantitative comparisons between experiment and theory have achieved only moderate precision (by the standards of atomic physics) owing to the spatial inhomogeneity and the uncertain temperature of the gases used in experiment. We identify a specific prediction for Bose-Hubbard systems that can be tested with high precision in spite of these otherwise limiting conditions. Specifically, we focus on a scaling hypothesis for the equation of state of Bose-Hubbard systems that applies equally to a variety of lattice geometries. By comparing the properties of gases loaded within the same experimental setup and into two different lattice geometries, specifically the two-dimensional triangular and the kagome geometries, this scaling hypothesis is tested quantitatively even with a non-zero-temperature and inhomogeneous gas. Somewhat surprisingly, we find the scaling hypothesis describes our data within the small (6%) uncertainty in our measurement [2].

Fourth, we present preliminary investigations of spatial correlations for strongly interacting bosons within a trimerized kagome lattice, a kagome-geometry lattice in which triangular plaquettes of one orientation have a much stronger tunneling energy (J) than those of the opposite orientation (J'). When a gas of bosons held in this lattice is driven to the strongly correlated regime, achieved by tuning the weak tunneling energy to be small compared to the onsite interaction, the nearest-neighbor spatial correlations in the lattice become strongly inversion asymmetric. These spatial correlations are measured by measuring and analyzing the momentum-space distribution of the gas. Their inversion asymmetry is measured interferometrically using a transient modification of the lattice potential.

[1] G.-B. Jo, J. Guzman, C.K. Thomas, P. Hosur, A. Vishwanath and D.M. Stamper-Kurn, Phys. Rev. Lett. **108**, 045305 (2012).

[2] C.K. Thomas, T.H. Barter, T.-H. Leung, M. Okano, G.-B. Jo, J. Guzman, I. Kimchi, A. Vishwanath and D.M. Stamper-Kurn, Phys. Rev. Lett. **119**, 100402 (2017).

[3] C.K. Thomas, T.H. Barter, T.-H. Leung, S. Daiss and D.M. Stamper-Kurn, Phys. Rev. A **93**, 063613 (2016).

Realization of a fractional period adiabatic superlattice

Dimitris Trypogeorgos[1], **R. P. Anderson**[2], **A. V. Curiel**[1], **Q.-Y. Liang**[1], **T. Andrijauskas**[3], **G. Juzeliūnas**[3], **and I. B. Spielman**[1]

[1] *Joint Quantum Institute, University of Maryland and National Institute of Standards and Technology, College Park, Maryland, 20742, USA*

[2] *School of Physics and Astronomy, Monash University, Melbourne, Victoria 3800, Australia*

[3] *Institute of Theoretical Physics and Astronomy, Vilnius University, Saulėtekio 3, LT-10222 Vilnius, Lithuania*

e-mail: *dtrypo@umd.edu*

We propose and realized a strongly sub-wavelength optical lattice for ultracold neutral atoms using N resonantly Raman-coupled internal atomic degrees of freedom. Although the Raman lasers had wavelength λ, the resultant lattice-period was $\lambda/2N$, a N-fold reduction as compared to the conventional $\lambda/2$ lattice period. We experimentally demonstrated this lattice using three hyperfine states in a ^{87}Rb Bose-Einstein condensate, and generated a lattice with a 132 nm period from $\lambda = 790$ nm lasers.

Our lattice derives from the N cyclically coupled internal atomic states labeled by $|n\rangle$ shown in Fig. 1. Two photon Raman transitions link consecutive states with matrix element $\Omega_n \exp(2ik_R\hat{x})\,|n+1\rangle\langle n|$, where $\hbar k_R = 2\pi\hbar/\lambda$ is the single photon recoil momentum from the underlying Raman lasers, counter propagating along $\mathbf{e}_x$. The resultant light-matter interaction term

$$\hat{V}(\hat{x}) = \sum_{n=1}^{N} \Omega_n e^{2ik_R\hat{x}}\,|n+1\rangle\langle n|$$

is manifestly invariant under spatial translations of $\delta x = m\lambda/2$. Remarkably this Hamiltonian is also invariant under sub-wavelength "translations" of $\delta x = m\lambda/2N$ implemented by $\hat{\mathcal{D}}(\delta x) = \hat{D}_x(\delta x)\hat{\Phi}(\delta x)$ that combines a spatial displacement from $\hat{D}_x(\delta x)$ and a spin-dependent phase shift from $\hat{\Phi}(\delta x) = \sum_n \exp(2ik_R n\delta x)\,|n\rangle\langle n|$. Transforming $\hat{V}(\hat{x})$ with $\hat{\Phi}(\hat{x})$ gives

$$\hat{V}'(\hat{x}) = \Omega_N e^{2Nik_R\hat{x}}\,|1\rangle\langle N| + \sum_{n=1}^{N-1} \Omega_n\,|n+1\rangle\langle n|$$

that explicitly exhibits the reduced unit cell. Because $\hat{\Phi}(\hat{x})$ depends on $\hat{x}$ this transformation also introduces a gauge term $\hat{A} = -2k_R\sum_n |n\rangle\langle n|$, similar to that appearing in 1D spin-orbit coupling experiments.

We change the period of the adiabatic lattice by coupling pairs of spin-states with an rf field instead of Raman. The rf field preserves the cyclical couplings but since it does not transfer any momentum, it leads to an increased lattice-period $\lambda/2(N-m)$, where m is the number of rf links. By linking a certain transition with both rf and Raman fields, we engineer subwavelength adiabatic superlattices, with two or three participating wavelengths.

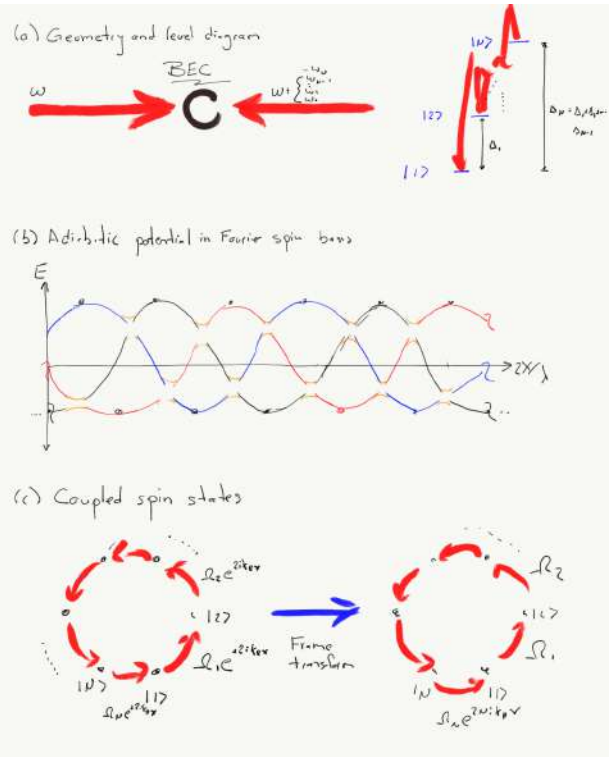


Figure 1: **a**. Experimental geometry showing a BEC illuminated by a pair of laser beams independently completing two photon Raman transitions between N internal states. The final "downgoing" transition requires an opposite detuning to provide the same momentum kicks as the "upgoing" transitions. **b**. Adiabatic potential computed for in the Fourier spin basis graphically illustrating the spatial subdivision of this lattice. **c**. Spin-state coupling diagram showing the laser induced phase factor associated with transitions between consecutively coupled states (left) and the coupling diagram following a spatial spin rotation with a single $\exp(2iNk_Rx)$ phase factor on a single link.

Optical visibility and core structure of vortex filaments in a three-dimensional bosonic superfluid

F. Dalfovo, R.N. Bisset, C. Mordini, G. Lamporesi, and G. Ferrari
INO–CNR BEC Center and Dipartimento di Fisica, Università di Trento, 38123 Trento, Italy
e-mail: *franco.dalfovo@unitn.it*

A rectilinear quantized vortex is a stationary solution of the Gross-Pitaevskii (GP) equation where all particles circulate with the same angular momentum $\hbar$ around a line where the density vanishes; the density recovers its asymptotic value n_0 over a length scale characterized by the healing length ξ, which is determined by n_0 and the strength of the interaction. Quantized vortices have been extensively studied in superfluid ^{4}He, which is a strongly correlated liquid; the core of the vortex in ^{4}He is only qualitatively captured by the GP equation and is inaccessible by experimental observation, the main reason being that the healing length in ^{4}He is of the same order as the atom size. Conversely, GP theory furnishes a very accurate description of dilute ultracold atomic gases in regimes of temperature and diluteness that are attainable in typical experiments with trapped Bose-Einstein condensates (BECs), where quantized vortices are routinely produced and observed with different techniques. However, no detailed quantitative comparison between theory and experiment for the structure of the vortex core in three-dimensional condensates has yet been performed, being strongly limited by effects of vortex bending and optical resolution.

In our experiments, we optically visualize the vortex filaments with enough accuracy to permit a direct comparison with the predictions of the GP theory. We produce large BECs of sodium atoms confined in a cigar-shaped harmonic magnetic trap and containing one or more vortices as a result of the Kibble-Zurek mechanism when cooling the gas across the BEC transition. The elongated shape of the condensate significantly reduces the bending of the vortex filaments, while at the same time keeping their local core structure three dimensional. Observations are performed by releasing the atoms from the trap and taking simultaneous absorption images of the full atomic distribution along the radial and axial directions after a long expansion in free space; a levitating magnetic field gradient prevents the BEC from falling. A vortex filament can be observed as a faint perturbation in the integrated density along the axial direction. By subtracting a fitted Thomas-Fermi profile we obtain the residual column density, from which we finally extract the shape, the width and the depth of the vortex.

We use the GP equation at zero temperature to simulate both the in-trap condensate with a vortex and its free expansion. The need to accurately describe the dynamics of the system on both the scale of the healing length and the scale of the width of the entire expanding condensate limits the simulations to condensates which are smaller than the experimental ones; however, in the Thomas-Fermi regime of our condensates, scaling laws can be safely used to interpolate between the GP results and the experimental conditions. We theoretically simulate and experimentally observe vortices in condensates with various atom numbers and we find that the observed shape of the vortex core in the residual column density after free expansion quantitatively agrees with the predictions of the Gross-Pitaevskii theory.

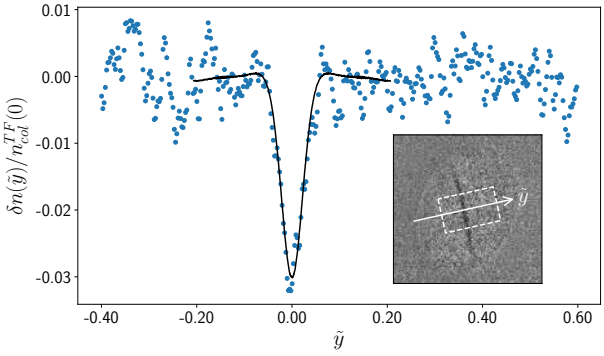


Figure 1: Example of residual column density after 150 ms of free expansion for a condensate with 2×10^7 sodium atoms containing a vortex. The inset shows the full residual column density in the y-z plane. The residual column density is averaged in the direction z, parallel to the vortex filament, within the rectangular box and the resulting values (blue points) are plotted in the main panel as a function of the rescaled coordinate $\tilde{y} = y/R_\perp$, where $R_\perp$ is the transverse Thomas-Fermi radius of the condensate. The solid line is the prediction of the Gross-Pitaevskii equation.

This work is dedicated to Lev P. Pitaevskii in celebration of his 85th birthday.

[1] F.Dalfovo, R.N.Bisset, C.Mordini, G.Lamporesi, and G.Ferrari, e-print arXiv:1804.03017.

Non-classical spin states with ultracold dysprosium atoms

T. Chalopin[1], **C. Bouazza**[1], **A. Evrard**[1], **V. Makhalov**[1], **D. Dreon**[1], **J. Dalibard**[1], **L. Sidorenkov**[1], **S. Nascimbène**[1]

[1] *Laboratoire Kastler Brossel, Collège de France, CNRS, ENS-PSL University, Sorbonne Université, 11 Place Marcelin Berthelot, 75005 Paris, France*

e-mail: *thomas.chalopin@lkb.ens.fr*

Non-classical spin states, such as spin squeezed states and quantum superpositions of coherent states with opposite magnetization (so-called cat states), are of great interest for modern quantum technologies, quantum metrology or quantum computing [1]. Cold atomic ensembles provide a sufficient degree of control and tunability for the realization of spin-squeezing, but the realization of mesoscopic superposition states remains challenging.

I will detail the latest experiments we have realized on our ultracold dysprosium gases experiment. We use non-linear light-spin interactions to coherently drive the large spin of bosonic dysprosium ($J = 8$ in the ground state) to a mesoscopic superposition of coherent spin-states with opposite magnetization, of the form

$$|\psi\rangle = \frac{|m_J = -J\rangle + |m_J = +J\rangle}{\sqrt{2}}.$$

The non-linear interactions stem from tensorial light-shifts induced by an off-resonant laser close to the narrow-line 626 nm transition [2].

We show that this superposition state provides a large sensitivity enhancement to external magnetic fields. We directly measure a quantum metrological gain (with respect to the standard quantum limit, achieved for a coherent spin-state) of $G = 13.9(11)$, close to the Heisenberg limit ($G = 16$ for $J = 8$). We also provide a full state tomography reconstruction (see figure 1) which shows strong non-classical features. We furthermore expose the intrinsic fragility of such a mesoscopic superposition by observing and characterizing its relatively fast (with respect to a coherent state) decoherence under environmental noise.

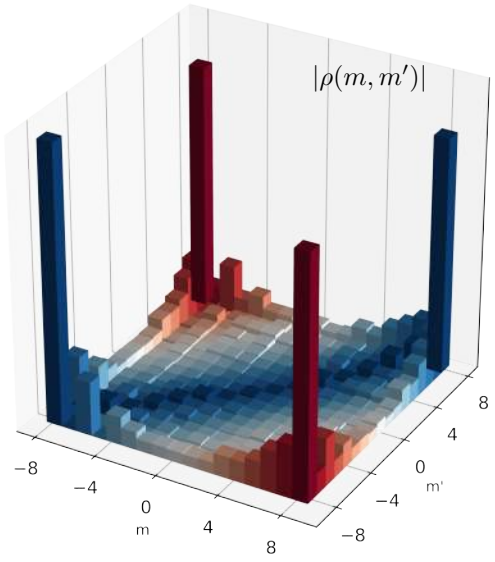


Figure 1: Density matrix corresponding to the realized mesoscopic superposition of opposite coherent spin-states, and reconstructed experimentally *via* full-state tomography. The color indicates the distance to the diagonal (populations in blue, coherences in red).

[1] L. Pezzè, A. Smerzi, M. K. Oberthaler, R. Schmied, and P. Treutlein, ArXiv:1609.01609 (2016).

[2] S. Chaudhury, S. Merkel, T. Herr, A. Silberfarb, I. H. Deutsch, and P. S. Jessen, Phys. Rev. Lett. **99**, 163002 (2007).

High Sensitivity Rf Spectroscopy of a Strongly-Interacting Fermi Gas

C. Shkedrov, Y. Florshaim, G. Ness, A. Gandman, Y. Sagi
Physics Department, Technion - Israel Institute of Technology, Haifa 32000, Israel
e-mail: *kostyas@technion.ac.il*

We report on a novel rf spectroscopy scheme with which we can detect very weak signals of only a few atoms [1]. We extend the experimentally accessible photon energies range by an order of magnitude compared to previous studies. Presented here are two main results: a universal power-law scaling of rf lineshape up to the interaction scale and a precision measurement of the binding energy of Feshbach molecules .

The experiment begins with preparing a quantum degenerate gas of ^{40}K atoms in a balanced mixture of the two lowest Zeeman sublevels. Rf pulse of frequency ν transfers a small fraction of the atoms from one of the states to a third Zeeman sublevel. By combining spin selection in a magntetic trap with a senstive fluorescence imaging in a magneto-optical trap, we measure the number of atoms in the third state. The result of this measurement is the rf transition rate $\Gamma(\nu)$, depicted in Fig. 1. Linear scaling shows that the data follows a power-law at high frequencies. The inset shows the power-law exponent extracted by fitting the tail of each dataset with c_1/ν^n. Our data shows that the universal power-law scaling resulting from contact-like interactions extends all the way up to the interaction scale in the vicinity of the Feshbach resonance for the two lowest states of ^{40}K.

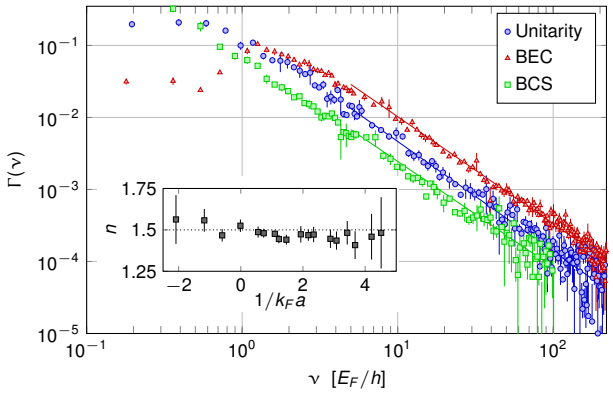


Figure 1: Rf lineshapes for three different interaction strengths in the BCS-BEC crossover: $1/k_F a = 0$ (unitarity), 0.49 (BEC) and -0.53 (BCS).

On the BEC side of the Feshbach resonance we measure the binding energy of a weakly bound Feshbach molecules which is related to the scattering length through $E_b = \frac{\hbar^2}{m(a-\bar{a})^2}$ (1), where $\bar{a}$ is a finite range correction constant [3]. This binding energy depends on a magnetic field through the scattering length $a(B) = a_{bg}\left(1 - \frac{\Delta B}{B-B_0}\right)$, with $a_{bg}, \Delta B, B_0$ the parameters of Feshbach resonance between the two lowest hyperfine levels of ^{40}K. We extract the binding energy from the position of the sharp rise in the molecular spectra, which marks the molecule dissociation threshold (inset of Fig. 2). Eq.(1) with the most recent calibration of the Feshbach resonance parameters given in Ref. [4] deviates from the data farther away from the resonance (dotted blue line). We fit our data with a two coupled channels calculation based on the model of Ref. [5] (solid red line) and extract a new calibration for the Feshbach resonance parameters. Eq.(1) with the new calibration fits the data well (dashed black line). Our new calibration shifts B_0 and Δ slightly relative to their values in Ref. [4] and improves their accuracy by a factor of 2 and 3.3, respectively.

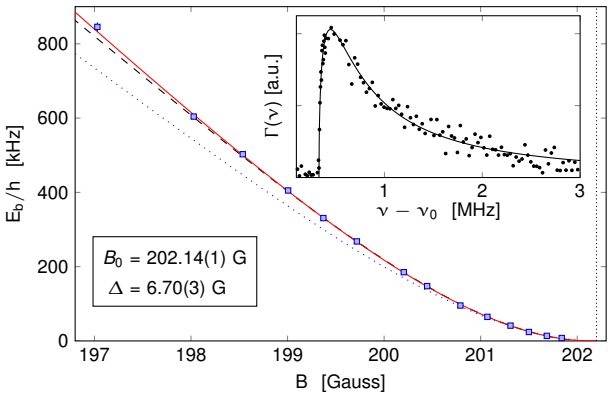


Figure 2: The binding energy (squares) of the Feshbach molecule at different magnetic fields close to the Feshbach resonance (dashed vertical line). Two coupled channel calculation (see text) is shown as solid red line. Eq.(1) is presented with previous (dotted blue line) and new (dashed black line) calibration. The inset shows a typical dataset from which we extract the binding energy.

[1] C. Shkedrov, Y. Florshaim, G. Ness, A. Gandman, and Y. Sagi, arXiv:1803.01770 (2018)

[2] W. Schneider and M. Randeria, Phys. Rev. A **81**, 021601 (2010)

[3] G. F. Gribakin and V. V. Flambaum, Phys. Rev. A **48**, 546 (1993)

[4] J. P. Gaebler, J. T. Stewart, T. E. Drake, D. S. Jin, A. Perali, P. Pieri, and G. C. Strinati, Nat. Phys. **6**, 569 (2010).

[5] M. H. Szymanska, K. Goral, T. Kohler, and K. Burnett, Phys. Rev. A **72**, 013610 (2005)

Experiment of Newton Cradle in One Dimensional Bose Gas

Xuzong Chen*
Chen Li, Tianwei Zhou, Qi Huang, Zijie Zhu, Wei Xiong and Xiaoji Zhou
School of Electronics Engineering and Computer Science, Peking University, Beijing 100871, China

Igor Mazets, Hans-Peter Stimming, Joerg Schmiedmayer**
Vienna Center for Quantum Science and Technology (VCQ), Atominstitut, TU-Wien, Stadionallee 2, 1020 Vienna, Austria

We study the dephasing and relaxation of 1D ultra-cold bosons in Newton Cradle scheme. In a setting similar to the Newton's cradle experiment by Kinoshita et al. [Nature 440, 900 (2006)] , the 1D Bose gases are excited in the longitude direction by coherent pulses, which stimulate the atoms to oscillate in the 1D gas tubes and to collide with each other. In principle, an integrable system, which is in a non-equilibrium state, will not thermalize over time. If the integrability is broken down, the time to reach thermal equilibrium is reduced. In the experiment, we demonstrated two case: (1) The initial energy of each atom is lower than the transverse excitation energy of the 1D system, it undergoes several hundred oscillation cycles to approach the thermalized state, which takes longer time than Kinoshita's experiment . (2) As the proportion of atoms in the transverse excitation state is higher than the transverse excitation energy of the 1D system, the integrability of the system is broke down, and the relaxation rate of the system is increased. These experimental results demonstrated integrability of 1D Bose gases and explain the reason the system will final reach the equilibrium. Detection were performed both in TOF and Band Mapping approaches.

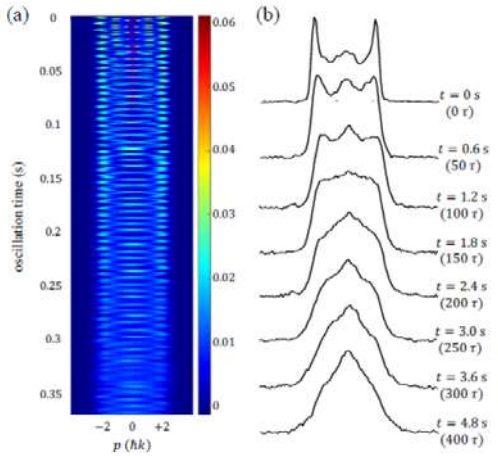


Fig1 Ocsillation of two clusts of BEC in 1D lattice (a) Evolution of the longitudinal momentum distribution of the atomic Newton's cradle in the first 30 periods (360ms) (b) Long time evolution of the period average momentum distribution.

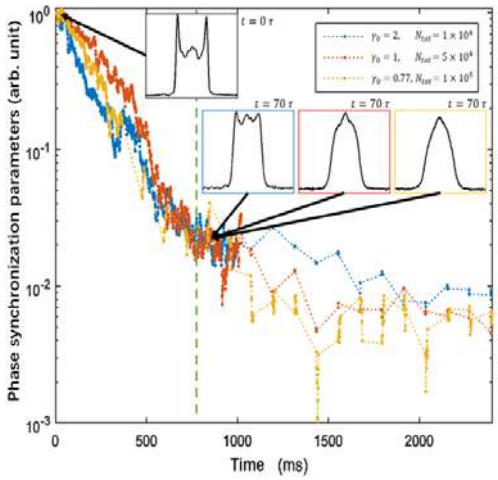


Fig2 Dephasing rate in the condition of only $\pm 2\hbar k$

Atom loading into a modulated optical dipole trap under Λ-enhanced gray molasses cooling

Min-Hsuan Wu[1,2], **Meng-Ju Tsai**[1,3], **and Ming-Shien Chang**[1,4,*]

[1] *Institut of Atomic and Molecular Sciences, Academia Sinica, 10617 Taipei, Taiwan*

[2] *Departament of Physics, National Taiwan University, 10617 Taipei, Taiwan*

[3] *Departament of Physics, National Taiwan Normal University, 11677 Taipei, Taiwan*

[4] *Departament of Physics, National Tsing Hua University, 30013 Hsinchu, Taiwan*

[*]e-mail: *msc@gate.sinica.edu.tw*

Optical dipole trap (ODT) is an essential and versatile tool for quantum gas production and quantum simulations. It, however, suffers small loading volume and shallow trap depth for direct loading laser cooled atoms, and sub-Doppler temperature is necessary. To improve laser cooling for ODT loading, we implemented Λ-enhanced gray molasses cooling of rubidium utilizing D_2 transition [1], and in free space we observed cooling down to 12 μK and phase space density raise by three-fold, compared with that achieved in temporal dark MOT. To further enhance loading into the ODT, we alternated gray molasses and optical trapping potential in time domain, and we observed increase of loading by 50%. We will report our most updated result and provide detailed understanding of our cooling and loading techniques.

This work has been supported by the MoST of Taiwan under Grant No. 106-2112-M-001-033-, and M.-H. Wu has been supported by the MoST-106-2813-C-001-009-M.

[1] Sara Rosi, Alessia Burchianti, Stefano Conclave, Devang S. Naik, Giacomo Roati, Chiara Fort & Francesco Minardi, Scientific Reports **8**, 1301 (2018).

Quantum reflection of ultracold atoms by a spherical surface

T. Yamaguchi[1], **R. Kanamoto**[1], **and D. Akamatsu**[2]
[1] *Department of Physics, Meiji University, Kawasaki, Kanagawa 214-8571, Japan*
[2] *National Institute of Advanced Industrial Science and Technology, Tsukuba, Ibaraki 305-8563, Japan*
e-mail: *kanamoto@meiji.ac.jp*

Determination of atom-surface interactions is crucial for building and control of nanoscale devices. Dispersion forces [1], such as the van der Waals (vdW) interaction and the Casimir-Polder (CP) interaction, have been calculated for various geometries and materials, and the precise measurements of these forces have made rapid progress in recent years [2].

Here we study the low-energy scattering of ultracold rubidium/cesium atoms by a dielectric nanosphere of silica glass levitated in a vacuum. It is well known that atoms moving toward a solid or a liquid surface firstly enter the region where the attractive interaction between the atoms and the surface is strong, and then inelastically collide with the surface. When the incident energy is sufficiently small, however, the wave character of atoms becomes significant and quantum effects manifest themselves, leading to a characteristic quantum phenomenon, called quantum reflection. Some of the atoms can be reflected in the "badlands" region and the other atoms that go through the badlands are accelerated by the interaction potential, and eventually adsorbed onto the surface [3].

In order to evaluate the elastic and absorption cross sections associated with these processes, we used the following expression for the atom-spherical surface interaction potential [4]

$$V_{\rm int}(r) = -\frac{\hbar^2}{2\mu}\left[\frac{r'^3}{\beta_3}v\left(\frac{r'}{L}\right)+\frac{r'^6}{\beta_6^4}v\left(\frac{r'}{L'}\right)\right]^{-1}\Bigg|_{r'=r-R},$$

where μ is the reduced mass, r the distance between the atom from the center of the sphere, R the radius of the sphere, and $r'=r-R$, respectively. The radius of the silica glass is set as $R=75$nm. The coefficients β_α ($\alpha=3,4,6,7$) are related to the vdW coefficients C_3, C_6 and the CP coefficients C_4, C_7 as $\beta_\alpha = \left(2\mu C_\alpha/\hbar^2\right)^{1/(\alpha-2)}$. The characteristic lengths are defined in terms of β_α as $L=\beta_4^2/\beta_3$, $L'=\beta_7^5/\beta_6^4$. The shape function $v(x)$ incorporates a geometry of the surface, and it asymptotically behaves as $v(x) \xrightarrow{x\ll 1} 1$, and $v(x) \xrightarrow{x\gg 1} x$. We evaluated the vdW and CP coefficients by using the one-oscillator model for the atomic polarizability, and the Lorentz model for the dielectric function of the sphere.

With the use of the potential $V_{\rm int}(r)$, we solved the radial Schroödinger equation for each partial wave to obtain the elastic cross section $\sigma_{\rm el}(k)$ and the absorption cross section $\sigma_{\rm abs}(k)$ for cesium and rubidium atoms,

$$\sigma_{\rm el}(k) = \sum_{l=0}^{\infty}\frac{(2l+1)\pi}{k^2}|1-S_l(k)|^2,$$
$$\sigma_{\rm abs}(k) = \sum_{l=0}^{\infty}\frac{(2l+1)\pi}{k^2}(1-|S_l(k)|^2),$$

where $S_l(k)$ are the diagonal elements of the S-matrix and k is the wavenumber of atoms. The lth partial-wave contributions for $\sigma_{\rm el}(k)$ and $\sigma_{\rm abs}(k)$ of cesium atoms are shown in Fig. 1 for $l=0,\ldots,8$.

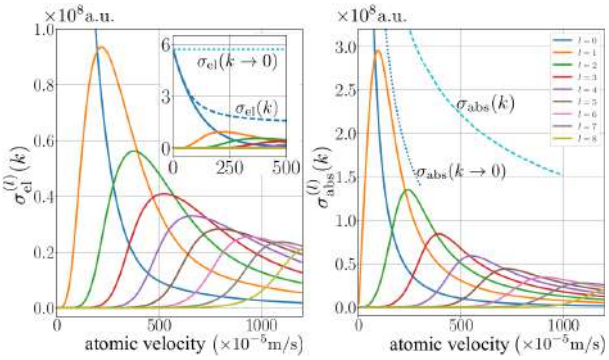


Figure 1: Partial wave contributions for the elastic (left panel) and absorption (right panel) cross sections $\sigma^{(l)}_{\rm el,abs}(k)$ of cesium atoms. The sum $\sigma_{\rm el,abs}(k)$ of them (dashed curves) and its threshold behavior $\sigma_{\rm el,abs}(k\to 0)$ (dotted curves) is also shown.

As future work, our results will be used for the experimental determination of the vdW and CP coefficients, as well as for the control of motional states of nanoparticle via atom-surface interaction.

References

[1] S.Y. Buhmann, *Dispersion Forces I* (Springer-Verlag, Berlin, 2012).

[2] For instance, P. Schneeweiss *et al.*, Nature Nanotech. **7**, 515 (2012); G. Winstone *et al.*, arXiv:1712.01426.

[3] H. Friedrich, *Scattering Theory* (Springer-Verlag, Berlin, 2012).

[4] F. Arnecke, H. Friedrich, and J. Madroñero, Phys. Rev. A **75**, 042903 (2007).

Roton in a many-body dipolar system

R. Ołdziejewski[1], **W. Górecki**[1], **K. Pawłowski**[1] **and K. Rzążewski**[1]

[1] *Center for Theoretical Physics, Polish Academy of Sciences - Al. Lotników 32/46, 02-668 Warsaw, Poland*

e-mail: *rafal@cft.edu.pl*

The roton quasiparticle is an object of interest of both theoretical and experimental physicists since early 40th when L. Landau introduced peculiar dispersion relation for excitations in Helium-II to explain the phenomenon of superfluidity. This topic has been broadly discussed, especially within the Bogoliubov approximation. However, the roton state has never been found as the exact solution of the many-body Hamiltonian in ultracold atom systems.

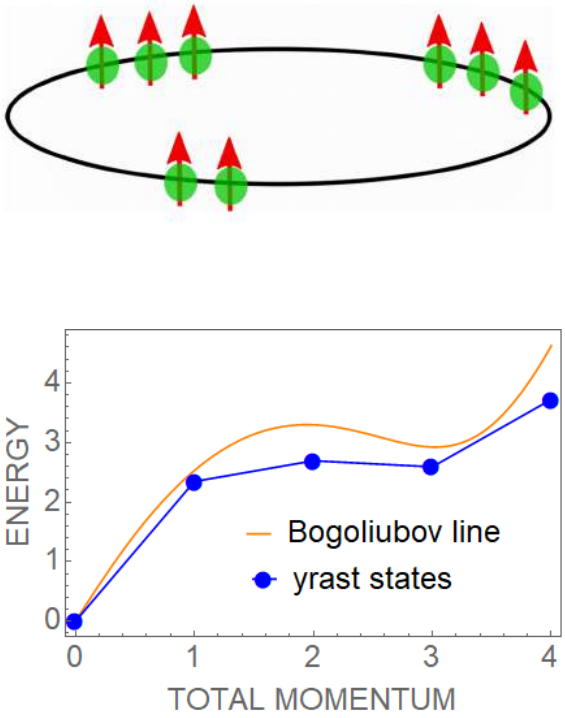


Figure 1: Upper panel: artist's view of the system of many dipolar atoms on the ring. Bottom panel: the dispersion relation for excitations is presented. The result of numerical calculations is compared with the Bogoliubov approximation.

In our work [1] we solve numerically exactly the many-body 1D model of atoms interacting via short-range attractive and long-range repulsive dipole-dipole forces. Periodic boundary conditions imply the conservation of total momentum. We find that the so-called yrast states, i.e. the lowest energy states with the fixed total momentum, may contain elementary excitations known from the Bogoliubov approximation. In particular, we identify the celebrated roton state. Moreover, with our methods, we go to stronger interactions, beyond the validity of Bogoliubov approximation. We also discuss a possibility of verifying our results by an experiment with dysprosium atoms. Especially, we observe that for the roton state the second order correlation function g_2 exhibits enhanced regular modulation.

References

[1] R. Ołdziejewski, W. Górecki, K. Pawłowski, K. Rzążewski, *arXiv:1801.06586* (2018).

Particle-Hole Character of Higgs and Goldstone Modes in Strongly Interacting Lattice Bosons

M. Di Liberto[1,2], **A. Recati**[1,3], **N. Trivedi**[4], **I. Carusotto**[1] **and C. Menotti**[1]

[1] *INO-CNR BEC Center and Dipartimento di Fisica, Università di Trento, 38123 Povo, Italy*

[2] *Center for Nonlinear Phenomena and Complex Systems, Université Libre de Bruxelles, CP 231, Campus Plaine, B-1050 Brussels, Belgium*

[3] *Arnold Sommerfeld Center for Theoretical Physics, Ludwig-Maximilians-Universität München, 80333 München, Germany*

[4] *Department of Physics, The Ohio State University, Columbus, OH 43210, USA*

e-mail: *mar.diliberto@gmail.com*

We study the low-energy excitations of the Bose-Hubbard model in the strongly-interacting superfluid phase using a Gutzwiller approach. We extract the single-particle and single-hole excitation amplitudes for each mode and report emergent mode-dependent particle-hole symmetry on specific arc-shaped lines in the phase diagram connecting the well-known Lorentz-invariant limits of the Bose-Hubbard model. By tracking the in-phase particle-hole symmetric oscillations of the order parameter, we provide an answer to the long-standing question about the fate of the pure amplitude Higgs mode away from the integer-density critical point. Furthermore, we point out that out-of-phase symmetric oscillations in the gapless Goldstone mode are responsible for a full suppression of the condensate density oscillations. Possible detection protocols are also discussed.

References

[1] M. Di Liberto, A. Recati, N. Trivedi, I. Carusotto, C. Menotti, Phys. Rev. Lett. **120**, 073201 (2018)

Fast rotating Bose gases in RF adiabatic potentials

M. de Goër de Herve, A. Kumar, Y. Guo, R. Dubessy, T. Badr, L. Longchambon, A. Perrin and H. Perrin

Laboratoire de Physique des Lasers, CNRS and Université Paris 13, Sorbonne Paris Cité, 93430 Villetaneuse, France

e-mail: *mathieu.degoerdeherve@univ-paris13.fr*

We study a Bose-condensed gas of ^{87}Rb atoms rotating in a highly oblate trap. The confinement is generated by RF-dressed adiabatic potentials [1], for which the atoms are placed at the surface of an ellipsoid. Around the potential minimum, located at the bottom of the ellipsoid, the trapping is approximately harmonic, but the bubble shape of the trap also generates higher order confinement, allowing to rotate the atoms at the trapping frequency and beyond while keeping them confined.

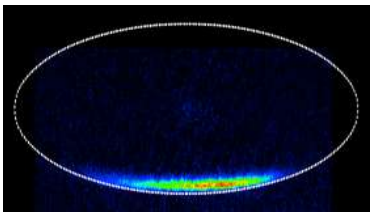


Figure 1: Atoms in a RF-dressed trap seen from the side; they are confined at the surface of an ellipsoid and attracted to its bottom due to gravity.

The rotation of a superfluid, due to its irrotational character, happens through the introduction of quantized vortices within the system. For small rotation rates, the vortices arrange in a triangular "Abrikosov" lattice [2]. Studying the regime of large rotation frequencies presents a fundamental interest; for example highly correlated states are predicted to appear for very fast rotation [3]. However, this regime has only been sparsely studied experimentally [4, 5].

In our experiment, we create an anisotropy in the radial potential that we rotate for a given time and frequency; we then go back to a rotationally invariant trap and let the atoms relax. We perform this experiment for various rotation frequencies Ω. The cloud radius increases with Ω, because the confinement is weakened: the radial potential, in the rotating frame, becomes:

$$V_{\mathrm{rot}}(r) = \frac{1}{2}M(\omega_{\mathrm{trap}}^2 - \Omega^2)r^2 + \alpha r^4 + ... \qquad (1)$$

We also see, after a time-of-flight expansion, the vortex lattice structure getting more and more distorted, which we analyze using Fourier transform and spatial autocorrelation of our data.

If we increase the rotation frequency up to and beyond the trapping frequency, the harmonic confinement vanishes in the rotating frame and even becomes repulsive. However, the higher order terms still keep the atoms trapped, similarly to [4]. The effective potential felt by the atoms then takes the shape of a mexican hat, and we end up with a stable, long-lived ring-shaped gas.

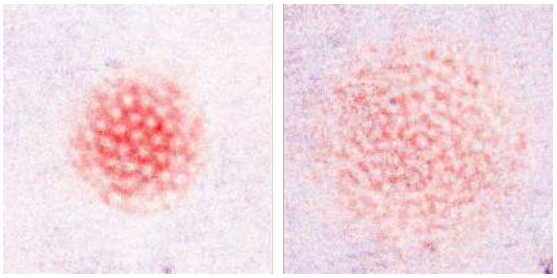


Figure 2: Time-of-flight picture of atoms rotating at the bottom of the ellipsoid, at around 26 Hz (left) and 32 Hz (right), for a trapping frequency of 34.1 Hz. On the right hand image, the vortices can still be clearly distinguished, but the lattice structure is highly disordered.

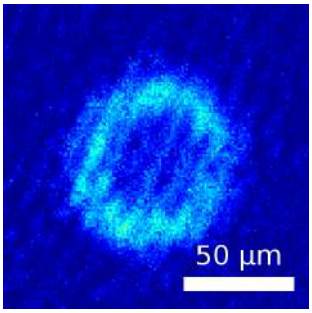


Figure 3: In situ picture of a fast rotating gas at the bottom of the RF-dressed trap, 30 s after excitation.

[1] K. Merloti *et al.*, New J. Phys. **15**, 033007 (2013).

[2] K.W. Madison *et al.*, Phys. Rev. Lett. **84**, 806 (2000).

[3] B. Paredes *et al.*, Phys. Rev. Lett. **87**, 010402 (2001).

[4] V. Bretin *et al.*, Phys. Rev. Lett. **92**, 050403 (2004).

[5] V.Schweikhard *et al.*, Phys. Rev. Lett. **92**, 040404 (2004).

Resummation of diagrammatic series with zero convergence radius for the unitary Fermi gas

R. Rossi[1], T. Ohgoe[2], K. Van Houcke[3] and F. Werner[4]

[1] *Center for Computational Quantum Physics, Flatiron Institute, 162 Fifth Avenue, New York, USA*

[2] *Department of Applied Physics, University of Tokyo, 7-3-1 Hongo, Bunkyo-ku, Tokyo, Japan*

[3] *Laboratoire de Physique Statistique, Ecole Normale Supérieure - Université PSL, CNRS, Sorbonne Université, Université Paris Diderot, Paris, France*

[4] *Laboratoire Kastler Brossel, Ecole Normale Supérieure - Université PSL, CNRS, Sorbonne Université, Collège de France, Paris, France*

e-mail: *ohgoe@solis.t.u-tokyo.ac.jp*

Feynman diagrams are powerful tools for studying various fields of physics. Still, the analysis usually involves some approximations, because some types of diagrams are neglected or only low-order diagrams are considered. However, the Monte Carlo method for unbiased sampling of Feynman diagrams has been recently developed[1, 2]. The method is called diagrammatic Monte Carlo method and it is one of the promising candidates for making predictions of various branches of many-body physics with high precision. On the other hand, the diagrammatic series sometimes have zero radius of convergence. The question is whether it is still possible to make accurate predictions by summing up Feynman diagrams.

In this work, we report high-precision results obtained by summing up Feynman-diagram series for a strongly-correlated continuous-space fermionic theory with zero convergence radius[3]. Specifically, we consider the unitary Fermi gas which is relevant to neutron matter as well as ultracold atom experiments. We first derived the large-order asymptotic behavior of the diagrammatic series. It was derived from a saddle point of a purely bosonic functinonal integral which was obtained by appling the Hubbard-Stratonovich transformation and then integrating out the fermionic degrees-of-freedom[4, 5]. As a result, we found out that it behaves as $a_N \sim (N/5)!A^{-N}\cos(4\pi N/5)$ for $N \to \infty$, where a_N is the sum of connected diagrams of order N. This immediately means that the radius of convergence is zero.

To properly resum the series with zero convergence of radius, we designed a conformal-Borel transformation that incorporates the large-order behavior and the knowledge of the analytical structure standing behind the series. Combining this new resummation method with diagrammatic Monte Carlo evaluation up to order 9, we obtain new results for the equation of state. Our results agree with the ultracold-atom experimental data, except for the 4-th virial coefficient for which our data point to the theoretically conjectured value of [6] (shown in Fig. 1). We will also present new data for Tan's contact and the momentum distribution.

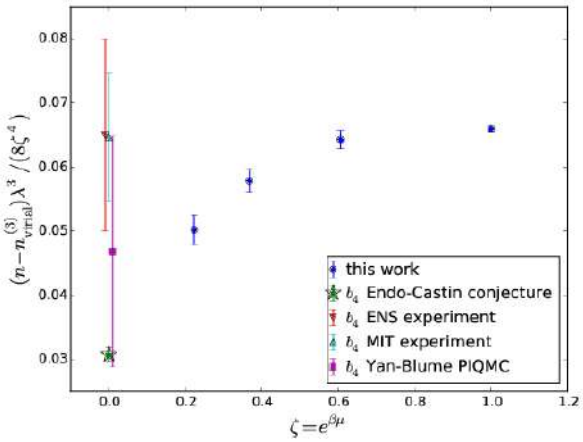


Figure 1: Equation of state and 4th virial coefficient: The difference between the density n and its 3rd order virial expansion $n^{(3)}_{\rm virial}$, divided by the appropriate factor, must tend to the 4th virial coefficient b_4 in the high-temperature limit $\zeta \to 0$

[1] K. Van Houcke, F. Werner, E. Kozik, N. Prokof ' ev, B. Svistunov, M. J. H. Ku, A. T. Sommer, L. W. Cheuk, A. Schirotzek, and M. W. Zwierlein, Nat. Phys. **8**, 366 (2012).

[2] R. Rossi, Phys. Rev. Lett. **119**, 045701 (2017).

[3] R. Rossi, T. Ohgoe, K. Van Houcke, F. Werner, arXiv:1802.07717.

[4] L. N. Lipatov, Zh. Eksp. Teor. Fiz. **72**, 411 (1977).

[5] G. Parisi, Phys. Lett. B **66**, 382 (1977).

[6] S. Endo and Y. Castin, J. Phys. A **49**, 265301 (2016).

Tunneling dynamics of a superfluid Bose-Fermi mixture in the Bose-Einstein-condensate-unitarity crossover

Zhenxia Niu[1], **Xiang Zhang**[2], **and Wei Zhang** [3]
[1] *Department of Physics, Renmin University of China, Beijing 100872, China*
e-mail: *niuzhx@ruc.edu.cn*

The tunneling dynamics of a superfluid Bose-Fermi mixture in BEC-unitarity crossover are numerically investigated by the mean-field method, where bosons confined in the double-well potential couple with fermions in a harmonic potential symmetrically positioned at the center of the double-well potential. We find that the coupling of the boson-boson, boson-dimer, and dimer-dimer interactions and the initial condition of population imbalance and relative phase determine together tunneling behaviors of bosons in this system. For weak boson-boson interaction, the boson-dimer interaction seems to induce a π phase difference to bosons in two wells and gives rise to the like-π-mode macroscopic quantum self-trapping (MQST). Moreover, the MQST for relatively small population imbalance can been realized through the boson-dimer and dimer-dimer interactions suppressing tunneling of bosons. While the relatively strong boson-boson interaction will dominate bosons to tunnel or be trapped whether the boson-dimer and dimer-dimer interactions are weak or strong.

Laser Cooling at Resonance

Y. Yudkin and L. Khaykovich
Department of Physics and QUEST Center, Bar-Ilan University, 5290002 Ramat Gan, Israel
e-mail: *yaakov.yudkin@gmail.com*

We show experimentally that 3-D laser cooling of lithium (^{7}Li) atoms on the D_2-line is possible when the laser light is tuned exactly to resonance with the dominant atomic transition (see black dots in Fig. 1). Since this contradicts the prediction of two-level atom Doppler cooling (blue dashed line) we build a more complex theoretical model to explain the phenomenon (orange region).

In order to verify the experimental observation the resonance position of the pump laser was determined with high precision as shown in Fig 2. In addition, the laser frequency stability was enhanced to ~ 60 kHz ($\sim 0.01\ \Gamma$, where Γ is the line width of the excited state) by locking the laser via the current that runs the lasing diode. All in all the experimental error in the frequency determination is estimated $\leq 0.05\ \Gamma$, which is the horizontal errorbar used in Fig. 1.

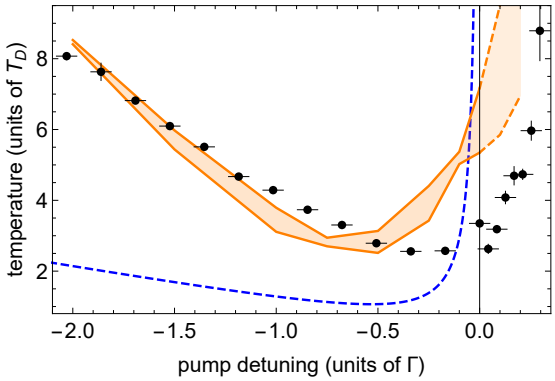


Figure 1: Plot of the temperature as a function of the pump laser detuning. The experimental results are compared to the standard two-level Doppler theory (blue dashed) and to the 24 level + polarization model (orange region) calculated in this work.

Qualitatively, the phenomenon of cooling at resonance can be understood by applying simple Doppler cooling arguments to the specific hyper-fine structure of the excited state of ^{7}Li which is both dense and inverted. However, to build a quantitative theory (orange region in Fig. 1) we must resolve to a full model which takes into account both the entire atomic structure of all 24 Zeeman sub-levels and the laser light polarization ($\sigma^+ - \sigma^-$). A careful analysis of the force and diffusion coefficient profiles shows that the fact, that the sub-Doppler cooling mechanism fails to work in ^{7}Li enhances Doppler cooling not only at resonance but also for large and negative detuning. Moreover, by means of Monte-Carlo simulations we show that coherent processes play an important role in showing consistency between the theory and the experimental results.

Cooling at resonance realizes a perfect combination of maximal photon scattering rate with effective cooling conditions. This can be directly applied in accurate atom counting experiments with single atom resolution [1] which would clearly benefit from this favorable combination.

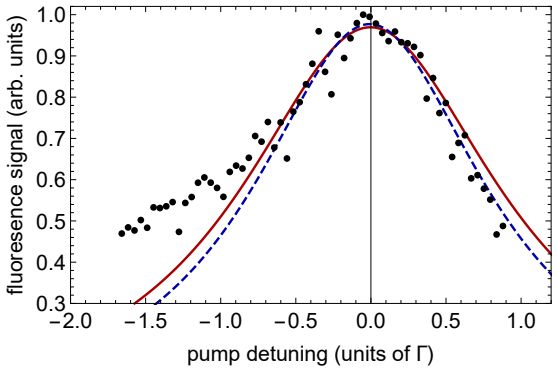


Figure 2: Fluorescence signal used to experimentally locate the position of the resonance. Due to the hyper-fine splitting of the excited state, the data is not symmetric it cannot be fitted to a Lorentzian on the entire range. We use only the central points and find a very low dependence of the position of the resonance on the range chosen. The red solid line is the fit to 21 central points while the blue dashed line uses 31 points. The shift in position of the fit maximum defines the uncertainty in resonance position.

This joint experimental and theoretical work was pulbished recently [2].

[1] D. B. Hume, I. Stroescu, M. Joos, W. Muessel, H. Strobel and M. K. Oberthaler, Phys. Rev. Lett. **111**, 253001 (2013).

[2] Y. Yudkin and L. Khaykovich, Phys. Rev. A **97**, 053403 (2018).

Quantum dark solitons in 1D quantum gases

J. Brand[1], **and S. S. Shamailov**[1,2]

[1] *New Zealand Institute for Advanced Study, Dodd-Walls Centre for Photonics and Quantum Technology, Centre for Theoretical Chemistry and Physics, Massey University, Private Bag 102904, North Shore, Auckland 0745, New Zealand*

[2] *Present address: Dodd-Walls Centre for Photonics and Quantum Technology, Department of Physics, University of Auckland, Private Bag 92019, Auckland, New Zealand*

e-mail: *j.brand@massey.ac.nz*

Dark and grey soliton-like states are shown to emerge from numerically constructed superpositions of translationally-invariant eigenstates of the interacting Bose gas in a toroidal trap. The exact quantum many-body dynamics reveals a density depression with superdiffusive spreading that is absent in the mean-field treatment of solitons (see Fig. 1). A simple theory based on finite-size bound states of holes with quantum-mechanical center-of-mass motion quantitatively explains the time-evolution of the superposition states and predicts quantum effects that could be observed in ultra-cold gas experiments. The soliton phase step is shown to be a key ingredient of an accurate finite size approximation, which enables us to compare the theory with numerical simulations. The fundamental soliton width, an invariant property of the quantum dark soliton, is shown to deviate from the Gross-Pitaevskii predictions in the interacting regime and vanishes in the Tonks-Girardeau limit.

In addition to the one-dimensional Bose gas in the Lieb-Liniger model [1], we also consider the one-dimensional Fermi gas with attractive delta-function interactions (Yang-Gaudin model) [2]. The corresponding Bethe-ansatz equations are solved for finite particle number and in the thermodynamic limit in order to obtain the *yrast* dispersion, i.e. the dispersion relation of the eigenstates of lowest energy for given momentum. Properties corresponding to the soliton-like nature of the yrast excitations are calculated including the missing particle number, phase step, and inertial and physical masses. The inertial to physical mass ratio, which is related to the frequency of oscillations in a trapped gas, is found to be unity in the limits of strong and weak attraction and fall to ≈ 0.78 in the crossover regime. This result is contrasted by one-dimensional mean field theory, which predicts a divergent mass ratio in the weakly attractive limit. By means of an exact mapping our results also predict the existence and properties of dark-soliton-like excitations in the super Tonks-Girardeau gas. The prospects for experimental observations are briefly discussed.

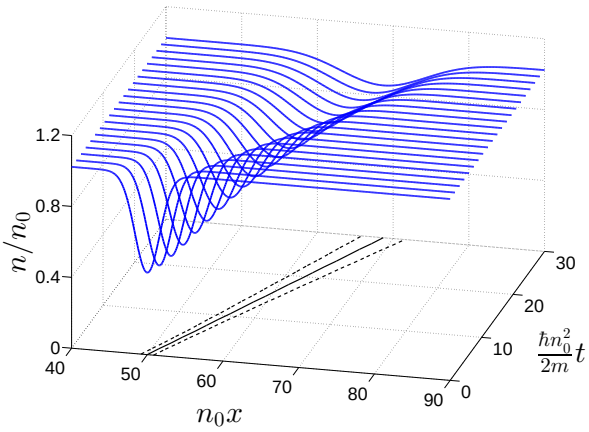


Figure 1: Time evolution of the quantum dark soliton constructed as a Gaussian superposition of yrast eigenstates of the Lieb-Liniger model with $N = 100$ particles at the intermediate interaction strength $\gamma = 1$, where $\gamma = c/n_0$ and $n_0 = N/L$. The superposition is prepared with $\Delta P = 2^{-3/2}\hbar n_0$ and $P_0 = 2\hbar n_0$. The solid line tracks the minimum of the dip and the dashed lines on either side of it are displaced by half of the soliton's width, i.e. by $\pm\Delta X/2$.

References

[1] Sophie S. Shamailov and Joachim Brand. Quantum dark solitons in the one-dimensional Bose gas. *arXiv:1805.07856*, 2018.

[2] Sophie S. Shamailov and Joachim Brand. Dark-soliton-like excitations in the Yang-Gaudin gas of attractively interacting fermions. *New J. Phys.*, 18(7):075004, jul 2016.

Excitation dynamics and dispersive shocks in spin-orbit-coupled Bose-Einstein condensates

Maren Mossman and Peter Engels
Department of Physics and Astronomy, Washington State University, Pullman, WA 99164
e-mail: *engels@wsu.edu*

Spin-orbit-coupled Bose-Einstein condensates (BEC) form a very rich framework for the investigation of quantum hydrodynamics. In the plane-wave phase, the single particle dispersion of a spin-orbit-coupled BEC features a region of negative effective mass, and the excitation spectrum can be either convex or concave depending on the direction of motion. We have developed a range of experimental tools to excite and probe dynamics from the linear to the nonlinear regime, and even in extreme regimes leading to dispersive shock waves. For example, by releasing a tightly confined BEC in the presence of a BEC background density, we can study the transition from sound to shock and show how the anisotropy of the spin-orbit coupling leads to strikingly different dispersive shock wave structures. As a second example, moving barriers can be used to effect spin flips with a spin-independent potential, leading to the concept of a unidirectional spin switch. The current status and future directions of this line of research will be discussed.

Staggered fluxes for Bose-Hubbard model in two leg ladder configuration

F. Metz[1], **R. Sachdeva**[1], **and T. Busch**[1]

[1] *Quantum Systems Unit, Okinawa Institute of Science and Technology Graduate University, Okinawa 904-0495, Japan*

e-mail: *friederike.metz@oist.jp*

We investigate the ground state properties of ultracold atoms trapped in a two leg ladder configuration in the presence of an artificial magnetic field in a staggered configuration. We focus on the strongly interacting regime, and using Landau theory of phase transitions in addition to mean field Gutzwiller variational method, we determine the stable superfluid phases in this system. We calculate the boundaries between the Mott-insulator and different superfluid phases as a function of magnetic flux and uncover regions of possibly new superfluid phases. In addition, we calculate the currents and momentum distribution of these superfluid phases, which clearly indicate the staggered vortex anti-vortex configuration per unit cell.

In the tight binding regime, neutral bosonic atoms confined in optical lattices are described by the single-band Bose-Hubbard model, which was already extensively analyzed and shown to give rise to two competing phases, the gapped Mott insulating phase and the compressible superfluid phase [1]. In recent years the influence of artificial gauge fields applied to these lattice systems has been progressively studied, which simulate the effect of an applied magnetic field on charged particles [2]. The case of a staggered magnetic flux in two-dimensional systems was studied as well, which, for certain flux strengths, gives rise to new superfluid phases with nontrivial momentum and current distributions [3].

As a next step we explore the effect of a staggered magnetic flux in one dimension only. Since at least two spatial degrees of freedom are needed to allow for a circular-like motion and therefore the potential creation of vortices, we restrict our system to a quasi-1D geometry of a ladder (see Fig. 1). The Bose-Hubbard Hamiltonian for a two-leg ladder with legs of the ladder denoted by a and b and with a staggered magnetic flux α (see Fig. 1) can be expressed by

$$H = -J\sum_j \left(e^{(-1)^j i\alpha}\hat{a}_j^\dagger \hat{a}_{j+1} + e^{(-1)^{j+1} i\alpha}\hat{b}_j^\dagger \hat{b}_{j+1} + h.c.\right)$$
$$-K\sum_j \left(\hat{a}_j^\dagger \hat{b}_j + h.c.\right) + \frac{U}{2}\sum_{j,p} \hat{n}_j^p\left(\hat{n}_j^p - 1\right) - \sum_{j,p}\mu\hat{n}_j^p.$$

The first term describes particles tunneling between different rungs of the lattice with strength J and an Aharonov-Bohm phase of $\pm\alpha$, with opposite signs for alternating lattice plaquettes. The second term refers to tunneling between the legs of the ladder with strength K, and the third term expresses the on-site interactions with a potential U.

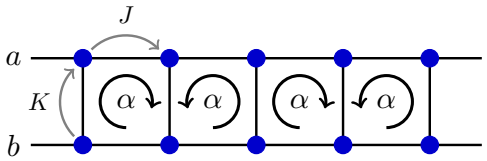


Figure 1: A two-leg ladder lattice subject to a staggered magnetic flux α.

We calculate the single-particle spectrum in the non-interacting limit which shows clear effects of the staggered flux. Next, we study the strongly interacting regime and use Landau theory to determine the different superfluid phases, which gives rise to the phase diagram shown in Fig. 2. The effect of the flux on the phase boundaries between the superfluid and the Mott-insulator is analyzed by performing a Gutzwiller variational method. Finally, the momentum and current distributions are computed to identify the distinct vortex configurations of the arising superfluids.

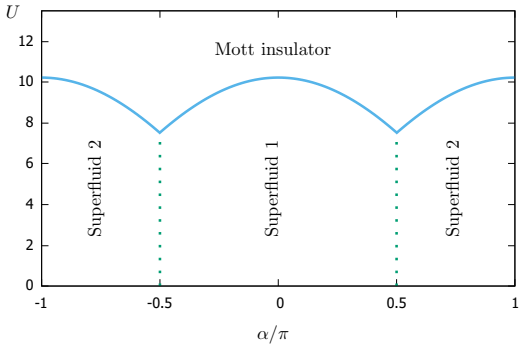


Figure 2: Critical interaction strength U plotted against flux α. The two superfluids are characterized by a staggered vortex anti-vortex configuration.

[1] M. Lewenstein, A. Sanpera, and V. Ahufinger, *Ultracold Atoms in Optical Lattices* (Oxford University Press, Oxford, 2012).

[2] N. Goldman, G. Juzeliūnas, P. Öhberg, and I. B. Spielman, Rep. Prog. Phys. **77**, 126401 (2014).

[3] L.-K. Lim, A. Hemmerich, and C. M. Smith, Phys. Rev. A **81**, 023404 (2010).

Light scattering by cold interacting two-level atoms

Ludovic Brossard[1], **Stephan Jennewein**[1], **Yvan R.P. Sortais**[1], **Patrick Cheinet**[2], **Pierre Pillet**[2], **Antoine Browaeys**[1]

[1] *Laboratoire Charles Fabry, Institut d'Optique, CNRS, Université Paris Sud, 2 Avenue Augustin Fresnel, 91127 Palaiseau cedex, France*

[2] *Laboratoire Aimé Cotton, CNRS, Université Paris Sud, Bât. 505 Campus d'Orsay, 91405 Orsay cedex, France*

e-mail: *ludovic.brossard@institutoptique.fr*

We study the problem of light scattering by a dense ensemble of cold atoms. When the medium is dense and the frequency of the light is tuned close to an atomic resonance, the light-induced dipoles interact. These resonant dipole-dipole interactions in turn modify the way the light is scattered. Besides being an interesting problem on its own, these studies are motivated by their potential applications. For example, these interactions may limit the accuracy of atomic based sensors (such as optical clocks).

We have shown recently that in the presence of these interactions, the *incoherent* response of a wavelength-sized and dense atomic cloud is no longer proportional to the number of atoms but is rather strongly suppressed [1]. The near-resonance *coherent* optical response of cold atomic gases is also modified by dipole-dipole interactions and has been at the focus of recent investigations by several groups including ours, both experimentally [2] [4] and theoretically [5] [6]. When comparing to the state-of-the-art coupled-dipole model, significant discrepancies between theory and experiment remain, possibly due to the multi-level structure of rubidium being improperly accounted for in the model.

This poster will present our latest measurement [3] of the coherent optical response of our microscopic dense ensemble but this time isolating a closed transition thanks to the application of a strong magnetic field. We thus realize a clean situation where the atoms are two-level systems. We developed a new model based on the Maxwell-Bloch equations which now shows good agreement with the data at low density and confirms the approach of the coupled-dipole model.

Nonetheless, significant deviations start to occur at higher density. This disagreement indicates that light scattering in dense, cold atomic ensembles is still not quantitatively understood, even in pristine experimental conditions. This conclusion motivated us to upgrade the experimental setup (Fig. 1). Indeed, as the collective response of a dense cold atomic cloud is supposed to depend dramatically on its geometry, we have added a second high resolution microscope axis in our setup, orthogonal to the first one. The goal of this second axis is to be able to control the geometry of our cloud by superimposing on it an interference pattern with adjustable interfrange distance, also called accordion [7]. In the medium-term, this feature, associated with spatial light modulator, will enable us to create arbitrary arrays of atoms and investigate experimentally strong-coupling between light and atoms as presented for example in [8]. This poster will present how we aligned and characterized the performance of these two confocal high resolution microscopes.

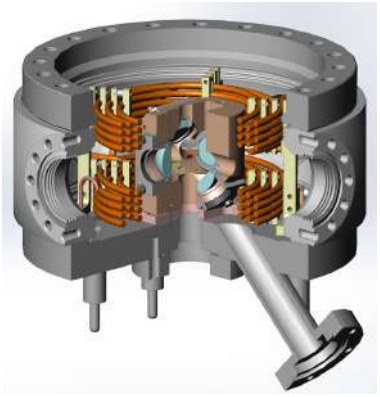


Figure 1: Three-dimensional view of the new vacuum chamber.

[1] J. Pellegrino *et al*, Phys. Rev. Lett. **113**, 133602 (2014).

[2] S. Jennewein *et al*, Phys. Rev. Lett. **116**, 233601 (2016).

[3] S. Jennewein *et al*, Phys. Rev. A **97**, 053816 (2018).

[4] L. Corman *et al*, Phys. Rev. A **96**, 053629 (2017).

[5] J. Javanainen, J Ruostekoski, Y. Li and S.-M. Yoo *et al*, Phys. Rev. Lett. **112**, 113603 (2014).

[6] J. Javanainen and J. Ruostekoski, Optics Express **24**, 993 (2016).

[7] J.L. Ville *et al*, Phys. Rev. A **95**, 013632 (2017).

[8] R.J. Bettles *et al*, Phys. Rev. Lett. **116**, 103602 (2016).

Droplet Phases in Dipolar and Rabi-Coupled Condensates

A. Cappellaro[1], **T. Macrì**[2], **F. Cinti**[3,4] **and L. Salasnich**[1,5]

[1] *Dipartimento di Fisica e Astronomia "G. Galilei" and CNISM, Universita' di Padova, via Marzolo 8, 35131 Padova, Italy*

[2] *Departamento de Fisica Teorica e Experimental, Universidade Federal do Rio Grande do Norte, and International Institute of Physics (IIP), 59078-970 Natal, Rio Grande do Norte, Brazil*

[3] *National Institute for Theoretical Physics (NITheP), Stellenbosch 7600, South Africa*

[4] *Institute of Theoretical Physics, Stellenbosch University, Stellenbosch 7600, South Africa* [5] *CNR-INO, via Nello Carrara, 150019 Sesto Fiorentino, Italy*

e-mail: *cappellaro@ipd.infn.it*

Droplets are very common in nature, from liquid water to superfluid Helium and nuclear matter. The structural properties of classical liquids can be understood by a thorough analysis of the inter-particles potential. The interplay between a repulsive core and a wider attractive tail plays a crucial role in determining the arising of self-bound states with a free surface. In 1995, Bose-Einstein condensation was experimentally achieved for the first time with ultracold alkali-atoms vapors. Since then, technical advances in magneto-optical trapping provided a wide variety of different quantum fluids [1] in extremely monitored environments.

We will discuss two examples of stable self-bound states arising in dipolar gases and Rabi-coupled BECs. Based on our Monte-Carlo calculations, we will provide the zero temperature phase diagram of dipolar bosons in free space [2], paying specific attention to the comparison with the experiments recently performed with Erbium and Dysprosium atoms [3]. Upon increasing the strength of the dipolar interaction, at sufficiently high densities, we find a wide region where filaments are stabilized along the direction of the external field. Most interestingly by computing the superfluid fraction we conclude that superfluidity is anisotropic and vanishes along the orthogonal plane. Based on Petrov proposal in collapsing bosonic mixtures [4, 5], this stabilization mechanism is enabled by the inclusion of quantum flucuations repulsive correction in the equation of state, balancing the attractive part of the dipole-dipole interaction.

In the second part we study the effects of quantum fluctuations on a Rabi-coupled binary Bose gas of interacting alkali atoms [6].

The divergent zero-point energy of gapless and gapped elementary excitations of the uniform system is properly regularized obtaining a meaningful analytical expression for the beyond-mean-field equation of state.

In the case of attractive inter-particle interaction we show that the quantum pressure arising from Gaussian fluctuations can prevent the collapse of the mixture with the creation of a self-bound droplet. We characterize the droplet phase and discover an energetic instability above a critical Rabi frequency provoking the evaporation of the droplet. We report the fact that droplet states have been recently observed in binary bosonic mixtures [7]. Implementing a coherent coupling between the components appears to be a natural extension of these experiments.

References

[1] F. Dalfovo, S. Giorgini, L. P. Pitaevskii and S. Stringari Rev. Mod. Phys. **71**, 463 (1999); I. Bloch, J. Dalibard and W. Zwerger, Rev. Mod. Phys. **80**, 885 (2008); J. Dalibard, F. Gerbier, G. Juliezunas and P. Ohberg, Rev. Mod. Phys. **83**, 1523 (2011).

[2] F. Cinti, A. Cappellaro, L. Salasnich and T. Macrì, Phys. Rev. Lett. **119**, 215302 (2017).

[3] H. Kadau, M. Schmitt, M. Wenzel, C. Wink, T. Maier, I. Ferrier-Barbut, and T. Pfau, Nature (London) **530**, 194 (2016); L. Chomaz, S. Baier, D. Petter, M. J. Mark, F. Wachtler, L. Santos, and F. Ferlaino, Phys. Rev. X **6**, 041039 (2016).

[4] D. S. Petrov, Phys. Rev. Lett. **115**, 155302 (2015).

[5] R. N. Bisset, R. M. Wilson, D. Baillie, and P. B. Blakie, Phys. Rev. A **94**, 033619 (2016).

[6] A. Cappellaro, T. T. Macrì, G. F. Bertacco and L. Salasnich, Sci. Rep. **7**, 13358 (2017).

[7] C. R. Cabrera et *al*, Science **106**, eaao5686-8 (2017); G. Semeghini et *al.*, arXiv:1710.10890v1 (2017).

Observation of the Higgs mode in a strongly interacting fermionic superfluid

M. Link[1], A. Behrle[1], T. Harrison[1], J. Kombe[2], K. Gao[1], J.-S. Bernier[2], C. Kollath[2] and M. Köhl[1]

[1] *Physikalisches Institut, University of Bonn, Wegelerstrasse 8, 53115 Bonn, Germany*
[2] *HISKP, University of Bonn, Nussallee 14-16, 53115 Bonn, Germany*
e-mail: *mlink@uni-bonn.de*

Higgs and Goldstone modes are possible collective modes of an order parameter upon spontaneously breaking a continuous symmetry. Whereas the low-energy Goldstone (phase) mode is always stable, additional symmetries are required to prevent the Higgs (amplitude) mode from rapidly decaying into low-energy excitations. In high-energy physics, where the Higgs boson has been found after a decades-long search, the stability is ensured by Lorentz invariance. In the realm of condensed-matter physics, particle-hole symmetry can play this role and a Higgs mode has been observed in weakly interacting superconductors. However, whether the Higgs mode is also stable for strongly correlated superconductors in which particle-hole symmetry is not precisely fulfilled or whether this mode becomes overdamped has been subject of numerous discussions. Experimental evidence is still lacking, in particular owing to the difficulty to excite the Higgs mode directly. Here, we observe the Higgs mode in a strongly-interacting superfluid Fermi gas. By inducing a periodic modulation of the amplitude of the superconducting order parameter Δ, we observe an excitation resonance at frequency $2\Delta/h$. For strong coupling, the peak width broadens and eventually the mode disappears when the Cooper pairs turn into tightly bound dimers signalling the eventual instability of the Higgs mode.

Local control of transport in an atomic quantum wire

P. Fabritius[1], **M. Lebrat**[1], **S. Häusler**[1], **D. Husmann**[1], **J.-P. Brantut**[2], **L. Corman**[1] **and T. Esslinger**[1]

[1] *Institute for Quantum Electronics, ETH Zürich, 8093, Switzerland*

[2] *Institute of Physics, École Polytechnique Fédérale de Lausanne, 1015 Lausanne, Switzerland*

e-mail: *philipfa@phys.ethz.ch*

We demonstrate the local control of fermionic lithium atoms flowing through a one-dimensional structure by imprinting holographically shaped optical potentials with a high-resolution microscope. In close analogy to the scanning gate technique applied to solid-state devices we image the transport through a quantum wire by scanning the position of a sharp, repulsive optical gate [1]. By measuring the variations in conductance we retrieve a high resolution map of transport with spatial resolution on the order of the Fermi wavelength in the channel. Imprinting more complex structures such as a series of indivually controlled barriers enables us to study the transport of neutral, fermionic atoms through a mesoscopic lattice. Building an increasingly longer lattice we observe the metal-insulator transition in a one-dimensional Fermi gas. We explore the influence of atom-atom interactions and find that the insulating state is robust when tuning the interactions from moderatley to strong attractive interactions, which supports the existence of a Luther-Emery liquid in the one-dimensional wire [2]. The flexibility of our setup makes it possible to project additional structures onto a wire or a quantum point contact. In particular close-to-resonance light which creates attractive or repulsive potentials depending on the internal state of the atoms can be holographically shaped and projected on the channel. Imprinting a single beam we observe a separation of the onset of conductance of the two spin states which corresponds to an effective magnetic field on the order of the Fermi temperature.

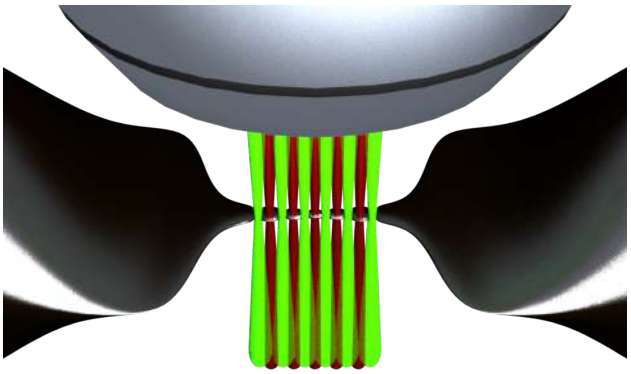


Figure 1: Sketch of one-dimensional lattices projected onto a quantum wire that connects two macroscopic atom reservoirs.

References

[1] S. Häusler, Shuta Nakajima, M. Lebrat, D. Husmann, Sebastian Krinner, J.-P. Brantut, and T. Esslinger, A scanning gate microscope for cold atomic gases, Phys. Rev. Lett. 119 030403 (2017)

[2] M. Lebrat, P. Grisins, D. Husmann, S. Häusler, L. Corman, T. Giamarchi, J.-P. Brantut, and T. Esslinger, Band and correlated insulators of cold fermions in a mesoscopic lattice, Phys. Rev. X. 8 011053 (2018)

Evolution of Few-Body Correlations in Bose Gases Quenched to Unitarity

S. Musolino[1], **V. E. Colussi**[1], **and S. J. J. M. F. Kokkelmans**[1]
[1] *Eindhoven University of Technology, P.O. Box 513, 5600 MB Eindhoven, The Netherlands*
e-mail: *s.musolino@tue.nl*

Recent experimental works [1, 2, 3, 4] highlight how signatures of few-body physics emerge in the observables of strongly-interacting atomic Bose gases. A critical challenge is to build up a theoretical model able to clarify how few-body physics evolves into the many-body problem [5]. In order to generalize many-body equations including few-body physics and finite-range potentials, we study the full-correlated (many-body) system in terms of cumulants [6]. A cumulant is a measure of a particular order of correlation in the system. These ideas are based on a successful model of the unitary Fermi gas, coined resonance superfluidity [7]. To compare directly theory and experiments, we mimic experimental magnetic-field sequences and simulate a quench from non-interacting regime to unitarity and vice versa, as illustrated in Fig. 1. We show how few-body phenomena, such as three-body recombination, influence the dynamics of few-body correlations.
Moreover, we consider the dependence of the observables on the rate of change of magnetic field (B) in time (t), that is $R = -dB/dt$. To do this, we analyze two different approaches. The total number of free atoms after a quench is reduced by the presence of compound molecules (in condensed-matter language, a sort of "Cooper pairs") or, in the other approach, dressed molecules [8], that are simultaneously in two different scattering channels. Importantly, the dressed-molecule equation of motion depends explicitly on R.
In conclusion, this work represents a basis for future studies of the three-body correlation function in a many-body context. This function contains the probability to find a three-body bound state, an Efimov state, in the presence of many particles.

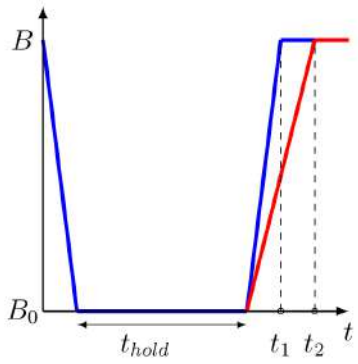


Figure 1: Schematic representation of experimental magnetic field (B) sequence as a function of time, t. First, the system is quenched to B_0, corresponding to unitarity, then it is held there for a t_{hold}, and finally ramped away from unitarity at a variable rate $R = -dB/dt$ (as represented by blue and red lines).

[1] P. Makotyn, C. E. Klauss, D. L. Goldberger, E. A. Cornell, and D. S. Jin, Nat. Phys. **10**, 116 (2014).

[2] R. J. Fletcher, R. Lopes, J. Man, N. Navon, R. P. Smith, M. W. Zwierlein, and Z. Hadzibabic, Science **355**, 377 (2017).

[3] C. E. Klauss, X. Xie, C. Lopez-Abadia, J. P. D'Incao, Z. Hadzibabic, D. S. Jin, and E. A. Cornell, Phys. Rev. Lett. **119**, 143401 (2017).

[4] C. Eigen, J. A. P. Glidden, R. Lopes, N. Navon, Z. Hadzibabic, and R. P. Smith, Phys. Rev. Lett. **119**, 250404 (2017).

[5] V.E. Colussi, S. Musolino, and S.J.J.M.F. Kokkelmans, arXiv:1805.06808 (2018).

[6] J. Fricke, Ann. Phys. (N.Y.) **252**, 479 (1996).

[7] S. J. J. M. F. Kokkelmans, J. N. Milstein, M. L. Chiofalo, R. Walser, and M. J. Holland, Phys. Rev. A **65**, 053617 (2002).

[8] R.A. Duine, and H.T.C. Stoof, Phys. Rev. A **68**, 013602 (2003).

Multi-second magnetic coherence in a single domain spinor Bose-Einstein condensate

Silvana Palacios[1], Pau Gomez[1], Simon Coop[1], Chiara Mazzinghi[1], Ferran Martin[1], Morgan Mitchell[1,2]

[1] *ICFO–Institut de Ciències Fotòniques, The Barcelona Institute of Science and Technology, 08860 Castelldefels, Spain*

[2] *ICREA–Institució Catalana de Recerca i Estudis Avançats, 08010 Barcelona, Spain* e-mail: *silvana.palacios@icfo.eu*

In ordinary spin systems, spin-destruction collision limit the coherence time of the system in general to the ms scale. In ultracold ensembles, these spin-spin interactions are fully coherent, and the relaxation time is expected to be unbounded. Here we show a polarized ferromagnetic single-domain spinor Bose-Einstein condensate (SD SBEC) exhibit no relaxation of the macroscopic spin state other than atoms losses [1]. To characterize the coherence properties, we use standard nomenclature: in a experiment with many spins (condensed or otherwise), the spin component along the field direction ($\mathbf{x}$), experiences the longitudinal relaxation time $\mathcal{T}_1$, defined by $\langle F_x\rangle \propto \exp[-t/\mathcal{T}_1]$. Similarly, the transverse components relax according to $\langle F_z\rangle \propto \exp[-t/\mathcal{T}_2^*]$ (and similar for $F_z \to F_y$, $\cos \to \sin$). $\mathcal{T}_2^*$ accounts for homogeneous effects, i.e., irreversible randomizations affecting all spins in the same way, and inhomogeneous effects, i.e., apparent randomization due to reversible effects such as differences in the local field. The lack of relaxation mechanisms in the SD SBEC implies $\mathcal{T}_2^* = \mathcal{T}_1$. There is another relaxation mechanism, loss of atoms, and this affects both F_x and $F_{y,z}$ in the same way, is truly irreversible, and affects all atoms in the same way. We assign the rate $1/\mathcal{T}_0$ to this loss of atoms: $N_A(t) \propto \exp[-t/\mathcal{T}_0]$.

We create SD SBECs with $N_A = 4\times10^4$ in a compact spherical trap of mean oscillation frequency 50 Hz. $\rho = 3\times10^{19}\,\mathrm{atoms/m^3}$. This system is well described by the single-mode approximation (SMA) provided the bias field is $B < 1\times10^{-4}\,\mathrm{T}$: the validity of the SMA depends on both, the spin interaction energy and the quadratic Zeeman energy, and is guaranteed when the condensate R is smaller than the bound $\lambda = h/\sqrt{2M(2|c_2|\rho+q)}$ [2], where ρ represents the mean density and for Rb^{87}, $M = 1.44\times10^{-25}\,\mathrm{kg}$, $c_2 = -2.39\times10^{-53}\,\mathrm{Jm^3}$ (spin-dependent interaction strength), and $q = (\gamma B)^2\hbar/\omega_{\mathrm{hf}}$ (quadratic Zeeman energy), $\omega_{\mathrm{hf}} = 2\pi\times6.83\,\mathrm{GHz}$ (hyperfine frequency splitting) and $\gamma = 2\pi(-7\,\mathrm{GHz/T})$ (gyromagnetic ratio). When the quadratic Zeeman energy dominates over the spin contact interaction energy, the SD SBEC is expected to follow a trivial precession about the magnetic field. We polarize the atoms in the $F = 1, m_F = 1$ state with a bias field $B = 29\,\mu\mathrm{T}$ defining the quantization axes along x. We then apply two MW pulses to prepare the state $(1,1,0)^T/\sqrt{2}$. Using non-destructive Faraday rotation probing we observe spin dynamics along z. The one-particle dynamics of this system is $f_z(t) = -\cos(\omega_L+\omega_Q)t/\sqrt{2}$. We observe the multi-particle system evolves as $N(t)[-\cos(\omega_L+\omega_Q)t/\sqrt{2}]$, as shown in Fig. 1 and therefore we associate $\mathcal{T}_2^* \equiv \mathcal{T}_0$. Using absorption imaging we have measured $N(t) = N_A\exp[-t/\mathcal{T}_0]$ with $\mathcal{T}_0 = 7.7\,\mathrm{s}$. This shows in our system only atom losses degrade the macroscopic spin polarization, giving a spin coherence time equal to the trap lifetime. At the used densities, the lifetime is set only by one-body losses. The trap lifetime time can in principle be extended with better vacuum conditions up to the three-body loss time $\approx 70\,\mathrm{s}$.

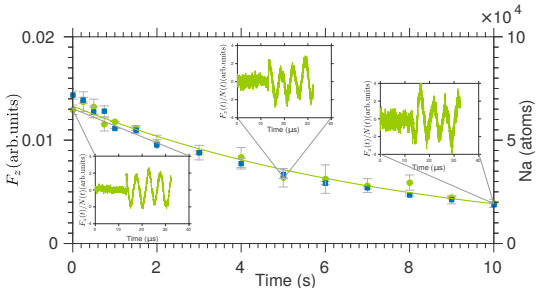


Figure 1: Amplitude of the Faraday signal $\propto F_z$ (circles, left axis) and N_A (squares, right axis) as a function of time. Insets: normalized Faraday signal $\propto F_z/N_A$ showing constant amplitude in time.

This result removes an important limitation of neutral atoms as decoherence is the most significant obstacle for applications in quantum information science. Demonstrating long coherence and scalability of the quantum system, would make the single domain SBEC interesting for long-lived entanglement or spin-squeezing. Additionally, one can profit from the small size of the condensate for applications such as high-resolution magnetic sensing.

[1] S. Palacios, S. Coop, P. Gomez, T. Vanderbruggen, N. Martinez de Escobar, M. Jasperse and M. W. Mitchell, New J. Phys. **20**, 053008 (2018).

[2] H. Mäkelä, M. Johansson, M. Zelan, and E. Lundh, Phys. Rev. A **84**, 043646 (2011).

Fermionic properties of two interacting bosons in a two-dimensional harmonic trap

P. Mujal[1,2], **A. Polls**[1,2], **and B. Juliá-Díaz**[1,2,3]

[1] *Departament de Física Quàntica i Astrofísica, Universitat de Barcelona, 08028 Barcelona, Spain*

[2] *Institut de Ciències del Cosmos (ICCUB), Universitat de Barcelona, Martí i Franquès 1, 08028 Barcelona, Spain*

[3] *Institut de Ciències Fotòniques, Parc Mediterrani de la Tecnologia, 08860 Castelldefels, Spain*

e-mail: *peremujal@fqa.ub.edu*

In one dimension, the Bose–Fermi mapping theorem [1] establishes that the systems of strong interacting bosons and noninteracting fermions, in the same trapping potential, have the same ground state energy. Furthermore, the ground state wave function of the strongly interacting bosonic system is obtained by symmetrizing the noninteracting fermionic one by taking the absolute value [1, 2].

In contrast, in two or more dimensions, the theorem does not apply. Only in one dimension the space is completely separated in two pieces by fixing the position of a particle [1]. However, the mechanism described by Girardeau whereby the particles can avoid feeling the interaction remains a possibility. The interaction induces correlations to the system of bosons in such a way that the probability of two particles being at the same position vanishes [3]. In this way, the expectation value of the interaction energy vanishes and then we say that the bosons avoid feeling the interaction, although it has a big effect on the system.

The system of two interacting identical bosons in a two-dimensional isotropic harmonic trap [4, 5] is described by the Hamiltonian [6, 7],

$$\mathcal{H} = \mathcal{H}_0 + V(|\vec{x}_2 - \vec{x}_1|), \tag{1}$$

where the noninteracting part of the Hamiltonian reads

$$\mathcal{H}_0 = \sum_{i=1}^{2} \left(-\frac{\hbar^2}{2m}\nabla_i^2 + \frac{1}{2}m\omega^2 \vec{x}_i^{\,2} \right), \tag{2}$$

and the interaction is modeled by means of a Gaussian-shaped potential,

$$V(\vec{x}_1, \vec{x}_2) = \frac{g}{\pi s^2} e^{-\frac{|\vec{x}_2 - \vec{x}_1|^2}{s^2}}. \tag{3}$$

The interaction strength is controlled by g, while s defines the interaction range. We always consider purely repulsive interactions, $g \geq 0$, and we concentrate on the dependence on both the strength g and the range s of the interaction.

We compare the numerical calculations for the ground state of two interacting bosons by exact diagonalization of the Hamiltonian with the properties obtained from the analytical wave functions that describe two noninteracting bosons,

$$\Psi_B(R, \varphi_R, r, \varphi_r) = \frac{1}{\pi} e^{-R^2 - \frac{r^2}{4}}, \tag{4}$$

two noninteracting fermions,

$$\Psi_F^{\pm}(R, \varphi_R, r, \varphi_r) = \frac{1}{\pi\sqrt{2}} e^{-R^2 - \frac{r^2}{4}} r e^{\pm i\varphi_r}, \tag{5}$$

and the corresponding symmetrized wave function,

$$\Psi_{|F|}(R, \varphi_R, r, \varphi_r) = \frac{1}{\pi\sqrt{2}} e^{-R^2 - \frac{r^2}{4}} r, \tag{6}$$

where $\vec{R} \equiv \frac{1}{2}(\vec{x}_1 + \vec{x}_2)$ is the center-of-mass coordinate, $\vec{r} \equiv \vec{x}_1 - \vec{x}_2$ is the relative coordinate and we have used harmonic oscillator units, i.e. the length in units of $\sqrt{\hbar/(m\omega)}$.

We show [7] that, for the two-boson system, $\Psi_{|F|}$ is a very good variational trial wave function and it provides an upper-bound very close to the ground state energy obtained by exact diagonalization in the short-range and strong interacting limit. Moreover, the distribution of the energy between the kinetic and harmonic potential parts in that limit also coincides. We show that some of the properties of the strong interacting two-boson system resemble the noninteracting fermionic ones. In particular, the density profile and the two-body correlation function [6, 7].

[1] M. Girardeau, J. Math. Phys. **1**, 516 (1960).

[2] M. D. Girardeau, E. M. Wright, and J. M. Triscari, Phys. Rev. A **63**, 033601 (2001).

[3] I. Romanovsky, C. Yannouleas, and U. Landman, Phys. Rev. Lett. **93**, 230405 (2004).

[4] T. Busch, B.-G. Englert, K. Rzazewski, and M. Wilkens, Found. Phys. **28**, 549 (1998).

[5] R. A. Doganov, S. Klaiman, O. E. Alon, A. I. Streltsov, and L. S. Cederbaum, Phys. Rev. A **87**, 033631 (2013).

[6] P. Mujal, E. Sarlé, A. Polls, and B. Juliá-Díaz, Phys. Rev. A **96**, 043614 (2017).

[7] P. Mujal, A. Polls, and B. Juliá-Díaz, Condens. Matter **3**(1), 9 (2018).

Non-linear resonnances in ^{23}Na spinor condensates

An QU, B. Evrard, K. Jiménez-Garcia, F. Gerbier, and J. Dalibard

Laboratoire Kastler Brossel, Collège de France, ENS-PSL, CNRS, Sorbonne Universités, 75005 Paris, France

e-mail: *an.qu@lkb.ens.fr*

We study coherent control of spin dynamics in a driven spinor condensate of Sodium atoms. Spin dynamics in a spinor condensate originates in spin-changing interactions that coherently convert atoms from the Zeeman state $m = 0$ to $m = +1$ and -1. In the single-mode regime, this dynamics is described by two equations and two energy scales, the quadratic Zeeman energy associated with the applied magnetic field and the spin-spin interaction energy. The equations of motion are analogous to the Josephson equations describing supercurrent dynamics in a superconducting weak link. In particular, a fast modulation of the magnetic field leads to the appearance of non-linear resonances, reminiscent of the "Shapiro spikes" in the AC-Josephson effect but more complex because of the non-linear phase evolution due to interactions (negligible in superconducting junctions). We observe the slow, non-linear dynamics associated with these resonances and characterize their properties in details.

Extended Bose-Hubbard Model with dipolar and contact interactions

Krzysztof Biedroń[1], **Mateusz Łącki**[1], **and Jakub Zakrzewski**[1]
[1] *Instytut Fizyki im. Mariana Smoluchowskiego, Uniwersytet Jagielloński, Kraków, Poland*
e-mail: *jakub.zakrzewski@uj.edu.pl*

Phase diagram of the one-dimensional boson gas trapped inside an optical lattice with contact and dipolar interaction taking into account next-nearest terms for both tunneling and interaction is presented. Using the density matrix renormalization group, we calculate changes of phase transitions regions with increasing dipolar interaction strength. We show an emergence of pair-correlated phases for large dipolar interaction strength and large density including a supersolid phase with an incommensurate density wave ordering manifesting the corresponding spontaneous breaking of the translational symmetry.

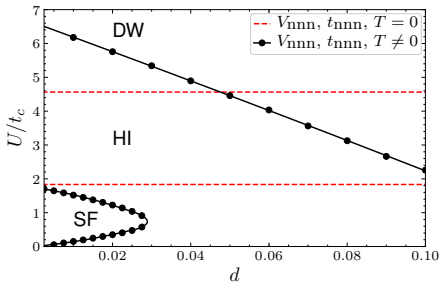


Figure 1: Critical values of U/t for DW-HI and HI-SF (superfluid) transitions, $V/U = 3/4$ (black, solid lines), same for model without next neighbors interactions and tunnelings (red, dashed lines). After [1].

Contrary to earlier treatments where parameters of the extended Bose-Hubbard models were varied at will, we take an experiment-inclined approach - we adjust the lattice depth and take realistic dipolar and contact interactions. The parameters of the resulting tight binding can be then obtained after evalutation of the Wannier functions.

This leads, for example, to significant changes of borders for the topological Haldane insulator (HI) and density wave (DW) phases as shown in Fig. 1. Importantly, novel phases appear for sufficiently high densities, compare Fig. 2. We observe both pair superfluid and supersolid phases but also an entirely novel phase, not discussed before, that we dub the incommensurate pair supersolid insulator (IPSS). It reveals intrinsic correlations between sites on a long range scale. The non-trivial spatial modulation of a density, single particle/pair/density-density correlation functions is confirmed by the peak in the structure factor, incommensurate with the lattice size.

In addition to sophisticated orderings, the IPSS phase is simply characterized by incommensurate modulations of the gas density.

The results are obtained using iTensor DMRG algorithms. When needed, we used a sine-square deformation method, thus implementing a smooth boundaries. This helped to avoid artifacts due to a dissonance between an incommensurate length scale of the IPSS and regular periodic or open boundaries.

Work supported by National Science Center (Poland) grant 2015/19/B/ST2/01028.

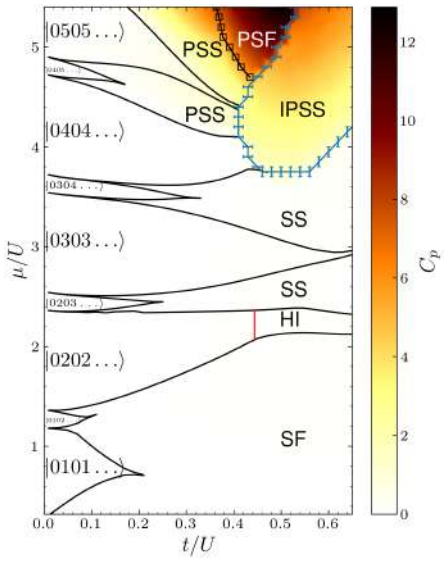


Figure 2: The phases for the system for a chosen dipole interactions parameter $d = 0.1$ at a fixed ratio $V/U = 0.75$ (ratio of nearest neighbor to on site interactions). Black lines show the boundaries of DW phases as obtained from OBC DMRG ($L = 200$). The black squares come from the so called sine-square deformation (SSD) DMRG (and show the transition points between pair-supersolid (PSS) and pair superfluid (PSF) phases. Blue error bars mark the boundaries of the newly discovered incommensurate pair supersolid phase (also SSD DMRG, $L = 100$). The value of pair-tunneling correlations parameter is plotted as a color map with a scale shown on the right. After [1].

[1] K. Biedroń, M. Łącki, and J. Zakrzewski, Phys. Rev. B *in press* (2018) .

Low-momentum Bragg Spectroscopy of a Unitary Fermi Gas

Carlos C. N. Kuhn, Sascha Hoinka, Ivan Herrera, Paul Dyke, Chris J. Vale
Centre for Quantum and Optical Sciences, Swinburne University of Technology, Melbourne 3122, Australia
e-mail: *cnoschangkuhn@swin.edu.au*

Bragg spectroscopy has been proven to be extremely useful in different areas of science. In this work, we use low-momentum Bragg spectroscopy to investigate elementary excitation in an ultracold cloud of ^{6}Li atoms at unitarity. In this regime, the scattering length goes to infinity and exact theoretical treatments are not available, meaning experiments are essential for obtaining quantitative understandings. Probing the homogeneous properties of such a system presents experimental challenges. Our Bragg system was designed to overcome these challenges by focusing the Bragg beams into the centre of the sample, which has recently been used to observe the Goldstone mode in an atomic Fermi superfluid [1]. Figure 1(a) shows a schematic illustrating how we probe the local excitation spectrum. Figure 1(b) and (c) are typical differential images showing the response as a result of these excitations in the cloud after a 4ms time of flight.

By perturbing the system through the transfer of momentum to the atoms, in units smaller than its natural units (Fermi momentum, k_F), we can excite first sound and extract its physical properties such as its speed and damping rate, which are related to the peak and width of the spectrum shown in Figure 1(d), respectively. We see a dramatic increase in damping above the critical temperature ($T_c = 0.167T_F$), indicated by the increased width, that signifies a change in shear viscosity.

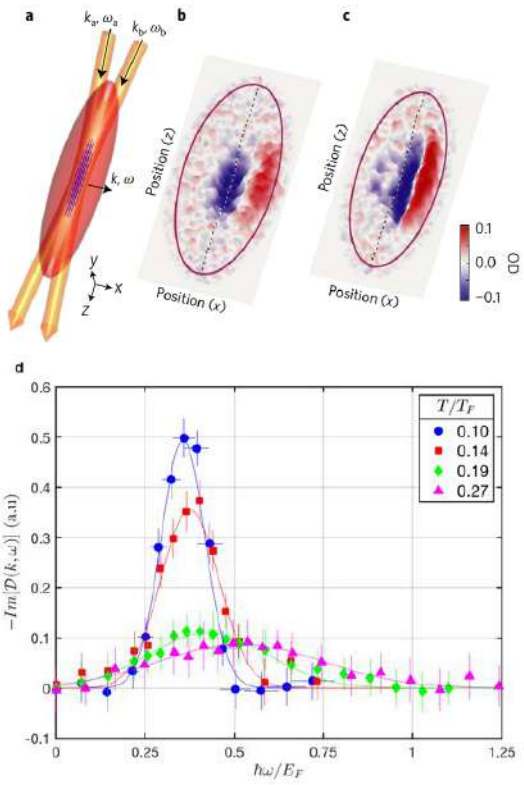


Figure 1: This figure (a) illustrates the configuration of our focused Bragg beams intersected in the centre of a harmonically trapped cloud of atoms. Figure (b) and (c) are examples of the local elementary excitation resulting in a displacement of the centre of mass of the cloud. (d) Bragg Spectrum for four different temperatures. The density-density response is normalised to the product of Bragg beam intensities. The perturbation energy is in units of Fermi energy.

[1] Sascha Hoinka, Paul Dyke, Marcus G. Lingham, Jami J. Kinnunen, Georg M. Bruun and Chris J. Vale, Nature Phys. **13**, pages 943 (2017).

Observation of a dynamical sliding phase superfluid with P-band bosons

Shengjie Jin[1], **Linxiao Niu**[1], **Xuzong Chen**[1], **Xiaopeng Li**[2], **and Xiaoji Zhou**[1*]

[1] *School of Electronics Engineering and Computer Science, Peking University, Beijing 100871, China*

[2] *State Key Laboratory of Surface Physics, Institute of Nanoelectronics and Quantum Computing, and Department of Physics, Fudan University, Shanghai 200433, China*

e-mail: *xjzhou@pku.edu.cn*

Sliding-phase superfluidity plays important roles in the fundamental understanding of coupled XY-models, however the experimental evidence so-far remains elusive. With field-theory analysis, the experimental challenge has been attributed to that the sliding-phase typically appears under extreme conditions for thermal-equilibrium systems or quantum ground-states. With synthetic quantum systems, recent experimental progress has achieved unprecedented approaches to investigate fascinating collective phenomena in controllable quantum dynamics, such as light-induced non-equilibrium superconductivity, time-crystals in trapped ion-qubits, correlated quantum kinematics in reduced-dimensional systems, and many-body localization with ultracold atoms in artificial light-crystals. While a complete theoretical framework to describe nonequilibrium phase-transition is still lacking, a formal analogy between temperature and time by comparing partition-function in the thermal-ensemble and unitary-evolution operator in quantum dynamics allows such concepts in statistical physics as many-body phases and condensation, to generalize to the time-domain.

Here, we report on an observation of a sliding-phase superfluid in a dynamical system of ultracold atoms loaded into the P-band of an optical lattice. Our work goes beyond previous studies in P-band optical lattices focused on static phases, by considering nonequilibrium quantum aspects. We have a three-dimensional quantum gas confined with a one-dimensional lattice, which can be thought as a series of "pancake"-shaped subsystems. Using an adiabatic short-passage [1, 2] to load atoms into the zero quasi-momentum state in the P-band of the lattice, the system is driven far-out-of-equilibrium. During the process of rethermalization, a metastable region is observed, where the atomic sample shows strong phase-coherence in the pancake directions, but no coherence in the lattice direction. These observations imply the first experimental discovery of the sliding-phase superfluid in the time-domain. This work would also shed light on the understanding of high-Tc mechanism in light-probed cooperates [3].

In order to characterize the real-time dynamics after P-band gets occupied, we measure momentum distributions in the lattice and pancake directions at the different holding-times (Fig. 2). From the time evolution, we identify three distinct dynamical regions. At early time—the first stage, the system has superfluid phase coherence in all three directions, which is clearly demonstrated through the sharp peaks observed in the momentum distribution. A bimodal fitting shows the system is coherent in all directions. At late time—the final stage, the quantum gas has rethermalized with a complete loss of phase-coherence, owing to the excessive energy in the atomic-gas. There is yet an intermediate time region with significant time-duration where the phase-coherence of the quantum system survives partially.

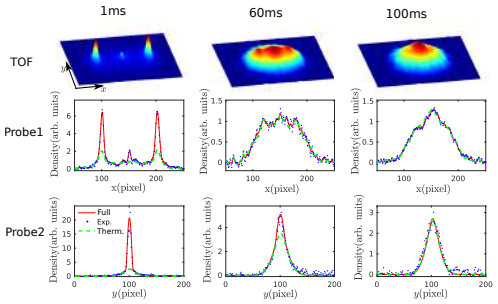


Figure 1: Momentum distributions measured at three different holding times $t = 1$ ms, 60 ms, 100 ms, along different directions. The images shown in the first row represent experimental TOF measurements in the xy-plane by Probe1 (see main text), and the corresponding momentum distribution in the central line along the $\hat{x}$-direction is given in the second row with blue dots. The red solid line gives a full fitting line while the green dashed line gives the distribution of thermal component. Atomic distribution in the S-band (P-band) is revealed in the first (second) Brillouin zone. The third row shows the atomic distribution along the central line in $\hat{y}$-direction for the experimental images in the yz-plane measured by Probe2.

[1] D. Hu, L. Niu, B. Yang, X. Chen, B. Wu, H. Xiong, and X. Zhou, *Phys. Rev. A* **92**, 043614 (2015).

[2] Xiaoji Zhou, Shengjie Jin, and Jörg Schmiedmayer, *New J. Phys.* **20**, 055005 (2018).

[3] Linxiao Niu, Shengjie Jin, Xuzong Chen, Xiaopeng Li, and Xiaoji Zhou arXiv:1805.03073 (2018).

Quantum Bose-Fermi droplets

D. Rakshit[1], **T. Karpiuk** [2], **M. Brewczyk**[2] **and M. Gajda**[1]
[1] *Institute of Physics, Polish Academy of Sciences, Aleja Lotnikw 32/46, PL-02668 Warsaw, Poland*
[2] *Wydział Fizyki, Uniwersytet w Białymstoku, ul. K. Ciołkowskiego 1L, 15-245 Białystok, Poland*
e-mail: *debraj@ifpan.edu.pl*

We study stability of a zero temperature mixture of attractively interacting degenerate bosons and spin-polarized fermions in free space. Our analysis shows that higher order corrections to the standard mean field energy of the system can lead to a formation of liquid droplets, which are self-bound incompressible systems in a three-dimensional space. In addition to the quantum Lee-Huang-Yang correction to the boson-boson interaction energy, a higher order correction term in the Bose-Fermi coupling constant plays crucial role in stabilizing these systems. We investigate various mixtures of species with different mass ratios as a function of the ratio of Bose-Fermi to Bose-Bose scattering length. We further support our analysis via numerical simulations of droplet formation dynamics starting with a trapped system which is subsequently released from the trap.

References

[1] T. Karpiuk, D. Rakshit, M. Brewczyk and M. Gajda, *Liquid quantum Bose-Fermi droplets*, arXiv:1801.00346.

Physics of ultracold Yb-^{6}Li and Yb-^{7}Li mixtures

F. Schäfer[1], **N. Mizukami**[2], **B. Koibuchi**[1], **A. Bouscal**[1,3], **and Y. Takahashi**[1]
[1] *Department of Physics, Graduate School of Science, Kyoto University, 606-8502 Kyoto, Japan*
[2] *Department of Physics, Faculty of Science, Kyoto University, 606-8502 Kyoto, Japan*
[3] *Department of Physics, École Normale Superiéure, Rue Lhomond 24, F-75231 Paris Cedex 05, France*
e-mail: *schaefer@scphys.kyoto-u.ac.jp*

We present our latest results on experiments on quantum degenerate mixtures of Ytterbium (Yb) and Lithium (Li). Both species feature stable bosonic isotopes, e.g. ^{174}Yb and ^{7}Li, and fermionic isotopes, ^{173}Yb and ^{6}Li. Of these, all possible Yb-Li mixture combinations were realized in our laboratory. Exploiting the different quantum statistics and the large mass imbalance between Yb and Li, $m_{\mathrm{Yb}}/m_{\mathrm{Li}} \approx 29$, we strive to address research topics raging from the simulation of impurity systems [1] to the realization of topological $p_x + i\,p_y$ superfluids [2].

A first set of experiments using fermionic ^{6}Li addressed fundamental questions concerning the simulation of impurity systems. Using a three-dimensional (3D) optical lattice a regime is accessible where only the heavy Yb, taking on the impurity role, is well localized in the lattice sites. Interest in such systems is based on a possible realization of Anderson localization [3], Anderson's orthogonality catastrophy [4] or the Kondo effect [5]. As a preparatory step a good understanding of the interspecies elastic and inelastic interactions in Yb(^{3}P$_2$)-^{6}Li is necessary. Here, the metastable ^{3}P$_2$ state of Yb has been chosen as this particular mixture was predicted to feature inter-species Feshbach resonances (FRs) with possibly favorable properties [6]. However, scanning a wide range of magnetic fields up to 800 G no FRs could be identified [7]. Instead, we could highlight the importance of proper initial hyperfine state preparation of the mixture for a suppression of inelastic losses [8]. Those results further lead to insight of the contribution of anisotropy in the inter-species potential to the scattering process.

A second set of experiments realized quantum degenerate Yb-Li mixtures using bosonic ^{7}Li. This was the first successful realization of such a system and inverses the situation previously found. While previously in the presence of a strong optical lattice mixed-dimensional systems with localized Yb and 3D fermionic ^{6}Li was realized, we now report on a situation with a bosonic 3D component that could be an important step towards the realization of a fermionic topological $p_x + i\,p_y$ superfluid in ultracold atomic systems [2]. To begin we realized both, a Boson-Boson ^{174}Yb^{7}Li and a Fermion-Boson ^{173}Yb^{7}Li mixture, with the latter being of central interest for the task at hand. Using cross thermalization measurements we performed a first characterization of the inter-species scattering lengths in both mixtures and found excellent agreement to earlier predictions [9]. The importance of the bosonic ^{7}Li background for a possible topological superfluid lies in the effective interactions mediated on ^{173}Yb by collective ^{7}Li Bogoliubov phonons. In order to better understand the robustness of such excitations with respect to distortions of the confining potential we further started to explore the ^{7}Li Bogoliubov spectrum.

To summarize, we present an exhaustive survey of the properties of quantum degenerate YbLi mixtures of profound interest for the quantum simulation of impurity systems and for the realization of topological superfluids.

[1] P. Massignan, M. Zaccanti, and G. M. Bruun, Rep. Prog. Phys. **77**, 034401 (2014).

[2] M. A. Caracanhas, F. Schreck, and C. M. Smith, New J. Phys. **19**, 115011 (2017).

[3] S. Ospelkaus *et al.*, Phys. Rev. Lett. **96**, 180403 (2006).

[4] M. Knap, A. Shashi, Y. Nishida, A. Imambekov, D. A. Abanin, and E. Demler, Phys. Rev. X **2**, 041020 (2012).

[5] Y. Nishida, Phys. Rev. A **93**, 011606 (2016).

[6] M. L. González-Martínez, and J. M. Hutson, Phys. Rev. A **88**, 020701 (2013).

[7] F. Schäfer, H. Konishi, A. Bouscal, T. Yagami, and Y. Takahashi, Phys. Rev. A **96**, 032711 (2017).

[8] F. Schäfer, H. Konishi, A. Bouscal, T. Yagami, and Y. Takahashi, New. J. Phys. **19**, 103039 (2017).

[9] D. A. Brue, and J. M. Hutson, Phys. Rev. Lett. **108**, 043201 (2012).

Single-particle properties and effective range corrections in a strongly interacting Fermi gas

H. Tajima

Quantum Hadron Physics Laboratory, RIKEN Nishina Center, Wako, Saitama 351-0198, Japan
e-mail: *hiroyuki.tajima@riken.jp*

We theoretically investigate single-particle properties of a strongly interacting Fermi gas in the presence of finite effective range. The effective range correction plays an important role when one considers the similarity between ultracold atomic gases and dilute neutron matter in a neutron star. Both systems are dominated by a strong attraction associated with the large scattering length. In this regard, an ultracold Fermi gas is expected to be a quantum simulator of neutron star matter in the low density region [1]. However, there is a crucial difference of magnitude of the effective ranges between these two systems since while the effective range in a cold atomic gas near the broad Feshbach resonance is usually negligible compared to its tunable scattering length, the effective range of neutron-neutron scatterings $r_{\rm nn} = 2.8$ fm is non-negligible compared to the scattering length $a_{\rm nn} = -18.5$ fm [2].

To obtain a unified understanding of these different interdisciplinary topics, we develop a strong-coupling theory for an ultracold Fermi atomic gas with finite negative effective range $r_{\rm e}$, which is realized near the narrow Feshbach resonance [3]. Within the framework of a many-body T-matrix approximation [4], we numerically calculate the single-particle spectrum, which is also relevant for the cooling mechanism of neutron stars [5], as a function of $r_{\rm e}$ in strongly interacting Fermi gases. In cold atom physics, it is known that single-particle excitations exhibit a pseudogap phenomenon in the normal phase near the superfluid phase transition temperature $T_{\rm c}$, where the single-particle density of states has a dip structure. Fig. 1 shows the calculated single-particle density of states at $T = T_{\rm c}$ in the intermediate coupling region with finite negative effective range. One can find that the pseudogap clearly appears near $\omega = 0$ in contrast to an ordinary single-particle density of states of ideal Fermi gases $\rho_0(\omega) = \frac{m}{2\pi^2}\sqrt{2m(\omega+\mu)}$ at $T = 0$, where ω is the single-particle energy measured from the chemical potential μ and m is the mass of a Fermi atoms.

In this presentation, we show that the pseudogap size becomes larger with increasing the negative effective range in the weak-coupling side and it decreases in the opposite side. This behavior is deeply related to effects of pairing fluctuations due to the strong attraction between atoms. We determine the effective range dependence of characteristic temperature $T_{\rm PG}$ where the pseudogap appears [4], at $(k_{\rm F}a)^{-1} = 0$ ($k_{\rm F}$ is the Fermi momentum). Finally, we obtain

$$\frac{T_{\rm PG}}{\varepsilon_{\rm F}} = 0.320 - 0.052 r_{\rm e} k_{\rm F} + O(r_{\rm e}^2 k_{\rm F}^2), \qquad (1)$$

which is expected to be valid even in the small positive effective range regime such as neutron matter. Eq. (1) indicates that the positive effective range suppresses pairing fluctuations. Such effects would also be evaluated by the cold atom experiments as well as quantum Monte-Carlo simulations. This presentation is based on our recent publication [6].

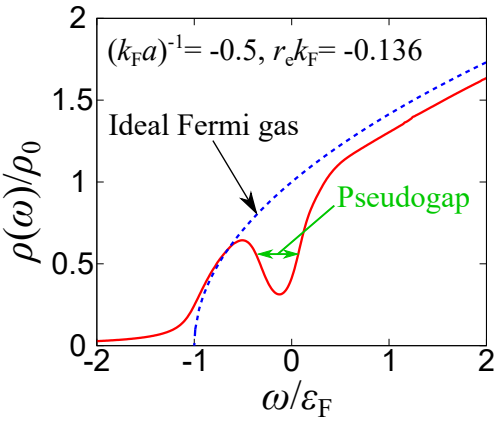


Figure 1: Calculated single-particle density of states $\rho(\omega)$ (ω is the single-particle energy) at $(k_{\rm F}a)^{-1} = -0.5, r_{\rm e}k_{\rm F} = -0.136$, where $a, r_{\rm e}$ and $k_{\rm F}$ are the scattering length, effective range, and Fermi momentum of atoms, respectively. The dashed line shows the single-particle density of states in an ideal Fermi gas at $T = 0$ and ρ_0 is that at $\omega = 0$. $\varepsilon_{\rm F}$ is the Fermi energy of atoms.

[1] P. van Wyk, H. Tajima, D. Inotani, A. Ohnishi, and Y. Ohashi, Phys. Rev. A **97**, 013601 (2018).

[2] R. B. Wiringa, V. G. J. Stoks, and R. Schiavilla, Phys. Rev. C **51**, 38 (1995).

[3] E. L. Hazlett, Y. Zhang, R. W. Stites, and K. M. O'Hara, Phys. Rev. Lett. **108**, 045304 (2012).

[4] S. Tsuchiya, R. Watanabe, and Y. Ohashi, Phys. Rev. A **80**, 033613 (2009).

[5] D. J. Dean and M. Hjorth-Jensen, Rev. Mod. Phys. **75**, 607 (2003).

[6] H. Tajima, Phys. Rev. A **97**, 043613 (2018).

Effect of a magnetic field on molecule-solvent angular momentum transfer

W. Rzadkowski[1] **and M. Lemeshko**[1]

[1] *Institute of Science and Technology Austria (IST Austria), Am Campus 1, 3400 Klosterneuburg, Austria*
e-mail: *wojciech.rzadkowski@ist.ac.at*

Recently it has been shown that a molecule exchanging angular momentum with the surrounding bosonic solvent can be described in terms of the 'angulon' quasiparticle [1]. Here, we extend the angulon theory to the case of molecules possessing an additional spin-1/2 degree of freedom and studied the behavior of the system in the presence of a static magnetic field [2].

Using a combination of variational and diagrammatic techniques, we get access to the full spectral function of the system (Fig. 2). Moreover, we calculate populations of bath phonons (Fig. 1), enabling us to study their emission in different angular momentum channels.

In particular, we demonstrate that exchange of angular momentum between the molecule and the bath can be altered by the field, even though the bath itself is not susceptible to the latter. In particular, we observed the possibility to control resonant emission of phonons with preordained orbital angular momentum using a magnetic field.

The formalism that we use, although exemplified for the case of linear molecules trapped in superfluid helium nanodroplets, is quite general, and can be in principle applied to any spin-1/2 impurity possessing rotational or orbital angular momentum, immersed into, in principle, any kind of a bosonic bath. Hence, the effects that we predict can also be applicable to Rydberg excitations in Bose-Einstein condensates or non-equilibrium magnetism in solids.

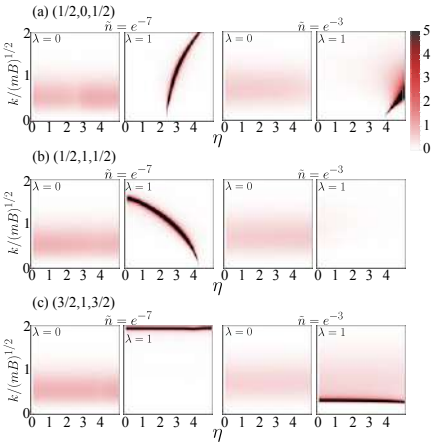


Figure 1: Dependence of the phonon populations vs. magnetic field (x-axis) and phonon wavenumber (y-axis). Figure adapted from Ref. [2].

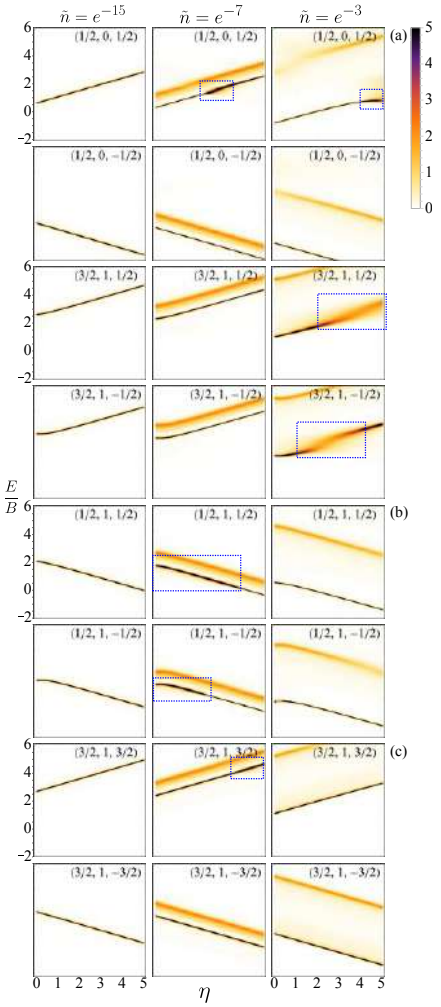


Figure 2: Dependence of the spectal function vs. magnetic field (x-axis) and energy (y-axis). Figure adapted from Ref. [2].

[1] M. Lemeshko, Quasiparticle Approach to Molecules Interacting with Quantum Solvents, Phys. Rev. Lett. 118, 095301 (2017)

[2] W. Rzadkowski and M. Lemeshko, Effect of a magnetic field on molecule-solvent angular momentum transfer, J. of Chem. Phys. 148, 104307 (2018)

Portable and flexible cold atom experiments

P. Ireland[1], **D. Bowman**[1], **P. F. Griffin**[2], **G. D. Bruce**[1], **and D. Cassettari**[1]
[1] *SUPA School of Physics and Astronomy, University of St Andrews, North Haugh, St Andrews, Fife, KY16 9SS, UK*
[2] *SUPA Department of Physics, University of Strathclyde, 107 Rottenrow, Glasgow, G4 0NG, UK*
e-mail: *pi8@st-andrews.ac.uk*

The drive to miniaturise atom-based metrological devices whilst maintaining the ability to probe the behavioural response of the atoms in novel geometries is becoming increasingly prevalent. Here, we report on our progress towards this goal.

Firstly, we have built a magneto-optical trap (MOT) that combines two key technological results with the intention of creating a compact, robust and transportable apparatus. The first of these is a laser locking technique as an alternative to the standard laboratory saturated absorption spectroscopy. The dichroic atomic vapour laser lock (DAVLL) technology [1] makes use of a longitudinal magnetic field to produce a large antisymmetric error signal centred on a typical Doppler-broadened absorption spectrum. The result is a robust locking mechanism with a significant recapture range that provides increased stability when using the portable MOT for outside a controlled lab environment. With an emphasis on reducing the total optical footprint, we combined the DAVLL technique with our homemade sideband generation electronics at 3GHz to supply the necessary repumper light to form a stable ^{85}Rb MOT of 10^7 atoms. The ability to generate the repumper power this way eliminates the need for a second laser to perform the repumper role, significantly reducing the amount of optics required. This setup has been utilised both as an undergraduate honours laboratory experiment and as part of a portable setup for outreach purposes to the general public. Additionally, in our outreach events we have reduced the optical setup further by using a micro-fabricated grating chip [2] (Figure 1a). This replaces a standard 6-beam MOT setup by forming an overlap volume from a single input laser beam and the resulting diffracted orders, which greatly simplifies both the optical setup around the glass cell and the alignment necessary.

Secondly, we describe our experimental progress of trapping cold atoms in arbitrary optical trap geometries using a phase-only spatial light modulator (SLM) combined with efficient hologram generation techniques. We report on the creation of multi-wavelength optical traps [3] using a single SLM, allowing different wavelength structures to overlap in the Fourier plane when the SLM is illuminated with co-propagating, overlapped laser beams, which may be desirable when optical access to a cold atoms experiment becomes limited. We also demonstrate simultaneous control of both the phase and amplitude of light in the output plane to produce high fidelity light patterns using a conjugate gradient (CG) minimisation routine [4, 5]. The phase constraint imposed on the output plane light in the CG routine is crucial for better control of the propagation of the SLM light, compared to hologram generation techniques that allow for phase freedom at the output plane. We incorporate this CG method to produce light patterns suitable for the trapping of cold atom ensembles, obtaining absorption images for atoms trapped e.g. in a gaussian line light pattern (Figure 1b), for studies of simultaneous trapping of atoms but also using a phase gradient to induce flow, and for a light pattern resembling two reservoirs connected by a shallow channel (Figure 1c), for investigations of transport through the two reservoirs. Further investigations will involve the use of a light sheet to act as a canvas for more complicated optical patterns, such as for investigations of the topological Kondo effect [6], aimed at emulating an impurity at a junction interacting with a gas of fermions in a set of one-dimensional external wires.

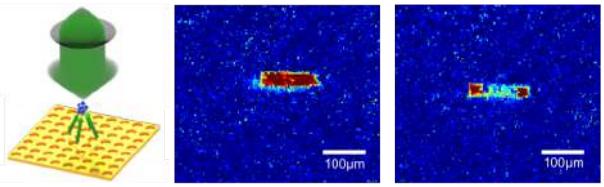


Figure 1: a) Schematic of the grating MOT operation; b) Absorption image of atoms confined in a gaussian line pattern; c) Absorption image of atoms confined in two reservoirs connected by a shallow channel.

[1] K. L. Corwin et al., *Appl. Opt.* **37**, 3295 (1998).

[2] C. C. Nshii et al., *Nature Nano.* **8**, 321 (2013).

[3] D. Bowman et al., *Opt. Express* **23**, 8365 (2015).

[4] T. Harte et al., *Opt. Express* **22**, 26548 (2014).

[5] D. Bowman et al., *Opt. Express* **25**, 11692 (2017).

[6] F. Buccheri et al., *New Journal of Physics* **18**, 075012 (2016).

Temperature dependence of the Bose Polaron in a Bose-Einstein condensate

M. G. Skou, N. B. Jørgensen, T. G. Skou, G. M. Bruun, and J. J. Arlt
Institut for Fysik og Astronomi, Aarhus Universitet, 8000 Aarhus C, Denmark
e-mail: *magnus.skou@phys.au.dk*

The interaction of an impurity with a surrounding medium is one of the most fundamental concepts in physics. A prime example is the electron placed in a crystal lattice. Here the interaction with the lattice phonons causes the formation of a quasiparticle coined the polaron [1]. Utilizing the versatile toolbox of Bose-Einstein condensates (BEC), the interaction may be tuned between impurity and medium, thus creating a platform for studying the polaron. This led to the very first observation of the Bose polaron in 2016 [2, 3].

In the Aarhus experiment the polaron is realized using two different spin states of ^{39}K. An interstate Feshbach resonance is employed to tune the interaction between the two states. This allows probing of both the attractive- and repulsive polaron branch by radio frequency spectroscopy.

Recent theoretic work have shown a nontrivial temperature dependence, where the Bose polaron state splits at finite temperature and attractive interaction between medium and impurity [4]. I will report on our recent experimental efforts in observing this splitting.

References

[1] L. D. Landau and S. I. Pekar, J. Exp. Theor. Phys. **18**, 419 (1948)

[2] N. B. Jørgensen, L. Wacker, K. T. Skalmstang, M. M. Parish, J. Levinsen, R. S. Christensen, G. M. Bruun, and J. J. Arlt, Phys. Rev. Lett. **117**, 055302 (2016).

[3] M.-G. Hu, M. J. Van de Graaff, D. Kedar, J. P. Corson, E. A. Cornell, and D. S. Jin, Phys. Rev. Lett. **117**, 055301, (2016)

[4] N.-E. Guenther, P. Massignan, M. Lewenstein, and G. M. Bruun, Phys. Rev. Lett. **120**, 050405 (2018).

Superfluid flow of an annular Bose gas

A. Kumar, M. de Goër de Herve, R. Dubessy, Y. Guo, T. Badr, A. Perrin, L. Longchambon, and H. Perrin

Laboratoire de Physique des Lasers, CNRS UMR 7538, Université Paris 13 Sorbonne Paris Cité, 93430 Villetaneuse, France

e-mail: *helene.perrin @ univ-paris13.fr*

Superfluidity is an intriguing property of quantum fluids, with spectacular manifestations such as the existence of a critical velocity or of persistent currents in a loop with a quantized circulation of the flow velocity. Quantum bosonic gases, which can be manipulated easily by light or magnetic fields and trapped in various geometries, allow the study of these features. In particular, ring traps have been developed to confined Bose-Einstein condensates in an annular configuration for the preparation and study of persistent superfluid flows [1].

In this work we present the trapping of a degenerate Bose gas in a ring trap and the preparation of a quantized circulation. The ring potential, as described in [2, 3], relies on intersecting two independent trapping potentials: a planar optical trap, confining the atoms at a given height, and a bubble-like trap produced by the dressing of atoms with a radio-frequency (rf) field [4, 5] in the presence of a quadrupolar magnetic field [6]. As a result, the atoms are confined to the intersection of an ellipsoid with a vertical symmetry axis and a horizontal plane, i.e. a circle, see Fig. 1. The radial confinement is thus ensured by the adiabatic potential while the vertical confinement is of optical nature.

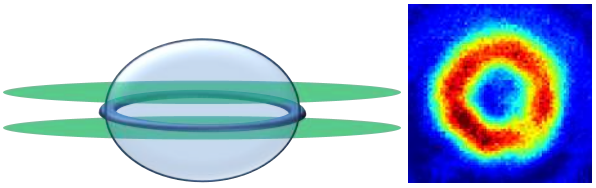


Figure 1: Left: principle of the ring trap. Right: absorption picture of atoms confined in the ring trap.

We present two methods to prepare a persistent current in this trap. First, we rotate an elliptical asymmetry obtained with the rf polarization as proposed in [3]. In this way, we are able to prepare a superfluid flow in the ring, with a velocity controlled by the rotation frequency of the ellipse axes.

The second method relies on phase imprinting an helicoidal intensity profile of a far-detuned laser, in the spirit of phase imprinting of solitonic waves [7, 8]. We propose a method to circumvent the necessarily finite resolution of the optical system resulting in a smoothened helicoidal profile by introducing an auxiliary barrier potential [9], see Fig. 2. We show by numerical simulations of the Gross-Pitaevskii equation

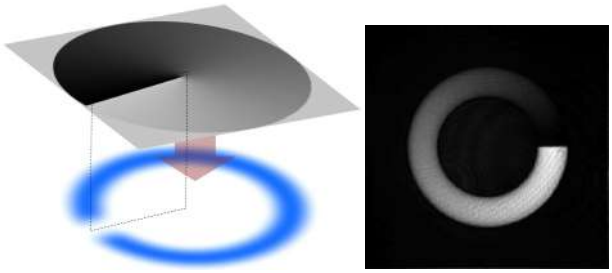


Figure 2: Left: Principle of the phase imprinting technique. Right: Experimental helicoidal intensity profile obtained with a SLM device.

that this process leads to a fast and efficient preparation of circulation states in realistic conditions.

[1] C. Ryu, M. F. Andersen, P. Cladé, Vasant Natarajan, K. Helmerson, and W. D. Phillips, Phys. Rev. Lett. **99**, 260401 (2007).

[2] O. Morizot, Y. Colombe, V. Lorent, H. Perrin, and B. M. Garraway, Phys. Rev. A **74**, 023617 (2006).

[3] W. H. Heathcote, E. Nugent, B. T. Sheard, and C. J. Foot, New J. Phys. **10**, 043012 (2008).

[4] B. M. Garraway and H. Perrin, J. Phys. B: At. Mol. Opt. Phys. **49**, 172001 (2016).

[5] H. Perrin and B. M. Garraway, Adv. At. Mol. Opt. Phys. **66**, 181–262 (2017).

[6] K. Merloti, R. Dubessy, L. Longchambon, A. Perrin, P.-E. Pottie, V. Lorent, and H. Perrin, New J. Phys. **15**, 033007 (2013).

[7] S. Burger, K. Bongs, S. Dettmer, W. Ertmer, K. Sengstock, A. Sanpera, G. V. Shlyapnikov, and M. Lewenstein, Phys. Rev. Lett. **83**, 5198 (1999).

[8] J. Denschlag, J. E. Simsarian, D. L. Feder, C. W. Clark, L. A. Collins, J. Cubizolles, L. Deng, E. W. Hagley, K. Helmerson, W. P. Reinhardt, S. L. Rolston, B. I. Schneider, and W. D. Phillips, Science **287**, 97 (2000).

[9] A. Kumar, R. Dubessy, T. Badr, C. De Rossi, M. de Goër De Herve, L. Longchambon and H. Perrin, Phys. Rev. A **97**, 043615 (2018).

Real and imaginary part of conductivity of strongly interacting bosons in optical lattices

B. Grygiel[1], **K. Patucha**[1], **and T. A. Zaleski**[1]

[1] *Institute of Low Temperature and Structure Research, Polish Academy of Sciences, ul. Okólna 2, 50-422 Wrocław, Poland*

e-mail: *b.grygiel@intibs.pl*

Optical-lattice systems filled with ultra-cold atomic gases have been an intensively studied subject in the recent years, especially thanks to the advancement in cooling and trapping techniques [1, 2]. These systems can be thought of as a counterpart of solid state systems, where the optical lattice plays the role of the ionic potential, while ultra-cold atoms act as the charge carriers. Thanks to the possibility of precise manipulation of their properties and the lack of defects, they can serve as quantum simulators of the solid state systems [3].

Methods, such as Floquet engineering or photon-assisted tunneling [4, 5], have allowed to introduce the artificial gauge fields and opened additional possibilities of control of behavior of particles under external potentials. Moreover, the techniques for measuring the tranport properties of ultracold atomic systems have been developed, leading to successful experiments, e.g. quantized conductance measurements in the cold-atom version of the quantum point contact [6] or a scanning gate microscopy method for ultracold gases [7], which can be applied to any cold-atom system.

These advances of the experimental techniques have motivated us to study the transport properties of strongly interacting bosons in optical lattice, also in the presence of the artificial magnetic field. To this end we use the Bose-Hubbard model in the quantum rotor approach, which allows us to take into account spatial dependencies, such as dimensionality, lattice geometry, and influence of the gauge potentials. We calculate the conductivity of bosons in a two-dimensional lattice in synthetic magnetic field. In such scenario, two types of conductivity can be distinguished, intra- and inter-band. The interband contribution, usually omitted in analysis of multiband systems, appears to have a crucial role in the transport properties as its values are a few orders of magnitude greater than the intraband one.

[1] C. Pethick and H. Smith, *Bose-Einstein Condensation in Dilute Gases* (Cambridge University Press, 2002)

[2] I. Bloch, J. Dalibard, and W. Zwerger, Rev. Mod. Phys. **80**, 885 (2008)

[3] M. Lewenstein, A. Sanpera, V. Ahufinger, B. Damski, A. Sen(De), and U. Sen, Adv. Phys. **56**, 243 (2007)

[4] G. Jotzu, M. Messer, R.Desbuquois, M. Lebrat, T. Uehlinger, D. Greif, and T. Esslinger, Nature **515**, 237 (2014)

[5] M. Aidelsburger, M. Atala, M. Lohse, J. T. Barreiro, B. Paredes, and I. Bloch, Phys. Rev. Lett. **111**, 185301 (2013)

[6] S. Krinner, D. Stadler, D. Husmann, J.-P. Brantut, and T. Esslinger, Nature **517**, 64 (2015)

[7] S. Häusler, S. Nakajima, M. Lebrat, D. Husmann, S. Krinner, T. Esslinger, and J.-P. Brantut, Phys. Rev. Lett. **119**, 030403 (2017)

Pinning Transition of Bose-Einstein Condensates in Optical Ring Resonators

S. C. Schuster[1], **P. Wolf**[1], **D. Schmidt**[1], **S. Slama**[1], **C. Zimmermann**[1]
[1] *Physikalisches Institut, Eberhard-Karls-Universität Tübingen, Auf der Morgenstelle 14, D-72076 Tübingen, Germany.*
e-mail: *simon.schuster@uni-tuebingen.de*

Cold atoms in optical resonators is a classic in quantum optics. While the majority of experiments are carried out with standing wave resonators, the specific properties of ring resonators are far less explored.

The here described experiment is based on a ^{87}Rb-Bose-Einstein condensate in a ring resonator that is longitudinally pumped in one direction (pump mode) [1]. In addition, some light is injected into the reverse propagating mode (probe mode). The interference between the pump mode and the probe mode generates a very weak periodic pinning potential that competes with the optical lattice generated by the atoms. We observe a new stable phase that appears if the resonator is detuned beyond a critical value, shown in Fig. 1. Below this value the self generated optical lattice of the atoms overrides the pinning potential and the system becomes unstable. The observations are well described by numerical simulations; however, a more physical explanation is possible by means of a geometric interpretation of the nonlinear equations of motion in the vicinity of the phase boundary [2].

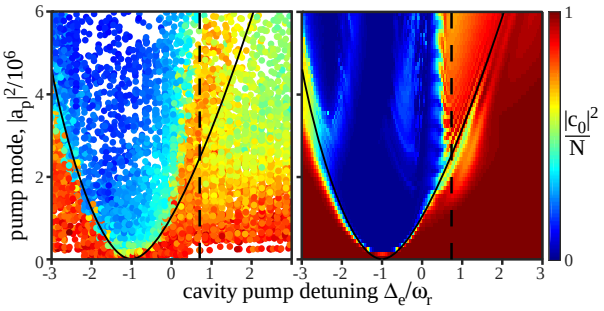


Figure 1: Phase diagram. Observed (left) and calculated (right) population of the zero momentum state after 1.5ms of interaction with the light in the resonator for various photon numbers in the pump mode and cavity pump detuning. The dashed line indicates the pinning transition in the limit of strong pumping. For negative detuning the experimental observations are well described by the phase boundary derived from a numerical simulation that does not include the pinning potential (solid line).

[1] D. Schmidt, H. Tomczyk, S. Slama, and C. Zimmermann, Phys. Rev. Lett. 112, 115302 (2014).

[2] S. C. Schuster, P. Wolf, D. Schmidt, S. Slama, C. Zimmermann, arXiv:1803.02293, submitted (2018).

Radiofrequency-Dressed Adiabatic Potentials to Observe Thermalisation of Two-Dimensional Quantum Gases

K. Luksch[1], **E. Bentine**[1], **A. J. Barker**[1], **S. Sunami**[1], **T. L.Harte**[2], **B. Yuen**[1] **and C. J. Foot**[1]
[1] *Clarendon Laboratory, University of Oxford, Oxford OX1 3PU, UK*
[2] *Cavendish Laboratory, University of Cambridge, JJ Thomson Avenue, Cambridge CB3 0HE, UK*
e-mail: *Kathrin.Luksch@physics.ox.ac.uk*

We have developed multiple-radiofrequency (MRF) dressed magnetic potentials [1], which create tuneable trapping geometries, such as a controllable double well (see Figure 1) or a broad single well, and can confine atomic motion to two dimensions. We have carried out radiofrequency (RF) spectroscopy to measure the MRF potentials and make a detailed comparison with calculations of the transition frequencies and relative amplitudes using the resolvent formalism [2].

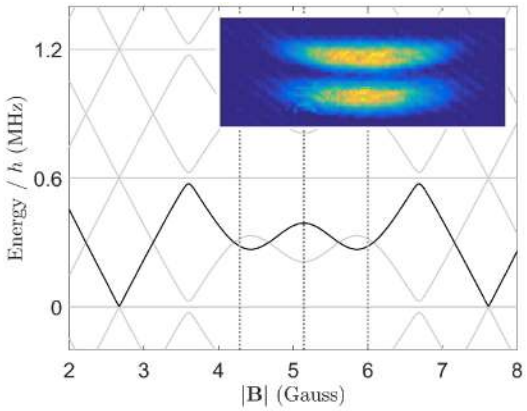


Figure 1: Eigenstates of atoms in a double well potential formed by dressing atoms with three RFs. Inset: Absorption image of thermal atoms trapped in such a potential.

These RF-dressed potentials are ideally suited for experiments to investigate thermalisation in a two-dimensional (2D) quantum-degenerate Bose gas close to a critical point, and to observe the out-of-equilibrium dynamics which drive the closed system towards a thermal state. We propose to split the condensate into two parallel 2D clouds with (approximately) zero relative phase, following which the phase fluctuations in each cloud evolve independently. The relative phase can be determined from the interference pattern that is formed when the clouds are released from the trap after a variable hold time, so that they expand and overlap, as illustrated in Figure 2. From the fringe pattern, we will determine how the relative phase evolves, under what conditions it thermalises, and the timescale for these processes [3].

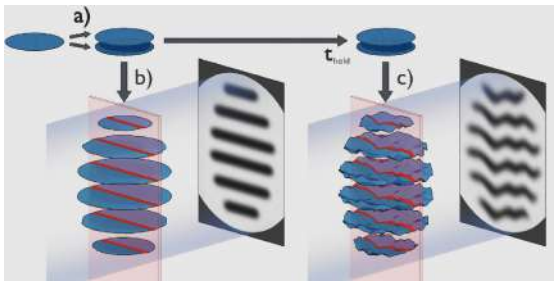


Figure 2: Visualisation of the proposed scheme to observe thermalisation of a 2D Bose gas. a) The gas is split and the two clouds overlapped after a variable hold time. b) After zero hold time, interference fringes will be flat corresponding to a constant relative phase. c) After some finite hold time, the fringes will be wavy, leading to a reduction of the integrated contrast.

[1] T. L. Harte, E. Bentine, K. Luksch, A. J. Barker, D. Trypogeorgos, B. Yuen, and C. J. Foot, Phys. Rev. A **97**, 013616 (2018).

[2] K. Luksch, E. Bentine, A. J. Barker, S. Sunami, B. Yuen, and C. J. Foot, *in preparation.*

[3] L. Mathey and A. Polkovnikov, Phys. Rev. A **81**, 033605 (2010).

2D Fermionic Dipoles at T = 0

R. Bombín[1], **J. Boronat**[1], **and F. Mazzanti**[1]

[1] *Universitat Politècnica de Catalunya, UPC - Dep. Física Campus Nord , 08034 Barcelona, Spain*

e-mail: *raul.bombin@upc.eu*

We analyse the ground state of a two-dimensional quantum system of fermionic dipoles in which all dipoles are polarized along the same direction in space. In our choice the dipole moments have X and Z spatial components. In this work,we use the diffusion Monte Carlo method that allows us to obtain ground state of the many body Schrödinger equation . We predict a phase transition from gas to solid at a critical density $nr_0^2 \sim 50$, which is five times lower than the one for the equivalent bosonic system. The existence of the stripe phase for hight polarization angles is also predicted and accurs at a lower density than in the bosonic case.

The interaction between two dipoles is anisotropic and for the two dimensional system of N particles restricted to move in the XY plane the Hamiltonian is written:

$$H = \frac{-\hbar^2}{2M}\sum_{j=1}^{N}\nabla_j^2 + \frac{C_{dd}}{4\pi}\sum_{i>j}^{N}\frac{1-3\lambda^2\cos^2\theta_{ij}}{r_{ij}^3}$$

Where M is the dipole mass, C_{dd} is proportional to the square of the magnetic ($C_{dd} = \mu_0 m^2$) or electric ($C_{dd} = p^2/\epsilon_0$) dipole moment, $\lambda = \sin\alpha$ and (r_{ij}, θ_{ij}) takes into account the separation between the ith and jth dipole in polar coordinates. The Hamiltonian may be rewritten in a dimensionless way, by introducing dipolar units: the characteristic length $r_0 = MC_{dd}/(4\pi\hbar^2)$ and energy scale $\varepsilon_0 = \hbar^2/mr_0^2$.

The T=0 phase diagram of the bosonic system has already been studied in the (n,α) plane[1] and it was shown that, not only there is a phase transition from the gas to the solid phase at high densities but, the anisotropic character of the dipolar interaction makes the system reach a stripe phase for certain conditions of density, n, and hihg enough polarization angle, α.

The superfluid properties of the different bosonic phases of the system have also been studied, showing that the system can exhibit a superstripe phase: one that exhibits both long range spacial order along one of the directions of the plane and superfluid behaviour. In this sense this phase shows both diagonal and off-diagonal long range order.[2]

The aim of this work is to draw the phase diagram for the fermionic system: the inclusion of Fermi statistics makes the dipolar gas more respulsive, which is reflected in the appeareance of structure in the gas phase at lower densities than for the bosonic system (see figure 1). Whereas in the solid phase the inclusion of antisymetry do not give rise to a relevant change in the energy of the system. The net effect in the gas to solid transition is that the critical density gets dramatically reduce its value: especifically, for the isotropic case the transition occurs at $nr_0^2 = 50(10)$[3], compared to $nr_0^2 = 290(30)$[1] for the analogous bosonic system. Current work is on the determination of the borders of the stripe phase region of the phase diagram by studying both stability and structural properties.

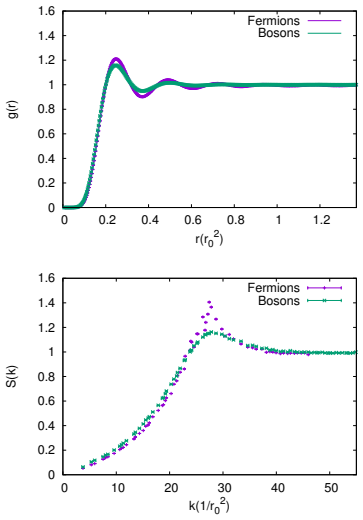


Figure 1: Radial distribution function (up), and static structure factor (down) for the isotropic system at a density nr_0^2= 16 compared for the bosonic and the fermionic system.

An open question is to determine if the system may exhibit a paramagnetic to ferromagnetic phase transition before the crystalization density is reached.

[1] A. Macia, J. Boronat and F. Mazzanti, Phys. Rev. A **90**, 061601R (2014)

[2] R. Bombin, J. Boronat and F. Mazzanti, Phys. Rev. Lett. **119**, 250402 (2017)

[3] N. Matveeva and S. Giorgini, Phys. Rev. Lett. **109**, 200401 (2012)

Variable Potentials for Thermalized Light and Coupled Condensates

David Dung[1], Christian Kurtscheid[1], Julian Schmitt[1,*], Tobias Damm[1], Frank Vewinger[1], Jan Klärs[1,], and Martin Weitz[1]**

[1] *Institut für Angewandte Physik, Universität Bonn, Wegelerstr. 8, 53115 Bonn, Germany*

[*] *present address: Department of Physics, University of Cambridge, United Kingdom*

[**] *present address: Faculty of Science and Technology, University of Twente, The Netherlands*

e-mail: *weitz@iap.uni-bonn.de*

Cold atoms in lattice potentials are an attractive platform to simulate phenomena known from solid state theory, as the Mott-insulator transition. In contrast, the field of photonics usually deals with non-equilibrium physics. Recent advances towards photonic simulators of solid state equilibrium effects include polariton double-site and lattice experiments, as well as the demonstration of a photon condensate in a dye-filled microcavity.

Here we report the creation of variable micropotentials for light within an ultrahigh-reflectivity mirror dye microcavity that is compatible with photon gas thermalization [1, 2]. For examples of microtrap configurations realized with our technique, see Fig. 1. By repeated absorption-emission cycles on the dye molecules photons thermalize to the temperature of the dye solution, and in a single microsite we observe a photon Bose-Einstein microcondensate (Fig. 2). Effective interactions between the otherwise nearly non-interacting photons are observed due to thermo-optic effects, and in a double-well system tunnel coupling between sites is demonstrated, as well as the hybridization of eigenstates. Prospects of the findings include photonic lattices in which cooling alone can produce entangled manybody states.

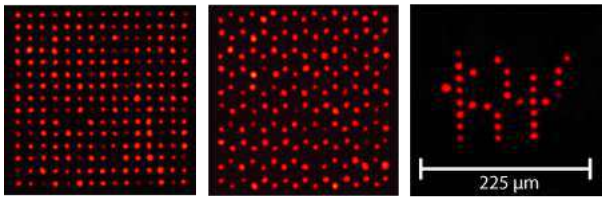


Figure 1: Experimentally observed images of the microcavity emission for two optical lattice potentials for the quantum gas with rectangular (left) and hexagonal (middle) geometry respectively and one non-periodic pattern showing the letters $\hbar\Psi$ (right), as generated by thermo-optical imprinting of the dye refractive index within the microcavity.

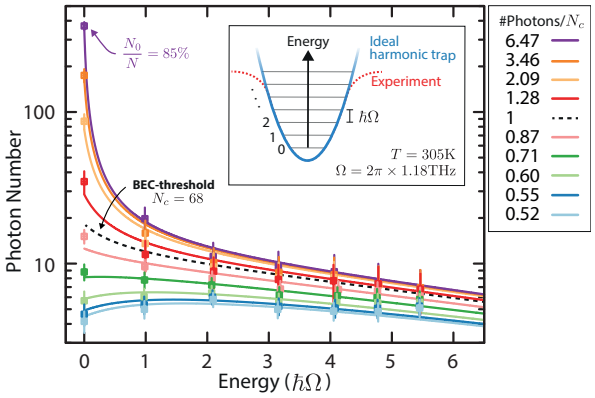


Figure 2: Spectrometer data of the microcavity emission for different total photon numbers N in units of the critical photon number, Nc (dots), together with theoretical expectations (lines). We observe a spectrally sharp condensate peak at the position of the cavity cutoff on top of a broad thermal cloud distributed over all bound seven trap levels.

[1] D. Dung, C. Kurtscheid, T. Damm, J. Schmitt, F. Vewinger, M. Weitz, and J. Klaers, Nature Photonics **11**, 565 (2017).

[2] C. Kurtscheid et al., to be published.

Induced transitions in the attractive Bose-Hubbard model

F. Hamodi, and L. Khaykovich

Department of Physics, QUEST Center and Institute of Nanotechnology and Advanced Materials, Bar-Ilan University, Ramat Gan, 5290002, Israel

e-mail: *lev.khaykovich@biu.ac.il*

We consider N particles distributed on a 1-D optical lattice with M sites and periodic boundary conditions. In the tight binding approximation the system is described by the Bose-Hubbard Hamiltonian:

$$\hat{H} = -J\sum_j(\hat{a}^\dagger_{j+1}\hat{a}_j + H.c.) + \frac{U}{2}\sum_j \hat{n}_j(\hat{n_j}-1), \quad (1)$$

where J is the tunnelling strength and U is the on-site interaction strength. The operator $\hat{a}^\dagger_j$ ($\hat{a}_j$) creates (annihilates) a particle on site j of the lattice. Here we consider the case of attractive interactions, i.e. $U < 0$. In the limit of small systems, the Hamiltonian (1) can be solved by exact diagonalization methods. An efficient approach, which we follow here, is according to Ref. [1].

When the interaction energy dominates ($|U/J| \geq 1$), the ground state of the system can be represented as a superposition of localized many-body states translated across the lattice. In this limit the energy spectrum is split into energy bands. The motion within the band corresponds to the center-of-mass motion of the localized many-body state as a whole. The band separation corresponds to the difference relative motion of the $N - N_f$ and the $N - N_f - 1$ atoms in the localized states respectively, where $N_f = 0, 1, ...$ and $N_f + 1$ are the number of free atoms in these 2 consecutive bands [1].

We consider induced transitions between consecutive energy bands. The system under study consists of 3 atoms distributed over lattices of different sizes (up to 149 sites). The knowledge of the exact eigenstates allows identification of the selection rules for transitions between different eigenstates. The very well known translational symmetry of the system imposes an obvious selection rule which is required by conservation of quasi-momentum. However, we identify subspaces in the total Hilbert space where parity symmetry dictates another and less obvious selection rule which is required by parity conservation. As the parity operator does not simultaneously commute with the Hamiltonian and the translation operator, we do not expect that this selection rule can be extended to the entire Hilbert space. Here we show that such a selection rule is obtained at zero quasi-momentum. Moreover, "near selection rules" conditions are obtained for other quasi-momenta and they show chaotic behaviour in the phase-space of U/J as can be seen in Fig. 1.

Direct application of these selection rules can be observed in the time dynamics of the system subject to resonant interband coupling. We start with the ground state, i.e. all 3 atoms are bound into a localized state. We then apply a weak modulation of the tunnelling strength in resonance with the energy difference to the second band where 2 atoms are bound and the third atoms is free:

$$h\nu = \frac{U}{2}\left(N(N-1) - (N-1)(N-2)\right). \quad (2)$$

Here ν is the oscillation frequency. The time dependent solution shows an exponential growth of the occupation probability of the excited band and after a few tenths of the tunnelling time the population is totally transferred to the first excited band (corresponding to one free atom and a two-atom bound state). Later the occupation probability of the second band decreases again and reaches minimum. This is the expected revival of the ground state population due to coherent time evolution in the finite-sized system. The interesting and unexpected feature in this revival is that its contrast is significantly better in the case of zero quasi-momentum than for other quasi-momenta. In this work we directly relate this revival contrast to the selection rules [2].

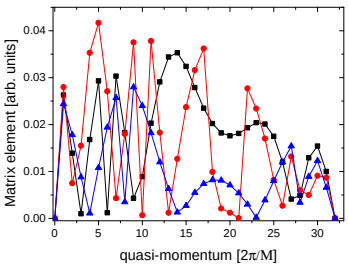


Figure 1: Matrix elements as a function of quasi-momentum for $M = 64$ and three different values of U/J : -7 (blue), -10 (black) and -15 (red). For each value of U/J, the matrix elements nearly vanishes for different quasi-momenta.

[1] O. S. Sørensen, S. Gammelmark, and K. Mølmer, *Relative and center-of-mass motion in the attractive Bose-Hubbard model*, Phys. Rev. A **85**, 043617 (2012).

[2] F. Hamodi and L. Khaykovich, in preparation.

Measurements with cold thulium atoms in optical dipole trap.

V. Khlebnikov[1], **I. Cojocaru**[1,5], **V. Tsyganok**[1,2], **D. Pershin**[1,2], **E. Davletov**[1,2,4], **A. Akimov**[1,3,5]
[1] *Russian Quantum Center, Business Center Ural, 100A Novaya Str., Skolkovo, Moscow, 143025, Russia*
[2] *Moscow Institute of Physics and Technology, Institutskii per. 9, Dolgoprudny, Moscow Region 141701, Russia*
[3] *PN Lebedev Institute RAS, Leninsky Prospekt 53, Moscow, 119991, Russia*
[4] *Center for Energy Systems, Skolkovo Institute of Science and Technology, 3 Nobel Street, Skolkovo, Moscow Region 143026, Russia*
[5] *Texas AM University, 4242 TAMU, College Station, Texas, 77843, USA*
e-mail: *breadoff@gmail.com*

On the way of creating a quantum simulator working on cold thulium atoms we have loaded $2{\cdot}10^6$ polarized thulium atoms at temperatures of 17μK into optical dipole trap. The degree of atomic polarization in the cloud as well as its dependence on experimental parameters were measured. Besides, low-field Fano-Feshbach resonances enabling control of the interatomic scattering length at various temperatures were detected. The temperature of the cloud was regulated via evaporative cooling.

Thulium atom belongs to rare-earth elements with open electronic f-shell submerged beneath a closed outer s-shell. This makes interatomic interactions anisotropic. Besides relatively high magnetic moment of μ=4 Bohr magnetons μ_B provides long-range magnetic dipole-dipole interactions. Exotic many-body quantum phases of these strongly interacting atoms can be investigated if cool them up to Bose-Einstein condensate.

At our setup emitted from oven hot atoms are firstly decelerated in Zeeman slower operating on strong 10 MHz blue 410.6 nm transition. Further cooling occurs in magneto-optical trap (MOT) working on narrow $\Gamma = 0.38$ MHz green 530.7 nm transition. It allows to capture up to $3{\cdot}10^7$ atoms at temperature of 13μK. Both aforementioned transitions are well cyclic enough to have no need in repumping lasers (more details on these cooling stages can be found in previous work [1]). We use over 15Γ far detuned green MOT as it automatically polarizes atoms to their energetically lowest magnetic sublevel. Predominantly one light polarization is absorbed by atoms if position of clouds center shifts from magnetic field zero. In far detuned regime such shift is caused by gravity. High degree of atoms polarization increases phase space density (PSD). Withal further heating and losses due to spin relaxation are minimized as cloud is being at magnetic ground state.

Prepared in such a way cloud is then loaded into 6W horizontally oriented optical dipole trap (ODT) operated on 532 nm light. Reload efficiency of 10% in atoms number is achieved when dipole beam is widened by high frequency sweeping of its spatial position with acousto-optic modulator (AOM). The depth of ODT is managed with the same AOM. Thus there is a tool for evaporatively cooling atoms. Several types of measurements were done in our ODT. Mean cloud polarization was measured with Stern-Gerlach type experiment. Strong dependence of cloud polarization degree on storage magnetic field and dipole beam light polarization was found. Also experiment confirms our theoretical modeling of degree of polarization at different MOT's detunings. Details of this work as well as procedure of MOTs to ODT reload are listed in [2].

Evaporation cooling optimization is made step-by-step by maximizing PSD trying to lose less atoms. Controlling evaporation allows to regulate temperature of atomic cloud. Thus, atomic cloud was made cold enough to detect s-wave Fano-Feshbach resonances which could be clearly separated from strong d-wave resonances by its temperature dependence. Analysis of the Fano-Feshbach resonances and corresponding temperature resonances spectrums allowed identification of the magnetic field leading to zero scattering length thus confirming tunability of the thulium-thulium interactions.

Further study of losses and investigation the reasons for short lifetime of our ODT are the nearest plans.

This research is supported by Russian Science Foundation grant #18-12-00266.

[1] I. Cojocaru, S. Pyatchenkov, et al. , Phys. Rev. A **95**, 012706 (2017).

[2] V. Tsyganok, V. Khlebnikov, et al., `arXiv:1804.09203`

Quantum scale anomaly and spatial coherence in a 2D Fermi superfluid

M. Holten[1], **L. Bayha**[1], **N. Defenu**[2], **A. C. Klein**[1], **P. A. Murthy**[1], **P. M. Preiss**[1], **T. Enss**[2], **and S. Jochim**[1]

[1] *Physics Institute, Heidelberg University, Germany*

[2] *Institute for Theoretical Physics, Heidelberg University, Germany*

e-mail: *mholten@physi.uni-heidelberg.de*

Quantum anomalies are violations of a classical symmetry in the corresponding quantized version of the theory. They appear in quantum field theories when a cut-off has to be introduced to regularize some divergent physical quantity. Quantum anomalies are typically associated only with high energy physics and their influence on experimental observables in other fields is difficult to discern.

On this poster, we report a striking manifestation of a quantum scale anomaly in the breathing mode dynamics of a 2D Fermi superfluid of ultracold atoms (see Fig. 1). In two independent measurements we have studied both the breathing frequency and the position and pair momentum distribution of the cloud during one breathing mode cycle.

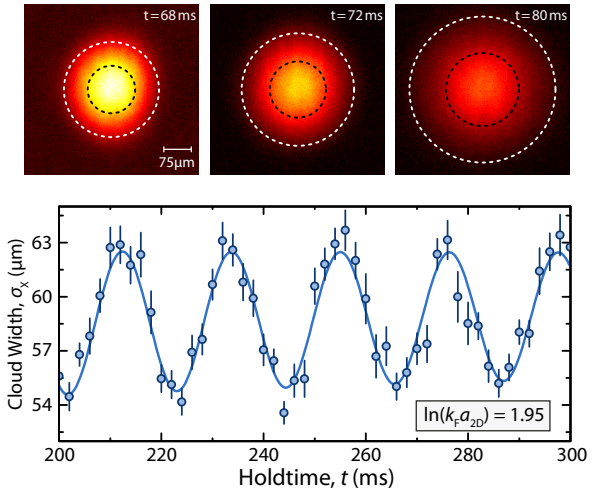


Figure 1: Observation of the breathing mode of a 2D Fermi superfluid in a harmonic confinement

The frequency of the breathing mode is fixed by the scale invariance of the classical Hamiltonian. Scale invariance is broken on the quantum mechanical level by introducing the two dimensional scattering length as a regulator. This leads to a shift of the frequency of the breathing mode of the cloud. We have studied this anomalous frequency shift for a two component Fermi gas in the strongly interacting regime. We find significant shifts away from the scale invariant result that depend strongly on both interactions and temperature [1].

A comparison of this result to the position and momentum distributions we measured in addition shows very good agreement. Whereas the atom distributions exhibit self-similar evolution in the weakly interacting BEC and BCS limits, we found the same violation in the strongly interacting regime. The signature of scale-invariance breaking is enhanced in the first-order coherence function. In particular, the power-law exponents that characterize long-range phase correlations in the system are modified due to this effect, indicating that the quantum anomaly has a significant influence on the critical properties of 2D superfluids [2].

[1] M. Holten, L. Bayha, A. C. Klein, P. A. Murthy, P. M. Preiss, and S. Jochim, arXiv:1803.08879 (2018).

[2] P. A. Murthy, N. Defenu, L. Bayha, M. Holten, P. M. Preiss, T. Enss, and S. Jochim, arXiv:1805.04734 (2018).

Spinor gases of fermionic erbium atoms

G. Natale[1], **S. Baier**[1], **D. Petter**[1], **A. Patscheider**[1], **L. Chomaz**[1], **M. J. Mark**[1,2], **F. Ferlaino**[1,2]
[1] *Institut für Experimentalphysik, Universität Innsbruck, Technikerstraße 25, 6020 Innsbruck, Austria*
[2] *Institut für Quantenoptik und Quanteninformation,Österreichische Akademie der Wissenschaften, 6020 Innsbruck, Austria*
e-mail: *Gabriele.Natale@uibk.ac.at*

Over the last decade, dipolar quantum gases have become an ideal system to study novel phenomena in ultracold quantum physics. Strongly magnetic species open fascinating possibilities to investigate dipole-dipole interaction and its impact on many-body quantum phases and spin physics.

In our experiment in Innsbruck, we evaporatively cool spin-polarized fermionic erbium (Er) atoms to quantum degeneracy, where the temperature of the cloud is as low as 0.1 of the Fermi temperature T_F. The ground state of the fermionic Er has a total angular momentum $F = 19/2$ giving rise to 20 different spin states. We load the spin-polarized sample into a three-dimensional optical lattice and ramp up a magnetic field of 40 G. Exploiting the quadratic Zeeman shift in combination with a radiofrequency pulse, spin mixtures between the two lowest m_f states with different population imbalances can be prepared. In a first set of experiments, we perform a Feshbach scan by reducing the magnetic field and loading the atoms back into an optical dipole trap. Interestingly, we find an interspin resonance centered around 690 mG where the lifetime of the spin mixture exceeds 150 ms even in the strongly interacting regime on resonance. In a second set of experiments, we keep the spin mixture in the lattice and perform modulation spectroscopy to map out the interspin s-wave scattering length over this entire resonance[1].

Our work opens the door to the investigation of the BEC-BCS crossover physics with dipolar atoms and to explore spin phases with highly magnetic atoms (see for example [2, 3, 4]).

References

[1] S. Baier et al., arXiv:1803.11445 (2018)

[2] O. Dutta et al., Reports on Progress in Physics, Volume 78, Number 6 (2015)

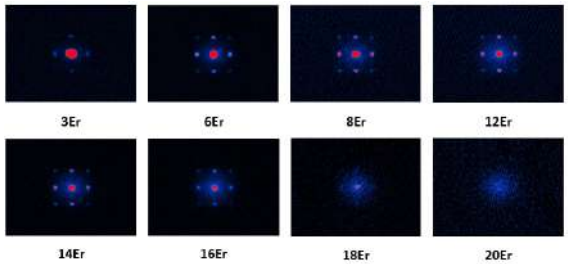
[3] M. A. Baranov et al., Chem. Rev. 112, 9, 5012-5061 (2012)

[4] A. Mazloom et al., Phys. Rev. A 96, 033602 (2017)

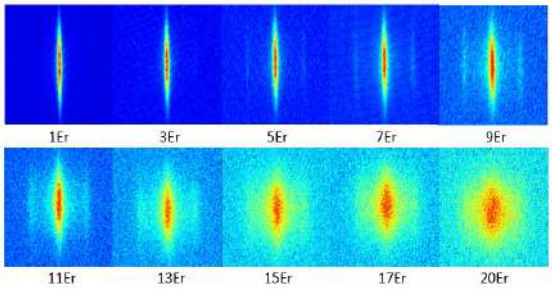
Progress on the research on prototype of Cold Atom Physics Rack for the Chinese Space Station

Jingxin Sun, Bo Fan, Yin Zhang , Wei Xiong and Xuzong Chen*,
School of Electronics Engineering and Computer Science, Peking University, Beijing 100871, China
e-mail: *xuzongchen@pku.edu.cn*

CAPR (Cold Atom Physics Rack) for the Chinese Space Station to be launched in 2022. We present the ground prototype of ultracold degenerate quantum gas experimental platform of CAPR. Using the new cooling approach proposed by our experimental team: Two Stage Crossed Beam Cooling (TSCBC, simplified TSC, Two Stage Cooling), the minimum temperature of 87Rb atomic gas is demonstrated to achieve below 4nK with full optical cross beam traps on the ground. We applied the magnetic levitation technique to levitate the gravity of atoms on the ground it means it will get further low temperature in the space. To prepare the conditions for future experiments, the 1D to 3D optical lattice is formed, phase transition from superfluid to MOTT insulator is demonstrated.



(a) Quantum Phase Transition from a Superfluid to a MOTT Insulator in a 3D Optical Lattice



(b) Quantum Phase Transition from a Superfluid to a MOTT Insulator in a 1D Optical Lattice

Figure 1: Quantum Phase Transition from a Superfluid to a MOTT Insulator

The prototype of CAPR is built, in order to meet the requirements for the operation of the space station, we designed the integrated degenerate quantum gas experimental platform that can be remotely controlled. The prototype needs to be fitted within the net size of 952mm*703mm*815mm, with 1500W power consumption. We designed a miniaturized vacuum system. Using beat-frequency lock-in technology to reduce the complexity of the light path and an FPGA-based control system enables remote operation and miniaturization of the control system.

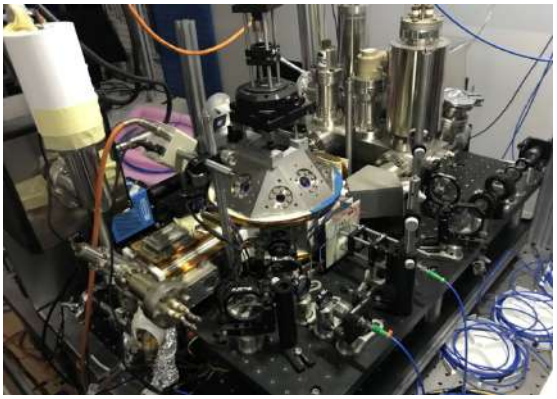


Figure 2: Real Physical Experriment Unit by size of 952mm*703mm*815mm

[1] Chen Li, Tianwei Zhou, Yueyang Zhai, Jinggang Xiang, Tian Luan, Qi Huang, Shifeng Yang, Wei Xiong, and Xuzong Chen, Rev.Sci.Instrum.88,053104(2017)

[2] H.Yao, T.Luan, C.Li, Y.Zhang, Z.Ma, and X.Chen, Opt.Commun.359,123(2016)

[3] T.Luan, H.Yao, L.Wang, C.Li, S.Yang, X.Chen, and Z.Ma, Opt. Express 23, 11378 (2015)

[4] L.Wang, P.Zhang, X.-Z.Chen, and Z.-Y.Ma, J.Phys.B:At.,Mol.Opt.Ph.46,195302(2013)

Pair condensation theory for systems of trapped cold fermionic atoms

J. Takahashi and Y. Yamanaka
Department of Electronic and Physical Systems, Waseda University, Japan
e-mail: *takahashi.j@aoni.waseda.jp*

The condensation of fermion pairs in trapped cold atomic systems is realized experimentally [1, 2]. We attempt to formulate the pair condensation theory for the systems in quantum field theory. Since the systems are translationally non-invariant and inhomogeneous due to the presence of the trapping potentials, the plane wave expansion of the field operator and the picture of the Cooper pair of fermions with opposite momenta in the BCS theory are not appropriate. We do not resort to the local approximation that the BCS theory for homogeneous systems is applied in a spatial region. Our formulation uses the expansion of the field operator in a complete set of Bogoliubov-de Gennes eigenfunctions corresponding with the presence of the trapping potential. Then the gap parameter should be position-dependent, $\Delta(\boldsymbol{x})$. From the systematic calculation of the Green's functions of quantum field theory, we derive the gap equation, i.e. the self-consistent equation for $\Delta(\boldsymbol{x})$. The gap equation is solved numerically.

Explicitly, we consider the following Hamiltonian

$$\hat{H} = \int d\boldsymbol{x} \left[\sum_{j=\uparrow,\downarrow} \hat{\psi}^{\dagger}_{H,j}(x) h_0(x) \hat{\psi}_{H,j}(x) - g \int d\boldsymbol{x} \hat{\psi}^{\dagger}_{H,\uparrow}(x) \hat{\psi}^{\dagger}_{H,\downarrow}(x) \hat{\psi}_{H,\downarrow}(x) \hat{\psi}_{H,\uparrow}(x) \right],$$

$$h_0 = -\frac{\nabla^2}{2m} + V(\boldsymbol{x}) - \mu,$$

where $V(\boldsymbol{x})$, m, g, and μ are the trapping potential, the mass of atoms, the coupling constant, and the chemical potential and $\hat{\psi}_{H,j}$ is the field operator in Heisenberg picture. In order to deal with the pair condensation for the inhomogeneous system, we take the following renormalized unperturbed Hamiltonian with the gap function $\Delta(\boldsymbol{x})$,

$$\hat{H}_u = \int d\boldsymbol{x} \left[\sum_{j=\uparrow,\downarrow} \hat{\psi}^{\dagger}_{j}(x) h_0(x) \hat{\psi}_{j}(x) + \Delta(\boldsymbol{x}) \left(\hat{\psi}^{\dagger}_{\uparrow}(x) \hat{\psi}^{\dagger}_{\downarrow}(x) + \hat{\psi}_{\downarrow}(x) \hat{\psi}_{\uparrow}(x) \right) \right] + \delta\hat{H},$$

where $\hat{\psi}_j$ is the field operator in interaction picture and $\delta\hat{H}$ is the energy counter term [3]

$$\delta\hat{H} = \int d\boldsymbol{x} d\boldsymbol{x}' \sum_{j=\uparrow,\downarrow} \hat{\psi}^{\dagger}_{in,j}(x) \delta\omega_j(\boldsymbol{x}, \boldsymbol{x}') \hat{\psi}_{in,j}(x').$$

The expansion of $\hat{\psi}_j$ in a complete set of Bogoliubov-de Gennes eigenfunctions leads to the daigonalized $\hat{H}_u$,

$$\hat{H}_u = \sum_i \omega^r_i \left(\hat{a}^{r,\dagger}_i \hat{a}^r_i + \hat{b}^{r,\dagger}_i \hat{b}^r_i \right),$$

and the vacuum of the system is defined by

$$\hat{a}^r_i |0\rangle = \hat{b}^r_i |0\rangle = 0.$$

The two-point causal Green's functions are calculated according to the Feynman diagram method, using the ladder approximation. The renormalization conditions on them give the self-consistent equation of $\Delta(\boldsymbol{x})$ and determine the energy counter term. Finally, we solve the derived gap equation numerically.

In this poster, we investigate physical implications of the numerical result of $\Delta(\boldsymbol{x})$ as well as the imposed renormalization conditions themselves. As in Ref. [4], quantum fluctuations of the zero mode becomes large in the condensation of trapped bosons and special care must be taken. The zero mode fluctuation bring physically observable effects in the alpha condensation of nuclear physics [5]. From this viewpoint, we also argue the pair condensation and the associated zero mode in the trapped fermionic system.

[1] C. A. Regal, M. Greiner, and D. S. Jin, Phys. Rev. Lett. **92**, 040403 (2004).

[2] M. W. Zwierlein et al, Phys. Rev. Lett. **92**, 120403 (2004).

[3] K. Kuwahara, Y. Nakamura, and Y. Yamanaka, Int. J. Mod. Phys. B **32**, 1850111 (2018).

[4] Y. Nakamura, J. Takahashi, and Y. Yamanaka, Phys. Rev. A. **89**, 013613 (2014).

[5] Y. Nakamura, J. Takahashi, Y. Yamanaka, and S. Ohkubo, Phys. Rev. C **94**, 014314 (2016).

Bose-Einstein Condensates with Rotating Dipole Moments

S. B. Prasad[1], **B. C. Mulkerin**[2], **and A. M. Martin**[1]
[1] *School of Physics, The University of Melbourne, Melbourne 3010, Australia*
[2] *Centre for Quantum and Optical Science, Swinburne University of Technology, Melbourne 3122, Australia*
e-mail: *sbad@student.unimelb.edu.au*

Dipolar quantum gases offer a novel platform for the study of several interesting phenomena that occur in strongly correlated quantum systems [1]. Previously, it has been suggested that the magnitude and sign of the dipole-dipole interaction strength, ϵ_{dd}, in a dipolar Bose-Einstein condensate (BEC), may be tuned by rapidly rotating the individual dipole moments [2]. In particular, the dipole-dipole potential resulting from a polarising field rotating about the z-axis, in the x-y plane, with an associated interaction strength ϵ_{dd}, is identical to the dipole-dipole potential for a polarisation along the z-axis with an associated interaction strength $-\epsilon_{dd}/2$, when time-averaged over one rotation cycle.

The system under consideration is a scalar Bose-Einstein condensate, with a relative dipolar interaction strength ϵ_{dd}, which is confined by a harmonic trapping potential with a cylindrically-symmetric trapping strength of $\omega_\perp$. The polarising field for the dipole moments is specified to be aligned in the x-y plane and rotating about the z-axis with an angular frequency of Ω. By analytically solving the Gross-Pitaevskii equation in the Thomas-Fermi limit, we obtain stationary states for arbitrary Ω and $\epsilon_{dd} \in [0, 1)$. In general, these solutions are qualitatively similar to the stationary Thomas-Fermi solutions for a non-dipolar BEC in a rotating, cylindrically asymmetric, harmonic trap [3]. However, when $\Omega \gg \omega_\perp$, the stationary solutions are found to closely match those of a dipolar BEC in an identical trapping geometry, but with non-rotating dipole moments aligned along the z-axis [4] and an associated relative dipolar interaction strength $-\epsilon_{dd}/2$, as demonstrated recently in an experiment [5].

We have also investigated the dynamical stability of the condensate with respect to collective oscillations arising from linearised perturbations about these stationary Thomas-Fermi solutions. The results of this procedure imply that, for $\Omega \geq \omega_\perp$, a dipolar condensate may be dynamically unstable above a threshold dipolar interaction strength $\epsilon'_{dd}(\Omega)$. This prediction, however, may not be matched by numerical solutions of the Gross-Pitaevskii equation in this regime, or by experiment.

[1] T. Lahaye et. al., Rep. Prog. Phys. 72, 126401 (2009).

[2] S. Giovanazzi, A. Görlitz and T. Pfau, Phys. Rev. Lett. 89, 130401 (2002)

[3] A. Recati, F. Zambelli and S. Stringari, Phys. Rev. Lett. 86, 377 - 390 (2001)

[4] C. Eberlein, S. Giovanazzi and D. H. J. O'Dell, Phys. Rev. A 71, 033618 (2005)

[5] Y. Tang, W. Kao, K-Y. Li and B. L. Lev, arXiv:1803.10867v1 (2018)

Further Cooling of Alkali Atomic Gas in "micro-gravity" on earth

Wei Xiong[1], **Chen Li**[1], **Tian Luan**[1], **Hui Li**[1], **Jiachen Yu**[1], **Henan Wang**[1] and **Xuzong Chen**[1]
[1] *School of Electronics Engineering and Computer Science, Peking University, Beijing 100871, China*
e-mail: *xuzongchen@pku.edu.cn*

We report a demonstration of further cooling ^{87}Rb atomic gas in "micro-gravity" under the condition of normal gravity on earth with a compact quantum gas setup . After generating an atomic cloud with Bose condensate and thermal background, the atomic gas is levitated by magnetic field and adiabatically released in an optical trap with much lower frequency. The atomic cloud can be further cooled to $3.6nK$, while the trap frequency achieves as low as $2.5Hz$. The apparatus also includes cooling scheme for degenerate Fermi gas ^{40}K, of which further cooling will soon be implemented. This system holds promise for many applications, such as atomic interferometry, atomic gyroscope, magnetometery, and many basic scientific research directions, such as quantum simulations, and atom optics.

[1] Chen Li, Tianwei Zhou, Yueyang Zhai, Jinggang Xiang, Tian Luan, Qi Huang, Shifeng Yang, Wei Xiong, and Xuzong Chen, Review of Scientific Instruments **88**, 053104 (2017)

[2] H. Yao, T. Luan, C. Li, Y. Zhang, Z. Ma, and X. Chen, Opt. Commun. **359**, 123 (2016)

[3] T. Luan, H. Yao, L. Wang, C. Li, S. Yang, X. Chen, and Z. Ma, Opt. Express **23**, 11378 (2015)

[4] L. Wang, P. Zhang, X.-Z. Chen, and Z.-Y. Ma, J. Phys. B: At., Mol. Opt. Phys. **46**, 195302 (2013)

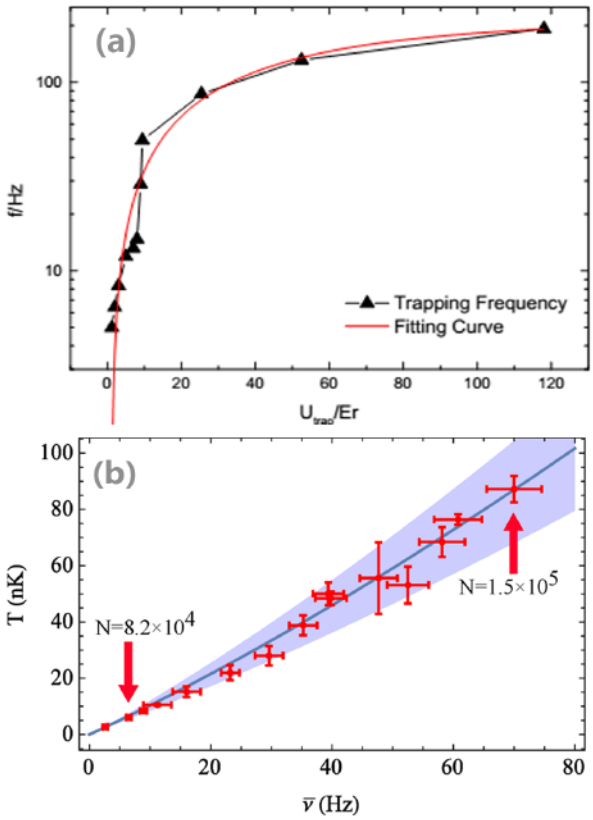


Figure 1: (a)As the depth of further cooling optical trap being tuned, the corresponding trapping frequency is measured, and it achieves as low as $2.5Hz$. (b)The temperature of the atomic gas is determined via measuring the condensate fraction, which is related to the temperature as $T/T_C = 1 - (N_C/N)^3$, where the critical temperature is $T_C = 0.94\hbar(\omega_x\omega_y\omega_z)^{1/3}N^{1/3}$, N is the total atom number of the atomic gas, N_C is the atom number of condensate, ω_x, ω_y and ω_z are the trap frequencies in three orthogonal directions.

Grassmann Phase Space Theory for Fermions

B. J. Dalton[1], N. Kidwani[1], J. Jeffers[2] and S. M. Barnett[3]

Centre for Quantum and Optical Science, Swinburne University of Technology, Melbourne, Victoria 3122,Australia[1]
Department of Physics, University of Strathclyde, Glasgow G4ONG, UK[2]
School of Physics and Astronomy, University of Glasgow, Glasgow G12 8QQ, UK[3]

bdalton@swin.edu.au

In both quantum optics and cold atom physics, the behaviour of bosonic photons and atoms is often treated using phase space methods, where mode annihilation and creation operators are represented by c-number phase space variables, with the density operator equivalent to a distribution function of these variables. The anti-commutation rules for fermion annihilation, creation operators suggests the possibility of using anti-commuting Grassmann variables to represent these operators. However, in spite of the seminal work by Cahill and Glauber [1] and a few applications [2], [3], [4] the use of Grassmann phase space methods in quantum - atom optics to treat fermionic systems is rather rare, though fermion coherent states using Grassmann variables are widely used in particle physics.

The theory of Grassmann phase space methods for fermions is developed, showing how the distribution function is defined and used to determine quantum correlation functions (QCF), Fock state populations and coherences via Grassmann phase space integrals, how the Fokker-Planck equations are obtained and then converted into equivalent Ito equations for stochastic Grassmann variables. The QCF etc are then given as stochastic averages of products of Grassmann stochastic variables. The number of c-number Wiener increments involved is $2n^2$, if there are n modes (for bosons there are only $2n$). Also, the sign for the drift term in the Ito equation is reversed and the diffusion matrix in the Fokker-Planck equation is anti-symmetric rather than symmetric. The un-normalised B distribution [2], [5], [6], [7] is of particular importance for determining Fock state populations and coherences, and as pointed out in [2], the drift vector in its Fokker-Planck equation only depends linearly on the Grassmann variables. The diffusion matrix has a bilinear dependence. Using these key features we show that the averages of products of Grassmann stochastic variables (that determine QCF etc) at a later time are related to those at the initial time (which are obtained from initial conditions) via a transformation matrix that only involves c-numbers - though these are stochastic. This resolves a major problem in carrying out numerical calculations based on Grassmann phase space theories of fermion systems, showing that calculations of QCF etc can be carried out without needing to represent anti-commuting Grassmann variables themselves on the computer.

As a simple test case we apply the B distribution theory and the Ito stochastic equations to determine the coherence between Cooper pair states in a four mode fermionic system involving spin conserving interactions between two spin 1/2 fermions, where modes with momenta $-k, +k$ - each associated with spin up, spin down states, are involved.

References

[1] K. E. Cahill and R. J. Glauber, Phys. Rev. A **59**, 1538 (1999).

[2] L. Plimak, M. J. Collett and M. K. Olsen, Phys. Rev. A **64**, 063409 (2001).

[3] B. J. Dalton, B. M. Garraway, J. Jeffers and S. M. Barnett, Ann. Phys. **334**, 100 (2013).

[4] E. A. Polyakov, Phys. Rev. A **94**, 062104 (2016).

[5] B. J. Dalton, J. Jeffers and S. M. Barnett, *Phase Space Methods for Degenerate Quantum Gases*, (Oxford University Press, Oxford, 2015).

[6] B. J. Dalton, J. Jeffers and S. M. Barnett, Ann. Phys. **370**, 12 (2016).

[7] B. J. Dalton, J. Jeffers and S. M. Barnett, Forts. Phys. **65**, 1600038 (2017).

Flat-band ferromagnetism of SU(N) Hubbard model on Tasaki lattice

Ruijin Liu[1], **Wenxing Nie**[2], **and Wei Zhang**[1,3]

[1] *Department of physics, Renmin University of China, 100872 Beijing, China*

[2] *College of Physical Science and Technology, Sichuan University, 610064 Sichuan, China*

[3] *Beijing Key Laboratory of Opto-electronic Functional Materials and Micro-nano Devices, Renmin University of China, 100872 Beijing, China*

e-mail: *wzhangl@ruc.edu.cn*

We study the fermion-Hubbard model on highly frustrated one and two-dimensional Tasaki lattice with an on-site $SU(N)$ symmetric repulsive interaction of strength $U > 0$. With specific ratio of hopping parameters along different paths on the lattice, the lowest-energy one-particle band will be completely dispersionless. By constructing localized many-particle ground states in the flat-band, the system can be mapped to a geometric site-percolation problem with a nontrivial, SU(N)-correlated weight for each configuration. In the thermodynamical limit, the occurrence of percolation indicates para-ferro magnetic transition. We obtain analytical results for 1D lattice through transfer-matrix method and numerical results for 2D lattice utilizing Metropolis Monte Carlo simulation. The transition point remains same for arbitrary $N = 3, 4, \cdots$, for 1D cases, while increases with N for 2D cases, due to the strength of effective repulsive interaction becomes stronger.

Entanglement and squeezing for two Bose Polarons

M.A. Garcia-March[1], **C. Charalambous**[2], **A. Lampo**[1], **M. Mehboudi**[1], **and M. Lewenstein**[1,2]
[1] *ICFO – Institut de Ciències Fotòniques, The Barcelona Institute of Science and Technology, 08860 Castelldefels (Barcelona), Spain*
[2] *ICREA, Lluis Companys 23, E-08010 Barcelona, Spain*
e-mail: *Miguel.Garcia-March@icfo.eu*

We study the out-of-equilibrium dynamics of two impurities immersed in a Bose-Einstein condensate (BEC) with an open quantum system formalism. Such an approach was introduced for a single impurity in an homogeneous [1] and inhomogeneous [2] BEC. This was a new approach to the Bose polaron problem. With this formalism, we show that the two impurities play the role of quantum Brownian particles interacting with a bath of oscillators corresponding to the Bogoliubov modes of the BEC. We characterize the dynamics of the Brownian impurities with a Langevin-like quantum stochastic equation. This equation is non-local in time, and thus the dynamics of both impurities in a BEC carry certain amount of memory. The Langevin equation is solved to evaluate the covariance matrix, namely a matrix which elements are all the position and momentum correlation functions. We find that the presence of the bath induces an interaction between the impurities which leads to entanglement among them. Particularly, we study entanglement as a function of the physical quantities of the system, such as temperature, impurity-gas coupling, gas interatomic interaction and density. These parameters may be experimentally tuned allowing to control the amount of entanglement between the impurities. We distinguish the situation in which the impurity is trapped in a harmonic potential and that where it is untrapped.

For the untrapped case, we obtain analytically all position and momentum correlation functions. We find entanglement at long times, which decreases linearly and disappears at long enough times. We study the dependence of the entanglement on the parameters of the system, which allows us to conjecture that the decreasing of entanglement is attributed to their interaction with the bath rather than them running away from each other.

For the trapped case, we obtain the covariance matrix elements numerically. We find that the bath induces entanglement between the two impurities at very low temperatures. This entanglement decreases as a function of temperature (see Fig. 1, where η_2 is the coupling strength between the second kind of impurity and the BEC). A detailed study of the entanglement dependence on the parameters of the system can be found in Ref. [3]. Squeezing also occurs in a regime of parameters which approximately coincides with that of entanglement.

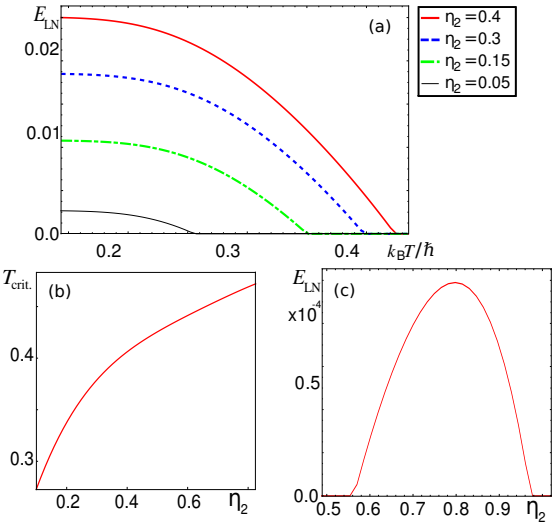


Figure 1: (a) temperature dependence of entanglement for various couplings. As shown increasing the interactions of second type of particles, η_2, enhances entanglement, at fixed T. For increasing T, entanglement decreases and eventually vanishes at certain $T_{\rm crit}$. (b) The $T_{\rm crit}$ increases with η_2. (c) the entanglement at fixed $T = 4.35nK$ increases for a range of η_2 and then decreases to zero. We considered impurities of potassium K in a bath of particles of Rubidium Rb, with trap frequency for the impurity of type 1, $\Omega_1 = 600\pi Hz$, and type 2, $\Omega_2 = 450\pi Hz$, $\eta_1 = 0.325$, density $n_0 = 350(\mu m)^{-1}$, coupling constant for the BEC $g_{\rm B} = 9.75 \cdot 10^{-39} J \cdot m$. Both traps for impurities 1 and 2 are located at the same position.

We emphasize that this study is performed for a realistic physical model: we avoid manipulating it by artificial Hamiltonian terms or by introducing arbitrarily conventional spectral densities. The parameters of the system used are within current experimental feasibility. These results on squeezing and entanglement are particularly interesting as they represent resources for quantum technologies.

[1] A. Lampo, S.H. Lim, M.A. Garcia-March, and M. Lewenstein, Quantum **1**, 30 (2017).

[2] A. Lampo, C. Charalambous, M.A. Garcia-March, and M. Lewenstein, arXiv:1803.08946.

[3] C. Charalambous, M.A. Garcia-March, A. Lampo, M. Mehboudi, M. Lewenstein, arXiv:1805.00709.

Design of an ultra-cold atom setup in microgravity

Bin Wang[1], Wei Xiong[2], Shuyu Zhou[1], Dijun Chen[1], Qiuzhi Qu[1],Tang Li[1], Lin Li[1], Tieqiang Song[1], Weibiao Chen[1], Xuzong Chen[2], and Liang Liu[1]

[1] *Key Laboratory for Quantum Optics, Shanghai Institute of Optics and Fine Mechanics, The Chinese Academy of Sciences, 201800 Shanghai, China*

[2] *School of Electronics Engineering & Computer Science, Peking University, 10087 Beijing, China*

e-mail: *wangbin@siom.ac.cn*

Cold Atom Physics Rack (CAPR) is scheduled for launch in 2022 as a multiuser ultra-cold atom setup locating in Science Module II of the Chinese Space Station to study cold atomic physics with Bose-Einstein condensates of bosonic ^{87}Rb and degenerate Fermi gases of ^{40}K. The purpose of the CAPR is to achieve quantum degenerate gases at picokelvin temperature and to implement a series of challenging experiments under the special condition of microgravity.

The CAPR includes a support rack and an ultra-cold atom setup. As shown in Fig.1(a), the ultra-cold atom setup located in the center of the support rack. The support rack consists of a rack thermal drawer and a rack control system which are located in the bottom of a rack main body. The rack thermal drawer is designed to provide two separate water cooling circuits for rack control system and ultra-cold atom setup, and the total maximum flow is 170 kg/hr. The rack control system manages the rack thermal drawer and communicate with the ultra-cold atom setup. The ultra-cold atom setup includes three parts: physics package, laser and experimental electronics subsystems. Each subsystem is mounted to the main body of the support rack.

As shown in Fig.1(b), the physic package with an UHV pumping system, an experiment chamber, a microwave/RF source and a laser splitting/combining module is located in the top of the support rack. The experiment chamber consists of a science chamber (3D-MOT), a differential pumping stage (DPS), a preparation chamber (2D-MOT) and a magnetic shielding. The vacuum pumps used in the science chamber are an ion pump with 20L/s and a SAES NEXTorr D500-5 compact pump, while another 2L/s ion pump is used in the preparation chamber. The science and preparation chambers have the target vacuum of 2×10^{-9} Pa and 10^{-7} Pa, respectively. The laser subsystem includes five laser modules which are used in ultra-cold atom setup and in the first-stage scientific mission. With modular and entire fiber-optical design, the laser modules can be updated independently in order to satisfy future follow-up scientific mission requirements in orbit, while the reliability and environmental temperature suitability of the laser subsystem will be improved. The electronics subsystem is designed to provide secondary power supply and manage the timing sequence of preparing the ultra-cold atoms and subsequently realizing the scientific tasks.

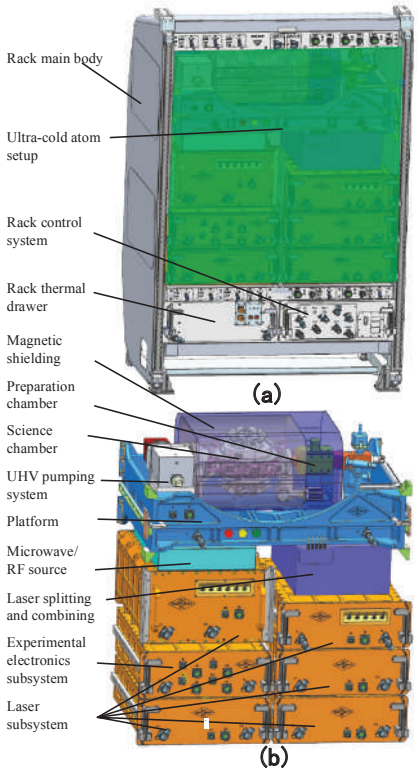


Figure 1: (a) CAPR consisting of a support rack and an ultra-cold atom setup. (b) Overview of ultra-cold atom setup. The physic package contains UHV pumping system, 2D-MOT, DPS , 3D-MOT, magnetic shielding, microwave/RF source and laser splitting/combining modoule, which are mounted on both sides of a platform. Laser subsystem and electronics subsystem are localed in the bottom of the ultra-cold atom setup.

[1] Xuzong Chen, Liang Liu, Weibiao Chen et al., Conference: 25th International Conference on Atomic Physics. **311**, (2016).

Prospects of reaching the quantum regime in Li/Yb$^+$

H. Fürst[1], **N. Ewald**[1], **H. Hirzler**[1], **J. Arias Espinoza**[1], **J. Joger**[1], **T. Secker**[2], **T. Feldker**[1], **M. Tomza**[3] **and R. Gerritsma**[1]

[1] *Institute of Physics, University of Amsterdam, Science Park 904, 1098 XH Amsterdam, Netherlands*
[2] *Eindhoven University of Technology, Post Office Box 513, 5600 MB Eindhoven, Netherlands*
[3] *Faculty of Physics, University of Warsaw, Pasteura 5, 02-093 Warsaw, Poland*
e-mail: *furst@uva.nl*

We report on the progress in our hybrid atom-ion experiment, where we overlap trapped laser-cooled Yb$^+$ ions with a cloud of cold ^{6}Li atoms as symbolically depicted in Fig. 1. This combination of species has recently been proposed to be the most suitable system to reach the quantum limit in atom-ion experiments [1], as its favorable mass ratio leads to suppressed intrinsic- and excess micromotion induced heating of the system [2].

Motivated by the idea of a buffer-gas cooled qubit, we observe the spin dynamics of single Yb$^+$ ions immersed in a cold cloud of spin-polarized ^{6}Li atoms. For a spin encoded in the Zeeman ground states of

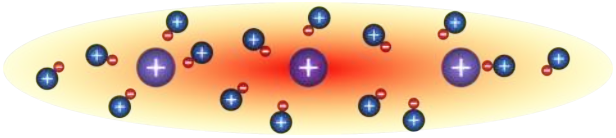


Figure 1: Symbolic picture of a trapped string of three ions, immersed in a cloud of atoms.

^{174}Yb$^+$, we find that the atomic environment polarizes the spin of the ion by 93(4) % after a few Langevin collisions, pointing to strong spin-exchange rates. For the hyperfine ground states of ^{171}Yb$^+$, we also find strong rates towards spin polarization. However, relaxation towards the $F = 0$ ground state occurs after 7.7(1.5) Langevin collisions. We investigate spin impurity atoms as possible source of apparent spin-relaxation leading us to interpret the observed spin-relaxation rates as an upper limit. Using *ab initio* electronic structure and quantum scattering calculations, we explain the observed rates and analyze their implications for the possible observation of magnetic Feshbach resonances between atoms and ions [3, 4].

A major requirement for the observation of these resonances are collision energies low enough to reach the s-wave (quantum) limit. Therefore the creation of an ultracold cloud of ^{6}Li atoms is necessary, which was recently achieved in our experiment employing a crossed optical dipole trap, overlapped with the ion trap. We present preliminary results on atom numbers and temperatures of the atomic cloud that can be used for the exploration of atom-ion Feshbach resonances.

Having ultracold atoms at hand, we estimate the accessibility of reaching s-wave collision energies within our experiment. Therefore we perform numerical simulations of trapped ^{171}Yb$^+$ ions that are buffer gas cooled by a cold cloud of ^{6}Li atoms [5]. Treating the atoms and ions classically, we compute that the collision energy indeed reaches below the quantum limit for a perfect linear Paul trap using the trapping parameters obtained from our experiment. We analyze the effect of imperfections that cause excess micromotion. We find that the suppression of excess micromotion required to reach the quantum limit should be within experimental reach [6]. We analyze the detection and suppression of excess micromotion in our setup and find collision energies that are a factor 2-11 larger than the quantum limit, indicating that modest improvements in micromotion detection and compensation are required to study atom-ion mixtures in the quantum regime.

[1] M. Cetina *et al.*, Phys. Rev. Lett. 109, **253201** (2012)

[2] Z. Meir *et al.*, Phys. Rev. Lett. 117, **243401** (2016)

[3] M. Tomza *et al.*, Phys. Rev. A 91, **042706** (2015)

[4] H. Fürst *et al.*, ArXiv e-prints, **arXiv:1712.07873** (2017)

[5] H. Fürst *et al.*, ArXiv e-prints, **arXiv:1804.04486** (2018)

[6] Härter A and Denschlag J H 2014 *Contemp. Phys.* **55** 33–45

Quantum Criticality and Tomonaga-Luttinger Liquid in One-dimensional Bose Gases

Bing Yang[1,3], **Yang-Yang Chen**[2], **Yong-Guang Zheng** [1,3], **Hui Sun**[1,3], **Han-Ning Dai**[1,3], **Xi-Wen Guan**[2], **Zhen-Sheng Yuan**[1,3] **and Jian-Wei Pan**[1,3]

[1] *Physikalisches Institut, Ruprecht-Karls-Universität Heidelberg, Im Neuenheimer Feld 226, 69120 Heidelberg, Germany*

[2] *State Key Laboratory of Magnetic Resonance and Atomic and Molecular Physics, Wuhan Institute of Physics and Mathematics, Chinese Academy of Sciences, Wuhan 430071, China*

[3] *Hefei National Laboratory for Physical Sciences at Microscale and Department of Modern Physics, University of Science and Technology of China, Hefei, Anhui 230026, China*

e-mail: *pan@ustc.edu.cn*

We experimentally investigate the quantum criticality and Tomonaga-Luttinger liquid (TLL) behavior within one-dimensional (1D) ultracold ^{87}Rb atoms. Based on the measured density profiles at different temperatures, the universal scaling laws of thermodynamic quantities are observed. The quantum critical regime and the relevant crossover temperatures are determined through the double-peak structure of the specific heat. In the TLL regime, we obtain the Luttinger parameter by probing sound propagation. Furthermore, a characteristic power-law behavior emerges in the measured momentum distributions of the 1D ultracold gas, confirming the existence of the TLL.

[1] Bing Yang, Yang-Yang Chen, Yong-Guang Zheng, Hui Sun, Han-Ning Dai, Xi-Wen Guan, Zhen-Sheng Yuan, and Jian-Wei Pan, Phys. Rev. Lett **119**, 165701 (2017).

[2] `https://journals.aps.org/prl/abstract/10.1103/PhysRevLett.119.165701`

Collisional cooling of trapped ions with ultracold atoms

, S.A. Rangwala[1], S. Dutta[1,2], R. Sawant[1,3], M. Niranjan[1], N. Joshi[1], S. Vashist[1], A. Prakash[1], A. Pandey[1]

[1] *Raman Research Institute, C. V. Raman Avanue, Sadashivanagar, Bangalore 560080, India*

[2] *Department of Physics, Indian Institute of Science Education and Research, Bhopal 462066, India*

[3] *Joint Quantum Centre (JQC) Durham-Newcastle, Department of Physics, Durham University, South Road, Durham DH1 3LE, United Kingdom*

e-mail: *sarangwala@rri.res.in*

The act of placing a single ion within a cloud of ultracold atoms creates a system with a distinct impurity [1, 2]. While both, trapped ultracold atoms and ions can be produced and manipulated with great precision, the hybrid combination of these traps have thrown up challenges in realizing the same level of control for hybrid systems [3, 4]. Ion-atom collision in traps, which is the fundamental two body process in such systems, exhibits complex behavior, which determines the cooling of the trapped ions [5].

We study alkali ions placed in a MOT of alkali atoms. For a parent-daughter relation between atoms and ions, the ions and atoms have equal mass. Nevertheless the ions are very effectively cooled in collision by the trapped atoms [5]. This is because the cold atom distribution is finite in its extent and is centered precisely at the bottom of the ion trap where the rotating saddle potential is centered.

Another consequence of the finite size of the atomic reservoir is that lighter mass ions can be collisionally cooled by heavier mass atoms. This is shown for K^+ ions with an Rb MOT and Rb^+ ions with a Cs MOT [6]. Further the limit of attainable temperature for the lighter ion is also decided by the spatial extent of the atom distribution and not the temperature of atoms, in the regime where collisions between ions and atoms can be treated classically.

In a 'parent atom - daughter ion' collision, symmetry allows the atomic valance electron to hop onto the ion with no energy cost. In such a process, while very little momentum may be exchanged between the initial ion and atom collision pair, the charge state can swap, and therefore post collision, a cold ion results at the center of the ion trap and a fast atom exits. This is the phenomenon of swap cooling and it manifests when the colliding ion-atom pair are identical, except for the extra electron [5, 7]. Experimentally, at room temperature values of the ion, it is found that a single swap collision is 100 times more efficient in cooling the ion than a generic elastic collision [7].

In order to systematically explore the regime where only a few partial waves describe the binary ion-atom collision, a new experiment is under development. Here the effort is to combine the experiments with alkali atoms and ions and the more conventional alkaline earth ions, which are readily laser cooled. The species of interest here are lithium and calcium. Experimental details and future prospects with these systems will be discussed.

References

[1] C. Zipkes, S. Palzer, C. Sias, and M.Köhl, Nature (London) 464, 388 (2010).

[2] S. Schmid, A. Härter, and J. Hecker Denschlag, Phys. Rev. Lett. 105, 133202 (2010).

[3] M. Cetina, A. T. Grier, and V. Vuletić, Phys. Rev. Lett. 109,253201 (2012).

[4] Z.Meir, T. Sikorsky, R. Ben-shlomi, N. Akerman, Y. Dallal, and R. Ozeri, Phys. Rev. Lett. 117, 243401 (2016).

[5] K. Ravi, S. Lee, A. Sharma, G.Werth, and S. A. Rangwala, Nat. Commun. 3, 1126 (2012).

[6] S. Dutta, R. Sawant, and S. A. Rangwala, Phys. Rev. Lett. 118, 113401 (2017).

[7] S. Dutta, and S. A. Rangwala, Phys. Rev. A 97, 041401(R) (2018),

Frequency comb cooling of atoms

N. Šantić[1], A. Cipriš[2], D. Buhin[1], D. Kovačić[1], I. Krešić[1], D. Aumiler[1], and T. Ban[1]
[1] *Institute of Physics, Bijenička cesta 46, 10000 Zagreb, Croatia*
[2] *Universit Côte dAzur, CNRS, Institut de Physique de Nice, Valbonne F-06560, France*
e-mail: *ticijana@ifs.hr*

Inducing mechanical action on atoms by continuous wave (CW) laser excitation has been a central topic in atomic physics for decades. Laser cooling and trapping of atoms, a technique that enables production of dense (ultra)cold atomic samples, was made available by employing radiation pressure and dipole forces. Furthermore, atomic self-organization and collective cavity cooling have been demonstrated in cavity-optomechanical systems with cold atomic ensembles. Yet, in contrast to the rich and fruitful field of CW-laser-induced optomechanics, the investigations of mechanical action on atoms due to interaction with trains of ultrashort laser pulses, i.e. frequency combs (FCs), are scarce in literature.

Laser cooling techniques are still limited to atoms with simple energy level structure and closed transitions accessible by current continuous wave (CW) laser technology. Laser cooling of more complex atomic species and molecules, or even simple atoms with strong cycling transitions in the vacuum ultraviolet (VUV) where generation of CW laser light is demanding, still remains an experimental challenge. The aforementioned problems can be approached by using mode-locked ultrashort lasers with high pulse repetition rates which produce stabilized optical FCs which simultaneously provide high peak powers needed for the efficient frequency conversion and the long coherence of CW lasers needed for the efficient cooling.

Employing the regular comb spectrum has been proposed for laser cooling of complex multilevel atoms and molecules [1] and for simultaneous cooling of multiple atomic species [2]. According to our knowledge, there are only two recent experiments where FC cooling was observed. FC cooling on the Rb two-photon transition at 778 nm has been demonstrated in the work by Jayich et al. [3]. Cooling is achieved through a coherent process in which multiple excitation pathways are excited by different combinations of comb modes. FC cooling of trapped magnesium ions has been achieved in the work by Rodriguez et al. [4], where the high peak powers of the FC is employed together with its long coherence, thus opening a route towards laser cooling of species with strong cycling transitions in the UV and VUV.

I will present our recent results on sub-Doppler cooling of rubidium atoms on a dipole-allowed transition at 780 nm by using a frequency comb [5]. Temperatures as low as 55 μK were measured in a one-dimensional FC cooling geometry using time-of-flight spectroscopy. We attribute the sub-Doppler temperatures observed in FC cooling to the same mechanisms that produce sub-Doppler temperatures when cooling with continuous-wave lasers. Laser cooling with FCs could enable achieving sub-Doppler temperatures for the atoms with dipole-allowed transitions in the vacuum ultraviolet. This can significantly improve the precision of optical frequency standards, enable measurements of fundamental constants with unprecedented accuracy, and open up the possibility to reach quantum degeneracy with atoms that have optical transitions unreachable by continuous wave lasers such as hydrogen, deuterium and antihydrogen.

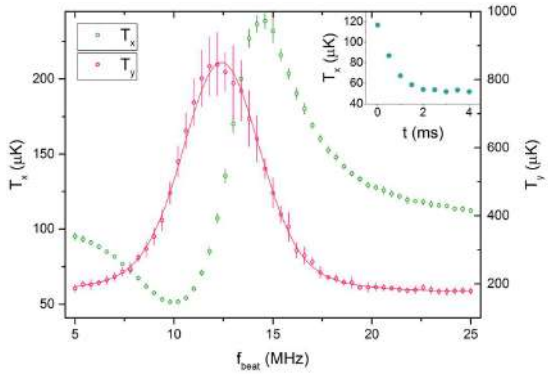


Figure 1: Temperatures obtained by TOF spectroscopy after 1D FC cooling in x direction as a function of FC detuning. Inset shows the dependence of the measured temperature on the FC cooling time.

[1] D. Kielpinski, Phys. Rev. A **73**, 063407 (2006).

[2] D. Aumiler and T. Ban, Phys. Rev. A **85**, 063412 (2012).

[3] A. M. Jayich, X. Long, and W. C. Campbell, Phys. Rev. X **6**, 041004 (2016).

[4] J. Davila-Rodriguez, A. Ozawa, T. W. Hänsch, and T. Udem, PRL **116**, 043002 (2016).

[5] N. Šantić, A. Cipriš, D. Buhin, D. Kovačić, I. Krešić, D. Aumiler, and T. Ban, in preparation.

Correlations of few-body quantum systems in position and momentum space

R. Klemt[1], **A. Bergschneider**[1], **V. M. Klinkhamer**[1], **J. H. Becher**[1], **P. M. Preiss**[1], **and S. Jochim**[1]

[1] *Physikalisches Institut der Universiät Heidelberg,*
Im Neuenheimer Feld 226, 69120 Heidelberg, Germany
e-mail: *klemt@physi.uni-heidelberg.de*

A general quantum many-body state is fully defined by the complete set of its correlation functions, where the most intriguing low-temperature phases are oftentimes characterized by strong correlations and large-scale entanglement of particular types or in specific bases. On the road towards studying such phases, great progress has been made over the last years, realizing low-entropy small- or medium-sized itinerant quantum systems with ultracold atoms and characterizing them either by phase, position or momentum correlations.

Our approach, which I will present on this poster, is based on three main ingredients: The deterministic preparation of fermionic few-body systems allows us to engineer specific strongly correlated quantum states of interest. In addition, a newly developed high fidelity, single atom and pseudo spin-resolved imaging system grants access to the measurement of correlations of in principle arbitrary order. Finally, as our imaging method works also in free space, we can access different measurement bases, in particular in real and momentum space, for the same quantum state.

Demonstrating our approach, I will present recent measurements on real and momentum space correlations induced by interactions in a Fermi-Hubbard dimer (Figure 1). Furthermore, I will present ongoing efforts utilizing these methods to study low entropy mesoscopic quantum systems both in 1D and 2D.

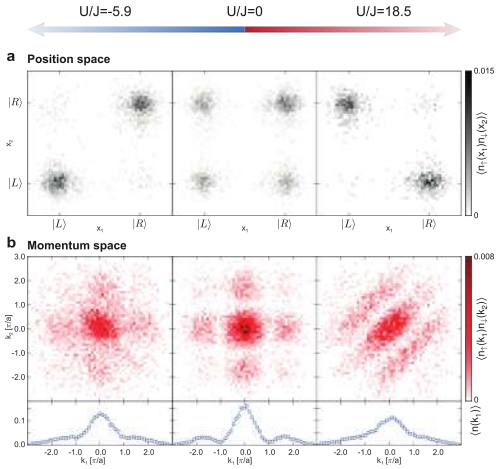


Figure 1: Correlations in a Fermi-Hubbard dimer. We prepare two fermions of different hyperfine state in the ground state of a double well potential. By tuning the on-site interaction strength U with respect to the tunnel coupling J we tune the system from strongly attractive to strongly repulsive. We measure correlations both in-situ (a) and in momentum space (b) with our free space single atom and spin-resolved imaging technique. This allows us to quantify correlations and certify entanglement in the system.

Dysprosium dipolar Bose-Einstein condensate with broad Feshbach resonances

L. Tanzi[1,2], **E. Lucioni**[1,2], **J. Catani**[1,3], **S. Gozzini**[2], **M. Inguscio**[1,3], **A. Fioretti**[2], **C. Gabbanini**[2], **and G. Modugno**[1,2]

[1] *LENS and Dip. di Fisica e Astronomia, Università di Firenze, 50019 Sesto Fiorentino, Italy*

[2] *CNR-INO, S.S. A. Gozzini di Pisa, via Moruzzi 1, 56124 Pisa, Italy*

[3] *CNR-INO, S.S. Sesto Fiorentino, 50019 Sesto Fiorentino, Italy*

e-mail: *luca.tanzi@ino.it*

We report on the production of a ^{162}Dy Bose-Einstein condensate and on the characterization of its scattering properties. We employ an innovative technique based on a resonator-enhanced optical trap that allows efficient loading from the magneto-optical trap. We use ultracold samples at temperatures just above condensation to investigate the Feshbach spectrum for magnetic fields between 6 and 30 G. Besides the chaotic distribution of narrow Feshbach resonances, typical of Lanthanides, we discover two rather isolated features at around 22 G and 27 G, with widths $\Delta \simeq 0.1$-1 G, comparable to the typical spacing between narrow resonances. A characterization with different complementary measurements (losses, thermalization, anisotropic expansion and molecular binding energy) points towards resonances of predominant s-wave character. Such resonances appear particularly appealing for a precise tuning of the contact interaction over a broad range, easing the investigation of quantum phenomena relying on the interplay between dipole and contact interactions.

Topological edge states and Aharanov-Bohm caging with ultracold atoms carrying orbital angular momentum

G. Pelegrí[1], A. M. Marques[2], R. G. Dias[2], J. Mompart[1], V. Ahufinger[1], A. J. Daley[3]

[1] *Departament de Física, Universitat Autònoma de Barcelona, E-08193 Bellaterra, Spain*

[2] *Department of Physics and I3N, University of Aveiro, 3810-193 Aveiro, Portugal*

[3] *Department of Physics and SUPA, University of Strathclyde, Glasgow G4 0NG, United Kingdom*

e-mail: *gerard.pelegri@uab.cat*

In recent years, the possibility of engineering complex couplings in systems of ultracold atoms in optical lattices has pushed forward the field of quantum simulation. To cite a few examples, the Hofstadter [1] and Haldane [2] models have been implemented and, through the synthetic dimension approach [3], topologically protected edge states analogous to those found in the context of quantum Hall physics have been demonstrated both for fermionic [4] and bosonic [5] atoms.

In this work, we consider a quasi-one-dimensional lattice with a diamond-chain shape whose sites are cylindrically symmetric (i. e., harmonic or ring-shaped) potentials. The lattice is loaded with non-interacting ultracold atoms that may occupy the two degenerate local Orbital Angular Momentum (OAM) $l = 1$ states of each of the sites. Due to the different relative orientations between the sites forming the lattice, some of the tunneling amplitudes that intervene in the tight-binding model acquire phases [6], giving rise to very rich physics. Through a series of exact mappings, we show that the model has a non-trivial topological nature, which is signalled by the presence of robust edge states. Furthermore, we demonstrate that the system can exhibit Aharanov-Bohm caging due to quantum interference between the tunneling processes with different phases. Recently, very similar models displaying analogous features have been successfully implemented in coupled photonic waveguide systems [7, 8].

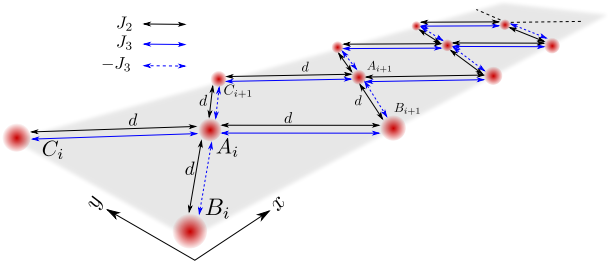


Figure 1: Schematic representation of the diamond-chain considered in this work, showing the directions along which some of the tunnelling amplitudes acquire phases.

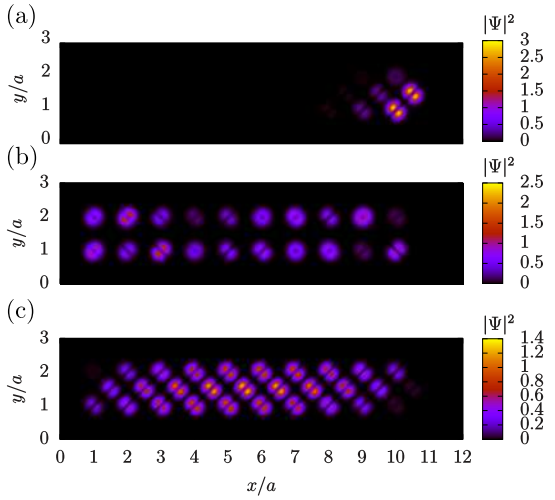


Figure 2: Real-space density plots of different eigenstates of the diamond chain. (a) Topologically protected edge state. (b) Zero-energy flat-band state. (c) State belonging to a dispersive band.

[1] M. Aidelsburger, M. Atala, M. Lohse, J. T. Barreiro, B. Paredes, and I. Bloch, *Phys. Rev. Lett.* **111**, 185301 (2013).

[2] G. Jotzu, M. Messer, R. Desbuquois, M. Lebrat, T. Uehlinger, D. Greif, and T. Esslinger, *Nature* **515**, 237 (2014).

[3] A. Celi, P. Massignan, J. Ruseckas, N. Goldman, I.B. Spielman, G. Juzeliūnas, and M. Lewenstein, *Phys. Rev. Lett.* **112**, 043001 (2014).

[4] M. Mancini, G. Pagano, G. Cappellini, L. Livi, M. Rider, J. Catani, C. Sias, P. Zoller, M. Inguscio, M. Dalmonte, and L. Fallani, *Science* **349**, 1510 (2015).

[5] B. K. Stuhl, H. I. Lu, L. M. Aycock, D. Genkina, and I. B. Spielman, *Science* **349**, 1514 (2015).

[6] J. Polo, J. Mompart, and V. Ahufinger, *Phys. Rev. A* **93**, 033613 (2016).

[7] S. Mukherjee, M. Di Liberto, P. Öhberg, R. R. Thomson, and N. Goldman, arXiv: 1805.03564.

[8] M. Kremer, I. Petrides, E. Meyer, M. Heinrich, O. Zilberberg, and A. Szameit, arXiv: 1805.05209.

Dynamical formation of the Bose polaron through impurity-bath decoherence

K. K. Nielsen[1], **L. A. Peña, Ardila**[1], **G. M. Bruun**[1] **and T. Pohl**[1]
[1] *Department of Physics and Astronomy, Aarhus University, Ny Munkegade, DK-8000 Aarhus C, Denmark*
e-mail: *kristianknakkergaard@phys.au.dk*

We study a single impurity immersed in a Bose-Einstein condensate in the perturbative regime to second order in the interaction. In the steady state it is well known that a quasiparticle forms, termed the Bose polaron. We systematically study this formation process and the relevant time scales. We show that the polaron forms due to decoherence between the impurity and the condensate – the bath. Further, we establish that the formation time depends strongly on the speed of the impurity, and that it diverges at the speed of sound of the condensate. At low momenta it is given by the ratio of the condensate coherence length and speed of sound. We show that below the speed of sound, the impurity only decoheres partially settling at the polaron residue. In the long time limit we recover the residue and polaron energy previously calculated, hereby benchmarking our results.

Non-equilibrium many-body dynamics is an outstanding challenge in quantum gases. Cold atoms provides a platform where the effect of the interactions can systematically be studied. The cold atoms platform has opened up for new fundamental questions. This includes probing many-body localization [1], linked to the breakdown of ergodicity [2, 3] and more generally non-equilibrium dynamics in cold atomic gases [4]. Until now the Bose polaron, an impurity residing in a Bose-Einstein condensate, has systematically been studied in the steady state using various theoretical techniques [5, 6, 7, 8, 9, 10, 11, 12]. As such the polaron energy and spectral signal is now well-studied and has successfully been measured experimentally [13, 14]. Some dynamics of the phononic dressing has also been studied in the strongly interacting regime [15] and recently the same group has further studied trajectories of impurities and polaron formation using a dynamical RG approach [16]. However, a well-understood picture of polaron formation and decoherence between the impurity and the condensate as a quantum reservoir is yet to be formulated.

[1] P. Bordia, H. Luschen, S. Scherg, S. Gopalakrishnan, M. Knap, U. Schneider, and I. Bloch, Phys. Rev. X **7**, 041047 (2017)

[2] P. W. Anderson, Phys. Rev. **109**, 1492 (1958)

[3] L. Fleishman and P. W. Anderson, Phys. Rev. B **21**, 2366(1980)

[4] E. Altman, ArXiv e-prints (2015), arXiv:1512.00870 [cond-mat.quant-gas]

[5] J. Tempere, W. Casteels, M. K. Oberthaler, S. Knoop, E. Timmermans, and J. T. Devreese, Phys. Rev. B **80**, 184504 (2009)

[6] S. P. Rath and R. Schmidt, Phys. Rev. A **88**, 053632 (2013)

[7] W. Li and S. Das Sarma, Phys. Rev. A **90**, 013618 (2014)

[8] W. Casteels and M. Wouters, Phys. Rev. A **90**, 043602 (2014)

[9] J. Levinsen, M. M. Parish, and G. M. Bruun, Phys. Rev. Lett. **115**, 125302 (2015)

[10] L. A. P. Ardila and S. Giorgini, Phys. Rev. A **92**, 033612 (2015)

[11] R. S. Christensen, J. Levinsen, and G. M. Bruun, Phys. Rev. Lett. **115**, 160401 (2015)

[12] F. Grusdt, R. Schmidt, Y. E. Shchadilova, and E. Demler, Phys. Rev. A **96**, 013607 (2017)

[13] N. B. Jrgensen, L. Wacker, K. T. Skalmstang, M. M. Parish, J. Levinsen, R. S. Christensen, G. M. Bruun, and J. J. Arlt, Phys. Rev. Lett. **117**, 055302 (2016)

[14] M.-G. Hu, M. J. Van de Graaff, D. Kedar, J. P. Corson, E. A. Cornell, and D. S. Jin, Phys. Rev. Lett. **117**, 055301 (2016)

[15] Y. E. Shchadilova, R. Schmidt, F. Grusdt, and E. Demler, Phys. Rev. Lett. **117**, 113002 (2016)

[16] F. Grusdt, K. Seetharam, Y. Shchadilova, and E. Demler, ArXiv e-prints (2017), arXiv:1711.03478 [cond-mat.quant-gas]

Quantum probe spectroscopy for cold atomic systems

A. Usui[1], **B. Buča**[2], **and J. Mur-Petit**[2]
[1] *Quantum Systems Unit, OIST Graduate University, Onna, Okinawa, Japan*
[2] *Clarendon Laboratory, University of Oxford, Oxford, United Kingdom*
e-mail: *jordi.murpetit@physics.ox.ac.uk*

We study a two-level impurity coupled locally to a quantum gas on an optical lattice. For state-dependent interactions between the impurity and the gas, we show that its evolution encodes information on the local excitation spectrum of gas at the coupling site. Based on this, we design a nondestructive method to probe the system's excitations in a broad range of energies by measuring the state of the probe using standard atom optics methods. We illustrate our findings with numerical simulations for quantum lattice systems, including realistic dephasing noise on the quantum probe, and discuss how a controllable dephasing rate on the quantum probe may enable distinguishing regular and chaotic spectra.

References

[1] A. Usui, B. Buča, and J. Mur-Petit, "Quantum probe spectroscopy for cold atomic systems", arXiv:1804.09237

Ultracold atoms in an optical kagome lattice

T.L. Harte, M. Melchner, D.G. Reed, F. Störtz , and U. Schneider
Cavendish Laboratory, J.J. Thomson Avenue, Cambridge CB3 0HE, UK
e-mail: *th558@cam.ac.uk*

Ultracold atoms confined in optical lattices can be used to simulate and explore emergent phenomena in condensed matter physics. We are building a quantum gas microscope experiment with which to study ultracold atoms in the flat band of an optical kagome lattice with single-site resolution.

A kagome lattice potential, illustrated in Fig. 1(a), has a trihexagonal tiling: a periodic structure of hexagons and triangles, created by the superposition of commensurate triangular optical lattices [1]. This creates a highly frustrated geometry ideal for studying long range correlations in quantum spin liquids. Solving the tight binding model for the kagome lattice yields three energy bands as pictured in Fig. 1(b). With a negative hopping term t in the tight-binding Hamiltonian, the lowest two bands are equivalent to those in graphene, and the uppermost band is flat; we will populate this non-dispersive flat band using a negative temperature state [2].

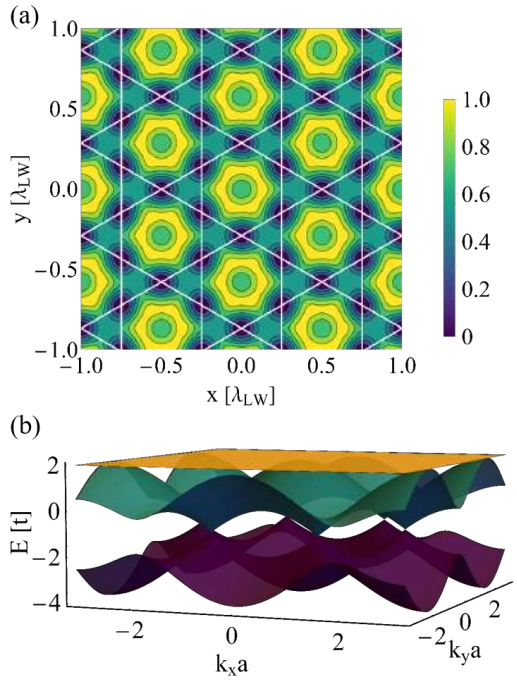


Figure 1: (a) The optical kagome potential created by overlapping two commensurate triangular lattices, with the kagome structure superimposed in white. (b) The corresponding tight-binding band structure, with hopping term $t < 0$. We aim to populate the flat band by creating a negative temperature state.

References

[1] G-B. Jo, J. Guzman, C. K. Thomas, P. Hosur, A. Vishwanath and D. M. Stamper-Kurn. Phys. Rev. Lett **108**, 045305 (2012).

[2] S. Braun, J. P. Ronzheimer, M. Schreiber, S. S. Hodgman, T. Rom, I. Bloch and U. Schneider, Science **339**(6115), 52-55 (2013).

Observation of Roton Mode Population in a Dipolar Quantum Gas

D. Petter[1], **L. Chomaz**[1], **S. Baier**[1], **G. Faraoni, J. H. Becher**[2], **M. J. Mark**[1,3] **and F. Ferlaino**[1,3]

[1] *Institute for Experimental Physics, University of Innsbruck, 6020 Innsbruck, Austria*

[2] *Physics Institute, Heidelberg University, 69120 Heidelberg, Germany*

[3] *Institute for Quantumoptics and Quantuminformation, Austrian Academy of Science, 6020 Innsbruck, Austria*

e-mail: *daniel.petter@uibk.ac.at*

Dipolar Bose-Einstein condensates (dBECs) offer an ideal playground for investigating novel aspects of many-body phenomena in the presence of dipole-dipole interactions (DDI). A seminal work in 2003 [1] predicted the existence of a roton mode (a minimum in the dispersion relation at a finite momentum k_{rot} with an energy Δ_{rot}) in the excitation spectrum of a dBEC, similar to the roton mode in superfluid He II. In contrast to He II, the roton mode in a dBEC does not require strong interactions, but rather arises from the momentum dependence of the DDI.

In our experiment, we use dBECs of ^{166}Er, confined in a cigar-shaped trap (Fig. 1a). In order to investigate the roton mode, we employ a Feshbach resonance to quench down the scattering length a_{s} into a regime, where Δ_{rot} vanishes and eventually becomes imaginary. At this point, the roton mode population starts to exponetially grow with time. We probe the roton mode in the momentum distribution of the atomic cloud and observe two distinct peaks at $\pm k_{\mathrm{rot}}$ appearing, when quenching below a critical a_{s} (Fig. 1b). From the time-resolved population (Fig. 1c) we are able to directly extract the imaginary Δ_{rot}. By repeating the measurements in different configurations, we experimentally probe the characteristic scalings of the roton mode with the trapping length scale along the diretion of the atomic dipoles and a_{s}. We compare our results with an analytical model and full real-time simulations, and unambigously confirm the roton nature of the observed mode [2].

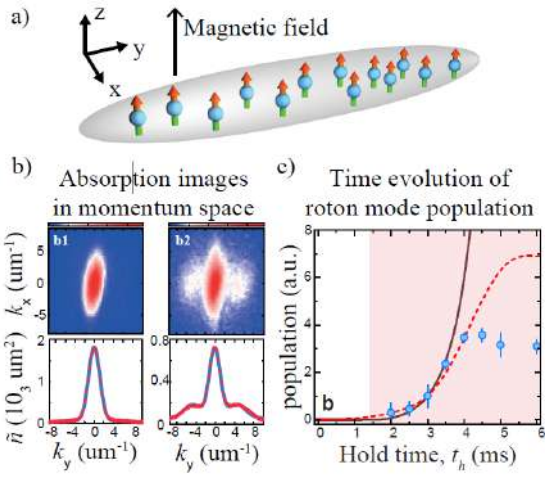


Figure 1: a) Experimental trapping configuration of the cigar-shaped dBEC with magnetic dipoles aligned along the z-direction. b) Absorption images of the atomic cloud's momentum distribution above (b1) and below (b2) a critical scattering length a_s. The latter case shows the emergence of distinct momentum peaks that are associated with population in the roton mode. c) Time evolution of the roton mode population. The Solid line shows the theoretical prediction from an analytical model and the dashed line the results obtained from numerical real-time simulations.

[1] L. Santos et. al., PRL 90, 250403 (2003)

[2] L. Chomaz, et. al., Nature Physics, 14, 442 - 446 (2018)

Controlling Spin Exchange of Single Impurities in a Bose-Einstein Condensate

F. Schmidt[1], D. Mayer[1], D. Adam[1], J. Koch[1], T. Lausch [1], J. Nettersheim [1], Q. Bouton[1], E. Tiemann[2] and A. Widera[1,3]

[1] *Fachbereich Physik und Landesforschungszentrum OPTIMAS, Technische Universitt Kaiserslautern, 67663 Kaiserslautern, Germany*

[2] *Institut für Quantenoptik, Leibniz Universität Hannover, 30167 Hannover, Germany*

[3] *Graduiertenschule Materials Science in Mainz, Gottlieb-Daimler-Str. 47, 67663 Kaiserslautern, Germany.*

e-mail: *widera@physik.uni-kl.de*

Individual, controllable neutral impurities in a quantum gas (see Fig.1) form a paradigm of quantum physics which allows experimentally studying questions of system-bath interaction and thermalization in nonequilibrium situations; single-atom aided, non-destructive local probing of quantum gases; or the formation and dynamics of quasi-particles in superfluids.

We realize this paradigm using single or few Cesium (Cs) atoms immersed in a Rubidium (Rb) Bose-Einstein condensate. Experimentally, a species-selective optical lattice yields independent position control over the Cs atoms, and we use the lattice to shuttle Cs into the Rb bath. For Raman-cooled Cs atoms we find a high probability for immersion of the impurity into the quantum gas.

In ultracold collisions, the system can either undergo a fully elastic collision, leaving the internal states of the atoms unchanged but leading to fast thermalization of the impurity; or hyperfine interaction can drive spin-exchange processes betwen Rb and Cs, where quantized angular momentum is exchanged betwen the impurity and one atom of the bath. We focus our analysis to the hyperfine ground states $F = 3$ ($F = 1$) for Cs (Rb).

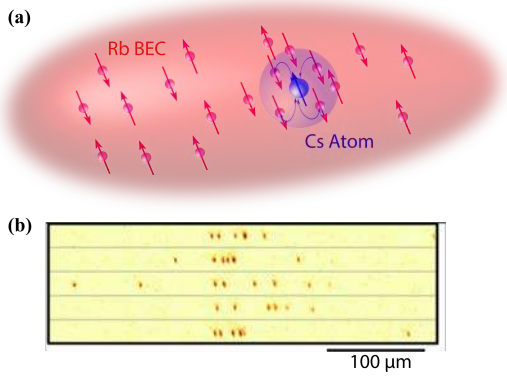


Figure 1: (a) Illustration of a single Cs impurity (blue) in a Rb Bose-Einstein condensate (red). The Cs atoms undergo spin-exchange collisions with atoms of the Rb bath. (b) False color fluorescence image of few Cs atoms trapped in an optical lattice.

Resolving the rich Zeeman manifold of the Cs ground state, we trace the spin population of individual impurities, initialliy prepared in the polarized state $m_F = 3$ being pumped by sucessive spin-exchange sollisions to the oposite Zeeman state $m_F = +3$. The spin-evolution observed is quantitatively in excellent agreement with theoretical predictions from numerical calculations of the Rb-Cs interaction potential. Importantly, the spin-exchange rate in general depends on the specific m_F values of Rb and Cs, i.e. the projection of the respective total angular momentum F onto the quantization axis.

Interestingly, we find a series of Feshbach resonances at magnetic fields below 1 G in different collisional channels. The interplay of Zeeman energy, adjusted via the external magnetic field, and the collision energy, adjusted via the bath temperature, allows controlling the spin dynamics of the Cs impurity in different regimes which will be discussed in detail.

Our work thus paves the way to the investigation of quasi-particle effects of spinful impurities and might fascilitate studying Bose-Kondo physics or polaron formation.

Experimental realization of driven interacting many-body systems

M. Messer[1], **F. Görg**[1], **K. Sandholzer**[1], **J. Minguzzi**[1], **G. Jotzu**[1,2], **R. Desbuquois**[1], **and T. Esslinger**[1]

[1] *Institute for Quantum Electronics, ETH Zurich, 8093 Zurich, Switzerland*

[2] *Max Planck Institute for the Structure and Dynamics of Matter, 22761 Hamburg, Germany*

e-mail: *messer@phys.ethz.ch*

Periodically driving a system of ultracold fermions in an optical lattice allows to implement a large variety of effective Hamiltonians including topological systems and artificial gauge fields. A crucial question remains, whether it is possible to extend this method to interacting systems or if heating limits the capabilities of Floquet engineering? Our tunable geometry optical lattice allows us to test different preparation protocols and to minimize coupling to higher bands. By using a two-body system we can control and adiabatically populate different Floquet states [1].

Furthermore, we present the successful implementation of a periodically driven Fermi-Hubbard model on a 3D hexagonal lattice (Fig. 1a) and explore the intriguing properties of Floquet many-body systems [2]. For near resonant modulation close to the interaction energy ($U \approx \hbar\omega$) our protocol realizes an effective tunneling energy which is density dependent (see schematics in Fig. 1b). By controlling the detuning between shaking frequency and interactions, we achieve independent control over the single particle tunneling and the magnetic exchange energy. We observe that antiferromagnetic correlations in a fermionic many-body system can be reduced, enhanced or even switched to ferromagnetic correlations.

This successful implementation offers the possibility to explore the complicated dynamics of periodically driven interacting systems and engineer new many-body phases. Although a theoretical analysis of such driven many-body Hamiltonians is inherently challenging, a deeper understanding of the underlying microscopic processes seems feasible by directly comparing calculations to our experiments.

[1] R. Desbuquois, M. Messer, F. Görg, K. Sandholzer, G. Jotzu, and T. Esslinger, Phys. Rev. A **96**, 053602 (2017).

[2] F. Görg, M. Messer, K. Sandholzer, G. Jotzu, R. Desbuquois, and T. Esslinger, Nature **553**, 481-485 (2018).

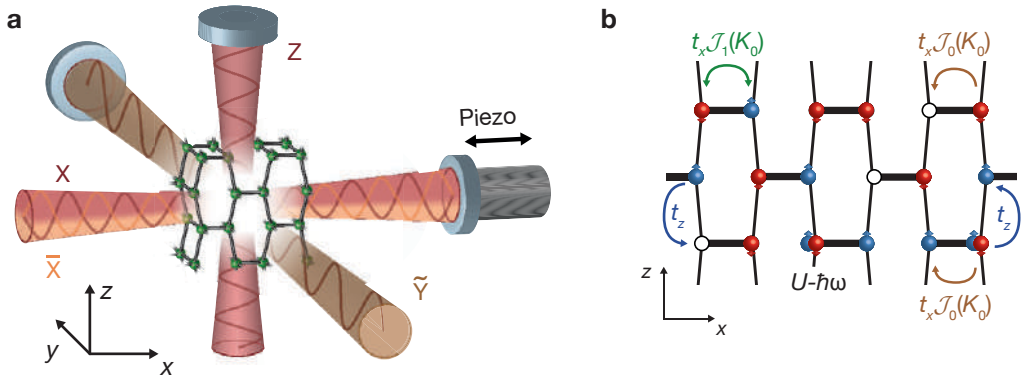


Figure 1: **(a)** A three dimensional tunable optical lattice with a sinusoidal modulation of the lattice position along the x-direction implements a driven Fermi-Hubbard model on a honeycomb lattice. **(b)** For near-resonant modulation ($U \approx \hbar\omega$), the effective Hamiltonian of the driven system is described by density-dependent tunneling processes. While single particles tunnel with $t_x\mathcal{J}_0(K_0)$, a tunneling process which changes the number of double occupancies is corrected by the first-order Bessel function $\mathcal{J}_1(K_0)$. In addition, the effective interaction becomes $U - \hbar\omega$. Adapted from Ref. [2].

Full-Contrast Fermionic Hanbury Brown-Twiss Interference

P. Preiss, J. H. Becher, R. Klemt, A. Bergschneider, V. Klinkhamer, S. Jochim
Physics Institute, Heidelberg University, 69120 Heidelberg, Germany
e-mail: *preiss@physi.uni-heidelberg.de*

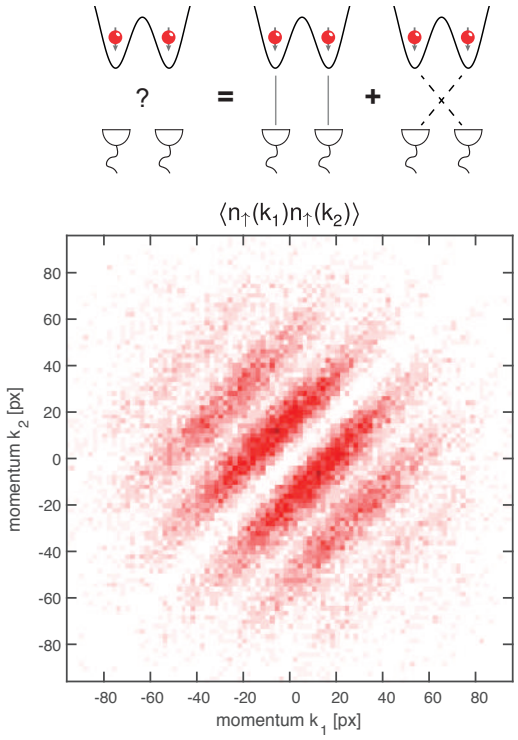


Figure 1: Hanbury Brown-Twiss interference occurs when indistinguishable quantum particles can interfere. All processes connecting the sources and detectors add coherently, introducing sensitivity to quantum statistics. We observe full-contrast correlations of two indistinguishable fermions released from optical tweezers. The fringe pattern in the momentum difference coordinate indicates high-contrast fermionic anti-bunching.

Intensity interferometry is a key technique to study spatial order at length scales not accessible by direct imaging. Within this approach, information about the structure of a source can be obtained from the correlations between particles arriving at distant detectors. The observed correlations depend on the particles' quantum statistics and are a paradigmatic example of two-particle interference, exhibiting bunching correlations for bosons and anti-bunching for fermions. Building on the stellar interferometry performed by Hanbury Brown and Twiss, intensity interferometry can be employed on vastly different energy scales ranging from ultracold atomic lattice systems to the quark-gluon plasma.

Here we demonstrate the high-contrast interference of ultracold fermionic atoms. We use deterministic single-atom sources realised by optical tweezers to study fermionic Hanbury Brown-Twiss correlations. In the experiment, non-interacting ^{6}Li atoms expand freely into a one-dimensional waveguide trap and are detected using single-particle sensitive fluorescence imaging in free space. We observe full-contrast fermionic anti-bunching, indicating excellent control over all degrees of freedom of the particles. Adding multiple sources to the system, we detect the presence of correlations at different length scales and observe the emergence of higher order correlation functions from the two-body correlator.

Our work demonstrates how to use high-contrast momentum space interference to characterise mesoscopic quantum systems of ultracold atoms.

One-dimensional ultradilute quantum liquids

G. E. Astrakharchik[1], **G. Guijarro**[1], **J. Boronat**[1], **A. Pricoupenko**[2], **and D. S.Petrov**[2]

[1] *Departament de Física, Campus Nord B4-B5, Universitat Politècnica de Catalunya, E-08034 Barcelona, Spain*

[2] *LPTMS, CNRS, Univ. Paris Sud, Université Paris-Saclay, 91405 Orsay, France*

e-mail: *grigori.astrakharchik@upc.edu*

We calculate the ground-state energy of a one-dimensional Bose-Bose mixture with attractive inter- and repulsive intraspecies interactions within quantum Monte Carlo method. By solving four- and six-body problems[1] we demonstrate that the dimer-dimer scattering length vanishes for some critical value of parameters. At the same point, the here-dimer interactions turns out to be repulsive. This provides a microscopic scenario of formation of a liquid, when dimer-dimer interaction is attractive while threee-dimer one is repulsive. We study the corresponding many-body problem and demonstrate the existence of such ultradilute liquid[2].

References

[1] G. Guijarro, G. E. Astrakharchik, J. Boronat, A. Pricoupenko, D. S. Petrov, arXiv:1803.08603 (2018)

[2] D. S. Petrov, G. E. Astrakharchik Phys. Rev. Lett. **117**, 100401 (2016)

Selective inter-band transition by pulse sequences in 1D bichromatic Bose lattices

T. Yamakoshi[1], **and S. Watanabe**[2]

[1] *Institute for Laser Science, University of Electro-Communications, 1-5-1 Chofugaoka, Chofu-shi, Tokyo 182-8585, Japan*

[2] *Department of Engineering Science, University of Electro-Communications, 1-5-1 Chofugaoka, Chofu-shi, Tokyo 182-8585, Japan*

e-mail: *t_yamakoshi@ils.uec.ac.jp*

Recently, the dynamics of ultracold atoms in higher bands has been gathering attention particularly after the theoretical observation of such fascinating phenomena as the orbital superfluidity, the swallowtail band structure at band edges, the Dirac cone-like dispersion, and so on. Our study focuses on the Dirac point, *i.e.* the Dirac cone in a one-dimensional bichromatic lattice system. It is realizable by varying the relative heights of the two optical lattices, thus by controlling the energy gap. This idea was theoretically suggested by [1] and experimentally demonstrated by [2] in 2011 using the Landau-Zener transition at the Dirac point in the presence of a harmonic dipole trap and the linear gravitational potential, the phenomenon is referred to as the Klein tunneling. However, the manipulation based on the linear potential causes diffusion of the wave packet, thus unsuitable for wave packet shaping.

Recently, two methods of coherent wave packet shaping are experimentally established, one based on the amplitude modulation and the other on the lattice pulse sequence. A recent experiment using the former method demonstrated the band spectroscopy of Fermionic atoms in a honeycomb lattice, proving it to be a powerful tool. However, the inter-band transition rate turned out rather low[3]. On the other hand, the monochromatic lattice pulse sequence has succeeded in producing the wave packets of Bosonic atoms [4] in the 1st-4th excited bands with high transition rate $\sim 90\%$.

In this poster, we present some numerical results based on the lattice pulse sequence with Bosonic atoms in a 1-dimensional bichromatic lattice system. Following the experimental paper[4], we begin with a Bose-Einstein condensate loaded onto a harmonic potential and examine the pulse sequence method. We consider the scaled Hamiltonian

$$\mathcal{H} = -\frac{\partial^2}{\partial x^2} + \nu x^2 \ + s_1 \sin^2(x) + s_2 \sin^2(2x). \quad (1)$$

The pulse sequence consists of two parts, namely, an on-duty cycle where $s_1, s_2 \neq 0$ and an off-duty cycle where $s_1 = s_2 = 0$. These two cycles are repeatedly applied pairwise to the initial ground state with appropriate durations until the wave packet reaches the target state.

The band gap goes to 0 when the lattice heights satisfy the condition $s_2 = s_1^2/16$ [1]. Therefore, we investigated the excitation dynamics from the ground to the 1st and 2nd excited bands with $s_1 = 10$, considering three typical cases centering around the resonance at $s_2 = 6.25$. First, we optimized the time duration of the on-duty cycle and that of the off-duty cycle as well as the lattice heights in the pulse sequence and found that the best transition rate of around 90% was achievable within 100μs. Furthermore, we studied the post-excitation dynamics of the wave packet in an external harmonic potential. In the resonant case $s_2 = 6.25$, the excited wave packet proves to be less dispersive than in the off-resonant case (see Fig. 1). Finally, we numerically examined effects of a weak atom-atom interaction included as the non-linear term in the Hamiltonian and confirmed that it does not alter the dynamics drastically. The study suggests that the pulse sequence method would be a powerful tool for the coherent wave packet shaping of ultracold atoms in an optical lattice system. Moreover, a combination with the amplitude modulation method may pave a new way to the physics of coherently accessing and controlling higher bands.

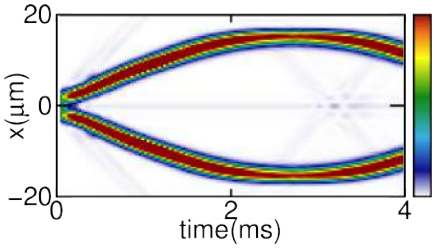


Figure 1: Density plot of the excited wave packet after the pulse sequence with $\nu = 1.2 \times 10^{-4}(2\pi \times 70\text{Hz})$, $s_1 = 10$, and $s_2 = 6.25$.

[1] D. Witthaut et. al., Phys. Rev. A **84**, 033601(2011).

[2] Tobias Salger et. al., Phys. Rev. Lett. **107**, 240401(2011).

[3] Nick Fläschner et. al., Phys. Rev. A **97**, 051601(R) (2018).

[4] Zhongkai Wang et. al., Phys. Rev. A **94**, 033624 (2016).

Spin current in spin-orbit coupling Bose-Fermi mixture

R. Sakamoto, E. Arahata, and H. Mori
Department of Physics, Tokyo Metropolitan University, Hachioji-shi, Tokyo 192-0397, Japan
e-mail: *sakamoto-ryohei@ed.tmu.ac.jp*

Spin current is a current of particles with different spins to an opposite direction. The study of spin-dependent electron transport phenomena in solid-state materials is called spintronics. Recently, various methods to induce and control a spin current have been proposed[1] and, particularly, it is known that spin current can be induced by a periodic magnetic field.

On the other hand, atoms trapped and cooled in ultra-low temperature exhibit a variety of quantum phenomena. One of useful features of the cold atoms is controllability of physical parameters including interaction strength between the atoms. Taking advantage of the features, we can create various interesting atom systems, such as spin-orbit (SO) coupled atom gases[2, 3, 4] and Bose-Fermi atom mixtures[7, 8].

Condensation of the SO coupled bosonic atoms is known to have a periodic spin structure[7, 8]. Therefore, in a mixture of spin-1/2 fermionic atoms and the SO coupled bosonic atoms, a spin current of the fermions can be induced, since the fermions feel the periodic magnetic field created by the periodic spin structure of the bosons. Furthermore, we expect that the induced spin current can be controlled by using the parameter control of the Bose-Fermi mixture system. In other words, the mixture system could be used as a novel spintronics device that allows control of spin current.

To pursue this possibility, we study a spin current of fermions in a mixture of spin-1/2 fermions and SO coupled bosons with focus on the controllability of the current[9]. We first derive the ground state phase diagram of the bosons in the mixture system using a variational method to clarify the parameter region where the bosons have a periodic spin structure (Fig. 1). Next we calculate the spin current of the fermions in the mixture and investigate the dependence of the spin current on the experimentally controllable parameters of the SO coupled bosons (Fig. 2). Details of the calculations and specific meaning of the parameters used in the figures are given in my poster.

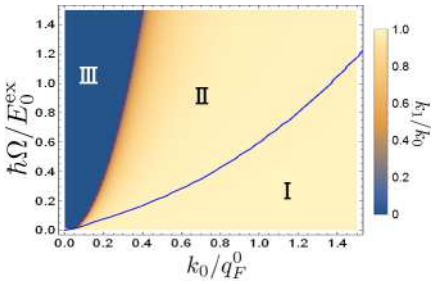


Figure 1: Ground state phase diagram of the bosons in the Bose-Fermi mixture at zero temperature. The vertical and horizontal axes show experimentally controllable parameters and k_1 is the variational parameter to determine the ground state wave function of the bosons.

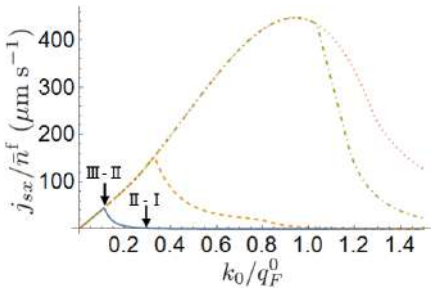


Figure 2: Spin current of the fermions for four different set of parameters. The vertical axis shows the value of the spin current and the horizontal axis shows the experimentally controllable parameter. The two arrows along the solid line show points of phase transitions of the bosons between Phases II and III and between I and II. (Definition of the phases is given in the poster).

[1] S. Maekawa, H. Adachi, K. Uchida, J. Ieda, and E. Saitoh, J. Phys. Soc. Jpn. **82**, 102002 (2013).

[2] Y. J. Lin, K. Jiménez-Garcí a, and I. B. Spielman, Nature **471**, 83 (2011).

[3] P. Wang, Z. Q. Yu, Z. Fu, J. Miao, L. Huang, S. Chai, H. Zhai, and J. Zhang, Phys. Rev. Lett. **109**, 095301 (2012).

[4] L. W. Cheuk, A. T. Sommer, Z. Hadzibabic, T. Yefsah, W. S. Bakr, and M. W. Zwierlein, Phys. Rev. Lett. **109** 095302 (2012).

[5] A. G. Truscott, K. E. Strecker, W. I. McAlexander, G. B. Partridge, and R. G. Hulet, Science **291**, 2570 (2001).

[6] G. Modugno, G. Roati, F. Riboli, F. Ferlaino, R. J. Brecha, and M. Inguscio, Science **297**, 2240 (2002).

[7] Y. Li, L. P. Pitaevskii, and S. Stringari, Phys. Rev. Lett. **108**, 225301 (2012).

[8] G. I. Martone, Y. Li, L. P. Pitaevskii, and S. Stringari, Phys. Rev. A **86**, 063621 (2012).

[9] R. Sakamoto, E. Arahata, and H. Mori, J. Phys. Soc. Jpn. (to be published).

Ultralow mechanical dissipation for quantum optomechanics

N. J. Engelsen[1], A. H. Ghadimi[1], S. A. Fedorov[1], M. J. Bereyhi[1], R. D. Schilling[1], D. J. Wilson[2], and T. J. Kippenberg[1]

[1] *Institute of Physics, École Polytechnique Fédérale de Lausanne, 1015 Lausanne, Switzerland.*

[2] *IBM ResearchZurich, 8803 Rschlikon, Switzerland.*

e-mail: *daw@zurich.ibm.com, tobias.kippenberg@epfl.ch*

Nano- and micromechanical oscillators are indispensable for navigation, timing, motion sensing and wireless communication. In the past decade, a technological and scientific revolution has enabled quantum control of mechanical devices by integrating them with electromagnetic cavities, forming the fields of cavity quantum electro/optomechanics [1]. The quality factor (Q) of the mechanical oscillator is an important figure of merit for these endeavors. Here we show how the Q of flexural modes of nanobeams can be greatly increased by exploiting insights from nanomechanics [2] and semiconductor physics [3].

Our oscillators are of particular interest from the prospective of quantum optomechanics, where thermomechanical noise is a major challenge. Though the central ideas of cavity optomechanics were theoretically proposed decades ago [4, 5], it is only within the last decade that experimental optomechanical systems can operate in a regime where the quantum nature of light has observable effects [6]. By integrating ultra-high Q mechanical oscillators with optical cavities, we seek to enter the regime where the oscillator's motion is dominated by radiation pressure shot noise at room temperature. Such a device could allow optical feedback cooling to the motional ground state and the observation of ponderomotive squeezing, until now only achieved at cryogenic temperatures.

The pursuit of resonators with ultra-high Q has led to intense study of dissipation dilution—an effect that increases the stiffness of a material without added loss. Interestingly, the paradigm has to date relied on weak strain produced during material synthesis—the use of geometric strain engineering techniques [3], capable of producing local stresses near the material yield strength, remains largely unexplored. By patterning doubly-clamped, Si_3N_4 nanobeams, we combine geometric strain with soft-clamping to produce exceptionally high Q nanomechanical oscillators, that can undergo tens of coherent oscillations at room temperature [7].

Loss due to curvature at the clamping points has been a major limiting factor in engineering of high Q mechanical oscillators. Soft-clamped resonators recently developed by Tsaturyan et al. [2] bypass this limitation by localizing the mode away from the clamping points. We adapt their technique to 1-dimensional nanobeams, using the geometries shown in Figure 1. The width corrugations in the nanobeam create a bandgap in the mechanical mode spectrum. By creating a defect in the center of the beam, a localized mode with enhanced quality factor is allowed to exist in the bandgap. Then, by tapering the overall width of the nanobeam, we increase the strain in the center of the beam to nearly four times the deposition stress. This combined strategy produces picogram-mass flexural modes with room-temperature Q factors as high as 800 million and Qf products of 10^{15} Hz—both unprecedented for a mechanical oscillator at room temperature (results shown in Fig. 1). Additionally, strain engineering allows us to tune the frequency of the ultra-high Q mode across a wide range of frequencies while retaining Qf products above 10^{14} Hz. At room temperature, the devices we study can have force sensitivities of $\mathrm{aN}/\sqrt{\mathrm{Hz}}$ and at the same time perform tens of oscillations within their thermal decoherence time. The extremely low dissipation and low effective mass of these devices make them promising for cavity quantum optomechanics experiments.

[1] M. Aspelmeyer, T. J. Kippenberg, F. Marquardt, Rev. Mod. Phys, **86**, 4, 1391-1452 (2014)

[2] Y. Tsaturyan, A. Barg, E. S. Polzik, and A. Schliesser, Nat. Nano., **12**, 8, 776-783 (2017)

[3] J. Li, Z. Shan, and E. Ma, MRS Bull., **39**, 2, 108-114 (2014)

[4] C. M. Caves, Phys. Rev. Lett, **45**, 2, 75-79 (1980)

[5] V. B. Braginsky and A. B. Manukin, Sov. Phys. JETP, **25**, 653-655 (1967)

[6] T. P. Purdy, R. W. Peterson, and C. A. Regal, Science, **339**, 6121, 801-804 (2013)

[7] A. H. Ghadimi et al., Science, **360**, 6390, 764-768 (2018)

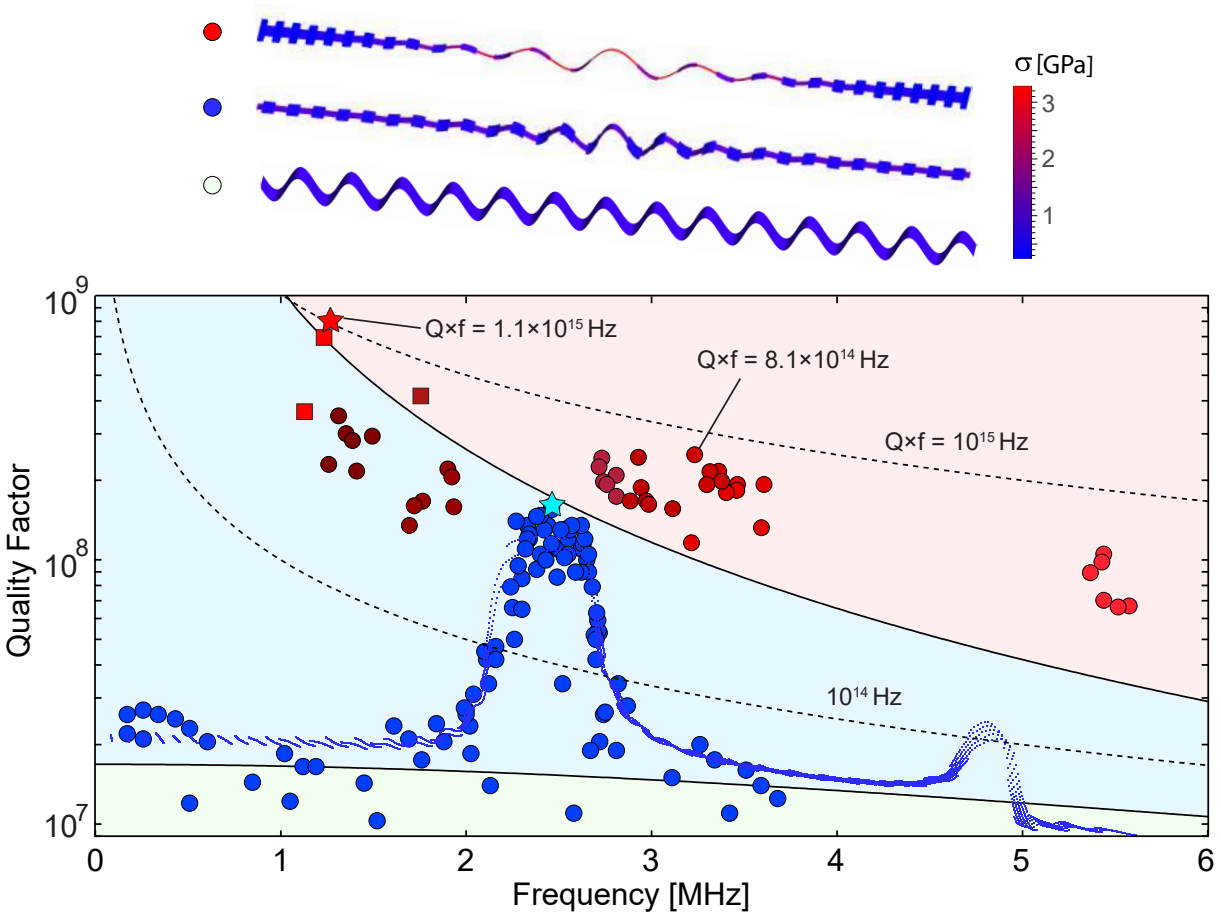


Figure 1: Q versus mode frequency of nanobeams with different geometries, as indicated above. Blue points correspond to modes of uniform, soft-clamped nanobeams. Red points correspond to defect modes of tapered beams. Color groups include the highest five Q-factors recorded for different beams. Red lines and blue dots are numerical models. The red star corresponds to a Q of 800 million and Qf-product of 1.1×10^{15} Hz.

Monochromatic thermal radiation from a sub-micron dielectric particle

M. Tachikawa, H. Odashima, R. Kanamoto, H. Tajima, and R. Morino
Department of Physics, Meiji University, Kawasaki 214-8571, Japan
e-mail: *tachikaw@meiji.ac.jp*

This is the LaTeX 2$_\varepsilon$ template for preparing a one-page abstract for the poster contribution to the 26th International Conference on Atomic Physics (ICAP-2018), to be held in July 2018 in Barcelona. Please ensure it is in the final publishable form.

Storage of Single Photons Generated from Cavity-enhanced Spontaneous Parametric Down Conversion in Cold Atomic Ensembles

Ying-Cheng Chen[1,2], **Ya-Fen Hsiao**[1,3], **and Pin-Ju Tsai**[1,4]

[1] *Institute of Atomic and Molecular Sciences, Academia Sinica, Taipei 10617, Taiwan*

[2] *Center for Quantum Technology, Hsinchu 30013, Taiwan*

[3] *Molecular Science and Technology, Taiwan International Graduate Program, Academia Sinica and National Central University, Taipei 10617, Taiwan*

[4] *Department of Physics, National Taiwan University, Taipei 10617, Taiwan*

e-mail: *chenyc@pub.iams.sinica.edu.tw*

We present an experimental study on the storage of single photons generated from cavity-enhanced spontaneous parametric down conversion (SPDC) in cold atomic ensembles based on electromagnetically induced transparency (EIT) scheme. In a recent work[1], we have developed a photon-pair source with a bandwidth of 6.6 MHz and with the frequency of the signal photons locked to cesium D_2 transition. At a relatively low optical depth and control intensity such that the EIT transparent bandwidth is less than the photon bandwidth, the temporal profile of the single photons in coincidence counting splits into two parts with one slow and one non-slow components after passing through the EIT media. By increasing the optical depth and control intensity, the output single photon profiles gradually evolve into a pure slow light component. We systematically study the dependence of both components with the optical depth, control intensity or the EIT bandwidth. The storage efficiency versus the optical depth will be presented. Future work to obtain a high storage efficiency[2] with a developing narrowband (<1 MHz) single photons at cesium D_1 transition will be discussed. Because the cavity-based SPDC photon-pair sources are relatively compact and easy to be copied, our demonstration of storage of single photons generated from cavity-SPDC source is an important step towards future realization of quantum repeater protocol based on photon-pair sources and multimode memories[3].

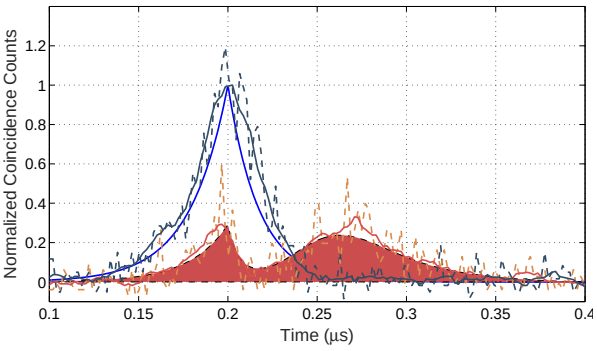


Figure 1: The single photon temporal profiles with (red) and without (black) passing through the EIT media. Dashed lines are the raw data and solid lines are the data with moving ageraging for 8 time bin with each bin width of 2 ns. The blue line is a calculation of the single photon profile with a bandwidth of 5.24 MHz. The red filled line is the calculation of the single photon pulse after passing through an EIT medium with an optical depth of 7.2 and a control Rabi frequency of $\Omega_c = 2.2\Gamma$. The total transmission containing both the slow and non-slow components is 67%. The value of 1 in y-axis is corresponding to 43 counts.

[1] P.-J. Tsai and Y.-C. Chen, Quantum Sci. Technol. **3**, 034005 (2018).

[2] Y.-F. Hsiao, P.-J. Tsai, H.-S. Chen, S.-X. Lin, C.-C. Hung, C.-H. Lee, Y.-H. Chen, Y.-F. Chen, I. A. Yu and Y.-C. Chen, Phys. Rev. Lett. **120**, 183602(2018).

[3] C. Simon, H. de Riedmatten, M. Afzelius, N. Sangouard, H. Zbinden and N. Gisin, Phys. Rev. Lett. **98**, 190503(2007).

Atom-chip interferometry with Bose-Einstein condensates

M. Gersemann[1], S. Abend[1], M. Gebbe[2], H. Ahlers[1], H. Müntinga[2], C. Schubert[1], C. Lämmerzahl[2], E. M. Rasel[1] and the QUANTUS team[1,2,3,4,5,6]

[1] *Institut für Quantenoptik, Leibniz Universität Hannover, 30167 Hannover, Germany*
[2] *ZARM, Universität Bremen, 28359 Bremen, Germany*
[3] *Institut für Physik, Humboldt-Universität zu Berlin, 10099 Berlin, Germany*
[4] *Institut für Quantenphysik, Universität Ulm, 89081 Ulm, Germany*
[5] *Institut für Angewandte Physik, Universität Darmstadt, 64289 Darmstadt, Germany*
[6] *Institut für Physik, JGU Mainz, 55122 Mainz, Germany*
e-mail: *gersemann@iqo.uni-hannover.de*

The small spatial and momentum width of ultracold atoms such as Bose-Einstein condensates (BEC) or delta-kicked collimated ensembles makes them very well suited for high precision atom interferometry [1]. As test masses where all relevant parameters are well known they are already used in geodesy and metrology, for example, measuring rotations, accelerations and fundamental principles of physics. In our atom-chip setup we benefit from a fast evaporation along with a compact design and reliably generate an ensemble of ultracold ^{87}Rb atoms. We employ different methods of coherent manipulation at high fidelity including state preparation as well as Bragg diffraction used as beam splitters and mirrors [2]. The sensitivity of atom interferometry experiments using a Mach-Zehnder sequence scales quadratically with the pulse separation time. Compact ground-based experiments have an intrinsic limitation of this time given by the free-fall baseline of the experimental setup. By combining a retro-reflected optical lattice with a double Bragg diffraction [3] pulse we developed a simple and versatile relaunch mechanism which allowed us to extend the interrogation time without increasing the baseline of the experiment. This ultimately led to the design of an atom-chip fountain gravimeter for compact volumes [4]. Another key technology for enhancing the sensitivity of atom interferometers is the implementation of large momentum transfer. For this reason we developed a new method for symmetric scalable large momentum separation using the combination of double Bragg diffraction and Bloch oscillations in a dual-lattice configuration. It is based on an initial splitting via double Bragg diffraction and a subsequent acceleration by Bloch oscillations. This sequence enables the transfer of up to $1008\,\hbar k$ in a single beam splitter and $408\,\hbar k$ when implemented in an atom interferometer, which is currently limited by technical constraints.

This work is supported by the German Space Agency (DLR) with funds provided by the Federal Ministry for Economic Affairs and Energy (BMWi) due to an enactment of the German Bundestag under grant number DLR 50WM1552-1557 (QUANTUS-IV-Fallturm), the Deutsche Forschungsgemeinschaft (DFG) in the scope of the SFB 1128 geo-Q and "Niedersächsisches Vorab" through the "Quantum- and Nano-Metrology (QUANOMET)" initiative.

[1] H. Müntinga et al., *Interferometry with Bose-Einstein Condensates in Microgravity*, Phys. Rev. Lett., **110**, 093602, (2013).

[2] E. Giese et al., *Light shifts in atomic Bragg diffraction*, Phys. Rev. A, **94.6**, 063619, (2016).

[3] H. Ahlers et al., *Double Bragg Interferometry*, Phys. Rev. Lett., **116**, 173601, (2016).

[4] S. Abend et al., *Atom-Chip Fountain Gravimeter*, Phys. Rev. Lett., **117**, 203003, (2016).

Phase Sensitive Amplification Enabled by Coherent Population Trapping

P. Neveu, C. Banerjee, J. Lugani, F. Bretenaker, E. Brion and F. Goldfarb
Laboratoire Aimé Cotton, Université Paris-Saclay, Bâtiment 505, 91405 Orsay, France
e-mail: *pascal.neveu@u-psud.fr*

Optical parametric amplification processes have been widely studied for their unique noise properties and their many possible applications in metrology, imaging and telecommunications. They have thus been implemented in different media such as nonlinear crystals and waveguides through three-wave mixing or fibers through four-wave mixing (FWM). In such processes, one or two strong driving pump field(s) Ω_c play the role of a reservoir of photons for a signal Ω_s and an idler Ω_i fields, where $\Omega_{c,s,i}$ are Rabi frequencies. Depending on the relative phase between these three fields, photons can be transferred from the pump(s) to the signal and idler fields or conversely. Such noiseless phase sensitive amplification (PSA) process allows the generation of squeezed states of light, which are of interest for quantum optics, atomic memories, entanglement swapping, and quantum information processing protocols. Very large quantum noise reduction up to 10 dB have been achieved using crystals, but down-converted photons are spectrally mismatched with atomic systems used for storage. PSA achieved directly through FWM in atomic systems does not have this drawback and is a subject of active interest [1].

In atomic systems, FWM efficiency can be boosted up using coherent population trapping (CPT) [2]. In this work, following the experimental results of [3], we isolate a novel FWM process, enabled by CPT, leading to efficient PSA through atomic superposition of states [4]. This process is permitted by the exploitation of two transitions starting from the same twofold degenerate ground state (Fig. 1.a). The D_1 transition is resonantly excited by a strong pump field that induces CPT, defining bright $|+\rangle_g$ and dark $|-\rangle_g$ states, where $|\pm\rangle_g = \left[|+1\rangle_g \pm |-1\rangle_g\right]/\sqrt{2}$. Ultra intense four-wave mixings can then be obtained from the dark state via the D_2 transition: signal and idler fields detuned by $\pm\delta$ from the pump (see Fig. 1b inset) are amplified through the following FWM paths

$$\text{via } |\pm2\rangle_2: \quad |-\rangle_g \overset{\Omega_c}{\to} |+\rangle_2 \overset{\Omega_{s,i}^*}{\to} |+\rangle_g \overset{\Omega_c}{\to} |0\rangle_1 \overset{\Omega_{i,s}^*}{\to} |-\rangle_g,$$
$$\text{via } |0\rangle_2: \quad |-\rangle_g \overset{\Omega_c}{\to} |0\rangle_2 \overset{\Omega_{s,i}^*}{\to} |+\rangle_g \overset{\Omega_c}{\to} |0\rangle_1 \overset{\Omega_{i,s}^*}{\to} |-\rangle_g.$$

where $|\pm\rangle_2 = \left[|+2\rangle_2 \pm |-2\rangle_2\right]/\sqrt{2}$.

This leads to a strong PSA (Fig. 1b) of the signal/idler fields even for low optical densities and out-of-resonance excitation of the D_2 transition. In our room-temperature metastable jelium cell of 2.7 optical depth, gain up to 9.3 dB are reachable. The

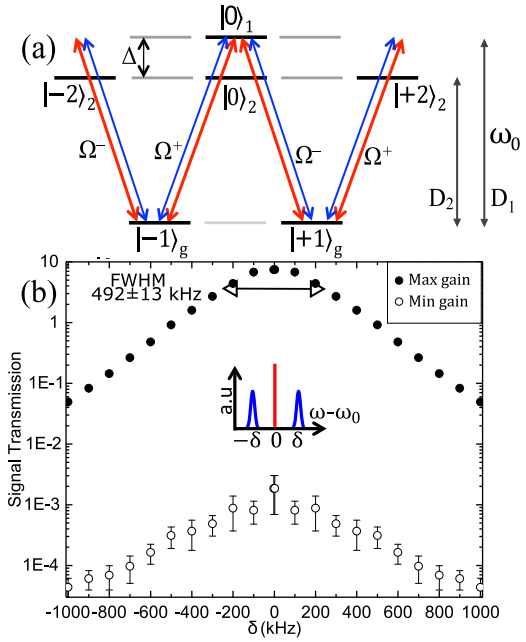


Figure 1: **(a)**: D_1 and D_2 transition of metastable helium, excited by a (red) pump and a (blue) signal/idler orthogonally and linearly polarized fields. Due to selections rules, grey levels are not relevant. $\Omega^\pm$ Rabi frequencies decomposition in the circular $\sigma_\pm$ basis. **(b)** Measurement of the signal/idler fields transmission, as function of their detuning δ from the pump. Scanning the relative phase between the fields, we extracted the maximum (•) and minimum (◦) gain. The bandwith of the process is the bandwith of the CPT induced by the pump.

enhancement of four-wave mixing can interpreted in the framework of the dark-state polariton formalism and we have develop an analytic treatment to extract the properties of the amplification process, and show that it has the properties of a perfect squeezer.

[1] N. V. Corzo, A. M. Marino, K. M. Jones, and P. D. Lett, Phys. Rev. Lett. **109**, 043602 (2012).

[2] S. E. Harris, J. E. Field, and A. Imamolu Phys. Rev. Lett. 64, 1107 (1990)

[3] J. Lugani, C. Banerjee, M.-A. Maynard, P. Neveu, W. Xie, R. Ghosh, F. Bretenaker, and F. Goldfarb, Opt. Lett. **41**, 4731-4734 (2016).

[4] P. Neveu, C. Banerjee, J. Lugani, F. Bretenaker, E. Brion and F. Goldfarb, arXiv:1803.05435.

Repulsive photons in a quantum nonlinear medium

A. Venkatramani[1], **S. Cantu**[2], **W. Xu**[2], **L. Zhou**[1], **M. Lukin**[1] **and V. Vuletić**[2]
[1] *Department of Physics, Harvard University, Cambridge, Massachusetts 02138, USA*
[2] *Department of Physics and Research Laboratory of Electronics, Massachusetts Institute of Technology, Cambridge, Massachusetts 02139, USA*
e-mail: *avenkatramani@g.harvard.edu*

Interacting quantum states of light offer possibilities in exploring new kinds of photonic matter and for use in quantum information. Photon interactions are generally weak, but we can engineer special media which can have strong photon-photon interactions. We achieve these strong interactions by coherently coupling light and Rydberg excitations in an ultracold atomic cloud. Such a system not only makes photons strongly interacting, but also gives them an effective mass. This has been used to create attractive photons which resulted in the observation of two and three photon bound states [1]. We now modify these interactions to create repulsive photons. We will present how the photon interactions can be controlled to make them repulsive and the measurements of few photon repulsion from correlation measurements. These basic ingredients of attraction and repulsion pave the way towards the realization, understanding, and control of strongly interacting quantum gases of light.

[1] Q-Y Liang *et. al. Science* **359**, 783-786 (2018).

Two-photon interferences with paired photons generation in a two-level atomic ensemble

Shuyu Zhou, Yuzhu Wang

Key Laboratory for Quantum Optics, Shanghai Institute of Optics and Fine Mechanics, The Chinese Academy of Sciences, 201800 Shanghai, China

e-mail: *syz@siom.ac.cn*

The usefulness of the paired-photon generated from four-wave mixing in a two-level atomic ensemble [1] has been demonstrated by implementing two-photon interference experiments. Rayleigh scatter of the pump provides a stable reference for obtaining normalized second-order correlation function, which makes it possible to compare theoretical predictions with experimental data quantitatively under unstable experimental conditions. This kind of light source can be used in quantum metrology in a robust way.

We prepare cold atomic ensemble in a ^{87}Rb magnetic-optical trap. A pair of counter-propagation laser beams, blue-detuned 54MHz from the transition $\left|5S_{1/2}, F=2\right\rangle \rightarrow \left|5P_{3/2}, F'=3\right\rangle$, excite atoms in a four-wave mixing process. Phase-matched counter-propagating photon pairs are generated and collected by a pair of polarization-maintaining (PM) single-mode fibers in opposed direction. Two polarizers in front of each fiber are set to insure the incident photons have the same linear polarization. We use two single photon detectors and a time-to-digital converter to obtain coincidence counts. The coincidence count, as showed in Fig. 1(a), has a damped oscillation and a flat background. The flat nonzero background is the accidental coincidence from uncorrelated Rayleigh scatter. Whereas for correlated photon pairs, $g^{(2)}(\tau)$ decay to zero for large τ. Therefore, we can use the coincident counts with large τ as the reference to get the normalized second-order correlation function, which is stable under fluctuant experimental conditions.

We perform the Hong-Ou-Mandel experiment which is similar to that in Ref. [2]. The photons are fed into a 50:50 beam splitter whose outputs are coupled to two PM single-mode fibers which connect to single-photon detectors. Damped oscillation coincidence peaks around $\tau = 0$ almost vanish due to two-photon destructive interference and the flat background maintains, as shown in Fig. 1(b). Then we investgate the case that two incident photons have orthogonal polarization. The effect due to distinguishable photons was observed by checking $g^{(2)}(\tau)$. We also measure autocorrelation of photons from one out-port of the HOM device. All these experimental results agree with theoretical predictions well.

Finally, we build a Mach-Zehnder interferometer which is composed of an electro-optic crystal and two polarization beam splitters. We find that balance

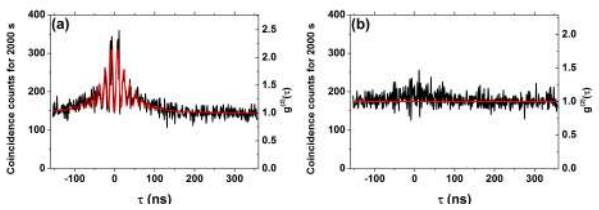


Figure 1: (a) Coincidence counts as a function of the time delay between detected photons for paired-photon generation in a two-state system. (b) HOM coincidence counts as a function of the time delay between detected photons.

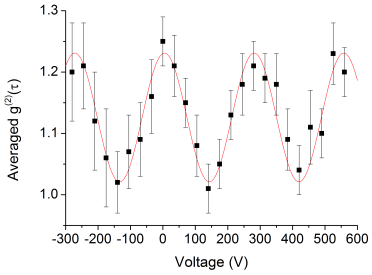


Figure 2: Two-photon interference signals in a Mach-Zehnder interferometer. We change the path-length difference by tuning the voltage on the electro-optic crystal.

input of Rayleigh scatter only provides a constant flat background which is independent with the optical path-length difference. The two-photon interference fringe is obtained by measuring averaged $g^{(2)}(\tau)$. As shown in Fig. 2, it is a sinusoidal signal superimposed on the background $g^{(2)}(\tau) = 1$.

[1] Shengwang Du, Jianming Wen, Morton H. Rubin, and G.Y. Yin, Phys. Rev. Lett. **98**, 053601 (2007).

[2] Chang Liu, J. F. Chen, Shanchao Zhang, Shuyu Zhou, Yoon-Ho Kim, M. M. T. Loy, G. K. L. Wong, and Shengwang Du, Phys. Rev. A **85**, 0218031 (2012).

Active temporal mode purification of quantum dots emission by quantum memory

S.Gao[1], O. Lazo-Arjona[1], B. Brecht[1,2], K. T. Kaczmarek[1,3], P. M. Ledingham[1], S. E. Thomas[1,4],J. Nunn[5],I. A. Walmsley[1],and D. J. Saunders[1]

[1] *Clarendon Laboratory, University of Oxford, Parks Road, Oxford OX1 3PU, United Kingdom*
[2] *Integrated Quantum Optics, Universität Paderborn, Warburger Strasse 100, 33098 Paderborn, Germany*
[3] *Groupe de Physique Appliquée, Université de Genève, CH-1211, Genève, Switzerland*
[4] *QOLS, Blackett Laboratory, Imperial College London, London SW7 2BW, United Kingdom*
[5] *Centre for Photonics and Photonic Materials, Department of Physics, University of Bath, Claverton Down, Bath BA2 7AY, United Kingdom*
e-mail: *dylan.saunders@physics.ox.ac.uk*

Single photon source (SPS) is required for many quantum information technologies. Semiconductor quantum dot (QD) is a promising SPS, which deterministically emits single photon with unprecedented brightness. However, QDs suffer from local environmental fluctuations as well as timing jitter. All these decrease the temporal-spectral purity of emitted photons. Further more, the full scalability of single photon sources requires identical photons from different QDs. However, producing, identical, scalable single-photons from semiconductor QD sources for quantum technologies remains a challenge. We propose a new technique "cascaded-absorption-buffer (CAB)" to transform impure quantum dot emission into identical pure state. We experimentally show that our device is noise-free and compatible with InGaAs-based QD, and we predict significant improvement in quantum dot performance using our CAB.

The emission from QD is a mixed state of spontaneous emission mode $|\phi(t_0,\omega_0)\rangle$ with central time (t_0) jitter and central frequency (ω_0) fluctuation:

$$\rho = \int p(t_0,\omega_0)|\phi(t_0,\omega_0)\rangle\langle\phi(t_0,\omega_0)|dt_0 d\omega_0 \qquad (1)$$

$p(t_0,\omega_0)$ is the probability distribution of ω_0 and t_0. The number density ρ can then be rewritten as a mixture of all its eigenmodes, $\rho = \sum \eta_k|\psi_k\rangle\langle\psi_k|$, with eigenvalues η_k and eigenmodes $|\psi_k\rangle$. A CAB is a modified ORCA memory[1] that can selectively absorb the main eigenmode with the largest eigenvalue and and then converts it to any wanted optical mode as the buffer's output after a short time of delay. All the other eigenmodes shall not be delayed so the output will be the most dominant pure state $|\psi_0\rangle$. We can also engineer the output of the buffers for different QDs to be the in the same optical mode, so that photons from distinct QDs will also be identical.

Such a quantum buffer requires four characteristics:

1. compatible with QD emission
2. noise free and high efficiency
3. mode selectivity
4. mode convertibility

we have experimentally shown the first one: it can work in the same frequency as InGaAs QD emission and the bandwidth match to each other, and the second: the device is free of noise and with high end-to-end efficiency. We also show that our model makes a good prediction of the behaviour of the CAB and with the model, we numerically explore the third and fourth requirement of our CAB.

We will also be discussing the imperfection of the CAB system and how to improve it. We predict the improvement on Indistinguishability of the QD to be much better than a ideal intensity filter.

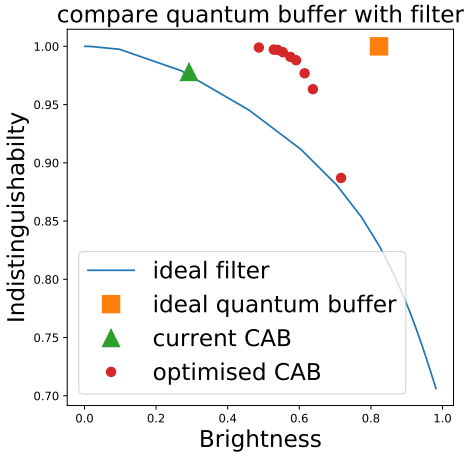


Figure 1: The improvement of a QD emission with initial Indistinguishaility of 0.69. Blue line is to use a intensity filter. the green triangle is the current CAB system. With pulse carving technique to optimize the CAB can make it outperform the ideal intensity filter (red circle). Orange square is the theoretical ideal performance

[1] K. T. Kaczmarek, P. M.Ledingham, B.Brecht, S.E.Thomas, G.S.Thekkadath, O.Lazo-Arjona, J.H. D.Munns, E.Poem, A.Feizpour, D.J. Saunders, J.Nunn, I,A, Walmsley, Phys. Rev. A **97**, 042316 (2018).

The fields of opto- and electromechanics have facilitated numerous advances in the areas of precision measurement and sensing, ultimately driving the studies of mechanical systems into the quantum regime. To date, however, the quantization of the mechanical motion and the associated quantum jumps between phonon states remains elusive. For optomechanical systems, the coupling to the environment was shown to preclude the detection of the mechanical mode occupation, unless strong single photon optomechanical coupling is achieved. Here, we propose and analyse an electromechanical setup, which allows us to overcome this limitation and resolve the energy levels of a mechanical oscillator. We find that the heating of the membrane, caused by the interaction with the environment and unwanted couplings, can be suppressed for carefully designed electromechanical systems. The results suggest that phonon number measurement is within reach for modern electromechanical setups.

Exploring Two Photon Processes Mediated by an Atom

V. Prakash[1], **L.C. Bianchet**[1], **N. Li**[1], **N. Bruno**[1], **and M.W.Mitchell**[1,2]
[1] *Institut de Ciències Fotòniques, The Barcelona Institute of Science and Technology, 08860 Castelldefels, Spain*
[2] *ICREA-Institució Catalana de Recerca i Estudis Avançats, 08015 Barcelona, Spain*
e-mail: *Vindhiya.Prakash@icfo.es*

We report on the development of a new experiment to study light matter interactions at the single particle level. The goal is to interface two narrowband entangled single photons with a single Rb^{87} atom (or a cloud of atoms), through strong coupling without the need for a cavity. This enables us to study non-linear effects at the single photon level, photon-photon interference effects mediated by an atom and atom-photon interactions involving indistinguishable entangled photons.

States containing one or a few photons have been used to elucidate many aspects of quantum mechanics and light-matter interactions such as multi-particle interference in the Hong-Ou-Mandel effect, linear-optics quantum computing [1] and ultra-sensitive quantum interferometry [2]. All these studies concern linear optics, in which each photon individually interacts with the material. Since single photons hardly interact with each other there is far less work in which small numbers of photons interact collectively with matter, i.e. nonlinear optics with single photons. Through coupling two resonant photons to a single atom we can explore the dynamics of the varied response of an atom to an input of two photons as opposed to one, the nonlinear response to the second photon due to saturation by the first and the quantum interference effects that will arise due to this nonlinearity along the lines of recent theory predictions [3]. Our source for frequency tuneable and correlated bi-photons also allows us to study fundamental processes such as stimulated emission and stimulated Raman transitions, which have not been previously studied at the level of of a single quantum emitter coupled to single photons. In this poster I describe the challenges for interacting multiple photons with the same material system, the solutions we are pursuing to meet this challenge and the fundamental questions we will investigate with our system.

Our experiment is novel in two aspects; firstly in that we develop a source for entangled, frequency-tuneable, pairs of photons whereby both photons can interact with the same atom. Secondly, the single atom is trapped in a dipole trap at the focus of 2 orthogonal pairs of lenses with a high numerical aperture of 0.5 and a focus of 1μm. This allows for the photons to interact through and be collected from two orthogonal spatial modes, thereby not only maximising the solid angle for accessing the atom but also opening the door to study previously unexplored aspects of atom-photon interactions. Our system is versatile such that not only can we trap a single atom but also a cloud of atoms to study collective interactions with photons.

With respect to the photons, the main experimental challenge is to generate them with sufficient brightness at a bandwidth smaller or equal to the unbroadened transition linewidth and in pairs that are time-frequency indistinguishable. The photons from Spontaneous Parametric Down Conversion (SPDC), a very broadband process,can be made compatible with narrowband atomic resonances through the addition of a cavity around the SPDC source. The cavity also enhances the brightness of the photon source through the Purcell effect; thus, the technique is referred to as Cavity Enhanced SPDC (CESPDC)[4]. We employ a Type II phase matched PPKTP crystal as the SPDC source for polarisation entangled photons.

Although the cavity reduces the bandwidth of the photons, the SPDC process generates photons spanning several free spectral ranges of the cavity. We can reduce the fraction of photons at unwanted frequencies through the clustering effect, which takes advantage of the birefringence induced differential path lengths experienced by the signal and idler. Since the free spectral ranges of the signal and idler are different, the condition for simultaneous resonance is satisfied only for those regions in the spectrum where the transmission peaks for both the signal and idler coincide. This reduces the number of modes coming out of the cavity to a large extent. We use an additional crystal to enhance the difference in the free spectral ranges and to control this simultaneous resonance. This gives an additional degree of control along with frequency tuneable interconnected locking schemes for the cavity and lasers involved, leading to a frequency versatile on demand system for narrowband, correlated, atom-resonant photons. Additionally we implement a tuneable filter cavity for a genuine single mode output.

[1] J. L. O'Brien, G. J. Pryde, A. G. White, T. C. Ralph, and D. Branning, Nature **426**, 264 (2003).

[2] F. Wolfgramm, C. Vitelli, F. A. Beduini, N. Godbout, and M. W. Mitchell, Nature Photonics **7**, 28 (2013).

[3] A. Roulet, H. N. Le, and V. Scarani, Physical Review A **93**, 033838 (2016).

[4] F. Wolfgramm, X. Xing, A. Cerè, A. Predojević, A. M. Steinberg, and M. W. Mitchell, Opt. Express **16**, 18145 (2008).

1D Atomic Lattices For Atom-Photon Physics

L. S. Peng[1], **A. P. Burgers**[1], **and H.J. Kimbles**[1]

[1] *Norman Bridge Laboratory of Physics MC12-33, California Institute of Technology, Pasadena, California 91125, USA*

e-mail: *lpeng@caltech.edu*

Integrating ultracold atoms with nanophotonics enables the exploration of new paradigms in quantum optics and many body physics. Low-loss dielectric structures can be fabricated to support guided mode (GM) light used to create stable trapping potentials for neutral atoms. The dispersion relation of a photonic crystal waveguide (PCW) structure can be engineered to study the physics of photon-mediated atom-atom interactions as well as collective atomic effects [1][2]. The central component of our device is the 'alligator' photonic crystal waveguide (APCW) [3], as shown in Fig.1. We utilize an optical lattice transport approach to achieve high fractional filling of the trap sites.

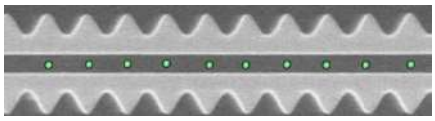


Figure 1: An 'Alligator' Photonic Crystal Waveguide (APCW), green dots indicate atom trap sites.

Trapping atoms near dielectric photonics crystal waveguides requires novel adaptations of standard atomic physics techniques. In our current system, a conveyor belt optical lattice is utilized for transport of atoms into the photonic crystal GM trap in a 'clocked' fashion. The 'clocked' transmission signal contains rich information of atomic movement near the PCW. We will present numerical simulations of atomic trajectories moving in the interference and diffraction patterns of the optical lattice beams with the APCW. A calculation of the transmission signal via transfer matrix model allows us to draw comparisons between simulation and experiment, an example is shown in Fig.2. Understanding the interaction between GM traps, optical lattice conveyor belt and atoms, constitutes a significant first step towards trapping several atoms along the waveguide and observing single, and collective atomic phenomena in an engineered photonic environment. For example, by manipulating the probe guided mode in simulations, atoms interact with different part of the APCW can be identified (Fig.3).

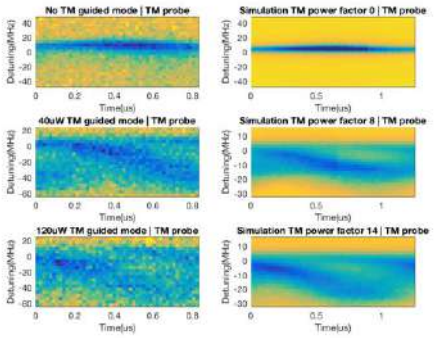


Figure 2: Comparison of simulation and experimental 'clocked' spectrum.

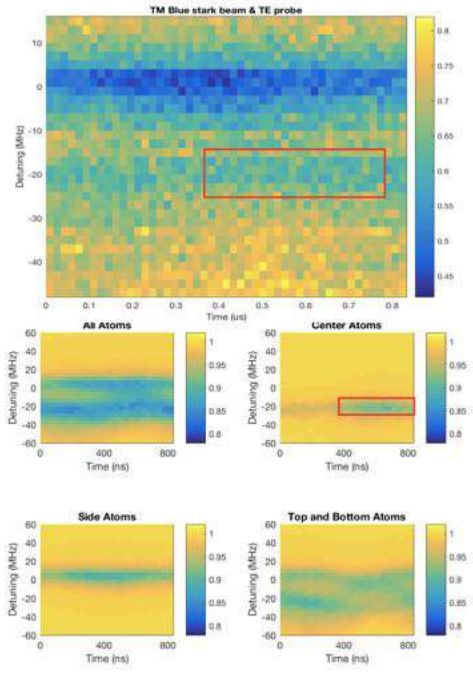


Figure 3: Experimental 'clocked' spectrum with four simulated spectrum with manipulated probe GMs. Boxes indicate the detuning and time relative to the lattice period where atoms couple most strongly to the APCW.

[1] C.-L Hung et al., PNAS. 133(34) E4946-E4955 (2016)

[2] A. Asenjo-Garcia et al., Phys. Rev. X. **7**, 031024 (2017).

[3] S.-P. Yu et al., Appl. Phys. Lett. **104**, 111103 (2014).

Deterministic quantum entanglement among three distant atomic ensembles

Zhihui Yan[1,2], **Liang Wu**[1], **Xiaojun Jia**[1,2], **Yanhong Liu**[1], **Ruijie Deng**[1], **Shujing Li**[1,2],**Hai Wang**[1,2], **Changde Xie**[1,2]**and Kunchi Peng**[1,2]

[1] *State Key Laboratory of Quantum Optics and Quantum Optics Devices, Institute of Opto-Electronics, Shanxi University, Taiyuan 030006, China.*

[2] *Collaborative Innovation Center of Extreme Optics, Shanxi University, Taiyuan 030006, China.*

e-mail: *zhyan@sxu.edu.cn*

In a quantum network, consisting of quantum nodes and quantum channels, it is essential to establish and store entanglement among multiple distant nodes and then release stored entanglement into quantum channels [1]. Especially atomic ensembles are one of ideal candidates of quantum nodes to store and process quantum information with advantage of the collective enhancement of light-atom interaction. The measurement-induced entanglement storing in four atomic memories as well as transferring the stored entangled state in the atomic ensembles into individual photonic state in quantum channel have been experimentally demonstrated in 2010 [2]. Deterministic quantum entanglement of continuous-variables (CVs) between two atomic ensembles has been produced by means of quantum-non-demolition measurement and dissipation mechanism, respectively [3, 4]. To date, deterministically entangling among more than two atomic ensembles still remains a challenge in CV regime.

Here we present an experimental demonstration on generation, storage and transfer of deterministic quantum entanglement among three atomic ensembles located 2.6 m apart from each other [5]. Schematic diagram for generation, storage and transfer of deterministic entanglement among among three nodes is demonstrated in Figure 1. The off-line prepared tripartite entanglement of optical modes is mapped into three distant atomic ensembles to establish the entanglement among atomic spin waves via Electromagnetically-Induced-Transparency (EIT) light-matter interaction. After a storage duration the stored atomic entanglement is transferred into a tripartite space-separated entangled state of light. By measuring combination of correlation variances among three submodes released from three atomic ensembles after a storage duration, the capacity of preserving multipartite entanglement in the presented system is experimentally verified. In our system this combination value is about is 0.96, which is less than quantum noise limit.

However, the high-fidelity quantum information application requires high quality entanglement among quantum nodes which is determined by the quality of input entangled optical modes and the CV quantum memory efficiency. And thus high efficiency

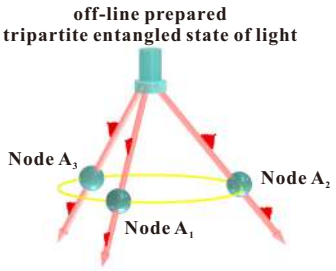


Figure 1: Schematic diagram for generation, storage and transfer of deterministic entanglement among among three nodes.

quantum memory is the key for the practical applications. And we are trying to improve the quadrature memory efficiency with the help of cavity-enhanced EIT dynamics. As well a high entangled degree among multiple atomic ensembles can be obtained by mapping the quantum state from multiple entangled optical modes into a collection of atomic spin waves inside optical cavities [6].

[1] H. J. Kimble, Nature **453**, 1023 (2008).

[2] K. S. Choi, A. Goban, et al. Nature **468**, 412 (2010).

[3] B. Julsgaard, A. E. Kozhekin, and E. S. Polzik, Nature **413**, 400 (2001).

[4] H. Krauter, C. A. Muschik, et al. Phys.Rev. Lett. **107**, 080503 (2011).

[5] Z. H. Yan, L. Wu, et al. Nature Commun. **8**, 718 (2017).

[6] Z. H. Yan, Y. H. Liu, et al. Phys.Rev. A **97**, 013856 (2018).

Four-wave-mixing and entanglement of spatially separated light

Wanxia Cao[1], **Jian Sun**[1], **Xingda Lu**[1], **Xin Meng**[1], **Heng Shen**[2], **and Yanhong Xiao**[1]
[1] *Department of Physics, Fudan University, Shanghai 200433, China*
[2] *Clarendon Laboratory, University of Oxford, Parks Road, Oxford, OX1 3PU, UK*
e-mail: *13110190001@fudan.edu.cn*

Entangled light beams are important resources in quantum information science and metrology, and they are commonly produced by wave mixing processes, for instance a double-Λ atomic system, which are mostly off-resonant to avoid absorption and noises. Here, we report nonlocal four wave mixing using resonant Λ-type electromagnetically induced transparency (EIT) configuration, but with two spatially separated optical channels coupled by moving atoms, which effectively form a double-Λ cycle. This scheme can enable steady state entanglement between spatially separated laser beams, and loosen requirement on energy levels and laser power.

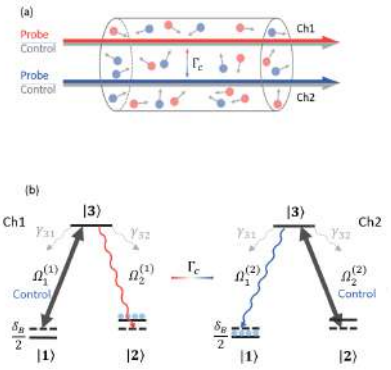


Figure 1: Experiment schematics.

The experiment schematics is shown in Fig. 1. The control (probe) fields in EIT for the two optical channels couple different transitions. Rapid coherence transport in the paraffin-coated ^{87}Rb cell effectively couple the two channels [1]. The two weak probes play the similar roles to that of the Stokes and anti-Stokes fields in four wave mixing (FWM). Intuitively, as the atomic coherence is being created in Ch1, the population is driven from $|1\rangle$ to $|2\rangle$; when this atom enters Ch2, the population is brought back to $|1\rangle$. The process is continuously boosted along with the coherence transfer. In our experiment, we proved that this coupled two channel system is nonlinear, and possesses the characteristics of conventional FWM system: phase-sensitive gain and phase matching behavior, as shown in Fig. 2. Also, our theoretical model predicts quantum correlations in the amplitude-quadrature and anti-correlations in the phase-quadrature of two probes. The entanglement criterion we will here is $I(\omega) < 1$, where the inseparability [2], [3] parameter is defined as $I(\omega) = 1/2(S_x{}^- + S_p{}^+)$. As shown in Fig. 3 , when the two channels are on two-photon resonance, the minimum $10\log_{10} I(\omega)$ is found to be -3 dB, near zero analysis frequency. Experimental verification of this entanglement is underway.

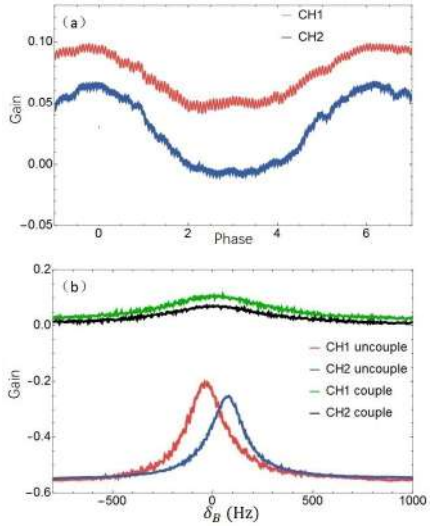


Figure 2: Experimental results. (a) Gain for the probes when the probe's phase in one channel is swept. (b) Probe gain as a function of two-photon detuning δ_B. Here, positive (negative) values stand for gain (absorption).

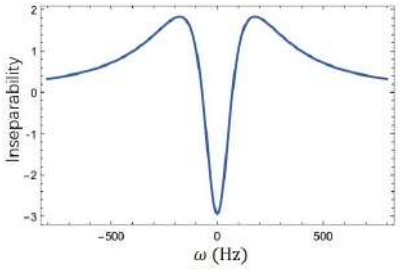


Figure 3: The calculated normalized inseparability spectrum.

[1] P. Peng, W. Cao, C. Shen, W.Qu, L. Jiang, J. Wen, and Y. Xiao, Nat. Phys. 12,1139 (2016).

[2] L. Duan, G. Giedke, J. I. Cirac, and P. Zoller, Phys. Rev. Lett. 84, 2722 (2000).

[3] R. Simon, Phys. Rev. Lett. 84, 2726 (2000).

Statistics of atom pair production by four wave mixing

C. I. Westbrook, M. Perrier, Z. Amodjee, P. Dussarrat, M. Cheneau, D. Boiron
Laboratoire Charles Fabry, Institut d'Optique Graduate School, CNRS, Universit ParisSaclay, 91127 Palaiseau cedex, France
e-mail: *christoph.westbrook@institutoptique.fr*

Photon pair generation via spontaneous parametric downcorversion has been a workhorse in the field of quantum optics for many years. Numerous fundamental effects have been demonstrated ranging from squeezing to teleportation. Consequently, the characteristics of downconversion sources has been extensively studied. It has been shown that in this situation, strong correlations are present between the beams, while each individual beam, after tracing over the other one is in a thermal state [1].

This feature has been verified experimentally by measuring the pair correlation function of the individual beams, and showing that the beam exhibits the same antibunching behavior as a single mode of a thermal source. Instead of correlation functions, one can alternatively examine the population distribution in a given mode to confirm its thermal nature. This type of measurement is less common in optics, although there are a few experiments which have been carried out [2, 3, 4, 5]. Part of the reason for the difficulty is the lack of practical detectors capable of distingushing multiple photon states.

An atomic analog of the pair production process, atomic four wave mixing has been used in several recent experiments inspired by quantum optics but atoms [6, 7]. Here too, pair correlation functions have been observed to exhibit atom bunching in individual modes [7, 8]. But atomic twin beam sources, being generated from initial BEC's have high spatial coherence and long coherence times, thus atom detectors, using either optical interactions or a microchannel plate (MCP) can directly measure populations in a single atomic mode. This feature has already been used in Ref. [9] to measure mode populations and in Ref. [10] to measure correlation functions up to the 6th order in a thermal atomic source. Here we use an MCP detector to directly measure populations in twin beams. We show that when the detection region is chosen to single out a single atomic mode, the population displays a thermal distribution, decreasing as a power law as predicted by the Boltzmann law. If the detection region is chosen to be much larger so that many modes contribute, the distribution begins to approach a Poissonian.

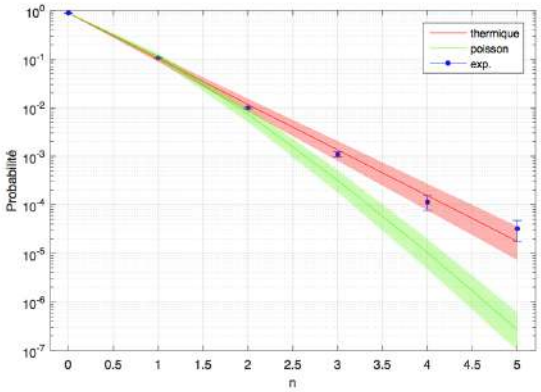


Figure 1: Count distribution of one mode of the output of the atom pair source, normalized to an integral of unity. The red line shows a thermal distribution with a mean detected atom number of 0.078. The red band shows a range of detected atom numbers varying by ±15%. The green band shows a Poisson distribution with the same mean.

[1] B. Yurke and M. Potasex, Phys. Rev. A 36, 3464 (1987).

[2] M. Vasilyev, S.-K. Choi, P. Kumar, and G. DAriano, Optics letters 23, 1393 (1998).

[3] A. Mosset, F. Devaux, G. Fanjoux, and E. Lantz, The European Physical Journal D - Atomic, Molecular and Optical Physics 28, 447 (2004).

[4] F. Paleari, A. Andreoni, G. Zambra, and M. Bondani, Optics Express 12, 2816 (2004).

[5] T. S. Iskhakov, A. Perez, K. Y. Spasibko, M. Chekhova, and G. Leuchs, Optics letters 37, 1919 (2012).

[6] R. Lopes et al., Nature 520, 66 (2015).

[7] R. I. Khakimov et al., Nature 540, 100 (2016).

[8] M. Bonneau et al, Physical Review A 87, 061603 (2013).

[9] A. Ottl, S. Ritter, M. Kohl, and T. Esslinger, Physical Review Letters 95 (2005).

[10] R. G. Dall et al., Nature Physics 9, 341 (2013).

Photons in the presence of parabolic mirrors

R. Jáuregui[1] **and R. Gutiérrez-Jáuregui**[2]

[1] *Instituto de Física, Universidad Nacional Autónoma de México, Apdo. Postal 20-364, 01000 Cd. de México, México*

[2] *The Dodd-Walls Centre for Photonic and Quantum Technologies, Department of Physics, University of Auckland, Private Bag 92019, Auckland, New Zealand*

e-mail: *rocio@fisica.unam.mx*

A vectorial analysis of the behavior of the electromagnetic field in the presence of boundaries with parabolic geometry is given [1]. Using the well known solutions for the scalar waves [2] and fully symmetrized Hertz potentials [3], the general expressions for the electromagnetic modes delimited by boundaries with parabolic shape are found. The modes are classified according to their relation to vector Hertz potentials $\vec{\pi}$: for $\mathcal{E}$-modes the electric field is given by $\vec{E} = \vec{\nabla} \times \vec{\pi}$, and for $\mathcal{B}$-modes the magnetic field is given by $\vec{B} = \vec{\nabla} \times \vec{\pi}$.

The elementary modes are obtained taking into account the symmetry transformations that distinguish the parabolic geometry. Polarization and phase related angular momenta of light have an essential role in the proper definition of the relevant generators, which correspond to the operator related to the component of the total angular momentum along the symmetry axis,

$$\hat{J}_3 \phi_r = -i(x_1 \partial_2 - x_1 \partial_2)\phi_r + \sum_{s=1,2,3} \widehat{\mathcal{S}}_{rs12} \phi_s, \quad (1)$$

and the kinetic part of the Runge Lenz vector along the same axis,

$$\hat{\mathfrak{A}}_3 \phi_r = \frac{1}{2} \sum_{s=1,2,3} \Big[\{\widehat{M}_{rs23}, \widehat{P}_2\} - \{\widehat{M}_{rs31}, \widehat{P}_1\} \Big] \phi_s. \quad (2)$$

Quantization of the electromagnetic field in terms of the resulting orthonormal elementary modes is performed. The scalar product used to determine this property is defined by the extrapolation of the expression of the EM energy density for two different modes. As a consequence, Einstein quantization can be directly implemented using these modes which define the quantum numbers of the corresponding photons.

The important case of a boundary defined by an ideal parabolic mirror is explicitly worked out. The presence of the mirror constrains the relative weights of the components of the Hertz potentials, and restricts the eigenvalues of $\mathfrak{A}_3$ available to the electric and magnetic fields of a given mode, via compact expressions. Modes previously reported in the literature [4] are particular cases of those described in this work.

The natural parabolic modes exhibit both electric and magnetic fields with a non trivial and rich topology: regions where the electric field has a magnitude different to the magnetic field, phase singularities, dislocation lines, vectorial vortices as well as strong gradients of the field components.

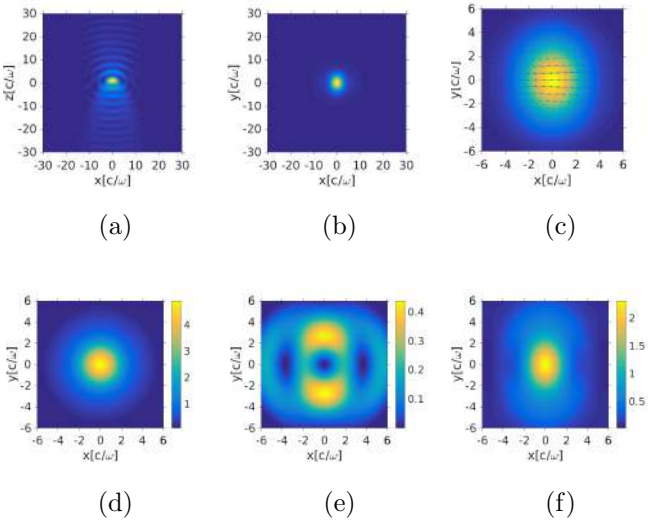


Figure 1: Illustrative example of the density of EM energy of a $\mathcal{E}$-mode for a mirror surface at $\zeta_0 = 35700c/\omega$ at the (a) plane defined by $x_2 = 0$ and at the (b) plane defined by $x_3 = 0$; (c) illustrates the electric field projection into the plane $x_3 = 0$;(d) $|\mathbf{E} \times \mathbf{e}_3|^2$; (e) $|\mathbf{E} \cdot \mathbf{e}_3|^2$; (f) $|\mathbf{B} \times \mathbf{e}_3|^2$ are illustrated at the $x_3 = 0$ plane.

The expected behavior of a cold atom trapped nearby the focus of a deep parabolic mirror is also discussed.

[1] R. Gutiérrez-Jáuregui and R. Jáuregui, *submitted to Phys. Rev. A.*

[2] C. P. Boyer, E. G. Kalnins, and W. Miller Jr., *Nagoya Math. J.* **60**, 35-80 (1976).

[3] A. Nisbet, *Proc. R. Soc. A* **231**, 250 (1955).

[4] G. Alber, J. Z. Bernád, M. Stobińska, L. L. Sánchez-Soto, and G. Leuchs, *Phys. Rev. A* **88**, 023825 (2013).

Optical nanoantennas for light - matter coupling through parallel multipolar mechanisms

P. Gładysz[1], **E. Rusak**[2], **J. Straubel**[2], **F. Weigend**[3], **C. Rockstuhl**[2], **K. Słowik**[1]

[1] *Institute of Physics, Faculty of Physics, Astronomy and Informatics, Nicolaus Copernicus University, Grudziadzka 5, 87-100 Torun, Poland*

[2] *Institut für Theoretische Festkörperphysik, Karlsruhe Institute of Technology, Germany*

[3] *Institut für Nanotechnologie, Institut für Physikalische Chemie Abteilung für Theoretische Chemie, Karlsruhe Institute of Technology, Germany*

e-mail: *pg@atomista.pl*

Optical nanoantennas are nanoscopic devices which dimensions are comparable to the visible light wavelengths. They are usually made of noble metals, dielectrics or even more exotic materials such as graphene [1]. In analogy to their macroscopic counterparts, they are able to mediate between electromagnetic radiation and localized regions of space. Quantum systems positioned at such regions are then subject to interaction with largely enhanced (even a few orders of magnitude) and spatially confined electromagnetic fields [2].

It is higly valuable to examine behaviour of quantum systems in these 'hot spots'. Increased modes density in such positions causes faster spontaneous emisson, higher frequency of Rabi oscillations or enlarge importance of multipole expansion terms beyond electric dipole. That means interaction is not only stronger than in a free space, but its character is also changed by admitting previously inavailable channels, e.g. magnetic dipolar or electric quadrupolar coupling [3].

I will present applications of nanoantennas neighbouring molecules or quantum dots, as efficient devices to control light-matter interaction through multiple mechanisms. These mechanisms are related to several electric and magnetic multipolar terms of the coupling Hamiltonian. In particular, the magnetic dipolar and electric quadrupolar terms become significant due to strong electromagnetic field enhancement and confinement near the nanoantenna. I will discuss nanoantennas tailored to selectively enhance individual interaction mechanisms, or to capitalize on their interference. Interference may cause an even stronger enhancement, but also it can strongly suppress a given transition. The suppression is achieved through tailoring the electromagnetic environment, usually discussed in terms of density of states, such that the spontaneous emission rate is decreased. An example of a nanoantenna geometry with properties described above is presented in the picture.

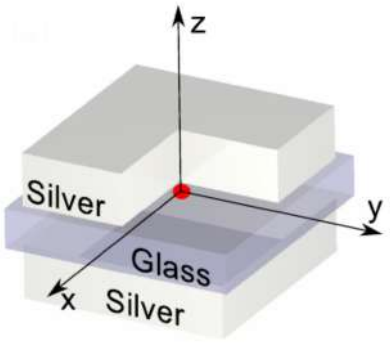


Figure 1: System composed of two silver plates separated by a glass layer with a molecule in its center.

[1] L. Novotny and N. Van Hulst. *Antennas for light*, Nature photonics 5(2), 83 (2011),

[2] G. M. Akselrod, et al. *Probing the mechanisms of large Purcell enhancement in plasmonic nanoantennas*, Nature Photonics 8(11), 835 (2014),

[3] R. Filter, S. Mühlig, T. Eichelkraut, C. Rockstuhl, and F. Lederer, *Controlling the dynamics of quantum mechanical systems sustaining dipole-forbidden transitions via optical nanoantennas*, Phys. Rev. B, 86(3), 035404 (2012).

Interaction of an asymmetric two-level quantum system with light

P. Gładysz, K. Słowik
Institute of Physics, Faculty of Physics, Astronomy and Informatics, Nicolaus Copernicus University, Grudziadzka 5, 87-100 Torun, Poland
e-mail: *pg@atomista.pl*

The subject of this contribution are quantum systems with broken inversion symmetry (Fig. 1) subject to a strong driving laser field, which can be used as an optically tunable radiation source.

A two-level quantum system characterized with inversion symmetry and coupled to a classical electromagnetic field undergoes Rabi oscillations where the population flips between the ground and excited levels.

I will demonstrate how the dynamics is modified if a system of broken inversion symmetry is exploited instead [1]. Then, the eigenstates are characterized with a permanent electric dipole moment originating from the polarisation of charges, which plays a significant role of an additional dipole source of radiation. The frequency of this radiation corresponds to the Rabi frequency of population transfer between the eigenstates [2], and could reach the terahertz domain if the quantum system is driven by strong electromagnetic fields, e.g. at close vicinity of plasmonic nanostructures [3]. What is more, the emission frequency would be tunable with a knob, by changing the intensity of the driving field.

I will discuss the effect in the density matrix formalism, taking into account various decoherence mechanisms, including spontaneous emission and collisional dephasing. Estimates of radiation intensity will be provided for experimentally feasible realistic systems, such as ensembles of asymmetric molecules.

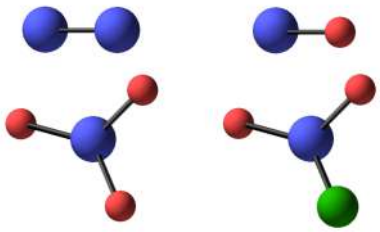


Figure 1: An example of systems with inversion symmetry (left) and without it (right).

[1] O. V. Kibis, G.Ya. Slepyan, S.A. Maksimienko, A. Hoffman, Matter Coupling to Strong Electromagnetic Fields in Two-Level Quantum Systems with Broken Inversion Symmetry, Physical Review Letters, 2009.

[2] P. Gładysz, Asymetryczny układ dwupoziomowy w oddziaływaniu ze światłem, bachelor's thesis, Toruń (2017).

[3] L. Novotny, N. van Hulst, Antennas for light, Nature Photonics, 5, 83–90 (2011).

Fast, noise-free memory for photon synchronization at room temperature

Ran Finkelstein[1], **Eilon Poem**[1], **Ohad Michel**[1], **Ohr Lahad**[1] **and Ofer Firstenberg**[1]
[1] *Department of Physics of Complex Systems, Weizmann Institute of Science, Rehovot 7610001, Israel.*
e-mail: *ran.finkelstein@weizmann.ac.il*

Future quantum photonic networks require coherent optical memories for synchronizing quantum sources and gates of probabilistic nature. We demonstrate a fast ladder memory (FLAME) mapping the optical field onto the superposition between electronic orbitals of rubidium vapor. Employing a ladder level-system of orbital transitions with nearly degenerate frequencies simultaneously enables high bandwidth, low noise, and long memory lifetime. We store and retrieve 1.7-ns-long pulses, containing 0.5 photons on average, and observe short-time *external* efficiency of 25%, memory lifetime ($\mathbf{1/e}$) of 86 ns, and below $\mathbf{10^{-4}}$ added noise photons. One immediate consequence is that coupling this memory to a probabilistic source would enhance the *on-demand* photon generation probability by a factor of 12, the highest number yet reported for a noise-free, room-temperature memory. This paves the way towards the controlled production of large quantum states of light from probabilistic photon sources [1].

As a next step, we are introducing a tapered fiber into the atomic vapor, yielding simultaneously both tightly focused beams with extremely high Rabi frequency and high OD. This would enable operating this scheme at an even higher bandwidth as well as extending the ladder scheme to high lying Rydberg states for quantum non-linear optics experiments.

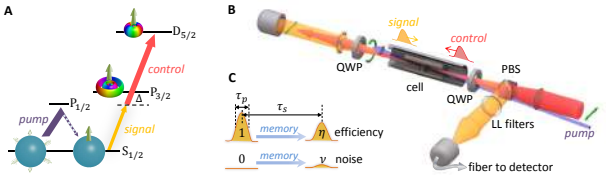


Figure 1: FLAME scheme. **(A)** A ladder level structure comprising purely orbital transitions (the surface colors display the phase structure of the orbitals $5s$, $5p$, and $5d$) is achieved by optical pumping (purple) of the nuclear and electronic spins (green arrows) to the maximally-polarized state. Nonzero detuning Δ from the intermediate level can be introduced. **(B)** Experimental setup. **(C)** The parameters governing the synchronization capability of the memory are pulse duration τ_p, memory lifetime τ_s, retrieval efficiency η, and noise ν.

[1] R. Finkelstein, E. Poem , O. Michel, O. Lahad, and O. Firstenberg. Fast, noise-free memory for photon synchronization at room temperature. Science Advances 4(1), eaap8598 (2018).

Interfacing single trapped atoms to a pair of indistinguishable photons

Natalia Bruno[1], **Lorena C. Bianchet**[1], **Vindhyia Prakash**[1], **Nan Li**[2] **and Morgan W. Mitchell**[1,3]

[1] *ICFO-Institut de Ciencies Fotoniques, The Barcelona Institute of Science and Technology, 08860 Castelldefels, Barcelona, Spain*

[2] *State Key Laboratory of Modern Optical Instrumentation, College of Optical Science and Engineering, Zhejiang University, Hangzhou 310027,China*

[3] *ICREA-Institucio Catalana de Recerca i Estudis Avancats, 08010 Barcelona, Spain*

e-mail: *natalia.bruno@icfo.eu*

We are building a system to interact tunable, atom-resonant photons from cavity-enhanced spontaneous parametric down-conversion (CE-SPDC) with individual atoms trapped at the focus of four high-numerical-aperture (NA) lenses. By combining resonant photon pairs with single atoms, we will be able to shed light on fundamental light-matter processes that to date have never been directly studied.

Promising applications of the study of isolated quantum systems can be found in quantum information science, e.g. for investigating quantum interference between atoms [1], or the scattering of photons generated in atom-based sources [3], or in down-conversion sources [4], but also for quantum simulation with arrays of Rydberg atoms [2].

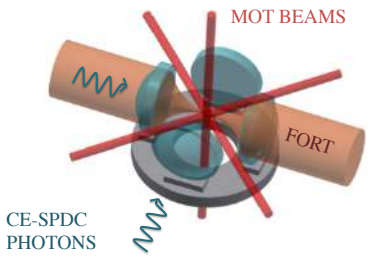


Figure 1: Sketch of the setup. Four aspheric lenses (NA=0.5) are aligned in a confocal configuration in order to focus a red-detuned far-off-resonance trapping beam (FORT) down to a waist of $\sim 1\mu$m and thereby trap a single ^{87}Rb atom loaded from a magneto-optical trap (MOT). Through the same lenses we probe it and efficiently collect scattered light. A CE-SPDC source is used to produce narrowband, atom-resonant and indistinguishable photons.

We use neutral alkali atoms such as ^{87}Rb using tightly focused far off resonance beams. High NA optics provides not only a simple tool for implementing micrometric optical dipole traps, but also an efficient interface between a single ^{87}Rb atom and resonant light. In particular, we have two pairs of aspheric lenses with high NA for strongly-focusing a far red detuned trapping beam, single-photon probing and collecting light from four different directions, as shown in Fig. 1, two more with respect to already existing setups.

The setup is novel and versatile, as it allows us to trap one or more atoms in the same potential or in an array of traps by means of a standing wave, and, interestingly, it allows us to probe the system and collect scattered light from an orthogonal direction. Moreover, merging a photon source with a trapped atom and having more optical access allows us to observe light matter interaction in the single-particle regime and paves the way for studying for the first time a wide range of phenomena involving atoms and quanta of light.

References

[1] A. Kaufman, B. Lester, C. Reynolds, M. Wall, M. Foss-Feig, K. Hazzard, A. Rey, and C. Regal. Two-particle quantum interference in tunnel-coupled optical tweezers. *Science*, 345(6194):306–309, 2014.

[2] H. Labuhn, D. Barredo, S. Ravets, S. de Léséleuc, T. Macrì, T. Lahaye, and A. Browaeys. Tunable two-dimensional arrays of single Rydberg atoms for realizing quantum Ising models. *Nature*, 534, June 2016.

[3] V. Leong, M. A. Seidler, M. Steiner, A. Cer, M. Foss-Feig, and C. Kurtsiefer. Time-resolved scattering of a single photon by a single atom. *Nature Communications*, 7(13716), 2016.

[4] C. Schuck, F. Rohde, N. Piro, M. Almendros, J. Huwer, M. W. Mitchell, M. Hennrich, A. Haase, F. Dubin, and J. Eschner. Resonant interaction of a single atom with single photons from a down-conversion source. *Phys. Rev. A*, 81:011802, Jan 2010.

Atom-phonon interaction in fiber-based optical traps

D. Hümmer[1,2], **P. Schneeweiss**[3], **A. Rauschenbeutel**[3,4], **and O. Romero-Isart**[1,2]

[1] *Institute for Quantum Optics and Quantum Information of the Austrian Academy of Sciences, 6020 Innsbruck, Austria*

[2] *Institute for Theoretical Physics, University of Innsbruck, 6020 Innsbruck, Austria*

[3] *Vienna Center for Quantum Science and Technology, TU Wien - Atominstitut, 1020 Vienna, Austria*

[4] *Institute of Physics, Humboldt-Universität zu Berlin, Germany*

e-mail: *daniel.huemmer@uibk.ac.at*

In recent years, it has become feasible to trap ensembles of individual atoms in the near-field of photonic nanoscale structures, such as tapered optical fibers. In the latter setup, evanescent fields surrounding a light-guiding nanofiber create an optical trapping potential a few hundred nanometers from the fiber surface. In experiments, a finite life-time of atoms in such fiber-based optical traps is being observed. One effect which may lead to the loss of a trapped atom is the heating of its center of mass motion by vibrations of the fiber itself.

We present a theoretical description of the effective interaction between the center of mass of the atom and vibrations of the fiber. The latter adiabatically change the optical fields surrounding the fiber, both by displacement of the fiber surface (radiation pressure), and by strain-induced inhomogeneity and anisotropy of the electric permittivity (strain-optical coupling). In consequence, the optical fluctuates, leading to an effective atom-phonon coupling. We derive a quantum description of the exchange of phononic excitations between a trapped atom and the fiber itself. The resulting model may be generalized to optical near-field traps based on other waveguide geometries. We estimate life-times for atoms in optical fiber traps, using parameters of existing experimental setups.

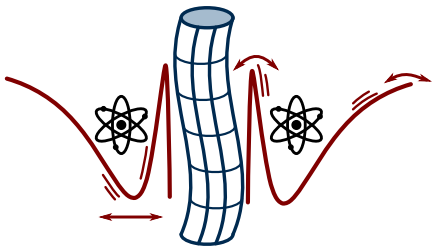


Figure 1: Visualization of atom-phonon interacton through radiation pressure (left) and strain-optical coupling (right).

Quantum optics in the hyperfine Paschen-Back regime (with STROLLing)

Renju S. Mathew,[1,*] **James Keaveney**,[1] **Daniel Whiting**,[1]
Francisco Ponciano-Ojeda,[1] and **Ifan G. Hughes**[1]

[1] *Joint Quantum Centre (JQC) Durham-Newcastle, Department of Physics, Durham University, South Road, Durham, DH1 3LE, United Kingdom*

The propagation of light through thermal atomic vapours subject to external magnetic fields continues to be a flourishing area of research interest [1]. Application of a sufficiently large magnetic field gives us access to the hyperfine Paschen-Back (HPB) regime [2, 3] (see Fig. 1), where the Zeeman splittings exceed the Doppler width. Applications of the quantitative understanding of atom-light interactions in the presence of a magnetic field range from devices (a compact optical isolator [4], narrow-line filters [5, 6], a Faraday laser [7]) to fundamental physics (single-photon interference due to motion in an atomic collective excitation [8], characterisation and modelling of the 4WM process [9]).

We have realised textbook four-wave mixing (4WM) signals that agree quantitatively with a simple four-level model [9] (see Fig. 2). Spontaneous 4WM leads to the creation of correlated pairs of photons; one photon of each pair can be used to herald the arrival of its partner. We are currently working towards characterising the resulting single-photon source. For this purpose we need to lock to a two-photon resonance, which we do by a novel method termed STROLLing (Simultaneous Two-Photon Resonant Optical Laser Locking). Details of the scheme and results characterising performance will be presented.

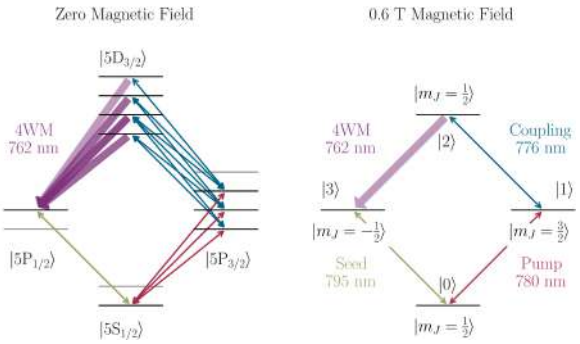


FIG. 1: Rubidium energy levels in the diamond-scheme in the absence (left) and presence (right) of a magnetic field of strength 0.6 T. Three beams (pump, seed & coupling) are added. When the phase matching condition is fulfilled, the four-wave mixing process generates a fourth beam (4WM). In the absence of a magnetic field, there is interference along multiple paths; the magnetic field removes the multiple-path interference.

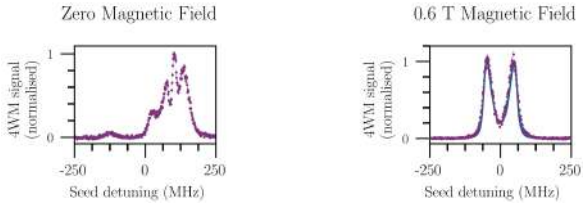


FIG. 2: Example experimental four-wave mixing spectra in the diamond-scheme in the absence (left) and presence (right) of a magnetic field of strength 0.6 T. In its absence, the four-wave mixing spectra are both highly sensitive to experimental conditions and difficult to model. Applying a magnetic field results in textbook four-wave mixing spectra that can be quantitatively modelled.

* r.s.mathew@durham.ac.uk

[1] D. Budker *et al.*, Rev. Mod. Phys. **74**, 1153 (2002)
[2] A Sargsyan *et al.*, Opt. Lett. **37**, 1379–1381 (2012)
[3] A Sargsyan *et al.*, J. Opt. Soc. Am. B **31**, 1046–1053 (2014)
[4] L. Weller *et al.*, Opt. Lett. **37**, 3405–3407 (2012)
[5] M. A. Zentile *et al.*, Opt. Lett. **40**, 2000-03 (2015)
[6] M. A. Zentile *et al.*, J. Phys. B. **48**(18), 185001 (2015)
[7] J. Keaveney *et al.*, Rev. Sci. Instr. **87**, 095111 (2016)
[8] D. J. Whiting *et al.*, Phys. Rev. Lett. **118**(25), 253601 (2017)
[9] D. J. Whiting *et al.*, J. Mod. Opt. **65** (2), 119-128 (2018)

A Fabry-Perot microcavity for an enhanced entangling rate in a diamond-based quantum network

S.B.van Dam[1,2], **M. Ruf**[1,2], **S. Bogdanovic**[1,2], **W. Westerveld**[1,2], **A. Galiullin**[1,2], **M. IJspeert**[1,2], **N. de Jong**[1,2], **J.H. van den Berg**[1,2], **M. Eschen**[1,2], **and R. Hanson**[1,2]

[1] *QuTech, Delft University of Technology, 2628 CH Delft, The Netherlands*

[2] *Kavli Institute of Nanoscience, Delft University of Technology, 2628 CH Delft, The Netherlands*

e-mail: *S.B.vanDam@tudelft.nl*

In a quantum network distant parties are connected via long-distance entanglement. The nitrogen-vacancy (NV) centre in diamond is a promising building block for such a quantum network. The electronic state of this defect centre combines a long-lived spin ground state with a coherent spin-photon interface that can be used for entanglement generation, while at the same time nearby nuclear spins are available as a quantum memory [1].

But the advancement towards larger quantum networks with multiple NV nodes is currently impeded by the low success probability of heralded entanglement generation: $\approx 10^{-8}$ over 1.3 km [2]. The success probability is for a large part limited by the coherent photon emission in the zero-phonon line ($\approx 3\%$) and subsequent collection efficiency. We address these limitations by embedding the NV center in an optical cavity at cryogenic temperature to benefit from the Purcell effect to enhance coherent photon emission and channel emitted photons into the cavity mode that can be efficiently collected.

A tunable Fabry-Perot microcavity with an embedded thin diamond membrane can have a small mode volume ($V \approx 10^2\lambda^3$) and high quality factor ($Q \approx 10^5$) providing an expected increase in entanglement success rate by three orders of magnitude [3, 4]. We present our latest results coupling NV centres to such microcavities.

[1] N. Kalb, et al., Science **356**, 928 (2017)

[2] B. Hensen, et al., Nature **526**, 682 (2015)

[3] S. Bogdanovic, et al., Appl. Phys. Lett. **110**, 171103 (2017)

[4] S. Bogdanovic, et al., APL Photonics **2**, 126101 (2017)

Coherent control of the spin of NV centers in levitating diamonds

T. Delord, P. Huillery, L. Nicolas, G. Hétet[1]

[1] *Laboratoire Pierre Aigrain, Ecole normale supérieure, PSL Research University, CNRS, Université Pierre et Marie Curie, Sorbonne Universités, Université Paris Diderot, Sorbonne Paris-Cité, 24 rue Lhomond, 75231 Paris Cedex 05, France* e-mail: *gabriel.hetet@lpa.ens.fr*

Experiments in the field of optomechanics showed control of macroscopic mechanical oscillators very close to their ground state of motion. These accomplishments provide opportunities to observe quantum superpositions with macroscopic systems. Due to clamping losses however, most of these experiments require cooling of the oscillators' internal degrees of freedom down to cryogenic temperatures. A solution to this is to optically levitate the macroscopic object [1]. There, the mechanical support is completely removed so one can reach very high quality factors. However, light scattering from the optically levitated object can significantly alter the optomechanical coupling strength at low vacuum pressures. One promising approach consists in using a non-invasive trap combined with a gentle way to probe the motion of levitating particles. In our group, we use a Paul trap for charged diamonds that contain NV centers, the electronic spin of which is used as a magnetometer to probe the diamond motion in the presence of a fixed magnetic field, as depicted in Fig. 1-a) [3].

The non-perturbative character of the trap on the diamond internal degrees of freedom was demonstrated in [2]. We will here present our recent observation of coherent control, namely Ramsey oscillations and spin echoes, with electrons spins in a levitating particle. Fig 1-b) shows Rabi oscillations taken at 1 mbars of vacuum pressure, where contrasted coherent oscillations are observed for up to μs. Fig. 1-c) shows spin echo and Ramsey (inset) measurements. The T_2^* is estimated to be around 40 ± 10 ns. Spin echoes show an exponential decay time of 3.3 μs showing no significant influence of the trap on the spin properties, even under this low vacuum level.

Observation of Ramsey and spin echoes under vacuum confirm that combining a Paul trap with spins in diamond is a viable option for spin-opto-mechanics, since the NV spins and the external and internal particle degrees of freedom are not significantly impacted and that long term angular stability of the levitating diamond can be achieved under vacuum [4].

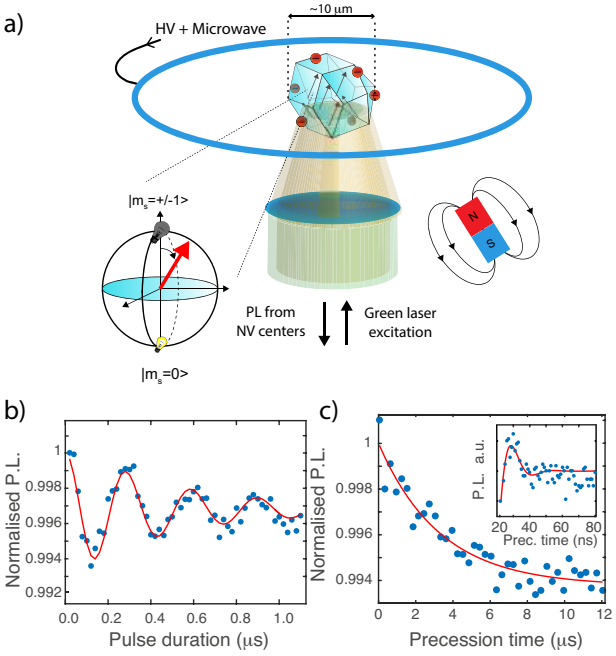


Figure 1: Coherent driving of NV centers' spins in a diamond levitating in the underdamped regime. a) Paul trap setup. b) Rabi oscillations and c) spin echo and Ramsey measurements (inset). All measurements are conducted under about 1 mbar of vacuum pressure.

[1] D. E. Chang *et al.* PNAS 107 1005-1010, (2010), O. Romero-Isart *et al.* Phys. Rev. A, 83 013803 (2011).

[2] T. Delord *et al.*, Applied Physics Letters, 111(1), 013101 (2017), G. P. Conangla, et al. Nano Letters, 05 (2018).

[3] Delord *et al.* New Journal of Physics, 19, 3 (2010).

[4] Delord *et al.* ArXiv : 1801.07798 (2018).

Quantum and nonlinear effects in transmission of light through planar arrays of atoms

R. J. Bettles[1], **M. D. Lee**[2], **S. A. Gardiner**[1], **and J. Ruostekoski**[3]

[1] *Joint Quantum Center (JQC) Durham–Newcastle, Department of Physics, Durham University, South Road, Durham, DH1 3LE, United Kingdom*
[2] *Mathematical Sciences, University of Southampton, Southampton, S017 1BJ, United Kingdom*
[3] *Physics Department, Lancaster University, Lancaster LA1 4YB, United Kingdom*

e-mail: *r.j.bettles@durham.ac.uk*

The optical properties of an ensemble of scatterers can be significantly modified when the scatterers interact, for example via the dipole–dipole interaction. Such *collective* behavior has been investigated extensively in recent years, exhibiting effects such as modified lifetimes and linewidths (superradiance and subradiance), energy shifts, and Fano-like interference lineshapes. In particular, dipolar lattices have been shown to provide a controllable environment for realizing strong collective behavior, including enhanced atom-light coupling via strong subradiance [1, 2], near-perfect optical reflection [1, 3, 4], and topological edge states [5, 6].

In this work [7] we investigate numerically the collective behavior of atomic lattices beyond the weak driving limit. In the presence of a saturating driving field, collective effects such as superradiance and energy shifts are modified significantly. This new regime requires careful consideration in how to correctly model the important effects, and presents new and exciting phenomena to be observed.

[1] R. J. Bettles, S. A. Gardiner, and C. S. Adams, Phys. Rev. Lett. **116**, 103602 (2016).

[2] G. Facchinetti, S. D. Jenkins, and J. Ruostekoski, Phys. Rev. Lett. **117**, 243601 (2016).

[3] S. D. Jenkins and J. Ruostekoski, Phys. Rev. Lett. **111**, 147401 (2013).

[4] E. Shahmoon, D. S. Wild, M. D. Lukin, and S. F. Yelin, Phys. Rev. Lett. **118**, 113601 (2017).

[5] R. J. Bettles, J. Minář, C. S. Adams, I. Lesanovsky, and B. Olmos, Phys. Rev. A **96**, 041603(R) (2017).

[6] J. Perczel, J. Borregaard, D. Chang, H. Pichler, S. F. Yelin, P. Zoller, and M. D. Lukin, Phys. Rev. Lett. **119**, 023603 (2017).

[7] R. J. Bettles, M. D. Lee, S. A. Gardiner, and J. Ruostekoski, *in preparation.*

Preparation and reconstruction of an entangled state of two microwave cavities

V. Métillon[1], **M. Brune**[1], **J.-M. Raimond**[1], **S. Haroche**[1], **P. Rouchon**[2] **and I. Dotsenko**[1]
[1] *Laboratoire Kastler Brossel, Collège de France, CNRS, ENS-Université PSL, Sorbonne Universités*
[2] *Centre Automatique et Systèmes, MinesParisTech, PSL Research University, Paris, France*
e-mail: *igor.dotsenko@lkb.ens.fr*

We report the preparation and full reconstruction of an entangled states of two microwave cavities separated by several centimeters and coupled by individual ^{85}Rb atoms prepared in circular Rydberg states. The tools available to us are resonant interaction, allowing exchange of quanta of energy between the atoms and the cavity fields, and dispersive interaction, allowing quantum non-demolition (QND) measurement of the parity of the microwave fields, which gives us the possibility to access directly the two-mode Wigner function of the field. By means of the controllable resonant interaction of a single excited atom with two cavities, we are able to prepare entangled superpositions of the type $(|10\rangle + |01\rangle)/\sqrt{2}$, where one photon is coherently shared between two fields, see Fig. 1.

The coherence of the above superposition can be probed through a suitable resonant interaction with a second probe atom [1], or can be accessed via a full tomography through Wigner measurements using a sequence of dispersively interacting atoms. In order to take into account each and every measurement result of different experimental realization, independent on the measurement nature, we have developed a reconstruction algorithm, based on a maximum likelihood estimation. It allows us to combine into the same reconstruction procedure the results of two types of measurement and to significantly reduce the amount of data acquisition necessary to get reliable information on the state [2].

The algorithm takes into account experimental imperfections and the system relaxation and decoherence during the measurement. Being very general and universal, it can be easily transposed to other systems, as long as a precise knowledge of the effect of the measurement in terms of a POVM is available.

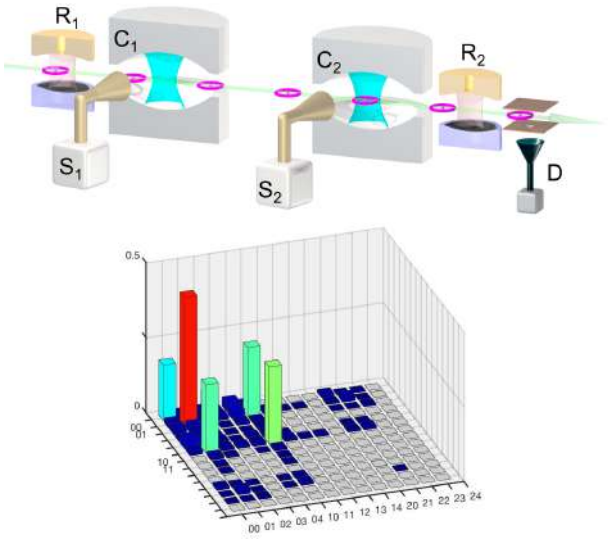


Figure 1: Preparation and quantum state reconstruction of a single photon shared between two cavities. (upper) Scheme of the experimental setup. Microwave fields of two high-finesse cavities, C_1 and C_2, are manipulated and probed by individual Rydberg atoms, toroids, state-selectively detected in D. Ramsey interferometer, R_1-R_2, provide QND measurment of the field parity. Together with two microwave sources, S_1 and S_2, it allos for the Wigner function measurement in a joint 4-dimentional phase space of two cavities. (lower) Reconstructed density matrix of an entagled two-cavity state (preliminairy). Single-cavity Hilbert space size is 5.

[1] A. Rauschenbeutel, P. Bertet, S. Osnaghi, G. Nogues, M. Brune, J.-M. Raimond, and S. Haroche, Phys. Rev. A **64**, 050301 (2001).

[2] V. Métillon *et al.*, in preparation (2018).

Controlling ultra-cold atomic ensembles with simultaneous radio-frequency and microwave dressing

G. Sinuco-Leon and B.M. Garraway
University of Sussex, Department of Physics and Astronomy, Brighton, BN1 9QH, United Kingdom
e-mail: *g.sinuco@sussex.ac.uk*

Following steady technical advances over the last two decades, ultra-cold (and cold) atomic ensembles of alkali atoms are consolidating as unparalleled playgrounds to investigate fundamental physical phenomena, as well as for developing sensing devices that surpass the performance of state-of-the-art technology [1]. The precise spatio-temporal control over the atomic internal and centre-of-mass degrees of freedom required by these applications can be achieved by applying electromagnetic fields (EM) tuned at frequencies determined by the atomic spectrum. In particular, the atomic population of ground state manifolds can be manipulated by a combination of low frequency EM fields [2, 3], where sub-wavelength tailoring of the field profile can be exploited in atom-chip configurations [4].

In this work we present a theoretical study of the use of radio-frequency (RF) and microwave (MW) fields for controlling atoms of 87Rb, applied to two typical experimental situations. Our starting point is a generic computational framework to evaluate the time-evolution of quantum systems with a discrete spectrum driven by several harmonically oscillating fields. With this tool, we define a generalised dressed picture and present details about how to compute observables in a dressed basis, the full time-evolution operator and the micro-motion operator.

As one application, we investigate the control over the population of the ground state manifold of RF-dressed 87Rb. A possible experimental sequence is shown in figure 1(a) [5]: atoms prepared initially in one state of the atomic ground manifold are adiabatically dressed by an RF field. Then, a short MW pulse flips the atomic population to the upper hyperfine manifold. We discuss how the driving of dressed states allows us to define sequences for fast and accurate control of atomic populations for applications in quantum information and sensing technologies.

As a second application, we study the manipulation of the spatial atomic potential landscape using a combination MW and RF radiation. We consider the effect of a MW field over the RF-dressed double well potential produced by a typical atom-chip configuration [2], which acquires additional features due to MW induced resonances between dressed states as shown in figure 1(b). We investigate how this double dressing scheme (RF+MW) can be used to achieve fine spatial tuning of the potential landscape to correct undesired features associated with finite size effects.

Finally, we relate this work to other relevant applications, in particular, qubit-gate optimisation [4], noise-protection of qubits and clock transitions and high precision measurement of RF fields [5], and we highlight the relevance of our findings to other experimental platforms pursuing applications in quantum technologies.

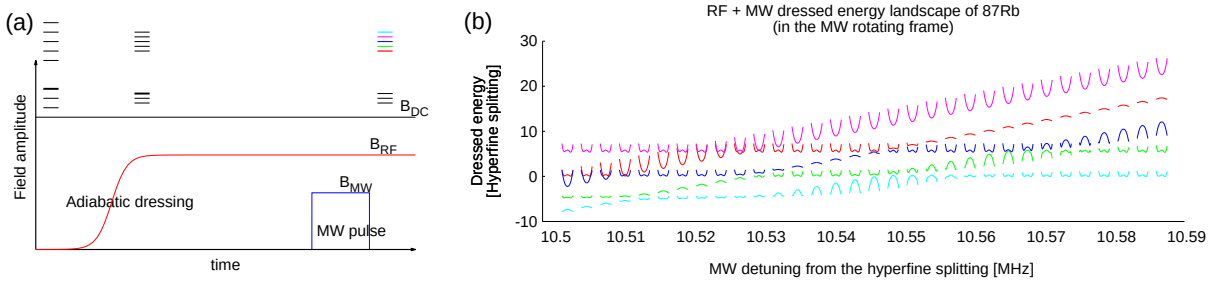


Figure 1: (a) Schematic of the sequence used to obtain a MW spectrum of RF dressed atoms. (b) Double dressed (RF + MW) energy landscape of 87Rb as a function of the MW frequency.

[1] K. Bongs, *et al.*, Proceedings of the Society of Photo-Optical Instrumentation Engineers: Quantum Optics, **9900**,990009 (2016).

[2] B. M. Garraway and H. Perrin, J. Phys. B **49**, 172001 (2016), H. Perrin and B. M. Garraway, Adv. in Atom, Mol. Opt. Phys. **66**, 181 (2017).

[3] T. L. Harte, *et al.*, Phys. Rev. A **97** 013616 (2018).

[4] G.A. Sinuco-Leon, *et al.*, Nat. Comm. **5**, 5289 (2014), G. A. Sinuco-Leon and B.M. Garraway, New J. Phys. **18**, 035009 (2016). C. L. Garrido Alzar, *et al.*, Phys Rev. A **74**, 0534131 (2012), B. E. Mischuck, *et al.*, Phys Rev. A **85**, 022302 (2012).

[5] W. von Klitzing, et al., *in preparation* (2018).

Fano resonance via $7F$ state in rubidium atom

M. Abe, R. Yasuda, and S. Tojo
Department of Physics, Chuo University, Tokyo 112-8551, Japan
e-mail: *abe@phys.chuo-u.ac.jp*

Rubidium atom is alkali metal, so that energy level is considerably simple. The atom is also attracted since laser cooling, Bose-Einstein condensation, and various quantum interferences are realized. Until now, rubidium laser spectroscopy has been mainly achieved in $5S$-$5P$, $5S$-$5D$, $5P$-$5D$, etc. On the other hand, transitions to F-states have been observed in few case [1, 2, 3]. They used three-step laser spectroscopy, i.e. S-P-D-F allowed transitions.

In this study, we have achieved the direct absorption measurement to $7F$ state in rubidium with only two laser. Rubidium energy levels are found in Ref. [4]. Figure 1 shows energy diagram in Rb up to 33000 cm^{-1}. Once exceited $5D$ state with two-photon absorption is pumped $7F$ state with a 1740 nm band laser additionally. We examine the transition, which is probably related to ionized rubidium atom with multi-photon excitation.

We employ a Ti:sapphire laser for producing $5D$ state with two-photon excitation. On the other hand, $5D$-$7F$ transition is induced by a 1740 nm band distributed feedback laser (DFB). The frequency of the Ti:sapphire laser is fixed on or near resonances. We obtain spectra by sweeping injection current of the DFB laser. Dichroic mirrors are used for addition and removal of 1740 nm light. A rubidium vaper cell is heated at about 100°C. Rubidium absorption is observed by transmitted 1740 nm light. Figure 2 shows the spectrum of $5D$-$7F$ transition. Lower trace is the

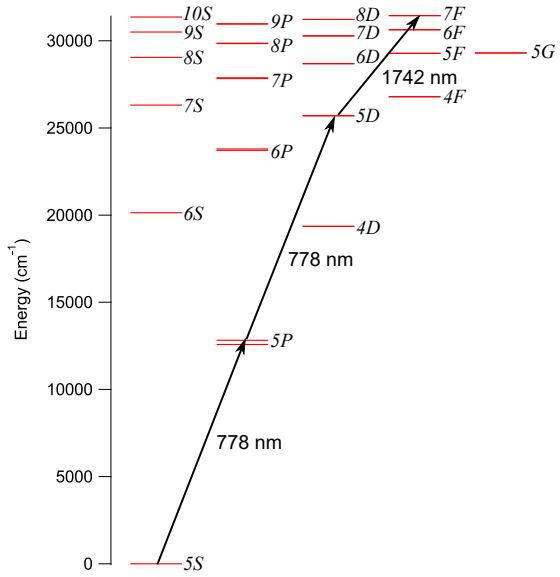


Figure 1: Energy level diagram of rubidium up to 33000 cm^{-1}. Arrow lines indicate used transitions.

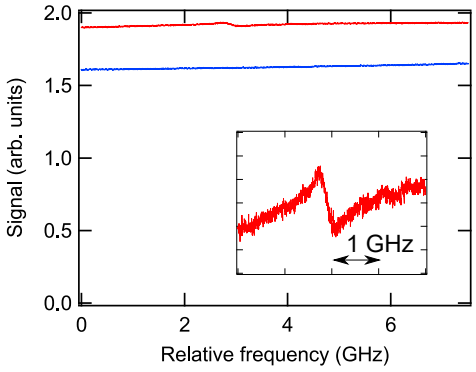


Figure 2: Acquired spectrum of $5D$-$7F$ transition. Lower and upper traces are the spectra without and with incident light of 778 nm. (Inset) Expanded upper trace near resonance.

spectrum without incident light of 778 nm and upper trace is the spectrum with 778 nm light. Upper trace has $5D$-$7F$ transition asymmetric profile at center (Fano profile). Additionally, upper trace increases background compared with lower trace. This indicated atom ionization and stimulated emission because we use a grating and an InGaAs detector after second dicroic mirror. Note that the overall slope is caused by output changing of the DFB laser associated with frequency sweeping and the frequency is roughly calibrated from a wavemeter.

We will set out the experimental detail in a poster. We will also present dependence on 778 nm pumping power and detuning, and discuss about the interaction of continuum states of rubidium atom.

[1] J. R. Brandenberger, C. A. Regal, R. O. Jung, and M. C. Yakes, Phys. Rev. A **65**, 042510 (2002).

[2] J. R. Brandenberger, and G. S. Malyshev, Phys. Rev. A **81**, 032515 (2010).

[3] L A M Johnson, H O Majeed, B Sanguinetti, Th Becker, and B T H Varcoe, New J. Phys. **12**, 063028 (2010).

[4] J. E. Sansonetti, J. Phys. Chem. Ref. Data **35**, 301 (2006).

High Precision Phase and Frequency Measurements in Rare Earth Doped Crystals for Probing Nanoresonator Behavior

N. Galland[1,2], **N. Lucic**[2], **S. Piccolomo**[2], **H. Alvarez-Martinez**[2], **R. Le Targat**[2], **A. Ferrier**[3,4], **J.-F. Motte**[1], **B. Fang**[2],**P. Goldner**[3], **S. Seidelin**[1,5], **Y. Le Coq**[2]

[1] *Université Grenoble Alpes and CNRS, Institut NEEL, F-38042 Grenoble, France*

[2] *LNE-SYRTE, Observatoire de Paris, Université PSL, CNRS, Sorbonne Université, 61 avenue de l'Observatoire 75014 Paris*

[3] *Université PSL, Chimie ParisTech, CNRS, Institut de Recherche de Chimie Paris, 75005, Paris, France*

[4] *Sorbonne Université, 75005, Paris, France*

[5] *Institut Universitaire de France, 103 Boulevard Saint-Michel, F-75005 Paris, France*

e-mail: *yann.lecoq@obspm.fr*

We here present an experiment concerning high precision spectroscopy of spectral holes in Eu^{3+} doped Y_2SiO_5 and the prospectives in the domain of frequency stabilization and micro-resonator behavior probing.

This experiment is based on $Eu^{3+} : Y_2SiO_5$ crystal that shows interesting properties at cryogenic temperatures. In this matrix, the $^7F_0 \rightarrow ^5 D_0$ transition of Eu^{3+} ions has a linewidth that can be as low as 1 kHz, and some measurement indicate a value reaching a few 100 Hz [1]. However, matrix inhomogeneities induce some local constraints on the ions that shift the frequency of this transition. As a consequence, the absorption spectrum of the crystal is broadened to several GHz. Below 7K, it is possible to place ions in metastable states, creating a hole in the absorption spectrum. The linewidth of this hole depends on the laser which is used to burn it and other experimental conditions (we typically reach 4kHz), and its lifetime can reach several hours.

To detect the spectral holes, a heterodyne method using two separate lasers is used. The frequency difference between the two lasers is chosen so that only one (the slave laser) is inside the 2 GHz wide absorption line and is able to burn and probe a spectral hole. The slave laser is beaten against the master (which is not affected strongly by the crystal) and the dephasing due to the dispersion signal of the hole is used as a frequency discriminator to measure the frequency difference between the slave and the hole center.

This experiment is currently used to make ultra-stable lasers using the frequency stability of the europium ions at low temperature [2].

Considering the absorption broadening process, a strong coupling between mechanical constraints on the crystal and hole frequency in the absorption spectrum is expected. Consequently, an accurate measurement of spectral hole frequency can provide a good monitoring of crystal deformations. This effect is intended to be used in order to probe the behaviour of a micro-resonator (see Figure 1) etched in a $Eu^{3+} : Y_2SiO_5$ crystal [3].

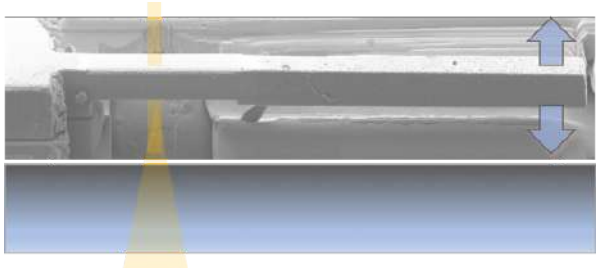


Figure 1: SEM image of a FIB-etched micro-resonator in $Eu^{3+} : Y_2SiO_5$ crystal. A 45° surface has been metal coated under the resonator so that a laser beam focused on the part close to cantilever attachment is deflected and does not go through the remaining bulk material.

In this poster, I will present the experimental setup in detail, show the preliminary results about laser stabilization and measured effect of mechanical stress on the spectral hole and discuss about future implementations concerning micro-resonator probing and laser stability improvement.

This project has received funding from Ville de Paris Emergence Program, First-TF Labex, Rgion Ile de France; European Unions Horizon 2020 research and innovation program under grant agreement No 712721 (NanOQTech); ANR under grant number 14-CE26-0037-01 DISCRYS; EMPIR 15SIB03 OC18 and from the EMPIR program co-financed by the Participating States.

[1] R. Yano et al., Opt. Lett. **16**, 1884-1886 (1991)

[2] O. Gobron et al. , Optics Express **25**(13), 15539-15548 (2017)

[3] K.Mølmer et al. , Phys. Rev. A **94**, 053804 (2016)

Towards a quantum-enhanced trapped-atom clock on a chip

M.-Z. Huang[1], **T. Mazzoni**[2], **C. L. Garrido Alzar**[2] **and J. Reichel**[1]

[1] *Laboratoire Kastler Brossel, ENS-Université PSL, CNRS, Sorbonne Université, Collège de France, 24 rue Lhomond, 75005 Paris, France*

[2] *LNE-SYRTE, Observatoire de Paris-Université PSL, CNRS, Sorbonne Université, 61 Avenue de l'Observatoire, 75014 Paris, France*

E-mail: *mengzi.huang@lkb.ens.fr*

The standard quantum limit (SQL), imposed by the quantum projection noise (QPN) when measuring uncorrelated atoms, has become a practically relevant noise source for state-of-the-art atomic clocks and atom interferometers. Nevertheless, entanglement, especially highly entangled states such as the spin-squeezed states [1], can introduce useful quantum correlations for collective measurements, enabling metrology beyond the SQL. Spin squeezing can be produced in a quantum non-destructive (QND) measurement of the collective spin [2, 3], particularly with cavity-quantum electrodynamical (QED) interactions [4, 5, 6].

Another major noise source which stems from the local oscillator (LO) phase noise, known as the Dick effect, puts stringent requirements on the LO quality. In particular, for applications seeking compact solutions, the Dick effect can be the dominant noise. The QND detection can also be tailored to alleviate the Dick effect [7, 8], by employing multiple weak interrogations on the same atomic ensemble, effectively reducing the dead time of the interferometer.

Despite the exceptional progress in achieving higher level of squeezing [6], showing the superiority of these quantum protocols at the metrological level remains a challenge. Here we present an on-going experiment, Trapped Atom Clock on a Chip (TACC), with the goal to test spin squeezing and QND detection in the metrological context. TACC is a microwave clock with trapped ultracold ^{87}Rb atoms, using an atom chip as a robust and miniature platform. The first-generation experiment has demonstrated a metrologically relevant performance [9] and spontaneous spin squeezing in a BEC [10]. In the second-generation apparatus, we have integrated two fiber Fabry-Perot cavities [11] on the clock chip (Fig. 1), realizing a platform for cavity-QED in the strong- and weak-coupling regimes respectively. In the preliminary clock measurements with atoms placed inside the cavity without light, we reached a fractional frequency stability of 6×10^{-13} at 1 s, with half of the noise contributed from the QPN. With further improvement of technical noises, we expect to enter a QPN limited regime. We also report the initial characterizations of the atom-cavity interaction.

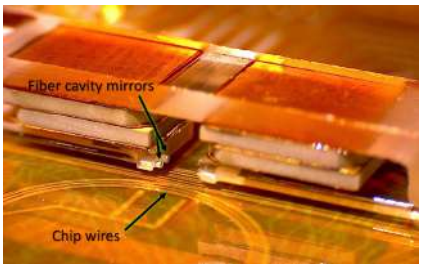


Figure 1: Photograph of the fiber cavities mounted on the clock chip.

[1] M. Kitagawa and M. Ueda, Phys. Rev. A **47**, 5138 (1993).

[2] J. Appel, P. J. Windpassinger, D. Oblak, U. B. Hoff, N. Kjærgaard and E. S. Polzik, PNAS **106**, 10960 (2009).

[3] M. H. Schleier-Smith, I. D. Leroux, and V. Vuletić, Phys. Rev. Lett. **104**, 073604 (2010).

[4] I. D. Leroux, M. H. Schleier-Smith, and V. Vuletić, Phys. Rev. Lett. **104**, 073602 (2010).

[5] J. G. Bohnet, K. C. Cox, M. A. Norcia, J. M. Weiner, Z. Chen, and J. K. Thompson, Nature Photonics **8**, 731 (2014).

[6] O. Hosten, N. J. Engelsen, R. Krishnakumar, and M. A. Kasevich, Nature **529**, 505 (2016).

[7] R. Kohlhaas, A. Bertoldi, E. Cantin, A. Aspect, A. Landragin, and P. Bouyer, Phys. Rev. X **5**, 021011 (2015).

[8] G. Vallet, E. Bookjans, U. Eismann, S. Bilicki, R. Le Targat and J. Lodewyck, New J. Phys. **19** 083002 (2017).

[9] R. Szmuk, V. Dugrain, W. Maineult, J. Reichel, and P. Rosenbusch, Phys. Rev. A **92**, 012106 (2015).

[10] T. Laudat, V. Dugrain, T. Mazzoni, M.-Z. Huang, C. L. Garrido Alzar, A. Sinatra, P. Rosenbusch, and J. Reichel, arXiv: 1804.07536.

[11] K. Ott, S. Garcia, R. Kohlhaas, K. Schüppert, P. Rosenbusch, R. Long, and J. Reichel, Optics Express Vol. **24**, 9839 (2016).

Measurement of magic wavelength for 1.14 μm clock transition in Tm atoms

D. Tregubov[1], **A. Golovizin**[1,2], **E. Kalganova**[1,2], **G. Vishnyakova**[1,2], **K. Khabarova**[1,2], **V. Sorokin**[1], **and N. Kolachevsky**[1,2]

[1] *P.N. Lebedev Physical Institute of the Russian Academy of Sciences, 119991 Moscow, Russia*

[2] *Russian Quantum Center, 143025 Moscow, Russia*

e-mail: *treg.dim@gmail.com*

We report measurement of a magic wavelength for the clock transition in thulium atoms, a promising candidate for optical clocks.

Best optical clocks based on ensembles of neutral atoms or single ions reach instability and uncertainty of about 10^{-18} [1, 2]. However, it is still necessary to search for other elements or methods one could use in order to achieve that level of precision, and even surpass it [3, 4]. Our group is involved in a study of a promising optical clock based on thulium atoms [5]. A distinguished feature of thulium in this case is expected low sensitivity of a clock transition to the black body radiation.

Accurate study of different frequency shifts is a key point for understanding the performance of any developing optical clock. For neutral atoms trapped in an optical lattice, frequency shift due to the lattice itself is of the foremost concern. A common technique usually employed here is to trap atoms in a lattice at a magic wavelength, at which both ground and excited states of a clock transition shift equally.

For the clock transition in thulium atoms, we theoretically predicted several possible magic wavelengths and decided that the region $806 - 815$ nm would be most convenient [5]. Accurate measurement of the magic wavelengths requires precise control and large range of lattice intensities, which we achieved with external cavity [6]. As a welcome side effect, it has also increased the efficiency of loading thulium atoms from magneto-optical trap into the optical lattice up to 60%.

In order to find the magic wavelength we have measured the frequency of the clock transition for different lattice powers for the range of wavelengths $806 - 845$ nm (Fig. 1). As a result, we have found two magic wavelengths with the one near 813.3 nm being a far better choice for the optical clock application, as it is further away from resonances and the frequency of the clock transition is less sensitive here to the lattice wavelength.

As a next step, we plan to measure differential polarisabilities in the extended region up to 860 nm, plus one point at 1.06 μm. These results would assist in extrapolation and allow us to determine the differential scalar static polarisability and to check theoretically predicted low sensitivity of the clock transition to the black body radiation.

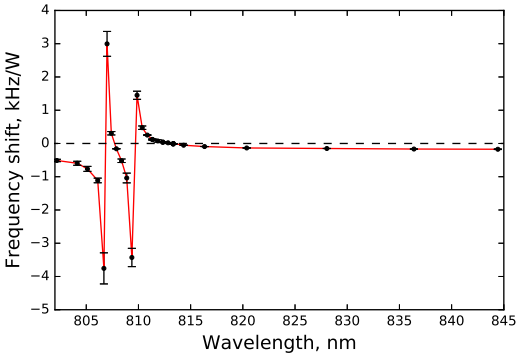


Figure 1: Frequency shift of the clock transition per unit of power of the optical lattice for different wavelength of the lattice. For each point, we have measured the frequency of the clock transition for 3 different lattice powers. Intersections with zero correspond to magic wavelengths.

[1] N. Hinkley, J. A. Sherman et al,Science **341**, 1215-1218 (2013).

[2] B. J. Bloom, T. L. Nicholson et al,Nature **506**, 71-75 (2014).

[3] C. J. Campbell, A. G. Radnaev et al,Physical review letters **108**, 120802 (2012).

[4] K. J. Arnold, R. Kaewuam et al,Nature communications **9** (2018).

[5] D. Sukachev, S. Fedorov et al,Physical Review A **94**, 022512 (2016).

[6] E. S. Kalganova, A. A. Golovizin et al,Quantum Electronics **48**(5), 415-418 (2018).

Cross-correlation measurement between two Ti:Sapphire optical frequency combs referencing a clock laser transferred via an optical fiber link

K. Nakashima[1], **T. Ikeda**[1], **E. Chae**[2], **T. Takano**[1], **I. Ushijima**[1,3], **N. Ohmae**[3,4], **T. Akatsuka**[3,5], **H. Katori**[1,3,4], **M. Kuwata- Gonokami**[6,7], **and K. Yoshioka**[2]

[1] *Department of Applied Physics, School of Engineering, The University of Tokyo, Bunkyo-ku, Tokyo, Japan*

[2] *Photon Science Center, The University of Tokyo, Bunkyo-ku, Tokyo, Japan*

[3] *Quantum Metrology Laboratory, RIKEN, Wako-shi, Saitama, Japan*

[4] *Center for Advanced Photonics, RIKEN, Wako-shi, Saitama, Japan*

[5] *NTT Basic Research Laboratories, Atsugi-shi, Kanagawa, Japan*

[6] *Institute for Photon Science and Technology, Graduate School of Science, The University of Tokyo, Bunkyo-ku, Tokyo, Japan*

[7] *Department of Physics, Graduate School of Science, The University of Tokyo, Bunkyo-ku, Tokyo, Japan*

e-mail: *nakashima@fs.t.u-tokyo.ac.jp*

A Ti:Sapphire mode-locked laser possesses beneficial properties such as high average power (> 500 mW), broad bandwidth (~ 300 THz after photonic crystal fiber), and visible wavelengths (450 nm to 1200 nm) compared with other types of mode locked lasers. Recently, we have established a 2.9 km-long phase-stabilized optical fiber link between Katori laboratory and Yoshioka laboratory at The University of Tokyo. An excitation laser for the clock transition (clock laser) for ^{87}Sr optical lattice clock [1] has been coherently transferred through the optical fiber link. One of the longitudinal modes of a Ti:Sapphire optical frequency comb (Ti:S OFC) in Yoshioka laboratory has been tightly phase-locked to the clock laser achieving a fractional instability of the order of 10^{-18} at 1 second [2]. As a result, all of the 3×10^6 modes are expected to have approximately the same linewidth as the clock laser.

In order to ascertain that all longitudinal modes have linewidths comparable to that of the clock laser, we conducted a cross-correlation measurement between two identically designed Ti:S OFCs, both of which were phase-locked to the same clock laser transferred via the optical fiber link (Fig. 1).

The obtained heterodyne beat spectrum around 700 nm is shown in Fig. 2. The linewidth of the beat signal was measured to be 1 Hz, which is limited by the resolution of the spectrum analyzer. Taking the additional contribution of optical fiber link to the linewidth into account, the absolute linewidth of one longitudinal mode of the Ti:S OFC was estimated to be approximately the same as that of the clock laser.

The achieved narrow linewidth of the Ti:S OFC, along with the inherent high power and short wavelengths, enables various applications. One of the applications would be ultra-broadband dual comb spectroscopy (DCS) [3] with a 300 THz bandwidth and the accuracy of the ^{87}Sr optical lattice clock. Since two Ti:S OFCs have mutual linewidth smaller than 1 Hz, the difference of f_{rep} can be set to 10 Hz in DCS. In that case, all the 3×10^6 modes spanning from green to infrared are available for DCS. Furthermore, frequencies of all the longitudinal modes are strictly determined referencing the ^{87}Sr optical lattice clock. In this contribution, the details of the experiment, the wavelength dependence of the linewidth of our combs, and the possibility of ultra-broadband/precision DCS will be discussed.

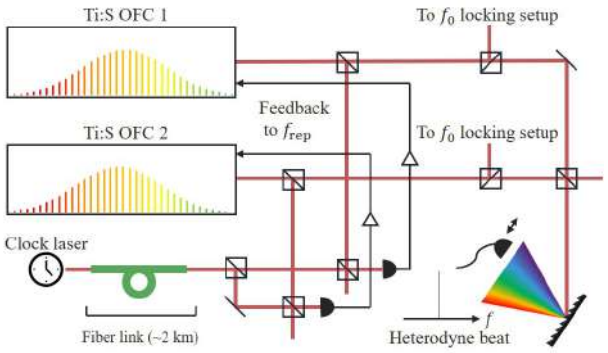


Fig. 1: Setup for cross-correlation measurement between two, phase-stabilized Ti:S OFCs.

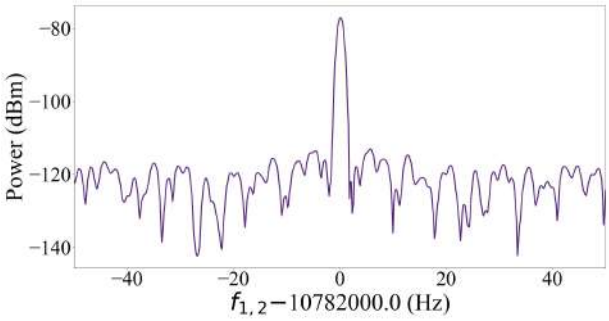


Fig. 2: Typical heterodyne beat between two Ti:S OFCs. Resolution bandwidth is 1 Hz.

We acknowledge the support from Photon Frontier Network Program of MEXT, Japan and JSPS KAKENHI Grant Number JP17H06205.

[1] M. Takamoto *et al*., Nature **435**, 321-324 (2005).

[2] E. Chae *et al*., in preparation.

[3] S. Schiller, Opt. Lett. **27**, 766-768 (2002)

Towards a second generation for the brazilian atomic fountain frequency standard: Tests with the new MOT chamber

S.T. Müller[1], C. Bueno[1], L.V.G. Tarelho[2], G.A. Garcia[2], V.S. Bagnato[3], and D.V. Magalhães[1]

[1] *São Carlos School of Engineering, University of São Paulo, Av. Trabalhador São-Carlense, 400, 13566-590, São Carlos, SP, Brazil*

[2] *National Institute of Metrology, Quality and Technology, Av. Nossa Senhora das Graças, 50, 25250-020, Duque de Caxias - RJ - Brazil*

[3] *São Carlos Institute of Physics, University of São Paulo, Av. Trabalhador São-Carlense, 400, 13566-590, São Carlos, SP, Brazil*

e-mail: *daniel@sc.usp.br*

Our research group is working in the second generation of the Brazilian Cesium Fountain (Br-CsF) [1], envisaging its operation as a national frequency standard. This work will discuss the opto-mechanical assembly and the new trap vacuum chamber. We used a squared section glass profile to build the region where the atoms are loaded and cooled using magneto-optical technique. The opto-mechanical system was reduced to increase stability and robustness. This newest Atomic Fountain is essential to contribute with time and frequency development in metrology systems and represents the efforts we have doing to the stablishment of reliable references [2].

One of the main aspects of this new design is the trap chamber in glass, to avoid undesired residual magnetic fields and also to maintain a small volume for the system. The optical system uses three lasers: a master laser to cool and trap atoms (TOPTICA TA100); repumping laser to recover atoms from forbidden transitions in the MOT and molasses phases (homemade); and detection laser used to perform the time-of-flight measurements after the microwave interrogation (Radiant Dyes). Both detection and repump lasers operate with intracavity interference filter in extended cavity.

Using a pair of coils to generate a quadrupole magnetic field and six laser beams, we can trap and cool an atomic cloud, using a mogneto-optical technique. Due to the reduced volume of the vacuum chamber, the nominal current for operating the coils is around 2 A. The trap region is shown in Fig. 1. For the Cesium reservoir three getters are placed, in order to provide longer operation autonomy. They operate with current up to 3 A each.

The characterization of the trap and loading times were done and is going to be presented in the poster. We are now working on the launch of atoms to the microwave interrogation region.

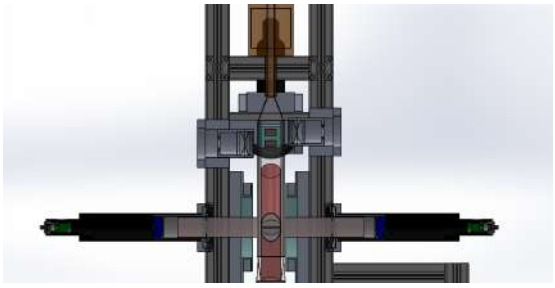


Figure 1: Trapping atoms region, using two coils and six beam expanders. The figure shows a pair of transverse beams.

The authors would like to acknwledge Grant 2013/07276-1, So Paulo Research Foundation (FAPESP), CAPES and CNPq for financial support

[1] C. Bueno, A. Rodriguez, S.T. Müller, V.S. Bagnato, D.V. Magalhães. Journal of Physics Conference Series, 975, 012071 (2017).

[2] Rodriguez, S. A.; Bagnato, V. S.; Bueno, C.; Pechoneri, R. D.; Müller, S. T.; Magalhães, D. V. 2016 IEEE International Frequency Control Symposium (2016).

Coherence properties of NV ensembles in HPHT diamond plates.

V.V. Vorobyov[2,3], O.R. Rubinas[1,2,3], V.V. Soshenko[2,3], S.V. Bolshedvorskii[2,3],V.N. Sorokin[2,3], A.N. Smolyaninov[3], V.G. Vins[4], A.P Yelisseyev[5], A.V. Akimov[2,3,6]

[1] *Moscow Institute of Physics and Technology, Institutskiy pereulok 9, Dolgoprudniy, Moscow region, Russia*

[2] *P.N. Lebedev Physical Institute of the Russian Academy of Sciences, Leninskiy prospect 53, Moscow, Russia*

[3] *LLC Sensor Spin Technologies, Nobelev Streeet 9, Moscow, Russia* [4] *LLSC Velman, Novosibirsk, Russia*

[5] *Sobolev Institute of Geology and Mineralogy SB RAS, Prospekt Akademika Koptyuga 3 , Novosibirsk, Russia*

[6] *Texas A&M University, 4242 TAMU, College Station, USA*

e-mail: *vadimvorobyov@gmail.com*

Modern state-of-the-art NV center sensor applications strongly depends on quality of the host diamond plates. Originated from shot noise limit the sensitivity of the device depends on number of NV centers and their coherence time [1]. It is hard to achieve simultaneously high coherence time and high number of NV centers due to various reasons [2]. Finding optimal balance between concentration and coherence time of the NV center ensemble requires careful optimization of diamond growing and post processing procedures.

We studied diamond plates made with high pressure high temperature method (HPHT) with various initial number of nitrogen impurities processed with slightly variable parameters [3]. As a result we measured coherence properties of all plates such as free induction decay time ($T^*_{2,FID}$), Rabi oscillation decay time ($T^*_{2,Rabi}$) and Hahn-Echo decay time ($T_{2,HE}$). We also measured concentration of NV^- centers and strain $E_\perp$ within diamond plates.

Our data shows, that properly processed HPHT diamonds plates could reach the unavoidable limits for $T^*_{2,FID}$ associated with natural abundance of ^{13}C and nitrogen p_1 center. We note that it correlates with transverse strain, measured in the plate with zero field technique [4].

The $T_{2,HE}$ coherence time in our plates was measured to be comparable with other works, however we found that due to some reason it saturates to 15 μs demonstrating other decoherence reason from nitrogen impurities, which should scale with 1/[N] law, reported in [2].

The sensitivity of an NV based device depends not exactly on concentration of NV centers but rather on number of photons one collect from it. Given the fact that usually the optical pumping power is limited at the level of several Watts one could be interested in the quantity of how many red NV^- photons diamond plate produces per one green photon (k). The practical important figure of merit in terms of sensitivity of the device in that sense become the product of $k \times T_2$. After sorting all plates with respect to this product we found that plates with higher NV concentration are best candidates for high sensitivity AC and DC magnetometry.

To increase the sensitivity of the NV ensemble sensor nuclear spin associated with ^{14}N could be utilized. In that sense it is of interest to measure collective nuclear spin ensemble coherence time.

In our plates nuclear FID coherence time was measured to be from 100 μs to 1000 μs for various diamond plates where nuclear polarization and coherent control was realized.

This paves the way towards utilization HPHT diamond plates as a promising platform for solid state ultraprecise sensors with a possibility to use nuclear spin memory as a resource to further increase its sensitivity.

[1] T. Wolf, P. Neumann, K. Nakamura, H. Sumiya, T. Ohshima, J. Isoya, J. Wrachtrup, Phys. Rev. X **4**,041001,5,(2015)

[2] E. Bauch, C. A. Hart, J. M. Schloss, M. J. Turner, J. F. Barry, P. Kehayias, S. Singh, and R. L. Walsworth, arXiv:1801.03793(2018).

[3] .R. Rubinas, V.V. Vorobyov, V.V. Soshenko, V.N. Sorokin, A.N. Smolyaninov, V.G. Vins, A.P Yelisseyev, A V Akimov 2018 in preparation.

[4] M.E. Trusheim, D. Englund NJP, (2016)

Rotation Sensing with an Atomic Clock

J. Johnson, F. Gentile, T. Pyragius, B. Foxon, K. Poulios, T. Fernholz.
School of Physics & Astronomy, University of Nottingham, University Park, Nottingham NG7 2RD, U.K.
e-mail: *jamie.johnson@nottingham.ac.uk*

The Sagnac effect manifests as a phase difference in the rotating frame of two counter-propagating observers when a difference in their path length around the interferometer has been traversed, as seen from the inertial frame. Matterwave Sagnac interferometry [1] promises orders of magnitude increase in the sensitivity over their optical counterparts by

$$\frac{\Phi_{atom}}{\Phi_{light}} = \frac{mc^2}{h\nu} \approx 10^{10} \quad (1)$$

where the mass m is taken to be ^{87}Rb and the frequency ν is within the optical range. The mass-energy ratio between atoms and photons provides a substantial lead to use atoms for rotation sensing. The fact that the Sagnac effect is also observed without free propagation of the atoms also provides an initiative to use guided matterwave interferometry which allows for the miniaturization of the setup. Progress in obtaining rotation sensing has been challenging, from designing PCB's and atom-chips allowing for the state dependent guiding of atoms, to state preparation via a sharp clock transition and a low noise detection scheme. We have theoretically and with most of the main experimental concepts achieved separately, shown that a durable guided Sagnac interferometer is obtainable with a target sensitivity of $10^{-9}\text{rad}/\sqrt{s}$ [2]. Here we present the scheme and basic theory of operation, the experimental progress and setup, along with some future outlooks combining multi-pole rf-dressing and ring quadrupole fields to create state dependently controlled ring lattices.

To guide the matterwaves around the paths, atoms are first split via a sharp microwave clock transition to two different internal atomic states which are then state dependently controlled around a ring via a guiding potential. This guiding potential is provided by rf-dressing and a static ring quadrupole field [3]. Guided matterwaves allow for atom-chip designs Fig.(1), that can miniaturize the setup and provide high trapping gradients for robust devices. Our 10 layer PCB produces magnetic fields required for transporting the atoms from the MOT to the matterwave guide supplied by the atom-chip, the chip uses current carrying wires to create a ring-quadrupole field which provides the quantization axis for the atoms. Both PCB and atom-chip are ready to be connected and put into the vacuum chamber. State dependent control has already been achieved by our collaborators with coherence times on the order of seconds. We have been able to produce state

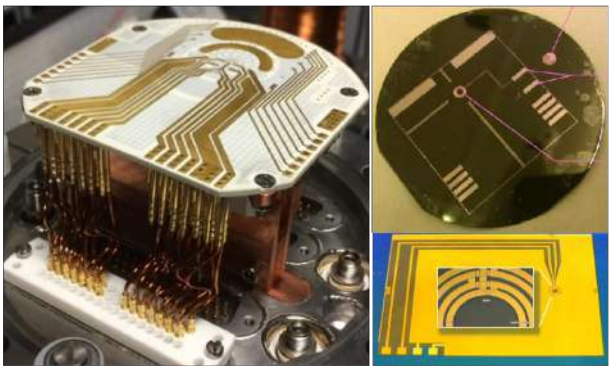


Figure 1: Left, the 10 layer PCB ready to be put into vacuum for testing. Right, electromagnetic and rf chips, the complete setup will see all three fixed together.

preparation of a dressed ^{87}Rb sample with a sharp clock transition from the $F = 1, m_F = -1$ to the $F = 2, m_F = 1$. A detection system for rf-dressed atoms that enables the simultaneous readout of the two states with low noise has been developed. The whole setup will sit on a rate table operating with a brushless DC-motor and air-bearing, capable of rotating at small $(10^{-5}\text{rad}/s)$ angular velocities.

We have also started looking beyond the initial concepts to include a new method of making ring lattices, this is done by exploiting rf-dressed potentials with multi-pole fields. This opens the possibility of increasing the area enclosed by the interferometer, as well as allowing for other potential ring lattice applications [4].

[1] B. Barrett, R. Geiger, I. Dutta, M. Meunier, B. Canuel, A. Gauguet, P. Bouyer, and A. Landragin, C.R. Phys. 15, 875-833

[2] R. Stevenson, M.R. Hush, T. Bishop, I. Lesanovsky, and T. Fernholz Phys. Rev. Lett. 115, 163001

[3] T. Fernholz, R. Gerritsma, P. Kru ger, and R. J. C. Spreeuw, Phys. Rev. A 75, 063406.

[4] F. Gentile, J. Johnson, K. Poulios, T. Fernholz, rf-dressed ring lattices. (In preparation)

Spin-Squeezing for Entanglement-Enhanced Matterwave Interferometers

Graham P. Greve[1], **Baochen Wu**[1], **Chengyi Luo**[1], **and James K. Thompson**[1]
[1] *JILA, NIST, and the University of Colorado-Boulder, Boulder CO, USA*
e-mail: *graham.greve@colorado.edu*

Quantum sensors such as atomic clocks, magnetometers, and matterwave interferometers operate by estimating the phase that accumulates between quantum states. The uncorrelated quantum projection noise of N unentangled atoms restricts the ultimate resolution of the accumulated phase to the standard quantum limit, $\Delta\phi_{\mathrm{SQL}} = 1/\sqrt{N}$. By engineering spin-squeezed states, correlations between atoms are introduced that can be used to cancel quantum noise, in principle extending the phase resolution to the Heisenberg limit, $\Delta\phi_{\mathrm{HL}} = 1/N$.

Quantum non-demolition measurements have been used to generate large amounts of spin-squeezing in atom-cavity systems (Fig. 1a) [1, 2]. In these systems, the correlation of internal atomic states has been particularly promising for operating an atomic clock beyond the standard quantum limit. However, implementation in a matterwave interferometer remains a major challenge.

One significant obstacle for matterwave interferometry involves mapping the previously-generated entanglement between internal atomic states onto entanglement between momentum states. We will discuss possible ways to accomplish this mapping using spin-dependent momentum kicks. In addition, most previous squeezing schemes have relied on spatially-inhomogeneous entanglement such that the enhancement in phase estimation is lost if atoms move. Using an effective intracavity dipole trap (Fig. 1b), we allowed atoms to fall along a cavity axis while retaining 11 dB of spin-squeezing by time-averaging their coupling to the probing laser [3]. These homogeneously entangled states are well-suited for release into the arm of a cavity-based matterwave interferometer.

With this poster, we place our past efforts at entanglement in context and discuss future prospects for enhanced matterwave interferometry. A new interferometer based around entangled rubidium atoms in a high finesse cavity is currently under construction.

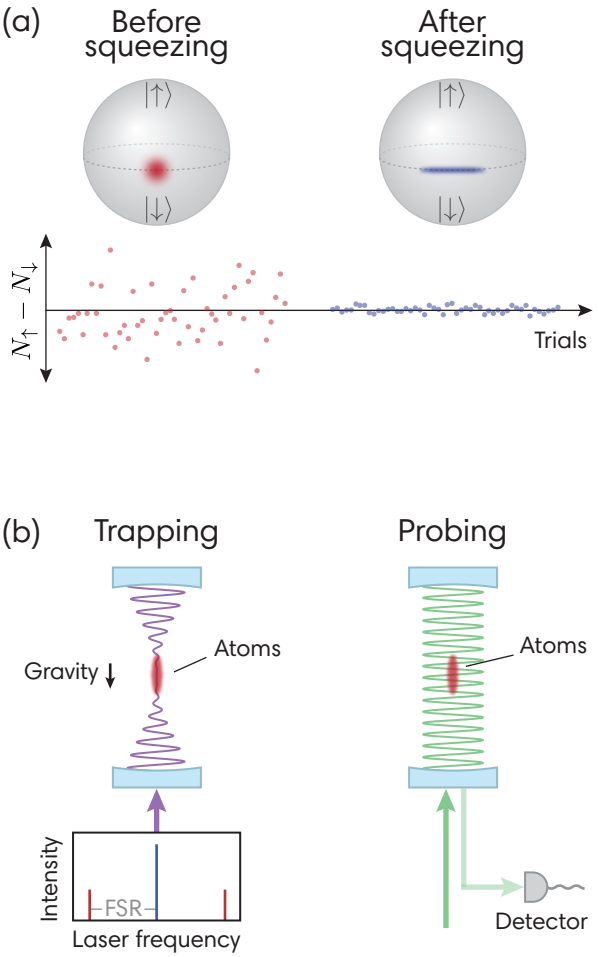


Figure 1: **(a)** Collective measurements of an atomic ensemble can be used to project the atoms into an entangled state. Atoms are initially in a coherent state (left) with population noise described by $\Delta\phi_{\mathrm{SQL}} = 1/\sqrt{N}$. After squeezing (right), the noise variance has been reduced by as much as 18 dB [1, 2]. **(b)** Injecting intracavity lattice laser tones separated by a free spectral range (FSR) allows atoms to fall axially while maintaining radial confinement. The collective spin state is then measured as the atoms average their coupling over multiple wavelengths of the probing laser. We expect to use a related technique to maintain squeezing during an interferometer sequence. The cartoon potentials are not drawn to scale.

[1] K. C. Cox, G. P. Greve, J. M. Weiner, and J. K. Thompson, Phys. Rev. Lett. **116**, 093602 (2016).

[2] O. Hosten, N. J. Engelsen, R. Krishnakumar, and M. A. Kasevich, Nature **529**, 505 (2016).

[3] K. C. Cox, G. P. Greve, B. Wu, and J. K. Thompson, Phys. Rev. A **94**, 061601 (2016).

Steady-state ultracold Sr with unity phase-space density

C. C. Chen, S. Bennetts, R. G. Escudero, B. Pasquiou, and F. Schreck
Van der Waals - Zeeman Institute, Institute of Physics, University of Amsterdam
e-mail: *c.c.chen@uva.nl*

We demonstrate a way to make a steady-state sample of ultracold strontium with a phase-space density approaching degeneracy. This long-standing goal within atomic physics represents a critical step towards demonstrating steady-state quantum gas devices such as atom lasers, interferometers and superradiant lasers which hitherto have only been possible in pulsed operation. Our machine tackles this goal by simultaneously cooling atoms in spatially separated regions on both the broad 30-MHz and narrow 7.4-kHz linewidth Sr transitions [1]. In this way we are able to continuously load a dipole trap at high phase-space density in which a Stark shift protected [2] dimple trap collects and concentrates the coldest atoms. We measure a steady-state atomic cloud with a phase-space density above unity. We discuss methods to characterize the atomic sample and search for signs of the existence of a steady-state Bose-Einstein condensate.

[1] S. Bennetts et al, Phys. Rev. Lett **119**, 223202 (2017).

[2] S. Stellmer et al, Phys. Rev. Lett **110**, 263003 (2013).

Ultra-stable laser based on a compact Fabry-Perot cavity

S. Denis[1], **A. Didier**[1,2], **J. Millo**[1], **B. Maréchal**[1], **C. Rocher**[1], **E. Rubiola**[1], **M. Ouisse**[1], **J. Delporte**[3], **C. Lacroûte**[1], **and Y. Kersalé**[1]

[1] *FEMTO-ST, Université de Bourgogne Franche-Comté, CNRS, ENSMM, 26 Rue de l'Epitaphe, 25030 Besançon cedex, France*

[2] *PTB, Bundesallee 100, 381 16 Braunschweig, Germany*

[3] *Centre National d'Etudes Spatiales (CNES), Toulouse, France*

e-mail: *severine.denis@femto-st.fr*

The use of a high Finesse Fabry-Perot cavity emerged in the last centry as a way to stabilize the frequency of a laser source fundamental for atomic optical clocks [1]. The improvement of such cavities also has a major stake for applications requiring the use of ultra-stable frequency referencies, such as high precision spectroscopy, or the synchronization of optical frequency combs for the transfer of the frequency fractional stability to the microwave domain [2].

However a Fabry-Perot cavity is subject to environmental constraints mainly vibrations and thermal fluctuations, that affect the resonant frequency of the cavity hence the frequency stability. This stability is generally improved by using complex systems such as cryocoolers or longer cavities, and requires many controls and bulky (> 1 m^3) isolations from the environmental constraints, in order to reduce the thermal noise limit to a 10^{-17} range [3]. These are responsible of a lack of transportability of the cavity system. To overcome this overall bulk, we developed a stabilized laser source based on a Fabry-Perot cavity confined in a compact vacuum chamber.

The presented Fabry-Perot cavity is made of a 25 mm long ULE glass spacer whose design is studied to reduce coefficients of vibration sensitivity, in order to avoid the use of an active vibration isolation system. The ULE glass is chosen as it is suitable for ultra-stable Fabry-Perot cavities because of its nulling point at room temperature. The length of 25 mm is a compromise between the thermal noise level of the cavity and its small size. This thermal noise limit is estimated to $\sim 10^{-15}$ in terms of fractional frequency stability. The cavity is held in a stainless steel support (Fig.1) and placed in a copper made shield, in order to reduce the sensitivity of the cavity to external temperature fluctuation, and both are contained in the 2.4 dm^3 vacuum chamber. The use of a Peltier module placed under the copper shield allows the control of temperature of the cavity.

The optical setup upstream to the cavity (Fig.2) is made of both free space and fibered optical elements. The laser light injected in the cavity is provided by a 1542 nm tunable fibered laser diode followed by a 90/10 coupler used to extract the ultra-stable laser signal. A fibered electro optical modulator (EOM) is placed before the free space part to provide a phase modulation for a Pound-Drever-Hall stabilization method. The free space part is made of two lenses and two mirrors, fixed to the vacuum chamber, that allow the alignment and mode matching inside the cavity. A beam splitter cube sends the light reflected by the cavity to a photodiode to adjust the working intensity and temperature of the laser diode.

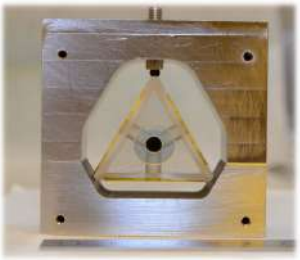


Figure 1: 25 mm long Fabry-Perot cavity in ULE glasse spacer, held on an stainless steel support with viton pads.

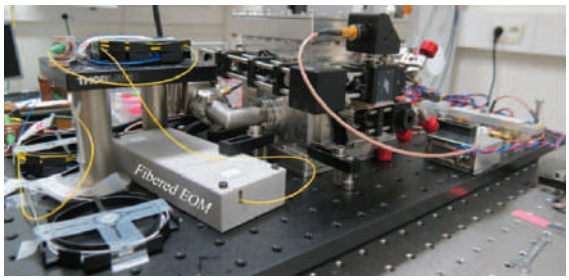


Figure 2: Experimental setup : fibered and free space optics adjoining the vacuum chamber, on a 6×3 dm^2 breadbord.

The presented compact ultra-stable laser, excluding electronics, fits in a 30 dm^3 volume. The fractional frequency stability of 7.5×10^{-15} at a 1 s integration time is consistent with the measured phase noise of 3 dB rad^2/Hz.

[1] A. D. Ludlow, *et al.*, Rev. Mod. Phys. **87**, 637 (2015).

[2] S. A. Diddams, *et al.*, Phys. Rev. Lett. **84**, 5102 (2000).

[3] T. Kessler, *et al.*, Nat. Photonics **6**, pages 687-692 (2012).

Measurement of ultracold atom velocity distributions by matterwave interferometry

Max Carey[1,2], **Jack Saywell**[1], **David Elcock**[1], **Mohammad Belal**[1], **and Tim Freegarde**[1]

[1] *School of Physics & Astronomy, University of Southampton, Highfield, Southampton SO17 1BJ, U.K.*

[2] *LP2N, Institut d'Optique d'Aquitaine, Rue François Mitterand, 34000 Talence, France*

e-mail: *tim.freegarde@soton.ac.uk*

We have previously shown how the velocity distribution within an ultracold atom cloud can be partially determined by quadrature Ramsey matterwave interferometry [1], but that the method's utility is limited by the finite duration and Doppler sensitivity of the Ramsey 'beam-splitter' pulses. We show here how, with the addition of a third interferometer pulse to form an asymmetric Mach-Zehnder interferometer, the method may be rendered general and practical.

The optical Ramsey pulses that form the beam-splitters of atom interferometers impart a momentum difference of a photon recoil between the interferometer states, and hence over the interferometer period τ result in an accrued phase

$$\Phi = \mathbf{k} \cdot \mathbf{v}\tau \tag{1}$$

where $\mathbf{v}$ is the atom's velocity and $\mathbf{k}$ the optical wavevector. For an atom cloud with velocity distribution $P(v_z)$ this results in an interferometer signal

$$\mathcal{S}(\phi, \tau) = \frac{1}{2} \int_{-\infty}^{\infty} P(v_z) \left[1 + \cos(k v_z \tau - \phi)\right] \mathrm{d}v_z \tag{2}$$

where ϕ is a phase difference that may be introduced between the two pulses to distinguish between positive and negative velocities, and k is taken to be in the z-direction. Quadrature measurements with $\phi = 0,\ \pi/2$ yield the 1-D velocity distribution from the Fourier transform of the complex quantity

$$\mathcal{S}(\tau) \equiv \mathcal{S}(0, \tau) + i\mathcal{S}(\pi/2, \tau). \tag{3}$$

In a pure Ramsey arrangement, τ is automatically positive, and indeed cannot be less than a value given by the small Doppler phase accrued during the beam-splitter pulses themselves. This truncates the interferometer data, distorting the derived velocity distribution. With the introduction of a third, 'mirror' pulse to form an asymmetric Mach-Zehnder interferometer, τ becomes the difference in time between the two interferometer periods, which may be swept smoothly from negative to positive values. The result is to provide the full Fourier transform data, from which the velocity distribution may be determined directly. The effects of Doppler sensitivity within the interferometer pulses are small, and may be corrected by applying a velocity-dependent scaling factor.

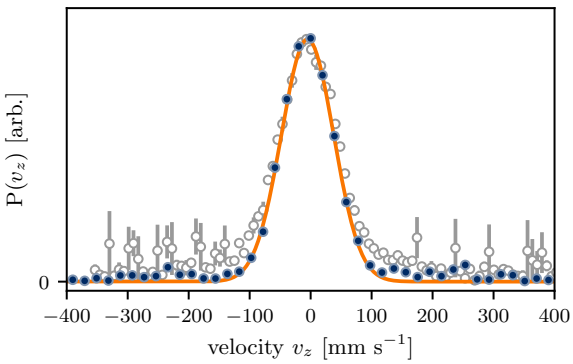


Figure 1: Interferometrically-determined velocity distribution (filled circles), overlaid upon Doppler Raman spectroscopic measurements (empty circles) taken under the same conditions. The solid line shows a Gaussian fit to the interferometric data with a temperature of 17 μK.

Results obtained for a cloud of ^{85}Rb atoms using this method are shown in Fig. 1, overlaid upon measurements determined by traditional Doppler Raman spectroscopy. The two measurements are in good agreement, with the interferometric method showing a rather better signal-to-noise ratio as the full sample effectively contributes to each data point.

We see a small but consistent difference between the interferometric and Doppler results in the wings of the distribution, which accords with some previous observations [2, 3, 4]. Measurements as a function of laser intensity suggest that broadening is an artefact of the conventional Doppler Raman method [5], perhaps due to off-resonant excitation [6].

[1] M. Carey et al., J. Mod. Opt. **65** (5-6), 657–666 (2018).

[2] P. D. Featonby et al., Phys. Rev. Lett. **81**, 495 (1998).

[3] L. P. Parazzoli, A. M. Hankin and G. W. Biedermann, Phys. Rev. Lett. **109** 230401 (2012).

[4] E. Maréchal et al., Phys. Rev. A **62**, 053603 (2000).

[5] M. Carey et al., `arxiv.org/1802.02190`, submitted (2018).

[6] I. G. Hughes, J. Mod. Opt. **65**, 640 (2018).

Developing a Transportable Ultra-cold Atomic Rotation Sensor

D. Elcock, M. Carey, J. Saywell, M. Belal and T. Freegarde
School of Physics and Astronomy, University of Southampton, SO17 1BJ, UK
e-mail: *dee1g12@soton.ac.uk*

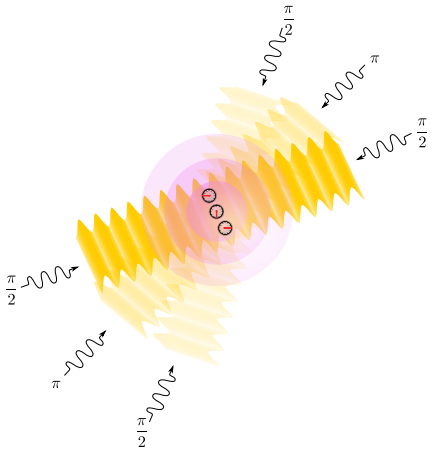


Figure 1: Mach-Zehnder sequence applied to an ultra-cold atomic cloud (purple). The cloud undergoes ballistic expansion during a (yellow) light-pulsed sequence.

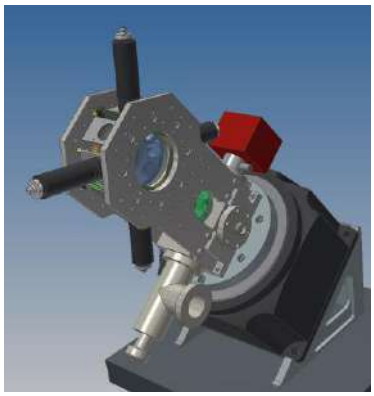


Figure 2: The proposed PSI design. A Magneto Optical Trap is formed inside a glass cell that is tested on a rotation stage. The entire apparatus is angled at Southampton's latitude.



Figure 3: Rack compatible Magneto Optical Trap laser optics shelf. Drift in laser frequency and power are reduced by thermal stabilisation and vibrational isolation from the suroundings. Acoustic isolation remains to be implemented.

Point Source Interferometry (PSI) has demonstrated sufficient inertial sensitivity to be useful for navigation applications [1]. The technique first developed by Dickerson *et al.* builds on the ballistic expansion of atomic clouds, which provide a direct map of the atom's velocity to the atom's spatial position [2]. Using a Mach-Zehnder light-pulse interferometric sequence, this map ensures a spatial-dependent state population across the cloud's cross-section. Absorption imaging of the expanded cloud provides the rotation rate and acceleration of the interferometer.

In the PSI, a expected cloud of $\sim 100\mu m$ width, $\sim 10\mu K$ ^{85}Rb atoms rotates (fig.1) relative to the rotating apparatus constructing a phase-shearing interferometer [3]. The new PSI (fig.2) is aimed having a short term rotation sensitiviy of $100\mu rad/\sqrt{Hz}$.

Transportability of the sensor is provided through populating a 870L rack with the laser systems and driving electronics. One such shelf of the control rack is shown in fig.3.

To improve the PSI performance, computational generated *composite pulses* [4] are being tested through thermal average fluorescence capturing. The current pulses under test make use of modified phase profiles during a pulse to counter the lowering diffraction envelope experienced by off-resonant matter-waves.

In this paper the preliminary experimental results from composite mirror pulses are shown along with progress on the new PSI.

[1] S. M. Dickerson, J. M. Hogan, A. Sugarbaker, D. M. S. Johnson and M. A. Kasevich, PRL **111**, [083001] (2013).

[2] G. W. Hoth, B. Pelle, S. Riedl, J. Kitching and E. A. Donley, Appl. Phys. Lett. **109**, [071113] (2016).

[3] A. Sugarbaker, S. M. Dickerson, J. M. Hogan, D. M. S. Johnson and M. A. Kasevich, Phys. Rev. Lett. **111**, [113002] (2013).

[4] J. Saywell, I. Kuprov, D. Goodwin, M. Carey and T. Freegarde, ArXiv [1804.04625], (2018). [Submitted for publication]

Near-Unitary Spin-Squeezing for Optical Clocks

S. Colombo[1], **B. Braverman**[1], **A. Kawasaki**[1], **E. Pedrozo**[1], **C. Shu**[1], **Z. Li**[1], **and V. Vuletić**[1]
[1] *Department of Physics, MIT-Harvard Center for Ultracold Atoms and Research Laboratory of Electronics, Massachusetts Institute of Technology, Cambridge, Massachusetts 02139, USA*
e-mail: *colombos@mit.edu*

State-of-the-art atomic sensors operate at or near the standard quantum limit, where the precision improves with the square-root of the number of involved atoms. A main goal of quantum metrology is to overcome this limit by engineering non-classical correlations between the atoms. Spin-squeezing techniques are actively investigated for the generation of these metrologically useful quantum states. However, most of these methods produce much more anti-squeezing than the minimum prescribed by the Heisenberg's uncertainty principle. The use of these highly non-unitary squeezed states significantly reduces the potential metrological gain of squeezing in atomic sensors.

We motivate our work by showing, with a theoretical model, the metrological advantages of unitary squeezing over non-unitary squeezing in optical clocks. We present the method and implementation for the generation of a near-unitary squeezed state in an ensemble of ^{171}Yb atoms mediated by a 'one-axis twisting' (OAT) interaction. In particular, we describe the engineering of the OAT Hamiltonian $\mathcal{H}=\hbar\chi S_z^2$ via cavity feedback [1] and we discuss the limits to the unitarity of the generated state. Probing photons sent to the atom-cavity system induce quantum back-action that generates the cavity feedback; however, they also carry some information about the quantum state of the atomic ensemble state. The atom-light entanglement, quantified by the quantum Fisher information of the effective resulting measurement, broadens the state along the squeezed direction.

We confirm the production of near-unitary squeezed states in our system both by conventional state tomography (Figure 1) and by a quantum magnification measurement. The deviation from unitarity of the generated quantum states is near (within a factor < 2) the predicted limit given by the Fisher information. This technique will not only allow for the creation of squeezed states with metrological gain on the clock transition of ^{171}Yb, but also those states offering the largest advantages for absolute improvements to optical clocks compared to previous work.

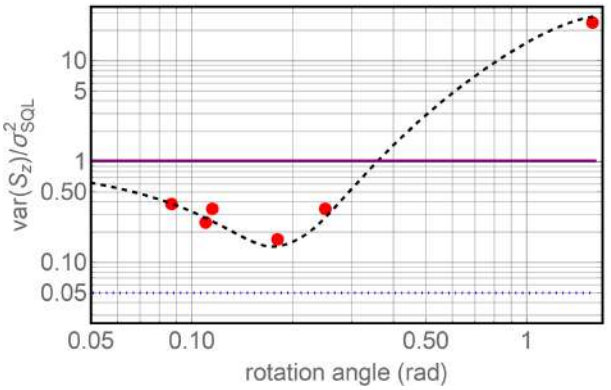


Figure 1: Tomography of a squeezed state of an ensamble of 250±20 ^{171}Yb atoms. After the squeezing process we rotate the state and measure its variance projected on the S_z axis. The solid line horizontal (purple) line shows the measured standard quantum limit variance while the dotted (blue) line represents the quality of our measurement. The dashed line is the theoretical model fitted with the parameters $Q = 5$ and $F = 1.5$, where $Q\propto\chi$ is the dimensionless shearing strength induced by the OAT interaction while F is the dimensionless Fisher information.

[1] M. H. Schleier-Smith, I. D. Leroux, and V. Vuletić, Phys. Rev. A **81**, 021804(R) (2010).

[2] I. D. Leroux, M. H. Schleier-Smith, and V. Vuletić, Phys. Rev. Lett. **104**, 073602 (2010).

Nondestructive measurement of trapped cold atoms

Xian Zhang[1,2], **XiaoXiao Ma**[1], **Kaikai Huang**[1], **and Xuanhui Lu**[1]
[1] *Department of Physics, Zhejiang University, 310017, Hangzhou, China*
[2] *Institute of Advanced Technology and Research, Zhejiang University, 310017, Hangzhou, China*
e-mail: *xhlu@zju.edu.cn*

We report a technology of detecting state populations of trapped atoms using a nondestructive interferometric measurement. The interferometer is in a Mach-Zehnder configuration. By recording the interferometer output, we extract the phase shift of an optical probe beam propagating through the cloud of ^{87}Rb atoms. The phase shift is induced by the complex index of refraction imposed on off-resonant light by an ensemble of cold multi-level atoms [1], as shown in fig 1 in the case of ^{87}Rb atoms.

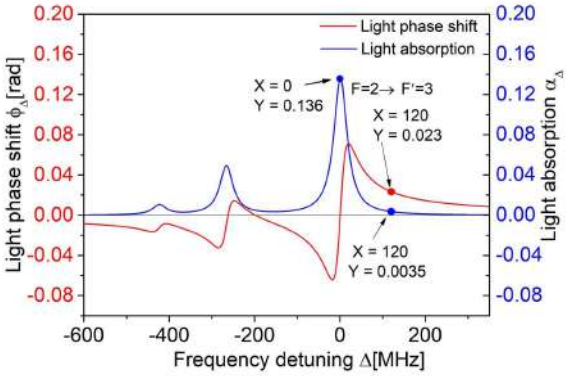


Figure 1: A theoretical simulation for ^{87}Rb atoms of light absorption (blue solid line) and phase shift (red solid line) versus probe light detuning.

Fig 2 shows the phase shift measurement according to a recorded interferometer output at certain probe laser frequency range. The data is consist with the numerical estimation based on the theoretical simulation as shown in fig 1. In the range of far detuning, the phase shift of probe laser is related to the density of atoms in the trap [2], while the absorption of photons is assumed to be low enough so that the state populations are not perturbed [3]. We are then able to monitor the state of atoms in real time with nondestructive measurement.

This technology can improve the efficiency of precision measurements with atoms in optical lattices or atom interferometers, where resonant fluorescence detection is usually needed and thus a dead time of measurement exists [4, 5]. Indeed, combing with a long life-time lattice, it is even possible to do continuous measurements of Bloch oscillations for inertial sensing [5].

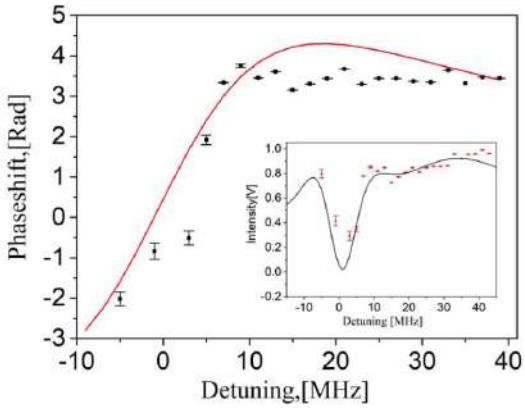


Figure 2: A measurement of atom-induced phase shift. The probe light is detuned by from the D2 line cycling transition of ^{87}Rb atoms. The black dots are the experimental data, and the Solid line the theoretical simulation of the phase shift in this case. The insert fig is the original data (red dots) and the numerical simulation (solid black line) of the output intensity of M-Z interferometer.

This work is supported by National Key Research and Development Program of China (Grant No. 2017YFA0304202 and the International Collaboration of Science and Technology of China (Grant No.11474254).

[1] I. I. Sobelman, *Atomic spectra and radiative transitions*, Springer, Berlin, 2nd editon(1992).

[2] J. Appel, P. J. Windpassinger, D. Oblak, U. B. Hoff, N. Kjærgaard, and E. S. Polzik, PNAS, **106**, 10961(2009).

[3] D. Oblak, P. G. Petrov, C. L. Alzar, W. Tittel, A. K. Vershovski, J. K. Mikkelsen, J. L. Sørensen, and E. S. Polzik, Phys. Rev. A, **71**, 045504, (2005).

[4] *Atom interferometry*, edited by G. M. Tino and M. A. Kasevich (Società Italiana di Fisica and IOS Press, Amsterdam, 2014).

[5] N. Poli, F.-Y. Wang, M. G. Tarallo, A. Alberti, M. Prevedelli, and G. M. Tino, Phys. Rev. Lett. **106**, 038501 (2011).

Development of a planar ion trap aimed at ion spacing control by anharmonic potential

H. Sasaki[1], **M. Kitao**[1], **K. Hayasaka**[2,1], **T. Mukaiyama**[1] **and U. Tanaka**[1,2]

[1] *Graduate School of Engineering Science, Osaka University, 1-3, Machikaneyama-cho, Toyonaka, Osaka, 560-8531, Japan*

[2] *National Institute of Information and Communications Technology, 588-2, Iwaoka, Iwaoka-cho, Nishi-ku, Kobe, 651-2492, Japan*

e-mail: *u005144i@ecs.osaka-u.ac.jp*

Laser-cooled atomic ions coupled to an optical cavity mode constitute an attractive quantum system that is expected to be applied to quantum interface [1] and optical frequency standards based on supperradiance, that is, active clocks [2]. In order to implement these applications, the coupling strength of interaction between the resonator mode and the large number of ions needs to be increased. As an effective approach for this realization, a new trap that localizes multiple ions at equal spacing in the optical resonator is conceivable. A general linear trap creates a harmonic potential, so that the ions are not equally spaced. For equally spaced ion strings, anharmonic potentials are required. However, such potentials are not easily created with conventional 3D traps because of limitation in machining accuracy.

In this study, we designed and evaluated a microfabricated planar trap which generates anharmonic potential to realize an isospaced ion string. In recent years, the potential for isospaced ion strings has been derived theoretically [3]. We created the desired potential by applying appropriate voltages to segmented DC electrodes.

Consider a planar trap consisting of rectangular electrodes, as shown in Fig. 1. When N ions are aligned at spacing d along the z-axis, the potential of the confinement along the z-axis can be expressed using the polygamma function [3].

By applying appropriate voltages to rectangular electrode pairs, we realize the desired potential. Let ϕ_{ij} be the potential at a position $z_i (1 < i < N)$ when a unit voltage is added to the jth electrode among the M electrodes. If the voltage added to the jth electrode is V_j, the potential Φ of the position z_i created by the applied voltage can be expressed by the following equation.

$$\Phi(z_i) = \sum_{j=1}^{M} \phi_{ij} V_j \qquad (1)$$

Simultaneous linear equations can be used to evaluate the voltage V_j that needs to be applied to achieve a target potential. However, if the number of electrodes is less than the number of ions, the simultaneous equations have no unique solution. Therefore, by obtaining V_j that minimizes the error, ideal potential can be achieved. Our trap consists of 12 pairs of DC electrodes to control the axial potential. We generated a potential for $N = 17$ and $d = 15$ μm. When generating an ion string, the trapping electric field is susceptible to the stray electric field and the electric field generated by the electrode is not equal to the designed field. Therefore, we developed a system which provides an electric field at each ion position from an ion string image and compensated the stray electric field. As shown in Fig. 2, we succeeded in realization of equally spaced 17 ions forming an ion string. A related work, using a different setup, has been reported by another research group [4]. In addition to these results, the possibility of strings with larger number of ions will be discussed.

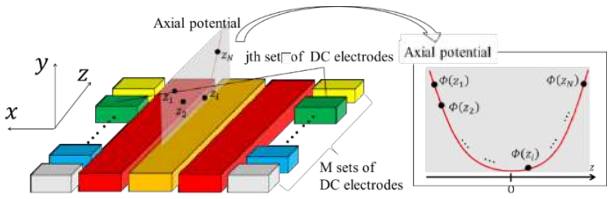


Figure 1: Potential generation by multiple electrodes.

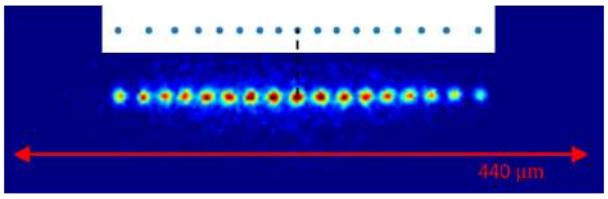


Figure 2: Equally spaced ion string. For comparison, the calculated position of each ion in the ion string at harmonic potential is shown above the image.

[1] H. J. Kimble, Nature **453**, 1023—30 (2008).

[2] D. Meiser *et al.*, Phys. Rev. Lett. **102**, 163601 (2009).

[3] M. Johanning, Appl. Phys. B **122**, 71 (2016).

[4] Y. Xie *et al.*, Phys. Rev. A **95**, 032341 (2017).

Pumped-Up SU(1,1) Interferometry

Stuart S. Szigeti[1], Robert J. Lewis-Swan[2] and Simon A. Haine[3]

[1] *Department of Quantum Science, The Australian National University, Canberra ACT 2601, Australia*
[2] *JILA, NIST, and Dept. of Physics, University of Colorado, 440 UCB, Boulder, CO 80309, USA*
[3] *Department of Physics and Astronomy, University of Sussex, Brighton BN1 9QH, United Kingdom*
e-mail: *stuart.szigeti@anu.edu.au*

Take a Mach-Zehnder interferometer and replace the beamsplitters with parametric amplifiers that create correlated particle pairs. This is an SU(1,1) interferometer (Fig. 1a). Researchers have recently been very excited by SU(1,1) interferometry since (a) it is ideally Heisenberg-limited (and so is an example of quantum-enhanced interferometry) and (b) good sources of correlated particles are now available to experimentalists (e.g. downconversion with light and spin-mixing collisions in Bose-Einstein condensates). However, the precision measurement community (e.g. LIGO) is less excited; SU(1,1) interferometers are routinely called "unconventional", yet are *never* described as "high precision". Although SU(1,1) interferometry is Heisenberg limited, this is with respect to the average number of correlated pairs created during the parametric process, which is generally much fewer than the total number of particles input into the interferometer. Consequently, the promise of Heisenberg-limited sensitivities is of little practical benefit, especially when sophisticated classical (shot-noise limited) interferometers display superior *absolute* sensitivities by many orders of magnitude.

Here [1] we propose an alternative 'pumped-up' approach that makes use of all input particles, and show how this can be implemented in spinor Bose-Einstein condensates (Fig. 1b) and hybrid atom-light systems (Fig. 1c) - both of which have experimentally realised SU(1,1) interferometry [2, 3]. We provide the optimal phase-estimation procedure (i.e. that saturates the quantum Cramer-Rao bound) and prove that pumped-up schemes can surpass the shot-noise limit with respect to the total number of particles, and are *never* worse than conventional SU(1,1) interferometry. We also incorporate the effect of losses and provide sub-optimal phase estimation procedures that are easier to implement in practice and furthermore are robust to irreversibilities that strongly limit the precision of SU(1,1) interferometers.

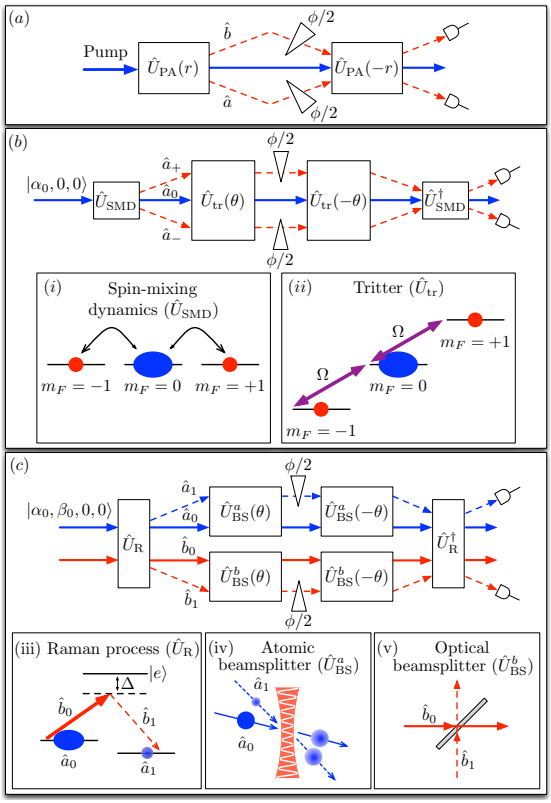


Figure 1: (a) SU(1,1) interferometry: Correlated particle pairs are created via parametric amplification: $\hat{U}_{\rm PA}(r) = \exp[-ir(\hat{a}\hat{b} + h.c.)]$. SU(1,1) interferometry is sensitive to the sum of phase shifts on both arms, ϕ_s. (b) Pumped-up SU(1,1) interferometry with spinor Bose-Einstein condensates. Parametric amplification is achieved using spin-changing collisions [$\hat{H}_{\rm SMD} = \hbar g(\hat{a}_0^2\hat{a}_+^\dagger\hat{a}_-^\dagger + h.c.)$ - see (i)], and the interferometer 'pumped-up' with tritter operation $\hat{U}_{\rm tr}(\theta) = \exp[-i\theta(\hat{b}^\dagger(\hat{a}_+ + \hat{a}_-) + h.c.)]$ [see (ii)]. (c) Pumped-up SU(1,1) interferometry in a hybrid atom-light system. Correlated atom-light pairs are created via a Raman process [$\hat{H}_{\rm R} = \hbar g(\hat{a}_0\hat{b}_0\hat{a}_1^\dagger\hat{b}_1^\dagger + h.c.)$ - see (iii)], and the interferometer pumped-up by independent mixing of the atomic modes $(\hat{a}_0, \hat{a}_1)$ and light modes $(\hat{b}_0, \hat{b}_1)$ via beamsplitters of angle θ [see (iv) and (v)].

References

[1] S. S. Szigeti, R. J. Lewis-Swan, and S. A. Haine. *Pumped-Up SU(1,1) Interferometry*. Phys. Rev. Lett. **118**, 150401 (2017).

[2] D. Linnemann, H. Strobel, W. Muessel, J. Schulz, R. J. Lewis-Swan, K. V. Kheruntsyan, and M. K. Oberthaler. *Quantum-Enhanced Sensing Based on Time Reversal of Nonlinear Dynamics*. Phys. Rev. Lett. **117**, 013001 (2016).

[3] B. Chen, C. Qiu, Cheng, S. Chen, J. Guo, L. Q. Chen, Z. Y. Ou, and W. Zhang. *Atom-Light Hybrid Interferometer*. Phys. Rev. Lett. **115**, 043602 (2015).

Simultaneous precision magnetic and inertial sensor based on spatial fringes using Bragg transitions

P. B. Wigley[1], **and N. P. Robins**[1], **K. S Hardman**[1]

[1] *Atomlaser and Quantum Sensors Group, Department of Quantum Science, Australian National University, Canberra 0200, Australia*

e-mail: *paul.wigley@anu.edu.au*

In recent years precision inertial sensors based on atom interferometry have become competitive with their traditional counterparts. Unlike these traditional sensors, those based on atom interferometry provide measurements based on fundamental properties of the atomic sources making them increasingly robust. These sources also offer additional degrees of freedom enabling measurements of other properties such as magnetic fields, magnetic gradients and time, with the potential for these measurements to be made simultaneously. Whilst these sensors typically use a thermal cloud of atoms as the source test mass, Bose-Einstein condensates (BECs) provide a number of advantages, primarily a larger spatio-temporal coherence. The spatial coherence of a BEC is equivalent to the size of the atomic cloud (100's of μm), larger than that of a thermal cloud which has a spatial coherence on the order of the de Broglie wavelength (100's nm). This increased spatial coherence provided by BECs makes these sources robust to systematics that reduce the fringe contrast [2]. A device utilizing a spinor BEC source and a Mach-Zehnder interferometer based on Bragg transitions is presented with the interferometer shown to operate on a superposition of three magnetic states $|m_F = 1,\, 0,\, -1\rangle$, facilitating a simultaneous measurement of the acceleration due to gravity and the magnetic field gradient with a 1000 run precision of $\Delta g/g = 1.45 \times 10^{-9}$ and $120pT/m$ respectively [1].

The spatial coherence provided by the BEC also gives rise to the possibility of precision atom-interferometers based on spatial fringes. These fringes arise from a temporal mismatch in the symmetry of the Mach-Zehnder pulse sequence resulting in sinusoidal modulation of the density envelope at the culmination of the interferometer. Unlike the symmetric version, this scheme enables a single shot phase readout while enabling longer Bragg-based interferometers by eliminating readout time that is typically needed to separate the states before measurement. By allowing the fringes to overlap constructively, the separation time is reduced while simultaneously improving the signal-to-noise. By addressing three magnetic substates, the asymmetric Mach-Zehnder interferometer could be used to simultaneously measure magnetic gradients, gravitational acceleration and rotations simultaneously. The plausibility and limitations of such a scheme are presented.

References

[1] K. Hardman, P. Everitt, G. McDonald, P. Manju, P. Wigley, M. Sooriyabandara, C. Kuhn, J. Debs, J. Close, and N. Robins. Simultaneous Precision Gravimetry and Magnetic Gradiometry with a Bose-Einstein Condensate: A High Precision, Quantum Sensor. *Physical Review Letters*, 117(13):138501, Sept. 2016.

[2] K. S. Hardman, C. C. N. Kuhn, G. D. McDonald, J. E. Debs, S. Bennetts, J. D. Close, and N. P. Robins. Role of source coherence in atom interferometry. *Physical Review A*, 89(2):023626, Feb. 2014.

AMBiT: A program for high-precision relativistic atomic structure calculations

J. C. Berengut and E. V. Kahl
School of Physics, University of New South Wales, Sydney NSW 2052, Australia
e-mail: *julian.berengut@unsw.edu.au*

We present AMBiT [1], a software package for fully relativistic, *ab initio* atomic structure calculations including energy levels, electric and magnetic multipole transition matrix elements, g-factors, hyperfine structure, and isotope shifts. AMBiT implements the particle-hole configuration interaction with many-body perturbation theory (CI+MBPT) method [2], which extends the CI+MBPT method [3, 4] to non-perturbatively include configurations with electron holes below the designated Fermi level.

Modern numerical methods and high-performance computing techniques employed by AMBiT allow for the calculation of open-shell systems with many valence-electrons ($N \geq 5$) to a high degree of accuracy and in a highly computationally efficient manner. The software is written in modern C++11, and can make use of both OpenMP and MPI to achieve demonstrated scalability from a personal notebook all the way up to state-of-the-art supercomputer clusters.

In order to reduce the size of the configuration interaction calculation, AMBiT makes use of "emu CI", a robust method of decreasing the matrix size without undermining the accuracy of the resulting atomic spectra. In this method matrix elements between high energy configurations are set to zero, with little effect on the accuracy of low lying levels (see Figure 1). The emu CI method makes it possible to saturate the CI matrix in atoms with many valence electrons. We have tested our method on the five-valence-electron atom tantalum [5] and ion Cr^+ [1], and verified the convergence of the calculated energies.

AMBiT has been used for many years to calculate low-lying spectra in atomic clock species, astrophysically relevant atoms and ions, and highly-charged ions. Recent calculations include Ta and Db [5], Sn^{7+} – Sn^{10+} [6], and Hg^+ [2]. AMBiT has the flexibility to calculate an enormous range of atomic species, has a relatively user-friendly interface, and is now an open source project that will serve the atomic physics community.

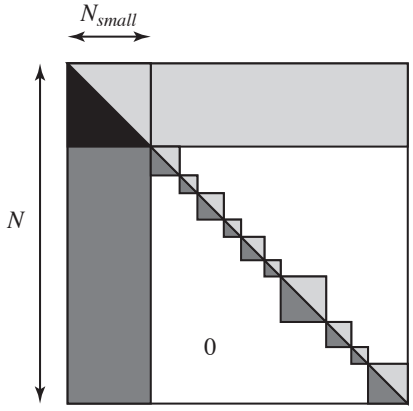


Figure 1: Structure of the CI matrix under the emu CI approximation. The most important configurations are in the upper left corner, while the shaded areas are the effective CI matrix. The unshaded area represents interactions between high energy states which are set to zero.

[1] E. V. Kahl and J. C. Berengut, arXiv:1805.11265 (2018); `https://github.com/drjuls/AMBiT`.

[2] J. C. Berengut, Phys. Rev. A **94**, 012502 (2016).

[3] V. A. Dzuba, V. V. Flambaum, M. G. Kozlov, Phys. Rev. A **54**, 3948 (1996).

[4] J. C. Berengut, V. V. Flambaum, M. G. Kozlov, Phys. Rev. A **73**, 012504 (2006).

[5] A. J. Geddes, D. A. Czapski, E. V. Kahl, J. C. Berengut, arXiv:1805.0661 (2018).

[6] F. Torretti *et al.*, Phys. Rev. A **95**, 042503 (2017).

Sensitivity limits of an atomic gravimeter using Raman atom interferometer

Sang-Bum Lee, Taeg Yong Kwon, Sang Eon Park, Myoung-Sun Heo,and Hyung-Gue Hong
Center for Time and Frequency, Korea Research Institute of Standard and Science, Daejeon, 34113, Korea
e-mail: *lsbum@kriss.re.kr*

An atomic interferometer using light-matter interaction has been attracting much attention as promising technology for multidisciplinary applications such as geophysics, geodesy, inertial navigation, and so on, as well as for high precision measurement in fundamental physics [1, 2, 3, 4, 5, 6, 7]. Especially, an atomic gravimeter using Raman atom interferometer is also a promising candidate for an absolute gravimeter with the uncertainty of sub-μGal [3, 4, 5, 6]. We introduce current experimental limits to the sensitivity of our gravimeter at developing and discuss intrinsic sensitivity limits of the gravimeter.

About 10^8 Rb-87 atoms are captured within 230 ms in a magneto-optical trap (MOT) with a period of about 0.5 s. They are cooled down to a temperature of about 2 μK by far-detuned optical molasses phase and adiabatically switching off, followed by a vertical velocity selection with a combination of microwave and Raman pulses. After atoms prepared in ground state $|F = 1, m_f = 0\rangle$ with narrow vertical velocity distribution free-fall, a Mach-Zehnder atom interferometer is realized by a sequence of three Raman pulses $\pi/2$-π-$\pi/2$ coupling two hyperfine ground states $|F = 1, m_f = 0\rangle$, $|F = 2, m_f = 0\rangle$ with a spacing of free evolution time 75 ms. We achieve a short-term sensitivity of 1.6×10^{-8} $g/\sqrt{\text{Hz}}$ and analyze elements which affect a long-term sensitivity as well as the short-term sensitivity. The most dominant element on the short-term sensitivity is analyzed as the intensity noise of a Raman laser which can be improved by power stabilization. One of two dominant elements on a long-term sensitivity are the position fluctuations of MOT atom clouds, which induce different phase offset resulting from undergoing different wave-front distortions of a Raman laser beam, and the other is the intensity drift of a Raman laser which shifts atomic levels by Stark effect [4]. The details for the elements and for a improvement will be discussed in the conference.

[1] A. Louchet-Chauvet, T. Farah, Q. Bodart, A. Clairon, A.G. Rosi, F. Sorrentino, L. Cacciapuoti, M. Prevedelli, and G. M. Tino, Nature (London) **510**, 518 (2014)..

[2] D. Schlippert, J. Hartwig, H. Albers, L. L. Richardson, C. Schubert, A. Roura, W. P. Schleich, W. Ertmer, and E. M. Rasel, Phys. Rev. Lett. **112**, 203002 (2014).

[3] A. Peters, K. Y. Chung, and S. Chu, Metrologia **38**, 25 (2001)

[4] A. Louchet-Chauvet, T. Farah, Q. Bodart, A. Clairon, A. Landragin, S. Merlet, and F. Pereira Dos Santos, New J. Phys.**13**, 065025 (2011

[5] V. Schkolnik, B. Leykauf, M.Hauth, C. Freier, and A. Peters Appl. Phys. B **120**, 311 (2015).

[6] R. Karcher, A. Imanaliev, S. Merlet, and F. Pereira Dos Santos, arXiv:1804.04909v1

[7] J. Le Gouet, T.E. Mehlstaubler , J. Kim, S. Merlet, A. Clairon, A. Landragin, , and F. Pereira Dos Santos, Appl. Phys. B **92**, 133 (2008)

Development of NPL's 2nd Generation Strontium Lattice Clock

W. Bowden[1,2], **R. Hobson**[1], **A. Vianello**[1,3], **M. Schioppo**[1], **A. Silva**[1], **I. R. Hill**[1], **P. Gill**[1,2,3], **and H. S. Margolis**[1,2]

[1] *National Physical Laboratory (NPL), Teddington, TW11 0LW, United Kingdom*
[2] *University of Oxford - Department of Physics, Oxford, OX1 3PU, United Kingdom*
[3] *Imperial College London - Department of Physics, London, SW7 2BB, United Kingdom*
e-mail: *william.bowden@npl.co.uk*

Over the past decade, optical lattice clocks have made significant improvements in performance to become a leading candidate systems for a possible redefinition of the SI second. We will present recent developments of Sr2, NPL's second generation strontium lattice clock, highlighting key design changes made to improve its performance with respect to our first generation system [1]. The main change has been to include the use of a pyramid MOT to simplify the optical system and reduce the required optical cooling power. The retro-reflector consists of six radial prism mirrors and a CaF_2 prism at the apex, see Fig. 1.

A key design feature is the addition of in-vacuum build up cavities for the optical lattice. The cavities are integrated into the pyramid MOT structure to form a single compact, monolithic device capable of both cooling and trapping the atoms. In addition to providing enhancement of the lattice used to confine the atoms, the high-reflective coatings extend to both of the principal laser cooling transitions and can therefore be used for non-demolition measurement of the atomic state [2].



Figure 1: Picture of the ^{88}Sr atoms trapped in pyramid MOT. The retro-reflector consists of six radial prism mirrors and a CaF_2 prism at the apex. ^{87}Sr, the fermionic isotope typically used for the clock, has also been trapped in the pyramid MOT with a lifetime exceeding 2 seconds.

Another important change to the system is the realization of a metastable triplet MOT operating on a closed transition between the $5s5p\ ^3P_2$ and $5s4d\ ^3D_3$ levels separated by 2.92 µm. Such a cooling scheme is currently being investigated as a possible alternative to the typically used second stage cooling at 689 nm. Already we have verified the MOT is capable of generating sufficiently cold samples to be loaded into the lattice, while a post-cooling molasses stage done in a bias field can spin polarize the atomic sample as needed for clock operation.

The addition of a second lattice clock in conjunction with our first generation system now allows for interleaved operation. In such a configuration, dead time in the experimental cycle, during which the local oscillator's frequency goes unmeasured, is eliminated [3]. This will greatly improve the performance as this dead time causes increased frequency instability via the Dick effect [4]. In addition, the Sr2 system will be integrated into Europe's existing optical clock network, connected via optical fibre link, so that it can be compared to other frequency standards to verify its performance while providing possible tests of fundamental physics [5].

[1] I.R. Hill, et al., Proceedings of the 8th Symposium on Frequency Standards & Metrology (2016).

[2] G. Vallet, et al., New Journal of Physics **19**, 083002 (2017).

[3] M. Schioppo, et al., Nature Photonics **11**, 48 (2017).

[4] G. Dick. Precise Time and Time Interval, 133-147, Redondo Beach, (1987).

[5] P. Delva et al. Phys., Rev. Lett. **118**, 221102 (2017).

A search for the low-energy ^{229}Th nuclear isometric transition using an "optical" pumping technique at 29-keV

S. Uetake[1], H. Hara[1], T. Hiraki[1], H. Kaino[1], Y. Kasamatsu[2], S. Kitao[3], K. Konashi[4], T. Masuda[1], Y. Miyamoto[1], K. Okai[1], N. Sasao[1], O. Sato[1], T. Schumm[5] , M. Seto[3], Y. Shigekawa[2], S. Stellmer[5], K. Suzuki[1], M. Watanabe[4], A. Yamaguchi[6], Y. Yasuda[2], Y. Yoda[7], A. Yoshimi[1], K. Yoshimura[1], M. Yoshimura[1]

[1] *Research Institute for Interdisciplinary Science, Okayama University, Okayama, Japan*
[2] *Department of Chemistry, Osaka University, Osaka, Japan*
[3] *Research Reactor Institute, Kyoto University, Osaka, Japan*
[4] *Institute for Materials Research, Tohoku University, Miyagi, Japan*
[5] *Institute for Atomic and Subatomic Physics, TU Wien, Vienna, Austria*
[6] *Quantum Metrology Laboratory, RIKEN, Saitama, Japan*
[7] *Japan Synchrotron Radiation Research Institute, Hyogo, Japan*
e-mail: *uetake@okayama-u.ac.jp*

Thorium-229 (^{229}Th) has remarkable features: (1) the first nuclear excited state of ^{229}Th ($3/2^+$) is long-lived metastable state (called nuclear isomer, ^{229m}Th); and (2) it is located in an extraordinarily low energy range of only a few eV. Such nuclear isometric state of ^{229}Th opens a new possibility of laser spectroscopy of *'nuclear transition'*. Also the small size of the nucleus leads to a small cross-section and sensitivity to ambient fields such as black-body radiation. Therefore nuclear isometric transition of ^{229}Th is expected to have longer coherence time than ordinary atomic clock transitions. It is also a promising candidate for an optical frequency standard of very high accuracy. Furthermore, it has 5-6 orders of magnitude higher sensitivity to detect possible time variations of the fine structure constants α and the strong interaction $m_q/\Lambda_{\rm QCD}$ than any other frequency standards[1].

In recent years much effort has been devoted to precise determination of its energy level, however, the present uncertainty of ± 0.5 eV (corresponds to ± 10 nm) is still fairly large to proceed the direct search by laser spectroscopy. This is because the transition wavelength is located in the VUV range ($\sim$ 160 nm) and there is no widely-tunable, narrow-linewidth VUV laser source so far. Therefore it is urgent to reduce the uncertainty in the isometric transition frequency.

We propose a new experimental method to determine the emission wavelength by detecting the VUV emission from ^{229m}Th. It is produced by "optical" pumping via the nuclear rotational excitation level ($5/2^+$) at 29.2 keV (step 1 and 2 in Fig. 1a). Then we detect the VUV emission through a monochromator (step 3 in Fig. 1a). In this case the energy of the observed light ($\sim$8 eV) is totally different from that of the pumping light (29 keV). Thus the strong pumping light does not affect detection of weak signal light, hence one can expect high signal-to-noise ratio. However, difficulties of this experiment are: (1) the lifetime of $5/2^+$ state is very short ($\sim$ 0.2 ns), and (2) branching ratio from $5/2^+$ to the ground state is small ($\sim$ 10%). Thus the X-ray fluorescence signal is estimated to be 10^{-7} smaller than the non-resonantly scattered background. In order to detect such weak and fast decay fluorescence in the presence of strong background scatter, one needs to develop a new X-ray detector that has very fast time response ($\sim$ 50 ps), high dynamic range ($> 10^7$), and large acceptance.

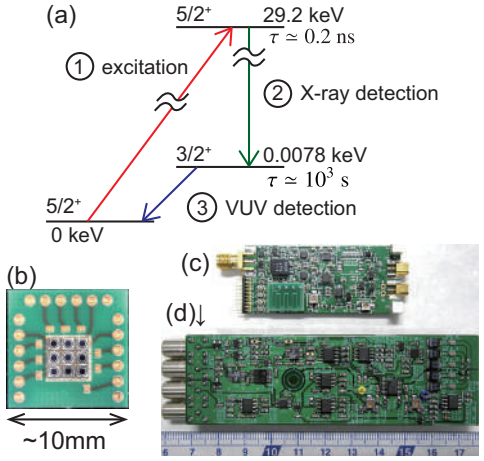


Figure 1: (a) Energy level of ^{229}Th. (b-d) Ultrafast X-ray detector system consists of (b) 9-ch APD array, (c) Constant Fraction Discriminator, and (d) Amplitude-to-Time Converter.

We have developed such X-ray detector system (Fig. 1(b-d) and [2]). We checked the ability of our new detector system with nuclear resonant scattering measurement of ^{201}Hg[3]. We have attempted to observe the VUV light emission from ^{229m}Th at SPring-8 synchrotron radiation facility. We show the present status of the experiment in the poster.

[1] V. V. Flambaum, PRL **97**, 092502 (2006).
[2] T. Masuda *et al.*, Rev. Sci. Instrum. **88**, 063105 (2017); T. Masuda *et al.*, in preparation
[3] A. Yoshimi *et al.*, PRC **97**, 024607 (2018).

A compact inertial sensor using atom interferometry: pushing towards high-dynamic range

I. Dutta, S. P. de Silva, X. Cheng, J. P. Stammers, T. B. Krastev, J. P. Cotter and E. A. Hinds

Centre for Cold Matter, Blackett Laboratory, Imperial College London, Prince Consort Road, London SW7 2AZ, United Kingdom

e-mail: *i.dutta@imperial.ac.uk*

Global navigation satellite systems (GNSS) presently provide sub-metre position accuracy, but during the absence of GNSS signal, conventional accelerometers and gyroscopes are used for navigation [1]. Navigation-grade devices are precise but over long times their accuracy is compromised by bias drift.

Cold atom interferometry promises an attractive solution to this problem. Inertial sensing based on cold atom interferometry benefits from long-term stability as the interferometer is referenced to the atomic transitions.

Here, we present our work towards a multi-axis cold atom accelerometer using Rubidium-87 atoms. Our cold atoms are prepared in a 2D + 3D magneto-optical trap, providing a thermal cloud of 6 μK temperature. These atoms are transferred to a magnetically-insensitive ground state, and then are selected in a narrow band of the velocity. A three pulse Mach-Zehnder ($\pi/2$ - π - $\pi/2$) interferometer using stimulated Raman transitions is used to measure the acceleration with high sensitivity. Our work has concentrated on measuring horizontal acceleration in the presence of the gravitational acceleration, g. A large operating range [3] can be achieved by combining the fine fringes of the atom interferometer with the coarser reading of a conventional MEMS accelerometer. This sets the system up to work as a high precision one-axis cold-atom hybrid accelerometer, with excellent rejection of ambient vibration noise.

The sensing head has a volume of 10 litres. The control electronics is mounted on a seperate racks that houses the lasers and electronics. The Raman beam optics, specially designed to deliver wavefront smoothness close to $\lambda/100$ uniformity, is mounted inside the ultra-high vacuum chamber together with the MEMS accelerometer. This combined set-up now gives us a one-axis sensitivity of 5 μ ms$^{-2}/\sqrt{\text{Hz}}$.

To be used in inertial navigation, the sampling by the interferometer has to be frequent enough that the loss of information introduced by the dead-time is negligible [2]. The dead time is currently 0.5 seconds. We next aim to achieve a repetition rate of 10 Hz to reduce the dead-time while maintaining a good signal-to-noise ratio. Currently, we are optimizing the system to reach a sensitivity of 1 μ ms$^{-2}/\sqrt{\text{Hz}}$ at a dynamic range of +/- 3 ms^{-2}. This will eventually be working as a standalone inertial navigation unit.

This application places extreme demands on the laser system which has been developed by M-Squared Lasers, and is described in a seperate poster.

[1] H. C. Lefvre, "The fiber-optic gyroscope, a century after Sagnacs experiment: The ultimate rotation-sensing technology?", Comptes Rendus Physique, 15, 851858, 2014

[2] C. Jekeli, "Navigation Error Analysis of Atom Interferometer Inertial Sensor", Navigation, 52: 114 (2005).

[3] J. Lautier, L. Volodimer, T. Hardin, S. Merlet, M. Lours, F. Pereira Dos Santos, and A. Landragin, "Hybridizing matter-wave and classical accelerometers", Appl. Phys. Lett. 105, 144102 (2014).

Atomic structure calculations and study the parameters of hyperfine constants, Landé g-factors and isotope shifts of Xe LIII

Dhia Elhak Salhi[1,2], **Pascal Quinet**[3,4] **and Haikel Jelassi**[1]

[1] *Laboratory on Energy and Matter for Nuclear Sciences Development, LR16CNSTN02, Tunisia. National Center for Nuclear Sciences and Technologies, Sidi Thabet Technopark 2020 Ariana Tunisia.*

[2] *Faculty of Sciences of Tunis, University Tunis El Manar Tunis, Tunisia.*

[3] *Physique Atomique et Astrophysique, Université de Mons, 7000 Mons, Belgium.*

[4] *IPNAS, Université de Liège, 4000 Liège, Belgium.*

e-mail: *salhidhiaelhak@gmail.com*

In recent years, there have been extensive spectroscopic studies, both experimental and theoretical, of helium isoelectronic sequence. An analysis of the spectra of solar, stellar and other astrophysical plasmas by many space missions, such as SOHO, Chandra and XMM Newton shows the presence of highly ionized atoms [1]. In addition, they are injected as impurities into tokamak plasmas [2, 3].

In particular, high Z elements of the fifth period are being increasingly used as injected impurities for tokamak fusion plasmas. Also, the inert gas atoms show a significant importance in the diagnostics of laboratory plasmas.

Furthermore, atomic data (namely energy levels, weighted oscillator strengths, radiative rates, lifetimes, hyperfine structure and landé g_j factors and isotope shifts) are required for many ions in order to estimate the power loss from the impurities in the forthcoming fusion reactors, such as ITER project [4].

We carry on in this study our previous work on He-like ions [5]. Energy levels, weighted oscillator strengths and transition probabilities, lifetimes, hyperfine interaction constants, Landé g_J factors and isotope shifts are calculated for all levels of $1s^2$ and $1snl$ ($n = 2-7$) configurations of He-like xenon ion ($Xe\ LIII$).

Multiconfigurational Dirac-Hartree-Fock (MCDHF) method is adopted for calculating these spectroscopic data. Comparisons are made with similar data obtained with FAC (Flexible Atomic Code) to assess the accuracy of the results. Transition probabilities are reported for all $E1$, $E2$, $M1$ and $M2$ transitions from the ground level. Breit interactions and quantum electrodynamics effects are estimated in extensive Relativistic Configuration Interaction (RCI) calculations.

Comparisons were made with the available data in the literature and good agreement was found which confirms the reliability of our results. The accuracy of the present calculations [6] is high enough to facilitate identification of many observed spectral lines.

[1] `http://www.chiantidatabase.org`.

[2] F. P. Keenan, S. M. McCann, Solar Physics **109** 01 (1987).

[3] K. J. H. Phillips, F. P. Keenan, L. K. Harra, S. M. McCann, E. Rachlew-Kallne, J. E Rice and M. Wilson, Journal of Physics B: Atomic, Molecular and Optical Physics **27** 10 (1994).

[4] A. J. H. Donne et al., Nucl. Fusion **47** S337 (2007).

[5] D. E. Salhi, H. Jelassi, Canadian Journal of Physics, **96** 3 (2018).

[6] D. E. Salhi, P. Quinet, H. Jelassi, Atomic Data and Nuclear Data Tables (Accepted).

Ultracold and ultrafast: Strong-field ionization of trapped alkali atoms

P. Wessels[1,2], **B. Ruff**[1,2], **T. Kroker**[1,2], **A. K. Kazansky**[3,4,5], **N. M. Kabachnik**[1,5,6], **K. Sengstock**[1,2], **M. Drescher**[1,2], **and J. Simonet**[2]

[1] *The Hamburg Centre for Ultrafast Imaging, 22761 Hamburg, Germany*

[2] *Center for Optical Quantum Technologies, University of Hamburg, 22761 Hamburg, Germany*

[3] *Departamento de Fisica de Materiales, UPV/EHU, 20018 San Sebastian/Donostia, Spain*

[4] *Ikerbasque, Basque Foundation for Science, 48011 Bilbao, Spain*

[5] *Donostia International Physics Center (DIPC), 20018 San Sebastian/Donostia, Spain*

[6] *Skobeltsyn Institute of Nuclear Physics, Lomonosov Moscow State University, Moscow 119991, Russia*

e-mail: *pwessels@physnet.uni-hamburg.de*

Charged particles in ultracold atomic ensembles offer appealing possibilities for fundamental research as well as advanced applications. For example, hybrid atom-ion quantum systems benefit from long-range Coulomb interactions and are promising candidates for a quantum information platform. Ultrashort laser pulses allow creating cold ions and electrons instantaneously. However, it is essential to understand the nature of this ionization process in detail since the subsequent dynamics strongly depend on the dominating ionization mechanism. A quantitative comparison between experimental data and theoretical models is notoriously difficult to achieve due to the nonlinearity in strong-field ionization.

The Keldysh parameter $\gamma = \sqrt{E_\mathrm{I}/(2U_\mathrm{p})}$ compares the binding energy of the electron E_I to the ponderomotive potential U_p and classifies the ionization regime into multiphoton ionization for large Keldysh parameters ($\gamma \gg 1$) and tunnel ionization for small Keldysh parameters ($\gamma \ll 1$). So far, experiments accessing the strong-field regime with alkali atoms have revealed that these commonly used models cannot be applied *a priori* which makes employing *ab-initio* calculations by solving the time-dependent Schrödinger equation (TDSE) inevitable.

In order to investigate the strong-field ionization of alkali atoms quantitatively, we take advantage of optically trapped ultracold atomic clouds. We use ground state ^{87}Rb atoms at temperatures of 100 nK, well beyond the temperatures achieved by laser cooling. As illustrated in Fig. 1, the cloud of ultracold atoms is exposed to a single femtosecond laser pulse in the intensity range between 1×10^{11} and 4×10^{13} W cm^{-2}. The pulse ionizes atoms in the center of the cloud and we measure the resulting atomic density by absorption imaging. Because the motion of the atoms is negligible at nanokelvin temperatures, regions of locally reduced atomic densities relate to *absolute* ionization probabilities [1]. The experimental data are in perfect agreement with TDSE calculations without any free parameters, both, for a nonresonant ionization process at 511 nm and resonant ionization at 1022 nm wavelength.

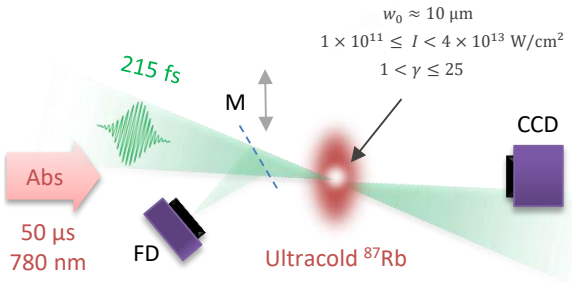


Figure 1: Probing strong-field ionization with ultracold atoms. A single femtosecond laser pulse is focused onto a cloud of ^{87}Rb atoms at nanokelvin temperatures. The remaining atomic density is measured by resonant absorption imaging, giving direct access to spatially resolved ionization losses. Additionally, the pulse energy as well as the focal intensity distribution are measured for calibrated peak intensities.

Our technique is precise enough to disclose subtle effects so that we can test commonly used strong-field ionization models. A multiphoton model based on lowest order perturbation theory agrees surprisingly well with our results, although such an agreement cannot be expected by default because the Keldysh parameter as well as the ionization probability are both close to unity. Furthermore, we find that including tunnel ionization losses within the Ammosov-Delone-Krainov (ADK) model clearly overestimate the observed ionization yield. This is indeed expected as ADK theory is strictly valid only for Keldysh parameters much smaller than unity ($\gamma \ll 1$) which means that the modification of the Coulomb barrier of the atom can *not* be regarded as adiabatic. Moreover, this renders the concepts of an over-the-barrier ionization intensity not applicable for alkali atoms.

We also present recent experimental progress on a spatially resolved detection of charged particles created out of quantum degenerate Bose-Einstein condensates and discuss future opportunities.

[1] P. Wessels, B. Ruff, T. Kroker, A. K. Kazansky, N. M. Kabachnik, K. Sengstock, M. Drescher, and J. Simonet, arXiv:1711.01875 (2018).

Extracting spectroscopic molecular parameters from short pulse photo-electron angular distributions

M. Telmini[1], **R. Chamakhi**[1], **R. Puthumpally-Joseph**[2], **and E. Charron**[3]

[1] *LSAMA, Department of Physics, Faculty of Science of Tunis, University of Tunis El Manar, 2092 Tunis, Tunisia*

[2] *Laboratoire Interdisciplinaire Carnot de Bourgogne, CNRS, Universite Bourgogne Franche-Comte, BP 47870, 21078 Dijon, France*

[3] *Institut des Sciences Moleculaires d'Orsay, CNRS, Univ. Paris-Sud, Universite Paris-Saclay, 91405 Orsay, France*

e-mail: *mourad.telmini@gmail.com*

Using a quantum wave packet simulation including the nuclear and electronic degrees of freedom, we investigate the femtosecond and picosecond energy- and angle-resolved photoelectron spectra of the E($^1\Sigma_g^+$) electronic state of Li_2. We find that the angular distributions of the emitted photoelectrons depend strongly on the pulse duration in the regime of ultrashort laser pulses.

This effect is illustrated by the extraction of a time-dependent asymmetry parameter whose variation with pulse duration can be explained by an incoherent average over different ion rotational quantum numbers. We then derive for the variation of the asymmetry parameter a simple analytical formula, which can be used to extract the asymptotic CW asymmetry parameters of individual transitions from measurements performed with ultra-short pulses.

The differential ionization probability can be written as

$$P(E,\theta) \propto \left[1 + \beta(\tau)\, P_2(cos\theta)\right] \qquad (1)$$

for an arbitrary pulse duration τ, where $\beta(\tau)$ is given by a weighted average of the CW β-values of the different individual exit channels N^+

$$\beta(\tau) = \frac{\sum_j \mu_j^2\, \tilde{f}_j\, \beta_j}{\sum_j \mu_j^2\, \tilde{f}_j}\,. \qquad (2)$$

where μ_j and $\tilde{f}_j$ denotes the dipole moments and the field amplitude at the frequency corresponding to the energy of the exit channel number j, respectively.

Indeed, with a limited number of measurements performed with very short laser pulses, it is possible to extract accurate values of some spectroscopic molecular parameters such as the asymmetry parameters of the different exit channels, thanks to the simplicity of Eq. (2) and therefore to the efficiency of the associated numerical fit.

For example, using the 5 values of β shown with green symbols in Fig 1 for $\tau = 4.5$ ps (on the left of the dashed vertical line), we obtained $\beta_0 = 0.2099$ instead of 0.2 (error $< 5\%$), $\beta_2 = 1.897$ instead of 1.9 (error $< 1\%$) and $\beta_4 = 0.2075$ (error $< 4\%$) instead of 0.2 for the initial state $N = 2$. For these very short pulses the rotation is not yet resolved in the kinetic energy spectrum, which shows a single broad peak (see poster for details). Indeed, for such ultrashort pulses, the pulse duration is smaller than the rotational period of both the neutral molecule and the ion.

The numerical values obtained with this fitting procedure for the relative electric dipole moments μ_j^2 are also correct within 5%.

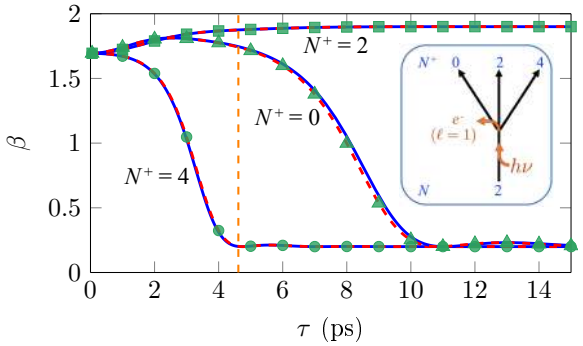


Figure 1: Asymmetry parameter $\tau = 50$ fs to $\tau = 15 =$ ps for the three peaks corresponding to $N^+ = 0$ ($E =$ 4674 cm^{-1}) , $N^+ = 2$ ($E = 4671$ cm^{-1}), and $N^+ = 4$ ($E = 4664$cm^{-1}). It includes the quantum simulation with green symbols and 2 curves: one for the analytical model with the exact parameters (solid blue lines) and one for the numerical fit (red dashed lines). The inset shows the three accessible ionization pathways in competition.

[1] R. Chamakhi, R. Puthumpally-Joseph, M. Telmini and E. Charron, J. Chem. Phys. **147**, 144304 (2017).

[2] E. Charron and M. Raoult, Phys. Rev. A **74**, 033407 (2006).

Wave packet motion analysis on the role of excited states in the multiphoton ionization

Shih-Da Jheng and T. F. Jiang
Institute of Physics, National Chiao-Tung University, 30010 Hsinchu, Taiwan
e-mail: *starr.py95g@nctu.edu.tw and tfjiang@nctu.edu.tw*

An electron of an atom can be ionized via multiphoton process in the strong laser field. The energy of the photoelectron can be estimated by the well-known rule : $E_k = n\hbar\omega - I_p - U_p$, where ω is the laser frequency, I_p is the ionization potential and U_p is the ponderomotive energy. The transition pathways can also be distinguished by selection rule. However, it is not easy to predict the ionization yield due to the existence of the excited states. The ionization yield can be enhanced or suppressed when the excited states are resonantly coupled during pulse time. Even if the resonance condition doesn't meet, the bound electron wave packet displays different motion in different laser wavelength region due to ac Stark effect and thus can also lead to different effect on the ionization yield [1]. These findings indicate there should be a competition between the components of the bound electron wave packet motion resulting from excited states induced by ac Stark effect and by resonantly coupling.

In this work, we numerically study the time dependent Schrödinger equation (TDSE) of a lithium atom interacting with the intense ultrashort laser pulse. By analysis of the bound electron wave packet motion caused by each excited states, we can provide pictures the role the excited states play in the multiphoton ionization process.

[1] Shih-Da Jheng and T. F. Jiang, J. Phys. B **50**, 195001 (2017).

Strong field approximation model for frustrated tunneling ionization and subsequent free induction decay

J. H. Mun[1], **I. A. Ivanov**[1], **Y. Hyeok**[1], **and K. T. Kim**[1,2]
[1] *Center for Relativistic Laser Science, Institute for Basic Science, Gwangju 61005, Korea*
[2] *Dept. of Physics and Photon Science,*
Gwangju Institute of Science and Technology, Gwangju 61005, Korea
e-mail: *mun1219@ibs.re.kr*

An atom or molecule can be excited in a strong laser field through tunneling. This process is known as frustrated tunneling ionization (FTI) [1]. Several theoretical approaches have been developed to describe the FTI process [1, 2]. These studies have focused on investigating the population in the excited states after the interaction with the strong laser field. In the present work, we focus our attention on the phase of the excited states. In order to describe the FTI process, we develop a quantum mechanical model. The strong field approximation (SFA) model developed by Lewenstein *et al.* [3] is extended to describe the FTI process. In our approach, we consider the ground and excited states of an atom in the strong laser field. The analytic expression for the transition from the ground to the excited states via the continuum states is derived.

A coherent extreme ultraviolet radiation can be emitted through free induction decay (FID) when an atom is coherently excited [6]. The FID radiation emitted from the atom excited through FTI has recently been observed [5], which we call the FTI emission. It is found that phase of the FTI emission is determined by the action of an electron accumulated during the excursion in the continuum states. We applied the attosecond lighthouse method [7] to investigate a spatial characteristics of the FTI emission. The FTI emissions calculated from an array of atoms distributed along the transverse direction with respect to the propagation direction of a laser beam is obtained using our SFA and the TDSE models as shown in Fig. 1. The Gaussian laser beams with (b) and without (a) a spatial chirp are compared in Fig. 1. The results from our SFA and the TDSE models are in a good agreement, supporting the validity of our SFA model.

The FTI process is one of the vital elements in understanding ultrafast electron dynamics in the strong laser field. Our SFA model provides an analytic expression that describes the transition from the ground state to the excited state via the continuum states within the duration of the laser pulse. Therefore, our approach would also be useful to study the excitation dynamics of atoms and molecules. In addition, the FTI emission would be useful as a new EUV source for imaging and lithography applications [5]. Since our extended SFA model provides an efficient, numerical-cost-effective method for describing the FTI, it could be applied for studying the phase matching and spatio-temporal coupling of the FTI emission.

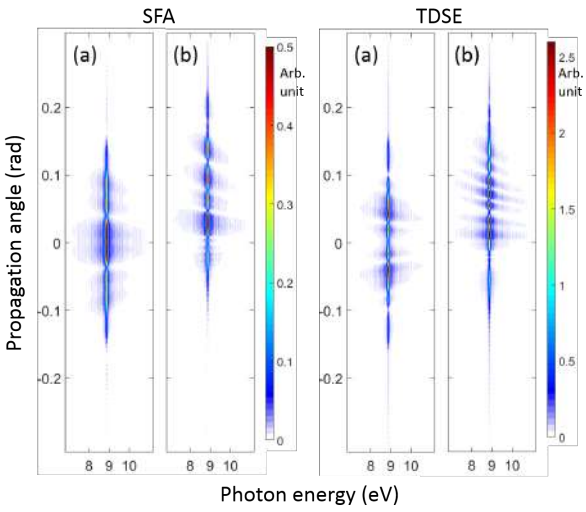


Figure 1: The far field profile of the FTI emission.

[1] T. Nubbemeyer, K. Gorling, A. Saenz, U. Eichmann, and W. Sandner, Phys. Rev. Lett. **101**, 233001 (2008).

[2] S. V. Popruzhenko, J. Phys. B At. Mol. Opt. Phys. **51**, 014002 (2018).

[3] M. Lewenstein, Ph. Balcou, M. Yu. Ivanov, Anne LHuillier, and P. B. Corkum, Phys. Rev. A **49**, 2117 (1994).

[4] G. L. Yudin and M. Y. Ivanov, Phys. Rev. A **64**, 013409 (2001).

[5] Y. Hyeok, J. H. Mun, S. I. Hwang, S. B. Park, I. A. Ivanov, C. H. Nam, and K. T. Kim (submitted)

[6] S. Beaulieu, E. Bloch, L. Barreau, A. Comby, D. Descamps, R. Gneaux, F. Lgar, S. Petit, and Y. Mairesse, Phys. Rev. A **95**, 041401 (2017).

[7] K. T. Kim, C. Zhang, T. Ruchon, J.-F. Hergott, T. Auguste, D. M. Villeneuve, P. B. Corkum, and F. Qur, Nat. Photonics **7**, 651 (2013).

Angle resolved photodetachment time delay

S. Saha[1], A. Mandal[2], P. C. Deshmukh[2,3], A. S. Kheifets[4], V. K. Dolmatov[5], and S. T. Manson[6]

[1] *Department of Physics, Indian Institute of Technology Madras, 600036 Chennai, India*
[2] *Department of Physics, Indian Institute of Science Education and Research Tirupati, 517507 Tirupati, India*
[3] *Department of Physics, Indian Institute of Technology Tirupati, 517506 Tirupati, India*
[4] *Research School of Physics and Engineering, The Australian National University, 0200 Canberra ACT, Australia*
[5] *Department of Earth Science, University of Northern Alabama, 35632 Florence, USA*
[6] *Department of Physics and Astronomy, Georgia State University, 30303 Atlanta, USA*
e-mail: *soumyajit147@gmail.com*

Advanced experimental techniques and theoretical tools enabled us to study the electron dynamics in their real time domain inside the atom over the last decade [1, 2, 3, 4]. Time delay measurement in atomic photoionization has gained enormous popularity as a probe in this particular study. In photodetachment process the negative ion gets neutralized upon the irradiation of photon pulse, results in absence of the long Coulomb tail in phase of the photoelectron. This helps in studying the time delay induced by the centrifugal barrier shape resonance [5, 6]. The time delay study in the region of shape resonance is expected to be a probe towards a complete analysis of shape resonance. The photoionization, in general, is anisotropic in nature and the delay in this process has a strong dependence on the angle between the momentum direction of the photoelectron and the laser polarization direction [7, 8]. In present work we study the photodetachment time delay for different angles, relative to the incident pulse polarization for Cl^- and Tm^- in the region of shape resonance. The delay has been studied for outer $np \rightarrow \varepsilon$d in Cl^- and outer nf$\rightarrow \varepsilon$g in Tm^-. The comparison has also been made with the results of their corresponding isoelectronic neutrals which are Ar (isoelectronic to Cl^-) and Yb (isoelectronic to Tm^-) respectively. Relativistic random phase approximation (RRPA) has been employed to do the calculations [9]. Tm^- is heavier ion and we expect to see significant relativistic effects in it compare to the results of Cl^-.

References

[1] M. Schultze et al., Science **328**, 1658 (2010).

[2] K. Klünder et al., Phys. Rev. Lett. **106**, 143002 (2011). (2010).

[3] A. S. Kheifets and I. A. Ivanov, Phys. Rev. Lett. **105**, 23 (2010).

[4] L. R. Moore et al., Phys. Rev. A **84**, 061404(R) (2011).

[5] S. Saha et al, BAPS **61 (8)**, 53 (2016).

[6] E. Lindroth and J. M. Dahlström, Phys. Rev. A **96**, 013420 (2017).

[7] J. Wätzel et al, J. Phys. B **48**, 025602 (2015).

[8] A. Mandal et al, Phys. Rev. A **96**, 053407 (2017).

[9] W. R. Johnson and C. D. Lin, Phys. Rev. A **20**, 964 (1979).

Interferences in photoelectron spectra - Holographic structures

S. D. López[1] **and D. G. Arbó** [1]

[1] *Institute for Astronomy and Space Physics, IAFE (CONICET-UBA), 1428 Buenos Aires, Argentina*
e-mail: *sebastlop@iafe.uba.ar*

When an intense short laser pulse interacts with an atom ionizing it, the photoelectron spectra present several structures that can be understood as double slit interferences in the time domain, namely intra- and inter-cycle interferences [1]. This type of structures are formed by electrons that emerge from the atom and follows directly to detector. There is another type of structures that requires interference of former direct electrons with other that interact with the parent core. In a classical picture, the latter returns to the parent ion driven by the laser field and rescatters off to the detector. It is well known that a short range potential is sufficient to understand the rescattering rings at high energy, formed by very hard interaction among electron and ion [2]. Other structures can be explained only when long range coulombic interactions take place. This type of structures can be interpreted as holograms, i.e. the interference pattern between the direct (reference) and the rescattered (signal beam) electrons. In this way, the information of the interaction is encoded in the interference pattern between the reference and the signal [3].

In this work we present a theoretical analysis of interferences using a numerical solution of the time dependent Schrödinger equation (TDSE) and semiclassical approaches, namely, quantum trajectory monte carlo (QTMC) and the semiclassical two step model (SCTS) [4]. We analyze the ionization of atomic hydrogen to characterize the role that the long range Coulomb interaction plays in the holographic stuctures. Particularly, we focus our analysis for very few cycle laser pulses allowing ionization in some parts, to turn on and off different kind of interferences. With semiclassical approaches we can examinate the trajectories that lead to different final conditions and get a deeper understanding of the electron kinematics associated to holographic structures.

In addition, by using short-range potentials as Yukawa potentials, we studied the effects of the Coulomb tail, and the screening parameter on the holographic structures. This allows us to interpret the electronic distribution as the dispersion of an electron wavepacket that crosses the region of interaction, and to establish relations with the shape of the potential.

We show in Figure 1 photoelectron distributions as function of parallel k_z and perpendicular k_x momentum to polarization axis calculated with SCTS model (upper pannel) and the TDSE (lower pannel). All the magnitudes are in atomic units. We observe interference patterns resembling a dispersion of an electron wave packet from a potential centered in the origin in both calculations.

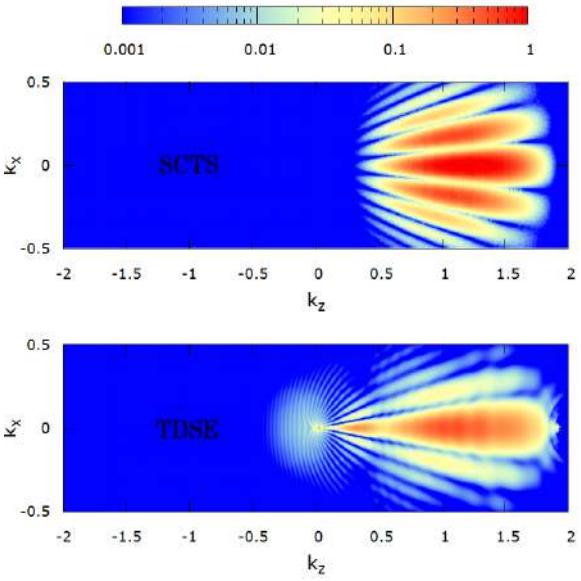


Figure 1: Photoelectron momentum distribution for ionization of atomic hydrogen by a short laser pulse of frequency ω=0.0575 a.u. and electric field amplitude F_0=0.05 a.u. calculated within the SCTS model for a single period laser pulse for SCTS (upper figure) and TDSE (lower figure).

This work was supported by the by CONICET (PIP100386) and ANPCYT (PICT-2016-0296 and PICT-2016-3029).

[1] Arbó, D. G., Ishikawa, K. L., Schiessl, K., Persson, E., and Burgdörfer, J. Phys. Rev. A **81**, 81, 021403 (2010)

[2] Lewenstein, M., Kulander, K. C., Schafer, K. J., and Bucksbaum, P. H., Phys. Rev. A **51**, 1495, (1995)

[3] Huismans, Y., Rouzée, A., Gijsbertsen, A., et al., Science,**331**, 61 (2011)

[4] Shvetsov-Shilovski, N. et al., Phys. Rev. A, **94**, 013415 (2016)

Time delays in $(\omega, 2\omega)$ above threshold ionization

S. D. López[1], **S. Donsa**[2], **S. Nagele**[2], **D. G. Arbó** [1] **and J. Burgdörfer**[2]

[1] *Institute for Astronomy and Space Physics, IAFE (CONICET-UBA), 1428 Buenos Aires, Argentina*

[2] *Institute for Theoretical Physics, Vienna University of Technology, Vienna, Austria, EU*

e-mail: *sebastlop@iafe.uba.ar*

Experiments employing either attosecond streaking or the complementary interferometric RABBIT technique have allowed to study photoemission from rare gas atoms and surfaces in the time-domain with attosecond precision. The experimental progress has triggered considerable theoretical efforts to understand photoionization from a time-dependent perspective (see [1] and references therein).

The experiment in atomic ionization by two-color $(\omega, 2\omega)$ lasers by Zipp *et al.* [2] has revealed that a pump-probe scheme can be used to characterize time delays in the emission of electrons in the above-threshold ionization regime for visible frequency of the pump. In this work, we perform a theoretical analysis of the time delays in Ar ionization by two-color laser for a typically $(\omega, 2\omega)$ configuration of Ti:sapphire laser (800 nm). To shed more light in ionization process we perform simulations with the time dependent Schrödinger equation and compare this results with the strong field and Coulomb-Volkov approximations. We find that time delays depend on the definition from electron momentum distributions. Besides, we also find a large discrepancy between the results predicted by the strong field approximation (zero delay for sidebands) and numerical solutions of time-dependent Schrödinger equation at the highest simulation energies. We also find that the strong assumption of additive time delays adopted in streaking or RABBITT techniques [3] needs to be revisited when applied to the case of $(\omega, 2\omega)$ lasers due to the multiplicity of coherent quantum paths leading to a final multiphoton peak. Finally, we explore simpler quantum paths to get a better understanding of the process. For this purpose we use Yukawa potentials fitting the electron binding energy to allow the absorption of a desired number of photons to reach the continuum. This analysis paves the way to understand the process and the time delays asociated to each path.

As an example, we show in Fig. 1 time delays obtained from asymmetries and forward emission, considering integrations over $\pm$z hemispheres. This is done for a single energy calculated from energy conservation, or by integrating in energy around the peak.

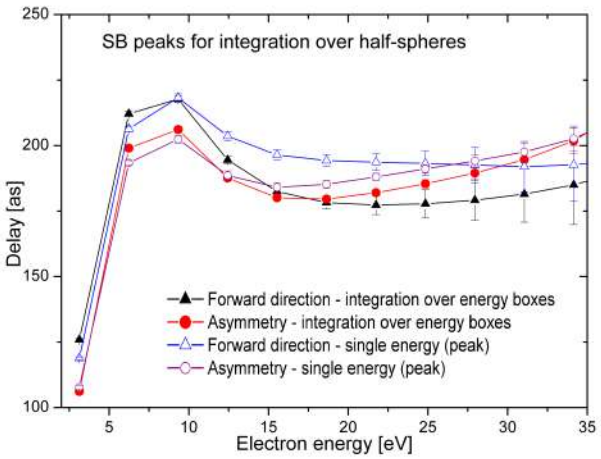


Figure 1: Delays calculated as a function of the emission energy for sidebands within the TDSE. The delays are calculated for forward emission (triangles) and asymmetry (circles). The calculations were performed integrating around peak energy (solid symbols) or considering only the peak energy (open symbols). The 2ω component intensity is 8×10^{13} W/cm^2 and the ω component is 4×10^{11} W/cm^2.

This work was supported by the FWF-Austria (SFB NEXTLITE, SFB VICOM), by CONICET (PIP100386), by ANPCYT (PICT-2016-0296 and PICT-2016-3029), by the OeAD (WTZ AR 03/2013), by the NSF through XSEDE resources (TG-PHY090031), and through computational resources at the Vienna Scientific Cluster (VSC).

[1] R. Pazourek, S. Nagele, and J. Burgdörfer, Rev. of Mod. Phys., **(2015)**, 87, 765 .

[2] L. J. Zipp, A. Natan, and P. H. Bucksbaum, Optica, **(2014)** 1, 361-364.

[3] J. Feist, O. Zatsarinny, S. Nagele, R. Pazourek, J. Burgdörfer, X. Guan, K. Bartschat and B. I. Schneider, Phys. Rev. A, **(2014)**, 89, 033417.

Theoretical modeling of the high-harmonic generation and ionization processes with a discrete representation of the continuum

P. Gniewek[1], **M. Jabłczyńska**[1], **M. Szczygieł**[1], **M. Lesiuk**[1], **D. K. Efimov**[2], **J. Zakrzewski**[2], **M. Lewenstein**[3], **R. Moszyński**[1]

[1] *Faculty of Chemistry, University of Warsaw, Pasteura 1, 02-093 Warsaw, Poland*

[2] *M. Smoluchowski Institute of Physics, Jagiellonian University, Łojasiewicza 11, 30-348 Kraków, Poland*

[3] *ICFO, The Barcelona Institute of Science and Technology, 08860 Castelldefels, Spain*

e-mail: *pgniewek@tiger.chem.uw.edu.pl*

1 Introduction

Theoretical description of processes in strong laser fields involves electrons occupying continuum states. Incorporation of continuum functions into a discrete basis set is still a considerable challenge [1]. To solve this problem we propose a new basis set composed of plane waves multiplied by Gaussian-type orbitals (GTOs). Our method is tested on the H and He atoms and can be straightforwardly extended to multielectron systems. We present comparisons with grid-based TDSE solutions in the QPROP code[2].

2 Basis set for the continuum

We base our description of the continuum on the Coulomb wave functions, which can be written as

$$\frac{e^{ik\cdot r}}{(2\pi)^{3/2}} \underbrace{\sum_l \mathcal{O}_l(k,r) \sum_m \mathcal{Z}^*_{lm}(k)\mathcal{Z}_{lm}(r)}_{\mathcal{O}(k,r)}, \qquad (1)$$

where $\mathcal{Z}_{lm}(r)$ are the regular solid harmonics. $\mathcal{O}(k,r)$ is the so-called overdrive function, which can be efficiently fitted by GTOs.

3 HHG and ionization of the hydrogen atom

The H atom in the laser field is governed by

$$\begin{aligned} i\frac{\partial\Psi(t)}{\partial t} &= \left(\hat{H}_0 + \hat{V}(t)\right)\Psi(t) \\ &= \left(-\frac{\nabla^2}{2} - \frac{1}{r} - iA(t)\frac{\partial}{\partial z}\right)\Psi(t), \end{aligned} \qquad (2)$$

where $\hat{H}_0$ is the time-independent Hamiltonian, $\hat{V}(t)$ is the interaction operator, and $A(t)e_z$ is the vector potential. Ionization is addressed by placing a complex absorbing potential (CAP) far enough from the nucleus [3]. The TDSE is solved by expanding $\Psi(t)$ into a linear combination of ψ_k, the ground and excited states of H_0. The latter are, in turn, assembled from a finite set of basis PW-GTO functions, χ_j:

$$\Psi(t) = \sum_{k=0} c_k(t)\psi_k, \qquad \psi_k = \sum_j d_{jk}\chi_j. \qquad (3)$$

The time evolution of $c(t)$ is given by

$$c(t+\Delta t) = e^{-i[H_0+V(t)]\Delta t}c(t). \qquad (4)$$

The exponential is calculated using the split operator technique. The HHG spectrum is extracted from the Fourier transform of the time-dependent dipole moment.

4 HHG of the helium atom

For the He atom H_0 and $V(t)$ are given by

$$\begin{aligned} H_0 &= -\frac{\nabla_1^2}{2} - \frac{\nabla_2^2}{2} - \frac{2}{r_1} - \frac{2}{r_2} + \frac{1}{r_{12}}, \\ V(t) &= -(z_1+z_2)E(t). \end{aligned} \qquad (5)$$

To solve the TDSE with the above operators we use the full configuration interaction (FCI) method, which is a standard approach of quantum chemistry and consists in the expansion of $\Psi(t)$ into antisymmetrized products of basis functions χ_j:

$$\psi_i = \sum_{j,k} d_{ijk}\big[\chi_j(\mathbf{r}_1)\chi_k(\mathbf{r}_2) + \chi_k(\mathbf{r}_1)\chi_j(\mathbf{r}_2)\big]. \qquad (6)$$

We use the highly-optimized He orbitals of Ref. [4] and PW-GTOs as the basis functions χ_j.

References

[1] E. Coccia *et al.*, Int. J. Quant. Chem. **116**, 1120 (2016).

[2] D. Bauer and P. Koval, Comput. Phys. Commun. **174**, 396 (2006).

[3] P. Krause *et al.*, J. Chem. Phys. **140**, 174113 (2014).

[4] W. Cencek*et al.*, J. Chem. Phys. **136**, 224303 (2012).

Multi-photon spectroscopy of the many-electron atoms and ions in a laser field with accounting for the Debye plasma effects

E. Ternovsky[2], **V. Buyadzhi**[1,2], *A.Glushkov*[1,2], *andO.Khetselius*[1,2]

[1] *Int. Research Centre for Quantum Optics and Laser Phys., Odessa State Environmental University, 65016 Odessa, Ukraine*

[2] *Departament of Applied Mathematics, Odessa State Environmental University, 65016 Odessa, Ukraine*

e-mail: *ternovskyev@gmail.com*

Besides, in our work we used generalized energy approach (EA) combined with the relativistic many-body perturbation theory [1,2] to studying spectroscopic parameters (the collision cross-sections, collision strengths, oscillators strengths) of the few-body atomic systems (ions) in plasmas with taking into account of a shielding effect (in a Debye shielding approximation) and inter-particle correlations within many-body perturbation theory. IA great number of physically different effects occur in atomic systems (ensembles) in dependence upon a intensity, frequency, multi-colority of laser field, energy spectrum structure of an atomic system etc. In the last decade a considerable interest has attracted studying of the elementary atomic processes in plasma environments because of the plasma screening effect on the plasma-embedded atomic systems. In this paper one-and two-color multi-photon spectroscopy of a number of transitions in a hydrogen, lithium and caesium atoms and ions (free and immersed in a Debye plasmas) is studied theoretically. The theoretical approach is based on the relativistic operator perturbation theory (PT) and relativistic energy approach [1,2]. The energy shift and width of the multiphoton resonances are calculated within an energy approach, which is based on the Gell-Mann and Low adiabatic formalism [2]. The plasmas medium effects are taken into account by introducing the Yukawa-type electron-nuclear attraction and electron-electron repulsion potentials into the electronic Hamiltonian for N-electron atom (ion) in a plasma [3]. There is studied a plasmas with typical corresponding parameters: the Debye lengths l=5a.u. (solar core: temperature T=10(7)K; density 10(32) 1/m(3)) and 25 a.u. (inertial confinement: temperature T=10(4)K; density 10(28) 1/m(3)) . It has been quantitatively determined a variation of the multi-photon resonance enhancement frequencies in dependence upon the plasmas parameters (the Debye length). For example, the corresponding values for the resonance enhancement frequencies r1, r2 and r3 for the 1s4f transition in the hydrogen for different Debye lengths (l=5-50 a.u.) are between 0.009 and 0.023a.u. The H-plasma data are compared with available other data [2]. We carried out a studying the transition energies, oscillators strengths, collision cross-sections for a number of low lying (incl. Rydberg) transitions in spectra of the -like ions with charge of a nucleus Z=26,36 and plasma parameters ne = 1022-1024cm^{-3}, T=0.5-2keV. A part of the data has been firstly presented. To test the results of calculations we have compared the obtained data for some Be-like ions with other alternative data by Li et al, Saha-Frische and others [2]. In table 1 we list the data of computing the energy shifts dE (cm^{-1}) for $2s^2 - [2s_{1/2}2p_{1/2,3/3}]1$ transitions.

Table 1. Energy shifts dE (cm^{-1}) for $2s^2 - [2s_{1/2}2p_{3/2}]1$ transition in spectra of the Be-like Ni for different values of ne (cm^{-3}), T (in keV)

Z	n_ekT	10^{22} Li et al	10^{24} Li et al	10^{22} Our data	10^{24} Our data
Ni^{24+}	0.5	31.3	2639.6	33.8	2655.4
	1.0	23.4	2030.6	25.7	2046.1
	2.0	18.0	1597.1	20.1	1612.5

[1] A. Glushkov, and L. Ivanov, Phys. Lett. A **170**, 33 (1992)

[2] Y. Li, J. Wu et al., J. Phys. B 41, 145002 (2008); S. Malinovskaya et al., IJQC. 111, 288 (2011).

[3] S. Malinovskaya, A. Glushkov, O. Khetselius, et al, Int.J.Quant.Chem. **111**, 288 (2011)

[4] S. Paul, and Y.K. Ho, J. Phys. B **43**, 065701 (2010)

Strong field three electron ionization - ab initio time-dependent study

Jan H. Thiede[1], Bruno Eckhardt[1], Dmitry K. Efimov[2], Jakub S. Prauzner-Bechcicki[1], and Jakub Zakrzewski[2]

[1] *Fachbereich Physik, Philipps-Universitat Marburg, Germany*

[2] *Instytut Fizyki im. Mariana Smoluchowskiego, Uniwersytet Jagiellonski, Krakow, Poland*

e-mail: *jakub.zakrzewski@uj.edu.pl*

We provide a first full *ab initio* quantum mechanical analysis of triple ionization for optical frequencies within the reduced dimensionality scheme. We analyse time-dynamics for two-cycle pulses and identify major ionization paths. The ionization yields obtained agree qualitatively with experimental results for Ne (with volume averaging). An appropriate Slater-like initial state allows us to identify spin resolved ionization channels.

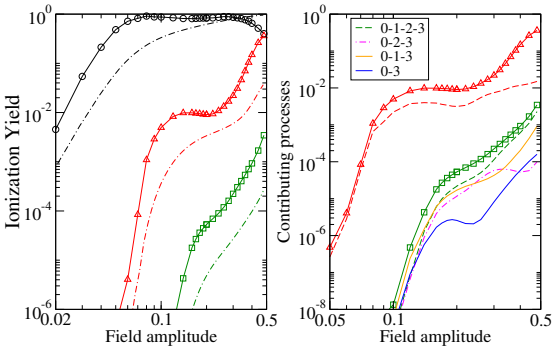


Figure 1: Ionization yields for a two-cycle pulse. Left panel: total yields for single ionization (SI, black circles), double ionization (DI, red triangles) and triple ionization (TI, green squares). The continuous lines are from the model, dash-dotted lines after integration over a Gaussian beam. SI saturates over a wide range of field strengths and DI shows a pronounced knee structure, TI a weak one. Right panel: Different contributions to DI and TI. The red dashed lines show the NSDI contribution to DI, which is overtaken by sequential processes for higher intensities. The legend identifies four contributions to TI, with the sequential process being the dominant and direct TI the weakest contribution, after [3].

Due to computer limitations grid-based method of *ab initio* strong-field ionization studies are typically limited to two active electron models. Here we report a simulation of the dynamics of triple ionization within the restricted dimensions (one degree of freedom per active electron). Instead of the Rochester model, we consider the "saddle-based" Hamiltonian coming from the classical dynamics analysis [1]:

$$H = \sum_{i=1}^{3} \frac{p_i^2}{2} + V(r_1, r_2, r_3) \qquad (1)$$

with

$$V(r_1, r_2, r_3) = -\sum_{i=1}^{3} \left(\frac{3}{\sqrt{r_i^2 + \epsilon}} + \sqrt{\frac{2}{3}} F(t) r_i \right) + \sum_{i,j=1 i<j}^{3} \frac{1}{\sqrt{(r_i - r_j)^2 + r_i r_j + \epsilon}} \qquad (2)$$

where a smoothing parameter $\epsilon = 0.83$ allows us to match the ionization potential for Ne. The initial state is taken as a Slater determinant with two electrons with spin up and the remaining one with spin down [2]. The time-dependent Schrödinger equation is solved on a spatial, equally spaced grid in three dimensions with Hamiltonian (1) by a standard FFT (split-operator) technique in an efficiently parallelized way (the same code yields the ground state by imaginary time propagation). By division of the configuration space into different sectors we identify regions for singly, doubly and triply ionized species. The resulting yields for two-cycle "$\sin^2$" pulse are depicted in Fig. 1. Not only the total yields or ionization paths can be identified - time dynamics analysis allows us to define spin-dependent rates, providing e.g. the information that after a single ionization the ion is predominantly left in a singlet state. For most interesting triple ionization event the sequential process dominates for strongest fields shown. For smaller fields otherprocesses takeover (see Fig. 1).

The ionization details strongly depend on the carrier pulse envelope (CPA, not shown) a behavior expected for very short pulses under study. Similarly we observe a significant variation with CPA of the harmonic sygnal generated during illuminating by laser pulse. Work supported by National Science Center (Poland) grant Symfonia 2016/20/W/ST4/00314.

[1] K. Sacha and B. Eckhardt, Phys. Rev. A 64, 053401 (2001).

[2] C. Ruiz, L. Plaja, and L. Roso, Phys. Rev. Lett. 94, 063002 (2005).

[3] J. H. Thiede, B. Eckhardt, D. K. Efimov, J. S. Prauzner-Bechcicki, and J. Zakrzewski, arXiv:1804.05773.

Laser Electron-Gamma-Nuclear Spectroscopy of Atoms and Multicharged Ions: Shake-Up and NEET Effects

O. Khetselius[2], **A. Glushkov**[1,2], **E. Ternovsky**[1,2], **V. Buyadzhi**[2]

[1] *Int. Research Centre for Quantum Optics and Laser Phys., Odessa State Environmental University, 65016 Odessa, Ukraine*

[2] *Departament of Applied Mathematics, Odessa State Environmental University, 65016 Odessa, Ukraine*

e-mail: *okhetsel@gmail.com*

A new class of problems has been arisen and connected with modelling the cooperative laser-electron-nuclear phenomena such as the electron shell shake-up and NEET or NEEC (nuclear excitation by electron transition or capture) effects in heavy neutral atomic/nuclear systems [1-5]. Though the shake-up effects in the neutral atoms (molecules) are quite weak (because of the weak coupling of the electron and nuclear degrees of freedom), the possibilities of their realization significantly change in a case of the multicharged ions (MCI). We present consistent, relativistic computational approach to calculation of the probabilities of the different cooperative laser electron-gamma-nuclear processes in the MCI (including the characteristics of the electron satellites in gamma-spectra of nuclei of the multicharged ions and the resonant NEET (NEEC) effects in heavy nuclei of MCI). The theory is based on the relativistic energy approach (S-matrix formalism of Gell-Mann and Low) and relativistic many-body perturbation theory [2-4,7]. Within the energy approach, decay and excitation probability (of the electron shell shake-up process or etc) is linked with the imaginary part of energy of the excited state for the electron shell-nucleus-photon system. We firstly present new data about intensities of the electron satellites in gamma-spectra of nuclei in the neutral (low lying transitions) and O-and F-like MCI for isotopes Fe, Cs, Yb, which demonstrate an existence of an new effect of the giant increasing (up 3 orders) electron satellites intensities (electron shell shake-up probabilities) at transition from the neutral atoms to the corresponding MCI.

We develop an advanced energy approach to the NEET (NEEC) process in the heavy MCI and list values of NEET probabilities in the nuclei of the Os, Ir, U, Ag of the O-and F-like MCI. The data listed demonstrate an effect of the significant changing the corresponding NEET probabilities under transition from the neutral atomic/nuclear systems to the corresponding MCI.

[1] L.N. Ivanov, and V.S. Letokhov, JETP.**93**, 396 (1987).

[2] A. Glushkov, Progr. Theor. Chem. Phys. **26**, 231 (2013)

[3] A. Glushkov, O. Khetselius, and S. Malinovskaya, Europ. Phys. J. **T160**, 195 (2008)

[4] A. Glushkov, O. Khetselius, and S. Malinovskaya, Europ. Phys. J. **108**, 1257 (2008)

[5] E.V. Tkalya, Phys.Rev.A. **75**, 022509 (2009).

[6] A. Palffy, Z. Harman, and W. Scheid, Phys. Rev.A **73**, 012715 (2006).

[7] O.Yu. Khetselius, Int. J. Quant.Chem. **109**, 3330(2009).

The effect of intermediate continuum states on two-photon ionization cross section

A. Mihelič[1]

[1] *Jožef Stefan Institute. Jamova cesta 39, SI-1000, Ljubljana, Slovenia*

e-mail: *andrej.mihelic@ijs.si*

Ionization of atoms and molecules using coherent light sources which operate in the extreme ultraviolet (XUV) or x-ray spectral regions, such as free electron lasers (FELs) or high-order harmonic generation (HHG) sources, often involves dealing with continuum-continuum transitions: when the incident photon flux is high enough, so that the probability for multiphoton ionization becomes non-negligible, continuum states may be encountered as both intermediate and final states of the multiphoton transition process.

In this work, the effect of intermediate atomic continuum (both unstructured and resonant) on the two-photon ionization cross sections is discussed using the formalism of exterior complex scaling (ECS) [1]. A novel, modified procedure for the calculation of partial two-photon ionization amplitudes and cross sections is presented. The modified procedure relies on a few-term linear least-squares fit of radial functions pertaining to different ionization channels of the second-order scattered wave.

As has become customary in the framework of the ECS method [2, 3], the second-order scattered wave is calculated by solving a set of driven Schrödinger equations. While for photon energies above the ionization threshold, the relevant driving term depends on the scaling radius, the second-order scattered wave has been seen to be independent of the scaling parameters in the non-scaled region of space. Since this region contains the complete information on the photoionization process, the least-squares fit represents a relatively simple way to extract the ionization amplitudes in the case of single-electron ejection. The method is applied to two-photon ionization of the helium atom (Fig. 1). The calculated two-photon partial and total cross sections agree well with the results found in the literature.

Finally, using a similar procedure, it is shown that partial photoionization cross sections of an atom in an autoionizing state may be defined in a meaningful way and calculated in a relatively straightforward manner using ECS. Such photoionization cross sections may turn useful in enhanced few-parameter models (e.g., see Refs. [4, 5, 6]) describing atom-light interaction in cases where a direct solution of the time-dependent Schrödinger equation becomes prohibitively lengthy.

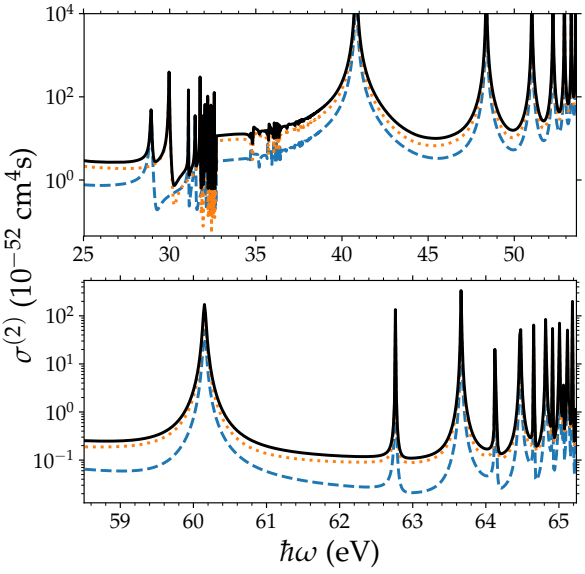


Figure 1: Top: two-photon ionization cross section of the He atom for photon energies in the region of the final $^1S^e$ and $^1D^e$ autoionizing states and core-excited resonances. Bottom: resonance-enhanced two-photon ionization cross section in the energy region of the $^1P^o$ autoionizing states below the second ionization threshold. The contributions of the $^1S^e$ and $^1D^e$ final states are plotted with a dashed blue and a dotted orange line, respectively, and their sum is plotted with a solid black line.

[1] C. W. McCurdy, F. Martín, J. Phys. B **37**, 917 (2004).

[2] D. A. Horner, F. Morales, T. N. Rescigno, F. Martín, C. W. McCurdy, Phys. Rev. A **76**, 030701 (2007).

[3] A. Palacios, T. N. Rescigno, C. W. McCurdy, Phys. Rev. A **79**, 033402 (2009).

[4] A. Jiménez-Galán, L. Argenti, F. Martín, Phys. Rev. Lett. **113**, 263001 (2014).

[5] A. Mihelič, M. Žitnik, Phys. Rev. A **91**, 063409 (2015).

[6] A. Mihelič, M. Žitnik, M. Hrast, J. Phys. B **50**, 245602 (2017).

Instantaneous ionization rate as a functional derivative

I. A. Ivanov[1], **C. Hofmann**[2], **L. Ortmann**[2], **A. S. Landsman**[2,3], **Chang Hee Nam** [1,4], **and Kyung Taec Kim**[1,4]

[1] *Center for Relativistic Laser Science, Institute for Basic Science, Gwangju 61005, Korea*

[2] *Max Planck Institute for the Physics of Complex Systems, Noethnitzer Strasse 38, 01187 Dresden, Germany*

[3] *Max Planck Center for Attosecond Science/Department of Physics, Pohang University of Science and Technology, Pohang 37673, Korea*

[4] *Department of Physics and Photon Science, GIST, Gwangju 61005, Korea*

e-mail: *igorivanov@ibs.re.kr*

The notion of the instantaneous ionization rate (IIR) proved extremely fruitful for understanding physics of tunneling ionization, the ionization regime characterized by small values of the Keldysh parameter $\gamma = \omega/E_0\sqrt{2|I|} < 1$ [1] (here ω, E_0 and I are the frequency, field strength and ionization potential of a target system expressed in atomic units). The fact that the IIR is a function which is sharply peaked near the local maxima of the electric field of the pulse underlies successful simulations of tunneling ionization phenomena, such as the classical trajectory Monte Carlo simulations (CTMC method) [2]. Recently, the temporarily localized ionization at the local maxima of the laser field has been used as a fast temporal gate to measure the laser field [3].

The notion of the ionization event occurring at a given time and, correspondingly, the notion of IIR are not free from certain ambiguity, however. We describe an approach to IIR which is based on the notion of a functional derivative.

Total ionization probability P can be considered as a functional $P[E]$ of the waveform $E(t)$. For a waveform which can be represented as $E(t) = E_f(t) + \delta E(t)$, with fundamental field $E_f(t)$ and signal field $\delta E(t)$, we can write:

$$\delta P = P[E_f + \delta E] - P[E_f] \approx \int_0^{T_1} \frac{\delta P}{\delta E_f(t)} \delta E(t) dt \ , \quad (1)$$

where the integral is calculated along the interval of the pulse duration. On the other hand, the integral on the r.h.s of Eq. (1) can be expressed as $\int_0^{T_1} \frac{dW_{\rm inst}(E_f(t))}{dE_f(t)} \delta E(t) dt$, where $W_{\rm inst}(E(t))$ is the IIR, which by definition depends on the instantaneous value $E(t)$ of the electric field. Taking into account that $\delta E(t)$ in Eq. (1) is arbitrary we can write:

$$\frac{\delta P}{\delta E_f(t)} \approx \frac{dW_{\rm inst}(E_f(t))}{dE_f(t)} \ . \quad (2)$$

The quantity on the l.h.s of this equation can be regarded as an unambiguous definition of the IIR. The definition of exact ionization rate in Eq. (1) is based on physically observable quantities: the electric field of the pulse and modulation of the total ionization probability. It is clearly gauge invariant.

We can compute the l.h.s of (2) from the solution of the time-dependent Schrödinger equation (TDSE) using a numerical procedure described in [4]. As an example we show in Figure 1 the first variation of the ionization probability and its contour lines for a single cycle pulse with carrier frequency $\omega = 0.02$ a.u. Any asymmetry of the contour lines about the midpoint of the pulse could be interpreted as a manifestation of the tunneling delay. The absence of any appreciable asymmetry in the Figure suggests that our definition of the IIR gives us an essentially zero time delay for the hydrogen atom.

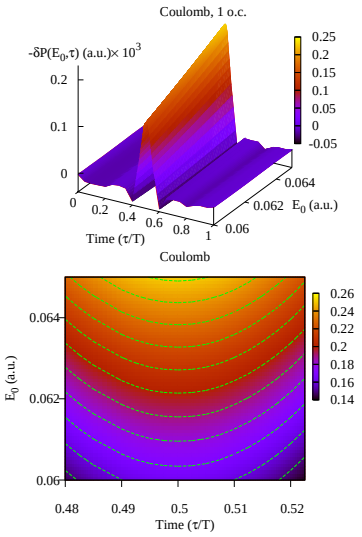


Figure 1: First variation of the ionization probability $\delta P(E_0, \tau)$ and its lines of constant elevation for Coulomb potential for the total pulse duration of 1 o.c.

[1] F. Krausz and M. Ivanov, Rev. Mod. Phys. **81**, 163 (2009).

[2] C. Hofmann *et al*, J. Phys. B **46**, 125601 (2013).

[3] S. B. Park *et al*, Optica **5**, 402 (2018).

[4] I. A. Ivanov, Phys. Rev. A **90**, 013418 (2014).

Creating and multiplying knots in the polarization state of light

E. Pisanty[1], **G. Jiménez**[1], **V. Vicuña**[1], **L. Rego**[2], **C. Hernández-García**[2], **L. Plaja**[2], **M. Maffei**[1], **A. Picón**[1,3], **A. Celi**[1,4], **J.P. Torres**[1,5] **and M. Lewenstein**[1,6]

[1] *Institut de Ciències Fotòniques, The Barcelona Institute of Science and Technology, 08860 Castelldefels, Spain*

[2] *Grupo de Investigacin en Aplicaciones del Láser y Fotónica, Departamento de Física Aplicada, University of Salamanca, E-37008, Salamanca, Spain*

[3] *Departamento de Química, Universidad Autónoma de Madrid, 28049, Madrid, Spain*

[4] *Institute for Theoretical Physics, University of Innsbruck, and Institute for Quantum Optics and Quantum Information, Austrian Academy of Sciences, Innsbruck, Austria*

[5] *Department of Signal Theory and Communications, Universitat Politecnica de Catalunya, Barcelona, Spain*

[6] *ICREA, Passeig de Lluís Companys, 23, 08010 Barcelona, Spain*

e-mail: `emilio.pisanty@icfo.eu`

The fundamental polarization singularities of monochromatic light are normally associated with invariance under coordinated rotations: symmetry operations that rotate the spatial dependence of an electromagnetic field by an angle θ and its polarization by a multiple $\gamma\theta$ of that angle. These symmetries are generated by mixed angular momenta of the form $J_\gamma = L + \gamma S$ and they give the beam polarization a Möbius-strip topology that, for monochromatic beams, restricts the coordination parameter γ to integer and half-integer values.

In this work we construct beams of light that are invariant under coordinated rotations for arbitrary rational γ, by exploiting the higher internal symmetry of 'bicircular' superpositions of counter-rotating circularly polarized beams at different frequencies (Fig. 1a). These beams exhibit a torus-knot polarization topology (Fig. 1b-e) which mirrors the embedding of the coordinated-rotations subgroup of $\mathrm{SO}(2) \times \mathrm{SO}(2)$ when seen as a flat torus (Fig. 1f). Moreover, this polychromatic polarization singularity can be characterized using the phase singularities of third- and higher-order field moment tensors, and it can be experimantally observed through nonlinear polarization tomography, exhibiting light beams with winding number $\pm n/3$.

In addition, we show that the torus-knot angular momentum J_γ of light (TKAM) is conserved in nonlinear interactions, by showing that TKAM beams can be used in high-harmonic generation to produce high-order harmonics that preserve the coordinated-rotation invariance and therefore have a topological charge $j_\gamma^{(q)} = q j_\gamma^{(1)}$ in the q^{th} harmonic that scales linearly with the harmonic order.

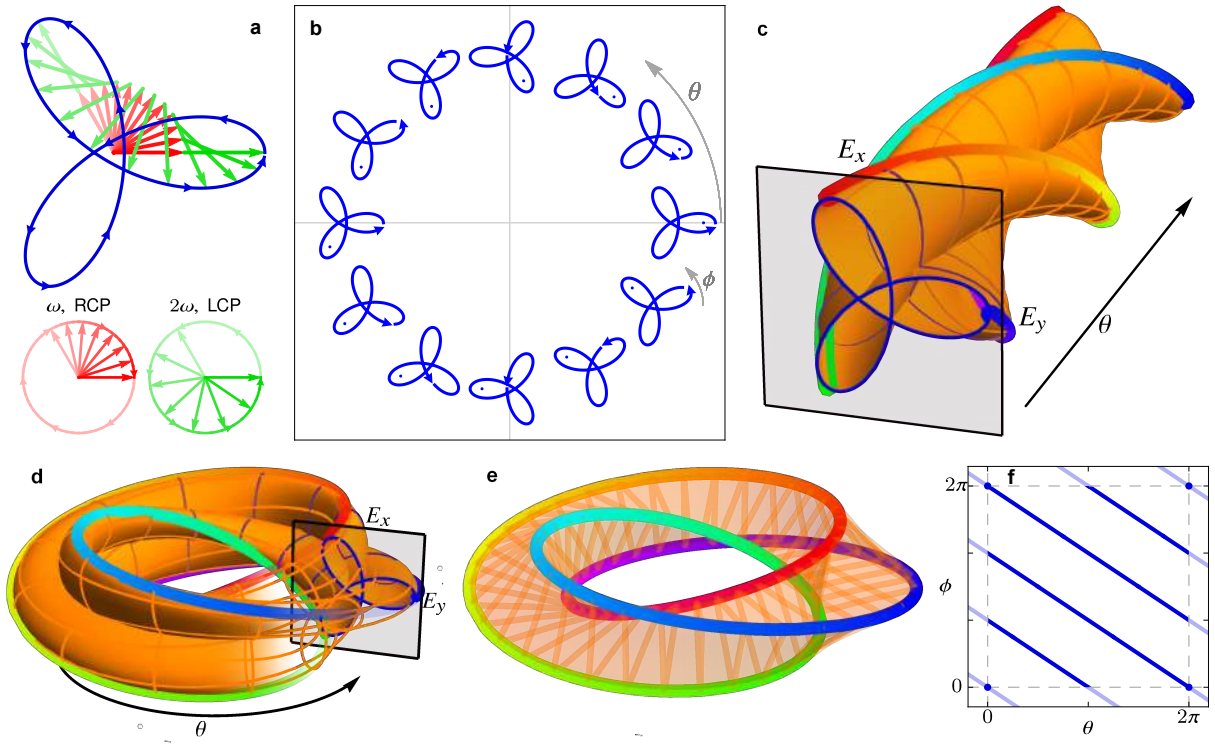


Fig. 1. Combining counter-rotating light beams at frequencies ω and 2ω gives a trefoil-shaped polarization (a), which can be combined in different orientations (by giving orbital angular momentum to the two components (b)) to give a torus-knot beam topology (c-e) that mirrors the figure's invariance group as a subset of the flat torus $\mathrm{SO}(2) \times \mathrm{SO}(2)$ (f).

Fast transport and spin control of atoms in moving traps

Q. Zhang[1,2,3] **and X. Chen**[1]**, and D. Guéry-Odelin**[2,3]

[1] *Department of Physics, Shanghai University, 200444 Shanghai, P. R. China*

[2] *Université de Toulouse, UPS, Laboratoire Collisions Agrégats Réactivité, IRSAMC, F-31062 Toulouse, France*

[3] *CNRS, UMR 5589, F-31062 Toulouse, France*

e-mail: *cherylqi@shu.edu.cn*

Fast and accurate control of spin and motion for atoms or atomic packets is quite demanding in atom interferometry, metrology and quantum information processing. Recently, the concept of shortcuts to adiabaticity enable us to speed up the conventional slow adiabatic process, and design the fast non-adiabatic protocols for expansion, rotation, transport and population transfer of internal states, see review [1].

In my talk, we first discuss the fast transport of an atom or a packet of atoms (see Fig. 1) by different kinds of non-harmonic traps including power-law trap ($U_n(x) = m\eta_n[x - x_0(t)]^{2n}/(2n)$ with $n \geq 1$ an integer where $x_0(t)$ denotes the trajectory of the bottom of the trap to be determined). We also consider now another type of non-harmonic potential that is the sum of a harmonic confinement and (i) a cubic anharmonicity: $m\omega_0^2 \left(x - x_0(t)\right)^3/3\xi$, or (ii) a quartic anharmonicity: $m\omega_0^2 \left(x - x_0(t)\right)^4/(4\xi^2)$, where ξ quantifies the strength of the anharmonicity. The study is based on the reverse engineering method. Firstly, exact results are obtained and applied to design robust transport protocols. Then, for both cubic anharmonic potential and quartic anharmonicities, the optimization of the transport trajectory is performed with classical trajectories, and remains valid for the transport of a wave packet. We also investigate the robustness of the transport of a packet of atoms in the framework of classical and quantum mechanics [2].

Secondly, we apply another strategy to transport atoms which is that we combine the invariant-based reverse engineering method, perturbation theory, and optimal control theory to design the fast and optimal transport. Since the actual optical traps are Gaussian rather than harmonic, we bound the relative displacement between the trap center and the center of the mass, and find the optimal trajectories for minimizing the average anharmonic perturbation energy to obtain high fidelity [3].

Finally, we consider the fast transport and spin control of spin-orbit coupled Bose-Einstein condense. Our starting point is the Hamiltonian is $H = p^2/2m + (1/2)m\omega^2[x - x_0(t)]^2 + \alpha(t)p\,\sigma_z$, where $\alpha(t)$ is a controllable SOC strength, adjusted by the geometry of two Raman lasers, ω is time-independent potential frequency and σ_z is the corresponding 2×2 Pauli matrix. We shall consider three cases. (i) When α is constant, the adiabatic transport with constant velocity and spin precession are illustrated. (ii) The counter-diabatic driving, implemented by compensating force, are exactly produced by such spin-orbit coupling, when $\alpha = \dot{x_0}$. (iii) More generally, we apply reverse engineering method to design the trap trajectory and spin-orbit coupling strength for fast transport and spin flip simultaneously, for spin-orbit-coupled Bose-Einstein condensates in a moving harmonic trap.

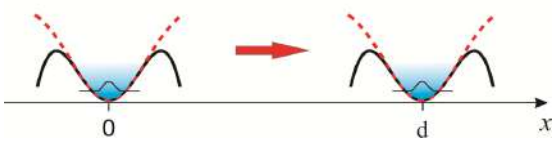


Figure 1: Schematic diagram of atomic transport in an effective one-dimensional Gaussian trap (dashed red line), approximated as a harmonic trap plus anharmonic quartic term (solid black line) from $x = 0$ to $x = d$.

All these results presented here will be compared with the new technique for designing the shortcuts based on inverse engineering combining with variational principle [5].

Acknowledgement Collabations with J. Gonzalo Muga and Jing Li.

[1] E. Torrontegui *et al.*, Adv. At. Mol. Opt. Phys. **62**, 117 (2013).

[2] Q. Zhang, X. Chen and D. Guéry-Odelin, Phys. Rev. A **92**, 043410 (2015).

[3] Q. Zhang, J. G. Muga and D. Guéry-Odelin and X. Chen, J. Phys. B: At. Mol. Opt. Phys. **49**, 125503 (2016).

[4] X. Chen, R.-L. Jiang, J. Li, Y. Ban, and E. Ya. Sherman, Phys. Rev. A **97**, 013631 (2018).

[5] J. Li, K. Sun, and X. Chen, Sci. Rep. **6**, 38258 (2016).

Turbulent cascades in out-of-equilibrium Bose gas

F. J. Vivanco, A. R. Fritsch, A. N. Novikov, P. E. S. Tavares, A. D. García-Orozco, G. D. Telles, V. S. Bagnato

Instituto de Física de São Carlos, Universidade de São Paulo, CP 369, 13560-970, São Carlos, SP, Brasil
e-mail: *gugs@ifsc.usp.br*

We studied a key concept of quantum turbulence taking place in inhomogeneous Bose-Einstein condensates driven out of equilibrium. We observed that turbulence in such systems manifests itself as a cascade characterized by anisotropic power-law distribution over the wave numbers k. It scales as $\sim k^{-3}$, and it is self-consistent with the existence of an inertial range matching the Kolmogorov-Zakharov analytical derived for weak-wave turbulence. This result is close enough to those observed in homogeneous quantum gases, which implies the independence of scaling from the spacial homogeneity of the system. We also analyze the evolution of the turbulent cascade for different regimes of excitation and identify a steady turbulent state that is relevant to previous experimental results, showing the transition to quantum turbulence in a finite size superfluid.

In classical fluids and gases turbulence is related to non dissipative energy transfer from large to small length scales of a system creating an energy cascade. One of the main features of this process is the spread of the kinetic energy over a wide range of wavenumbers, k, following the Kolmogorov power-law, $E(k) \sim k^{-5/3}$ [2]. Unlike the classical fluids, superfluids do support quantized vortices with characteristic sizes given by the healing length, ξ, together with random vortex tangles associated to the quantum turbulence definition, according to Feynmann [1]. Nowadays the quantum turbulence phenomena stands for a much broader class of turbulent behavior [2] such as Kolmogorov (semiclassical), Vinen (ultra-quantum) and weak-wave turbulence [3].

Figure 1 presents an overview of the emergence of quantum turbulence in a Bose gas perturbed for $t_{exc} \approx 32$ ms with $A \approx 330$ mG/cm amplitude. On top, the plane projection of the momentum distribution, $\tilde{n}(k_r)/\Delta\theta$, is shown for the long (red line) and short (blue line) axes. In both directions we observe a power-law taking place into the range marked by the two vertical green lines lying well into the physically meaningful bound $k_R < k_r < k_\xi$. The spatial anisotropy of the cloud affects the evolution of the momentum distributions by shifting the relevant inertial range towards the lower wave numbers. Despite the distinct non isotropic shape, in any case, $\tilde{n}(k_r)/\Delta\theta$ shows the same power law scaling, $\tilde{n}(k_r) \sim k^{-\gamma_{2D}}$, with the exponent $\gamma_{2D} \approx 2.1$.

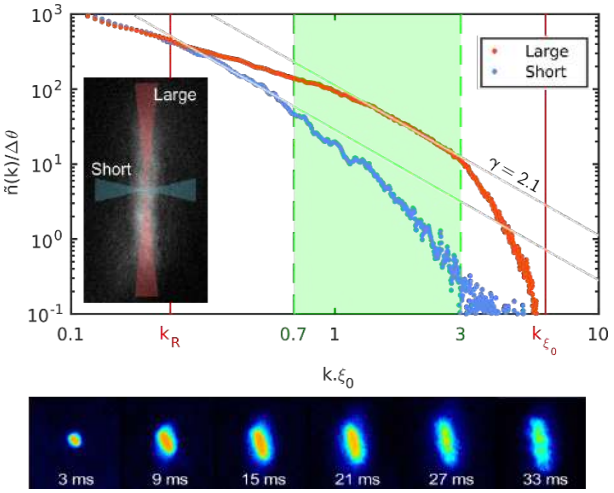


Figure 1: Top: In-plane momentum distributions $\tilde{n}(k_r)/\Delta\theta$ determined for the different sections of the strongly perturbed atomic cloud, namely: long axis (red dots), short axis (blue dots), and the total, integrated, cloud (black dots). The boundaries of the inertial range are marked with the vertical red lines. The green area shows the sub-range where the power-law is more clearly spotted and it is set as the fitting constraints to determine the power-law exponent. The solid gray lines are just eye-guides to help following the cascade exponent slope. As is seen, $\gamma_{2D} = 2.1$ is the same for all the measurements. Inset: a typical (normalized) absorption image of the perturbed Bose gas with its long and short axes. Bottom: non isotropic self-similar expansion of the excited quantum gas during the time of flight.

[1] R.P. Feynman, Prog. Low Temp. Phys. **1**, 17 (1955).

[2] C.F. Barenghi, L. Skrbekb and K.R. Sreenivasan, Proc. Natl. Acad. Sci. **111**, Supl. 1, 4647 (2014).

[3] G.V. Kolmakov, P.V.E. McClintock, S.V. Nazarenko, Proc. Natl. Acad. Sci. **111**, Supl. 1, 4727 (2014).

Creating a superfluid by kinetically driving a Mott insulator

G. Pieplow, F. Sols, and C.E. Creffield
Dpto. de Física de Materiales, Universidad Complutense de Madrid, E-28028, Spain
e-mail: *c.creffield@fis.ucm.es*

We study the effect of time-periodically varying the hopping amplitude (which we term "kinetic driving") in a one-dimensional Bose-Hubbard model, such that the time-averaged hopping is zero [1]. By using Floquet analysis, we derive the static effective Hamiltonian that arises in the limit of high driving frequency. This Hamiltonian has the novel feature that nearest-neighbor single-particle hopping processes are suppressed, but all even higher-order processes are allowed, and can be arbitrarily long-ranged. Unusual many-body features arise from the combined effect of the nonlocal interactions and correlated tunneling. In particular, at a critical value of the driving, the system passes from a Mott insulator to a superfluid formed by two quasi-condensates with opposite nonzero momenta, as shown in Fig.1. This fragmented superfluid consists of a coherent superposition of the two condensates, forming a Schrödinger cat-like state, whose properties can be described well as a Luttinger liquid. We extract the spectrum of the system's collective excitations, and locate the critical driving strength by evaluating the Luttinger liquid parameter K_b, which takes the universal value $K_b = 1/2$ at the phase transition. We further verify that this point coincides with the vanishing of the superconducting gap and the macroscopic occupation of the two condensates.

This work thus shows how driving of the hopping energy provides a novel form of Floquet engineering, which enables atypical Hamiltonians and exotic states of matter to be produced and controlled.

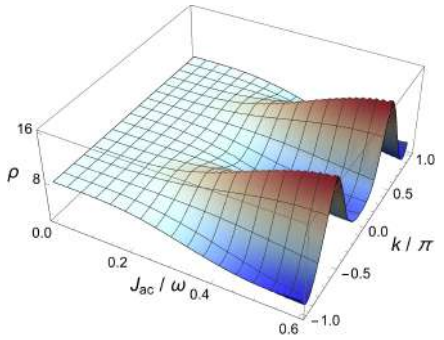


Figure 1: Single-particle momentum density over the first Brillouin zone, for an 8-site system, as the amplitude of the driving $J_{\rm ac}$ is varied. In the absence of driving ($J_{\rm ac} = 0$) the momentum density is flat, corresponding to a Mott insulator state. As $J_{\rm ac}$ is increased, peaks appear at $\pm\pi/2$, indicating the formation of condensates centered at these moment.

[1] G. Pieplow, C.E. Creffield, and F. Sols, arXiv:1706.04864.

Revealing missing charges with generalised quantum fluctuation relations

J. Mur-Petit[1], **A. Relaño**[2], **R. A. Molina**[3], **and D. Jaksch**[1,4]
[1] *Clarendon Laboratory, University of Oxford, Oxford, United Kingdom*
[2] *Departamento de Física Aplicada I and GISC, Universidad Complutense de Madrid, Madrid, Spain*
[3] *Instituto de Estructura de la Materia, IEM-CSIC, Madrid, Spain*
[4] *Centre for Quantum Technologies, National University of Singapore, Singapore*
e-mail: *jordi.murpetit@physics.ox.ac.uk*

The non-equilibrium dynamics of quantum many-body systems is one of the most fascinating problems in physics. Open questions range from how they relax to equilibrium, to how to extract useful work from them. A critical point lies in assessing whether a system has conserved quantities (or 'charges'), as these can drastically influence its dynamics [1], as highlighted by a number of recent experiments in cold atomic systems [2, 3, 4, 5, 6].

We have designed a general protocol to reveal the existence of charges from non-equilibrium measurements, based on a set of exact relations between out-of-equilibrium fluctuations and equilibrium properties of a quantum system [7]. As an example, we have applied our *generalised quantum fluctuation relations* to a trapped-ion quantum simulator subject to a series of quenches. **Fig. 1** shows how the amount of work done on the system by a highly non-equilibrium process is affected by the presence of charges. Our findings also indicate the relevance of charges to obtain unbiased temperature estimates in ultracold atomic systems from non-equilibrium measurements, which can have a direct impact in the interpretation of quantum simulation experiments.

More generally, our results will shed light on the interplay of quantum and thermal fluctuations in quantum non-equilibrium dynamics and the transition from integrability to chaos, and in the design of new quantum devices.

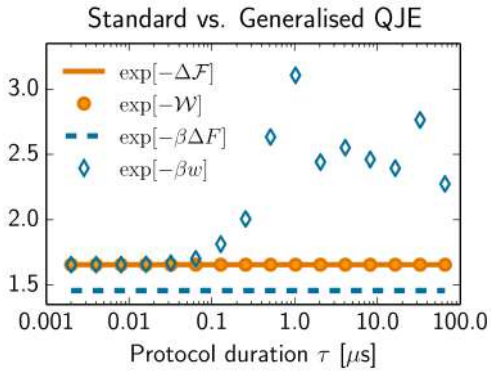


Figure 1. Average exponentiated work, $\langle\exp(-\beta w)\rangle$ (diamonds), and average exponentiated generalised work, $\langle\exp(-\mathcal{W})\rangle$ (circles), done on $N = 7$ ions, as a function of the free evolution time τ between two quenches of the intensity of red- and blue-sideband lasers. According to the quantum Jarzynski equality (QJE), these averages should not depend on τ (solid and dashed lines): the deviation of the standard work average (diamonds) indicates the existence of conserved charges in the system. *Figure adapted from Ref. [7].*

References

[1] B. Sutherland, *Beautiful Models. 70 Years of Exactly Solved Quantum Many-Body Problems* (World Scientific, 2004).

[2] T. Kinoshita, T. Wenger, and D. S. Weiss, Nature **440**, 900 (2006).

[3] M. Gring *et al.*, Science **337**, 1318 (2012).

[4] S. Trotzky *et al.*, Nature Phys. **8**, 325 (2012).

[5] J. P. Ronzheimer *et al.*, Phys. Rev. Lett. **110**, 205301 (2013).

[6] T. Langen *et al.*, Science **348**, 207 (2015).

[7] J. Mur-Petit, A. Relaño, R. A. Molina, and D. Jaksch, Nature Comms. **9**, 2006 (2018), doi: 10.1038/s41467-018-04407-1.

Weakly interacting Bose gases far from thermal equilibrium - Engineering condensation with a hot needle

Alexander Schnell[1], **Daniel Vorberg**[1], **Roland Ketzmerick**[1,2], **André Eckardt**[1]

[1] *Max-Planck-Institut für Physik komplexer Systeme, Nöthnitzer Straße 38, 01187 Dresden, Germany*

[2] *Technische Universität Dresden, Institut für Theoretische Physik and Center for Dynamics, 01062 Dresden, Germany*

e-mail: *schnell@pks.mpg.de*

We investigate theoretically [1] a one-dimensional ideal Bose gas that is driven into a steady state far from equilibrium via the coupling to two heat baths: a global bath of temperature T and a "hot needle", a bath of temperature $T_h \gg T$ with localized coupling to the system (see sketch in Fig. 1). Remarkably, this system features a crossover to finite-size Bose condensation at temperatures T that are orders of magnitude larger than the equilibrium condensation temperature.

This counterintuitive effect is explained by a suppression of long-wavelength excitations resulting from the competition between both baths. Moreover, for sufficiently large needle temperatures ground-state condensation is superseded by condensation into an excited state, which is favored by its weaker coupling to the hot needle (see Fig. 1). Our results suggest a general strategy for the preparation of quantum degenerate nonequilibrium steady states with unconventional properties and at large temperatures.

For the ideal gas a simple description of this open system is given by the Born-Markov approximation. Within this framework, the bath induces quantum jumps between energy eigenstates. Taking into account temperature-dependent dissipation for the interacting gas is challenging. Already on the level of a simple mean field approximation, it requires the diagonalization of the mean field Hamiltonian in every step of the time integration.

We propose and test a scheme to circumvent this problem by treating the system–bath coupling semiclassically. To this end, we decompose the system into bins and approximate that the bath may only drive transitions between wavelets that localize in such a bin (see sketch in Fig. 2). We thus find a description of the action of the dissipative bath interaction that is independent of the mean field potential. This provides a perfect tool to study far from equilibrium gases, whose steady state density profile in general is not known ab-initio. We apply this formalism to the "hot needle" scenario and find that our main findings for the ideal gas are robust against weak interactions.

[1] A.Schnell, D. Vorberg, R. Ketzmerick, and A. Eckardt, Phys. Rev. Lett. **119**, 140602

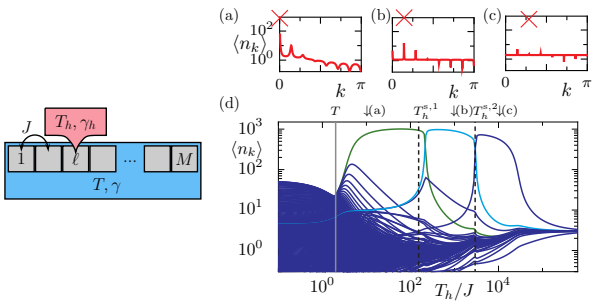


Figure 1: Left: Sketch of the setup. Right: Mean occupations in the non-equilibrium steady state for the non-interacting Bose gas (d) as a function of the temperature of the needle. Although the system does not feature condensation in equilibrium $T_h = T$ (grey line), by increasing the temperature of the needle a ground state condensate is forming. At a given temperature of the needle we find switching into an excited state condensate. Corresponding momentum distributions are shown in panel (a-c), where the crosses mark the condensate occupation.

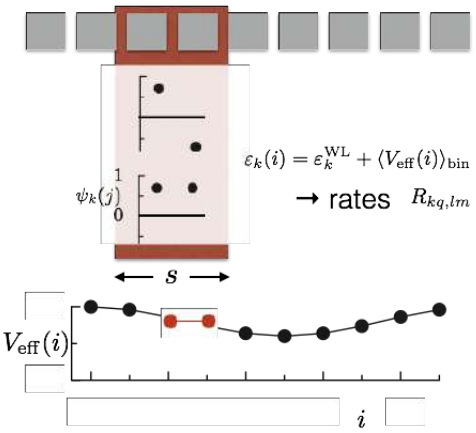


Figure 2: Sketch: Semiclassical treatment of the bath interaction. We propose that the bath may drive transitions only locally with in a bin of size s. Within this bin, the mean field potential V_{eff} only varies weakly, such that the local basis and corresponding energies can be assumed to be independent of the potential.

Quench dynamics in a two-particle system with a combination of synthetic spin-orbit coupling and Raman coupling

A. Usui, Th. Fogarty, and Th. Busch
Quantum Systems Unit, Okinawa Institute of Science and Technology Graduate University, Onna, Okinawa 904-0495, Japan
e-mail: *ayaka.usui@oist.jp*

Since Bose-Einstein condensation in a cold alkali gas was first observed, systems of cold atoms have been attracting attention, and particularly the realisation of the isolated system has motivated one to investigate non-equilibrium phenomena and quantum thermodynamics.

We study a system of two bosons in one dimension in the presence of synthetic spin-orbit (SO) coupling. The two bosons are described by two identical atoms with different hyperfine states, and can therefore be regarded as a two-level system with a pseudo-spin. We investigate quench dynamics given by the sudden switching on of the Raman coupling, and calculate the time-dependent coefficients of the corresponding eigenstates, Loschmidt echo (LE), Quantum Fisher information (QFI), and von Neumann entropy (vNE) in order to characterise the dynamics. These tools allow me to examine the generation of entanglement as a result of the quench dynamics. Especially, it is interesting to calculate the vNE because there are two types of vNE which can be defined in the system, one of which is a function $S(x_1, x_2)$ of continuous variables which are positions of particles, and other of which is a function $S(\uparrow, \downarrow)$ of discrete variables which are up-spin and down-spin of the pseudo-spin.

To start with, we show the Hamiltonian of the system. Here, let us consider two interacting particles in a harmonic trap with Raman coupling resulting in SO coupling where the contact interaction is dependent on the species of the two-component BEC. The Hamiltonian of the system can be expressed as Fig. 1 in the pseudo-spin basis $|\uparrow\uparrow\rangle, |\uparrow\downarrow\rangle, |\downarrow\uparrow\rangle, |\downarrow\downarrow\rangle$ and using the coordinates of the centre-of-mass $X = (x_1 + x_2)/\sqrt{2}$ and the relative motion $x = (x_1 - x_2)/\sqrt{2}$.

Here, we represent Hamiltonian of centre-of-mass and relative motion as

$$H_{\rm com}(X) = -\frac{\hbar^2}{2m}\frac{\partial^2}{\partial X^2} + \frac{1}{2}m\omega^2 X^2, \tag{1}$$

$$H_{\rm rel}^{jk}(x) = -\frac{\hbar^2}{2m}\frac{\partial^2}{\partial x^2} + \frac{1}{2}m\omega^2 x^2 + \frac{g_{jk}}{\sqrt{2}}\delta(x), \tag{2}$$

with trap frequency ω and interaction coefficient g_{jk}, and we show SO coupling terms as

$$H_{\rm com}^{\rm soc} = \frac{i\sqrt{2}\hbar^2 k}{m}\frac{\partial}{\partial X}, \tag{3}$$

$$H_{\rm rel}^{\rm soc} = \frac{i\sqrt{2}\hbar^2 k}{m}\frac{\partial}{\partial x} \tag{4}$$

with the strength of SO coupling k , and the strength of Raman coupling Ω. The eigenstates and eigenenergies of the system are obtained by diagonalising the Hamiltonian.

For the preliminary research, we have investigated the ground state and the energy spectrum as a functuon of Ω. It is confirmed that in the energy spectrum the crossing points become decreasing with increasing k , which is the same behaviour as Ref. [1]. It is also seen that for strong interactions the degeneracy at $\Omega = 0$ is lifted, which results in a non-trivial energy spectrum due to the competing spin-orbit and contact interactions.

[1] Q. Guan, X.Y. Yin, S.E. Gharashi, and D. Blume, J. Phys. B: At. Mol. Opt. Phys. **47**, 161001 (2014).

$$H = \sum_{k,l,m,n=\uparrow,\downarrow} |k,l\rangle \langle k,l|H|m,n\rangle \langle m,n|$$
$$= \begin{bmatrix} H_{\rm com} + H_{\rm rel}^{\uparrow\uparrow} + H_{\rm com}^{\rm soc} & \hbar\Omega/2 & \hbar\Omega/2 & 0 \\ \hbar\Omega/2 & H_{\rm com} + H_{\rm rel}^{\uparrow\downarrow} + H_{\rm rel}^{\rm soc} & 0 & \hbar\Omega/2 \\ \hbar\Omega/2 & 0 & H_{\rm com} + H_{\rm rel}^{\downarrow\uparrow} - H_{\rm rel}^{\rm soc} & \hbar\Omega/2 \\ 0 & \hbar\Omega/2 & \hbar\Omega/2 & H_{\rm com} + H_{\rm rel}^{\downarrow\downarrow} - H_{\rm com}^{\rm soc} \end{bmatrix}$$

Figure 1: The Hamiltonian explained in the text.

Impact of geometry on many-body localization

D. Wiater[1,2] **and J. Zakrzewski**[2,3]

[1] *Institute of Physics, Polish Academy of Sciences, Aleja Lotnikow 32/46, PL-02668 Warsaw, Poland*

[2] *Instytut Fizyki imienia Mariana Smoluchowskiego, Uniwersytet Jagielloński, ulica Łojasiewicza 11, PL-30059 Kraków, Poland*

[3] *Mark Kac Complex Systems Research Center, Uniwersytet Jagielloński, Kraków, Poland*

e-mail: *wiater.dariusz@gmail.com*

The impact of geometry on many body localization is studied on simple, exemplary systems amenable to exact diagonalization treatment [1]. The crossover between ergodic and MBL phase for uniform as well as quasi-random disorder is analyzed using statistics of energy levels. It is observed that the transition to many-body localized phase is correlated with the number of nearest coupled neighbors. The crossover from extended to localized systems is approximately described by the so called plasma model [2]. All calculations are performed for the same Heisenberg model [3]:

$$H = \sum_{<i\neq j>} [J(S_i^x S_j^x + S_i^y S_j^y) + J_z S_i^z S_j^z] + \sum_i h_i S_i^z \quad (1)$$

We consider two cases [4]. For the "uniform disorder" $h_i \in [-W, W]$ is drawn from the uniform random distribution. We consider also the case of quasi-periodic disorder defined in the 1D chain as:

$$h_i = W\cos(2\pi\tau i + \phi) \quad (2)$$

where: W is the disorder amplitude, i the site number, $\tau = \frac{1+\sqrt{5}}{2}$ and a phase: $\phi \in [-\pi, \pi]$. Each realization corresponds to a fixed ϕ, The definition of quasi-periodic disorder has to be modified for 2D models. In particular for the ladder system (with eight rows and two columns) let us define index i as a pair j, k with j numbering rows and k - columns. Then we take: $h_i = W\cos(2\pi\tau j + \phi_k)$, where: $\tau = \frac{1+\sqrt{5}}{2}$, and the phases: $\phi_k \in [-\pi, \pi]$ are independent for each column. The same construction holds for the square lattice model (4x4) with four independent ϕ_k for each realization. For a triangular lattice model case there is a need to define a model of disorder which could be realized in a cold-atom experiment. We assume that the quasi-random disorder in the triangular lattice is created by adding a weak incommensurate lattice:

$$V(r) = \frac{1}{2}W[\cos(2\pi\tau\mathbf{b}_3\cdot\mathbf{r} - \phi_1) + \cos(2\pi\tau\mathbf{b}_2\cdot\mathbf{r} - \phi_2) + \cos(2\pi\tau\mathbf{b}_1\cdot\mathbf{r} + \phi_1 - \phi_2)] \quad (3)$$

where direction vectors $\mathbf{b}_1 = (0, -\sqrt{3})$, $\mathbf{b}_2 = (3/2, -\sqrt{3}/2)$, $\mathbf{b}_3 = (3/2, \sqrt{3}/2)$ and $\mathbf{r} = (x, y)^T$

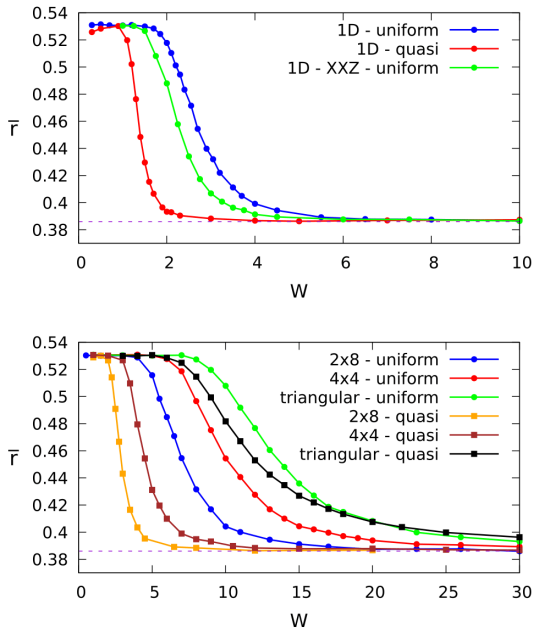


Figure 1: Average gap ratio $\bar{r}$ (4) averaged over 800-1500 realizations of uniform or quasi-disorder for eigenvalues included in $\varepsilon \in (0.49, 0.51)$ is presented for mentioned lattices, where $\varepsilon = (E - E_{max})/(E_{max} - E_{min})$.

with random phases: $\phi_1, \phi_2 \in [-\pi, \pi]$. Fig.1 presents dimensionless gap ratio defined as the ratio of consecutive level spacings:

$$r_n = \frac{\min(s_n, s_{n-1})}{\max(s_n, s_{n-1})}. \quad (4)$$

For a given disorder it is the number of neighbors that play the decisive role in deciding how large the amplitude of the disorder is needed to observe the transition.

[1] D. Wiater and J. Zakrzewski, arXiv:1805.07383

[2] M. Serbyn and J. E. Moore, Phys. Rev. B 93, 041424 (2016).

[3] D. J. Luitz, N. Laflorencie, and F. Alet, Phys. Rev. B 91, 081103 (2015).

[4] V. Khemani, D. N. Sheng, and D. A. Huse, Phys. Rev. Lett. 119, 075702 (2017).

Collective modes and quantum thermalisation with tilted dipoles

L. Gabardos[1,2], **S. Lepoutre**[1,2], **K. Kechadi**[1,2], **B. Naylor**[1,2], **E. Maréchal**[1,2], **O. Gorceix**[1,2], **B. Zhu**[3,4], **L. Isaev**[3], **J. Schachenmayer**[5], **P. Pedri**[1,2], **A. M. Rey**[3], **L. Vernac**[1,2] and **B. Laburthe-Tolra**[1,2]

[1] *Laboratoire de Physique des Lasers, Université Paris 13, Sorbonne Paris Cité, 93430 Villetaneuse, France*
[2] *CNRS, UMR No. 7538, LPL, 93430 Villetaneuse, France*
[3] *JILA, NIST, and Department of Physics, University of Colorado, Boulder, Colorado 80309, USA*
[4] *ITAMP, Harvard-Smithsonian Center for Astrophysics, Cambridge, MA 02138, USA*
[5] *CNRS, UMR 7504, IPCMS; UMR 7006, ISIS; and Université de Strasbourg, Strasbourg, France*
e-mail: *lucas.gabardos@univ-paris13.fr*

We study out-of-equilibrium spin dynamics of an ensemble of chromium atoms. This atomic species has a large $S = 3$ spin in its ground state, resulting in a large magnetic dipole moment of 6 μ_B (with μ_B the Bohr magneton) which induces significant dipole-dipole interactions between atoms.

We start with a quantum gas of ^{52}Cr in the $|S = 3, m_S = -3\rangle$ absolute ground state. We trigger the dynamics by rotating the spins of all atoms, thus creating a ferromagnetic coherent state tilted by an angle θ with respect to the external magnetic field. The evolution of the system is then characterized by monitoring the populations of the 7 spin components after Stern-Gerlarch separation.

In the superfluid case of a BEC [1, 2], the population dynamics is governed by the interplay between spin-dependent contact interactions, dipole-dipole interactions, and spin-orbit coupling provided by magnetic field gradients. It is well described by a mean-field model, where each spin precesses around the field created by all other dipoles. We found that the ferromagnetic character of the condensate (characterised by the local spin length) is conserved. This protection of ferromagnetism is a universal feature arising due to an energy gap created by the spin-dependent contact interactions [1]. Provided the magnetic field gradient is small enough, the quantum gas thus behaves like a quantum ferrofluid. In this regime, the observed spin dynamics is associated with the excitation of a collective mode coupling the spin and the orbital degrees of freedom, a trapped magnon mode (Fig. 1). These observations are well described by classical hydrodynamic equations [2].

In the case of a Mott insulating state [3], the atoms now solely interact via long-range dipole-dipole interactions, realizing a spin-3 XXZ Heisenberg model for a unit filled array of 10^4 atoms. Mean-field simulations fail to account for the observed dynamics, which is, on the other hand, well reproduced by a model adapted from the truncated Wigner approximation (Generalized Discrete Truncated Wigner Approximation [4], GDTWA). This indicates the emergence of quantum correlations between atoms. Our observations are consistent with quantum thermalisation of an isolated many-body system, where entanglement between particules leads to thermal statistics for individual spin components.

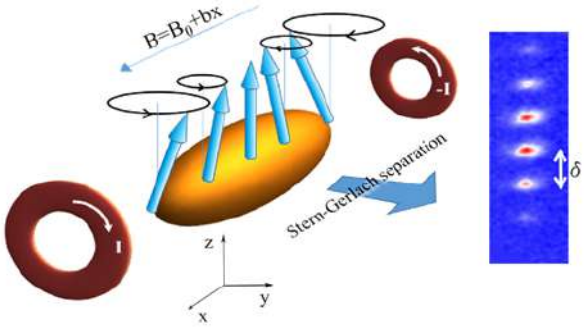


Figure 1: A BEC is initially polarized perpendicular to the external magnetic field. Spin collective modes are excited by a magnetic field gradient. In the rotating frame, these modes correspond to spins oscillating around their initial direction with an amplitude which linearly depends on the position x.

[1] S. Lepoutre, K. Kechadi, B. Naylor, B. Zhu, L. Gabardos, L. Isaev, P. Pedri, A. M. Rey, L. Vernac, and B. Laburthe-Tolra, Phys. Rev. A **97**, 023610 (2018).

[2] S. Lepoutre, L. Gabardos, K. Kechadi, P. Pedri, O. Gorceix, E. Marechal, L. Vernac, B. Laburthe-Tolra, https://arxiv.org/abs/1804.10254

[3] S. Lepoutre, J. Schachenmayer, L. Gabardos, B. Zhu, B. Naylor, E. Maréchal, O. Gorceix, A. M. Rey, L. Vernac, and B. Laburthe-Tolra, https://arxiv.org/abs/1803.02628

[4] J. Schachenmayer, A. Pikovski, and A. M. Rey, Phys. Rev. X **5**, 011022 (2015).

Monitoring squeezed collective modes of a 1D Bose gas after an interaction quench using density ripples analysis

M. Schemmer[1], **A. Aisling**[1], **and I. Bouchoule**[1]

[1] *Laboratoire Charles Fabry, Institut d'Optique, 2 Avenue Augustin Fresnel, 91127 Palaiseau, France*

e-mail: *maximilian.schemmer@institutoptique.fr*

We investigate the out-of-equilibrium dynamics following a sudden quench of the interaction strength, in a one-dimensional quasi-condensate trapped at the surface of an atom chip. Within a linearized approximation, the system is described by independent collective modes and the quench squeezes the phase space distribution of each mode, leading to a subsequent breathing of each quadrature. We show that the collective modes are resolved by the power spectrum of density ripples which appear after a short time of flight. This allows us to experimentally probe the expected breathing phenomenon. The results are in good agreement with theoretical predictions which take the longitudinal harmonic confinement into account

Experimentally, we prepare at $t = 0$ a cloud of ^{87}Rb atoms in the 1D quasi-condensate regime. The effective 1D coupling constant g can then be controlled by the transverse trapping frequency $\omega_\perp$ ($g \propto \omega_\perp$). We perform quenches of g by quickly changing $\omega_\perp$, and investigate the post-quench behavior at different time t after the quench. For this purpose, we analyze the density ripples that arise after a short time of flight, following a sudden switch off of the the confinement: Interactions are effectively quickly turned off by the transverse expansion of the gas and the subsequent free evolution transforms phase fluctuations into density fluctuations. We show that long wavelength density ripples resolve the Bogoliubov excitations: The component $\langle|\rho(q)|^2\rangle$ of the density power spectrum is proportional to $\langle\theta_q^2\rangle$, the square width of the phase quadrature of the Bogoliubov mode at wavevector q. These excitations are characterized by a linear dispersion relation $\omega_q = cq$, with c the speed of sound and $\langle\theta_q^2\rangle$ is expected to oscillate at $\sin(2\tau)$, where $\tau = cqt$, with an amplitude proportional to the quench strength $\kappa = \omega_\perp^{\text{final}}/\omega_\perp^{\text{initial}} - 1$. Thus all $\langle|\rho(q)|^2\rangle(\tau)/\langle|\rho(q)|^2\rangle(0)$ are expected to collapse on the same function, denoted as $\bar{J}$. Fig. 1 shows the time evolution of $\bar{J}$ obtained gathering the experimental data (see [2] for details). The observed oscillations reveal the predicted breathing of the Bogoliubov modes.

For a precise comparison with theory we take into account the effect of the trapping potential in a local density approach, where one introduces a local speed of sound. The spatial spread in speed of sound is responsible for a dephasing leading to a damping of the function $\bar{J}$. The predicted damping (see dashed lines in Fig. 1) is in agreement with the experimentally observed damping (solid line).

The effect of the quench could also be monitored by observing the one-body correlation function $g_1 = \langle\Psi(z)^\dagger\Psi(z)\rangle$, whose evolution shows a thermalization behavior in the form of a light cone, as observed in [1]. Our analysis reveals ongoing dynamics beyond the characteristic thermalization time of the g_1 function (see Fig. 1 inset red points).

Details about this work can be found in [2]

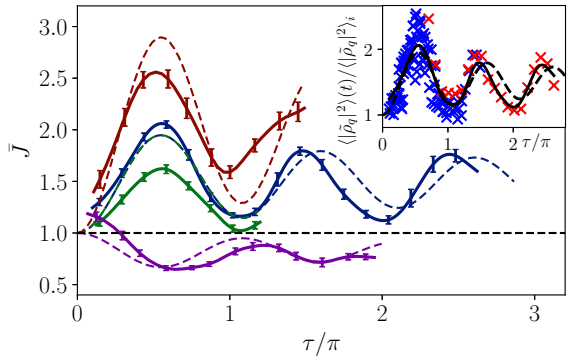


Figure 1: The time evolution of squeezed collective modes produced by an interaction strength. The smoothed normalized density ripples power spectrum $\bar{J}$ is plotted versus the reduced time $\tau = cqt$ with the speed of sound c for different data sets. The initial transverse oscillation frequency is 1.5 kHz, except for the green curve for which it is 3 kHz. Quench strengths are $\kappa = 4$ (red data), $\kappa = 2$ (blue and green) data and $\kappa = 0.7$ (purple data). Dashed lines are theoretical predictions for quench strengths. The inset shows the raw (unsmoothed) data corresponding to each measurement time t and discrete q values, for a data set corresponding to the blue curve J in black and its theoretical predictions. Points in blue correspond to $t < t_{th}^{g_1}$ and red to $t < t_{th}^{g_1}$

[1] T. Langen, et al., Nature Physics **9.10**, 640 (2013).

[2] M. Schemmer, A. Johnson and I. Bouchoule, arXiv:1712.04642 (2017)

Probing many-body localization in the presence of a quantum bath

A. Rubio-Abadal[1], **J-y. Choi**[1,2], **J. Zeiher**[1], **S. Hollerith** [1], **J. Rui**[1], **I. Bloch**[1,3], **and C. Gross**[1]

[1] *Max-Planck-Institut für Quantenoptik, 85748 Garching, Germany*

[2] *Department of Physics, Korea Advanced Institute of Science and Technology, Daejeon 3414, Korea*

[3] *Fakultät für Physik, Ludwig-Maximilians-Universität München, 80799 München, Germany*

e-mail: *antonio.rubio@mpq.mpg.de*

An isolated quantum many-body system driven out of equilibrium will generically evolve into a state locally described by a thermal ensemble. Such a relaxation can, however, fail to take place in systems with quenched disorder, leading to the phenomenon of many-body localization (MBL), in which the conditions of an initially prepared state can survive for arbitrarily long times, even in the presence of interactions [1]. One of the fundamental open questions in the field of quantum thermalization concerns the stability of MBL in higher dimensions, and it is tightly linked to the problem of coupling an MBL system to a bath with few degrees of freedom. The numerical simulation of such small-bath scenarios is extremely challenging and out of scope for systems with two or more dimensions, calling for the use of ultracold atoms as quantum simulators to provide an answer to this question [2, 3].

In our recent work [4], we studied an out-of-equilibrium mixture of ultracold bosonic atoms immersed in a two-dimensional optical lattice with a species-dependent disordered potential (see Fig. 1). When preparing all atoms in a state which experiences the disorder (dirty component), the system relaxed to a state which partially preserved the initially prepared density pattern, which we identify as many-body localization. If we instead prepared a system with an atomic state insensitive to the disorder (clean component), the initial distribution rapidly relaxed until it became inappreciable. When mixing the two components, which strongly interact with each other, the clean one plays the role of a small bath, and the outcome of the dynamics in such a hybrid system will depend on their relative populations. Our results show that MBL becomes unstable as we increase the size of the bath, but for small enough baths, localization can survive, potentially hinting at either the localization of the bath component or to the coexistence of a localized and a thermal phase.

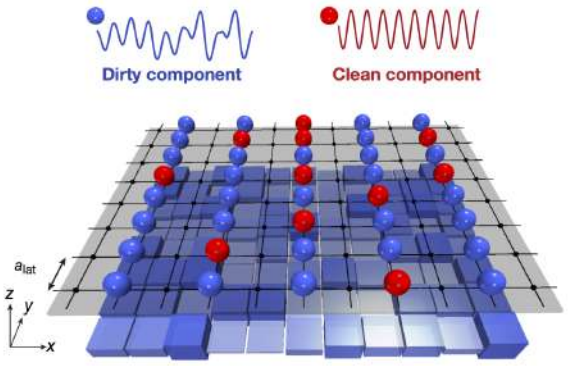


Figure 1: Schematic of the two-component mixture prepared at the beginning of our experiment. The system consists of a square optical lattice with a state-dependent potential in which two different hyperfine spin states are prepared. The clean component (red spheres) experiences only the lattice potential, while the dirty component (blue spheres) is additionally affected by a random on-site potential. The initial state displays a short-scale density modulation along the x-direction.

[1] R. Nandkishore and D.A. Huse, Annu. Rev. Condens. Matter Phys. **6** 15-38 (2015)

[2] M. Schreiber, S. S. Hodgman, P. Bordia, H.P. Lüschen, M.H. Fischer, R. Vosk, E. Altman, U. Schneider and I. Bloch, Science **349** 842 (2015)

[3] J.-y. Choi, S. Hild, J. Zeiher, P. Schauß, A. Rubio-Abadal, T. Yefsah, V. Khemani, D.A. Huse, I. Bloch and C. Gross, Science **352**, 1547 (2016)

[4] A. Rubio-Abadal, J.-y. Choi, J. Zeiher, S. Hollerith, J. Rui, I. Bloch and C. Gross, arXiv:1805.00056 (2018)

Dynamical Phase Transition in the Collective Heisenberg Model

Scott Smale[1*], Peiru He[2*], Ben A. Olsen[1], Kenneth G. Jackson[1], Haille Sharum[1], Stefan Trotzky[1], Jamir Marino[2], Ana Maria Rey[2], Joseph H. Thywissen[1]

[1] *Department of Physics, University of Toronto, Ontario M5S 1A7, Canada*

[2] *JILA, NIST, and the University of Colorado, Boulder, CO 80309, USA*

e-mail: *kjackson@physics.utoronto.ca*

The Heisenberg spin model is a textbook model for magnetism and superconductivity [1]. We simulate the collective Heisenberg model with 3×10^4 fermionic potassium atoms in a three-dimensional harmonic oscillator potential. In the weak scattering regime [2], atoms are frozen in single-particle harmonic oscillator modes, and mode-changing collisions are suppressed during the timescale of the experiment. Oscillator modes thus serve as lattice sites, and we simulate a lattice spin model without a physical lattice [3, 4, 5, 6, 7]. Due to the density-density overlap of harmonic oscillator wavefunctions, lattice interactions are long range.

Beginning with a system fully magnetized in the transverse direction, we measure the dynamics of the magnetization and observe a dynamical phase transition from ferromagnetic dynamics in which the transverse magnetization is stabilized, to a paramagnetic phase, where the magnetization decays quickly. Near the dynamical phase transition [8, 9, 10, 11], interactions open an energy gap that protects against dephasing and causes oscillations in the magnetization, which slowly damp. We find excellent agreement with mean-field theory of the collective Heisenberg Hamiltonian (Eq. 1) that includes exchange interactions J_{ij} between spins $\hat{\mathbf{s}}_i$, and an inhomogeneous axial field h_i (due to an effective magnetic field curvature):

$$\hat{H}/\hbar = \sum_i h_i \hat{s}_i^Z - \sum_{i,j} J_{ij} \hat{\boldsymbol{s}}_{\boldsymbol{i}} \cdot \hat{\boldsymbol{s}}_{\boldsymbol{j}}. \qquad (1)$$

We map out the dynamical phase diagram by tuning the inhomogeneity of h_i and the interaction strength (using an s-wave Feshbach resonance). We also observe the failure of the spin model at larger scattering lengths where mode-changing collisions become significant, and perform a many-body echo to find a region in which the spin model is valid [12]. To summarize, we show that weakly interacting Fermi gases can simulate the non-equilibrium dynamics of the collective Heisenberg model.

References

[1] Auerbach, A. (Springer-Verlag, New York, 1994).

[2] Du, X., Luo, L., Clancy, B. & Thomas, J. E. *Phys. Rev. Lett.* **101**, 150401 (2008).

[3] Martin, M. J. *et al. Science* **341**, 632 (2013).

[4] Zhang, X. *et al. Science* **345**, 1467 (2014).

[5] Rey, A. M. *et al. Ann. Phys. (NY)* **340**, 311 (2014).

[6] Swallows, M. D. *et al. Science* **331**, 1043 (2010).

[7] Bromley, S. L. *et al. Nature Physics* **14**, 399 (2018).

[8] Eckstein, M., Kollar, M. & Werner, P. *Phys. Rev. Lett.* **103**, 056403 (2009).

[9] Schiró, M. & Fabrizio, M. *Phys. Rev. Lett.* **105**, 076401 (2010).

[10] Sciolla, B. & Biroli, G. *Phys. Rev. Lett.* **105**, 220401 (2010).

[11] Gambassi, A. & Calabrese, P. *EuroPhys, Lett.* **95**, 66007 (2011).

[12] Widera, A. *et al. Phys. Rev. Lett.* **100**, 140401 (2008).

Quantum master equation in paired degenerate subspace of finite-size dissipative Dicke model

R. Imai and Y. Yamanaka
Department of Electronic and Physical Systems, Waseda University, Tokyo 169-8555, Japan
e-mail: *rimai@asagi.waseda.jp*

The Dicke model that describes a collection of identical two-level atoms interacting with a single electromagnetic mode in an optical cavity is an appealing theoretical model because of a phase transition to superradiance. After an experimental realization was proposed by Dimer *et al.* [2], the experiments of the cold atomic system in an optical cavity that corresponds to the Dicke model system have been conducted, showing the superradiant phase [3, 4]. The experimental system with an additional driving force is dissipative and open.

In this work, we study the *finite-size* Dicke model with *photon leakage* and show that the leakage stabilizes the symmetry breaking states that reduce to the superradiant states in the thermodynamic limit [1].

The Hamiltonian of the finite-size Dicke model is defined by

$$\hat{H} = \omega_0 \hat{J}^{(3)} + \omega \hat{a}^\dagger \hat{a} + \frac{\lambda}{\sqrt{2J}} \left(\hat{a} + \hat{a}^\dagger\right) \left(\hat{J}^+ + \hat{J}^-\right),$$

where $\hat{a}$ denotes the bosonic annihilation operator for the cavity mode with frequency ω, and $\hat{J}^{(i)}$ $(i = 1, 2, 3)$ are pseudospin operators, describing a collection of finite N atoms with level spacing ω_0. The quantity J represents the magnitude of the pseudospin and is related to N via $N = 2J$. We consider the situation in which the level spacing of atoms is sufficiently small. Then, the ground and the first excited states are constructed as states, or a symmetric and an antisymmetric superpositions of coherent states, respectively, which are also even-parity and odd-parity states [1]. The energy gap between them decreases exponentially as N increases, if λ goes beyond a critical value λ_c, $\lambda > \lambda_c$, and the ground and first excited states form an almost degenerate pair [1, 5].

In order to take account of the photon leakage properly, we consider an external photon reservoir coupled to the optical cavity mode in $\hat{H}$. Under the Born approximation, we derive the quantum master equation for the open Dicke system. When the level spacing of atoms is sufficiently small, we can show that the state subspace spanned by the ground and first excited states are separated dynamically from the complementary state space in the leading order of the level spacing [1]. Thus the master equation closed in the subspace of the almost degenerate pair is derived and its solution tells us about the phases of the system and the phase transition. For $\lambda > \lambda_c$, which is called the superradiant region, it can be shown that the master equation of the almost degenerate pair naturally has a Markovian form due to the vanishing gap energy [1]. Using this Markovian equation, we observe the dephasing process in which the initial parity eigenstates change into the symmetry breaking states [1]. This provides, without taking the thermodynamic limit, an alternative way to interpret the results of the experiments of cold atomic Dicke systems in an optical cavity. In contrast to the superradiant region, the finite gap exists in the normal region, $\lambda < \lambda_c$. Then it is imagined that the quantum master equation remains in the non-Markovian form and that the non-Markovian property makes the temporal development of the system more complicated than in case of the superradiant region. In particular, the dephasing process in the normal region may be affected by the non-Markovicity.

We shall solve the quantum master equation numerically and investigate the behaviors that the solutions show. We discuss the problem mainly from the viewpoints of the superradiant transition in the open system, and of Markovicity or non-Markovicity of the quantum master equation.

[1] R. Imai and Y. Yamanaka, `arXiv:1801.05954`.

[2] F. Dimer, B. Estienne, A. S. Parkins and H. J. Carmichael, Phys. Rev. A **75**, 013804 (2007).

[3] K. Baumann, C. Guerlin, F. Brennecke, T. Esslinger, Nature **464** 1301, (2010).

[4] K. Baumann, R. Mottl, F. Brennecke, T. Esslinger, Phys. Rev. Lett. **107** 140402, (2011).

[5] J. Larson and E. K. Irish, Journal of Physics A: Mathematical and Theoretical **50**, 174002 (2017).

Nontrivial Bloch oscillations in an optical lattice due to spin-orbit coupling

Lu Zhou[1], **Wei Ji**[1], **and Weiping Zhang**[2]

[1] *Department of Physics, School of Physics and Material Science, East China Normal University, 200241 Shanghai, China*

[2] *Department of Physics and Astronomy, Shanghai Jiaotong University, 200240 Shanghai, China*

e-mail: *lzhou@phy.ecnu.edu.cn*

Our model is based on the recent experiment [1] with a ^{87}Rb BEC prepared in a one-dimensional optical lattice along the z-direction, inside which the effective SO interaction is induced via coupling the $|1,-1\rangle$ ($|\downarrow\rangle$) and $|1,0\rangle$ ($|\uparrow\rangle$) hyperfine states with Raman lasers. In addition to that, a constant external force F is exerted on the atoms via either tilting the optical lattice or introducing a linearly time-dependent frequency difference $\Delta\nu\,(t)$ between the two lattice beams. The effective single-particle Hamiltonian reads

$$\hat{H}=\frac{\left(\hat{p}_z-\hat{A}\right)^2}{2m}+\frac{\hbar\Omega}{2}\hat{\sigma}_x+\frac{\hbar\delta}{2}\hat{\sigma}_z+U_0\sin^2\left(k_l\hat{z}\right)-F\hat{z}, \tag{1}$$

in which the SO coupling is embodied in the effective vector potential $\hat{A}=-m\alpha\hat{\sigma}_z$ ($\alpha=\hbar k_R/m$ characterizes SO coupling strength with k_R the Raman beam wavevector), Ω is the Raman coupling strength with δ the two-photon detuning. The periodic potential is characterized by the depth U_0 and period $d=\pi/k_l$.

By performing lowest energy band truncation and assuming tight binding approximation, Hamiltonian (1) can be expanded in the σ-Wannier basis $|j,\sigma\rangle$ as

$$\begin{aligned}\hat{H}=\sum_j\Bigg\{\Bigg[&-\frac{J}{2}\cos\left(\pi\gamma\right)\sum_\sigma|j,\sigma\rangle\langle j+1,\sigma|\\&+i\frac{J}{2}\sin\left(\pi\gamma\right)\left(|j,\uparrow\rangle\langle j+1,\uparrow|-|j,\downarrow\rangle\langle j+1,\downarrow|\right)\\&+\frac{\hbar\Omega}{2}|j,\uparrow\rangle\langle j,\downarrow|+H.c.\Bigg]-Fd\sum_\sigma j\,|j,\sigma\rangle\langle j,\sigma|\\&+\frac{\hbar\delta}{2}\left(|j,\uparrow\rangle\langle j,\uparrow|-|j,\downarrow\rangle\langle j,\downarrow|\right)\Bigg\}\end{aligned} \tag{2}$$

in which the spin-dependent hopping matrix element $\hat{T}=J\exp\left(-i/\hbar\int\hat{A}dl\right)/2$ is obtained through Peierls substitution, J is the tunneling amplitude without SO coupling, $\gamma=k_R/k_l$. J can be calculated as

$$J=-2\int dz w_{j+1}\left(z\right)\left[-\frac{d^2}{dz^2}+U_0\sin^2\left(k_lz\right)\right]w_j\left(z\right), \tag{3}$$

with $w_j\left(z\right)=w_j\left(z-z_j\right)$ is the Wannier state of the lowest energy band at the j-th site which can be obtained numerically. Here we consider the case of $U_0>0$ with $z_j=jd$.

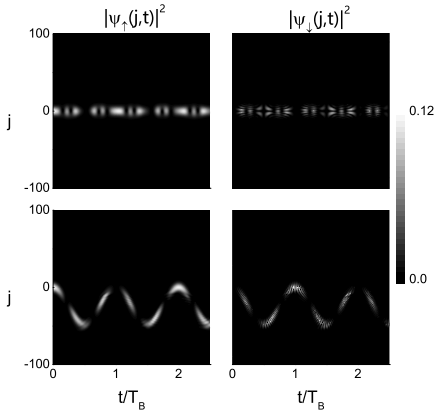


Figure 1: Dynamics of $|\psi_\uparrow|^2$and $|\psi_\downarrow|^2$. The atoms are initially prepared in a Gaussian wavepacket centered at the lattice site $j=0$.

Based on the model we calculate the Bloch oscillation dynamics, the results are shown in Fig. 1, which display nontrivial properties.

[1] C. Hamner, Y. Zhang, M. A. Khamehchi, M. J. Davis, and P. Engels, Phys. Rev. Lett. **114**, 070401 (2015).

Turning-off two-body and generating three-body interactions between ultracold neutral bosonic atoms

Philip R. Johnson[1], **Saurabh Paul**[2], **and Eite Tiesinga**[2]

[1] *Dept. of Physics, American University, Washington DC 20016 USA*

[2] *Joint Quantum Institute and Center for Quantum Information and Computer Science, National Institute of Standards and Technology and University of Maryland, Gaithersburg MD 20899 USA*

e-mail: *pjohnson@american.edu*

We discuss our recent work showing how the effect of pair-wise (two-body) interactions between ultracold neutral bosonic atoms can be suppressed, to generate a low-energy Hamiltonian in which attractive three-body interactions are dominant. Our results rely on either adjusting the strength of a trapping potential or exploiting a Feshbach resonance such that there is a cancellation between the influence of the scattering length and effective range contributions to two-body interactions, while leaving an effective three-body interaction that is of sufficient magnitude to be experimentally observed. For van-der-Waals potentials, which for example describe scattering of alkaline-earth atoms, we find that turning off pair-wise interactions requires atoms with a small negative scattering length (e.g., the Sr88 isotope is a possible candidate). For atoms with collisional magnetic Feshbach resonances this restriction does not apply, and we show examples involving several known narrow resonances between alkali-metal as well as chromium atoms. Using these results, we simulate the coherent collapse-and-revival dynamics of ultracold bosons with dominant three-body interactions in optical lattices, and discuss experimental observables.

Scale-dependent anomalous diffusion in spatially disordered environments

G. Muñoz-Gil[1], **M.A. Garcia-March**[1], **and M. Lewenstein**[1,2]

[1] *ICFO – Institut de Ciències Fotòniques, The Barcelona Institute of Science and Technology, 08860 Castelldefels (Barcelona), Spain*

[2] *ICREA, Lluis Companys 23, E-08010 Barcelona, Spain*

e-mail: *gorka.munoz@icfo.eu*

The understanding of the diffusion of particles in complex environments is of key interest in many fields of science, from classical to quantum physics, chemistry, biology,... The study of such motion provides information both from the particle and the environment where it moves. An example is the motion of impurities in ferromagnetic materials, which allows for interesting behaviors not only from the impurities, but also of the materials, due to the back reaction.

It is usual to simulate such materials with the Ising model, which offers a simple playground from which one can understand very complex systems. In Ref. [1] we studied how the coupling between a particle and an Ising environment gives rise to anomalous, non-ergodic diffusion of the particle. When anomaly diffusing, the motion can be sub(super)diffusive when the variance of the position grows non-linearly in time as

$$\langle x^2(t)\rangle \propto t^{\alpha}, \tag{1}$$

with $0 < \alpha < 1$ ($\alpha > 1$).

In systems where the particle moves through a complex environment, its motion is closely related to their interaction. In Ref. [1] we illustrated this for a complex Ising environment where the presence of stochasticity in the particle-environment interaction causes the particle to diffuse anomaly. Such findings can be used to explain many experimental observations, from particles moving in Bose-Einstein condensates to proteins in cell membranes. In this contribution we investigate a simple mechanism able to justify the interaction between particle and the Ising environment postulated in [1]. This is, a random walk of a particle in an environment with random length/area compartments, just as the cluster distribution of the Ising model. The compartments are separated by boundaries of random transmittance. In this work, we show how the presence of a spatial scale in the system gives rise to different prediction on the type of diffusion, depending on the scale it is measured.

Concretely, the system under consideration comprises a compartmentalized environment, where each compartment has a given size L (see blue indicators in Fig. 1). Moreover, we consider that the boundary between compartments has a certain transmittance T. One can then calculate the exit time of a particle

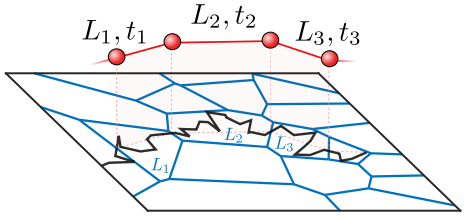


Figure 1: Two dimensional example of the system under consideration: a particle moving in a compartmentalized space. The motion of the particle can be characterized by in the microscopic (black) or macroscopic (red) scale.

inside a compartment as

$$\phi(t|T,L) = \frac{T}{L}\exp\left(-t\frac{T}{L}\right), \tag{2}$$

which holds for 1D and can be extended to more dimensions by means of normalization constants.

Now, one can characterize the motion of the particle in two scales. In the first scale, the *macroscopic* scale (red line in Fig.1), one considers that we can only retrieve information from the position of the party when it exits a compartment. The behavior of the particle is then characterized as Lévy Walk with step size the size of the compartment and step time given by Eq. (2). As an example, we consider that the size of the compartments has a PDF $g(x) = x^{-1-\beta}$ (notice here that for the 2D case this corresponds to the cluster size distribution from a critical Ising environment); on top of this we assume that the transmittances of the boundaries follow a PDF $P(q) = q^{-1-\alpha}$. With this, the variance of the position is

$$\langle x^2(t)\rangle_M \propto t^{2-\beta+\min(\alpha,\beta)}. \tag{3}$$

In the second scale, the *microscopic* scale, one considers that we can track the position of the particle at every time step. Our work shows that, if one considers a system with spatial disorder, such as the one presented in Eq. (3), there will be a mismatch in the variance of the position between the two scales. Particularly, for the previous example, one finds for the microscopic scale

$$\langle x^2(t)\rangle_\mu = \sqrt{\langle x^2(t)\rangle_M}. \tag{4}$$

[1] G. Muñoz-Gil *et al.*, Phys. Rev. E **96**, 052140 (2017).

Quantum noise in a transversely pumped cavity Bose–Hubbard model

Dávid Nagy, Gábor Kónya, Peter Domokos, and Gergely Szirmai
Institute for Solid State Physics and Optics, Wigner Research Centre for Physics, Hungarian Academy of Sciences, H-1525 Budapest P.O. Box 49, Hungary
e-mail: *szirmai.gergely@wigner.mta.hu*

We investigate the quantum measurement noise effects on the dynamics of an atomic Bose lattice gas inside an optical resonator. We describe the dynamics by means of a hybrid model consisting of a Bose–Hubbard Hamiltonian for the atoms and a Heisenberg–Langevin equation for the lossy cavity field mode. We assume that the atoms are prepared initially in the ground state of the lattice Hamiltonian and then start to interact with the cavity mode. We show that the cavity field fluctuations originating from the dissipative outcoupling of photons from the resonator lead to vastly different effects in the different possible ground state phases, i.e., the superfluid, the supersolid, the Mott- and the charge-density-wave phases. In the former two phases with the presence of a superfluid wavefunction, the quantum measurement noise appears as a driving term leading to depletion of the ground state. The time scale for the system to leave the ground state is presented in a simple analytical form. For the latter two incompressible phases, the quantum noise results in the fluctuation of the chemical potential. We derive an analytical expression for the corresponding broadening of the quasiparticle resonances.

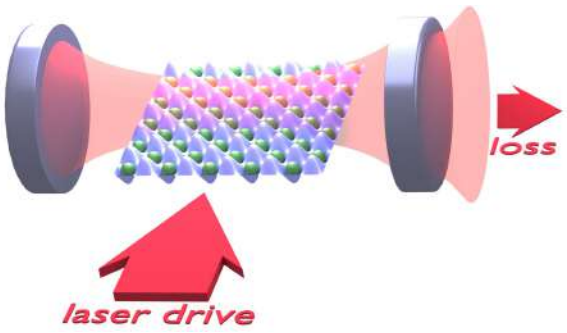


Figure 1: Schematic plot of the system. Ultracold bosons are loaded into an optical lattice, which is inside a single-mode Fabry-Prot resonator. The optical lattice is formed by external laser drives. The wavelength of the lattice matches that of the single-mode of the cavity. The cavity is pumped transversely, through the atoms, by an additional laser, detuned slightly below resonance.

[1] D. Nagy, G. Kónya, P. Domokos, and G. Szirmai, Phys. Rev. A (accepted), arXiv:1803.06014

Out-of-equilibrium many-body systems: a numerical approach based on non-equilibrium Green's functions

N.W.Talarico[1], **S. Maniscalco**[1,2], **and N. Lo Gullo**[1]

[1] *QTF Centre of Excellence, Turku Centre for Quantum Physics, Department of Physics and Astronomy, University of Turku, 20014 Turku, Finland*

[2] *QTF Centre of Excellence, Department of Applied Physics, Aalto University, FI-00076 Aalto, Finland*

e-mail: *natale.talarico@utu.fi*, *nicolino.logullo@utu.fi*, *sabrina.maniscalco@utu.fi*

In recent years there has been a growing interest in the study of the dynamics of many-body quantum systems. The reasons are manifold, ranging from purely theoretical interests in the behavior of complex quantum systems when brought out-of-equilibrium to the possibility of exploiting unusual quantum mechanical properties in technological applications. Non-equilibrium Green's functions theory provides a versatile approach to study out-of-equilibrium systems in correlated matter starting from a microscopic description[1]. The power of the method relies on the possibility to study a wide range of different phenomena: from the time-dependent quantum transport in nanosystem, to the post-quench dynamics in ultracold atomic gases, to driven quantum systems which are useful in modeling, for instance, quantum heat engines. The technique is based on the self-consistent solution of the Dyson equation for the interacting single-particle Green's function once a proper choice of the self-energy, which is a functional of the single-particle Green's function itself, has been made[2]. For our purpose, we use the second Born approximation to describe strongly correlated system where the dominant contribution to particle-particle interaction is short-range in nature. This scheme is then implemented numerically by a parallelized code which exploits the symmetries of the different quantities and the structure of the equations of motion. We show how this method gives access to different physical and experimentally relevant quantities such as the steady-state density, the density of states, and the spectral function. As an application of our approach we present two studies: 1) the thermalization process of an interacting quantum dot coupled with an infinite non-interacting reservoir[3], as well 2) the spreading of correlation of interacting electrons in a one dimensional lattice with an incommensurate Aubry-André potential[4].

[1] G. Stefanucci and R. van Leeuwen, Nonequilibrium Many-Body Theory of Quantum Systems: A Modern Introduction (Cambridge University Press, 2013).

[2] A. Stan, N. E. Dahlen, and R. v. Leeuwen, J. Chem. Phys. 130, 224101 (2009).

[3] C. D. Spataru, M. S. Hybertsen, S. G. Louie, and A. J. Millis, Phys. Rev. B 79, 155110 (2009).

[4] H.P. Lschen, P. Bordia, S. Scherg, F. Alet, E. Altman, U. Schneider, and I. Bloch, Phys. Rev. Lett. 119, 260401 (2017).

A many-ion quantum simulator of the Dicke model for probing entanglement, chaos and information scrambling

R. J. Lewis-Swan[1], **A. Safavi-Naini**[1], **and A. M. Rey**[1]

[1] *JILA, NIST and University of Colorado, 440 UCB, Boulder, CO 80309, USA*

[2] *Center for Theory of Quantum Matter, University of Colorado, Boulder, CO 80309, USA*

e-mail: *robert.lewisswan@colorado.edu*

The Dicke Hamiltonian is an iconic model in cavity QED, describing the coupling of a (large) spin and an oscillator, which is of broad interest as it exhibits rich physics including quantum phase transitions and non-ergodic behaviour. We recently reported an implementation of the Dicke model in a quantum simulator using a two-dimensional planar crystal of ~ 70 ions [1]. We accomplished this by using a pair of lasers to couple the vibrational (phonon) modes of the crystal to the ions (spins) in the presence of an external transverse field. We benchmarked our quantum simulator by measuring full spin distribution functions for slow quenches across the quantum phase transition between the normal and superradiant phases. We benchmark the quantum dynamics by experimentally measuring full spin distribution functions, whilst also inferring the build-up of spin-phonon correlations.

The Dicke model is known to show chaos in the related classical model, thus our trapped-ion quantum simulator opens the way for investigation of a range of related phenomena such as quantum chaos, thermalization, entanglement propagation and the scrambling of quantum information. In particular, we propose to study these features using 'out-of-time-order' correlations (OTOCs) accessible, as recently demonstrated, by time-reversal of the quantum dynamics [2].

We find the ergodic/non-ergodic transition is characterised by the build-up (or absence) of entanglement between the spin and phonon degrees of freedom, whilst thermalization is signalled by extensive 'volume-law' entanglement in more general bipartitions of the system. Crucially, we find that both features are also apparent in experimentally measurable OTOCs. We show this result is a consequence of an intimate and striking correspondence between OTOCs and the Renyi entanglement entropy, paving the way for potentially detailed characterisation of entanglement in large many-body quantum systems.

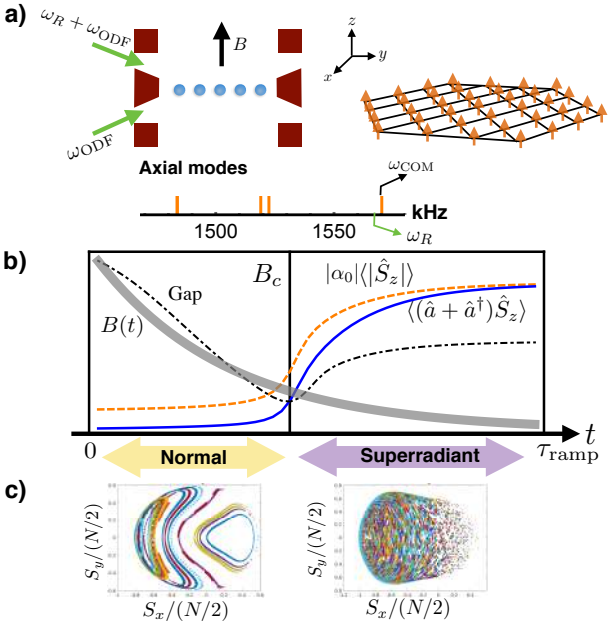


Figure 1: Implementation and dynamical protocol. (a) The Dicke model is engineered with a Penning trap ion crystal of $N \sim 70$ ions by applying an optical dipole force, resonant only with the center of mass mode (which generates spin-phonon interactions) and resonant microwaves (which generates the transverse field). The system is initially prepared in the normal phase where all the spins point along the transverse field and are decoupled from the phonons. (b) As the transverse field is slowly turned off [using linear or exponential ramp (shown here) profiles] the system enters the superradiant phase after crossing the quantum critical point at $B(t_{\text{crit}}) = B_c$ where the gap closes. The superradiant phase with macroscopic phonon population, ferromagnetically aligned spins and large spin-phonon entanglement is described by the order parameter $\langle(\hat{a}+\hat{a}^\dagger)\hat{S}_z\rangle$, which is tracked closely by the re-scaled spin observable $|\alpha_0|\langle|\hat{S}_z|\rangle$. (c) The classical model is known to exhibit chaos, characterised by a transition between ergodic and regular dynamics coinciding with the superradiant and normal phases respectively. We illustrate this with representative Poincare sections for a fixed energy E above the ground state configuration of the two phases.

[1] A. Safavi-Naini, R. J. Lewis-Swan, *et. al.*, *Verification of a many-ion simulator of the Dicke model through slow quenches across the quantum critical point*, Submitted to Phys. Rev. Lett.

[2] M. Gärttner *et. al.*, *Measuring out-of-time-order correlations and multiple quantum spectra in a trapped ion quantum magnet*, Nat. Phys., **13**, 781 (2017)

Relaxation dynamics of non-equilibrium quantum gas in a uniform box potential

Jinyi Zhang [1], **Christoph Eigen** [1], **Robert Smith** [1], **Zoran Hadzibabic** [1]**and Nir Navon**[1,2]
[1] *Cavendish Laboratory, University of Cambridge, J. J. Thomson Avenue, Cambridge, CB3 0HE, UK*
[2] *Department of Physics, Yale University, New Haven, Connecticut 06511, USA*
e-mail: *jz439@cam.ac.uk*

Turbulent flow remains as the most important unsolved problem of classical physics as Feynman pointed out. In 1941, Kolmogorov and Obukhov [1, 2] introduced the universality hypothesis for inertial range where no dissipation occurs. This idea gives rise to a dimensional argument and the famous Kolmogorov−Obukhov spectrum can be predicted, which was a landmark in the theoretical framework of turbulence.

Recently, ultracold atomic gases have emerged as a novel platform for studies of vortex turbulence [3, 4, 5, 6, 7] and wave turbulence [8], which offers new experimental possibilities. In our previous experiment, we prepare a ^{87}Rb Bose−Einstein condensate (BEC) in a homogeneous box trap [9] and drive it out of equilibrium via a continuous oscillating magnetic gradient force along the axial direction, which leads to a turbulent atomic cloud and meanwhile momentum distribution reveals the direct cascade characterised by an isotropic power-law distrubition [8].

Right now, in the ongoing project, we would like to investigate the relaxation process after the strongly shaking process, i.e. relaxation of non-equilibrium state. A general conceptual understanding for the relaxation dynamics of quantum many−body system prepared far out of equilibrium remains a largely open question [10]. Especially, it is intriguing to ask to what extent analogues of the universal behaviour arising from the equilibrium theory of critical phenomena may exist for non−equilibrium systems. We study the coherence reemerging during the phase ordering formation of BEC after shaking. For that reason, we measure spatial two point correlation function to characterise the relaxation dynamics from non-equilibrium state to equilibrium BEC state. In the experiment, a pair of Bragg pulses (Ramsey type pulses) can be utilized to measure correlation function [11, 12], therefore, correlation length for different relaxation time is extracted. We plot the correlation length as a function of relaxation time in the double logarithmic coordinates for different parameters, which strongly demonstrates a universal scaling behaviour of the growth of correlation length $l(t) \sim t^{1/z}$, where the exponent $1/z$ is around 1.1.

[1] Kolmogorov, A. N. Dokl. Akad. Nauk SSSR 30, 299−303 (1941)

[2] Obukhov, A. Dokl. Akad. Nauk SSSR 32, 22−24 (1941)

[3] E. A. L. Henn, J. A. Seman, G. Roati, K. M. F. Magalhes, and V. S. Bagnato, Phys. Rev. Lett. 103, 045301 (2009)

[4] T. W. Neely, A. S. Bradley, E. C. Samson, S. J. Rooney, E. M. Wright, K. J. H. Law, R. Carretero-González, P. G. Kevrekidis, M. J. Davis, and B. P. Anderson, Phys. Rev. Lett. 111, 235301 (2013)

[5] Woo Jin Kwon, Geol Moon, Jae-yoon Choi, Sang Won Seo, and Yong-il Shin, Phys. Rev. A 90, 063627 (2014)

[6] Shaun P. Johnstone, Andrew J. Groszek, Philip T. Starkey, Christopher J. Billington, Tapio P. Simula, Kristian Helmerson, arXiv:1801.06952 (2018)

[7] Guillaume Gauthier, Matthew T. Reeves, Xiaoquan Yu, Ashton S. Bradley, Mark Baker, Thomas A. Bell, Halina Rubinsztein-Dunlop, Matthew J. Davis, Tyler W. Neely, arXiv:1801.06951 (2018)

[8] Nir Navon, Alexander L. Gaunt, Robert P. Smith, Zoran Hadzibabic, Nature 539, 72 (2016)

[9] Alexander L. Gaunt, Tobias F. Schmidutz, Igor Gotlibovych, Robert P. Smith, and Zoran Hadzibabic, Phys. Rev. Lett. 110, 200406 (2013)

[10] Isara Chantesana, Asier Piñeiro Orioli, Thomas Gasenzer, arXiv:1801.09490 (2018)

[11] E. W. Hagley, L. Deng, M. Kozuma, M. Trippenbach, Y. B. Band, M. Edwards, M, Doery, P. S. Julienne, K. Helmerson, S. L. Rolston, and W. D. Phillips, Phys. Rev. Lett. 83, 3112 (1999)

[12] Nir Navon, Alexander L. Gaunt, Robert P. Smith, Zoran Hadzibabic, Science 347, 167 (2015)

Nonlinear damping of quantum gas at ultra−low temperature in a cylindrical box potential

Jinyi Zhang [1], **Wei Zheng** [1], **Christoph Eigen** [1], **Robert Smith** [1], **Nigel Cooper** [1], **Zoran Hadzibabic** [1] **and Nir Navon** [1,2]

[1] *Cavendish Laboratory, University of Cambridge, J. J. Thomson Avenue, Cambridge, CB3 0HE, UK*
[2] *Department of Physics, Yale University, New Haven, Connecticut 06511, USA*
e-mail: *jz439@cam.ac.uk*

Damping of low−energy excitation of a Bose−Einstein condensate (BEC) in a trap is one of the most fascinating peculiarities in the physics of quantum degenerate gases, such as Landau damping [1, 2, 3] and Beliaev damping [4] have been extensively experimentally investigated in the harmonic trap.

In our previous experiment, we investigate the lowest-lying, axial mode [5, 6] of a BEC confined in a cylindrical box trap [7]. This mode in the hydrodynamic regime was previously exploited as a route to wave turbulence [6].

Here, we would like to investigate the nonlinear damping [8] of shaking quasi pure BEC in the box trap, where nonlinear damping means damping rate depends on shaking strength. In the experiment, we both focus on frequency domain gives rise to the nonlinear stroboscopic spectrum and time domain leads to time series (non)linear response function. In the stroboscopic spectrum, we show driven oscillation versus shaking strength (ΔU) and observe increasing ΔU both shifts and broaden the resonance, especially for very large ΔU, which demonstrates the system to be a nonlinear oscillator. In the time series, we measure the response functions. Appealing to linear response theory (Kubo formula) for linear regime, center of mass (CoM) position is directly related to the global optical conductivity of the system [9, 10]. While, in the nonlinear regime, breathing mode signals can be extracted from Fourier analysis to the transverse width of the atomic cloud.

In the theory aspect, we employ Keldysh formalism to understand the nonlinear damping mechanism. Shaking the box can inject energy to the system and excite dipole mode in the axial direction. Since the dipole mode is the lowest−lying mode, Beliaev damping is prohibited. Meanwhile, dipole mode couples to the transverse breathing mode via nonlinear interaction due to the box shape. Thus, two dipole modes annihilate and two breathing modes create, vice versa. Therefore, it leads to effective two−body loss for the dipole mode, and furthermore, gives rise to the nonlinear damping which is satisfied with the experimental emerging of breathing mode.

[1] D. S. Jin, M. R. Matthews, J. R. Ensher, C. E. Wieman, and E. A. Cornell, Phys. Rev. Lett. 78, 764 (1997)

[2] M.-O. Mewes, M. R. Andrews, N. J. van Druten, D. M. Kurn, D. S. Durfee, C. G. Townsend, and W. Ketterle Phys. Rev. Lett. 77, 988 (1996)

[3] D. M. Stamper-Kurn, H.-J. Miesner, S. Inouye, M. R. Andrews, and W. Ketterle, Phys. Rev. Lett. 81, 500 (1998)

[4] N. Katz, J. Steinhauer, R. Ozeri, and N. Davidson, Phys. Rev. Lett. 89, 220401 (2002)

[5] S. J. Garratt, C. Eigen, J. Zhang, P. Turzák, R. Lopes, R P. Smith, Z. Hadzibabic and N. Navon, preparing

[6] Nir Navon, Alexander L. Gaunt, Robert P. Smith, Zoran Hadzibabic, Nature 539, 72 (2016)

[7] Alexander L. Gaunt, Tobias F. Schmidutz, Igor Gotlibovych, Robert P. Smith, and Zoran Hadzibabic, Phys. Rev. Lett. 110, 200406 (2013)

[8] Yu. Kagan and L.A. Maksimov, Physics Letters A 317 477 (2003)

[9] Zhigang Wu, Edward Taylor, Eugene Zaremba, EPL 110, 26002 (2015)

[10] Rhys Anderson, Fudong Wang, Peihang Xu, Vijin Venu, Stefan Trotzky, Frdric Chevy, Joseph H. Thywissen, arXiv:1712.09965

Floquet-Gibbs state for dissipative quantum systems

Tatsuhiko Shirai[1], **Takashi Mori**[2], **and Seiji Miyashita**[2]
[1] *Institute for Solid State physics, University of Tokyo, Japan*
[2] *Department of Physics, University of Tokyo, Japan*
e-mail: *shirai@exa.phys.s.u-tokyo.ac.jp*

Time periodic driving field provides one of the typical non-equilibrium situations, and it is implemented in wide range of fields such as quantum optics, condensed matter physics, and cold atom physics. The Hamiltonian is given by

$$H(t) = H(t+T), \tag{1}$$

where T is the period of the driving field. Due to the time periodicity of the Hamiltonian, we can introduce a time-independent Hamiltonian called the Floquet Hamiltonian $H_{\rm F}$, which is defined by a time-evolution operator over one period, i.e.,

$$e^{-\frac{i}{\hbar}H_{\rm F}T} \equiv \mathcal{T} e^{-\frac{i}{\hbar}\int_0^T H(t)dt}, \tag{2}$$

where $\mathcal{T}$ is a time-ordering operator. The Floquet Hamiltonian $H_{\rm F}$ gives a full description of the coherent dynamics at stroboscopic times, i.e. $t = nT (n \in \mathbb{Z})$, and thus it is relevant for the description of the *isolated* periodically driven systems. The design of $H_{\rm F}$ with a well-controlled driving field now provides a new method to control macroscopic phases [1, 2].

In this presentation we discuss a *thermodynamic* relevance of the Floquet Hamiltonian. Namely, we introduce the Floquet-Gibbs state,

$$\rho_{\rm FG} \equiv \frac{e^{-\beta H_{\rm F}}}{{\rm Tr}[e^{-\beta H_{\rm F}}]}, \tag{3}$$

and discuss whether or not the driven system in contact with a thermal bath is relaxed to this state after a sufficiently long time. The general asymptotic states of the periodically driven systems are extremely complex, but we found that in some class of models the Floquet Hamiltonian is thermodynamically relevant.

The theoretical framework for the relaxation dynamics is formulated by considering a thermal bath in addition to the system of interest. The reduced system with a weak system-bath coupling obeys a Markovian quantum master equation:

$$\frac{d\rho(t)}{dt} = -\frac{i}{\hbar}[H(t), \rho(t)] + \gamma\Gamma[\rho(t)], \tag{4}$$

where $\rho(t)$ is the reduced density matrix of the system of interest. The second term of r.h.s. represents the dissipation effects due to the coupling to the thermal bath, and the strength of the dissipation is denoted by γ. After a sufficiently long time, the reduced density matrix approaches a time-periodic state, which is here compared with the Floquet-Gibbs state.

We first discuss quantum systems with infinitesimal system-bath coupling $\gamma \to 0$. We obtain the sufficient conditions for the realization of the Floquet-Gibbs state as follows [3]:

1. The driving frequency is much larger than the spectral width of the system Hamiltonian
2. The driving Hamiltonians commute with itself at different instants of time
3. The driving Hamiltonian and the system-bath interaction Hamiltonian commute.

These conditions severely restrict a class of suitable physical models attaining the Floquet-Gibbs state. The condition 1 restricts the system with a relatively small Hilbert space and the condition 3 requires a fine tuning of the system-bath coupling. With the aid of a truncated Floquet Hamiltonian in the Floquet-Magnus expansion and without the rotating wave approximation, we lift the condition of the infinitesimal coupling strength and extend the idea of the Floquet-Gibbs state to a broader class of open quantum systems with finite dissipation effect, i.e. finite γ effects. We show in a numerical simulation that the conditions 1 and/or 3 can be lifted by imposing conditions on timescales of the three constituents, the system of interest, thermal bath, and driving field [4].

[1] M. Bukov, L. D'Alessio, and A. Polkovnikov, Adv. Phys. **64**, 139 (2015).

[2] A. Eckardt and E. Anisimovas, New journal of physics **17**, 093039 (2015).

[3] T. Shirai, T. Mori, and S. Miyashita, Phys. Rev. E **91**, 030101 (2015).

[4] T. Shirai, J. Thingna, T. Mori, S. Denisov, P. Hänggi, and S. Miyashita, New Journal of Physics **18**, 053008 (2016).

Formulation of quantum field theory for driven-dissipative Bose–Einstein condensation

Takahiro Oyama[1], **Ryosuke Imai**[1], **and Yoshiya Yamanaka**[1]

[1] *Department of Electronic and Physical Systems, Waseda University, Tokyo 169-8555, Japan*

e-mail: *dice-o.soeztf@fuji.waseda.jp*

It is reported in recent years that Bose–Einstein condensates in driven-dissipative nonequilibrium systems have been created experimentally. In particular, the exciton-polariton condensates were observed in the experiments using quantum well excitons and microcavity photons [1, 2, 3]. Then, the systems with a driving force and photon dissipation are in nonequilibrium, and the condensation is called as nonequilibrium Bose-Einstein condensation (BEC) in distinction from the BEC in equilibrium.

So far the nonequilibrium BEC has been studied mainly within the mean-field approximation, namely by the phenomenological dissipative Gross-Pitaevskii (GP) equation, which is obtained by adding driven-dissipative terms to the ordinary GP equation for an isolated system. In order to go beyond the mean-field theory that ignores some quantum fluctuations, we employ quantum field theory (QFT) for a description of the driven-dissipative system rather strictly. The formulation in QFT promotes discussions on symmetries of the system. In QFT, BEC is interpreted as the spontaneous symmetry breaking (SSB) whether for equilibrium or nonequilibrium, and then there must exist a zero excitation energy mode, called zero mode, according to Nambu-Goldstone's theorem [4, 5]. We emphasize that the quantum fluctuation of the zero mode becomes large for finite-size and that the zero mode is relevant then. For an isolated system, we have proposed a new formulation to take the zero mode into account properly [6]. The formulation can be extended straightforwardly to the driven-dissipative system. This way we can investigate the BEC of the driven-dissipative finite-size system, based on QFT with SSB and the zero mode.

To deal with the open nonequilibrium system in QFT, we start from the Gorini-Kossakowski-Lindblad-Sudarshan (GKLS) equation [7], which describes a Markovian temporal evolution of the density operator. Using the superoperator correspondence [8], GKLS equation can be reformulated in Thermo Field Dynamics (TFD) [9, 10] that is a real-time canonical formalism of QFT in thermal situations (both of equilibrium and nonequilibrium). We adopt TFD because of its clear and definite quasi-particle picture, which is an important concept in QFT. In TFD formalism we consider BEC, which implies that an original field operator $\hat{\psi}(\boldsymbol{x},t)$ is divided into the order parameter $\xi(\boldsymbol{x},t)$ and a new field operator $\hat{\phi}(\boldsymbol{x},t)$, $\hat{\psi}(\boldsymbol{x},t) = \xi(\boldsymbol{x},t) + \hat{\phi}(\boldsymbol{x},t)$. We introduce the TFD Hamiltonian that gives the driven-dissipative GP equation at the level of the mean-field approximation. The field operator $\hat{\phi}(\boldsymbol{x},t)$, whose Heisenberg equation is also derived from the TFD Hamiltonian, describes the excitation modes on BEC and the zero mode. The diagonalization of the Hamiltonian for $\hat{\phi}(\boldsymbol{x},t)$ determines the spectrum of the excitation modes. We can also argue on the dynamical behaviors of the zero mode and its quantum fluctuation.

In this study, we introduce the formulation of QFT for the driven-dissipative BEC and analyze the effects of quantum fluctuations and the zero mode, comparing to the corresponding isolated system.

[1] J. Kasprzak, et al., Nature (London) **443**, 409 (2006).

[2] K. G. Lagoudakis, et al., Nat. Phys. **4**, 706 (2008).

[3] G. Roumpos, et al., Proc. Natl. Acad. Sci. USA **109**, 6467 (2012).

[4] Y. Nambu and G. Jona-Lasinio, Phys. Rev. **122**, 345 (1961).

[5] J. Goldstone, A. Salam, and S. Weinberg, Phys. Rev. **127**, 965 (1962).

[6] J. Takahashi, Y. Nakamura, and Y. Yamanaka, Phys. Rev. A **92**, 023627(2015).

[7] V. Gorini and A. Kossakowski, J. Math. Phys. **17**, 821 (1976).

[8] Z. Schmutz, Z. Phys. B. **30**, 97 (1978).

[9] H. Umezawa, *Advanced Field Theory — Micro, Macro, and Thermal Physics* (AIP, New York, 1993).

[10] Y. Nakamura and Y. Yamanaka, Ann. Phys. **331**, 51 (2013).

Non-equilibrium phase structure and dynamics of driven-dissipative Rydberg spin systems

S. Helmrich[1], **A. Arias**[1,2], **G. Lochead**[1,2], **M. Buchhold**[3], **S. Diehl**[4], **S. Whitlock**[1,2]

[1] *Physikalisches Institut, Universität Heidelberg, Im Neuenheimer Feld 226, 69120 Heidelberg, Germany*

[2] *IPCMS and ISIS, University of Strasbourg and CNRS, 67000 Strasbourg, France*

[3] *Department of Physics and Institute for Quantum Information and Matter, California Institute of Technology, Pasadena, CA 91125, USA*

[4] *Institut für Theoretische Physik, Universität zu Köln, 50937 Cologne, Germany*

e-mail: *helmrich@physi.uni-heidelberg.de, whitlock@ipcms.unistra.fr*

Statistical mechanics provides a powerful framework for understanding and classifying states of matter close to thermal equilibrium. However, many systems found in nature are not in thermodynamic equilibrium, as, for instance, their inevitable coupling to the environment can give rise to fundamentally new behaviour. Understanding open quantum many-body systems poses a significant challenge, since theoretical methods capable of dealing with such scenarios are less developed and it is experimentally difficult to devise observables capable of distinguishing their vastly different types of behaviour.

Here we experimentally investigate the long-time dynamics and phase structure of an open quantum spin system [1]. This system consists of a cloud of ultracold atoms laser-excited from the ground state to a Rydberg state, leading to a strong interplay between coherent driving, dissipation (e.g. due to spontaneous decay) and interactions [Figure 1(a)]. We demonstrate that the overall rate of population loss due to the decay of excited states provides a convenient macroscopic observable for the many-body state. We discover that this observable exhibits approximate power law scaling as a function of the Rabi frequency of the driving field (with exponent α). By combining our experimental observations with mean field and many-body rate equation simulations, we map out the non-equilibrium phase diagram of this system [Figure 1(b)]. It exhibits crossovers to two distinct many-body regimes: (i) from the dissipation-dominated regime to a critical regime governed by collectively enhanced atom-light interactions, and (ii) an instability which drives the system to an active regime that is linked to the presence of an absorbing state phase transition [2].

Furthermore we explore the full dynamics of the driven-dissipative system under the conditions of facilitated excitation and slow loss of excited atoms out of the system. In contrast to previous studies which treated loss as something to be avoided, we show that the non-conservation of population is a crucial ingredient of the nonlinear dynamics that drives the system to a stationary state that is independent of the initial conditions. Our measurements show that this state exhibits scale invariance and a strong response to external perturbations characteristic of self-organised criticality [3].

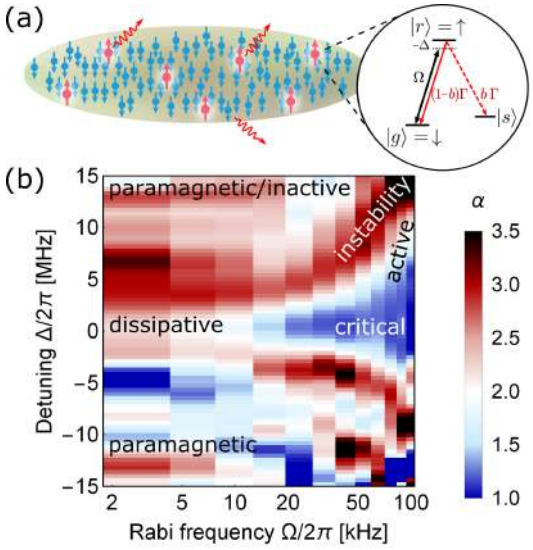


Figure 1: (a) Rydberg spin system comprising a cloud of atoms in the ground state (blue arrows) laser-driven to Rydberg states (red arrows). (b) Non-equilibrium phase diagram determined from the local scaling exponent α (adapted from [1]).

These experiments establish Rydberg atoms as a well controlled platform for exploring non-equilibrium phases of matter and for testing fundamental concepts of non-equilibrium statistical mechanics with unprecedented access to the underlying microscopic properties of the system.

This research is supported by the DFG Collaborative Research Center "SFB 1225 (ISOQUANT)" and the "Investissements d'Avenir" programme through the Excellence Initiative of the University of Strasbourg.

[1] S. Helmrich, A. Arias and S. Whitlo5ck arXiv:1605.08609.

[2] R. Gutiérrez, C. Simonelli, M. Archimi et al, Phys. Rev. A 96, 041602(R) (2017).

[3] P. Bak, C. Tang, and K. Wiesenfeld, Phys. Rev. Lett. 59, 381 (1987).

Exploring extreme nonequilibrium dynamics with ultracold atoms

T. Shimasaki, R. Senaratne, S. V. Rajagopal, K. M. Fujiwara, K. Singh, Z. A. Geiger, P. E. Dotti, M. Lipatov, Q. Simmons, and D. M. Weld
University of California Santa Barbara, 93106 California, USA
e-mail: *weld@ucsb.edu*

We report recent results from several nonequilibrium dynamics experiments performed in the Weld group at UC Santa Barbara.

First, we will discuss the experimental realization of a physical quantum simulator of ultrafast phenomena, in which a time-varying force on neutral atoms in a tunable optical trap emulate the electric eld of a pulsed laser acting on electrons or nuclei in a binding potential [1]. The simulator operates in regimes equivalent to those of ultrafast and strong- eld pulsed-laser experiments, opening up a hitherto unexplored application of quantum simulation techniques and a complementary path towards investigating open questions in ultrafast science. Counterintuitively, this approach emulates some of the fastest processes in atomic physics with some of the slowest, giving rise to a temporal magni cation factor of up to twelve orders of magnitude [2]. The correspondence with ultrafast science is demonstrated by a sequence of experiments: we perform nonlinear spectroscopy of a many-body bound state, control the excitation spectrum by shaping the potential, observe sub-cycle unbinding dynamics during strong few-cycle pulses, and directly measure carrier-envelope phase dependence of the response to an ultrafast-equivalent pulse.

Second, we report on experiments studying phasonic spectroscopy in a tunable quantum quasicrystal. The phasonic degrees of freedom of solid-state quasicrystals (analogues of phonon modes in a regular crystal) are typically not dynamically accessible, and yet are believed to have signi cant e ects on thermal and electronic transport. We directly drive such a phason mode in a bichromatic lattice and observe the atomic excitation as a function of drive parameters. We identify new features of phasonic spectroscopy which distinguish it from the familiar phononically driven excitations of ground band atoms.

In addition to this strontium work we will also report on experiments with ultracold ^{7}Li in a strongly driven optical lattice. In one experiment, we realized and studied a harmonic oscillator in the relativistic regime [3]. The oscillator is composed of ultracold lithium atoms in the third band of an optical lattice, which have an energy-momentum relation nearly identical to that of a massive relativistic particle, with a reduced e ective mass and speed of light. We observed dynamics that are in quantitative agreement with longstanding but hitherto-untested relativistic predictions [4].

Next, we will report a study of Floquet band engineering, in which a driven lattice is used to hybridize and tune the properties of the static Bloch bands. In the absence of driving, we observed position-space center-of-mass Bloch oscillations [5], which allow direct imaging of the band structure. Strikingly, when a drive is applied, we observe that the interplay of momentum-space and real-space evolution in a Floquet-Bloch band leads to large-scale rapid coherent atomic transport across thousands of lattice sites. This "giant Floquet-Bloch oscillation" can be understood as a consequence of reversible Landau-Zener tunneling to and from higher bands with relativistic dispersion. Transport can be precisely regulated via the drive frequency and strength, o ering a simple and powerful tool for atomic control and opening up the possibility of more complex band hybridization.

Finally, we discuss the response of many-body quantum systems to strong driving. The stabilization or destabilization of new states of matter by variation of drive parameters can be encapsulated in Floquet phase diagrams; these maps of system properties as a function of drive parameters can be viewed as a nonequilibrium generalization of thermodynamic phase diagrams. We report on experimental exploration of a Floquet phase diagram using ultracold bosonic lithium in a strongly-driven optical lattice. As the drive frequency and amplitude are tuned into previously unexplored regions, we observe a crossover between stable and unstable behavior, and the onset and destruction of Floquet prethermalization. We explore the e ect of Feshbach-tunable interactions and variable tunneling on the properties of this Floquet phase diagram, and compare the results to classical and quantum theories.

References

[1] R. Senaratne, *et al.*, Nat. Comm. 9, 2065 (2018).

[2] S. Sala *et al.*, Phys. Rev. A 95, 011403 (2017)

[3] K. M. Fujiwara et al., arXiv:1712.09501 [cond-mat.quant-gas] (2017).

[4] W. Moreau *et al.*, Am. J. Phys. 62, 531 (1994).

[5] Z. A. Geiger *et al.*, Phys. Rev. Lett. 120, 213201 (2018).

Universal phase fluctuations in low dimensional quantum systems

Ryan Plestid[1,2] **and D.H.J. O'Dell**[1]

[1] *Department of Physics and Astronomy, McMaster University, 1280 Main St. West, Hamilton, Canada*

[2] *Perimeter Institute for Theoretical Physics, 31 Caroline St. North, Waterloo, Canada*

e-mail: *plestird@mcmaster.ca*

Low-dimensional systems are well known to be characterized by enhanced fluctuations due to the increased density of low energy states. Of particular importance in systems with bosonic elementary excitations are fluctuations of the phase, which are typically maximal (i.e. uniform over the unit circle) for low-dimensional systems. This behaviour has importance consequences such as the destruction of Bose-Einstein condensates for $d \leq 2$ which related to the Mermin-Wagner theorem [**?**]. A natural question to ask is what the consequences of such large fluctuations are for the resultant quantum many-body dynamics and the associated correlation functions.

A similar question has been asked by Berry in the context of optics [2]. In this scenario monochromatic light impinges upon a random phase screen which imprints a phase profile upon the wave being given by $\exp(\mathrm{i}k[z - \Phi(x,t)])$. The limit of large phase fluctuations, at least in this context, is naturally associated with the limit of physical optics, and as a consequence can lead to universal and *non-Gaussian* statistics in the moments of the intensity distribution.

This universality is a consequence of *catastrophe theory* [3] wherein the variations in the intensity can be found by considering the trajectories traced out by random phases on a torus. These eventually "pileup" leading to caustic patterns.

Furthermore, upon including the effects of diffraction these caustic patterns predict universal critical exponents with which the moments of the intensity distribution diverge

$$\lim_{k\to\infty} \langle I^n \rangle \sim k^\nu. \tag{1}$$

Catastrophe theory guarantees that these kinds of statistics are generic, and represent an emergent universal behaviour in the limit of *large* fluctuations in contrast to the Gaussian statistics that emerge due to small fluctuations.

Are there analogous results for quantum many-body systems with large phase fluctuations? In this poster we investigate the role of catastrophe theory in controlling phase fluctuations in low dimensional quantum systems. We examine the possibility of universal, but non-Gaussian, statistics emerging in the limit of strong phase fluctuations.

[1] V. Popov, *Functional integrals and collective excitations*, Cambridge University Press (1987)

[2] M. Berry, J. Phys. A **10**, 12, 2061 (1977).

[3] T. Potson and I. Stewart, *Catastrophe theory and its applications*, Dover Publications, (1977).

Dynamics in an isolated disordered Heisenberg spin system

A. Signoles[1], R. Ferracini Alves[2], T. Franz[2], M. Ferreira-Cao[2], A. Piñeiro Orioli[3], M. Gärttner[4], J. Berges[5,6], S. Whitlock[7], G. Zürn[2], and M. Weidemüller[2,8]

[1] *Institut d'Optique, 2 avenue Augustin Fresnel, 91127 Palaiseau, France*
[2] *Physikalisches Institut, Universität Heidelberg, INF 226, 69120 Heidelberg, Germany*
[3] *JILA, University of Colorado/NIST, 440 UCB, Boulder, CO 80309*
[4] *Kirchhof Institut für Physik, Universität Heidelberg, INF 227, 69120 Heidelberg, Germany*
[5] *Institut für Theoretische Physik, Universität Heidelberg, Philosophenweg 16, 69120 Heidelberg, Germany*
[6] *ExtreMe Matter Institute EMMI, Planckstraße 1, 64291 Darmstadt, Germany*
[7] *IPCMS (UMR 7504) and ISIS (UMR 7006), UNISTRA and CNRS, 67000 Strasbourg, France*
[8] *Hefei National Laboratory for Physical Sciences at the Microscale and Department of Modern Physics, and CAS Center for Excellence*
e-mail: *zuern@uni-heidelberg.de*

Out of equilibrium spin systems with disorder can show extremely slow dynamics as for example known from spin glasses where the magnetization relaxes over several orders of magnitude in time [1]. To investigate such dynamics in the presence of quantum fluctuations we implement an isolated disordered spin system composed of long-range interacting Rydberg atoms [2] which can be described by a Heisenberg XXZ spin model.

Here we present an experiment which disentangles the role of fluctuations stemming from disorder and from quantum fluctuations. Therefore we initially prepare all spins aligned in x-direction which is an eigenstate of the XXZ mean field Hamiltonian (see figure 1). We find strong deviation from this static mean field prediction of the magnetization which instead evolves with a non-exponential decay much slower than the timescale associated to the exchange coupling strength. This is in good agreement with a discrete truncated Wigner approximation [4] revealing that the quantum fluctuations of the initial state determine the time evolution of the magnetization.

By applying a transverse field during the time evolution we observe a sharp asymmetric structure of the magnetization around zero field at long times. This cusp-like behavior can be understood in terms of the explicit symmetry breaking of the XXZ Hamiltonian originally invariant under spin rotations around the z-axis. By comparing our results to predictions of several statistical ensembles we find qualitative disagreement with the prediction of a canonical ensemble indicating that our disordered spin system does not reach thermal equilibrium.

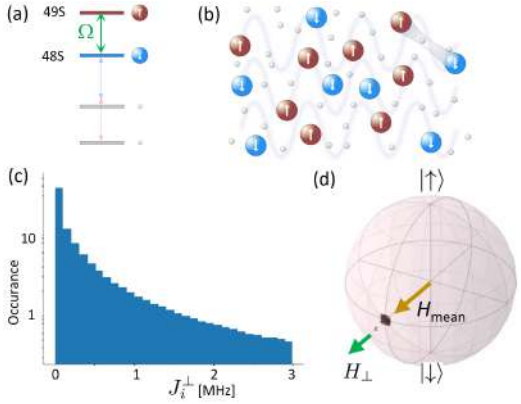


Figure 1: (a) Rydberg spins composed of the atomic states $|48S\rangle = |\downarrow\rangle$ and $|49S\rangle = |\uparrow\rangle$ prepared by laser excitation of ^{87}Rb atoms. Using a two-photon microwave coupling an arbitrary superposition state of $|\uparrow\rangle$ and $|\downarrow\rangle$ can be realized. (b) Sketch of the spatial distribution of the approximately 2000 Rydberg spins with a minimum pair distance of 5 μm determined by the blockade radius of the laser excitation [3]. c) Disorder distribution of the maximum exchange coupling strength $J_i^\perp = \mathrm{Max}\left[\left(J_{ij}^\perp\right)_j\right]$ of each spin derived from the spatial distribution and from the Van der Waals interaction strength between the Rydberg atoms. (d) Initial state of the experiment with all spins prepared in x-direction illustrated by its mean field H_{mean} (orange arrow). Additionally a transverse field $H_\perp = \Omega \sum_i S_i^x$ (green arrow) either aligned or anti-aligned with the initial state can be applied.

[1] J. Bouchaud, Journal de Physique I **2**, 1705-1713 (1992)

[2] A. Piñeiro Orioli et al., Phys. Rev. Lett. **120**, 63601, (2018).

[3] M. Lukin et al., Phys. Rev. Lett. **87**, 037901 (2001)

[4] J. Schachenmayer, et al., Phys. Rev. X **5**, 11022, (2015).

A model for strong-coupling, finite-time and finite-size interactions: the Gaussian Otto cycle

Alejandro Pozas-Kerstjens[1], Eric Brown[1], Karen Hovhannisyan[1,2]

[1] ICFO-Institut de Ciencies Fotoniques, The Barcelona Institute of Science and Technology, E-08860 Castelldefels (Barcelona), Spain

[2] Department of Physics and Astronomy, Ny Munkegade 120, Aarhus University, DK-8000 Aarhus, Denmark

In this talk I will present results characterizing the full dynamics of a quantum harmonic Otto engine, in which the working body is a harmonic oscillator and the heat baths are collections of oscillators. By harmonically interacting the working body with the baths we are able to exactly solve the system dynamics during an engine stroke, and thus the dynamics of the cycle as a whole. With this approach we are able to study the efficiency and total work output of the engine, and how these are impacted by finite bath sizes, the strength of the working body-bath coupling, and the timescale of the interaction. We also analyse the correlations that build up between the working oscillator and the baths, and correlations that build between the baths themselves, and how these impact the workings of the engine. In this way we are starting to get a grasp on many of the destabilizing effects that are to be expected in any real laboratory implementation of a quantum Otto engine, and the avenues available for their minimization.

Kapitza stabilization of a repulsive Bose-Einstein condensate in an oscillating optical lattice

J. Martin[1], **B. Georgeot**[2], **D. Guéry-Odelin**[3], **and D. L. Shepelyansky**[2]

[1] *Institut de Physique Nucléaire, Atomique et de Spectroscopie, CESAM, Université de Liège, Belgium*

[2] *Laboratoire de Physique Théorique, IRSAMC, Université de Toulouse, CNRS, UPS, France*

[3] *Laboratoire Collisions, Agrégats, Réactivité, IRSAMC, Université de Toulouse, CNRS, UPS, France*

e-mail: *jmartin@uliege.be*

The striking example of the inverted pendulum (or Kapitza pendulum) shows that an oscillating force with zero average can lead to the phenomenon of Kapitza stabilization, with transformation of an unstable fixed point into a stable one [1]. In this work, we show that the Kapitza stabilization can occur in the context of nonlinear quantum fields [2]. Through this phenomenon, an amplitude-modulated optical lattice can stabilize a Bose-Einstein condensate (BEC) with repulsive interactions and prevent the spreading for long times (see Fig. 1). We present a classical and quantum analysis in the framework of Gross-Pitaevskii equation (GPE). In reduced variables, GPE for our system reads

$$\frac{i}{4\pi}\dot{\Psi} = R_{0\ell}\left(-\hbar_{\rm eff}\partial_X^2 + \frac{\cos(2\pi T)\cos X}{8\hbar_{\rm eff}} + \frac{\bar{g}|\Psi|^2}{2}\right)\Psi$$

where X and T stands respectively for the position in units of the lattice spacing and the time in units of the driving period, $R_{0\ell}$ is the ratio between the natural oscillation frequency of a particle in one of the potential wells of the optical lattice and its driving frequency, $\dot{\Psi} = \partial_T\Psi(X,T)$, $\hbar_{\rm eff}$ is an effective Planck constant that only depends on the depth of the lattice, and $\bar{g}$ quantifies the interatomic interaction strength (see [2] for more details). We specify the parameter region where stabilization occurs. Effects of nonlinearity lead to a significant increase of the stability domain compared with the classical case. Our theoretical proposal can be experimentally realized with current cold atom technology. Besides its fundamental interest, it should provide new tools for the long-time manipulation of BECs.

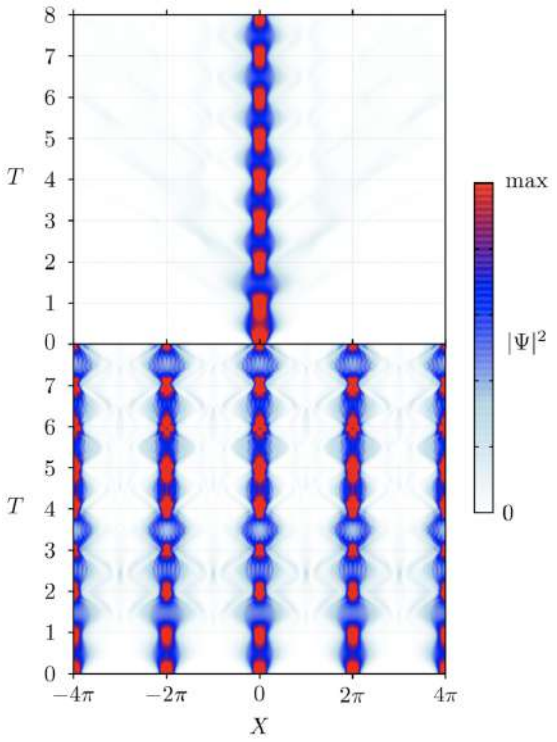


Figure 1: Density plot of the probability density $|\Psi(X,T)|^2$ as a function of position X and time T for a BEC with repulsive interactions ($\bar{g} = 0.6$) for $R_{0\ell} = 0.6$, and $\hbar_{\rm eff} = 0.035$. Top panel: initial state is a single Gaussian wave packet centred at $X = 0$. Bottom panel: initial state is the periodic ground-state wave function of GPE with static optical lattice.

[1] P. L. Kapitza, *Dynamic stability of the pendulum with vibrating suspension point*, Sov. Phys. JETP **21**, 588 (1951).

[2] J. Martin, B. Georgeot, D. Guéry-Odelin, and D. L. Shepelyansky, *Kapitza stabilization of a repulsive Bose-Einstein condensate in an oscillating optical lattice*, Phys. Rev. A **97**, 023607 (2018).

Direct measurement of localization and logarithmically-slow correlation dynamics in the many-body-localized phase

Matthew Rispoli[1], Alexander Lukin[1], Robert Schittko[1], Sooshin Kim[1], M. Eric Tai[1], Vedika Khemani[1], Adam M. Kaufman[2], Julian Leonard[1], Markus Greiner[1]

[1] *Department of Physics, Harvard University, Camridge, MA 02138, USA*

[2] *JILA, NIST and University of Colorado, and Department of Physics, University of Colorado, Boulder, Colorado 80308, USA*

e-mail: *rispoli@physics.harvard.edu*

An interacting quantum system that is subject to disorder may cease to thermalize due to localization of its constituents, thereby marking the breakdown of thermodynamics. The key to our understanding of this phenomenon lies in the system's entanglement, which is experimentally challenging to measure. We realize such a many-body-localized system in a disordered Bose-Hubbard chain and characterize its entanglement properties through particle fluctuations and correlations. We observe how the particles become localized, preventing subsystems from thermalizing with the remaining system and suppressing transport in the system. Intriguingly, we observe how the system develops non-local correlations, whose evolution is consistent with a logarithmic growth of entanglement entropy. Our work experimentally establishes many-body localization as a qualitatively distinct phenomenon from localization in non-interacting, disordered systems.

Probing microscopic models for system-bath interactions via parametric driving

A. S. D. Dietrich[1], **M. Kiffner**[2,1], **and D. Jaksch**[1,2]
[1] *Clarendon Laboratory, University of Oxford, Parks Road, Oxford OX1 3PU, United Kingdom*
[2] *Centre for Quantum Technologies, National University of Singapore, 3 Science Drive 2, Singapore 117543*
e-mail: *anastasia.dietrich@physics.ox.ac.uk*

Driving condensed matter systems with intense terahertz radiation opens up unprecedented possibilities to manipulate their quantum dynamics. Examples include the melting of charge density waves, the generation of synthetic magnetic fields, control of heterointerfaces or even the controlled creation of transient superconductivity [1]. However, exact microscopic models for the interaction of these systems with their environment are often unknown, and thus one has to resort to phenomenological models. In order to optimize the coherent control of these systems even further, it would be highly desirable to improve our understanding of their system-bath interactions.

Recently, it has been shown that strongly driven systems can enter the intriguing regime of environment-governed dynamics [2] (EGD) where the system dynamics is predominantly determined by the details of the system-bath interaction, e.g., the form of the coupling operator. This strongly-driven regime can be described within the framework of the Floquet-Markov master equation approach [3], which combines ideas from open quantum systems with Floquet theory. A fascinating question is thus whether the environment-dependent dynamics in the regime of EGD can be employed to infer microscopic details about the system-bath interaction.

We show that strong parametric driving of a quantum harmonic oscillator coupled to a thermal bath (Fig. 1) allows one to distinguish between different microscopic models for the oscillator-bath coupling. We consider a bath with an Ohmic spectral density and a model where the system-bath interaction can be tuned continuously between position and momentum coupling via the coupling angle α. We derive a master equation for the reduced density operator of the oscillator in Born-Markov approximation and investigate its quasi-steady state as a function of the driving parameters, the temperature of the bath and the coupling angle α. We find that the driving introduces a strong dependence of the time-averaged variance of position and momentum on these parameters. In particular, we identify parameter regimes that maximise the α-dependence and provide an intuitive explanation of our results.

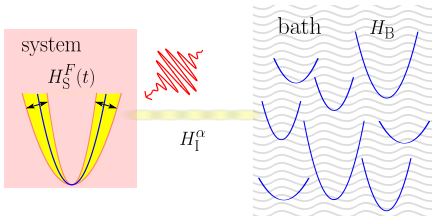


Figure 1: The system of interest is comprised of a parametrically driven harmonic oscillator and a bath of harmonic oscillators with Hamiltonians $H_S^F(t)$ and H_B, respectively. The system-bath interaction is described by the interaction Hamiltonian H_I^α, where the parameter α allows one to continuously adjust the interaction from position ($\alpha = 0$) to momentum coupling ($\alpha = \pi/2$). The parametric driving affects both the system and dissipation mechanism as indicated by the red arrow.

[1] D. Nicoletti and A. Cavalleri, Adv. Opt. Photonics **8**, 401 (2016).

[2] S. Gasparinetti, P. Solinas, S. Pugnetti, R. Fazio, and J. P. Pekola, Phys. Rev. Lett. 110, 150403 (2013).

[3] S. Kohler, T. Dittrich, and P. Hänggi, Phys. Rev. E 55, 300 (1997).

[4] arXiv:1803.07785

Optical conductivity of a quantum gas

P.Xu[1], R.Anderson[1], F.Wang[1], V.Venu[1], S.Trotzky[1], F.Chevy[2], and J.H.Thywissen[1]
[1] *Department of Physics, University of Toronto, M5S 1A7, Canada*
[2] *Laboratoire Kastler Brossel, ENS-PSL Research University, CNRS, UPMC-Sorbonne Universités, Collège de France*
e-mail: *pxu@physics.utoronto.ca*

Optical conductivity measurements are generally used to study transport dynamics, and are basic characterizations of materials. In materials, typical dynamical frequencies on the THz scale make infrared light a natural probe. Here we realize analogous experiments with ultracold atoms, known as quantum simulations, where the natural frequencies are on the Hz to kHz scale. In a quantum simulator composed of a quantum gas in an optical lattice, atoms are governed by physics comparable to that of electrons in materials, so the quantum simulator provides a straightforward system to investigate conductivity properties. A powerful feature of quantum simulations is the ability to control initial conditions, observe dynamics, and tune experimental parameters including temperatures, chemical potentials and interaction strength between atoms. With the help of this ability, and the property that there is no impurity or defect in the quantum simulator, we can get to some experimental regimes that are unreachable for real materials. So quantum simulations can lead us to some additional insights.

Here we measure the optical conductivity of charged neutral fermionic ^{40}K atoms in a cubic optical lattice. To perform the measurements, proposed by Wu *et al.*[1], a periodic force is applied to the atoms by sinusoidally displacing the crossed dipole trap beams. The global displacement of atoms, characterized by the centre of mass (COM) of the cloud, is captured in-situ by a high-resolution fluorescence imaging system as illustrated in Fig.1. The COM motion with respect to time is understood as the mass current response to the force, and the complex optical conductivity is then deduced as the ratio of the global mass current to the force. We can also obtain the full conductivity tensor, with the ability to detect both on-axis and off-axis conductivity.

The first feature we observe from the measurements is the melting of Kohn response [2] with the presence of a lattice. According to Kohn, the bulk COM response should be independent of particle interactions in a translationally invariant space. If a lattice is applied, translational symmetry will be broken and the Kohn theorem should no longer be valid. The feature manifests as a shift in the peak

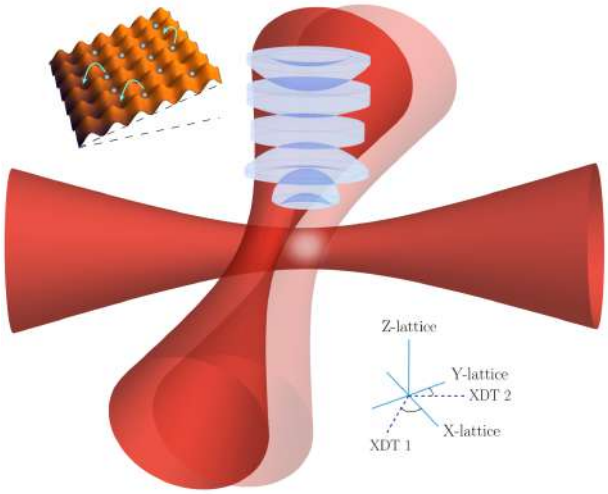


Figure 1: One or both of the crossed dipole traps (XDT) are displaced sinusoidally in the x-y plane to create periodic forces, and the global displacement of atoms is observed with a high-resolution imaging system.

response, a loss of spectral weight and a broadening as the lattice depth increased.

We also explore the effect of changing the on-site interaction strength by tuning the scattering length with a Feshbach resonance, and changing the density of particles. We find that the conductivity spectrum broadens, as increased rates of collisions between the particles speed the decay of the induced currents. Our data are consistent with a transport time that scales with $1/U^2$ scaling for small U, where U is the interaction strength, and with a perturbative calculation based on Fermi's golden rule. However, the calculated f-sum reveals that spectral weight is not lost: interactions merely redistribute conductivity among other frequencies in the optical conductivity spectrum.

[1] Z. Wu, E. Taylor, and E. Zaremba, Europhys. Lett. 110, 26002 (2015).

[2] W. Kohn, Phys. Rev. 123, 1242 (1961).

Two-electron atoms: The Greens function approach to the Fock expansion calculations

E. Z. Liverts[1], **and N. Barnea**[1]
[1] *Racah Institute of Physics, The Hebrew University of Jerusalem, 91904, Israel*
e-mail: *liverts@phys.huji.ac.il*

The helium-like atoms represent the two-electron atomic systems which can serve as an excellent model for testing and verifying quantum theories. It was V. Fock who proposed the following expansion [1] of the corresponding wave function in the vicinity of the triple coalescence point ($R \to 0$)

$$\Psi(R,\alpha,\theta) = \sum_{k=0}^{\infty} R^k \sum_{p=0}^{[k/2]} \psi_{k,p}(\alpha,\theta)(\ln R)^p. \qquad (1)$$

The important feature of the Fock expansion (1) in the hyperspherical coordinates R, α, θ is including the logarithmic function of the hyperspherical radius R, what provides the correct behavior of the wave function near the two- and three-particle coalescences.

It was shown in [2, 3, 4] that the angular Fock coefficients (AFC) $\psi_{k,p}$ can be separated into the components

$$\psi_{k,p}(\alpha,\theta) = \sum_{j=p}^{k-p} \psi_{k,p}^{(j)}(\alpha,\theta) Z^j, \qquad (2)$$

and any component $\psi_{k,p}^{(j)}$, associated with a definite power of the nucleus charge Z (of the considered atomic system), can be represented by a single series of the form

$$\psi_{k,p}^{(j)}(\alpha,\theta) = \sum_{l=0}^{\infty} \omega_l^{(k,p;j)}(\alpha)(\sin\alpha)^l P_l(\cos\theta), \qquad (3)$$

where $P_l(x)$ are the Legendre polynomials.

The authors applied different methods for calculating the AFCs. One of the methods is solving the (so called) individual Fock recurrence relations

$$\left[\Lambda^2 - k(k+4)\right] \psi_{k,p}^{(j)}(\alpha,\theta) = h_{k,p}^{(j)}(\alpha,\theta), \qquad (4)$$

where the explicit forms of the angular momentum operator Λ^2 and the rhs $h_{k,p}^{(j)}$ can be found in [5].

The powerful method (applied by Fock) using the Green's functions was undeservedly forgotten. Application of the corrected Green's function approach [5] yields the following formula for calculation of the AFC-components in case of the collinear arrangement (the angle between the radius-vectors of the electrons, $\theta = 0$) of the particles

$$\psi_{k,p}^{(j)}(\alpha',0) = \frac{1}{8}\int_0^{\pi} d\alpha \sin^2\alpha \int_0^{\pi} d\theta \sin\theta\; h_{k,p}^{(j)}(\alpha,\theta) \frac{\zeta(\gamma)\cos\left[\left(\frac{k}{2}+1\right)\gamma\right]}{\sin\gamma}, \qquad (5)$$

where $$\zeta(\gamma) = \begin{cases} 1 & k \quad odd \\ 1-\gamma/\pi & k \quad even \end{cases}, \qquad (6)$$

$$\cos\gamma = \cos\alpha\cos\alpha' + \sin\alpha\sin\alpha'\cos\theta. \qquad (7)$$

Note that the electron-nucleus ($\alpha' = 0$) and electron-electron ($\alpha' = \pi/2$) coalescences are the particular cases of the collinear arrangement with $\theta' = 0$.

It is very important that Eqs.(5)-(7) enable us to calculate the α-dependent functions $\omega_l^{(k,p;j)}(\alpha)$ of the general expansion (3) (see [5]).

It can be shown that formula (5)-(7) cannot be used if the rhs $h_{k,p}^{(j)}$ is proportional to one of the hyperspherical harmonics $Y_{kl}(\alpha,\theta)$ $(l = 0, 1, ...k/2)$. For this case, the required solution can be found in the form

$$\psi_{k,p}^{(j)}(\alpha,\theta) = \widetilde{\psi}_{k,p}^{(j)}(\alpha,\theta) - \sum_{l=0}^{k/2} C_l F_{k,l}(\alpha,\theta), \qquad (8)$$

where $\widetilde{\psi}_{k,p}^{(j)}$ being obtained by the violent orthogonalization [5] can be calculated by formula (5)-(7). The orthogonalization coefficients $C_l \equiv C_l^{(k,p;j)}$ are defined in [5]. The explicit form of the functions $F_{k,l}$ is

$$F_{k,l}(\alpha,\theta) = \frac{P_l(\cos\theta)}{\sin\alpha} \begin{cases} g_{k,l}(\alpha) & 0 \le \alpha \le \pi/2 \\ \pm g_{k,l}(\pi-\alpha) & \pi/2 \le \alpha \le \pi \end{cases} \qquad (9)$$

where $g_{k,l}(\alpha) = G_l(k/2+1,\alpha)$ which for the simplest case of $l = 0$ reduces to the form

$$G_0(n,\alpha) = \frac{1}{16n^2} \begin{cases} 2n\alpha\cos(n\alpha) - 2\sin(n\alpha) & n \; even \\ 2n\alpha\cos(n\alpha) - \sin(n\alpha) & n \; odd \end{cases} \qquad (10)$$

whereas the corresponding results for $l > 0$ are presented in [5].

[1] V. A. Fock, Izv. Akad. Nauk SSSR Ser.Fiz. **18**, 161 (1954).

[2] E. Z. Liverts and N. Barnea, Phys. Rev. A **92**, 042512 (2015).

[3] E. Z. Liverts, Phys. Rev. A **94**, 022504 (2016).

[4] E. Z. Liverts, Phys. Rev. A **94**, 022506 (2016).

[5] E. Z. Liverts and N. Barnea, J. Phys. A: Math. Theor. **51**, 085204 (2018).

A fibre-tip Fabry-Pérot cavity for deterministic, strong atom-photon interactions

M. Mohammed, T. Doherty, N. Holland, K. Theophilo, D. Stuart, J. Dong and A. Kuhn
University of Oxford, Clarendon Laboratory, Parks Road, Oxford, OX1 3PU, UK
e-mail: *marwan.mohammed@physics.ox.ac.uk*

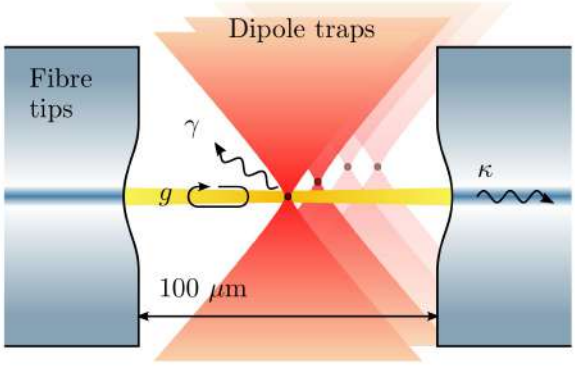


Figure 1: Atom-cavity interactions. Tightly-focused dipole traps move atoms into the cavity field. g, κ and γ represent atom-cavity coupling strength, the decay rates from cavity field to mirrors and from non-cavity field to environment respectively.

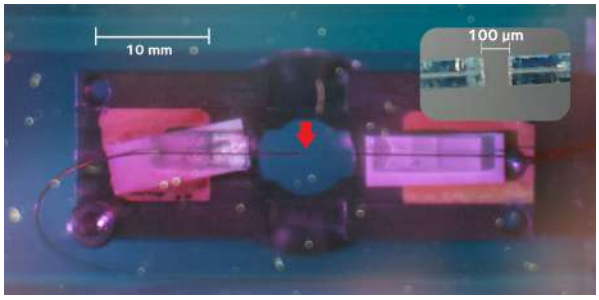


Figure 2: Top-down view of an assembled fibre-tip Fabry-Pérot cavity. The fibres are glued into V-grooves on top of shear piezos that modulate the cavity length. A red arrow indicates the position of the cavity. *Inset*: magnified view of the cavity.

Optical fibre-tip Fabry-Pérot cavities [1] can be used for strong coupling of an atom's electronic state and the cavity's photon state, allowing for a reversible and controllable quantum interface [2]. With atoms as stationary qubits and photons as flying qubits, this deterministic interface can be used both as a single-photon source and as a quantum memory, and therefore as a node in quantum networks [3].

Besides the benefit of coupling the light directly to the fibre, the small fibre-tip diameter allows for optical access with numerical apertures as strong as 0.6, making possible the use of tightly focused dipole traps that hold single atoms at cavity standing-wave anti-nodes [4]. Circumventing the fixed configuration of atoms trapped in optical lattices, we use optical tweezers combined with a spatial light modulator to produce reconfigurable 2D arrays of trapped ^{87}Rb atoms [5]. Single atoms can be moved using the same scheme [6].

This work focuses on the implementation of the cavity. Our symmetric confocal fibre cavity is formed of two single-mode fibres, with a finesse of 100,000, a length of 100 µm and a predicted co-operativity of 29. Whilst there are constraints on the mode-matching efficiency and mirror parameters of these cavity types, we are developing hybrid cavities formed of a fibre-tip and a superpolished micromirror and a mirror shaping technique combining focused ion beam milling and laser ablation that will overcome these constraints. The deterministic nature and strength of the atom-photon interaction will be particularly useful for photonic quantum networks.

[1] D. Hunger, T. Steinmetz, Y. Colombe, C. Deutsch, T. W. Hänsch and J. Reichel, New. J. Phys. **12**, 065038 (2010).

[2] A. Kuhn, *Engineering the Atom-Photon Interaction: Controlling Fundamental Processes with Photons, Atoms and Solids* (Springer, Cham, 2015)

[3] S. Ritter, C. Nölleke, C. Hahn, A. Reiserer, A. Neuzner, M. Uphoff, M. Mücke, E. Figueroa, J. Bochmann and G. Rempe, Nature **484**, 195 (2012).

[4] C. Muldoon, L. Brandt, J. Dong, D. Stuart, E. Brainis, M. Himsworth and A. Kuhn, New. J. Phys. **14**, 073051 (2012).

[5] N. Holland, D. Stuart, O. Barter and A. Kuhn, arXiv:1711.07845.

[6] D. Stuart and A. Kuhn, New J. Phys. **20**, 023013 (2018).

Polarised Single-Photons from a Cavity-Enhanced Atom-Light Interface in Photonic Quantum Networks

T. D. Barrett[1], **A. Rubenok**[2], **D. Stuart**[1], **O. Barter**[1], **A. Holleczek**[1], **J. L. O'Brien**[2], **J. C. F. Matthews**[2] **and A. Kuhn**[1]

[1] *University of Oxford, Clarendon Laboratory, Parks Road, Oxford, OX1 3PU, UK*

[2] *Quantum Engineering Technology Labs, H. H. Wills Physics Laboratory and Department of Electrical and Electronic Engineering, University of Bristol, Merchant Venturers Building, Woodland Road, Bristol, BS8 1UB, UK*

e-mail: *thomas.barrett@physics.ox.ac.uk*

Entanglement is a key resource for quantum information processing (QIP). Mutually entangled cluster states are inherently more robust than pairwise chains of entangled qubits, however it is particularly difficult to create these in non-local networks where bringing together distant nodes is often impractical. Instead, quantum networks of interlinked stationary (typically single atoms or ions) and flying (photonic) qubits offer a scalable route to bridging these physical distances [1], but necessitate a reliable interface between these quantum elements. A single atom strongly coupled to a single mode of the electric field, where the internal spin state of the atom is entangled to the emitted photon polarisation, is then an ideal architecture for realising such a system. Probabilistic entanglement of distant atoms can be achieved by entanglement swapping acting on photons emitted from each atom [2, 3]. Here we discuss the essential first step, an *a priori* non-probabilistic source of polarised single-photons, that utilises the unparalleled control over the photonic states provided by the cavity-enhanced interaction with a single ^{87}Rb atom [4].

In particular we consider using cavity-sourced photons to operate a 4×4 multimode interferometer (MMI) integrated onto a photonic chip [5, 6]. Non-classical correlations between photon detection events show no loss of coherence when interfering pairs of these photons through the MMI in comparison a direct measurement of the two-photon visibility taken using Hong-Ou-Mandel interference. This demonstrates the real-world ability of an integrated MMI to mediate the entanglement of remote nodes in a photonically-linked quantum network.

Additionally we present a theoretical and experimental investigation of the novel effects of non-linear Zeeman shifts on this system [7]. The hitherto unexplored operation of our vacuum-stimulated Raman adiabatic passage (V-STIRAP) process in the regime of intermediate magnetic fields, required for a polarised process but leading to a breakdown of the atomic hyperfine structure, is key to explaining experimentally observed asymmetries and to informing the next steps for such systems.

The authors are grateful for the contributions of K. Poulios, G. D. Marshall and A. Politi to the development of the integrated MMI chips used in this work, and to P. B. R. Nisbet-Jones, and J. Dilley for their work with cavity-based single-photon sources. We acknowledge support for this work through the quantum technologies programme (NQIT hub).

[1] S. Ritter *et al.*, Nature **484**, 195 (2012).
[2] D. Moehring *et al.*, Nature **449**, 68 (2007).
[3] S. Olmschenk *et al.*, Science **323**, 486 (2009).
[4] A. Kuhn, in *Engineering the Atom-Photon Interaction* (Springer, 2015) pp. 3–38.
[5] A. Peruzzo *et al.*, Nat. Commun. **2**, 224 (2011).
[6] T. D. Barrett *et al.*, arXiv:1803.10222 (2018).
[7] T. D. Barrett *et al.*, arXiv:1804.10455 (2018).

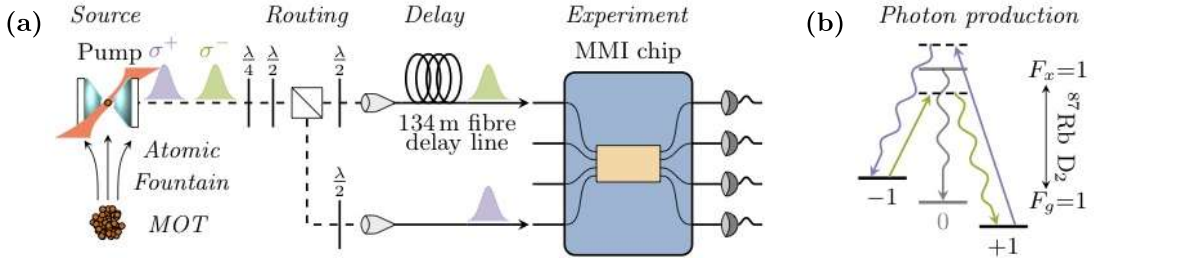


Figure 1: (a) Experimental set-up of the hybrid source-chip system showing the routing of polarised photons into paths of different length such that pairs of photons are simultaneously delivered to the MMI chip. (b) Energy level diagram of the V-STIRAP process between magnetic sublevels of the ^{87}Rb D$_2$ line.

From Reservoir Engineering with Trapped Ions to GKP Coding State and Phonon Lasing

T. L. Nguyen[1], **C. Flümann**[1], **D. Kienzler**[1], **M. Marinelli**[1], **V. Negnevitsky**[1], **K. Mehta**[1], **J. Home**[1]

[1] *Institute for Quantum Electronics, ETH Zürich, Otto-Stern-Weg 1, 8093 Zürich, Switzerland*
e-mail: *nguythan@phys.ethz.ch*

Quantum reservoir engineering (QRE), involving active control of the coupling of a quantum system to its environment, has recently been shown to be a resource for robust quantum state preparation and quantum computing. The implementation of QRE in our recent works allows us to stabilize squeezed states on the vibrational motion of a single trapped ion [1], and create superposition of these squeezed wave-packets such as the squeezed Schrödinger's cat [2] and GKP states useful for quantum error correction [3].

In addition, QRE provides the possibility to study quantum phase transitions driven by dissipation, in which a system abruptly changes its steady state as a function of the strength of the dissipation. We will explore such dissipative phase transitions using the vibrational motion of trapped ion chains, which are among the most precisely controlled quantum systems available to physics today. As a starting point for this research direction, we will realize both standard and squeezed phonon lasing deep in the quantum regime using newly available resources of mixed-species ion control and our pioneering works on QRE. This novel device can be applied for ultra-sensitive metrology, with the potential enhancement due to squeezing.

[1] D. Kienzler et al., Science **347**, 53 (2015).

[2] H.-Y. Lo et al., Nature **521**, 336 (2015).

[3] D. Gottesman et al., Phys. Rev. A **64**, 012310 (2001).

Demonstration of a passive photon-atom swap gate

A. Borne[1], O. Bechler[1], S. Rosenblum[1,2], G. Guendelman[1], O. Mor[1], M. Netser[1], T. Ohana[1], Z. Aqua[1], N. Drucker[1], R. Finkelstein[1], Y. Lovsky[1], R. Bruch[1], D. Gurovich[1], E. Shafir[1] and B. Dayan[1]

[1] *AMOS and Department of Chemical Physics, Weizmann Institute of Science, Rehovot 76100, Israel.*
[2] *Departments of Physics and Applied Physics, Yale University, New Haven, CT 06520, USA*
e-mail: *adrien.borne@weizmann.ac.il*

Deterministic quantum interactions between single photons and single quantum emitters are a vital building block towards the distribution of quantum information between remote systems [1]. Deterministic photon-atom state transfer has previously been demonstrated by using protocols that include active feedback or synchronized control pulses [2, 3, 4, 5]. Here we demonstrate a completely passive swap operation between the states of a single photon and a single atom. The underlying mechanism is single-photon Raman interaction (SPRINT) [6, 7], an interference-based effect in which a photonic qubit deterministically controls the state of a material qubit encoded in the two ground states of a Λ system, and vice versa. Using a nanofiber-coupled microsphere resonator coupled to single Rb atoms, we swap a photonic qubit into the atom and back (see Fig. 1), demonstrating fidelities exceeding the classical threshold of 2/3 in both directions. Requiring no control fields, this single-step gate takes place automatically at the timescale of the atoms cavity-enhanced spontaneous emission time. Applicable to any waveguide-coupled Λ system, this mechanism, which can also be modified to construct universal gates such as $\sqrt{\text{SWAP}}$ [8], provides a versatile building block for the modular scaling up of quantum information processing systems.

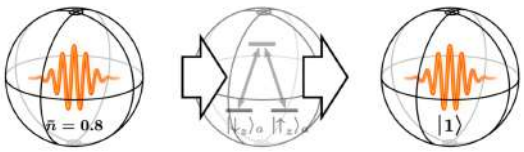


Figure 1: A photonic qubit is written on an atom using SPRINT, then extracted from the atom by sending a probe pulse and analyzed in the write basis.

[1] H. J. Kimble, Nature **453**, 1023-1030 (2008).

[2] L.-M. Duan and H. J. Kimble, Phys. Rev. Lett. **92**, 127902 (2004).

[3] A. D. Boozer, A. Boca, R. Miller, T. E. Northup and H. J. Kimble, Phys. Rev. Lett. **98**, 193601 (2007).

[4] H. P. Specht *et al.*, Nature **473**, 190 (2011).

[5] A. Reiserer, N. Kalb, G. Rempe and S. Ritter, Nature **508**, 237 (2014).

[6] D. Pinotsi and A. Imamoglu, Phys. Rev. Lett. **100**, 93603 (2008).

[7] S. Rosenblum, A. Borne and B. Dayan, Phys. Rev. A **95**, 33814 (2017).

[8] K. Koshino, S. Ishizaka and Y. Nakamura, Phys. Rev. A **82**, 10301 (2010).

High-fidelity Single-Qubit Gates of a Neutral-Atom Qubit in a Magic-Intensity Optical Dipole Trap

Cheng Sheng[1,2,3], Xiaodong He[1,2,*], Ruijun Guo[1,2], Kunpeng Wang[1,2], Peng Xu[1,2], Zongyuan Xiong[1,2], Min Liu[1,2], Jin Wang[1,2], and Mingsheng Zhan[1,2,3,*]

[1] *State Key Laboratory of Magnetic Resonance and Atomic and Molecular Physics, Wuhan Institute of Physics and Mathematics, Chinese Academy of Sciences, Wuhan 430071, China*

[2] *Center for Cold Atom Physics, Chinese Academy of Sciences, Wuhan 430071, China*

[3] *Wuhan National Laboratory for Optoelectronics, Wuhan 430074, China*

e-mail: *hexd@wipm.ac.cn*

mszhan@wipm.ac.cn

We demonstrate high fidelity single-qubit Clifford gates of a single neutral atom trapped in magic-intensity optical dipole trap (MI-ODT) with an activity stabilized magnetic field. The MI-ODT efficiently mitigates the detrimental effects of light shifts thus sufficiently improves the performance of single qubit-gates. The fidelity of microwave-driven gates is characterized by using Randomized Benchmarking method. We obtain an average error per Clifford gate of $3.0(7)\times10^{-5}$ which surpasses the error threshold (10^{-4}) for fault-tolerance. This error is found to be dominated by qubit dephasing, and the corresponding coherence time relevant to the Clifford gates is also measured experimentally. Additionally, due to the advantage that the gates fidelity is robust to the atom temperature and the trap depth in MI-ODT, we could implement highly uniform global single-qubit gates in atom array. This work is an essential step toward the construction of a scalable quantum computer with neutral atoms.

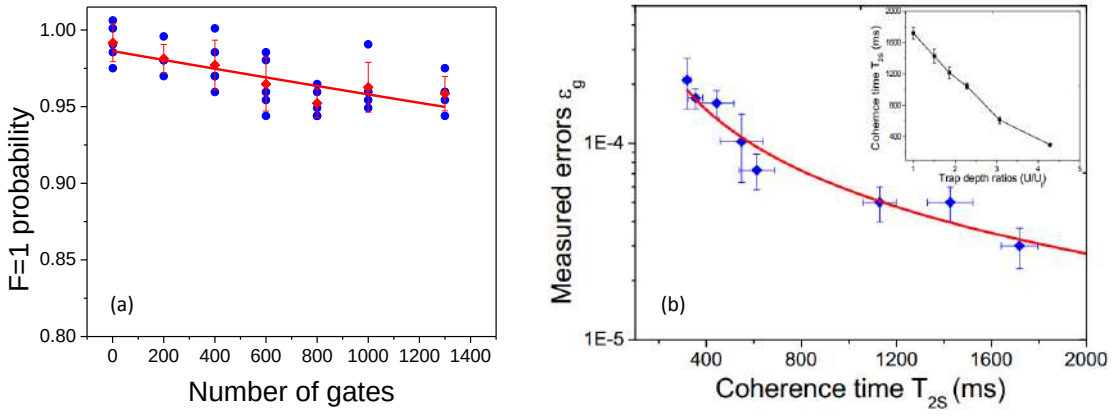


Figure 1: (a) Results of Randomized Benchmarking method to characterize single-qubit Clifford gates in MI-ODT. The average error per gate is $\varepsilon_g \approx 3.0(7) \times 10^{-5}$ (state preparation and readout errors $d_{if} \approx 0.03 \pm 0.01$). (b) Dependence of values of error per gate on the homogeneous coherence times T_{2s}. All the accompanying error bars of coherence times and values of error per gate are fitting errors.The inset shows dependence of coherence time T_{2s} on ratio of varied trap depths U to magic working trap depth U_I.

[1] Cheng Sheng, Xiaodong He, Ruijun Guo, Kunpeng Wang, Peng Xu, Zongyuan Xiong, Min Liu, Jin Wang, and Mingsheng Zhan, High-fidelity Single-Qubit Gates of a Neutral-Atom Qubit in a Magic-Intensity Optical Dipole Trap, arXiv:1712.06306.

[2] Jiaheng Yang, Xiaodong He, Ruijun Guo, Peng Xu, Kunpeng Wang, Cheng Sheng, Min Liu, Jin Wang, Andrei Derevianko, and Mingsheng Zhan, Coherence Preservation of a Single Neutral Atom Qubit Transferred between Magic-Intensity Optical Traps, Phys. Rev. Lett. **117**, 123201 (2016).

Using and reusing coherence to realize quantum processes

María García Díaz[1], **Kun Fang**[2], **Xin Wang**[2], **Matteo Rosati**[1], **Michalis Skotiniotis**[1], **John Calsamiglia**[1] **and Andreas Winter**[1,3]

[1] *Física Teòrica: Informació i Fenòmens Quàntics, Departament de Física, Universitat Autònoma de Barcelona, ES-08193 Bellaterra (Barcelona), Spain*

[2] *Centre for Quantum Software and Information, University of Technology Sydney, NSW 2007, Australia*

[3] *ICREA—Institució Catalana de Recerca i Estudis Avançats, Pg. Lluis Companys, 23, ES-08001 Barcelona, Spain*

e-mail: *maria.garcia.diaz@uab.cat*

Coherent superposition is a key feature of quantum mechanics that underlies the advantage of quantum technologies over their classical counterparts. Recently, coherence has been recast as a resource theory in an attempt to identify and quantify it in an operationally well-defined manner. Here we study how the coherence present in a state can be used to implement a quantum channel via incoherent operations and, in turn, to assess its degree of coherence. We introduce the robustness of coherence of a quantum channel—which reduces to the homonymous measure for states when computed on constant-output channels—and prove that: i) it quantifies the minimal rank of a maximally coherent state required to implement the channel (setting of Fig. 1a); ii) its logarithm quantifies the amortized cost of implementing the channel provided some coherence is recovered at the output (setting of Fig. 1b); iii) its logarithm also quantifies the zero-error asymptotic cost of implementation of many independent copies of a channel. We also consider the generalized problem of imperfect implementation with arbitrary resource states. Using the robustness of coherence, we find that in general a quantum channel can be implemented without employing a maximally coherent resource state. In fact, we prove that *every* pure coherent state in dimension larger than 2, however weakly so, turns out to be a valuable resource to implement *some* coherent unitary channel. We illustrate our findings for the case of single-qubit unitary channels.

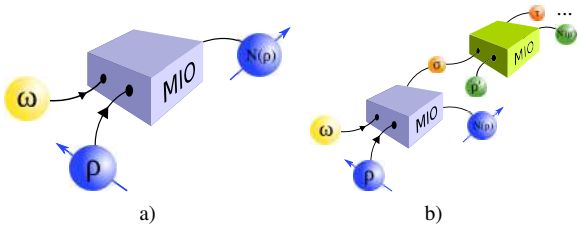


Figure 1: Different protocols for implementing a quantum channel $\mathcal{N}$ using a MIO $\mathcal{M}$ and a coherent resource ω. **a)** The implementation destroys completely the input resource, $\mathcal{M}(\omega \otimes \rho) = \mathcal{N}(\rho)$. **b)** After the implementation, a degraded resource σ is recovered and ready to be recycled: $\mathcal{M}(\omega \otimes \rho) = \sigma \otimes \mathcal{N}(\rho)$. For example it can be used to implement another channel $\mathcal{N}'$: $\mathcal{M}'(\sigma \otimes \rho') = \tau \otimes \mathcal{N}'(\rho')$.

[1] F. G. S. L. Brandão and G. Gour, Phys. Rev. Lett. **115**, 070503 (2015).

[2] T. Baumgratz, M. Cramer, and M. B. Plenio, Phys. Rev. Lett. **113**, 140401 (2014).

[3] J.Åberg, arXiv:quant- ph/0612146 (2006).

[4] E.Chitambar and G.Gour, Phys. Rev. Lett. **117**, 030401 (2016).

[5] C. Napoli, T. R. Bromley, M. Cianciaruso, M. Piani, N. Johnston, and G. Adesso, Phys. Rev. Lett. **116**, 150502 (2016).

[6] A. Streltsov, G. Adesso, and M. B. Plenio, Rev. Mod. Phys. **89**, 041003 (2017).

[7] E. Chitambar and M.-H. Hsieh, Phys. Rev. Lett. **117**, 020402 (2016).

[8] K. Ben Dana, M. García Díaz, M. Mejatty, and A. Winter, Phys. Rev. A **95**, 062327 (2017).

[9] J. Watrous, Theory of Computing **5**, 217 (2009).

[10] A. Mani and V. Karimipour, Phys. Rev. A **92**, 032331 (2015).

[11] K. Bu, A. Kumar, L. Zhang, and J. Wu, Phys. Lett. A **381**, 1670 (2017).

[12] M. García-Díaz, D. Egloff, and M. B. Plenio, Quantum Information & Computation **16**, 1282 (2016).

[13] Q. Zhao, Y. Liu, X. Yuan, E. Chitambar, and X. Ma, Phys. Rev. Lett. **120**, 070403 (2018).

[14] A. Winter and D. Yang, Phys. Rev. Lett. **116**, 120404 (2016).

Photonic quantum state engineering using single-photon Raman interaction

Z. Aqua[1], **M. S. Kim**[2], **and B. Dayan**[1]

[1] *AMOS and Department of Chemical Physics, Weizmann Institute of Science, Rehovot 76100, Israel*

[2] *QOLS, Blackett Laboratory, Imperial College London, London SW7 2AZ, United Kingdom*

e-mail: *ziv.aqua@weizmann.ac.il*

The control over the quantum state of light is highly sought after in many fields such as quantum information processing in photonic circuits [1], quantum metrology [2] and quantum communication [3]. In this work we present a theoretical scheme for the efficient generation of nonclassical states of light. The underlying mechanism is single-photon Raman interaction (SPRINT) [4–7] - in which a photonic qubit deterministically controls the state of a material qubit encoded in the two ground states of a Λ system, and vice versa. In addition, the scheme assumes a single-photon source, towards which a significant progress has recently been made [8]. Utilizing SPRINT as a building block, a theoretical multi-step protocol for the efficient manipulation of the quantum state of light is introduced; in particular, the heralded generation of arbitrary photon-number Fock states from coherent pulses is presented. Requiring no control fields or feedback, the protocol occurs automatically with each step taking place at the timescale of the cavity-enhanced spontaneous emission time.

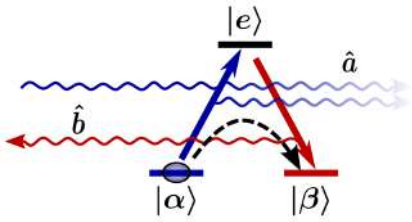


Figure 1: The basic principle of SPRINT. Upon an incident single-photon in mode $\hat{a}$ and an atom prepared in $|\alpha\rangle$, destructive interference forces the atom to emit back the photon in mode $\hat{b}$ and undergo a Raman transition to state $|\beta\rangle$.

[1] E. Knill, R. Laflamme, and G. J. Milburn, Nature (London) 409, 46 (2001).

[2] M. J. Holland and K. Burnett, Phys. Rev. Lett. 71, 1355 (1993).

[3] M. Hillery, V. Buzek, and A. Berthiaume, Phys. Rev. A 59, 1829 (1999).

[4] I. Shomroni, S. Rosenblum, Y. Lovsky, O.Bechler, G. Guendelman, and B. Dayan, Science 345, 903 (2014).

[5] S. Rosenblum, O. Bechler, I. Shomroni, Y. Lovsky, G. Guendelman, and B. Dayan, Nat. Photon. 10, 19 (2016).

[6] S. Rosenblum, A. Borne, and B. Dayan, Phys. Rev. A 95, 033814 (2017).

[7] O. Bechler et al., (under review). arXiv:1711.10974 (2017).

[8] N. Somaschi et al., Nat. Photonics 10, 340 (2016).

Sub-Megahertz Single Photon Source Suitable for Quantum Memories

[1] **M. Rambach, W. Y. Sarah Lau[1], A. Nikolova[1], S. Laibacher[2], V. Tamma[3,2], A. G. White[1] and T. J. Weinhold[1]**

[1] *ARC Centres for Engineered Quantum Systems and Quantum Computation & Communication Technology, School of Mathematics and Physics, University of Queensland, Australia*

[2] *Institut für Quantenphysik and Center for Integrated Quantum Science and Technology (IQ^{ST}), Universität Ulm, Germany.*

[3] *Faculty of Science, SEES and Institute of Cosmology & Gravitation, University of Portsmouth, UK.*

e-mail: *w.y.s.lau@uq.edu.au*

The use of secure quantum communication protocols over long distances relies on the construction of quantum repeater networks, of which a quantum memory is an integral part. This is the interface that brings together the benefits of two unique quantum architectures; atomic qubits offer excellent readout and storage capabilities, while photons are highly mobile and can be easily transmitted. For efficient interaction between these two systems, and thereby an efficient memory, the spectral properties of the photons must be matched to the resonances of the atomic species. Unfortunately, the atomic transition usually has a much narrower bandwidth than single photons generated by spontaneous parametric down-conversion (SPDC), the current gold standard of producing high-purity heralded single photons at flexible wavelengths. The challenge therefore remains to significantly reduce the single photon emission spectra to fulfill the requirements of quantum memory candidates. We try to achieve this by using an optical cavity to enhance the probability of creating the photons in the spectral and spatial resonator mode.

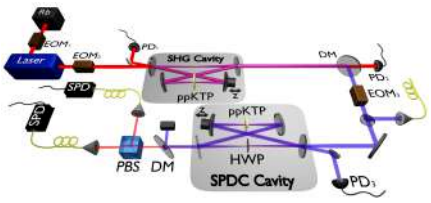


Figure 1: Schematic experimental setup. The laser is stabilised to a second harmonic generation (SHG) cavity which itself is stabilised to the Rubidium spectroscopy cell's D_1 transition for absolute frequency stability. The generated light at 397.5nm is separated from 795nm light at a dichroic mirror (DM) and pumping the type-II SPDC cavity. Finally the single photons are split on a polarising beam splitter (PBS) and fibre-coupled for further processing.

Previous cavity-based SPDC sources have achieved bandwidths comparable to atomic linewidths, but their operation time is divided into stabilization and photon production phases, resulting in typical duty cycles <50%. The current narrowest photons from SPDC have bandwidths still well above a MHz [1], and only one source has demonstrated 100% duty cycle [2].

We report 100% duty cycle generation of sub-MHz single photon pairs at the Rubidium D_1 line using cavity-enhanced SPDC [3], a schematic of which can be found in Fig. 1. The single photons exhibit a bandwidth of 429 ± 10kHz. This is, to our knowledge, the narrowest single photon bandwidth from SPDC to date. A new method of placing a half-wave plate inside the cavity helps to achieve triple resonance between pump, signal and idler photon, reduces the bandwidth and simplifies the locking scheme. Additionally, stabilisation of the cavity to the pump frequency enables the 100% duty cycle. The quantum characteristic of the single photon source is shown by measuring the idler-triggered second-order autocorrelation function $g^2(0)$. We observe antibunching below 0.5 up to heralding rates of 250kHz with a minimum measured $g^2(0) = 0.016 \pm 0.002$ for a heralding rate of 5kHz.

The indistinguishability of the single photons can be quantified by measuring a Hong-Ou-Mandel (HOM) dip. With no time delay between two photons, a HOM dip had a visibility of $98.4 \pm 1.7\%$. The unique temporal shape of the photons also results in repeated HOM dips when one of the photons are physically delayed an effective cavity round trip time in fibre. The longest delay, equivalent to approximately 348ns, still produced a HOM dip with a visibility of $55 \pm 3\%$.

The narrow bandwidth, in combination with the tunability, makes our system the perfect source for integration with Rubidium-based systems, such as the gradient echo memories (GEM) [4, 5], one of the most promising candidates for quantum memories to date. This work is currently in progress. The photons from this source are also suitable for combination with hollow-core glass fibers filled with rubidium gas [6] to allow the construction of novel quantum logic gates.

[1] J. Fekete, D. Rieländer, M. Cristiani and H. de Reidmatten, "Ultranarrow-Band Photon-Pair

Source Compatible with Solid State Quantum Memories and Telecommunication Networks", Phys. Rev. Lett. **110**, 220502 (2013).

[2] M. Scholz, L. Koch and O. Benson, "Statistics of Narrow-Band Single Photons for Quantum Memories Generated by Ultrabright Cavity-Enhanced Parametric Down-Conversion", Phys. Rev. Lett. **102**, 063603 (2009).

[3] M. Rambach, A. Nikolova, T. J. Weinhold and A. G. White, "Sub-Megahertz Single Photon Source", APL Photonics **1**, 096101 (2016).

[4] M. Hosseini, B. M. Sparkes, G. Hètet, J. J. Longdell, P. K. Lam and B. C. Buchler, "Coherent optical pulse sequencer for quantum applications", Nature **461**, 241-245 (2009).

[5] Y.-W. Cho, G. T. Campbell, J. L. Everett, J. Bernu, D. B. Higginbottom, M. T. Cao, J. Geng, N. P. Robins, P. K. Lam, and B. C. Buchler, Optica **3**, 100 (2016)

[6] C. Perrella, P. S. Light, J. D. Anstie, T. M. Stace, F. Benabid, and A. N. Luiten, "High-resolution two-photon spectroscopy of rubidium within a confined geometry", Phys. Rev. A **87**, 013818 (2013)

Repeated multi-qubit readout and feedback with a mixed-species trapped-ion register

M. Marinelli*, V. Negnevitsky*, K. Mehta, H-Y. Lo, C. Flühmann, and J. P. Home
Institute for Quantum Electronics, ETH Zürich, Otto-Stern-Weg 1, 8093 Zürich, Switzerland
e-mail: *mmatteo@phys.ethz.ch*

Quantum error correction involves repeated rounds of error detection and recovery, involving multi-qubit non-demolition measurements along with conditional feedback [2]. This requires the use of systems in which, measurement and decision times are short compared to relevant decoherence timescales, and in which the act of measurement does not destroy subspace coherence or disrupt future operations. Using a mixed-species ion chain, we demonstrate up to 50 sequential measurements of correlation between two beryllium ion qubits coupled to a co-trapped calcium ion. State readout of the calcium ancilla has no direct effect on the internal states of beryllium. Using the ability to rapidly make in-sequence processing in our classical computer control, we perform feedback on the beryllium qubits conditioned on the ancilla readout, which we use to prepare and stabilize Bell states and parity subspaces. The methods demonstrated here could be applied to quantum error correcting codes as well as quantum metrology and are key ingredients for realizing a hybrid universal quantum computer based on trapped ions [3].

* These authors contributed equally to this work.

[1] V. Negnevitsky*, M. Marinelli*, K. Mehta, H-Y Lo, C Flühmann, J P. Home, arXiv:1804.09703

[2] D. Gottesman, Physical Review A 57, 127 (1998).

[3] D. Leibfried, M. D. Barrett, T. Schaetz, J. Britton,J. Chiaverini, W. M. Itano, J. D. Jost, C. Langer, andD. J. Wineland, Science 304, 1476 (2004)

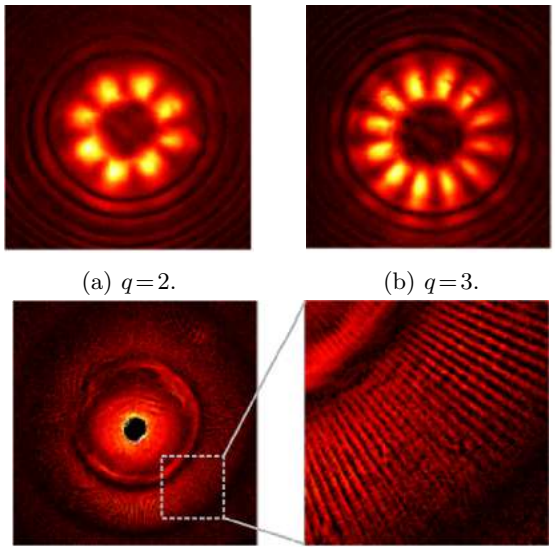
Spatially dependent Electromagnetically Induced Transparency

F. Castellucci,N. Radwell, A. Selyem, S. M. Barnett, and S. Franke-Arnold
SUPA, School of Physics and Astronomy, University of Glasgow, Glasgow G12 8QQ, U K
e-mail: *Francesco.Castellucci@glasgow.ac.uk*

We demonstrate the rise of Spatially dependent Electromagnetically Induced Transparency (SEIT) in a sample of cold atoms, where light beams with Orbital Angular Momentum (OAM) are used to locally modify the atoms absorption, and therefore their transparency [1]. In a typical EIT configuration, two lower atomic states are coupled to a common upper state with two near-resonant laser beams. EIT is often characterised by scanning a laser beam across the atomic transition, with transparency occurring for two-photon resonance. Here, on the other hand, we show that EIT also depends on the relative phase between the two driving laser beams, so that a beam with locally varying phase structure results in spatially varying dark states, and hence spatially varying EIT. Typical EIT is not phase dependent. In our case, however, the two lower states are coupled by a residual transverse magnetic field, resulting in a closed atomic system in which light absorption is dependent to the angle between the phase of the beam and the direction of the magnetic field. To achieve SEIT in our lab we prepare a ^{87}Rb atomic sample with $2\cdot10^{11}\mathrm{cm}^{-3}$ density in the lower $F=1$ ground state. A magnetic field of about 0.1 G is directed mainly along the propagation direction of the beam, with only a fraction in the transverse plane. This transverse component gives rise to a Hanle-type coupling of the lower levels. We structure the phase of our EIT beams by use of q-plates [2], which for a charge of $q=\ell/2$, and linearly polarized input light generate a field with opposite OAM in the right and left handed polarization component

$$\sigma_+ e^{-i2q\phi} + \sigma_- e^{+i2q\phi}. \tag{1}$$

This means that from linearly polarized light passing through the q-plate comes out a beam with correlations between polarization and azimuthal angle of the probe laser, which also results in the generated beams containing OAM. The interaction between this shaped light beam and the atoms is analysed from the absorption imaging, of which the figures below are examples. The number of lobes in each picture is 2ℓ, where ℓ is the OAM value of the beam. In addition the variation of the direction of the magnetic field, and the ratio between the longitudinal and transverse component cause a rotation of the pattern and the splitting of the 2ℓ lobes, respectively.
We have shown theoretically and experimentally that the absorption pattern changes as a function of both the transverse and the longitudinal direction of the magnetic field, that we can fully control: this implies that we can "write" an image in the cloud of cold atoms. In the future we aim to extend furter the duration time of the stored image inside the cloud, leading us to the development of an effective quantum memory.



(a) $q=2$. (b) $q=3$.

(c) $q=100$, with a zoom of the marked section.

Figure 1: Absorption patterns for different q values, each showing a $4q$-fold symmetry. All absorption patterns arise from single shot images.

References

[1] N. Radwell, T.W. Clark, B. Piccirillo, S. M. Barnett, and S. Franke-Arnold, PRL 114, 123603 (2015)

[2] L. Marrucci, C. Manzo, and D. Paparo, PRL 96, 163905 (2006)

Photonic quantum state transfer between a cold atomic gas and a crystal

Nicolas Maring[1*], **Pau Farrera**[1], **Kutlu Kutluer**[1], **Margherita Mazzera**[1], **Georg Heinze**[1], **Hugues de Riedmatten**[1,2]

[1] *Institut de Ciències Fotòniques, The Barcelona Institute of Science and Technology, 08860 Castelldefels, Spain*

[2] *ICREA-Institució Catalana de Recerca i Estudis Avançats, 08015 Barcelona, Spain*

e-mail: *nicolas.maring@icfo.eu*

The interconnection of fundamentally different quantum platforms via photons is a key requirement to build future hybrid quantum networks [1]. Such heterogeneous architectures hold promise to offer more powerful capabilities than their homogeneous counterparts, as they would benefit from the individual strengths of different quantum matter systems.

We report on interfacing a cold atomic ensemble of Rubidium atoms with a rare-earth ion-doped crystal. The first one, beside being an excellent quantum memory (QM) and single photon source [2], also gives access to quantum processing via Rydberg excitation, while the second system offers multiplexed long-lived quantum state storage [3].

In this experiment we demonstrate storage in the solid state memory of a paired single photon, emitted from the atomic cloud [4]. As both systems exhibit very different optical transitions, we apply cascaded frequency conversion techniques to bridge the wavelength gap and moreover transmit the single photon at telecom wavelength, favorable for long distance communication. We demonstrate that the coherence of the single photon is preserved through frequency conversion, storage and retrieval (Fig. 1a). Finally, we show time-bin qubit transfer between the two fundamentally different QM systems with a conditional fidelity of 85 %, surpassing the classical threshold (Fig. 1b).

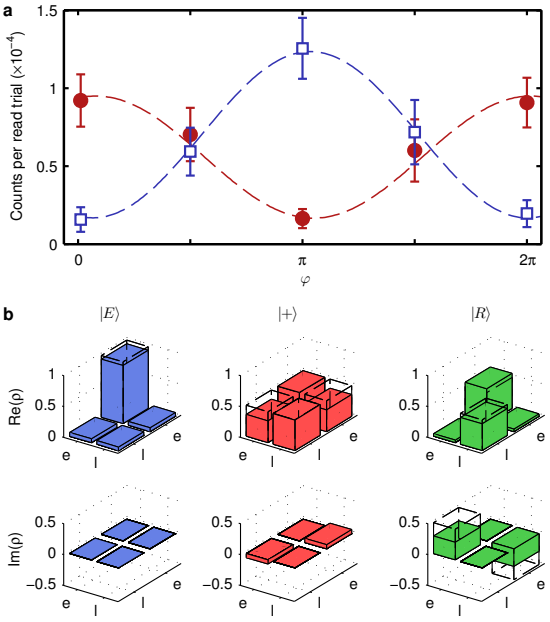


Figure 1: **Single photon qubit transfer.** (a) Interference fringes from a single time-bin photon $|\Psi_{\mathrm{eq}}\rangle = \frac{1}{\sqrt{2}}(|early\rangle + e^{i\varphi}|late\rangle)$ generated by the cold atomic cloud and stored in the crystal. The solid state memory is also used to analyze the qubits in different bases (e.g. red dots and blue open squares). (b) Real and imaginary parts of the reconstructed density matrices measured after the crystal for 3 different input qubits.

[1] Walmsley, I. A. and Nunn, J. Editorial: "Building Quantum Networks." Physical Review Applied 6, 040001 (2016).

[2] Sangouard, N., Simon, C., de Riedmatten, H. and Gisin, N. "Quantum repeaters based on atomic ensembles and linear optics". Review of Modern Physics 83, 3380 (2011).

[3] Hedges, M. P., Longdell, J. J., Li, Y. and Sellars, M. J. "Efficient quantum memory for light." Nature 465, 1052-6 (2010).

[4] N. Maring, P. Farrera, K. Kutluer, M. Mazzera, G. Heinze, and H. de Riedmatten, "Photonic quantum state transfer between a cold atomic gas and a crystal", Nature 551, 485–488 (2017).

Energy-time entanglement between a single photon and a spin wave in a solid state quantum memory

K. Kutluer[1], **E. Distante**[1], **M. Mazzera**[1], **and H. de Riedmatten**[1,2]

[1] *Institut de Ciències Fotòniques, The Barcelona Institute of Science and Technology, 08860 Castelldefels, Spain*

[2] *Institutió Catalana de Recerca i Estudis Avançats, 08015 Barcelona, Spain*

e-mail: *margherita.mazzera@icfo.eu*

Light matter entanglement plays a fundamental role in the development of quantum technologies, as quantum cryptography and quantum computation. It can be achieved, for example, by generating photonic entanglement with external sources and storing it in long lived quantum memories. Another technique consists in generating entanglement directly with the quantum memory, following the DLCZ protocol [1]. While this technique has been extensively used with atomic gases since 2005, very few attempts have been done with solid-state atomic ensembles, demonstrating continuous variable entanglement [2] and quantum correlation between photons and spin waves [3, 4].

Here we report on the direct generation of energy-time entanglement between a photonic qubit and a single collective spin excitation (spin wave) in an ensemble-based solid-state quantum memory. Also we demonstrate that the matter qubit can be read out on-demand after an arbitrary delay, in form of a second photonic qubit. The entanglement is verified by violating a Bell inequality. The chosen platform is Pr^{3+}: Y_2SiO_5, which has already demonstrated outstanding capabilities of light storage [5, 6]. We implement a modified version of the DLCZ protocol, where an atomic frequency comb (AFC) [7] is prepared by hole burning in the ensemble of Pr^{3+} ions, with the scope of maintaining the coherence of the collective atomic excitations [8] (see Fig. 1(a)). We first demonstrate that the joint protocol provides strongly non-classically correlated photon pairs with controllable delay [3]. Contrary to the original scheme, the AFC-DLCZ enables the storage of several temporal modes thanks to the inherent temporal multimodality of the AFC protocol [7]. We thus exploit this powerful capability to demonstrate energy-time entanglement between the photons of the pair by measuring two-photon quantum interference with visibilities above 80%, and by violating a CHSH inequality. Notably, our setup, sketched in Fig. 1(b), does not require largely unbalanced interferometers, whose stabilization would prove extremely challenging. In fact, besides the crystal used as a quantum memory, our setup includes a second, almost identical, crystal that we exploit as a spatially multiplexed and tunable spectral filter [3]. To demonstrate entanglement, we prepare in this filter crystal two spatially

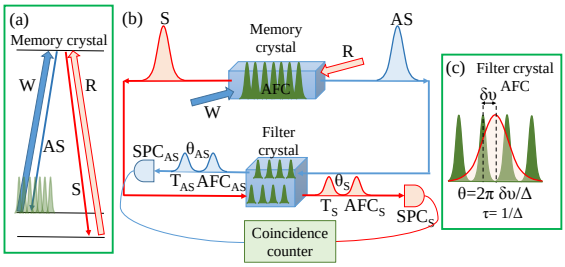


Figure 1: (a) Energy level and pulse scheme for the AFC-DLCZ protocol: W, write pulse; S, Stokes photon; R: read pulse; AS, anti-Stokes photon. (b) Experimental setup: SPC, single photon counter; θ, phase difference between the transmitted part of the pulse through the AFC (T) and the AFC echo. (c) AFC in the filter crystal used as interferometer: $\delta\nu$, detuning between the photon central frequency and the AFC peaks; τ, AFC storage time; Δ, periodicity of the comb.

separated AFCs that act as unbalanced interferometers for the two photons of the pair [7], where the short (long) arm corresponds to the photon being transmitted through (stored in) the AFC (see Fig. 1(c)). Our experiment opens prospects for the implementation of scalable quantum networks architectures using multimode solid state quantum memories.

[1] L.-M. Duan *et al.*, Nature **414**, 413 (2001).

[2] K. Ferguson *et al.*, Phys. Rev. Lett. **117**, 020501 (2016).

[3] K. Kutluer *et al.*, Phys. Rev. Lett. **118**, 210502 (2017).

[4] C. Laplane *et al.*, Phys. Rev. Lett. **118**, 210501 (2017).

[5] M. P. Hedges *et al.*, Nature **465**, 1052 (2010).

[6] G. Heinze *et al.*, Phys. Rev. Lett. **111**, 033601 (2013).

[7] M. Afzelius *et al.*, Phys. Rev. A **79**, 52329 (2009).

[8] P. Sekatski *et al.*, Phys. Rev. A **83**, 053840 (2011).

Multiplexed storage and real-time manipulation based on a multiple-degree-of-freedom quantum memory

Tian-Shu Yang[1,2], **Zong-Quan Zhou**[1,2], **and Chuan-Feng Li**[1,2]

[1] *CAS Key Laboratory of Quantum Information, University of Science and Technology of China, Hefei, 230026, China*

[2] *Synergetic Innovation Center of Quantum Information and Quantum Physics, University of Science and Technology of China, Hefei, 230026, P.R. China*

e-mail: *yts11@mail.ustc.edu.cn*

Quantum light-matter interfaces lie at the heart of photonic quantum information processing [1]. The faithful storage and coherent manipulation of quantum states with matter-systems enable the construction of large-scale quantum networks based on quantum repeater. To achieve useful communication rates, highly multimode quantum memories will be required to construct a multiplexed quantum repeater. Here, through the combination of this spatial degree-of-freedom with temporal and spectral degrees of freedom, we create a multiple-degree-of-freedom quantum memory at the single-photon-level with high multimode capacity. We further demonstrate that this quantum memory can be used to realize essentially arbitrary spectral and temporal manipulations of spatial-qutrit-encoded photonic pulses in real-time.

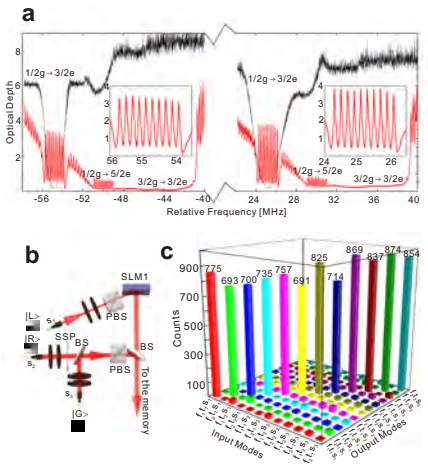


Figure 1: Multiplexed quantum storage in three DOF. **a**, The double AFC structure (red) in the MC and the double filter structure (black) in the FC. **b**, Three independent spatial modes carrying different OAM states are employed for spatial multiplexing. **c**, A demonstration of temporal, spectral and spatial multiplexing.

Here, we show that our solid-state memory can be simultaneously multiplexed in temporal, spectral and spatial DOF. As shown in Figure 1a, two AFC are created in the MC with an interval of 80 MHz between them to achieve spectral multiplexing. We employed two temporal modes. The spatial multiplexing is realized by using three independent paths as input as shown in Figure 1b. These paths, s_1, s_2 and s_3, correspond to the OAM states as $|L\rangle$, $|R\rangle$, and $|G\rangle$ defined above. By combining all three DOF together, we obtain $2 \times 2 \times 3 = 12$ modes in total.

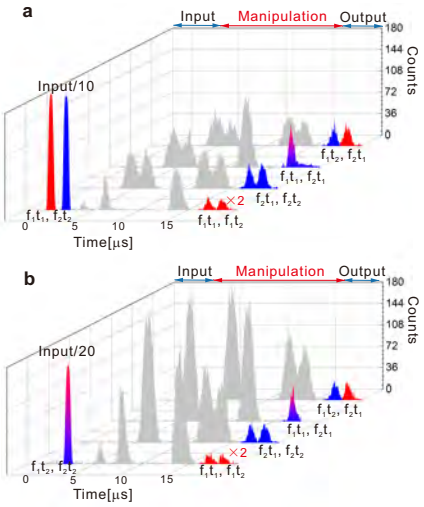


Figure 2: Four typical operations are presented for two different input states. **a**, The OAM qutrit state $|\psi_1\rangle$ encoded on the f_1t_1 and f_2t_2 modes. **b**, The OAM qutrit state $|\psi_2\rangle$ encoded on the f_1t_2 and f_2t_2 modes.

As an example, we prepared the OAM qutrit state $|\psi_1\rangle = (|L\rangle + |G\rangle + |R\rangle)/\sqrt{3}$ in the f_1t_1 and f_2t_2 modes (Figure 2a) as the input. Four typical operations were demonstrated, i.e., exchange of the readout times for the f_1 and f_2 photons, the simultaneous retrieval of the f_1 and f_2 photons at t_1, shifting the frequency of f_1 photons to f_2 but keeping the frequency of f_2 photons unchanged and temporal beam splitting the f_1 photons but filtering out the f_2 photons. These operations correspond to output of $|\psi_1\rangle_{f_1t_2, f_2t_1}$, $|\psi_1\rangle_{f_1t_1, f_2t_1}$, $|\psi_1\rangle_{f_2t_1, f_2t_2}$ and $|\psi_1\rangle_{f_1t_1, f_1t_2}$, respectively. Another example was implemented with the OAM qutrit state $|\psi_2\rangle = (|L\rangle + |G\rangle - i|R\rangle)/\sqrt{3}$ encoded in the f_1t_2 and f_2t_2 modes as the input, as shown in Figure 2 with same output.

[1] Sangouard, M., Simon, C., de Riedmatten, H. & Gisin, N. Quantum repeaters based on atomic ensembles and linear optics. *Rev. Mod. Phys.* **83**, 33-80 (2011).

Speeding Up Reinforcement Learning on a Trapped Ion Quantum Computer

Th. Sriarunothai[1], S. Wölk[1,2], G. S. Giri[1], N. Friis[3,2], V. Dunjko[2,4], H. J. Briegel[2,5], and C. Wunderlich[1]

[1] *Department of Physics, School of Science and Technology, University of Siegen, 57068 Siegen, Germany*
[2] *Institute for Theoretical Physics, University of Innsbruck, Technikerstraße 21a, 6020 Innsbruck, Austria*
[3] *Institute for Quantum Optics and Quantum Information, Austrian Academy of Sciences, Boltzmanngasse 3, 1090 Vienna, Austria*
[4] *Max Planck Institute for Quantum Optics 85748 Garching, Germany*
[5] *Department of Philosophy, University of Konstanz, 78457 Konstanz, Germany*
e-mail: *christof.wunderlich@uni-siegen.de*

The development of quantum computing and of novel methods for machine learning have, thus far, advanced nearly independently. However, recently fruitful interactions between the research fields of quantum information science and artificial intelligence lead to experiments overcoming the boundaries of these two fields.

Here, we report the first demonstration of the deliberation process of a learning agent in the framework of reinforcement learning on a quantum computer [1]. We show that decision making is sped up quadratically as compared to a classical agent using reflecting projective simulation (RPS) for reinforcement learning. Also, by varying over a wide range the initial relative probabilities for obtaining a desired action, it is shown that the experiment preserves these probabilities.

These experiments are carried out on a fully programmable 2-qubit quantum computer based on electrodynamically trapped $^{171}Yb^{+}$ ions. All coherent operations are carried out employing radio frequency (RF) radiation taking advantage of magnetic gradient induced coupling (MAGIC) between hyperfine states of individual ions. The quantum computer's register can be reconfigured on-the-fly to act as a quantum memory, or a processor carrying out conditional quantum dynamics, or both simultaneously, by simply applying RF pulses [2]. Different ion species are not required for this purpose.

RF-driven atomic ions and MAGIC, as used in these experiments, are a promising approach for realizing scalable quantum computing using interconnected modules containing quantum processors [3]. Transport of trapped ions is a prerequisite for this and other [4] scalable strategies for quantum computing with trapped ions. We have shown, by shuttling a single $^{171}Yb^{+}$ ion 22×10^6 times and quantifying the coherence of its hyperfine qubit, that the quantum information stored in this qubit is preserved with a fidelity of $99.9994(+6-7)\%$ during transport of the ion over a distance of 250 μm [5].

References

[1] Th. Sriarunothai, S. Wölk, G.S. Giri, N. Friis, V. Dunjko, H. J. Briegel, and C. Wunderlich, arXiv:1709.01366v2 [quant-ph].

[2] C. Piltz, T. Sriarunothai, S. S. Ivanov, S. Wölk and C. Wunderlich, Science Advances **2**, e1600093 (2016).

[3] B. Lekitsch, S. Weidt, A. G. Fowler, K. Mølmer, S. J. Devitt, C. Wunderlich and W. K. Hensinger, Science Advances **3** (2017).

[4] D. Kielpinski, C. Monroe and D. J. Wineland, Nature **417**, 709 (2002).

[5] P. Kaufmann, T. F. Gloger, D. Kaufmann, M. Johanning and C. Wunderlich, Phys. Rev. Lett. **120**, 010501 (2018).

Scaling of electric field noise in surface ion traps

C. Matthiesen, C. Noel, M. Lewin-Berlin, D. An, E. Urban and H. Häffner
Department of Physics, University of California, Berkeley, California 94720, USA
e-mail: *cm467@berkeley.edu*

In the canonical trapped ion approach to quantum computing, the motional modes serve as a quantum bus for the transfer of information between the ions. For instance, entanglement between ions in the same trap takes advantage of their coupling to a common motional mode in this scheme. High-fidelity gates then require a high degree of coherence of the ion motion. Electric fields fluctuating at the trap frequency lead to decoherence, placing a limit on achievable fidelities.

With the advance of small chip-based radio-frequency Paul traps, or surface traps, ions are routinely trapped at distances of tens to hundreds of micrometers from the nearest surface. At these distances, electric field noise emanating from the trap chip is the dominant source of motional decoherence. The measured noise amplitude is orders of magnitude larger than expected from Johnson noise from the metallic trap electrodes.

Some surface treatment techniques [1] and cooling ion traps to cryogenic temperatures [2] have yielded large reductions in electric field noise, pointing to the importance of the trap surface. However, after more than a decade of research and a wealth of proposed mechanisms, unifying explanations for the surface noise have not been found [3].

Surface noise is typically characterised by its dependence on three parameters, namely frequency ω, distance to nearest surface d, and temperature T and written as a power law

$$S_{\mathrm{E}} \propto \omega^{-\alpha} d^{-\beta} T^{+\gamma}\,, \tag{1}$$

where S_{E} is the spectral noise density of the electric field. Here, we study pairs of these parameters in two separate traps. S_{E} is measured through the ion heating rates, which are proportional to S_{E}. Both traps use 1-μm-thick aluminium-copper electrodes on a fused silica substrate. The first trap employs a five-electrode linear surface trap design, and is mounted on a heating element inside the ultra-high-vacuum chamber. Heating rates show a non-trivial dependence on the trap temperature, ruling out technical noise sources, and several of the proposed noise mechanisms. In fact, to the best of our knowledge the only consistent model is that of thermally-activated fluctuators. The model predicts a temperature-dependent noise frequency scaling which we confirm in our experiment.

In the second experiment, we employ a novel trap design allowing us to tune the ion-electrode separation using static fields. With this trap we measure electric field noise both parallel and perpendicular to the trap surface for ion-surface distances between 50 and 300 μm. The distance scaling $\sim d^{2.5}$ suggests a surface noise correlation length of tens of microns, in contrast to recent other experiments [4, 5]. At low trapping heights, the electric field noise scales more favourably with trap miniaturisation than expected from the commonly assumed d^{-4} dependence.

[1] D. A. Hite, Y. Colombe, A. C. Wilson, K. R. Brown, U. Warring, R. Jördens, J. D. Jost, K. S. McKay, D. P. Pappas, D. Leibfried and D. J. Wineland, Phys. Rev. Lett. **109**, 103001 (2012).

[2] J. Labaziewicz, Y. Ge, P. Antohi, D. Leibrandt, K. R. Brown and I. L. Chuang, Phys. Rev. Lett. **100**, 013001 (2008).

[3] M. Brownnutt, M. Kumph and P. Rabl and R. Blatt, Rev. Mod. Phys. **87**, 1419 (2015).

[4] I. A. Boldin, A. Kraft, and C. Wunderlich, Phys. Rev. Lett. **120**, 023201 (2018).

[5] J. A. Sedlacek, A. Greene, J. Stuart, R. McConnell, C. D. Bruzewicz, J. M. Sage, and J. Chiaverini, Phys. Rev. A **97**, 020302(R) (2018).

Progress towards entanglement of atomic ensemble qubits via Rydberg blockade

Minho Kwon[1], **Christopher Young**[1], **Matthew Ebert**[1], **Thad Walker**[1] **and Mark Saffman**[1]
[1] *Department of Physics, University of Wisconsin-Madison*
1150 University Ave, Madison WI 53706, USA
e-mail: *mkwon22@wisc.edu*

We report on progress towards Rydberg-mediated deterministic preparation and control of atomic ensemble qubits. Collectively enhanced atom-light coupling[1–4] and robustness against particle loss[5] make ensemble qubits promising candidates for quantum information processing[6, 7]. Our previous demonstration[8] of the preparation of an ensemble qubit into W-state, or symmetric and singly excited state, was limited to moderate fidelity <60%. We surmise that short-range interactions between atom-atom pairs lead to Rydberg blockade leakage. In order to restrict unwanted molecular resonance channels[9], we insert a blue-detuned 1-D lattice superimposed over an existing red-detuned dipole trap, thereby imposing constraints on the minimal interatomic distance. We study the effect of lattice insertion on the fidelity of ensemble state preparation and Rydberg-mediated gates, as well as altered atom collision rates. In the context of quantum memory applications, cooperative scattering[10–14] of single photons from 1D atom chains is studied and we present preliminary calculations on the altered decay rate and emission modes from such atomic ensembles. Technical advances on an automatic alignment system, to improve the pointing stability of the tightly focused Rydberg excitation beams, are also presented.

*This research was supported by the NSF under award PHY-1521374.

[1] R. Heidemann, U. Raitzsch, V. Bendkowsky, B. Butscher, R. Low, L. Santos, and T. Pfau, Phys. Rev. Lett. **99**, 163601 (2007).

[2] A. Gaetan, Y. Miroshnychenko, T. Wilk, A. Chotia, M. Viteau, D. Comparat, P. Pillet, A. Browaeys, and P. Grangier, Nature Phys. **5**, 115 (2009).

[3] Y. O. Dudin, L. Li, F. Bariani, and A. Kuzmich, Nature Phys. **8**, 790 (2012).

[4] M. Ebert, A. Gill, M. Gibbons, X. Zhang, M. Saffman, and T. G. Walker Phys. Rev. Lett. **112**, 043602 (2014).

[5] E. Brion, K. Mølmer, and M. Saffman, Phys. Rev. Lett. **99**, 260501 (2007).

[6] M. D. Lukin, M. Fleischhauer, R. Cote, L. M. Duan, D. Jaksch, J. I. Cirac, and P. Zoller, Phys. Rev. Lett. **87**, 037901 (2001).

[7] M. Saffman and T. G. Walker, Phys. Rev. A **72**, 042302 (2005).

[8] M. Ebert, M. Kwon, T. G. Walker, and M. Saffman, Phys. Rev. Lett. **115**, 093601 (2015).

[9] A. Derevianko, P. Kómár, T. Topcu, R. M. Kroeze, and M. D. Lukin, Phys. Rev. A **92**, 063419 (2015).

[10] M. Saffman and T. G. Walker, Phys. Rev. A **66**, 065403 (2002).

[11] Robert J. Bettles, Simon A. Gardiner, and Charles S. Adams, Phys. Rev. A **94**, 043844 (2016).

[12] S.J. Roof, K.J. Kemp, M.D. Havey, and I.M. Sokolov, Phys. Rev. Lett. **117**, 073003 (2016).

[13] Anatoly A. Svidzinsky, Jun-Tao Chang, and Marlan O. Scully, Phys. Rev. A **81**, 053821 (2010).

[14] Martin Hebenstreit, Barbara Kraus, Laurin Ostermann, and Helmut Ritsch, Phys. Rev. Lett. **118** 143602 (2017).

Independent gate operations on two adjacent atomic qubits in a 532-nm 1D optical lattice

Hyok Sang Han, Hyun Gyung Lee, Seokchan Yoon and D. Cho
Department of Physics, Korea University, Seoul 02841, Korea
e-mail: *cho@korea.ac.kr*

Spin state of an atomic qubit at a specific site of a 1D optical lattice is manipulated without affecting coherence of a qubit in an adjacent site when separation between the sites is only 532 nm. We use the $|2S_{1/2}, F = 1, m_F = 1\rangle$ and $|2S_{1/2}, F = 2, m_F = 2\rangle$ states of ^{7}Li as the qubit states. Site-specific addressing is achieved by using a site-dependent Zeeman shift under a 1.6 G/cm magnetic field gradient. See Fig. 1. Difference in Zeeman shift between the adjacent sites is 180 Hz. We reduce inhomogeneous broadening of the ground hyperfine transition, which has been a major obstacle in this approach, to less than 10 Hz by using magic polarization [1] for the lattice. We also employ a low-expansion mounting system to avoid drift in position of a target site with respect to B gradient, a three-layer magnetic shield to reduce effect of ambient field, and a network of stabilization systems that allow a long-term data taking. Transition frequency at a specific site stays constant to within 1 Hz for a few hours.

The experiment consists of two parts: one is the loading of a single atom to a specific site, and the other is to use the atom to demonstrate site-specific operation. For the single atom loading, (i) atoms are loaded to the 1D lattice from a double MOT system, (ii) they are Doppler cooled and optically pumped to the $|2S_{1/2}, F = 2, m_F = 2\rangle$ state, (iii) π pulse transition to the $|2S_{1/2}, F = 1, m_F = 1\rangle$ state at a specific site is driven by a 803-MHz RF pulse under the B gradient, (iv) atoms in $F = 2$ state are blown away by a push beam, and finally (v) probe fluorescence is monitored to confirm presence of a single atom. Success probability for the loading is less than 50% and the process may have to be iterated. The octagonal glass chamber for the lattice and a single-atom image is shown in Fig. 2.

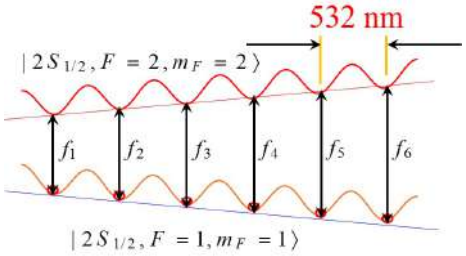


Figure 1: Site-dependent Zeeman shift of the qubit transition in 1D optical lattice under a magnetic field gradient.

For the site-specific gate operations, using the single atom loaded to the target site (i) apply a short $\pi/2$ pulse so that atoms are driven to a superposition state regardless of its position, (ii) apply a long gate pulse, which is specific to the target site, (iii) apply another short $\pi/2$ pulse with a varying phase shift from the first pulse, and (iv) detect the final spin state of the atom. Measurements are made with a single atom at either the target site or its adjacent site. Effect of the long-pulse gate operation shows up only for the target qubit, and the adjacent qubit shows a usual Ramsey signal from the two short $\pi/2$ pulses. We will present quantitative results at the Conference.

With this ability to coherently address individual qubits and the new ideas such as a superlattice and Feshbach-enhanced cold collisional interaction, we may revisit a 1D optical lattice to realize its full potential as the simplest nontrivial platform for quantum information processing.

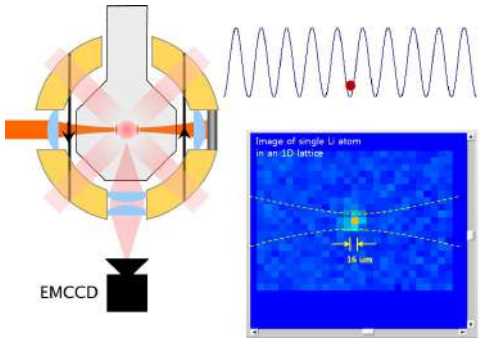


Figure 2: Octagonal glass chamber where the second MOT and the optical lattice are formed. The image is that of a single atom taken by an electron-multiplying charge-coupled device (EMCCD).

[1] Huidong Kim, Hyok Sang Han, and D. Cho, Phys. Rev. Lett **111**, 243004 (2013).

Modular segmented ion trap with an integrated optical cavity

S. Ragg[1], **T. Lutz**[1], **K. Theophilo**[2], **C. Decaroli**[1] **and J. P. Home**[1]

[1] *Trapped Ion Quantum Information Group, Institute for Quantum Electronic, ETH Zurich, 8093 Zurich, Switzerland*

[2] *Grupo de Optica, Instituto de Fisica de São Carlos (IFSC), Universidad de São Paulo, 13566-590 São Carlos, Brasil*

e-mail: *raggs@phys.ethz.ch*

Atomic ions trapped in radio frequency traps and cooled by laser light are a leading candidate for a quantum information processor. Scaling such a system by controlling a large number of ions confined in a single trap presents immense technical challenges. A possible solution is to link a large number of well controlled modular ion trap processors through optical interconnects to form a scalable ion trap quantum architecture [1].

I will present work towards an ion trap that could serve as such a module. The trap will be built using fused silica wafers which are etched after laser ablation [3], allowing us to create arbitrary electrode configurations and shapes. The trap design provides optical access for a high-finesse cavity, while shielding the ions from possible effects of dielectric mirror charging. Furthermore, it provides precise and foolproof relative alignment of the trap wafers. Figure 1 shows one of the newly developed trap wafers. In contrast to previous approaches, our trap is fully encapsulated, optical access into the trapping region for laser light and cavity mode is only provided along tailored channels. As a result, trap size and cavity length are highly correlated.

An initial run will use a fiber cavity at 854 nm, with a length of around $400\mu m$.

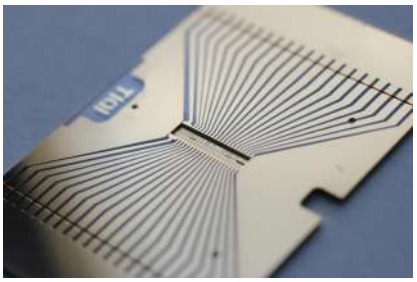


Figure 1: New developed trap chip.

Tests with fiber-tips [2] with ROC of around 200 μm have shown that we can reach the targeted cavity length while at the same time maintaining a Finesse of at least 65 000. Using fibers with ROC between 300 μm and 450 μm will give us a stable cavity of length longer than 400 μm and provide high ion-photon coupling.

[1] C. Monroe et al., Phys. Rev. A **89**, 022317 (2014).

[2] The fibers are provided by T. Northup from University of Innsbruck.

[3] `https://www.femtoprint.ch`

Towards a temporally multiplexed quantum repeater node based on laser-cooled atoms

L. Heller[1], **P. Farrera**[1], **G. Heinze**[1] **and H. de Riedmatten**[12]

[1] *Institut de Ciències Fotòniques, The Barcelona Institute of Science and Technology, 08860 Castelldefels, Spain*

[2] *ICREA-Institució Catalana de Recerca i Estudis Avançats, 08015 Barcelona, Spain*

e-mail: *lukas.heller@icfo.eu*

A global quantum network involves the efficient transfer and storage of information encoded in quantum states of light. Direct end-to-end transmission of single photons is not possible within reasonable time scales, mainly due to various sources of losses in the communication channel. To overcome this limitation, quantum repeater architectures have been proposed [1] that rely on entanglement preparation and swapping mechanisms and quantum memories. To further boost the performance of the quantum repeater, namely to greatly enhance entanglement rates, different forms of multiplexing have been proposed and implemented experimentally. These include for example spatial, frequency and temporal multiplexing [2]. For $N_m P_0 \ll 1$, N_m beeing the number of stored modes and P_0 the entanglement generation probability, the gain in entanglement rates scales linearly with the number of modes that can be stored in the memory.

We want to demonstrate a temporally multiplexed quantum repeater in a laser-cooled cloud of ^{87}Rubidium atoms. We employ the DLCZ protocol [3] where pairs of photons and collective spin excitations are created. The latter can then be efficiently transferred into a single photon. The implementation of DLCZ in cold gases does not posses intrinsic temporal multiplexing capabilities. In order to achieve this multiplexing we make use of controlled reversal of inhomogeneous broadening techniques (CRIB) to distinguish different temporal modes [4]. An inhomogenous broadening can be achieved by means of a magnetic field gradient that acts on the Zeeman sublevels of the atomic transitions. This broadening can then be reversed in a controlled way by reversing the magnetic field gradient. The storage of two modes combining DLCZ and controlled rephasing has already been shown by the group [5]. However, an important limitation is that the error due to increasing noise scales linearly with the number of modes.

For the present work, a low-finesse cavity was build around the atoms in order to suppress background noise from spin waves created in other time bins. It is resonant with the write photons but does not alter the read photon decay probabilities. An upper limit of the number of modes that can be stored, compared to the case without cavity, is given by the cavity's finesse and the inhomogeneous broadening [4]. We will report on the CRIB technique and initial results when the quantum memory is combined with the cavity.

The successful implementation of temporal multiplexing in a laser-cooled DLCZ storage medium will pave the way to both highly-efficient and long-lived quantum memories with multiplexing capabilities at hand. A device with such characteristics is a crucial key element of any quantum repeater architecture and may enable the distribution of quantum states of light over long distances in the future.

[1] H-J. Briegel, W. Dür, J. I. Cirac and P. Zoller, Phys. Rev. Lett. **81**, 5932 (1998).

[2] N. Sangouard, C. Simon, H. de Riedmatten and N. Gisin, Rev. Mod. Phys. **83**, 33 (2011).

[3] L.-M. Duan, M. Lukin, J. I. Cirac, and P. Zoller, Nature (London) **414**, 413 (2001).

[4] C. Simon, H. de Riedmatten and M. Afzelius, Phys. Rev. A **82**, 010304(R) (2010).

[5] B. Albrecht, P. Farrera, G. Heinze, M. Cristiani and H. de Riedmatten, Phys. Rev. Lett. **115**, 160501 (2015).

Quasi-continuous variable quantum computation with collective spins in multi-path interferometers

T. Opatrný

Optics Department, Palacký University, 17. Listopadu 12, 77146 Olomouc, Czech Republic

e-mail: *opatrny@optics.upol.cz*

For quantum computation with continuous variables (CVs) one needs (i) a sufficiently large set of single CV modes each of which can be initialized in a suitable quantum state, (ii) a suitable set of single-mode Hamiltonians capable to be combined into more complicated Hamiltonians realizing arbitrary polynomials of the CV, and (iii) a suitable interaction Hamiltonian of different CVs. As shown in [1], having in each mode k a conjugate pair of variables q_k and p_k commuting as $[q_k, p_k] = i$, any polynomial Hamiltonian of q_k and p_k can be constructed if a Hamiltonian of at least third power of q_k or p_k is available, as well as some simpler Hamiltonians realizing, e.g., displacements or rotations in the phase space. Hamiltonians containing higher powers of q and p are generated by cascaded application of commutators of lower power Hamiltonians.

Based on the spin squeezing experiments [2], a scheme of quasi-CV quantum computation working with collective spins of large atomic samples is proposed [3]. The collective spin components commute as $[X, Y] = iZ$, etc., and interact via optical fields in multi-path interferometers. Although spin is a discrete variable, for large N and nearly polarized atomic samples the spin components perpendicular to the polarization direction have similar properties as the CVs position and momentum of a harmonic oscillator. Visualizing collective spin states on a Bloch sphere, the computationally relevant states are localized in a confined area where the geometry is close to that of a flat phase space. On the other hand, the curved geometry brings a special advantage in that already quadratic Hamiltonians typically used to generate spin squeezing are sufficient to generate higher power Hamiltonians by commutators. This is achieved by a sequence of rotations (linear Hamiltonian) and squeezing operations (quadratic) which can realize, e.g.,

$$X^3 = \frac{i}{4}\left[(Z^2 - Y^2), (YZ + ZY)\right] + \frac{i}{4}\left[(XZ + ZX), (XY + YX)\right] + \frac{1}{4}X.$$

Moreover, if the atomic samples are placed in optical resonators mutually coupled to form an interferometer, the off-resonant atom-light interaction can mediate quantum non-demolition (QND) interaction between various samples. By changing resonator lengths and optical phases between the resonators, one can select the modes to interact. Thus, multi-mode polynomial Hamiltonians can be realized. To realize quantum computation, the system is initialized by squeezing the atomic spins in each resonator, and at the end the results are read-off by measuring the relevant spin components as in the cavity spin squeezing experiments.

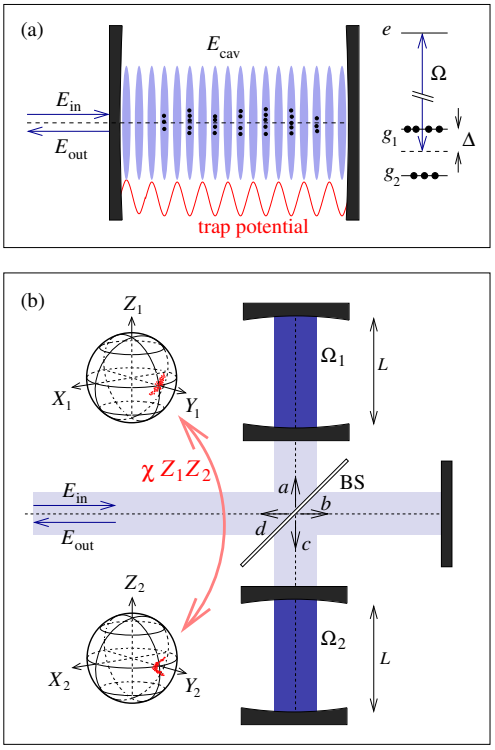


Figure 1: (a) Scheme of the resonator with trapped atoms. (b) Michelson-like interferometer with two resonators. Difference of atomic numbers in states g_1 and g_2 corresponds to the spin coordinate Z. Phase of each resonator influences the intensity in both of them. The QND interaction rotates sphere 1 around the Z_1 axis in dependence on the value of Z_2 and vice versa.

[1] S. Lloyd and S. L. Braunstein, Phys. Rev. Lett. **82,** 1784 (1999).

[2] M. H. Schleier-Smith, I. D. Leroux, and V. Vuletić, Phys. Rev. Lett. **104,** 073604 (2010).

[3] T. Opatrný, Phys. Rev. Lett. **119,** 010502 (2017)

Eliminating Noise from a Broadband and Single-Mode Quantum Memory

T. M. Hird[1,2], **S. E. Thomas**[1,3], **J. H. D. Munns**[1,3], **K. T. Kaczmarek**[1], **O. L. Arjona**[1], **S. Gao**[1], **J. Nunn**[4], **B. Brecht**[1], **D. J. Saunders**[1], **P. M. Ledingham**[1], **and I. A. Walmsley**[1]

[1] *Clarendon Laboratory, University of Oxford, Parks Road, Oxford OX1 3PU, United Kingdom*

[2] *Department of Physics and Astronomy, University College London, London WC1E 6BT, United Kingdom*

[3] *Blackett Laboratory, Imperial College London, London SW7 2BW, United Kingdom*

[4] *Department of Physics, University of Bath, Claverton Down, Bath, BA2 7AY, United Kingdom*

e-mail: *thomas.hird@physics.ox.ac.uk*

Single-mode broadband quantum memories provide unique capabilities that can enhance and expand the performance of future quantum networks. On the one hand, they facilitate the temporally multiplexed generation of pure single photons at high clock rates, which dramatically increases photon generation rates [1]. On the other hand, they can serve as special quantum mechanical beam splitters that can operate on novel bases for information encoding. One such basis are temporal modes complex temporal amplitudes of pulsed single photons which have been identified as appealing high-dimensional basis states for integrated quantum networks[2].

Our system of choice is a quantum memory in warm atomic Caesium vapour, based on an off-resonant Raman scattering protocol [3], which combines operation at ambient conditions, high storage efficiencies, GHz bandwidth storage, and single-mode operation [4].

Previous implementations of the Raman memory have suffered from four-wave mixing noise (Figure 1a) where the control couples to the populated state to produce a noise photon by Anti-Stokes scattering. This noise contaminates the retrieved fields with thermal noise, destroying the non-classical statistics of stored quantum states. This has been identified as the key limiting factor in reaching quantum level operation[5].

Here we demonstrate a novel technique to suppress the four-wave mixing noise by creating an absorption feature for the noise, thereby preventing that process. This is achieved by arranging the detuning such that it is resonant with an atomic transition (Figure 1a and 1b) [6]. Using this technique we have shown a nearly an order of magnitude reduction in noise photons when using this suppression method (Figure 1c).

With the elimination of this noise pathway, the Raman memory is a technically simple broadband and single mode memory capable of selectively storing an arbitrary and user chosen quantum state. Therefore, with further engineering, the Raman memory is a promising candidate for temporal-mode selection and multiplexed photon generation in future quantum networks.

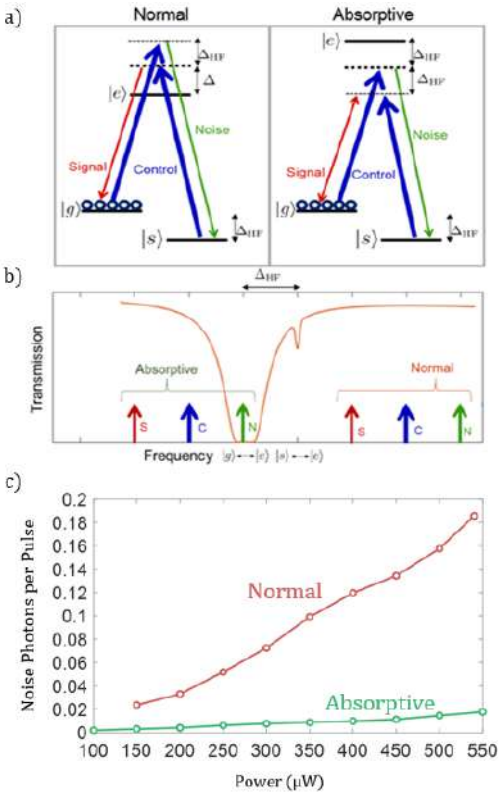


Figure 1: a) Energy level diagram showing the fields involved in the Raman memory, including the four-wave mixing process. b) Transmission spectra of Caesium showing the position of the fields in the normal operation of the Raman memory and when in the absorptive suppression scheme. c) Noise photons produced per pulse in the two regimes as a function of control field power that is, memory operation strength.

References

[1] J Nunn et al. *Phys. Rev. Lett.*, 110(13):133601, 2013.

[2] B Brecht et al. *Physical Review X*, 5(4):041017, 2015.

[3] J Nunn et al. *Phys. Rev. A*, 75(1):011401, 2007.

[4] JHD Munns et al. In preperation.

[5] PS Michelberger et al. *New Journal of Physics*, 17(4):043006, 2015.

[6] G Romanov et al. *Journal of Modern Optics*, 63(20):2048–2057, 2016.

High-Dimensional Temporal Mode Manipulation using Quantum Memories

S. E. Thomas[1,2], **J. H. D. Munns**[1,2], **M. Hynes**[1], **T. M. Hird**[1,3], **P. M. Ledingham**[1], **D. J. Saunders**[1], **J. Nunn**[4], **B. Brecht**[1], **and I. A. Walmsley**[1]

[1] *Clarendon Laboratory, University of Oxford, Parks Road, Oxford, OX1 3PU, UK*

[2] *Blackett Laboratory, Imperial College London, London SW7 2BW, UK*

[3] *Department of Physics and Astronomy, University College London, London WC1E 6BT, UK*

[4] *Centre for Photonics and Photonic Materials, University of Bath, North Road, Bath, BA2 7AY, UK*

e-mail: *sarah.thomas@physics.ox.ac.uk*

There are many architectures for quantum information processing, each with their own distinct advantages and drawbacks, and the route towards scalable quantum technologies is likely to involve combining these unique advantages in a hybrid system. Photons are a promising platform for quantum communication and for interfacing different nodes of a quantum network. However, to optimally couple different devices and components of a quantum network we require the capability to engineer and manipulate the spectral-temporal wavepacket of pulsed photons, the so-called temporal mode (TM) [1].

Here we demonstrate a temporal mode manipulation device which can separate and reshape arbitrary temporal wavepackets of light. We show TM manipulation of weak coherent pulses in a Raman quantum memory in warm atomic caesium vapour [2]. The Raman interaction can be described as a time non-stationary light-matter beam splitter that acts on a single temporal mode [3], and therefore the shapes of the stored and retrieved TM are defined by the temporal amplitudes of the strong control pulses used to drive the memory. This enables storage, delay and re-shaping of a user-defined TM in one single device.

The Raman memory operates on pulses in the MHz and GHz regime, and can therefore interface narrowband atomic systems with fast GHz-bandwidth communication networks. We demonstrate bandwidth conversion of ns-duration Gaussian pulses by increasing and decreasing the bandwidth by a factor of 25, as shown in Figure 1(a). We compare the efficiency of this process to that of using a bandwidth filter, and find that the memory can outperform a filter at large compression factors.

Furthermore, TMs have been identified as an appealing basis for quantum information science as they form a high dimensional basis that is compatible with single-mode fibres [1]. By selecting the TM of the storage and retrieval control pulses of the Raman memory, we can fully determine which mode is stored and then retrieved from the memory, allowing us to separate and convert TMs. We demonstrate conversion between different Hermite-Gaussian modes and Figure 1(b) shows that we can fully convert between the first five basis states, and the efficiency of the conversion (storage and retrieval) is around 35% for all state transformations.

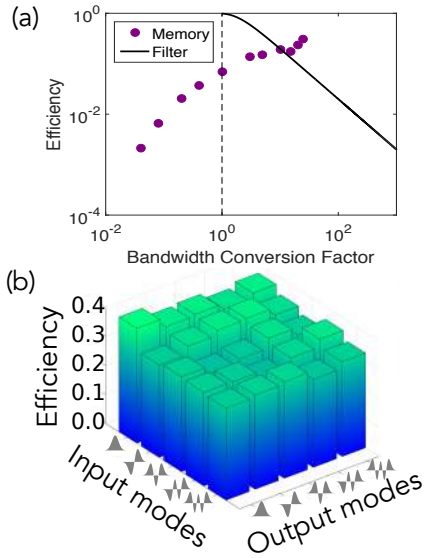


Figure 1: (a) Efficiency of bandwidth conversion using the Raman memory. The solid line shows the equivalent efficiency for a bandwidth filter. (b) The efficiency of conversion between different Hermite-Gaussian temporal modes.

We have shown that the Raman memory is a versatile device for temporal mode manipulation. Its applications include interfacing different solid state systems such as atoms and quantum dots, where you require not only bandwidth conversion but also re-shaping (temporal inversion) of the temporal wavepacket. It also will enable quantum key distribution using temporal modes as a high dimensional encoding alphabet to realise fibre-compatible qudits. This highlights its potential as a key device in future quantum networks.

[1] B. Brecht et al. hoton temporal modes: A complete framework for quantum information science. *Physical Review X*, 5(041017), 2015.

[2] K. F. eim et al. Single-photon-level quantum memory at room temperature. *Physical Review Letters 107*, 107(053603), 2011.

[3] J. Nunn et al. apping broadband single-photon wave packets into an atomic memory. *Physical Review A*, 75(011401), 2007.

Microfabricated optical elements towards a photonic interface for ion microtrap arrays

Matthew Day[1,2,3], **Kaushal Choonee**[3], **Zachary Chaboyer**[4], **Simon Gross**[4], **Michael Withford**[4], **Alastair G. Sinclair**[3], **Graham D. Marshall**[1]

[1] *Quantum Engineering Technology Labs, University of Bristol, BS8 1TL, UK*

[2] *Quantum Engineering Centre for Doctoral Training, University of Bristol, BS8 1TL, UK*

[3] *National Physical Laboratory, Teddington, TW11 0LW, UK*

[4] *Centre for Ultrahigh bandwidth Devices for Optical Systems (CUDOS), MQ Photonics Research Centre, Macquarie University, NSW 2109, Australia*

e-mail: *matt.day@bristol.ac.uk*

Trapped ions are a useful resource for protocols in quantum information processing and quantum metrology. Scaling to large numbers of entangled ions in a segmented microtrap array requires laser addressing of multiple trapping segments. Each segment needs one or more wavelengths with specific propagation vectors for operations such as photoionisation, laser cooling and qubit control. One approach is to use microfabricated optics such as planar waveguides with focusing couplers [1] or diffractive lenses [2]. We propose a novel method based on laser-written waveguides (with a 3D topology) and diffractive microlenses. In this work we have demonstrated the principles of the constituent optical components.

We have investigated a variety of techniques for the fabrication of diffractive microlenses (DMLs) for focusing 405 nm radiation, which is the shortest required wavelength for $^{88}Sr^{+}$ operation. Focused ion beam milling was used to shape continuous surface-relief DMLs in BK7 glass [3], demonstrating a maximum diffraction efficiency of 84.0% with background intensities of -40 dB away from the beam focus. A grayscale electron beam lithography (EBL) process was developed for fabricating continuous-relief profiles of DMLs in poly(methyl methacrylate) (PMMA). This enabled rapid prototyping of lens designs and demonstrates maximum diffraction efficiencies of 93.8% and 76.8% for on-axis and 20° off-axis lenses respectively. We have also established the principle of transferring PMMA surface-reliefs into thin-film titania substrates using reactive-ion etching, which includes compensation (during EBL writing) of the non-linear nature of the etch process. We measure maximum diffraction efficiencies of on-axis titania microlenses of 89.5%; fabrication of off-axis microlenses in titania is underway.

Trapped $^{88}Sr^{+}$ ions require specific wavelengths in the range from 405 to 1092 nm for full operation. We developed buried laser written waveguides with a 3D topology, in aluminosilicate glass, for single-mode guidance of blue and near-IR wavelengths. A laser-written waveguide chip as a component of an optical system, designed to couple to trapped $^{88}Sr^{+}$ ions in two neighbouring segments of a monolithic microtrap [4], was then fabricated. The waveguide chip contains 10 waveguides in total, including 3 at 422 nm (Doppler cooling), 1 at 1033 nm (qubit state quencher), and 1 at 1092 nm (cooling repumper) for two individual segments. The waveguide chip has been coupled, and bonded, to a fibre array with < 3 dB loss in all 10 waveguides.

We have demonstrated the principle of combining the waveguide chip with a microlens array for focusing independent waveguide outputs to a single point (e.g. the centre of a microtrap segment). The waveguide chip was successfully coupled to a PMMA DML array designed to overlap 3 blue beams with the required k-vectors. The overlapping of the full beam sets is still a work in progress, as is the realisation of the microlens array in titania.

The effects of the proximity of dielectric material to the RF trapping field is has been numerically studied. We found that a grounded conductive coating is required around the microlenses to alleviate charge accumulation. This allows a microlens array to be placed ≥ 1 mm from the trap centre without uncontrolled displacement of the trapping potential minimum. Bringing the optics to ≥ 400 μm of the trap centre requires modest voltages (< 4 V) on the DC compensation electrodes to correct for the displacement of the ion position.

The viability of the designed optical assembly will be discussed, based on the demonstrated optical components in this work. The eventual integration of the optical assembly into the vacuum chamber remains the largest challenge and we will present our proposed solutions.

[1] K. K. Mehta *et al.*, "Integrated optical addressing of an ion qubit," *Nat. Nano.*, vol. 11, pp. 1066–1070, Dec 2016.

[2] E. W. Streed *et al.*, "Imaging of trapped ions with a microfabricated optic for quantum information processing," *Phys. Rev. Lett.*, vol. 106, p. 010502, 2011.

[3] M. Day *et al.*, "Continuous-relief diffractive microlenses for laser beam focusing," *Opt. Express*, vol. 25, no. 22, pp. 26987–26999, 2017.

[4] G. Wilpers *et al.*, "A monolithic array of three-dimensional ion traps fabricated with conventional semiconductor technology," *Nat. Nano.*, vol. 7, no. 9, pp. 572–576, 2012.

Electron and Nuclear spin dynamics of Kramers ion at Subkelvin Temperatures

Pei-yun Li[1,2], Chao Liu[1,2], Zong-quan Zhou[1,2], Xiao Liu[1,2], Zong-feng Li[1,2], Tian-shu Yang[1,2], Jun Hu[1,2], Yu Ma[1,2], Peng-jun Liang[1,2], Xue Li[1,2], Chuan-feng Li[1,2], and Guang-can Guo[1,2]

[1] *CAS Key Laboratory of Quantum Information, University of Science and Technology of China, Hefei, 230026, China*

[2] *Synergetic Innovation Center of Quantum Information and Quantum Physics, University of Science and Technology of China, Hefei, 230026, P.R. China*

e-mail: *lpyzz@mail.ustc.edu.cn*

Rare Earth ions doped in crystal hosts has been recognized as a promising solid-state system for optical quantum technology due to their long optical and spin coherence time. Optical memory with storage time of 1 minute [1] quantum memory with high efficiency [2], high fidelety [3], on-demand [4] and multimode capacity [5] has been realized in this system. Nuclear spin coherence time as long as 6 hours has been acheived in Eu^{3+}:Y_2SiO_5 [6].

Kramers ions with unquenched electronic magnetic moment are endowed with a further interface to microwave photonsmaking them attractive candidates for microwave memory [7] and quantum transducers [8]. However, the large electronic magnetic moment also induces severe decoherence effect due to phonon-miediated relaxation process and magnetic dipole-dipole interaction. Such disadvantages can be significantly alleviated via reducing the temperature of the sample [9].

Here, we combine an X-band pulsed EPR spectrometer (Bruker Elexsys 580) with a dilution refrigerator to explore the spin dynamics of $^{143}Nd^{3+}$:Y_2SiO_5 at subkelvin temperatures.

To clarify the hyperfine level structures, the highly anisotropic Zeeman **g** matrix and hyperfine **A** matrix were deduced by gathering the EPR spectrograms as the crystal rotates in three orthogonal planes (b,D1), (b,D2), and (D1,D2) where magnetic field B_0 is contained. A home-made program based on *MATLAB* and *EasySpin* was used for the simulation. The simulated annealing algorithm was employed to minimize the deviation between experimental data and simulated result. At last, we got a average deviation of 18.4 Gauss for a single experimental data point. The best fit **g** tensor in D1D2b frame is:

$$g = \begin{pmatrix} -1.03 & -2.48 & 0.44 \\ -2.49 & -2.19 & -0.14 \\ 0.44 & -0.14 & 1.39 \end{pmatrix}$$

The best fit **A** tensor in D1D2b frame is (in MHz):

$$A = \begin{pmatrix} 495.7 & 687.4 & -232.8 \\ 687.4 & 751.8 & 165.8 \\ -232.8 & 165.8 & -338.3 \end{pmatrix}$$

The electron spin coherence time T_{2e} has increased from 33μs at 6K to 205μs at 0.1k. The growth momentum significantly alleviates below 2.5K due to instantaneous diffusion. Nevertheless, with the much smaller magnetic momentum, coherence time of nuclear spin increases quickly below 1K, reaching 43ms at 0.1K. Data curve is given in Fig. 1.

References

[1] Georg Heinze, Christian Hubrich, and Thomas Halfmann. *Phys. Rev. Lett.*, 111:033601, Jul 2013.

[2] Mahmood Sabooni, Qian Li, Stefan Kröll, and Lars Rippe. *Phys. Rev. Lett.*, 110:133604, Mar 2013.

[3] Zong-Quan Zhou, Wei-Bin Lin, Ming Yang, Chuan-Feng Li, and Guang-Can Guo. *Phys. Rev. Lett.*, 108:190505, May 2012.

[4] Alessandro Seri, Andreas Lenhard, Daniel Rieländer, Mustafa Gündoğan, Patrick M. Ledingham, Margherita Mazzera, and Hugues de Riedmatten. *Phys. Rev. X*, 7:021028, May 2017.

[5] Zong-Quan Zhou, Yi-Lin Hua, Xiao Liu, Geng Chen, Jin-Shi Xu, Yong-Jian Han, Chuan-Feng Li, and Guang-Can Guo. *Phys. Rev. Lett.*, 115:070502, Aug 2015.

[6] Manjin Zhong, Morgan P Hedges, Rose L Ahlefeldt, John G Bartholomew, Sarah E Beavan, Sven M Wittig, Jevon J Longdell, and Matthew J Sellars. *Nature*, 517(7533):177, 2015.

[7] S. Probst, H. Rotzinger, A. V. Ustinov, and P. A. Bushev. *Phys. Rev. B*, 92:014421, Jul 2015.

[8] Christopher O'Brien, Nikolai Lauk, Susanne Blum, Giovanna Morigi, and Michael Fleischhauer. *Phys. Rev. Lett.*, 113:063603, Aug 2014.

[9] D. D. Sukachev, A. Sipahigil, C. T. Nguyen, M. K. Bhaskar, R. E. Evans, F. Jelezko, and M. D. Lukin. *Phys. Rev. Lett.*, 119:223602, Nov 2017.

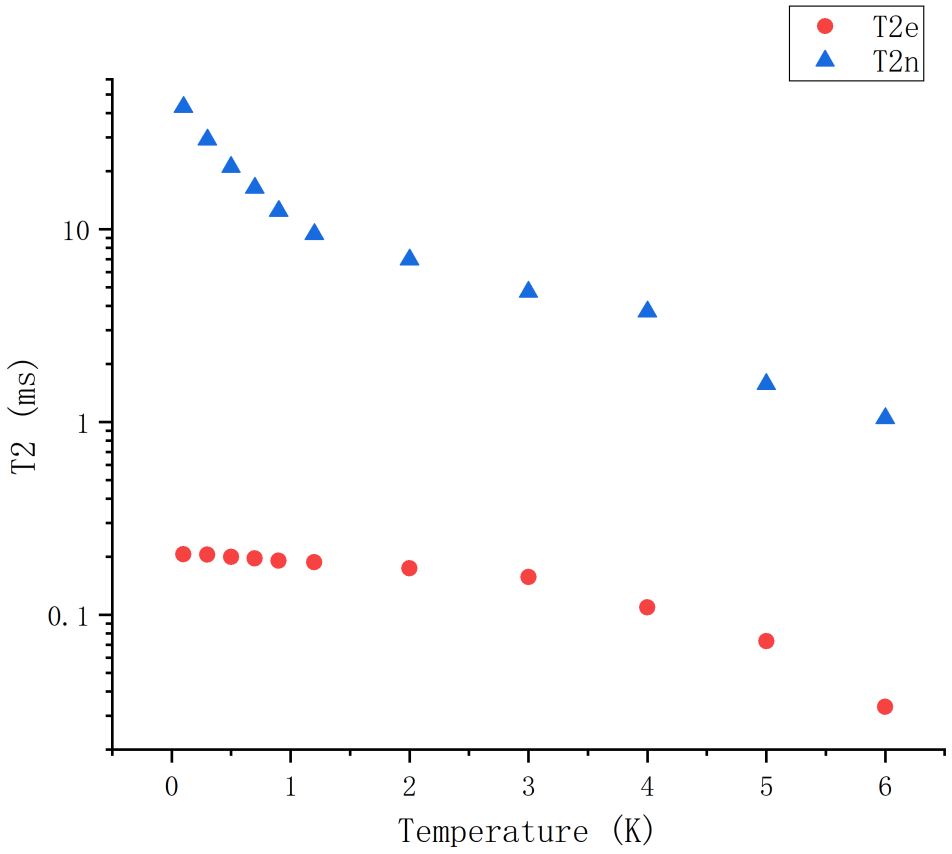


Figure 1: temperature dependence of electron and nuclear coherence time

Highly-Efficient Quantum Memory for Polarization Qubits in a Spatially-Multiplexed Cold Atomic Ensemble

M. Cao, P. Vernaz-Gris, K. Huang, A. S. Sheremet, and J. Laurat

Laboratoire Kastler Brossel, Sorbonne Université, CNRS, ENS-Université PSL, Collège de France, 4 place Jussieu, 75005 Paris, France

e-mail: *mingtao.cao@lkb.upmc.fr*

Quantum memory for flying optical qubits is a key enabler for a wide range of applications in quantum information science and technology, such as long-distance optical communication and all-optical quantum computation [1]. In this context, our group focuses on the demonstration of such interfaces based on large cold atom ensembles. In recent years, we demonstrated for instance the implementation of a quantum memory for quantum bits encoded in the orbital angular momentum (OAM) degree of freedom, which provides an essential capability for future networks with multimode capability [2]. We also realized multiple-degree-of-freedom memory, which can find applications in classical data processing but also in quantum network scenarios where states structured in phase and polarization have been shown to provide promising attributes [3].

In all these realizations, a critical figure of merit is the overall storage-and-retrieval efficiency. Theoretically, the retrieval efficiency can be improved with the increase of the optical depth (OD). Efficient optical memory has been demonstrated with large OD, however, high efficiency qubit storage had not been demonstrated. Here, we demonstrate a faithful quantum memory for polarization qubits with a storage-and-retrieval efficiency close to 70% [4]. Our implementation is based on electromagnetically-induced transparency (EIT) in a single spatially- multiplexed ensemble of cold cesium atoms featuring a large optical depth. The reported efficiency approaches the maximal performance achievable on the D2 line transition used here, as shown by a comprehensive model that includes all the involved atomic transitions. Relative to previous works, this advance has been possible by combining a high OD medium, efficient spatial multiplexing and low-noise operation.

More specifically, to obtain an ensemble with large optical depth, our experiment is based on an elongated 2D magneto-optical trap (MOT) of cesium atoms. Thanks to the large OD achieved here, we could investigate the scaling behaviour of the storage-and-retrieval efficiency. The maximal efficiency achieved here reaches 69 ± 1%. This represents a record on the cesium D2 line and, more importantly, the highest achievable value in this configuration. We have demonstrated a highly-efficient memory for optical qubits by successfully operating a large OD elongated atomic ensemble in a dual-rail configuration. This combination enables the reversible mapping of arbitrary polarization states not only with fidelities well above the classical benchmark but also with an overall storage-and-retrieval efficiency close to 70%. This value represents the highest efficiency to date for the storage and readout of optical qubits in any physical platforms and is more than double of the previously reported values. It also outperforms the important 50% threshold required to beat the no-cloning limit without post-selection.

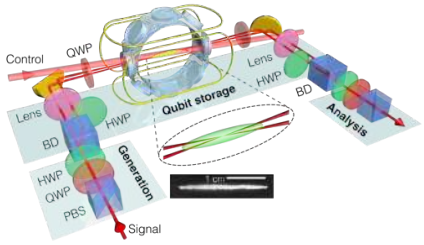


Figure 1: Highly-efficient quantum memory for polarization qubits in a spatially-multiplexed cold atomic ensemble.

Besides the aforementioned network architecture scalability and potential loss-tolerant schemes, the achieved efficiency opens the way to first tests of advanced quantum networking tasks where the storage node efficiency plays a critical role, such as in certification protocols or unforgeable quantum money. Moreover, the designed platform is directly compatible with recent works based on spatially structured photons and multiple-degree-of- freedom storage and can now yield to very efficient realizations to boost high-capacity network channels.

[1] K. Heshami, D. G. England, P. C. Humphreys, P. J. Bustard, V. M. Acosta, J. Nunn, and B. J. Sussman, J. Mod. Opt. **23**, 2005 (2016).

[2] A. Nicolas, L. Veissier, L. Giner, E. Giacobino, D. Maxein, and J. Laurat, Nat. Photon. **8**, 234 (2014).

[3] V. Parigi, V. D′Ambrosio, C. Arnold, L. Marrucci, F. Sciarrino, and J. Laurat, Nat. Comm. **6**, 7706 (2015).

[4] P.Vernaz-Gris, K. Huang, M. Cao, A. S. Sheremet, and J. Laurat, Nat. Comm. **9**, 363 (2018).

Electron and Nuclear spin dynamics of Kramers ion at Subkelvin Temperatures

Pei-yun Li[1,2], Chao Liu[1,2], Zong-quan Zhou[1,2], Xiao Liu[1,2], Zong-feng Li[1,2], Tian-shu Yang[1,2], Jun Hu[1,2], Yu Ma[1,2], Peng-jun Liang[1,2], Xue Li[1,2], Chuan-feng Li[1,2], and Guang-can Guo[1,2]

[1] *CAS Key Laboratory of Quantum Information, University of Science and Technology of China, Hefei, 230026, China*

[2] *Synergetic Innovation Center of Quantum Information and Quantum Physics, University of Science and Technology of China, Hefei, 230026, P.R. China*

e-mail: *lpyzz@mail.ustc.edu.cn*

Rare Earth ions doped in crystal hosts has been recognized as a promising solid-state system for optical quantum technology due to their long optical and spin coherence time. Optical memory with storage time of 1 minute [1] quantum memory with high efficiency [2], high fidelety [3], on-demand [4] and multimode capacity [5] has been realized in this system. Nuclear spin coherence time as long as 6 hours has been acheived in Eu^{3+}:Y_2SiO_5 [6].

Kramers ions with unquenched electronic magnetic moment are endowed with a further interface to microwave photonsmaking them attractive candidates for microwave memory [7] and quantum transducers [8]. However, the large electronic magnetic moment also induces severe decoherence effect due to phonon-miediated relaxation process and magnetic dipole-dipole interaction. Such disadvantages can be significantly alleviated via reducing the temperature of the sample [9].

Here, we combine an X-band pulsed EPR spectrometer (Bruker Elexsys 580) with a dilution refrigerator to explore the spin dynamics of $^{143}Nd^{3+}$:Y_2SiO_5 at subkelvin temperatures.

To clarify the hyperfine level structures, the highly anisotropic Zeeman **g** matrix and hyperfine **A** matrix were deduced by gathering the EPR spectrograms as the crystal rotates in three orthogonal planes (b,D1), (b,D2), and (D1,D2) where magnetic field B_0 is contained. A home-made program based on *MATLAB* and *EasySpin* was used for the simulation. The simulated annealing algorithm was employed to minimize the deviation between experimental data and simulated result. At last, we got a average deviation of 18.4 Gauss for a single experimental data point. The best fit **g** tensor in D1D2b frame is:

$$g = \begin{pmatrix} -1.03 & -2.48 & 0.44 \\ -2.49 & -2.19 & -0.14 \\ 0.44 & -0.14 & 1.39 \end{pmatrix}$$

The best fit **A** tensor in D1D2b frame is (in MHz):

$$A = \begin{pmatrix} 495.7 & 687.4 & -232.8 \\ 687.4 & 751.8 & 165.8 \\ -232.8 & 165.8 & -338.3 \end{pmatrix}$$

The electron spin coherence time T_{2e} has increased from 33μs at 6K to 205μs at 0.1k. The growth momentum significantly alleviates below 2.5K due to instantaneous diffusion. Nevertheless, with the much smaller magnetic momentum, coherence time of nuclear spin increases quickly below 1K, reaching 43ms at 0.1K. Data curve is given in Fig. 1.

References

[1] Georg Heinze, Christian Hubrich, and Thomas Halfmann. *Phys. Rev. Lett.*, 111:033601, Jul 2013.

[2] Mahmood Sabooni, Qian Li, Stefan Kröll, and Lars Rippe. *Phys. Rev. Lett.*, 110:133604, Mar 2013.

[3] Zong-Quan Zhou, Wei-Bin Lin, Ming Yang, Chuan-Feng Li, and Guang-Can Guo. *Phys. Rev. Lett.*, 108:190505, May 2012.

[4] Alessandro Seri, Andreas Lenhard, Daniel Rieländer, Mustafa Gündoğan, Patrick M. Ledingham, Margherita Mazzera, and Hugues de Riedmatten. *Phys. Rev. X*, 7:021028, May 2017.

[5] Zong-Quan Zhou, Yi-Lin Hua, Xiao Liu, Geng Chen, Jin-Shi Xu, Yong-Jian Han, Chuan-Feng Li, and Guang-Can Guo. *Phys. Rev. Lett.*, 115:070502, Aug 2015.

[6] Manjin Zhong, Morgan P Hedges, Rose L Ahlefeldt, John G Bartholomew, Sarah E Beavan, Sven M Wittig, Jevon J Longdell, and Matthew J Sellars. *Nature*, 517(7533):177, 2015.

[7] S. Probst, H. Rotzinger, A. V. Ustinov, and P. A. Bushev. *Phys. Rev. B*, 92:014421, Jul 2015.

[8] Christopher O'Brien, Nikolai Lauk, Susanne Blum, Giovanna Morigi, and Michael Fleischhauer. *Phys. Rev. Lett.*, 113:063603, Aug 2014.

[9] D. D. Sukachev, A. Sipahigil, C. T. Nguyen, M. K. Bhaskar, R. E. Evans, F. Jelezko, and M. D. Lukin. *Phys. Rev. Lett.*, 119:223602, Nov 2017.

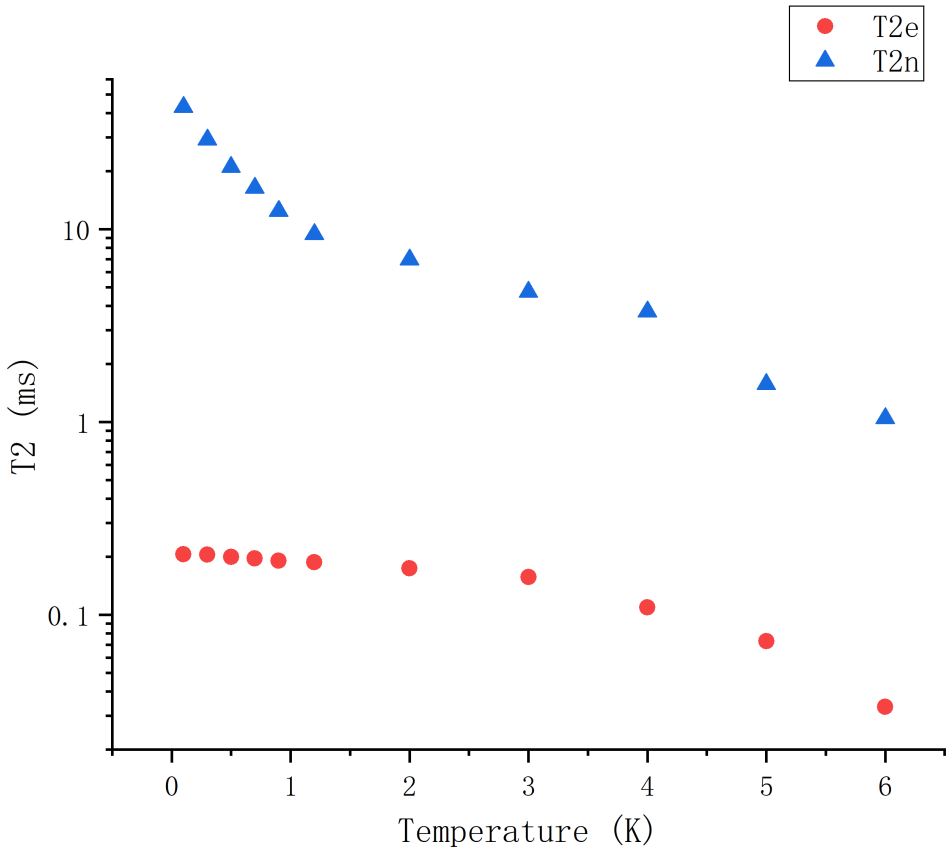


Figure 1: temperature dependence of electron and nuclear coherence time

Spiral bandwidth of four-wave mixing in rubidium vapour

Rachel F. Offer[1], Dalius Stulga[1], Erling Riis[1], Sonja Franke-Arnold[2] and Aidan S. Arnold[1]
[1] *Department of Physics, SUPA, University of Strathclyde, Glasgow G4 0NG, United Kingdom*
[2] *School of Physics and Astronomy, SUPA, University of Glasgow, Glasgow G12 8QQ, United Kingdom*
e-mail: *aidan.arnold@strath.ac.uk*

Structured light, and in particular orbital angular momentum (OAM), is an important tool for optical manipulation, processing, imaging and both classical and quantum communication [1, 2]. We explore the transfer of OAM in an e cient four-wave mixing process in rubidium vapour [3]. Conservation of OAM determines the total OAM carried by the two generated fields – at 420 nm and 5.2 μm – but not how it is distributed between them [4, 5, 6]. A small pump OAM is transferred almost entirely to the 420 nm light, allowing e cient OAM frequency conversion and addition [7]. For larger pump OAM, the OAM spectrum of the generated light becomes broadened, indicating that the two generated fields, which have widely disparate wavelengths, are OAM entangled. We infer the available spiral bandwidth of this state by performing a full mode decomposition on the 420 nm light for a range of pump OAM [7].

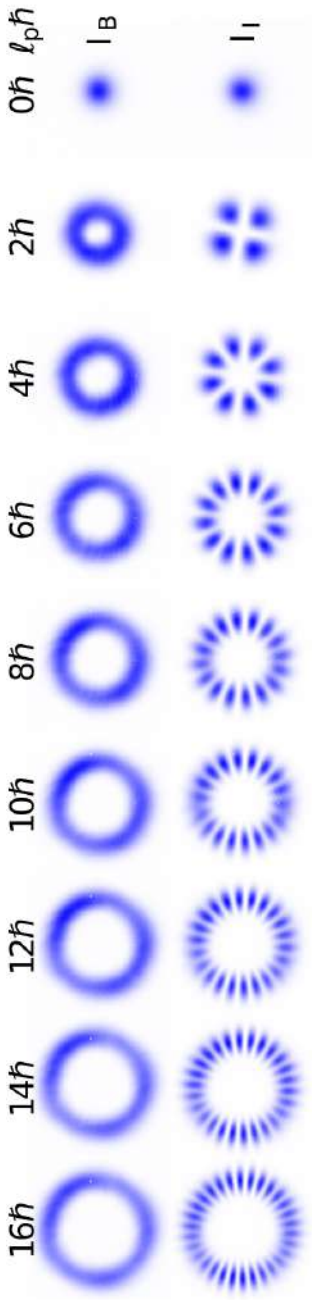


Figure 1: Intensity profile, I_B, and interferogram, I_I, of the generated 420 nm light for increasing total pump OAM, $\ell_p\hbar$. As ℓ_p increases, the visibility of the interference fringes along the vertical axis of the interferogram decreases, indicating broadening of the OAM spectrum.

[1] S. Franke-Arnold and N. Radwell, Opt. Phot. News, June, 28 (2017).

[2] A. Mair, A. Vaziri, G. Weihs and A. Zeilinger, Nature **412**, 313 (2001).

[3] A. S. Zibrov, M. D. Lukin, L. Hollberg and M. O. Scully, Phys. Rev. A **65**, 051801 (2002).

[4] G. Walker, A. S. Arnold and S. Franke-Arnold, Phys. Rev. Lett. **108**, 243601 (2012).

[5] A. M. Akulshin, I. Novikova, E. E. Mikhailov, S. A. Suslov, and R. J. McLean, Opt. Lett. **41**, 1146 (2016).

[6] R. N. Lanning, Z. Xiao, M. Zhang, I. Novikova, E. Mikhailov, and J. P. Dowling, Phys. Rev. A **96**, 013830 (2017).

[7] R. F. Offer, D. Stulga, E. Riis, S. Franke-Arnold, and A. S. Arnold, arxiv:1805.08190.

Superconducting qubit-qutrit circuit: A toolbox for efficient quantum gates

T. Bækkegaard[1], **L.B. Kristensen**[1], **N.J.S. Loft**[1,†], **C.K. Andersen**[2], **D. Petrosyan**[3], **N.T. Zinner**[1,4]

[1] *Department of Physics and Astronomy, Aarhus University, DK-8000 Aarhus C, Denmark*
[2] *Department of Physics, ETH Zürich, CH-8093 Zürich, Switzerland*
[3] *Institute of Electronic Structure and Laser, FORTH, GR-71110 Heraklion, Greece*
[4] *Aarhus Institute of Advanced Studies, Aarhus University, DK-8000 Aarhus C, Denmark*
[†] *Present address: Research Laboratory of Electronics, Massachusetts Institute of Technology*
e-mail: *t_b@phys.au.dk*

As classical computers struggle to keep up with Moore's law, quantum computing may represent a big step in technology and yield significant improvement over classical computing for many important tasks [1]. Over the last decade, superconducting circuits have steadily improved to become one of the most promising candidates for the realization of scalable quantum computing [2], with recent coherence times of above 50 µs [3]. Building a quantum computer, however, requires good control but also good isolation from the environment to minimize decoherence. It is therefore important to realize quantum gates e - ciently, using as few operations as possible, to reduce the amount of required control and operation time and thus improve the quantum state coherence.

We propose a superconducting circuit, shown in figure 1, which implements an effective tunable spin chain consisting of a qutrit (three-level system) coupled to two qubits (spin-1/2). In our paper [4] we show the derivation leading to the effective spin-model system which has highly tunable qutrit energy levels and Heisenberg XXZ -like interactions between the three effective degrees of freedom. Our system can e ciently accomplish various quantum information tasks, including entanglement of the two qubits and conditional three-qubit quantum gates such as the famous Toffoli (double-conditional NOT, CCNOT) and Fredkin (conditional SWAP, CSWAP) gates, which are universal for reversible classical computation. The CCNOT is implemented using a single-operation three-qubit CCZ (phase) gate and two Hadamard gates. The CSWAP gate is implemented as a resonant exchange between the qubits and can be seen as a conditional iSWAP, but with a phase that is easier removed by a single CCZ gate, resulting in the full CSWAP gate. Furthermore, our system realizes a conditional geometric (holonomic) non-adiabatic quantum gate.

These implementations show how utilization of the third, qutrit, level in conjunction with the usual qubits can drastically improve the e ciency of implementation of several important tasks for quantum computing. Furthermore the e ciency, robustness, and universality of our circuit makes it a promising candidate to serve as a building block for larger spin networks capable of performing involved quantum computational tasks.

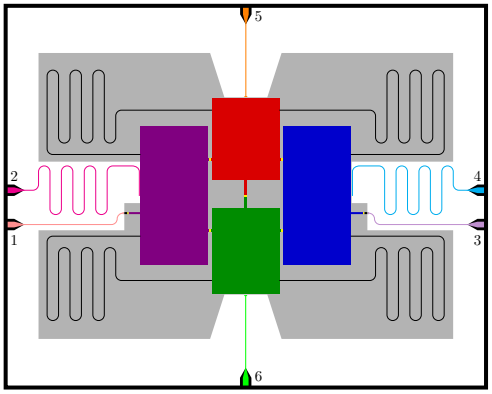


Figure 1: Sketch of the proposed circuit. Each colored box is a superconducting island corresponding to a node in a lumped circuit element model, with the two middle nodes combining to give a highly tunable effective qutrit. Josephson junctions are shown as narrow yellow strips. Bent black wires are inductors. The numbered colored lines are controls for readout and driving of the circuit.

References

[1] P. W. Shor. Polynomial-time algorithms for prime factorization and discrete logarithms on a quantum computer. *SIAM Journal on Computing*, 26(5):1484–1509, 1997.

[2] M. H. Devoret and R. J. Schoelkopf. Superconducting circuits for quantum information: An outlook. *Science*, 339(6124):1169–1174, 2013.

[3] A. Kandala, A. Mezzacapo, K. Temme, M. Takita, M. Brink, J. M. Chow, and J. M. Gambetta. Hardware-e cient variational quantum eigensolver for small molecules and quantum magnets. *Nature*, 549:242–246, Sep 2017.

[4] T. Bækkegaard, L. B. Kristensen, N. J. S. Loft, C. K. Andersen, D. Petrosyan, and N. T. Zinner. Superconducting qutrit-qubit circuit: A toolbox for e cient quantum gates. *ArXiv e-prints*, feb 2018.

Optimal condition for a cavity QED-based quantum gate

R. Asaoka[1], **R. Kanamoto**[1], **Y. Tokunaga**[2], **and T. Aoki**[3]
[1] *Department of Physics, Meiji University, Kawasaki, Kanagawa 214-8571, Japan*
[2] *NTT Secure Platform Laboratories, NTT Corporation, Musashino 180-8585, Japan*
[3] *Department of Applied Physics, Waseda University, 3-4-1 Okubo, Shinjuku, Tokyo 169-8555, Japan*
e-mail: *r_asaoka@meiji.ac.jp*

Cavity quantum electrodynamics (QED) has been extensively studied for decades as one of the promising candidates for the realization of quantum computing and quantum network. For example, the controlled phase flip gate between photons assisted by cavity-QED systems was proposed in 2004 [1] and demonstrated recently [2].

However, fault-tolerant quantum computing with cavity-QED-based techniques remains a challenging problem due to the infidelity and the losses originated from various dissipative processes; the cavity decay, the atomic decay, and the other imperfections such as the channel losses outside the cavity. Minimizing the error associated with these processes and relaxing the fault-tolerant conditions are thus both important issues for realizing quantum information processing.

Goto *et al.,* [3] proposed to use the quantum gate between atoms by cavity-assisted scattering of a mediated photon [4] as a probabilistic quantum gate and succeeded to significantly relax the fault-tolerant condition. In their paper, they also optimized the external coupling rate of the cavity to minimize the photon loss probability by taking account of the cavity internal loss rate and the atomic decay rate. That is, they showed the possibility of cavity-QED-based fault-tolerant quantum computing within current technologies under the optimized condition.

Recently, a novel optical cavity system, a nanofiber cavity system has been developed using an optical nanofiber sandwiched by two fiber-Bragg-grating mirrors [5]. The extraordinary small mode area contributes to achieve the strong coupling regime even with considerably larger internal cavity loss rate compared to that of the free-space cavity systems. Further technological improvement of the nanofiber cavity systems may accelerate the realization of cavity-QED-based quantum information processing.

Motivated by such a recent development of cavity-QED systems, in this work, we theoretically investigate optimal conditions for the cavity-QED-based quantum gate in more detail. By considering the pulse width and the channel losses outside the cavity in addition to the parameters in [3], we investigate the optimal conditions of controllable experimental parameters to achieve high fidelity and low losses for fault-tolerant quantum computing. We consider the typical experimental values of the nanofiber cavity-QED system as a promising candidate for the near future development.

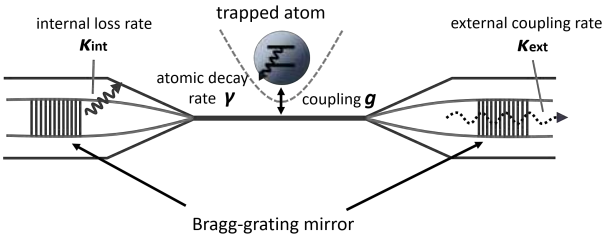


Figure 1: Nanofiber cavity QED system and its parameters.

[1] L.-M. Duan and H. J. Kimble, Phys. Rev. Lett. **92**, 127902 (2004).

[2] B. Hacker, S. Welte, G. Rempe, and S. Ritter, Nature **536**, 193 (2016).

[3] H. Goto and K. Ichimura, Phys. Rev. A **82**, 032311 (2010).

[4] L.-M. Duan, B. Wang, and H. J. Kimble, Phys. Rev. A **72**, 032333 (2005).

[5] S. Kato and T. Aoki, Phys. Rev. Lett. **115**, 093603 (2015).

RF-induced evaporative cooling in an optical trap

Meungho Seo, Sooyoung Park, and D. Cho
Department of Physics, Korea University, Seoul 02841, Korea
e-mail: *mhseo0609@gmail.com*

We evaporatively cool ^{87}Rb atoms in a 1D optical lattice using an energy-selective hyperfine transition followed by a state-selective push-out process. The scheme is illustrated in Fig. 1. Evaporation using RF transition followed by ejection from a trap - known as an RF knife edge method - has been successfully applied to a magnetic trap to reach a Bose-Einstein condensation. In an optical trap, however, the method has never been applied because there is no obvious energy-selective transition to use. Instead, simple lowering of a well depth - known as forced evaporation - has been the cooling method of choice in an optical trap at the expense of loosening the trap and consequent reduction in the atom-number or phase-space density.

In order to render a ground hyperfine transition energy sensitive, we use a circularly polarized lattice beam. An ac Stark shift of an alkali-metal atom in its ground state, $|nS, F, m_F\rangle$ induced by a laser field with an amplitude $\mathcal{E}$ is

$$U = \alpha_F|\mathcal{E}|^2 + \beta_F\eta g_F m_F|\mathcal{E}|^2, \qquad (1)$$

where α_F and β_F are the scalar and vector polarizabilities, respectively, η is the degree of circularity of the laser polarization, and g_F is the Lande g factor. We optically pump the atoms trapped in a 1D optical lattice to the $|5S_{1/2}, F = 1, m_F = 1\rangle$ state and use the hyperfine transition to the $|5S_{1/2}, F = 2, m_F = 2\rangle$ state. Well depths for the two states differ by $(3/2)\beta_F|\mathcal{E}|^2$ for a circularly polarized lattice beam, and as a consequence vibration frequencies for the center-of-mass motion are different. This gives rise to an inhomogeneous broadening. Fig.2. shows lineshapes for the inhomogeneously broadened $|F = 1, m_F = 1\rangle \rightarrow |F = 2, m_F = 2\rangle$ transition and the clock transition without a broadening. The asymmetry reflects the Maxwell Boltzmann distribution and the long tail on red side is contributed by high-n atoms, n being a vibration quantum number.

We use the method of adiabatic passage to drive transitions from broad range of high n states. Simple RF pulse to drive Rabi transitions is not effective in this application because we need to induce transitions over large range of resonance frequency and Rabi frequency. Once a high-n atom makes a transition to the $|F = 2, m_F = 2\rangle$ state, we apply a right circularly polarized push beam tuned to the $|5S_{1/2}, F = 2\rangle$ to $|5P_{3/2}, F = 3\rangle$ cycling transition along the quantization axis. The atoms are ejected with 99% e ciency in 50 μs with negligible off-resonant transition from the $|5S_{1/2}, F = 1, m_F = 1\rangle$ state.

The experiment is in progress and we will report quantitative results at the Conference.

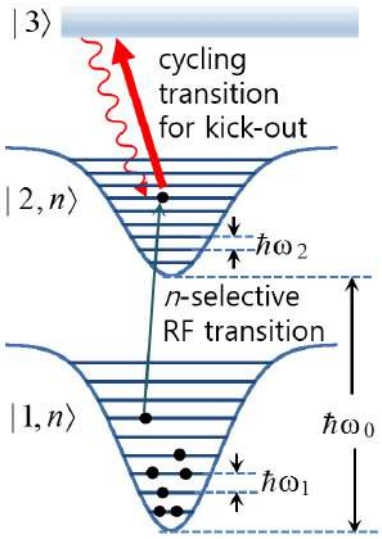


Figure 1: RF-induced evaporative cooling in an optical trap. Circularly polarized lattice beam makes the transition frequency dependent on motional quantum number via vector polarizability.

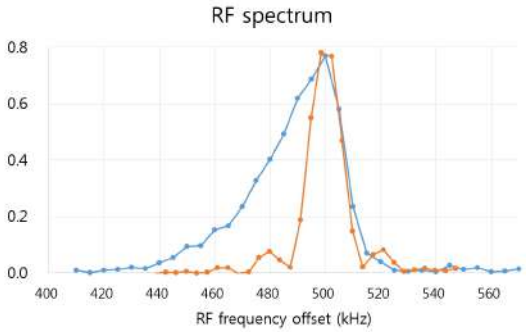


Figure 2: RF spectra of the inhomogeneously broadened $|F = 1, m_F = 1\rangle \rightarrow |F = 2, m_F = 2\rangle$ transition and the clock transition without a broadening.

A novel integrated platform for quantum storage of heralded single photons

A. Seri[1], **G. Corrielli**[2], **D. Lago-Rivera**[1], **A. Lenhard**[1], **H de Riedmatten**[1,3], **R. Osellame**[2] **and M. Mazzera**[1]

[1] *Institut de Ciències Fotòniques, The Barcelona Institute of Science and Technology, 08860 Castelldefels, Spain*

[2] *IFN - Istituto di Fotonica e Nanotecnologie, CNR and Dipartimento di Fisica, Politecnico di Milano, 20133 Milano, Italia*

[3] *ICREA - Institució Catalana de Recerca i Estudis Avançats, 08015 Barcelona, Spain*

e-mail: *alessandro.seri@icfo.eu*

The e cient and reversible mapping of quantum states of light into collective atomic excitation is a promising route towards the realization of quantum memories. Rare earth doped crystals offer long lived spin states and are naturally suitable for miniaturization and integration of several quantum memories onto a single substrate, e.g. in form of waveguides. The latter would greatly facilitate the scalability and, thanks to the tight confinement of light, would lead to a strong enhancement of the light matter interaction. Pr^{3+}:Y_2SiO_5 is currently one of the best systems for quantum memory. With this crystal very e cient storage of weak coherent states [1] has been demonstrated, as well as the longest storage time ever demonstrated in any system (in the regime of 1 minute for classical images) [2]. We recently proposed to create integrated quantum memories in Pr^{3+}:Y_2SiO_5 using femtosecond laser micromachining (FLM) [3]: a fs-pulsed laser is highly focused in the crystal to create pairs of parallel damage tracks. As a consequence of a positive change of refractive index between the two tracks, the light is guided (type II waveguide). In this approach, beside an improved light-matter interaction, the storage with on-demand retrieval was performed with bright light pulses, demonstrating the first implementation of an integrated on-demand optical memory [3].

Here [4], we propose a new platform for integrated optical memories, based again on FLM: we fabricate a single mode *type I* waveguide in Pr^{3+}:Y_2SiO_5 , by creating just one modified track along the crystal in which the positive change of refractive index coincides with the track itself. *Type I* waveguides provide stronger confinement than type II without increasing the losses, thus further increasing the light-ions interaction. Moreover they can be potentially connected with fibers and standard glass chips. We demonstrate that the coherence properties of the material are of the same order of magnitude as for the bulk, despite the invasive fabrication process. To prove that this platform is suitable for being used as a quantum memory, we perform storage of ultra-narrowband single visible photons (signals), using the partial atomic frequency comb protocol (AFC). The photons are generated by spontaneous parametric down conversion (SPDC) and with telecom heralding (idlers). Fig. 1a shows an experimental trace of the storage, and Fig. 1b the measured second-order cross-correlation function $g^{(2)}_{AFC,i}$ between the idler and the stored and retrieved signal photons versus the storage time τ. The dotted line is the classical upper bound. For all the storage times investigated, the $g^{(2)}_{AFC,i}$ is clearly above the classical bound, thus proving that laser written memories can operate in the quantum regime. Taking advantage of the large inhomogeneous broadening of the ions in Pr^{3+}:Y_2SiO_5 and of the strong light-matter interaction in the waveguide, we also demonstrated recently the storage of a frequency multiplexed photon. This device opens new perspectives for the implementation of miniaturized and integrated quantum memories, with possibilities to create memory enhanced photonic circuits in 3 dimensions.

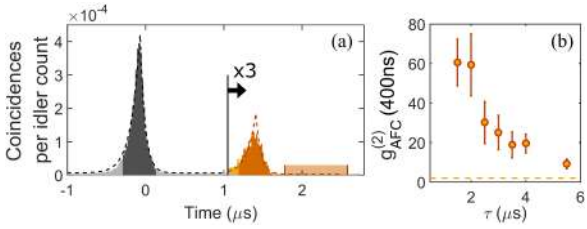


Figure 1: (a) Time-resolved histograms of the idler-signal coincidences for signal photons before the storage (gray histogram) and stored for $\tau = 1.5\,\mu$s (orange histogram); (b) $g^{(2)}_{AFC,i}$ of the correlations between idler photons and stored signal photons for different storage times τ. The orange dotted line is the classical upper bound.

[1] M. P. Hedges, et al. Nature **465**, 1052 (2010).

[2] G. Heinze, et al. Phys. Rev. Lett. **111**, 033601 (2013).

[3] G. Corrielli, et al. Phys. Rev. Applied **5**, 054013 (2016).

[4] A. Seri, et al. ArXiv: 1805.02494 (2018).

Efficient single-photon collection for long-distance entanglement of atoms

Robert Garthoff[1], **Timon Hummel**[1], **Kai Redeker**[1], **Tim van Leent**[1], **Paul Koschmieder**[1], **Wei Zhang**[1],**Wenjamin Rosenfeld**[1,2], **and Harald Weinfurter**[1,2]

[1] *Fakultät für Physik, Ludwig-Maximilians-Universität München, D-80799 München, Germany*

[2] *Max-Planck-Institut für Quantenoptik, D-85748 Garching, Germany*

e-mail: *robert.garthoff@physik.uni-muenchen.de*

Entanglement between distributed quantum systems forms the basis of future quantum networks and thus will be essential for secure quantum communication and distributed quantum computing. The only suitable candidate to interconnect separate quantum memories is the photon. Currently, e cient collection of photons from the quantum memory limits the generation of remote entanglement in schemes based on entanglement swapping.

Here we present the experimental details and results of the optimization of the photon collection e ciency from a single trapped Rb-87 atom used as a quantum memory. Based on spontaneous decay we can obtain entanglement between the internal states of an atom and the polarisation of an emitted photon. Starting with atom-photon entanglement in two traps, the entanglement swapping protocol is employed to generate heralded entanglement between the atoms over a distance of 400m [1]. The remote entanglement rate scales quadratically with the single-photon collection e ciency. Using custom designed microscope objectives with a high numerical aperture and corrected for our specific geometry, we aim at an threefold increase of collection e ciency and thereby at an improvement of remote entanglement rate by one order of magnitude relative to that achieved in our previous measurements [2].

The next goal is to extend the distance between the entangled atoms. This involves minimizing losses in the optical fibers by converting photons to telecom wavelengths and increasing the coherence time of the atomic state. We estimate that the gain in photon collection e ciency with the new optics will compensate for the losses of the photon conversion to telecom wavelengths, thus allowing to achieve entanglement over distances of a few 10 km at a reasonable rate , Fig. 1.

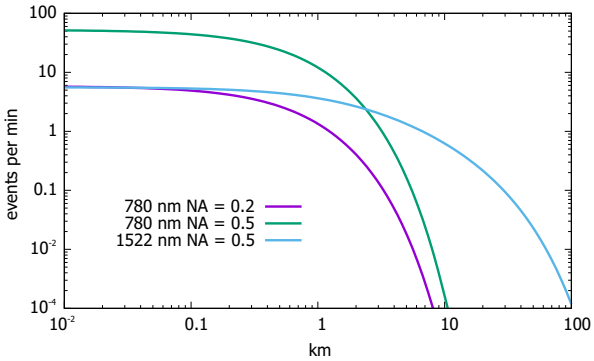


Figure 1: Estimated remote entanglement rates

[1] J. Hofmann, Science **337**, 72 (2012).

[2] W. Rosenfeld, Phys. Rev. Lett. **119**, 010402 (2017).

Towards quantum interfaces based on trapped $^{25}Mg^{+}$ ions

A. S. Borisenko[1,2], **I. V. Zalivako**[1,2], **I. A. Semerikov**[1,2], **K. Yu. Khabarova**[1,2], **and N. N. Kolachevsky**[1,2]

[1] *Russian Quantum Center, 143025 Moscow, Russia*

[2] *P. N. Lebedev Physical Institute, Russian Academy of Sciences, 119991 Moscow, Russia*

e-mail: *alexander.borisenko@yandex.ru*

High isolation from the environment, strong confinement, and Coulomb interaction are the features of trapped and laser-cooled ions that make them ideal candidates for implementation of e cient quantum memory, quantum computers, and quantum simulators. A qubit can be formed using a pair of hyperfine components of a ground state in case of microwave driving field or utilizing a well-controlled optical transition. Entanglement of the qubits is usually achieved through common degrees of freedom of the particles in a trap potential. Extremely long coherence times of ionic qubits were demonstrated as well as high-fidelity single-qubit and two-qubit gates [1]. The ion qubits are completely identical what sets them apart from superconducting and neutral-atom qubits. Quantum information processing methods can also be used for precision spectroscopy of ions whose states cannot be read out directly [2].

Our group is working on a development of e - cient quantum interfaces based on trapped and laser-cooled $^{25}Mg^{+}$ ions. The advantages of magnesium ion for application in quantum logic include its simple energy level structure and the availability and a small number of laser sources that are necessary [3]. A transition between hyperfine components of the ground state of an ion is convenient to use as a qubit. Here we present first results on the way to $^{25}Mg^{+}$ based quantum interfaces.

A linear Paul trap for capturing magnesium ions was created and a laser system for Doppler cooling was developed. The laser system contains a commercial diode laser and two home-built second-harmonic generators, which generate ultraviolet radiation at 280 nm. A Doppler cooling of $^{24}Mg^{+}$ ions was performed as a preliminary step before operating with $^{25}Mg^{+}$ isotope due to its simpler energy structure. After Doppler cooling, the ion temperature below 40 mK was achieved (which is the conservative estimation). A secular frequency spectrum of simple ion crystals, such as a single $^{24}Mg^{+}$ ion and a $^{24}Mg^{+}$ ion pair was investigated. The results indicate high harmonicity of the trap potential, which is important for the achievement of low heating rates of the ions. Targeted vibrational mode excitation was demonstrated (Fig. 1).

We propose a new trap loading method which involving usage of an ultraviolet light-emitting diode. This method does not require an expensive and complex laser system, although is not isotope selective. This method can be modified for simple and e cient loading of arrays of ion traps for quantum information processing applications.

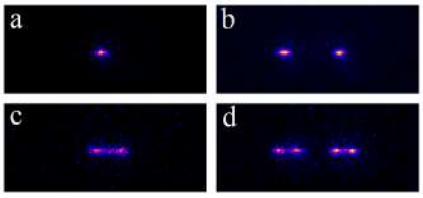


Figure 1: Images of elementary $^{24}Mg^{+}$ crystals with excited axial vibrational mode: a single ion (a $\rightarrow$ c) and a pair of ions (b $\rightarrow$ d).

[1] J. P. Gaebler *et al*, Phys. Rev. Lett., **117**, 1 (2016).

[2] P. O. Schmidt, T. Rosenband, C. Langer, W. M. Itano, J. C. Bergquist, D. J. Wineland, Science, **309**, 749 (2005).

[3] B. Hemmerling, F. Gebert, Y. Wan, D. Nigg, I. V. Sherstov, P. O. Schmidt, Appl. Phys. B, **104**, 583 (2011).

Tomography of a Raman Quantum Memory for Temporal Modes

J.H.D. Munns,[1,2] **S.E. Thomas**,[1,2] **T.M. Hird**,[1,3] **P.M. Ledingham**,[1] **D.J. Saunders**,[1]
J. Sperling,[1] **J. Nunn**,[4] **B. Brecht**,[1] **and I.A. Walmsley**[1]

[1] *Clarendon Laboratory, University of Oxford, OX1 3PU, United Kingdom*
[2] *Blackett Laboratory, Imperial College London, SW7 2AZ, United Kingdom*
[3] *Department of Physics & Astronomy, University College London, WC1E 6BT, United Kingdom*
[4] *Department of Physics, University of Bath, BA2 7AY, United Kingdom*
e-mail: *joseph.munns@physics.ox.ac.uk*

Practical, scalable, architectures for networked quantum information processing draw upon the strengths of different media: for instance in which one exploits the precision and controllability of quantum states and interactions in material systems and photonic systems which exhibit only weak interaction with their environment (and other photons). The former facilitate information processing, whereas the latter are ideal for the transmission of information between nodes of a quantum network. Temporal modes (TMs) of light are an appealing encoding for photonic quantum information processing [1]. To interface with these, two prerequisites are to be able to firstly prepare – and verify – these states, and secondly to selectively adress, and separate out, a chosen temporal mode. We present the means to address the both of these criteria.

To interface with TMs, the quantum pulse gate (QPG) based upon sum-frequency generation, enables a time non-stationary beam-splitter interaction to be implemented [2]. By appropriately tuning the pump pulse, a chosen temporal mode may be selectively mapped to a different frequency (and temporal mode, determined by the phase matching conditions). However, such devices are also subject to a lower limit of bandwidths of ∼100 GHz, and are not compatible with quantum light sources operating in the MHz-GHz regime.

The Raman memory [3] also constitutes a platform which implements a time non-stationary beam-splitter interaction, whereby a chosen signal may be mapped into (and retrieved from) an atomic excitation, whilst orthogonal modes are transmitted. We demonstrate selective storage of ns duration weak coherent state TMs in a Raman quantum memory in warm caesium vapour. The $6S_{1/2}(F = 3, 4)$ hyperfine levels are used as the ground/storage states, respectively; and the control pulse drives a two-photon Raman transition between these via the $6P_{3/2}$ manifold. Pulses are carved from a continuous wave diode laser using a fibre-integrated Mach-Zehnder electro-optic modulator driven by two AWGs enabling full control of the output amplitude and phase.

At elevated e ciencies, the "broadband beam-splitter" interaction becomes multimode and the Schmidt modes become destorted [4]. To verify the usefulness of a device for interfacing with TMs, we reconstruct the modal structure of the memory interaction by probing the storage e ciency of an ensemble of prepared input signals. With this we are able to establish the eigenmodes and extract the mode-selectivity of the interaction.

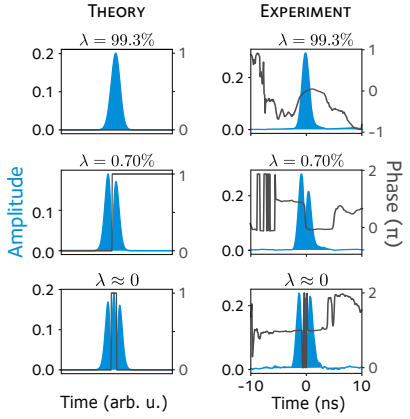


Figure 1: Eigenmodes of the memory interaction, theory (L.) and extracted from a typical experiment (R.). The singular values indicate a separability of 99%.

Additionally, to verify the states which are sent to the memory, one requires access to the amplitude and phase of the pulses. Existing pulse characterisation techniques [5, 6, 7] based upon spectral methods do not have the resolution to access the ns scale pulses used here. We demonstrate a single-shot, self-referenced protocol that operates instead in the temporal domain, *Temporal Amplitude & Phase: Algorithmic Reconstruction via Time-domain Interferometry* (TeAPARTI).

We have demonstrated the TM-selective operation of the Raman memory which provides the basis for using this a device for the manipulation of TMs.

[1] B. Brecht *et al.*, Phys. Rev. X **5**, 041017 (2015).
[2] B. Brecht *et al.*, Phys. Rev. A **90**, 1 (2014).
[3] J. Nunn *et al.*, Phys. Rev. A **75**, 011401 (2007).
[4] A. Christ *et al.*, New J. Phys. **15**, 053038 (2013).
[5] D. Kane *et al.*, IEEE J. Quantum Elect. **29**, 571 (1993).
[6] C. Iaconis *et al.*, Opt. lett. **23**, 792 (1998).
[7] C. Bourassin-Bouchet *et al.*, Opt. lett. **38**, 5299 (2013).

Towards heralded entanglement of single atoms over long distances

Tim van Leent[1], **Robert Garthoff**[1], **Kai Redeker**[1], **Matthias Bock**[2], **Timon Hummel**[1], **Paul Koschmieder**[1], **Wei Zhang**[1], **Christoph Becher**[2], **Wenjamin Rosenfeld**[1,3], **and Harald Weinfurter**[1,3]

[1] *Fakultät für Physik, Ludwig-Maximilians-Universität München, D-80799 München, Germany*
[2] *Universität des Saarlandes, Fachrichtung Physik, 66123 Saarbrücken, Germany*
[3] *Max-Planck-Institut für Quantenoptik, D-85748 Garching, Germany*
e-mail: *t.van.leent@physik.uni-muenchen.de*

The concept of quantum repeaters paves the way towards a scalable quantum network, which is essential for large scale quantum communication and distributed quantum computing. The basis of a quantum network is entanglement between separated quantum memories. One of the current experimental challenges is to achieve entanglement over long distances.

Currently, we operate an experimental setup which employes the entanglement swapping protocol to generate entanglement between two Rubidium 87 atoms separated by a distance of 400 meters [1]. Here we report on results increasing this distance by at least an order of magnitude. Milestones on this path are converting photons to telecom wavelengths, increasing the event rate, and improving the coherence time of the atomic state.

Any fiber based photonic quantum state distribution beyond 2 km makes conversion to telecom wavelengths indispensable. To preserve the polarization state during the conversion, which is initially entangled with the atomic state, we are implementing a quantum frequency converter using a nonlinear waveguide crystal in a Sagnac-type interferometer configuration [2, 3].

To overcome losses during the frequency conversion and hence retain the current event rate (1-2 events per min), a new photon collection optics is being implemented. We report on tests of a custom made microscope objective (NA 0.5), which will increase the collected number of the spontaneous emitted photons by a factor of 3-5, for both setups.

Another crucial point to achieve entanglement over longer distances is improving the coherence time of the atomic state, currently limited by small magnetic field fluctuations and longitudinal field components of the strongly focussed optical dipole trap. For entanglement generation over 20 km one needs coherence times of the order of 1 ms. To achieve such long times we develop a standing wave optical dipole trap to compensate for the longitudinal field components.

[1] W. Rosenfeld et al., Phys. Rev. Lett. **119**, 010402 (2017)

[2] M. Bock et al., Nat. Comm. **9**, 1998 (2018)

[3] R. Ikuta et al., Nat. Comm. **9**, 1997 (2018)

Optimized Entangled State Retrieval from Quantum Memories for Networking

Siddhartha Santra[1], **Liang Jiang**[2], **and Vladimir S. Malinovsky**[1]
[1] *US Army Research Laboratory, Adelphi, Maryland 20783, USA*
[2] *Department of Applied Physics, Yale University, New Haven, Connecticut 06520, USA*
e-mail: *sidsantra1@gmail.com*

Quantum repeaters provide distributed entanglement for quantum information processing tasks such as communications, cryptography, sensing and interferometry [1]. The performance of these tasks is limited by the rate at which a quantum repeater can distribute remotely entangled states. The essential idea for establishing long-distance entanglement is to create and store entangled states in quantum memories over smaller segments and then use entanglement swapping operations to increase the spatial range of the states. However, the inevitable decoherence in the memories degrades the distributed states and reduces the effective rate at which entanglement can be distributed [2].

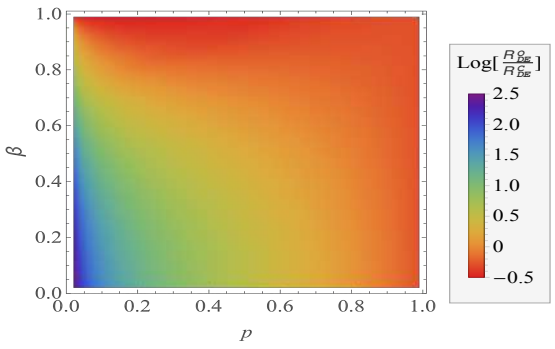


Figure 1: Logarithm (base 10) of the ratio of entanglement generation rate in the optimized protocol, R^O_{DE}, to that in the canonical protocol, R^C_{DE}. The optimized protocol performs better in most of the parameter space. The maximum advantage with the optimized protocol is seen for low p, β regions.

In our work we propose an optimized protocol of state retrieval from quantum memories that mitigates the effect of decoherence [3]. Entanglement generation and swapping are performed during a fixed window of time, the access time, after which the quantum memories are reset. We determine the size of this optimal access time depending on the probability of generating entanglement between the quantum memories, p, and the memory quality parameter, β. The optimal access time is obtained in units of the classical communication time required to verify that entangled states are available in both segments for a swapping operation to proceed. Our protocol maximizes the rate of distillable entanglement R^O_{DE}, in the average accessed state. Compared to a canonical

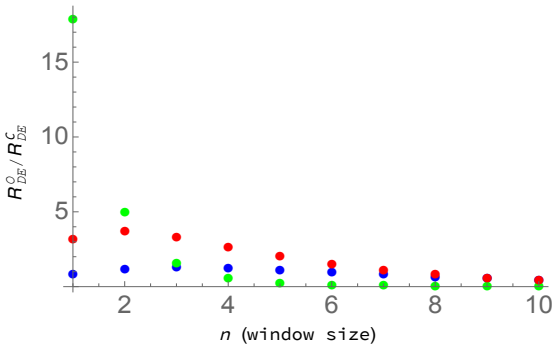


Figure 2: The optimal wait-window size in the optimized protocol depends on the location in parameter space. Shown here is the ratio of entanglement generation rates for $(p, \beta) = (0.1, 0.9)$ in blue, $(0.05, 0.8)$ in red and $(0.1, 0.4)$ in green with their maximum at $n_{\text{opt}} = 3, 2, 1$ respectively.

protocol the optimized state retrieval protocol can achieve orders of magnitude improvement in entanglement generation rates for successive nesting levels of a quantum repeater, Figure 1, particularly in the technologically relevant, low entanglement generation probability and low memory quality region, $(p \to 0, \beta \to 0)$.

We show that the size of the optimal access-time window depends on the operating point of the repeater in the (p, β) parameter space. The window size scales as $n_{\text{opt}}(p, \beta) \sim p^{-1}(\log \beta)^{-1}$ in units of the classical communication time, Figure 2. Various levels in a nested repeater architecture have their own optimal access times. We propose a repeater architecture where all nesting levels can follow an optimized state retrieval protocol. The rates achievable with the optimized protocol are much higher than those based on the canonical protocol for all nesting levels when realistic swapping success probabilities and technologically feasible entanglement generation probability and memory quality is considered.

[1] Van Meter, R., *Quantum Networking*, John Wiley & Sons Ltd., 2014.

[2] Razavi, M., Piani, M., Lütkenhaus, N. *Quantum repeaters with imperfect memories: Cost and scalability*, Phys. Rev. A., 80, 3, 032301, 2009.

[3] Santra, S., Jiang, L., Malinovsky, V. S., *Quantum repeater architecture with hierarchically optimized access-times*, In Preparation.

Engineering the components of a quantum cryptographic network enhanced by quantum memories

S. Gera[1], **S. Sagona-Stophel**[1], **M. Namazi**[1], **M. Flament**[1], **A. Scriminich**[2], **B. Jordaan**[1], **R. Shahrokhshahi**, [1] **G. Vallone**[2], **P. Villoresi**[2], **and E. Figueroa**[1]

[1] *Stony Brook University, 100 Nicolls Rd, Stony Brook, NY 11794, USA*

[2] *Department of Information Engineering, University of Padova, Via Gradenigo 6b, 35131 Padova, Italy*

e-mail: *sonali.gera@stonybrook.edu*

Introduction. Creating a memory assisted quantum communication network requires unconditional quantum memories that can support the technical demands of outside-of-the-laboratory quantum communication channels.

We report the creation of such an elementary quantum network which has these desired properties and present individual experiments addressing various challenges in order to create the quantum connectivity needed to perform long distance communication with random polarization qubits and entanglement by combining several different quantum modules: random polarization qubit generators, free space/fiber quantum communication channels, warm vapor quantum memories, atom-tuned quantum light and quantum state measurement set ups.

Ultra-low noise room temperature quantum memories. We have shown an ultra-low noise regime of operation in a simple quantum memory in warm ^{87}Rb atomic vapor. By modeling the quantum dynamics of four-level room temperature atoms, retrieval fidelities >98% for single-photon level polarization qubits have been obtained. [1].

Employing noise-reduction techniques permits the use of higher optical depths and control field powers, leading to storage e ciencies above 50%, and improved achievable storage times at the few-photon-level, with storage times of $\sim$ 1 ms already within reach. We also pioneered memory-integrated photon-shaping techniques necessary to interface several quantum memories e ciently [2].

A cryptographic network with quantum memories. We have interconnected several quantum modules: (i) two independent random polarization qubit generators, (ii) two portable quantum memories and (iii) a qubit decoder and reading station. After storage and retrieval the qubits are analyzed in a four-detector polarization setup [3]. The corresponding quantum bit error rates (QBER's) of $\sim$ 3% fulfill all the requirements needed to perform the BB84 and memory-assisted measurement-device-independent QKD protocols [4].

Evolution towards a quantum repeater node. Towards optimization of all components to reach the parameters needed for a long-distance entanglement distribution, we are building four high-duty-cycle fully-portable room temperature quantum memories.

"Atom-tuned" quantum light. In addition, we are engineering a quantum device to generate entanglement and other forms of non-classical light. Using Spontaneous Parametric Down Conversion in a non-linear crystal placed inside a cavity, we generate non-classical light tuned to Rubidium transitions and within the bandwidth of the Electromagnetically-Induced Transparency window making it compatible with quantum memories. We have performed real-time state reconstruction of the output quantum light using Quantum State Tomography via a homodyne detector. The cavity is maintained at a constant length using a Pound-Drever-Hall(PDH) Lock whose error signal is used to incorporate fluctuation-correction by correcting quadrature values.

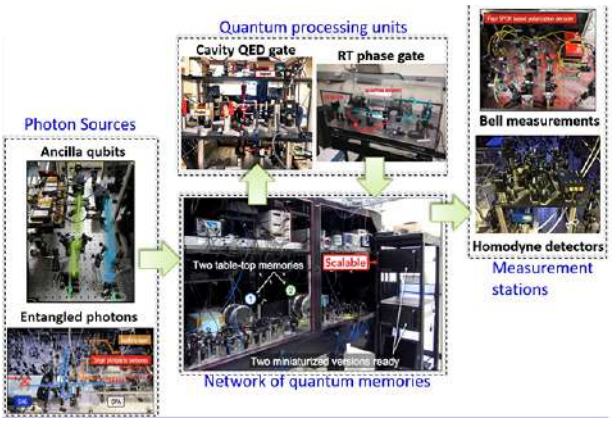


Figure 1: The components of a quantum network: **Photon Sources**, **Light-Matter Interfaces**, **Measurement Devices**

References

[1] M. Namazi, *et al.*, Phys. Rev. App. **8**, 034023 (2017)

[2] M. Namazi, *et al.*, Phys. Rev. A **92**, 033846 (2015).

[3] M. Namazi, *et al.*, arXiv 1609.08676 (2017). Accepted for publication in Phys. Rev. App.

[4] C. Panayi, *et al.*, New Journal of Physics **16**, 043005 (2014).

Cubic Hamiltonian in few steps

Š.Bräuer, T. Opatrný
Optics Department, Faculty of Science, Palacký University
17. Listopadu 12, 77146 Olomouc, Czech Republic
e-mail: *simon.brauer@seznam.cz*

In experiments, the action of linear and quadratic orders of the components of the collective spin operator $J_k, k = x, y, z$ have well-defined mechanisms for implementation, but it is non-trivial to do the same for cubic and higher orders. A continuous variable universal quantum computer in principle however requires Hamiltonians with arbitrary powers of J_k^n. The commutators allow expression of a cubic operator in terms of linear and quadratic ones [1][2], and the Suzuki–Trotter expansion can be utilized $e^{-iAt}e^{-iBT}e^{iAt}e^{iBT} \approx e^{[A,B]t^2}$ to do a effective implementation of cubic operators. However, in practice a literal implementation of this requires very high number of incremental operations, with up to thousands of iterations necessary to get at least 90% fidelity. So a different approach is taken here where the quadratic and linear operators are alternately applied, and the sequence optimized. This led to a sequence of just 26 such operations replicating the action of a cubic operator J_x^3 with 97.4% fidelity.

[1] S. Lloyd and S. L. Braunstein, Phys. Rev. Lett.**82**, 1784(1999).

[2] T. Opatrný, Phys. Rev. Lett **119**, 010502 (2017).

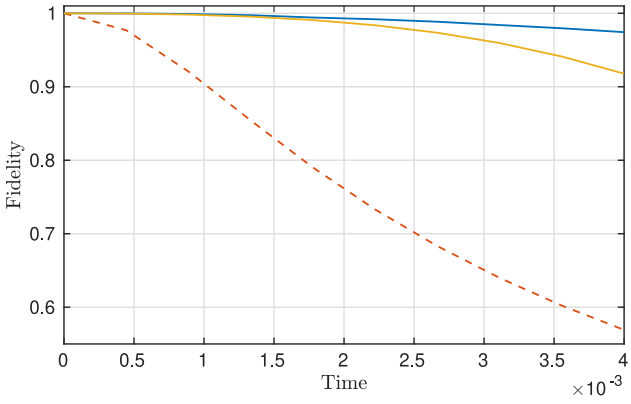


Figure 1: We present fidelities of states prepared with different interaction modes in respect to a state prepared using ideal hamiltionan .Blue curve - emulated cubic operator (26 steps). Yellow curve - cubic operator (commutator method, 1000 iterrations). Orange curve - squeez initial state without interaction.

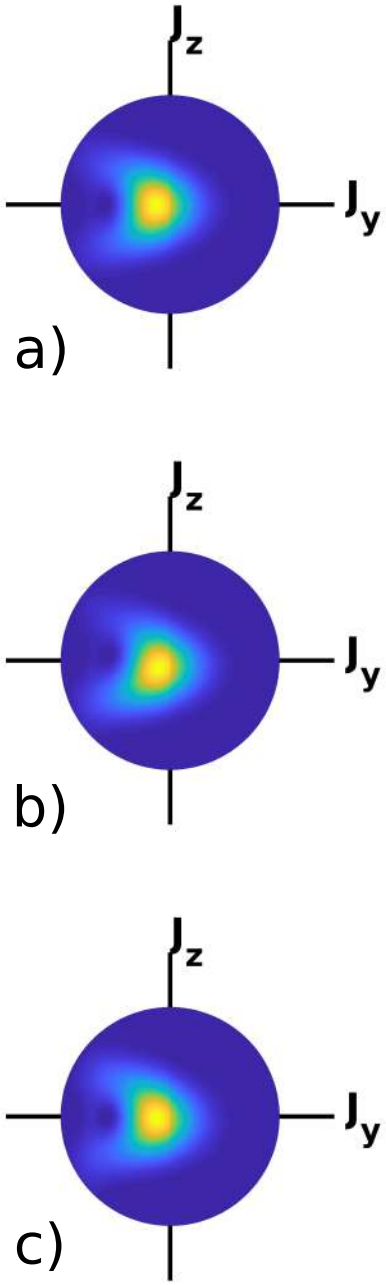


Figure 2: Bloch sphere. Cubic operators acting on squeezed spin state. Exact cubic operator a), cubic operator - commutator method (1000 iterations) b), emulated cubic oparator - 26 steps c).

Modal Properties of the Off-resonant Cascaded Absorption Memory

O. Lazo-Arjona[1], **K. T. Kaczmarek**[2], **S. Gao**[1], **G. S. Thekkadath**[1], **D. J. Saunders**[1], **J. Nunn**[3], **I. A. Walmsley**[1]

[1] *Clarendon Laboratory, University of Oxford, United Kingdom*
[2] *Group of Applied Physics, University of Geneva, Switzerland*
[3] *Department of Physics, University of Bath, United Kingdom*
e-mail: *oscar.lazoarjona@physics.ox.ac.uk*

We present a theoretical analysis of the recently-proposed ORCA quantum memory [1] for storing broadband single photons as orbital excitations in atomic vapour. The Maxwell-Bloch equations for a ladder-type system are derived under linear and adiabatic approximations. We show that in the long-cell limit these equations have an analytic solution for square control pulses, while in the short-cell limit the equations are equivalent to those of the previously studied lambda-type off-resonant memory [2]. The condition for unit e ciency is derived in the long-cell limit, and a detailed analysis of the modal properties in both regimes is made, and compared with numerical solutions to the equations.

[1] K. T. Kaczmarek, Physical Review A, vol. 97, Iss.4 - April 2018.

[2] Nunn J, Walmsley I, Raymer Met al., Physical ReviewA, 75(1):011401, 2007.

Broadband Light-Matter Interactions with an Atomic Frequency Comb in a Rare-Earth-Ion-Doped Crystal

P. M. Ledingham[1], **M. Nicolle**[1,2], **J. N. Becker**[1], **and I. A. Walmsley**[1]

[1] *Clarendon Laboratory, University of Oxford, Parks Road, Oxford, OX1 3PU, United Kingdom*

[2] *Quantum Engineering Technology Labs, H. H. Wills Physics Laboratory & Department of Electrical and Electronic Engineering, University of Bristol, BS8 1FD, United Kingdom*

e-mail: *patrick.ledingham@physics.ox.ac.uk*

Harnessing quantum physics promises to lead to powerful technologies, such as guaranteed secure data transmission for communications, and accelerated processing beyond the reach of any conceivable classical computer [1]. One of the promising candidate platforms for the implementation of these revolutionising technologies is photonics, where quantum information is encoded, processed and distributed using the same physical resource – photons. Like all platforms, building up a network based on photons faces the challenge of scalability; the generation and manipulation of single photons is non-deterministic, while long-distance distribution of them suffers from the inherent loss of communication channels. Therefore, the success probability of any composite system falls exponentially with the number of quantum elements and channels comprising the system.

A quantum memory for light (QM) provides a potential solution. This light-matter based interaction can be engineered to store and recall quantum photonic states on demand, facilitating temporal multiplexing for the synchronisation of non-deterministic events. A QM can be used to store photons output from successful operations while the remaining components of the composite system are run. Once each component has successfully executed, the photons can be released from the QMs simultaneously and the next quantum task can proceed.

A promising system to implement a QM are rare-earth-ion-doped solids at cryogenic temperatures, in particular praseodymium doped yttrium orthrosilicate (Pr^{3+}:Y_2SiO_5). This system offers long-lived optical coherence times ($\sim 100\,\mu s$) [2], while the spin coherence time has been demonstrated to approach the minute timescale [3]. Furthermore, a crystal field interaction inhomogeneously broadens the optical line to several GHz [2]. This line can be specifically tailored using spectral hole-burning techniques, allowing for the creation of complex spectral features required for QM protocols, such as the atomic frequency comb protocol (AFC) [4]. Many experiments have used Pr^{3+}:Y_2SiO_5 with the AFC protocol, demonstrating e cient storage and recall of classical light [5], storage of single photons [6], and by mapping to a long-lived spin coherence, storage of time-bin qubits [7] and single photons [8]. So far, these demonstrations have taken advantage of the narrowly split hyperfine levels, and have thus been limited to MHz bandwidth photons.

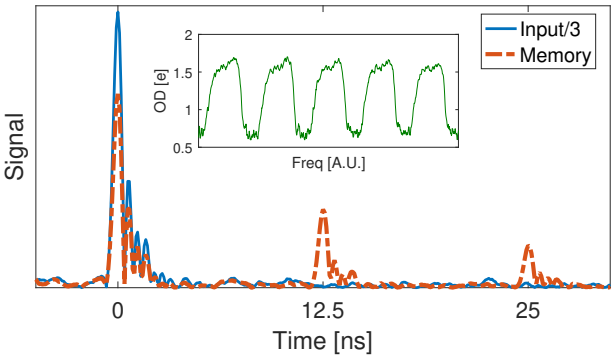


Figure 1: Broadband AFC rephasing. The thin solid line shows the input/3 centered at time 0. The thick dashed line shows the AFC memory showing rephasing at 12.5 ns and 25 ns. Inset: A section of the AFC showing 5 teeth separated by 80 MHz.

In this work we demonstrate the first broadband implementation of the AFC memory protocol in Pr^{3+}:Y_2SiO_5 (see fig. 1). We use an 80 MHz mode-locked laser to pump a dye laser to produce an optical frequency comb of ~ 4 GHz band, allowing to imprint an AFC of this bandwidth into the Pr^{3+}:Y_2SiO_5 line. Optimising over detuning, preparation time and power, we see an AFC echo echo e ciency of up to 10 % at a 12.5 ns delay time. Further, we also witness multiple rephasings (up to 10 in some cases) due to imperfect comb preparation; when summing over all outputs, we witness a total e ciency of up to 20 %. These results open up the possibility for a broadband and long-lived QM on a solid-state platform.

[1] M. F. Riedel, et. al., Quantum Sci. Technol. **2**, 030501 (2017).

[2] R. W. Equall, et al., PRB **52**, 3963 (1995).

[3] G. Heinze, et al., PRL 111, 033601 (2013).

[4] M. Afzelius, et al., PRA 79, 052329 (2009).

[5] M. Sabooni, et al., PRL **110**, 133604 (2013).

[6] D. Rieländer, PRL **112**, 040504 (2014).

[7] M. Gündoğan, et al., PRL **114**, 230501 (2015).

[8] A. Seri, et al., PRX **7**, 021028 (2017).

Storing single photons emitted by a quantum memory on a highly excited Rydberg state

E. Distante[1], P. Farrera[1], A. Padrón-Brito[1], D. Paredes-Barato[1], G. Heinze[1] and H. de Riedmatten[1,2]

[1] *Institut de Ciències Fotòniques, The Barcelona Institute of Science and Technology, 08860 Castelldefels, Spain*

[2] *ICREA - Institució Catalana de Recerca i Estudis Avançats, 08015 Barcelona, Spain*

e-mail: *apadron@icfo.net*

Photons are very good candidates to carry quantum information since they interact weakly with the environment. However, this prevents strong photon-photon interactions, which are needed to process photonic quantum information. To overcome this issue, we need to map the information carried by photons into a medium where it is possible to process it.

Non-linearities at the level of single photons have been demonstrated by using Rydberg atoms, which are atoms excited to states with a high principal quantum number. However, previous experiments with Rydberg atoms have been implemented with weak coherent input states of light, hence the coupling with true single photons is, so far, an outstanding goal.

Strong interactions between two single photons are also very useful for quantum repeater applications. A quantum repeater is a complex device that allows the distribution of quantum information over long distances, establishing entanglement between two separated particles by a process known as entanglement swapping [1]. Each of the separated particles comes from a different entangled pair, so their entangled mates find each other in a middle location. The entanglement swapping is performed by a joint measurement in the Bell-states basis over the entangled mates. The success probability of this operation can be highly increased if the Bell-state measurement is performed deterministically. In the case of photons, it requires mapping them in a highly non-linear medium.

In this work, we have demonstrated the storage and retrieval of a paired single photon on a highly non-linear medium based on atoms excited to Rydberg levels. The single photons are generated in a source based on a quantum memory located in a separated cold atomic ensemble.

The source is based on the Duan-Lukin-Cirac-Zoller scheme [2]. It generates pairs of correlated photons, called *write* and *read*, with a controllable delay between them in a cloud of cold ^{87}Rb atoms. The *write* photon is generated probabilistically via spontaneous Raman scattering by sending a series of weak coherent pulses (*write* pulses). The detection of a *write* photon heralds a single collective excitation known as spin wave. The excitation can be deterministically readout after a storage time by sending a strong, counter-propagating *read* pulse, which generates a single *read* photon. The *read* photon is then, coupled into a 10 m fibre and sent to a separated cloud of cold ^{87}Rb atoms. There, the *read* photon reaches the atomic cloud with a strong counter-propagating coupling beam which allows the excitation to a Rydberg state (n=60) via electromagnetically-induced transparency. By switching off the coupling beam while the *read* photon travels inside the medium, we can store the photon as a Rydberg excitation and then retrieve it by switching the coupling beam back on.

The non-linearity in the Rydberg ensemble is also characterized, finding that the number of stored photons saturates at the level of tens of photons. We are currently working on increasing the non-linearity towards the single-photon level by using a smaller and denser ensemble in an optical dipole trap. This will allow the storage of an single photon in a medium with single-photon non-linearity.

Our results show that nonclassical correlations between *read* and *write* photons persist after retrieval from the Rydberg ensemble, as well as the single photon statistics of the stored *read* photon [3]. This is an important step towards the creation of a building block for deterministic Bell-state measurements in quantum repeaters

[1] N. Sangouard, C. Simon, H. de Riedmatten, and N. Gisin, Rev. Mod. Phys. **83**, 33 (2011).

[2] L.-M. Duan, M. Lukin, J. I. Cirac, and P. Zoller, Nature **414**, 413 (2001).

[3] E. Distante, P. Farrera, A. Padrón-Brito, D. Paredes-Barato, G. Heinze, and H. de Riedmatten, Nat. Comm. **8**, 14072 (2017).

Quantum compilation optimized for experiments with multi-qubit gates

L.Y. Ding[1], **X. Zhang**[1], **and W. Zhang**[1]
[1] *Department of Physics, Renmin University of China, Beijing, China*
e-mail: *tin@ruc.edu.cn*

There is increasing interest in implementing quantum algorithms via simpler and shorter experimental operations for building universal quantum computers. Here, we present a general quantum computation compiler, which maps arbitrary quantum algorithm to an optimal quantum circuit consisting of a sequential set of universal gates which is feasible to operate directly in experiment with atomic qubits by lasers. We implement several methods, including matrix elementary decomposition, cosine-sine decomposition, quantum Shannon decomposition and Cartans KAK decomposition, to transform the quantum algorithm into a series of one-bit gates and specific two-bit or multi-bit gates. The compiler optimizes experimental gate sequence by heuristically applying mirroring and merging tricks. Moreover, we extend numerical optimization method in [1] to compile unitaries using native multi-bit gates, i.e., Ising gates, which significantly reduce gate numbers. The compilation technique is practically favorable and will be used in our following experiment based on trapped ions.

References

[1] Esteban A Martinez et al 2016 New J. Phys. **18** 063029

A novel quantum memory protocol for coherent storage and manipulation of broadband photons via dynamically controlled Autler-Townes absorption

A. Rastogi[1], **E. Saglamyurek**[1], **T. Hrushevskyi**[1], **L. Cooke**[1], **S. Hubele**[1], **K. Heshami**[2], **L. J. LeBlanc**[1,3]

[1] *Department of Physics, University of Alberta, Edmonton, Alberta T6G 2E1, Canada*
[2] *National Research Council of Canada, 1200 Montreal Road, Ottawa, Ontario K1A 0R6, Canada*
[3] *Canadian Institute for Advanced Research, Toronto, Ontario M5G 1M1, Canada*
e-mail: *rastogi1@ualberta.ca*

Optical quantum memories facilitate coherent and reversible transfer of quantum information between light fields and matter. These memories will play a key role in the development of quantum information processing devices. Different approaches to quantum memories have been realized and implemented in many systems [1] including atomic platforms [2, 3, 4, 5]. Despite significant advances, the realization of practical quantum memories featuring e cient, broadband and long-lived storage is still a challenge due to the inherent and system-specific limitations of established light-matter interaction protocols. Here, we describe a novel quantum memory technique that allows for coherent storage and on-demand retrieval of broadband optical pulses, together with robust and high-speed signal processing capabilities. Our approach relies on the resonant absorption of a weak signal (probe) field in the presence of a strong control (coupling) field via dynamically controlled Autler-Townes split (ATS) lines. Using this 'ATS-protocol', the dynamically controlled absorption mediates the reversible exchange of coherence between the signal photonic state and a long-lived spin state of an atomic ensemble.

We experimentally demonstrated a proof-of-principle of this ATS memory scheme by storing short (nanoseconds long) pulses in a collective spin-wave excitation of laser-cooled ^{87}Rb atoms for a period of upto 1 microsecond. We also demonstrated the coherent manipulation of broadband pulses through temporal-spectral pulse compression and stretching, temporal-beam-splitting, wavelength-conversion via dynamic control of storage bandwidth and atom-based interferometry [6]. In addition, we demonstrated storage and retrieval of broadband signals at the single-photon level by using attenuated laser pulses consisting, an average of less than one photon per pulse. Our results show the inherent broadband nature of the ATS scheme and hold great promise for interfacing an ATS memory with single photon sources.

Furthermore, our analysis using the Maxwell-Bloch equations [7], show that compared to established memories (EIT, off-resonant Raman, photon-echo techniques), the ATS-scheme is favorable for practical implementations of broadband pulse storage and manipulation in the fast operation, low optical-depth regime. ATS memory offers significantly relaxed requirements in terms of optical depth, power of the control field, technical complexity and robustness to decoherence. Finally, the ATS-protocol can be readily applied to any generalized three-level system and hence should find application in various domains of quantum technologies.

References

[1] A. I. Lvovsky, B. C. Sanders, and W. Tittel. "Optical quantum memory". In: *Nature photonics* 3.12 (2009), p. 706.

[2] K. Reim et al. "Towards high-speed optical quantum memories". In: *Nature Photonics* 4.4 (2010), p. 218.

[3] Y.-H. Chen et al. "Coherent optical memory with high storage e ciency and large fractional delay". In: *Physical review letters* 110.8 (2013), p. 083601.

[4] G. Hétet et al. "Photon echoes generated by reversing magnetic field gradients in a rubidium vapor". In: *Optics letters* 33.20 (2008), pp. 2323–2325.

[5] H. De Riedmatten et al. "A solid-state light–matter interface at the single-photon level". In: *Nature* 456.7223 (2008), p. 773.

[6] E. Saglamyurek et al. "Coherent storage and manipulation of broadband photons via dynamically controlled Autler-Townes splitting". In: *arXiv preprint arXiv:1710.08902* (2017).

[7] A. V. Gorshkov et al. "Photon storage in Λ-type optically dense atomic media. II. Free-space model". In: *Physical Review A* 76.3 (2007), p. 033805.

Strong upper bounds for the classical capacity on Gaussian quantum channels

K. Jeong[1,2,*] **and H. H. Lee**[1]

[3] *IMDARC, Department of Mathematical Sciences, Seoul National University, 08826 Seoul, Korea*
[2] *School of Computational Sciences, Korea Institute for Advanced Study, Seoul 02455, Korea*
e-mail*: *kgjeong6@snu.ac.kr*

Abstract
Most natural way to describe an information-carrying system involving a specific additive-noise is given by a model known as the additive white Gaussian-noise (AWGN) channel. In bosonic quantum Gaussian case, although the classical information capacity for a phase-insensitive thermal-noise channel under the proof of minimal-output entropy conjecture is additive, still we have several open questions. Here, by generalizing the Gaussian noisy model, we rigorously revisit and calculate strong upper bounds on the information capacity for the single-mode and general Gaussian-noise channel via the quantum entropy power inequality (QEPI). In this frame we have found a new formula for finding upper bound on the information capacity over bosonic Gaussian-noise channels.

A central goal in quantum Shannon theory, as a quantum analogue of information theory, is to determine the channel capacity on quantum communication systems or quantum channels. The channel capacity for a communication channel is generally defined as the maximal rate of information-transmission at which certain information can be reliably transmitted through the channel within vanishing errors, and it is practically organized as the electromagnetic systems. To date we can use a communication system characterized by quantum optical channel, which is modeled by an input bosonic quantum state transformed into another output bosonic state with its external thermal-noise (via Gaussian unitaries), and it is called as bosonic Gaussian-noise (or thermal-noise) channel. Here we restrict quantum channel described only by Gaussian operations over bosonic Gaussian states and the bosonic Gaussian-noise.

Recently one way to obtain the tight upper bound on information capacity for a (single-mode) bosonic Gaussian-noise channel is suggested by proving their Gaussian minimal-output entropy conjecture. This implies that Gaussian information capacity on Gaussian-noise channel is additive, since it saturates to the Holevo capacity. On the other hand, universal upper bound on the capacity can be obtained by exploiting the new notion of quantum entropy power inequality (QEPI) in the Gaussian regime [1, 2]. Formally, for independent two input Gaussian signals ρ_X and ρ_Y, the QEPI is given by

$$S(\rho_Z) \geq \tau S(\rho_X) + (1-\tau)S(\rho_Y), \qquad (1)$$

where $S(\cdot)$ denotes the von Neumann entropy and ρ_Z an output state through a beamsplitter with its mixing parameter $\tau \in [0,1]$. Due to a potential role of Gaussian entanglement such as non-additivity of Gaussian information capacity, we here take care of the upper bound given by the notion of QEPI [3]. Actually, we still believe that there exists some additivity violation for the bosonic Gaussian-noise channels, whenever any entangled (or squeezed) encodings in the Gaussian regime are possible. If not, Gaussian channels are may useless in the view point of increasing the channel capacity for Gaussian communications via quantum entanglement. This is one of reason why we seriously consider the upper bounds on the information capacity through the QEPI.

Here we consider a bosonic Gaussian channel including *general* Gaussian-noise case. Here, we explicitly calculate its universal upper bounds of the information capacity for the general Gaussian-noise channels, and derive a new formula. That is, we suggest an exact formula to restrict universal upper bounds for the Gaussian information capacity on the bosonic Gaussian channel, where the lower bound naturally comes from well-known Holevo-Schumacher-Westmoreland theorem. The universal upper bounds generally come from the Smith and König's previous works in Refs. [1, 2] together with this research [3].

Acknowledgments
This work was supported by the National Research Foundation of Korea (NRF) through a grant funded by the Korean government (Ministry of Science and ICT) (NRF-2017R1E1A1A03070510 & NRF-2017R1A5A1015626).

[1] R. König and G. Smith, Nat. Photon. **7**, 142 (2013).

[2] R. König and G. Smith, Phys. Rev. Lett. **110**, 040501 (2013).

[3] K. Jeong and H. H. Lee, submitted (2018).

Investigation of the Hyperfine Structure of the Electronically Excited State through Raman Heterodyne Detection

Yu Ma[1,2], Zong-Quan Zhou[1,2], Chao Liu[1,2], Yong-Jian Han[1,2], Tian-Shu Yang[1,2], Tao Tu[1,2], Yi-Xin Xiao[1,2], Peng-Jun Liang[1,2], Pei-Yun Li[1,2], Yi-Lin Hua[1,2], Xiao Liu[1,2], Zong-Feng Li[1,2], Jun Hu[1,2], Xue Li[1,2], Chuan-Feng Li[1,2] and Guang-Can Guo[1,2]

[1] *CAS Key Laboratory of Quantum Information, University of Science and Technology of China, 230026 Hefei, P. R. China*

[2] *Synergetic Innovation Center of Quantum Information and Quantum Physics, University of Science and Technology of China, 230026 Hefei, P. R. China*

e-mail: *mayu@mail.ustc.edu.cn*

The ground-state spin coherence time of $^{151}Eu^{3+}$ in Y_2SiO_5 crystal in a critical magnetic field was extended to six hours in a recent work [1], which paved the way for constructing quantum memory with long storage time. In order to select a three-level system for quantum memory applications, information about the excited-state energy level structures is required for optical pumping. In this work, we experimentally characterize the hyperfine interaction of the optically-excited state $^5D_0$ using Raman heterodyne detection of nuclear magnetic resonance (NMR). The NMR spectra collected in 201 magnetic fields are well fitted. The results can be used to predict the energy level structures in any given magnetic field, thus enabling the design of optical pumping and three-level quantum memory in that field.

Raman heterodyne detection of NMR, as an RF-optical double-resonance technique based on the coherent Raman effect, is a useful tool for observing NMR [2]. Measurements of the ground-state hyperfine structure $^7F_0$ of $^{151}Eu^{3+}$ at site 1 in Y_2SiO_5 were covered elsewhere [3], which provide a stepping stone towards hour-long spin coherence time. Here we present the characterization of the hyperfine interaction of the excited state $^5D_0$ of $^{151}Eu^{3+}$ at the same site using a similar approach.

The hyperfine energy level diagram in zero magnetic field is shown in Fig. 1(a). A sample of Eu^{3+}:Y_2SiO_5 is placed inside a cryostat for spectrum measurements. The XYZ coils outside the cryostat are used to provide a magnetic field. An RF field is produced by a coil wrapped around the sample along the C_2 axis. Two laser beams from a frequency-doubled semiconductor laser tuned to be resonant with the $^7F_0 \rightarrow {}^5D_0$ transition are incident on the sample. The probe beam propagates along the crystal C_2 axis. The transmitted light which carries the Raman heterodyne signal is detected with a photodetector.

The Raman heterodyne signal is generated when the RF field is resonant with the hyperfine transition either in the excited- or ground-state manifold. The signal stems from a beat between the transmitted probe laser and the Raman scattered light.

For more experimental details and results, see our original paper posted on arXiv [4].

[1] M. Zhong, J. J. Longdell and M. J. Sellars *et al.*, Nature **517**, 177180 (2015).

[2] J. Mlynek, N. C. Wong, R. G. DeVoe, E. S. Kintzer and R. G. Brewer, Phys. Rev. Lett. **50**, 993996 (1983).

[3] J. J. Longdell, A. L. Alexander and M. J. Sellars, Phys. Rev. B **74**, 195101 (2006).

[4] Y. Ma, Z. Q. Zhou, C. F. Li and G. C. Guo *et al.*, arXiv:1711.01814v2 (2018).

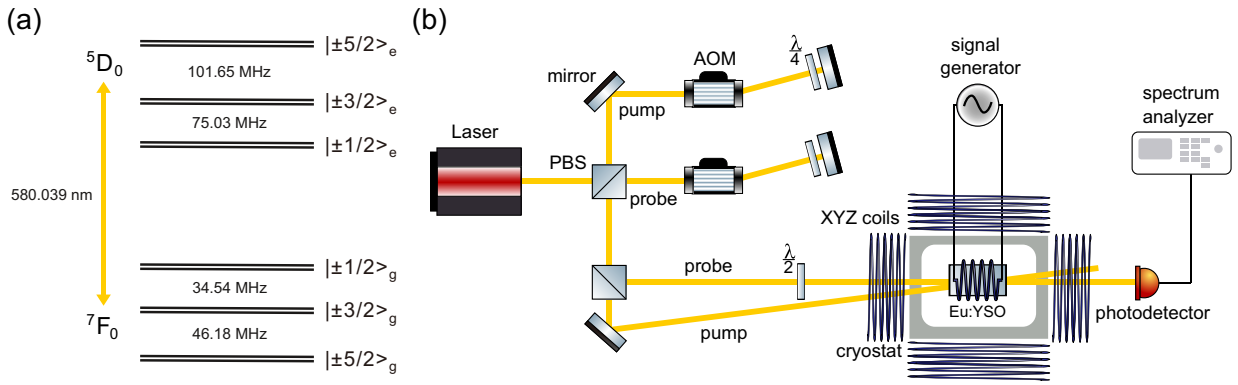


Figure 1: Energy level diagram and experimental setup.

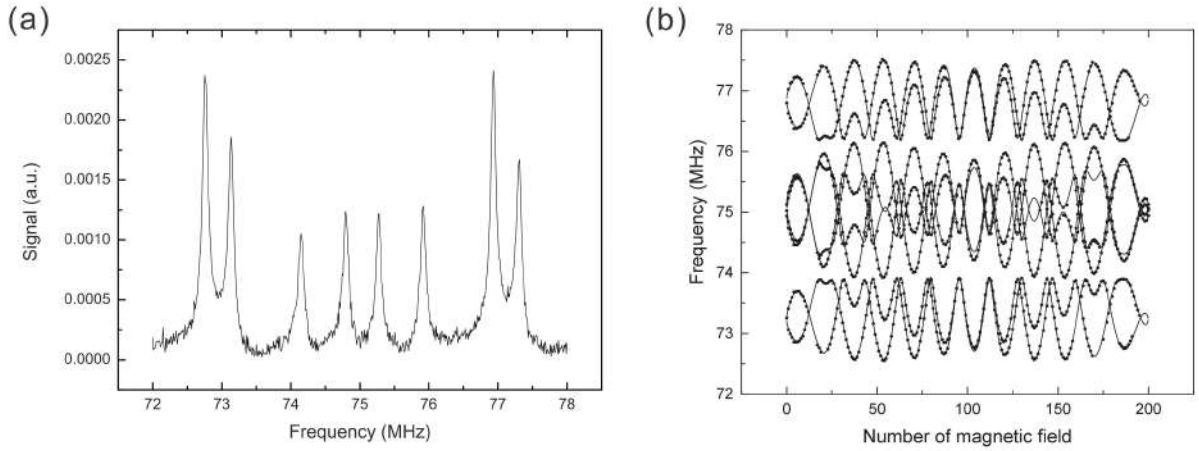


Figure 2: (a) A typical excited-state Raman-heterodyne spectrum collected in a magnetic field. Eight NMR peaks can be clearly located with high signal-to-noise ratio. (b) The experimental data and fit curves for the excited-state hyperfine transitions in 201 magnetic fields. The dots represent the NMR peak positions detected in the experiment, and the solid lines are the fit curves of the experimental data.

Genuinely entangled symmetric states with no N-partite correlations

J. Martin[1], **S. Designolle**[2], **and O. Giraud**[3]

[1] *Institut de Physique Nucléaire, Atomique et de Spectroscopie, CESAM, Université de Liège, Belgium*

[2] *Groupe de Physique Appliquée, Université de Genève, CH-1211 Genève, Switzerland*

[3] *LPTMS, CNRS, Univ. Paris-Sud, Université Paris-Saclay, 91405 Orsay, France*

e-mail: *jmartin@uliege.be*

We investigate genuinely entangled N-qubit states with no N-partite correlations (see, e.g., [1, 2, 3]) in the case of symmetric states. Using a tensor representation for mixed symmetric states [4], we obtain a simple characterization of the absence of N-partite correlations [5]. We show that symmetric states with no N-partite correlations cannot exist for an even number of qubits. We fully identify the set of genuinely entangled symmetric states with no N-partite correlations in the case of three qubits, and in the case of rank-2 states. We present a general procedure to construct families for an arbitrary odd number of qubits [5].

In particular, we show that symmetric three-qubit states with no N-partite correlations are represented, in the symmetric Dicke states basis, by a matrix of the form

$$\rho = \frac{1}{8}\mathbb{1}_4 + \frac{3}{8}\sum_{a,b=1}^{3} A_{ab} J_{ab}, \tag{1}$$

with $\mathbb{1}_4$ the 4×4 identity matrix, J_{ab} given by

$$J_{ab} = \frac{J_a J_b + J_b J_a}{3} - \frac{\delta_{ab}}{2}\mathbb{1}_4, \tag{2}$$

with J_a the 4×4 angular momentum matrices, and A the 3×3 real symmetric matrix of two-partite correlations, $A = (\langle\sigma_{ab}\rangle_\rho)_{1\leq a,b\leq 3}$, with $\sigma_{ab} = \sigma_a \otimes \sigma_b \otimes \mathbb{1}_2$ and $\langle\sigma_{ab}\rangle_\rho = \mathrm{tr}(\rho\,\sigma_{ab})$ and σ_a the Pauli matrices. Figure 1 shows, in the space of eigenvalues of A, the region containing all symmetric three-qubit genuinely entangled states with no 3-partite correlations.

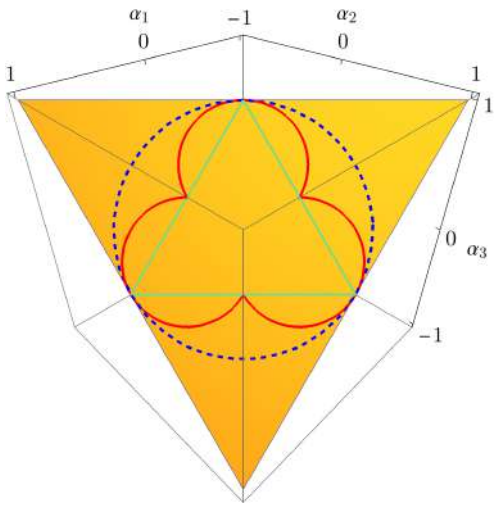


Figure 1: Three-qubit symmetric states of the form (1) in the space of eigenvalues α_i of the two-partite correlation matrix $A = (\langle\sigma_{ab}\rangle_\rho)_{1\leq a,b\leq 3}$ (see text). Points outside the green triangle up and inside the dashed blue circle correspond to genuinely entangled states [5].

[1] D. Kaszlikowski, A. S. De, U. Sen, V. Vedral, and A. Winter, *Quantum Correlation without Classical Correlations*, Phys. Rev. Lett. **101**, 070502 (2008).

[2] C. Schwemmer, L. Knips, M. C. Tran, A. de Rosier, W. Laskowski, T. Paterek, and H. Weinfurter, *Genuine Multipartite Entanglement without Multipartite Correlations*, Phys. Rev. Lett. **114**, 180501 (2015).

[3] M. C. Tran, M. Zuppardo, A. de Rosier, L. Knips, W. Laskowski, T. Paterek, and H. Weinfurter, *Genuine N-partite entanglement without N-partite correlation functions*, Phys. Rev. A **95**, 062331 (2017).

[4] O. Giraud, D. Braun, D. Baguette, T. Bastin, and J. Martin, *Tensor Representation of Spin States*, Phys. Rev. Lett. **114**, 080401 (2015).

[5] S. Designolle, O. Giraud, and J. Martin, *Genuinely entangled symmetric states with no N-partite correlations*, Phys. Rev. A **96**, 032322 (2017).

Observing the quantum interference and entanglement of electron-nuclear system on Bloch sphere by Wigner distribution

Heng Shen[1], **Bing Chen**[2], **and Nanyang Xu**[2]

[1] *Clarendon Laboratory, University of Oxford, Parks Road, Oxford, OX1 3PU, UK*

[2] *School of Electronic Science and Applied Physics,Hefei University of Technology, Hefei, Anhui 230009, China*

e-mail: *heng.shen@physics.ox.ac.uk*

Quantum state tomography of a system from measurements is an important topic in the emerging field of quantum technology. Through full state reconstruction, we can estimate the properties of quantum systems such as entanglement and purity, and furthermore determine their potential application in fields of quantum metrology[1, 3], quantum simulation[4, 6, 5] and quantum computation[7, 8]. As a counterpart of density matrix reconstruction, Wigner function is convenient for longer spins, where the density matrix reconstruction with maximum likelihood estimation[9] in practice become problematic.

We present the experimental reconstruction of the Wigner function of a two-level electron single spin and electron-nuclear two spins in diamond. This spherical Wigner function contains the same information as the density matrix for any spin- j system. As an example, we experimentally measure the Wigner function of a single qubit undergoing a nearly pure dephasing process. The extracted fidelities of spin state at different time points show the same decay rate as dephasing process, which agrees with theoretical prediction. Then our method is applied to two qubit system in Bell state to present the entanglement behavior. Furthermore, it can be applied straightforwardly to multi-atom systems for measuring the Wigner function of their collective spin state, such as trapped ions.

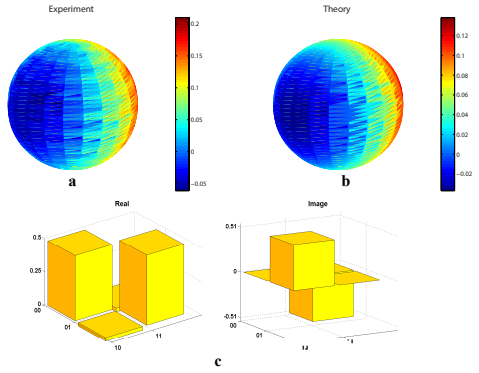


Figure 1: Experimental(a) and theoretical(b) WF of a qubit in state of $|x\rangle = \frac{|0\rangle+|1\rangle}{\sqrt{2}}$. (c).The density matrix elements reconstructed through quantum state tomography.

[1] J. Appel, P. J. Windpassinger, D. Oblak, U. B. Hoff, N. Kjærgaard and E. S. Polzik, Mesoscopic atomic entanglement for precision measurements beyond the standard quantum limit, Proc. Natl Acad. Sci. USA 106 10960 (2010).

[2] C. Gross, T. Zibold, E. Nicklas, Estéve J and M. K. Oberthaler, Nonlinear atom interferometer surpasses classical precision limit, Nature (London) 464 11659 (2010).

[3] A. Friedenauer, H. Schmitz, J. T. Glueckert, D. Porras and T. Schaetz, Simulating a quantum magnet with trapped ions, Nat. Phys. 4 757(2008).

[4] K. Kim, M.-S. Chang, S. Korenblit, R. Islam, E. E. Edwards, J. K. Freericks, G.-D. Lin, L.-M. Duan and C. Monroe, Quantum simulation of frustrated Ising spins with trapped ions, Nature (London) 465, 590 (2010).

[5] B. P. Lanyon, C. Maier, M. Holzäpfel, T. Baumgratz, C. Hempel, P. Jurcevic, I. Dhand, A. S. Buyskikh, A. J. Daley, M. Cramer, M. B. Plenio, R. Blatt and C. F. Roos, E cient tomography of a quantum many-body system, Nat. Phys. 13, 1158 (2017).

[6] D. Leibfried, E. Knill, S. Seidelin, J. Britton, R. B. Blakestad, J. Chiaverini, D. B. Hume, W. M. Itano, J. D. Jost, C. Langer, R. Ozeri, R. Reichle and D. J. Wineland, Creation of a six-atom 'Schrödinger cat' state, Nature (London) 438, 639 (2005).

[7] J. Benhelm, G. Kirchmair, C. F. Roos and R. Blatt, Towards fault-tolerant quantum computing with trapped ions, Nat. Phys. 4 463 (2008).

[8] Mi. Ježek, J. Fiurášek, and Z. Hradil, Quantum inference of states and processes, Phys. Rev. A 68, 012305 (2003).

Verifying high-fidelity multi-particle processes in an ion-trap quantum computer

A. Erhard[1], **R. Stricker**[1], **L. Postler**[1], **M. Meth**[1], **E. Martinez**[1], **P. Schindler**[1], **T. Monz**[1] and **R. Blatt**[1]

[1] *Institute for Experimental Physics, Universtity of Innsbruck, Austria*

e-mail: *alexander.erhard@uibk.ac.at*

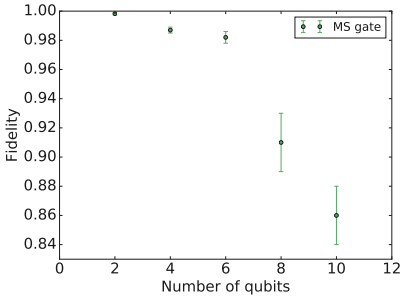


Figure 1: Entangling Molmer-Sorensen (MS) gate fidelity on increasing number of qubits.

Fully characterizing a quantum process is a daunting task. Even for two-level systems, one requires 12^N measurement settings to gather su cient information to reconstruct the full process acting on N particles. However, it is possible to verify certain quantum processes e ciently. A prominent example of a class of e ciently verifiable processes are operations from the Clifford group, whose error rates can be estimated using Randomized Benchmarking. These operations are crucial in quantum information science as they provide a set of operations that enable a fault tolerant quantum computer. Exact knowledge of the error rate is one of the keys in an experimental quantum computer, as it is directly linked to the fault tolerant threshold that enables arbitrary long quantum algorithms. We implement multiple benchmarking protocols in our trapped-ion multi-qubit system and compare these results with gate set tomography. In the case of two qubits we measure error rates of less than 1 %. We also investigate the scaling of error rates with increasing number of qubits and obtain error rates for entangling operations below 15 % with 10 qubits (see figure 1).

Half-Deterministic Atom-Photon Entanglement for Quantum Repeaters

Jun Li[1,2,3], **Ming-Ti Zhou**[1,2,3], **Chao-Wei Yang**[1,2,3], **Xiao-Hui Bao**[1,2,3] **and Jian-Wei Pan**[1,2,3]

[1] *Hefei National Laboratory for Physical Sciences at Microscale and Department of Modern Physics, University of Science and Technology of China, Hefei, Anhui 230026, China*

[2] *CAS Center for Excellence and Synergetic Innovation Center in Quantum Information and Quantum Physics, University of Science and Technology of China, Hefei, Anhui 230026, China*

[3] *CAS-Alibaba Quantum Computing Laboratory, Shanghai 201315, China*

e-mail: *jlee@ustc.edu.cn*

In recent years, Rydberg blockade mechanism has been introduced into atomic ensembles to deterministically generate singly excited collective states [1, 2, 3] and it has been proposed to be used for realizing efficient quantum repeaters [4]. In this work, taking advantage of Rydberg blockade, we propose and experimentally demonstrate a scheme that prepares the entanglement between a single photon and a collective atomic excitation with an intrinsic efficiency of 50%, which we call "half-deterministic".

The essence of our scheme is to take advantage of Rydberg blockade between two collective atomic excitations in one atomic ensemble for entanglement generation, while the momentum degree of freedom is introduced to map the atomic excitaitons onto phase-matched single photons in different spatial modes, such that the emission path of the first read-out photon is entangled with the momentum mode of the remaining atomic excitation. The success probability of the scheme is 50%. In the experiment, we observe the nonlinearity arising from Rydberg blockade between collective excitation pairs that results in a $\sqrt{2}$ factor compared with single excitations. With a specified $\pi/\sqrt{2}$ pulse, the entanglement is obtained. By varying the relative phase in the aotom-photon entanglement system, we observe the coincidence patterns of the converted photons in the eigen basis (H/V) and the superposition basis ($+45°/-45°$), as shown in Fig. 1, where $n_\perp = n_{\mathrm{HV}(+-)} + n_{\mathrm{VH}(-+)}$ and $n_\parallel = n_{\mathrm{HH}(++)} + n_{\mathrm{VV}(--)}$ are the corresponding coincidence count summations that have been normalized by setting the summations of all coincidence counts as 1 unit. Then the entanglement fidelity is measured to be 0.901(8), and $g^2(0)$ of the photons converted from the two atomic excitations are 0.114(14) and 0.120(17) respectively. It proves the two parts of the entanglement are both genuine single photons, which is critical in the implementations of quantum repeaters. The half-deterministic photon-atom entanglement source is definitely suitable for robust quantum repeaters based on two-photon interference detection [5]. Using this kind of entanglement source in quantum repeaters instead, we can reduce the complexity of the quantum network and speed up the quantum repeater working effeciency compared with probabilistic schemes [6, 7]. And the half-deterministic entanglement source will promote the complete realization of fully deterministic entanglement sources in the near future.

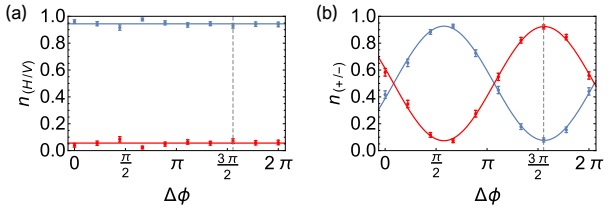


Figure 1: Measurement of polarization correlations of the two photons. With the additional phase shift $\Delta\phi$ varying, in H/V basis (a) $n_\perp$ (blue) and $n_\parallel$ (red) keep as constants approximating to unity and zero respectively, while in $+/-$ basis (b) $n_\perp$ (blue) and $n_\parallel$ (red) exhibit sinusoidal oscillations in a complementary manner with a period of $\simeq 2\pi$. The error bars represent ± 1 SD.

[1] M. D. Lukin, M. Fleischhauer, R. Cote, L. M. Duan, D. Jaksch, J. I. Cirac, and P. Zoller, Phys. Rev. Lett. **87**, 037901 (2001).

[2] M. Saffman, T. G. Walker, and K. Mølmer, Rev. Mod. Phys. **82**, 2313 (2010).

[3] Y. O. Dudin and A. Kuzmich, Science **336**, 887 (2012).

[4] B. Zhao, M. Müller, K. Hammerer, and P. Zoller, Phys. Rev. A **81**, 052329 (2010).

[5] Z.-S. Yuan, Y.-A. Chen, B. Zhao, S. Chen, J. Schmiedmayer, and J.-W. Pan, Nature **454**, 1098 (2008).

[6] L.-M. Duan, M. Lukin, J. I. Cirac, and P. Zoller, Nature **414**, 413 (2001).

[7] B. Zhao, Z.-B. Chen, Y.-A. Chen, J. Schmiedmayer, and J.-W. Pan, Phys. Rev. Lett. **98**, 240502 (2007).

Quantum memory for light: beyond the three-level Λ-scheme approximation

A.S. Sheremet, P.Vernaz-Gris, K. Huang, M. Cao, J. Raskop, N.V. Corzo, and J. Laurat
Laboratoire Kastler Brossel, Sorbonne Université,
CNRS, ENS-PSL Research University, Collège de France, 4 place Jussieu, 75005 Paris, France
e-mail: *alexandra.sheremet@lkb.upmc.fr*

The processes of light interaction with optically dense atomic ensembles allow the creation of a controllable quantum optics interface, which can be a building block for many applications in quantum information science [1]. For example, quantum memory implements the controllable and reversible mapping of a quantum state of light onto a quantum state of matter [2]. In recent years, the physical implementation of such interfaces has been at the focus of a very intense research. A critical figure of merit is the overall storage-and-retrieval e ciency, which is mainly determined by technical losses and the storage e ciency, and depends on the storage mechanism and matter properties. Collective and cooperative effects manifestable in an atomic ensemble could provide essential enhancement of the coupling strength between the light and atomic subsystems. In this context, one of the strongest requirement to obtain a high e ciency is a large optical depth (OD), which can be achieved by increasing the size of the atomic system or atomic density in the system. In addition, the interaction between light and atoms can be enhanced by trapping atoms in the vicinity of a nanoscale waveguide due to strong confinement of the light [3]. However, some nonlinear optical effects become significant at a large OD and lead to reduce the storage-and-retrieval e ciency.

In this context, here we present the theoretical description of quantum memory based on electromagnetically induced transparency (EIT) and Duan-Cirac-Lukin-Zoller protocol (DLCZ) [4] in an ensemble of cold cesium atoms featuring a large optical depth. Additionally, we present a model of control of light propagation based on EIT in a system of trapped atoms in the vicinity of an optical nanofiber.

As it was mentioned above, we consider different mechanisms of quantum memory. The processes of light-matter interaction for the optically dense, but spatially dilute atomic medium can be described with the formalisms of Maxwell-Bloch equations (for EIT-based memory) or with Heisenberg-Langevin equations (for DLCZ memory). Both techniques allow us to take into account the complex structure of atomic levels. In our theoretical models we include interaction of optical fields with the full D_2-line structure of ^{133}Cs atoms. In addition to all the excited levels, we also include the Zeeman sublevels to compare implementations with and without optical pumping. These models show that at a large OD, as required, the non-resonant coupling of the driving fields with hyperfine sublevels of the excited state results in significant modification of atomic response compared to the standard Λ-scheme approximation. This non-resonant coupling leads to additional effective atomic ground state decoherence and limits the storage e - ciency.

Moreover, spatially dense atomic ensembles (i.e. up to one atom in a volume of radiation wavelength) allow obtaining effective light-matter interface and reliable light storage with essentially fewer atoms than in can be achieved in dilute gases. Futhermore, nanofiber-based optical dipole traps, in which ensembles of a few thousand atoms are trapped in the evanescent field can lead to cooperative effects which have important implications for quantum memory. The presence of an optical nanofiber strongly modifies the character of atomic interaction and results in long-range dipole-dipole coupling between atoms not only via the vacuum, but also through the waveguide mode. We describe the process of light-atoms interaction in presence of a nanofiber using the standard T-matrix and Resolvent operator formalism.

In conclusion our models allow to estimate the highest storage-and-retrieval e ciency for chosen polarization configuration and atomic transitions. Moreover, our results of EIT-based memory in free space are in perfect agreement with the highest e ciency memory (70%) demonstrated for optical qubits in a large-OD elongated atomic ensemble [5].

References

[1] K. Hammerrer, A.S. Sørensen, and E.S. Polzik, Rev. Mod. Phys. **82**, 1041 (2010).

[2] H.J. Kimble, Nature **453**, 1023 (2008).

[3] V.I. Balykin, K. Hakuta, F. Le Kien, et al., Phys. Rev. A **70**, 011401(R) (2004).

[4] L.-M. Duan, M.D. Lukin, J.I. Cirac and P. Zoller, Nature **414**, 413 (2001).

[5] P. Vernaz-Gris, K. Huang, M. Cao, A.S. Sheremet, and J. Laurat, Nat. Comm. **94**, 363 (2018).

[6] B. Gouraud, D. Mexein, A. Nicolas, O. Morin, J. Laurat, Phys. Rev. Lett. **114**, 180503 (2015).

Negative-mass effects in spin-orbit coupled Bose-Einstein condensates

David Colas[1], **Fabrice P. Laussy**[2,3], **and Matthew J. Davis**[1]

[1] *ARC Centre of Excellence in Future Low-Energy Electronics Technologies (FLEET), School of Mathematics and Physics, University of Queensland, St Lucia, Queensland 4072, Australia*

[2] *Faculty of Science and Engineering, University of Wolverhampton, Wulfruna St, WV1 1LY, UK*

[3] *Russian Quantum Center, Novaya 100, 143025 Skolkovo, Moscow Region, Russia*

e-mail: *d.colas@uq.edu.au*

Negative effective masses for wave packets can be achieved by engineering the dispersion relation in a range of quantum systems. Examples include holes within semiconductors, exciton-polaritons in 2D microcavities, or atomic spin-orbit coupled Bose-Einstein condensates (SOCBEC). An interesting feature known as Self-Interfering Packet (SIP) can appear when these systems are excited near an inflection point in the dispersion relation. This linear effect has been originally predicted theoretically in exciton-polariton systems [1] and recently observed in an atomic SOCBEC [2, 3]. An example of SIP dynamics is shown in Fig. 1(a) where a narrow condensate trapped at the bottom of the lower branch of the SOCBEC dispersion (see inset) is released and expands. As the condensate diffuses, interference fringes appear and are bounded in space in a well defined cone d_1-d_2 determined by the shape of the dispersion. This result is obtained from a simple Schrödinger equation modified with the SOCBEC dispersion and without any need of interaction. However, we show how the presence of interaction can favour the SIP formation by increasing the condensate's momentum, thus populating the region of negative mass. We also investigate configurations accessible in SOCBECs when both mass parameters controlling the condensate's propagation and diffusion are negative, producing counter-propagating self-interfering packets [3]. We show that the Wavelet Transform (WT)

$$\mathbb{W}(x,k) = \frac{1}{\sqrt{|k|}} \int_{-\infty}^{+\infty} \psi(x) \mathcal{G}^* \left(\frac{x - x_0}{k} \right) \mathrm{d}x \qquad (1)$$

brings unique insights into the complex wave packet dynamics, being a more physical spectral representation than the Fourier Transform. Figure 1(b) shows the WT of the condensate wave function taken at $t = 35$ μm. One sees how different k-components of the condensate travel with the same velocity within the diffusion cone and yield an interference pattern in real space. The WT provides a clear understanding of the SIP effect, and can also be applied to understand other experiments exhibiting effects related to non-parabolic dispersion. An interesting case study is the X-wave, a type of non-spreading wave packet appearing when the system's dispersion relation is hyperbolic or locally hyperbolic. X-waves have been observed in the early 2000s in atomic systems [4] and more recently in polariton system [5].

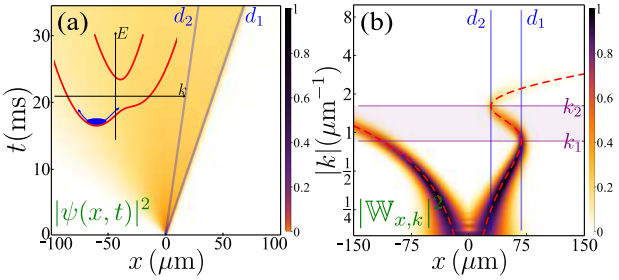


Figure 1: (a) The condensate density $|\psi(x,t)|^2$ exhibits interference fringes bounded by a diffusion cone d_1-d_2 defined by the shape of the dispersion (shown as inset). (b) Corresponding wavelet transform $|\mathbb{W}(x,k)|^2$, showing the energy density of the field displayed in *(x-k)* space, and following the k-dependent packet group velocity (red dashed line).

[1] D. Colas and F. P. Laussy, Phys. Rev. Lett., **116**, 026401 (2016).

[2] M. A. Khamehchi *et al.*, Phys. Rev. Lett., **118**, 155301 (2017).

[3] D. Colas, F. P. Laussy and M. J. Davis, arXiv:1801.04779 (2018).

[4] C. Conti and S. Trillo, Phys. Rev. Lett., **92**, 120404 (2004).

[5] A. Gianfrate *et al.*, Light: Sci. and. appl., **7**, 17119 (2018).

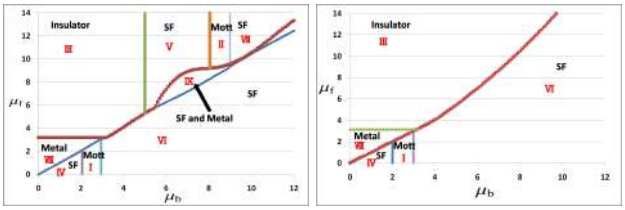
Quantum Phases and Excitations in Bose-Fermi Mixtures in a Three-Dimentional Optical Lattice

R. Hatsuda[1], **E. Arahata**[2]
[1] *Faculty of Science and Engineering, Tokyo Metropolitan University, Hachioji, Tokyo* 192 − 0397*, Japan*
[2] *Department of physics, Tokyo Metropolitan University, Hachioji, Tokyo* 192 − 0397*, Japan*
e-mail: *hatsuda-rei@ed.tmu.ac.jp*

Recently, a superfluid of Bose-Fermi mixture in which both Bose and Fermi gases are superfluids, has been realized by ENS group [1]. This experiment has renewed interest in a superfluid of Bose-Fermi mixtures. In particular, quantum phases in Bose-Fermi mixtures in a 3D optical lattice have attracted a lot of attention both theoretically and experimentally. Bose-Fermi mixtures in a optical lattice [2, 3] can be well described by the so-called tight binding Bose-Fermi Hubbard model which has been derived in Ref.[3]. This model is expected as new quantum simulator because many body effect of difference from statistic is enhanced. The parameters, such as the effective interaction between Bose and Fermi gases, the total filling factor, the ratio of bosons and fermions, can be turned experimentally [4]. Such variability of physical parameters can make quantum phases very rich. In particular, the existence of coexisting Mott insulator phase has been reported theoretically, which the total number of bosons and fermions is an integer value but both bosons and fermions take some intermediate values. However most theoretical studies have concentrated on the filling factor of bosons and fermions in optical lattices. The effect of turning of the other parameters has not given in any detail so far.

In Ref. [5], investigated the phase diagrams of Bose-Fermi mixtures in a three dimensional optical lattice by dynamical mean field theory (DMFT) with limited interaction parameters. However it is necessary to study with turning of variable parameters in order to find a novel phase diagram. In order to understand such a novel phase, it is important to reveal the details of the excitations of Bose-Fermi mixtures in a three dimensional optical lattice. Experimentally the excitation spectra have been observed by the Bragg spectroscopy. It is expected that elementary excitations of Bose-Fermi mixtures will be observed and be able to characterize the different phase.

We study the quantum phase and the excitation properties in Bose-Fermi mixture in a 3D optical lattice at zero temperature using the Gutzwiller approximation by turning of variable parameters. We first determine the ground-state phase diagrams in Fig. 1 for finding phases which we should focus on. Second, we investigate the excitations by extending the method for calculating excitation spectra to Bose-Fermi mixtures. We found the existence of coexisting Mott insulator phase and the typical excitation spectra from this phase .



(a) (b)

Figure 1: Phase diagrams in Bose-Fermi mixture spanned by the chemical potentials $\mu_{\rm b}$and $\mu_{\rm f}$ for (a) $U_{\rm bb} = 6$, $U_{\rm bf} = 6$, (b) $U_{\rm bb} = 6$, $U_{\rm bf} = 12$.
Region I represent Mott insulator phase for pure bosons. II, Mott insulator phase for bosons and fermions. III, Insulator phase for pure fermions. IV, superfluid phase for pure bosons($n_{\rm b} < 1$). V, superfluid phase for bosons($n_{\rm b} < 1$) and insulator fermions. VI, superfluid phase for pure bosons($n_{\rm b} > 1$). VII, superfluid phase for bosons($n_{\rm b} > 1$) and insulator fermions. VIII, metal phase for pure fermions. IX, coexisting phase of superfluid bosons and metal fermions.

We shall also discuss how the excitation spectra changed for several characteristic phases in detail.

[1] I. Ferrier-Barbut, M. Delehaye, S. Laurent, A. T. Grier, M. Pierce, B. S. Rem, F. Chevy, C. Salomon Science 345, 6200 (2014).

[2] Th. Best, S. Will, U. Schneider, L. Hackermuller, D. van Oosten, I. Bloch, and D.-S. Luhmann Phys. Rev. Lett. 102, 030408 (2009).

[3] D. Jaksch, C. Bruder, J.I. Cirac, C. W. Gardiner, and P. Zoller, Phys. Rev. Lett, 81. 15 (1998).

[4] D. van Oosten, P. van der Straten, and H. T. C. Stoof, Phys. Rev. A 63, 053601 (2001).

[5] Q.M. Liu, X. Dai, Z. Fang, J.-N. Zhuang, Y. Zhao, Appl. Phys. B 99, 639-650 (2010).

Magnetic phases of spin-1 lattice gases with random interactions

K. D. McAlpine[2], S. Paganelli[2], S.Ciuchi [2,3], A. Sanpera[4,5] and G. De Chiara[1]

[1] *Centre for Theoretical Atomic,Molecular, and Optical Physics, School of Mathematics and Physics, Queen' s University Belfast, Belfast BT7 1NN, United Kingdom*

[2] *Dipartimento di Scienze Fisiche e Chimiche, Universitá dell'Aquila, via Vetoio, I-67010 Coppito-L'Aquila, Italy*

[3] *Consiglio Nazionale delle Ricerche (CNR-ISC) Via dei Taurini, I-00185 Rome, Italy*

[4] *ICREA, Pg. Lluís Companys 23, E-08010 Barcelona, Spain*

[5] *Departament de Física, Universitat Autònoma de Barcelona, 080193 Bellaterra, Spain*

e-mail: *simone.paganelli@univaq.it*

A spin-1 atomic gas [1] in an optical lattice, in the unit-filling Mott insulator (MI) phase and in the presence of disordered spin-dependent interaction, is considered.

The system is well described by a Bose-Hubbard model, consisting of two competing terms: the hopping between lattice sites and the repulsive interaction produced by local scattering [2, 3]

$$H = \frac{U_0}{2}\sum_i n_i\left(n_i-1\right) + \frac{1}{2}\sum_i U_{2i}\left(\mathbf{S}_i^2 - 2n_i\right) - \mu\sum_i n_i - t\sum_{i,\sigma}\left(a^\dagger_{i,\sigma}a_{i+1,\sigma} + a^\dagger_{i+1,\sigma}a_{i,\sigma}\right). \quad (1)$$

If the spin orientation is fixed by an external magnetic field, as happens when the gas is confined in a magnetic trap, a scalar model is su cient to describe the system [4, 5]. Conversely, if the spin orientation is not externally constrained, as in the case of optical trapping, the spinor character of the gas has to be taken into account.

At zero temperature, the phase diagram of interacting spin-1 bosons on a lattice consists of the Mott insulator (MI) lobes as in the scalar case while for smaller interactions the system is superfluid (SF) [3]. In the MI phase, density fluctuations are suppressed while the spin degrees of freedom give rise to a variety of possible magnetic phases. In order to explore the magnetic behavior inside the MI phase, it is possible to map the problem into a spin Hamiltonian by a perturbative expansion in the hopping parameter.

We study the case of a spin-1 system in the MI phase with one boson per site, when disorder mixes locally ferromagnetic and antiferromagnetic interactions. By mapping the spin-1 Bose-Hubbard system into the corresponding spin model (bilinear-biquadratic),

$$H_{BB} = \sum_{i=1}^{L-1} J_i(\cos\theta_i(\mathbf{S}_i\cdot\mathbf{S}_{i+1}) + \sin\theta_i(\mathbf{S}_i\cdot\mathbf{S}_{i+1})^2), \quad (2)$$

we find numerically the ground state of the system for each disorder realization using the density matrix renormalization group (DMRG).

To identify the possible phases of the model, we analyze the ferromagnetic and the dimer order parameters, together with a normalized Edwards-Anderson (EA) order parameter. Our results indicate that the phase diagram consists of three phases: a ferromagnetic phase, a random singlet phase with a nonzero dimer order parameter, and an intermediate phase between the first two phases. This intermediate phase exhibits nonvanishing EA parameter and we argue that it can be identified as a disordered "large-spin" regime [6]. By studying the entanglement entropy between two half chains, we exclude the existence of random singlet ordering in the large-spin phase. A linear scaling with the system size of the ferromagnetic domain walls suggests that the intermediate phase could be a locally disordered ferromagnet containing microscopic magnetized droplets.

References

[1] D. M. Stamper-Kurn and M. Ueda, Rev. Mod. Phys. **85**, 1191 (2013).

[2] A. Imambekov, M. Lukin, and E. Demler, Phys. Rev. A **68**, 063602 (2003).

[3] M. Rizzi, D. Rossini, G. De Chiara, S. Montangero, and R. Fazio, Phys. Rev. Lett. **95**, 240404 (2005).

[4] M. P. A. Fisher, P. B. Weichman, G. Grinstein, and D. S. Fisher, Phys. Rev. B **40**, 546 (1989).

[5] J. K. Freericks and H. Monien, EPL **26**, 545 (1994).

[6] V. L. Quito, J. A. Hoyos, and E. Miranda, Phys. Rev. Lett. **115**, 167201 (2015).

[7] K. D. McAlpine, S. Paganelli, S.Ciuchi, A. Sanpera and G. De Chiara, Phys. Rev. B **95**, 235128 (2017).

Laser cooling of ^{87}Rb to quantum degeneracy

A. Urvoy[1], **Z. Vendeiro**[1], **J. Ramette**[1], **J. Hu**[1], **and V. Vuletić**[1]

[1] *Department of Physics and Research Laboratory of Electronics, Massachusetts Institute of Technology, Cambridge, Massachusetts 02139, USA*

e-mail: *urvoy@mit.edu*

Raman sideband cooling has proven to be a very fast and reliable way of cooling atoms to sub-Doppler temperatures [1]. However, as virtually all methods of optical cooling, it has so far only reached a maximum phase-space density two orders of magnitude below that required for Bose-Einstein condensation [2].

We have recently reached quantum degeneracy with Raman sideband cooling in a 2D optical lattice [3]. The key ingredient is optical pumping light that is far detuned to the red of atomic transition. In particular, we observed just a few favorable red detunings with limited light-induced losses. We also discuss the influence of the one-dimensional geometry of the atomic ensembles on losses and thermalization.

Finally we will present recent developments towards the creation of a large, single Bose-Einstein Condensate, by means of Raman sideband cooling in a 1D lattice and Raman cooling in an optical dipole trap.

[1] A. J. Kerman, V. Vuletić, C. Chin and S. Chu, Phys. Rev. Lett. **84**, 439 (2000).

[2] D.-J. Han, S. Wolf, S. Oliver, C. McCormick, M. T. DePue, and D. S. Weis, Phys. Rev. Lett. **85**, 724 (2000).

[3] J. Hu, A. Urvoy, Z. Vendeiro, V. Crépel, W. Chen, and V. Vuletić, Science **358**, 1078 (2017).

Measurement of interorbital spin-exchange interaction of ytterbium atoms

K. Ono[1], J. Kobayashi[2], Y. Amano[1], K. Sato[1], N. Oda[3] and Y. Takahashi[1]

[1] *Department of Physics, Graduate School of Science, Kyoto University, Kyoto 606-8502, Japan*

[2] *PRESTO, Japan Science and Technology Agency, Kyoto 606-8502, Japan*

[3] *Faculty of Science, Kyoto University, Kyoto 606-8502, Japan*

e-mail: *koukiono3@yagura.scphys.kyoto-u.ac.jp*

Ultracold atomic gases have been successfully used to study quantum many-body systems owing to a high degree of controllability. In particular, alkaline-earth-like atoms have received much attention in recent years as an important experimental platform for unique quantum simulations of strongly correlated fermions. One of remarkable properties of two-electron atoms is the existence of the metastable state $|e\rangle = |^3\mathrm{P}_0\rangle$ as well as the ground state $|g\rangle = |^1\mathrm{S}_0\rangle$. Alkaline-earth atoms in the $^1\mathrm{S}_0$ and $^3\mathrm{P}_0$ states trapped in an optical lattice can be described by two-orbital SU(N) Hubbard Hamiltonian, including the spin-exchange interaction term between $|g\uparrow\rangle$ and $|e\downarrow\rangle$, where the arrows show the arbitrary nuclear spin I [1].

The two-orbital system is a candidate for the quantum simulation of the Kondo effect [2]. One of essential ingredients for the emergence of the Kondo effect is an antiferromagnetic coupling. Scattering properties between the $^1\mathrm{S}_0$ and $^3\mathrm{P}_0$ states in the fermionic isotopes of ^{173}Yb($I = 5/2$) and ^{87}Sr($I = 9/2$) were previously investigated, and the interorbital spin-exchange interactions were found to be ferromagnetic [3, 4]. A tunable spin-exchange interaction of ^{173}Yb using a confinement-induced resonance was successfully demonstrated, with the particle loss from the trap [5].

In this work, we report on the measurement of the interorbital spin-exchange interaction of fermionic isotope of ^{171}Yb($I = 1/2$). We successfully cool the ^{171}Yb atoms down to the temperature around 0.2 T_F by the sympathetic cooling with ^{173}Yb atoms, where T_F represents the Fermi temperature. The clock transition spectroscopy was performed after loading the atoms into a 3D optical lattice with a magic wavelength of 759 nm. A typical result is shown in Fig. 1, in which we successfully measure the resonances from singly occupied sites ($n = 1$) and doubly occupied sites ($n = 2$). A systematic measurement of the resonances at various magnetic fields will enable us to obtain $a_{eg}^{+(-)}$, which is the s-wave scattering length in the nuclear spin-singlet (-triplet) state $|eg^{\pm}\rangle$. These are important parameters to know whether the spin-exchange interaction between the two orbital states is antiferromagnetic or ferromagnetic, and this measurement will pave the way to the quantum simulation of the Kondo effect.

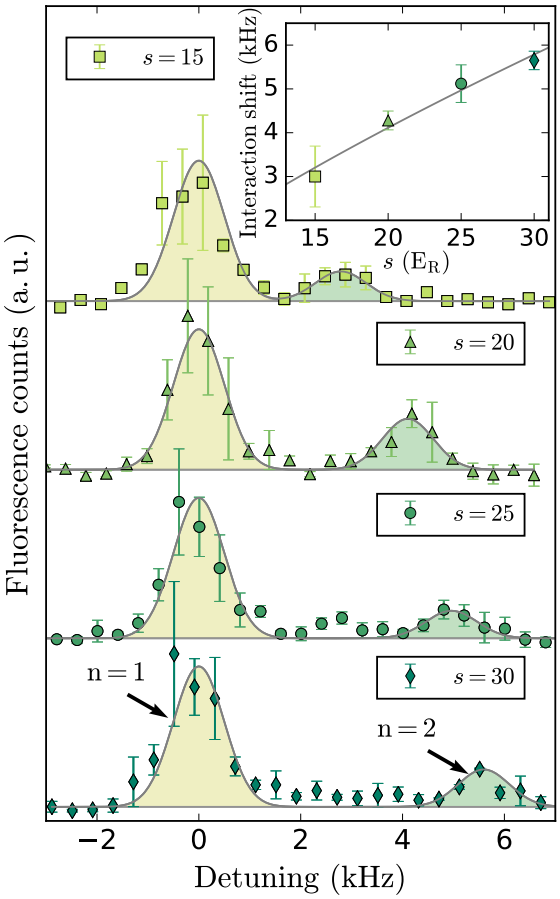


Figure 1: Clock transition spectroscopy in a 3D optical lattice. Error bars show the standard deviation of the mean obtained by averaging three measurement. Inset shows the interaction shift as a function of s, which denotes the lattice depth scaled by the recoil energy $E_R = \hbar^2/2m\lambda_L^2$, λ_L and m being the lattice wavelength and the mass of ^{171}Yb. Error bars are 95 % confidence intervals of resonance position fits.

[1] A. V. Gorshkov *et al.*, Nature Phys. **6**, 289-295 (2010).

[2] M. Foss-Feig *et al.*, Phys. Rev. Lett. **81**, 051603 (2010).

[3] F. Scazza *et al.*, Nature Phys. **10**, 779-784 (2014).

[4] X. Zhang *et al.*, Science **345**, 1467-1473 (2014).

[5] L. Riegger *et al.*, Phys. Rev. Lett. **120**, 143601 (2018).

Shear viscosity of a strongly-interacting Fermi gas

Daichi Kagamihara, Daisuke Inotani, and Yoji Ohashi
Department of Physics, Keio University, 3-14-1 Hiyoshi, Kohoku-ku, Yokohama 223-8522, Japan
e-mail: *dkagamih@rk.phys.keio.ac.jp*

We theoretically investigate the shear viscosity η, as well as the entropy density s, in the BCS-BEC crossover regime of an ultracold Fermi gas, to assess the so-called Kovtun-Son-Starinets(KSS) conjecture about the existence of the lower bound of the ratio η/s[1]. In our theory, we include strong pairing fluctuations within the framework of a self-consistent T-matrix approximation (SCTMA)[2]. We evaluate the shear viscosity η by using the linear response theory, where the self-energy and vertex corrections are treated in a consistent manner within SCTMA[3].

Starting from the BCS weak coupling regime, we find that the shear viscosity η gradually decreases with increasing the interaction strength, as well as with decreasing the temperature, as shown in Fig 1. In the BCS-BEC crossover region, the minimum value of η is obtained at the superfluid phase transition temperature $T_{\rm c}$ when $(k_{\rm F}a_{\rm s})^{-1} \sim 0.4$, which is consistent with the recent experiment on an ultracold ^{6}Li Fermi gas[4].

However, although the ratio η/s also takes a minimum value around $(k_{\rm F}a_s)^{-1} = 0.4$, this minimum is realized is, *not* at $T_{\rm c}$, but slightly above $T_{\rm c}$ ($T/T_{\rm F} \sim 0.25$), as shown in Fig. 2. The minimum value η/s is about 5 times larger than the KSS bound, $\hbar/4\pi k_{\rm B}$.

We will also discuss the importance of an effective interaction between preformed Cooper pairs in considering the shear viscosity, as well as the ratio η/s, especially in the strong-coupling BEC side. Our results would provide useful information about where the ratio η/s becomes the closest to the KSS bound ($= \hbar/4\pi k_{\rm B}$), in the phase diagram of an ultracold Fermi gas in terms of the temperature and the interaction strength.

[1] P. K. Kovtun, D. T. Son, and A. O. Starinets, Phys. Rev. Lett. **94**, 111601 (2005).

[2] R. Haussmann, Z. Phys. B **91**, 291 (1993).

[3] T. Enss, R. Haussmann, and W. Zwerger, Ann. Phys. **326**, 770 (2011).

[4] E. Elliott, J. A. Joseph, and J. E. Thomas, Phys. Rev. Lett. **113**, 020406 (2014).

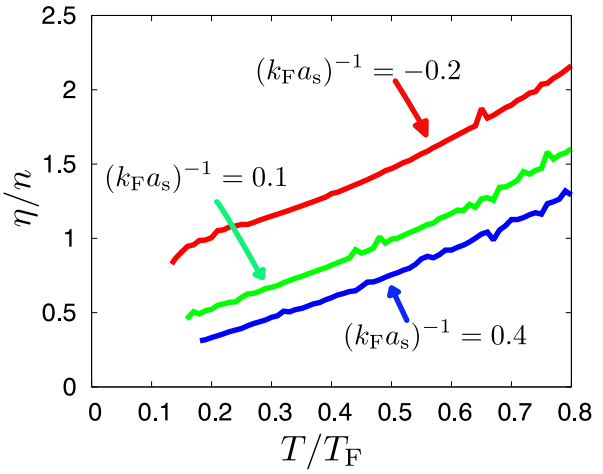


Figure 1: Calculated shear viscosity $\eta(T)$, as a function of the temperature T. The interaction strength is measured in terms of the inverse scattering length $(k_{\rm F}a_s)^{-1}$, normalized by the Fermi wavelength $k_{\rm F}$. $T_{\rm F}$ is the Fermi temperature, and n is the number density of Fermi atoms.

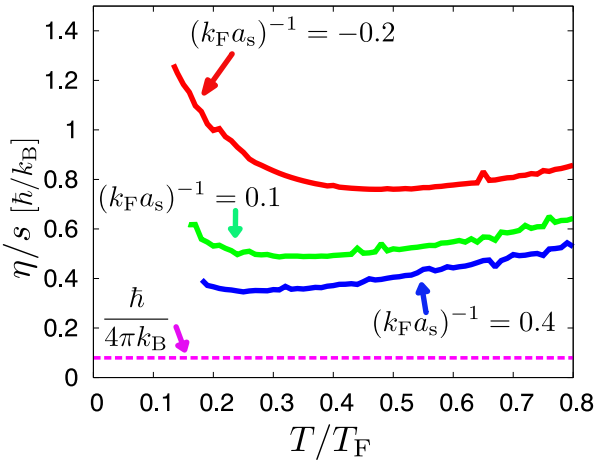


Figure 2: Calculated ratio η/s of the shear viscosity η to the entropy density s, as a function of the temperature T. The KSS bound $\hbar/4\pi k_{\rm B}$ is also shown.

Sound Propagation excited by Density Perturbation in a Bose-Fermi Mixture Superfluid at Finite Temperatures

Yosuke Ono, Rei Hatsuda, Kenta Shiina, Hiroyuki Mori, and Emiko Arahata
Department of physics, Tokyo Metropolitan University, 1-1 Minamiosawa, Hachioji, Tokyo 192-0372, Japan
e-mail: *ono-yosuke@ed.tmu.ac.jp*

A Bose-Fermi mixture superfluid which a cold bosonic and fermionic gas are simultaneous superfluidity has been realized by ENS group in 2014 [1]. This experiment provide us a platform on which we can directly investigate phenomena caused by the coupling between bosons and fermions.

The dynamics of superfluid at finite temperatures is described by Landau's two-fluid hydrodynamics [2] when a system is the local equilibrium. Two-fluid hydrodynamics consist of equations of a superfluid component and a normal-fluid component, and predict two hydrodynamic modes referred to as first-sound and second-sound. In superfluid ^{4}He, first sound is a pressure wave, and second sound is a temperature wave. Therefore, second sound is not excited by density perturbation. However, in a cold atomic Bose or Fermi superfluid gas, second sound can be excited by density perturbation since hybridization of sound modes is expected. These sound modes predicted by two fluid hydrodynamic have been observed [3].

We study sound propagation exited by density perturbation in a Bose-Fermi mixture superfluid in collision-dominated hydrodynamic regime where the system is the local equilibrium. We found that there are three sound modes in a Bose-Fermi mixture superfluid [4], and these amplitudes can be described in term of weight of the density response function obtained from linear response theory. We show the amplitudes of three sound modes as a function of temperature in Fig. 1. We can see three sound modes have appreciable weight in almost all temperatures. This results indicates three sound modes can be excited by density perturbation. Figure 2 shows the amplitudes as a function of interaction between bosons and fermions. Remarkably, the amplitude W_2 is a negative where a Bose-Fermi interaction is repulsive. We will discuss the reason why the amplitude become negative in detail. We shall also discuss how the three sound modes propagate by sudden modification external potential.

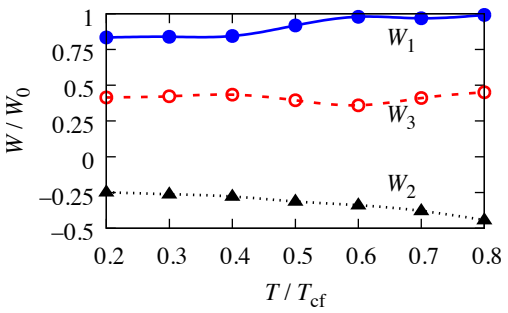


Figure 1: Amplitudes of three sound modes as a function of temperature. T_{cf} is a Fermi superfluid critical temperature, and W_0 is an average of W_1, W_2 and W_3.

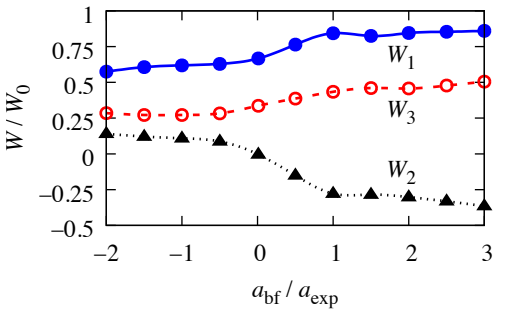


Figure 2: Amplitudes of three sound modes as a function of Bose-Fermi interaction. a_{bf} is a scattering length between bosons and fermions, a_{exp} is a experimental parameter in Ref. [1],

[1] I. Ferrier-Barbut, *et al.*, Science **345**, 1035 (2014).

[2] L. D. Landau, J. Phys. (USSR) **5**, 71 (1941).

[3] J. Joseph, *et al.*, Phys. Rev. Lett. **98**, 170401 (2007). R. Meppelink, S. B. Koller, and P. van der Straten, Phys. Rev. A **80**, 043605 (2009). L. A. Sidorenkov, *et al.*, Nature **498**, 78 (2013).

[4] Y. Ono, R. Sakamoto, H. Mori, and E. Arahata, J. Phys. Soc. Jpn. **85**, 065004 (2016).

Observation of Atom Number Fluctuations in a Bose-Einstein Condensate

M. A. Kristensen[1], M. B. Christensen[1], M. Iglicki[2], K. Pawłowski[2], C. Klempt[3], J. F. Sherson[1], K. Rzażewski[2], A. J. Hilliard[1], J. J. Arlt[1]

[1] *Institut for Fysik og Astronomi, Aarhus Universitet, Ny Munkegade 120, 8000 Aarhus C, Denmark*
[2] *Center for Theoretical Physics, Polish Academy of Sciences, Al. Lotników 32/46, 02-668 Warsaw, Poland*
[3] *Institut für Quantenoptik, Leibniz Universität Hannover, Welfengarten 1, 30167 Hannover, Germany*
e-mail: *arlt@phys.au.dk*

Particle number fluctuations play a central role in our understanding of the statistical properties of bosonic systesms. While the fluctuations are well understood for many quantum systems at zero temperature, the case of an interacting quantum system at finite temperature still poses numerous experimental and theoretical challenges. Despite the intense investigation of Bose-Einstein condensates (BECs), the fluctuations between the BEC and the thermal component have therefore not been investigated. Here we report the observation of these fluctuations. Our experiments are based on stabilization technique which allows for the preparation of ultracold thermal clouds at the shot noise limit, eliminating numerous technical noise sources. Moreover we utilize the correlations established by the evaporative cooling process to determine the fluctuations and the sample temperature precisely. Thus the telltale signature of these fluctuations, a sudden increase close to the critical temperature, was observed. We compare our result with theoretical predictions for the ideal gas and find good agreement.

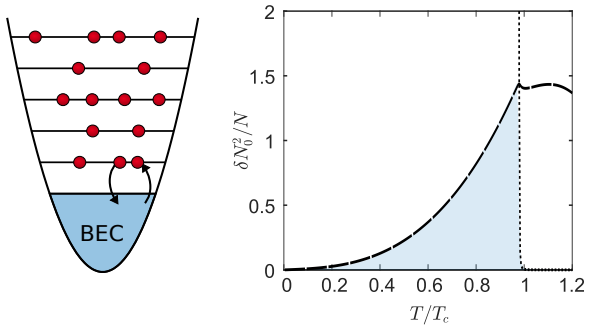


Figure 1: Left: Redistribution of excitations leads to thermal fluctuations of the BEC atom number. Right: Fluctuations calculated based on the grand canonical ensemble (dotted line) are unphysical large below the critical temperature. Here a better estimate is obtained by an alternate approach, where the condensate is treated as a reservoir for thermal excitations. The shaded area indicates the fluctuations obtained by an exact canonical calculations.

Isothermal Compresibility and Strong Coupling Effects in an Ultracold Fermi Gas

R. Sato, D. Kagamihara, K. Manabe, D. Inotani, and Y. Ohashi
Department of Physics, Keio University, 3-4-1 Hiyoshi, Kohoku-ku, Yokohama 223-8522, Japan
e-mail: *r.s.08030803@gmail.com*

We theoretically investigate strong-coupling corrections to the isothermal compressibility $\kappa(T)$ in the normal state of an ultracold Fermi gas. While $\kappa(T)$ is a fundamental thermodynamic quantity, it is known to *unphysically* diverge at the superfluid phase transition temperature $T_{\rm c}$, when it is treated within the non-self-consistent T-matrix approximation[1], because of the ignorance of an effective interaction between preformed Cooper-pairs. To overcome this theoretical difficulty, we deal with strong pairing fluctuations in the BCS-BEC crossover region within the framework of the self-consistent T-matrix approximation (SCTMA)[2] in which a molecular interaction is taken into account in the normal state[3]. We then evaluate $\kappa(T)$ consistently in the sense that the vertex corrections to $\kappa(T)$ are included within the same approximation level as the SCTMA self-energy in the single-particle Green's function.

As expected, the calculated compressibility no longer diverges at $T_{\rm c}$, as shown in Fig. 1. In the BEC regime (panel (a)), where the system properties are dominated by tightly bound molecules, $\kappa(T)$ is found to be well described by the compressibility in a repulsively interacting molecular Bose gas with the molecular scattering length $a_{\rm M} = 2a_s$[2], where a_s is the s-wave scattering length for a Fermi-Fermi attractive interaction. In the weak-coupling BCS regime (panel (c)), $\kappa(T)$ is reduced to that in a free Fermi gas. In the unitarity limit, our result quantitative agrees well with the recent experiment on a ^{6}Li Fermi gas[4].

Since the compressibility is sensitive to the interaction between preformed pairs, our results would be useful for the study of such a molecular interaction in a strongly interacting Fermi gas.

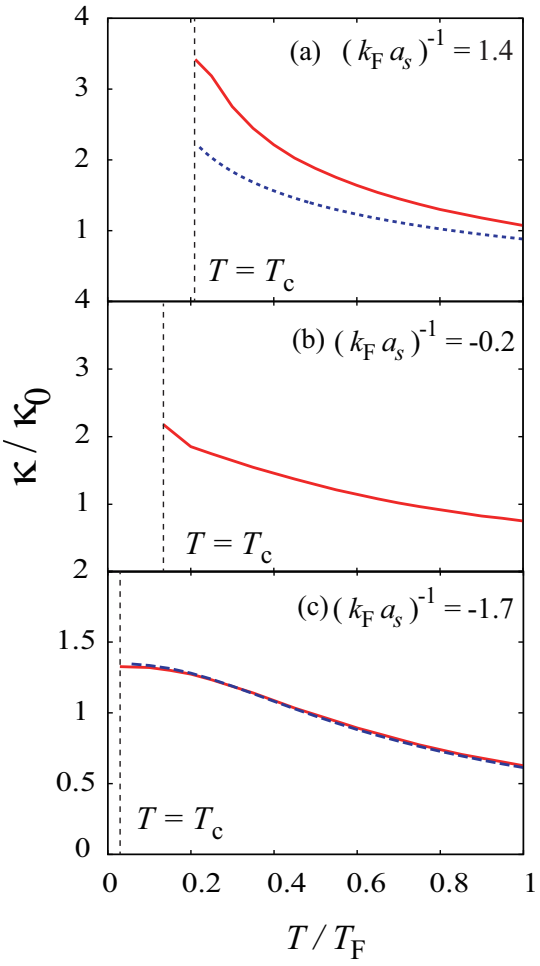


Figure 1: Calculated isothermal compressibility $\kappa(T)$ (solid line). (a) Strong-coupling BEC regime. The dotted line shows the results for a repulsively interacting molecular Bose gas with the Bose scattering length $a_{\rm M} = 2a_s$, where a_s is the s-wave scattering length for an attractive interaction between Fermi atoms. (b) Unitarity regime. (c) Weak-coupling BCS regime. The dashed line shows the result in a free Fermi gas, where the Fermi chemical potential is determined in SCTMA. The vertical dashed line shows $T_{\rm C}$. κ_0 is the isothermal compressibility in a free Fermi gas at $T = 0$, $T_{\rm F}$ is the Fermi temperature, and $k_{\rm F}$ is the Fermi momentum.

[1] A. Perali, P. Pieri, G. C. Strinati, and C. Castellani, Phys. Rev. B **66**, 024510 (2002).

[2] R. Hausmann, Z. Phys. B. **91**, 291 (1993).

[3] P. Pieri and G. C. Strinati, Phys. Rev. B **61**, 15370 (2000).

[4] M. J. H. Ku, A. T. Sommer, L. W. Cheuk, and M. W. Zwierlein, Science **335**, 563 (2012).

Photoemission Spectrum in an Ultracold Bose-Fermi Mixture with a Hetero-Pairing Interaction

Koki Manabe, Daichi Kagamihara, Daisuke Inotani, and Yoji Ohashi
Department of Physics, Keio University, 3-14-1Hiyoshi,Kohoku-ku,Yokohama 223-8522, Japan
e-mail: *k.manabe.rikou@keio.jp*

We theoretically investigate single-particle properties of a mass-imbalanced Bose-Fermi mixture with a hetero-nuclear Feshbach resonance. This work is an extension of some of the authors' previous work[1] for the mass-balanced case, to include realistic mass difference between the two species. Including strong Bose-Fermi hetero-pairing fluctuations induced by a tunable pairing interaction associated with a Feshbach resonance within the framework of the improved T-matrix approximation[1], we clarify strong-coupling corrections to single-particle spectral weight (SW) in existing ^{23}Na-^{40}K and ^{87}Rb-^{40}K gas mixtures. We also examine how these strong-coupling effects can be observed by the photoemission-type experiment[2].

In the mass-balanced case shown in Fig.1(a1), SW exhibits (A) a sharp upward peak along the single-particle Fermi atomic dispersion, (B) a broad downward peak in the negative energy region, and (C) a sharp peak along the dispersion of a composite Fermi molecule composed of a Bose and Fermi atoms. While this character succeeds to the mass-imbalanced case shown in Figs. 1(a2) and (a3), effects of mass difference on the detailed spectral structure differently appear, depending on which component is heavier. That is, in a ^{23}Na-^{40}K mixture ($m_{\rm B} < m_{\rm F}$, where $m_{\rm B}$ ($m_{\rm F}$) is a mass of Bose (Fermi) atom), the molecular branch (C) is pronounced, compared to the downward broad peak (B) (see panel (a2)). In the case of a ^{87}Rb-^{40}K mixture ($m_{\rm B} > m_{\rm F}$), the opposite tendency is obtained, as shown in panel (a3).

We point out that the three-peak structure of the single-particle spectral weight (SW), as well as the above-mentioned effects of mass imbalance on SW, remain to be observed in the photoemission spectrum (PES), as shown in the right panels in Fig. 1. Since such a spectral structure is not observed in strongly interacting Fermi-Fermi mixtures (^{40}K-^{40}K mixture and ^{6}Li-^{6}Li mixture), our results would be useful in understanding how the quantum statistics of atoms (fermion or boson) affects strong-coupling properties of a two-component gas mixture.

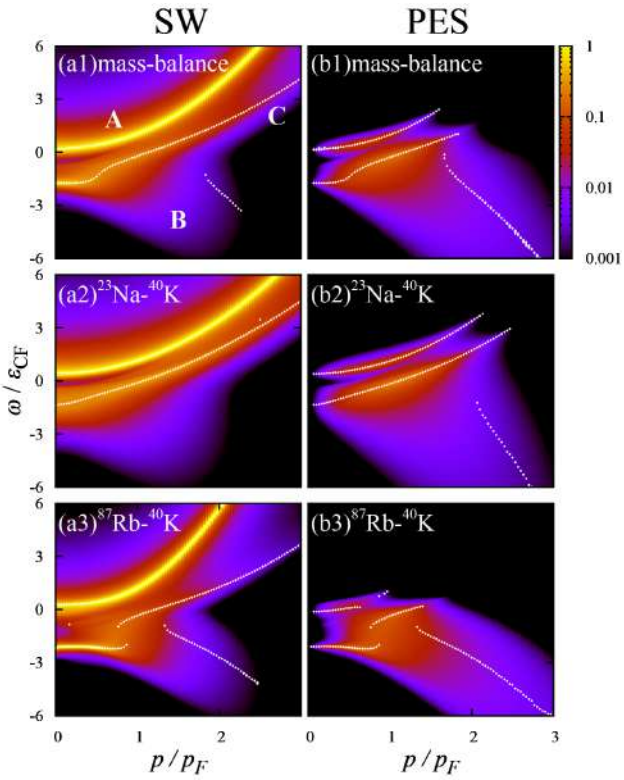


Figure 1: Calculated intensity of (a1)-(a3) Fermi single-particle spectral weight (SW), and (b1)-(b3) the corresponding photoemission spectrum (PES), in the unitary regime ($(k_{\rm F}a_{\rm BF})^{-1} = 0.2$) of a Bose-Fermi mixture at the Bose-Einstein condensation temperature $T_{\rm BEC}$. (a1) and (b1): mass-balanced case. (a2) and (b2): ^{23}Na-^{40}K mixture. (a3) and (b3): ^{87}Rb-^{40}K mixture. $a_{\rm BF}$ is an s-wave scattering length for an inter-species interaction, and $k_{\rm F}$ is the atomic Fermi wavelength. $\varepsilon_{\rm CF}$ is the Fermi energy of composite Fermi molecules consisting of a Bose and a Fermi atom. In each panel, white dotted lines show peak positions of the spectral intensity.

[1] D. Kharga, D. Inotani, R. Hanai, and Y. Ohashi, J. Phys. Soc. Jpn. **86**, 084301 (2017).

[2] Y. Sagi, T. E. Drake, R. Paudel, R. Chapurin, and D. S. Jin, Phys. Rev. Lett. **114**, 075301 (2015).

Phase-separated state in a repulsive Bose-Fermi mixture: Interface structure and breathing mode

B. Huang[1], **R. S. Lous**[1,2], **I. Fritsche**[1,2], **F. Lehmann**[1,2], **M. Jag**[1,2], **E. Kirilov**[2], **J. T. W. Walraven**[1], **and R. Grimm**[1,2]

[1] *Institut für Quantenoptik und Quanteninformation (IQOQI), Österreichische Akademie der Wissenschaffen, 6020 Innsbruck, Austria*

[2] *Institut für Experimentalphysik, Universität Innsbruck, 6020 Innsbruck, Austria*

e-mail: *bo.huang@uibk.ac.at*

We produce a degenerate Bose-Fermi mixture with a ^{41}K BEC immersed in a large single-component degenerate Fermi gas of ^{6}Li. Both elements are trapped in an elongated optical dipole trap while the interspecies contact interaction is manipulated by a magnetic Feshbach resonance between the lowest spin state of both elements near 335 G. When the interspecies repulsive interaction increases, the two components start to repel each other, i.e. the BEC density is enhanced while the fermions are depleted at the trap center, and finally become spatially separated when the interaction is su ciently strong.

We probe the interface between the small BEC residing in the large Fermi Sea [1]. We quantify the residual spatial overlap between the two components by measuring three-body recombination losses for variable strength of the interspecies repulsion. A comparison with a numerical mean-field model highlights the importance of the kinetic energy term for the condensed bosons in maintaining the thin interface far in the phase-separated regime. Our results demonstrate a corresponding smoothing of the phase transition in a system of finite size.

Across this transition to a phase-separated state, we also measure the frequencies of BEC collective oscillations and observe a striking change of the frequency of the radial breathing mode. We construct several mean-field models beyond the Thomas-Fermi approximation with different treatments for the fermions. The comparison between the models and the observations suggests an adiabatic behaviour of the Fermi sea when the components are miscible, and the adiabaticity of the fermion cloud remains approximately valid in the phase-separated regime.

[1] R. Lous, I. Fritsche, M. Jag, F. Lehman, E. Kirilov, B. Huang, and R. Grimm, arXiv:1802.01954 (2018)

An experiment for the study of small Hubbard models with rapid repetition rate

M. Schlederer[1], **P. Wieburg**[1], **A. Mozdzen**[1], **T. Lompe**[1], **and H. Moritz**[1]
[1] *Institute for Laser Physics, University of Hamburg, Luruper Chaussee 149, 22761 Hamburg, Germany*
e-mail: *mschlede@physnet.uni-hamburg.de*

We present an experiment to study small scale Fermi-Hubbard systems using optical microtraps. This bottom-up approach shall provide us with a better understanding of the basic processes governing the Fermi-Hubbard model. We present the experimental progress including grey molasses cooling and loading into a two-dimensional optical lattice as well as into optical tweezers.

The development of quantum gas microscopes has enabled the study of ultracold atoms in optical lattices with single site, single atom resolution. In these experiments, the gases are typically cooled evaporatively and loaded into a large optical lattice formed by interfering laser beams. Here, we will report on the present status of an experimental setup designed to follow a complementary approach [1] where small Fermi-Hubbard type systems are assembled site by site using optical microtraps.

We have lasercooled K40 atoms to sub-Doppler temperatures using magneto-optical trapping and grey molasses cooling. After magnetic transport to the science region the atoms are loaded into optical lattices and subsequently into optical tweezers. Both in the lattice and in the tweezers, we perform further Raman-sideband cooling. The fluorescence light emitted during this process serves to image the atoms. Our setup features two high NA in-vacuo microscopes which will be used to create small scale structures such as 2x2 site plaquettes and to image the atoms. The technique combines fast experimental cycle times with single site addressability and detection and will allow to study the fundamental processes governing the Fermi-Hubbard model in a bottom-up approach.

[1] A.M. Kaufman et al., Physical Review X **2**, 041014 (2012).

Temperature-dependent break-down of disorder-induced localization for interacting fermions coupled to a thermal bath

Ling-Na Wu[1], **Alexander Schnell**[1], **Giuseppe De Tomasi**[1], **Markus Heyl**[1], **and André Eckardt**[1]
[1] *Max Planck Institute for the Physics of Complex Systems, D-01187 Dresden, Germany*
e-mail: *lnwu@pks.mpg.de*

We study the temperature dependent transport of interacting fermions through a disordered tight-binding chain in the presence of a thermal bath of temperature T. This model describes electronic systems coupled to phonons and can also be realized with ultracold fermionic atoms immersed in a Bose gas. By employing two different methods, quantum-jump Monte-Carlo simulations and mean-field theory, we find different regimes with respect to temperature. For low temperatures, we encounter a (many-body) localized regime, where the transport is temperature-independent and decreases exponentially with the system size. Above a system-size dependent threshold temperature, a bath-assisted temperature-dependent conductivty σ is found. It is described by Mott's law for variable-range hopping, $\sigma \sim \exp(-\sqrt{T_0/T})$. Weak repulsive (attractive) interactions are found to enhance (lower) T_0.

Collisional Properties of Ultracold Potassium in the Vicinity of a D-Wave Feshbach Resonance

Markus Bohlen[1], **Thomas Reimann**[1], **Cédric Enesa**[1], **Julian Struck**[1], **Tarik Yefsah**[1], **Christophe Salomon**[1] **and Frédéric Chevy**[1]

[1] *Laboratoire Kastler Brossel, ENS-Université PSL, CNRS, Sorbonne Université, Collège de France, 24 rue Lhomond, 75005 Paris, France*

e-mail: *markus.bohlen@lkb.ens.fr*

The large impact of ultracold atoms on modern physics is founded in the great versatility they offer to explore new quantum phenomena. Most notably, Feshbach resonances represent a formidable tool in order to smoothly tune the scattering length and with it the interactions between atoms (Figure 1). Originally conceived in the context of nuclear physics by Herman Feshbach [1], it has, since then, found numerous other applications in several fields, including atomic and molecular physics as well as condensed matter physics. In particular, high partial wave Feshbach resonances ($l > 1$) have been predicted to give access to complex order parameters and quantum phase transitions, as Cooper pairs with p- or d-wave symmetry arise in p-wave superfluids like ^{4}He or d-wave high-T_C superconductors respectively [2, 3]. Here, we report on our progress on studying the temperature dependent collisional properties of a Fermi gas of ^{40}K in the vicinity of a new d-wave Feshbach resonance. To this end, we first characterize the nature of the two-body losses before analyzing the dynamical evolution of the spin composition while reaching thermal equilibrium.

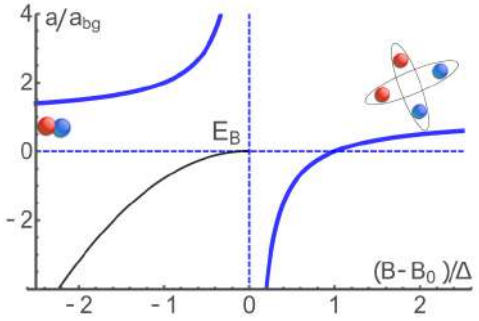


Figure 1: Scattering length across a Feshbach resonance for Fermions.

[1] H. Feshbach, Ann. Phys. **5**, 357 (1958)

[2] D.M. Lee, Rev. Mod. Phys.**69**, 645 (1997)

[3] C.C. Tsuei and J. R. Kirtley, Phys. Rev. Lett. **85**, 182 (2000)

Long-range interactions and symmetry-breaking in quantum gases through optical feedback

Yong-Chang Zhang[1], **Valentin Walther**[1], **and Thomas Pohl**[1]

[1] *Department of Physics and Astronomy, Aarhus University, Ny Munkegade 120, 8000 Aarhus C, Denmark*
e-mail: *yczhang@phys.au.dk*

A lot of recent attention has been focused on long-range interaction in dipolar atoms and in cavity-assisted systems. Yet, it is an open challenge to engineer long-range interaction between atoms without large dipole moment in free space. Here, we propose to generate an exotic type of long-range interaction between ultracold atoms using a simple single-mirror optical feedback setup [1]. We show that this effective interaction gives rise to a rich spectrum of ground states (see Fig. 2). In particular, we find that it can cause the spontaneous contraction of the quasi two-dimensional condensate to form a self-bound one-dimensional chain of mesoscopic quantum droplets.

As shown in Fig. 1(a), a quasi-2D BEC is illuminated by a laser light that is back-reflected by a mirror and thereby generates optical feedback in the degenerate atom cloud. The light scattering generates an effective atomic interaction [see Fig. 1(b)]. Interestingly, in the large distance limit ($d \to \infty$), this potential takes the form

$$U(\mathbf{r}) = -\cos(r^2/4), \tag{1}$$

which oscillates with a growing frequency.

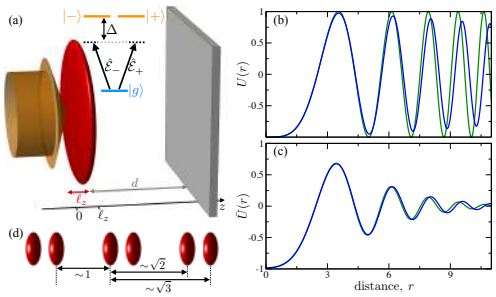


Figure 1: (a) Schematic illustration of the considered setup. (b) Effective long-range potential induced by the feedback. The blue and green line depict the potential for $kd = 20$ and in the limit $kd \to \infty$, respectively, where k is the wavenumber of the optical field. Panel (c) shows the average interaction between two Gaussian clouds separated by a distance r. The peculiar form of the interaction can stabilize a 1D lattice of quantum droplets that is illustrated in panel (d).

Within the mean-field theory, we explore the ground states triggered by this unusual interaction using the following Gross-Pitaevskii equation

$$i\frac{\partial}{\partial t}\psi(\mathbf{r}) = -\frac{1}{2}\nabla_\perp^2\psi(\mathbf{r}) + g|\psi(\mathbf{r})|^2\psi(\mathbf{r}) + 2\alpha\beta\int |\psi(\mathbf{r}')|^2 U(\mathbf{r}-\mathbf{r}')\mathrm{d}^2\mathbf{r}'\psi(\mathbf{r}), \tag{2}$$

where g and $\alpha\beta$ are the strengths of the contact interaction and the effective long-range interaction. More details can be found in [1]. As exhibited in Fig.2(a), we find different ground states, from an infinitely extended flat BEC for strong contact interactions to a single localized quantum droplet [Fig.2(e)] for dominating non-local interactions, $U(\mathbf{r})$. In between these limiting cases, there exist two-dimensional regular structures as shown in Fig.2(g), and one-dimensional droplet chains as depicted in Fig.2(f).

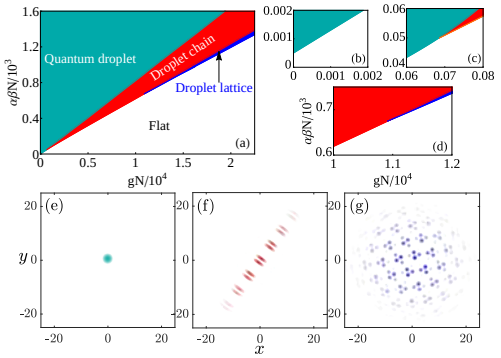


Figure 2: Ground state phase diagram of the driven BEC, determined by the competition between the contact and long-range interaction, respectively. Panels (b-d) zoom in the phase diagram around the critical points. Panels (e-g) illustrate the different solutions and depict the density profile of the (e) single-droplet state, (f) droplet chain state, and (g) droplet lattice state.

We have also studied the real dynamics of the system using relevant parameters within the reach of current experimental capabilities, which shows that all of our predictions are experimentally feasible.

[1] Y.-C. Zhang, V. Walther, and T. Pohl, arXiv:1805.03422 (2018).

Dynamical control of phases in a Driven-Dissipative Bose-Einstein Condensate in an Optical Cavity

Jayson G. Cosme[1,2], **Christoph Georges**[1], **Andreas Hemmerich**[1,2], **and Ludwig Mathey**[1,2]

[1] *Zentrum für Optische Quantentechnologien and Institut für Laserphysik, Universität Hamburg, 22761 Hamburg, Germany*

[2] *The Hamburg Centre for Ultrafast Imaging, Luruper Chaussee 149, 22761 Hamburg, Germany*

e-mail: *cosme.jayson@physik.uni-hamburg.de*

One intriguing phenomenon in nature is the rich interplay between coexisting phases or competing orders in various complex systems. To gain insights to possible fundamental nature of such interplay, we consider a system consisting of a driven Bose-Einstein condensate inside a high-finesse optical cavity. This system exhibits a well-known phase transition from a spatially homogeneous condensed (BEC) phase to a self-organized superradiant phase reminiscent of a charge density wave (CDW) order as the strength of the transverse pump beam is increased [1, 2]. By modulating the pump beam strength, we demonstrate dynamical control of this phase transition. In particular, we show that periodic driving of the pump beam suppresses density order, and that condensate formation is restored, in analogy to emergence of superconductivity due to suppression of density order. We perform a high-frequency expansion of the Hamiltonian to show that the enhancement can be explained by a reduction in the atom-cavity coupling parameter after a modulation of the pump field. This kind of pump field modulation can be realized by simply adding laser beams which are detuned from the pump beam as depicted in Fig. 1. Furthermore, we show that new dynamical phases with higher CDW order may arise by finely tuning the driving frequency to resonantly match the frequencies of relevant atomic momentum states. Finally, we observe the emergence of chaotic dynamics for strong driving.

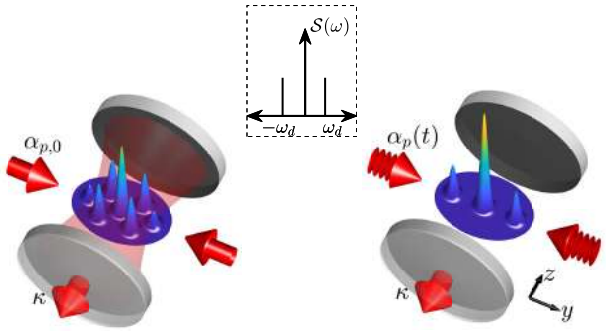


Figure 1: (Left) For constant transverse pump strength $\alpha_{p,0}$, the system is in a CDW phase characterized by occupation of the cavity mode and the higher momentum states. (Right) By modulating the pump strength $\alpha_p(t)$, the CDW phase is suppressed and the BEC is restored as signaled the by increase in the central peak density and the absence of cavity mode population. For the driven case, the intensity of the pump beam $|\alpha_p(t)|^2$ is effectively modulated due to the additional frequency sidebands $\pm\omega_d$ as shown in the power spectrum $\mathcal{S}(\omega)$.

[1] K. Baumann, C. Guerlin, F. Brennecke, and T. Esslinger, Nature 464, 1301 (2010).

[2] J. Klinder, H. Keler, M. Wolke, L. Mathey, and A. Hemmerich, Proc. Natl. Acad. Sci. USA 112, 3290 (2015).

2D and 3D Grating Magneto-Optical Traps as Cold Atom Sources

O. Burrow[1], **A. Arnold**[1], **E Riis**[1] **and P. Griffin**[1]
[1] *Department of Physics, University of Strathclyde, Glasgow G4 0NG, United Kingdom*
e-mail: *oliver.burrow@strath.ac.uk*

Making the core technologies of magneto-optical trapping more compact and robust is a crucial step for enabling portable cold atom quantum sensors. The grating magneto-optical trap (MOT) simplifies the optical requirements to a single beam and diffraction grating element per MOT [1]. The planar nature of the grating MOT allows for optimal optical access and atom temperatures of 3 μK are achieved [2]. In this work a double-chambered 2D to 3D grating MOT system is demonstrated (figure 1) with a loading rate of 10^8 per second ^{87}Rb atoms. This system is assembled around a double-chambered glass experimental cell only 200 mm in length and will be used as a starting point for rapid formation of Bose-Einstein condensates.

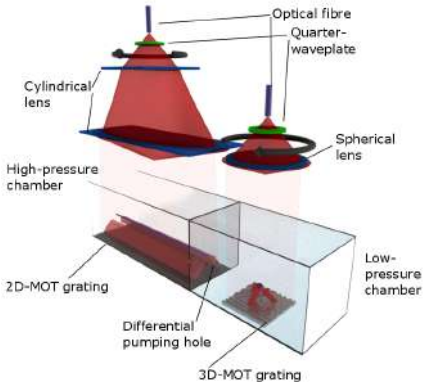


Figure 1: **2D and 3D grating MOT concept.** The system is based around a partitioned double-chambered cell. The left chamber is at higher pressure and contains the 2D grating MOT. Cold atoms flow through the differential pumping hole to the right hand chamber, which is maintained at ultra-high vacuum and a 3D grating MOT is formed. Each MOT has a circularly polarised beam, collimated from a fibre; the 2D- MOT beam is elliptical and illuminates a planar grating, whilst the 3D-MOT is a circular beam illuminating a 'TRI' design grating.

[1] C. C. Nshii, M. Vangeleyn, J. P. Cotter, P. F. Gri n, E. A. Hinds, C. N. Ironside, P. See, A. G. Sinclair, E. Riis and A. S. Arnold, Nature Nanotechnology **8**, 321 (2013)

[2] J. McGilligan, P. Gri n, R. Elvin, S. Ingleby, E Riis and A. Arnold, Scientific Reports **7**, 384 (2017)

Doppler-sensitive holographic Microscopy of cold atoms

Yuzhuo Wang, Jian Zhao, Yizun He, Liyang Qiu and Saijun Wu
Department of Physics, State Key Laboratory of Surface Physics and Key Laboratory of Micro and Nano Photonic Structures (Ministry of Education), Fudan University, Shanghai 200433, China
e-mail: *saijunwu@fudan.edu.cn*

Abstract

Developments of cold atom based quantum sensors [1] and many-body simulators [2] rely on e cient imaging methods for atomic state preparation and detections. In contrast to the widely used absorption and fluorescence imaging methods, holographic imaging method [3] has the unique advantage of being able to resolve both the amplitude and the phase of the scattered probe light, allowing quantitatively sensing the complex optical response of atoms due to certain perturbations. In this work, we demonstrate sensing Doppler effect on D2 transition of ^{39}K atoms with holographic microscopy. By reconstructing elastically scattered light from moving atoms, we are able to resolve velocity for laser-accelerated atomic sample at $\delta v \sim 0.15$ m/s along the probe direction while maintaining $\delta x \sim 2$ μm transverse spatial resolution at the same time. The method may be combined in EIT configuration with substantially improved velocity resolution for output state detection in atom interferometer.

[1] T. Kovachy, P. Asenbaum, et al. , Nature, 528(7583): 530 (2015).
R. H. Parker, C. Yu, et al. Science, 360(6385): 191-195 (2018).

[2] M. F. Parsons, A. Mazurenko, et al. Science,353(6305): 1253-1256 (2016).
L. Riegger, N. D. Oppong, Phys. Rev. Lett, 120(14): 143601 (2018).
S. Kuhr, Quantum-gas microscopes: Nat. Sci. Rev. 3(2): 170-172 (2016).

[3] L. Turner, K. Domen, R. Scholten, Phys. Rev. A 72(3): 031403 (2005).
J. P. Sobol, and S. Wu, New J. Phys, 16(9): 093064(2014).

Superfluid weight and Berezinskii-Kosterlitz-Thouless temperature of spin-imbalanced and spin-orbit-coupled Fulde-Ferrell phases in lattice systems

A. Julku[1], **L. Liang**[1], **and P. Törmä**[1]
[1] *Department of Applied Physics, Aalto University School of Science, FI-00076 Aalto, Finland*
e-mail: *aleksi.julku@aalto.fi*

The Fulde-Ferrell (FF) superfluid states, identified by finite center-of-mass Cooper pair momenta, have gained widespread interest in the context of ultracold gases. Initially proposed accessible via the population imbalance of two pairing Fermion species [1], FF phases have been recently predicted to exist also by applying spin-orbit coupling (SOC) and Zeeman fields [2, 3]. Furthermore, it has been argued that SOC-induced FF states could support topologically non-trivial phases and existence of Majorana fermions both in continuum and in lattice systems [2, 3, 4]. Such topological FF states are conceptually new superconductive phases of matter.

Despite theoretical studies supporting the existence of FF phases, the experimental realization of such exotic superfluid states has been problematic due to a need of low dimensional systems which are required to reach FF phases [1]. In particular in 2D systems, phase transitions to superfluid states is defined by the Berezinskii-Kosterlitz-Thouless (BKT) transition temperature, T_{BKT}, which usually is extremely low. For a superconducting system the BKT temperature in turn depends on the superfluid weight D^s which is responsible for the dissipationless electric current and the Meissner effect - the fundamental properties of superconductors [5].

In our work [6] we study D^s and T_{BKT} in case of FF states in 2D lattice systems. We consider spin-imbalanced systems with and without SOC accompanied with Zeeman fields. In earlier studies FF phases have been predicted to exist in lattice geometries but the stability of these states against thermal phase flucutations has not been investigated before. By applying mean-field theory, we derive general equations for D^s and T_{BKT} in the presence of SOC and the Zeeman fields for 2D Fermi-Hubbard lattice models, and apply our results to a 2D square lattice. We show that conventional spin-imbalanced FF states without SOC can be observed at finite temperatures and that FF phases are further stabilized against thermal fluctuations by introducing SOC, see Fig. 1. We also propose how topologically non-trivial SOC-induced FF phases could be identified experimentally by studying the total density profiles. Furthermore, the relative behavior of transverse and longitudinal superfluid weight components and the role of the geometric superfluid contribution are discussed.

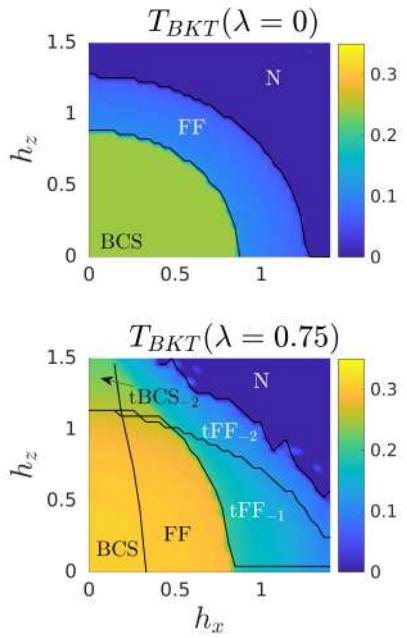


Figure 1: BKT temperature T_{BKT} as a function of the in-plane Zeeman and out-of-plane Zeeman fields, h_x and h_z, for zero SOC $\lambda = 0$ (upper panel) and for finite SOC $\lambda = 0.75$ (lower panel). By applying SOC, T_{BKT} of FF states can be increased and topologically non-trivial phases (indicated by tFF$_x$ or tBCS$_x$ where x is the Chern number) reached.

[1] J. J. Kinnunen, J. E. Baarsma, J.-P. Martikainen and P. Törmä, Rep. Prog. Phys. **81**, 046401 (2018)

[2] C. Qu, Z. Zheng, M. Gong, Y. Xu, L. Mao, X. Zou, G. Guo and Chuanwei Zhang, Nat. Commun. **4**, 2710 (2013)

[3] W. Zhang and W. Yi, Nat. Commun. **4**, 2711 (2013)

[4] L.-F. Guo, P. Li, and S. Yi, Phys. Rev. A **95**, 063610 (2017)

[5] A. Julku, S. Peotta, T. I. Vanhala, D.-H. Kim, and Päivi Törmä, Phys. Rev. Lett. **117**, 045303 (2016)

[6] A. Julku, L. Liang, P. Törmä, arXiv:1804.11063 (2018)

Out-of-time-ordered correlator of quenched state in many-body localization

J. Lee[1] **and D.-H. Kim**[1]

[1] *Department of Physics and Photon Science, Gwangju Institute of Science and Technology, 61005 Gwangju, Republic of Korea*

e-mail: *dongheekim@gist.ac.kr*

We study an out-of-time-ordered correlator (OTOC) of a pure state in many-body localization (MBL). Recent researches related to the OTOC in MBL are focused on the thermal ensemble in high temperature [1, 2, 3, 4]. We compare the OTOC of the pure state with the thermal ensemble average to find the typical states that describe thermal ensemble well. Here, We consider pure states in quenched states which are randomly sampled under a certain constraint.

We define the OTOC of a pure state given by

$$F(t) = \langle\psi|W(t)VW(t)V|\psi\rangle \tag{1}$$

where $|\psi\rangle$ is a quenched state and $W(t)$, V are local operators. The quenched state is prepared in a product of randomly oriented spin states whose size of projection onto z-axis is fixed to v. We make sets of quenched states with the same value of v.

The local operator, $W(t) = e^{iHt}We^{-iHt}$, is evolved under the Hamiltonian H, which describes an XXZ spin chain with random on-site fields. The random field strength is within the fixed range defined by disorder strength parameter. We set strong disorder strength to induce the many-body localization on the system.

We compare the OTOC of the quenched state to the thermal ensemble average of OTOC in Fig. 1. While we follow the average scheme presented in [3], we average the result over the quenched states within the set instead of average over the thermal ensemble. We find that the OTOC of the set of $v = 0$ well agrees to the thermal ensemble average in the localized system. As v increases, the average within the corresponding set slightly deviates from the thermal ensemble result. The set of $v = 1$ shows a significant difference to the thermal ensemble.

We discuss that the result of the OTOC also appears in an inverse participation ratio (IPR) of the quenched state over eigenstates of the Hamiltonian. In Fig. 2, we observe that the states of the smaller v are more likely to have the lower IPR. The lower IPR indicates more even superposition of the eigenstates. A state of low IPR has an expectation value of an operator close to the thermal ensemble average of the operator, which is consistent with the result of the OTOC in Fig. 1.

We have confirmed that the thermal ensemble average of the OTOC is well represented by the random product states composed with spins in the XY-plane. We suggest possible applications for experimental measurement of OTOC in a trapped ion system.

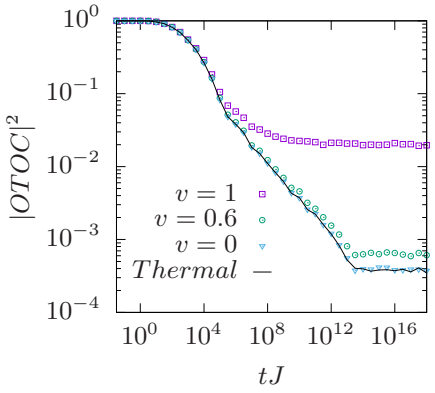


Figure 1: Time evolution of OTOC in many-body localized system with system size $L = 12$. 1000 disorders are realized and 30 states are prepared.

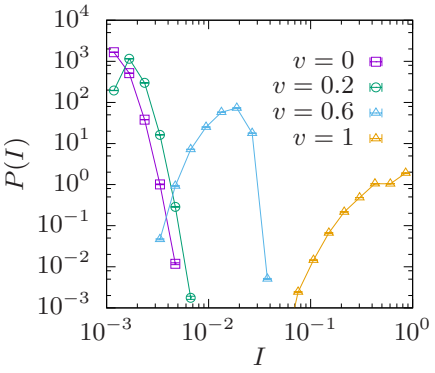


Figure 2: Probability distribution of inverse participation ratio across disorder realizations with system size $L = 10$. 10000 disorders are realized and 100 states are prepared.

[1] Y. Huang, Y.-L. Zhang, and X. Chen, Annalen der Physik **529**, 1600318 (2016).

[2] R. Fan, P. Zhang, H. Shen, and H. Zhai, Science Bulletin **62** (10), 707-711 (2017).

[3] X. Chen, T. Zhou, D. A. Huse, and E. Fradkin, Annalen der Physik **529**, 1600332 (2016).

[4] R.-Q. He and Z.-Y. Lu, Phys. Rev. B **95**, 054201 (2017).

Collisionless sound in a uniform Bose gas

Miki Ota[1], Fabrizio Larcher[1,2], Franco Dalfovo[1], Lev Pitaevskii[1,3], Nikolaos P. Proukakis[2], and Sandro Stringari[1]

[1] *INO-CNR BEC Center and Dipartimento di Fisica, Università di Trento, 38123 Trento, Italy*

[2] *Joint Quantum Centre Durham–Newcastle, School of Mathematics and Statistics, Newcastle University, Newcastle upon Tyne, NE1 7RU, United Kingdom*

[3] *Kapitza Institute for Physical Problems RAS, Kosygina 2, 119334 Moscow, Russia*

e-mail: *miki.ota@unitn.it*

Using linear response theory within the Random Phase Approximation (RPA), we investigate the propagation of sound in a uniform Bose gas in the collisionless regime, both in two-dimensional (2D) [1] and three-dimensional (3D) configurations. Recently, propagation of sound in a weakly-interacting 2D Bose gas has been measured, both below and above the superfluid Berezinskii-Kosterlitz-Thouless (BKT) transition [2]. While the observed speed of sound is well described by Landau's two-fluid hydrodynamic theory in the superfluid regime, it does not exhibit the predicted jump [3] at the phase transition temperature T_c. Instead, the measured velocity remains finite, with a large damping rate. In our work, we study the dynamical behaviour of a 2D Bose gas in absence of collisions, with special emphasis to the region above the BKT transition. We show that sound can propagate also in this case, due to mean-field interaction effects.

Experimentally, sound wave is excited by suddenly removing a static density modulation applied to the system. According to linear response theory, such perturbation induces a density fluctuation given by

$$\delta n(t) \propto \int_{-\infty}^{\infty} \mathrm{d}\omega \frac{\chi''(\omega)}{\omega} e^{i\omega t}, \qquad (1)$$

where $\chi''(\omega)$ is the imaginary part of the response function, evaluated within RPA. Using Eq. (1) we can estimate the velocity of sound c and its damping rate Γ. Our results are shown in Fig. 1 and we find good agreement with the experimental points of [2]. In particular, our RPA model correctly describes the Landau damping mechanism, at the origin of the observed strong damping of sound mode above T_c. The RPA results are confirmed by a comparison with the predictions of the stochastic (projected) Gross-Pitaevskii equations (SGPE) [1].

We further extend our analysis to the 3D case and point out the crucial role played by the Bose-Einstein condensate, absent in 2D as a direct consequence of the Hohenberg-Mermin-Wagner theorem. In contrast to 2D, the 3D collisionless sound is found to vanish at the critical temperature T_c and to lie close to the hydrodynamic second sound in the whole range of temperature $T < T_c$.

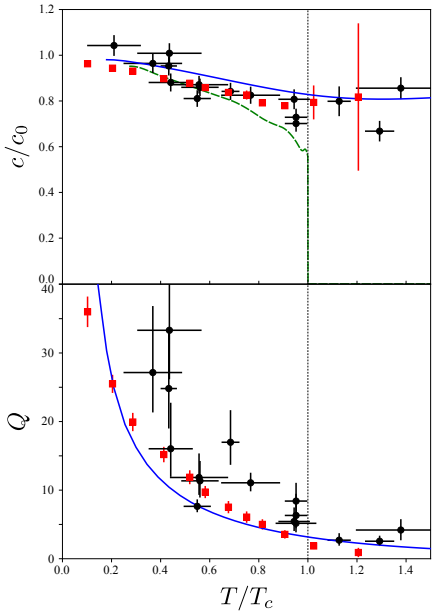


Figure 1: Upper panel: Sound velocity in units of the zero-temperature Bogoliubov sound $c_0 = \sqrt{g_{2D}n/m}$ with coupling constant $g_{2D} = 0.16\hbar^2/m$. The blue solid line is the RPA prediction for the sound velocity, extracted from Eq. (1). The green dashed line is the second sound predicted by Landau's two-fluids hydrodynamics [3]. The red squares are the results of SGPE simulations. The black circles are experimental points of Ref. [2]. Lower panel: Quality factor $Q = c/\Gamma$. The blue solid line is the RPA prediction. The red squares and the black circles are SGPE and experimental [2] results, respectively.

References

[1] M. Ota, F. Larcher, F. Dalfovo, L. Pitaevskii, N. P. Proukakis, and S. Stringari, arXiv:1804.04032.

[2] J. L. Ville, R. Saint-Jalm, E. Le Cerf, M. Aidelsburger, S. Nascimbène, J. Dalibard, and J. Beugnon, arXiv:1804.04037.

[3] T. Ozawa and S. Stringari, Phys. Rev. Lett. **112**, 025302 (2014).

Fast manipulation of Bose-Einstein condensates with an atom chip

R. Corgier[1,2], **S.Amri**[2], **Waldemar Herr**[1], **Holger Ahlers**[1], **David Guéry-Odelin**[3], **E. Charron**[2], **E.M. Rasel**[1], **and N. Gaaloul**[1]

[1] *Institut für Quantenoptik, Leibniz Universität Hannover, Welfengarten 1, D-30167 Hannover, Germany*

[2] *Institut des Sciences Moléculaires d'Orsay, Université Paris-Saclay, 91405 Orsay Cedex, France*

[3] *Laboratoire de Collisions - Agrégats - Réactivité, Université Paul Sabatier - Toulouse 3, 31062 Toulouse Cedex 9, France*

e-mail: *corgier@iqo.uni-hannover.de*

Recent proposals in the field of fundamental tests of foundations of physics propose Bose-Einstein condensates (BEC) as sources of atom interferometry sensors [1]. Atom chip devices have allowed to build transportable BEC machines with high repetition rates as demonstrated in the QUANTUS project [2]. The proximity of the atoms to the chip surface is, however, limiting the optical access and the available interferometry time necessary for precision measurements. In this context, a fast and perturbation-free transport of the atoms is required. We present a detailed theoretical analysis of the implementation of shortcut-to-adiabaticity protocols for the fast transport of neutral atoms with atom chips [3]. The objective is to engineer transport ramps with durations not exceeding a few hundred milliseconds to provide metrologically-relevant input states for an atomic sensor. Aided by numerical simulations of the classical and quantum dynamics, we study the behavior of a Bose-Einstein condensate in an atom chip setup with realistic anharmonic trapping. We detail the implementation of fast and controlled transports over large distances of 1-2 millimeters, *i.e.* distances 1000 times larger than the size of the atomic cloud. A subsequent optimized release and collimation step demonstrates the capability of our transport method to generate ensembles of quantum gases with expansion speeds in the picokelvin regime as illustrated in the figure. With such low expansion rates, atom interferometry experiments with seconds of drift time are possible. The performance of this procedure is analyzed in terms of collective excitations [4] reflected in residual center of mass and size oscillations of the condensate. We further evaluate the robustness of the protocol against experimental imperfections. Such a procedure has been applied in the Quantus 2 experiment leading to only 5 micrometers of residual dipole oscillation amplitude in the final trap after a 1.5mm transport during 150ms ramp [5] and allows an e cient delta-kick-collimation (DKC) [6, 7] to the pK level. Thanks to the optimal control theory, we highlight how one can extend this method for the double species transport problem relevant for universality of free fall tests.

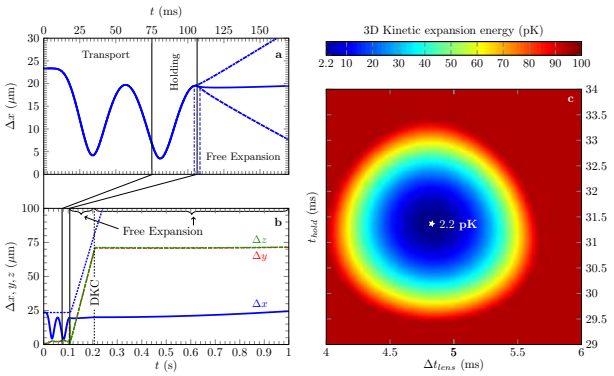


Figure 1: Transport, holding, release and magnetic lensing of a BEC to pK expansion velocities. Panel (a): Effect of the collective excitations during the holding trap in the weak trapping direction x for different timing. Panel (b): Full sequence with transport, holding, release and delta-kick collimation leading to an average, over the three spatial directions, expansion rate at the pK level: 2.2 pK. Without the collective excitations (*i.e.* for an adiabatic transport in the x direction, thin blue dotted curve representing Δx as a function of time), the collimation performance is much worse, leading to a global expansion temperature of 555 pK. Panel (c): Optimal parameters search by scanning the holding and lens durations. The white star marks the optimal values leading to an expansion temperature of 2.2 pK shown in (b).

[1] D. N. Aguilera et al. Class. Quantum Grav. **31**,115010 (2014)

[2] J. Rudolph et al. New J. Phys. **17**, 079601 (2015)

[3] R. Corgier, et al., arXiv1712.04820v1 (2017).

[4] S. Stringari, Phys. Rev. Lett. **77**, 2360 (1996)

[5] Rudolph J 2016 Matter-Wave Optics with Bose-Einstein Condensates in Microgravity Ph.D. thesis Leibniz University of Hanover

[6] H. Müntinga et al. Phys. Rev. Lett. **110**, 093602 (2013)

[7] T. Kovachy et al. Phys. Rev. Lett. **114**, 143004 (2015)

Spatially distributed genuine multipartite entanglement enables EPR steering of Bose-Einstein condensates

P. Kunkel[1], **M. Prüfer**[1], **H. Strobel**[1], **D. Linnemann**[1], **A. Frölian**[1], **T. Gasenzer**[1], **M. Gärttner**[1], **and M. K. Oberthaler**[1]

[1] *Kirchhoff-Institut für Physik, Universität Heidelberg, 69120 Heidelberg, Germany*

e-mail: *philipp.kunkel@kip.uni-heidelberg.de*

Heisenberg's uncertainty relation poses a fundamental limit on the simultaneous knowledge of two noncommuting observables. Yet, quantum mechanics allows for nonlocal correlations between two systems such that a measurement in one system allows for prediction of the outcome in the other one with a precision beating the local uncertainty limit which is known as Einstein-Podolsky-Rosen (EPR) steering [2]. These nonclocal correlations are one of the key resources for quantum technologies. Here, we experimentally show that entanglement, which is produced in a Bose-Einstein condensate (BEC) by local contact interactions in a single spatial mode, can be spatially distributed to yield nonlocal correlations which we verify by demonstrating EPR steering (see Fig. 1). Our experiment illustrates that entanglement of indistinguishable particles can be mapped to individually addressable subsystems, which has been proposed recently [3, 4]. This kind of entanglement is therefore as useful, in the sense of the LOCC (local operation and classical communication) paradigm, as entanglement between distinguishable particles.

We start our experiment with a BEC consisting of $N \approx 11,000$ ^{87}Rb atoms held in a crossed optical dipole trap. The atoms are prepared in the magnetic substate $m_\mathrm{F} = 0$ of the $F = 1$ hyperfine manifold. We use spin mixing to coherently populate the states $m_\mathrm{F} = \pm 1$ with atom pairs which is equivalent to spin nematic squeezing [5]. Since the atoms of the BEC are in principle indistinguishable, the correlations are shared among all atoms in the atomic cloud. By switching off the longitudinal confinement, the BEC expands in the remaining wave-guide potential and the entanglement is distributed in space. After expansion, we read out the relevant spin observable by applying a resonant rf-pulse followed by state selective absorption imaging. The high optical resolution of our imaging system enables the definition of distinct systems by partitioning the absorption signal. We measure two noncommuting spin observables and find in each partition that the fluctuations well exceed the local uncertainty constraint. Yet, we show that the measurement outcome in one subsystem of the atomic cloud can be used to infer the result in the remaining part better than allowed by the fundamental local uncertainty, which verifies that these parts are EPR entangled.

By partitioning the absorption signal into three parts of equal length we demonstrate that each part is steered by the remaining ones. This confirms three-way steering. To further elucidate the multipartite character of the generated entanglement, we construct a witness which connects the inference value of bipartite EPR steering to genuine multipartite entanglement. With this witness we reveal up to genuine five-partite entanglement.

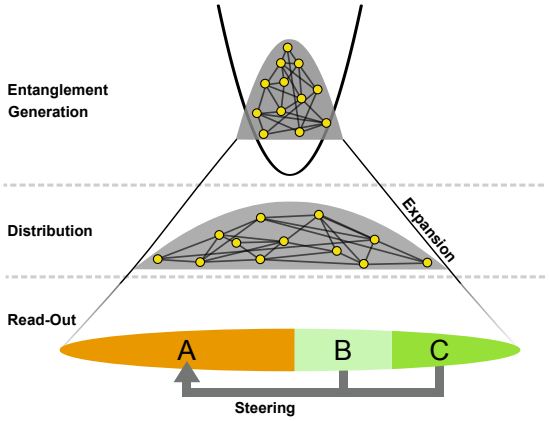


Figure 1: Experimental scheme to distribute entanglement in space [1].

[1] P. Kunkel et al., Science **360**, 413–416 (2018).

[2] M. D. Reid et al., Rev. Mod. Phys. **81**, 1727–1751 (2009).

[3] P. Hyllus, L. Pezzé, A. Smerzi, and G. Tóth, Phys. Rev. A **86**, 012337 (2012).

[4] N. Killoran, M. Cramer, and M. Plenio, Phys. Rev. Lett. **112**, 150501 (2014).

[5] C. D. Hamley, C. S. Gerving, T. M. Hoang, E. M. Bookjans, and M. S. Chapman, Nat. Phys. **11**, 167–172 (2015)

Coherent splitting and recombination of bright solitary matter waves

A. Rakonjac[1], **O. J. Wales**[1], **T. P. Billam**[2], **J. L. Helm**[3], **S. A. Gardiner**[1], **and S. L. Cornish**[1]

[1] *Joint Quantum Centre (JQC) Durham–Newcastle, Department of Physics, Durham University, South Road, Durham DH1 3LE, UK*

[2] *Joint Quantum Centre (JQC) Durham–Newcastle, School of Mathematics and Statistics, Newcastle University, Newcastle upon Tyne NE1 7RU, UK*

[3] *Dodd-Walls Centre for Photonic and Quantum Technologies, Department of Physics, University of Otago, 730 Cumberland Street, Dunedin 9016, New Zealand*

e-mail: *ana.rakonjac@durham.ac.uk*

We report on the controlled creation, splitting, and recombination of bright solitary matter waves formed from Bose-Einstein condensates of ^{85}Rb atoms. These solitary wavepackets, or solitons, are long-lived, with lifetimes of over 20 seconds, and can propagate without observable dispersion over macroscopic distances. Following our previous work on classical reflection of solitons from a broad repulsive barrier [1] and quantum reflection from a narrow attractive well [2], we extend our investigations to solitons incident on a narrow repulsive gaussian barrier [3]. When the kinetic energy of the soliton wavepacket is comparable to the barrier height, we observe controllable splitting of the soliton into two daughter solitons. The splitting proportion varies according to incident velocity and barrier height with good agreement with 1-D and 3-D Gross-Pitaevskii simulations.

After allowing the daughter solitons to oscillate in a weak harmonic potential, they recombine on the barrier. Experiments are performed with two barrier widths, $\omega_{\mathrm{wide}} \approx 11$ μm and $\omega_{\mathrm{narrow}} \approx 4.7$ μm. The outcome of a recombination event depends crucially on the barrier size. For ω_{wide}, splitting and apparent recombination is classical, with velocity filtering dominating the outcome. For ω_{narrow}, tunneling dominates and the daughter solitons are coherently recombined. Qualitatively, the difference manifests clearly: for the wide barrier case, the "recombined" soliton travels in the "reflected" direction (Fig. 1a), and for the narrow barrier, the recombined soliton travels in the "transmitted" direction (Fig. 1b), which is not possible in the classical regime.

The coherent splitting and recombination of solitons as well as their long lifetime leads the way to using such a scheme for soliton-based interferometry in a variety of configurations [4]. In particular, the scheme can be utilised in a ring geometry for Sagnac interferometry [5]. Future work includes implementing a soliton Sagnac interferometer using a 2-D painted ring potential and further experimental studies of bright matter-wave soliton dynamics that can be used to elucidate the wealth of theoretical work in the field, as well as to explore, for example, the realisation of Schrödinger cat states [6, 7] and the study of short-range atom-surface potentials [8].

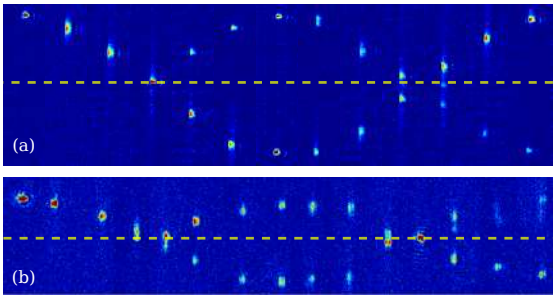


Figure 1: A series of destructive absorption images showing splitting and recombination on a (a) wide and (b) narrow barrier. The barrier position is indicated by the dashed line.

[1] A. L. Marchant, T. P. Billam, T. P. Wiles, M. M. H. Yu, S. A Gardiner, and S. L. Cornish, Nat. Commun. **4**, 1865 (2013)

[2] A. L. Marchant, T. P. Billam, M. M. H. Yu, A. Rakonjac, J. L. Helm, J. Polo, C. Weiss, S. A. Gardiner, and S. L. Cornish, Phys. Rev. A **93**, 021604(R) (2016)

[3] J. L. Helm, T. P. Billam, and S. A. Gardiner, Phys. Rev. A **85**, 053621 (2012)

[4] A. D. Cronin, J. Schmiedmayer, and D. E. Pritchard, Rev. Mod. Phys. **81**, 1051 (2009)

[5] J. L. Helm, S. L. Cornish, and S. A. Gardiner, Phys. Rev. Lett. **114**, 134101 (2015)

[6] C. Weiss and Y. Castin, Phys. Rev. Lett. **102**, 010403 (2009)

[7] A. I. Streltsov, O. E. Alon, and L. S. Cederbaum, Phys. Rev. A **80**, 043616 (2009)

[8] S. L. Cornish, N. G Parker, A. M. Martin, T. E. Judd, R. G. Scott, T. M. Fromhold, and C. S. Adams, Physica D **238**, 1299 (2009)

Bilayer system of dipolar bosons: few-body bound state

Grecia Guijarro Gámez[1], **Gregory Astrakharchik**[1], **and Jordi Boronat Medico**[1]
[1] *Universitat Politècnica de Catalunya, UPC - Física i Enginyeria Nuclear*
Campus Nord UPC, 08034 Barcelona, Spain
e-mail: *grecia.guijarro1@upc.edu*

Quantum Monte Carlo methods provide a powerful tool for predicting quantitatively the properties of many-body quantum system [1]. At the level of few-body physics, existence of bound-states (trimers, tetramers, etc.) for dipolar molecules in a bilayer is an open and controversial question. Anisotropy of the dipolar interaction (which can be attractive or repulsive) complicates the study but leads to rich physics [2]. The problem of two and three dipolar molecules can be solved analytically, the last one with more effort. However, as the number of dipoles is increased, the problem becomes essentially intractable using standard approaches. At this point Quantum Monte Carlo methods become highly competitive. We use Diffusion Monte Carlo method [3] to obtain the ground state energy and spatial distribution function of a bilayer system of dipolar bosons, where dipoles are oriented perpendicularly to the parallel planes. Interaction between dipoles in same layer is purely repulsive, while interlayer interaction is attractive at short distances. Tunneling of bosons between layers is not allowed.

The Hamiltonian of the dipolar system is given by

$$H = -\frac{\hbar^2}{2m}\sum_{i=1}^{N_A}\nabla_i^2 - \frac{\hbar^2}{2m}\sum_{\alpha=1}^{N_B}\nabla_\alpha^2 + \sum_{i<j}\frac{d^2}{r_{ij}^3} + \sum_{\alpha<\beta}\frac{d^2}{r_{\alpha\beta}^3} + \sum_{i\alpha}\frac{d^2(r_{i\alpha}^2-2h^2)}{(r_{i\alpha}^2+h^2)^{5/2}},$$

where d is the dipole moment of particles of mass m and h is the distance between the two layers. N_A and N_B are the number of dipoles in the top and bottom layer, respectively. The dipolar length $r_0 = md^2/\hbar^2$ is used as a unit of length and $E_0 = \hbar^2/(mr_0^2)$ as unit of energy. The in-plane distance between pairs of particles in the top (bottom) layer is $r_{ij(\alpha\beta)} = |\mathbf{r}_{i(\alpha)} - \mathbf{r}_{j(\beta)}|$ and the distance between the projections onto any of the layers of the positions of the α-th and i-th particle is $r_{\alpha i} = |\mathbf{r}_\alpha - \mathbf{r}_i|$.

It is known that a dimer exists for *arbitrary* separation between layers [4]. For three and four dipoles, the bound state does not exist for small separation between the two layers. We find the critical value of the interlayer separation at which the trimer and tetramer appear. For the trimer, we have found that the dominant structure close to the critical separation is halo state, where two dipoles are close to each other while the third is far away (see Fig. 1). Five- and six-body bound states also exist (work in progress).

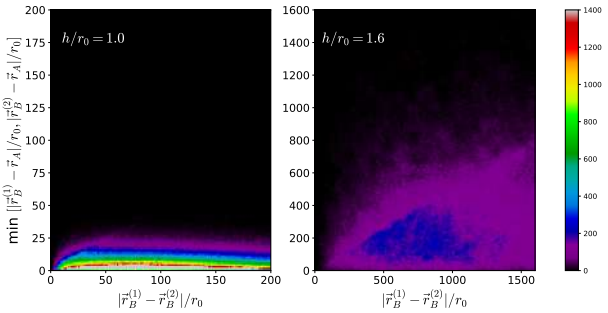


Figure 1: Spatial distributions of the trimer for two different values of the separation between layers.

[1] R. Guardiola, "Monte Carlo Methods in Quantum Many-Body Theories" (1998). In: J. Navarro, A. Polls (eds), "Microscopic Quantum Many-Body Theories and Their Applications". Lecture Notes in Physics, **510**, Springer, Berlin, Heidelberg (2007).

[2] A. Macia, G. E. Astrakharchik, F. Mazzanti, S. Giorgini, and J. Boronat, Phys. Rev. A, **90**, 043623 (2014).

[3] J. Boronat and J. Casulleras, Phys. Rev. B **49**, 8920 (1994).

[4] M. A. Baranov, A. Micheli, S. Ronen, and P. Zoller, Phys. Rev. A, **83**, 043602 (2011).

A new apparatus for the study of Sodium spinor BECs in highly stable magnetic field environment

A. Farolfi[1], **G. Colzi**[1,2], **E. Fava**[1], **C. Mordini**[1], **G. Lamporesi**[1,2], **G. Ferrari**[1,2]
[1] *INO-CNR BEC Center and Dipartimento di Fisica, Universitá di Trento, Povo 38123, Italy*
[2] *Trento Institute for Fundamental Physics and Applications, INFN, Povo 38123, Italy*
e-mail: *arturo.farolfi@unitn.it*

The dynamics of two-component superfluid systems have been studied in different experiments. In particular the Sodium $|F = 1, m_F = \pm 1\rangle$ mixture is interesting because of its miscibility and the absence of buoyancy. This allowed us to observe clean spin-dipole oscillations [1] and to demostrate spin superfluidity [2]. Theoretical predictions show that when the two components are resonantly coupled via an external field, new dynamics set in. Among them, a stationary domain wall in the relative phase[3], magnetic solitons[4] and confinement of vortex pairs[5].

Accessing the spin dynamics requires in practice coherent coupling of the order of one second requiring magnetic field stability at the μG level. To achieve this we developed a passive magnetic shield made of four layers of high magnetic permeability alloy (μ-metal), that will encase the science chamber of the apparatus while allowing optical access. The effect of this shield has been numerically simulated and then experimentally characterized using a high-precision magnetic field probe and its performance are excellent, with an attenuation factor of $10^{-4} - 10^{-5}$.

We developed a source of ultracold sodium atoms, made of a Zeeman slower and a 2D magneto-optical trap (MOT) in a separate chamber, from which we produce samples in the science chamber of $4 \cdot 10^9$ atoms trapped in a 3D Dark-Spot MOT. The atoms are then cooled using gray molasses [6] down to $\approx 14\mu$K before being loaded into a hybrid trap, that has been specifically designed for operating with the magnetic shield can sustain. The hybrid trap consists of a quadrupole magnetic trap (QMT) and a tight optical dipole trap (ODT) focused close to the center of the QMT[7]. The ODT is slowly loaded with atoms coming in the QMT, increasing the phase-space density by three orders of magnitude as well as preventing spin-flips at the center of the QMT. Performing evaporative cooling ramping down the ODT power we achieve condensation of $6 \cdot 10^6$ atoms[8].

In the near future we will install the magnetic shield, characterize the magnetic field stability in terms of coherence time of the BEC and move towards the experimental study of the confinement behaviour.

[1] Serafini et al., Phys. Rev. A, **94**, 063652 (2016)

[2] E. Fava et al., Phys. Rev. Lett. **120**, 170401 (2018)

[3] D.T. Son and M. A. Stephanov, Phys. Rev. A **65**, 063621 (2002)

[4] Qu et al., Phys. Rev. A **95**, 033614 (2017)

[5] M. Tylutki et al., Phys. Rev. A **93**, 043623 (2016)

[6] Colzi et al., Phys. Rev. A **93**, 023421 (2016)

[7] Lin et al., Phys. Rev. A **79**, 063631 (2009)

[8] Colzi et al. Phys. Rev. A **97** 053625 (2018)

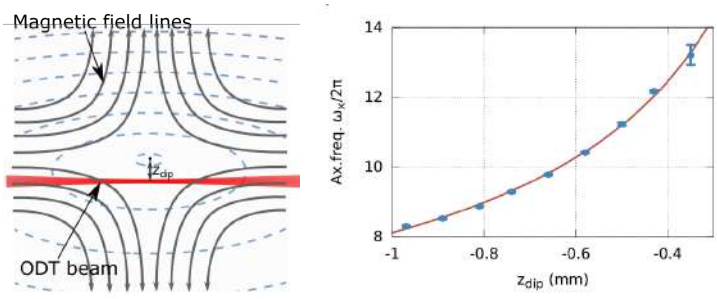


Figure 1: Schematic rapresentation of the hybrid trap and axial trapping frequency dependence on z_{dip}, showing the robustness of this trapping configuration

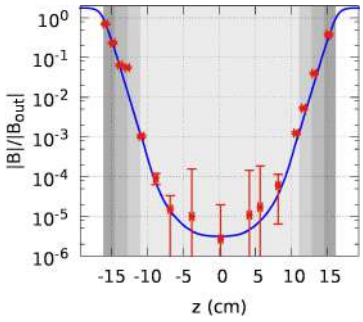


Figure 2: Experimental characterization of the magnetic shield

A Spinor BEC co-magnetometer for phase resolving spin amplification

Pau Gómez Kabelka[1], **F. Martin**[1], **C. Mazzinghi**[1], **S. Coop**[1], **S. Palacios**[1] **and M.W. Mitchell**[12]
[1] *ICFO Institut de Ciències Fotòniques, 08860 Castelldefels, Barcelona, Spain.*
[2] *ICREA Institució Catalana de Recerca i Estudis Avanats,08015 Barcelona, Spain.*
e-mail: *pau.gomez@icfo.es*

The *co-magnetometer* is a technology developed for rotation sensing [1] and searches for physics beyond the standard model [2], consisting of two different magnetically-sensitive systems operating in the same volume and thus experiencing the same magnetic field. A differential measurement can then reject true magnetic influences (which typically are strong and noisy), while sensitively detecting small signals that differently affect the two components.

Here we report on a ^{87}Rb spinor BEC (SBEC) co-magnetometer, with the two components being the F=1 and F=2 ground state populations, an extension of our recently-reported single-domain magnetic SBEC [3]. The collective spin of each hyperfine manifold is independently detected using Faraday rotation probing [4]. We study spin oscillation and spin amplification in F=2, using the F=1 component as a reference. This novel scheme gives accurate information on both the amplitude and phase of the F=2 SBEC as it rotates in a magnetic field, allowing tomographic study of spontaneous symmetry breaking, spin squeezing, and quantum entropy generation in a magnetically-polarized system.

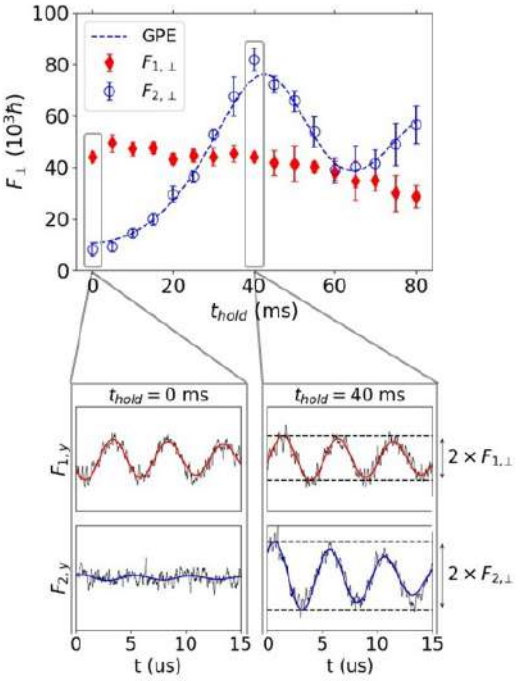


Figure 1: Temporal evolution of the transverse magnetizations in the F=1 and F=2 manifolds under a magnetic field of $B_z = 283\ mG$. The F=2 component experiences strong spin amplification (left, circles) while the slowly varying F=1 component keeps track of the rotating reference frame (left, diamonds). The combined measurement results in a phase sensitive spin amplifier.
For each hold time, the raw Faraday signals (right) reveal simultaneously the oscillating (200 kHz) spin components along the y-direction ($F_{1,y}$ and $F_{2,y}$). The respective transverse magnetizations ($F_{1,\perp}$ and $F_{2,\perp}$) are given by the observed oscillation amplitudes. Note that the orientation of the rotating reference frame is extracted from the initial phase in the $F_{1,y}$ signal.

References

[1] T. W. Kornack *et al. Nuclear Spin Gyroscope Based on an Atomic Comagnetometer.* PRL **95**: 230801 (2005).

[2] M. Smiciklas *et al. New Test of Local Lorentz Invariance Using a ^{21}Ne-Rb-K Comagnetometer.* PRL **107**: 171604 (2011).

[3] S. Palacios *et al. Multi-second magnetic coherence in a single domain spinor BEC.* New Journal of Physics **20.5**: 053008 (2018).

[4] M. Koschorreck *et al. Sub-projection-noise sensitivity in broadband atomic magnetometry.* PRL **104.9**: 093602 (2010).

Anomalous momentum diffusion in a Bose-Hubbard gas

R. Bouganne, M. Bosch Aguilera, A. Ghermaoui, J. Beugnon and F. Gerbier

Laboratoire Kastler-Brossel, Collège de France, CNRS, ENS-PSL University, Sorbonne Université, 11 place Marcelin Berthelot, 75005 Paris, France

e-mail: *raphael.bouganne@lkb.ens.fr*

Decoherence is a frequent limitation to the creation and manipulation of quantum systems. Much effort has been devoted in the recent years to understand the mechanisms at play, but the case of many-body systems of interacting particles remains challenging.

In this work, we investigate the decoherence dynamics of a two-dimensional Bose-Hubbard gas submitted to spontaneous emission. Spontaneous emission destroys spatial coherences in the gas, which in turns leads to a broadening of the momentum distribution [1]. For independent particles in free space, due to the inherent randomness in spontaneous emission directions, the photon scattering translates into momentum diffusion with a momentum width scaling as $t^{1/2}$.

In the case of strongly interacting bosonic atoms in optical lattices, we observe a drastic slowing down of the relaxation. Spatial coherences decay algebraically in time and momentum space dynamics becomes subdiffusive with a momentum width scaling as $t^{1/4}$ (see Fig. 1).

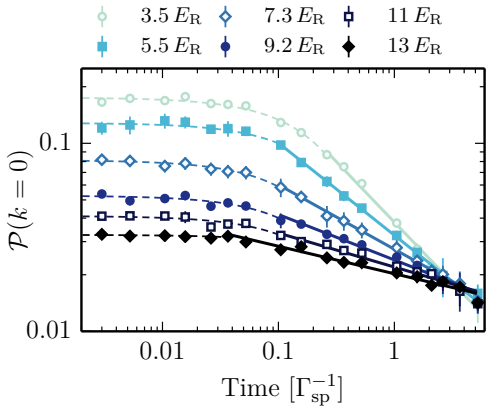


Figure 1: Fraction of atoms at zero-momentum $\mathcal{P}(k=0)$ versus dissipation time (Γ_{sp} is the spontaneous emission rate) for various lattice depths. The solid lines are fits with a power law, with a slope decreasing with lattice depth.

We explain these observations with a model proposed by Poletti et al. [2, 3], where the decoherence dynamics is understood in terms of a diffusion in Fock space. Dissipation leads to the formation of on-site clusters of atoms with higher occupancy than on average. These clusters decay slowly due to the energy mismatch provided by interatomic interactions. We use three-body losses as a probe of on-site statistics, and provide a direct evidence of this anomalous diffusion in Fock space which underlies the anomalous momentum diffusion.

[1] Cohen-Tannoudji C., Lectures at Collège de France, unpublished (1989).

[2] D. Poletti *et al.*, Phys. Rev. Let. **109**, 045302 (2012)

[3] D. Poletti *et al.*, Phys. Rev. Let. **111**, 195301 (2013)

Quantized circular dichroism in ultracold atoms

D.T. Tran[1], N. Goldman[1]
[1] *Center for Nonlinear Phenomena and Complex Systems.*
Université Libre de Bruxelles, CP231, Campus Plaine, B-1050 Brussels, Belgium
e-mail: *ducttran@ulb.ac.be*
Collaboration with: L. Asteria, N. R. Cooper, A. Dauphin, N. Fläschner, A. G. Grushin, T. Ozawa, B. S. Rem, K. Sengstock, M. Tarnowski, C. Weitenberg and P. Zoller

In the last decades, the relation between geometry, topology and quantum physics has been intensively investigated in solid-state systems, which has led to the discovery of novel states of matter. Building on their universal nature, topological properties are currently studied in an even broader context, ranging from ultracold atomic gases to photonics, where distinct observables and probes offer a novel view on topological quantum matter.

In this poster, I will discuss how the topology of quantum states can be revealed using an universal scheme based on excitation-rate measurements upon periodic driving [1]. When applied to Chern insulators or Landau levels, this approach leads to a topological dissipative response, which is revealed through an intriguing quantized circular dichroism [1, 2]. The poster will also report on the first experimental observation of this quantized dichroism effect in an ultracold Fermi gas [3].

References

[1] D. T. Tran, A. Dauphin, A. G. Grushin, P. Zoller, and N. Goldman. Probing topology by "heating": Quantized circular dichroism in ultracold atoms. *Science Advances*, 3(8), 2017.

[2] D. T. Tran, N.R. Cooper, and N. Goldman. Quantized Rabi oscillations and circular dichroism in quantum Hall systems. *ArXiv e-prints*, 2018.

[3] L. Asteria, D. T. Tran, T. Ozawa, M. Tarnowski, B. S. Rem, N. Fläschner, K. Sengstock, N. Goldman, and C. Weitenberg. Measuring quantized circular dichroism in ultracold topological matter. *ArXiv e-prints*, 2018.

Speed of sound in a superfluid 2D Bose gas

R.Saint-Jalm[1], **J.-L. Ville**[1], **M. Aidelsburger**[2], **É. Le Cerf**[1], **S. Nascimbène**[1], **J. Dalibard**[1] **and J. Beugnon**[1]

[1] *Laboratoire Kastler Brossel, Collège de France, CNRS, ENS-PSL University, Sorbonne Université, 11 place Marcelin Berthelot, 75005 Paris, France.*

[2] *Fakultät für Physik, Ludwig-Maximilians-Universität München, Schellingstr. 4, 80799 Munich, Germany.*

e-mail: *raphael.saint-jalm@lkb.ens.fr*

The propagation of sound is an important feature for the understanding of superfluid systems. In liquid helium the two-fluids model has predicted the existence of two sound modes, which have been then observed [1]. The first mode corresponds to the in-phase oscillation of the density of the superfluid and of the normal phase, whereas the second mode corresponds to the out-of-phase oscillation of their entropies.

In dilute quantum fluids, the propagation of sound has also been of huge interest. In the case of strongly interacting Fermi gases the picture is similar to liquid helium because of their small compressibility [2, 3, 4]. In that respect, the case of weakly interacting Bose gases is different and the nature of the two modes is modified [5]. The second sound is mainly due to superfluid part of the gas and its study is helpful to gain information about the superfluid properties of the gas.

The dimensionality of the gas is an important parameter for the propagation of sound, as it influences the thermodynamics of the gas. In a three-dimensional Bose gas, the superfluid fraction goes continuously from 1 at $T = 0$ to 0 at $T = T_c$, and the speed of secound sound goes from the Bogoliubov speed of sound to zero. In a two-dimensional Bose gas, because of the Berezinskii-Kosterlitz-Thouless transition, the superfluid fraction reaches a non-zero value right below the critical point and disappears right above it, and so does the predicted speed of sound of the second mode [6].

I will present the experiments that we have been performing with two-dimensional uniform Bose gases: We observe the propagation of sound and measure its velocity and its damping rate from a highly degenerate regime to above the critical temperature. The sound we observe is corresponding to the second sound of the two-fluids model. Below T_c, our observations are in good agreement with the theoretical values of the two-fluids model. Above T_c, we still observe the propagation of sound, which we attribute to non-isentropic sound.

For temperatures where the damping of the sound is low, we also excite standing waves in our trap to corroborate our measurements.

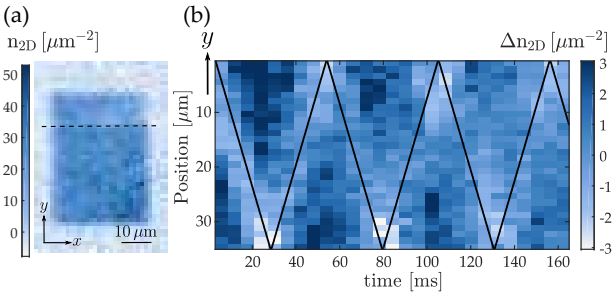


Figure 1: Propagation of a soundwave. (a): We add a local potential to create a density dip on one side of the cloud. (b) We remove abruptly the potential. After a variable propagation time we integrate the density along the x axis to see the propagation of the density dip. The black line shows the wavefront and gives a good measurement of the speed of sound.

References

[1] R.J. Donnelly, The two-fluid theory and second sound in liquid helium, Phys. Today **62**, 3439 (2009).

[2] E. Taylor, H. Hu, X.-J. Liu, L. P. Pitaevskii, A. Gri n, and S. Stringari, First and second sound in a strongly interacting Fermi gas, Phys. Rev. A **80**, 053601 (2009).

[3] J. Joseph, B. Clancy, L. Luo, J. Kinast, A. Turlapov, and J. E. Thomas, Measurement of sound velocity in a Fermi gas near a Feshbach resonance, Phys. Rev. Lett. **98**, 170401 (2007).

[4] L.A. Sidorenkov, M.K. Tey, R. Grimm, Y.-H. Hou, L. Pitaevskii, and S. Stringari, Second sound and the superfluid fraction in a Fermi gas with resonant interactions, Nature **498**, 7881 (2013).

[5] A. Gri n and E. Zaremba, First and second sound in a uniform Bose gas, Phys. Rev. A **56**, 48394844 (1997).

[6] T. Ozawa and S. Stringari, Discontinuities in the first and second sound velocities at the Berezinskii-Kosterlitz-Thouless transition, Phys. Rev. Lett. **112**, 025302 (2014).

Non-demolition quantum thermometry of BECs in the sub-nK domain

M. Mehboudi[1,2], **A. Lampo**[1], **C. Charalambous**[1], **L. A. Correa**[3], **M. A. García-March**[1], **and M. Lewenstein** [1,4]

[1] *ICFO—Institut de Ciències Fotòniques, The Barcelona Institute of Science and Technology, 08860 Castelldefels (Barcelona), Spain*

[2] *Departament de Física, Universitat Autònoma de Barcelona, E-08193 Bellaterra, Spain*

[3] *School of Mathematical Sciences and Centre for the Mathematics and Theoretical Physics of Quantum Non-Equilibrium Systems, The University of Nottingham, University Park, Nottingham NG7 2RD, United Kingdom*

[4] *ICREA, Lluis Companys 23, E-08010 Barcelona, Spain*

e-mail: *mohammad.mehboudi@icfo.eu*

The precise knowledge of temperature of a Bose Einstein condensate (BEC) is of fundamental and technological interest, for instance in order to operate them as quantum simulators [1]. Here, we propose a novel protocol to measure the temperature of the BEC, that remains reasonably precise even at the sub-nK domain, while it minimally perturbs the BEC [2]. The method is based on using a Bose-polaron impurity as the temperature probe or *thermometer*. The impurity is embedded inside the BEC, and thanks to its interaction with the BEC, it reaches a steady state. Such steady state is recently explored within the framework of quantum open systems, and by means of quantum Langevin equations [3].

Crucially, the temperature of the BEC has a prominent role in the steady state of the impurity. In particular, it is determinant in the statistics of the position $\hat{x}$ and momentum $\hat{p}$ of the impurity. That being the case, we naturally explore a temperature estimate that uses the outcomes of measuring position and/or momentum of the polaron. Any such estimate is minimally perturbing the BEC, as it is performed only on the impurity. For a more rigorous quantification of the performance of the aforementioned measurements, we benefit from the emerging field of *quantum thermometry*, that brings together toolboxes from quantum metrology, and open quantum systems, to estimate ultra-low temperatures.

Firstly, our results identify the most precise temperature measurement, and quantify its performance through the *quantum Cramér-Rao* bound. This optimal measurement is a linear combination of $\hat{x}^2$ and $\hat{p}^2$. We find that—in the temperature domain $0.3\ \text{nK} \leq T \leq 2\ \text{nK}$—one can achieve a relative error $[\delta T/T]_{\min} = 10\%$, with a number of measurements that is as few as 100. Secondly, and more importantly, we quantify the precision of position and momentum measurements and benchmark them against the optimal one. We observe that position measurements over-perform momentum measurements. What is more, their overall performance is similar, and reasonably close to the optimal measurements.

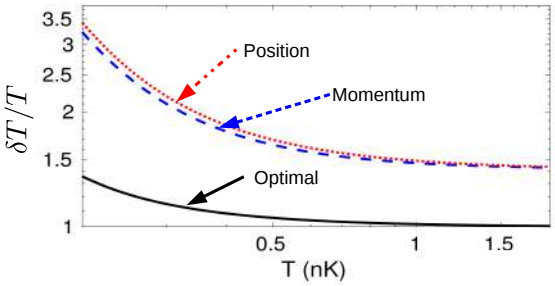


Figure 1: The relative error (per-measurement) of temperature estimation vs. temperature. The blue-dashed and red-dotted curves represent measuring the position and momentum of the polaron impurity, respectively. The black-solid curve depicts the minimum possible relative error—that is the relative error optimized over all possible measurements on the impurity. A detailed description of the model and the parameters used can be found in [2].

In particular, one can achieve a relative error of about 10% with 400 measurements (see Fig. 1).

Our results are very generic, and can be applied to any impurity and any 1D BEC—and extended to higher dimensions. Hence, many of the current experimental set ups will benefit from them. We illustrated the method with particular BEC of K atoms and Yb impurity, but we expect similar results for other atomic species

References

[1] M. Lewenstein, A. Sanpera, and V. Ahufinger, *Ultracold atoms in optical lattices*, Vol. 143 (Oxford University Press Oxford, 2012).

[2] M. Mehboudi, C. Charalambous, A. Lampo, L. A. Correa, M. Á. García-March, and M. Lewenstein, in preparation (2018).

[3] A. Lampo, C. Charalambous, M. Á. García-March, and M. Lewenstein, arXiv:1803.08946 (2018).

Two-dimensional Condensation of Polar Molecules in a Synthetic Gauge Field

I-Kang Liu and Shih-Chuan Gou

Department of Physics and Graduate Institute of Photonics, National Changhua University of Education, Changhua 50058, Taiwan

e-mail: *ligetern@gmail.com*

In this presentation, we theoretically investigate groundstate properties of a two-dimensional ultracold polar molecule gas in the condensate phase and subjected to an effective vector potential induced by the Raman coupling between two rotational levels of the molecule [**?**]. The interaction between molecules is considered to be dominant by the effective dipole moment induced by the Raman coupling [**?**, **?**], and the dipole moments are aligned by a DC field in the direction perpendicular to that of the two counterpropagating Raman beams. Based on the previous studies [**?**, **?**, **?**], such setup can facilitate to engineer an effective long-range interaction featuring not only the standard dipolar form [**?**, **?**] but also a spatial dependence on the relative phase between two coupled rotational states. Under the mean-field approximation, three phases can be found by the variational ansatz. Two of phases are governed by the coupling, and in the interaction dominant regime the system energetically favours a Stoner-type ferromagnetic state with a spatial phase modulation showing $\pm\pi/2$ phase jump in its relative phase. The numerical solutions computed by solving Gross-Pitaevskii equation (GPE) agree with the variational approach, and the dynamical stability of the Stoner-type phase is examined by GPE real-time simulation with perturbed initial condition.

References

[1] J.-H. Zheng, B. Xiong, G. Juzeliūnas, and D.-W. Wang, Phys. Rev. A **92**, 013604 (2015).

[2] A. Micheli, G. Pupillo, H. P. Böchler, and P. Zoller, Phys. Rev. A **76**, 043604 (2007).

[3] H. P. Böchler, E. Demler, M. Lukin, A. Micheli, N. Prokofév, G. Pupillo, and P. Zoller, Phys. Rev. Lett. 98, 060404 (2007).

[4] C.-H. Lin, Y.-T. Hsu, H. Lee, and D.-W. Wang, Phys. Rev. A **81**, 031601(R) (2015).

Non-linear relaxation of interacting bosons coherently driven on a narrow optical transition

M. Bosch Aguilera[1], **R. Bouganne** [1], **A. Dareau** [2], **M. Scholl** [3], **Q. Beaufils** [4], **J. Beugnon** [1] **and F. Gerbier** [1]

[1] *Laboratoire Kastler Brossel, Collège de France, ENS-PSL Research University, Sorbonne Université, CNRS, 11 place Marcelin-Berthelot, 75005 Paris, France*

[2] *Vienna Center for Quantum Science and Technology, TU Wien Atominstitut, Stadionallee 2, 1020 Vienna, Austria*

[3] *FARO Scanner Production GmbH, Lingwiesenstrasse 11/2, D-70825 Korntal-Münchingen*

[4] *Laboratoire PhLAM, Bt. P5 - USTL, F-59655 Villeneuve d'Ascq*

e-mail: *manel.bosch@lkb.ens.fr*

Two-electron atoms, such as Ytterbium, feature ultranarrow optical transitions that are nowadays largely exploited in metrology laboratories to build optical clocks. These transitions, nearly free of spontaneous emission, are not only interesting for metrological applications, but also provide a good tool to investigate many-body physics with atomic quantum gases, and therefore offer new instruments for quantum simulation and quantum information.

Here, I will present the coherent driving of Rabi oscillations on the doubly forbidden $^1S_0 \rightarrow {}^3P_0$ optical clock transition in a ^{174}Yb Bose Einsten Condensate (BEC) loaded in an optical dipole trap [1]. Spontaneous emission being negligible, the dynamics of the relaxation of these oscillations is strongly influenced by the following effects: asymmetric elastic interactions (due to different values in intra- and inter-state scattering lengths) [2, 3], inelastic losses and Doppler broadening due to the finite momentum width imposed by the confinement.

In particular, we observe the transition between two regimes (cf. Fig.1): a first one, when the driving strength prevails with respect to the relaxation processes, in which Rabi oscillations are observed, to an irreversible decay when the relaxation takes over. This crossover is reminiscent of the textbook problem of a discrete level coupled to a continuum: in the case of a broad continuum the evolution leads to an irreversible Weisskopf-Wigner decay, whereas if the continuum is so narrow that can be approximated by a discrete state, Rabi oscillations are observed. We compare our observations to a two-component Gross-Piatevskii (GP) model and we conclude that for moderate values of interactions, the main damping source is the finite momentum width of the BEC, while inelastic losses lead to a non-exponential decay of populations.

The GP model shows excellent agreement for the regime of small interactions. However, we find that for larger values of interactions it fails to reproduce the observed damping of the oscillations, pointing to the existence of beyond mean-field phenomena.

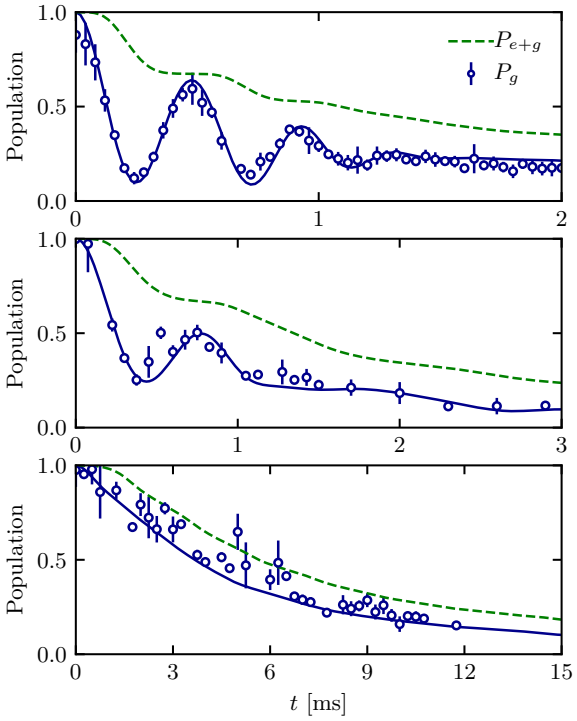


Figure 1: Population dynamics vs. pulse duration for decreasing Rabi frequencies. The transition between the oscillating regime and the irreversible decay is observed as the Rabi frequency is decreased. From top to bottom the Rabi frequencies are $\Omega_L/2\pi = 2.1\,\mathrm{kHz}$, $1.1\,\mathrm{kHz}$ and $200\,\mathrm{Hz}$. The Doppler width is $\Delta_D/2\pi = 600\,\mathrm{Hz}$ for all of them and the chemical potential $\mu/h = 1\,\mathrm{kHz}$.

[1] M. Bosch Aguilera et al, in preparation.

[2] R. Bouganne et al, *New J. Phys.* **19** (2017) 113006.

[3] L. Franchi et al, *New J. Phys.* **19** (2017) 103037.

Observation of Spin Superfluidity in a Bose Gas Mixture

C. Mordini[1,2], **E. Fava**, **T. Bienaimé**, **G. Colzi**[1,2], **C. Qu**[1,*], **S. Stringari**[1,2], **G. Lamporesi**[1,2], **and G. Ferrari**[1,2]

[1] *INO-CNR BEC Center and Dipartimento di Fisica, Universita di Trento, 38123 Povo, Italy*
[2] *Trento Institute for Fundamental Physics and Applications, INFN, 38123 Povo, Italy*
e-mail: *carmelo.mordini@unitn.it*

Spin-superfluidity and spin-transport phenomena play a key role in condensed matter physics both experimentally and theoretically. Even in systems where spin is conserved, the behavior of spin transport is highly nontrivial since, at finite temperature, collisions between different spin species yield relaxation of the spin current, a phenomenon known as spin drag. So far the study of superfluidity at finite temperature has mainly concerned the density channel, where both the number of particles and total current are conserved. The dynamics in atomic Bose mixtures present additional features related to interactions an the miscibility of superfluids, which might cause the demixing of the superfluids. For this reason until recently spin-transport measurements in atomic Bose mixtures were limited to the thermal phase [1], and only in the last two years they extended to the superfluid phase in the zero temperature limit [2, 3] exploiting the highly miscible sodium $|F = 1, m_F = \pm 1\rangle$ two-state mixture. The latter measurements showed that for harmonically trapped systems undamped spin oscillations can indeed be observed, their dynamics is heavily affected by interactions [2], and the spin superflow rapidly damps when it exceeds a critical value [3].

Here we present measurements of spin-dipole (SD) oscillations at finite temperature on sodium $|F = 1, m_F = \pm 1\rangle$ mixtures [4] resolving the superfluid from the thermal components, both in the collisionless (collisional rate lower than oscillation frequency, $\gamma_{\rm coll} < \omega_{\rm x}$) and in the collisional regime ($\gamma_{\rm coll} > \omega_{\rm x}$). We find that while the SD oscillation of the thermal fraction exhibits damping on the timescale of the classical collisional time, the superfluid SD dynamics is undamped and not affected by finite-temperature effects, hence revealing the effects of spin superfluidity.

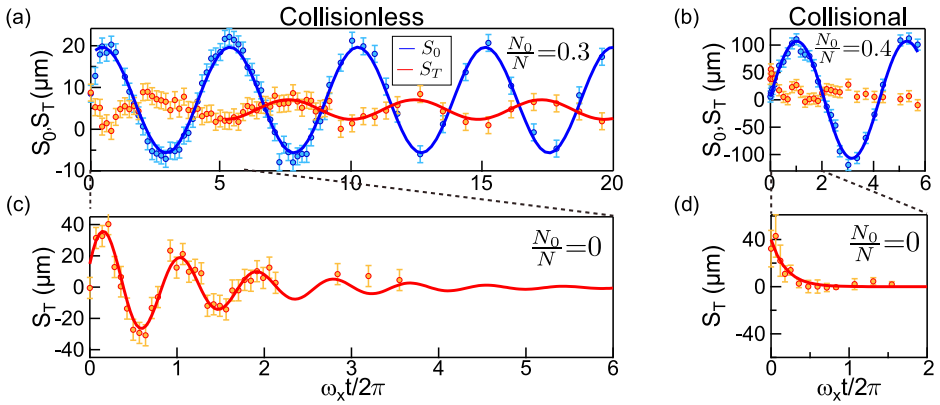


Figure 1: Spin oscillations for the thermal S_T (red) and condensed S_0 (blue) in the collisionless and collisional regimes: (a) and (c) finite temperature below T_c, (b) and (d) $T > T_c$.

* present address: JILA, Department of Physics, University of Colorado, Boulder, CO 80309, USA

[1] S. B. Koller, A. Groot, P. C. Bons, R. A. Duine, H. T. C. Stoof, P. van der Straten, New J. Phys. **17**, 113026 (2015).

[2] T. Bienaimé, E. Fava, G. Colzi, C. Mordini, S. Serafini, C. Qu, S. Stringari, G. Lamporesi, G. Ferrari, Phys. Rev. A **94**, 063652 (2016).

[3] J. H. Kim, S. W. Seo, Y. Shin, Phys. Rev. Lett. **119**, 185302 (2017).

[4] E. Fava, T. Bienaimé, C. Mordini, G. Colzi, C. Qu, S., G. Lamporesi, G. Ferrari, Phys. Rev. Lett. **120**, 170401 (2018).

Synthetic dimensions in ultracold polar molecules: From topology to quantum strings

Bhuvanesh Sundar[1], **Matthew Thibodeau**[1], **Yuxin Wang**[2], **Zhiyuan Wang**[1], **Kaden R. A. Hazzard**[1], **and Bryce Gadway**[3]

[1] *Rice University, Houston, USA*

[2] *University of Science and Technology, Anhui Sheng, China*

[3] *University of Illinois at Urbana Champaign, Urbana, USA*

e-mail: *bs55@rice.edu*

Synthetic dimensions alter one of the most fundamental properties in nature, the dimension of space. We show that rotational states of ultracold molecules can be used as synthetic dimensions extending to many – potentially hundreds of – synthetic lattice sites. Microwaves coupling rotational states drive fully controllable synthetic inter-site tunnelings, enabling, for example, topological band structures. We show that interactions leads to even richer behavior: when molecules are frozen in a real space lattice with uniform synthetic tunnelings, dipole interactions cause the molecules to aggregate to a narrow strip in the synthetic direction beyond a critical interaction strength, resulting in a quantum string or a membrane, with an emergent condensate that lives on this string or membrane. We explore the properties of these phases using mean field, exact, and density-matrix-renormalization-group solutions. All the phases above can be detected using measurements of rotational state populations.

Universality of liquid Bose-Bose mixture of ultracold atoms

V. Cikojević, L. Vranješ Markić[1], and J. Boronat[2]

[1] *Faculty of Science, University of Split, Ruđera Boškovića 33, HR-21000 Split, Croatia*

[2] *Departament de Física, Universitat Politècnica de Catalunya, Campus Nord B4-B5, E-08034 Barcelona, Spain*

e-mail: *leandra@pmfst.hr*

We have studied dilute Bose-Bose mixtures of atoms with attractive interspecies and repulsive intraspecies interaction using quantum Monte Carlo methods at T=0. Using different interaction models we determine conditions for the universal equation of state of the liquid mixture. It is shown that Lee-Huang-Yang correction is sufficient only very close to the mean-field limit provided the range of the interaction potential is not large.

Modeling atom diffraction beyond the weakly-diffracting limit

B. T. Beswick[1], **I. G. Hughes**[1], **and S. A. Gardiner**[1]

[1] *Joint Quantum Centre (JQC) Durham–Newcastle, Department of Physics, Durham University, Durham DH1 3LE, United Kingdom*

e-mail: *b.t.beswick@durham.ac.uk*

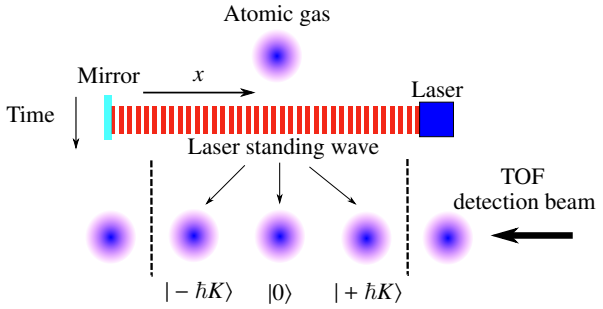


Figure 1: Schematic of a standing-wave-pulse atom-diffraction setup, an ultracold atomic gas is subjected to some number of lattice pulses N, before a time of flight beam measures the atomic population in each of the allowed momentum states. The gas is diffracted into an (in principle infinite) discrete ladder of momentum states $|n\hbar K\rangle$, $n \in \mathbb{Z}$, where K is twice the laser wavenumber k_{L}. The dashed lines enclose the three relevant momentum states in the weakly-diffracting case, where the lattice depth is sufficiently small ($\sim 0.01 E_{\mathrm{R}}$, where $E_{\mathrm{R}} = \hbar^2 k_{\mathrm{L}}^2 / 2M$ and M is the atomic mass).

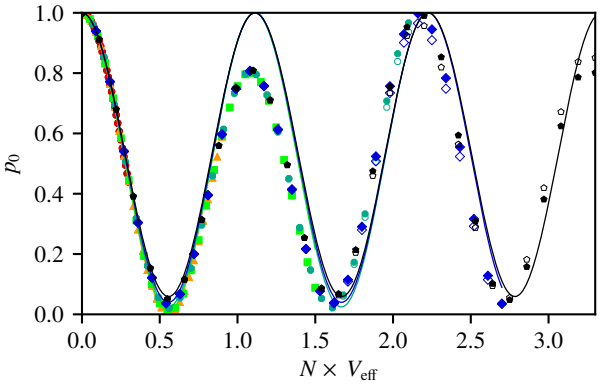


Figure 2: Plot of population in the $|0\hbar K\rangle$ momentum state, p_0, versus the number of pulses N (30 in total for each curve), as calculated analytically using a three state basis (solid lines), and numerically using a five state basis (solid markers), and a 2048 state basis (hollow markers). Each coloured curve corresponds to a specific value of the effective lattice depth V_{eff}, by which the bottom axis has been scaled to reveal an approximate universality. Beyond $NV_{\mathrm{eff}} \sim 0.7$ the three state model ceases to agree, though for values of NV_{eff} up to ~ 1.7 the five state model (in principle analytically solveable) is clearly sufficient.

Precision measurement of lattice depths is important in many areas of interest in atomic physics, most notably in quantum simulation, atom interferometry and for accurate calculation of transition dipole matrix elements. In such experiments, lattice depths are often measured by exposing an ultracold atomic gas to a series of off-resonant laser-standing-wave pulses, and fitting theoretical predictions for the fraction of atoms found in each of the allowed momentum states by time of flight measurement after some number of pulses N (See Fig. 1).

However, for the case of 'weak' lattice depths ($\sim 0.01E$ for any atom, where $E = \hbar^2 k_{\mathrm{L}}^2 / 2M$), the precision on such measurements can be hampered by signal to noise issues. Recently, the work of Herold et al. [1] has suggested that this complication can be mitigated by alternating each standing-wave pulse with a free evolution-stage, both with duration equal to half the Talbot time, $T_T/2 = 2\pi M/\hbar K^2$, where K is twice the laser wavenumber k_{L}, and M is the atomic mass [2]. The modeling approach taken in [1], is valid for a weak lattice which is pulsed a small number of times, corresponding to the 'weakly-diffracting limit'. We present a full analytic model for the time evolution of the atomic populations of the $|0\hbar K\rangle$ and $|\pm\hbar K\rangle$ states, which is su cient for a 'weak' lattice, as well as numerical simulations incorporating higher momentum states at both strong ($>0.1E$) and weak lattice depths, both of which are compared for typical experimental values in Fig. 2. We also explore the role of finite-temperature effects in such experiments. Finally we use the same techniques to explore the case where either the standing wave is left continuously on, or the free-evolution stage is transformed away by employing a 'walking wave' technique [3]. We conclude that, especially for a finite-temperature gas, we should expect this modified approach to provide a more precise measurement of lattice depths both in and out of the weakly-diffracting limit.

[1] C. D. Herold, V. D. Vaidya, X. Li, S. L. Rolston, J. V. Porto, M. S. Safronova Phys. Rev. Lett. **109**, 243003 (2012)

[2] Y. Zhai, C. H. Carson, V. A. Henderson, P. F. Gri n, E. Riis, A. S. Arnold, Optica **5**, 80 (2018)

[3] M. Saunders, P. L. Halkyard, S. A. Gardiner, K. J. Challis, Phys. Rev. A **79**, 023423 (2009)

Quantum Monte Carlo simulations of spin-orbit coupled systems

Andrii Gudyma[1], **Leandra Vranješ Markić**[1]
[1] *Faculty of Science, University of Split, Ruđera Boškovića 33, HR-21000 Split, Croatia*
e-mail: *agudyma@pmfst.hr*

Quantum Monte Carlo methods are based on solving the Schrodinger equation stochastically and provide an extremely powerful numerical tool for studying the static properties of quantum systems. We propose to modify the diffusion Monte Carlo algorithm in order to incorporate additional spin-orbit coupling terms. For this purpose we use exact mapping of the spinor system on a scalar system resulting in an effective Hamiltonian without nonlocal interactions.

Our methodology can be applied to cold atomic gases with synthetic spin-orbit coupling (SOC). In order to test our approach we study interacting many-body systems with Rashba and Dresselhaus SOC of equal strengths. Even in one dimensional geometry such a system demonstrates rich and interesting physics, e.g. degenerate ground state and stripe phases [1]. For the degenerate ground state stripe phase may or may not emerge depending on the strength of interparticle interaction. In cases of strong repulsion condensate polarises to one of ground state functions and thus this phase is called magnetized or separated phase. In this phase no stripe behaviour is observed.

[1] Zhu, C. et al. Journal of Physics B: Atomic, Molecular and Optical Physics **49**, 145301 (2016)

Raise and fall of a bright soliton in an optical lattice

P. Naldesi[1], **J. P. Gomez**[1], **B. Malomed** [23], **M. Olshanii** [4], **A. Minguzzi**[1], **and L. Amico** [56789]

[1] *Université Grenoble-Alpes, LPMMC, F-38000 Grenoble, France and CNRS, LPMMC, F-38000 Grenoble, France*

[2] *Department of Physical Electronics, School of Electrical Engineering, Faculty of Engineering, Tel Aviv University, P.O.B. 39040, Ramat Aviv, Tel Aviv, Israel*

[3] *Center for Light-Matter Interaction, Tel Aviv University, P.O.B. 39040, Ramat Aviv, Tel Aviv, Israel*

[4] *Department of Physics, University of Massachusetts Boston, Boston, MA 02125, USA*

[5] *Dipartimento di Fisica e Astronomia, Via S. Sofia 64, 95127 Catania, Italy*

[6] *Centre for Quantum Technologies, National University of Singapore, 3 Science Drive 2, Singapore 117543, Singapore*

[7] *MajuLab, CNRS-UNS-NUS-NTU International Joint Research Unit, UMI 3654, Singapore*

[8] *CNR-MATIS-IMM & INFN-Sezione di Catania, Via S. Sofia 64, 95127 Catania, Italy*

[9] *LANEF 'Chaire d'excellence', Universitè Grenoble-Alpes & CNRS, F-38000 Grenoble, France*

e-mail: *piero.naldesi@lpmmc.cnrs.fr*

We study an ultracold atomic gas with attractive interactions in a one-dimensional optical lattice. We find that its excitation spectrum displays a quantum soliton band, corresponding to N-particle bound states, and a continuum band of other, mostly extended, states. For a system of a finite size, the two branches are degenerate in energy for weak interactions, while a gap opens above a threshold value for the interaction strength. We find that the interplay between degenerate extended and bound states has important consequences for both static and dynamical properties of the system. In particular, the solitonic states turn out to be protected from spatial perturbations and random disorder. We discuss how such dynamics implies that our system effectively provides an example of a quantum many-body system that, with the variation of the bosonic lattice filling, crosses over from integrable non-ergodic to non-integrable ergodic dynamics, through non-integrable non-ergodic regimes.

A full version of our work can be found here [1]

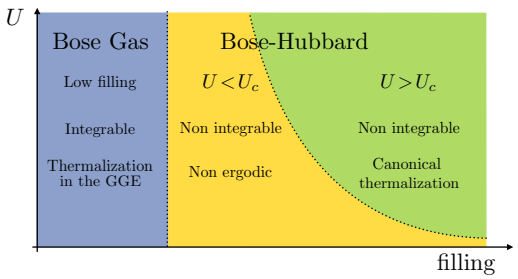


Figure 1: Integrability of a condensates composed of attractive bosons in one-dimensional lattices as a function of the filling and interaction strength. At low fillings, the system is well described by the Bose-gas field theory in the continuum. The integrability of this model makes the system thermalize towards a Generalized Gibbs Ensemble. In the opposite regime, at larger fillings and $U > U_c$, the Bose-Hubbard model is not integrable and it thermalizes to the micro-canonical ensemble. For intermediate fillings and $U > U_c$, as the bound and scattering states may be degenerate, the system is non-integrable and non-ergodic.

References

[1] Naldesi, P., Polo Gomez, J., Minguzzi, A., et al. 2018, arXiv:1804.10133

Towards ultracold erbium-potassium quantum gas mixtures

J. Ang'ong'a and B. Gadway
University of Illinois at Urbana-Champaign
e-mail: *angonga2@illinois.edu*

Emergent phenomena in strongly interacting systems are challenging to study since the complexity of the system grows rapidly with the size of the system. Quantum simulators, naturally realizing the Hamiltonian of the system of interest through particle-particle interactions, can in many cases explore system sizes well beyond what can be numerically simulated. Direct observation of the evolution of a system of trapped quantum gases provides access to parameter regimes that are intractable in classical simulators.

This works aims to realize trapped and cooled erbium and potassium gas mixtures for the study of strongly interacting systems. Due to relatively large dipole moment and consequently strong dipole-dipole interaction, a gas of ultracold erbium atoms provides a natural platform for the simulation of strongly interacting systems. Existence of Feshbach resonances for both potassium and erbium atoms allows for possible investigation of tunable interspecies interactions. Additionally, we hope to explore novel phenomena associated with mixtures of alkali and dipolar gases such as anomalous supersolidity [1].

In this work we present initial developments towards the realization of a system of trapped and cooled erbium and potassium mixtures i.e.

- Results on the study of a polarization spectroscopy signal of erbium atoms in a hollow cathode lamp for the frequency stabilization of a laser beam at 400.91 nm [2].
- Construction of double MOT system and initial results on optimization of a 3D MOT of potassium atoms.
- Initial plans and developments towards implementation of sub-Doppler laser cooling of potassium atoms using the gray molasses technique.
- Transport of potassium atoms from one part of the vacuum chamber to another using *Optotune* focus tunable lens [3].

References

[1] R. M. Wilson, W. E. Shirley, and S. S. Natu, Phys. Rev. A 93, 011605(R) (2016).

[2] J. Ang'ong'a and B. Gadway, J. Phys. B: At. Mol. Opt. Phys. 51, 045003 (2018)

[3] `https://www.optotune.com`

Quantum liquid droplets in a mixture of Bose-Einstein condensates

C. R. Cabrera, L. Tanzi, J. Sanz, B. Naylor, P. Thomas, P. Cheiney and L. Tarruell
Institut de Ciències Fotòniques, The Barcelona Institute of Science and Technology
08860 Castelldefels (Barcelona), Spain
e-mail: *cesar.cabrera@icfo.es*

Dilute quantum droplets are liquid-like clusters of ultra-cold atoms self-trapped by attractive mean-field forces, and stabilized against collapse by repulsive beyond mean-field many-body effects. Originally predicted for mixtures of Bose-Einstein condensates with attractive interactions [1], these systems have been recently realized in dipolar quantum gases. In my poster, I will present the first experimental demonstrations of quantum droplets in Bose-Bose mixtures, exploiting a mixture of two ^{39}K Bose-Einstein condensates.

In a first series of experiments [2], we realize quantum liquid droplets in a system with only vertical confinement. We directly measure the droplet size and ultra-low density via high-resolution in situ imaging, and experimentally confirm their self-bound nature (see Fig. 1 top and central panel). We demonstrate that the very own existence of these droplets is a striking manifestation of quantum fluctuations, negligible in single-component condensates with only contact interactions (see Fig. 1 bottom panel). Finally, we observe that for small atom numbers quantum pressure dissociates the droplets and drives a liquid-to-gas transition, which we map out as a function of interaction strength.

These first measurements open an intriguing question: the difference existing between droplets and solitons. In a second series of experiments [3], we address it by placing the mixture in an optical waveguide, realizing a system that contains both composite bright solitons and quantum liquid droplets. In analogy to non-linear optics, the former can be seen as one-dimensional matter-wave solitons stabilized by dispersion, whereas the latter correspond to high-dimensional solitons stabilized by a higher order non-linearity. We find that depending on atom number, interaction strength and confinement, solitons and droplets can be smoothly connected or remain distinct states coexisting only in a bi-stable region. We measure their spin composition, extract their density for a broad range of parameters, and map out the boundary of the region separating solitons from droplets.

Our experiments demonstrate a novel type of ultra-dilute quantum liquid, stabilized only by contact interactions. They provide an ideal platform for benchmarking complex quantum many-body theories beyond the mean-field approximation in a quantum simulation approach. Furthermore, they constitute a novel playground to explore experimentally self-bound states stabilized by unconventional higher order non-linearities, relevant in non-linear optics.

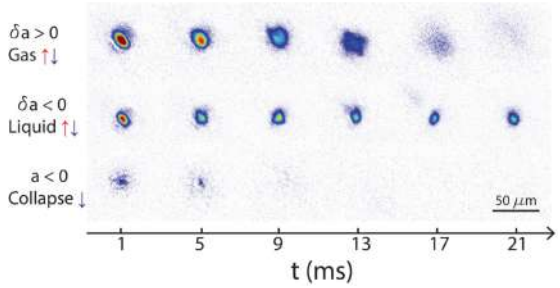


Figure 1: Time evolution of a Bose-Bose mixture with effective repulsive (top panel) and attractive interactions (central panel). The manifestation of a self-bound state (*quantum droplet*) is due to the presence of quantum fluctuations. In a single component BEC (bottom panel) the attractive mean-field interactions dominate and the system collapses.

[1] D. S. Petrov, Phys. Rev. Lett. **115**, 155302 (2015).

[2] C. R. Cabrera, L. Tanzi, J. Sanz, B. Naylor, P. Thomas, P. Cheiney, and L. Tarruell, Science **359**, 6373 (2018).

[3] P. Cheiney, C. R. Cabrera, J. Sanz, B. Naylor, L. Tanzi, and L. Tarruell, Phys. Rev. Lett. **120** 135301 (2018).

Many-body effects in synthetic lattices

Fangzhao Alex An*, **Eric J. Meier, and Bryce Gadway**
Department of Physics, University of Illinois at Urbana-Champaign, Urbana, IL 61801-3080, USA
e-mail: *faan2@illinois.edu*

Ultracold atoms in optical lattices have seen success in simulating and studying many-body phenomena. The method of using discrete atomic internal or external states as sites in a "synthetic lattice" has further expanded the capabilities of cold atom quantum simulation, enabling experiments on disordered and topological systems. Here, we provide the first clear signature of interaction effects in synthetic lattices, utilizing atoms in a lattice of coupled discrete momentum states to study the physics of a bosonic Josephson junction array.

Due to our momentum-space lattice setup, we are able to initialize atoms in a highly out-of-equilibrium state (i.e., confined to one or two lattice sites) and subsequently detect lattice population after dynamics in a site-resolved manner. Interactions exist in our momentum-space system, and have been discussed in depth in Ref. [1]. While the interactions are generally nontrivial, we consider a mean-field regime. Here, we present three closely-related results:

1. Direct observation of many-body localization with increasing ratio of interaction to tunneling U/t. Some related works have been performed in Refs. [2, 3].

2. Increasing asymmetry in Bloch oscillations with increasing U/t.

3. Dynamics after initializing equal population in two modes with variable relative phase. Current switching should occur at large enough interaction strength.

[1] F. A. An, E. J. Meier, J. Ang'ong'a, and B. Gadway, *Phys. Rev. Lett.* **120**, 040407 (2018).

[2] R. Labouvie, B. Santra, S. Heun, S. Wimberger, and H. Ott, *Phys. Rev. Lett.* **115**, 050601 (2015).

[3] A. Reinhard, J.-F. Riou, L. A. Zundel, D. S. Weiss, S. Li, A. M. Rey, and R. Hipolito, *Phys. Rev. Lett.* **110**, 033001 (2013).

Dynamics and Thermodynamics of Strongly Interacting Homogeneous Bose Gases

Timon Hilker[1], **Christoph Eigen**[1], **Jake Glidden**[1], **Lena Bartha**[1], **Raphael Lopes**[1], **Nir Navon**[1,2], **David Clément**[3], **Eric Cornell**[4], **Robert Smith**[1,5], **and Zoran Hadzibabic**[1]

[1] *Cavendish Laboratory, University of Cambridge CB3 0HE, United Kingdom*

[2] *Departament of Physics, Yale University, New Haven, Connecticut 06511, USA*

[3] *Laboratoire Charles Fabry, Institut dOptique, Université Paris-Saclay, 91127 Palaiseau, France*

[4] *JILA, NIST, University of Colorado, and Department of Physics, Boulder, Colorado 80309-0440, USA*

[5] *Claredon Laboratory, University of Oxford, Oxford OX1 3PU, United Kingdom*

e-mail: *tah48@cam.ac.uk*

We study homogeneous ^{39}K Bose gases with tunable contact interactions and we give an overview of recent experimental and theoretical research topics.

We present measurements of the dynamics of Bose gases quenched to unitarity, where the s-wave scattering length diverges. Our work includes measurements of the atom loss, molecular correlation and momentum (re)distribution dynamics [1, 2]. In particular, we study the coherent time evolution at short times before heating and losses dominate [1]. In degenerate samples we observe universal post-quench dynamics in agreement with the emergence of a pre-thermal state. In thermal gases, dynamics and thermodynamic properties generically depend on both the gas density n and temperature T, but we find that they can still be expressed in terms of universal dimensionless functions.

We also present our results of the quantum depletion of a Bose-Einstein condensate due to interactions [3], which confirm the 70-year-old theory of Bogoliubov.

Finally, we discuss the surprising fact that three-body loss can lead to the cooling and even the purification of Bose gases.

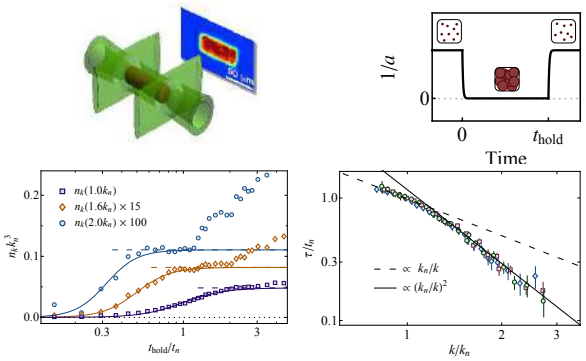


Figure 1: After a BEC is quenched to unitarity, the dynamics per mode k shows two separated timescales: a fast, coherent dynamics and a slower heating rate connected to losses [1]. We analyse the coherent evolution and find a universal description in terms of the Fermi length scale $k_n = (6\pi n)^{1/3}$ and Fermi time $t_n = 2m/\hbar k_n^2$. Scaled by these numbers, the initial growth time τ is given by a low and high k algebraic scaling.

References

[1] C. Eigen, J. A. P. Glidden, R. Lopes, E. A. Cornell, R.P. Smith, Z. Hadzibabic, ArXiv 1805.09802 (2018)

[2] C. Eigen, J. A. P. Glidden, R. Lopes, N. Navon, Z. Hadzibabic, R. P. Smith, Phys. Rev. Lett. **119** 250404 (2017)

[3] R. Lopes, C. Eigen, N. Navon, D. Clément, R. P. Smith, Z. Hadzibabic, Phys. Rev. Lett. **119** 190404 (2017)

Supersolid Phase with Ultracold Bose Gases in an Optical Lieb Lattice

Hisashi Kawaguchi, Daisuke Yamamoto, and Nobuo Furukawa

Department of Physics and Mathematics, Aoyama-Gakuin University, Sagamihara, Kanagawa 252-5258, Japan

e-mail: *h-kawaguchi@phys.aoyama.ac.jp*

Supersolid is an exotic phase of matter that possesses both diagonal (solid) and off-diagonal (superfluid) long-range orders. For lattice systems, the previous numerical simulations [1] and theoretical considerations [2] on extended Bose-Hubbard models have demonstrated the importance of long-range interactions between particles for realizing stable supersolids. On the other hand, Huber and Altman have shown that a supersolid state can be stabilized even in the absence of explicit long-range interactions for a frustrated kagome system with a dispersionless energy band (flat band) [3].

Recently, Takahashi's group at Kyoto has realized the Lieb-lattice geometry with an optical lattice [4], and has succeeded in coherent transfer of a Bose-Einstein condensate of ^{174}Yb atoms into the first excited energy band, which is completely dispersionless. Motivated by this seminal experiment, here we theoretically study the quantum phases of bosonic particles loaded into the flat band of the Lieb optical lattice. We consider the following Bose-Hubbard model:

$$\mathcal{H} = -\sum_{\langle i,j\rangle} J_{i,j} \hat{b_i}^\dagger \hat{b_j} + \frac{U}{2}\sum_i \hat{n_i}(\hat{n_i}-1) - \mu \sum_i \hat{b_i}^\dagger \hat{b_i}, \tag{1}$$

where $J_{i,j}$ takes $(1+\delta)J$ and $[(1-\delta)J]$ for the thick [thin] bonds shown in Fig. 1(a). Diagonalizing the non-interacting part of the Hamiltonian, we obtain the three energy bands of the Lieb lattice. We can see in Fig. 1(b) that the first excited band is completely dispersionless with respect to the wave vector $\boldsymbol{k}$. This indicates the existence of single-particle eigenstates localized on a loop consisting of several sites [see Fig. 1(a)]. Such localized single-particle states do not feel the one-site interaction U as long as they overlap each other. Therefore, any direct-product arrangement of localized single-particle states constitutes an exact eigenstate of the whole Hamiltonian (1). At $\nu = \nu_c$, the lattice is close-packed with the smallest (four-site) localized single-particle states, which can be regarded as a solid (Wigner crystal) with a discrete translational symmetry breaking.

For the density $\nu > \nu_c = 1/6$, we employ the projection method that has been used for the kagome system by Huber and Altman [3]. We project the Hamiltonian onto the flat Bloch band on the basis of the Wannier function given as the eigenstate for the flat energy band. In order to make the flat band more isolated [see Fig. 1(b)] and improve the effective description with the well-localized Wannier function, we introduce a finite gap Δ with $\delta \neq 0$ [5]. Applying the standard mean-field approximation to the effective model, we calculate the superfluid and solid order parameters Ψ and $\nu_{\rm solid}$ to identify the quantum state as a function of the particle doping $\delta\nu = \nu - \nu_c$ on the solid. In the poster presentation, we present the obtained phase diagram in the plane of δ versus $\delta\nu$, and discuss a possible formation of supersolid states due to the flat band.

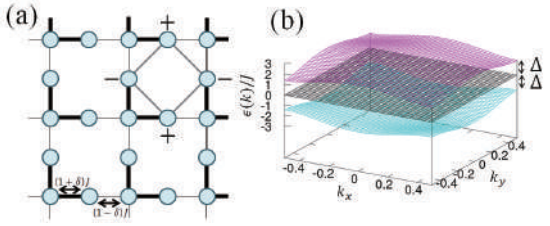


Figure 1: (a)The Lieb lattice. We introduce a staggered moderation in the hopping amplitude to open a band gap. (b) The three branches of the energy band of the Lieb lattice with the band gap $\Delta = 2\sqrt{2}\delta$.

[1] B. Capogrosso-Sansone *et al.*, Phys. Rev. Lett. **104**, 125301 (2010); L. Pollet *et al.*, Phys. Rev. Lett. **104**, 125302 (2010).

[2] D.Yamamoto, A. Masaki, and I. Danshita, Phys. Rev. B **86**, 054516 (2012).

[3] S. D. Huber and E. Altman, Phys. Rev. B **82**, 184502 (2010).

[4] S. Taie *et al.*, Sci. Adv. **1**, 1500854 (2015).

[5] A. Julku *et al.*, Phys. Rev. Lett. **117**, 045303 (2016).

Squeezed field description of second sound in Bose-Einstein condensates

L. Mathey, Ilias M. H. Seifie, Vijay Pal Singh
Zentrum für Optische Quantentechnologien, Universität Hamburg, 22761 Hamburg, Germany
Institut für Laserphysik, Universität Hamburg, 22761 Hamburg, Germany
The Hamburg Center for Ultrafast Imaging, Luruper Chaussee 149, Hamburg 22761, Germany
e-mail: *lmathey@physnet.uni-hamburg.de*

We study the second sound mode of Bose Einstein condensates in the weakly interacting regime. We explicitly take the dynamics of the squeezing of the order parameter into account which results in a extended effective action. By considering the classical trajectory, which constitutes a generalization of the Gross-Pitaevskii equation, we recover both the Bogolyubov mode and its dispersion, as well as a second excitation mode which we identify with the second sound mode. We discuss the generality of this approach, which gives a new perspective on condensate dynamics and other many-body systems.

Universal few-body correlations in a Bose polaron

S. Endo[1], **S. M. Yoshida**[2], **J. Levinsen**[3], **and M. M. Parish**[3]

[1] *Frontier Reserach Institute for Interdisciplinary Science and Department of Physics, Tohoku University, 6-3 Aoba, Aramaki-aza, Aobaku, Sendai, Japan*

[2] *Department of Physics, University of Tokyo, 7-3-1 Hongo, Bunkyo-ku,Tokyo, Japan*

[3] *School of Physics and Astronomy, Monash University, 19 Rainforest Walk, Clayton, VIC, Australia*

e-mail: *shimpei.endo@nucl.phys.tohoku.ac.jp*

We study physical properties of an atom embedded in condensates of bosonic atoms. This system has recently been realized in cold atom experiments and is referred to as the "Bose polaron" [1, 2]. In contrast to Fermi polaron systems [3, 4], the Bose system can show Efimov physics [5, 6, 7], so that 3-body and associated few-body clusters can appear. We investigate how these Efimov physics can affect quantum many-body behavior in the Bose polaron system. In particular, with a recently developed variational wave function [8], we theoretically study how the Efimov states and their associated length scale can characterize the Bose polaron, and unveil the crucial role of few-body correlations in the Bose polaron.

[1] M. G. Hu, *et al.* Phys. Rev. Lett. 117, 055301 (2016).

[2] N. Jorgensen, *et al.* Phys. Rev. Lett. 117, 055302 (2016).

[3] A. Schirotzek, *et al.* Phys. Rev. Lett. 102, 230402 (2009).

[4] M. Cetina, M. Jag, R.S. Lous, I. Fritsche, J.T. M. Walraven, R. Grimm, J. Levinsen, M.M. Parish, R. Schmidt, M. Knap, E. Demler, Science 354, 96 (2016).

[5] V. Efimov, Phys. Lett. B, 33, 563 (1970).

[6] P. Naidon, S. Endo, Rep. Prog. Phys. 80, 056001 (2017).

[7] C. H. Greene, P. Giannakeas, J. Perez-Rios, Rev. Mod. Phys. 89, 035006 (2017).

[8] J. Levinsen, M.M. Parish, G. M. Bruun, Phys. Rev. Lett. 115, 125302 (2015).

Spin-dependent artificial magnetic fields and superfluidity in Bose-Einstein condensates

B. D. Smith[1], **L. C. Clark**[1], **A. Rastogi**[1], **T. Hrushevskyi**[1], **E. Saglamyurek**[1], **and L. J. LeBlanc**[1]

[1] *Department of Physics, University of Alberta, Edmonton AB T6G 2E1, Canada*
e-mail: *lindsay.leblanc@ualberta.ca*

The exquisite control available in ultracold quantum gas experiments has enabled the emulation of many different quantum systems and allowed us to better understand the many-body states of quantum matter [1]. Among the many tools for manipulating atoms in these experiments is the ability to tailor the kinetic energy terms in the Hamiltonian, which opens up the possibility for artificial gauge fields [2].

In this project, we consider a spatially- and spin-dependent gauge potential $\vec{\mathcal{A}}_\sigma(\vec{r})$, where the kinetic energy is modified from the free-particle value ($\mathcal{H} = \hbar^2\vec{k}^2/2m$) to

$$\mathcal{H} = \frac{\hbar^2\left[\vec{k} - \vec{\mathcal{A}}_\sigma(\vec{r})/\hbar\right]^2}{2m^*}, \qquad (1)$$

where $\sigma = (\uparrow, \downarrow)$ denotes the spin. When $\vec{\mathcal{A}}_\sigma(\vec{r}) = \vec{\mathcal{A}}(\vec{r})\check{\sigma}_z$ (the gauge potential's sign depends on the spin) and $\vec{\mathcal{A}}(\vec{r}) = (-\mathcal{B}y, 0, 0)$ (the Landau gauge), the system has a spin-dependent magnetic field

$$\vec{\mathcal{B}}_\sigma = \mathcal{B}\check{\sigma}_z. \qquad (2)$$

. In the limit of strong-enough $\mathcal{B}$, vortices should enter the system [3, 4] but will have opposite circulation for each spin. This raises several questions: Can vortices of opposite rotation be introduced into the same condensate? Is the threshold for vortex nucleation the same as a single-component system? What are the stable spatial configurations of vortices? How do inter-spin interactions affect all of these?

We first investigate the effects of a spin-dependent artificial magnetic field in a BEC using numerical simulations of the Gross-Pitaevskii equation, including evaluating the onset of vortex nucleation in the ground state, and evaluating the vortex nucleation for different interspin interactions.

Next we have begun experiments in our laboratory, where we make optically trapped Bose-Einstein condensates of ^{87}Rb atoms (Fig. 1). Using Raman transitions, we couple the Zeeman sublevels of the ground state to transfer momentum in a spin-dependent way and realize a spin-dependent gauge potential. Using this, we are working towards the creation of a spin-dependent artificial magnetic field, which, in analogy to Raman-induced artificial magnetic field [5], we use real magnetic field gradients to make the spin-orbit coupled system spatially dependent, thus introducing a spin-dependent artificial magnetic field [6]. We will discuss our progress towards studying the superfluid properties of the BEC in this environment, including the development and dynamics of spin-dependent vortices. In light of our preliminary GPE calculations, possible states that we will prepare to measure include those of paired vortices, phase separation, and/or stripes. In future experiments, we plan to use a species with an accessible Feshbach resonance (^{39}K) to emulate the effects of different interspin interactions, with the expectation that this will lead to an even richer collection of many-body phases.

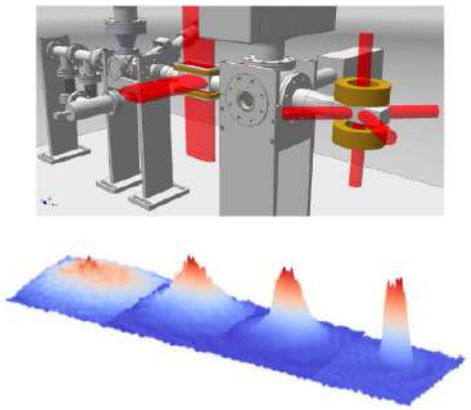


Figure 1: Experiment. Top: Schematic of Rb-K BEC apparatus. Bottom: Momentum distributions during progression to condensation of 10^5 ^{87}Rb atoms from above the transition temperature (left) to below (right).

[1] I. Bloch, J. Dalibard, and S. Nascimbène, Nat. Phys. **8**, 267 (2012).

[2] N. Goldman, G. Juzeliunas, P. Öhberg, and I. B. Spielman, Reports Prog. Phys. **77**, (2014).

[3] Y. J. Lin, K. Jiménez-García, and I. B. Spielman, Nature **471**, 83 (2011).

[4] J. Radić, T. A. Sedrakyan, I. B. Spielman, and V. Galitski, Phys. Rev. A **84**, 063604 (2011).

[5] Y. J. Lin *et al.*, Nature **462**, 628 (2009).

[6] M. C. Beeler *et al.*, Nature **498**, 201 (2013).

Collective oscillations of a strongly interacting 2D Fermi gas

P. Dyke[1,2], **I. Herrera**[1], **C. N. Kuhn**[1,2], **S. Hoinka**[1,2], **and C. J. Vale**[1,2]

[1] *Swinburne University of Technology, Centre for Quantum and Optical Science, Melbourne, Australia, 3122*

[2] *ARC Centre of Excellence in Future Low-Energy Electronics Technologies, Australia*

e-mail: *pdyke@swin.edu.au*

The ability to tune the interactions and dimensionality in ultracold gases of fermionic atoms provides a versatile platform to study many-body quantum phenomena; allowing new ways to investigate condensed matter physics in an environment free of defects. One example is a two-component two dimensional (2D) Fermi gas with tunable interactions that will allow the study of the Berezinskii-Kosterlitz-Thouless mechanism in Fermi superfluids.

In our experiments, ultracold 2D Fermi gases of ^{6}Li atoms are formed between the antinodes of a cylindrically focused, blue detuned, TEM_{01} mode laser beam potential combined with a weak magnetic field curvature. This produces a highly oblate trapping potential and provides tight and highly harmonic confinement, allowing us to routinely produce clouds with an aspect ratio of >250 [1], as shown in Fig. 1.

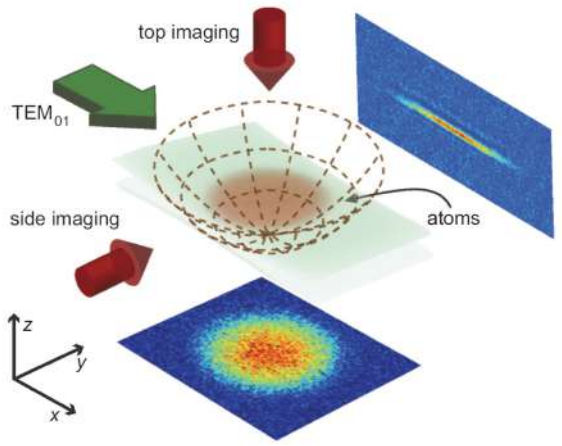


Figure 1: Experimental setup for producing 2D clouds.

We present our measurements of collective oscillations, specifically the breathing mode frequency of a 2D Fermi gas of ^{6}Li atoms throughout the 2D to 3D crossover. The breathing mode corresponds to an oscillation in the radial width, changing the overall volume of the cloud and can be used to probe the adiabatic compressibility and hence the thermodynamic equation of state of the gas, which depends on the dimensionality, interactions and temperature. We also present measurements verifying the existence of a quantum anomaly in the deep 2D regime [2, 3]. A scaling symmetry of the classical theory is broken in the renormalised quantum theory that leads to an upshift in the frequency of the breathing mode from its scale invariant value of $2\omega_r$ [4].

[1] P. Dyke, K. Fenech, T. Peppler, M. G. Lingham, S.Hoinka, W. Zhang, S.-G. Peng, B.Mulkerin, H. Hu, X.-J. Liu, and C. J. Vale, Phys. Rev. A. **93**, 011603(R) (2016).

[2] M. Olshanii, H. Perrin, and V. Lorent, Phys. Rev. Lett. **105**, 095302 (2010).

[3] J. Hofmann, Phys. Rev. Lett. **108**, 185303 (2012).

[4] T. Peppler, P. Dyke, M. Zamorano, S. Hoinka, and C. J. Vale, preprint at https://arxiv.org/abs/1804.05102 (2018)

Bistability and non-equilibrium condensation in a driven-dissipative atomic superfluid

Matthew T. Reeves[1] **and Matthew J. Davis**[1]

[1] *Australian Research Council Centre of Excellence in Future Low-Energy Electronics Technologies, School of Mathematics and Physics, University of Queensland, St Lucia, QLD 4072, Australia.*
e-mail: *m.reeves@uq.edu.au*

Dissipation and decoherence are often undesirable in quantum systems, as they tend to wash out interesting quantum inteference effects. However, in recent years it has been realized that adding controlled sources of dissipation to many-body quantum systems can allow engineering of novel quantum states of matter. For example, appropriate environment coupling can generate robust entangled states [1], or enable dissipative quantum computation protocols [2]. Further, the addition of driving allows controlled study of non-equilibrium steady-states, which can exhibit emergent and exotic properties that cannot be achieved at or near equilibrium [3]. Ultracold atomic gases, simultaneously offering high experimental control and tractable theoretical models, naturally serve as ideal simulators for exploring these non-equilibrium phenomena. In a recent experiment Labouvie *et al.* [4] studied a prototypical non-equilibrium quantum system: a driven-dissipative Josephson junction array. The system was comprised of an atomic BEC loaded in a one-dimensional optical lattice, with dissipation introduced by a focussed electron beam, and driving provided by the neighbouring sites [Fig. 1].

We develop a minimal model of this system within the framework of c-field theory, describing the lossy site dynamics in terms of an AC-driven and dissipative stochastic Gross-Pitaevskii equation. The c-field model is found to reproduce the key features of the experiment that were not captured by Josephson or single-particle models, namely: i) bistability, ii) the associated non-equilibrium phase diagram and iii) critical slowing down in the lower branch of the bistable region. Our model suggests the critical slowing down is due to a non-equilibrium condensation phenomenon occurring into an excited harmonic oscillator mode, occuring at sufficiently large driving frequencies. A clear signature appears as a distinct peak in the atom number fluctuations, and should thus be readily detectable in current cold atoms experiments. Our model is closely related to the so-called Lugiato-Lefever equation, and thus draws new connections between nonequilibrium dynamics of ultracold atoms with nonlinear optics, exciton-polaritons [5, 6], and driven-damped sine-Gordon systems [7].

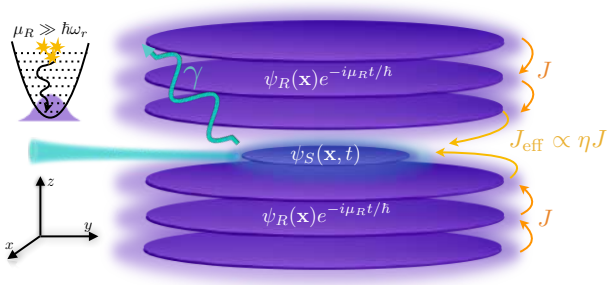


Figure 1: Schematic of the system. A large prolate BEC loaded into a 1D optical lattice produces a long chain of quasi-2D condensates. Dissipation at a rate γ is introduced to a single site by an electron beam, and driving by the neighbouring sites which act as a particle resevoir. The effective driving is filling dependent, determined by both the lattice tunnelling rate J and the radial overlap η. The chemical potential of the driving reservoirs, μ_R, is much larger than the radial harmonic oscillator spacing; for a nearly depleted site, particles are too energetic to access the groundstate, and instead must tunnel to a nearby excited state and relax via collisions.

[1] G. Kordas, S. Wimberger, and D. Witthaut, EPL (Europhysics Letters) **100**, 30007 (2012).

[2] F. Verstraete, M. M. Wolf, and J. I. Cirac, Nature physics **5**, 633 (2009).

[3] National Research Council and Solid State Sciences Committee and others, Condensed-Matter and Materials Physics: The Science of the World Around Us, Vol. 4 (National Academies Press, 2008).

[4] R. Labouvie, B. Santra, S. Heun, and H. Ott, Phys. Rev. Lett. **116**, 235302 (2016).

[5] S. Rodriguez, A. Amo, I. Sagnes, L. Le Gratiet, E. Galopin, A. Lemaître, and J. Bloch, Nature communications **7**, 11887 (2016).

[6] M. Foss-Feig, P. Niroula, J. T. Young, M. Hafezi, A. V. Gor- shkov, R. M. Wilson, and M. F. Maghrebi, Phys. Rev. A **95**, 043826 (2017).

[7] M. A. Ferré, M. G. Clerc, S. Coulibally, R. G. Rojas, and M. Tlidi, The European Physical Journal D **71**, 172 (2017).

Synthetic Frustrated Antiferromagnets with Coherently-Coupled Binary Fermi Gases in a Triangular Optical Lattice

D. Yamamoto[1], **G. Marmorini**[2], **M. Tabata**[1], **K. Sakakura**[1], **and I. Danshita**[3]

[1] *Department of Physics and Mathematics, Aoyama Gakuin University, Sagamihara, Kanagawa 252-5258, Japan*

[2] *Research and Education Center for Natural Sciences, Keio University, Kanagawa 223-8521, Japan*

[3] *Department of Physics, Kindai University, Higashi-Osaka, Osaka 577-8502, Japan*

e-mail: *d-yamamoto@phys.aoyama.ac.jp*

In recent years, many theoretical and experimental attempts have been made to emulate some fundamental models in condensed-matter physics, such as the Hubbard model, with cold atomic gases in an optical lattice. For instance, the frustrated classical XY model has been realized with bosonic atoms in a triangular optical lattice [1]. More recently, Greiner's group at Harvard emulated the Hubbard model on the square lattice with a binary mixture of ultracold fermions and realized the long-range Néel order [2].

Motivated by the success in Ref. [2], we further push the cold-atom simulator to the next step by investigating a quantum simulation of frustrated magnetism. Here we consider an "optical synthesis" of triangular-lattice antiferromagnets with a two-component ($\sigma =\uparrow,\downarrow$) mixture of Fermi atomic gases trapped into a triangular optical lattice [3]. The Hamiltonian of the model is given by

$$\hat{\mathcal{H}} = -\sum_{\langle i,j\rangle,\sigma} t_\sigma \left(\hat{c}^\dagger_{i\sigma}\hat{c}_{j\sigma} + \text{H.c.}\right) + U\sum_i \hat{n}_{i\uparrow}\hat{n}_{i\downarrow} + \Omega\sum_i \left(\hat{c}^\dagger_{i\uparrow}\hat{c}_{i\downarrow} + \hat{c}^\dagger_{i\downarrow}\hat{c}_{i\uparrow}\right)/2, \quad (1)$$

where we introduce component-dependent hoppings t_σ, intercomponent repulsion U, and coherent coupling Ω between the two components. This Hamiltonian can be engineered in the laboratory with the combination of the currently available techniques.

In order to discuss the frustrated magnetism of the model, we first derive an effective spin model for dominant interactions ($U/t_\sigma \gg 1$),

$$\hat{\mathcal{H}} = \sum_{\langle i,j\rangle}\left(J\hat{S}^x_i\hat{S}^x_j + J\hat{S}^y_i\hat{S}^y_j + J_z\hat{S}^z_i\hat{S}^z_j\right) - H\sum_i \hat{S}^x_i, \quad (2)$$

in which the hopping imbalance $J/J_z \equiv 2t_\uparrow t_\downarrow/(t_\uparrow^2 + t_\downarrow^2)$ and $H = -\Omega$ play the roles of the XXZ-type exchange anisotropy and transverse magnetic fields, respectively, in the spin language. Using the numerical cluster mean-field method with cluster-size scaling [4], we demonstrate that the ground-state phase diagram shows a rich variety of quantum magnetic phases [Fig. 1(a)], in contrast to the featureless phase diagram for the classical counterpart of the same spin model [Fig. 1(b)]. The difference between the quantum and classical diagrams stems from the order-by-disorder mechanism. We also perform Monte-Carlo simulations, and find that thermal fluctuations induce an unexpected two-step transition with partial symmetry restoration. The estimated transition temperature is smaller but in the same order of magnitude as the currently achievable temperature (~ 0.45 of the spin exchange energy [2]), which provides a guidepost for future developments of cold-atom quantum simulators for frustrated magnetism.

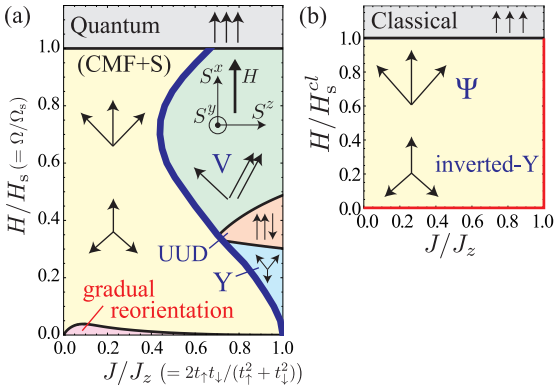


Figure 1: (a) Quantum and (b) classical ground-state phase diagrams of the spin Hamiltonian (2). The three arrows of each magnetic phase illustrate the spin moments on the three sublattices.

[1] J. Struck *et al.*, Science **333**, 996 (2011).

[2] A. Mazurenko *et al.*, Nature **545**, 462 (2017).

[3] D. Yamamoto, G. Marmorini, M. Tabata, K, Sakakura, and I. Danshita, in preparation.

[4] D. Yamamoto, G. Marmorini, and I. Danshita, Phys. Rev. Lett. **112**, 127203 (2014); *ibid*, **112**, 259901 (2014).

Self-bound Bose mixtures

Clemens Staudinger[1], **Ferran Mazzanti**[2], **and Robert E. Zillich**[1]
[1] *Institute for Theoretical Physics, Johannes Kepler University, Altenbergerstrasse 6 9, 4040 Linz, Austria*
[2] *Departament de Física i Enginyeria Nuclear, Campus Nord B4-B5, Universitat Politècnica de Catalunya, E-08034 Barcelona, Spain*
e-mail: *robert.zillich@jku.at*

Ultracold quantum gases usually require a trapping potential to hold the cloud of atoms together. An exception is the case of dipolar quantum gases which can form self-bound droplets, but recent experiments [1, 2] found that also binary Bose mixtures can form such self-bound ultra-dilute liquid droplets, confirming the predictions [3, 5] based on a beyond mean-field approxiamtion [4], see also [6]. In the liquid regime, the inter-species attraction overcompensates the intra-species repulsion resulting in a small net attraction and hence a self-bound ground state.

We proceed beyond the beyond-mean-field approximation, and study liquid Bose mixtures using a variational *pair density* functional theory, the hypernetted-chain Euler Lagrange (HNC-EL) method. The HNC-EL methods accounts for correlations non-perturbatively by using a multi-component Jastrow-Feenberg ansatz [7]

$$\Psi_0 = \exp\left[\frac{1}{4}\sum_{\alpha,\beta}\sum_{i,j}{}' u_{\alpha,\beta}(|\mathbf{r}_{i,\alpha} - \mathbf{r}_{j,\beta}|)\right]$$

where a Greek index labels the component and a Latin index numbers the atoms. The correlations $u_{\alpha,\beta}$ are obtained by functional optimization $\delta e/\delta g_{\alpha,\beta}(r) = 0$ of the energy per particle e, where $g_{\alpha,\beta}(r)$ is the pair distribution function, and closure of the resulting equations is achieved by summation of Meyer cluster diagrams in the hyper-netted chain approximation. The HNC-EL energy functional is real also in the liquid regime, unlike in the beyond-mean-field approximation which yields complex energies.

We focus on the case of a mixture of uniform density, as it would be realized inside large saturated droplets, a regime not yet reach in experiments [1, 2]. Using ^{39}K and values for the scattering lengths as the experiments, we study the conditions for stability against evaporation of one of the components, i.e. both chemical potentials μ_1 and μ_2 need to be negative, and against liquid-gas phase separation (the "spinodal instability" driven by infinitesimal density fluctuations), the latter being accompanied by a vanishing speed of sound. Dilute Bose mixtures are stable only in a very narrow regime of partial densities ρ_1 and ρ_2, near an optimal ratio ρ_1/ρ_2 and near the total energy minimum, which defines the equilibrium (Fig. 1). We find that, despite the low density, the equilibrium densities and energies depend also on the effective ranges, not just universally on the s-wave scattering lengths [8].

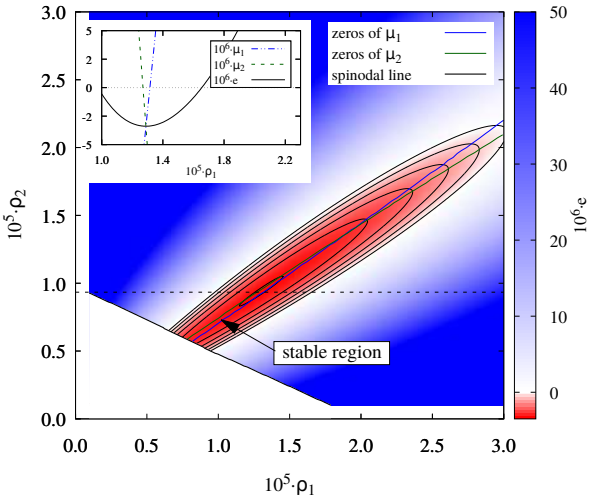


Figure 1: Total energy per particle e as function of ρ_1 and ρ_2. The lines indicate the spinodal instability (black), and the zeroes of the chemical potentials μ_1 (blue) and μ_2 (green). Only in the narrow region pointed at by the arrow the mixture is stable against evaporation. The inset shows e and the chemical potentials μ_1 and μ_2 along the dashed line intersecting the energy minimum.

[1] C. R. Cabrera, L. Tanzi, J. Sanz, B. Naylor, P. Thomas, P. Cheiney, and L. Tarruell, Science 359, 301 (2018).
[2] G. Semeghini, G. Ferioli, L. Masi, C. Mazzinghi, L. Wolswijk, F. Minardi, M. Modugno, G. Modugno, M. Inguscio, and M. Fattori, ArXiv e-prints (2017), arXiv:1710.10890 [cond-mat.quant-gas].
[3] D. S. Petrov, Phys. Rev. Lett. 115, 155302 (2015).
[4] D. M. Larsen, Ann. Phys. 24, 89 (1963).
[5] D. S. Petrov and G. E. Astrakharchik, Phys. Rev. Lett. 117, 100401 (2016).
[6] V. Cikojevic, K. Dzelalija, P. Stipanovic, L. Vranjes Mar- kic, and J. Boronat, Phys. Rev.

B 97, 140502 (2018).
[7] M. Hebenstreit, M. Rader, and R. E. Zillich, Phys. Rev. A 93, 013611 (2016).
[8] C. Staudinger, F. Mazzanti, and R. E. Zillich, ArXiv e-prints (2018), arXiv:1805.06200 [cond-mat.quant-gas].

Superfluidity of Light in an atomic vapor

Quentin Fontaine, Alberto Bramat, Tom Bienaimé, Quentin Glorieux
Laboratoire Kastler Brossel, Sorbonne Université, ENS-PSL Research University, Collège de France, CNRS
4 place Jussieu Case 74, F-75005 Paris, France
quentin.glorieux@lkb.ens.fr

Abstract: We investigate the dispersion relation of small amplitude density waves propagating on top of a photon fluid. We also present two ongoing experiments to study dispersive shock waves and observe superfluidity of light.
OCIS codes: (020.0020) Atomic and molecular physics; (190.0190) Nonlinear optics

1. Introduction and experimental platform

Recently, the field of quantum fluids of light demonstrated several milestone results such as photon condensation, light superfluidity and the observation of topological excitations (solitons and vortices) [1]. Up to now, these experiments rely on confined geometries (semiconductor micro-cavities or cavities filled with dye molecules).

In our experiment, we develop an alternative platform to study quantum fluids of light where light propagates inside a nonlinear Kerr medium rather than being trapped inside a cavity. In this case, the dynamics of the system is conservative in contrast to the driven-dissipative nature of micro-cavity setups. Such systems have been implemented in photorefractive crystals [2] and thermo-optic nonlinear medium [3]. Our platform consists in a laser

$$i\frac{\partial A}{\partial z}=-\frac{1}{2k_0}\nabla_\perp^2 A-\gamma|A|^2 A,$$

field propagating through a hot rubidium atomic vapor [4]. In the paraxial approximation the evolution of the transverse electric field envelope A is described by a 2D Gross-Pitaevskii equation [5]:

where z is the direction of propagation, $\lambda=2\pi/k_0$ is the wavelength of light and $\gamma=k_0 n_2$ describes the strength of photon-photon interactions. Experimentally, we can access to the "temporal-like" evolution of the photon fluid by imaging different transverse planes along the direction of propagation (see Fig. 1). As such, this system is a promising platform to study phenomena related to Bose-Einstein condensation and superfluidity of light.

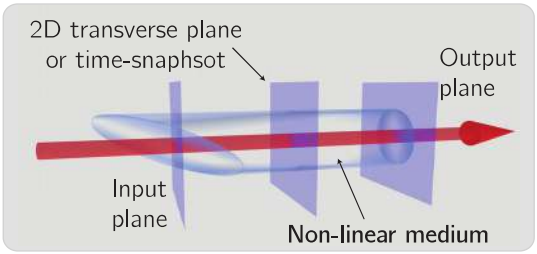


Fig. 1. Scheme of the experimental setup.

2. Bogoliubov dispersion relation and shock-wave dynamics

20 years ago, Chiao and Boyce theoretically investigated the problem of the Bogoliubov dispersion relation for a weakly interacting photon gas trapped inside a cavity [6]. Interestingly, no experiments were reported thereafter. Here, we measure the dispersion relation of small amplitude density waves propagating on top of a photon fluid. Fig. 2 a) shows a preliminary experimental curve. We obtain a dispersion relation of Bogoliubov type [7]:

$$k(q)=\sqrt{\frac{q^2}{k_0}\left(\frac{q^2}{4k_0}+\gamma I\right)},$$

where I is the intensity of the background photon fluid. This dispersion is linear at small wave vector, as expected in the superfluid regime, and "particle-like" (quadratic) at larger wave vectors. In the superfluid regime, we

characterize the dependence of the sound velocity with intensity (photon density) and compare our results with theoretical predictions.
When the perturbation on top of the photon fluid becomes large, it can propagate faster than the local speed of sound. This leads to the generation of dispersive shock waves as seen in Fig. 2 b). We discuss and analyze the

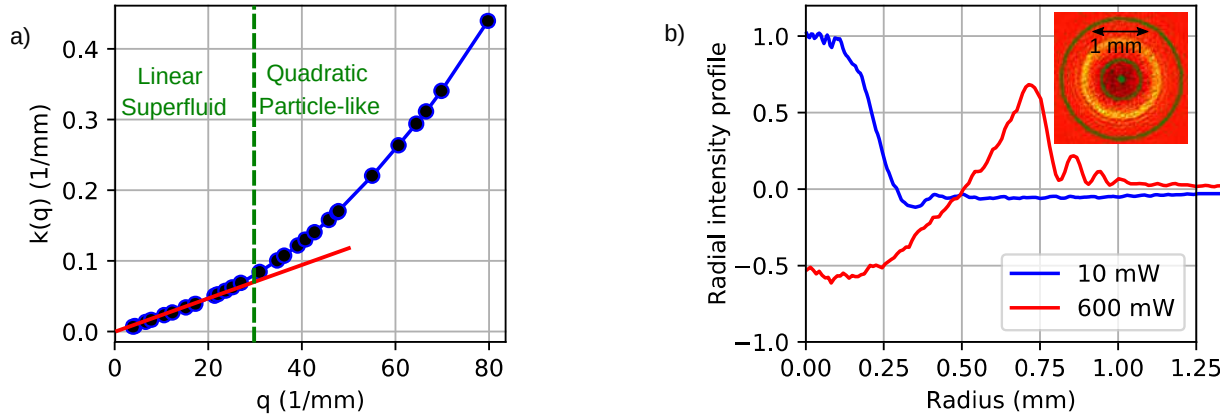


Fig. 2. a) Dispersion relation of small amplitude density waves propagating on top of a photon fluid. b) Radial intensity profiles (superfluid background substracted) at the output plane of the cell at low (blue) and high (red) intensities. At high intensity, dispersive shock waves are observed. Inset: 2D intensity profile at high intensity – radial averaging around the green marker leads to the red curve.

peculiar dynamics of these waves and confront our observations to analytical and numerical models.

3. Outlook: optomechanical signature of light superfluidity

Observing a linear dispersion relation at low momentum is a necessary but not sufficient condition to characterize a superfluid state. A "smoking gun" evidence of superfluidity is the cancellation of the drag force on a defect. This effect was recently investigated in a bulk photo-refractive crystal using an optical defect [8].
We present an ongoing experiment to test light superfluidity by studying the drag force that a photon fluid exerts on a material mobile obstacle. This experiment is based an nanofiber, immersed in an atomic vapor so that the refractive-index mismatch provides a constant potential. A light beam hitting the nanofiber tip at a small angle, will create a flow around the impurity, or in optics language, a radiation pressure force resulting in the optomechanical deformation of the obstacle. We expect to observe a cancellation of this "optical drag force" at high intensity indicating a superfluid flow of photons around the obstacle. In terms of optics, this leads to a non-intuitive cancellation of the radiation pressure thanks to nonlinear interactions [9].

[1] I. Carusotto and C. Ciuti, "Quantum fluids of light", Rev. Mod. Phys. **85,** 299-366 (2013).

[2] W. Wan, S. Jia, and J. W. Fleischer, "Dispersive superfluid-like shock waves in nonlinear optics", Nat. Phys. **3**, 46-51 (2007).

[3] D. Vocke, T. Roger, F. Marino, E. M. Wright, I. Carusotto, M. Clerici, and D. Faccio, "Experimental characterization of nonlocal photon fluids", Optica **2**, 484-490 (2015).

[4] N. Šantic, S. Salem, J. Garnier, A. Fusaro, A. Picozzi, and R. Kaiser , "Non-equilibrium precondensation of classical waves propagating through atomic vapors", Phys. Rev. Lett. **120**, 055301 (2018).

[5] I. Carusotto, "Superfluid light in bulk nonlinear media", Proc. R. Soc. A **470,** 20140320 (2014).

[6] R.Y. Chiao and. J Boyce, "Bogoliubov dispersion relation and the possibility of superfluidity for weakly interacting photons in a two-dimensional photon fluid", Phys. Rev. A **60**, 4114 (2014).

[7] P.E. Larré, S. Biasi, F. Ramiro-Manzano, L. Pavesi, and I. Carusotto, "Pump-and-probe optical transmission phase shift as a quantitative probe of the Bogoliubov dispersion relation in a nonlinear channel waveguide", Eur. Phys. J. D **71**, 146 (2017).

[8] C. Michel, O. Boughdad, M. Albert, P.-É. Larré, and M. Bellec, "Experimental Observation of the Drag Force Suppression in a Flow of Superfluid Light*"*, arXiv:1710.03081 (2017).

[9] P.E. Larré and I. Carusotto, "Optomechanical signature of a frictionless flow of superfluid light", Phys. Rev. A **91**, 053809 (2015).

Interaction control and interorbital molecules exploiting clock transition in two electron atoms

L. Franchi[1,3], L. F. Livi[1,2,3], D. Tusi[1], D. Benedicto-Orenes[2], G. Cappellini[1,2,3], M. Inguscio [2,1,4], J. Catani[2,4,3] and L. Fallani[1,2,3,4]

[1] *Dipartimento di Fisica e Astronomia, Università degli Studi di Firenze, I-50019 Sesto Fiorentino, Italy*

[2] *INO-CNR Istituto Nazionale di Ottica del CNR, Sede di Sesto Fiorentino, I-50019 Sesto Fiorentino, Italy*

[3] *INFN Istituto Nazionale di Fisica Nucleare, Sezione di Firenze, I-50019 Sesto Fiorentino, Italy*

[4] *LENS European Laboratory for Nonlinear Spectroscopy, I-50019 Sesto Fiorentino, Italy*
e-mail: *catani@lens.unifi.it*

Exploiting the recently-proposed mechanism of orbital Feshbach resonance (OFR) in two electron fermions [1, 2] we experimentally investigated the emergence of a strongly interacting regime [3] in a degenerate gas of ^{173}Yb atoms in different nuclear and electronic states and characterized the position of the resonance and its scaling with the magnetic field accordingly to fermionic Yb SU(N) symmetry. To this scope we make use of the optical clock transition typical of this kind of atoms.

The demonstration of the OFR mechanism has then allowed us to produce orbital molecules which we realized by means of clock-transition-based photoassociation in a 3D lattice. Optical coherent manipulation of the orbital molecules has then been employed to address free-to-bound and bound- to-bound processes connecting the molecular states with two unbound atoms in the first case and to molecules with different spin composition in the second case. In particular, bound-to-bound processes enabled by Raman transitions have been used as a detection tool of the molecular state, allowing us to characterize the molecular lifetime in a quasi-2D setting.

[1] R. Zhang, Y. Cheng, H. Zhai, and P. Zhang Phys. Rev. Lett. **115**, 135301 (2015).

[2] Y. Cheng, R. Zhang, and P. Zhang, Phys. Rev. A **95**, 013624 (2017).

[3] G. Pagano, M. Mancini, G. Cappellini, L. Livi, C. Sias, J. Catani, M. Inguscio, and L. Fallani Phys. Rev. Lett. **115**, 265301 (2015). *See related results in* M. Höfer et. al., Phys. Rev. Lett. **115**, 265302

Strong-coupling effects on p-wave contacts in an ultracold Fermi gas with a p-wave interaction

D. Inotani[1], **Y. Ohashi**[1]

[1] *Department of Physics, Keio University, 3-14-1 Hiyoshi, Kohoku-ku, Yokohama 223-8522, Japan*
e-mail: *dinotani@rk.phys.keio.ac.jp*

We theoretically investigate p-wave contacts, as well as asymptotic behavior of high momentum distribution in an ultracold Fermi gas with a uniaxially anisotropic p-wave interaction in the normal state[1]. Including p-wave pairing fluctuations within a strong-coupling theory developed by Nozières and Schmitt-Rink[2], we calculate the p-wave contacts defined from the adiabatic energy relations as $C_v^{(i)} = -2m\left(\frac{\partial\Omega}{\partial v_i^{-1}}\right)_{T,\mu}$ and $C_R^{(i)} = -2m\left(\frac{\partial\Omega}{\partial R_i^{-1}}\right)_{T,\mu}$, in a wide interaction and temperature region above the superfluid transition temperature T_c. Here Ω is the thermodynamic potential, m is the atomic mass, and v_i and R_i $(i = x, y, z)$ are the scattering volume and the effective range, respectively, of the p_i-wave interaction. We also obtain the asymptotic form of the high momentum distribution averaged over p_x-direction $\bar{n}(\rho)$ within our theoretical frame work as $\bar{n}(\rho) \to \frac{3\pi\bar{C}_v}{\rho} + \frac{3\pi\left(\bar{C}_R+\delta\right)}{2\rho^3}$ which has been experimentally observed[3]. Here $\rho = \sqrt{p_y^2 + p_z^2}$, $\bar{C}_v = C_v^{(x)} + \sum_{i=y,z} C_v^{(i)}/2$, and $\bar{C}_R = C_R^{(x)} + \sum_{i=y,z} 3C_R^{(i)}/2$ (Noting that we take x-axis being parallel to the Feshbach magnetic field). We find that an additional term which is not related to the thermodynamic potential appears in the sub-leading behavior in the high momentum distribution.

Figure 1 shows the temperature dependence of the p-wave contacts $\bar{C}_v$, $\bar{C}_R$, and the coefficient of the sub-leading term of the high momentum distribution. Although in low-temperature regime near T_c the effects of the additional term δ is negligible, as increasing the temperature δ gradually dominates the sub-leading behavior of the high momentum distribution even in the weak-coupling regime.

We also directory compare our theoretical predictions with the recent experimental results[3] by including the effects of the trap potential within the local density approximation. We find that our approximation qualitatively describes the experimental results in the weak- and intermediate-coupling region.

Since the p-wave contacts connect the thermodynamic properties with the microscopic properties of the p-wave interacting Fermi gas, our results are helpful for understanding of the strong-coupling effects in this unconventional strongly correlated Fermi system.

[1] D. Inotani, Y. Ohashi, arXiv:1804.06529 (2018).

[2] P. Nozières, and S. Schmitt-Rink, J. Low Temp. Phys. **59**, 195 (1985).

[3] C. Luciuk, S. Trotzky, S. Smale, Z. Yu, S. Zhang, and J. H. Thywissen, Nature Phys. **12**, 599 (2016).

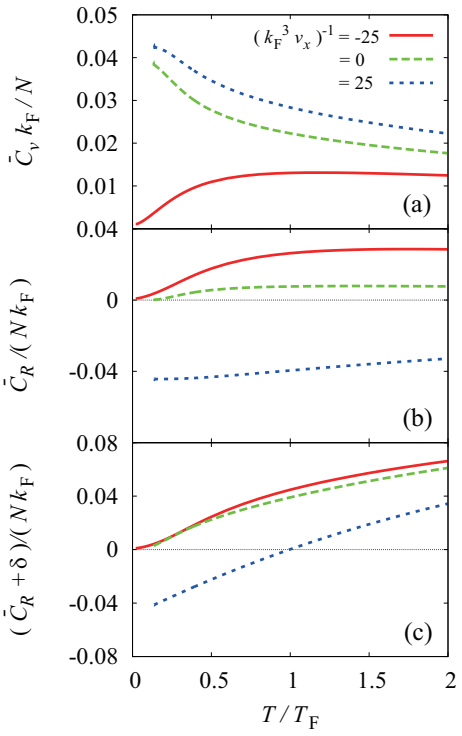


Figure 1: Calculated p-wave contacts in an ultracold Fermi gas with an attractive p-wave interaction (a) $\bar{C}_v$ and (b) $\bar{C}_R$, which are defined from the adiabatic energy relations, in the normal state. (c) Coefficient of the sub-leading term of the high momentum distribution, $\bar{C}_R + \delta$. Here δ is an additional term which is not related to the total energy of the system. $N = k_F^3/(6\pi^2)$ is the total number of Fermi atoms, k_F is the Fermi momentum, and v_i $(i = x, y, z)$ is the scattering volume of the p_i-wave interaction. For the anisotropy of the p-wave interaction, we set $\delta v^{-1} = v_x^{-1} - v_y^{-1} = v_x^{-1} - v_z^{-1} = 8k_F^3$, where we take x-axis being parallel to the Feshbash magnetic field.

Precision imaging of cold atoms with high resolution holographic microscopy

J. Zhao[1], **Y. Wang**[1], **Y. He**[1], **L. Qiu**[1], **M. Kang**[1], **Y. Fang**[1], **J. Sobol**[2], **and S. Wu**[1]

[1] *Key Laboratory of Surface Physics and Department of Physics, Fudan University, 200433 Shanghai, China*

[2] *Keit Spectrometers, Rutherford Appleton Laboratory, OX11 0QX Oxfordshire, UK*

e-mail: *saijunwu@fudan.edu.cn*

Abstract

Methods for in situ phase imaging of dense atomic samples are of unique importance for non-destructive probing quantum states and dynamics of ultracold atoms. In contrast to widely applied phase imaging techniques [1], we introduce a simpler, aberration-free technique that retrieves high resolution complex phase shift images of atomic sample from a single hologram [2] [3]. Speckles in the hologram, a typical noise source in holographic microscopy associated with the laser coherence length, are fully characterized to recover the probe wave front for faithful atomic signal reconstruction. We demonstrate the method by holographically imaging a ^{39}K sample in a micrometer-size dipole trap, with a spatial resolution of 2.6 μm, with nearly photon shot-noise limited phase shift sensitivity of about 4 mrad, and by retrieving high quality phase shift and absorption spectroscopic data from the images.

References

[1] M. Andrews et al, Phys. Rev. Lett **79**, 553 (1997).

[2] D. Gabor, Nature **161**, 777 (1948).

[3] J. Sobol et al, New J. Phys **16**, 093064 (2014).

Drag force and superfluidity in the supersolid stripe phase of a spin-orbit-coupled Bose-Einstein condensate

G. I. Martone[1] **and G. V. Shlyapnikov**[2,3,1,4,5,6]

[1] *LPTMS, CNRS, Univ. Paris-Sud, Université Paris-Saclay, Orsay 91405, France*

[2] *Russian Quantum Center, Skolkovo, Moscow 143025, Russia*

[3] *SPEC, CEA, CNRS, Université Paris-Saclay, CEA Saclay, Gif sur Yvette 91191, France*

[4] *Van der Waals-Zeeman Institute, Institute of Physics, University of Amsterdam, Science Park 904, 1098 XH Amsterdam, The Netherlands*

[5] *Wuhan Institute of Physics and Mathematics, Chinese Academy of Sciences, 430071 Wuhan, China*

[6] *Russian Quantum Center, National University of Science and Technology MISIS, Moscow 119049, Russia*

e-mail: *giovanni.martone@u-psud.fr*

The phase diagram of a Bose gas with equal Rashba and Dresselhaus spin-orbit coupling includes a supersolid stripe phase, which is featuring density modulations along the direction of the spin-orbit coupling [1, 2, 3]. This phase has been recently found experimentally [4]. In our recent work [5] we characterize the superfluid behavior of the stripe phase by calculating the drag force acting on a moving impurity. Because of the gapless band structure of the excitation spectrum [3], the Landau critical velocity vanishes if the motion is not strictly parallel to the stripes, and energy dissipation takes place at any speed. Moreover, due to the spin-orbit coupling, the drag force can develop a component perpendicular to the velocity of the impurity. Finally, by estimating the time over which the energy dissipation occurs, we find that for slow impurities the effects of friction are negligible on a time scale up to several seconds, which is comparable with the duration of a typical experiment.

[1] T.-L. Ho and S. Zhang, Phys. Rev. Lett. **107**, 150403 (2011).

[2] Y. Li, L. P. Pitaevskii, and S. Stringari, Phys. Rev. Lett. **108**, 225301 (2012).

[3] Y. Li, G. I. Martone, L. P. Pitaevskii, and S. Stringari, Phys. Rev. Lett. **110**, 235302 (2013).

[4] J. Li, J. Lee, W. Huang, S. Burchesky, B. Shteynas, F. Ç. Top, A. O. Jamison, and W. Ketterle, Nature (London) **543**, 91 (2017).

[5] G. I. Martone and G. V. Shlyapnikov, arXiv:1805.12552, to appear in JETP.

Towards weakly-destructive, real-time transport measurements of interacting Fermi Gas

B. Cilenti[1], **K. Roux**[1], **H. Konishi**[1], **V. Helson**[1] **and J-P. Brantut** [1]
[1] *Institut de Physique, École Polytechnique Fédérale de Lausanne , 1015 Lausanne, Switzerland*
e-mail: *barbara.cilenti@epfl.ch*

Over the last decades an intensive research has been conducted on ultracold atoms, inspired by their good isolation from the environment and ease in manipulation.
As a result a very high degree of control is now accessible, including the tuning of inter-atomic interactions, the possibility to organize them in defined geometrical patterns or in lower dimensions. For these reasons, ultracold atoms can simulate a large variety of many-body quantum system that cannot be studied theoretically directly [1].
Among the open problems in many-body physics, the study of the transport properties has gained popularity in the past years, and several experiments have been realized to study the phenomenon under different perspectives. In particular, simulation of conductance in mesoscopic devices has been performed, by connecting two macroscopic reservoirs of ultracold fermions via a channel and observing the current induced by a controlled unbalance of the two reservoirs [2]. These experiments are usually limited in sensitivity by the noise associated to the preparation of a new sample after each measurement.
The aim of the experiment that we have set up in Lausanne is to overcome this limitation to the sensitivity by integrating a high finesse cavity in the experimental set-up to perform weakly-destructive measurements of current [3]. This feature will allow us to observe the dynamics of the system in real time and, as a consequence, to reduce the preparation noise.
A pictorial representation of the technique is shown in Fig 1.

When designing the cavity as a tool to perform weakly destructive probing of the atoms, the most crucial parameter to be selected is its finesse. In fact it has been shown that, for a fixed destructivity of the measurement, the signal to noise ratio increases like the square root of the finesse [4]. We thus planned a value of 50000, as a compromise between high signal to noise ration and experimental complexity. Our experimental setup will combine cavity assisted measurements with a tunable Fermi gas of ^{6}Li atoms.
A picture of the high finesse cavity integrated in the main chamber is shown in Fig. 2.
In my poster I will give a detailed description of the current status of the experimental setup with a focus on the integrated high finesse cavity.

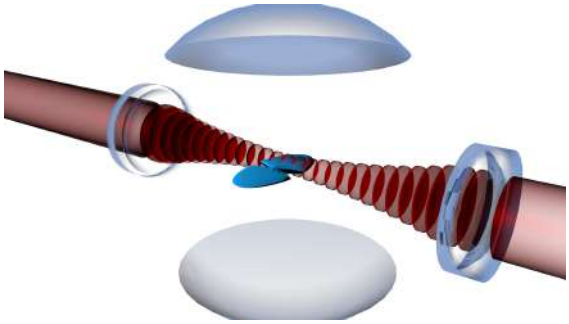


Figure 1: Working principle of the weakly destructive measurement: a probe, far from resonance beam is shone on one of the reservoir produced inside the cavity. The information on the number of atoms, and consequently on the current flowing, can be retrieved in real-time from the phase of the probe beam leaking out of the cavity.

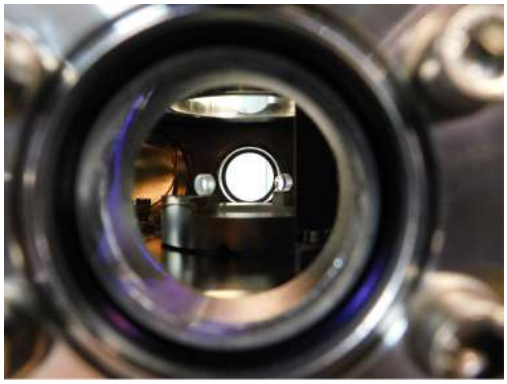


Figure 2: Picture of the actual cavity inside the vacuum chamber of the experiment, seen from one of the available optical access. The two mirrors are spaced by 4cm to allow the passage of the MOT beams at the center, facilitating the loading of the atoms in the cavity-based dipole trap

[1] I. Bloch, J. Dalibard, and W. Zwerger, Rev. Mod. Phys 80, 885 (2008)

[2] J-P. Brantut, J. Meinke, D. Stadler, S. Kinner and T. Esslinger, Science 337, 6098 (2012)

[3] S. Uchino, M. Ueda, J-P. Brantut, arXiv:1802.04024 (2018)

[4] J. E. Lye, J. J. Hope, and J. D. Close, Phys. Rev. A 67, 043609 (2003)

Feshbach resonances and Feshbach molecules in an ultracold ^{6}Li-^{133}Cs mixture

B. Zhu[1], **M. Gerken**[1], **B. Tran**[1], **M. Neiczer**[1], **J. Matthies**[1], **E. Lippi**[1], **L. Klaus**[1], **and M. Weidemüller**[1,2]

[1] *Physikalisches Institut, Universität Heidelberg, Im Neuenheimer Feld 226, 69120 Heidelberg, Germany*
[2] *Hefei National Laboratory for Physical Sciences at the Microscale and Department of Modern Physics, and CAS Center for Excellence and Synergetic Innovation Center in Quantum Information and Quantum Physics, University of Science and Technology of China, Hefei, Anhui 230026, China*
e-mail: *bzhu@physi.uni-heidelberg.de*

Feshbach resonance (FR) has been a main workhorse in ultracold atomic physics for the past two decades. One of the important applications is to form the so-called Feshbach molecules from atomic clouds, which is a prerequisite for the creation of ultracold polar molecules via Raman processes [1]. Here we present our understanding of FRs in an ultracold mixture of fermionic ^{6}Li and bosonic ^{133}Cs atoms, focusing on the investigation of substructures of p-wave ($l = 1$) FRs (see an example shown in Fig. 1). Instead of the well-know doublet splitting due to spin-spin interaction [2], we observe a triplet substructure in our system and attribute the further splitting to spin-rotation coupling. We also present our experimental efforts towards the formation of ultracold ^{6}Li^{133}Cs Feshbach molecules near s-wave ($l = 0$) FRs. One particularly interesting question is to study the atom-dimer collisions, where the Efimov effect [3] manifests itself as loss resonances at the positive scattering length side.

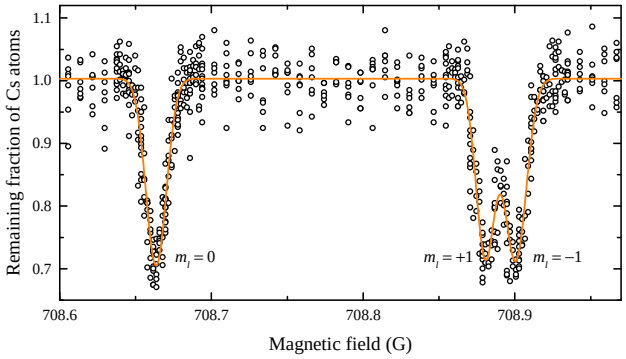


Figure 1: Substructures of a p-wave FR in ^{6}Li -^{133}Cs system. Here we show the trap-loss spectroscopy, where the loss of atoms is recorded with respect to an external magnetic field (open dots). The resonant features are identified as FRs with different m_l, the projection of pair rotational angular momentum l along the external magnetic field. The solid line is a fit with multi-Gaussian function to extract the resonance positions and widths.

[1] Steven A. Moses, Jacob P. Covey, Matthew T. Miecnikowski, Deborah S. Jin, and Jun Ye, Nat. Phys. **13**, 13-20 (2017).

[2] C. Ticknor, C. A. Regal, D. S. Jin, and J. L. Bohn, Phys. Rev. A **69**, 042712 (2004).

[3] S. H afner, J. Ulmanis, E. D. Kuhnle, Y. Wang, C. H. Greene, and M. Weidemüller, Phys. Rev. A **95**, 062708 (2017)

Long range interactions in time lattices

K. Giergiel[1], **A. Miroszewski**[2], **and K. Sacha**[1,3]

[1] *Instytut Fizyki imienia Mariana Smoluchowskiego, Uniwersytet Jagielloński, ulica Profesora Stanisława Łojasiewicza 11, PL-30-348 Kraków, Poland*

[2] *National Centre for Nuclear Research, ul.Hoża 69, PL-00-681 Warsaw, Poland*

[3] *Mark Kac Complex Systems Research Center, Uniwersytet Jagielloński, ulica Profesora Stanisława Łojasiewicza 11, PL-30-348 Kraków, Poland*

e-mail: *krzysztof.giergiel+icap@gmail.com*

Time crystals are many-body systems which spontaneously self-organize their motion in a periodic way in time by analogy with the formation of crystalline structures in space in solid state physics. Time crystal behavior can be investigated in periodically driven systems if the driving is resonant with unperturbed motion of particles. Wide class of condensed matter problems can be realized in the time domain if single-particle or many-body systems are resonantly driven. It opens up unexplored territory for investigation of condensed matter physics in time and for invention of novel "time devices" because time is our new ally.

In the poster it will be shown how to create time lattices similar to optical (space) lattices. In this new type of systems almost any long range interactions in an effective Bose-Hubbard Hamiltonian can be engineered [1]. This can be achieved in ultra-cold atoms if s-wave scattering length is periodically modulated in time by means of the Feshbach resonance. In Figures 1-2 an example9 is presented where the magnitude of the interactions of a particle located at a given site with other particles located at the same or distant sites is nearly the same, but their repulsive or attractive character changes in an oscillatory way. We focus on ultra-cold atoms bouncing on an oscillating atom mirror. Time crystal behavior is such a system still awaits experimental demonstration, but our analysis of the experimental conditions shows that it is easily attainable in current laboratories [2].

[1] Giergiel, K., Miroszewski, A. & Sacha, K. 2018, Phys. Rev. Lett., 120, 140401.

[2] KGiergiel K., Kosior A., Hannaford P., Sacha K., preprint https://arxiv.org/abs/1805.05718

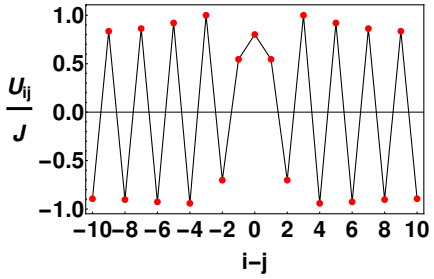


Figure 1: Example of a system with exotic interactions: ultra-cold atoms bouncing on a harmonically oscillating mirror. The 20:1 resonance condition between the mirror oscillation frequency and the frequency of atom motion is fulfilled and the many-body system is described by the Hamiltonian $\hat{H}_{\rm eff} = -\frac{J}{2}\sum_{\langle i,j\rangle}\hat{a}_i^\dagger\hat{a}_j + \frac{1}{2}\sum_{i,j}U_{ij}\ \hat{a}_i^\dagger\hat{a}_j^\dagger\hat{a}_j\hat{a}_i,$. The interactions of a particle located at a given site with other particles located at the same or distant sites is nearly the same, but their repulsive or attractive character changes in an oscillatory way.

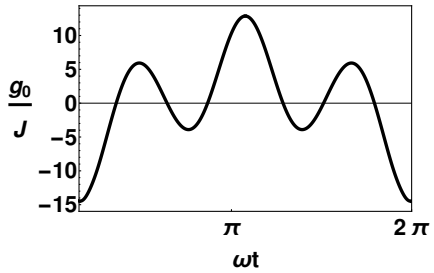


Figure 2: Scattering length $g_0(t)$, that creates the interaction profile from Fig. 1. Time scale corresponds to the mirror oscillations frequency ω. This type of scattering length behavior can be crated by time dependent magnetic field close to Feshbach resonance.

Quantum phase transition of a frustrated Bose-Hubbard model on triangular lattice: Density matrix renormalization group study

Y. Saiki[1], **D. Yamamoto**[1], **S. Goto**[2], **and N. Furukawa**[1]

[1] *Department of Physics and Mathematics, Aoyama Gakuin University, Sagamihara, Kanagawa, 252-5258, Japan*

[2] *Department of Physics, Kindai University, Higashi-Osaka, Osaka, 577-8502, Japan*

e-mail: *y-saiki@phys.aoyama.ac.jp*

We study the quantum phase transition of Bose gases loaded into an optical lattice with geometrical frustration in local phase configuration. In 2002, the superfluid (SF)-to-Mott insulator (MI) transition has been experimentally observed in an optical-lattice system of ultracold atoms [1]. The physics of the transition can be captured by the Bose-Hubbard model with the onsite repulsion between atoms and the hopping from one site to another neighboring site. More recently, it has been proposed that a frustrated Bose-Hubbard model with sign-inverted hopping could exhibit an exotic intermediate phase, called chiral Mott insulator (CMI), in between the chiral superfluid (CSF) and standard MI phases [2, 3]. In this case, the transition is accompanied with two successive symmetry breakings about the U(1) global phase rotation and a discrete chiral degree of freedom. Also in the context of magnetism, a similar successive transition with an intermediate phase has been predicted in the $S = 1$ Heisenberg model with easy-plane single-ion anisotropy on the triangular lattice [4].

Here we study the quantum phase transition of a frustrated Bose-Hubbard model on the triangular lattice, using the density matrix renormalization group method (DMRG). The Hamiltonian of the model is

$$\hat{\mathcal{H}} = \sum_{\langle i,j \rangle} \left(t\hat{b}_i^\dagger \hat{b}_j + \text{H.c.} + V\hat{n}_i\hat{n}_j \right) + \frac{U}{2}\sum_i \hat{n}_i(\hat{n}_i - 1) - \mu \sum_i \hat{n}_i. \quad (1)$$

Recent development of experimental techniques has enabled inverting the sign of the hopping integral t from negative sign to positive [5]. For such sign-inverted hopping $t > 0$, the relative phase of local condensate order parameters at neighboring lattice sites tends to be π in analogy with antiparallel alignment of antiferromagnetic spins. However, the geometry of the triangular lattice does not allow the staggered (0 or π) configuration of the local phase, and as a result, the so-called three-sublattice 120° structure is formed as in triangular antiferromagnets. The condensates with the 120° local phase structure, referred to as CSF, breaks the $\mathbb{Z}_2$ symmetry about the configuration of the chirality defined in each triangle (Fig. 1) as well as the U(1) symmetry.

The existence of the CMI phase with only $\mathbb{Z}_2$ chiral symmetry breaking in between the CSF and MI phases has been examined by a variational analysis [2, 3] for the triangular-lattice system. We perform here the two-dimentional DMRG calculations to study the succesive transition from CSF to CMI, and then to MI. In the DMRG analysis, we adopt finite-size rhombic clusters of $3m^2 (m = 2, 3, 4 \cdots)$ sites with the periodic boundary condition. The structure factors for the particle-particle and chirality-chirality correlations are calculated to locate the transition points. We also disscuss the critical phenomena at each transition.

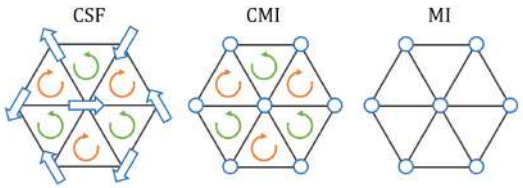


Figure 1: Illustrations of CSF, CMI, and MI phases. The arrows in CSF indicate the local phase of the condensate. The loop currents in each triangular are also depicted.

[1] M. Greiner, O. Mandel, T. Esslinger, T. Hansch, and I. Bloch, Nature **415**, 39 (2002)

[2] M. P. Zaletel, S. A. Parameswaran, A. Rüegg, and E. Altman, Phys. Rev. B **89**, 155142 (2014)

[3] C. Romen and A. M. Läuchli, arXiv:1711.01909 (2017)

[4] Z. Wang, A. E. Feiguin, W. Zhu, O. A. Starykh, A. V. Chubukov, and C. D. Batista , Phys. Rev. B **96**, 184409 (2017)

[5] A. Eckardt, C. Weiss, and M. Holthaus, Phys. Rev. Lett. **95**, 260404 (2005); H. Lignier, C. Sias, D. Ciampini, Y. Singh, A. Zenesini, O. Morsch, and E. Arimondo, Phys. Rev. Lett. **99**, 220403 (2007).

Observation of semimetal phase for ultracold fermions with 2D spin-orbit coupling in an optical lattice

Chengdong He[1], Zejian Ren[1], Bo Song[1], Elnur Hajiyev[1], Qianhang Cai[1], Gyu-Boong Jo[1]1

[1] *Department of Physics, Hong Kong University of Science and Technology Clear Water Bay, Hong Kong*

Spin-orbit (SO) coupling is an essential ingredient in realizing exotic band structures for ultracold atoms. Especially SO coupling in higher dimensions (e.g. 2D or 3D) allows us to explore a new class of topological phases corresponding to topological insulators and superconductors in solids. Nevertheless, the experimental realization of high dimensional SO coupling still remains unexplored for ultracold fermions in an optical lattice. Here, we demonstrate for the first time the realization of 2D SO coupling for ultracold fermions in an optical lattice and investigate the SO driven semimetal phases. In the experiment, we combine the 2D optical Raman lattice [2], formed in the x-y plane, with the Raman-induced SO coupling [1] along the z direction, resulting in 3D topological band structure. With the highly tunable SO coupling, a novel nodal-line topological semimetal, as formed by stacking 2D Dirac semimetals along z direction, can be achieved in the 3D configuration. While to map out the 3D topological band structure is an open challenge, we successfully resolve the 2D Dirac points for a specific dominating k_z-plane through both equilibrium spin-texture imaging and quench dynamics after loading fermions into the nodal-line semimetal. In particular, in the quench from a deep trivial regime to topological semimetal phase, we observe in the quench spin dynamics the band inversion lines which are bulk counterparts of Fermi arc states and connect the Dirac points. On the band inversion lines the Bloch states exhibit resonant spin oscillations induced by SO coupling, yielding zero time-averaged spin polarization, which provides a signature of the nontrivial band topology. The observations are well consistent with the theoretical predictions and show the feasibility in the study of novel topological quantum physics and quantum far-from-equilibrium dynamics with SO coupled ultracold atoms.

Funding support:
Hong Kong Research Grants Council(ECS26300014, GRF16300215, GRF16311516, GRF16305317, N HKUST601-17)
Croucher Foundation (Croucher Innovation Grants).

References

[1] Bo Song, Chengdong He, Shanchao Zhang, Elnur Hajiyev, Wei Huang, Xiong-Jun Liu, and Gyu-Boong Jo. Spin-orbit-coupled two-electron fermi gases of ytterbium atoms. *Phys. Rev. A*, 94:061604, Dec 2016.

[2] Bo Song, Long Zhang, Chengdong He, Ting Fung Jeffrey Poon, Elnur Hajiyev, Shanchao Zhang, Xiong-Jun Liu, and Gyu-Boong Jo. Observation of symmetry-protected topological band with ultracold fermions. *Science Advances*, 4(2), 2018.

[1] gbjo@ust.hk

Two-photon spectroscopy of ultracold rubidium atoms in magnetic field

Ryo Yasuda, Ryohei Itoyama, Masashi Abe, and Satoshi Tojo
Department of Plhysics, Chuo University, 112-8551, Tokyo, Japan
e-mail: *tojo@phys.chuo-u.ac.jp*

Two-photon transition spectroscopy is one of useful methods for precise measurements, which can exclude Doppler broadening [1]. Nonlinear phenomena including collision broadenings observed in Rb two-photon spectra in high density of atoms [2]. Two-photon transition spectroscopy is classified as off-resonance and on-resonance via an intermediate state. In Rb atoms, the off-resonance spectroscopy has good advantages of canceling for undesired effects from intermediate $5P$ state such as heating trapped atoms. The transition needs high intensity of excited laser due to off-resonance of 1 THz from the $5P_{3/2}$ state.

We study two-photon spectroscopy of ultracold ^{87}Rb atoms in a magnetic field. The atoms are excited from the $5S_{1/2}$ ground state to the $5D_{5/2}$ excited state via off resonant $5P_{3/2}$ state using 778 nm laser as shown in Fig. 1(a). We observe transition spectra by counting the number of trapped atoms using the absorption imaging method. Figure 1(b) shows a configuration of an optical path diagram in this research including trapping lasers, an excitation laser, and a probe laser. The excitation laser is set to around 778 nm in terms of wavelength by lock system which uses two-photon spectra at a room temperature cell with an applied magnetic field, and is swept in the range of 64 MHz by acousto optic modulator (AOM). We use a crossed far-off-resonance optical trap (crossed-FORT) with the wavelength of 1064 nm with these total intensities of 15 W, and prepare 10^6 atoms with 10 μK in initial.

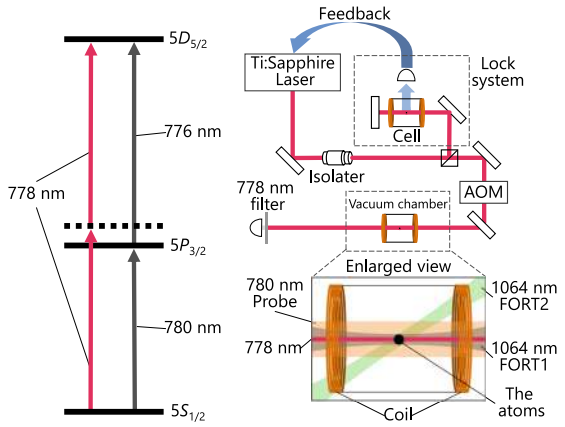


Figure 1: (a) Energy level diagram for ^{87}Rb in $5S_{1/2}$-$5D_{5/2}$ excitation. (b) Configuration of experimental setup of our optical path diagram.

Figure 2 shows two-photon transition spectra from $5S_{1/2}$ (F= 1) to $5D_{5/2}$ (F'= 1, 2, 3) in the absence of a magnetic field. We set the resonant frequency of $5S_{1/2}$ (F= 1) to $5D_{5/2}$ (F'= 2) to be zero; observed dips in lower and higher frequencies correspond to F'= 3 and F'= 1, respectively, and we measure the remained atoms in the trap after irradiation of 778 nm light with 100 ms. The laser intensity is sufficiently low with 0.4 mW for measurement of linear phenomena. The full widths at half maximum of the spectra correspond to 2.52 MHz (F'= 1), 3.13 MHz (F'= 2) and 3.43 MHz (F'= 3), respectively. As a reference, the widths at room temperature in our measurement including the transit-time broadening are 6.43 MHz (F'= 1), 6.44 MHz (F'= 2) and 5.67 MHz (F'= 3), respectively.

We have observed sharp spectra of ultracold ^{87}Rb atoms. The results indicate that our trap-loss measurement using ultracold atoms have sufficient resolution for observing spectral splitting when applying a magnetic field of about several gausses. We will report on two-photon excitation spectra of ultracold Rb atoms in magnetic field of several gausses.

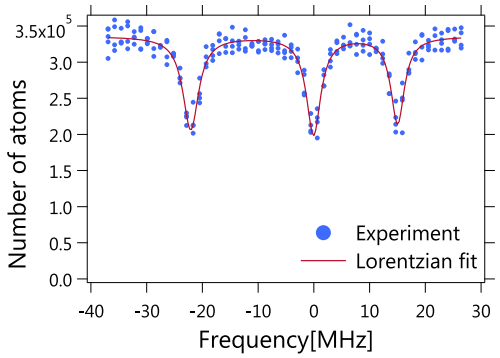


Figure 2: Spectra $5S_{1/2}$ (F= 1)-$5D_{5/2}$ (F'= 1, 2, 3). The solid line is Lorentzian fitting to experiments.

[1] R. E. Ryan, L. A. Westling, and H. J. Metcalf, J. Opt. Soc. Am. B **10**, 1643 (1993).

[2] F. Nez, F. Biraben, R. Felder, and Y. Millerioux *et al.*, Opt. Comm. **102**, 432-438 (1993).

[3] D. A. Steck, Rubidium 87 D Line Data, Los Alamos National Laboratory (2003).

Observation of Superradiant Decay of Cold Atoms via the 350 Hz Intercombination Line of Calcium

H. Winter, T. Laske, and A. Hemmerich
Institut für Laserphysik, Universität Hamburg, Luruper Chaussee 149, 22761 Hamburg, Germany
e-mail: *hwinter@physnet.uni-hamburg.de*

The standard approach for producing narrow-band light sources is to stabilize a laser with respect to an ultra stable high-Q cavity. As this approach reaches fundamental limits (thermal fluctuations in mirror coatings and the cavity spacer) a novel laser concept has recently been subject to intense investigations: So called superradiant lasers make use of ultra narrow optical transitions (for example clock transitions in alkaline earth metals) [1]. In the superradiant limit, the linewidth of such a laser becomes independent of small fluctuations of the cavity length and is reduced below the natural linewidth of the used atomic transition. This has been successfully observed by Thompson et. al. in a superradiant laser based on ^{87}Sr Atoms [2]. The cooperativity of the atoms can be substantially increased using an optical cavity resonant with the atomic transition. In order to operate in the superradiant regime, the decay rate of the cavity field is chosen to be orders of magnitude larger than the natural atomic decay rate.

We are presently investigating superradiant lasing with Calcium atoms. We prepare a sample of ^{40}Ca atoms inverted with respect to the intercombination line $^1S_0 \rightarrow {}^3P_1$, which has a natural linewidth of 350 Hz. To minimize any line broadening due to atomic motion or shifts of the used atomic energy levels, the atoms are trapped using a deep magic optical lattice, where the magic wavelength in our case is approximately 800 nm. Su cient lattice depth is achieved by power enhancement due to a cavity, which at the same time is resonant with respect to the atomic transition to support the collective decay of the atoms, resulting in superradiance. We are able to prepare a pure ensemble of $^3P_1$-Atoms (i.e. full inversion) trapped inside the cavity mode. By measuring the subsequent photon emission rate behind the cavity, we analyze the atomic decay. The observation of smaller decay times (76 μs) than the natural life time of the $^3P_1$ state (431 μs) is an indication for superradiance.

[1] D. Meiser, Jun Ye, D. Carlson, and M. Holland, Physical Review Letters, 102(16):163601, Apr 2009.

[2] Matthew A. Norcia and James K. Thompson. Physical Review X, 6(1):1, Mar 2016.

Blue light emission from ultracold rubidium atoms via optical double resonance

Sakura Seta, Go Tanaka, Taro Mashimo, Masashi Abe, and Satoshi Tojo
Department of Physics, Chuo University, Tokyo 112-8551, Japan
e-mail: *tojo@phys.chuo-u.ac.jp*

Double resonance is one of powerful tools for change in wavelengths and control of quantum states in the range from radio frequency to optical frequency. It can be investigated for the researches of the four-wave mixing and dressed state. By use of ultracold atoms, these localization, density, and degree of vacuum are much higher than those at room temperature, so that precise measurement such as lengthening of coherence time and narrowing of spectra is possible. In view of optical-optical double resonance, blue fluorescence emission at 420 nm corresponding to $6P_{3/2}$ to $5S_{1/2}$ transition can be detected through doubly excited to $5D_{5/2}$ state and decay to $6P_{3/2}$ state as shown in Fig. 1. In vapor experiments, blue light emission of Rb atoms has been investigated for change in color, generation of collimated light, especially, four-wave mixing with 780 and 776 nm lasers. For laser-cooled experiment, blue light emission has been achieved in use of cold magneto-optical trap (MOT) with irradiation light of 780 nm as a cooling laser and 776 nm as an optical double resonance (ODR) laser.

In our experiment, we have captured cold Rb atoms in MOT and irradiated ODR light. The ODR light source has been locked to a Rb gas cell with a counterpart irradiation of controlled 780 nm laser by use of absorption spectra. Due to the frequency modulation technique, we have observed dispersive Doppler-free absorption spectra and locked ODR laser into $5P_{3/2}(F' = 3)$ to $5D_{5/2}(F'' = 4)$ transition through a lock-in system. The ODR beam axis is coaxial to one of the MOT light. Thanks to large difference between cooling (780 nm) and ODR (776 nm) wavelengths, blue light emission can be easily detected by use of the band pass filter. The frequency of the ODR light is swept by the acousto-optic-modulator with the laser frequency set to zero for $5P_{3/2}(F' = 3)$ to $5D_{5/2}(F'' = 4)$ transition. We have confirmed blue light emission of fluorescence at 420 nm as shown in Fig. 2. We have observed three blue emission spectra and fitted them by the Lorentzian functions (solid line in Fig. 2). The peaks at lower and zero frequencies correspond to $5D_{5/2}(F'' = 3)$ and $(F'' = 4)$ transition, respectively. The peak in higher frequency indicates a closed cycle of $5P_{3/2}(F' = 3) - 5D_{5/2}(F'' = 4)$ transition since the center frequency of the profile is independent of detunings of the cooling laser.

In our poster, we will report on blue emission at 420 nm with several dependences of the detuning of the cooling laser, the intensities of ODR laser, and polarization of light in MOT and an optical trap.

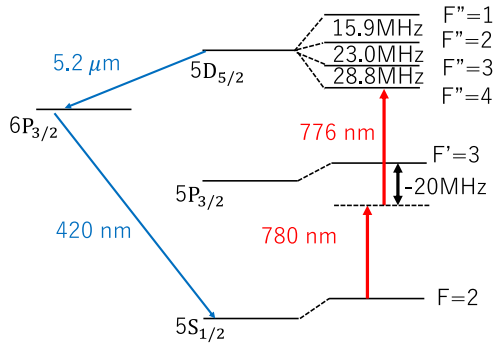


Figure 1: Grotrian diagram of ^{87}Rb

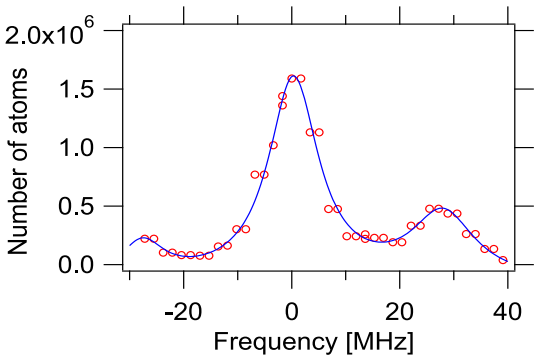


Figure 2: Blue fluorescence spectrum from MOT with irradiation of 776 nm detunings.

[1] A. S. Zibrov *et al.,* Phys. Rev. A **65**, 051801 (R) (2002).

[2] D. V. Sheludko *et al.,* J. Phys. Conf. Ser. **80**, 012040 (2007); R. Kumar *et al.,* Phys. Rev. A **91**, 053842 (2015).

[3] M. H. Anderson *et al.,* Science **269**, 198 (1995).

[4] T. T. Grove *et al.,* Physica Scripta **52**, 3 (1995).

[5] K. B. Davis *et al.,* Phys. Rev. Lett. **75**, 3969 (1995).

Coupled order parameters with ultracold atoms in two crossed cavities

P. Zupancic[1], **A. Morales**[1], **J. Léonard**[1], **X. Li**[1], **A. Baumgärtner**[1], **D. Dreon**[1], **T. Esslinger**[1], **and T. Donner**[1]

[1] *Institute for Quantum Electronics, ETH Zurich, Zurich, Switzerland*

e-mail: *zupancic@phys.ethz.ch*

The concept of intertwined order describes the simultaneous existence of independent order parameters and can therefore allow materials to feature multiple properties. Examples include multiferroic materials that have coexisting ferroelectric and ferromagnetic orders leading to enhanced functionalities, and materials that are superconducting at high temperatures due to intertwining between charge- and spin-order.

I will report on our recent experimental realization of an intertwined ordered phase in a quantum gas where we can control the interaction between the atoms at the microscopic level. Our system is realized by a BEC placed at the mode crossing of two optical cavities. Being coherently driven by a photon pump, the atoms can transit into self-organized phases. The tunability of pump strength and frequency as well as the cavity and atomic detunings allow us to explore wide parameter ranges with various phases and different dynamics.

For vanishing inter-order coupling we realize a supersolid phase of matter by symmetry enhancement of the composite order parameter to a $U(1)$ symmetry [1]. This phase supports Higgs and Goldstone modes, whose energy we measure spectroscopically across the normal–supersolid phase transition. We observe their amplitude and phase character in real time [2]. Increasing the inter-order coupling, this symmetry breaks down to a $\mathbb{Z}_2 \times \mathbb{Z}_2$, and we observe the emergence of an extended intertwined phase arising from the coupling of the individual order parameters. This coupling enables us to increase or decrease the critical point of one order by controlling the other [3] (see Fig. 1).

[1] J. Léonard, A. Morales, P. Zupancic, T. Esslinger, T. Donner, Nature, 543, 87-90 (2017)

[2] J. Léonard, A. Morales, P. Zupancic, T. Donner, T. Esslinger, Science, 358, 1415-1418 (2017)

[3] A. Morales, P. Zupancic, J. Léonard, T. Esslinger, T. Donner, arXiv:1711.07988 (accepted in Nature Materials)

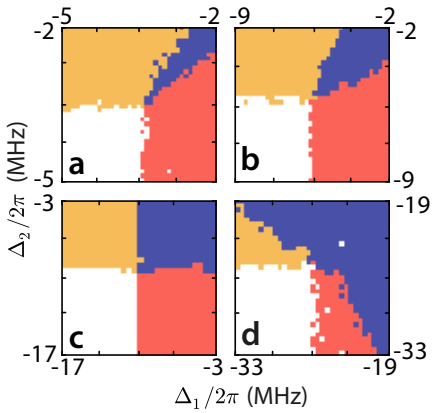


Figure 1: Phase diagrams as a function of the the cavity detunings Δ_1 and Δ_2 for increasing inter-order coupling (**a-d**). White indicates the normal phase, red and orange the self-organized phase of cavity 1 and 2 resp., and blue the intertwined phase.

Two photon spectroscopy of ultracold rubidium atoms near dielectric surface

Taro Mashimo, Go Tanaka, Sakura Seta, Masashi Abe, and Satoshi Tojo
Department of Physics, Chuo University, Kasuga, Bunyo-ku, Tokyo 112-8551, Japan
e-mail: *taro.mashimo@gmail.com*

At near dielectric surface, there are various interaction between atoms and surface, such as van der Waals effect and Casimir-Polder effect [1,2]. In the area below several tens of nanometers from the surface, there are the effects which cause remarkable energy shift and change in spectra profiles due to the dielectric surface. Recently, transferred atoms near the surface have been realized and observed rebound behaviors. In this research, we use far-off-resonance trap [3], and transport ultracold rubidium atoms to near dielectric surface.

We prepare ultracold rubidium atoms with 2 μK and 10^7 atoms by laser cooling method. We also construct the system for effective loading of ultracold rubidium from magneto-optical trap (MOT) into far-off-resonance trap [4] and transporting atoms stably to the dielectric surface by using the optical trap. Thank to retro-reflection regime, the optical lattices are generated with parallel to the dielectric surface. The transported rubidium atoms are held in the optical lattices with each interval of 7 μm as shown in Fig.1(a). Then, the atoms are irradiated with 780 nm laser and excited from $5S$ state to $5P$ state in the optical lattices. We have taken fluorescences of resonant ($5S$-$5P$) transition as shown in Fig.2. Concurrently above experiment, we also observed absorption spectrum of on-resonant ($5S$-$5P$-$5D$) transitions for ultracold Rb atoms in MOT (Fig.1(b)).

We have investigated observing the absorption spectrum of on-resonant ($5S$-$5P$-$5D$) transitions for ultracold rubidium atoms by using irradiation of 776 nm and 780 nm lasers. By comparing absorption spectrum near the surface to those in an optical trap in free space, we will discuss the non-linear interaction between atom and dielectric surface.

In our poster, we will report on the spectrum of two photon ($5S$-$5D$) transition in an optical trap near the surface and in free space. We will also reveal the interaction on the surface and demonstrate a light shift of $5S$-$5D$ transition in optical lattice.

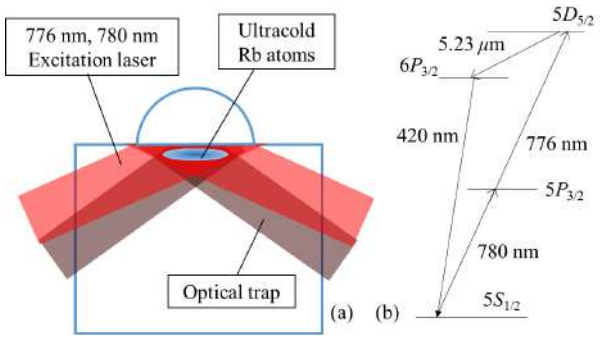


Figure 1: (a) Experiment setup to observe the spectrum of $5S$-$5P$-$5D$ transitions near dielectric surface. (b) Energy level of rubidium atoms and on-resonant ($5S$-$5P$-$5D$) transitions used in our experiments.

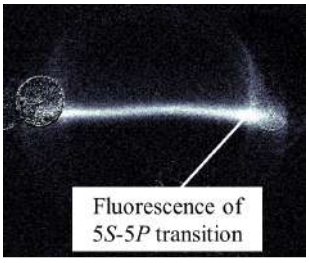


Figure 2: Fluorescence of $5S$-$5P$ transition of ultracold rubidium atoms near dielectric surface

[1] H. Bender, Ph. W. Courteille, C. Marzok, C. Zimmermann, and S. Slame, Phys. Rev. Lett. **104**, 083201 (2010).

[2] A. Landragin, J. -Y. Courtois, G. Labeyrie, N. Vansteenkiste, C. I. Westbrook, and A. Aspect, Phys. Rev. Lett. **77**, 1464 (1996).

[3] J. D. Miller, R. A. Cline, and D. J. Heinzen Phys. Rev. **47**, R4567(R) (1993).

[4] K. Shibata, S. Yonekawa, and S. Tojo, Phys. Rev. A. **96**, 013402 (2017).

Observation of the $5^2P_{3/2}$ - $6^2P_{3/2}$ forbidden transition in laser-cooled rubidium atoms

Miki Fukui[1], **Masashi Abe**[1], **and Satoshi Tojo**[1]
[1] *Department of Physics, Chuo University, Tokyo 112-8551, Japan*
e-mail: *tojo@phys.chuo-u.ac.jp*

Optical forbidden transition has advantages to realize tests of fundamental symmetries of nature, and can be investigated for parity nonconserving and precise spectroscopies. The alkali metal atoms such as rubidium (Rb) as hydrogen-like are useful for search for quantum state analytically. Therefore, experimental results are consistent with theoretical ones, and are realized to proof for novel phenomena by using laser spectroscopy. Figure 1 shows energy level diagram of ^{87}Rb. For doubly excited experiments, in use of $5^2S_{1/2}$ - $5^2P_{3/2}$ - $5^2D_{5/2}$ excitation. Fluorescence observation of 420 nm in cooled atoms is used to observed relaxation process $6^2P_{3/2}$ - $5^2S_{1/2}$ via allowed transition $5^2D_{5/2}$ - $6^2P_{3/2}$ [1]. Recently, the fluorescence observation in a vapor cell experiment with the transition from $5^2P_{3/2}$ - $6^2P_{3/2}$ has been achieved though the forbidden transition corresponding to magnetic dipole and electric quadrupole transitions [2]. For laser-cooled atoms, optical forbidden Na $3^2P_{3/2}$ - $4^2P_{1/2}$ transition in a magneto-optical trap (MOT) has been observed with multiphoton excitation by photoionization for probe this forbidden transition [3].

In this study, we irradiate laser-cooled rubidium atoms with 911 nm laser beam corresponding to optical forbidden $5^2P_{3/2}$ - $6^2P_{3/2}$ transition accompanied by direct fluorescence of 420 nm of $6^2P_{3/2} - 5^2S_{1/2}$ transition. We briefly describe our experimental setup. The laser-cooled atoms of ^{87}Rb are generated by a typical MOT system. The forbidden 911 nm laser beam is incident with focused into the cold atomic cloud. The beam axis is coincide to one of the light axis of MOT. The fluorescence of 420 nm is observed with a CCD camera with a 420 nm band pass filter. The 911 nm laser source is a hand-made single mode diode laser (DL) system. Frequency sweep of DL is performed by changing in injection current with an external function generator with a small modulation. The laser frequency is calibrated with a precise wavemeter, which has accuracy of 60 MHz.

Figure 2 shows the pictures of 420 nm fluorescence; (b) indicates fluorescence with on-resonance from Rb MOT cloud while (a) with off-resonance. We have found the resonant frequency corresponding to $5^2P_{3/2}$ ($F = 3$) - $6^2P_{3/2}$ ($F = 3$) state is 329053.6 GHz with the irradiation power of 60 mW.

In our poster, we will report on the emission spectra of 420 nm changing in the optical forbidden 911 nm DL frequency with several dependence on laser detunings and power. We would like to thank Jose Jiménez-Mier for useful supports about the laser source and fruitful discussion.

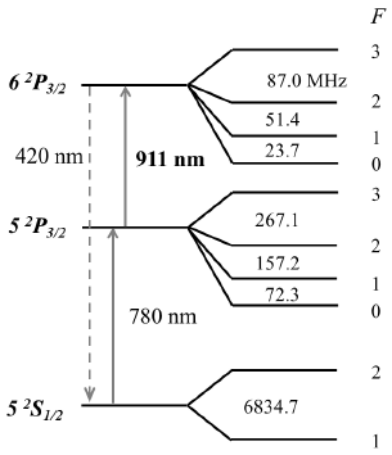


Figure 1: Energy levels with hyperfine separation of ^{87}Rb atom in MHz.

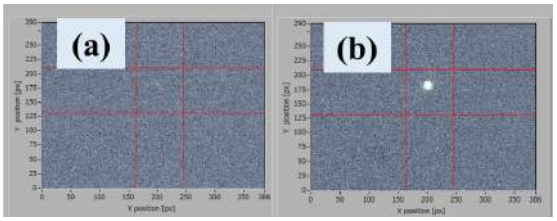


Figure 2: Picture of 420 nm fluorescence observation. (a) off resonance, (b) on resonance corresponding to $5^2P_{3/2}$ ($F = 3$) to $6^2P_{3/2}$ ($F = 3$) transition.

[1] R. Kumar, V. Gokhroo, K. Deasy, and S. N. Chromaic, Phys. Rev. A **91**, 053842 (2015).

[2] F. Ponciano-Ojeda *et al.*, AIP Conf. Proc. **1950**, 030001 (2018).

[3] M. Bhattacharya, C. Haimberger, and N. P. Bigelow, Phys. Rev. Lett. **91**, 213004 (2003).

A two-dimensional box trap for ultracold ^{39}K atoms with tuneable interactions

P. Christodoulou[1], **M. Galka**[1], **J. Man**[1], **R. Lopes**[1], **J. Schmitt**[1], **R.P. Smith**[1], **and Z. Hadzibabic**[1]

[1] *Department of Physics Cavendish Laboratory, University of Cambridge, Cambridge CB3 0HE, UK*
e-mail: *pc558@cam.ac.uk*

Ultracold atomic gases constitute a powerful platform to study strongly-correlated many-body physics due to the high level of control of their confinement, interactions and dimensionality. It has long been known, that dimensionality profoundly modifies the behaviour in the quantum degenerate regime. While three-dimensional Bose gases manifest Bose-Einstein condensation below a finite critical temperature, thermal fluctuations suppress the emergence of true long-range order in a two-dimensional (2D) homogeneous gas. For su ciently high phase-space densities, however, the 2D Bose gas exhibits an infinite-order topological phase transition to a superfluid, known as the Berezinskii-Kosterlitz-Thouless (BKT) transition, which crucially depends on the strength of the interparticle interactions and is associated with an algebraic decay of the first-order spatial correlations. In the harmonic traps used in previous experimental work, the inhomogeneous atomic density has complicated quantitative studies of the thermodynamics, spatial correlations and out-of-equilibrium dynamics, prompting uniform 2D Bose gases with tuneable interactions promising candidates to shed light on the BKT phase.

Here we report on an experimental implementation of a 2D uniform trap for bosonic ^{39}K atoms by sculpting an optical box trap. The 2D confinement of the gas is realised using a digital micromirror device (DMD) in Fourier configuration that can dynamically change the axial trap frequency of a far-blue detuned light sheet trap at 532 nm. The in-plane circular box potential is derived from a spatial light modulation technique using blue-detuned light near 760 nm, which generates stiff, repulsive walls separated by a variable distance [1]. We have performed a characterisation of the optical box trap, which includes the loading e ciency of the ^{39}K BEC to the box with and without a DMD-controlled optical accordion, the achievable vertical trapping frequencies up to 12.9 kHz, the in-plane homogeneity, trap depth and the power-law associated with the potential walls. Importantly, our ^{39}K sample allows us to tune the atomic interactions by employing a wide magnetic Feshbach resonance for atoms in the $|1,1\rangle$ hyperfine state near 402.70 G [2]. In a first step, we address the collapse of a 2D degenerate Bose gas by tuning to attractive interactions. Unlike 3D systems, where a counterbalance of kinetic and interaction energy promotes a metastable BEC even for negative s-wave scattering lengths (below a critical value), the 2D uniform Bose gas is prone to collapse or stabilise without the existence of a metastable state. By investigating the critical scattering length for collapse as a function of the box parameters and axial trapping frequencies, we expect to connect genuine two- and three-dimensional physics.

In the future, we plan to use our uniform 2D Bose gas with tuneable interactions to provide insight into the behaviour of second sound near the BKT phase transition under hydrodynamic conditions [3], which might reveal the associated universal jump of the superfluid density [4]. Moreover, we intend to implement a Bragg interferometric technique to measure the first-order spatial correlations of the gas and exploit the high-speed control of the DMD as well as the ability to rapidly quench interactions to study lower-dimensional out-of-equilibrium physics, which are expected to reveal clearly pronounced features in a 2D uniform gas.

[1] A.L. Gaunt et al., PRL 110, 200406 (2016)

[2] R.J. Fletcher et al., Science 355, 377(2017)

[3] R.J. Fletcher et al., submitted (2018)

[4] M. Ota and S. Stringari, PRA 97, 033604 (2018)

Lifetime of a chiral superfluid in an orbital optical lattice

R. Eichberger[1,2], **R. Büchner**[1], **M. Hachmann**[1] **and A. Hemmerich**[1,2]

[1] *Institut für Laser-Physik, Universität Hamburg, Luruper Chaussee 149, 22761 Hamburg, Germany*

[2] *The Hamburg Center for Ultrafast Imaging, Luruper Chausee 149, 22761 Hamburg, Germany*

We study bosons in metastable higher bands of an optical square lattice, where the composition of local orbitals with different nodal geometry and orientation can lead to wavefunctions with highly complex patterns of the local phase. In the second band the ground state wavefunction comprises local p_x and p_y-orbitals. If the lattice beams are precisely controlled to provide 4-fold rotation symmetry, p_x and p_y-orbitals are degenerate and repulsive interaction favors a complex superposition $p_x \pm ip_y$. Hence, a complex wavefunction arises with a staggered vortex phase pattern. If due to lattice imperfections a small energy difference on the order of several nanokelvin of p_x and p_y-orbitals is adjusted, only the energetically lower of the p-orbitals is populated and a real striped phase pattern arises.

We present a novel optical lattice setup, which utilizes a Michelson-Sagnac interferometer. It enables the excitation to higher bands and a precise control of even fine details of the bandstructure. The lifetime of excited metastable states in higher bands is limited by binary collisions and depends sensitively on the details of the band structure. Close to $p_x \pm ip_y$-order the lifetime is expected to significantly increase due to negative interference of different relaxation channels. We report first measurements demonstrating this effect.

One-dimensional spinor Bose gases: Spin-domain formation and giant spin-dipole polarizability

Karina Jimenez-Garcia , Andrea Invernizzi, Bertrand Evrard, Camille Frapolli, Jean Dalibard, and Fabrice Gerbier

Laboratoire Kastler Brossel, College de France, CNRS, ENS-PSL Research University, Sorbonne Universite, 11 Place Marcelin Berthelot, 75005 Paris, France

e-mail: *fabrice.gerbier@lkb.ens.fr*

Spinor Bose-Einstein condensates (BEC), quantum systems with spin degree of freedom, are excellent candidates to investigate the interplay between magnetism and superfluidity in quantum systems. Spinor BECs in reduced dimensions are particularly interesting to study both the spatial organization of spins in equilibrium, as well as non-equilibrium dynamics after a quench.

Here we present the experimental study of a spin-1 BEC in a quasi-1D geometry. We use a single red-detuned laser beam to produce a highly elongated trapping potential, that, to a very good approximation, is independent on the internal state of the atoms (Zeeman states: $m_F = 0, +1, -1$).

We observe a phase transition (fig. 1), from a $m_F = \pm 1$ mixture favored by anti-ferromagnetic interactions to a $m_F = 0, +1$ phase separated state, energetically favored at high magnetic field, due to the quadratic Zeeman effect. In that later case, we observe the spontaneous formation of spin-domains.

Spin-domains have been previously observed in the presence of magnetic forces [1]. In our experiment, we work with su ciently small magnetic field gradients, so that the formation and spatial arrangement of the domains inside the trap is primarily driven by the spin-dependent interactions [2]. At su ciently high field in the absence of external forces the mF=0 domain tends to be localized at the center of the trap, surrounded by polarized mF=+1 domains (fig. 1).

In a second experiment, we measure a significant increase of the linear response to a magnetic field gradient – the so-called spin-dipole polarizability – for a partially polarized and phase-separated spinor gas compared to a completely polarized system.

Finally, we study the evolution of spin domains after the sudden cancellation of a strong magnetic force.

References

[1] J. Stenger, S. Inouye, D. M. Stamper-Kurn, H. J. Miesner, A. P. Chikkatur, and W. Ketterle, Spin domains in ground-state Bose-Einstein condensates, Nature **396**, 345348 (1998).

[2] Michal Matuszewski, Ground states of trapped spin-1 condensates in magnetic field, Phys. Rev. A **82**, 053630 (2010).

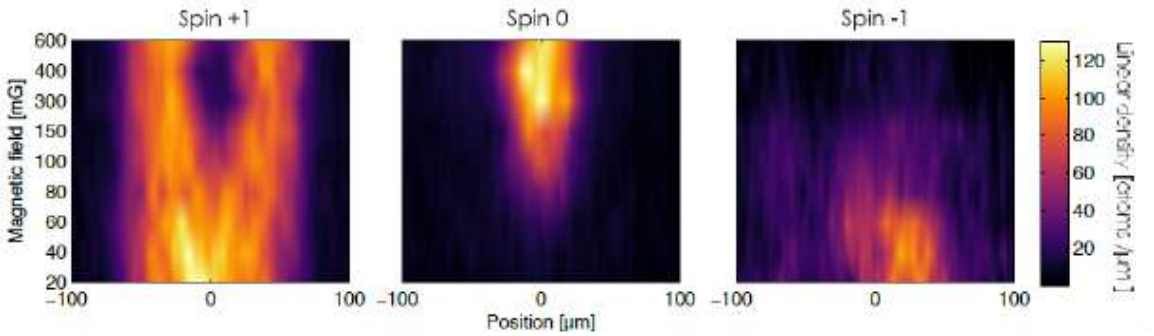


Figure 1: Magnetic phase transition in a spin-1 BEC

Nanosecond geometric control of electric dipole

Yizun He, Yuzhuo Wang, Jian Zhao, Liyang Qiu and Saijun Wu
Department of Physics, State Key Laboratory of Surface Physics and Key Laboratory of Micro and Nano Photonic Structures (Ministry of Education), Fudan University, Shanghai 200433, China
e-mail: *saijunwu@fudan.edu.cn*

Abstract

We report high fidelity coherent control of electric dipole moment of a strong optical transition using shaped nanosecond laser pulses. A combination of adiabatic and diabatic manuvours prepare laser-cooled ground state ^{39}K atoms into various quantum states with uniformly oriented D1 electric dipoles. Geometric gate operations with operation time as short as 2 nanosseconds are realized by quasi-adiabatially evolving the states with nullified dynamic phases [1]. Fidelity of gate operations is retrieved by measuring the photon recoil associated with optical excitations. We realize all the gates in the Clifford group with fidelity $f = 84\% \sim 91\%$. We discuss extension of this work, with straightforward improvements, for manipulation of sub-radiant dipole excitation in dense gases, as well as for fast matterwave acceleration [2] in laser cooling and atom interferometry.

[1] S-L. Zhu and Z. D. Wang, Phys. Rev. Lett. **097902**, 89 (2002).

[2] X. Miao, E. Wertz, M. G. Cohen and H. Metcalf, Phys. Rev. A. **011402**, 75 (2007).

Optical switching in Doppler broadened multilevel atomic systems

K. Yadav* **and A. Wasan**
Department of Physics, Indian Institute of Technology, Roorkee 247 667, India
e-mail: *kadphdph@iitr.ac.in*

One of the most promising mediums to study the light atom interaction for coherent control are multilevel atoms. Multilevel atoms serve as effective hosts for the multi-photon interactions and higher order nonlinear processes. Electromagnetically induced transparency (EIT), a quantum interference phenomenon causes the cancellation of the absorption of a weak probe field in the presence of a strong control field for a medium composed of a multilevel system [1]. Therefore, the optical response of the medium can be manipulated owing to the ability to induce coherence using the laser fields. EIT transparency is associated with a normal dispersion while enhanced absorption results in an anomalous dispersion at the line center. Ever since the initial studies of EIT extensive work has been done employing EIT. Originally EIT was investigated in simple three-level systems named as Λ, Ξ and V. However, in recent times, modification of EIT and its applications with the inclusion of an additional fourth level have also been of burgeoning interest and are widely explored.

Depending on the nature of decay pathways, various interesting features are observed in the Ξ system contrary to the other two systems. We study two type of four-level systems by adding an extra level in the three-level Ξ system named as inverted-Y and $\Xi-\Lambda$ for ^{87}Rb atom. Adding one more level increases the degree of freedom of the EIT phenomenon that further enhances the EIT controllability. These complex multilevel systems can be employed for optical switching applications. We elucidate the EIT phenomenon in these multilevel systems and examine optical switching applications theoretically. The probe absorption can be turned on and off in the considered multilevel systems on varying the chosen parameters. EIT transparency is associated with normal dispersion and enhanced absorption results in an anomalous dispersion at the line center [2]. The normal and anomalous dispersion lead to sub- and super-luminal light propagation, respectively. In an inverted-Y type system which is composite of Ξ and Λ subsystems, wavelength mismatching effects are taken into account [3]. The mixing of Doppler-free (Λ) and Doppler-broadened (Ξ) systems is borne out to be favorable and splitting is observed in the absorption and the dispersion profiles. Narrow absorption peaks are observed on both the sides of the resonance and the slope behavior changes from positive at the line center to negative just near the line center. Our numerical results show that both types of light propagation can be obtained by the experimental realization of our system. The variation of group index with the coupling field shows switching from sub-luminal to super-luminal and again back to sub-luminal when the first coupling field is slightly detuned. This switching behavior is most prominent in the Rydberg state with largest mismatching factor among all the discussed states

However, in the $\Xi-\Lambda$ system enhanced absorption is observed at the line center [4]. In $\Xi-\Lambda$ system, transparency switches into absorption when the third field is applied. In our system, the three-photon resonance condition is not fulfilled for the moving atoms always. Atoms moving with some specific velocities, contribute to the absorption at the zero detuning. Optical switching is more prominent in the moving atoms as compared to the stationary atoms. The transient behavior displays enhanced absorption on applying the drive field and can be utilized for optical switching. This enhanced absorption is modified for optimum strength of the control field and can facilitate the absorptive optical switching applications. A correlation is observed due to the three-photon coherence between the FWM and the TPEIA. Our theoretical study helps to get a deeper insight into the three-photon effects in multilevel systems.

References

[1] M. Fleischhauer, A. Imamoglu, J. P. Marangos, Rev. Mod. Phys. **77**, 633 (2005).

[2] V. Bharti and V. Natrajan, Opt. Commun. **392**, 180 (2017).

[3] K. Yadav, A. Wasan, Phys. Lett. A **381**, 3246 (2017).

[4] K. Yadav, A. Wasan, J. Phys. B: At. Mol. Opt. Phys. **51**, 105501 (2018).

Highly bright polarization-entangled photon-pairs from a Doppler-broadened ladder-type atomic ensemble

Jiho Park, Heonoh Kim, and Han Seb Moon*
Department of physics, Pusan National University, Busan, Korea
*e-mail: *hsmoon@pusan.ac.kr*

Quantum entanglement was to be at the heart of quantum mechanics and most counter-intuitive phenomena in the classical world. The generation of entangled photons is a very important key technology in areas of quantum communication, quantum simulation, quantum computing, and quantum metrology. The most popular method for the generation of polarization-entangled photon pairs is the spontaneous parametric down-conversion (SPDC) process in $\chi^{(2)}$ nonlinear crystals. SPDC sources are highly bright photon pairs, but their coherence time is short. Recently, the generation of polarization-entangled photon pairs has been demonstrated using the spontaneous four-wave mixing (SFWM) process in cold atomic ensemble [1]. The coherence time of SFWM sources in an atomic system is greater than that of SPDC sources, but the photon-pair generation rate of SFWM sources is low [2].

We report on an e cient experimental scheme for producing bright CW-mode Sagnac source of polarization entangled photon pairs with a coincidence counting rate per input power (cps/mW) of tens of thousands, obtained via spontaneous four-wave mixing from a Doppler-broadened atomic ensemble of the $5S_{1/2}$-$5P_{3/2}$-$5D_{5/2}$ transition of ^{87}Rb. The photon-pair generation rate is enhanced by the two-photon coherence contributions from almost all he atomic velocity groups in the Doppler-broadened ladder-type atomic system. We obtained the violation of the Cauchy-Schwarz inequality by a factor of 10,000 and confirmed the polarization correlation of the paired signal and idler photons. We believe that our scheme for highly bright paired photons is important as a useful quantum light source for quantum entanglement swapping between completely autonomous sources.

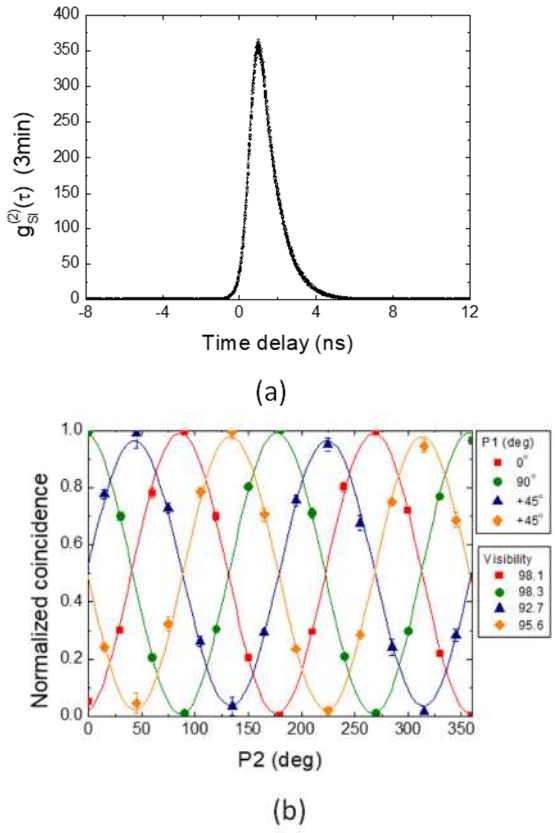


Figure 1: (a) Normalized temporal cross-correlation fuction between signal and idler photons. (b) Polarization correlation of the paired signal and idler photons.

[1] K. Liao, H Yan, J. He, S. Du, Z.-M. Zhang, and S.-L. Zhu, Phys. Rev. Lett **112**, 243602 (2014).

[2] Y.-S. Lee, S. M. Lee, H. Kim, and H. S. Moon, Opt. Express **24**(24), 28083 (2016).

Bidirectional lasing with cold atoms in a ring cavity

J. Goldwin, B. Megyeri, G. Harvie, and A. Lampis
School of Physics & Astronomy, University of Birmingham, Edgbaston, Birmingham B15 2TT, United Kingdom
e-mail: *j.m.goldwin@bham.ac.uk*

We describe the experimental realisation of a bidirectional ring laser using cold atoms as the gain medium. A magneto-optical trap of potassium-39 atoms is formed at the waist of a triangular ring cavity. The standard conditions of cooling and trapping also generate gain, which triggers lasing into the counter-propagating cavity modes without the need for any additional fields. Measurements of the gain spectrum identify Mollow gain as the underlying mechanism. Threshold measurements with increasing atom number show that the laser operates in the collective strong coupling regime of cavity QED [1]. Lasing is further evidenced by a transition from photon bunching to second-order optical coherence. The laser exhibits bistability, with random switching between emission directions. A nonreciprocity is manifest as a relative shift between the resonant cavity lengths for the two emission directions.

[1] R. Culver, A. Lampis, B. Megyeri, K. Pahwa, L. Mudarikwa, Ph.-W. Courteille, and J. Goldwin, New J. Phys. **18**, 113403 (2016).

A simple approach to quantum dispersive light through single-particle quantum mechanics

Niclas Westerberg[1,2], **Angus Prain**[2,1], **Daniele Faccio**[2,1] **and Patrik Öhberg**[1]

[1] *Institute of Photonics and Quantum Sciences, Heriot-Watt University, EH14 4AS Edinburgh, UK*

[2] *School of Physics and Astronomy, University of Glasgow, Glasgow G12 8QQ, UK*

e-mail: *nkw2@hw.ac.uk*

Macroscopic quantum electrodynamics is one of the cornerstones of theoretical physics, and has been used to study a wide range of topics: Examples include Casimir-Polder forces [1], sonoluminescence [2] and photon production in ε-near-zero mateirals [3]. It is an accurate description of electromagnetism in dielectric media, but being a phenomenological model, there has been many approaches at varying levels of complexity. In general however, taking dispersion into account makes calculations prohibitively complex. In this work [5], we quantise electromagnetism coupled to a dielectric medium, represented as a continuum of oscillators, in a simple manner, reducing the problem to that of a set of complex quantum harmonic oscillators.

Summarised, we consider a quasi-microscopic action describing electromagnetism coupled to a set of oscillators:

$$
\begin{aligned}
S_\gamma &= \int_{t_i}^{t_f} dt \int d^3x \, \frac{1}{2}\left[\dot{\mathbf{A}}^2 - (\boldsymbol{\nabla}\times\mathbf{A})^2\right] \\
S_R &= \sum_i \int_{t_i}^{t_f} \int d^3x \, \frac{\rho}{2}\left[\dot{\mathbf{R}}_i^2 - \Omega_i^2(\mathbf{x},t)\mathbf{R}_i^2\right] \\
S_{\text{int}} &= \sum_i \int_{t_i}^{t_f} \int d^3x \; (-\rho q_i)\; \dot{\mathbf{A}}\cdot\mathbf{R}_i, \qquad (1)
\end{aligned}
$$

where ρ is the density of oscillators. Each of the natural oscillation frequencies $\Omega_i^2(\mathbf{x},t)$ is in general space- and time-dependent. This action is inspired by the Hopfield model employed in Ref. [4]. We then quantise this action in a path integral formalism, and by transforming into polariton field-coordinates we reduce the problem to that of complex harmonic oscillators in two-time potentials. From this, we calculate the probability to excite two back-to-back polaritons for a realistic scenario, when modulating the medium with two frequencies. This is illustrated in Fig. 1.

[1] W. M. Simpson and U. Leonhardt, *Forces of the quantum vacuum: An Introduction to Casimir Physics* (World Scientific, 2015).

[2] C. Eberlein, PRL **76**, 3842 (1996)

[3] A. Prain, ... , N.W. *et al*, PRL **118**, 133904

[4] R. Y. Chiao *et al*, PRA **69**, 063816 (2004)

[5] N.W. *et al*, arXiv preprint: to appear soon

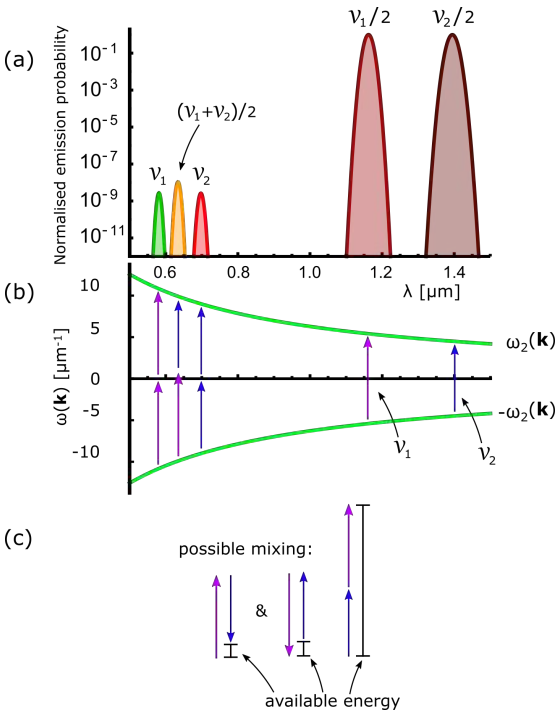


Figure 1: **(a)** The probability of exciting two polaritons back-to-back from the vacuum when modulating fused silica. Here we used $\delta n \simeq 10^{-4}$ by modulating the Ω_2-resonance (near-visible-ultaviolet) at frequencies $\nu_1 = \Omega_2/5$ and $\nu_2 = \Omega_2/6$ for $N = 50$ periods (100-250fs depending on wavelength). We also normalised to the maximum probability of $\sim 10^{-8}$: The absolute numbers are not important for this study. The peaks are labelled identifying each process, and we have ignored peaks that are outside the optical/infrared window. The spectrum is in *vacuum* wavelengths. Note in particular the $(\nu_1+\nu_2)/2$ peak: This would be absent in a dispersionless medium. **(b)** The polariton branch of interest as a function of vacuum wavelength. The excitation processes always involve a polariton-antipolariton pair, the latter living at negative frequency: The time-modulation provides the energy that couples the pair, here denoted as coloured arrows. Importantly, the total energy of the polariton-antipolariton pair ($2\omega_\alpha$) must be matched by the energy supplied by the time-modulation. **(c)** Illustration of the possible mixing processes at second order in perturbation theory.

Direct frequency-comb-driven Raman transitions in the terahertz range

C. Solaro[1], **S. Meyer**[1], **K. Fisher**[1], **M. V. DePalatis**[1] **and M. Drewsen**[1]
[1] *Department of Physics and Astronomy, Aarhus University, DK-8000 Aarhus C, Denmark*
e-mail: *solaro@phys.au.dk*

I will present our recent results on the use of a femtosecond frequency comb to coherently drive stimulated Raman transitions between terahertz-spaced energy levels [1]. More specifically, we address the $3d\ ^2D_{3/2}$ and $3d\ ^2D_{5/2}$ fine structure levels of a single trapped $^{40}Ca^+$ ion. We achieved Rabi oscillations with 99.3(6)% contrast and milliseconds coherence time (see figure 1)! We also show that the population dynamics of frequency-comb-driven Raman transitions can be fully predicted from the spectral properties of the femtosecond frequency comb.

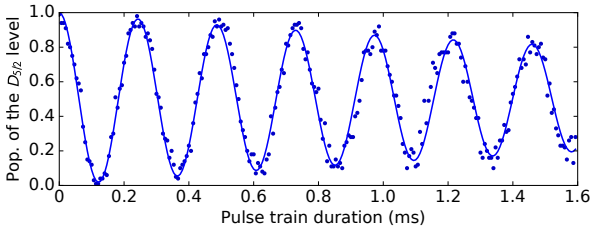


Figure 1: Frequency comb driven Raman Rabi flopping between the ~ 1.8 THz fine structure split $3d\ ^2D_{3/2}$ and $3d\ ^2D_{5/2}$ states of a single trapped $^{40}Ca^+$ ion.

Furthermore, we spectroscopically resolve the $3d\ ^2D_{3/2} \leftrightarrow 3d\ ^2D_{5/2}$ transition frequency with a relative accuracy of 5.5×10^{-12} (see figure 2)! The achieved accuracy is nearly a factor of five better than the previous best Raman spectroscopy [2], and is currently limited by the inaccuracy of our atomic clock reference.

Using direct frequency comb Raman spectroscopy on four other isotopes $^{42,44,46,48}Ca^+$, in combination with precise measurements of the $4s\ ^2S_{1/2} - 3d\ ^2D_{5/2}$ transition, will eventually allow us to improve bounds on new physics beyond the standard model [3,4].

The technique can easily be generalized to transitions in the sub-kHz [5] to tens of THz range and should be applicable for driving, e.g., spin-resolved rovibrational transitions in molecules and hyperfine transitions in highly charged ions, opening up paths towards new qubit systems for quantum technologies.

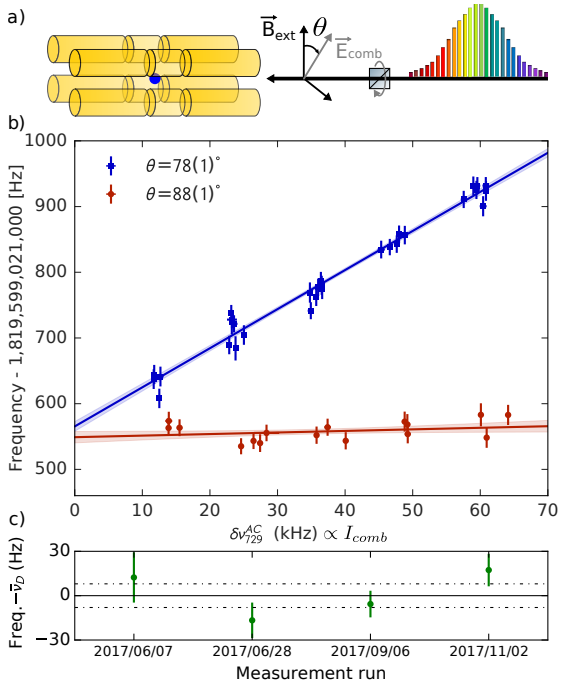


Figure 2: a) Schematic of the linear Paul trap showing the frequency comb polarization with respect to the applied external magnetic field. b) Measured transition frequency as a function of frequency comb intensity for two different polarizations of the frequency comb. The differential AC-Stark shift induced by the frequency comb cancels for a given "magic polarization". c) Absolute frequency measurements performed over five months used to determine the fine structure level separation $\bar{\nu}_D = 1{,}819{,}599{,}021{,}534 \pm 8$ Hz. The dashed lines correspond to the 8 Hz standard deviation of the mean.

[1] C. Solaro et al. arXiv:1712.07429, accepted for publication in PRL (2018)
[2] R. Yamazaki et al. PRA 77,012508 (2008)
[3] S. Meyer et al. in preparation
[4] J.C. Berengut et al. PRL 120,091801 (2018)
[5] D. Hayes et al. PRL 104,140501 (2010)

Excitation enhancement in optical forbidden transitions near nano structure

Satoshi Tojo[1], **Taro Mashimo**[1], **Masashi Abe**[1], **and Daniel Bloch**[2]
[1] *Department of Physics, Chuo University, 112-8551 Tokyo, Japan*
[2] *Laboratoire de Physique des Lasers, UMR 7538 du CNRS, Universite Paris 13-Sorbonne-Paris-Cite, F93430 Villetaneuse, France*
e-mail: *tojo@phys.chuo-u.ac.jp*

We have investigated optical forbidden, namely electric and magnetic multipole, transitions of atoms in the vicinity of a nano-structure. We calculate excitation efficiencies of optical forbidden transitions in alkali atoms with scale and angle dependences of a scattered electro-magnetic field generated by a nanostructure. Due to strong field gradients depending on both scales and angles, the excitation efficiencies of the electric and magnetic multipoles reach 5 orders of magnitude larger than that in free space regime.

Local fields in the vicinity of a nano-structured surface are one of powerful tools for generation of high intensity, high field gradient, and strong localization below a diffraction limit of light. The spatial localization of light leads to the inhomogeneous large spatial modulation or electric field gradient more than that of a homogeneous field in free space. Recently, electric and magnetic multipole transitions are investigated due to these multipole, such as an electric quadrupole (E2) and a magnetic dipole (M1), transitions depending explicitly on the wave vector [1] or the field gradient of the excitation light field [3, 4].

The excitation efficiencies of electric dipole (E1), quadrupole (E2), and octupole (E3) transitions were calculated in use of a 2D rectangular silver with nanoscale curvature R irradiated by a θ-angled light for incident light with linear polarization at 389 nm corresponding to rubidium $5^2S_{1/2}$–$5^2D_{5/2}$ transition as shown in Fig.1(a). Figure 1(b) shows calculation results of excitation efficiencies in E1, E2, and E3 transitions near the nano structured surface at various curvatures being 2, 10, and 50 nm at $\theta = 0$ degree. The efficiency of E2 and E3 transitions in the range of 5 to 200 nm can be explained by $(1/R)^2$ dependence while that of E1 transition has small change. The large multipole excitation efficiencies near an edge can be understood in the frame of the spherical harmonics basis. In general, a scattered field is given as the solution of the Helmholtz equation $(\nabla^2 + k^2)f(\mathbf{r}) = 0$ and the solution $f(\mathbf{r})$ can be expanded to the radial and spherical harmonics such as atomic wave functions [2]. The excitation efficiencies depend not only on the curvatures but on angles due to the change of the scattered electric field. In the case of E2 transition, the enhancement factor which is the excitation efficiency normalized by the oscillator strength has strong angle dependence,

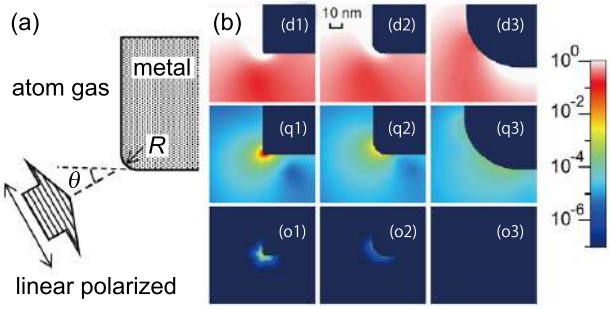


Figure 1: (a) Schematic geometry of a nanostructure and incident light. (b)Two-dimensional plots of the excitation efficiencies of (d1)-(d3) E1, (q1)-(q3) E2, (o1)-(o3) E3 transitions with curvatures of (d1), (q1), (o1) 2 nm, (d2), (q2), (o2) 10 nm, and (d3), (q3), (o3) 50 nm.

and the factor around $\theta = 15$ degrees reaches 1 order, totally 5 orders, of magnitude larger than that at $\theta = 0$. The results indicate that excitation efficiencies of multipole transitions close up those of dipole transitions due to several orders of magnification near the nano-structured surface, and the enhanced multipole transition may give aid to high sensitive detections and novel developments for high efficiency devices.

Simulations were performed with the finite-difference time-domain (FDTD) method, using a freely available software package [5]. We would like to thank Kosuke Shibata for his early work. The work was supported by Grants-in-Aid for Scientific Research from JSPS and the MAEDI/SAKURA Program for Japan-France bilateral project.

[1] S. Tojo, M. Hasuo, and T. Fujimoto, Phys. Rev. Lett. **92**, 053001 (2004).

[2] K. Shibata, S. Tojo, and D. Bloch, Opt. Express. **25**, 9476 (2017).

[3] V. V. Klimov, D. Bloch, M. Ducloy, and J. R. Rios Leite, Phys. Rev. A **85**, 022501 (2012).

[4] K. Deguchi *et al.,* J. Phys. Soc. Jpn. **78**, 024301 (2009); A. M. Kern and O. J. F. Martin, Phys. Rev. A **85**, 022501 (2012).

[5] A. Taflove and S. C. Hagness, *Computational Electrodynamics:* The Finite-Difference Time-Domain Method (Artech; Norwood, MA, 2000).

A versatile neutral-atom microtrap using high NA optics to study light-matter interaction

Lorena C. Bianchet[1], **Vindhiya Prakash**[1], **Nan Li**[2], **Natalia Bruno**[1] **and Morgan W. Mitchell**[1,3]

[1] *Institut de Ciències Fotòniques, Barcelona Institute of Science and Technology, 08860 Castelldefels (Barcelona), Spain*

[2] *State Key Laboratory of Modern Optical Instrumentation, College of Optical Science and Engineering, Zhejiang University, Hangzhou 310027, China*

[3] *ICREA-Institució Catalana de Recerca i Estudis Avançats, 08010 Barcelona, Spain*

e-mail: *lorena.bianchet@icfo.eu*

We describe the design and experimental status of a versatile system for studying atom-photon, atom-atom, and photon-photon interactions at the single-particle level. The system uses high-NA lenses to achieve strong atom-photon interactions and individual-atom microtrapping without cavities, as in [1, 2, 3]. In contrast to those works, high-NA access is obtained in four directions, opening new possibilities, including structured atomic potentials, trapping of multiple atoms, and study of multi-photon processes, e.g. stimulated emission at the single-photon level.

The system consists of a strongly-focused far-off-resonance trap (FORT) loaded from a magneto-optical trap (MOT) of ^{87}Rb (scheme and picture in Figures 1 a and b). Because of the geometry constraints due to the small distance between the lenses (NA = 0.5) MOT beams are placed in the space in between the lenses. With 0.7mm diameter beams in the horizontal directions and 2mm in the vertical ones, the obtained micro-MOT has 100μm size.

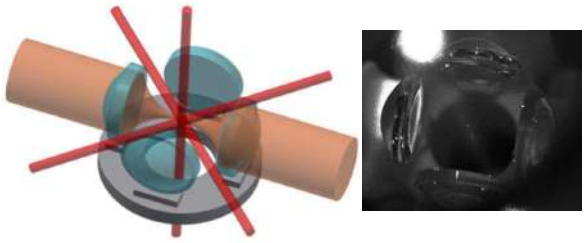


Figure 1: *Left* Geometry of the experiment. Four aspherical lenses (NA=0.5) with MOT beams and FORT beams. *Right* Picture of the experiment.

Strong focusing of the FORT beam (down to 1μm waist size) produces a very small trap that, due to light-induced collisions, can hold at most one atom. This process is evidenced in the Figure 2, where we show the presence of either zero or one atoms in the trap (and a short presence of a second trapped atom) by measuring its fluorescence with an APD.

A standing wave in the dipole trap beam can produce an arrangement of multiple single atom traps

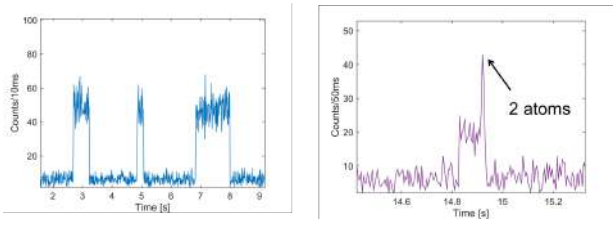


Figure 2: *Left* Discrimination of the number atoms in the trap . *Right* Detection of a second atom falling in the trap (double fluorescence rate) and subsequently both atoms leaving the trap due to light assisted collisions.

allowing for non-destructive atomic correlations measurements [3].

The lenses have been aligned and glued onto a macor base one by one following a precise protocol of optical metrology developed in our group, in order to optimize the wavefront at the waist position. Aberrations due to the commercial lenses used (that are designed to work with a cover slip) were optically compensated with the divergence of the trap beams.

This setup allows matching of the atomic dipole pattern to a travelling optical beam, leading to a significant probability of atomic excitation even with only one incident photon.

Due to this strong interaction, most optical processes carry very low power requirements, which allowed us to develop an extremely stable experiment based on DBR lasers and a FPGA control system.

[1] M. K. Tey et al., *Nature Physics*, vol. 4, no. 12, pp. 924-927, 2008.

[2] A. M. Kaufman et al., *Science*, vol. 345, no. 6194, pp. 306-309, 2014.

[3] D. Barredo et al., *Science*, vol. 354, no. 6315, pp. 1021-1023, 2016.

Microscale atom-photon junction

E. Da Ros[1], **N. Cooper**[1], **and L. Hackermüller**[1]
[1] *School of Physics & Astronomy, University of Nottingham, United Kingdom*
e-mail: *elisa.daros@nottingham.ac.uk*

Interfacing atoms and photons is of fundamental interest in the implementation of quantum networks [1]. The potential for storing photons in atomic ensembles or generating single photons from atomic ensembles has already been proven [2], therefore the interaction between the atomic ensemble and the light can act as a node for the storage and processing of quantum information. However, quantum information processes require e cient transfer of the information. The e ciency of information transfer can be improved by tight focussing of the light onto the atoms, as well as by the use of optical cavities. Direct interfacing of cold atoms with the guided mode of a fibre is therefore an attractive mechanism by which to create atom-photon interfaces, as the small mode area increases the interaction rate. Furthermore, optical cavities can be readily implemented via the use of in-fibre Bragg gratings.

We have developed a microscopic atom-photon junction (Fig. 1) capable of coherently interfacing cold atoms with light guided through a single mode optical fibre. Our system relies on the interaction between photons guided through a single-mode optical fibre and an ensemble of cold Caesium atoms tightly confined by an optical dipole trap, formed in a microscopic void that has been laser-drilled through the fibre itself, see Fig. 2. We demonstrate loading of a cold cloud of Caesium atoms into the fibre's void and investigate the interaction between the atoms and a probe beam coupled into the fibre.

An advantage of the laser drilling technique over alternative methods for forming such a junction is that it can be implemented not only in a single optical fibre, but also at any desired point within a 2D waveguide chip. This allows direct integration of cold atoms into existing photonic circuits.

With a view towards longer term quantum information applications, we have also carried out numerical simulations of light transmission across waveguide junctions of this type. In work to be published shortly [3], we show that shaping of the hole interfaces using laser micro-machining has the potential to substantially enhance transmission across such junctions, as well as to create an even tighter focus for the guided light when it reaches the atoms. Both of these help to make the system a more viable candidate for integrated quantum information processing.

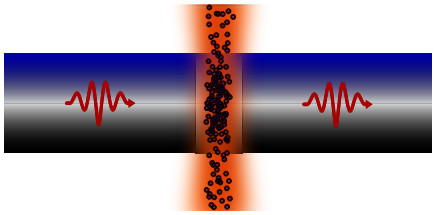


Figure 1: Simplified diagram of the fibre junction. Photons guided through the fibre mode interact with the atoms trapped in the fibre void and are collected back into the fibre mode.

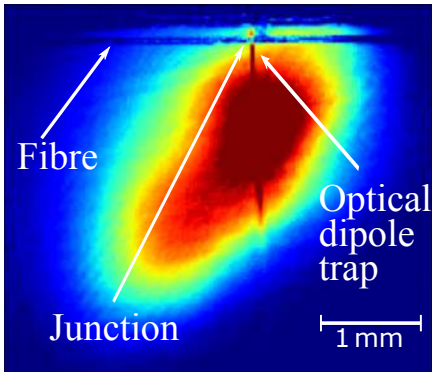


Figure 2: Absorption imagining of the Caesium cloud trapped in the vertical optical dipole trap that is aligned with the fibre void.

[1] H. J. Kimble, Nature **453**, 10231030 (2008).

[2] B. Gouraud, D. Maxein, A. Nicolas, O. Morin, and J. Laurat Phys. Rev. Lett. **114**, 180503 (2015).

[3] C. Briddon, E. Da Ros, V. Naniyil, M. Greenaway, N. Cooper, and L. Hackermüller (In Preparation).

Tuning dipole-dipole interactions in atomic vapours via cavities

Helge Dobbertin[1] **and Stefan Scheel**[1]

[1] *Institut für Physik, Universität Rostock, Albert-Einstein-Straße 23, D-18059 Rostock, Germany*

e-mail: *helge.dobbertin@uni-rostock.de*

When resonant atoms are confined inside a volume smaller than the transition wavelength λ cubed, they couple strongly via dipole-dipole interactions. Here we study the resulting transmission spectra, line shifts and line broadenings by means of a microscopic coupled dipole model [1] for hot and cold atomic vapours. We incorporate the influence of a Fabry-Perot nanocavity on single atom properties (Casimir-Polder and Purcell effect) and atom-atom interactions. As a result, cavity parameters such as length and finesse can be used to tailor spectra and line shifts. Our approach may help to explore the origin of line shifts recently observed in dense thermal vapours confined in nano-cells [2, 3]. For changing cavity parameters, collisional interactions between atoms as well as atoms and surface do not vary strongly. Hence, our approach may help to discriminate dipole-dipole induced effects from other contributions to the spectra. Finally, the microscopic modelling can be used to study the emergence of macroscopic vapour properties from microscopic atomic properties in different temperature regimes.

References

[1] J. Javanainen et al., Phys. Rev. A **96**, 033835 (2017).

[2] J. Keaveney et al., Phys. Rev. Lett. **108**, 173601 (2012).

[3] T. Peyrot et al., Phys. Rev. Lett. in print, arXiv:1801.01773v2 (2018).

Towards a quantum interface between cold atoms and a nano membrane

Chun Tat Ngai[1], **Thomas M. Karg**[1], **Baptiste Gouraud**[1], **Gianni C. Buser**[1], **Klemens Hammerer**[2], **and Philipp Treutlein**[1]

[1] *Department of Physics, University of Basel, Klingelbergstrasse 82, 4056 Basel, Switzerland*

[2] *Institute for Theoretical Physics, Leibniz University Hannover, Callinstrasse 38, 30167 Hannover, Germany*

e-mail: *c.ngai@unibas.ch*

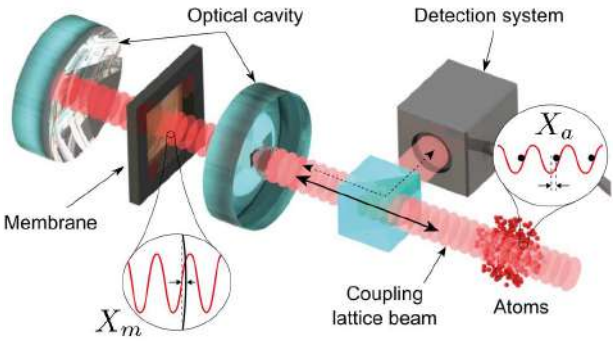


Figure 1: Sketch of the experimental setup

Hybrid systems in which a mechanical degree of freedom is coupled to a microscopic quantum system promise control and detection of mechanical motion at the quantum level. By reaching the quantum regime, fundamental test of creating a macroscopic quantum state and applications in precision sensing and quantum signal transduction can be realized [1, 2].

In our experiment, we study a hybrid system (Fig. 1) that consists of a cold atomic ensemble and a membrane oscillator inside an optical cavity separated at the metre-scale. A long-distance two-way quantum bus between the subsystems is established by coupling them with a common optical mode. Using the atoms as a coolant, our group has demonstrated sympathetic cooling of the macroscopic oscillator from room temperature to below 1 Kelvin [3]. Moreover, we observed light-mediated collective atomic motion in the optical lattice, inducing atom-membrane self-oscillations in the hybrid system [5].

Here we will report on experimental progress towards operation of the system in the quantum regime. On the one hand, we have built and characterized a membrane-in-the middle setup in a liquid Helium flow cryostat designed for large optomechanical cooperativity in the non-resolved sideband regime. This regime allows fast transfer of information between the two systems.

On the other hand, we have realized a light-matter interface where the collective atomic spin (in contrast to its center of mass position from previous experiments) is coupled to the polarization state of light via the vector Stark shift. Recently, we have observed the first Faraday rotation signal from the atomic spins.

We couple the spins of the atoms to the motional degree of freedom of the membrane oscillator using a scheme inspired by [4]. Experimentally, this is implemented in the following way: The magnetic population difference is imprinted on the laser as a Faraday rotation. Subsequent polarization optics converts the atomic signal into amplitude modulation of the light field entering the optomechanical cavity, hence modulating the radiation pressure force on the membrane. The membrane imparts a phase modulation to the light reflected on it, converted via polarization interferometry to circular polarization. The circular polarization of the light field then sent to the atoms is seen as an effective magnetic field around which the atoms can precess. Combining the two directions of remote coupling, the scheme allows to create an effective Hamiltonian interaction. We now work towards the realization of coherent coupling between atomic spin and mechanical resonator.

References

[1] K. Hammerer et al., Physical Review Letters **102**, 020501 (2009).

[2] P. Treutlein et al., in: Cavity Optomechanics, ed: M. Aspelmeyer, T. J. Kippenberg, and F. Marquardt (Springer, Berlin 2014) pp. 327-351.

[3] A. Jöckel et al., Nature Nanotechnology **10**, 55-59 (2015).

[4] B. Vogell et al., New Journal of Physics **17**, 043044 (2015).

[5] A. Vochezer et al., Phys. Rev. Lett. 120, 073602 (2018).

Two-mode intensity squeezing using OAM-carrying pump and probe beams

N. Prajapati[1], **N. Super**[1], **and I. Novikova**[1]

[1] *Department of Physics, The College of William and Mary, Williamsburg, VA 23185, USA*

e-mail: *nprajapati@email.wm.edu*

Light carrying optical angular momentum (OAM) is of particular interest in quantum information technologies due to its potential for increasing channel capacity [1], as multiple OAM states can be encoded onto a single beam or even individual photons [2]. Here we investigate the possibility of generating quantum-correlated optical fields with controllable OAM in a FWM process, shown in Fig. 1(a). Previous studies have shown that OAM, added to the initial control or probe field, can be used to manipulate the spatial mode of the generated Stokes field, while maintaining the high degree of quantum correlations [3].

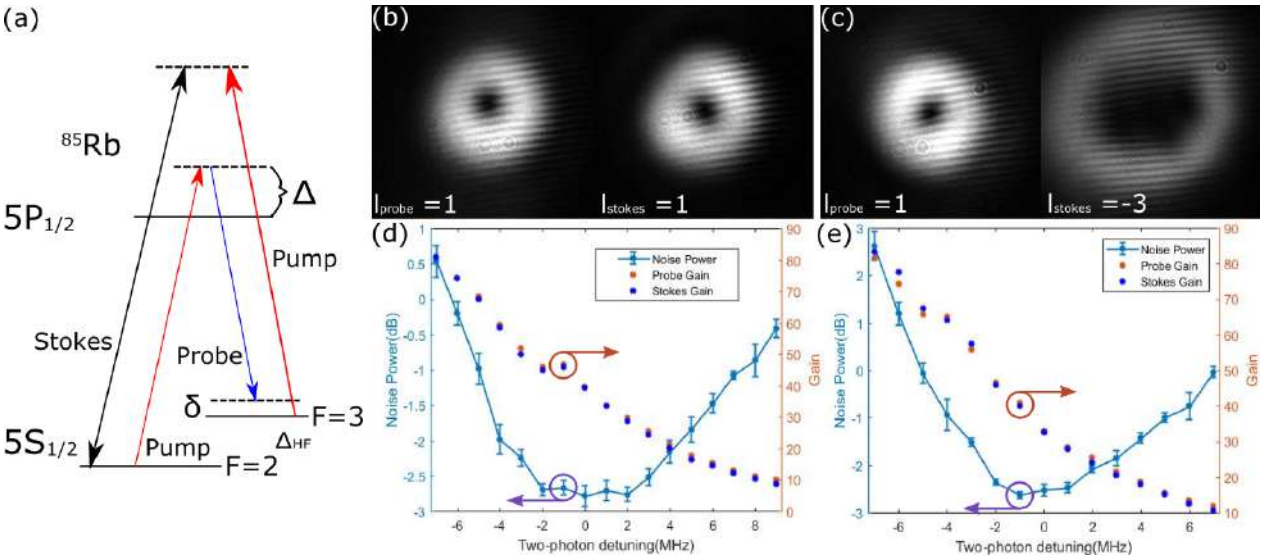


Figure 1: *(a)* FWM interaction scheme, showing the pump (red), probe (blue), and Stokes (black) optical fields interacting with the D_1 line of the ^{85}Rb atoms. The laser (one-photon) detuning $\Delta \approx 1$ GHz. *(b,c)* Spatial profiles of the amplified probe and generated Stokes beams for equal $l_{probe} = l_{pump} = 1$ *(b)* or opposite $l_{probe} = -l_{pump} = 1$ *(c)* OAM charges of the input pump and probe beams. *(d,e)* shows the corresponding differential intensity noise power relative to the shot noise (left axis) and probe and Stokes gain (right axis) as a function of two-photon detuning δ.

The focus of our experiment is to extend the parameter space of accessible OAM modes by placing OAM in both the pump and probe optical fields, and observing its effect on measured squeezing. The OAM of the input pump and probe beams were controlled independently using separate vortex masks. With this, two configurations were tested: when pump and probe optical fields had the same ($l_{probe} = l_{pump} = 1$) or opposite ($l_{probe} = -l_{pump} = 1$) OAM charges.

In the first configuration, the Stokes beam was generated in the same mode as the input beams $l_{Stokes} = 1$ in [Fig. 1(b)], as expected from the OAM conservation in a FWM process, $2l_{pump} = l_{probe} + l_{Stokes}$ (1). In the other configuration, where the two input beams had opposite OAM, the Stokes was generated in the $l_{Stokes} = -3$ mode, shown in Fig. 1(c). Not only did we observe e cient transfer of OAM in the two configurations, we saw that two-mode intensity squeezing was maintained at -2.7 dB in both configurations, shown in Fig. 1(d) and (e), respectively. This value was lower than the -3.9 dB of squeezing seen with Gaussian-shaped input beams, but the increase in noise for the OAM pump field could be attributed to the scattering off the vortex mask. In conclusion, we have demonstrated that the independent control of the OAM state of input fields shows great promise in quantum communications since it increases the number of accessible modes and maintains two-mode intensity squeezing even when there is a large OAM mode mismatch between the amplified probe field and generated Stokes field.

[1] G. Gibson, J. Courtial, M. Padgett, M. Vasnetsov, V. Pas'ko, S. Barnett, and S. Franke-Arnold, Opt. Express **12**, 5448–5456 (2004).

[2] G. Molina-Terriza, J. P. Torres, and L. Torner, Phys. Rev. Lett. **88**, 013 601 (2001).

[3] A. M. Marino, V. Boyer, R. C. Pooser, P. D. Lett, K. Lemons, and K. M. Jones, Phys. Rev. Lett. **101**, 093 602 (2008).

Quantum Mechanics in Technicolor; Analytic Expressions for a Spin-Half Particle Driven by Polychromatic Light

B. Yuen[1]

[1] *University of Oxford, Clarendon Laboratory, Parks Road, Oxford, OX1 3PU, UK*

e-mail: *benjamin.yuen@physics.ox.ac.uk*

Our experience of the world is shaped by the way light and matter interact. This interaction is described by the Jaynes Cummings or Rabi models, which can be solved analytically when limited to light of a single frequency [1, 2]. These models apply to a diverse range of systems in quantum optics and describe the underlying processes in many emerging quantum technologies. A logical step forward is to generalise the theory to find solutions of the polychromatic Rabi model. Such solutions are likely to highlight new ways to control and excite atoms, generate squeezed states and investigate decoherence as the light approaches a continuous, broadband spectrum.

I present analytic expressions for the time evolution of a spin-half particle interacting with a polychromatic field, together with a general method to find approximate analytic solutions to the polychromatic Rabi model [3]. This method extends the monochromatic dressed atom picture in which one views atoms and photons together in the eigenbasis of the interacting system [4]. For polychromatic fields, atom-photon states are dressed progressively by the interaction with each field mode, one at a time. In this polychromatic dressed atom picture the time evolution operator takes a simple approximate form. It can be transformed back to the undressed picture where it contains terms which accurately describe resonant, near resonant and far off-resonant interactions.

The complexity of the polychromatic system is reduced by working in the non-degenerate basis presented. Furthermore, the time evolution operator for the atom can be simplified greatly by retaining only the leading order terms in the field amplitudes when making the transformations between the dressed and undressed pictures. The simplified result still gives a remarkably good description of the atomic excitation when the coupling of the spin half to each mode is weak compared to frequency separation between modes.

[1] E. T. Jaynes and F. W. Cummings, Proceedings of the IEEE 51, **89** (1963).

[2] D. Braak, *Physical Review Letters* **107**, 100401 (2011). Q.-H. Chen, C. Wang, S. He, T. Liu, and K.-L. Wang, Phys. Rev. A **86**, 023822 (2012). H. Zhong, Q. Xie, M. T. Batchelor, and C. Lee, Journal of Physics A: Mathematical and Theoretical **46**, 415302 (2013).

[3] B. Yuen, arXiv preprint arXiv:1805.05922 (2018).

[4] C. Cohen-Tannoudji and S. Haroche, CR Acad. Sc. Paris B **262**, 37 (1966).

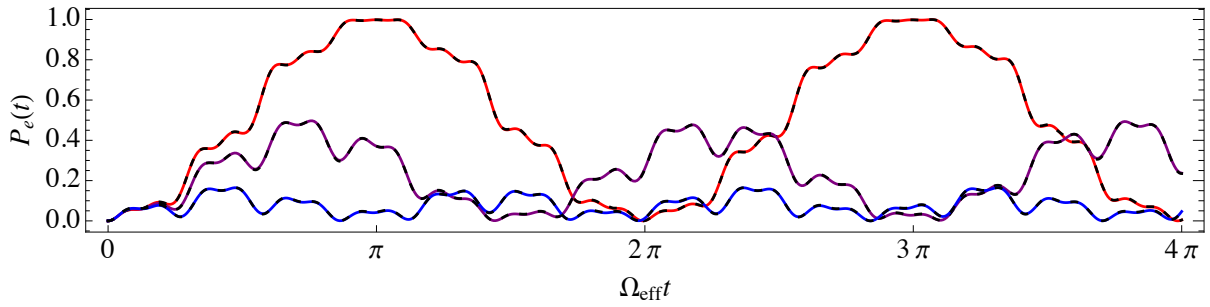


Figure 1: An example of a comparison between the analytic and numerical expressions for the excitation probability $P_e(t)$ of a spin half particle driven by a polychromatic light field. The figure shows $P_e(t)$ for a particle initially in the ground state, and a field with three modes separated evenly by frequency ω_f. The amplitude of modes are equal and correspond to a Rabi frequency of $\Omega = \omega_f/7$ when isolated from the other modes. Analytic results are shown by the red, purple and blue lines, where the spin-half is either resonant or red detuned by Ω or 2Ω from resonance with the highest frequency mode respectively. Numerical results are shown by the black dashed lines overlaid, and are in very close agreement to the analytic results.

Spatially-multiplexed coherent beamsplitter for squeezed light

Jian Sun[1], **Weizhi Qu**[1], **Eugeniy Mikhailov**[2], **Irina Novikova**[2], **Heng Shen**[3], **and Yanhong Xiao**[1]

[1] *Department of Physics, Fudan University, Shanghai 200433, China*
[2] *Department of Physics, College of William and Mary, Williamsburg, Virginia 23185, USA*
[3] *Clarendon Laboratory, University of Oxford, Parks Road, Oxford, OX1 3PU, UK*
e-mail: *12110190043@fudan.edu.cn*

Quantum imaging with high spatial resolution are of interest in optical quantum information processing and quantum metrology. Significant efforts have been made to reach and even beat the quantum noise limit [1, 2], which defines a measurement-independent absolute limit to the sensitivity that may in principle be achieved with a given number of uncorrelated photons. Although quantum-correlated light with amplitude noise squeezed below the vacuum level were used there to perform the precision measurement and the quantum shot noise limit was surpassed, the generation of squeezed light arrays, which promises the high spatial resolution, is still unexplored. Here, we report the realization of spatially-multiplexed coherent beamsplitter for squeezed light in an anti-relaxation coated ^{87}Rb vapor cell. In our scheme, the presence of squeezed state in the target optical channel is fully controlled by a spatially separated light beam, mediated by the flying atoms with long-lived ground state coherence [3]. The control beam serves as the optical pumping beam to create the spin wave, and further leads to the generation of squeezed light. Intrinsic strong nonlinearity associated with light-atom interaction and the ground state coherence transfer are the keys to the demonstration of our protocol. The demonstrated scheme can be extended to the creation of one-dimension and two-dimension arrays of squeezed light with the requirement of low laser power $\sim$ mW, which is underway.

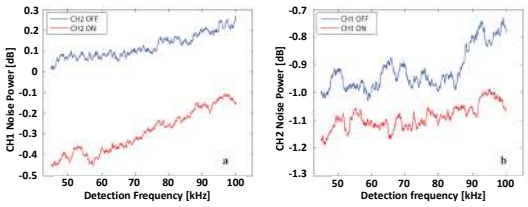


Figure 1: Squeezed quadrature noise spectra of (a) CH1 measured with and without CH2, and (b) CH2 measured with and without CH1 as a function of the detection frequency.

To demonstrate our protocol, we perform the experiment in the regime of low intensity at ^{87}Rb D1 line. Four-wave mixing (FWM) of the double-Λ system of ^{87}Rb D1 line, or polarization self-rotation (PSR), leads to the generation of squeezed light field, which is detected via phase-retarding plate (PRP) configuration [4, 5]. It is expected that the long-lived ground state coherence established in one optical channel can spread out in the entire cell, and enhance the FWM, thus improve the squeezing in the other channel. The result of a proof-of-principle experiment is shown in Figure.1, which confirms that the minimum noise in one channel can be reduced with the presence of the other channel via motional averaging of the atoms. Compared to shot-noise-level output of channel 1 (CH1), there is 0.4 dB squeezing of CH1 at the detection frequency of 40 kHz when the strong beam channe 2 (CH2) is on. Meanwhile, the noise power of CH2 is reduced as well, which enables the spatially-multiplexed coherent beamsplitter for squeezed light.

Furthermore, we investigate the dependence of noise reduciton on laser detuning. As shown in Fig.2, squeezing enhancement varies with one-photon detuning due to the competition between the saturation effect and the squeezing process.

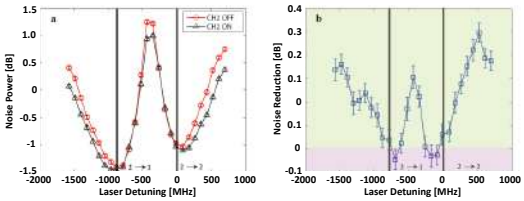


Figure 2: Laser detuning dependence of the noise reduction in quadrature with minimum variance. (a) Laser detuning dependence of the squeezed quadrature of CH1 and (b) enhancement measured with and without CH2.

[1] M. A. Taylor, et. al, Nat. Photon. 7, 229 (2013).

[2] F. Wolfgramm, et. al, Phys. Phys. Lett. 105, 053601 (2010).

[3] Y. Xiao, et. al, Phys. Phys. Lett. 101, 043601 (2008).

[4] I. Novikova, et. al, Phys. Rev. A 91, 051804(R) (2015).

[5] T. Horrom, et. al, J. Phys. B 45, 124015(2012).

Narrowband four photon entanglement swapping

Zong-Feng Li[1,2], **Xiao Liu**[1,2], **Zong-Quan Zhou**[1,2], **and Chuan-Feng Li**[1,2]

[1] *CAS Key Laboratory of Quantum Information, University of Science and Technology of China, Hefei, 230026, China*

[2] *Synergetic Innovation Center of Quantum Information and Quantum Physics, University of Science and Technology of China, Hefei 230026, China*

e-mail: *cfli@ustc.edu.cn*

We report the experimental realization of entanglement swapping with narrow band photons. By realizations of a Bell state measurement, entanglement is generated and distributed between two photons, which come from two independent entangled photon pairs. In the experiment we use Type-II parametric down conversion (PDC) to generate the photon pair in largest polarization entangled state, and the two pairs are created in spatially separated sources although pumped by the same laser.

The SPDC photon always has a wide bandwidth, which lead to a low interaction e ciency with material. Contrary to the previous swapping experiments involving multi photons [1, 2], the photon bandwidth has a magnitude of gigahertz.

[1] H. de Riedmatten *et al.*, Phys. Rev. A **71**, 050302(R) (2005).

[2] Alexander M. Goebel *et al.*, Phys. Rev. Lett **101**, 080403 (2008).

Towards a BEC-ONF Interface

C. A. Alampounti, **R. A. Jenkins**, and **S. Eriksson**
Department of Physics, College of Science,
Swansea University, SA2 8PP, Swansea, UK and
e-mail: c.a.alampounti.651871@swansea.ac.uk

Optical nanofibers (ONF) have recently shown remarkable promise in multiple aspects of atomic physics and quantum communications. They have been established as excellent imaging tools with single atom sensitivity [1] and have shown promise as ultra-high sensitivity molecular detectors [2–4], chemical and biological sensors [5] and even more recently they have shown development in the fields of quantum information and quantum cryptography [6–8]. Advances have also been shown in the study of fundamental physics including quantum chiral optics [9].

Trapping a quantum degenerate gas in the presence of the evanescent field of an ONF would open up new avenues in fundamental physics. For example, artificial gauge fields could be generated near the ONF [10]. The correlation function of light scattered into the ONF by ultra-cold atoms has been measured, from which information about the atoms themselves can be derived [11]. With some refinement, this method could be used to reconstruct the correlation function of atoms in a degenerate quantum gas with the potential to study exotic phases [12].

In this work, we report the observation of a magnetic trap of ^{87}Rb atoms near an ONF. The trapped atoms have a temperature of 73 μK and can be held in the magnetic trap with at least 1×10^7 remaining after 1 second. In this experiment the position of the magnetic trap is such that the ONF occupies some of the trap volume. A detailed lifetime analysis is in progress at the time of writing. Our experiment has the capability of employing a dimple trap, which provide short evaporation times [13]. We note that recently, it has been shown that quantum degeneracy can be reached dy direct laser cooling rubidium in only 300 ms[14]. Such developments are paving a promising path towards a BEC-ONF interface.

Our next steps involve evaporative cooling of the atoms in various potential-well configurations and studying the behaviour as the atoms are brought closer to the fibre.

The optical nanofiber described here was created at TU Wien. We gratefully acknowledge Arno Rauschenbeutel and his group for their help.

[1] K. P. Nayak and K. Hakuta, New J. Phys. **10**, 053003 (2008).
[2] F. Warken, E. Vetsch, D. Meschede, M. Sokolowski, and A. Rauschenbeutel, Opt. Express **15**, 11952 (2007).
[3] R. Garcia-Fernandez, W. Alt, F. Bruse, C. Dan, K. Karapetyan, O. Rehband, A. Stiebeiner, U. Wiedemann, D. Meschede, and A. Rauschenbeutel, Appl. Phys. B **105**, 3 (2011).
[4] A. Stiebeiner, O. Rehband, R. Garcia-Fernandez, and A. Rauschenbeutel, Opt. Express **17**, 21704 (2009).
[5] T. Vo-Dinh and P. Kasili, *Anal. Bioanal. Chem.*, **382**, 918 (2005).
[6] R. Kumar, V. Gokhroo, and S. N. Chormaic, New J. Phys. **17**, 123012 (2015).
[7] R. Kumar, V. Gokhroo, and S. N. Chormaic, New J. Phys. **17**, 123012 (2015).
[8] C. Sayrin, C. Clausen, B. Albrecht, P. Schneeweiss, and A. Rauschenbeutel, Optica **2**, 353 (2015).
[9] P. Lodahl, S. Mahmoodian, S. Stobbe, A. Rauschenbeutel, P. Schneeweiss, J. Volz, H. Pichler, and P. Zoller, Nature **541**, 473 (2017).
[10] R. Sachdeva and T. Busch, Phys. Rev. A **95**, 033615 (2017).
[11] J. A. Grover, P. Solano, L. A. Orozco, and S. L. Rolston, Phys. Rev. A - At. Mol. Opt. Phys. **92**, 013850 (2015).
[12] Á. Rapp, G. Zaránd, C. Honerkamp, and W. Hofstetter, Phys. Rev. Lett. **98**, 160405 (2007).
[13] H. P. Mishra, A. S. Flores, W. Vassen, and S. Knoop, Eur. Phys. J. D **69**, 52 (2015).
[14] J. Hu, A. Urvoy, Z. Vendeiro, V. Crépel, W. Chen, and V. Vuletić, Science (80-.). **358**, 1078 (2017).

Transverse and Upstream Motion of Photons in Moving Atomic Media

Akbar Safari[1], **Boris Braverman**[1], **and Robert W. Boyd**[1,2]
[1] *Department of Physics, University of Ottawa, Ottawa, ON, K1N 6N5, Canada*
[2] *Institute of Optics, University of Rochester, Rochester, New York, 14627, USA.*
e-mail: *asafa055@uOttawa.ca*

Photons propagating in a moving medium acquire a transverse speed if the medium is moving normal to the light propagation direction. This transverse motion is however very small and di cult to measure. The first experimental observation of the transverse drag effect was in the 1970s using a rapidly rotating glass plate [1, 2]. The transverse drag effect should be independent of the pulse duration and stay the same even in the limit of highly monochromatic light. This led Rayleigh in his work on the velocity of light in 1881 [5] to conclude that the transverse aether drag (stellar aberration) depends only on the wave velocity, not the group velocity of light. After being challenged by Ehrenfest in 1910, he pointed out that the transverse drag effect also depends on the group index [6].

The transverse displacement of the photons is predicted to be dramatically enhanced in a highly dispersive medium [3, 4];

$$x = \frac{vL}{c}\left(n_g - \frac{1}{n}\right), \qquad (1)$$

where v is the speed of the medium of length L, with refractive index and group index of n and n_g, respectively. The effect of dispersion on the transverse drag appears even for monochromatic light. We are performing an experiment using electromagnetically induced transparency (EIT) in a rubidium vapor cell to achieve a group index as large as one million [7]. A Rb cell moves transverse to the light propagation direction and a large shift in the transverse direction is expected. Since the refractive index of atomic vapors is very close to unity, the entire shift can be attributed to the effect of dispersion.

In addition, by tuning the laser frequency and using electromagnetically induced absorption, a large negative group index can be achieved [8, 9]. In this case, photons are expected to move opposite to the motion of the atoms. We investigate the possibility of this upstream motion of photons for the first time.

The enhanced transverse drag effect has potential applications in sensing transverse motions. Moreover, the light drag effect can contribute to the resolution of the famous Abraham-Minkowski dilemma concerning the momentum of a photon inside a dielectric medium [10]. In a transversely moving medium, the two momenta are different not only in magnitude, but also in direction.

[1] R. V. Jones, *Proc. R. Soc. Lond. A.* **328**, 337-352 (1972).

[2] R. V. Jones, *Proc. R. Soc. Lond. A.* **345**, 351-364 (1975).

[3] M. A. Player, *Proc. R. Soc. Lond. A.* **345**, 343-344 (1975).

[4] I. Carusotto, M. Artoni, G. C. La Rocca, and F. Bassani, *Phys. Rev. A.* **68**, 063819 (2003).

[5] Rayleigh, *Nature, Lond* **24**, 382 (1881).

[6] Rayleigh, *Phil. Mag.* **22**, 130-134 (1911).

[7] M. M. Kash, V. A. Sautenkov, A. S. Zibrov, L. Hollberg, G. R. Welch, M. D. Lukin, Y. Rostovtsev, E. S. Fry, and M. O. Scully, *Phys. Rev. Lett.* **82**, 5229 (1999).

[8] A. M. Akulshin, S. Barreiro, and A. Lezama, *Phys. Rev. Lett.* **83**, 4277 (1999).

[9] E. E. Mikhailov, V. A. Sautenkov, I. Novikova, and G. R. Welch, *Phys. Rev. A.* **69**, 063808 (2004).

[10] P. W. Milonni and R. W. Boyd, *Adv. Opt. Photon.* **2**, 519-553 (2010).

Multi-mode state retrodiction from optodynamical measurements of collective atomic dynamics

J. Kohler[1], **J. A. Gerber**[1], **E. Dowd**[1], **J. Wolf**[1], **and D. M. Stamper-Kurn**[1,2]
[1] *Department of Physics, University of California, Berkeley, California 94720, USA*
[2] *Materials Sciences Division, Lawrence Berkeley National Laboratory, Berkeley, California 94720, USA*
e-mail: *jkohler@berkeley.edu*

Optical cavities enable quantum-limited measurement of the dynamics of diverse systems, from the motion of mechanical oscillators [1] to the precession of atomic spins [3]. The cavity mode can also be used to mediate long-range interactions through coherent autonomous feedback, facilitating tunable exchange [2] and pair-creation [4] interactions within multi-mode optodynamical systems. One challenge for exploring interacting many-body systems in cavity optodynamics is to perform e cient state readout, multiplexed through the single-mode output field of the optical cavity.

In this poster, we describe our recent experimental application of matched filters for estimating the two-mode covariance of correlated states, produced through a negative-mass instability realized in a collective spin-orbit coupled atomic ensemble [4]. We present a theoretical analysis of multi-mode state retrodiction for oscillator dynamics sensed through an optical cavity, using matched filters applied to the continuous optical measurement of their subsequent free evolution. Estimation of the past state of each oscillator from its observed trajectory is perturbed by measurement noise and diffusion of the oscillators' states during observation, driven by thermal motion and measurement backaction. Using an optimal filter, derived from both the coherent oscillator response and its noise driven diffusion, we show that estimation of the past state approaches the standard quantum limit (SQL) in the limit of high-cooperativity measurement. We further demonstrate additional constraints on reaching the SQL for optimal state estimation from simultaneous readout of multiple, frequency resolved oscillators.

We will also present preliminary results on stabilization of a non-equilibrium state of collective atomic spin precession, through continuous measurement and optodynamical feedback.

[1] M. Aspelmeyer, T. J. Kippenberg, and F. Marquardt, Rev. Mod. Phys. **86**, 1391 (2014).

[2] N. Spethmann, J. Kohler, S. Schreppler, L. Buchmann, and D. M. Stamper-Kurn, Nat. Phys. **12**, 27 (2015).

[3] J. Kohler, N. Spethmann, S. Schreppler, and D. M. Stamper-Kurn, Phys. Rev. Lett. **118**, 63604 (2017).

[4] J. Kohler, J. A. Gerber, E. Dowd, and D. M. Stamper-Kurn, Phys. Rev. Lett. **120**, 013601 (2018).

Heralded entanglement in a spinor gas in an optical cavity

S. J. Masson[1] **and A. S. Parkins**[1]

[1] *The Dodd-Walls Centre for Photonic and Quantum Technologies, Department of Physics, The University of Auckland, New Zealand*

e-mail: *smas176@aucklanduni.ac.nz*

Gases of ultracold Bose atoms possessing internal spin degrees of freedom - spinor Bose gases - offer a remarkable variety of possibilities for the investigation of quantum fluids and many-body quantum dynamics. Tremendous experimental progress has been made using Bose-Einstein condensates (BECs) in which all magnetic sub-levels of a single hyperfine ground state are condensed [1]. In such systems, the interplay of spin collisional dynamics and magnetic field shifts governs the dynamics. This has led to the generation of quantum spin squeezing and many-body entanglement, and the study of quantum phase transitions and other quantum many-body phenomena. We proposed a method to 'manufacture' spinor physics using cavity-assisted Raman transitions instead of spin collisions [2].

Our scheme borrows from earlier engineered effective Dicke models for ensembles of two-level systems strongly coupled to a quantised cavity mode [3], but generalises it to integer spins. This model allows for the study of the Dicke model equivalently to two-level systems, with such an approach having been demonstrated in a study of non-equilibrium phase transitions in an imbalanced Dicke model [4].

We discuss how such an integer-spin system (e.g. $s = 1$) with all N atoms initiated in the $m = 0$ state can be projected by cavity output measurement into an entangled state. Considering an effective Tavis-Cummings model (TCM), each spin length present in the initial state should produce a distinct photon number in the cavity output field. Therefore, an ideal photon detector will perfectly project out a spin state of the form $|S, -S\rangle$. We show that in this case then the average run can be shown to have Heisenberg limited metrological sensitivity. A non-ideal detector still produces entanglement with metrological sensitivity better than the standard quantum limit. By implementing a sequence of TCM and anti-TCM interactions and measuring the consequent output pulses, it is also possible to regain the ideal case.

The cavity-assisted Raman transitions we use to implement the effective Dicke model can be detuned such that the cavity mode may be adiabatically eliminated. We are then left with a system of interacting spins described by an effective Hamiltonian very similar to that of collisional dynamics in a spinor BEC under the single mode approximation (i.e., where the spatial degrees of freedom are frozen out). This allows us to emulate certain experiments performed in spinor BECs such as the production of spin-nematic squeezing [2]. However, since the system is both open and engineered, these methods provide greater flexibility than collisional dynamics.

Here, we discuss a particular scheme used to prepare a heavily entangled ground state of the collisional Hamiltonian: a macroscopic spin singlet. By beginning in an easily prepared ground state and adiabatically altering the relevant parameters of the Hamiltonian, one can in theory prepare the spin singlet perfectly. However, due to the time scales involved, this is not practical experimentally [5]. However, a 'quasi-adiabatic' parameter change can greatly enhance the overlap of the atomic state with the spin singlet [6].

We show that performing such a sweep is also possible with our methods. However, due to the presence of the cavity-mediated damping, we have another option of preparing the spin singlet. Simply put, such a state is a dark state of the system. Therefore, evolution of the system conditioned on a null measurement of the cavity output signals the preparation of a very high fidelity spin singlet. Such a scheme works with a probability proportional to the overlap between the initial ensemble and the spin singlet, which is $1/(N + 1)$ with all atoms initially in $m = 0$. If instead the input state is the result of a quasi-adiabatic sweep as described above, then the probability of success can be raised to much more manageable numbers.

[1] Y. Kawaguchi and M. Ueda, Phys. Rep. **520**, 253 (2012). D. M. Stamper-Kurn and M. Ueda, Rev. Mod. Phys. **85**, 1191 (2013)

[2] S. J. Masson, M. D. Barrett and A. S. Parkins, Phys. Rev. Lett. **119**, 213601 (2017)

[3] F. Dimer, B. Estienne, A. S. Parkins and H. J. Carmichael, Phys. Rev. A **75**, 013804 (2007). S. Morrison and A. S. Parkins, Phys. Rev. Lett. **100**, 040403 (2008). S. Morrison and A. S. Parkins, Phys. Rev. A **77**, 043810 (2008)

[4] Z. Zhiqiang, C. H. Lee, R. Kumar, K. J. Arnold, S. J. Masson, A. S. Parkins and M. D. Barrett, Optica **4**, 424 (2017)

[5] T. M. Hoang et al, PNAS. **113**, 34 (2016)

[6] X-Y. Luo et al, Science. **355**, 6325 (2017)

What filter do you need for your heralded single photon source?

Daniel R. Blay[1], **Michael J. Steel**[1], **and Lukas G. Helt**[1,2]

[1] *Department of Physics and Astronomy, Macquarie University, New South Wales 2109, Australia*
[2] *Department of Physics, Engineering Physics and Astronomy, Queen's University, Kingston, ON K7L 3N6, Canada*
e-mail: *daniel.blay@mq.edu.au*

Spectrally pure single photons are a necessity for many quantum information protocols. They must be produced on-demand and at high rates. The two most common sources of such photons are atom-like systems (e.g. quantum dots) and nonlinear optical (NLO) sources (e.g. spontaneous parametric down conversion [SPDC]). Presently the latter platform is the workhorse of laboratory sources worldwide, as they achieve high rates and are easily integrated into existing optical technologies. These NLO sources generate pairs of photons, one of which is detected to "herald" the presence of the other. Typically these sources have spectral correlations between the pairs of photons, and as such the heralding process projects the remaining single photon into a mixture of frequency states, degrading the purity. To prevent this loss of purity the correlations can be removed with narrowband spectral filters, at the cost of greater loss [1]. This trade-off between purity and heralding probability, while well-known in the narrowband limit, has not been fully explored. Earlier work has focused on other regimes [2, 3, 4], and has not thoroughly investigated the photon pair spectral correlation space, or been well-connected to experiments.

We provide an in-depth examination of the effects of spectral filtering on the purity and heralding probability of heralded photon sources. We present parallel schemes. First, a method involving the direct integration of the two photon joint spectrum $\Phi(\omega,\omega')$, useful for finding analytical expressions within certain limits. Second, a more detailed treatment in the spectral mode basis using the Schmidt decomposition of the joint spectrum $\Phi(\omega,\omega') = \sum_\mu \sqrt{p_\mu}\Gamma_\mu(\omega)\Theta_\mu(\omega')$, teasing apart the multimode physics. These methods provide us with the following expressions for the heralding probability,

$$\mathcal{S} = \int \mathrm{d}\omega\mathrm{d}\omega' \left|t(\omega')\right|^2 \left|\Phi(\omega,\omega')\right|^2 = \sum_\mu Q_{\mu\mu}p_\mu, \quad (1)$$

where $Q_{\mu\nu} = \int \mathrm{d}\omega \left|t(\omega)\right|^2 \Theta_\mu(\omega)\Theta_\nu^*(\omega)$ are the overlaps between the Schmidt modes and the filter transmission $|t(\omega)|^2$. Similarly, the purity is given by

$$\begin{aligned}\mathcal{P} =& \mathcal{S}^{-2} \int \mathrm{d}\omega\mathrm{d}\omega'\mathrm{d}\omega''\mathrm{d}\omega''' \left|t(\omega')\right|^2 \left|t(\omega''')\right|^2 \\ &\times \Phi(\omega,\omega')\Phi^*(\omega'',\omega')\Phi^*(\omega,\omega''')\Phi(\omega'',\omega''') \quad (2)\\ =& \mathcal{S}^{-2} \sum_{\mu\nu} \left|Q_{\mu\nu}\right|^2 p_\mu p_\nu.\end{aligned}$$

These expressions apply to any state described by $\Phi(\omega,\omega')$. For a discretized joint spectrum the Schmidt decomposition can be evaluated quickly numerically with a singular value decomposition, as well as any derived quantities. For states that are well-described by a product of Gaussians with widths σ_1, σ_2, and orientations θ_1, θ_2 [5], as well as Gaussian filters of centre ω_0 and bandwidth σ_f, the direct integration method yields analytical expressions for the purity and heralding probability. This is a powerful tool for exploring a very broad class of states, allowing us to show that purities as high as 90% are available for heralding probabilities of $\sim 20\%$.

We can directly connect the parameters of the double Gaussian with experimental quantities. We identify that $(\sigma_1,\sigma_2,\theta_1,\theta_2) = (\Delta\omega_\mathrm{p}/\sqrt{\ln 2}, \Delta\omega_\mathrm{pm}/\sqrt{\ln 2}, \theta_\mathrm{p}, \theta_\mathrm{pm})$, where p refers to the pump and pm to the phasematching. The pump angle in the spectral domain $\theta_p = \pi/4$ is determined by energy conservation, and for pump pulses of duration τ, the pump bandwidth is $\Delta\omega_\mathrm{p} = 1/\tau$. For an SPDC source, the phasematching angle is

$$\theta_\mathrm{pm} = \tan^{-1}\left[\left(v_g^p(\omega_p) - v_g^s(\frac{\omega_p}{2})\right)/\left(v_g^p(\omega_p) - v_g^i(\frac{\omega_p}{2})\right)\right] \quad (3)$$

and the phasematching bandwidth is

$$\frac{\Delta\omega_\mathrm{pm}}{2\pi} = \frac{s\pi^{-1}L^{-1}}{\sqrt{\left[v_g^p(\omega_p) - v_g^s(\frac{\omega_p}{2})\right]^2 + \left[v_g^p(\omega_p) - v_g^i(\frac{\omega_p}{2})\right]^2}}, \quad (4)$$

where $s \approx 1.392$, and $v_g^{p,s,i}$ is the group velocity of the pump, signal or idler. For a specific periodically poled KTP source [2], the filter necessary to achieve 90% purity is narrower than the pump or phasematching bandwidth (see fig. 1), unlike what one might naively expect. This demonstrates a need to carefully select the appropriate filter for a given heralded photon source.

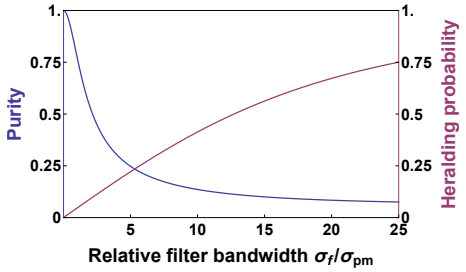


Figure 1: The purity and heralding probability for a periodically poled KTP SPDC source [2] with parameters $(6.0\,\mathrm{ps}^{-1}, 0.70\,\mathrm{ps}^{-1}, \pi/4\,\mathrm{rad}, 0.97\,\mathrm{rad})$, for varying filter widths.

[1] M. M. Weston *et al*, Opt. Express **24**, 10871 (2016).
[2] A. M. Brańczyk *et al*, New J. Phys. **12**, 063001 (2010).
[3] S. Du, Phys. Rev. A **92**, 043836 (2015).
[4] A. Christ *et al*, Phys. Rev. A **90**, 023823 (2014).
[5] M. V. Fedorov *et al*, J. Phys. B. At. Mol. Opt. Phys. **39**, S467 (2006).

Atom-light interaction in thermal Rubidium vapours confined to a volume less than λ^3

William J. Hamlyn,[1,*] James Keaveney,[1] Jan Renger,[2] Ifan G. Hughes,[1] Vahid Sandoghdar,[2] and Charles S. Adams[1]

[1] *Joint Quntum Centre (JQC) Durham-Newcastle, Department of Physics, Durham University, Durham, DH1 3LE, UK*
[2] *Max Planck Institute for the Science of Light (MPL), D-91058 Erlangen, Germany*

We present a study of bespoke thermal vapour cells of Rubidium with nano-scale internal dimensions. Our cells are produced in house with a glue-free design that allows for a high degree of optical access and long lifetime (>1 yr). Via two-photon excitation our detection sensitivity allows us to operate at room temperature in the pursuit of low atom number. We demonstrate that the size and shape of the vapour cavities is sufficient to perturb the atomic diffusion, both through changes in vapour density, and velocity distribution. Our platform allows for transmission spectrosopy, total internal reflection fluorescence, confocal microscopy, fluorescence imaging, and photon statistics measurements, and thus offers a robust environment for the study of novel atomic physics, and the control of few quantum emitters.

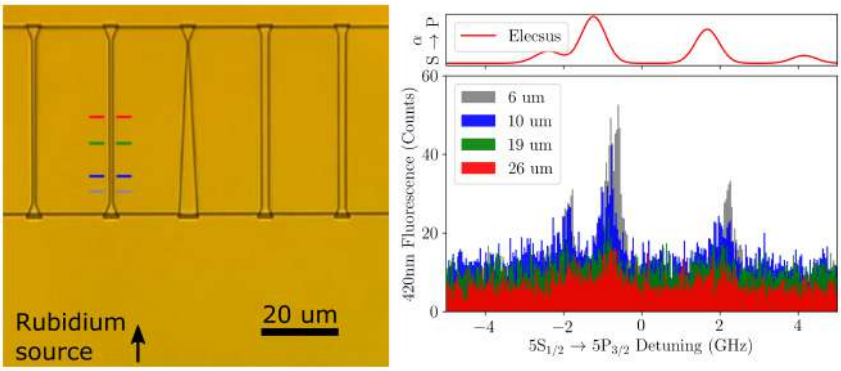


FIG. 1. **Left:** A bright field image of 1-dimensional vapour channels in fused silica substrate.
Right: 420 nm fluorescence signal at progressive distances into the 1D channel, showing the atomic density gradually diminishing.

[1] M. A. Zentile et al. Comp. Phys. Comm. 189, 162 (2015)
[2] K. A. Whittaker et al. J. Phys.: Conf. Ser. 635 12206 (2015)

* william.j.hamlyn@durham.ac.uk; http://www.jqc.org.uk/

Electromagnetically induced transparency (EIT), absorption(EIA) and Autler Townes(AT) splitting in N-type system

B. C. Das[1*], **A. Das**[1], **D. Bhattacharyya**[2], **S. Chakrabarti**[1] **and S. De**[1]
[1] *Saha Institute of Nuclear Physics, HBNI, 1/AF, Bidhannagar, Kolkata – 700064, India.*
[2] *Department of Physics, Santipur College, Santipur, Nadia, West Bengal, 741404, India.*
e-mail: **bankim.das@saha.ac.in*

Electromagnetically induced transparency (EIT), electromagnetically induced absorption (EIA) and Autler Townes (AT) splitting has been studied experimentally and theoretically in a N-type system.

We have chosen ^{85}Rb-D_2 transition in order to make the N-type system. The coupling beam is locked to the closed transition $F = 3 \rightarrow F' = 4$ and the probe beam is downshfited by $-120MHz$ with an acousto optic modulator(AOM) so that it can be locked to the transition $F = 3 \rightarrow F' = 3$. In this way a V-type system is formed maintaining phase coherency. In order to make the N-type system, the pump beam is introduced in between the transition $F = 2 \rightarrow F' = 3$. The pump beam has no phase coherency with the probe and the coupling beam. In our experiment we have scanned the pump beam and locked the probe and the coupling beam in order to get rid of the Doppler background[1]. We have studied how the probe transmission modified with the variation of the coupling beam power taking the pump power as a parameter.

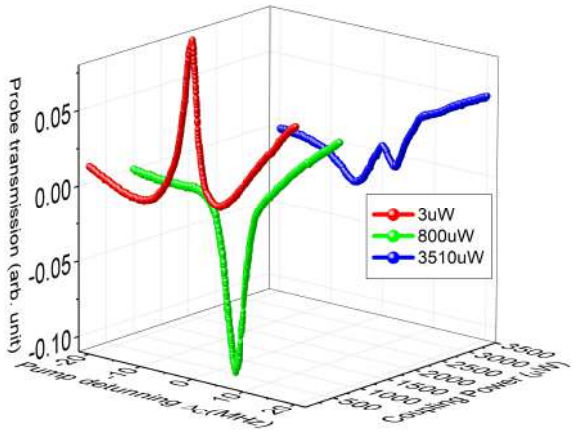


Figure 1: Probe transmission vs pump detunning Δ_c for the pump power $1.25mW$. The red, green and blue curves represent EIT, EIA and AT respectively. Corresponding coupling beam powers are written in the legend.

We have observed EIT, EIA and AT splitting depending upon the coupling beam powers.
To explain the three beam spectroscopy results we took three different approaches. In the first appraoch, we have solved the density matrix solution in steady state condition considering the thermal velocity. For analytical solution we have assumed the velocity distribution to be a Lorentzian [2]. We solved an analytical solution for the susceptibility in order to study the line-shapes of probe transmission.
In the second approach we have solved the time dependent density matrix solution numerically in order to understand the population dynamics of different states and the interference contributions in order to attribute the EIT, EIA and AT splitting effects in the system. Then we took the dressed state approach as the thrid one to explain the underlying physical mechanism for the three different regimes depending only on the coupling power variations.

When the coupling beam is off or its power is less, the system behaves like a *Lambda*-type system. So, EIT will be observed in the probe transmission. All the population will be trapped in the dark state i.e. $F = 3 \rightarrow F' = 3$. When the coupling beam is introduced in between the states $F = 3 \rightarrow F' = 4$, we are basically destroying the dark state and changing it to another superposition state. Now we can expect the EIT to be diminished as we increase the coupling power. Here Λ-type contribution will be less and the system behaves like a N-type system. At a certain power, i.e coupling Rabi frequency $\Omega_b \approx$ pump Rabi frequency Ω_c, the EIT will be transformed to an EIA. On further increase of the coupling power EIA will start to split again. We termed it as AT splitting . Since $\Omega_b >> \Omega_c$, the V-type system is dominating over the Λ-type system. So, for the high power case we will see the AT splitting which is shown in figure 1. If the coupling power is further increased, the separation between the AT peaks will also increase linearly.This is a signature of AT splitting.

[1] B.C. Das et *al.* The Journal of Chemical Physics 145, 224312 (2016);

[2] A. Javan, O. Kocharovskaya, H. Lee, and M. O. Scully, Phys. Rev. A **66**, 013805 (2002).

Pulse delay and group velocity dispersion measurement in V-type electromagnetically induced transparency of hot ^{85}Rb atom

B. C. Das[1*], **D. Bhattacharyya**[2],**A. Das**[1],**S. Saha**[1], **S. Chakrabarti**[1] **and S. De**[1]
[1] *Saha Institute of Nuclear Physics, HBNI, 1/AF, Bidhannagar, Kolkata – 700064, India.*
[2] *Department of Physics, Santipur College, Santipur, Nadia, West Bengal, 741404, India.*
e-mail: [*] *bankim.das@saha.ac.in*

Pulse delay with the group velocity dispersion(GVD) characteristics is studied in the V-type electromagnetically induced transparency(EIT) in the hyperfine levels of ^{85}Rb atoms with a closed system configuration. We studied these characteristics with the variation of the pump laser intensity taking temperature as a parameter.

The pump beam is locked to the closed transition $F = 3 \rightarrow F' = 4$ of ^{85}Rb-D_2 transition and the probe beam is down shifted by $-120MHz$ with acousto optic modulator(AOM) so that it can be locked to the transition $F = 3 \rightarrow F' = 3$. In this way a V-type system is formed maintaining the phase coherence between the two laser beams. For our experiment, we have used the probe beam as a pulsed beam and the pump beam as a continuous beam. Part of the probe pulse is taken as a reference pulse before the cell. The reference pulse goes through free space and the probe pulse goes through the medium, i.e. Rb cell. The reference pulse and the probe pulse are detected simultaneously by a pair of photo detectors after covering the same distance.

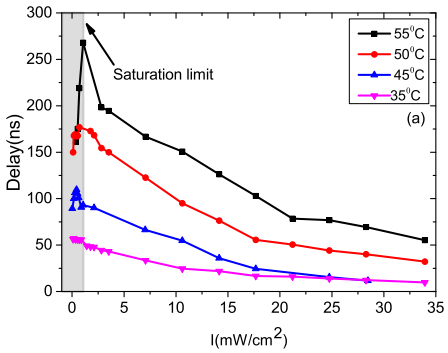


Figure 1: Variation of the pulse delay with pump intensity for different cell temperatures. The lines are drawn for guidance of eye.

We have studied both experimentally and theoretically, the dispersive property of ^{85}Rb. It is observed that if we increase the number density of the atoms by increasing the temperature, the delay will increase as shown in figure 1. The GVD characteristics is found to be opposite to the pulse delay characteristics.We observed a maximum of 268 ns pulse delay for 1.06 mW/cm^2 pump intensity at 55^0C temperature of the cell. For a better understanding of the experimental results we have derived an analytical solution for the delay characteristics considering the thermal averaging [1]. The analytical solution is derived for a three level V-type system. The theoretical plots (figure 2) of the delay $(1 + \frac{\omega_0}{2}\frac{d\chi}{d\omega}|_{\omega_o})/c$ and the group velocity dispersion $\frac{\omega_0}{2c}\frac{d^2\chi}{d\omega^2}|_{\omega_0}$ show the same characteristics as observed in the experiment. We further found out that these results are similar to the numerically solved results.

We observed that for a particular temperature,

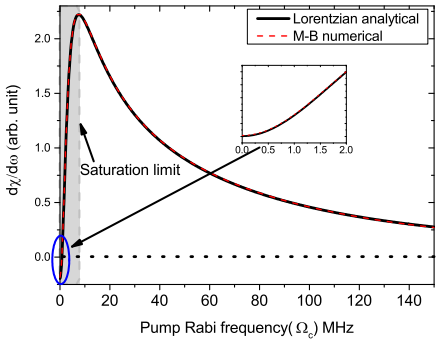


Figure 2: Simulated plots for $\frac{d\chi}{d\omega}|_{\omega_0}$ vs pump Rabi frequency Ω_c using both the analytical solution considering Lorentzian distribution and the numerical solution considering Maxwell-Boltzmann distribution. Shaded region in the figure is the below saturation regime.

if we increase the pump intensity up to a certain value, the delay will increase and after reaching a maximum value, the delay will decrease if the pump intensity is increased further. It implies that till the saturation limit, the slope of the dispersion will increase and correspondingly the delay will increase. After reaching the maximum delay the pump power broadening starts to dominate resulting in a decreased slope of dispersion. Theoretically we have derived an asymptotic solution for this phenomena. When the intensity of the pump or the pump Rabi frequency $\Omega_c \rightarrow 0$, we found that the pulse delay is increasing with Ω_c^2 dependency and when $\Omega_c \rightarrow \infty$, it decreases following a $\frac{1}{\Omega_c^2}$ relationship.

[1] A. Javan, O. Kocharovskaya, H. Lee, and M. O. Scully, Phys. Rev. A **66**, 013805 (2002).

Angular momentum spacial symmetry transformation in rubidium ground-state

M. Auzinsh[1], **R. Ferber**[1], **A. Mozers**[1], **L. Kalvans** [1]
[1] *Laser Centre, University of Latvia, Rainis Boulevard 19, LV-1586 Riga, Latvia*
e-mail: *arturs.mozers@lu.lv*

We studied angular momentum spacial symmetry transformation in rubidium ground-state caused by combined action of linearly polarized exciting laser radiation and an external magnetic field. The linearly polarized light first creates an aligned state and the external magnetic field transforms the angular momentum spacial distribution into an oriented state. It means that the aligned state, which had a determined axis, now has also preferred spacial direction. This angular momentum spacial symmetry transformation is also known as alignment-to-orientation conversion (AOC). We present results from a theoretical investigation of ground-state angular momentum alignment-to-orientation conversion (AOC) by observing laser-induced fluorescence (LIF) signals of rubidium atoms at D_1 excitation. This can be detected by observing circularly polarized light as circularity is direct evidence of angular momentum orientation. The excitation and observation geometry for creating and observing AOC stands as follows: the magnetic field **B** defines the quantization axis and the exciting linearly polarized laser radiation **E** forms an angle of $\pi/4$ with respect to the magnetic field **B**, observation direction is in the direction perpendicular to both **E** and **B**. In the previous work [1], where the same excitation and observation geometry was used, the AOC phenomenon was studied in the excited state where due to the nonlinear Zeeman effect of the excited state magnetic sublevel crossings occurred thus allowing for linearly polarized light to create coherence among sublevels that differ in value by 1 ($m_F = 1$). In contrast, there is no magnetic sublevel crossings in the ground state and one would not expect to observe AOC. But due to the nonlinear dependencies of the energies of ground-state magnetic sublevels, the angular momentum alignment, created by linearly polarized light, can be partially converted to orientation. The ground-state AOC occurs at relatively high magnetic field values around 2000 gauss, because of relatively large hyperfine splitting in the ground-state — 3.0 GHz for ^{85}Rb.

The theoretical model is based on the optical Bloch equations and takes into account all nearby transitions, the coherence properties of the exciting laser radiation, and the mixing of magnetic sublevels in an external magnetic field and also includes averaging over the Doppler profile [2]. We used the theoretical model to calculate two opposite circularly polarized light components (σ^+ and σ^-) of LIF signal dependencies on hyperfine transition, Rabi frequency of the atom-light interaction and laser linewidth. The results show that peculiar curves suggest about 1% of circularity at around 1500 gauss (Fig. 1). In near future the theoretical curves will be compered with experimentally obtained ones.

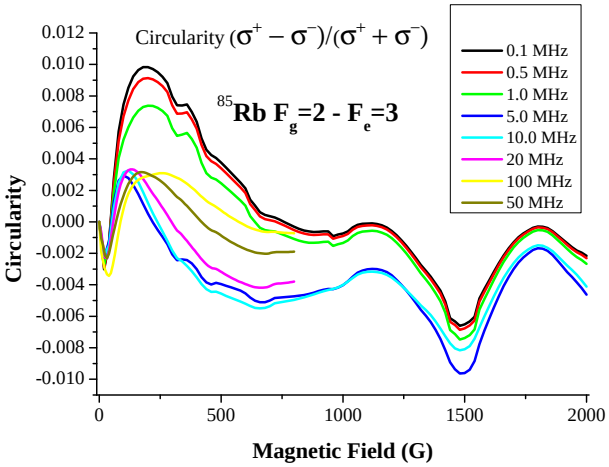


Figure 1: Calculated circularity of LIF signal dependency on magnetic field for the $F_g = 2 \longrightarrow F_e = 3$ transition of the D_1 line of ^{85}Rb. Various colors denote different Rabi frequencies characterizing atom-light interaction.

We gratefully acknowledge the financial support from the Base/Performance Funding Project No. AAP2016/B013, ZD2010/AZ27. A. Mozers acknowledges support from ERAF PostDoc Latvia project No. 1.1.1.2/16/117 "Experimental and theoretical signals of ground-state angular momentum alignment-to-otientation conversion by the influence of laser radiation and external magnetic field in atomic alkali metal vapour".

[1] M. Auzinsh, A. Berzins, R. Ferber, F. Gahbauer, L. Kalvans, A. Mozers, and A. Spiss, Phys. Rev. A **91**, 053418 (2015).

[2] M. Auzinsh, R. Ferber, F. Gahbauer, A. Jarmola, and L. Kalvans, Phys. Rev. A **79**, 053404 (2009).

Designing regular atomic arrays as 'free-space' photonic quantum link

P.-O. Guimond[1,2], **A. Grankin**[1,2], **D. V. Vasilyev**[1,2], **B. Vermersch**[1,2], **F. Robicheaux**[3,4,5], **M. Saffman**[5], **and P. Zoller**[1,2]

[1] *Institute for Theoretical Physics, University of Innsbruck*

[2] *Institute for Quantum Optics and Quantum Information, Austrian Academy of Sciences, Innsbruck, Austria*

[3] *Department of Physics and Astronomy, Purdue University, West Lafayette, Indiana 47907, USA*

[4] *Purdue Quantum Center, Purdue University, West Lafayette, Indiana 47907, USA*

[5] *Department of Physics, University of Wisconsin-Madison, 1150 University Avenue, Madison, Wisconsin 53706, USA*

e-mail: *pierre-olivier.guimond@uibk.ac.at*

We present the design of a free-space interface between light and single atoms, where the aim is to connect atoms as qubits using photons propagating in free space. With this interface, deterministic and probabilistic protocols for 'on-chip' quantum communication can be realized e ciently between two trapped distant atomic qubits ($a = 1, 2$), with two long-lived electronic states $|G\rangle_a$ and $|E\rangle_a$. In particular, quantum state transfer, realizing the coherent process $|\psi\rangle_1|G\rangle_2 \to |G\rangle_1|\psi\rangle_2$ with $|\psi\rangle$ an arbitrary qubit state [1], can be achieved with high success probability. This is obtained by coupling each qubit in a laser-assisted process to an array of atomic emitters with subwavelength spacings, as represented in Fig. 1(a,b). Using lasers to control the phases in these couplings, the atomic arrays are engineered to emit and absorb photons propagating only in a single paraxial gaussian mode of the radiation field.

We provide two different strategies to achieve a high qubit connectivity using this setup. First, in certain regimes the two atomic arrays support a long-lived delocalized subradiant state as collective excitation [2]. This 'dark' state behaves as a high-finesse single-mode resonator, which can be used to mediate coherent interaction between qubits. Remarkably, this can be realized using for each atomic array a single layer with a slight curvature [see Fig. 1(c)]. Second, using instead two layers, each atomic array can be engineered such that they absorb and emit photons propagating in a single direction [3]. In this regime the arrays act as 'chiral' phased-array optical antennas, mediating the interaction of qubits with unidirectional photons [4].

For both strategies, we present an effective quantum optical model and demonstrate how the success probability for quantum state transfer, limited by diffraction, depends on the number of atoms and their geometric arrangement. Even for as few as a hundred atoms in total, the state of the first qubit can be transferred to the second one with high probability for separation lengths L of a few dozen wavelengths. Finally, we discuss experimental considerations in the implementation of this model based on laser-assisted Rydberg interactions.

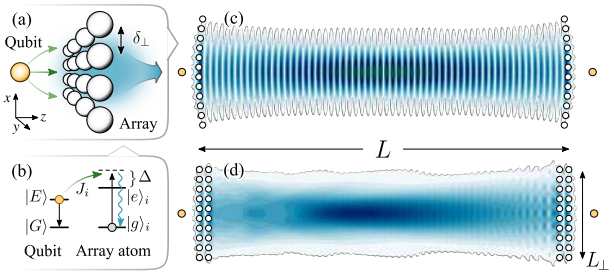


Figure 1: *Free-space photonic quantum link between two qubits.* (a,b) Sketch and level scheme of the setup. (c) Interaction mediated by a long-lived subradiant mode, with electric field profile in blue. (d) Cascaded configuration with atomic arrays as chiral antennas.

[1] T. E. Northup, and R. Blatt, *Quantum information transfer using photons*, Nature Photonics **8**, 356 (2014)

[2] P.-O. Guimond, A. Grankin, D. V. Vasilyev, B. Vermersch, F. Robicheaux, M. Saffman, and P. Zoller, unpublished.

[3] A. Grankin, D. V. Vasilyev, P.-O. Guimond, B. Vermersch, and P. Zoller, *A 'Few-Atom' Quantum Optical Antenna*, arXiv:1802.05592 (2018).

[4] P. Lodahl, S. Mahmoodian, S. Stobbe, A. Rauschenbeutel, P. Schneeweiss, J. Volz, H. Pichler, and P. Zoller, *Chiral quantum optics*, Nature **541**, 473 (2017)

Heralding of a single collective excitation in a 1D atomic array coupled to an optical nanofiber

J. Raskop, N. V. Corzo, A. Chandra, A. S. Sheremet and J. Laurat
Laboratoire Kastler Brossel, Sorbonne Université, CNRS, ENS-Université PSL, Collège de France
e-mail: *jeremy.raskop@lkb.upmc.fr*

Developing light-matter interfaces is a crucial capability with unique applications to quantum optics and quantum information networks. In this context, our group focuses on the study of interactions between photons guided by nanoscale waveguides and arrays of trapped atoms. Nanoscale waveguides offer a compelling platform because of the tight transverse confinement of the propagating light, the strong photon-atom coupling in single pass, and the potential long-range atom-atom interaction mediated by the guided photons.

Our setup consists in a two-color compensated dipole trap located around an optical nanofiber in a ultra-high vacuum chamber. Cesium atoms are trapped in two 1D arrays above and below the nanofiber with a trap lifetime of 25ms. An optical depth of over 100 is achieved with only a few thousand atoms. Here, we present three of our most recent results using this light-matter interface.

The first one is the demonstration of a fibered optical memory at the single photon level [1]. Using Electromagnetically Induced Transparency (EIT), we store a single photon pulse with a total storage-retrieval e ciency of $\eta = 10.0 \pm 0.5\%$ and a signal to noise ratio in the retrieved pulse of more than 20.

The second result is the observation of large Bragg reflection by the ordered atoms [2]. Contrary to previous experimental results with atoms around nanofibers which were obtained with a disordered or incommensurate array of atoms, and only relied on the resulting optical depth of the medium, in this experiment we realize collective effects arising from atoms trapped in a close-to-commensurate optical lattice. By engineering the atomic distance in the chains to be almost half of the atomic transition wavelength, we create conditions to observe a large Bragg reflection. Using this configuration, strong reflection, as high as 70% for single–photon pulses, is achieved with only 2000 atoms in the 1D atomic chains.

And finally, our latest study concerns the generation and characterization of a single collective excitation in the 1D atomic array. The excitation is heralded by the detection of a Raman scattered photon directly in the nanofiber. We are then able to retrieve a single photon in the guided mode after a tunable delay with an e ciency of up to 25%.

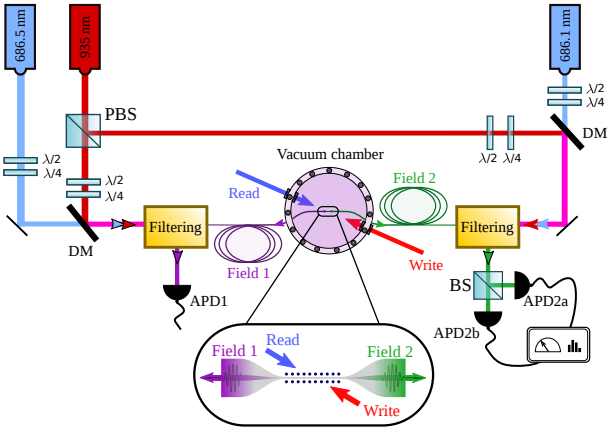


Figure 1: Experimental setup for single collective excitation generation. Via external Write and Read beams, a collective entangled state with one 'spin-flip' excitation can be heralded and read out as a single photon emitted into the guided mode. A filtering stage allows us to filter the dipole trap beams and characterize the output signal with APDs at the single-photon level.

This work provides a first demonstration of a heralded single collective excitation in a 1D atomic array coupled to a nanoscale waveguide in the context of the emerging waveguide-QED approach.

[1] B. Gouraud, D. Maxein, A. Nicolas, O. Morin and J. Laurat, Phys. Rev. Lett. **114**, 180503 (2015)

[2] N. V. Corzo, B. Gouraud, A. Chandra, A. Goban, A. S. Sheremet, D. V. Kupriyanov and J. Laurat, Phys. Rev. Lett. **117**, 133603 (2016).

[3] N. V. Corzo, J. Raskop, A. Chandra, A. S. Sheremet, B. Gouraud and J. Laurat, *submitted*

Measurement of the hyperfine structure of the $5s5d\ ^3D_3$ state in ^{87}Sr using a hollow cathode lamp

T. Sato, Y. Hayakawa, T. Aoki, and Y. Torii
Institute of Physics, The University of Tokyo, Tokyo 153-8902, Japan
e-mail: *t-sato@g.ecc.u-tokyo.ac.jp*

Laser frequency stabilization for the cooling transition of Sr ($5s^2\ ^1P_0$–$5s5p\ ^1P_1$, see Fig. 1) can be easily performed by Doppler-free spectroscopy using a hollow cathode lamp (HCL) [1, 2]. The HCL provides Sr atoms in the ground state ($5s^2\ ^1S_0$) based on a sputtering process. The optical transitions which include the metastable $5s5p\ ^3P_J (J = 0, 1, 2)$ states as the lower level are also important for repumping. Recently, Norcia and Thompson demonstrated Doppler-free spectroscopy for the $5s5p\ ^3P_2 - 5s6s\ ^3S_1$ (707 nm) transition using a commercial see-through HCL (Hamamatsu L2783-38Ne-Sr) filled with a Ne gas of 5-10 Torr and succeeded in stabilizing the laser frequency to this transition [3]. However, as the mean free path of Sr atoms was of the order of 10 μm in the commercial HCL, the population of sputtered Sr atoms was small at the center of the hollow cathode, where metastable Sr atoms were created [2]. If we reduce the buffer gas pressure, the mean free path of Sr atoms would be longer, and eventually the population of metastable Sr atoms would be increased.

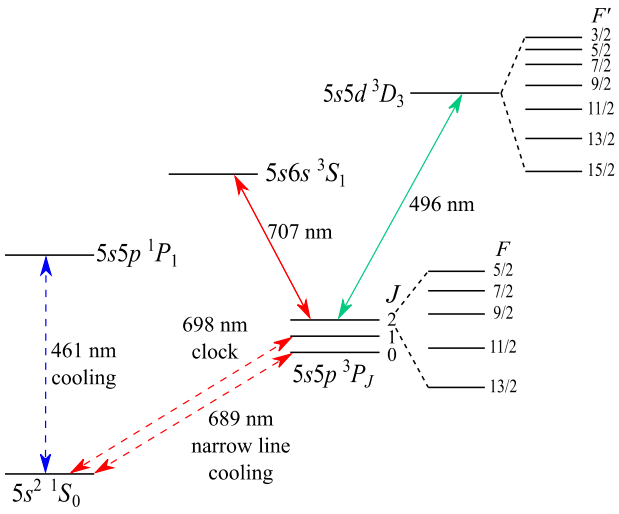


Figure 1: Relevant energy levels of ^{87}Sr. Transitions indicated by solid arrows are investigated in Ref. [3] (707 nm) and our study (496 nm). The cooling and clock transitions are indicated by dashed arrows.

We demonstrated Doppler-free spectroscopy of the $5s5p\ ^3P_2 - 5s5d\ ^3D_3$ (496 nm) transition using a custom HCL which is filled with a buffer gas of a reduced pressure (0.5 Torr Ne and 0.5 Torr Xe) to increase the populations in all of the $5s5p\ ^3P_J (J = 0, 1, 2)$ metastable states [4]. Figure 2 shows the signal of frequency modulation spectroscopy on the $5s5p\ ^3P_2 - 5s5d\ ^3D_3$ (496 nm) transition. In addition to the large dispersion signal from ^{88}Sr, we clearly observed the hyperfine transitions of ^{87}Sr with a nuclear spin $I = 9/2$. We determined the magnetic dipole constant $A = -157.0(3)$ MHz and the electric quadrapole constant $Q = -9(10)$ MHz, which are in good agreement with the values reported in Ref. [5], in which magnetically trapped ^{87}Sr atoms were used.

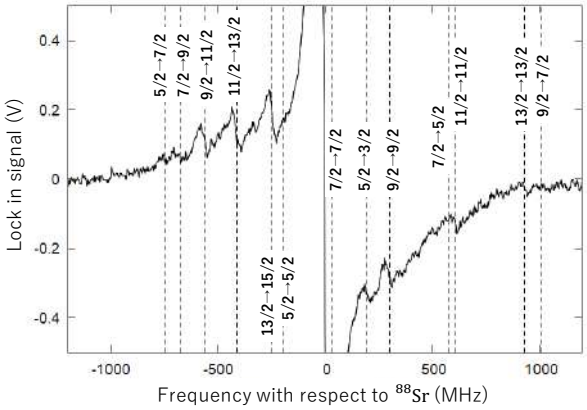


Figure 2: Signal for the $5s5p\ ^3P_2(F) - 5s5d\ ^3D_3(F')$ transition by frequency modulation spectroscopy using a custom HCL. The positions of the hyperfine transitions are indicated by dashed lines with labels $F \to F'$.

[1] T. Aoki, K. Umezawa, Y. Yamanaka, N. Takemura, Y. Sakemi, and Y. Torii, J. Phys. Soc. Jpn. **81**, 034401 (2012).

[2] Y. Shimada, Y. Chida, N. Ohtsubo, T. Aoki, M. Takeuchi, T. Kuga, and Y. Torii, Rev. Sci. Instrum. **84**, 063101 (2013).

[3] M. A. Norcia and J. K. Thompson, Rev. Sci. Instrum. **87**, 023110 (2016).

[4] Y. Hayakawa, T. Sato, C. Watanabe, T. Aoki, and Y. Torii, Appl. Opt. **57**, 1450 (2018).

[5] S. Stellmer and F. Schreck, Phys. Rev. A **90**, 022512 (2014).

Progress in the stability and frequency uncertainty of strontium optical lattice clocks at NPL

R. Hobson[1], **W. Bowden**[1,2], **M. Schioppo**[1], **A. Vianello**[1,3], **I. R. Hill**[1], **A. Silva**[1], **P. Gill**[1,2,3], **and H. S. Margolis**[1,2]

[1] *National Physical Laboratory, Teddington, TW11 0LW, United Kingdom*
[2] *University of Oxford - Department of Physics, Oxford, OX1 3PU United Kingdom*
[3] *Imperial College London - Department of Physics, London, SW7 2BB, United Kingdom*
e-mail: *richard.hobson@npl.co.uk*

Optical lattice clocks have emerged as a leading technology within the field of frequency metrology. In two of the most important attributes of an atomic clock—the frequency instability and the systematic frequency uncertainty—optical lattice clocks now demonstrate fractional performance of a few parts in 10^{18}. Through the effect of gravitational time dilation, the unprecedented precision of these clocks allows us to probe geodesy at a resolution of just a few cm [1, 2].

Here, we present work on two strontium optical lattice clocks at NPL. The first clock, "Sr1", has been operational for three years [3]. For this system, we present a characterization of systematic frequency shifts with a total fractional uncertainty of 1×10^{-17}. We also describe the nearly twofold improvement in the frequency instability of Sr1 to $1 \times 10^{-15}/\sqrt{\tau}$, achieved using a new local oscillator based on an ultra-stable, 48.5 cm long ULE optical cavity [7]. The improved instability is visible on frequency ratios with other optical clocks within the European fibre network, enabling us to perform more precise tests of geodesy and relativity [4, 2].

A second optical lattice clock at NPL, "Sr2", has recently become operational for the first time. Several details of its novel design, including a hexagonal pyramid MOT, two in-vacuum optical cavities, and a metastable cooling stage at 2.92 μm, are being presented separately at this conference [8]. Here we focus on the status of one particular experiment being implemented in Sr2: cavity-enhanced non-destructive detection of the atomic excitation fraction. Our scheme for non-destructive detection builds on the work of the SYRTE group [5], but with important modifications intended to improve signal to noise ratio and decrease atomic heating and decoherence. The first goal of our work is to carry out non-destructive detection in the classical sense, where the atoms remain trapped in the lattice after detection, and can therefore be immediately recycled for repeated interrogation of the clock transition. A second goal is to carry out quantum non-destructive measurement of the excitation fraction, potentially enabling the preparation of spin squeezed collective atomic states [6]. Each of these milestones could potentially improve the frequency instability of our optical lattice clock by an order of magnitude.

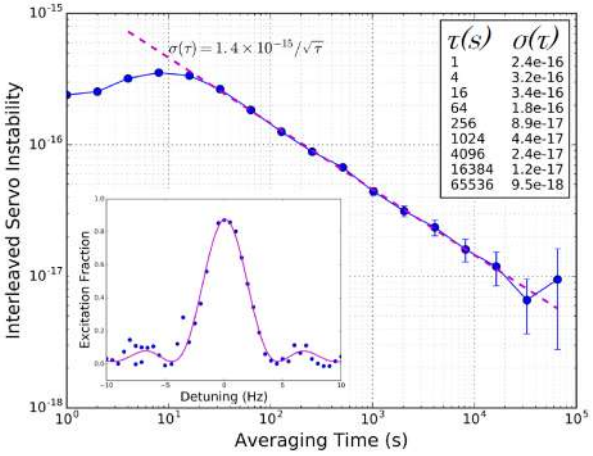


Figure 1: Fractional frequency instability of an interleaved self-comparison using the Sr1 optical lattice clock at NPL. *Inset:* A scan over the clock transition using a 300 ms Rabi pulse.

[1] T. Takano et al., Nature Photonics **10**, 662666 (2016).

[2] C. Lisdat et al., Nature Communications **7**, 12443 (2016).

[3] I. R. Hill et al., Journal of Physics: Conference Series **723**, 012019 (2016).

[4] P. Delva et al., Physical Review Letters **118**, 221102 (2017).

[5] G. Vallet et al., New Journal of Physics **19**, 083002 (2017).

[6] O. Hosten et al., Nature **529**, 505-508 (2016).

[7] M. Schioppo et al., ICAP poster (2018).

[8] W. Bowden et al., ICAP poster (2018).

Search for biomagnetism in venus-flytrap plants

A. Fabricant[1], **L. Bougas**[1], **Y. Hu**[1,2], **and D. Budker**[1,2,3]
[1] *Johannes Gutenberg-Universität Mainz, 55128 Mainz, Germany*
[2] *Helmholtz-Institut Mainz, 55128 Mainz, Germany*
[3] *University of California, Berkeley, California 94720, USA*
e-mail: *afabrica@uni-mainz.de*

In this experiment, we attempt to detect the magnetic fields produced by living plants, using sensitive atomic magnetometers. Our group previously conducted gradiometric measurements on a blooming titan arum, also known as the "corpse flower", at the Berkeley Botanical Garden in California [1]. As far as we know, the only successful detection of magnetic fields produced by intact plants was published in 2000 [2]—an array of SQUID magnetometers was used to measure signals from wounded bean plants in a magnetically shielded room.

After consultation with plant biologists at the University of Würzburg, we have chosen to launch a new biomagnetism experiment using the venus flytrap, Dionaea muscipula (Fig. 1). This carnivorous plant is relatively easy to stimulate mechanically, and one can generate action potentials (APs) consistently. So far we have successfully set up surface-electrode measurements for AP monitoring (Fig. 2), and we are currently conducting preliminary magnetometry measurements in a small magnetic shield with commercial QuSpin magnetometers. We are also in the process of acquiring our own magnetically shielded room, to which the experiment will eventually be moved. Our future goal is to develop a robust system for measuring biomagnetic signals from a variety of living plants (e.g. agricultural species), based on compact atomic sensors.

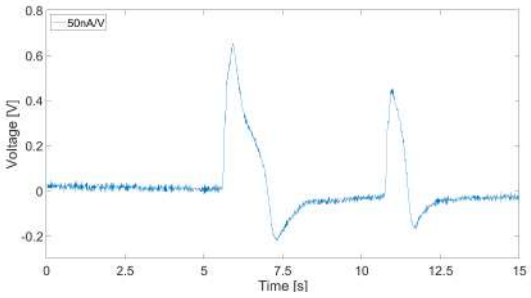


Figure 2: Electric signals produced by a trap after mechanical stimulation of its trigger hairs. Each peak corresponds to a single stimulation.

[1] E. Corsini, V. Acosta, N. Baddour, J. Higbie, B. Lester, P. Licht, B. Patton, M. Prouty, and D. Budker, J. Appl. Phys. **109**, 074701 (2011).

[2] V. Jazbinsek, G. Thiel, W. Müller, G. Wübbeler, and Z. Trontelj, Eur. Biophys. J. **29**, 515-522 (2000).



Figure 1: One of our venus-flytrap specimens in the lab.

A geometrically asymmetric optical cavity for a spin squeezed ^{171}Yb optical atomic clock

E. Pedrozo[1], **B. Braverman**[1], **A. Kawasaki**[1], **S. Colombo**[1], **C. Shu**[1], **Z. Li**[1], **and V. Vuletić**[1]

[1] *Department of Physics, MIT-Harvard Center for Ultracold Atoms and Research Laboratory of Electronics, Massachusetts Institute of Technology, Cambridge, Massachusetts 02139, USA*

e-mail: *epedrozo@mit.edu*

Optical cavities are widely used to enhance the atom-light interaction. Two major features that an optimal optical cavity should have are a tight waist, for a strong enhancement of the interaction between atoms and light, and a large mode volume for convenient atomic ensembles' loading. Achieving these two goals with commonly used geometrically symmetric cavity designs is challenging because they are strongly sensitive to misalignment.

To overcome this di culty, we designed and built a geometrically asymmetric standing-wave cavity, consisting of mirrors with very different radii of curvature. The resulting cavity mode has a small waist and a large mode volume while maintaining a high mechanical stability and robustness. Moreover, the mode width varies a lot if we move along the longitudinal axis of cavity resulting thus in a position dependent effective cooperativity. As shown in Figure 1, for our asymmetric design, the tunable range exceed 10^3 while for symmetric cavities the transversal mode diameter varies by a factor 2, resulting in a maximal tuning of the cooperativity of 4.

We demonstrate a wide range of single-atom cavity effective cooperativities ranging from $\eta = 0.03$ to $\eta = 20$, directly loading between 10^2 and 10^4 ^{171}Yb atoms from a mirror magneto-optical trap directly into a one-dimensional optical lattice along the cavity mode. In this system, we anticipate the production of a variety of exotic entangled states of mesoscopic atomic ensembles through collective measurements and we demonstrate the engineering of squeezed state of atomic ensembles via cavity feed-back.

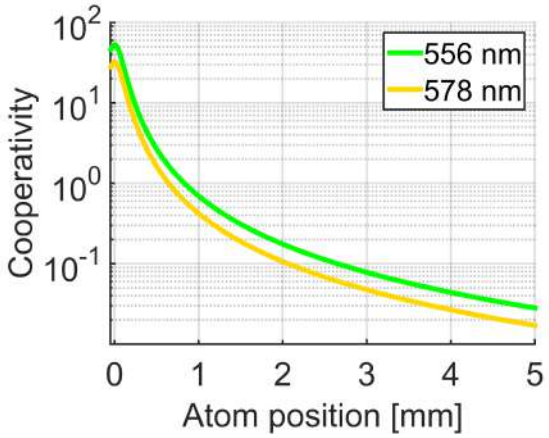


Figure 1: Theoretical cooperativity for squeezing light (556nm) and clock-transition light (578nm) as a function of atoms position.

[1] W. Chen, J. Hu, Y. Duan, B. Braverman, H. Zhang, and V. Vuletić, Phys. Rev. Lett. **115**, 250502 (2015).

Quantum metrology with Rydberg atoms

S. Gleyzes[1], **A. Larrouy**[1], **R. Richaud**[1], **J.M. Raimond**[1], **and M. Brune**[1]

[1] *Laboratoire Kastler Brossel, Collège de France, CNRS, ENS-Université PSL, Sorbonne Université, 11, place Marcelin Berthelot, 75005 Paris, France*

e-mail: *gleyzes@lkb.ens.fr*

Rydberg states correspond to electron wave function localized at a very large distance from the nucleus. These giant atoms are thus extremely sensitive to their electromagnetic field environment. It is possible to prepare state with very large electric dipole to probe the amplitude of the electric field, or states with very large angular momentum, able to detect very small magnetic field. As often in quantum metrology experiment, the limit of the sensitivity is set by the quantum fluctuations associated with the state of the atom. To reach the ultimate sensitivity set by the law of quantum mechanics, called the Heisenberg limit, it is necessary to prepare the atom in a non-classical states, like a Schrdinger cat state.

Our system is a Rydberg atom with a large quantum principal number $n \sim 50$. In the presence of a small electric field defining the quantization axis, the degeneracy between levels with the same n is lifted. The new eigenstates, called Stark levels, are defined by the magnetic quantum number m, which remains a good quantum number, and the parabolic quantum number n_1, with $0 \leq n_1 \leq n - |m| - 1$. Since m remains a good quantum number, it is possible, using a radio frequency field with a well-defined $\sigma+$ polarization, to restrict the evolution of the atom to a subspace of the Stark manifold where the system behaves like a large spin $J = (n-1)/2$, whose frequency is proportional to the local amplitude of the electric field. We have used this effective spin to perform a quantum-enabled measurement of the static electric field. We prepare a Schrödinger cat state of the Rydberg atom, quantum superposition of two classically distinct wavefunction with very different polarizability, and observe how the relative phase between the two components of the quantum superposition provides a very sensitive signal to measure the variation of the static electric field. We achieve a precision that exceeds the SQL and approaches the fundamental Heisenberg limit (HL). The single-shot sensitivity reaches 0.3 mV/cm for a 200 ns interaction time, (8 microvolt/cm/$\sqrt{\text{Hz}}$ at a 3 kHz repetition rate). This highly sensitive, non-invasive space- and time-resolved field measurement extends the realm of electrometric techniques and could have important applications. Driving the Rydberg atom with a combination of $\sigma+$ and $\sigma-$ polarization would also open the way to explore the full set of Stark level, and in particular prepare quantum superposition of state with same parabolic number but opposite value of m. Such states are very interesting for magnetic metrology, as they would correspond to microscopic probe with up to 100 μ_B magnetic moment, while at the same time being impervious to electric field noise.

References

[1] A. Facon, *et al*, Nature **535**, 262 – 265 (2016).

Tunable phase-locked laser system for quantum sensing applications

J. Thom[1], J. I. Malcolm[1], J. Hughes[1], A. Kelly[1], K. Craig[1], S. Webster[1], N. Hempler[1], G. T. Maker[1], G. P. A. Malcolm[1], I. Dutta[2], S. P. de Silva[2], X. Cheng[2], J. P. Stammers[2], D. T. Krastev[2], J. P. Cotter[2] and E. A. Hinds[2].

[1] *M Squared Lasers Ltd., West of Scotland Science Park, Maryhill Road, Glasgow, G20 0SP, UK*

[2] *Centre for Cold Matter, Blackett Laboratory, Imperial College London, London, SW7 2AZ, UK*

e-mail: *joseph.thom@m2lasers.com*

Quantum sensors using atom interferometry can significantly enhance the precision and accuracy of applications such as gravimetry and inertial navigation. Whilst laboratory-based interferometers have been demonstrated with very high sensitivities [1, 2], much work is now focused on engineering sensing devices suitable for field applications. Cold atom quantum sensors require finely tuned optical pulses for laser cooling, state preparation, implementing stimulated Raman transitions and state readout. Each of these steps requires specific optical frequencies covering a range of several GHz, necessitating either multiple lasers and optical modulators, or a simplified system with a high degree of frequency agility. A laser system for a cold atom sensor must also be sufficiently portable and robust to be viable for practical applications.

We have developed a phase-locked laser system that provides all of the optical pulses for a ^{87}Rb atom interferometer in a fully integrated and automated setup. The system consists of two M Squared SolsTiS Ti:Sapphire lasers operating at 780 nm in a 'master' and 'slave' configuration by means of a phase-lock at 6.834 GHz. The master laser is referenced to an ^{85}Rb transition via a tunable offset lock. By varying the offset frequency over a range of ∼1-2 GHz, both lasers are tuned between the optical frequencies required for laser cooling and Raman transitions in less than 3 ms. With > 8 W of combined optical power, the system is ideally suited to meet the requirements of large beam diameter and short pulse durations that must be fulfilled for the highest possible sensitivities. An out-of-loop measurement of phase noise, a critical factor in determining the sensitivity limits of an atom interferometer, reveals a phase variation of < 7 mrad for Raman pulses separated by 25 ms. This result is limited by the oscillator used as a reference frequency in the phase lock.

An M Squared DCS sequencer module permits complex pulse sequences at cycle rates over 10 Hz and rapid update of sequence parameters, essential features for operating atom interferometers in dynamic environments. The phase locking is provided by an M Squared Ice Bloc instrumentation unit that enables highly accurate phase shifts between interferometer pulses and fast chirping of the phase-lock frequency at rates up to 100 MHz/s for Doppler shift compensation.

We present a full characterisation of the system and report on its application in two ^{87}Rb systems: a quantum gravimeter at M Squared Lasers and a horizontal quantum accelerometer at Imperial College London. By taking advantage of the broad emission range of the SolsTiS platform, the principles of this laser system could be adapted to other atomic species commonly used in atom interferometers such as Caesium at 852 nm [3], Potassium at 767 nm [4], and Sodium at 589 nm [5].

A detailed description of the quantum accelerometer at Imperial College London, which uses this laser system, is given in a complimentary poster.

[1] S. Dickerson, Phys. Rev. Lett. **111**, 083001 (2015).

[2] Z-K. Hu, et. al, Phys. Rev. A. **88**, 043610 (2013).

[3] A. Peters, K. Y. Chung and S. Chu, Metrologia **38**, 25 (2001).

[4] A. N. Dinkelaker, et. al, Appl. Opt. **56**, 1388 (2017).

[5] M. Kasevich and S. Chu, Phys. Rev. Lett. **67**, 181 (1991).

Development of Yb optical lattice clocks at KRISS

D. H. Yu, H. Kim, C. Y. Park, M.-S. Heo, W.-K. Lee, and S. E. Park
Korea Research Institute of Standards and Science, Daejeon 34113, Rep. of Korea
e-mail: *dhyu@kriss.re.kr*

Optical clocks using the narrow optical transitions of neutral atoms and ions are promising candidates for the redefinition of SI second. Yb optical lattice clocks using one-dimensional optical lattices are under development at KRISS (Korea Research institute of Standards and Science) and we reported the measured absolute frequency of the optical clock transition $^1S_0(F = 1/2)$ - $^3P_0(F = 1/2)$ of ^{171}Yb atoms as 518 295 836 590 863.38(57) Hz [1]. Recently, the systematic uncertainty of the first Yb optical lattice clock (Yb1) reached the total systematic uncertainty of 8.3×10^{-17}.

Since the expected accuracy of Yb1 is limited by the BBR (Black Body Radiation) shift due to lack of isolation from inhomogeneous thermal environments, we are developing the second Yb clock (Yb2) that has a specially designed BBR temperature shield chamber (Fig.1).

The chamber has eleven 16-mm-daiameter apertures with BK7 windows (4.5 mm thickness) or BK7 lenses (10 mm edge thickness), two open apertures with 10 mm diameter, and two smaller open apertures with 4 mm diameter. In order to reduce the BBR shift uncertainty, the temperature of the BBR chamber is controlled actively slightly higher than those of surroundings and possible temperature distributions should be considered. In addition, there are other heat sources such as an atomic beam oven, a Zeeman slower, and a heated window for a Zeeman slowing laser, etc. Hence the performance of the BBR chamber were verified by using a 10-mm-diameter black copper ball with a platinum resistance thermometer (black ball PRT) as a radiation detector at the center of the BBR chamber as shown in Fig. 1. The black ball PRT was coated by a black material with absorptivity of 90 % over wavelengths of 1 to 30 micrometer. Temperatures of other parts of the chamber were measured using ten calibrated PRTs. The radiation on the surface of the ball was a dominant source of the energy flux on the black ball PRT over the conduction via wires and the self-heating of the PRT. With an energy rate equation and the specific heat of copper, the temperature of the black ball PRT could be calculated. Fig.2 shows the measured temperature due to the radiation from the heated window for the Zeeman slowing laser input together with the simulatied result from the modeled equation. Using parameters fitted to experimental data, the radiation intensity at the position of the atom trap was evaluated with equivalent accuracy of 40 mK for the blackbody temperature which corresponded to 1.3×10^{-18} uncertainty for the clock transition of ^{171}Yb.

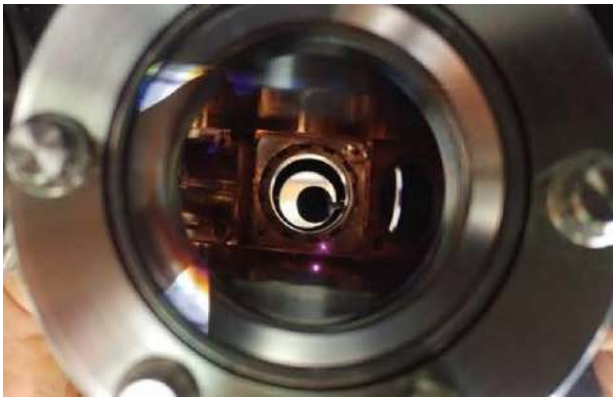


Figure 1: Black ball PRT installed in the BBR chamber.

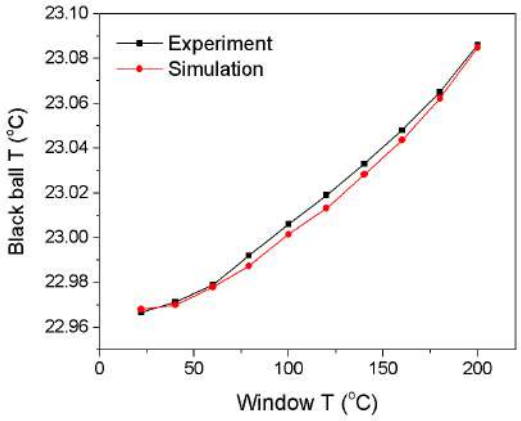


Figure 2: Temperature increase of black ball PRT and simulation result due to the radiation from the heated window for the Zeeman slowing laser input.

[1] H. Kim et al., Jpn. J. Appl. Phys. **56**, 050302, (2017).

A compact grating magneto-optical trap for ultracold ^{171}Yb

R.J. Fasano[1,2], **R. Fox**[1], **W.F. McGrew**[1,2], **D. Nicolodi**[1], **X. Zhang**[1], **K. Beloy**[1], **and A.D. Ludlow**[1]

[1] *National Institute of Standards and Technology, 325 Broadway, Boulder, CO 80305, USA*
[2] *Department of Physics, University of Colorado, Boulder, CO 80309, USA*
e-mail: *robert.fasano@nist.gov*

A ubiquitous element in a cold-atom experiment is the magneto-optical trap (MOT), conventionally formed from three pairs of red-detuned laser beams intersecting at the center of a quadrupole magnetic field [1]. A considerable reduction in complexity is offered by the grating MOT (gMOT), which forms a tetrahedral atom trap at the intersection of a single input beam and three diffracted beams above a nanofabricated grating chip [2]. Though gMOTs have demonstrated atom numbers rivaling conventional MOTs with rubidium, they have not yet been realized with group-II atoms such as ytterbium or strontium. The doubly-forbidden $^1S_0 \rightarrow {}^3P_0$ transition in these species is useful in many applications, including optical lattice clocks [3] and long-lived qubit encoding [4].

Extending gMOT technology to the alkaline earth atoms is non-trivial due to the two-stage cooling common to these atoms, typically using the broad $^1S_0 \rightarrow {}^1P_1$ transition to cool to several mK, followed by cooling to several uK on the $^1S_0 \rightarrow {}^3P_1$ intercombination line. The zeroth diffracted order, which destabilizes the vertical force balance, can be eliminated for only a single wavelength by controlling the etching depth of the grating. Moreover, because the two colors diffract at different angles, the groove spacing must be chosen to optimize the overlap region of the two wavelengths while maintaining adequate trapping force along all axes. An additional complication is that the nonuniformity inherent to Gaussian beam profiles greatly diminishes the capture volume and radial trapping strength relative to a uniform-intensity beam. While this has already impacted single-wavelength grating MOTs [5], the problem is magnified in an overlapped two-color MOT. Finally, loading the trap from a beam instead of vapor presents di culties due to the requirement for atoms to traverse a region of severely unbalanced radiation pressure before entering the capture region; for instance, the negative-order diffracted beams and unbalanced input beam shown in Figure 1 will deflect atoms below a critical velocity, limiting the velocity capture range of the MOT. By rotating the grating appropriately, one negative-order diffracted beam can be used for additional slowing and to counteract the unbalanced downwards force of the incident beam, significantly improving the trapping e ciency of the gMOT.

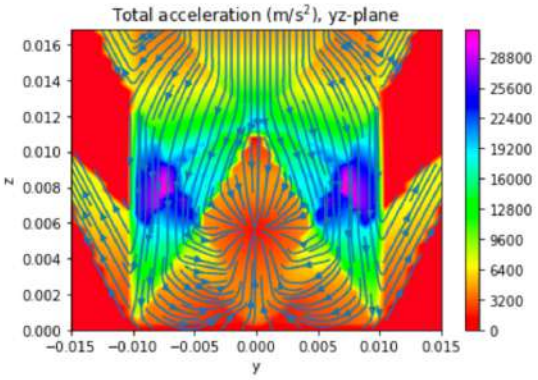


Figure 1: Acceleration profile of a grating MOT with an input beam of 10 mm radius. The color and vector streamlines correspond to the acceleration experienced by a stationary atom. A balanced optical molasses forms in the central diamond-shaped region.

We have developed a three-dimensional force model permitting estimation of atom number in diverse experimental conditions, including variation of the magnetic field, beam height relative to the grating, and grating diffraction angle. I will report on valuable insights gleaned from these simulations, as well as early results from a grating MOT experiment at 399 nm aiming to thoroughly characterize gMOTs for use with group-II atoms. Additionally, I will report on steps towards a portable optical lattice clock aimed at 10^{-18} uncertainty, highlighting a compact, modular design and active compensation for uncontrolled environmental variables.

[1] E.L. Raab et al. Phys. Rev. Lett., 59(23):2631, 1987.

[2] M. Vangeleyn et al. Opt. Lett., 35(20):34533455, 2010.

[3] A.D. Ludlow et al. Rev. Mod. Phys., 87(2):637, 2015.

[4] A.J. Daley. Quantum Inf. Process., 10(6):865884, 2011.

[5] Imhof, Eric, et al. Phys. Rev. A 96.3 (2017): 033636.

Towards a spin-squeezed atomic gradiometer with multipass cells

Vito Giovanni Lucivero[1], **Wonjae Lee**[1], **N. D. McDonough**[1], **Nezih Dural**[1] **and M. V. Romalis**[1]

[1] *Department of Physics, Princeton University, Princeton New Jersey 08544, USA*

e-mail: *lucivero@princeton.edu*

A major challenge in atomic quantum metrology is the use of squeezing to beat classical sensitivity of atomic sensors under optimal conditions i.e. within a high-density regime. In the context of optical magnetometry, it has been recently predicted [1] that, in the presence of nonlinear spin-exchange relaxation, spin squeezing induced by a quantum-non-demolition (QND) measurement can improve the long-term magnetometer sensitivity. Here we report recent progress towards the experimental implementation of spin squeezing to improve the sensitivity of an atomic gradiometer using multipass cells. We report nonlinear evolution of 87Rb dense ensembles, with strong polarization and high spin correlation, by using a new generation of multipass cells.

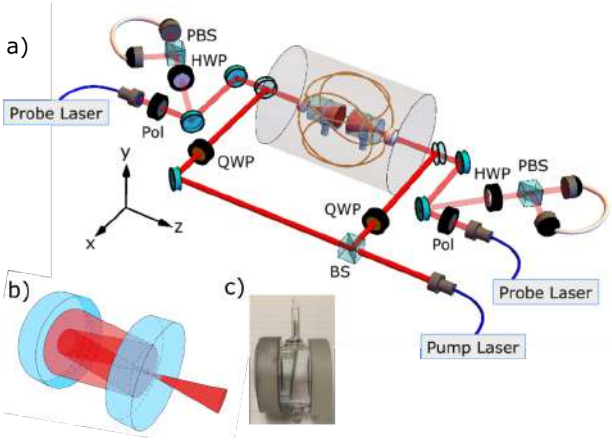


Figure 1: a) Experimental setup. b) Probe beam geometry inside the cell. c) Vapor cell side view.

A schematic of the experimental setup is shown in Fig. 1 (a). Two ^{87}Rb multipass cells are placed at 2 cm distance within a ceramic oven and enclosed in 5 μ-metal layers of magnetic shielding. Differently from prior work in our group [2], we use a new generation of multipass cells which contain atoms just in the half where the probe beam is expanded (see Fig. 1 (b-c)). This design maintains a large effective interaction volume and significantly reduces the decay time of the diffusion component of the spin noise correlation function [3], being the latter a requirement for the suppression of atomic spin noise by spin squeezing. After generating strong initial atomic polarization with a strong pulsed beam we measure the free precession around the magnetic field with a second probe beam in a collinear geometry, to ensure quantum back-action evasion and QND probing scheme. The probe is focused through a 200 μm hole and, by making 32 passes between the mirrors inside the cell [2], undergoes paramagnetic Faraday rotation, which is detected by shot-noise-limited balanced polarimeters. The signals from the two cells are fed into a frequency counter which provides the difference between the two precession frequencies. Alternatively we directly fit the sinusoidal signals, acquired with a digital oscilloscope.

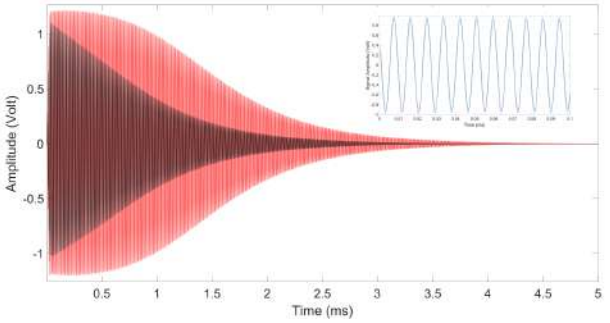


Figure 2: (a) Optical rotation signal for large (red) and small (black) initial polarization.

In Fig. 2 we show signals from one cell in the case of large (red) and small (black) initial polarization at a temperature of $T = 120°$C. In the first case the decay of the transverse spin polarization is nonlinear due to partial suppression of spin-exchange collisions because of the strong initial atomic polarization. In contrast, for small initial polarization the transverse relaxation decay is faster and exponential. Such nonlinearity causes the spin coherence to be preserved for longer time, making the described experiment a good candidate for quantum-enhancement by spin squeezing. We will report current technical limitations approaching the projection noise magnetic sensitivity.

[1] G. Vasilakis, V. Shah, and M. V. Romalis, Phys. Rev. Letter. **106**, 143601 (2011)

[2] D. Sheng, S. Li, N. Dural, and M. V. Romalis, Phys. Rev. Letter. **110**, 160802 (2013).

[3] V. G. Lucivero, N. D. McDonough, N. Dural, and M. V. Romalis Phys. Rev. A **96**, 062702 (2017)

MEMS fabrication and operation of 3D ion microtraps

G. Wilpers[1], **M. Akhtar**[1,2], **K. Choonee**[1], **S. Thomas**[1,2], **E. Riis**[2] **and A. G. Sinclair**[1]
[1] *National Physical Laboratory, Teddington, TW11 0LW, UK*
[2] *Department of Physics, University of Strathclyde, Glasgow, G4 0NG, UK*
e-mail: *alastair.sinclair@npl.co.uk*

Trapped ions are of significant interest for research in quantum technologies such as simulation, information processing and metrology. Ion microtrap devices are seen as a viable route to scaling up to more complex systems with larger numbers of ions.

Building on our earlier work [1, 2], we have demonstrated parallel, wafer-scale, MEMS fabrication of monolithic ion trap chips. The microtrap devices (figure 1) have a near-ideal, three-dimensional electrode geometry, and an ion-electrode distance of 240 μm. These devices contain a linear microtrap array consisting of a remote, shielded loading zone and 7 operation segments. We have performed the first 5 (out of a total of 6) fabrication stages at wafer level (with 100 mm diameter wafers). The fabrication process results in mechanically intact, microstructured chips and can achieve up to 90 % of chips on the wafer to within $\pm$ 3 % of geometric design targets. Upon dicing into individual chips, an automated die-attach process completes the electronic package in a modified ceramic chip carrier, which also serves as a UHV electrical feedthrough.

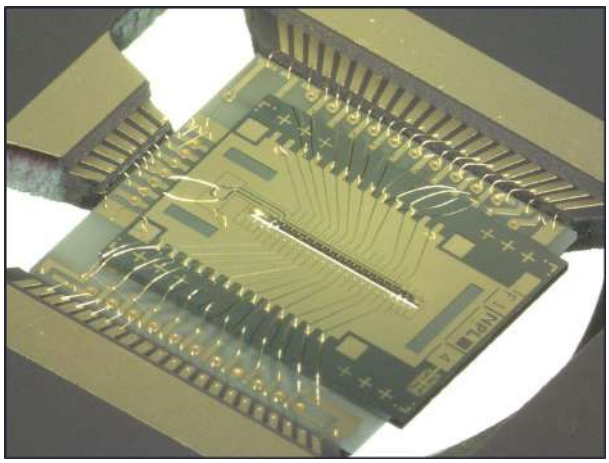


Figure 1: Example of 3D microtrap chip.

Applying a high-voltage, RF amplitude to a microtrap chip is essential to achieve confinement of ions at the Lamb-Dicke limit and realise motional frequencies of a few MHz. We developed an apparatus for assessing such electrical performance of chips in a resonant circuit. We find optical imaging to be a more sensitive discriminant of the onset of RF breakdown via surface flashover, in comparison to electrical means. Operation in the range 250 V to 300 V without flashover is routinely observed across a sample of chips. Tests with process modifications have indicated that amplitudes up to 500 V are feasible.

A first chip from this fabrication batch has undergone trapping tests using a Doppler-cooled $^{88}Sr^{+}$ ion. An initially cold ion can be stored for up to 1.5 hrs without active cooling. Coherent spectroscopy on the optical qubit/clock transition ($5s\ ^2S_{1/2}$ - $4d\ ^2D_{5/2}$) shows Lamb-Dicke confinement. Resolved sideband cooling to the ground state has been performed. The initial heating rate of a ground state ion was measured to be 2.6(2) quanta/s (axial mode at $\omega_z/2\pi = 1.05$ MHz), which is a factor of 100 improvement over our earlier work [1, 2]. Note that this is achieved with the device operating at room temperature, which is in contrast to scalable microtraps with a 2D electrode geometry. Such a low heating rate is important for maximising coherence.

To take advantage of the low-noise microtrap, other sources of decoherence in the wider apparatus have been minimised. The trap is enclosed in a magnetic shield ($\sim$ 59 dB attenuation of amplitude at 50 Hz) and we have implemented an ultrastable laser (linewidth $\sim$ 1 Hz) which can be intensity-stabilised at the position of the trap [3]. Optical spectroscopy for evaluating the limits to coherence is in progress, as is a more detailed study of ion heating rates; latest results will be presented. Following this, the system will be used to prepare an entangled 2-ion string using a bichromatic optical field via the Mølmer-Sørensen scheme. In the longer term, this work aims to realise quantum-enhanced spectroscopy with entangled ions in a scalable device with minimal motional decoherence.

[1] G. Wilpers *et al*, Nat. Nanotechnol. **7**, 572 (2012).

[2] P. See *et al*, J. Microeletromech. Syst. **22**, 1180 (2013).

[3] J. Thom *et al*, Appl. Phys. B (2018) `https://doi.org/10.1007/s00340-018-6955-4`

Crossover from quantum cats to classical mixtures in ultra-cold atom interferometers

S. P. Kelly[1], **E. Timmermans**[2] **and S. W. Tsai**[3]
[1] *University of California Riverside, Los Alamos National Labs*
[2] *Los Alamos National Labs*
[3] *University of California Riverside*
e-mail: *skell013@ucr.edu*

The classical phase space of the two-mode description of the N-boson double well potential and of the internal state Josephson-coupled BEC systems, exhibits a separatrix that separates orbits of distinct dynamics: self-trapping and traditional Josephson oscillations. As suggested previously by others[1], the (temporary) separation of neighboring trajectories in the near-separatrix classical phase space dynamics may be experimentally exploited to dynamically create Shrodinger cat states. We discuss the experimental characterization and the temperature dependence of such dynamically created cats. The two peak structure,(Fig. 1) that is suggestive of macroscopic quantum entanglement, survives to higher temperatures whereas the macroscopic (scaling faster than $1/\sqrt{N}$ with particle number N) quantum sensitivity, that makes the cat a candidate for quantum enhanced measurements, does not.

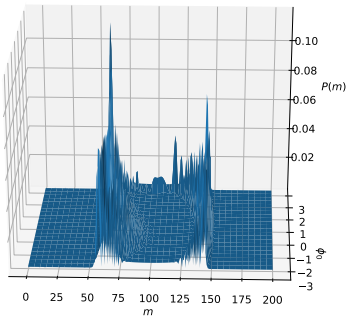


Figure 1: Two peak structure of cats generated by seperatrix. P_m is the probability of finding m particles in the left well. ϕ_0 parameterizes where on the separatrix the cat is generated

The experimental protocol we propose is designed so the quantum enhanced sensitivity, quantified by the Fisher information, relies directly on the particular form of entanglement suggested by the double-peak, and thus confirms the double peak is a product of a macroscopic quantum phenomenon. We then show how to directly observe and quantify the interference of the dead and alive cat when they meet up again in classical phase space. Both the interference and the sensitivity undergo a quantum to classical cross-over as the temperature of the initial state is increased. Since the characterization procedures are based on the fisher information we are also able to quantify the enhanced interferometric sensitivity of any of the dynamically evolved states. We demonstrate that states prepared entirely in the self-trapping sector also evolve into macroscopically entangled states.

[1] A. Micheli, D. Jaksch, J. I. Cirac, and P. Zoller, Phys. Rev. A **67**, 013607 (2003).

Novel atom interferometers with ultra-cold alkaline-earth atoms

N. Poli[1,2], **L. Hu**[1,3], **L. Salvi**[1], **E. Wang**[1] **and G.M. Tino**[1,4]

[1] *Dipartimento di Fisica e Astronomia and LENS - Università di Firenze, INFN - Sezione di Firenze, Via Sansone 1, 50019 Sesto Fiorentino, Italy*

[2] *Consiglio Nazionale delle Ricerche, Istituto Nazionale di Ottica (INO), Largo E. Fermi 6, 50125 Firenze, Italy*

[3] *ICTP, Trieste, Italy*

[4] *CNR-IFAC, Sesto Fiorentino, Italy*

e-mail: *nicola.poli@unifi.it*

Today, matter-wave interferometers as clocks and gravimeters allow for precision measurements of time and gravity at an unprecedented level. In all these sensors, indeed, the exquisite control of both internal (electronic) and external (center of mass motion) degrees of freedom of ultra-cold atomic samples, enable us to study interactions at their most basic, quantum level, paving the way for new tests of fundamental physics [1, 2].

Although most atomic inertial sensors are based on alkali atoms, very recently there has been an increasing interest in the use of alkaline-earth-like atoms. These atoms offer interesting properties toward high sensitivity and high accuracy gravimeters and gradiometers. Taking advantage of the ultra-narrow intercombination transitions in these atoms, which are currently employed in highest precision optical lattice clocks, novel atom interferometry schemes towards a new detector of gravitational waves have been proposed. Here, some of most the recent results obtained by our group in this field are presented, showing the first experimental tests performed on a Bragg gravimeter using the dipole allowed transition [3, 4] and the dipole intercombination transitions of strontium isotopes (^{88}Sr-^{87}Sr) [5, 6].

Although the first demonstration of the power of non-classical atomic sources in clocks has been demonstrated, the application of similar techniques in atom interferometry has not been shown experimentally. A novel scheme for the production of spin-squeezed momentum states with direct application to Bragg interferometers will also be presented [7].

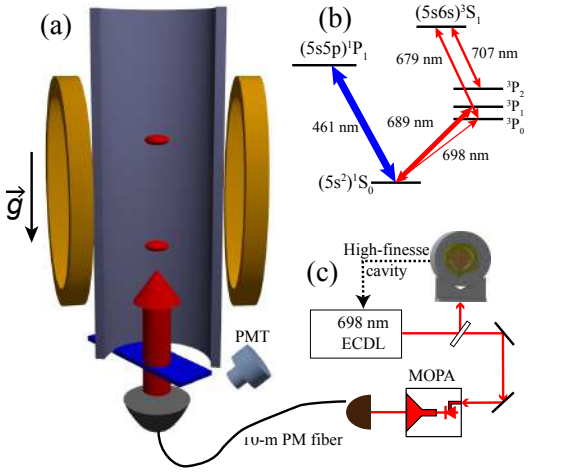


Figure 1: (a) Experimental setup for an atom gradiometer based on strontium clock transition. (b) Electronic level system and relevant optical transitions in strontium atoms. (c) High power frequency stabilized clock laser based on master diode laser and tapered amplifier.

References

[1] N. Poli, F.-Y. Wang, M. G. Tarallo, A. Alberti, M. Prevedelli and G. M. Tino , Phys. Rev. Lett. **106**, 038501 (2011)

[2] M. G. Tarallo, T. Mazzoni, N. Poli, D. V. Sutyrin, X. Zhang, and G. M. Tino, Phys. Rev. Lett. **113**, 023005 (2014)

[3] T. Mazzoni, X. Zhang, R. Del Aguila, L. Salvi, N. Poli, and G. M. Tino, Phys. Rev. A **92**, 053619 (2015)

[4] X. Zhang, R. P. del Aguila, T. Mazzoni, N. Poli, and G. M. Tino, Phys. Rev. A **94**, 043608 (2016)

[5] L. Hu, N. Poli, L. Salvi and G. M. Tino, Phys. Rev. Lett. **119**, 263601 (2017)

[6] R. P. del Aguila, T. Mazzoni, L. Hu, L. Salvi, G. M. Tino and N. Poli, New. J. Phys. **20**, 043002 (2018)

[7] L. Salvi, N. Poli, V. Vuletić and G. M. Tino, Phys Rev. Lett. 120, 033601 (2018)

Ramsey Spectroscopy with Frequency Displaced Jumps

M. Shuker[1,2], J. W. Pollock[1,2], R. Boudot[1,3], V. I. Yudin[3,4,5], A. Taichenachev[3,4,5], J. Kitching[1,2] and E. A. Donley[1,2]

[1] *National Institute of Standards and Technology, Boulder, Colorado 80305, USA*

[2] *University of Colorado, Boulder, Colorado 80309-0440, USA*

[3] *FEMTO-ST, CNRS, 26 rue de l'epitaphe 25030 Besancon, France*

[4] *Novosibirsk State University, ul. Pirogova 2, Novosibirsk, 630090, Russia*

[5] *Institute of Laser Physics SB RAS, pr. Akademika Lavrent'eva 13/3, Novosibirsk, 630090, Russia*

[6] *Novosibirsk State Technical University, pr. Karla Marksa 20, Novosibirsk, 630073, Russia*

e-mail: *moshe.shuker@nist.gov*

Ramsey spectroscopy is a technique widely used for precision measurements. A series of a preparation pulse, a dark-period and a reading pulse is applied to the sample resulting in narrow spectroscopic features. Ramsey spectroscopy minimizes probe field duration, by introducing the dark period in which the sample is free from the influence of the fields. However, even the short interrogation pulses in the Ramsey sequence result in light shifts, limiting the accuracy of the spectroscopic measurement. In the long-term, these shifts may lead to instability due to changes in the interrogation fields properties.

Ramsey spectroscopy is commonly applied for atomic clocks both in the microwave and the optical domains. Typically, two Ramsey measurement are performed on the two sides of the spectroscopic feature, generating the error signal required for steering the clock frequency. This is realized by either changing the frequency between the two Ramsey measurements (frequency-jumps) or by changing the phase of the interrogation field (by $\pm\pi/2$) between the preparation and reading pulses (phase-jumps).

Recently, an auto-balanced Ramsey (ABR) interrogation scheme was suggested and implemented for atomic clocks [1, 2, 3]. In the ABR scheme, two phase-jump Ramsey cycles are performed consecutively, with different dark periods but otherwise identical parameters. The two error signals obtained are used to control the clock frequency and a second control parameter (the concomitant parameter). By properly selecting the control equations, smaller sensitivity of the clock frequency to various shifts is achieved, resulting in improved long-term stability.

Here, we suggest and demonstrate an ABR scheme that uses frequency-jumps (FJABR) rather than phase-jumps. We use two frequency-jump Ramsey cycles with different dark periods, and introduce a second control parameter - the frequency displacement, a correction to the value of the frequency jumps. Since both control parameters, as well as the error signal generation, use the interrogation frequency, only a single physical variable is controlled in order to implement this scheme (compared with both the frequency and the phase of the interrogation field in other schemes). This may allow for easier implementation of this scheme in future devices.

Figure 1 depicts the energy level scheme, experimental apparatus and experimental sequence of FJABR. We used a cold-atom CPT clock apparatus in the Lin || Lin configuration (see [4] for details). We applied a sequence comprised of four Ramsey measurements, two with short $T_1 = 4$ ms dark period, and two with long $T_2 = 16$ ms dark period, with interrogation frequencies as detailed in Fig. 1.C. It is important to notice that although both control parameters use the same physical variable, the frequency displacement is not the same for the short and long cycles, but it is scaled as the inverse of the Ramsey dark period (unlike the clock frequency). This causes any shift that is inversely proportional to the Ramsey dark period to affect mainly the frequency displacement, leaving the clock frequency stable. We used the short error signal to control the frequency displacement and the long error signal to control the clock frequency.

Figure 2 depicts the average clock frequency with standard Ramsey and FJABR, at different intensity ratios of the CPT fields. By changing this ratio we change the off resonant light shift, causing a shift of about 0.4 Hz in standard Ramsey interrogation [5]. It is evident that the clock frequency with FJABR remains nearly stable, unlike the standard Ramsey spectroscopy. The concomitant parameter, the frequency displacement (also depicted in fig. 2) adapts to compensate for the shift. The rejection of the shift with FJABR is better than an order of magnitude. The clock frequency with FJABR stabilizes near the 2^{nd} order Zeeman shift, since this shift does not scale with the dark period.

In conclusion, we suggest and demonstrate Ramsey spectroscopy with displaced frequency jumps. In this method some of the shifts to the spectroscopic feature, that are induced by the interrogation, are rejected from the clock frequency and affect a second, concomitant, control parameter. This may allow for improved long-term stability. This method requires the control of only a single physical variable, the interrogation field frequency, which might reduce the complexity of its implementation in future devices.

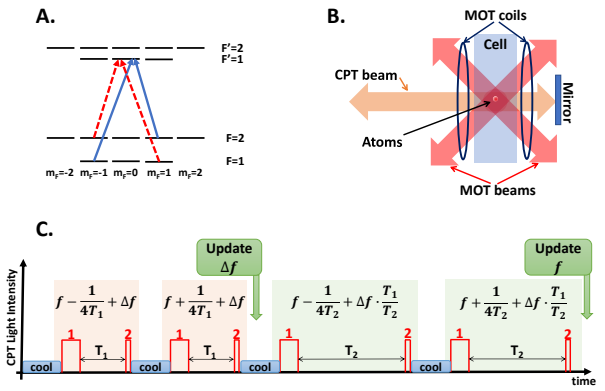


Figure 1: A. Energy level scheme of Lin || Lin CPT interrogation. B. Experimental setup of cold-atom CPT clock. C. Experimental sequence of the Ramsey spectroscopy with displaced frequency jumps.

[1] C. Sanner et al., Phys. Rev. Lett. **120**, 053602 (2018).

[2] V. I. Yudin et al., Phys. Rev. Appl. **9**, 054034 (2018).

[3] M. Abdel Hafiz et al., accepted for publication in Phys. Rev. Appl. (2018).

[4] X. Liu et al., Phys. Rev. Appl. **8**, 054001 (2017).

[5] J. W. Pollock et al., arXiv:1805.06029v1 (2018).

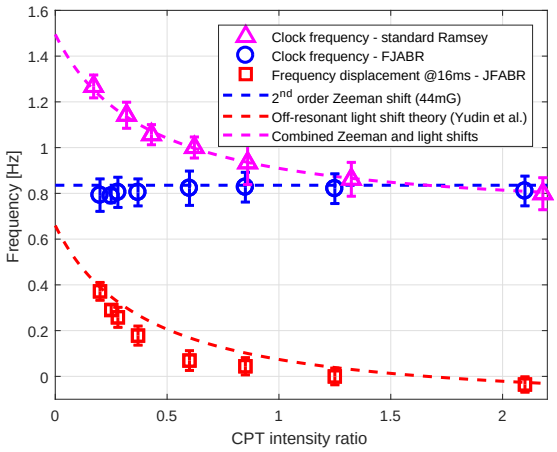


Figure 2: The average clock frequency (deviation from the generally accepted value) for standard Ramsey spectroscopy (triangles) and FJABR (circles) vs. the CPT intensity ratio. Changing this ratio affects the clock frequency in the standard Ramsey spectroscopy (due to off resonant light shift), however the clock frequency in the FJABR is nearly constant. The average value of the concomitant parameter in the FJABR (frequency displacement, squares) adapts to compensate for the light shift.

Spin self-rephasing in the system of several atoms

K. Szymański[1]

[1] *Marian Smoluchowski Institute of Physics, Jagiellonian University, Kraków, Poland*
e-mail: *konrad.szymanski@uj.edu.pl*

In this work a system consisting of a number of atoms evolving under the influence of external magnetic field is analyzed. Due to the inhomogenities of the external field, the atomic spins undergo dephasing: classically, since each atom feels different field along its trajectory, the spin rotation differs as well and the average spin decays. In a quantum mechanical context this corresponds to entanglement of spin and spatial degrees of freedom; additionally, two other modes of dephasing are possible: formation of internally (spin-spin) entangled state and population transfer to antisymmetric spin state.

The spin dephasing can be prevented by tuning the interaction between the atoms: such an effect, called spin self-rephasing has been observed experimentally [1] and can increase the coherence time by a large factor.

While such systems have been studied from a semiclassical point of view, a quantum mechanical description does not exist yet. In this work we fill in the gap by providing a numerical simulation of the behavior of the quantum mechanical system of several interacting, indistiguishable particles in the presence of inhomogenous magnetic field and analysis of the spin rephasing and coherence.

[1] C. Deutsch et al., Physical Review Letters **105.2**, 020401 (2010)

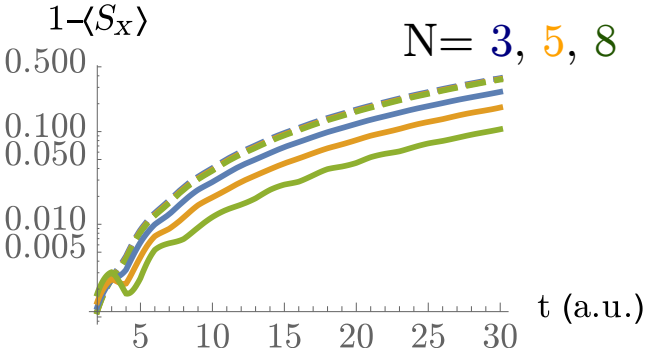


Figure 1: Envelope of visibility $\langle S_x \rangle$ for different number of particles. The parameters expressed in oscillator units are: temperature $T = 0.1$, interaction strengths $g_{\downarrow\downarrow} = 0.0099, g_{\uparrow\uparrow} = 0.011, g_t = 0.01$, and magnetic field $B(x) = 0.03x^2$. Solid line denotes presence of particle-particle interactions, dashed – interaction-free case. Progressively better (with growing number of particles) coherence protection is visible: already for $N = 8$ the coherence time is increased by factor of 5 (note the logarithmic scale).

Ytterbium optical lattice clocks supporting 1×10^{-18} frequency comparisons

W. F. McGrew[1,2], **X. Zhang**[1], **R. J. Fasano**[1,2], **S. A. Schaffer**[1], **K. Beloy**[1], **D. Nicolodi**[1], **R. C. Brown**[1], **N. Hinkley**[1,2], **G. Milani**[1], **M. Schioppo**[1], **T. H. Yoon**[1], **and A. D. Ludlow**[1]

[1] *National Institute of Standards and Technology, 325 Broadway, Boulder, CO 80305, USA*

[2] *Department of Physics, University of Colorado, Boulder, CO 80309, USA*

e-mail: *wfm@nist.gov*

Time and its inverse, frequency, can be measured more precisely than any other physical quantity, with the current generation of optical atomic clocks reporting fractional performance below one part in 10^{17} [1, 2, 3, 4, 5]. General relativity dictates that clocks exhibit sensitivity to gravitational potential. Here we demonstrate two opitcal lattice clocks based on ytterbium with performance that exceeds the present-day capability to determine the gravitational redshift between distant clocks. This performance is manifest in unprecedented levels of clock uncertainty, instability, and reproducibility - three fundamental figures of merit for clock performance. Though gravitational redshifts could degrade the performance of these optical clocks as terrestrial standards of time, this same sensitivity allows clocks to serve as probes of geopotential [5, 6, 7, 8]. We measure for the first time in an optical lattice clock the shift from background gas collisions and *s*-wave collisions arising from imperfect spin-polarization. We also present updates on an ongoing campaign of optical frequency comparisons with the Al^+ single-ion clock at NIST and the Sr optical lattice clock at JILA, as well as an absolute frequency measurement of the Yb $^1S_0 \rightarrow {}^3P_0$ transition frequency.

[1] Chou, C. W., Hume, D. B., Koelemeij, J. C. J., Wineland, D. J. and Rosenband, T. Frequency comparison of two high-accuracy Al^+ optical clocks. Phys. Rev. Lett. **104**, 070802 (2010).

[2] Nicholson, T. L. et al. Systematic evaluation of an atomic clock at 2×10^{-18} total uncertainty. Nat. Commun. **6**, 6896 (2015).

[3] Huntemann, N., Sanner, C., Lipphardt, B., Tamm, C. and Peik, E. Single-ion atomic clock with 3×10^{-18} systematic uncertainty. Phys. Rev. Lett. 116, 63001 (2016).

[4] Schioppo, M. et al. Ultra-stable optical clock with two cold-atom ensembles. Nat. Photonics 11, 48–52 (2016).

[5] Takano, T. et al. Geopotential measurements with synchronously linked optical lattice clocks. Nat. Photonics 10, 662–666 (2016).

[6] Chou, C. W., Hume, D. B., Rosenband, T. and Wineland, D. J. Optical clocks and relativity. Science 329, 1630–1633 (2010).

[7] Delva, P. and Lodewyck, J. Atomic clocks: new prospects in metrology and geodesy. Acta Futur. 7, 67–78 (2013).

[8] Grotti, J. et al. Geodesy and metrology with a transportable optical clock. Nat. Phys. (2018). doi:10.1038/s41567-017-0042-3.

Entanglement, interferometric sensitivity, and macroscopic superposition states by scanning through quantum phase transitions in spinor Bose-Einstein condensates

P. Feldmann[1], **L. Pezzè**[2], **M. Gessner**[2], **M. Gabbrielli**[2,3], **C. Klempt**[4], **L. Santos**[1], **A. Smerzi**[2]

[1] *Institut für Theoretische Physik, Leibniz Universität Hannover, Appelstraße 2, DE-30167 Hannover, Germany*

[2] *QSTAR, INO-CNR, and LENS, Largo Enrico Fermi 2, IT-50125 Firenze, Italy*

[3] *Dipartimento di Fisica e Astronomia, Università degli Studi di Firenze, via Sansone 1, I-50019 Sesto Fiorentino, Italy*

[4] *Institut für Quantenoptik, Leibniz Universität Hannover, Welfengarten 1, DE-30167 Hannover, Germany*

e-mail: *polina.feldmann@itp.uni-hannover.de*

Spinor Bose Einstein condensates (BECs) exhibit different ground state phases, when a tunable magnetic field or microwave dressing is applied as a control parameter. Some of them are experimentally well accessible. Others, in contrast, feature strong multipartite entanglement. Thus, driving the system from the former to the latter is a promising approach to the preparation of exciting, highly entangled many-body states. That this can be put into praxis, though the gap between the ground state and the first excited state closes at the critical points, has been recently demonstrated in [1, 2].

Encouraged by these results, which have been obtained within the $f = 1$ manifold of ^{87}Rb, we elaborate on the opportunities offered by the quasiadiabatic crossing of quantum phase transitions (QPTs) in a ferromagnetic spin-1 BEC. For separable states the sensitivity of atom interferometers is fundamentally limited by the standard quantum limit (SQL), which scales as $1/\sqrt{N}$ with the particle number N. Employing multipartite entanglement allows to shift this bound towards the Heisenberg limit $\propto 1/N$. Entanglement that facilitates to surpass the SQL is unambiguously witnessed by the quantum Fisher information (QFI, F_Q). An evaluation of the QFI across all three ground state phases of a ferromagnetic spin-1 BEC unveils an unexpected regime, the state in the center of the broken axisymmetry phase (CBA state), which provides Heisenberg scaling of the QFI and is separated from the experimentally initial state by only one QPT. We identify optimal unitary transformations and an experimentally feasible optimal measurement prescription that maximize the interferometric sensitivity.

Investigating why the CBA state is so particularly sensitive leads up to an intriguing connection to macroscopic superposition (MS) states. A spin-1 system accommodates three magnetic modes, labeled by $m_f \in \{0, \pm 1\}$. By a change of basis (corresponding to radio-frequency and microwave techniques), $m_f = \pm 1$ can be transformed into their (anti)symmetric combinations tagged by $g(h)$. As illustrated in Fig. 1, projecting the CBA state onto the particle number in one of these modes, say N_h, mostly yields highly entangled two-mode states resembling NOON states. The large contribution of suitable N_h to the CBA state allows for a probabilistic preparation of MS states being heralded by N_h.

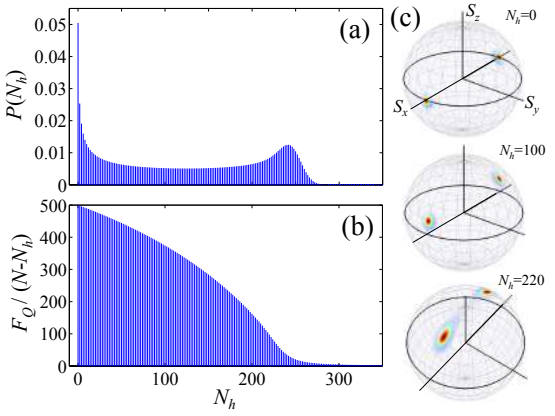


Figure 1: Macroscopic superposition states accommodated by the CBA state of a spin-1 BEC. N_h is the particle number in the antisymmetric mode. (a) With high probability P a measurement of N_h results in a state with (b) large quantum Fisher information F_Q. (c) The Husimi distribution of the projected two-mode states resembles NOON states. Here $N = 500$.

A crucial question in the context of quasiadiabatic state preparation is its stability with respect to a finite driving speed. We show that both the FI and the MS features are well preserved under realistic conditions. Sub-SQL interferometry with the CBA state has by now been demonstrated in [2]. This further emphasizes that the preparation of MS states in spin-1 BECs is brought into reach of current technology by the high stability of the enclosing CBA state.

[1] X.-Y. Luo et al., Science **355**, 620 (2017).

[2] Yi-Quan Zou et al., arXiv:1802.10288.

[3] P. Feldmann et al., arXiv:1712.03896.

[4] L. Pezzè et al., arXiv:1712.03864.

Towards Quantum Logic Spectroscopy of Highly Charged Ions

P. Micke[1,2], S. A. King[1], T. Leopold[1], S. Kühn[2], J. Nauta[2], L. Schmöger[1,2], M. Schwarz[1,2], J. Stark[2], J. R. Crespo López-Urrutia[2], and P. O. Schmidt[1,3]

[1] *Physikalisch-Technische Bundesanstalt, Bundesallee 100, 38116, Braunschweig, Germany*

[2] *Max-Planck-Institut für Kernphysik, Saupfercheckweg 1, 69117, Heidelberg, Germany*

[3] *Institut für Quantenoptik, Leibniz Universität Hannover, Welfengarten 1, 30167 Hannover, Germany*

e-mail: *Piet.Schmidt@quantummetrology.de*

Highly charged ions (HCIs) are promising candidates for frequency metrology as they are less sensitive to external perturbations than neutral or singly-charged systems. Furthermore, they offer a great variety of forbidden optical transitions, some of which are predicted to be extremely sensitive to a change of the fine-structure constant or the electron-proton mass ratio [1]. However, high temperatures inherent to their production impede high-precision spectroscopy. Recently, this obstacle was overcome by re-trapping HCIs in a cryogenic Paul trap, CryPTEx [2] where they were sympathetically cooled by a Coulomb crystal of laser-cooled beryllium ions [3, 4]. We have set up an evolved version of CryPTEx at the German National Metrology Institute (PTB) with improved magnetic shielding and vibration damping for HCI spectroscopy in the Lamb-Dicke regime (see Fig. 1). HCIs are produced with a novel room-temperature Heidelberg compact electron beam ion trap [5], extracted, decelerated, pre-cooled, and transferred to the Paul trap. There, a two-ion crystal composed of one HCI and an auxiliary Be^+ ion is prepared and cooled to its motional ground state, enabling quantum logic spectroscopy [6] on HCIs with unprecedented frequency resolution and accuracy. We will present the first steps towards applying this method to the $2p_{1/2}$-$2p_{3/2}$ M1 line at 441 nm in Ar^{13+} [7].

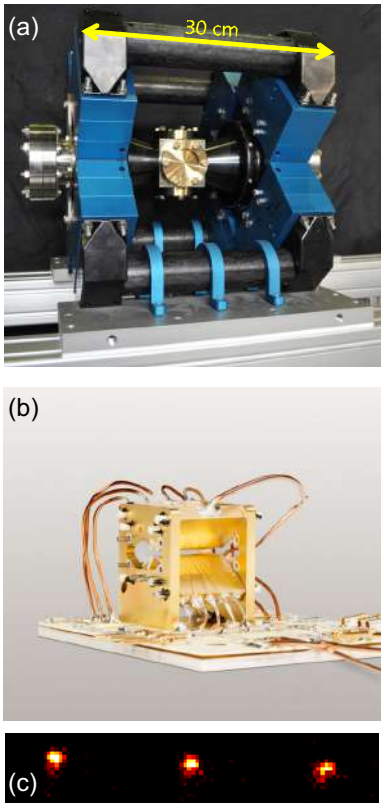


Figure 1: Components of the PTB HCI experiment. (a) Compact electron beam ion trap. (b) Cryogenic Paul blade trap. (c) Three-ion crystal of fluorescing Be^+.

[1] M. G. Kozlov, *et al.*, *Highly Charged Ions: Optical Clocks and Applications in Fundamental Physics*, arXiv:180306532 (2018).

[2] M. Schwarz, *et al.*, *Cryogenic Linear Paul Trap for Cold Highly Charged Ion Experiments*, Rev. Sci. Instrum. **83**, 083115–083115–10 (2012).

[3] L. Schmöger, *et al.*, *Coulomb Crystallization of Highly Charged Ions*, Science **347**, 1233–1236 (2015).

[4] L. Schmöger, *et al.*, *Deceleration, Precooling, and Multi-Pass Stopping of Highly Charged Ions in Be+ Coulomb Crystals*, Rev. Sci. Instrum. **86**, 103111 (2015).

[5] P. Micke, *et al.*, *The Heidelberg Compact Electron Beam Ion Traps*, Review of Scientific Instruments p. accepted (2018).

[6] P. O. Schmidt, *et al.*, *Spectroscopy Using Quantum Logic*, Science **309**, 749–752 (2005).

[7] V. Mäckel, *et al.*, *Laser Spectroscopy on Forbidden Transitions in Trapped Highly Charged Ar^{13+} Ions*, Phys. Rev. Lett. **107**, 143002 (2011).

Dynamics of a Strontium Cold Atom Laser

M. Tang, S. A. Schäffer, M. R. Henriksen, A. A. Jørgensen, and J. W. Thomsen
The Niels Bohr Institute, University of Copenhagen, Blegdamsvej 17, 2100 Copenhagen, Denmark
e-mail: *cmv967@alumni.ku.dk*

The forbidden ${}^1S_0{-}{}^3P_1$ transition of Sr-88 has a narrow linewidth of $\Gamma = 2\pi \cdot 7.5$ kHz, making it of great interest in the development of active frequency references with high stability. One idea is to interrogate the atomic transition in the bad cavity regime, so the narrow atomic spectral features dominate, even if the cavity is more noisy experimentally [1]. In our experimental setup, we cool a thermal ensemble of Sr-88 atoms on the ${}^1S_0{-}{}^1P_1$ transition to a few mK with a Magneto-Optical Trap (MOT). The MOT lasers are then turned off, and the ensemble is subjected to a π pump pulse on the ${}^1S_0{-}{}^3P_1$ transition after some microseconds. Due to experimental limitations, only about 70% of the population in the cavity mode is transferred to ${}^3P_1$. The atoms are coupled to a cavity in the bad cavity regime ($\kappa = 2\pi \cdot 620$ kHz), and following the pump pulse, we observe lasing on the ${}^1S_0{-}{}^3P_1$ transition, causing a pulse in cavity output power.

We model the dynamics of the atoms coupling to the pump pulse and cavity mode, including thermal velocities, and compare the model to experimental results in different regimes - e.g. a detuned cavity, where we observe ringings in the cavity output power (see Fig. 1). We interpret the dynamics in terms of different atomic velocity classes moving in a standing wave cavity field - examples of simulated population dynamics can be seen in Fig. 2. For a cavity near resonance, atoms with low velocities along the cavity axis interact the most with the standing wave and build up an initial cavity field. As the cavity field intensifies, faster-moving, excited atoms interact more with the cavity mode, and amplify the field. For a detuned cavity, atoms with certain velocities (E.g. Bennet hole/Doppleron resonances [2]) interact most with the cavity mode even at lower intensities, which can lead to more synchronized dynamics of different velocity groups. Experimentally, a detuned cavity will result in a more uniform distribution of strongly interacting velocity groups over the duration of the emission pulse.

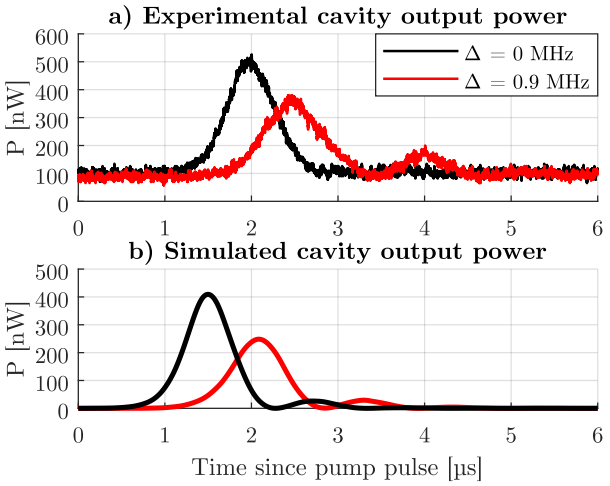


Figure 1: Examples of observed (Fig. a) and simulated (b) cavity output power, for a resonant and detuned cavity. The 100 nW offset for experimental data is due to far-detuned light used to lock the cavity length.

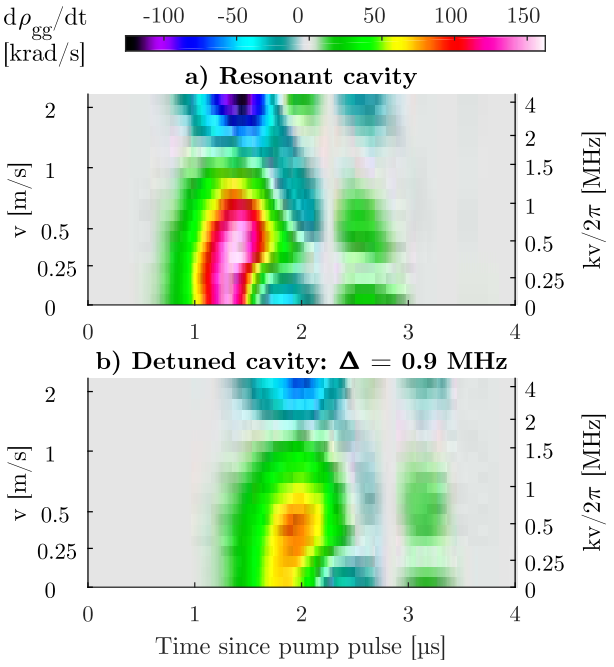


Figure 2: Simulated population dynamics: Red/blue colors represent the change in ${}^1S_0$ population due to emission and absorption of photons in the cavity mode (compare simulation of Fig. 1b). The ensemble is divided into 20 equally populated groups based on their speed (v) along the cavity axis. In Fig. a, the cavity is near resonance; in Fig. b, the cavity is detuned.

References

[1] G. A. Kazakov and T. Schumm, Phys. Rev. A **87**, 013821 (2013)

[2] A. Tallet, J. Opt. Soc. Am. B **11**, 1336-1349 (1994)

Route to a Portable Optical Clock

P. K. Molony[1], M. R. Aldous[1], M. Gellesch[1], J. Bass[1], D. Morris[1], M. Menchetti[1], Q. Obaid[1], S. Viswam[1], I. R. Hill[2], P. Gill[2], Y. Singh[1] and K. Bongs[1]

[1] *Department of Physics and Astronomy, Birmingham University, United Kingdom*

[2] *National Physical Laboratory, Teddington, London, United Kingdom*

e-mail: *p.k.molony@bham.ac.uk*

Portable atomic clocks have a wide range of applications, from geodesy and navigation [1], to space-based master clocks [2], to tests of fundamental physics [3]. Optical clocks offer higher accuracy and stability, and shorter averaging times than radio-frequency clocks. Strontium lattice clocks are especially attractive because the large number of atoms allows fast averaging.

However, a compact clock presents unique technical challenges. The cooling lasers are all in the visible range where laser diodes are still an emerging technology, and they must be stabilised to sub-kHz linewidth. The clock transition also has large blackbody radiation shifts, so the atoms must be held in a stable and well-characterised thermal environment.

Here we present our progress towards a suitcase-scale strontium lattice clock. We develop a compact direct-diode laser system with board-level integrated electronics, in $< 1L$ per laser. These are locked to a single reference cavity. We use lasers based on volume holographic gratings and interference filters, but the system would also work with DBR and DFB lasers to cover a huge range of wavelengths.

We also develop a compact vacuum chamber and physics package based on a single-beam pyramid MOT. A room-temperature source of thermal atoms avoids the use of an oven and the associated BBR shifts [4]. We demonstrate that millions of strontium atoms from the vapour can be captured in a magneto-optical trap (MOT) in a fully controlled manner and with several Hz repetition rate.

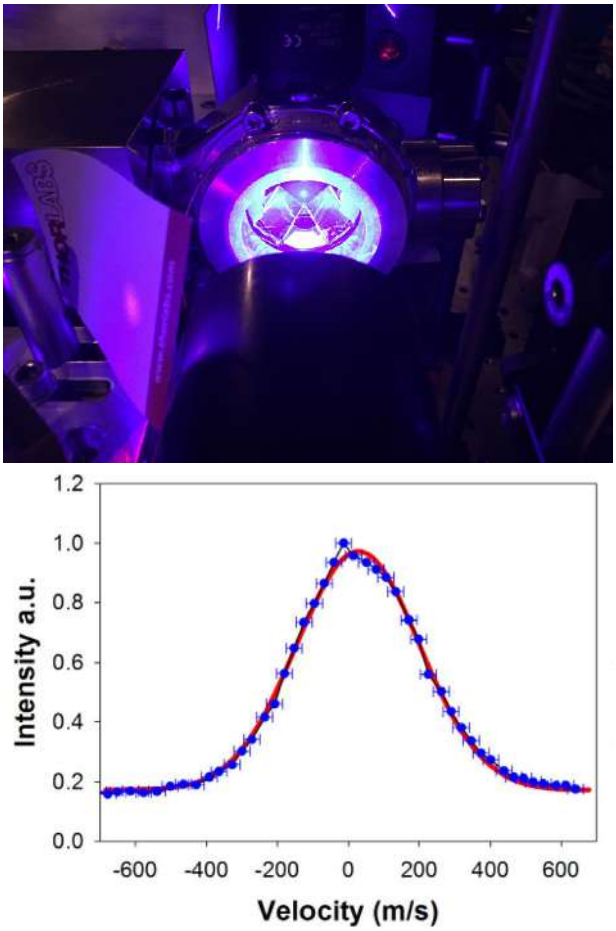


Figure 1: Top: cold Strontium atoms in the single-beam pyramid MOT developed for this project. Bottom: non-thermal velocity distribution of atoms emitted by laser ablation of SrO.

[1] J. Grotti *et al.*, "Geodesy and metrology with a transportable optical clock", Nature Physics (2018)

[2] S. Schiller *et al.*, "Development of high-performance transportable and breadboard optical clocks and advanced subsystems", European Frequency and Time Forum (EFTF) 412-418 (2012)

[3] R. M. Godun *et al.*, Frequency Ratio of Two Optical Clock Transitions in $^{171}Yb^{+}$ and Constraints on the Time Variation of Fundamental Constants, Phys. Rev. Lett. **113**, 210801 (2014)

[4] O. Kock *et al.*, Scientific Reports **6**, 37321 (2016)

Precision Measurements with Trapped-Ion Optical Clocks at NIST

D. B. Hume[1], **S. M. Brewer**[1], **J. S. Chen**[2], **C. W. Chou**[1], **E. Clements**[1,3], **A. M. Hankin**[1], **D. J. Wineland**[1,3,4], **J. C. Bergquist**[1] **and D. R. Leibrandt**[1,3]

[1] *National Institute of Standards and Technology, Boulder, CO 80305, USA*

[2] *Present address: IonQ, Inc., College Park, MD 20740*

[3] *University of Colorado, Boulder, CO 80309*

[4] *Present address: University of Oregon, Eugene, OR 97403*

e-mail: *david.hume@nist.gov*

In recent years, atomic clocks based on optical resonances in single trapped ions have demonstrated fractional instabilities and inaccuracies below the level of 1×10^{-17} [1, 2]. At NIST we have developed optical clocks based on $^{199}Hg^{+}$ and $^{27}Al^{+}$. Previous frequency ratio measurements between these two clocks place a stringent constraint on the time-variation of the fine structure constant [3]. I will review general features of the $^{27}Al^{+}$ standard, which uses sympathetic cooling and quantum-logic spectroscopy, and describe recent progress in its performance. The total inaccuracy of this clock has now been reduced to 1.0×10^{-18} primarily by suppressing uncertainty due to time dilation [4, 5]. I will report on the latest accuracy evaluation and present preliminary results of recent frequency comparison measurements between the $^{27}Al^{+}$ clock and the NIST optical lattice clocks based on ^{87}Sr [6], and ^{171}Yb [7]. We have observed fractional frequency instability in these comparisons at the level of $1.2 \times 10^{-15}/\sqrt{\tau}$ and long-term reproducibility below the level of 1×10^{-17}. We anticipate that these measurements will establish optical frequency ratios, which can be compared internationally, at a new level of uncertainty. Further analysis of this data, including historical data from $^{199}Hg^{+}/^{27}Al^{+}$ comparisons, can place constraints on models of dark matter as ultralight bosons [8, 9].

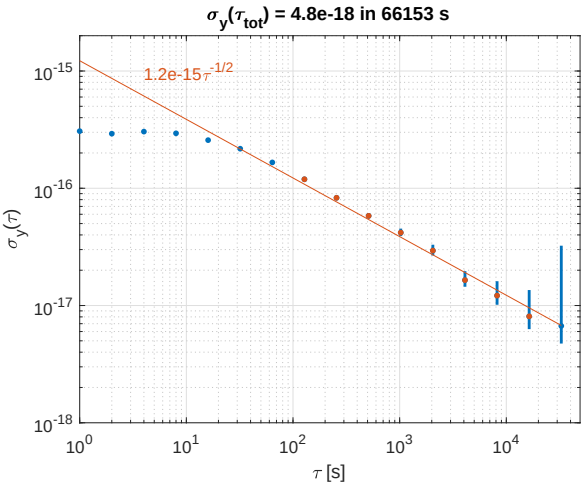


Figure 1: Example long-term stability of frequency ratio measurement between the aluminum-ion and ytterbium-lattice optical clocks.

[1] C. W. Chou, D. B. Hume, J. C. J. Koelemeij, D. J. Wineland, and T. Rosenband, *Phys. Rev. Lett.*, **104**, 070802, (2010)

[2] N. Huntemann, C. Sanner, B. Lipphardt, C. Tamm, and E. Peik,*Phys. Rev. Lett.*, **116**, 063001, (2016)

[3] T. Rosenband, D. B. Hume, P. O. Schmidt, C. W. Chou, A. Brusch, L. Lorini, W. H. Oskay, R. E. Drullinger, T. M. Fortier, J. E. Stalnaker, S. A. Diddams, W. C. Swann, N. R. Newbury, W. M. Itano, D. J. Wineland, and J. C. Bergquist, *Science*, **319**, 1808, (2008)

[4] J.-S. Chen, S. M. Brewer, C. W. Chou, D. J. Wineland, D. R. Leibrandt, and D. B. Hume, *Phys. Rev. Lett.*, **118**, 053002, (2017)

[5] J.-S. Chen, PhD thesis, University of Colorado, Boulder, (2017)

[6] T. L. Nicholson, S. L. Campbell, R. B. Hutson, G. E. Marti, B. J. Bloom, R. L. McNally, W. Zhang, M. D. Barrett, M. S. Safronova, G. F. Strouse, W. L. Tew, and J. Ye, *Nat. Comm.*, **6**, 6896, (2015)

[7] M. Schioppo, R. C. Brown, W. F. McGrew, N. Hinkley, R. J. Fasano, K. Beloy, T. Yoon, G. Milani, D. Nicolodi, J. Sherman, *et al.*, *Nat. Phot.*, **11**, 48, (2017)

[8] K. Van Tilburg, N. Leefer, L. Bougas, and D. Budker, *Phys. Rev. Lett.*, **115**, 011802, (2015)

[9] A. Arvanitaki, J. Huang, and K. Van Tilburg, *Phys. Rev. D*, **91**, 015015, Jan (2015)

Two clock transitions in neutral Yb for the highest sensitivity to variations of the fine-structure constant

M. S. Safronova[1,2], S. G. Porsev[1,3], C. Sanner[4], and J. Ye[4]

[1] *Department of Physics and Astronomy, University of Delaware, Newark, Delaware 19716, USA*

[2] *Joint Quantum Institute, National Institute of Standards and Technology and the University of Maryland, Gaithersburg, Maryland 20742, USA*

[3] *Petersburg Nuclear Physics Institute of NRC "Kurchatov Institute", Gatchina 188300, Russia*

[4] *JILA, NIST, and Department of Physics, University of Colorado, Boulder, Colorado 80309, USA*

e-mail: *sporsev@gmail.com*

We propose a new frequency standard based on a $4f^{14}6s6p\ ^3P_0 - 4f^{13}6s^25d\ (J = 2)$ transition in neutral Yb. This transition has a potential for high stability and accuracy and the advantage of the highest sensitivity among atomic clocks to variation of the fine-structure constant α. We find its dimensionless α-variation enhancement factor to be $K = -15$, in comparison to the most sensitive current clock (Yb^+ E3, $K = -6$), and it is 18 times larger than in any neutral-atomic clocks (Hg, $K = 0.8$). Combined with the unprecedented stability of an optical lattice clock for neutral atoms, this high sensitivity opens new perspectives for searches for ultralight dark matter and for tests of theories beyond the standard model of elementary particles. Moreover, together with the well-established $^1S_0 - {}^3P_0$ transition one will have two clock transitions operating in neutral Yb, whose interleaved interrogations may further reduce systematic uncertainties of such clock-comparison experiments.

Fringe Visibility, Which-Way Information and Weak Value

Minsu Kim[1] **Sang Wook Kim**[2]

[1] *Department of Physics, Pusan National University, Busan 609-735, Korea*

[2] *Department of Physics, Kyung Hee University, Seoul 02447, Republic of Korea*

e-mail: [1] *shuypigel@gmail.com*, [2] *swkim0412@gmail.com*

We show how to obtain both complete which-way information and a perfect interference pattern simultaneously in a double-slit experiment using a quantum weak value scheme.

I. Complementarity and Motivation

The wave-particle duality is expressed as a trade-off relation

$$\mathcal{D}^2 + \mathcal{V}^2 \leq 1, \tag{1}$$

where $\mathcal{D} = \frac{1}{2}\mathrm{tr}\left|U_+\rho_D^{(i)}U_+^\dagger - U_-\rho_D^{(i)}U_-^\dagger\right|$ (distinguishability) and $\mathcal{V} = \frac{p_\phi^{\max}-p_\phi^{\min}}{p_\phi^{\max}+p_\phi^{\min}}$ (visibility) with $p_\phi = \frac{1}{2}\mathrm{tr}\left[(1-\hat{\sigma}_z)\rho^{(f)}\right]$.

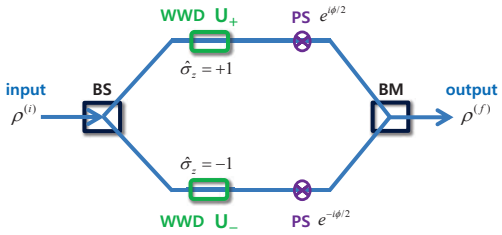


Figure 1: Schematic of a two-way interferometer.

In this presentation we show that

$$\mathcal{D}^2 + \langle\mathcal{V}\rangle_w^2 \leq 2, \tag{2}$$

where $\langle\rangle_w$ denotes the weak value, is achieved in a certain condition.

II. Main idea

One might imagine overcoming the uncertainty principle, a kind of duality; First he measures an observable A very weakly, and consequently its conjugate observable B strongly. No matter how small the weak measurement is, however, it must disturb the initial state. Thus it is impossible to precisely measure both A and B as is well-known. Now we introduce a trick; the weak measurement outcomes of A are averaged only over the post- selected ensemble of B. This is called the weak value. Depending on what is post-selected, we obtain counter-factual information. The weak value is defined as the average of outcomes of the weak measurement of an observable O in the pre- and post-selected ensemble,

$$\langle O\rangle_w = \frac{\langle\psi_i|O|\psi_f\rangle}{\langle\psi_i|\psi_f\rangle} \tag{3}$$

III. Our trick to overcome the duality using weak values

Our scheme is as follows. First, an electron passes through the double slits to form a superposition state, namely $1/\sqrt{2}\,(|L\rangle + |R\rangle)$, where $|L\rangle$ ($|R\rangle$) denotes the state through which the electron passes the left (right) slit, which is the initial state. Second, we obtain the precise which-way information so that we unambiguously know which slit the electron passes through, implying $\mathcal{D} = 1$. Third, we weakly measure the position of the electron and store it to construct the interference fringes later. Finally, we perform a projection measurement to select only the case that the final state collapses to the original initial state, $1/\sqrt{2}\,(|L\rangle + |R\rangle)$, which contains no which-way information. Only over these selected cases we average the outcomes of the weak measurement, which we call $\mathcal{V}_w$. We then obtain $\mathcal{D}^2 + \mathcal{V}_w^2 = 2$.

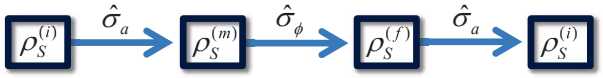


Figure 2: Schematic diagram of our generalized set-up. The initial state $|+\rangle_x$ is measured by $\hat{\sigma}_a$ with the strength α so that the pre-selected state is $\rho_S^{(m)}$. It is then measured by $\hat{\sigma}_\phi$ with the strength α', and the final state is $\rho_S^{(f)}$. It is post-selected on $|+\rangle_x$ by measuring $\hat{\sigma}_x$.

Note that the weak value of the density operator is obtained using

$$\mathrm{tr}\left[\hat{\sigma_\phi}\rho_S^{(i)}\right] = \mathrm{tr}\left[\rho_S^{(m)}\hat{\sigma_\phi}\rho_S^{(i)}\right]/\mathrm{tr}\left[\rho_S^{(m)}\rho_S^{(i)}\right] \tag{4}$$

IV. Conclusion and remarks

The maximum visibility of which-way interference pattern can be recovered even after the projection measurement on the which-way is done. We use a trick of weak value, where the interference is measured very weakly and only the post-selected data are exploited to construct the interference pattern. It does not mean that we truly achieve both complete which-way information and the maximum visibility violating the wave-particle duality since we use only part of the measurement outcomes.

Sympathetic cooling of trapped ions for high resolution spectroscopy

J. Heinrich[1], **M. Baghdad**[1], **J.-Ph. Karr**[1,2], **L. Hilico**[1,2] **and T. Louvradoux**[1]

[1] *Laboratoire Kastler Brossel, UPMC-Univ. Paris 6, ENS, CNRS, Collège de France, 4 place Jussieu, F-75005 Paris, France.*

[2] *Université d'Evry-Val d'Essonne, Boulevard F. Mitterrand, F-91000 Evry, France.*

e-mail: *thomas.louvradoux@lkb.upmc.fr*

The hydrogen molecular ion H_2^+ and its isotopomers HD^+ and $D_2{}^+$ are the simplest molecules. Extremely precise energy levels can be predicted in the frame of QED. The relative inaccuracy on rovibrational transition frequencies is 3×10^{-11} and should reach 10^{-12} [1] This opens the route towards molecular bound state QED tests, fundamental constant measurement such as the electron to proton mass ratio or the proton radius [2], and tests of new physics beyond the standard model [3, 4].

The overall goal of our experiment is to yield a direct measurement of the fundamental constant the proton to electron mass ratio μpe and to test the theory of QED. In order to determine μpe we plan to measure a ro-vibrational Doppler-free two-photon transition ($v = 0$, $L = 2$ to $v = 1$, $L = 2$) in the the molecular hydrogen H_2^+. The precision of the measurement is limited by the second order Doppler effect. In order to reduce this effect the H_2^+ ions need to be trapped and cooled. Since molecular ions cannot be directly laser-cooled, sympathetic cooling via laser-cooled Be^+ ions was implemented. The poster will show how the $313\,nm$ laser source for Be^+ cooling is implemented, then how we create H_2^+ in the $v = 0$, $L = 2$ state through resonance-enhanced multiphoton ionization (REMPI) via a $303\,nm$ dye laser. Then how both species are trapped a linear radio frequency trap. Then show how the spectroscopy will be conduct via resonance-enhanced multiphoton dissociation [5] (REMPD) using a QCL at $9.17\,\mu m$ for spectroscopy and a $213\,nm$ commercial pulse laser for dissociation (Fig. 1). The poster will overall present the status of the experiment on H_2^+ in Paris as well as some results in the form of Coulomb crystals (Fig. 2).

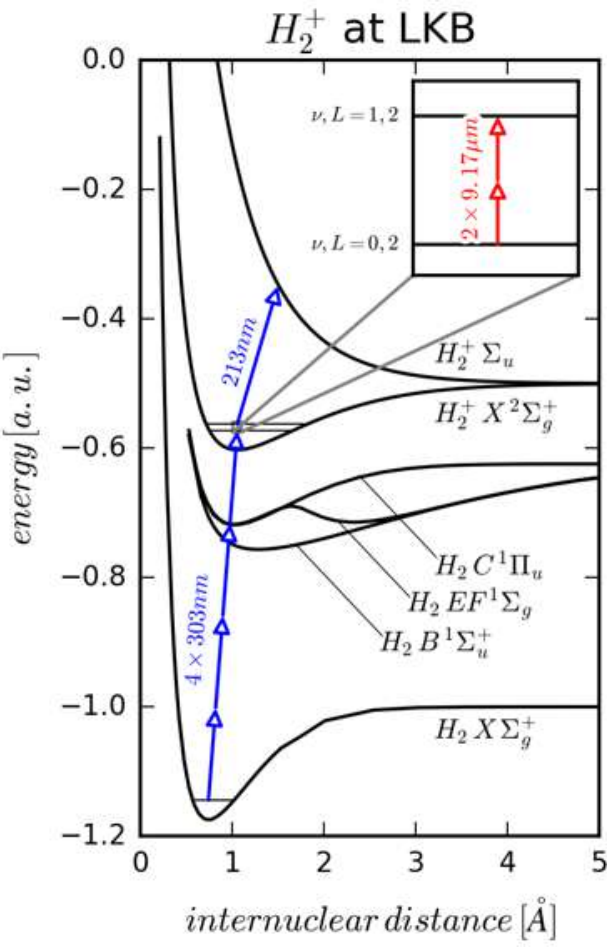


Figure 1: Electronic states in the Born-Oppenheimer approximation for H_2 and H_2^+ and transitions as planned at LKB.

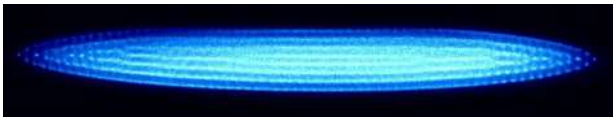


Figure 2: Coulomb crystal of around 15 000 laser cooled Be^+.

[1] V. I. Korobov & al., Phys. Rev. A **89**, 032511 (2014).

[2] R. Pohl & al. Nature **466**, 213216 (2010).

[3] J. Biesheuvel & al., Nature Comm. **7**, 10385 (2016).

[4] J.-Ph. Karr, J. Mol. Spectrosc. **300**, 37 (2014).

[5] Y. Weijun, R. Alheit and G. Werth. Z. Phys D **28**, 87 (1993).

Anderson Localisation Experiments with Ultracold Atoms in a 2D Programmable Potential

M. D. Hoogerland[1], T. A. Haase[1], D. H. White[1,†], A. V. H. McPhail[1], and D. J. Brown[1]

[1] *Dodd-Walls Centre for Photonic and Quantum Technologies, Department of Physics, University of Auckland, Private Bag 92019, Auckland, New Zealand*

[†] *Current Address: Department of Applied Physics, Waseda University, 3-4-1 Okubo, Shinjuku-ku, Tokyo 169-8555, Japan*

e-mail: *alexander.mcphail@auckland.ac.nz*

Anderson localisation is a quantum mechanical effect in which the diffusive transport of waves through a disordered medium is suppressed [1]. In this study, we investigate Anderson localisation in two-dimensions, which has yet to be observed with matter-waves. Previous work conducted by de Saint Vincent *et al.* [2] on expanding a two-dimensional ultracold degenerate gas into a laser speckle pattern resulted in the observation of reduction of diffusive transport, attributed to classical trapping effects due to the high percolation threshold in speckle.

Our experiment generates a BEC of 2×10^4 atoms, using an all-optical set-up. Conducting an expansion experiment results in a dilute sample over the expected localised area, which we are unable to image directly. To overcome this, we conduct transmissive experiments to study the impact of Anderson localisation on the atom conduction. We utilise an SLM [3] to trap the atoms in a 'dumbbell' potential (Fig. 1(a)) [4], loading the atoms into the right-most reservoir and projecting a controllable point-like disorder into the connecting channel (Fig. 2(b,c,d)). By applying the atomtronic RCL model [5, 6, 7] to describe the system dynamics, we represent the conduction of atoms through an effective resistance of the channel. We present our results of the experiments modifying both the geometry of the channel and amount of disorder.

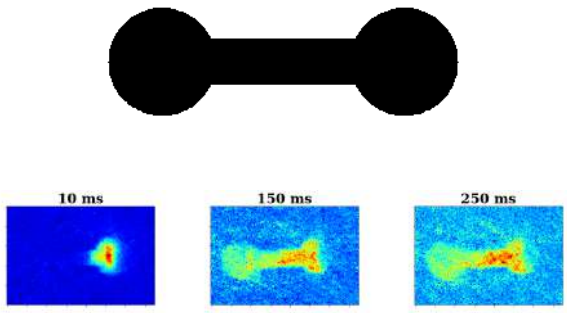


Figure 1: (a) Dumbbell potential. (b,c,d) Migration of atoms through dumbbell potential. The atoms are initially loaded into the right-hand reservoir. Shots are taken of the migration of the atoms through the channel at different times. After 250 ms it can be seen that atoms are filling the left-hand reservoir.

As can be seen in Figure 1, the atoms migrate from the initial reservoir on the right hand side and after 150 ms occupy both the channel and the left-hand reservoir. We introduce point-like disorder into the channel of our circuit (Fig. 2). We monitor the transport of the atoms through the disordered channel and find signatures characteristic of Anderson localisation. Figure 2 shows that with the introduced disorder the atoms diffusive transport is halted and the atoms migrate half-way down the channel.

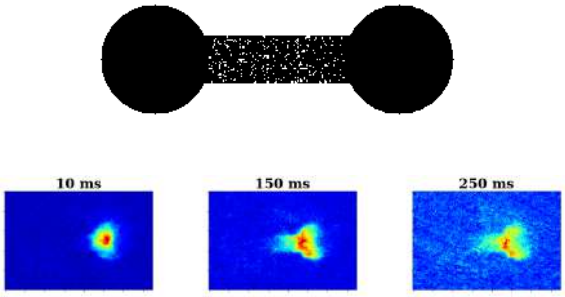


Figure 2: (a) 2D dumbbell potential with point disorder. (b,c,d) Migration of atoms through dumbbell potential with point disorder. It can be seen that the atoms do not migrate to the left-hand reservoir and are instead localised to the right-hand side of the circuit.

[1] P. W. Anderson, Phys. Rev. **109**(5), 1492–1505 (1958).

[2] M. R. de Saint Vincent *et al.*, Phys. Rev. Lett. **104**, 220602

[3] T. A. Haase *et al.*, Rev. Sci. Inst. **88**, 113102 (2017).

[4] A. Li *et al.*, Phys. Rev. A **94**, 023626 (2016).

[5] B. T. Seaman *et al.*, Phys. Rev. A **75**, 023615 (2007).

[6] S. Krinner *et al.*, Phys. Rev. Lett. **110**, 100601

[7] S. Eckel *et al.*, Phys. Rev. A **93**, 063619

Atomic diffraction through nano grating for a novel Casimir-Polder potential measurement

F. Correia[1], **H. Bricha**[1], **F. Perales**[1], **M. Ducloy**[1] **and G. Dutier**[1]
[1] *Laboratoire de Physique des Lasers, Institut Galilée, Université Paris 13, France*
e-mail: *dutier@univ-paris13.fr*

Casimir-Polder potential between a moving atom and solid matter is a fascinating configuration for multiple physical issues from QED to 5th force constraint at very short scale [1]. Numerous experiments have been done in several configurations: cold atoms bounce, quantum reflection, hot vapor in thin cell and transmission nanogratings in supersonic atomic beams. All of them were able to measure the Casimir-Polder potential (van der Waals, London) with a reasonable agreement. However, they all encounter a limitation due to the small atom-surface interaction potential regards to the total measured signal e.g. optical potential, geometrical diffraction or selective reflection signal.

We have done a novel experimental configuration with a transmission nanograting and a low velocity tunable metastable Argon beam, which is a new atomic tool [2]. The grating is made up of 50 nm slits, 100 nm pitch and 130 nm depth in silicon nitride (Si_3N_4). The argon beam is prepared in the $^3P_2$ metastable state with velocities ranging from 20 to 150 m/s with a natural velocity dispersion of 3%. Additional post-treatments allow accuracy down to 0.1% on the velocity selection and 0.1% for velocity dispersion. A 8 cm diameter chevron channel plates (MCP) followed by a delay line detector allow a time-position recording. In such a configuration, the diffraction picture is a combination between the signal of an atomic wave packet passing through a nanograting and the effect of the Casimir-Polder potential on atoms traveling through the nanograting. The atom-surface interaction becomes particularly large when the velocity decreases. The reason is a longer traveling time inside the nanograting, which induces a larger atomic wave packet dephasing and consequently a larger diffraction picture. Between 560 m/s (thermal velocity of Argon) and for example 20 m/s, the factor 28 in the de Broglie wavelength is also found in the diffraction spectra angular aperture: from 1 to 30 mrad. Such an enormous size at low velocity allows a much better angular resolution, which consequently leads to spectrum with much better accurate shapes than the ones done with previous experiments.

As we know the geometry of the nanograting with a reasonable accuracy, the atom surface potential introduced in the theoretical model is more constrained in our apparatus than for older experiments. At intermediate velocities (namely from 70 to 150 m/s), we have an excellent agreement between our measurements and a model using the semi-classical approach (potential energy smaller than kinetic energy) with a standard calculated potential [3]. We find an accuracy on the potential in the range of 5% at 34 m/s for 3 hours of data acquisition (Fig. 1). Such a result corroborates a previous experiment of a complete nanograting interferometer with a supersonic beam [4].

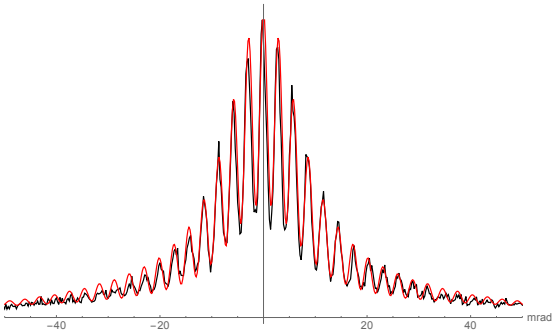


Figure 1: Diffraction picture of atomic argon beam at $v = 34$ m/s through a nano grating of 50 nm slit width and 100 nm pitch. In black, experimental points and in red theoretical calculation.

Our experimental device opens the way to of a more rigorous theoretical models which could lead to an unprecedented Casimir-Polder potential measurement accuracy. An agreement in the range of 1% is expected and would give a novel constrain at very short distances for the hypothetical 5th force.

[1] I. Antoniadis *et al.*, C. R. Physique **12**, 755 (2011)

[2] T Taillandier-Loize *et al.*, J. Phys. D: Appl. Phys. **49**, 135503 (2016)

[3] R. E. Grisenti, *et al.*, Phys. Rev. Lett. **88** 1755 (1999)

[4] S. Lepoutre *et al.*, Eur. Phys. J. D **62**, 309 (2011)

EDM^3: a new search for the electron electric dipole moment using molecules in a matrix

E. A. Hessels[1], **A. C. Vutha**[2], **M. Horbatsch**[1], **G Koyanagi**[1], **M. C. George**[1], **J. T. Singh**[3], **R. Fournier**[1], **A. Ragyanszki**[1], **C. H. Storry**[1], **Z. A. Corriveau**[1], **N. McCall**[1], **J. Perez Garcia**[1], **F. Fang**[3], **K. Saltoun**[1], **and H. Yau**[1]

(EDM^3 collaboration)

[1] *York University, Toronto, ON, Canada*

[2] *University of Toronto, Toronto, ON, Canada*

[3] *Michigan State University, East Lansing, MI, U.S.A.*

e-mail: *hessels@yorku.ca*

Improved measurements of the electron electric dipole moment (eEDM) will strongly constrain the parameter space of new physics theories. Such experiments are especially important due to the dearth of new physics observations at high-energy colliders. Over the last decade, polar molecules have become established as the most promising systems for eEDM searches, due to the large internal electric fields experienced by an eEDM in these molecules. The sensitivity of eEDM searches is determined by the coherence time available for measuring eEDM-induced electron spin precession, as well as the total number of molecules available over the course of a measurement. We present a new method which uses polar molecules oriented within a rare gas matrix. We refer to this method as EDM^3 (for Electric Dipole Measurements using Molecules in a Matrix). The method combines long coherence times (of up to 1 s) and large molecule numbers (of up to 10^{13}), allowing for the possibility of an eEDM search experiment with improved precision by many orders of magnitude beyond the current eEDM limit [1, 2] of 7×10^{-29} e cm. The EDM^3 method also offers an array of reversals and controls for cleanly suppressing systematic effects to a level commensurate with the improved statistical precision. This measurement precision will test physics well beyond the reach of collider physics.

The first version of the EDM^3 experiment will use BaF molecules that are created by neutralizing a 1-eV beam of isotopically-pure BaF^+ ions. The molecules will be embedded in solid argon at 4 kelvin, which will align the molecules along the three axes of its cubic structure. In the Ar matrix, the BaF molecule can no longer rotate, with its rotational motion being replaced by librational motion. Because of the temperature of the sample, all molecules will thermalize into the lowest electronic, vibrational and librational state.

Radiofrequency-assisted optical pumping will prepare the molecules into one hyperfine state. The molecule will be put into its precessing state (a linear combination of the $m_f = -1$ and $m_f = 1$ states in a small magnetic field) using rf pulses. Because the matrix maintains the orientation of the molecules, no applied electric field is needed during the precession period. Further rf pulses are followed by laser cycling transitions ($^2\mathrm{X}^+(\nu = 0)$ to $^2\mathrm{A}_{3/2}(\nu = 0)$). Interspersed upward- and downward-pointing molecules simultaneously precess and have their signals differenced, allowing for a determination of the eEDM contribution while canceling the effect of magnetic fields.

[1] J. Baron, W. C. Campbell, D. DeMille, J. M. Doyle, G. Gabrielse, Y. V. Gurevich, P. W. Hess, N. R. Hutzler, E. Kirilov, I. Kozyryev, B. R. O'Leary, C. D. Panda, M. F. Parsons, E. S. Petrik, B. Spaun, A. C. Vutha, and A. D. West (ACME collaboration) Science **343**, 269 (2014).

[2] W. B. Cairncross, D. N. Gresh, M. Grau, K. C. Cossel, T. S. Roussy, Y. Ni, Y. Zhou, J. Ye, and E. A. Cornell, Phys. Rev. Lett. **119**, 153001 (2017).

Development of a hybrid atom chip.

Julien Alibert, Maxime Bordoux, Baptiste Allard, Alexandre Gauguet
LCAR Laboratoire Collisions Agrégats et Réactivité UMR 5589, Université Paul Sabatier, 31062 Toulouse, France
e-mail : *alibert@irsamc.ups-tlse.fr*

We present the development of an hybrid (optic-magnetic) atom chip to reach the Bose-Einstein condensation of rubidium 87 and 85 in the framework of atom interferometry. We realised a first prototype and trapped 6×10^9 atoms of both species in a millimeter scale magnetic trap [1]. Moreover, we present studies on atom chip to improve the stiffness of the trap.

Atom interferometry has shown its interest for high precision measurements, such as inertial sensors, tests of fundamental physics or fundamental constant measurements. A way to improve sensitivity of such device is to reduce velocity spread of the atomic cloud. The use of ultra-cold atoms allows longer interrogation time and larger spatial separation between the interferometer arms. We are building a new atom interferometer with separated arms at the *LCAR*. This new set-up will meet two objectives. One is to study and develop a new double species Bose-Einstein condensate *BEC* source for atom interferometry with rubidium 87 and 85. This *BEC* source relies on the atom chip technology to cool down and manipulate atoms. This technology is compact and low power consuming, therefore suitable for transportable applications in space. A second aim is to use this interferometer to fix new bounds on the experimental value of atom neutrality thanks to the scalar Aharonov-Bohm effect.

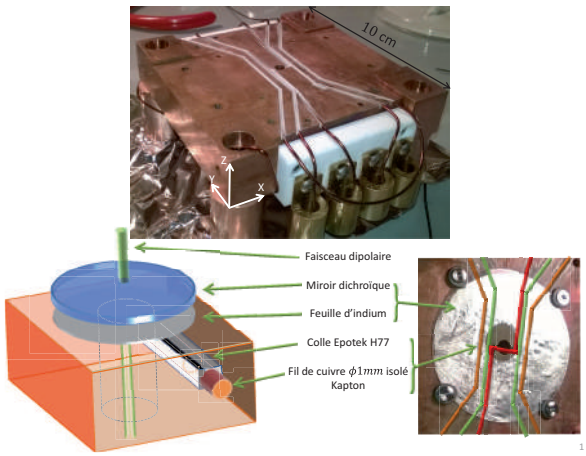


FIGURE 1: Setup of the millimter scale magnetic trap.

We realised a millimeter scale magnetic trap, Fig. 1. The surface is covered by a dichroïc coating allowing to realise a mirror magneto-optical trap *mMOT* and the dipolar beam to pass through the surface. Below the surface, millimetric copper wires provide the magnetic trapping and a radio frequency antenna which is used for the evaporative cooling. This first prototype allows the loading of 4×10^{10} atoms of both species in a *mMOT* within 1.8 s. After laser cooling stages we trap 6×10^9 atoms in the magnetic trap.

This millimeter scale trap will help loading atoms into micrometer size magnetic trap in order to compress the cloud and cool it down to the Bose-Einstein condensation. We are developing a new atom chip based on the deposition of copper wires on top of AlN substrate. The atom chip will be fixed on top of the millimetric structure and we will realise a gratting *MOT* on its surface. The design of the conductive tracks, that we present, will allow to reach transversal trapping frequencies of the order of 2 kHz and therefore an evaporation time less than 500 ms. In this poster we will present the first tests and the design of this new hybrid (magnetic and optic) atom chip.

[1] Alibert, J. and Décamps, B. and Bordoux, M. and Allard, B. and Gauguet, A., *Review of Scientific Instruments*, vol. 88, p. 113–115, (2017).

Precision microwave measurement of the $n = 2$ triplet P_1 to P_2 fine structure interval of atomic helium

K. Kato, T. D. G. Skinner, N. Bezginov, T. Valdez, and E. A. Hessels
Department of Physics and Astronomy, York University, Toronto, Ontario, Canada
e-mail: *hessels@yorku.ca*

The 2^3P_1-to-2^3P_2 fine structure interval in atomic helium is measured using the frequency-offset separated oscillatory fields (FOSOF) technique [1]. This is the first use of the FOSOF technique for a precision measurement. Significant improvements in experimental design have been made to the previous microwave measurement of the same transition performed in 2009. Details of the experimental apparatus and a study of major systematic effects are presented.

A beam of metastable helium atoms is produced in a liquid-nitrogen-cooled DC-discharge source, and is intensified using a two-dimensional magneto-optical trap (2D-MOT). Atoms in the 2^3S_1 state are optically pumped into the 2^3S_1 (m=+1) state prior to entering the main experiment region. These atoms are excited to the 2^3P_1 (m=+1) state by a short pulse of linearly polarized 1083-nm laser light inside the microwave region, where they undergo a FOSOF experiment sequence. The 2^3P_1-to-2^3P_2 transition is excited by two time-separated microwave fields. Atoms that undergo the microwave transition during the first pulse accumulate a different quantum-mechanical phase from the ones that make the transition during the second pulse. Interference between the probability amplitudes for the two cases gives rise to a transition lineshape whose width is proportional to the inverse of the time separation between the two microwave fields. Shortly after the FOSOF sequence is completed, 447-nm and 1532-nm laser pulses excite atoms in the 2^3P_2 state up to the 18P Rydberg state. These Rydberg atoms are Stark-ionized and counted. This background-free ion detection method is only sensitive to the atoms that experience a complete FOSOF sequence, eliminating the major systematic effects of previous experiments [2]. The detection method has also led to a substantial improvement in the signal-to-noise ratio of collected data.

The excellent signal-to-noise ratio allowed us to quickly investigate various systematic effects (pressure shifts, quadratic Zeeman shifts, light shifts, etc). Amongst all of the systematic effects being studied, the most subtle effect observed in our experiment was a small shift in linecenter caused by phase and amplitude distortions at the beginning and end of the microwave pulses due to RF switching imperfections. Microwave pulses are monitored on an oscilloscope, and the traces of the pulses are used for numerical integration of the Schrödinger equation. The numerical integration shows that the linecenter shift depends linearly on the microwave power, the inverse of the time separation between two pulses (T), and the pulse duration (D). The consistent behavior of linecenters between simulation and experiment allows us to use extrapolations to zero microwave power to determine the linecenters. Excellent agreement in extrapolation results among various T, D combinations was observed.

Recent results in laser and microwave spectroscopy of the 2^3P_1 to 2^3P_2 transition [3, 2, 4, 5] use various experimental systems with different systematic effects. Our new measurement obtains an improved measurement precision, and will allow for an even more precise test of two-electron quantum electrodynamics (QED) theory in the helium n=2 triplet P system. This measurement is an important step towards obtaining a precise determination of the fine structure constant.

[1] A. Vutha and E. A. Hessels, Phys. Rev. A **92**, 052505 (2015).

[2] J. S. Borbely, M. C. George, L. D. Lombardi, M. Weel, D. W. Fitzakerley, and E. A. Hessels, Phys. Rev. A **79**, 060503 (2009)

[3] X. Zheng, Y. R. Sun, J.-J. Chen, W. Jiang, K. Pachucki, and S.-M. Hu, Phys. Rev. Lett. **118**, 063001 (2017)

[4] J. Castillega, D. Livingston, A. Sanders, and D. Shiner, Phys. Rev. Lett. **84**, 4321 (2000).

[5] T. Zelevinsky, D. Farkas, and G. Gabrielse, Phys. Rev. Lett. **95**, 203001 (2005).

Parity-nonconserving interaction-induced light shifts in the $7S_{1/2} - 6D_{3/2}$ transition of the ultracold ^{210}Fr atoms to probe new physics beyond the standard model

T. Aoki[1], Y. Torii[1], B. K. Sahoo[2], B. P. Das[3], K. Harada[4], T. Hayamizu[4], K. Sakamoto[4], H. Kawamura[4,5], T. Inoue[4,5], A. Uchiyama[4], S. Ito[4], R. Yoshioka[4], K. S. Tanaka[4], M. Itoh[4], A. Hatakeyama[6], and Y. Sakemi[7]

[1] *Institute of Physics, The University of Tokyo, Tokyo 153-8902, Japan*
[2] *AMO Physics Division, Physical Research Laboratory, Ahmedabad 380009, India*
[3] *IRCS and Department of Physics, Tokyo Institute of Technology, Tokyo 152-8550, Japan*
[4] *CYRIC, Tohoku University, Sendai, Miyagi 980-8578, Japan*
[5] *FRIS, Tohoku University, Sendai, Miyagi 980-8578, Japan*
[6] *Applied Physics, Tokyo University of Agriculture and Technology, Tokyo 184-8588, Japan*
[7] *CNS, The University of Tokyo, Wako, Saitama 351-0198, Japan*
e-mail: *aoki@phys.c.u-tokyo.ac.jp*

Studies of atomic parity nonconservation effects have the potential to probe new physics beyond the standard model (SM) of particle physics and to measure the nuclear anapole moment (NAM) which is an unusual property of the nucleus [1, 2]. There are mainly two sources of parity nonconservation(PNC) interactions in atomic systems. One is due to the neutral current weak (NCW) interactions by the exchange of the Z_0 boson between the nucleus and electrons, while the other is due to the interaction of the NAM with the electrons. The NCW interaction can be classified into nuclear spin independent (NSI) and nuclear spin-dependent (NSD) PNC interactions. It is possible in principle to gain insights into new physics beyond the SM of particle interactions by investigating the NSI PNC interaction. The most accurate data on atomic PNC currently comes from the $6S_{1/2} - 7S_{1/2}$ transition in cesium [3]. To obtain a more accurate value of the nuclear weak charge $Q_{\rm W}$, many other atomic systems such as Yb [4], Ba^+ [5], Ra^+ [6], and Yb^+ [7] have been proposed.

We present an experimental technique to measure light shifts due to the NSI PNC interaction in the $7S_{1/2} - 6D_{3/2}$ transition in ultracold ^{210}Fr atoms (Fig. 1). The approach we propose is similar to the one by Fortson [5] to measure the PNC-induced light shift which arises from the interference of parity nonconserving electric dipole transition and electric quadrupole transition amplitudes. A relativistic coupled-cluster method has been employed to calculate the electric dipole transition amplitudes arising from the PNC interactions. Based on these calculations, we have evaluated the PNC-induced light shifts for transitions between the hyperfine levels of the $7S_{1/2}$ and $6D_{3/2}$ states and suitable transitions are identified for carrying out PNC measurements. We shall be able to extract a precise value of weak charge $Q_{\rm W}(^{210}{\rm Fr})$ from the measurement of the light shifts. It is possible in principle to probe new physics beyond the SM with our proposed experimental scheme. The sensitivities of masses for new particles are TeV/c^2 scale [8].

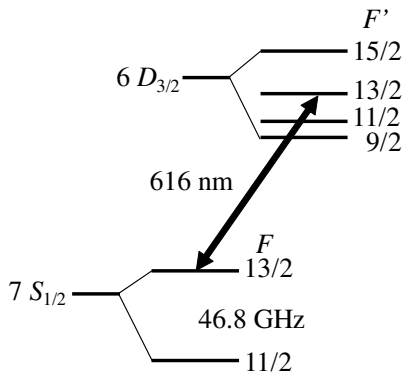


Figure 1: Schematic hyperfine energy level diagrams of ^{210}Fr. Arrow indicates the laser-induced transition to observe the E2 light shift and PNC-induced light shift from the $7S_{1/2}$ state to the $6D_{3/2}$ state.

[1] M.A. Bouchiat, C. Bouchiat, Rep. Prog. Phys. **60**, 1351 (1997).

[2] J. S. M. Ginges, V. Flambaum, Phys. Rep. **397**, 63 (2004).

[3] C. S. Wood *et al.*, Science **275**, 1759 (1997).

[4] K. Tsigutkin, D. Dounas-Frazer, A. Family *et al.*, Phys. Rev. Lett. **103**, 071601 (2009).

[5] N. Fortson, Phys. Rev. Lett. **70**, 2383 (1993).

[6] L. W. Wansbeek, B. K. Sahoo, R.G.E. Timmermans *et al.*, Phys. Rev. A **78**, 050501(R) (2008).

[7] B. K. Sahoo, B. P. Das, Phys. Rev. A **84**, 010502(R) (2011).

[8] T. Aoki, Y. Torii, B. K. Sahoo, B. P. Das, K. Harada *et al.*, Appl. Phys. B **123**, 120 (2017).

Optical dipole force trapping of rubidium atoms for a dual-isotope co-magnetomter toward the electron electric dipole moment measurement

A. Uchiyama[1], K. Harada[1], T. Inoue[2,3], H. Kawamura[4,1], K. S. Tanaka[1], M. Itoh[1], T. Aoki[5], A. Hatakeyama[6], Y. Takahashi[7], and Y. Sakemi[8]

[1] *Cyclotron and Radioisotope Center, Tohoku University, 980-8575 Miyagi, Japan*
[2] *RIKEN Cluster for Pioneering Research, 351-0198 Saitama, Japan*
[3] *RIKEN Nishina Center for Accelerator-Based Science, 351-0198 Saitama, Japan*
[4] *Frontier Research Institute for Interdisciplinary Sciences, Tohoku University, 980-8575 Miyagi, Japan*
[5] *Institute of Physics, The University of Tokyo, 153-8902 Tokyo, Japan*
[6] *Department of Applied Physics, Tokyo University of Agriculture and Technology, 184-8588 Tokyo, Japan*
[7] *Department of Physics, Kyoto University, 606-8502 Kyoto, Japan*
[8] *Center for Nuclear Study, The University of Tokyo, 351-0198 Saitama, Japan*
e-mail: *uchiyama@cyric.tohoku.ac.jp*

The permanent electric dipole moment (EDM) of an elementary particle is a good candidate to search for the physics beyond the standard model [1]. The electron EDM has been searched for by measuring the energy splitting of atoms and molecules in an electric field [2, 3]. In such experiments, laser cooling and trapping can prolong the interaction time and suppress systematic errors, which is an improvement over conventional atomic beam experiments. At the Cyclotron and Radioisotope Center, Tohoku University, an experimental effort to measure the electron EDM using laser-cooled and trapped francium (Fr) atoms is ongoing [4, 5]. Fr is an unstable alkali metal with a large enhancement factor for the electron EDM [6, 7].

In this study, the frequency difference between the resonance transition of the Fr atom in a static electric field parallel to the static magnetic field is compared with that in an electric field anti-parallel to the magnetic field. For accurate and precise EDM measurement, measurements of the Zeeman shift caused by the applied magnetic field and the light shift caused by an optical dipole force trap (ODT) or optical lattice (OL) are required. The dual Rb isotope co-magnetometer, which uses both ^{85}Rb and ^{87}Rb isotopes, is utilized for measuring the Zeeman shift and the light shift for Rb atoms simultaneously.

For the long coherence time required for a highly sensitive magnetometer, it is necessary to trap atoms in ultra-high vacuum. Therefore, we constructed a double magneto-optical trap (MOT) system which combines two MOTs (first MOT, second MOT) for ^{85}Rb and ^{87}Rb. The MOT beams for ^{85}Rb and ^{87}Rb are red-detuned 18 MHz from the resonances of ^{85}Rb $5S_{1/2}, F = 3 \rightarrow 5P_{3/2}, F' = 4$ and ^{87}Rb $5S_{1/2}, F = 2 \rightarrow 5P_{3/2}, F' = 3$, respectively and repumping light beams are resonant to the respective resonances ^{85}Rb $5S_{1/2}, F = 2 \rightarrow 5P_{3/2}, F' = 3$ and ^{87}Rb $5S_{1/2}, F = 1 \rightarrow 5P_{3/2}, F' = 2$. These laser beams are generated by an external cavity diode laser with inputting three RF signals to an electro-optic modulator [8]. ^{85}Rb and ^{87}Rb atoms are simultaneously transported from the first MOT to the second MOT by pushing light, which is tuned to the transition of $F = 3 \rightarrow F' = 4$ for ^{85}Rb and $F = 2 \rightarrow F' = 3$ for ^{87}Rb. Figure 1 shows the absorption spectrum of ^{85}Rb and ^{87}Rb trapped in the second MOT obtained by scanning a probing laser frequency. We are currently developing the polarization gradient cooling (PGC) system for ^{85}Rb and ^{87}Rb to load them into ODT or OL efficiently. In this presentation, we report the progress in the development of the dual-isotope PGC and ODT.

[1] M. Pospelov and A. Ritz, Ann. Phys. **318**, 119 (2005).
[2] J. Baron *et al.*, Science **343**, 269 (2014).
[3] B. C. Regan *et al.*, Phys. Rev. Lett. **88**, 071805 (2002).
[4] H. Kawamura *et al.*, Rev. Sci. Instrum. **87**, 02B921 (2016).
[5] K. Harada *et al.*, Appl. Opt. **55**, 1164 (2016).
[6] D. Mukherjee *et al.*, J. Phys. Chem. A **113**, 12549 (2009).
[7] T. M. R. Byrnes *et al.*, Phys. Rev. A **59**, 3082 (1999).
[8] V. M. Valenzuela *et al.*, J. Opt. Soc. Am. B **30**, 1205 (2013).

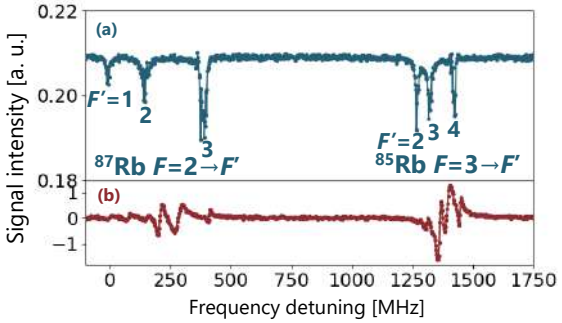


Figure 1: (a) Absorption spectrum of trapped ^{85}Rb and ^{87}Rb. (b) Saturated absorption spectrum of Rb vapor cell measured with frequency-modulated light.

Diffraction Phases in Large Momentum Separation Contrast Interferometry with Yb Bose-Einstein condensates*

K. McAlpine[1], **D. Gochnauer**[1], **B. Plotkin-Swing**1 **and S. Gupta**[1]
[1] *University of Washington, Seattle, Washington 98195, USA*
e-mail: *kem37@uw.edu*

We perform experiments with a symmetric three-path matter-wave interferometer using a ^{174}Yb Bose-Einstein condensate (BEC) atom source with a goal of obtaining precision measurements of the fine-structure constant. We recently achieved 112 photon recoil momenta ($112\hbar k$) momentum separation for the outer paths and demonstrated a phase evolution rate as large as 7 x 10^7 rad/s while still observing phase stability. For path acceleration, third-order Bragg pulses were used. Due to the momentum-dependent AC Stark effect, while in the presence of the pulse light, the phase of the atoms evolves at a rate different than the rate for free space evolution. The difference in phase accumulated due to the light is called diffraction phases and can be a source of systematic error. We we wish to use Bloch oscillations for acceleration because they can have higher e ciencies, however they can produce larger diffraction phases. We construct a model for diffraction phases then test the model by measuring the diffraction phase for different lattice depths, atom momenta, and pulse orders. The model can be used to inform a future experimental design to minimize the effect of diffraction phases.
*This work is supported by NSF Grant No. PHY-1707575.

[1] B. Plotkin-Swing et al, arXiv:1712.06738.

Dephasing due to Gravitational Interaction in Atomic Interferometer

Sohitri Ghosh[1], **Daniel Carney**[2,3] **and Jacob M. Taylor**[2,3,4]
[1] *Department of Physics, University of Maryland, College Park, MD 20742*
[2] *Joint Quantum Institute, College Park, MD 20742*
[3] *Joint Center for Quantum Information and Computer Science, College Park, MD 20742*
[4] *National Institute of Standards and Technology, Gaithersburg, MD 20899*
e-mail: *sohitri@umd.edu*

Atomic interferometers are based on the same principle as optical interferometers. With atomic interferometry we can look at the phase difference between matter-waves from a particular source, following separate paths to recombine at the end, which is a function of the difference between the applied potential through those paths. Atomic interferometers with cutting edge technologies are being proposed as potential tools in search for dark matter [1] and also for gravitational waves[2], especially to look at the gravitational decoherence in an atomic interferometer due to the scattering of stochastic gravitational waves [3]. Here, we look at the dephasing in an atomic interferometer due to the gravitational interaction of the matter-wave with an ideal gas-like mass distribution in thermal state at a certain distance from the interferometer. Introduction of longer separation between interferometer arms and bigger test mass with current technologies would make the signal stronger. We explain how the time-time correlation function of the gradient of gravitational potential sourced by the mass distribution makes contribution to the noise of the atomic interferometer signal and consequently derive analytic expressions for this correlation function.

[1] A. A. Geraci, A. Derevianko, Phys. Rev. Lett. 117, 261301 (2016)

[2] S. Dimopoulos,P. W.Graham, J. M.HoganMark, A. Kasevich, S, Rajendran, Physics Letters B, Volume 678, Issue 1, 2009, Pages 37-40, ISSN 0370-2693

[3] B. Lamine, M. Jaekel, S. Reynaud, Eur.Phys.J. D20 (2002) 165-176.

Directional detection of dark matter using spectroscopy of crystal defects

R. Walsworth[1,2], **M. Lukin**[2], **D. Phillips**[1], **S. Rajendran**[3], **and A. Sushkov**[4]

[1] *Harvard-Smithsonian Center for Astrophysics, Cambridge, MA 02138 USA*

[2] *Department of Physics, Harvard University, Cambridge, MA 02138 USA*

[3] *Department of Physics, Univ. of California-Berkeley, Berkeley, CA 94720 USA*

[4] *Department of Physics, Boston University, Boston, MA 02215 USA*

e-mail: *rwalsworth@cfa.harvard.edu*

We propose a method to identify the direction of weakly interacting massive particle (WIMP) dark matter via induced nuclear recoil. The method is based on spectroscopic interrogation of quantum defects in macroscopic solid-state crystals, such as NV centers in diamond. When a WIMP scatters in a crystal, the induced nuclear recoil creates a tell-tale damage track, localized to about 100 nm, with an orientation to the track that correlates well with the direction of the recoil and hence the incoming WIMP. This damage track induces strain in the crystal, shifting the energy levels of nearby quantum defects. These level shifts can be measured optically making it possible to detect the damage track and determine its orientation. To localize the damage track to a millimeter-scale region within a large volume solid-state detector (about a cubic meter), one can use conventional WIMP detection techniques such as the collection of ionization/scintillation. This method could allow for directional detection of WIMP-induced nuclear recoils at solid-state densities, enabling probes of WIMP parameter space below the floor set by coherent neutrino scattering.

Towards deployable atomic gravimeters for geophysics

Z. Pagel[1], **X. Wu**[1], **B. S. Malek**[1], **J. Dudley**[1], **P. Canoza**[1], **H. Müller**[1,2]
[1] *University of California at Berkeley, Berkeley, CA 94720, US*
[2] *Lawrence Berkeley National Laboratory, Berkeley, CA 94720, US*
e-mail: *zpagel@berkeley.edu*

Many types of gravimeters are used in geophysics for gravity surveying, mineral prospecting, seismology and natural disaster monitoring. Atomic gravimeters use mater-wave interferometry, and are more accurate and have better long-term stability than gravimeters based on springs, superconducting coils or falling cubes. Since current atomic gravimeters are too complicated to operate outside a well-controlled laboratory, we have implemented an atom interferometer using only one laser diode and a pyramidal mirror, allowing for the instrument to be simple, compact and transportable. The pyramidal mirror is used to create a magneto-optical trap (MOT), and this reduces the number of incident laser beams on the MOT region to a single retro-reflected beam. Operating as a gravimeter, we have achieved sensitivities of 6 $\mu m/s^2/\sqrt{(}Hz)$ [1]. To ensure better transportability and reliability, we are developing an upgraded pyramid-based atomic gravimeter. Our simple and transportable design will open up applications in geodesy and geology.

[1] X. Wu, F. Zi, J. Dudley, R. Bilotta, P. Canoza, and H. Muller, Optica 4(12),1545-1551 (2017).

Reflecting on an alternative (parity-time-symmetric) quantum theory, and its analog in optics

Ray-Kuang Lee[1,2]

[1] *Department of Physics, National Tsing Hua University, Hsinchu, Taiwan*

[2] *Physics Division, National Center for Theoretical Sciences, Hsinchu, Taiwan*

e-mail: *rklee@ee.nthu.edu.tw*

By no-signaling principle, we showed that parity-time ($\mathcal{PT}$)-symmetric quantum theory as an extension of quantum theory to non-Hermitian Hamiltonians is either a trivial extension or likely false as a fundamental theory [4]. In addition to the implementation $\mathcal{PT}$-symmetric optical systems by carefully and actively controlling the gain and loss, we show that a 2×2 $\mathcal{PT}$-symmetric Hamiltonian has a unitarily equivalent representation without complex optical potentials in the resulting optical coupler. Through the Naimark dilation in operator algebra, passive $\mathcal{PT}$-symmetric couplers can thus be implemented with a refractive index of real values and asymmetric coupling coe cients. Moreover, with a phase-space representation on the vicinity of an exceptional point, we show that a $\mathcal{PT}$-symmetric phase transition from an unbroken $\mathcal{PT}$-symmetry phase to a broken one is a second-order phase transition.

With spatial reflection and time reversal, $\mathcal{PT}$-symmetry has a special place in studies of non-Hermitian operators, as it exists the possibility with purely real or complex mixed spectra. It is known that there exist spontaneous $\mathcal{PT}$-symmetry-breaking points, where the eigen-states of the system are no longer the eigenstates of $\mathcal{PT}$-operator. Based on Wigner distribution function, we present a phase-space study of a non-Hermitian Hamiltonian with $\mathcal{PT}$-symmetry [2]. For an arbitrary complex potential, we derive a generalized continuity equation for the Wigner function flow and calculate the related circulation values. Studying the vicinity of an exceptional point, we show that a $\mathcal{PT}$-symmetric phase transition from an unbroken $\mathcal{PT}$-symmetry phase to a broken one is a second-order phase transition.

Our studies of Wigner function flow present the the correspondence between phase transition and $\mathcal{PT}$-symmetry breakdown. By calculating the flux through volume or surface integrals and quantitatively distinguishes cases of unbroken and broken $\mathcal{PT}$-symmetry. It provides a quantitative measure, which allows us to distinguish the cases of broken and unbroken $\mathcal{PT}$-symmetry. Moreover, we develope a continuity equation for Wigner function flow and calculate the corresponding circulation values, for generalized quantum harmonic oscillators with $\mathcal{PT}$-symmetry, or with parametric optical process.

Exploiting the correspondence between the Wigner distribution function and the frequency-resolved optical gating (FROG) measurement, we experimentally demonstrate the existence of chessboardlike interference patterns with a time-bandwidth product smaller than that of a transform-limited pulse in the phase-space representation of compass states. Using superpositions of four electric pulses as the realization of compass states, we have shown via direct measurements that displacements leading to orthogonal states can be smaller than limits set by uncertainty relations. In the experiment we observe an exactly chronocyclic correspondence to the sub-Planck structure in the interference pattern appearing for the superposition of two Schrodinger-cat-like states in a position-momentum phase space [3].

In addition to the implementation of parity-time($\mathcal{PT}$) symmetric optical systems by carefully and actively controlling the gain and loss, we show that a 2×2 $\mathcal{PT}$-symmetric Hamiltonian has a unitarily equivalent representation without complex optical potentials in the resulting optical coupler [1]. Through the Naimark dilation in operator algebra, passive $\mathcal{PT}$-symmetric couplers can thus be implemented with a refractive index of real values and asymmetric coupling coe cients. This opens up the possibility to implement general $\mathcal{PT}$-symmetric systems with state-of-the-art asymmetric slab waveguides, dissimilar optical fibers, or cavities with chiral mirrors.

[1] Yi-Chan Lee, Jibing Liu, You-Lin Chuang, Min-Hsiu Hsieh, and Ray-Kuang Lee, "Passive $\mathcal{PT}$-symmetric couplers without complex optical potentials," Phys. Rev. A **92**, 053815 (2015).

[2] Ludmila Praxmeyer, Popo Yang, and Ray-Kuang Lee, "Phase-space representation of a non-Hermitian system with PT-symmetry," Phys. Rev. A **93**, 042122 (2016).

[3] Ludmila Praxmeyer, Chih-Cheng Chen, Popo Yang, Shang-Da Yang, and Ray-Kuang Lee, "Direct measurement of time-frequency analogs of sub-Planck structures," Phys. Rev. A **93**, 053835 (2016).

[4] Yi-Chan Lee, Min-Hsiu Hsieh, Steven T. Flammia, and Ray-Kuang Lee, "Local $\mathcal{PT}$-Symmetry Violates the No-Signaling Principle," Phys. Rev. Lett. **112**, 130404 (2014).

Development of Multi-shell Magnetic Shields for Atomic Spin Gyroscope

Z. Kim, T. H. Kim, S. H. Yim, S. Lee, and K. M. Shim
Agency for Defense Development, Daejeon 34186, Republic of Korea
e-mail: *zkim@add.re.kr*

We have developed magnetic shields for atomic gyroscope and magnetometer [1], which require high magnetic shield to decouple from environmental fields and improve the stability. Studying the performance of the high permeable thin material for spherical shell and infinitely long cylindrical shell theoretically gives insight into designing shield layers for atomic gyroscope and magnetometer. Measured shield factors of a four-layers shield ranges from 10^5 to 10^7, which are possibly limited by the sensitivity of the commercial flux-gate magnetometer. Preliminary results of the atomic gyroscope will be also discussed.

Consider a spherical shell under uniform external magnetic field such as Fig. 1 of inner(outer) radius $a(b)$ with no current and permeability of $\mu = \mu_0\kappa_m$, where μ_0 is vacuum permeability and κ_m is relative permeability.

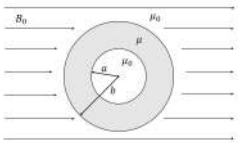


Figure 1: Schematic of spherical shell.

Defining the shield factor as the ratio of the external field to the field inside, comparison between the analytic [2] and the finite element method shows differences less than 0.2% (See Fig. 2).

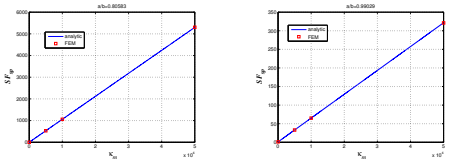


Figure 2: Simulated shield factors for the spherical shell as a function of κ_m from FEM (red squares) and analytic method (blue line) for $a/b = 0.81$ (left) and $a/b = 0.99$ (right).

For an infinitely long cylindrical shell under external B field along transverse direction and for finite cylindrical shell with end caps along the longitudinal direction, the analytic solution is given by [2] and [3], respectively.

Unlike the case of the spherical shell, the analytic method and the finite element method (FEM) produce quite different shield factors each other of about 2% for the transverse direction and 20% for the longitudinal direction, especially (Fig. 3), which implies the analytic solution along the longitudinal direction should be applied carefully.

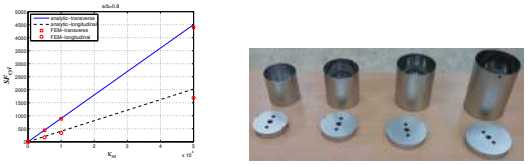


Figure 3: (left) Simulated shield factors for the cylindrical shell as a function of κ_m from FEM and analytic method, (right) picture of cylindrical multi-shell shields.

Figure 4 shows measured shield factors along transverse and longitudinal directions with external B field from 610 mG to 13 G. By multiplying shield factors of each shield layer, expected shield factors of 4 layer shields are more than 10^7 for the longitudinal direction and 10^9 for the transverse direction. Measured shield factors, however, with 4 layer shields range from 10^5 to 10^7 and from 10^6 to 10^7 for the longitudinal and transverse directions, respectively. In the poster, the preliminary data of the atomic gyroscope will be also presented.

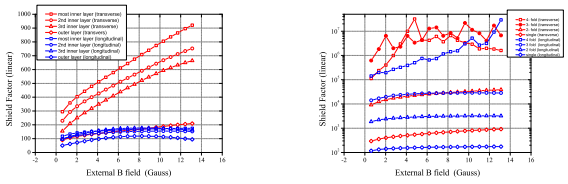


Figure 4: (left) Measured shield factors from each shield layer, (right) measured shield factor from multi shield layers.

[1] E. A. Donley, E. Hodby, L. Hollberg, J. Kitching, Review of Scientific Instruments **78**, 083102 (2007).

[2] J. D. Jackson, *Classical Electrodynamics*, 3rd edition.

[3] A. J. Mager, IEEE Trans. Magn. **6**, 67 (1970).

Investigating Particle Indistinguishability with a Freely Rotating Coulomb Crystal

E. Urban[1], **N. Glikin**[1], **B. Hemmerling**[1,2], **and H. Haeffner**[1]
[1] *University of California - Berkeley, Department of Physics, Berkeley, California, USA*
[2] *University of California - Riverside, Department of Physics, Riverside, California, USA*
e-mail: *urbaneg@berkeley.edu*

The symmetrization postulate of identical particles is a fundamental tenant of quantum mechanics, placing strict limits on the allowed states systems identical particles may occupy compared to their distinguishable counterparts. This is true for both fundamental and composite particles. The physical manifestation of these restrictions has been observed several physical systems such as large ensembles of homonuclear diatomic molecules.

Here we describe an experiment that would extend these results to a model system with a pair of well-separated, identical particles, $^{40}Ca^{+}$ ions, through direct exchange of the particles. Using a surface Paul trap with cylindrical symmetry, we engineer the Hamiltonian of a trapped diatomic homonuclear molecule confined to a plane. We show that we are able to spatially split the wave function of a two ion crystal in a 2D rigid rotor potential. This splitting allows the two particles to be exchanged while remaining spatially anti-correlated from each other at all times. Using this capability, we hope to study the emergence of indistinguishably under controlled conditions even for particles which are always separated by many micrometers.

Experimental probe of the tunneling time for ultra-cold atoms

R. Ramos[1], **D. Spierings**[1], **I. Racicot**[1], **and A.M. Steinberg**[1,2]

[1] *Centre for Quantum Information and Quantum Control and Institute for Optical Sciences, Department of Physics, University of Toronto, 60 St. George Street, Toronto, Ontario M5S 1A7, Canada*

[2] *Canadian Institute For Advanced Research, MaRS Centre, West Tower 661 University Ave., Toronto, Ontario M5G 1M1, Canada*

e-mail: *jramonra@physics.utoronto.ca*

We present an experiment studying the time it takes unbound Rubidium atoms to tunnel through an isolated potential barrier. We cool ^{87}Rb atoms to 900 $\pm$ 200 pK, leading to a significant probability for single-pass tunneling through a 1.3 μm barrier. We employ a Larmor clock measurement to determine time: we use a pair of magnetic-field-insensitive states of the ground-state manifold as a pseudo-spin 1/2, and a pair of Raman beams to connect these states. The barrier itself serves as the Raman beams; therefore, the pseudo-spin rotates only while the atoms are under the barrier. The rotation angle thus constitutes a measurement of the time atoms spend in the forbidden region before being transmitted.

Additionally, the light for the optical barrier is close to one of the rubidium tuned-out wavelengths at 421.09 nm, which gives us the flexibility of changing the barrier height without modifying the strength of the Raman coupling. We expect this measurement can be extended to investigate measurement back-action [1, 2] and how atomic interactions affect this process.

[1] A. M. Steinberg, Phys. Rev. Lett. **74**, 2405 (1995)

[2] A. M. Steinberg, Phys. Rev. A **52**, 32 (1995)

Precision Search for CP Violation with Polyatomic Molecules

N. R. Hutzler[1], **A. Jadbabaie**[1], **A. Periwal**[1], **and N. Pilgram**[1,2]
[1] *Division of Physics, Mathematics, and Astronomy.*
California Institute of Technology, Pasadena, CA, USA.
[2] *Division of Engineering and Applied Science.*
California Institute of Technology, Pasadena, CA, USA.
e-mail: *hutzler@caltech.edu*

Polar molecules are extremely sensitive platforms to search for physics Beyond the Standard Model, especially CP-violating electromagnetic moments that are amplified by large internal molecular fields. Molecule-based searches for the electron EDM are already probing the TeV scale, and their strong robustness against systematic errors via internal co-magnetometer states means that they can reach even higher energy scales in multiple sectors. Many molecular precision measurements are limited largely by interaction time, and could be enhanced by many orders of magnitude if suitable molecules could be cooled and trapped like their atomic counterparts. Laser-cooling of molecules is advancing rapidly, but current techniques only work for molecules with particular electronic structures that conflict with the requirements for internal co-magnetometers in diatomic molecules. However, polyatomic molecules have mechanical modes that can be used to realize internal co-magnetometer states, while still offering the electronic structure required for laser-cooling and maintaining sensitivity to new physics [1]. Polyatomic molecules such as YbOH and YbOCH3 are therefore candidates for long coherence time precision measurements of CP-violation at the PeV scale with laser-cooling, trapping, and internal co-magnetometers. We will discuss the interesting physics of laser cooling and polyatomic molecules that makes this possible, and present an update on experimental progress.

This work is supported by the Heising-Simons Foundation.

[1] I. Kozyryev and N. R. Hutzler, Phys. Rev. Lett. **119**, 133002 (2017).

Realization of a 12 m atom fountain and suppression of wave-front-aberration phase noise in atom interferometers

C. He[1,2], W. T. Duan[1,2], J. G. Hu[1,2], B. Tang[1,3], L. Zhou[1,3], X. Chen[1,3], J. Wang[1,3*] and M. S. Zhan[1,3†]

[1] *State Key Laboratory of Magnetic Resonance and Atomic and Molecular Physics, Wuhan Institute of Physics and Mathematics, Chinese Academy of Sciences - Wuhan National Laboratory for Optoelectronics, Wuhan 430071, China*

[2] *School of Physics, University of Chinese Academy of Sciences, Beijing 100049, China*

[3] *Center for Cold Atom Physics, Chinese Academy of Sciences, Wuhan 430071, China*

e-mail: ∗ *wangjin@wipm.ac.cn*, † *mszhan@wipm.ac.cn*

Atom fountains are important tools both for the frequency standard and the interferometry. Fountain type atom interferometers (AIs) have been used in precision measurements. One of the main parameters that limits the accuracy of AIs is the integration time between the Raman pulses (that is free fall time of atoms). In order to achieve longer free fall time, it is necessary to develop a large atom fountain which can provide enough space for atoms to undergo a free fall. Dimopoulos *et al.* proposed a plan for WEP test experiment based on long-baseline AIs [1]. There are many scientific and technical challenges in the construction of long-baseline fountain-type AIs. In 2011, we designed and completed a long-baseline AI for WEP test, and experimentally realized atom fountains with launch height of 6 m [2]. In 2013, Dickerson *et al.* demonstrated the realization of atom fountain with launch height approaching 10 m [3]. Hartwig *et al.* proposed a new plan for WEP test experiment based on long-baseline AIs [4]. In 2015, we demonstrated a 10^{-8} level test of WEP using ^{85}Rb-^{87}Rb dual-AIs under the free fall time of $2T = 141.92$ ms [5]. Recently, we demonstrate the experimental realization of a large atom fountain, the fountain height exceeds 12 m, the free fall time of atoms for the Mach-Zehnder type atom interferometer in the 10-meter uniform magnetic field area is 2.8 s. The temperature and the atom number of fountains with different height are measured.

However, there are still key problems in long-baseline AIs, one of the most prominent of these problems is the wave-front aberration of Raman beams [6]. When Raman beams interact with atoms, the wave-front aberration is printed on the atomic wave function, and thus induces the phase shift in AIs. To further solve this problem, we theoretically analyze the wave-front aberration phase noise (WAPN) in WEP tests using dual-species atom interferometers, and propose an expansion-rate-selection method to suppress the WAPN in both isotopic and non-isotopic atom interferometers. The suppression ratio is about 10 at the expense of half number of atoms. The simulation based on appropriate experimental parameters shows that, the standard deviations to the Eötvös coefficient caused by wave-front aberration in WEP tests using ^{85}Rb-^{87}Rb and ^{41}K-^{87}Rb are 1.3×10^{-14} and 3.0×10^{-13} [7], respectively. Better results can be obtained by improving the wave-front quality and utilizing atom cloud with lower temperature.

References

[1] S. Dimopoulos, P. W. Graham, J. M. Hogan, M. A. Kasevich, Phys. Rev. Lett. **98**, 111102 (2007)

[2] L. Zhou, Z. Y. Xiong, W. Yang, B. Tang, W. C. Peng, K. Hao, R. B. Li, M. Liu, J. Wang, M. S. Zhan, Gen. Relativ. Gravit. **43**, 1931(2011)

[3] S. M. Dickerson, J. M. Hogan, A. Sugarbaker, D. M. S. Johnson, M. A. Kasevich, Phys. Rev. Lett. **111**, 083001(2013)

[4] J. Hartwig, S. Abend, C. Schubert, D. Schlippert, H. Ahlers, K. Posso-Trujillo, N. Gaaloul, W. Ertmer, E. M. Rasel, New J. Phys. **17**, 035011(2015)

[5] L. Zhou, S. T. Long, B. Tang, X. Chen, F. Gao, W. C. Peng, W. T. Duan, J. Q. Zhong, Z. Y. Xiong, J. Wang, Y. Z. Zhang, M. S. Zhan, Phys. Rev. Lett. **115**, 013004(2015)

[6] D. N. Aguilera, H. Ahlers, B. Battelier *et al.*, Class. Quantum Grav. **31**, 115010 (2014).

[7] J. G. Hu, X. Chen, J. Fang, L. Zhou, J. Q. Zhong, J. Wang and M. S. Zhan, Phys. Rev. A **96**, 023618 (2017).

Generation of Atomic Beams of Highly Refractory Elements for Laser Spectroscopy

A. Castro, J. H. Bartlett, and V. Lebedev
Los Alamos National Laboratory, Los Alamos, New Mexico, USA
e-mail: *acx@lanl.gov*

We present a novel compact design for a multi-channel micro-crucible which generates collimated atomic beams of highly refractory elements for laser spectroscopy (Fig. 1). We use 50-μm tantalum foil folded in an origami-like fashion to form the appropriate crucible shape, which can be easily attached to vacuum compatible electrical feedthrough connectors. Our crucible exhibits a high thermal e - ciency due to minimization of its surface area, and is capable of achieving temperatures up to 2500 °C when resistively-heated by 200 W of applied electrical power. As a result, the design does not require any active cooling and is compact enough to allow for its incorporation into a variety of instruments and vacuum systems.

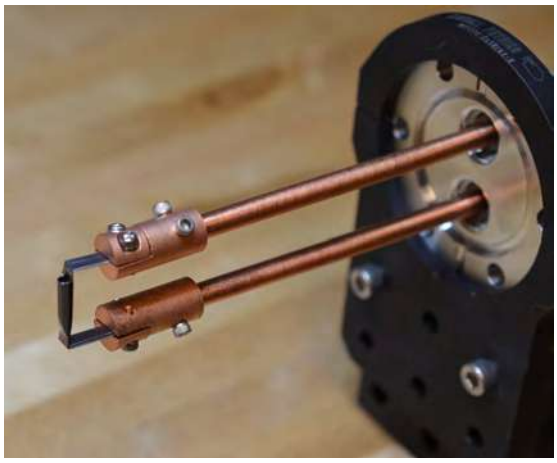


Figure 1: Tantalum foil micro-crucible mounted on copper feedthroughs.

Using this micro-crucible, we demonstrate laser spectroscopy of the 400.91 nm transition of erbium ($4f^{12}6s^2\,{}^3H_6 \rightarrow 4f^{12}({}^3H_6)6s6p({}^1p_1^o)(6,1)_7^o, 0 \rightarrow 24943.272\ cm^{-1}$)[1] at 1300 °C, and also the 861.031 nm transition of uranium ($f^3ds^2\,{}^5L_6 \rightarrow f^2d^2s^2\,{}^5K_5, 0 \rightarrow 11613.977\ cm^{-1}$)[2] at 2200 °C with improved isotopic resolution with respect to single-channel designs (Fig. 2). We expect that this new oven design will find applications in experimental areas that require the e cient generation of atomic beams, such as cold atoms, and atomic clocks.

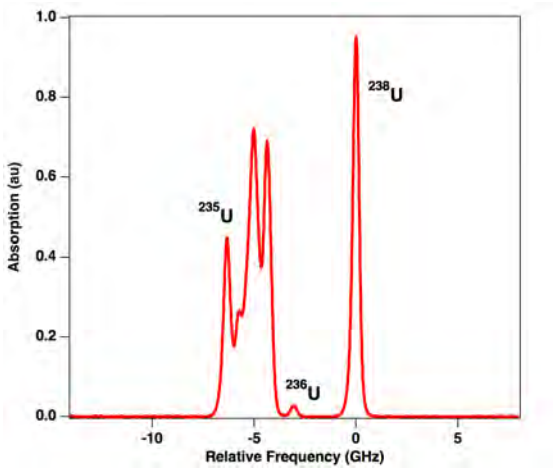


Figure 2: Uranium spectrum at 861.031 nm.

[1] N. Spector, J. Opt. Soc. Am. 57, 308 (1967).

[2] J. Blaise and L. J. Radziemski, Jr., J. Opt. Soc. Am. 66, 644 (1976).

High Sensitivity Ring Laser Gyroscopes for Geodesy and Fundamental Physics

N. Beverini[1,2], **G. Carelli**[1,2], **A. Di Virgiio**[1], **U. Giacomelli**[1,2], **E. Maccioni**[1,2], **and F. Stefani**[1,2]
[1] *INFN, Sezione di Pisa, 56127 Pisa, Italy*
[2] *Dipartimento di Fisica, Università di Pisa, 56127 Pisa, Italy*
e-mail: *nicolo.beverini@unipi.it*

Ring Lasers Gyroscopes (RLG), based on the Sagnac effect, are very reliable instruments with extended bandwidth and very high duty cycle. The most advanced RLG devices with an area of tens of square meters are used in rotational seismology and they are considered in the geodetic community suitable for measuring the fast variations (daily and subdaily) of the Earth rotation rate [1]. The purpose of GINGER (Gyroscopes IN GEneral Relativity) is to measure the General Relativity (GR) components of the Earth gravito-magnetic field at 1% [2]. Following GR, the gravito-magnetic and gravito-electric fields act on the RLG cavity as non-reciprocal effects [3] and the RLG rotational signal contains additional terms of the order of 10^{-13} rad/s, very close to the present best sensitivity in one day of integration time. In this scheme the GR terms would be evaluated by comparison with the kinetic Earth rotation rate, independently measured with high accuracy by IERS (International Earth Rotation Service). This will provide the first measurement of a GR dynamic effect of the gravitational field on the Earth surface. It would be a direct local measurement, independent of the global distribution of the gravitational field, and not an average value as in the case of space experiments.

The whole information on angular vector requires a 3-dimensional array of gyroscopes. A ring with the axis oriented parallel to Earth rotation axis is especially suited to measure the fluctuation of the rotational speed, while rings lying in horizontal or in vertical plane would give information on the fluctuations of axis direction (polar motion) [4].

A pilot-prototype for GINGER is the single axis apparatus called GINGERino that has been installed deep underground (Fig.1), inside the Gran Sasso Laboratories, far from surface perturbations [5]. This installation is working unattended with a duty cycle larger than 90% since one year. It tested the local seismic noise, providing at the same time unique information for geophysics [6]. The measured power spectrum of the rotational signal is shown in Fig. 2. An analysis of the data taken over 90 days of continuous operation is presented in [7].

Optimising the quality of the optical cavity mirrors and increasing ring dimension up to 6-7 m can greatly reduce quantum noise limit, while the active control of the geometry, presently under investigation on GP-2 (a smaller RLG located in INFN laboratory in Pisa), will improve the long-term stability. Eventually, we can estimate that GINGER will achieve a sensitivity at the level of GR terms in a few days of measurement.



Figure 1: GINGERINO apparatus.

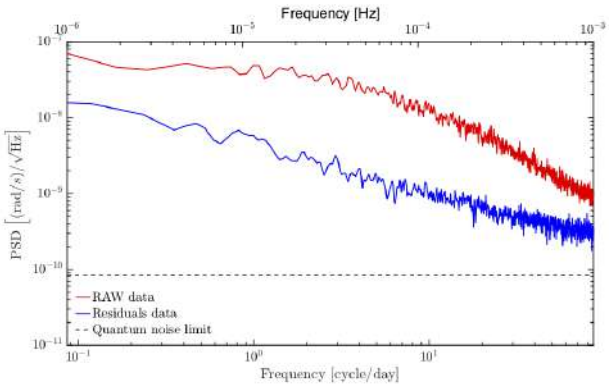


Figure 2: Power spectral density of GINGERINO from raw data (*in red*) and after reduction for laser dynamics (*in blue*).

[1] T. Nilsson et al., J. Geodynamics **62**, 69 (2012)

[2] F. Bosi et al., Phys. Rev. D **84**, 122002 (2011)

[3] A.Tartaglia, et al., Eur. Phys. J. Plus **132**, 73 (2017)

[4] A. Di Virgilio, et al., Eur. Phys. J. Plus **132**, 157 (2017)

[5] J.Belfi, et al, Rev.Sci.Instrum. **88**,034502 (2017)

[6] A. Simonelli, et al., Geophys. J. Intern. *ggy*186 (2018)

[7] J. Belfi, et al., https://arxiv.org/abs/1804.02569

Towards high-precision spectroscopy of the 1S–2S transition in He^+

F. Schmid[1], **A. Ozawa**[1], **J. Weitenberg**[1,2], **T. W. Hänsch**[1,3], **and Th. Udem**[1,3]
[1] *Max Planck Institute of Quantum Optics, Garching, Germany*
[2] *Fraunhofer Institute for Laser Technology ILT, Aachen, Germany*
[3] *Ludwig Maximilian University, Munich, Germany*
e-mail: *fabian.schmid@mpq.mpg.de*

The simplicity of hydrogen and hydrogen-like systems allows for extremely accurate predictions of their energy levels using bound-state quantum electrodynamics (QED). These theory values contain fundamental constants, most importantly the Rydberg constant and the nuclear size. By comparing theory and experiment, these constants can be determined and the validity of the theory itself can be tested.

The frequency of the extremely narrow 1S–2S two-photon transition was measured in atomic hydrogen with a relative uncertainty below 10^{-14} [1, 2]. This value can be combined with measurements of other transitions in order to extract values for the Rydberg constant and the proton size [3].

We are currently setting up an experiment to do spectroscopy of the 1S–2S transition in the simplest hydrogen-like ion, He^+. This could give new insights into a so-far unresolved discrepancy between different determinations of the proton charge radius which is known as the *proton radius puzzle* [4]. Furthermore, interesting higher-order QED corrections scale with large exponents of the nuclear charge which makes this measurement much more sensitive to these corrections compared to the hydrogen case [5]. Finally, He^+ ions are charged particles that can be trapped and cooled in an ion trap. This greatly reduces systematic effects due to particle motion that dominate the uncertainty in the hydrogen measurements.

However, driving the 1S–2S transition in He^+ requires narrow-band radiation at 61 nm. This lies in the extreme ultraviolet (XUV) range where no refractive optics and no laser sources exist. We will therefore perform direct frequency comb spectroscopy by converting an infrared high power frequency comb to the XUV using high harmonic generation in a gas target. The He^+ ions will be trapped in a Paul trap and sympathetically cooled by co-trapped Be^+ ions.

[1] C. G. Parthey *et al.*, Phys. Rev. Lett. **107**, 203001 (2011).

[2] A. Matveev *et al.*, Phys. Rev. Lett. **110**, 230801 (2013).

[3] A. Beyer *et al.*, Science **358**, 79 (2017).

[4] A. Antognini *et al.*, Science **339**, 417 (2013).

[5] M. Herrmann *et al.*, Phys. Rev. A **79**, 052505 (2009).

Tune-out wavelength for the $1s2s\ ^3S$ state of helium

Gordon W.F. Drake and Jacob Manalo
Department of Physics, University of Windsor, Windsor Ontario N9B 3P4 Canada
e-mail: *gdrake@uwindsor.ca*

The tune-out wavelength is the wavelength at which the frequency dependent polarizability of an atom vanishes. For the helium $1s2s\ ^3S$ state this occurs around 413 nm. It can be measured to very high precision by means of an interferometric comparison between two beams. This paper is part of a joint theoretical/ experimental project with K. Baldwin et al. (Australian National University) [1] and L.-Y. Tang et al. (Wuhan Institute of Physics and Mathematics) [2] to perform a high precision comparison between theory and experiment as a probe of atomic structure, including relativistic and quantum electrodynamic effects. We will report the results of calculations for the tune-out wavelength that is closest to the $1s2s\ ^3S - 1s3p\ ^3P$ transition of ^{4}He at 413 nm. Our result for the $M = 0$ and $M = \pm 1$ magnetic substates, obtained with a fully correlated Hylleraas basis set, are 413.084 23(1) nm and 413.09010(1) nm respectively as shown in Table 1, where the figures in brackets indicate the uncertainty. This includes a leading relativistic contribution of $-0.059\,218\,5(16)$ nm from the Breit interaction as a perturbation (for $M = 0$), and a relativistic recoil contribution of $-0.000\,044\,47(17)$ nm. A leading QED correction of 0.004 150 93 nm is also included, together with estimates of higher-order terms from Ref. [2]. Accurate calculations of the higher-order and finite wavelength corrections are in progress. However at present, theory and experiment differ by nearly two standard deviations (see Table 1).

Comparisons will also be made with previous high-precision calculations for the helium ground state [3,4].

Table 1: Nonrelativistic, relativistic, and QED contributions to the tune-out wavelength for the ^{4}He $1s2s\ ^3S_m$ state, including relativistic recoil of $O(\alpha^2\mu/M)$. Here $m = 0$ or $m = \pm 1$ in parentheses the first column is the magnetic quantum number.

Terms included	λ_t (nm)	Zhang [2]
Nonrelativistic	413.038 304 39(4)	413.038 28(3)
NR + Rel. (0)	413.079 958(2)	413.080 00(1)
NR + Rel. (± 1)	413.085 828(2)	413.085 89(1)
α^3 QED	0.004 1531	0.004 145 56
α^4 QED	0.000 072 08 [a]	0.000 072 08
$\alpha^3\ \delta\ln(k_0)$	0.000 04(1) [a]	0.000 04(1)
Nuclear size	0.000 002 75 [a]	0.000 002 75
Total (0)	413.084 23(1)	413.084 26(4)
Total (± 1)	413.090 10(1)	413.090 15(4)
Expt. (± 1) [b]	413.093 8(9_{stat})(20_{sys})	
Difference	0.0037(9_{stat})(20_{sys})	

[a] From Zhang et al. [2] and private communication.
[b] From Ref. [1].

[1] B. M. Henson, R. I. Khakimov, R. G. Dall, K. G. H. Baldwin, L.-Y. Tang, and A. G. Truscott, Phys. Rev. Lett. **115**, 043004 (2015).

[2] Y.-H. Zhang, L.-Y. Tang, X.-Z. Zhang, and T.-Y. Shi, Phys. Rev. A **93**, 052516 (2016).

[3] J. Sapirstein and K. Pachucki, Phys. Rev. A **63**, 012504, (2000).

[4] M. Puchalski, K. Piszczatowski, J. Komasa, B. Jeziorski, and K. Szalewicz, Phys. Rev. A **93**, 032515 (2016).

Contribution to resolution of the proton radius puzzle via measurement of the $n = 2$ Lamb shift in atomic hydrogen.

N. Bezginov[1], **T. Valdez**[1], **A. C. Vutha**[2], **K. Kato**[1], **T. D. G. Skinner**[1], **and E. A. Hessels**[1]
[1] *Department of Physics and Astronomy, York University, 4700 Keele St, M3J 1P3, Toronto, ON, Canada*
[2] *Department of Physics, University of Toronto, M5S 1A7, Toronto, ON Canada*
e-mail: *nibezg@yorku.ca*

Since 2010 measurements of the $n = 2$ Lamb shift in muonic hydrogen [1, 2] have resulted in an extracted proton rms charge radius that is different from the accepted CODATA value [3] by six standard deviations. This discrepancy is known as the proton radius puzzle [4, 5, 6], and remains unsolved.

To contribute to the resolution of the puzzle, we perform a measurement of the $n = 2$ Lamb shift in atomic hydrogen ($2S_{1/2}$ $F = 0$ to $2P_{1/2}$ $F = 1$), which was last measured by Lundeen and Pipkin [7] in 1981. The reduced mass of the proton-electron system is 186 times smaller compared to that of muonic hydrogen, leading to much weaker influence of the finite proton radius on the wavefunction of the $2S$ state.

Our experiment begins with a beam of protons moving at approximately $0.01c$ that undergoes charge exchange with hydrogen gas to produce a fast beam of atomic hydrogen, with some fraction of the hydrogen atoms being in the metastable $2S$ state. A section of electric field is used to deflect the protons and to quench higher-n states by mixing them with the short-lived nP states. Microwave cavities quench the $2S_{1/2}$ $F = 1$ atoms by driving them to $2P_{1/2}$ states. The atoms travel through two coherently driven microwave regions, where we utilize the novel technique of frequency offset separated oscillatory fields (FOSOF) [8]. The surviving $2S$ population passes through a large DC electric field, where a superposition of $2S$ and $2P$ states is formed and quickly decays to ground state. The emitted photons are observed using a large-solid-angle Lyman-alpha detector.

We present the latest experimental results from this experiment, along with an analysis of our systematic studies.

[1] R. Pohl, et al., Nature **466**, 13 (2010).

[2] A. Antognini, et al., Science **339**, 417 (2013).

[3] P. J. Mohr, D. B. Newell, and B. N. Taylor, J. Phys. Chem. Ref. Data **45**, 043102 (2016).

[4] J. C. Bernauer, and R. Pohl, Scientific American **310**, 32 (2014).

[5] R. Pohl, R. Gilman, G. A. Miller, and K. Pachucki, Ann. Rev. of Nucl. and Part. Science **63**, 175 (2013).

[6] C. E. Carlson, Progress in Part. and Nucl. Phys. **82**, 59 (2015).

[7] S. R. Lundeen and F. M. Pipkin, Phys. Rev. Lett. **46**, 232 (1981).

[8] A. C. Vutha, and E. A. Hessels, Phys. Rev. A **92** 052504 (2015).

Repulsive self-generated lattice from a BEC in an optical resonator

D. Dreon[1], **P. Zupancic**[1], **A. Morales**[1], **X. Li**[1], **A. Baumgärtner**[1], **T. Esslinger**[1] **and T. Donner**[1]

[1] *Institute for Quantum Electronics, ETH Zurich, Zurich, Switzerland*
e-mail: *dreond@phys.ethz.ch*

The interaction of a Bose-Einstein condensate (BEC) with the electromagnetic field of an optical cavity is known to exhibit a superradiant phase transition to a self-organized phase. In our experiment, a ^{87}Rb BEC is placed at the mode crossing of two optical cavities. The BEC is illuminated with a pump laser beam whose detuning from the D_2 atomic line determines the interaction regime.

We recently explored different red atomic detunings, where the system reduces its potential energy spontaneously forming an attractive lattice in the cavity mode. There, we have observed a supersolid phase [1, 2] and a phase with coupled order parameters [3]. In contrast, in the blue-detuned case the energy of the atoms is increased by the presence of an optical lattice, which intuitively could suppress self-organisation.

I will report on our most recent experimental results on the blue side of the atomic resonance, where we observe that self-organization is still possible. In addition, the repulsive lattice induces non-trivial modifications to the system's band structure, which affect the extent of the self-organised phase. We measure the phase diagram of the system and explain our findings with simple energy arguments.

[1] J. Léonard, A. Morales, P. Zupancic, T. Esslinger, and T. Donner, Supersolid formation in a quantum gas breaking a continuous translational symmetry. Nature **553**, (2017)

[2] J. Léonard, A. Morales, P. Zupancic, T. Donner, and T. Esslinger, Monitoring and manipulating Higgs and Goldstone modes in a supersolid quantum gas. Science, **358**(6369), 1415-1418 (2017)

[3] A. Morales, P. Zupancic, J. Léonard, T. Esslinger, and T. Donner, Coupling two order parameters in a quantum gas. preprint arXiv:1711.07988 (2017).

Vortex Lattice Formation in a Stirred Bose-Einstein Condensate

E. M. Gutierrez[1], **P. E. S. Tavares**[1], **H. V. Duque**[1], **P. L. Mazo**[1], **G. A. Neto**[1], **J. A. Scarpin**[1], **K. M. Farias**[1] **and V. S. Bagnato**[1]

[1] *São Carlos Institute of Physics, University of São Paulo, PO Box 369, 13560-970, São Carlos, SP, Brazil*
e-mail: *emmidv91@gmail.com*

Bose-Einstein condensate (BEC) are still a powerful system to study important properties of matter. One of these properties is superfluidity, a fluid with zero viscosity. If we add angular momentum to this kind of system it is possible to create quantum vortices and study the evolution of the vortex lattice until reach a turbulent system. In this work we show the vortex nucleation process in a BEC of sodium using a stirring beam to add angular momentum to the system. We produce a BEC of sodium with around 1.5×10^6 atoms at 100 nK in a crossed optical dipole trap (ODT)with frequencies $\omega_r = 80$ Hz and $\omega_z = \sqrt{2}\omega_r$. The atoms are stirred with a red detuned beam (532 nm) while they are in the ODT during 200 ms and then release in TOF for 40 ms. The vortex appears as hole of density in the cloud in which the vortex number depends on stirring frequency (Figure 1).

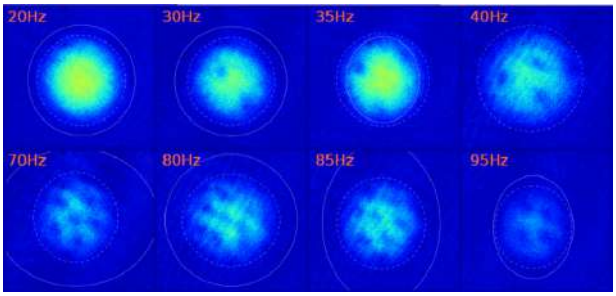


Figure 1: vortex lattice in a crossed dipole trap for different frequencies

As we can see in the figure the number of vortices increases as we increase the Stirring frequency, however, when the frequency comes into resonance with the frequency of the trap the number of atoms decreases as a result of exciting modes in the atomic cloud.

A versatile apparatus for quantum simulation with ultracold dipolar Erbium atoms

Bojeong Seo[1], **Bowen Sun**[1], **Ziting Chen**[1], **Jinho Kim**[1], **Gyu-boong Jo**[1]
[1] *Department of Physics, The Hong Kong University of Science and Technology, Hong Kong*
e-mail: *gbjo@ust.hk / bseo@connect.ust.hk*

Lanthanide atoms such as dysprosium and erbium isotopes with a large angular momentum provide various cold-atom toolkits such as the Feshbach resonance, the strong magnetic dipole moment, a narrow-line optical transition and a meta-stable excited state [1]. In this poster, we present our new versatile apparatus for quantum simulation with ultracold dipolar Erbium atoms. We build a bi-chromatic magneto-optical trap scheme to enhance the repetition rate of ultracold dipolar gas [2]. Furthermore, our bitter-type electromagnet design helps us to generate the magnetic field of 500G to tune the Feshbach resonace. In our experiment, we use our home-made 401nm ECDL for broad singlet transition and home-made high temperature effusion cell to generate atomic beam. A high-resolution optical imaging system would lead us to experimentally simulate many-body physics in optical lattices including extended Bose(Fermi)-Hubbard model. In addition, we plan to investigate interacting topological states in spin-orbit-coupled optical lattices utilizing a narrow optical transition and the Feshbach resonance available in erbium fermions. Moreover, tuning a s-wave scattering length by Feshbach resonance shows us the quantum droplet phenomena.

[1] A. Frisch, Dipolar Quantum Gas of Erbium(PhD thesis). University of Innsbruck, Austria

[2] J. Lee et al., Phys. Rev. A, 91 053405 (2015).

Funding support : Croucher Innovation Awards from the Croucher Foundation

Few-Mode Treatment of Interacting Bose Gases with Spin-Orbit Coupling

J. Cabedo*, **J. Mompart, and V. Ahufinger**
Departament de Física, Universitat Autònoma de Barcelona, 08193 Bellaterra, Spain
*e-mail: *josep.cabedo@uab.cat*

Spin-orbit coupling (SOC) links a particle's spin to its motion and has a crucial role in the electronic properties of many condensed-matter systems, being at the basis of phenomena such as the spin-Hall effect and topological insulators. The high level of control of ultracold atoms makes them ideal candidates to engineer SOC in neutral systems [1]. In particular, by dressing two atomic spin states of a Bose-Einstein condensate (BEC) with a pair of lasers in a Raman configuration, spin-1/2 SOC can be realized, with equal Rashba and Dresselhaus contributions. Its phase diagram is characterized by the existence of three phases: the stripe, the plane-wave and the single-minimum phase, which merge in a characteristic tricritical point [2–4]. Furthermore, larger spin SOC can be realized by dressing three or more internal atomic states with simultaneous Raman transitions, which at weak coupling lead to a many-wells-shaped lowest band of the single-atom dispersion relation [5,6].

However, the study of these many-body systems beyond mean-field approaches is widely unexplored. Here we investigate the properties of interacting Bose gases with arbitrary spin SOC following a few-mode approximation [7], where only low energy contact interactions are considered. We derive the Hamiltonian for the weakly interacting and weakly-trapped gas, which is numerically and analytically studied.

Due to the coupling between internal and external degrees of freedom in the system, each s-wave collision is weighted by the overlaps of the spin-states of initial and final states coupled by the interaction. In the low-energy limit, such overlaps decrease with the distance in momentum space. The many-wells structure of the lowest band together with such selection rules for the interaction processes leads to a certain degree of localization of the interactions in quasimomentum space.

Notably, an effective two-particle tunneling between the well-states of the lowest band becomes relevant at this regime for spins larger than 1/2, which supposes a marked deviation from the position space many-wells analogy. This term is responsible for the appearance of avoided crossings in the lowest eigenenergies spectrum when evaluated as a function of the interaction strength. The energy gap at the avoided crossings can be closed by conveniently manipulating the external electromagnetic fields, yielding a ground state presenting a step-like behaviour in several observables as the relative strength of the interactions is modified (Figure 1).

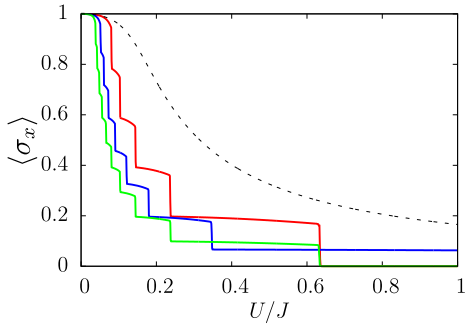


Figure 1: Mean transverse spin polarization of the ground state of the SOC spin-1 gas, $\langle\sigma_x\rangle = \frac{1}{\sqrt{2}}\left\langle(\hat{b}^\dagger_\uparrow + \hat{b}^\dagger_\downarrow)\hat{b}_\leftrightarrow + h.c.\right\rangle$, as a function of the relative strength of the interactions, at very weak-trapping regime, for $N = 10$ (red line), $N = 15$ (blue line) and $N = 20$ (green line) particles. For comparison, the dashed line shows the behavior of the analogous position space triple well potential problem. Here, the energy of the central well is positively shifted to close the energy gap at the discontinuities.

References

[1] Y. Zhang, M. E. Mossman, Th. Busch, P. Engels and C. Zhang, *Frontiers of Physics* **11**, 118103 (2016).

[2] Yun Li, G. I. Martone and S. Stringari, *Annual Review of Cold Atoms and Molecules*, Vol.**3** (World Scientific, 2015), Chap. 5, pp. 201-250.

[3] Y.-J. Lin,K. Jiménez-García and I. B. Spielman, *Nature* **471**, 83 (2011).

[4] Jun-Ru Li *et al.*, *Nature* **543**, 91 (2017).

[5] Z. Lan and P. Öhberg, *Phys. Rev. A* **89**, 023630 (2014).

[6] G. I. Martone, F.V. Pepe, P. Facchi, S, Pascazio and S. Stringari, *Phys. Rev. Lett* **177**, 125301 (2016).

[7] J. Higbie and D. M. Stamper-Kurn, *Phys. Rev. A* **69**, 053605 (2004).

Progress toward single atom microscopy for ultracold Yb atoms in optical lattice

Jongchul Mun[1], **Jae Hoon Lee**[1], **Won-Kyu Lee**[1], **and Dai-Hyuk Yu**[1]
[1]*Korea Research Institute of Standards and Science, Daejeon, Korea*
e-mail: *jcmun@kriss.re.kr*

We report our progress toward single lattice site resolution microscopy for ultracold Yb atoms.

First, we present our experimental apparatus for production of quantum gas using Yb isotopes. Our experimental apparatus consists of Zeeman slower, main MOT chamber, and auxiliary science chamber. We employed core-shell magneto-optical trap scheme[1], where the broad transition ($^1S_0 \longleftrightarrow {}^1P_1, \lambda \sim 399$ nm), and narrow intercombination transition ($^1S_0 \longleftrightarrow {}^3P_1, \lambda \sim 556$ nm) are spatially arranged into a core-shell configuration. This scheme significantly enhances the loading rate(∼100-fold) and captured atom number(∼10-fold) leading to faster experimental cycle for quantum gas realization.

Quantum degenerate gas of Yb atoms is produced in the main chamber by typical evaporative cooling scheme using optical dipole trap of 532 nm laser light. After the realization of quantum gas, it is transported to the auxiliary science chamber by moving the optical trap using our zoom lens system. We present our design for the optically compensated zoom lens system.

After moving to the science chamber, the quantum gas is loaded in optical lattice for single site imaging. The experimental designs of science chamber, optical lattice setup and single site microscope lens system are discussed in this presentation.

[1] Jeongwon Lee, Jae Hoon. Lee, Jiho Noh, and Jongchul Mun, Phys. Rev. A **91**, 053405 (2015).

Towards ultracold potassium-cesium mixture.

P. Arciszewski[1], **M. Bochenski**[1], **J. Dobosz**[1], **B. Szczerba**[1], **and M. Semczuk**[1]
[1] *Faculty of Physics, University of Warsaw, Pasteura 5, 02-093 Warsaw, Poland*
e-mail: *msemczuk@fuw.edu.pl*

We present progress towards creating a new experimental setup for laser cooling of cesium and potassium atoms. The apparatus will be used to explore ultracold, heteronuclear mixtures in species selective potentials and will enable production of ground state molecules of KCs.

The magneto-optical traps for both species are loaded from the background gas with the help of light induced atomic desorption. A novel laser system is designed for laser cooling of all stable isotopes of potassium (i.e. ^{39}K, ^{40}K and ^{41}K). The switching between isotopes is done without any moving parts, is computer controlled and can be reliably performed in less than 1 ms, limited only by the settling time of the tapered amplifiers used in the setup. Due to seeding of optical amplifiers with either D1- or D2-line light, two stage cooling can be implemented using D1-line gray molesses thanks to the built-in phase coherence between the cooling and repumping beams. Though not implemented here, the laser system can also provide light for a 2D-MOT.

A light sheet beam located 34 cm below the trapping region will enable single atom resolved detection of dilute clouds after long expansion times exceeding 250 ms.

The project is funded by the National Science Centre grant no. 2015/16/S/ST2/00425 and 2016/21/D/ST2/02003, and by the Fundation for Polish Science (Homing Programme).

Dynamics in the Dissipative Fermi-Hubbard Model

L. Freystatzky[1,3], **K. Sponselee**[1], **B. Abeln**[1], **M. Diem**[1], **B. Hundt**[1], **A. Kochanke**[1], **T. Ponath**[1], **B. Santra**[1], **K. Sengstock**[1,2,3], **C. Becker**[1,2] **and L. Mathey**[1,2,3]

[1] *Zentrum für Optische Quantentechnologien, Universität Hamburg, Luruper Chaussee 149, 22761 Hamburg, Germany*

[2] *Institut für Laserphysik, Universität Hamburg, Luruper Chaussee 149, 22761 Hamburg, Germany*

[3] *The Hamburg Centre for Ultrafast Imaging, Luruper Chaussee 149, 22761 Hamburg, Germany*

e-mail: *lfreysta@physnet.uni-hamburg.de*

Coherent evolution and formation of quantum ground-states is often hindered by dissipation, which is one of the biggest obstacles for research on realistic quantum systems in general and in particular for the realisation of new devices based on quantum technology. The relevance of dissipation in quantum systems is therefore of uppermost importance and under certain conditions it has been predicted that carefully engeneered dissipation can be employed for robust quantum state preparation and protection with high fidelity.

We study the decay dynamics of ^{173}Yb atoms in a one dimensional lattice, which realizes a dissipative Fermi-Hubbard model. The dynamics consists of unitary dynamics driven by the Hubbard terms, and of a two-atom decay process which creates well-defined dissipation in the system. We model this system with a Master equation approach, and observe that the atomic sample is quickly driven into a space of dark states, which we identify as highly entangled Dicke states. We observe a qualitatively similar result in experiment, and study the dependence of the particle number of the steady state on various parameters, motivated by the experimental findings.

We find very similar dynamics, showing that the creation of strongly correlated states is a robust and universal phenomenon. This offers interesting opportunities for precision measurements.

References

Sponselee, K. et al. (May 2018). "Dynamics of Ultracold Quantum Gases in the Dissipative Fermi-Hubbard Model". In: *ArXiv e-prints*. arXiv: `1805.11853 [cond-mat.quant-gas]`.

Global thermodynamic susceptibilities for harmonic trapped gases

F. J. Poveda-Cuevas, I. Reyes-Ayala, J. A. Seman, and V. Romero-Rochín
Instituto de Física, Universidad Nacional Autónoma de México, Apartado Postal 20-364, 01000 Ciudad de México, Mexico
e-mail: *jacksonpc@fisica.unam.mx*

From the point of view of thermodynamics, a second-order or high-order phase transition is manifested when there is an abrupt change in the susceptibilities or their derivatives. The proposal of this work is to show the behavior the critical properties of a harmonically confined Bose gas around the phase transition from the normal to the superfluid condensate. We premise formulate a model [1, 2] for the density in the normal region, which is a function of chemical potential μ and temperature T is of the form of the Bose ideal gas, restricting ourselves to an isotropic harmonic trap of frequency ω, for $\mu - \frac{1}{2}m\omega^2 r^2 > 0$

$$\rho(\mathbf{r};\mu,T) = \frac{1}{\lambda^3} g_{\frac{3}{2}}\left(\frac{\mu - \frac{1}{2}m\omega^2 r^2}{kT}\right). \qquad (1)$$

In the superfluid region we have an expression for $\mu - \frac{1}{2}m\omega^2 r^2 \leq 0$

$$\rho(\mathbf{r};\mu,T) = \frac{1}{g}\sqrt{\left(\mu - \frac{1}{2}m\omega^2 r^2 + bg\right)^2 - (bg)^2} + \frac{\zeta_{3/2}}{\lambda^3}, \qquad (2)$$

which is it approaches asymptotically to Thomas-Fermi regime for $T \to 0$. Here $\lambda = h/(2\pi mkT)^{1/2}$ is the thermal de Broglie wavelength with h Planck constant, k Boltzmann constant, m the atomic mass, $g = 4\pi\hbar^2 a_s/m$, a_s is the atomic scattering length, ζ_ν is the Riemann zeta function, and $g_\nu(\mu/kT)$ the Bose function. This model is addressed with the knowledge of an equation of state of the underlying homogeneous Bose fluid, where the density profile is modified by means of *local density approximation*. Although it is not a strict thermodynamic requirement, we impose a restriction to be continuous on the derivative of density in order to fix the coe cient $b(T)$, therefore

$$b(T) = \frac{4\pi}{\lambda^3}\frac{a_s}{\lambda}. \qquad (3)$$

This identification completely determines the equation of state in terms of a_s and T.

The fundamental relations in Eqs. 1 and 2 formulate a mean-field like model which is completely analytic and let us to compute all the susceptibilities plotted in the Figs. 1 and 2. The presence of the confinement trap arrests the usual divergences of the susceptibilities, the critical behavior manifests itself now in the divergence of its derivatives. Around the transition the critical properties matches with the ideal Bose gas, preserving the *global* properties of the harmonically confined gas. We discuss how these properties can be experimentally tested.

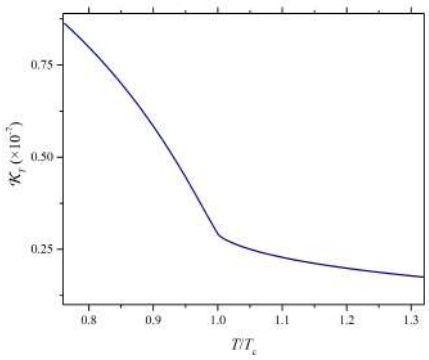


Figure 1: Global isothermal compressibility as function of T/T_c, where T_c is the critical temperature.

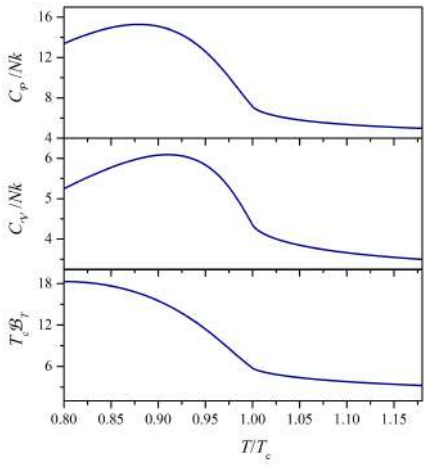


Figure 2: The heat capacities at constant pressure (above) and constant volume (middle), the expansion coefficient (below) at constant temperature as function of T/T_c.

[1] I. Reyes-Ayala, et al, J. Stat. Mech. Th. Exp. 073101, (2017)

[2] F. J. Poveda-Cuevas, et al, AIP Conf. Proc. **1950**, 030006 (2018).

Coherent inflation in Bose Einstein condensate.

Sicong Ji[1], **Bernhard Rauer**[1], **Thomas Schweigler**[1], **Federica Cataldini**[1], **Mohammadamin Tajik**[1], **Joao Sabino**[1] **and Jörg Schmiedmayer**[1]

[1] *Vienna Center for Quantum Science and Technology, Atominstitut, TU Wien, Stadionallee 2, 1020 Vienna, Austria.*

e-mail: *sicong.ji@tuwien.ac.at*

The quantum delocalization gives many fascinating possibilities. One is the unexplored gravitationally induced decoherence. To arrive at this destination, overcoming many inevitable decoherence (scattering of background gas, balck-body radiation) and fast preparing high purity coherence states with large spatial size are crucial but still challenging. In this work, we experimentally realize the squeezing of coherence state of Rubidium 87 using exponentially speed-up quantum dynamics in an inverted magnetic harmonic trap [1] and further prepare the large scale coherrent states with a subsequent time-of-flight. The study of the connection between the decoherence effect and the excitation in longitude direction in one-dimentional system is also intriguing.

[1] H. Pino, J. Prat-Camps, K. Sinha, B. P. Venkatesh, O. Romero-Isart, Quantum Sci. Technol. **3**, 25001 (2018).

Time resolved study of competing instabilities on a Fermi gas quenched to strong repulsion

A. Amico[1,2], **F. Scazza**[1,2], **P. E. S. Tavares**[1,2,4], **G. Valtolina**[1,2,3], **G. Del Pace**[1,2], **W. Kwon**[1,2], **M. Inguscio**[1,2], **M. Zaccanti**[1,2], **and G. Roati**[1,2]

[1] *LENS and Dipartimento di Fisica e Astronomia, Università di Firenze, 50019 Sesto Fiorentino, Italy*
[2] *Istituto Nazionale di Ottica del Consiglio Nazionale delle Ricerche (INO-CNR), 50019 Sesto Fiorentino, Italy*
[3] *JILA, University of Colorado, Boulder, CO 80309, USA* [4] *Instituto de Física de São Carlos, Universidade de São Paulo, Caixa Postal 369, 13560-970 São Carlos, SP, Brazil*
e-mail: *amico@lens.unifi.it*

We investigate the out-of-equilibrium dynamics of a two-component Fermi gas of ultracold atoms, following a quench to strong repulsive interactions. By means of time-resolved pump-probe RF spectroscopy, we study the evolution of the repulsive interaction shift and the paired fraction. We observe a strong suppression of the interaction energy over a timescale that is shorter than the pairing one, revealing the emergence of strong short-range spin correlations. By means of optical spin density noise-correlation measurements, we directly probe the presence of spin inhomogeneities, finding for su ciently strong interactions a substantial increase of spin fluctuations after the quench. By measuring the density-density correlation function, we estimate the characteristic length of the fluctuations to be shorter than few interparticle spacing. Finally, we study the relaxation of the system for longer time after the quench, observing a suppression of pairing for strong repulsive interactions.

Matter wave speckle observed in an out-of-equilibrium quantum fluid

P. E. S. Tavares[1], **A. R. Fritsch**[1], **G. D. Telles**[1], **M. S. Hussein**[2], **F. Impens**[3], **R. Kaiser**[4] and **V. S. Bagnato**[1]

[1] *São Carlos Institute of Physics, University of São Paulo, PO Box 369, 13560-970, São Carlos, SP, Brazil*
[2] *Departamento de Física, Instituto Tecnológico de Aeronaútica, DCTA, São José dos Campos, SP, Brazil*
[3] *Instituto de Física, Universidade Federal do Rio de Janeiro, C.P. 68528, Rio de Janeiro, RJ, Brazil*
[4] *Université Nice Sophia Antipolis, Institut Non-Linéaire de Nice, CNRS UMR 7335, Valbonne, France*
e-mail: *pedro.ernesto.tavares@usp.br*

In recent years, significant progress concerning matter-wave creation and manipulation has been achieved. Fresnel diffraction, atom lasers, and nonlinear matter wave phenomena, are just a few examples of recent interesting research topics. There have also been quite a lot of studies related to the propagation of matter waves interacting with disordered potentials, but not as much concerning the disorder existing into the matter wave itself. In the present study, we analyze the disorder imprinted into a Bose-Einstein condensate (BEC), and its characteristic spatial evolution afterwards. We performed careful analyses and traced a few analogies that took us to the conclusion that the perturbed BECs evolve very much in a speckle-like manner, in close analogy with a traveling light (optical) speckle.

The properties of a turbulent trapped atomic superfluid were investigated by taking into account its matter wave nature. The quantum turbulent regime is achieved by perturbing a ^{87}Rb Bose-Einstein condensate (BEC), produced in a QUIC trap, with a time oscillating magnetic field [1, 2]. The randomness of amplitude and phase observed in free-expanding turbulent BEC (disordered matter wave) were found to have strikingly similar properties to those of a traveling speckle light field (disordered optical wave), Fig. 1(a)-(d). More specifically, we observed that the divergence of both propagating waves present strong similarities, and diffraction is at the origin of the wave divergence. In addition, the second-order (spatial) correlation function was evaluated, Fig. 1(e) and (f), again resulting in essentially the same qualitative behavior for both waves [3]. The analogy in between the light and the matter waves may create new perspectives to study disordered quantum matter states. Finally, the study of the propagation of a three-dimensional matter wave speckle might bring some new insights to better understand the light speckle phenomenon in higher dimensions (beyond 2D), expanding the horizons of this phenomena.

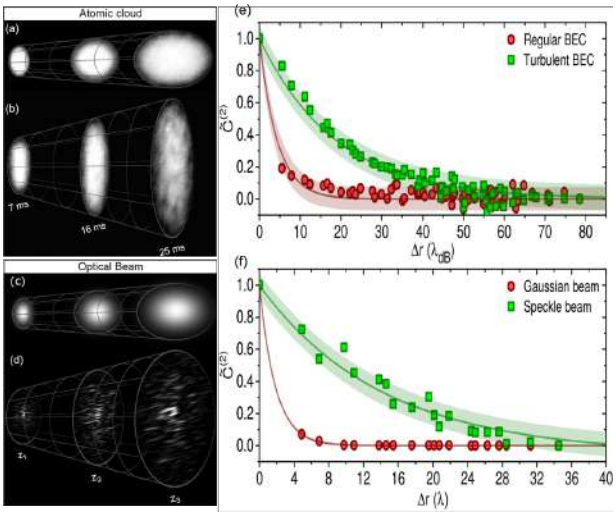


Figure 1: Atomic cloud expansion, optical beam propagation and Second-order correlation function. (a) Time-of-flight expansion of a regular BEC and (b) turbulent cloud. (c) Propagation of a Gaussian and (d) Speckle beam. (e) Second-order correlation function for an atomic cloud (matter wave) and (f) optical beam.

[1] E. A. L. Henn, J. A. Seman, G. Roati *et al.*, Phys. Rev. Lett. **103**, 045301 (2009).

[2] A. Bahrami, P. E. S. Tavares, A. R. Fritsch*et al.*, J. Low Temp. Phys. **180**, 126 (2015).

[3] P. E. S. Tavares, A. R. Fritsch, G. D. Telles *et al.*, PNAS **114**, 12619 (2017).

A two species superfluid system to study quantum phases transitions in an atomic vortex lattice

P. E. S. Tavares[1], **E. D. M. Gutierrez**[1], **H. V. Duque**[1], **P. L. Mazo**[1], **G. A. Neto**[1], **J. A. Scarpin**[1], **K. M. Farias**[1] **and V. S. Bagnato**[1]

[1] *São Carlos Institute of Physics, University of São Paulo, PO Box 369, 13560-970, São Carlos, SP, Brazil*
e-mail: *pedro.ernesto.tavares@usp.br*

A new experimental apparatus has been built to product a trapped two-species Bose-Einstein condensates of sodium (^{23}Na) and potassium (^{41}K). Where we propose to implement a route to produce and study ultracold atoms immersed in a BEC vortex lattice, exploring different intraspecies interaction regimes. The vortex lattice will be produced in the ^{23}Na condensate using the stirring beam technique, without perturbing the potassium atomic cloud. By changing the interaction between the two species, we pretend to demonstrate that a vortex lattice is equivalent to an optical lattice to trap ultracold atoms. This study could provide a new tool for simulating systems and models in condensed matter physics. Specifically, by using ultracold atoms immersed in an atomic vortex lattice we will experimentally simulate the Bose-Hubbard model for a static lattice and the extended Bose-Hubbard model for a out-of-equilibrium lattice, as theoretically propose by [1]. In this study, they considered a ultracold bose gas mixture, trapped in a quasi-2D potential, formed by species A (which contains the vortex lattice) and species B, this model results is a Bose-Hubbard hamiltonian (BH). By tunning the intraspecies interaction using Feshbach ressonances a quantum phase transition from Mott-insulator (MI) to a superfluid phase (SF) can be observed in such system.

Figure 1 shows the phase boundary between the Mott-insulator and the superfluid phase for the two lattices type: (a) on a static triangular lattice, where different boundaries are obtained through mean-field theory, processchain approach and the quantum Monte Carlo technique (QMC); (b) on a dinamic triangular lattice obtained by QMC simulation

[1] Chaviguri, R. H. *et al.*, Phys. Rev. A **95**, 053639 (2017).

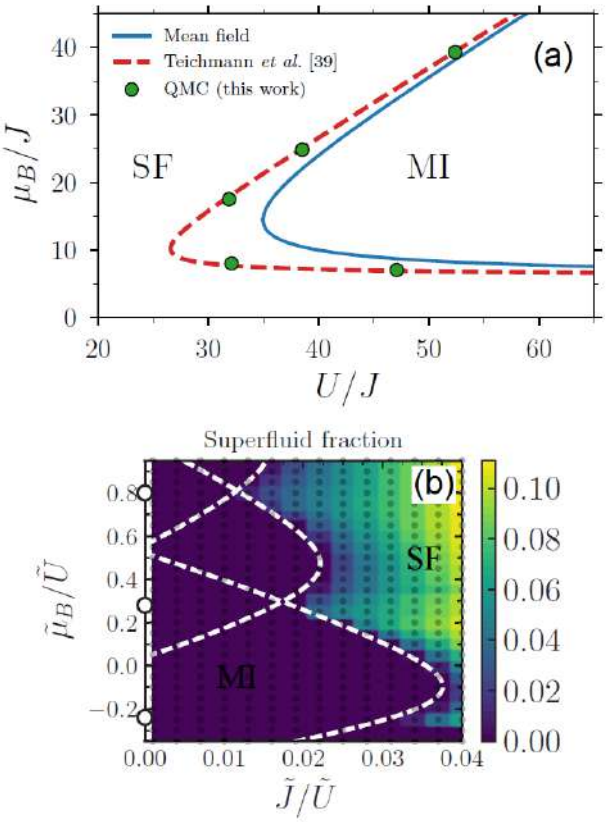


Figure 1: Phase boundary between the Mott-insulator (MI) lobe and the superfluid phase (SF). (a) on a twodimensional static triangular lattice. Different boundaries are obtained through mean-field theory (blue solid line), processchain approach (dashed red line), and the quantum Monte Carlo technique (green circles). (b) on a dinamic triangular lattice obtained by QMC simulation. Dashed white lines are phase boundaries of the Mott insulators with differents filling factors ($g = 1, 2, 3$). Adapted from reference [1].

Large arrays of bosonic atoms in optical tweezers

M. O. Brown, T. Thiele, C. H. Kiehl, B. J. Lester, Y. Lin, C. A. Regal

JILA, National Institute of Standards and Technology and University of Colorado, and Department of Physics, University of Colorado, Boulder, Colorado 80309, USA

e-mail: *Mark.O.Brown@colorado.edu*

Single neutral atoms trapped by arrays of optical tweezers has proved to be promising platform for atomic physics, quantum information processing, and quantum simulation. We previously developed this platform for the ground-state cooling and control of single neutral ^{87}Rb atoms trapped in arrays of optical tweezers, where we have demonstrated versatile control of atomic tunneling between tweezers and multi-atom contact interactions. We used these tools to demonstrate HOM interference between two ground-state atoms and then we demonstrated and characterized entanglement between two atoms via spin-exchange.

More recently, we extracted a spin-entangled state of two neutral atoms via postselection based on a measurement of their spatial configuration [1]. Typically, entangled states of neutral atoms are engineered via atom-atom interactions. In contrast, in our work, we used Hong-Ou-Mandel interference and postselection to identify a spin-singlet state after overlapping two atoms in distinct spin states on an effective beam splitter. We verify the presence of entanglement and determine a bound on the postselected fidelity of a spin-singlet state of (0.62 ± 0.03). The experiment has direct analogy to creating polarization entanglement with single photons and hence demonstrates the potential to use protocols developed for photons to create complex quantum states with noninteracting atoms.

We also discuss our progress in developing several single-atom imaging techniques. Traditionally, we use polarization-gradient-cooling-based imaging. However, this imaging is not state-selective and is sensitive to unevenness in the tweezer depths. To address these issues, we have implemented a lossless state-selective imaging technique [2] to detect the atomic spin-state without loss, and a flashing technique. By quickly flashing between the trapping and imaging light, we effectively image the atoms while in free-space. This both minimizes the effect of the unevenness of the traps and simultaneously avoids anti-trapping the atom while the atom is in its excited state.

We now report on our recent progress in extending our platform to larger arrays of 100 or more optical tweezers, and in swiftly rearranging the atoms therein using a different time-averaged flashing technique. To compensate for the probabilistic atom loading, the atoms are rearranged to create arbitrary configurations in a 2D grid [3]. The array of traps is created by using two orthogonal large-bandwidth acousto-optical modulators (AOMs). We rapidly switch (1 MHz) the two orthogonal AOMs between generating a static array of tweezers, which holds the majority of the atoms in place, and one or more deeper moving tweezers which shuttle the atoms between tweezers. The resulting time-averaged potential is capable of moving atoms between tweezers in about 60 μs. In addition, we implement new features such as such as the parallelization of the moves, which can considerably decrease the time taken for the rearranging process [4, 5].

We also present our plans to use the the creation and control of large ordered arrays of atoms for studies of collective behavior in the interaction of an ordered array with nearly resonant laser light and as well as increasingly sophisticated experiments harnessing the tunneling of bosonic atoms.

[1] B. J. Lester, Y. Lin, M. O. Brown, A. M. Kaufman, R. J. Ball, E. Knill, A. M. Rey, and C. A. Regal, Phys. Rev. Lett. 120, 193602 (2018).

[2] A. Fuhrmanek, R. Bourgain, Y. R. P. Sortais, and A. Browaeys, Phys. Rev. Lett. 106, 133003 (2011).

[3] B. J. Lester, N. Luick, A. M. Kaufman, C. M. Reynolds, and C. A. Regal, Phys. Rev. Lett. 115, 073003 (2015).

[4] D. Barredo, S. de Lsleuc, V. Lienhard, T. Lahaye, and A. Browaeys, Science 354, 1021 (2016).

[5] M. Endres, H. Bernien, A. Keesling, H. Levine, E. R. Anschuetz, A. Krajenbrink, C. Senko, V. Vuletic, M. Greiner, and M. D. Lukin, Science aah3752 (2016).

Complex Networks on Quantum States: From Quantum Phase Transitions to Emergent Dynamics of Quantum Cellular Automata

Lincoln D. Carr[1], **Marc Andrew Valdez**[1], **Daniel Jaschke**[1], **David L. Vargas**[1], **Bhuvanesh Sundar**[2,3], **and Kaden Hazzard**[2,3]

[1] *Department of Physics, Colorado School of Mines, Golden, Colorado, U.S.A.*

[2] *Department of Physics and Astronomy, Rice University, Houston, Texas, U.S.A.*

[3] *Rice Center for Quantum Materials, Rice University, Houston, Texas, U.S.A.*

e-mail: *lcarr@mines.edu*

Complex networks defined on quantum states via quantum mutual information turn out to give a surprising level of new insight on physical problems ranging from quantum critical phenomena to far-from-equilibrium quantum dynamics. We first show how measures well-known to the complex network theory community, such as clustering and disparity, serve to rapidly and e ciently identify quantum critical points for workhorse many-body models such as the transverse quantum Ising model and Bose-Hubbard model, as studied in present quantum simulator experiments [1]. Then we extend our work to finite temperature states to elucidate correlation structure in the quantum critical fan for the transverse Ising model [2]. Finally, we show how a small modification of such models allows one to produce entangled quantum cellular automata [3]. Complex network-based averages and dynamics serve as key quantifiers for emergent complexity along with localized robust dynamical structures and entropy fluctuations. They show that a new class of highly entangled yet also highly structured quantum states arise out of dynamics just a short step away from present experimental protocols. They also identify a set of simple criteria, called Goldilocks Rules, which consistently produce complexity independent of the details of the protocol. Thus complex network theory not only presents a useful new tool we can apply to present quantum simulator experiments, but also suggests significant new directions and new physics to be discovered.

References

[1] Marc Andrew Valdez, Daniel Jaschke, David L. Vargas and Lincoln D. Carr, "Quantifying Complexity in Quantum Phase Transitions via Mutual Information Complex Networks," Phys. Rev. Lett., **119**, 225301 (2017).

[2] Bhuvanesh Sundar, Marc Andrew Valdez, Lincoln D. Carr, and Kaden R. A. Hazzard, "A complex network description of thermal quantum states in the Ising spin chain," Phys. Rev. A, **97**, 052320 (2018).

[3] Matthew T. Jones, L. E. Hillberry, P. Rall, David L. Vargas, N. Yunger Halpern, N. Bao, S. Montangero, and Lincoln D. Carr "Entangled Quantum Cellular Automata, Physical Complexity, and Goldilocks Rules," to be submitted (2018).

Mixtures in radiofrequency-dressed potentials

E. Bentine[1], **A. Barker**[1], **K. Luksch**[1], **S. Sunami**[1], **T. Harte**[2], **B. Yuen**[1] **and C. J. Foot**[1]
[1] *Department of Physics, University of Oxford, Parks Road OX1 3PU, United Kingdom*
[2] *Cavendish Laboratory, Department of Physics, University of Cambridge, CB3 0HE, United Kingdom*

D. J. Owens[3], **J. M. Hutson**[3]
[3] *Joint Quantum Centre (JQC) Durham-Newcastle, Department of Chemistry, Durham University, South Road, Durham DH1 3LE, United Kingdom.*
e-mail: *elliot.bentine@physics.ox.ac.uk*

Radiofrequency(rf)-dressed potentials have become established as a technique to trap and manipulate ultracold gases due to their smoothness and extremely low heating rates. These potentials are species-selective when the magnetic dipole moment differs between species. They can independently manipulate mixtures of hyperfine states [1] and/or isotopes [2], for which optical methods are poorly-suited due to the similar electronic structure and thus optical transitions of these species. Here, we experimentally demonstrate rf-dressed manipulations for a mixture of the isotopes ^{85}Rb and ^{87}Rb.

However, experiments with mixtures also require collisional stability, which has not previously been investigated for isotopic mixtures in rf-dressed potentials. We observe fast inelastic loss between a mixture of ^{85}Rb and ^{87}Rb atoms that we identify as due to two-body collisions. Our measured rate constants are comparable to spin-exchange processes, and vary with detuning from the rf resonance. We explain the loss by invoking the concept of a rotating frame [3], and compare our measurements to quantitative predictions from a coupled channel model (defined in [4]) that includes the rf field.

[1] I. Lesanovsky, T. Schumm, S. Hofferberth, L. M. Andersson, P. Krüger, J. Schmiedmayer, Phys. Rev. A, **73** 033619 (2006).

[2] E. Bentine, T. L. Harte, K. Luksch, A. J. Barker, J. Mur-Petit, B. Yuen, C. J. Foot, J. Phys. B **50**, 094002 (2017).

[3] A. J. Moerdijk, B. J. Verhaar, T. M. Nagtegaal, Phys. Rev. A, **53** 4343 (1996).

[4] D. Owens, J. M. Hutson, Phys. Rev. A **96**, 042707 (2017).

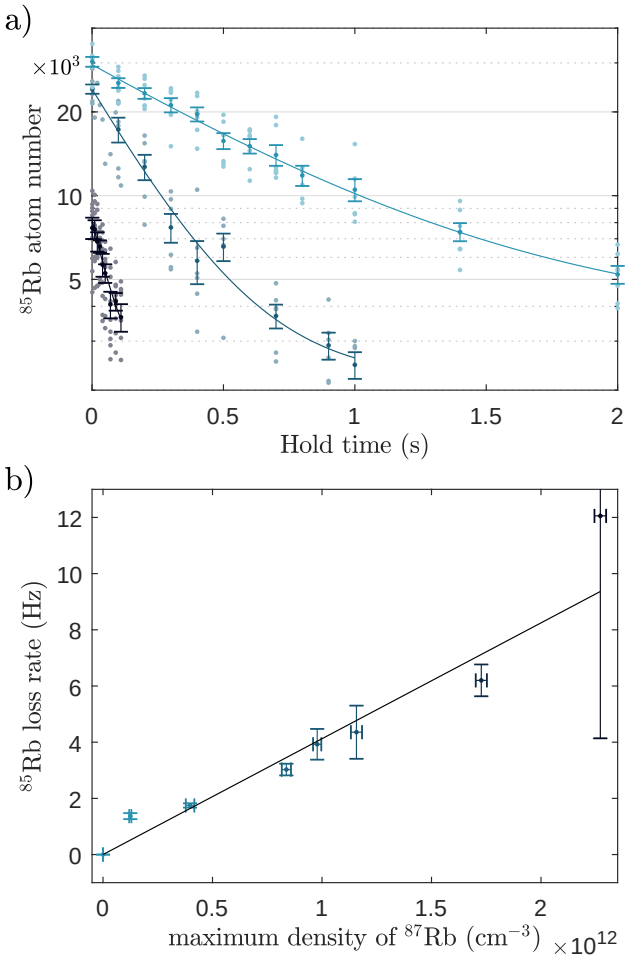


Figure 1: Inelastic loss occurs in an rf-dressed potential for a mixture of ^{85}Rb and ^{87}Rb. a) Total ^{85}Rb atom number as a function of time for three different densities of ^{87}Rb. b) The loss rate of ^{85}Rb increases linearly with the density of ^{87}Rb.

Magnetically tunable Feshbach resonances in ultracold gases of europium atoms and mixtures of europium and alkali-metal atoms

K. Zaremba-Kopczyk[1], **P. Żuchowski**[2], **and M. Tomza**[1]

[1] *Faculty of Physics, University of Warsaw, Pasteura 5, 02-093 Warsaw, Poland*

[2] *Faculty of Physics, Astronomy and Informatics, Nicolaus Copernicus University in Torun, Grudziadzka 5, 87-100 Toruń, Poland*

e-mail: *k.kopczyk@student.uw.edu.pl*

Tunable Feshbach resonances serve as an effective means of manipulating the interatomic interactions and scattering properties characterizing an ultracold quantum gas, and thus open up possibilities for producing highly controllable quantum systems.

With the advances in atom cooling, it is has become possible to investigate ultracold species more complex than the alkali metals, for which Feshbach resonances had already been accurately characterized [1], such as highly magnetic chromium [2], dysprosium [3], or erbium [4] atoms.

For the ultracold gases of dysprosium and erbium, it was shown that the highly anisotropic interaction between constituent atoms leads to chaotic scattering [5, 6]. It was speculated that the scattering spectra of other magnetic lanthanides might also exhibit chaotic behavior [6], however, non-chaotic scattering was predicted for the mixture of erbium and lithium [7].

At the same time, the buffer-gas cooling and magnetic trapping of cold europium atoms were already demonstrated [8]. It was also predicted that EuK, EuRb and EuCs molecules should possess both large electric and magnetic dipole moments [9]. Thus, ultracold europium and its mixtures with alkali-metal atoms may be next interesting systems to study.

In this work we investigate magnetically tunable Feshbach resonances between ultracold europium atoms and between europium and alkali-metal atoms. For an ultracold gas of europium atoms both homonuclear ^{153}Eu+^{153}Eu and heteronuclear ^{151}Eu+^{153}Eu systems are investigated. Calculations for mixtures of europium and alkali-metal atoms are carried out for prototype systems of ^{153}Eu+^{87}Rb and ^{153}Eu+^{7}Li. We analyze the prospects for magnetoassociation into ultracold polar and paramagnetic molecules, observation of quantum chaotic behavior, and control of scattering properties in the investigated systems. Presented results may be useful for realization and application of dipolar atomic and molecular quantum gases based on europium atoms in many-body physics.

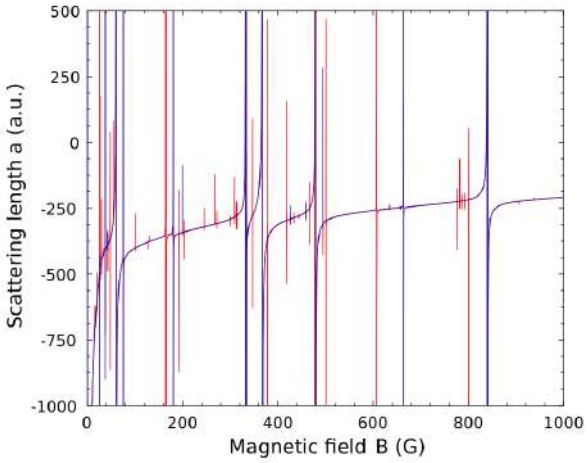


Figure 1: Scattering length dependence on the magnetic field for ultracold collisions between ^{153}Eu and ^{87}Rb and for the projection of total angular momentum $M_{TOT} = 0$. The blue lines show scattering lengths without the dipole-dipole interaction included and the red lines – with the dipole-dipole interaction included.

[1] C. Chin, R. Grimm, P. Julienne, and E. Tiesinga, Rev. Mod. Phys. **82**, 1225 (2010).

[2] A. Griesmaier, J. Werner, S. Hensler, J. Stuhler, and T. Pfau, Phys. Rev. Lett. **94**, 160401 (2005).

[3] M. Lu, N. Q. Burdick, S. H. Youn, and B. L. Lev, Phys. Rev. Lett. **107**, 190401 (2011).

[4] K. Aikawa, A. Frisch, M. Mark, S. Baier, A. Rietzler, R. Grimm, and F. Ferlaino, Phys. Rev. Lett. **108**, 210401 (2012).

[5] A. Frisch, M. Mark, K. Aikawa, F. Ferlaino, J. L. Bohn, C. Makrides, A. Petrov, and S. Kotochigova, Nature (London) **507**, 475 (2014).

[6] T. Maier *et al.*, Phys. Rev. X **5**, 041029 (2015).

[7] M. L. González-Martnez, and P. S. Żuchowski, Phys. Rev. A **92**, 022708 (2015).

[8] C. I. Hancox, S. C. Doret, M. T. Hummon, L. Luo, and J. M. Doyle, Nature **431**, 281 (2004).

[9] M. Tomza, Phys. Rev. A **90**, 022514 (2014).

Studying Quantum Turbulence in Two Species Superfluid: The State of the Art of NaK System

Kilvia M. Farias[1], Emmanuel D. M. Gutierrez[1], Patricia C. M. Castilho[1], Pedro E. S. Tavares[1], Humberto V. Duque[1], Giacomo Roati[2] and Vanderlei S. Bagnato[1]

[1] *São Carlos Institute of Physics, University of São Paulo, PO Box 369, 13560-970, São Carlos, SP, Brazil*

[2] *INO-CNR and LENS, Università di Firenze, 50019 Sesto Fiorentino, Italy*

e-mail: *kilvia@ifsc.usp.br*

Quantum turbulence in cold atoms is a very interesting phenomenon that has been studied recently. Its diagnosis and related effects are being developed and bringing new insights to the field. Our observation of superfluid turbulence in ^{87}Rb [1] introduced the experimental tools of atomic optics into the world of quantum fluid dynamics. In this work, we present the state of the art of our experiment for a mixture of Na and K Bose-Einstein Condensates. The specific case of Na-K mixtures is of particular interest due to its large flexibility. Both, Bose-Bose and Bose-Fermi mixtures could be produced by changing the potassium isotope and the different miscibility regimes explored with the tuning of the interspecies interactions via the Feshbach resonances for each combination. We are going to investigate effects related to two different species as effects of transferring quantum excitations, vortices and lattices formation, and quantum turbulence, as well using this flexibility.

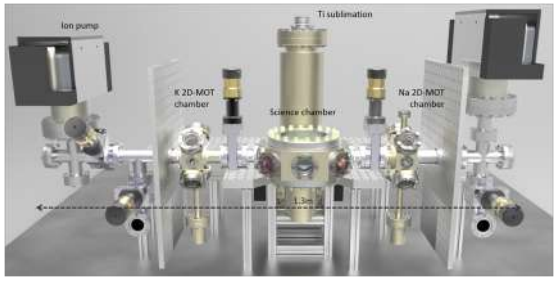


Figure 1: Front view of the compact vacuum system designed for the production of the ^{23}Na-^{41}K Bose-Bose superfluid mixture.

Our experimental system is a composition of two independently atomic sources attached to the main chamber, which is the Science chamber. In Fig. 1, we show how the system was built. Our experimental apparatus is very compact compared to traditional systems and its details will be discussed in this presentation and also published soon[3]. We produce magneto-optical traps (MOT) of Na [2] and K atoms from 2D MOTs, which utilize a novel Zeeman slower configuration. For the case of K, it is the first time that technique is implemented. In our case, we can manipulate both ^{39}K and ^{41}K.

We will present how we lead with the two conservative traps we have: the optically plugged Quadrupole trap and the crossed Optial Dipole Trap. In Fig. 2 we have a vertical section of our vacuum chamber, where we show the laser access and magnetic field lines.

We are running the Na BEC from the Optical Trap and started the first experiments on Vortices Lattices formation using a stirring beam. Results also related to K will be presented here, as the process using Gray Molasses [4] to deeply cooling it. As this is a large project, we will also have more detailed presentations for different aspects of our work in this conference.

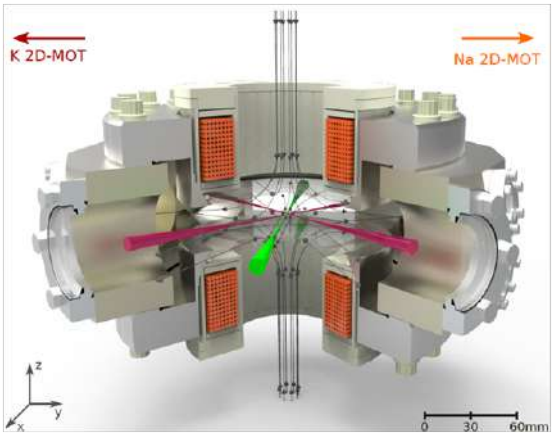


Figure 2: Vertical cut of Science Chamber showing optical access and magnetic field lines.

[1] E. A. L. Henn, J. A. Seman, G. Roati, K. M. F. Magalhes, and V. S. Bagnato, Physical Review Letters 103, 045301 (2009).

[2] G. Lamporesi, S. Donadello, S. Serafini, and G. Ferrari, Review of Scientific Instruments 84, 063102 (2013).

[3] Patricia C. M. Castilho, et al. To be published. A compact experimental machine for studying tunable Bose-Bose superfluid mixtures.

[4] D. Boiron, C. Triche, D. R. Meacher, P. Verkerk and G. Grynberg, Phys. Rev. A 52, R3425 (1995).

Bright Soliton to Quantum Droplet Transition in a Mixture of Bose-Einstein Condensates

P. Cheiney, C. R. Cabrera, J. Sanz, B. Naylor, L. Tanzi, and L. Tarruell
Institut de Ciències Fotòniques, The Barcelona Institute of Science and Technology
08860 Castelldefels (Barcelona), Spain
e-mail: *julio.sanz@icfo.es*

Self-bound states are ubiquitous in nature, and appear in contexts as diverse as solitary waves in channels, optical solitons in nonlinear media, and liquid He droplets. Their binding results from a balance between attractive forces, which tend to make the system collapse, and repulsive ones, which stabilize it to a finite size. Bose-Einstein condensates with attractive meanfield interactions constitute ideal systems to explore in the same setting different self-bound states like bright solitons and quantum droplets. While solitons are stabilized due to the interplay with quantum pressure, quantum droplets are stabilized by a repulsive many-body beyond mean-field effect [1]. In analogy to non-linear optics, the former can be seen as one-dimensional matter-wave solitons stabilized by dispersion, whereas the latter correspond to high-dimensional solitons stabilized by a higher order nonlinearity. The observation of quantum droplets in the context of Bose-Bose mixtures [2, 3] has opened the question about the similarities and differences between this two kinds of self-bound states.

In this poster, we address this question both theoretically and experimentally with a spin mixture of ^{39}K BECs in a wave-guide geometry [4]. We find that depending on atom number, interaction strength and confinement, solitons and droplets can be smoothly connected or remain distinct states coexisting only in a bi-stable region, see Fig. 1. We measure their spin composition, extract their density for a broad range of parameters, and map out the boundary of the region separating solitons from droplets.

Future experimental directions include the study of metastability and hysteresis when crossing the soliton-to-droplet transition from different directions. Another interesting possibility is to perform collisions between two self-bound states, which are expected to display very different behavior in the soliton and droplet limits. Finally, spin imbalanced systems offer the possibility to explore finite temperature effects in a well controlled setting, exploiting the excess component as a thermal bath.

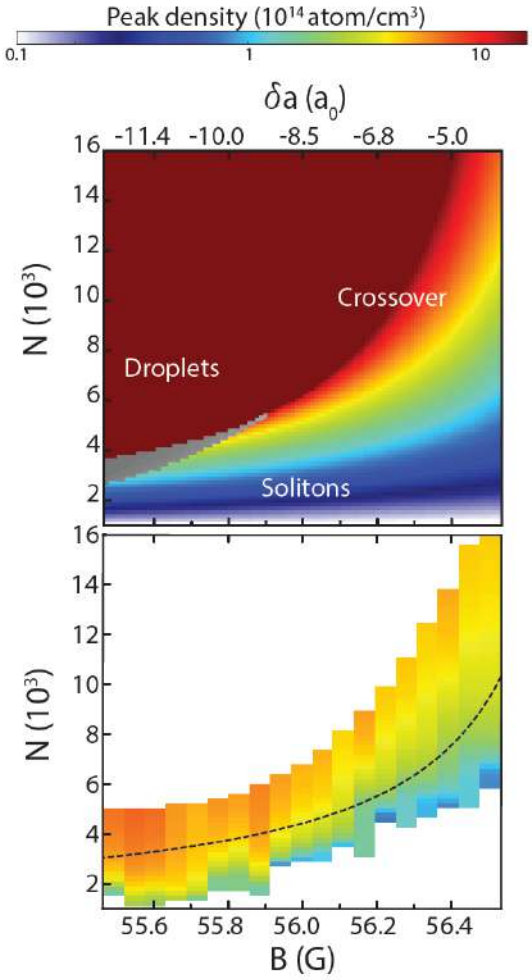


Figure 1: Top panel: Ground state peak density vs atom number N and magnetic field B computed numerically from an extended Gross-Pitaevskii equation where we have included the effect of quantum fluctuations as an effective repulsion. Solitons and droplets are distinct solutions, which coexist in a bistable region (gray area) and become smoothly connected in the crossover above $B_c \sim 55.85G$. Bottom panel: Peak density extracted experimentally by means of three-body decay measurements. Interestingly, self-bound states exist above the mean-field collapse threshold (dashed line).

[1] D. S. Petrov, PRL **115**, 155302 (2015).

[2] C. R. Cabrera et al., Science **359**, 6373 (2018).

[3] G. Semeghini et al., PRL **120**, 235301 (2018)

[4] P. Cheiney et al., PRL **120** 135301 (2018).

Anomalous expansion of turbulent Bose-Einstein condensates

A. D. García-Orozco, A. R. Fritsch, A. N. Novikov, P. E. S. Tavares, G. Roati[0], G. D. Telles, V. S. Bagnato

Instituto de Física de São Carlos, Universidade de São Paulo, CP 369, 13560-970, São Carlos, SP, Brasil

e-mail: *gugs@ifsc.usp.br*

The standard expansion of the ultracold matter waves is observed to be suppressed by the disorder onset. We explored this interest phenomenon with a turbulent Bose condensates, by carefully studying the experimental bimodal density profiles and observed a clear transition from the standard Gaussian to a single exponential tail shape dominated by the higher momentum atoms. This suggests the onset of locking in mass transport properties of the quantum gas, caused by the presence of a turbulent core. We investigated the transition in between different excitation conditions and concluded that, unlike the previous experimental observations where the expanded cloud expands in a static potential, our system is more dynamical though it still preserves the universal behavior of stopping the matter spread in the presence of disorder.

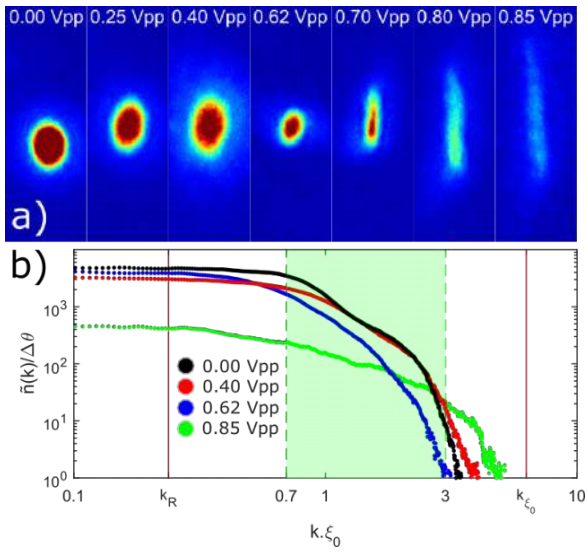


Figure 1: (a) Images of the atomic clouds taken after the BEC was perturbed for 31.7 ms then released from the trap and free fell for 28 ms. (b) Typical momentum spectra acquired from the images showing the effects of perturbing the BECs with different amplitudes.

Essentially, we start with samples of trapped turbulent ultracold cloud, produced under different and controlled conditions, then we suddenly shut the trap off allowing for its free expansion, and study the expanding atom density in free fall. It was observed that, under certain experimental conditions, a clear transition from Gaussian to the single exponential is observed to take place in the wings of the typical bimodal atomic distribution [1].

A typical sequence of images of the turbulent atomic clouds is presented in Fig. 1, resulting from different perturbing amplitudes. Depending on the values of the perturbing parameters such as amplitude and time, different stages of turbulence are reached. Actually, nearly any excitation seems to take the system out-of-equilibrium, though we observed that the cloud irreversibly evolves to turbulence only after a certain threshold amplitude is reached. Once turbulence emerges, there a few signs showing its onset. The most important is the power law dependence observed in the momentum density distribution plotted as a function of the wave numbers. Essentially, it implies the existence of an energy cascade associated with dissipation, and less energy is being transferred from the large to the small scales. As a result, a high momentum turbulent cloud will present larger number of atoms with high momentum. Recently, The cascade mechanism is considered as an universal characteristic of turbulence [2].

Currently, our understanding is that the interplay between a single, high-momentum, atom and the core of turbulent superfluid is physically equivalent to the interaction of that atom with a random potential comprising the spatial density fluctuations, where multiple scattering cloud take place, leading to the highly anisotropic expansion observed. Such modification indicates the variation of the transport depending on the degree of disorder introduced into the superfluid.

[1] L. Sanchez-Palencia *et al.*, Phys. Rev. Lett. **98**, 210401(2007); J. Billy *et al.*, Nature **453**, 891(2008); G. Roati *et al.*, Nature **453**, 895(2008).

[2] K.J. Thompson *et al.*, Laser Phys. Lett. **11**, 015501(2014); N. Navon *et al.*, Nature **539**, 72(2016).

[0]Permanent Address: LENS and Dipartimento di Fisica, Universitá di Firenze, 50019 Sesto Fiorentino, Italy

Thermodynamic measurement of the sound velocity of a Bose gas across the Bose-Einstein condensation

A. R. Fritsch, P. E. S. Tavares, F. A. J. Vivanco, G. D. Telles, V. S. Bagnato, and E. A. L. Henn

Instituto de Física de São Carlos, Universidade de São Paulo, CP 369, 13560-970, São Carlos, SP, Brasil
e-mail: *gugs@ifsc.usp.br*

We present an alternative method for determining the sound velocity in atomic Bose-Einstein condensates, based on thermodynamic global variables. The total number of trapped atoms was as a function of temperature carefully studied across the phase transition, at constant volume. It allowed us to evaluate the sound velocity resulting in consistent values from the quantum to classical regime, in good agreement with previous results found in literature. We also provide some insight on which fraction (BEC/thermal) rules the sound mode at different temperature ranges.

We took a different approach to investigate the sound velocity in a Bose gas at finite temperature across the Bose-Einstein condensation (BEC) transition. Essentially, we directly evaluate the global thermodynamic variables [1], from unperturbed BEC samples prepared following slightly different evaporation ramps. The total number of atoms in each BEC sample was varied together with the final temperatures in a constant trap volume (constant global volume parameter), and then the change in the global pressure as a function of the number density was used to determine the sound velocity. This method allows us to directly compare the results to the original thermodynamic sound velocity derived for quantum gases. Furthermore, we were able to determine the contribution of two-component Bose gas separately at each temperature range, which is not possible by the previous methods [2].

Figure 1 shows the partial components of the sound velocity. In figure 1(a) one can see the range where each fraction rules the first sound: below ≈ 90 nK the BEC fraction takes over the small thermal fraction, while above 100 nK the thermal cloud rules. The inset shows the lowest temperature range to emphasize each fraction's lead. We also determine the independent sound velocities, as shown in figure 1(b), to show even more clear that the sound velocity in the thermal fraction varies linearly with the temperature all the way from zero temperature.

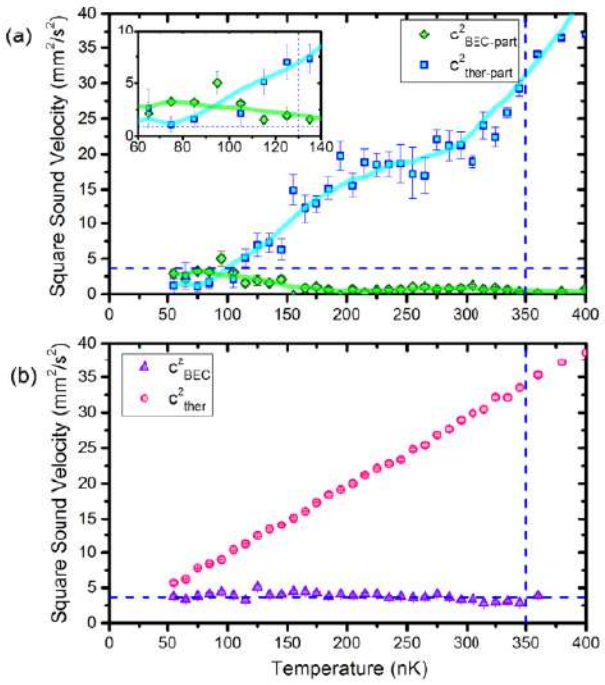


Figure 1: (a) Partial components of the first sound velocity, given by the BEC (green diamonds) and thermal parts (blue squares). (b) 'Single fluid' sound velocity of the BEC (purple up-triangles) and thermal fluids (magenta circles). The solid lines in both (a) and (b) are guides to the eye following the points. The horizontal dashed line is the theoretical predicted $T = 0$ first sound velocity and the vertical dashed line is the approximate limit above which no BEC fraction is detected at our experiments.

[1] V. Romero-Rochín *et al.*, Phys. Rev. A **85**, 023632 (2012); V. Romero-Rochín, Phys. Rev. Lett. **94**, 130601 (2005).

[2] A. R. Fritsch *et al.* J. Stat. Mech. **18**, 053108 (2018).

Few-Photon-Level Atom-Mediated Cross-Phase Modulation at Room Temperature

S. Sagona-Stophel[1], **R. Shahrokhshahi**[1], **M. Namazi**[1], **B. Jordaan**[1] **and E. Figueroa**[1]
[1] *Stony Brook University, 100 Nicolls Rd, Stony Brook, NY 11794, USA*
e-mail: *steven.sagona-stophel@stonybrook.edu*

Introduction. Developing atom-mediated systems capable of interaction strengths su cient to achieve photon-photon gate operations is a considerable challenge. While the strength of photon-induced phase shifts has been the primary figure-of-merit over the last decade of experiments[1, 2], it is critical for the development of quantum processes to have an experimental framework that can perform a full quantum characterization of the phase-shifted light.

We both demonstrate the first room-temperature implementation in which simultaneously propagating pulses of single-photon-level light create π phase shifts, while also performing a quantum characterization of the phase-shifted output state[3]. To achieve this, we use a double-Λ [4] atomic system in a warm ^{87}Rb ensemble, in which both individual Λ subsystems exhibit electromagnetically-induced transparency (EIT), as indicated in the figure.

Phase Extraction using Homodyne Quadratures. By sending an alternating pulse sequence of three $2\mu s$ long probe pulses with $20\mu s$ interpulse delay into our homodyne detector, we can simultaneously obtain an accurate measurement of the phase-shift of our output light while also recovering quadrature statistics for quantum state reconstruction, as seen in the figure.

Quantum State Reconstruction. Using the assembled quadrature statistics extracted from our pulse sequences and the techniques for identifying and binning by output phase shifts, we perform maximum-likelihood estimation to reconstruct density matrices of the underlying quantum states, sorted by their post-selected, phase-shifted values. Despite being mediated by a room-temperature FWM process, the phase-shifted quantum state's overlap with input state reaches values as high as 94% with a phase shift of 1.29 radians for the probe and signal simultaneously at the few-photon level.

Analysis of Four-wave Mixing Contribution. Having such a large fidelity is surprising for a room-temperature system, as fundamental four-wave-mixing effects have been observed to destroy fidelities of quantum memories at the single-photon level. To observe this, we reconstruct the quantum state of the four-wave mixing and observe that it is fundamental to the generation of our phase-shifted light. We observe that this generated FWM light in the Fock state basis does not get substantially distorted and remains as a pure state.

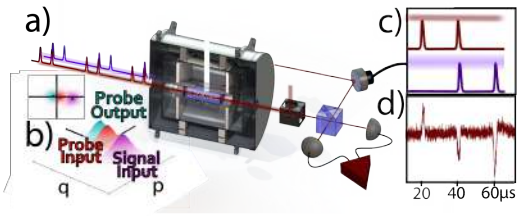


Figure 1: **a) Experimental setup. b)**Wigner functions of reconstructed input and output states from quadrature data. **c,d) Illustration and output quadratures of pulse sequences:** The first, second and third pulses in the sequence measure the probe output light's phase and quadrature values produced by the reference EIT, the full-double lambda system, and four-wave mixing respectively.

Future Work. While such a system has immediate applications for all-optical computing, with recent theoretical developments [5], we envision a similar scheme, incorporating weak nonlocalities, to be the first candidate for a high-fidelity, room-temperature photon-photon gate. We are currently working towards two-mode quantum process characterization of similar systems. With the recent success quantum memories at room-temperature[6], warm atomic systems are becoming a particularly promising emergent architecture to achieve large quantum processing networks.

[1] D. Tiarks, S. Schmidt, G. Rempe, and S. Durr, Science Advances **2**, 1600036 (2016).

[2] Z.-Y. Liu, Y.-H. Chen, Y.-C. Chen, H.-Y. Lo, P.-J. Tsai, I. A. Yu, Y.-C. Chen, and Y.-F. Chen, Phys. Rev. Lett. 117, 203601 (2016).

[3] R. Shahrokhshahi, S. Sagona-Stophel, B. Jordaan, M. Namazi, E. Figueroa `https://arxiv.org/abs/1803.07012` (2018).

[4] M. Artoni and A. Zavatta, Phys. Rev. Lett. 115, 113005 (2015).

[5] B. Viswanathan and J. Gea-Banacloche Phys. Rev. A 97, 032314 (2018).

[6] M. Namazi, C. Kupchak, B. Jordaan, R. Shahrokhshahi, and Eden Figueroa Phys. Rev. Applied 8, 034023

Dark State Optical Lattice with a Subwavelength Spatial Structure

Y. Wang[1], S. Subhankar [1],P. Bienias[1], M. Łącki[3,4,5], T-C. Tsui[1], M. A. Baranov[3,4], A. V. Gorshkov[1,2], P. Zoller[3,4], J. V. Porto[1], and S. L. Rolston[1]

[1] *Joint Quantum Institute, National Institute of Standards and Technology and the University of Maryland, College Park, Maryland 20742 USA*

[2] *Joint Center for Quantum Information and Computer Science, National Institute of Standards and Technology and the University of Maryland, College Park, Maryland 20742 USA*

[3] *Institute for Quantum Optics and Quantum Information of the Austrian Academy of Sciences, A-6020 Innsbruck, Austria*

[4] *Institute for Theoretical Physics, University of Innsbruck, A-6020 Innsbruck, Austria*

[5] *Jagiellonian University, Institute of Physics, Łojasiewicza 11, 30-348 Kraków, Poland*

e-mail: *sarthaks@umd.edu*

Optical dipole potentials are used extensively in ultracold atomic physics for dipole trapping, engineering exotic lattice geometries, study of many-body physics, etc. These potentials, however, are constrained by the diffraction limit of the trapping light to have minimum spatial features of order the optical wavelength. Using the non-linear atomic response of a three-level atom, one can engineer optical potentials based on spatially dependent atomic dark states [1,2]. These potentials arise as effective geometric scalar potentials experienced by three-level atoms in the Λ configuration in a spatially varying dark state, and result in repulsive barriers that can be of the order of tens of nanometers in width.

We report on the experimental demonstration of such a lattice of ultranarrow barriers with widths less than 10 nm, well below the wavelength of the trapping light. Using this technique we physically realize a Kronig-Penney(KP) potential using ^{171}Yb [3]. Even on resonance, the observed lifetimes of atoms trapped in the lattice is 44 ms, nearly 10^5 times the excited state lifetime, and could be further improved with more laser intensity. The experimental realization of such a system can allow for the realizations of sharp walled optical box traps, detection of topological edge states, narrow tunnel junctions for atomtronics applications, stroboscopically generated lattice with sub-wavelength spacings, etc.

In line with the scope of this work [4,5], we also report on progress to perform super-resolution imaging of a wavefunction. The non-linearity of the atomic response allows the spin composition of the dark state wavefunction to change at sub-wavelength scale. We use this nonlinearity to locally flip the spin of a spatial slice of a target wavefunction and image the population of atoms in that slice using spin-selective imaging. The measured population is a direct measure of the probability density of the wavefunction at that spatial position. By stacking the measured population of contiguous spatial slices together, we effectively map out the target wavefunction.

References

[1] M. Łącki, M.A. Baranov, H. Pichler, and P. Zoller, Phys. Rev. Lett. 117, 233001(2016)

[2] F. Jendrzejewski, S. Eckel, T. G. Tiecke, G. Juzeliūnas, G.K. Campbell, Liang Jiang, and A.V. Gorshkov, Phys. Rev. A 94, 063422(2016)

[3] Y. Wang, S. Subhankar, P. Bienias, M. Łącki, T-C. Tsui, M.A. Baranov, A.V. Gorshkov, P. Zoller, J.V. Porto, and S.L. Rolston, Phys. Rev. Lett. 120, 083601 (2018).

[4] D.D. Yavuz, N. A. Proite, Phys. Rev. A 76, 041802(R) (2007).

[5] D. Yang, C. Laflamme, D. V. Vasilyev, M. A. Baranov, and P. Zoller, Phys. Rev. Lett., 120, 133601 (2018)

Quantum Monte Carlo description of dipolar droplets

F. Mazzanti[1], **R. Bombin**[1], **J. Sánchez-Baena**[(1)] **and J. Boronat**[1]
[1] *Departament de Física, Universitat Politècnica de Catalunya, 08034 Barcelona, Spain*
e-mail: *ferran.mazzanti@upc.edu*

Recent experiments [1, 2] have reported on the formation of stable quantum droplets containing approximately from several hundreds to several thousands of ^{164}Dy atoms in the region of mean-field collapse. In these systems, beyond-mean-field effects become very important and dramatically limit the stability of the formed droplets through the compensation of attractive and repulsive forces, be means of a mechanism similar to the one described in [4].

From a theoretical point of view, these droplets have been analyzed in the framework of the extended Gross-Pitaevskii equation [3], which incorporates Lee-Huang-Yang corrections to the energy functional but still provides a mean-field picture of the system. In this work we use the Path Integral Ground State (PIGS) [5] method to describe the formation of droplets of dipolar bosons. Starting from a sensible model wave function of the many-body problem, stochastic propagation in imaginary time leads to an unbiased decryption of the exact ground state without further approximations. In this sense, the result is *exact* within statistical uncertainties. We analyze the critical number of atoms required to form a droplet as a function of the initial trapping aspect ratio, using a model two-body interaction that describes the known scattering properties of the Dy-Dy potential. Parameters such as the scattering length are fixed by solving the T-matrix problem corresponding to the combined two-body isotropic potential and the dipole-dipole force.

References

[1] H. Kadau, M. Schmitt, M. Wenzel, C. Wink, T. Maier, I. Ferrier-Barbut, and T. Pfau, Nature 530, 194 (2016).

[2] I. Ferrier-Barbut, H. Kadau, M. Schmitt, M. Wenzel and T. Pfau, Phys. Rev. Lett.**116**, 215301 (2016).

[3] I. Ferrier-Barbut, M. Wenzel, M. Schmitt, F. Böttcher and T. Pfau, Phys. Rev. A **97**, 011604(R) (2017).

[4] D.S.Petrov, Phys. Rev. Lett.115, 155302 (2015).

[5] A. Sarsa and K. E. Schmidt, J. Chem. Phys.**113**, 1366 (2000).

Dynamical transfer of vortex states between two coupled Bose-Hubbard rings

M. Guilleumas[1,2], **A. Escrivà**[1,2], **and B. Juliá Díaz**[1,2]
[1] *Departament de Física Quàntica i Astrofísica, Universitat de Barcelona, 08028 Barcelona, Spain*
[2] *Institut de Ciències del Cosmos, Universitat de Barcelona, 08028 Barcelona, Spain*
e-mail: *muntsa@fqa.ub.edu*

We consider two coupled Bose-Hubbard rings [1, 2] with two different tunneling strengths populated by ultracold bosons with repulsive interactions. The atoms can either tunnel between the sites of the same ring, with a given inter-ring coupling, or between the sites of different rings coupled via the rungs by an intra-ring coupling. By solving the corresponding Bose-Hubbard Hamiltonian we obtain the many-body ground state for different values of the interaction and tunneling strengths. We characterize the static properties of the ground state by means of coherence, correlations and entanglement.

We have studied the transfer of quantized vortex states between the two rings as a function of the tunneling parameters and atom-atom interaction strength by direct diagonalization of the Hamiltonian. We have identified two different regimes: i) for large interactions the chiral current is suppressed forming a Meissner-like phase [3, 4] (no vortex transfer) and the system fragments, and ii) for small interactions the system remains coherent, the behaviour of the chiral current is periodic and the mean-field approximation provides a good description [5].

[1] D. Aghamalyan, L. Amico and L. C. Kwek, Phys. Rev. A **88**, 063627 (2013).

[2] T. Haug, L. Amico, R. Dumke and L.-C. Kwek, e-print arXiv:1612.09109 (2018).

[3] M. Atala, M. Aidelsburger, M. Lohse, J.T. Barreiro, B. Paredes and I. Bloch, Nat. Phys. **10**, 237208 (2014).

[4] A. Richaud and V. Penna, Phys. Rev. A **96**, 13620 (2017).

[5] A. Gallemí, A. Muñoz Mateo, R. Mayol and M. Guilleumas, New J. Phys. **18**, 015003 (2016).

Matter Wave Subradiance with Bose-Einstein Condensates in an Optical Ring Resonator

P. Wolf[1], **S. C. Schuster**[1], **D. Schmidt**[1], **S. Slama**[1] **and C. Zimmermann**[1]
[1] *Universität Tübingen, Physikalisches Institut, 72076 Tübingen, Germany*
e-mail: *philip.wolf@uni-tuebingen.de*

We experimentally demonstrate matter wave subradiance with ^{87}Rb Bose-Einstein condensates inside an optical ring resonator with sub recoil resolution. The atoms are pumped transversally with laser light that contains two frequency components that resonantly drive cavity assisted Raman-transitions A,B between three discreet atomic momentum states $c_{0,1,2}$ (see Fig. 1).

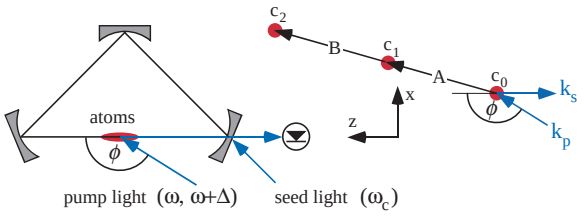


Figure 1: Scheme for matter wave subradiance. The three level system of atomic momentum is indicated as red dots in momentum space (right subplot). The sequence of momentum states is limited to three with respect to the small field decay rate of the high-finesse cavity. Pump light with two components of frequency ω and $\omega + \Delta$ is scattered into the same optical mode of a recoil resolving ring resonator. The scattered photons induce the decay of the atomic population $|c_n|^2$ from $n = 0$ to $n = 1$ (transition A) and $n = 1$ to $n = 2$ (transition B). The wave vectors of pump and scattered light for transition A are shown as blue arrows.

Within a few hundred micro seconds, the system evolves into a stationary subradiant state leaving the atoms in a superposition of the three momentum states. The relative population of the three states and the scattered light field into the cavity a is shown in Fig. 2. A series of subradiant states for amplitude ratios $\varepsilon = E_1/E_0$ of the two pump components between 0 and 2.1 have been observed with up to 50% of the atoms remaining in the initial zero momentum state.

By turning off one of the frequency components in the pump beam the subradiant state can be destroyed and the system fully decays. Furthermore, the decay dynamics in and out of the subradiant state can be triggered by a resonant seed pulse. For the future it will be interesting to study quantum correlations of the subradiant state [1] and explore possible applications for storage of quantum information [2].

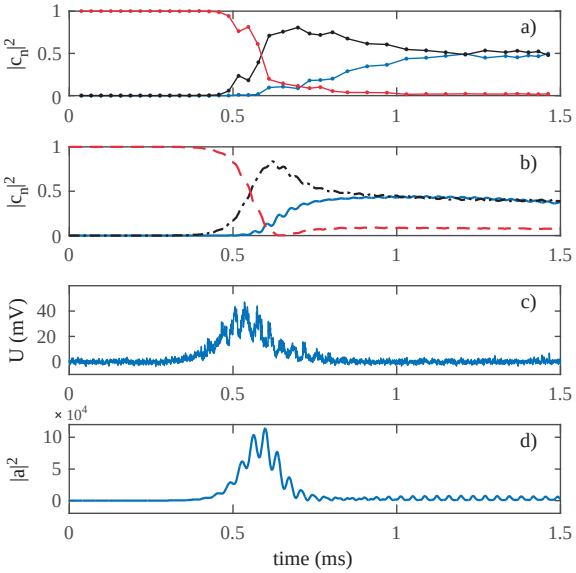


Figure 2: Relaxation into the subradiant state. a) Observed relative population $|c_n|^2$ of the momentum states with $n = 0, 1, 2$ (red, black, blue dots) for various holding times after turning on the pump beams. The amplitude ratio $\varepsilon = 0.6$ and the total pump power amounts to 1.9 mW. Each data point shows an average over six experimental cycles. b) Simulation for the populations for the parameters of a) with $n = 0, 1, 2$ (red dashed, black dash-dotted, and blue solid line). c) Power in the cavity mode during a typical cycle ($\varepsilon = 0.6$) and d) simulation.

References

[1] M. M. Cola, D. Bigerni, and N. Piovella, Phys. Rev. A 79, 053622 (2009).

[2] Hans J. Briegel and Robert Raussendorf, Phys. Rev. Lett. 86, 910.

Non-linear spin dynamics in atomic magnetometers

R. Gartman[1], V. Guarrera[1], G. Bevilacqua[2], W. Chalupczak[1]

[1] National Physical Laboratory, Hampton Road, Teddington, TW11 0LW, United Kingdom
[2] Università di Siena, Siena, Italy

Atomic magnetometers create a versatile platform for magnetic field measurement with applications ranging from fundamental physics, navigation, and chemical analysis to security and medical screening. The simplicity of the experiment instrumentation is matched by the richness of the linear and non-linear couplings between system components (atomic vapour and pump/probe lasers).

We are going to show experimental studies indicating that the couplings introduced by the pump beam, the optical probe as well as spin-exchange collisions could generate non-linear atomic spin dynamics. This might lead to an increase in the coherence lifetime and generation of atomic spin squeezing. The former will be demonstrated and discussed in context of so-called spin maser, and the latter in a framework of parametric excitation in Bell-Bloom pumping process, where the atomic coherences are created by the train of optical excitation pulses.

[1] W. Chalupczak, and P. Josephs-Franks, *Phys. Rev. Lett.* **115**, 033004 (2015).

Studying Quantum Turbulence in Two Species Superfluid: Cooling Process for Potassium Specie

H. V. Duque[1], E. D. M. Gutierrez[1], P. E. S. Tavares[1], P. L. Mazo[1], G. A. Neto[1], J. A. Scarpin[1], K. M. Farias[1] and V. S. Bagnato[1]

[1] *São Carlos Institute of Physics, University of São Paulo, PO Box 369, 13560-970, São Carlos, SP, Brazil*
e-mail: *hum_vargas@hotmail.com*

We present an experimental apparatus to produce a Bose-Einstein Condensate (BEC) of two atomic species, ^{23}Na e ^{41}K. BEC Mixtures are important to study many properties and phenomena of matter in quantum state, such as miscible/immiscible phase diagram for trapped two species BEC, vorticity transmission between species, quantum turbulence in the two specie BEC and so on.

As part of the apparatus described on Castilho [1], we have a system dedicated to generate cold atom Potassium that is interchangeable between its most abundant isotopes, ^{41}K and ^{39}K. The small energy between their transitions makes easier to transitate from ^{39}K to its isotope ^{41}K, it is an advantage once we can maximize the flux of atoms using its more abundant isotope ^{39}K, with 93,26% abundance, while the second most abundant has 6,73%.

The atoms comes from an oven heated to about 140 ^{o}C whom in a pre-cooling stage we use an Adapted 2 Dimensional Magnetico-Optical Trap Zeeman-Slower (2D-MOT-ZS) technique. This technique is based on that described by E. Pedrozo-Peafiel [2] for the Sodium System in the present Apparatus. In that configuration the hot atoms are cooled down by the use of counter-propagating light to the atom beam, which combined with a spatially dependent magnetic field, that changes the energy transition due to the Zeemann effect, compensate the Doppler shift caused by the atoms deceleration. This technique, called Zeemann-Slower, keeps the atoms in a decreasing velocity process over the path to the 2D MOT. After losing energy due to the Zeemann Slower, the confining of neutral atoms is done by using the combination of an inhomogeneous magnetic eld and circular polarized light near-resonant to a cycling transition in a 2-dimensional configuration, 2D-MOT. Note here we use the same magnetic field for both techniques, once the requirements of the magnetic field for the 2D-MOT are met by adjusting a zero in the center of the crossed beam and opposites directions in the vertical.

The atoms that were cooled down in the 2D-MOT-ZS are transferred using a laser beam that pushes the atoms through the nontrapable direction of the 2D-MOT to the 3D-MOT.

Before transfer the atoms to the Quadrupole conservative trap to achieve high phase-space densities we perform a Gray Molasses technique with light close to the D1 line transition [3]. With the much cooler cloud of Sodium atoms, we will use the sympathetic cooling process [4], to reach lower temperatures with Potassium. This will them be sufficient to finally perform the evaporative cooling and obtain the Two Species BEC.

[1] Patricia C. M. Castilho *et al.*, To be published. A compact experimental machine for studying tunable Bose-Bose superfluid mixtures.

[2] E Pedrozo-Peafiel *et al.*, Laser Physics Letters **13**, 065501 (2016).

[3] Hao-Ze Chen *et al.*, Phys. Rev. A **94**, 033408 (2016).

[4] Modugno *et al.*, Science **294**, 1320-1322 (2001).

Vortex lattices in binary Bose-Einstein condensates with dipole-dipole interactions

R. Kishor Kumar[1], L. Tomio[2], B. A. Malomed[3] and A. Gammal[1]
[1] *Instituto de Física, Universidade de São Paulo, 05508-090 São Paulo, Brazil*
[2] *Instituto de Física Teórica, Universidade Estadual Paulista, 01156-970 São Paulo, SP, Brazil*
[3] *Department of Physical Electronics, School of Electrical Engineering, Faculty of Engineering, Tel Aviv University, Tel Aviv 69978, Israel*
e-mail: *kishor@if.usp.br*

We study the structure and stability of vortex lattices in two-component rotating Bose-Einstein condensates with intrinsic dipole-dipole interactions (DDIs) and contact interactions. To address experimentally accessible coupled systems, we consider ^{164}Dy-^{162}Dy and ^{168}Er-^{164}Dy mixtures, which feature different miscibilities. The corresponding dipole moments are $\mu_{\rm Dy} = 10\mu_{\rm B}$ and $\mu_{\rm Er} = 7\mu_{\rm B}$, where $\mu_{\rm B}$ is the Bohr magneton. For comparison we also discuss a case where one of the species is non dipolar. Under a large aspect ratio of the trap, we consider mixtures in the pancake-shaped format, which are modeled by effective two-dimensional coupled Gross-Pitaevskii equations, with a fixed polarization of the magnetic dipoles. Then, vortex-lattice structures are studied, by varying the coe cients of the contact interactions (assuming the use of the Feshbach-resonance mechanism) and the rotation frequency. We present phase diagrams for several types of lattices in the parameter plane of the rotation frequency and ratio of inter- and intra-species scattering lengths. The vortex structures are found to be diverse for the more miscible ^{164}Dy-^{162}Dy mixture, with a variety of shapes, whereas for the less miscible case of ^{168}Er-^{164}Dy, the lattice patterns mainly feature circular or square formats.

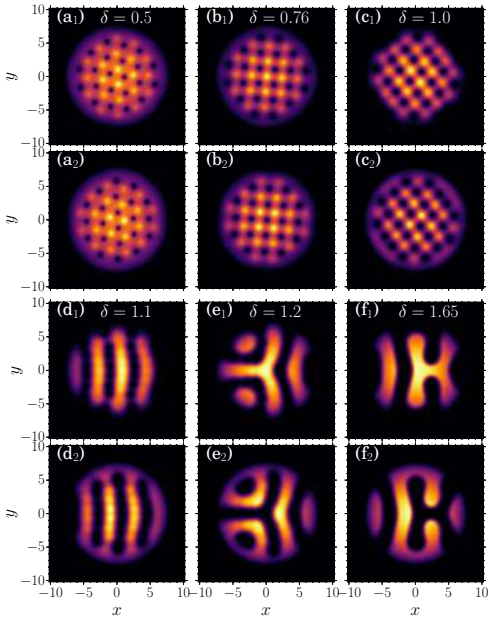


Figure 1: 2D component densities, $|\psi_j|^2$ [(a_j) to (f_j), with j =1,2], for the ^{164}Dy-^{162}Dy mixture in different patterns of stable vortices, for $\delta = a_{12}/a_{11}$ varying from 0.5 to 1.65, as indicated. The lattices are triangular ($a_{j=1,2}$), squared ($b_{j=1,2}$), rectangular ($c_{j=1,2}$), striped ($d_{j=1,2}$), and with domain walls [($e_{j=1,2}$) and ($f_{1,2}$)]. Other parameter are: $N_{j=1,2} = 10^4$, $\lambda = \omega_z/\omega_\rho = 20$, $a_{12} = 50a_0$, and $\Omega = 0.4$.

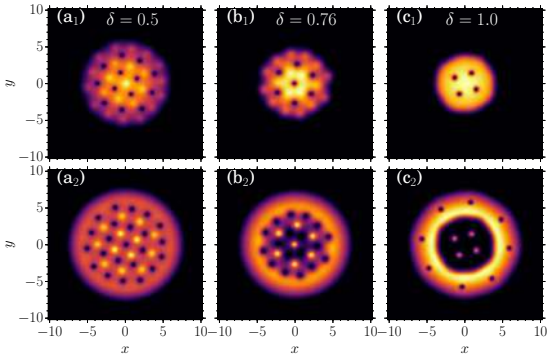


Figure 2: 2D component densities, $|\psi_j|^2$ [(a_j) to (c_j), with j =1,2], for the ^{168}Er-^{164}Dy mixture, we have the 2D densities $|\psi_j|^2$, for several values of δ and rotation frequency $\Omega = 0.4$, with the other parameters given by $N_{j=1,2} = 10^4$, $\lambda = 20$ and $a_{12} = 50a_0$.

[1] R. K. Kumar, L. Tomio, B. A. Malomed, and A. Gammal, Phys. Rev. A **96**, 063624 (2017).

[2] R. K. Kumar, L. E. Young-S, D. Vudragović, A. Balaž, P. Muruganandam and S. K. Adhikari, Comput. Phys. Commun. **195**, 117-128 (2015).

Ultracold collisional magnetic gradiometer

K. Jachymski[1], **T. Wasak**[2], **A. Negretti**[3], **and T. Calarco**[4]

[1] *Institute for Theoretical Physics III, University of Stuttgart, Germany*

[2] *Faculty of Physics, University of Warsaw, Poland*

[3] *Center for Optical Quantum Technologies, University of Hamburg, Germany* [3] *Institute for Complex Quantum Systems, University of Ulm, Germany*

e-mail: *jachymski@itp3.uni-stuttgart.de*

Feshbach resonances, which allow for tuning the interactions of ultracold atoms with an external magnetic field, have been widely used to control the properties of quantum gases. We propose a scheme for using scattering resonances as a probe for external magnetic fields, showing that by carefully tuning the parameters it is possible to reach a sensitivity of the order of 1 nT for the field strength and 100 nT/mm for its gradient.

The working principle of our sensor is schematically presented in Fig. 1. We consider an ensemble of noninteracting atoms (red wave packets on the left-hand side). Each atom is being injected into its corresponding quasi-one dimensional waveguide (blue cylinders). Such a setup can be experimentally realized by means of a deep three-dimensional (3D) optical lattice with single-site access, which is relaxed in the longitudinal direction in a controlled way. In the centre of each waveguide there is a tightly confined atom (green spheres). The collision can lead to transmission or reflection of the incoming atoms by the impurity. Transmitted and reflected atoms are then detected. The sensitivity of the measurement on the magnetic field is due to a Feshbach resonance that controls the interaction strength between the atom and the impurity. It is possible to tune the parameters in such a way that the probability of reflecting the colliding atom back from the impurity strongly depends on the local value of the magnetic field. The spatial spread of the waveguides allows to gather information about the average magnetic field strength at their positions, therefore providing information about the field gradient.

In order to calculate the transmission of atoms through the waveguide we employ the solution of the scattering problem for quasi-1D systems. The external trap leads to series of confinement-induced resonances which can be extremely narrow. The high precision of the protocol makes use of these resonances.

We derive the metrological bounds for the achievable precision of the sensor using multiparameter estimation theory. In particular, for a single atom the precision of the measurement is bounded by the Fisher information, which can be expressed in terms of the probability distribution of different outcomes

$$F = \sum_{s=\pm 1} \frac{1}{P(s|B)} \left(\frac{\partial P(s|B)}{\partial B} \right)^2 , \qquad (1)$$

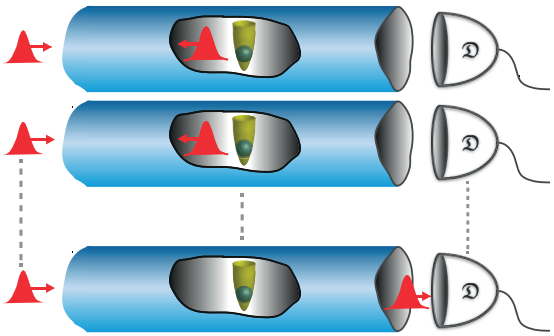


Figure 1: Schematic idea of the collisional sensor.

where the transmission probability is $P(+1|B) \equiv T(B)$, and the probability of reflecting the atom is $P(-1|B) \equiv 1 - T(B)$.

Then we show that for our collisional setup it is possible to saturate the quantum precision bound with a simple measurement protocol. This can be intuitively understood as follows: After the collision the particle is in a superposition of being transmitted or reflected with respective probability amplitudes. The modulus and phase of these amplitudes depend on the magnetic field. The transmission measurement we propose is only capable of determining the moduli of the amplitudes, while the information about the field encoded in the phases is lost. However, the phases of the amplitudes are always equal and form a common phase factor which cannot improve the precision.

[1] K. Jachymski *et al*, Phys. Rev. Lett. **120**, 013401 (2018)

[2] T. Wasak *et al*, arXiv:1803.03024 (2018).

A three-mode treatment of spin-1 ultra-cold quantum gases with spin-orbit coupling

J. Cabedo*, **J. Mompart, and V. Ahufinger**
Departament de Física, Universitat Autònoma de Barcelona, 08193 Bellaterra, Spain
*e-mail: *josep.cabedo@uab.cat*

Spin-orbit coupling (SOC) links a particle's spin to its motion and has a crucial role in the electronic properties of many condensed matter systems, being at the basis of phenomena such as the spin-Hall effect and topological insulators. The high level of control of ultracold atoms makes them ideal candidates to engineer spin-orbit coupling in neutral systems [1]. In particular, by dressing two atomic spin states of a Bose-Einstein condensate (BEC) with a pair of lasers in a Raman configuration, spin-1/2 SOC can be realized, with equal Rashba and Dresselhaus couplings. Its phase diagram is characterized by the existence of three phases: the stripe, the plane-wave and the single-minimum phase, which merge in a characteristic tricritical point [2–4]. Furthermore, larger spin SOC can be realized by dressing three or more internal atomic states [5] [6].

Spin-1 SOC can be engineered by two simultaneous Raman transitions, which at weak coupling lead to a triple-well in the lowest band of the single-atom dispersion relation. Here we investigate the properties of spin-1 SOC quantum gases following a three-mode approximation [7]. We derive a many body Hamiltonian for a trapped and dressed weakly interacting gas, which is numerically and analytically studied. The non-locality in momentum space of the two-body interaction processes gives rise to interaction-mediated tunneling-like terms. Notably, an effective two-particle tunneling dominates at weak trapping regime, which supposes a marked deviation from the position space triple-well many-body problem (Fig. 1). This term is responsible for step-like variations in several observables, such as the transverse spin polarization, the condensed fraction and the quantum correlations in the ground state of the system as the strength of the interactions is increased (Fig. 2).

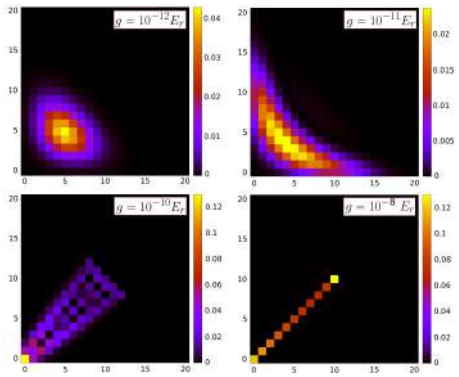


Figure 1: Population distribution of the ground state of the triple-well system in momentum space in the left- and right-well Fock for 20 particles, for different values of the interaction strength g, scaled to the recoil energy E_r. The trapping frequency is set to $10^{-2} E_r$.

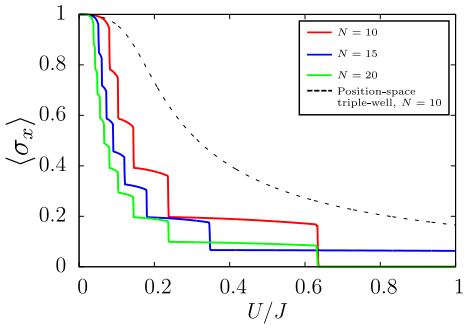


Figure 2: Mean transverse spin polarization $\langle \sigma_x \rangle = \frac{1}{\sqrt{2}} \left\langle (\hat{b}_R^\dagger + \hat{b}_L^\dagger)\hat{b}_M + h.c. \right\rangle$ of the ground state as a function of the interaction-tunneling coefficients ratio U/J, at weak-trapping regime, for $N = 10$, $N = 15$ and $N = 20$ particles.

References

[1] Y. Zhang, M. E. Mossman, Th. Busch, P. Engels, and C. Zhang, *Frontiers of Physics* **11**, 118103 (2016).

[2] Yun Li, G. I. Martone, S. Stringari, *Annual Review of Cold Atoms and Molecules*, Vol.**3** (World Scientific, 2015), Chap. 5, pp. 201-250.

[3] Y.-J. Lin,K. Jiménez-García, and I. B. Spielman, *Nature* **471**, 83 (2011).

[4] Jun-Ru Li *et al.*, *Nature* **543**, 91 (2017).

[5] Z. Lan, P. Öhberg, *Phys. Rev. A* **89**, 023630 (2014).

[6] G. I. Martone, F.V. Pepe, P. Facchi, S, Pascazio, S. Stringari, *Phys. Rev. Lett* **177**, 125301 (2016).

[7] J. Higbie and D. M. Stamper-Kurn, *Phys. Rev. A* **69**, 053605 (2004).

Tomography of Correlation Functions in Sodium Bose-Einstein Condensates

H.-Y. Liang[1], **Y.-B. Yang**[1], **T. Tian**[1], **H.-X. Yang**[1], **L.-Y. Qiu**[1], **A.-J. Chu, Y.-M. Liu**[2], **and L.-M. Duan**[1,3]

[1] *Center for Quantum Information, IIIS, Tsinghua University*
[2] *Department of Physics, Oklahoma State University*
[3] *Department of Physics, University of Michigan, Ann Arbor*
e-mail: *lianghy15@mails.tsinghua.edu.cn*

We present a novel experimental scheme for reconstructing single-particle correlation functions of ultracold atoms from absorption images taken after various time of flights. We plan to experimentally demonstrate the e ciency of this scheme in two different systems, i.e., a sodium Bose-Einstein condensate (BEC) with an imprinted phase controlled by a digital mirror device, and a quasi-one-dimensional Bose gas of ultracold sodium atoms. This scheme is independent of atomic species, and may thus be applicable to other ultracold atomic systems.

Spin-orbit coupling in quantum systems: a quantum Monte Carlo approach

J.Sánchez-Baena[1], **F.Mazzanti**[1], **and J.Boronat**[1]
[1] *Departament de Física, Universitat Politècnica de Catalunya, 08034 Barcelona, Spain*
e-mail: *juan.sanchez.baena@upc.edu*

The interplay between an electron's spin and its momentum, denoted as spin-orbit coupling (SOC), is an effect of major relevance when studying a wide variety of systems in the field of solid-state physics, such as Majorana fermions [1], spintronic devices [2] or topological insulators [3]. The realization in the last few years of a synthetic SOC interaction in ultracold atomic gases represents an important achievement, as the high controllability of these systems allows for a better understanding of the nature of SOC.

We present two different Diffusion Monte Carlo algorithms to deal with Hamiltonians featuring synthetic spin-orbit coupling interactions: the T-moves DMC [4] [5] and an original method created in our group, the Spin-rotation DMC. While an effective Hamiltonian must be defined in the T-moves approach to cure a sign problem in the propagator, we overcome this issue with the Spin-rotation DMC by propagating the spin-integrated wave function in imaginary time. Because of this, we are able to get an energy estimation closer to the ground state energy. We present a comparison between our DMC method and the T-moves DMC (Fig. 1). As a check for the viability of the method, we also compare the DMC energies with results obtained with other numerical algorithms, finding very good agreement between both estimations (Figs. 1, 2)

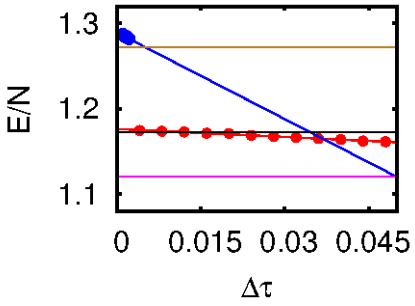


Figure 1: Diffusion Monte Carlo energies as a function of the time step (lines with points, red for the spin-rotation DMC and blue for the T-moves DMC) vs imaginary time evolution energies (straight lines, magenta for the ground state, black for the fixed phase energy and orange for the effective Hamiltonian, fixed phase energy) for a system of two interacting particles in a harmonic trap with Rashba SOC. The energy estimation is linear with $\Delta\tau$ for the T-moves DMC, although it can not be seen in the Figure because of the small time step needed in the simulations.

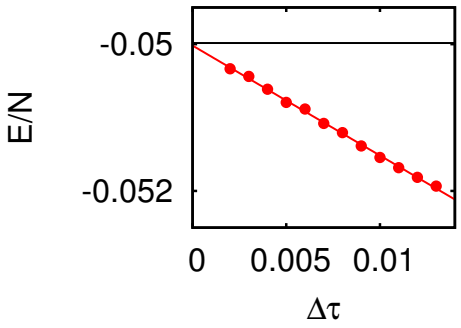


Figure 2: Spin rotation Diffusion Monte Carlo energies as a function of the time step (red line with points) vs fixed phase Gross-Pitaevskii equation energy estimation (black straight line) for a system of forty interacting particles with Raman SOC in the dilute regime.

[1] F. Wilczek, Nat. Phys. **5**, 614 (Sep, 2009).

[2] J. D. Koralek, C. P. Weber, J. Orenstein, B. A. Bernevig, S.-C. Zhang, S. Mack, and D. D. Awschalom, Nature. **458**, 610 (2009).

[3] M. Z. Hasan and C. L. Kane, Rev. Mod. Phys. **82**, 3045 (2010).

[4] Cody A. Melton, M. Chandler Bennett and L. Mitas, J. Chem. Phys. **144**, 244113 (2016)

[5] M. Casula, S. Moroni, C. Filippi, S. Sorella, J. Chem. Phys. **132**, 154113 (2010)

Experimental determination of the equation of state of an interacting one-dimensional Bose gas.

F. Salces-Cárcoba[1], **C. J. Billington**[1], **A. Putra**[1], **Y. Yue**[1], **E. Altuntas**[1], **I.B. Spielman**[1]
[1] *Joint Quatum Institute, National Institute of Standards and Technology, and University of Maryland College Park, Gaithersburg, Maryland, 20899, USA*
e-mail: *pacosc@terpmail.umd.edu*

We realize individual trapped 1D Bose gases and compare their observed equation of state with the predictions of Yang-Yang thermodynamics [1]. We combine calibrated confining potentials with *in-situ* density profiles to obtain the equation of state.

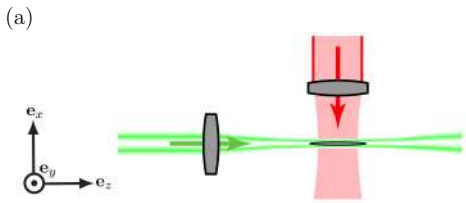


Figure 1: Schematic of the crossed dipole trap formed by a z-propagating blue-detuned LG_{01} beam and an x-propagating red-detuned gaussian beam.

Our realization helps breach the gap between 2D-optical lattice and chip-based experiments that also study 1D Bose gases by enabling the possibility of studying individual single and multi-component interacting systems.

Our experiment is benchmarked against the exact infinite-system 1D thermodynamic solutions under the local density approximation which has allowed us to identify a breakdown of adiabaticity in our loading procedure. We discuss some of the implications of this for future experiments.

[1] C. P. Yang and C. N. Yang, Journal of Mathematical Physics **10**, 7, 1115-1122 (1969).

Towards Quantum Many-Body Physics with Strontium in Optical Lattices

André Heinz[1], Annie Jihyun Park[1], Fabian Finger[1], Stepan Snigirev[1], Jean Dalibard[2], Immanuel Bloch[1], and Sebastian Blatt[1]

[1]*Max-Planck-Institut für Quantenoptik, Hans-Kopfermann-Straße 1, 85784 Garching, Germany*
[2]*Laboratoire Kastler Brossel, Collège de France, ENS-PSL Research University, CNRS, UPMC-Sorbonne Universités, 11 place Marcelin Berthelot, 75005 Paris, France*
e-mail: *sebastian.blatt@mpq.mpg.de*

Within the last decade, fermionic strontium atoms in optical lattices have become a platform for precision measurements [1], culminating in the realization of a Sr optical lattice clock with the currently highest stability and accuracy at the 2×10^{-18} level [2]. In the meantime, quantum degenerate gases of all bosonic and fermionic isotopes of Sr have been realized [3]. With the extension of the quantum gas microscopy technique to fermionic alkali metal atoms, experiments with quantum degenerate gases in optical lattices have taken another step towards full control over the internal and external degrees of freedom of fermions in optical lattices [4, 5, 6, 7].

One of the crucial technical advances in the development of optical lattice clocks was the introduction of optical lattices at a wavelength where the polarizabilities of both clock states are matched — the so-called magic wavelength [8]. In the Sr atom, many other interesting polarizability ratios exist at easily-accessible wavelengths from the near ultraviolet to the near infrared. For instance, at so-called tuneout wavelengths, only one of the clock states is trapped and the other state can move freely [9]. Because of the (in principle) exact cancellation of the ground (excited) clock state polarizability at the $^1S_0$ ($^3P_0$) tuneout wavelength ~689 nm (~633 nm) [9], we will be able to realize such spin-dependent lattices with high fidelity.

Here, we report on our progress towards a new experiment to realize such internal-state-dependent control of the atomic motion: Ultracold Sr atoms will be trapped in a two-dimensional optical lattice in the plane of a high-resolution imaging system. The lattice wavelength is chosen at the $^3P_0$ tuneout wavelength such that the ground state atoms experience a standard red-detuned optical lattice, but the excited state atoms move freely. To this optical lattice, we propose to add another optical trap (e.g. optical tweezers) at the tuneout wavelength for the $^1S_0$ state.

The combination of optical traps at both tuneout wavelengths enables high-fidelity, state-dependent control of the atomic position, a key ingredient to realize collisional phase gates for quantum computation [10, 11], or quantum simulation schemes [12, 13, 14] involving spin-orbit coupling [15, 16]. In combination with magnetic field gradients and patterned excitation, it should become possible to create single-site- and single-atom-resolved images of optical lattices with sub-wavelength spacing.

An enabling technology for high-fidelity experiments of this type are deep and homogeneous optical lattice potentials. We report on progress towards an in-vacuum optical cavity (see Fig. 1) supporting two crossed modes with large waists ~0.5 mm. The cavity spacer is made from ultralow-expansion glass with optically contacted cavity mirrors.

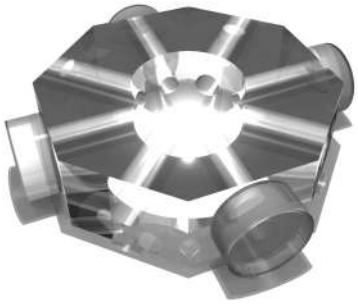


Figure 1: Monolithic, in-vacuum buildup cavity with 50 mm length supporting two crossed modes for optical lattices spanning ~1 mm^3.

[1] A. Ludlow, *et al.*, Rev. Mod. Phys. **87**, 637 (2015).
[2] T. L. Nicholson, *et al.*, Nat. Comm. **6**, 6896 (2015).
[3] S. Stellmer, *et al.*, Ann. Rev. of Cold Atoms and Molecules **2**, World Scientific (2014).
[4] L. W. Cheuk, *et al.*, Phys. Rev. Lett. **114**, 193001 (2015).
[5] M. F. Parsons, *et al.*, Phys. Rev. Lett. **114**, 213002 (2015).
[6] E. Haller, *et al.*, Nature Physics **11**, 738 (2015).
[7] A. Omran, *et al.*, Phys. Rev. Lett. **115**, 263001 (2015).
[8] J. Ye, *et al.*, Science **320**, 1734 (2008).
[9] M. S. Safronova, *et al.*, Phys. Rev. A **92**, 040501 (2015).
[10] A. J. Daley, *et al.*, Phys. Rev. Lett. **101**, 170504 (2008).
[11] A. J. Daley, Quant. Inf. Proc. **10**, 865 (2011).
[12] F. Gerbier and J. Dalibard, N. J. Phys. **12**, 03307 (2010).
[13] A. González-Tudela and J. I. Cirac, Phys. Rev. Lett. **119**, 143602 (2017).
[14] L. Krinner, *et al.*, arXiv:1712.07791 (2017).
[15] S. Kolkowitz, *et al.*, Nature **542**, 66 (2016).
[16] L. F. Livi, *et al.*, Phys. Rev. Lett. **117**, 220401 (2016).

Effective two-mode description of the dynamics of interacting bosons confined in a double-well trap

J. Dobrzyniecki[1] **and T. Sowiński**[1]

[1] *Institute of Physics of the Polish Academy of Sciences, Al. Lotników 32/46, 02-668 Warsaw, Poland*

e-mail: *jacek.dobrzyniecki@ifpan.edu.pl*

Typically, when the dynamics of a few bosons in a double-well potential is studied, one uses a two-mode model which assumes that particles can occupy the lowest orbitals localized in the left or the right well. Consequently all excited orbitals are neglected. A typical two-mode Hamiltonian, taking into account the tunneling between wells and the interactions between bosons, has the Bose-Hubbard form:

$$H = -J(\hat{a}_L^\dagger \hat{a}_R + \hat{a}_R^\dagger \hat{a}_L) + \frac{U}{2}(\hat{a}_L^\dagger \hat{a}_L^\dagger \hat{a}_L \hat{a}_L + \hat{a}_R^\dagger \hat{a}_R^\dagger \hat{a}_R \hat{a}_R)$$

where the operators $\hat{a}_L, \hat{a}_R$ annihilate a boson in a particular (left or right) well.

This traditional model is sufficient to describe the system for sufficiently deep wells and in a weakly interacting regime, i.e., where the interaction energy per particle is much smaller than the single-particle excitation energy. However, the model rapidly becomes inaccurate as the interparticle interaction strength grows, since couplings to higher bands become non-negligible.

In this work we show that, even for quite strong interactions, the dynamical properties of the system can be recovered accurately in the framework of a two-mode description if appropriate effective modifications are made. We describe two different approaches to this problem.

In the first method [1], we describe the system in terms of a specific basis of effective wave functions, uniquely tailored to the problem under study. The basis modes are directly derived from the many-body Hamiltonian. The shapes of the resulting basis wave functions take into account the interaction-induced modifications of the natural orbitals. This effective model gives accurate predictions over a wider range of interactions than the traditional model (Fig. 1b).

The second method [2], which can be used if the number of particles is larger than two, involves extending the many-body Hamiltonian with effective three-body interaction terms. These terms effectively account for various corrections that arise from virtual transitions to excited energy states. Two such terms, an on-site three-body interaction and an interaction-induced single-particle tunneling, are sufficient to recover the exact dynamics with excellent accuracy (Fig. 1c).

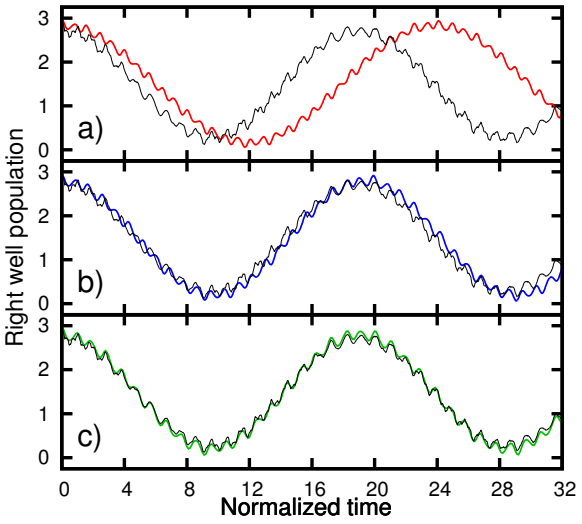


Figure 1: Time evolution of the population in the right well, for a system of three strongly interacting bosons initially occupying the chosen well, predicted by different models: an exact multi-mode model (thin black), the traditional two-mode model (solid red), the improved two-mode model using effective wave functions (solid blue), and the two-mode model extended with effective three-body interactions (solid green). The improved models proposed are clearly more accurate than the traditional two-mode model.

[1] J. Dobrzyniecki and T. Sowiński, Phys. Lett. A **382**, 394 (2018).

[2] J. Dobrzyniecki, X. Li, A. E. B. Nielsen, and T. Sowiński, Phys. Rev. A **97**, 013609 (2018).

Confinement-Induced Resonance of Alkaline-Earth-Metal Atoms in Anisotropic Quasi-one Dimensional Geometry

Q. Ji[1], **R. Zhang**[2], **and W. Zhang**[1,3]

[1] *Department of Physics, Renmin University of China, Beijing 100872, China*

[2] *Department of Applied Physics, School of Science, Xi'an Jiaotong University, Shanxi 710049, China*

[3] *Beijing Key Laboratory of Opto-electronic Functional Materials and Micro-nano Devices, Renmin University of China, Beijing 100872, China*

e-mail: *jiqinghappy@ruc.edu.cn*

We study the confinement-induced resonance(CIR) of alkaline-earth-metal atoms in anisotropic quasi-one-dimensional tube. Starting with solving the scattering problem, we present the location of CIR for various anisotropy and magnetic field in ^{173}Yb atoms. Our results show the anisotropy strength of the trapping potential can serve as a knob to shift the location of CIR. In particular, one can shift the location of CIR to the region attainable in current experiment. We also study the energy spectrum of such system and analysis the properties of CIR from the perspective of bound state. Considering the Zeeman energy difference between $|g\uparrow;e\downarrow\rangle$ and $|g\downarrow;e\uparrow\rangle$ channel, we define two threshold energies with different energy. It is found that CIR happens when the closed channel bound state energy is equal to either the higher or lower threshold energy.

Entanglement and dynamical phase transition in a spin-orbit-coupled Bose-Einstein condensate

F. X. Sun[1,2], **W. Zhang**[3,4], **Q. Y. He**[1,2] **and Q. H. Gong**[1,2]

[1] *State Key Laboratory of Mesoscopic Physics, School of Physics, Peking University, Collaborative Innovation Center of Quantum Matter, Beijing 100871, China*

[2] *Collaborative Innovation Center of Extreme Optics, Shanxi University, Taiyuan 030006, China*

[3] *Department of Physics, Renmin University of China, Beijing 100872, China*

[4] *Beijing Key Laboratory of Opto-Electronic Functional Materials and Micro-Nano Devices, Renmin University of China, Beijing 100872, China*

e-mail: *sunfengxiao@pku.edu.cn*

Characterizing quantum phase transitions through quantum correlations has been deeply developed for a long time, while the connections between dynamical phase transitions (DPTs) and quantum entanglement is not yet well understood. In this work, we show that the time-averaged two-mode entanglement in the spin space reaches a maximal value when it undergoes a DPT induced by external perturbation in a spin-orbit-coupled Bose-Einstein condensate. We employ the von Neumann entropy $\bar{E}$ and a correlation-based entanglement criterion $\bar{E}_{HZ}$ as entanglement measures and find that both of them can infer the existence of DPT, which is shown in Fig. 2. While the von Neumann entropy works only for a pure state at zero temperature and requires state tomography to reconstruct, the experimentally more feasible correlation-based entanglement criterion acts as an excellent proxy for entropic entanglement and can determine the existence of entanglement for a mixed state at finite temperature, making itself an excellent indicator for DPT. Our work provides a deeper understanding about the connection between DPTs and quantum entanglement and may allow the detection of DPT via entanglement become accessible as the examined criterion is suitable for measuring entanglement.

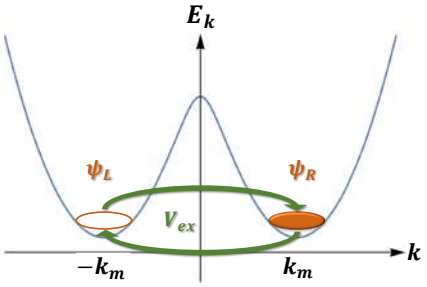


Figure 1: The external perturbation V_{ex} can induce resonant couplings between the two magnetized phases, marked as ψ_R and ψ_L at k_m and k_m , respectively.

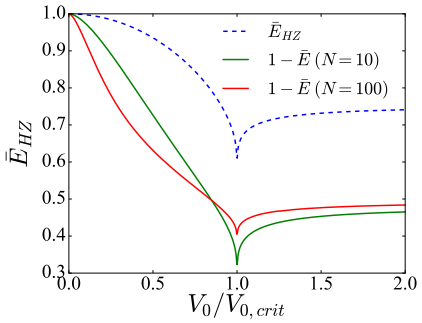


Figure 2: The time-averaged entropic entanglement measure $\bar{E}$ and correlation-based entanglement criterion $\bar{E}_{HZ}$shows a discontinuity in the first-order derivative, which signifies the occurrence of DPT.

[1] F. X. Sun, W. Zhang, Q. Y. He, Q. H. Gong, Phys. Rev. A **97**, 012307 (2018).

Finite-range Efimov physics in strongly-interacting Bose gases

P. M. A. Mestrom[1], **T. Secker**[1], **and S. Kokkelmans**[1]
[1] *Eindhoven University of Technology, P.O. Box 513, 5600 MB Eindhoven, The Netherlands*
e-mail: *p.m.a.mestrom@tue.nl*

Recent experimental progress has opened the door for exploration of the unitary Bose gas, which would lead to a deeper understanding of quantum many-body physics. This strongly interacting Bose gas is profoundly influenced by three-body phenomena such as the universal Efimov effect. Experiments with ultracold atomic gases revealed that the range of the two-body potentials is very important in the context of Efimov physics. We study finite-range effects on the universal Efimov spectrum for three identical spinless bosons interacting via several two-body potentials. First of all, we consider a square well potential and several separable approximations for this potential. Such two-body approximations are often used to go from few to many-body systems in the strongly interacting regime. We test the validity of these separable approximations on the three-body level in the context of Efimov physics and we show the limitations of such simple models. An example of such comparisons can be found in figure 1 which illustrates the Efimov spectrum for a shallow square well potential.

Secondly, we consider interactions with a Van der Waals tail. We calculate the three-body recombination rate at zero collision energy by solving the Faddeev equations in the momentum-space representation. We also study ultracold atom-dimer scattering processes. The Efimov features related to these three-body scattering processes are studied in a way which has not been done before. Our methods allow us to switch off any part of the considered interaction model without affecting the unitarity of the scattering matrix and to study the corresponding effects on the three-body observables. In particular, we show how d-wave dimer states modify the Efimov spectrum and the related observables. For example, figure 2 shows how well the results of our methods agree with those of the adiabatic hyperspherical approach. It also shows that we can relate features in the recombination rate to specific dimer states.

[1] P. M. A. Mestrom, J. Wang, C. H. Greene, and J. P. D'Incao, Phys. Rev. A **95**, 032707 (2017).

[2] J. Wang, J. P. D'Incao, Y. Wang, and C. H. Greene, Phys. Rev. A **86**, 062511 (2012).

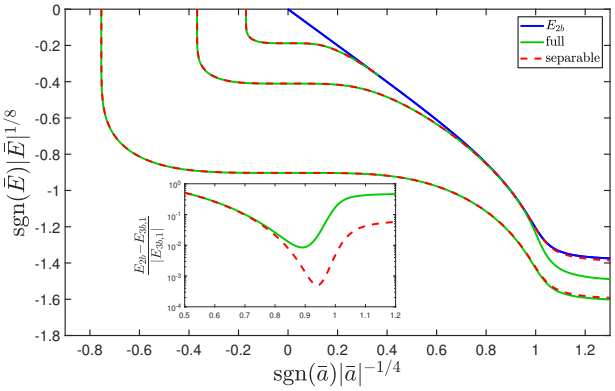


Figure 1: Energy of the lowest three Efimov states (green and red curves) calculated near the first potential resonance of the square well potential. The green curves involve the full square well potential as two-body interaction, whereas the red dashed curves involve a separable approximation for the square well potential. The blue line is the binding energy corresponding to the s-wave dimer state. The inset shows the relative energy difference between the energies of the s-wave dimer state and the second Efimov state as a function of the inverse scattering length.

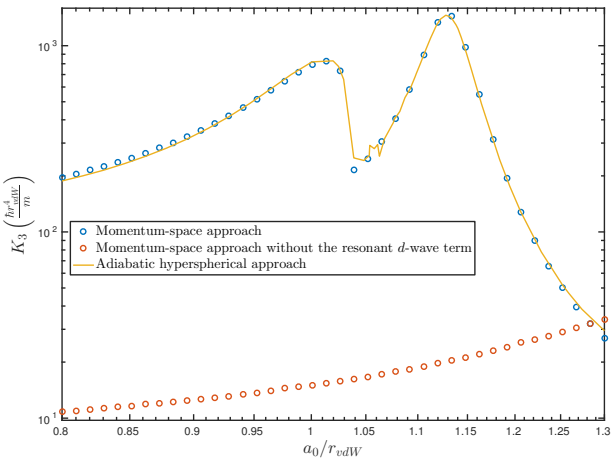


Figure 2: Zero-energy limit of the three-body recombination rate as a function of the two-body scattering length near the first potential resonance of the Lennard-Jones potential. The red data points correspond to a Lennard-Jones potential from which the expansion term which includes the (almost) bound d-wave dimer state is removed. This shows that the two peaks are related to this (almost) bound d-wave dimer state. The yellow curve is the data from Ref. [1] which is obtained from the adiabatic hyperspherical approach. Our results (blue data points) agree well with this position-space approach. More details of these features of K_3 can be found in Ref. [2].

Josephson oscillation and self-trapping in momentum space

Yi Zheng, Shiping Feng, and Shi-Jie Yang
Department of Physics, Beijing Normal University, Beijing 100875, China
e-mail: *yangshijie@tsinghua.org.cn*

The recent realization of synthetic dimension and gauge field in neutral atomic gases has intrigued exploration of fundamental many-body physics and band topology in lattice systems. A two-leg ladder with uniform flux provides a basic platform for simulating the Harper-Hofstadter Hamiltonian. Such system holds promise for investigating exotic physics such as (fractional) quantum Hall effects, chiral currents (which characterize the Meissner phase and the vortex phase), etc.

The two chains play the role of pseudo-spins which are coupled to the momentum via the gauge field. The energy-band structure reveals two local minima in the vortex phase. The macroscopic quantum systems condensed in these two minima can be regarded as a double-well model in momentum space (MS). On the other hand, the density oscillations of BECs in a double-well trap is regarded as the atomic Josephson effect (JE). Such effect, signified by the generalized Josephson current and the macroscopic quantum self-trapping (MQST), has been observed in experiments with ultra-cold atoms.

To generate the two-mode macroscopic quantum systems in momentum space as well as their coupling with modulated lattice gases. We propose a Creutz ladder in the presence of unconventional flux induced by complex tunneling rates along and between the two legs. The interaction in the effective two-mode model is related to the on-site interaction, which allows for a quantitative understanding of the Josephson effect and the self-trapping in momentum space.

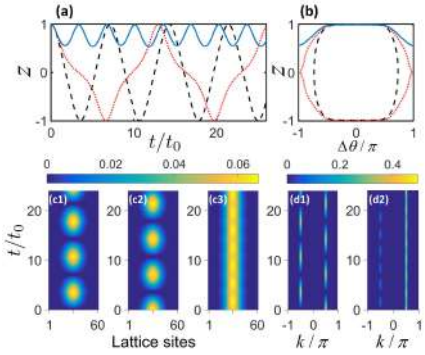


Figure 1: (a) The temporal evolution of population imbalance z for $U = 0.3$ (black dashed curve), $U = 0.475$ (red dotted curve) and $U = 0.6$ (blue solid curve), respectively. (b) The corresponding trajectories of (a) in phase space spanned by z and the phase difference $\Delta\theta$. Lower left panel: The density evolutions in the upper (c1), the lower (c2), and both chains (c3), which corresponds to the dashed black curve ($U = 0.3$) in (a). Lower right panel: The density evolutions in momentum space which reveals (d1) the Josephson oscillation for $U = 0.3$ and (d2) the self-trapping effect for $U = 0.6$. The evolutions in (d1) and (d2) respectively correspond to the dashed black curve and the blue solid curve in (a). Here we set $t_0 = 100/t_{\|}$ ($\hbar = 1$) as the unit of time.

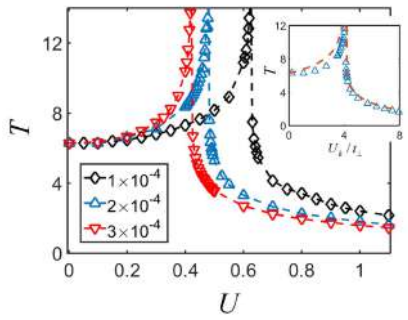


Figure 2: The Josephson oscillating period T (in units of $t_0 = 100/t_{\|}$) versus on-site interaction U with initial conditions $z(0) = 1$ and $\Delta\theta(0) = 0$. The data are from numerical simulations of the time-dependent DNLS equation with trap $V_{\rm trap} = 1 \times 10^{-4}$ (diamond), 2×10^{-4} (triangle) 2×10^{-4} (inverted triangle), respectively. The dashed curves are a guide to the eye. Inset: T versus $U_k/t_\perp$ with the interaction rescaled by $U_k = U/\lambda$. The dashed curve in the inset is the analytical solution.

[1] Yi Zheng, Shiping Feng, and Shi-Jie Yang, Chiral Bloch oscillation and nontrivial topology in a ladder lattice with magnetic flux. Phys. Rev. A. **96**, 063613 (2017).

[2] Yi Zheng, Shiping Feng, and Shi-Jie Yang, Josephson oscillation and self-trapping in momentum space. Phys. Rev. A. **97**, 043627 (2018).

Efimov physics in the dynamical formation of unitary Bose gases

V. E. Colussi[1], **S. Musolino**[1], **and S. J. J. M. F. Kokkelmans**[1]
[1] *Eindhoven University of Technology, 5600 MB Eindhoven, The Netherlands*
e-mail: *v.colussi@tue.nl*

Three identical bosons interacting with infinite s-wave scattering length, a, may form a series of three-body bound states famously studied by Efimov [1]. Recently, a macroscopic population of Efimov molecules was measured for the first time in a Bose-condensed gas quenched to the unitary regime $na^3 \to \infty$, where n is the atomic density [2]. In this highly-correlated regime, pairwise interactions are as strong as possible, leading to sequential clustering of excitations as the gas evolves towards metastability [3]. Through the method of cumulants [4, 5], we study two and three-body physics in the many-body context to understand the dynamical constitution of unitary Bose gas. Our results demonstrate quantitatively the sensitivity of two- and three-body bound clusters to the background buildup of quantum depletion on the scale of the interparticle spacing shown in Fig. 1. This leads to an evolution of scaling laws at the microscopic level within the depletion. The formation of weakly-bound two-body clusters scaling universally with the density provides a pathway for universal inelastic losses, which have been recently observed experimentally [6].

We find also that Efimov clusters extended at the scale of the interparticle spacing transition between discrete and universal, continuous scaling laws. This study sets the stage for a quantitative study of three-body correlations dynamics and manifestations of Efimov physics in the quenched unitary Bose-condensed gas, which has been studied to date only during the earliest stages of evolution in the unitary regime [3, 7].

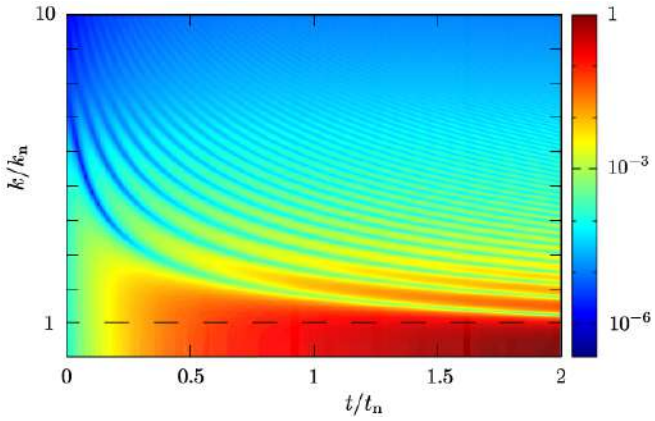


Figure 1: Universal evolution of the density of excitations within the depletion as the quenched Bose gas evolves in the unitary regime. The density plot is scaled in "Fermi units" $k_n = (6\pi^2 n)^{1/3}$, $t_n = 2m/(\hbar k_n^2)$ where n is the atomic density and m is the atomic mass.

[1] V. Efimov, Sov. J. Nucl. Phys. **29**, 546 (1979).

[2] C. E. Klauss, X. Xie, C. Lopez-Abadia, J. P. D'Incao, Z. Hadzibabic, D. S. Jin, E. A. Cornell, Phys. Rev. Lett. **119** (14), 143401 (2017).

[3] V. E. Colussi, J. P. Corson, and J. P. D'incao, Phys. Rev. Lett. **120**, 100401 (2018).

[4] T. Köhler and K. Burnett, Phys. Rev. A **65**, 033601 (2002).

[5] M. Kira, Nat. Comm., **6**, 6624, (2015).

[6] C. Eigen, J. A. P. Glidden, R. Lopes, N. Navon, Z. Hadzibabic, and R. P. Smith, Phys. Rev. Lett. **119**, 250404 (2017).

[7] J. P. D'Incao, J. Wang, and V. E. Colussi, arXiv:1804.05912 (2018).

Generation of Bose-Einstein Condensates' Ground State Through Machine Learning

Yong-Sheng Zhang[1], **Xiao Liang**[1], **Sheng Liu**[1], **and Yan Li**[2]

[1] *Laboratory of Quantum Information, University of Science and Technology of China, Hefei, 230026, China*

[2] *Department of Physics, East China Normal University, Shanghai, 200241, China*

e-mail: *yshzhang@ustc.edu.cn*

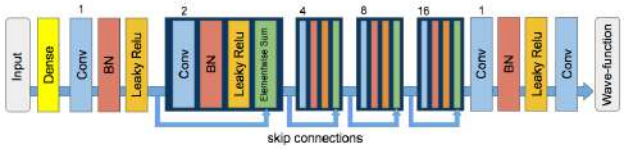


Figure 1: Our neural network is made up of several blocks. Each block consists of a convolutional layer, batch normalization and the Leaky relu activation. The input is the feature that we are interested in the Hamiltonian, such as the coupling coeffcient. The input is transformed into a high dimensional vector by a dense layer, namely, a fully connected layer. The convolutional layer in the first and the last block has the dilation rate of identity, and the convolutional layers in the intermediate blocks has the dilation rate of 2, 4, 8 and 16. Dilation rate that is greater than identity is benefit to learn the wave-functions in the larger scale. The last convolutional layer outputs the wave-function densities, and it has the dilation rate of identity. The output channel of the last layer is either one for single-component BEC or two for two-component BECs. Since the network has eight layers in total, we use elementwise sum after each block to keep gradients flowing properly.

We show that both single-component and two-component Bose-Einstein condensates' (BECs) ground states can be simulated by deep convolutional neural networks of the same structure. We trained the neural network via inputting the coupling strength in the dimensionless Gross-Pitaevskii equation (GPE) and outputting the ground state wave-function. After training, the neural network generates ground states faster than the method of imaginary time evolution, while the relative mean-square-error between predicted states and original states is in the magnitude between 10^{-5} and 10^{-4}. We compared the eigen-energies based on predicted states and original states, it is shown that the neural network can predict eigen-energies in high precisions. Therefore, the BEC ground states, which are continuous wave-functions, can be represented by deep convolution neural networks.

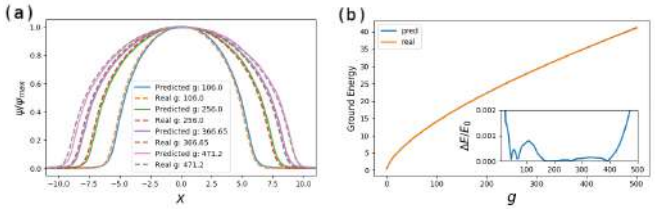


Figure 2: Single component BEC wave-function comparison between neural network generated and imaginary time evolution.

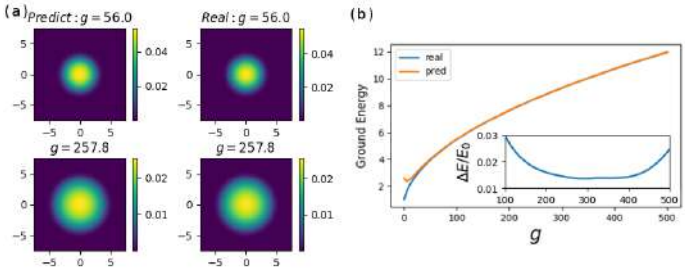


Figure 3: Single component two dimensional BEC wave-function comparison between neural network generated and imaginary time evolution.

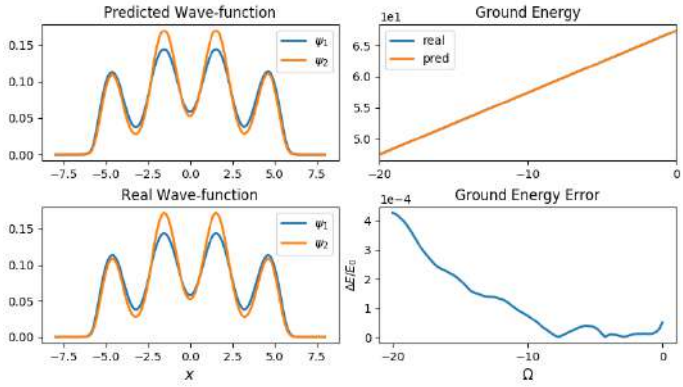


Figure 4: Two component BEC wave-function comparison between neural network generated and imaginary time evolution.

Self-bound quantum droplets of atomic mixtures in free space

G.Ferioli[1,2], **G. Semeghini**[1,2], **L. Masi**, [1,2], **L. Wolswijk**[1], **C. Mazzinghi**[1], **F.Minardi** [2,1], **M. Modugno**[3,4],**G. Modugno**[1,2], **M. Inguscio**[2,1] **and M. Fattori**[1,2]

[1] *LENS and Dipartimento di Fisica e Astronomia, Universitá di Firenze, 50019 Sesto Fiorentino, Italy*

[2] *CNR Istituto Nazionale Ottica, 50019 Sesto Fiorentino, Italy*

[3] *Depto. de Física Teórica e Hist. de la Ciencia, Universidad del Pais Vasco UPV/EHU, 48080 Bilbao, Spain*

[4] *IKERBASQUE, Basque Foundation for Science, 48011 Bilbao, Spain*

e-mail: *ferioli@lens.unifi.it*

Quantum droplets have been recently discovered as a new liquid-like phase in the context of ultracold atomic systems [1, 2, 3, 4, 5, 6]. In analogy with the known classical and quantum liquid droplets, they are indeed self-bound and incompressible, but still much more dilute. The self-binding mechanism arises from the balance of the attractive mean-field (MF) energy and the repulsive first-order correction due to quantum fluctuations, the so called Lee-Huang-Yang (LHY) energy. This liquid-like phase has been so far observed in dipolar condensates [2, 3] and only recently in bosonic mixtures [4, 5, 6]. In our experiment we use potassium-39 atoms in two different hyperfine states with tunable scattering lengths to produce a bosonic mixture in the desired interaction regime [6]. We implement a time-averaged optical potential in order to compensate gravity without providing an external confinement along any direction. In this way we can prove the existence of self-bound droplets and study their properties in free space. We characterize the critical conditions for their existence as well as their size and composition. Our results are in good agreement with the theoretical model that first predicted the liquid-like phase [1]. We also study the dynamics observed in the formation and time evolution of the droplet, by comparing our experimental data to the results of a numerical simulation. We consider a system of two coupled Gross-Pitaevskii equations which include the LHY energy as described in [1] and three-body losses. Interestingly, we find that while the mixture loses atoms due to three-body recombination, the size of the droplet decreases in order to keep a constant density, as expected for an incompressible system. This work paves the way to the study of the peculiar features of this new phase, among which is the unprecedented capability to spontaneously expel excitations and reach zero temperature [1].

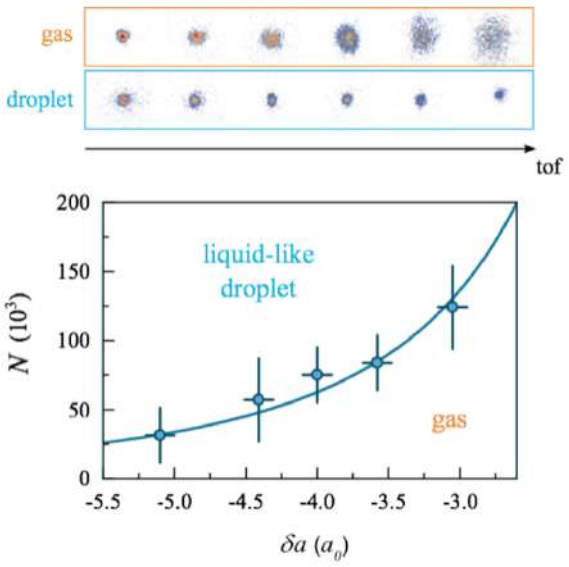


Figure 1: Phase diagram for the attractive mixture as a function of the atom number and of the effective scattering length $\delta a = a_{12} + \sqrt{a_{11}a_{22}}$, where a_{ij} are the intra/inter-species scattering lengths. The data represent the minimum atom numbers for the creation of liquid-like droplets, which are self-bound as shown by the time of flight (tof) evolution reported above.

[1] D.S. Petrov, Phys. Rev. Lett. **115**, 155302 (2015).

[2] M. Schmitt, M. Wenzel, F. Böttcher, I. Ferrier-Barbut, and T. Pfau, Nature **539**, 259 (2016).

[3] L. Chomaz, S. Baier, D. Petter, M.J. Mark, F. Wächtler, L. Santos, and F. Ferlaino, Phys. Rev. X **6**, 041039 (2016).

[4] C. R. Cabrera, L. Tanzi, J. Sanz, B. Naylor, P. Thomas, P. Cheiney, and L. Tarruell, Science **359**, 301 (2018).

[5] P. Cheiney, C. R. Cabrera, J. Sanz, B. Naylor, L. Tanzi, and L. Tarruell, arXiv:1710.11079 (2017).

[6] Semeghini, G., Ferioli, G., et al. , arXiv:1710.10890 (2017).

Atoms, or Electrons and Nuclei? ISRE Nuclear and Electron Spin Waves in Spin-Polarized Atomic Hydrogen

L. Lehtonen[1], **O. Vainio**[1], **J. Ahokas**[1], **J. Järvinen**[1], **S. Sheludyakov**[2], **K.-A. Suominen**[1], **S. Vasiliev**[1], **V. Khmelenko**[2], **and D. M. Lee**[2]

[1] *Departament of Physics and Astronomy, University of Turku, 20014 Turku, Finland*

[2] *Institute for Quantum Science and Engineering, Department of Physics and Astronomy, Texas A&M University, College Station, TX, 77843, USA*

e-mail: *laanle@utu.fi*

Spin waves in spin-polarized atomic hydrogen exist due to the Identical Spin Rotation Effect (ISRE). Both nuclear[1] and electron spin waves[2] have been observed to date, and recent experiments suggest that one may treat these spin waves as quasiparticles which undergo Bose-Einstein condensation[3]. Theoretically ISRE spin waves are treated based on the work of Lhuillier and Laloë[4], who consider a spin-1/2 system with the other spin degree of freedom frozen. Another approach for atomic hydrogen by Bouchaud and Lhuillier[5] splits the atom into a nucleus and an electron for proper symmetrization of the wave function and to account for electron transfer during scattering. We find that these approaches yield very similar results in the experimentally accessible regime, aside from a key sign difference[6]. We discuss this sign difference in light of experimental magnetic resonance spectra.

[1] B. R. Johnson ,J. S. Denker , N. Bigelow , L. P. Lévy , J. H. Freed, and D. M. Lee, Physical Review Letters **52** 15081511 (1984)

[2] O. Vainio, J. Ahokas, S. Novotny, S. Sheludyakov, D. Zvezdov, K.-A. Suominen, and S. Vasiliev Physical Review Letters **108** 185304 (2012)

[3] O. Vainio, J. Ahokas, J. Järvinen, L. Lehtonen, S. Novotny, S. Sheludyakov, K.-A. Suominen, S. Vasiliev, D. Zvezdov, V. V. Khmelenko, and D. M. Lee Physical Review Letters **114** 125304 (2015)

[4] C. Lhuillier and F. Lalo, Journal de Physique **43** 197-241 (1982)

[5] J.-P. Bouchaud and C. Lhuillier, Journal de Physique **46** 11011112 (1985)

[6] L. Lehtonen, O. Vainio, J. Ahokas, J. Järvinen, , S. Novotny, S. Sheludyakov, K.-A. Suominen, S. Vasiliev, V. V. Khmelenko, and D. M. Lee `http://arxiv.org/abs/1804.10431` (2018)

Singular loops and their non-Abelian geometric phases in ultracold spin-1 atoms

H. M. Bharath[1], **M. Boguslawski**[1], **M. Barrios**[1], **L. Xin**[1] **and M. S. Chapman**[1]
[1] *School of Physics, Georgia Institute of Technology*
e-mail: *bharath.hm@gatech.edu*

Non-Abelian and non-adiabatic variants of Berry's phase have been pivotal in the recent advances in holonomic quantum gates, while Berry's phase itself is at the heart of the study of topological phases of matter. Here we use ultracold atoms to study the unique properties of spin-1 geometric phase [1]. The spin vector of a spin-1 system, unlike that of a spin-1/2 system, can lie anywhere on or inside the Bloch sphere representing the phase space. This suggests a generalization of Berry's phase to include closed paths that go inside the Bloch sphere. In [2], this generalized geometric phase was formulated as an SO(3) operator carried by the spin fluctuation tensor, developing on m=0 spin geometric phases [3] . Under this generalization, the special class of loops that pass through the center, which we refer to as singular loops are significant because their geometrical properties are qualitatively different from the nearby non-singular loops, making them akin to critical points of a quantum phase transition. Here we use coherent control of ultracold 87Rb atoms in an optical trap to experimentally explore the geometric phase of singular loops in a spin-1 quantum system [1].

For instance, in a system of spin-1/2 fermions in a 1-dimensional Kitaev chain, the ground state at the critical point is represented by a Singular loop inside the Bloch sphere [4]. In the momentum basis, the ground state is a loop on the Bloch sphere. At finite temperature, however, the ground state is mixed and is represented by a loop inside the Bloch sphere. A phase transition in this system is characterized by a discontinuous change in the number of windings of this loop around the center of the Bloch sphere. In ref. [4], it has been shown that the critical point of the transition from zero to one winding is a singular loop, where the ground state passes through the center.

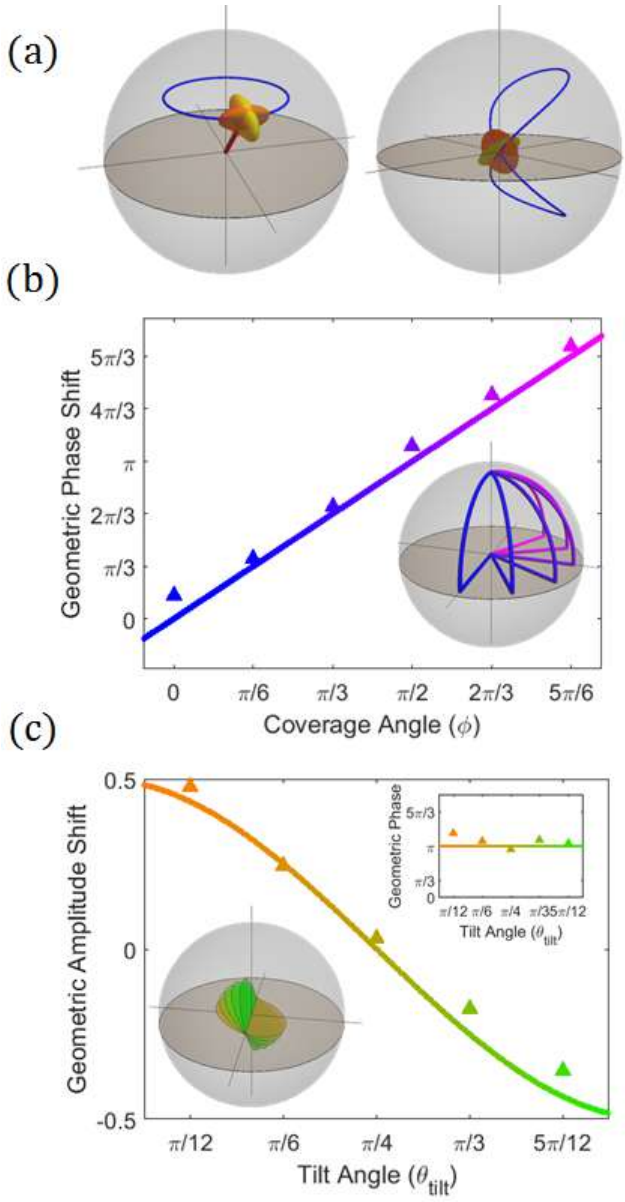


Figure 1: (a) shows a non-singular and a singular loop inside the Bloch sphere together with the spin fluctuation tensor represented by an ellipsoid, being parallel transported along the loops. (b) shows a comparison of the experimentally observed geometric phase with the theoretical prediction for the chosen loops, shown in the inset. (c) shows a comparison of the experimentally observed geometric phase with the theoretical prediction for various initial orientations of the spin fluctuation tensor.

References

[1] H. M. Bharath, M. Boguslawski, M. Barrios, Lin Xin and M. S. Chapman, arXiv:1801.00586 (2018).

[2] H. M. Bharath, arXiv:1702.08564 (2017).

[3] J. M. Robbins, M. V. Berry, *Journal of Physics A: Mathematical and General* **27**, L435 (1994).

[4] O. Andersson, I. Bengtsson, M. Ericsson and E. Sjöqvist, *Philosophical Transactions of the Royal Society of London Series A* **374**, 20150231 (2016).

Bosonic Mixture of Sodium and Potassium

A Zenesini[1], **K. K. Voges**[1], **P. Gersema**[1], **T. Hartmann**[1], **T. A. Schulze**[1], **E. Tiemann**[1], **and S. Ospelkaus**[1]

Institute for Quantum Optics, Leibniz University Hannover, 30167 Hannover, Germany
e-mail: *zenesini@iqo.uni-hannover.de*

Mixtures of alkali atoms are multi-talented tools, which allow a variety of investigations, from mixture phenomena to molecules, from spectroscopy to chemistry. Sodium and potassium mixtures have recently attracted much interest due to the different isotope combinations and to the large dipole moment of the rovibrational electronic ground state molecules. The fermionic mixture has so far received major attention and Feshbach spectroscopy and molecular association have been successfully performed [1, 2, 3].

We focus our effort on the ^{23}Na^{39}K bosonic mixture, a still overlooked combination. We first prove the possibility to perform sympathetic evaporation of potassium both in magnetic and optical dipole trap down to double degenerate mixture [4]. Extended Feshbach resonance spectroscopy in different spin mixtures reveals several resonances previously only theoretically predicted [**?**]. Our measurements lead us to improve the existent singlet molecular potential model and to additionally revise the fermionic one.

We identify several ranges of magnetic fields with different combinations of negative and positive, intra- and inter-species scattering length; see Fig.1. Miscible, immiscible and collapsing regime can easily been reached and this shows that the ^{23}Na^{39}K collisional properties are a promising starting point for a large variety of investigations, both in direction of dipolar molecules and toward the investigation of beyond mean-field effects in degenerate mixtures [6].

Technical solutions for molecular preparation and detection are also presented, with particular emphasis on novel imaging schemes.

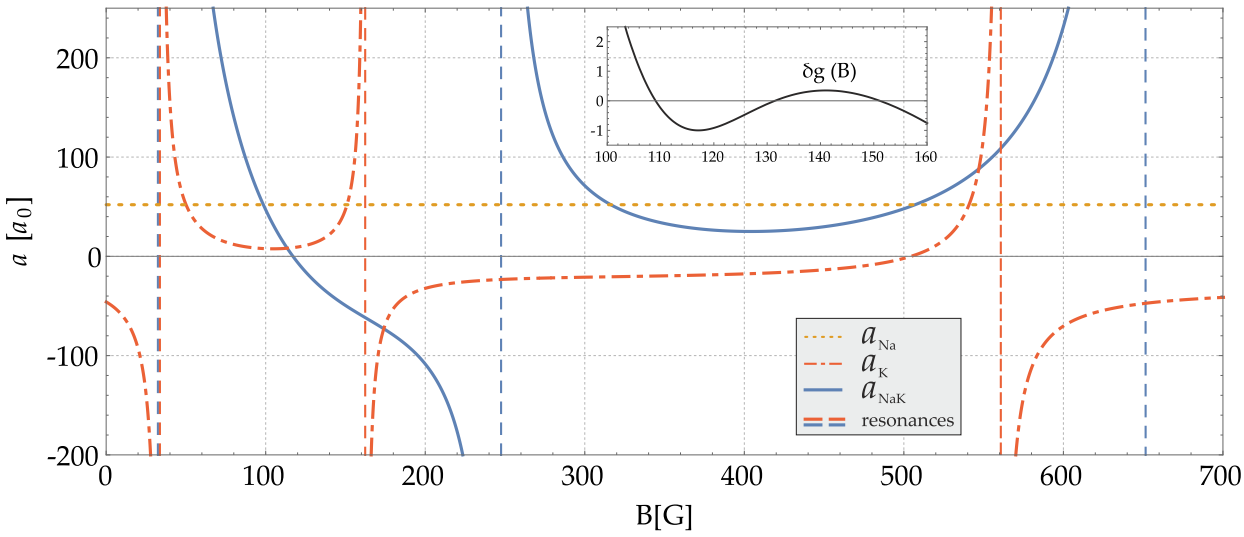


Figure 1: Hetero- and homonuclear scattering length in bosonic sodium and potassium mixtures ($|F = 1, m_f = -1\rangle_{Na} + |F = 1, m_f = 1\rangle_K$). *Inset* Miscibility parameter between 100 and 160 G.

[1] Park et al, Phys. Rev. A 85, 051602(R) (2015)

[2] Zhu et al, Phys. Rev. A 96, 062705 (2017)

[3] Seesselberg et al, Phys. Rev. A 97, 013405 (2018)

[4] Schulze et al, Phys. Rev. A 97, 023623 (2018)

[5] Hartmann et al, In preparation

[6] Petrov, Phys. Rev. Lett. 115, 155302 (2015)

Effective interactions in a quantum Bose-Bose mixture

O. I. Utesov[1], M. I. Baglay[2], and S. V. Andreev[2]
[1] *National Research Center "Kurchatov Institute" B. P. Konstantinov Petersburg Nuclear Physics Institute, Gatchina 188300, Russia*
[2] *ITMO University, Saint Petersburg 197101, Russia*
e-mail: *Serguey.Andreev@gmail.com*

Application of the methods of Quantum Electrodynamics (QED) to a system of bosons at absolute zero temperature put forward by Spartak Beliaev in 1958 [1] has been one of the most powerful analytical methods in studies of Bose-Einstein condensates. The Beliaev theory provides a prescription of replacement of the actual microscopic interaction by an effective potential which can be used for perturbative expansion of the many-body Hamiltonian. Originally designed for one-component systems, the method has recently been applied to binary Bose mixtures in the context of supersolidity [2] and stabilization of collapsing Bose-Einstein condensates by quantum fluctuations [3, 4, 5].

The present work [6] is aimed at investigation of legitimacy of extrapolation of the Beliaev prescription to two-component systems. We show that quantum scatterings of different components, which until now have been assumed independent, can interfere due to the Andreev-Bashkin entrainment effect. The effect manifests itself in renormalization of the elementary excitations of the system. This result has escaped the earlier considerations based on the Fourier expansion of small-amplitude oscillations of the order parameter. We explain how one can account for the effect by using a properly generalized Bogoliubov approach. In 3D the effect appears in the second order of the perturbation theory, which makes possible using the concept of effective potential in this case. The entrainment arises due to dressing of magnons with Bogoliubov phonon modes, by analogy with the physics of a Bose polaron. We exploit this fruitful analogy to speculate on possible formation of a magnon crystal in the strongly-interacting regime.

In 2D the polaronic effects contribute to the magnon dispersion already in the first approximation. This reflects the enhancement of quantum fluctuations in reduced dimensionality and calls for refinement of the results for the LHY correction to the energy of the mixture obtained in [4].

I acknowledge the support by Russian Science Foundation (Grant No. 18-72-00013).

References

[1] S. T. Beliaev, Zh. Eksp. Teor. Fiz. **34**, 417 (1958) [Sov. Phys. JETP **7**, 289 (1958)]; Zh. Eksp. Teor. Fiz. **34**, 433 (1958) [Sov. Phys. JETP **7**, 299 (1958)].

[2] S. V. Andreev, Phys. Rev. B **94**, 140501(R) (2016).

[3] D. S. Petrov, Phys. Rev. Lett. **115**, 155302 (2015).

[4] D. S. Petrov and G. E. Astrakharchik, Phys. Rev. Lett. **117**, 100401 (2016).

[5] C. R. Cabrera, L. Tanzi, J. Sanz, B. Naylor, P. Thomas, P. Cheiney and L. Tarruell, Science **359**, 301 (2018); G. Semeghini, G. Ferioli, L. Masi, C. Mazzinghi, L. Wolswijk, F. Minardi, M. Modugno, G. Modugno, M. Inguscio, and M. Fattori Phys. Rev. Lett. **120**, 235301 (2018).

[6] O. I. Utesov, M. I. Baglay and S. V. Andreev, Phys. Rev. A **97**, 053617 (2018).

Second sound in the BEC-BCS crossover

Vijay Pal Singh[1,2], **Daniel Kai Hoffmann**[3], **Thomas Paintner**[3], **Wolfgang Limmer**[3], **Johannes Hecker Denschlag**[3], **and Ludwig Mathey**[1,2]

[1] *Zentrum für Optische Quantentechnologien, Universität Hamburg, 22761 Hamburg, Germany*

[2] *Institut für Laserphysik, Universität Hamburg, 22761 Hamburg, Germany*

[3] *Institut für Quantenmaterie, Universität Ulm, 89081 Ulm, Germany*

e-mail: *vsingh@physnet.uni-hamburg.de*

We report on the first and second sound measurements across the BEC-BCS crossover and their theoretical analysis. The measurements are performed in a cigar-shaped three-dimensional cloud of ^{6}Li atoms and molecules. First sound is excited by an external potential that couples to the density, while second sound is excited by a potential modulation resulting mainly in local heating. The velocity of first and second sound is extracted from the propagation of the excited density wave. We find that the second sound velocity is reduced with decreasing cloud density and vanishes at the superfluid-thermal boundary, whereas the first sound velocity is only weakly affected by the cloud density. We compare the experiments on the BEC side of the crossover to numerical simulations and find good agreement.

How does a binary mixture separate in a three-well potential?

A. Richaud[1] **and V. Penna**[1]
[1] *Dipartimento di Scienza Applicata e Tecnologia - Politecnico di Torino*
e-mail: *andrea.richaud@polito.it*

Spatial phase separation of the atomic species forming a binary bosonic mixture represents a rather intuitive phenomenon in which a suciently strong inter-species repulsion is able to localize the two components in separated domains [1]. We show that, depending on the ratio between the inter- and the intra-species interactions, a binary mixture trapped in a three-well potential with periodic boundary conditions exhibits three macroscopic ground-state configurations which differ in the degree of mixing. Accordingly, the corresponding quantum states feature either delocalization or a Schrödinger cat-like structure. The two-step phase separation occurring in the system, which is smoothed by the activation of tunnelling processes, is confirmed by the analysis of the energy spectrum that collapses and rearranges at the two critical points. In such points, we show that also Entanglement Entropy, a quantity borrowed from quantum-information theory, features singularities, thus demonstrating its ability to witness the double mixining-demixing phase transition. The developed analysis, which is of interest to both the experimental and theoretical communities, opens the door to the study of the demixing mechanism in complex lattice geometries [2].

The model. We consider a bosonic binary mixture trapped in a three-well potential with periodic boundary conditions (closed trimer). Making use of the Continuous Variable Picture [3], one can reduce the search for the ground state of the relevant Bose-Hubbard Hamiltonian $\hat{H}$ to the one for the minimum of an effective potential V_*.

Two mixing-demixing phase transitions. The configuration $(\vec{x}, \vec{y})$ which minimizes the effective potential V_* is determined, at first, when the tunnelling T is suppressed. In this situation, in fact, it is possible to carry out a fully analytic study, based on the exploration of the polytope-like domain of V_*. In Figure 1, one can recognize the presence of three different quantum phases, which qualitatively differ in the degree of mixing. It is clear that $W/U = 1, 2$ represent critical values where two different mixing-demixing phase transitions occur. The presence of a tunnelling $T > 0$ is responsible for the rightward translation of critical points and for the smoothing of the transition. The border between the first and the second phase region has been analytically determined to be $W/U = 1 + 9T/(2UN)$.

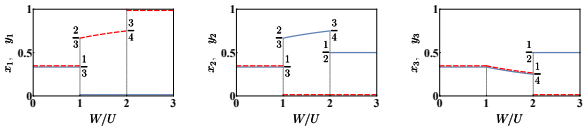


Figure 1: Normalized semiclassical bosonic populations in each of the three wells for varying W/U and for $T = 0$. Each panel corresponds to a site of the trimer, while blue solid (red dashed) lines are associated to bosonic species a (b).

Schrödinger cats. Of course, due to the symmetry of the trimer system, no well is favoured compared to the others, and, as a consequence, there are multiple macroscopic congurations which minimize the effective potential V_*. Indeed, they are equal up to a cyclic permutation of the site labels, and/or species-label swapping. Quantum-mechanically, the degeneracy associated to m minimum-energy congurations leads to the formation of a non-degenerate ground state $|\Psi_0\rangle$ which is a m-sided Schrödinger cat.

Entanglement Entropy as a critical indicator. The entanglement entropy (EE) quanties the quantum correlation between two parts of a physical system through the Von Neumann entropy of a suitably defined sub-system [4]. In this work, the physical system is of course the binary mixture, the two parts correspond to the two different atomic species and, therefore, the EE describes the quantum correlation between them. Such indicator features the presence of peaks where the transitions occur and approaches the limiting value $\log_2 6$ (where 6 is the number of cat's faces) for $W/U \gg 2$.

Spectrum. The energy levels are shown to collapse and rearrange where the two mixing-demixing phase transitions occur.

[1] H. Pu and N. Bigelow, Phys. Rev. Lett. **80**, 1130 (1998).

[2] V. Penna and A. Richaud, `https://arxiv.org/abs/1803.05467`.

[3] F. Lingua. and V. Penna, Phys. Rev. E **95**, 062142 (2017).

[4] F. Lingua, V. Penna and A. Richaud, Entropy, **20,** 84 (2018).

[5] F. Lingua et al, J. Phys. B **49**, 205005 (2016).

Andreev-reflection and Aharonov-Bohm dynamics in atomtronic circuits

T. Haug[1], **R. Dumke**[1,2,3], **L.-C. Kwek**[1,3,4,5], **and L. Amico**[1,3,6,7,8]

[1] *Centre for Quantum Technologies, National University of Singapore, 3 Science Drive 2, Singapore 117543, Singapore*

[2] *Division of Physics and Applied Physics, Nanyang Technological University, 21 Nanyang Link, Singapore 637371, Singapore*

[3] *MajuLab, CNRS-UNS-NUS-NTU International Joint Research Unit, UMI 3654, Singapore*

[4] *Institute of Advanced Studies, Nanyang Technological University, 60 Nanyang View, Singapore 639673, Singapore*

[5] *National Institute of Education, Nanyang Technological University, 1 Nanyang Walk, Singapore 637616, Singapore*

[6] *Dipartimento di Fisica e Astronomia, Via S. Sofia 64, 95127 Catania, Italy*

[7] *CNR-MATIS-IMM & INFN-Sezione di Catania, Via S. Sofia 64, 95127 Catania, Italy*

[8] *LANEF 'Chaire d'excellence', Universitè Grenoble-Alpes & CNRS, F-38000 Grenoble, France*

e-mail: *tobias.haug@u.nus.edu*

Atomtronics seeks to realize circuits of cold-atoms guided with laser light or magnetic fields. This technology can create arbitrary potentials, which for example can be used to study the atom analogue of the superconducting quantum interference device[1] or realize quantum phases[2]. The Aharonov-Bohm, and its dual, the Aharonov-Casher effect have been extremely fruitful in physics and are of central importance for quantum technologies. With an Atomtronic setup, these effects can be realized in a ring system with neutral cold atoms and an artificial magnetic field (see Fig.1 or [4]).

Here, we study the quantum transport for interacting bosons through two specific atomtronic circuits: a ring condensate coupled to leads and a Y-junction[3].

In the ring system, the transport through the ring depends on various parameters like Aharonov-Bohm flux, atom-atom interaction, properties of the lead reservoirs, and coupling strength between ring and leads. We study the dynamics and the current of this system using analytic methods, tDMRG and an open system approach. We find that the propagation of low-energy excitations exhibits a peculiar interplay of the Aharonov-Bohm effect, Mott-insulator transition and persistent current of the condensate. For non-equilibrium quenches, the steady-state is independent of flux, however the dynamics towards the steady-state is affected by flux.

Further, we study the dynamics of interacting bosons in a Y-junction. This system displays Andreev-like reflections with negative amplitude at the junction. We study the cross-over from Andreev-like reflections to regular reflections depending on the coupling strength of the Y-junction.

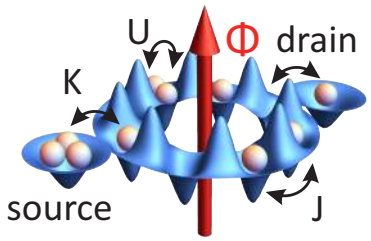


Figure 1: Atomtronic setup consisting of a superfluid condensate in a ring lattice with two attached leads. The dynamics is controlled by Aharonov-Bohm flux Φ and ring-lead coupling K. Particles tunnel between ring sites with rate J and particles interact on-site with strength U.

[1] T. Haug, J. Tan, M. Theng, R. Dumke, L.-C. Kwek, and L. Amico, Phys. Rev. A 97, 013633 (2018).

[2] T. Haug, L. Amico, R. Dumke, and L.-C. Kwek, Quantum Sci. Technol. (2018).

[3] T. Haug, R. Dumke, L.-C. Kwek, L. Amico, et al., to be published (2018).

[4] T. Haug, H. Heimonen, R. Dumke, L.-C. Kwek, and L. Amico, arXiv:1706.05180 (2017).

Chaotic and regular spin-orbit entanglement of ultracold atoms

Wenhua Hai

Department of Physics and Key Laboratory of Low-dimensional Quantum Structures and Quantum Control of Ministry of Education, Hunan Normal University, Changsha 410081, China

e-mail: *whhai2005@aliyun.com*

We study the spatially chaoticity-dependent spin-motion entanglement of a spin-orbit (SO) coupled Bose-Einstein condensate (BEC) [1]. The BEC was loaded into a quasi-one-dimensional optical superlattice potential of large length L in a stationary regime $x_0 \leq x \leq L$ with a source of ultracold atoms maintained a persistent incident current [2] at the site $x = L$ or $x = x_0$. The spin-orbit entangled state reads $|\Psi(x,t)\rangle = \langle x|\Psi(t)\rangle = \langle x|\Psi_1(t)\rangle|\uparrow\rangle + \langle x|\Psi_2(t)\rangle|\downarrow\rangle = \Psi_1(x,t)|\uparrow\rangle + \Psi_2(x,t)|\downarrow\rangle$ with the spin-up and spin-down internal states $|\uparrow\rangle$ and $|\downarrow\rangle$ and the macroscopic wave function $\Psi_j(x,t)$, which is governed by the coupled nonlinear Gross-Pitaevskii (GP) equations [3] with the superlattice potential $V(x) = V_1 \sin^2(kx) + V_2 \sin^2(2kx)$ and the SOC strength γ. Given the stationary GP equations, we make the mathematical equivalency between them and a pair of nonlinear dynamical equations by using the time variable t to replace the spatial coordinate x. Then we construct the equivalent phase space and seek the regular and chaotic "orbits" which are associated with the corresponding atomic spatial distributions. We let the starting point of the many-site superlattice be $x_0 = 0$ which corresponds to the initial time of the equivalent dynamical system such that we can employ the well-known dynamical method to investigate the spatial chaos.

Taking the stationary state $|\Psi_j(x,t)\rangle = [R_1(x)|\uparrow\rangle + R_2(x)|\downarrow\rangle]e^{i[\theta(x)-\mu t]}$ with the chemical potential μ and synchronized phase $\theta(x)$, and applying the Melnikov chaos criterion, we analytically demonstrate that (a) the phase synchronization results in decouple of the GP equations and the SO coupling (SOC) leads to the generation of spin-motion entanglement; (b) as shown in Fig. 1, the area of the high-chaoticity parameter region inversely relates to the SOC strength which renormalizes the chemical potential; and (c) the highchaoticity is associated with the lower chemical potential and the larger ratio of the short-lattice depth to the longer-lattice depth. Then, we numerically generate the Poincaré sections to pinpoint that the chaos probability is enhanced with the decrease in the SOC strength and/or the spin-dependent current components $J_j = R_j^2[\theta_x + (-1)^{3-j}\gamma]$ for $j = 1, 2$. The existence of chaos is confirmed again by computing the corresponding largest Lyapunov exponents. For an appropriate lattice depth ratio, the complete stop of one of (or both) the current components is related to the full chaoticity. The results mean that the weak SOC and/or the small current components can enhance the chaoticity. Based on the insensitivity of chaos probability to initial conditions, we propose a feasible scheme to manipulate the ensemble of chaotic spin-orbit entangled states, which may be useful in coherent atom optics with chaotic atom transport.

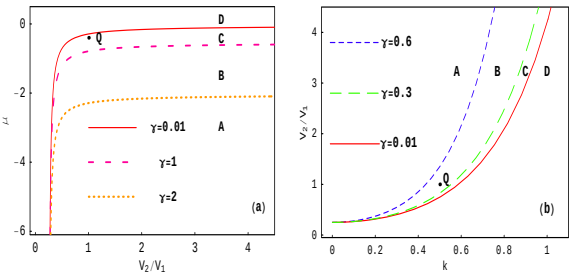


Figure 1: The chaotic regions on the different parameter planes. (a) Chemical potential μ as a function of depth ratio V_2/V_1 for the parameters $k = 0.5$ and $\gamma = 2$ (dotted curve), $\gamma = 1$ (long-interval short dashed curve) and $\gamma = 0.01$ (solid curve). (b) Depth ratio (V_2/V_1) versus k for the parameters $\mu = -0.4$ and $\gamma = 0.6$ (short dashed curve), $\gamma = 0.3$ (long dashed curve) and $\gamma = 0.01$ (solid curve). The parameter planes are divided into different regions by these boundary curves, which are labeled by A, B, C and D. The letter Q labels the parameter point $Q(\mu, k, V_2/V_1) = Q(-0.4, 0.5, 1)$.

We also study coherent control of regular spin-motion entanglement of spin-orbit-coupled single atoms held in a driven optical bipartite lattice [4]. Under the high-frequency limit and nearest-neighbor tight-binding approximation, we find a new decoupling mechanism between states with the same (different) spins, which leads to two sets of analytical solutions describing dynamical localization and directed transport with (without) spin-orbit entanglement.

[1] C. Kong, H. Chen, C. Li, W. Hai, *Chaos* **28**, 023115 (2018).

[2] T. Paul, K. Richter, and P. Schlagheck, *Phys. Rev. Lett.* **94**, 020404 (2005).

[3] Y. S. Cheng, G. H. Tang, and S. K. Adhikari, *Phys. Rev. A* **89**, 063602 (2014).

[4] Y. Luo, G. Lu, C. Kong, W. Hai, *Phys. Rev. A* **93**, 043409 (2016).

Uncover Topology by Quantum Quench Dynamics

W. Sun[1,2,3], **C.-R. Yi**[1,2,3], **B.-Z. Wang**[1,2,4,5], **W.-W. Zhang**[6], **B. C. Sanders**[1,7,8], **X.-T. Xu**[1,2,3], **Z.-Y. Wang**[1,2,3], **J. Schmiedmayer**[9], **Y. Deng**[1,2,3], **X.-J Liu**[4,5], **S. Chen**[1,2,3], **and J.-W. Pan**[1,2,3]

[1] *Shanghai Branch, National Laboratory for Physical Sciences at Microscale and Department of Modern Physics, University of Science and Technology of China, Shanghai 201315, China*

[2] *Chinese Academy of Sciences Center for Exellence: Quantum Information and Quantum Physics, University of Science and Technology of China, Hefei Anhui 230326, China*

[3] *CAS-Alibaba Lab for quantum computation, Shanghai 201315, China*

[4] *International Center for Quantum Materials, School of Physics, Peking University, Beijing 100871, China*

[5] *Collaborative Innovation Center of Quantum Matter, Beijing 100871, China*

[6] *Centre for Engineered Quantum Systems, School of Physics, The University of Sydney, Sydney, NSW 2006, Australia*

[7] *Institute for Quantum Science and Technology, University of Calgary, Calgary, Alberta, Canada T2N 1N4*

[8] *Program in Quantum Information Science, Canadian Institute for Advanced Research, Toronto, Ontario M5G 1Z8, Canada*

[9] *Vienna Center for Quantum Science and Technology, Atominstitut, TU Wien, Stadionallee 2, 1020 Vienna, Austria*

Topological quantum states are characterized by nonlocal invariants, and their detection is intrinsically challenging. Various strategies have been developed to study topological Hamiltonians through their equilibrium states. We present a fundamentally new, high-precision dynamical approach, revealing topology through the unitary evolution after a quench from a topological trivial initial state with a two-dimensional Chern band realized in an ultracold ^{87}Rb atom gas. The emerging ring structure in the spin dynamics uniquely determines the Chern number for the post-quench band and enables probing the full phase diagram of the band topology with high precision as well as the complex band structure. Our dynamical approach provides a way towards observing a universal bulk-ring correspondence, which has broad applications in exploring topological quantum matter.

Highly controllable and Robust 2D Spin-Orbit Coupled Topological Bose Gas

W. Sun[1,2], B.-Z. Wang[1,2,3,4], X.-T. Xu[1,2], C.-R. Yi[1,2], L. Zhang[3,4], Z. Wu[1,2], Y. Deng[1,2], X.-J Liu[3,4], S. Chen[1,2], and J.-W. Pan[1,2]

[1] *Shanghai Branch, National Laboratory for Physical Sciences at Microscale and Department of Modern Physics, University of Science and Technology of China, Shanghai 201315, China*

[2] *Chinese Academy of Sciences Center for Exellence: Quantum Information and Quantum Physics, University of Science and Technology of China, Hefei Anhui 230326, China*

[3] *International Center for Quantum Materials, School of Physics, Peking University, Beijing 100871, China*

[4] *Collaborative Innovation Center of Quantum Matter, Beijing 100871, China*

We report the realization of a robust and highly controllable two-dimensional (2D) spin-orbit (SO) coupling with topological non-trivial band structure. By applying a retro-reflected 2D optical lattice, the phase tunable Raman couplings are formed into the anti-symmetric optical Raman lattice structure, and generate the 2D SO coupling with precise inversion and C_4 symmetries. Due to these symmetries, the topological region is considerably enlarged, and the life time of the 2D SO coupled Bose-Einstein condensate reaches several seconds, which enable to explore the fine tuning interaction effects. These essential advantages of the present new realization open the door to explore exotic quantum many-body effects and non-equilibrium dynamics with novel topology.

Ramsey interferometry with trapped motional quantum states

Linxiao Niu[1], **Shengjie Jin**[1], **Xuzong Chen**[1], **Jörg Schmiedmayer**[2] **and Xiaoji Zhou**[1*]

[1] *School of Electronics Engineering and Computer Science, Peking University, Beijing 100871, China*

[2] *Vienna Center for Quantum Science and Technology, Atominstitut, TU Wien, Stadionallee 2, 1020 Vienna, Austria*

e-mail: *xjzhou@pku.edu.cn*

Interferometers employing separated oscillating fields to create and probe superpositions of states, also known as Ramsey interferometery (RI), have originaly been developed for magnetic resonance to measure transition frequencies and were then extended to a general tool of spectrocopy and matter wave interferometry. Typical sequences consist of two $\pi/2$ pulses separated by an time for free evolution or a $\pi/2-\pi-\pi/2$ sequence. Ramsey interferometers using internal electronic or nuclear states already have played an important role in accurate quantum state engineering and quantum metrology. In general, echo techniques are used in RIs to suppress de-phasing for significantly increasing the coherent time [1]. Even though motional states of particles are on the same footing as internal states in current quantum technologies, conventional echo-RIs rarely exploit the quantum interference of trapped motional states. Recently, an RI with trapped motional states of a Bose-Einstein condensate trapped in an anharmonic potential has been demonstrated with 92% contrast for several cycles [2]. This proof-of-principle experiment holds great promises for studying quantum many-body physics out of equilibrium, quantum metrology with non-classical motional states and quantum information processing with motional qubits.

We demonstrate a RI with trapped motional quantum states (TMQS) of atoms employing the S- and D-bands in an optical lattice [3]. Due to the lack of selection rules for lattice band transition, a key challenge for constructing this RI is to realise π- and $\pi/2$-pulses analogous to those in conventional RIs. Using a shortcut loading method, we have designed sequences of optical pulses [4], analogous to a π- or $\pi/2$-pulse, to e ciently prepare a superposition of atoms in S- and D-band states in the optical lattice at zero quasi-momentum with high fidelity within tens of microseconds, which is much shorter than the characteristic time scales of the decay process. Keeping the lattice on, we observe state interference and measure the decay of the coherent oscillations.

Experimental results on the time evolution of the atom population in D band with the lattice time $p_D(t_{OL})$ are shown in Fig. 1(a) for $V_0 = 10E_r$ and $T = 50$ nK with two $\pi/2$-pulses. Fig. 1(c) shows the measured contrast decay versus time for the different initial temperatures of condensates. The horizontal dashed line indicates the contrast drops to the value

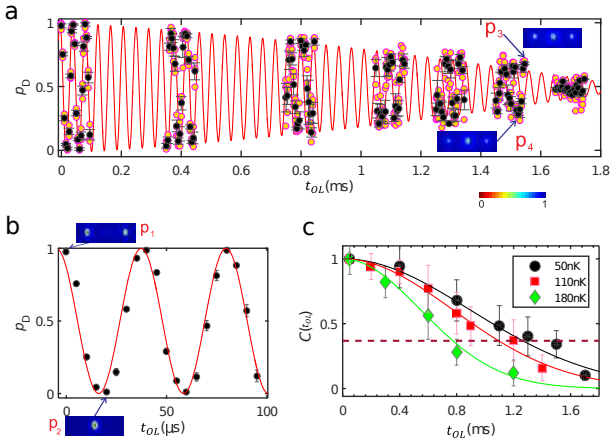


Figure 1: a) The oscillation of the population of atoms in the D band p_D at $T = 50$ nK, for single measurement(red circle), the mean value (dots with errorbars), and also the corresponding fitting curve(red solid line). b) Detail of the oscillation at begining. Insets: TOF images. c) The decay of the contrast at different temperatures.

of $1/e$, which is used to define a coherence time τ.

In summary, we have demonstrated a RI for atoms within an optical lattice. We further employ a band echo technique to enhance the coherence time by one order of magnitude and identified the mechanisms leading to the contrast decay for the RI signal. The contrast decay is closely related to the homogeneity of the optical lattice, laser intensity fluctuation, interaction-induced transverse expansion, and finite temperature dynamics of a condensate. All except for the effects of finite temperature can be suppressed by a matter-wave band echo sequence. Thus the damping from thermal fluctuations is well uncovered.

[1] A. D. Cronin, J. Schmiedmayer, and D. E. Pritchard, *Rev. Mod. Phys.* **81**, 1051(2009).

[2] S. van Frank, A. Negretti, T. Berrada, S. Montangero, J. F. Schaff,T. Schumm,T. Calarco and J. Schmiedmayer, *Nat. Comm.* **5**, 4009 (2014).

[3] D. Hu, L. X. Niu, S. J. Jin, X. Z. Chen, G. J. Dong, J. Schmiedmayer, and X. J. Zhou, arXiv preprint arXiv:1712.07520 (2017).

[4] D. Hu, L. Niu, B. Yang, X. Chen, B. Wu, H. Xiong, and X. Zhou, *Phys. Rev. A* **92**, 043614 (2015).

Stability and excitations of droplet phases in dipolar and two-component condensates

T. Macrì[1], **A. Cappellaro**[2], **F. Cinti**[3], **L. Salasnich**[2,4]

[1] *Departamento de Física Teórica e Experimental, Universidade Federal do Rio Grande do Norte, and International Institute of Physics, Natal-RN, Brazil*

[2] *Dipartimento di Fisica e Astronomia "Galileo Galilei", Università di Padova, via Marzolo 8, 35131 Padova, Italy*

[3] *National Institute for Theoretical Physics (NITheP), Stellenbosch 7600, South Africa*

[4] *CNR-INO, via Nello Carrara, 1 - 50019 Sesto Fiorentino, Italy*

e-mail: *macri@fisica.ufrn.br*

Droplets are very common in nature, from liquid water to superfluid Helium and nuclear matter. In this talk I will discuss two examples of stable self-bound solutions exist in dipolar gases and Rabi-coupled BECs. In the first part I will present the zero temperature phase diagram of bosons interacting via dipolar interactions in three dimensions in free space. Upon increasing the strength of the dipolar interaction and at su ciently high densities we find a wide region where filaments are stabilized along the direction of the external field. Most interestingly by computing the superfluid fraction we conclude that superfluidity is anisotropic and vanishes along the orthogonal plane. In the second part I will focus on the case of two-component Bose condensates coupled via a laser field. We study the effects of quantum fluctuations on a Rabi-coupled two-component Bose gas of interacting alkali atoms. The divergent zero-point energy of gapless and gapped elementary excitations of the uniform system is properly regularized obtaining a meaningful analytical expression for the beyond-mean-field equation of state. In the case of attractive inter-particle interaction we show that the quantum pressure arising from Gaussian fluctuations can prevent the collapse of the mixture with the creation of a self-bound droplet. We characterize the droplet phase and discover an energetic instability above a critical Rabi frequency provoking the evaporation of the droplet. Finally, we suggest an experiment to observe such quantum droplets using Rabi-coupled internal states of 39K atoms and measure their collective excitations.

[1] A. Cappellaro, T. Macrì, and L. Salasnich, Collective modes across the soliton- droplet crossover in binary Bose mixtures, To appear in Phys. Rev. A (2018).

[2] A. Cappellaro, T. Macrì, G. F. Bertacco and L. Salasnich, Equation of state and self-bound droplet in Rabi-coupled Bose mixtures, Scientific Reports **7**, 13358 (2017).

[3] F. Cinti, A. Cappellaro, L. Salasnich and T. Macrì, Superfluid filaments of dipolar bosons in free space, Phys. Rev. Lett. **119**, 215302 (2017).

We create and study a homogeneous Fermi gas with strong interactions in uniform trapping potentials. Here we present three current research themes, and outlook for future experiments. We study the temperature dependence of spin impurities and observe a polaron to bare particle crossover, observe quantum limited sound attenuation by local density modulation, and present measurements of the temperature dependence of the contact. Furthermore, we detail progress on upgrading our apparatus for achieving a uniform 2d Fermi gas with strong interactions.

Continuum of classical-field ensembles from canonical to grand canonical and the onset of their equivalence

J. Pietraszewicz[1], **E. Witkowska**[1], **P. Deuar**[1]

[1] *Institute of Physics, Polish Academy of Sciences, Aleja Lotników 32/46, 02-668 Warsaw, Poland*
e-mail: *pietras@ifpan.edu.pl*

The canonical and grand-canonical ensembles are two usual marginal cases for ultracold Bose gases, but real collections of experimental runs commonly have intermediate properties. We have studied the continuum of intermediate cases and look into the appearance of ensemble equivalence as interaction rises for mesoscopic 1D systems. We have demonstrated how at sufficient interaction strength the distributions of condensate and excited atoms become practically identical, regardless of the ensemble used. Importantly, we have found that features that are fragile in the ideal gas and appear only in a strict canonical ensemble can become robust in all ensembles when interactions become strong. As evidence, the steep cliff in the distribution of the number of excited atoms is preserved in GCE.

To make this study, a straightforward approach for generating canonical and intermediate classical field ensembles using a modified stochastic Gross-Pitaevskii equation (SGPE) was developed.

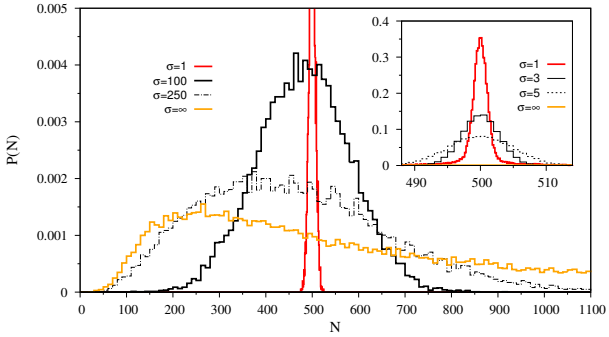


Figure 1: The plot presents the change of the probability distribution of the total number of atoms on the path between CE → GCE. To obtain the intermediate ensemble statistics, an external parameter σ of modified SGPE was varied. The inset shows ensembles for which the properties are very close to an ideal canonical Bose gas.

[1] J. Pietraszewicz, E. Witkowska, P. Deuar, Phys. Rev. A **96**, 033612 (Sep 2017).

Experimental realization of a supersolid-like stripe-phase in a spin-orbit-coupled Bose-Einstein condensate enabled by momentum-space hopping

Sean Mossman, Thomas Bersano, Vandna Gokhroo and Peter Engels
Department of Physics and Astronomy, Washington State University, Pullman, WA 99164
e-mail: *sean.mossman@wsu.edu*

We investigate a spin-orbit-coupled Bose-Einstein condensate in which the two spin-orbit dispersion minima are coupled by additional lattice-assisted tunneling. Numerical simulations show that this system exhibits stripe-phase behavior, such as a pronounced fine-grained density modulation. We observe coherent Rabi oscillations between the relevant momentum states and experimentally verify the ground state phase diagram as a function of tunneling strength and spin-orbit detuning. This arrangement provides a flexible and long-lived experimental platform for further investigation of the properties of the stripe-phase in the context of a spin-orbit-coupled Bose-Einstein condensate.

Matter-wave optics with thermal and quantum degenerate atoms

I. Drougkakis[1,3], **S. Pandey**[1,3], **H. Mass**[1,2], **G. Vasilakis**[1], **V. Bolpasi**[1] **and W. von Klitzing**[1]

[1] *Foundation For Research and Technology Hellas, Institute of Electronic Structure and Laser,71110 Heraklion, Greece*

[2] *Department of Physics, University of Crete, Heraklion 70113, Greece*

[3] *Department of Materials, Science and Technology, University of Crete, Heraklion 70113, Greece*

e-mail: *drougakis@iesl.forth.gr*

Matter-wave optics concerns itself with the manipulation of atomic beams in free space, for example, the focusing of an atomic cloud into a tight spot. One of the goals in the field of atom optics is to realize atom-optical elements that are analogous to conventional optical devices, such as mirrors[1], 3D lenses [2] and beam-splitters [3]. This can drive advances in several fields such as precision measurements [4], nanolithography and detection of small condensate fractions [5].

Initially, atom optics used thermal beams created by the supersonic expansion of a buffer gas. The development of laser-cooling and trapping then allowed the preparation of thermal samples of atoms down to nano Kelvin temperatures [6]. More recently, Bose Einstein condensation (BEC) led to the development of coherent atom beams an atom lasers [7, 8], giving the opportunity to investigate macroscopic quantum phenomena in dilute atomic gases. [9]

The scope of this work is to investigate the factors limiting the quality and size of the final image obtained in focusing experiments using time dependent magnetic lenses; to identify the sources of aberration; and finally to reach diffraction-limited focusing of atomic patterns.

We are using a BEC of Rubidium atoms as the initial source that guarantees near perfect spatial coherence. This matter wave will be manipulated using an optically generated phase mask, and then imaged using magnetic lenses. We present preliminary results of condensate focusing using Quadrupole-TOP (QTOP) magnetic lenses.

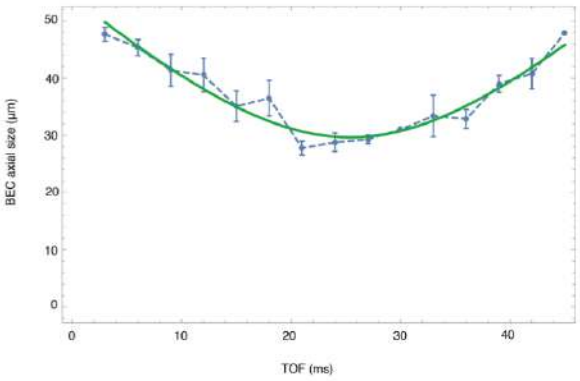


Figure 1: BEC focusing using a QTOP lens

References

[1] Hansch T. W., Opt. Lett 18, 450452 (1993)

[2] Cornell E A, Monroe C and Wieman C E Phys. Rev. Lett. 67 2439 (1991)

[3] Chu S., Phys. Rev. Lett. 66, 2297 (1991)

[4] Foot C.J., Physical Review A 83 043408 (2011)

[5] Walraven T. M., Phys. Rev. Lett.89, 270404 (2002)

[6] Cohen-Tannoudji C N, Rev. Mod. Phys. 70 707 (1998)

[7] Von Klitzing W., N.J. Physics 16, 033036 (2014)

[8] Rolston S.L. and Phillips W.D., Nature 416, 219 (2002)

[9] Esslinger T., Phys. Rev. Lett. 95, 090404 (2005)

An experiment for dipolar quantum mixtures of erbium and dysprosium atoms

C. Politi[1], **P. Ilzhöfer**[1,2], **G. Durastante**[1,2], **A. Patscheider**[1,2], **M. Sohmen**[1,2], **A. Trautmann**[1], **M. J. Mark**[1,2] **and F. Ferlaino**[1,2]

[1] *Institut für Quantenoptik und Quanteninformation, Österreichische Akademie der Wissenschaften, 6020 Innsbruck, Austria*

[2] *Institut für Experimentalphysik, Universität Innsbruck, TechnikerstraSSe 25, 6020 Innsbruck, Austria*

e-mail: *claudia.politi@oeaw.ac.at*

Strongly magnetic atoms allow the study of few- and many-body effects arising from long-range, anisotropic dipole-dipole interactions. Up to now, experiments with dipolar lanthanoids focus on the single-species operation. We present an experimental setup which for the first time combines the two highly magnetic atoms, erbium and dysprosium, in a three-chamber apparatus. In the main experimental chamber we cool and trap the mixture in a two-species magneto-optical trap (MOT), which operates on an intercombination line. We demonstrate a novel MOT configuration which, due to the narrow-line character together with gravity, employs only five beams in an orthogonal *open-top* configuration [1]. The atoms are then transferred into an optical dipole trap for evaporative cooling to the degenerate phase. Our experiment plans to investigate Bose-Bose, Bose-Fermi and Fermi-Fermi mixtures with imbalanced dipolar strength and to study the unexplored interspecies scattering physics with dipolar atoms. A second chamber will allow us to investigate the Rydberg physics with our multi-electron atoms which feature an optically active core. Furthermore, an additional chamber is dedicated to explore the fascinating quantum phases predicted for dipolar atoms in optical lattices. For this, we plan to build a quantum gas microscope with single-site resolution in a highly-controllable magnetic environment. Atoms will be transported from one chamber to the others in an optical tweezer covering a total distance of around 80 cm. After the realization of the two-species magneto-optical trap and the Bose-Einstein condensation of Er and Dy, the experiment is currently at the stage of investigating the interspecies scattering physics.

[1] P. Ilzhöfer *et al.*, A two-species five-beam magneto-optical trap for highly magnetic Er and Dy atoms, Phys. Rev. A, volume 97, 2018.

Experiments with dipolar Bose-Einstein condensates: quantum droplets, self-organization and superfluidity

T. Langen[1], **I. Ferrier-Barbut**[1], **M. Wenzel**[1], **F. Boettcher**[1], **J.-N. Schmidt**[1], **M. Eisenmann**[1], **M. Isoard**[2], **S. Stringari**[2], **and T. Pfau**[1]

[1] *5. Physikalisches Institut and Center for Integrated Quantum Science and Technology IQST, Universität Stuttgart, Pfaffenwaldring 57, 70550 Stuttgart, Germany*

[2] *INO-CNR BEC Center and Dipartimento di Fisica, University of Trento, 38123 Povo, Italy*

e-mail: *t.langen@physik.uni-stuttgart.de*

We present a series of recent results in the study of dipolar dysprosium quantum gases.

Firstly, we study self-organized structure formation in these gases, which is similar to the Rosensweig instability in classical ferrofluids [1]. The corresponding phase-transition is characterized by the formation of self-bound droplets that are stabilized by beyond mean-field effects [2]. While the ground state of the system in 3D is a single droplet, we find theoretically that under strong anisotropic confinement the ground state becomes a striped state that consists of multiple droplets [3]. Experimentally we show that such self-organized stripes can indeed be generated, likely in a metastable excited state. We outline prospects to experimentally reach a phase coherent supersolid ground state.

Secondly, we report on the observation of the scissors mode of a single self-bound droplet [4]. The existence of this mode is due to the breaking of the rotational symmetry by the dipole-dipole interaction, which is fixed along an external homogeneous magnetic field. By modulating the orientation of this magnetic field, we excite the scissors mode and observe clear signatures of its non-linear coupling to other low frequency modes (see Figure 1).

Finally, we study the superfluid properties of a dipolar BEC [5, 6]. By moving an attractive laser beam through the condensate we observe an anisotropic critical velocity for the breakdown of dissipationless flow, which, in the spirit of the Landau criterion, can directly be connected to the anisotropy of the underlying dipolar excitation spectrum. Our observations are in excellent agreement with simulations based on the Gross-Pitaevskii equation and highlight the effect of dipolar interactions on macroscopic transport properties.

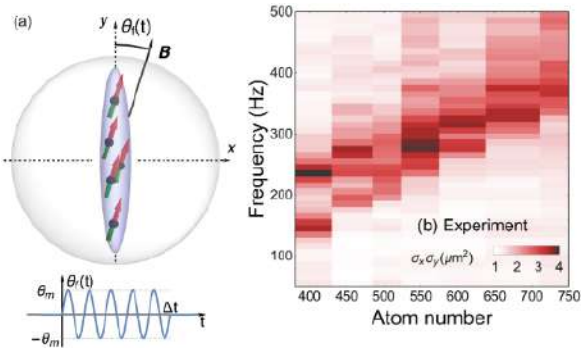


Figure 1: (a) Experimental method to excite the scissors mode of a self-bound quantum droplet. The droplet is held in a cylindrically symmetric trap (around z) and the orientation of the field is modulated around its mean value along y for Δt at variable frequency. (b) Experimental response measured as a growth in the visible size of the droplet as a function of atom number and modulation frequency [4].

[1] Kadau et al., Nature **530**, 194 (2016)

[2] Schmitt et al., Nature **539**, 259 (2016)

[3] Wenzel et al., Phys. Rev. A **96**, 053630 (2017)

[4] Ferrier-Barbut et al., Phys. Rev. Lett. **120**, 160402 (2018)

[5] Ticknor, Wilson and Bohn, Phys. Rev. Lett. **106**, 065301 (2011)

[6] Wenzel et al., arxiv:1804.04552 (2018)

Ultradilute quantum liquid drops

V. Cikojević[1], **K. Dželalija**[1], **P. Stipanović**[1], **L. Vranješ Markić**[1], **J. Boronat**[2]

[1] *Faculty of Science, Unirsity of Split, Ruđera Boškovića 33, HR-21000 Split, Croatia*

[2] *Departament de Física, Universitat Politècnica de Catalunya, Campus Nord B4-B5, E-08034 Barcelona, Spain*

e-mail: *viktor.cikojevic@pmfst.hr*

We report diffusion Monte Carlo results of dilute Bose-Bose mixtures with repulsive intraspecies interaction $g_{11} = g_{22}$ and attractive interspecies interaction g_{12} [7]. The calculations are exact within some statistical noise and thus go beyond previous perturbative estimations. We determine the critical attractive scattering length needed to form a self-bound droplet. The ground-state energies and the density profiles for increasing numbers of particles are determined. Deviations from the mean-field prediction as a function of the ratio of $g_{12}^2/(g_{11}g_{22})$ are discussed. Observation of a self-bound drop agrees with recent experimental findings[3].

Mean-field theory of Bose-Bose mixtures predicts miscible gas phase for $g_{12}^2 < g_{11}g_{22}$ and a collapsed state for $g_{12}^2 > g_{11}g_{22}$. Adding a LHY correction [1] to the mean-field, Petrov predicted stable liquid-like droplets at $g_{12}^2 \approx g_{11}g_{22}$ [2]. Liquid-like droplets are also predicted in 1D and 2D [4]. Going beyond perturbation theory, using quantum Monte Carlo, we study droplets far from mean-field critical point. We determine critical interaction strength required to self-bind finite particle drops (1), density profiles of self-bound drops, (2) dependence of system properties with the number of particles and the behavior of a collapse with the increase of $|a_{12}|$.

A N-particle Hamiltonian for a mixture is given by

$$H = -\frac{\hbar^2}{2m_1}\sum_{i=1}^{N_1}\nabla_i^2 - \frac{\hbar^2}{2m_2}\sum_{j=1}^{N_2}\nabla_j^2 + \frac{1}{2}\sum_{\alpha,\beta=1}^{2}\sum_{i_\alpha,j_\beta=1}^{N_\alpha,N_\beta} V^{(\alpha,\beta)}(r_{i_\alpha j_\beta}) \ , \quad (1)$$

We use square well for the interspecies attraction and a hard core for the intraspecies repulsion. To reduce the number of variables in the problem, we restrict to a scenario where $m_2 = m_1$ and $a_{11} = a_{22}$. We use exact DMC method accurate to second-order in the time step [5]. Distribution functions are obtained using the pure estimators [6].

Comparison between the Bose-Bose drops and superfluid ^{4}He drops show their unique properties. For a typical value of a_{11} used in ultracold mixtures of ^{39}K, $a_{11} = 50a_0$, with a_0 the Bohr radius,the saturation densities shown in Fig. 2 are $\sim 10^{-6}$ and $1.6 \cdot 10^{-6}$Å^{-3}. The saturation density of liquid ^{4}He is $2.2 \cdot 10^{-2}$Å^{-3}, meaning that the Bose-Bose drops can be as dilute as $\sim 10^4$ times the ^{4}He.

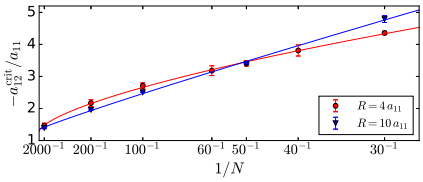


Figure 1: Dependence of critical a_{12} on the number of particles N for two different interaction models.

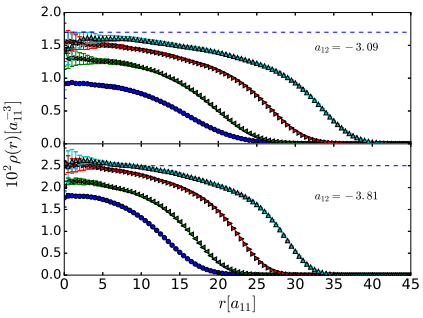


Figure 2: Density profiles for fixed a_{12}. From small to large drops, $N = 200$, 400, 1000, and 2000. Dashed lines represents equilibrium bulk density obtained by DMC.

References

[1] T. D. Lee, K. Huang, and C. N. Yang, Phys. Rev. 106, 1135 (1957)

[2] D.S. Petrov, Phys. Rev. Lett. 115, 155302, (2015)

[3] C. R. Cabrera *et al.*, Science 359, 301(2018)

[4] D. S. Petrov, G. E. Astrakharchik, Phys. Rev. Lett. 117, 100401 (2016)

[5] J. Boronat and J. Casulleras, Phys. Rev. B 49 8920 (1994)

[6] J. Casulleras and J. Boronat, Phys. Rev. B 52, 3654 (1995)

[7] V. Cikojević, K. Dželalija, P. Stipanović, L. Vranješ Markić, and J. Boronat, Phys. Rev. B 97, 140502 (2018).

Non-Linear Two-Dimensional Atomic Mirrors

M. Moreno-Cardoner[1], **M. T. Manzoni**[1], **A. Asenjo-Garcia**[1,2,3], **D. E. Chang**[1,4]
[1] *ICFO-Institut de Ciencies Fotoniques, The Barcelona Institute of Science and Technology, 08860 Castelldefels (Barcelona), Spain*
[2] *Norman Bridge Laboratory of Physics MC12-33, California Institute of Technology, Pasadena, CA 91125, USA*
[3] *Institute for Quantum Information and Matter, California Institute of Technology, Pasadena, CA 91125, USA*
[4] *ICREA-Institució Catalana de Recerca i Estudis Avançats, 08015 Barcelona, Spain*
e-mail: *mariona.moreno@icfo.eu*

It is known that a single layer of atoms ordered in a two-dimensional array can reflect light as a perfect mirror, if the atoms are placed at close enough distances. This represents a beautiful example of how the cooperative response of a collection of atoms, arising from strong interference and long-range rescattering in light emission, can give rise to surprising behavior that is in contrast to our daily experience (where large amounts of material are needed to construct a mirror).

While the linear optical properties of dipole arrays have been relatively well studied, a feature unique to atoms is the ability to generate strong interactions between photons, such as by the excitation of an atom to a Rydberg state through photon absorption. Indeed, the influence on quantum light propagation due to Rydberg blockade in disordered atomic ensembles has generated intense interest.

Here, we investigate the qualitatively different physics that can occur when Rydberg interactions are added to an ordered 2D array. We find that this system offers exciting possibilities, such as creating a non-linear optical mirror, which responds very differently depending on the number of photons of the incident light beam, and the generation of non-classical spatial correlations between scattered photons.

To calculate these effects, we employ a quantum interacting dipole-dipole model to capture the dynamics of atomic internal states as they interact via electromagnetic modes, while all of the emitted field properties are related to correlations of the atoms via a novel quantum input-output relation.

Quantum Batteries: Fundamental bounds and spin-system architecture

S.Julia Farre[1], T.Salamon[1,2] A.Riera[1], M.Bera[1] and M. Lewenstein[1]

[1] *Institut de Ciències Fotòniques, The Barcelona Institute of Science and Technology, 08860 Castelldefels, Spain*

[2] *Institute for Theoretical Physics, Albert-Einstein-Allee 11, Universitat Ulm, D-89069 Ulm, Germany*

e-mail: *tymoteusz.salamon@icfo.eu*

The lack of significant progress in capacity and power of classical, electrochemical batteries is a big obstacle to development of new transport and energy storage technologies. While the range of modern electric cars is becoming competitive with petrol-powered ones the charging process is still at least on order of magnitude greater then filling up the fuel tank.

Quantum batteries gained much interest in 2012 as a result of Alicki and Fannes paper [1] in which the concept of maximal reversibly extractable work(capacity) was discussed as well as reaching the thermodynamical limit of capacity by using entangling charging operations.

In 2015 Binder et al. presented the new charging protocol for quantum battery[2]. It has been shown that an array of N qubits with energy gap E_1 (the battery) with total energy described by battery Hamiltoninan $H_B = \sum_{i=1}^{N} \frac{1}{2}\sigma_z^i$ which is transformed (charged) from the state $|0\rangle^{\otimes N} \rightarrow |1\rangle^{\otimes N}$ by the Hamiltonian of the form $H_C^{global} = NE_1(|0\rangle^{\otimes N}\langle 1|^{\otimes N} + h.c)$ will perform such an evolution n times faster (power(P) of the battery n times greater) then by independent (parallel) charging of each qubit with the Hamiltonian of the form: $H_C^{parallel} = \sum_{i=1}^{N} E_1\sigma_x^i$ providing these two charging processes have the same amount of energy (NE_1) available for battery charging. However such a global operation as given by H_C^{global} is difficult to realize. In 2017 Campaioli et al. [3] proved that for any charging process based on k-body interactions with each qubit interacting with max. m other qubits the maximal power advantage Γ comparing to $H_C^{parallel}$ is upper-bounded by $\Gamma = \gamma(k^2(m-1)+k)$, where γ was a size-independent coefficient.

We present the theoretical approach for fundamental bounds on power of quantum batteries based on analysis of quantum state's dynamics in both Hilbert and energy space. We assume that quantum power advantage comparing to parallel charging can be obtained either by increased speed of evolution in energy space which is an equivalent of Fisher information or by following shortened trajectory in the energy space which corresponds to non-locality of the battery Hamiltonian and which is described by energy fluctuations of the state of the system, namely $\delta^2 H_B = \sqrt{\mathrm{Tr}\{H_B^2\rho\} - \mathrm{Tr}\{H_B\rho\}^2}$. We also derive fundamental bound on power based on Cauchy-Schwarz inequality and above mentioned assumptions.

We also present possible realization of the quantum batteries based on spin chains. We restrain ourselves to 2-body interactions with various symmetries and range regimes within Lipkin-Meshkov-Glick[4, 5, 6, **?**] model governed by Hamiltonian of the form:

$$H_{LMG} = -h\sum_i \sigma_z^i - \frac{\lambda}{N}\sum_{i<j}(\sigma_x^i\sigma_x^j + \gamma\sigma_y^i\sigma_y^j). \quad (1)$$

We then analyze and measure above mentioned theoretical quantities to check if LMG for any symmetry/range configuration can saturate fundamental power bounds.

References

[1] R. Alicki and M. Fannes, Phys. Rev. E **87**, 042123 (2013).

[2] F. Binder *et. al.*, New J. Phys **17**, 075015 (2015).

[3] F. Campaioli *et. al.*, Phys. Rev. Lett **118**, 150601 (2017).

[4] H. J. Lipkin, N. Meshkov, and A. J. Glick, Nucl. Phys **118**, 150601 (2017).

[5] N. Meshkov, A. J. Glick, and H. J. Lipkin, Nucl. Phys **188**, 188 (1965).

[6] A. J. Glick, H. J. Lipkin, and N. Meshkov, Nucl. Phys **62**, 199 (1965).

[7] J. I.Lattore, R.Orus, E. Rico, J. Vidal, Phys. Rev. A **71**, 101103 (2004).

Energy exchange between atoms and a Quartz Crystal μ–balance

A. Chavarría-Sibaja[1,2], A. Godínez-Sandí[1,2], K. Hernández-Jiménez[1,2], S. Thiel-Pizarro[1,2], M. Guevara-Bertsch[3], and O.A. Herrera-Sancho[1,2,4]

[1] *Escuela de Física, Universidad de Costa Rica, 2060 San Pedro, San José, Costa Rica*

[2] *Centro de Investigación en Ciencia e Ingeniería de Materiales, Universidad de Costa Rica, 2060 San Pedro, San José, Costa Rica*

[3] *Institut für Quantenoptik und Quanteninformation, Österreichische Akademie der Wissenschaften, Technikerstr. 21a, 6020 Innsbruck, Austria*

[4] *Centro de Investigación en Ciencias Atómicas Nucleares y Moleculares, Universidad de Costa Rica, San José 2060, Costa Rica*

e-mail: *oscar.herrerasancho@ucr.ac.cr*

"Never measure anything but frequency!" was the motto of Arthur Schawlow [1], referring to the physical quantity that can be measured with the highest precision and accuracy. Inspired by this idea, we propose an experimental method to fully characterize the energy exchange of particles in their physical vapor state in order to study the dynamics of the first atoms colliding with an oscillator. Our approach is based on the careful observation of perturbations induced by interaction of particles with the oscillation frequency of a Quartz Crystal μ-balance (QCM). Therefore, we are able to measure the momentum exchange between atoms and the QCM during the evaporation process and determine the energy distribution of the particles [2]. Our goal is to apply our experimental approach to characterize the cooling dynamics of our Zeeman Slower [3].

Furthermore, we are able to follow the desorption dynamics of particles immediately after a thin layer has been formed at the QCM. As is well known, the first layers of any material are the bridge of communication between the bulk and the environment that surrounds it. Consequently, these layers have a key role in the comprehension and control of the properties of any material [4]. Our experimental results are in close relation to the surface binding energy of the evaporated material, as they also offer a better control to obtain the desired properties of the thin surface layer. We therefore applied experimentally our technique to investigate the physical vapor evaporation process for diverse elements, usually implemented in contemporary technological development of thin film surface layer, such as Cu, W, Au, Gd, and In. Our results support the observations reported by A. Jasik using other techniques such as low temperature photo luminescence in rather complicated measurement systems like a liquid He cryostat [5].

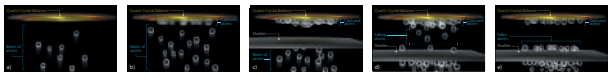


Figure 1: Artistic visualization of the perturbations induced by interaction of particles with the oscillation frequency of a Quartz Crystal μ-balance (QCM). Panel a) shows the resonant oscillation frequency of the crystal and the beam of atoms. Panel b) demonstrates the interactions of the beam of atoms with the QCM. Panel c), d) and e), on the other hand, shows the time–scale–dynamics where the beam of atoms is abruptly stopped with a shutter.

[1] T.W. Hänsch, Annalen der Physik 15 (2006) 627-652.

[2] A. Godínez-Sandí, A. Chavarría-Sibaja, M. Guevara-Bertsch, O.A. Herrera-Sancho, to be published (2018).

[3] M. Guevara-Bertsch, L. Salfenmoser, A. Chavarría-Sibaja, E. Avendaño, and O.A. Herrera-Sancho, Rev. Mex. Fis 62 (2016) 175-182.

[4] M. Guevara-Bertsch, G. Ramírez-Hidalgo, A. Chavarría-Sibaja, E. Avendaño, J.A. Araya-Pochet, and O.A. Herrera-Sancho, AIP Advances 6 (2016) 035317.

[5] A. Jasik, A. Wnuk, J. Gaca, M. Wójcik, A. Wójcik-Jedlińska, J. Muszalski, W. Strupiński, Journal of Crystal Growth **311**, (2009): 4423-4432.

Nanophotonic cavity QED with individually trapped atoms

T. Dordevic[1], **P. Samutpraphoot**[1], **P. Ocola**[1], **H. Bernien**[1], **V. Vuletic**[2], **M. D. Lukin**[1]
[1] *Department of Physics, Harvard University, Cambridge, MA 02138,USA*
[2] *Department of Physics and Research Laboratory of Electronics, Massachusetts Institute of Technology, Cambridge, MA 02139, USA*
e-mail: *tamaradordevic@g.harvard.edu*

Engineering interactions between individual photons and matter qubits is a central theme in quantum optics and an essential prerequisite for future quantum technologies such as quantum networks. We achieve such interactions by using a hybrid approach in which we couple individually trapped atoms to a nanophotonic crystal cavity [1]. Using nanophotonic cavities allows for small mode volumes and high quality factors, as well as high collection e ciency of the reflected photons.

Here we demonstrate strong coupling between single atoms and photons (Fig. 1). We use this coupling to read out the internal state of the atoms in a single shot. Furthermore, we show our results on controlling the internal states of the atoms close to the cavity, as well as our progress towards preparing an entangled state of the two atoms mediated by the cavity photons. We discuss the prospects of scalable and efficient quantum gates with applications in integrated quantum networks.

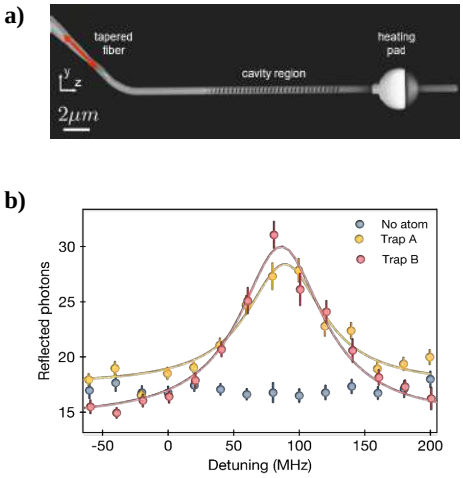


Figure 1: **a**) SEM image of the nanophotonic cavity used in this experiment. **b**) Cavity reflection spectrum with atoms in individual traps (A and B) coupled to the cavity mode. Increased reflectivity on resonance is a signature of strong atom-photon coupling.

[1] T. G. Tiecke, J. D. Thompson, N. P. de Leon, L. R. Liu, V. Vuletic and M. D. Lukin, Nature **508**, 241 (2014).

Subradiance and radiation trapping in large ensembles of cold atoms

P. Weiss[1], **M. O. Araùjo**[1], **A. Cipris**[1], **W. Guerin**[1] **and R. Kaiser**[1]

[1] *Institut de Physique de Nice, Universitè Côte d'Azur, CNRS, 1361 Route des Lucioles, 06560 Valbonne, France*

e-mail: *patrizia.weiss@inphyni.cnrs.fr*

Coherent effects in light scattering triggered a lot of studies, experimental and theoretical, since the seminal paper on "Coherence in spontaneous radiation processes" by Dicke [1]. Beside a variety of steady state experiments recent studies explore also the temporal dynamics of light scattering [2]. A lot of studies focused on fast decay dynamics, superradiance, first in a high excitation case and in the last years also in the low excitation limit (linear optics regime). The slow dynamics, subradiance, became topic of intense research recently. For example, it has been proposed to use subradiant states for photon storage [3, 4] or metrology [5].

We present the study of the temporal decay dynamics of a large atomic ensemble weakly excited (linear optic regime) by a series of light pulses. Due to cooperative effects the decay is modified compared to the single atom decay of the excited state. We show the experimental observation of subradiance in a large ensemble of N cold atoms [6]. Although our ensemble is dilute and much larger compared to the excitation wavelength, which is in contrast to Dicke's initial assumptions, subradiante states are still present. The decay time of the longest lived, visible subradiant mode behaves independently of the detuning and scales linearly with the on-resonant optical thickness of the sample. The independence with the light detuning to the atomic resonance excludes the possibility of multiple scattering causing the slow decay.

Further we studied the effect of radiation trapping or slow diffusion of light due to classical multiple scattering [5], which at first glance mimics subradiance as it also shows a slow decay for atomic ensembles with large optical thickness. With well chosen parameters of the exciting beam both effects can occur together [8].

We demonstrate the different physical origins of both effects and show how to discriminate between radiation trapping and subradiance. Due to the different physical mechanisms the decay time scaling dependencies are different and allow to distinguish between both effects. The interpretation of the effects is supported by numerical simulations done with the coupled dipole model and a random walk model [8].

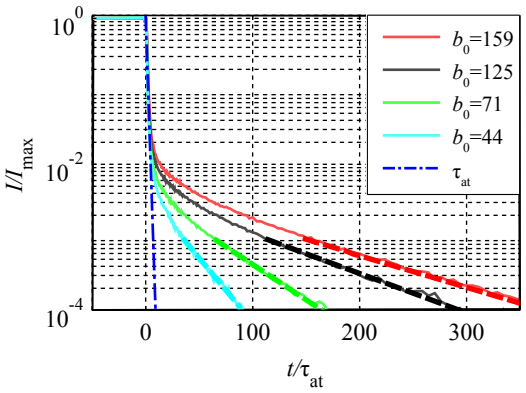


Figure 1: Experimental decay curves for different on-resonance optical depths b_0. The atomic cloud was weakly excited with a large detuned laser pulse $\delta = -3.15\Gamma$.

[1] R. H. Dicke, Phys. Rev. **93**, 99–110 (1954).

[2] M. O. Scully, E. S. Fry, C. H. Raymond Ooi and K. Wódkiewicz, Phys. Rev. Lett. **96**, 010501 (2006).

[3] G., Facchinetti S. D. Jenkins and J. Ruostekoski, Phys. Rev. Lett. **117**, 243601 (2016)

[4] A. Asenjo-Garcia, M. Moreno-Cardoner, A. Albrecht, H. J. Kimble and D. E. Chang, Phys. Rev. X **7**, 031024 (2017)

[5] L. Ostermann, H. Ritsch, and C. Genes, Phys. Rev. Lett. **111**, 123601 (2013)

[6] W. Guerin, M. O. Araújo, and R. Kaiser, Phys. Rev. Lett. **116**, 083601 (2016).

[7] G. Labeyrie, E. Vaujour, C.A. Müller, D. Delande, C. Miniatura, D. Wilkowski, R.Kaiser, Phys. Rev. Lett. **91**, 223904 (2003).

[8] P. Weiss, M. O. Araújo, R. Kaiser and W. Guerin, New J. Phys. accepted for publication (2018).

Atomic memory using higher-order nonlinear processes

G. C. Borba[1], **D. Felinto**[1], **and J. W. R. Tabosa**[1]
[1] *Departamento de Física, Universidade Federal de Pernambuco, Recife-PE, 50670-901, Brazil*
e-mail: *gabrielborba@df.ufpe.br*

Quantum memories are essential for many tasks in quantum information, especially for long-distance quantum communication protocols, where optical memory would be essential to the synchronization of the different segments of a linear chain of pairs of entangled atomic ensembles. Successful implementation of atomic-ensemble quantum memory has been carried out using different techniques. Many of them employ essentially first-order ground-state coherences to store the phase information of the incident fields, being the overall nonlinear process of storage retrieval characterized by the third-order nonlinear susceptibility $\chi^{(3)}$ of the atomic medium, which is connected to four-wave mixing.

The present work explores new possibilities for the selective storage of higher order nonlinearity in a sample of cold atoms confined in a magneto-optical trap. Particularly, we demonstrate the storage of a third-, fifth-, and seventh-order nonlinear atom-light interaction into the hyperfine cesium $6S_{1/2}$, $F = 3$ ground state. The writing process creates gratings associated with higher-order nonlinear processes, which can be selectively read by the beam R after a controlled storage time. In each process the atom interacts with a specific number of photons leading to special features in the signal of each order [1]. We also demonstrated that such memories were able to both store and manipulate the orbital angular momentum of an input field, obtaining outputs with topological charges that were algebraic functions of the input topological charge [2]. For example, one can retrieve double or triple input topological charge for the memory based on $\chi^{(5)}$ or $\chi^{(7)}$ processes, respectively.

Since such higher-order nonlinearities are associated with processes involving a larger number of photons, this kind of memory can in principle be used to generate multiple quantum-correlated photons, opening the possibility to extend the capability of many quantum information protocols.

[1] G. C. Borba, D. Felinto, and J. W. R. Tabosa, J. Opt. Soc. Am. B **34**, 2528 (2017).

[2] R. A. de Oliveira, G. C. Borba, W. S. Martins, S. Barreiro, D. Felinto, and J. W. R. Tabosa, Opt. Lett. **40**, 4939 (2015).

Atom-light interactions in photonic crystal waveguides

A. P. Burgers[1], **L. Peng**[1], **and H. J Kimble**[1]
[1] *California Institute of Technology, Pasadena, CA, United States*
e-mail: *aburgers@caltech.edu*

Integrating cold atoms with nanophotonics enables the exploration of new paradigms in quantum optics and many body physics. Advanced fabrication capabilities for low-loss dielectric materials provide powerful tools to engineer band structure and light-matter couplings between photons and atoms. The current system at Caltech to explore such phenomena consists of a quasi-one-dimensional photonic crystal waveguide whose band structure arises from periodic modulation of the dielectric structure [1]. The waveguide design gives rise to stable trap sites for atoms at each unit cell of the crystal (150 sites for the 1D waveguide). Atoms localized in these traps will interact with one another via guided modes of the waveguide creating a versatile system that can be utilized for both quantum memories and quantum simulation [2, 3, 4] .

A detailed understanding of the atomic delivery near the device is required before any trap sites within the waveguide can be loaded. To deliver atoms to the structure they are first confined into a 1D lattice using two counter-propagating, free-space dipole beams. By chirping the frequency of a single lattice beam the atoms are transported to the structure ∼2cm from the lattice loading site. A guided mode probe, resonant with the atoms, in the photonic crystal structure signals the atom arrival to the device. The intensity maxima of the 1D lattice (where the atoms are trapped) pass through the device at a temporal spacing given by the inverse of the chirp frequency. So, by temporally registering the probe data between the lattice intensity maxima we build a histogram of the atom arrival in one lattice period. Figure 1 shows the kind of spectrum we are able to obtain by utilizing this technique. These time vs. detuning spectra convey important information about atomic trajectories near the device and inform the ultimate goal of trapping along the photonic crystal waveguide. To better understand the atomic delivery we conducted detailed simulations of atomic trajectories near the structure including calculations of the atomic spectra in the presence of guided mode fields. These guided mode fields will ultimately be used to create the desired trapping potentials, so a detailed understanding of the atomic interaction with such fields and drawing direct correspondence between simulation and experiment is essential. Figure 1 shows the comparison between simulation and experiment for a single guided mode field used to Stark shift atoms interacting with different regions

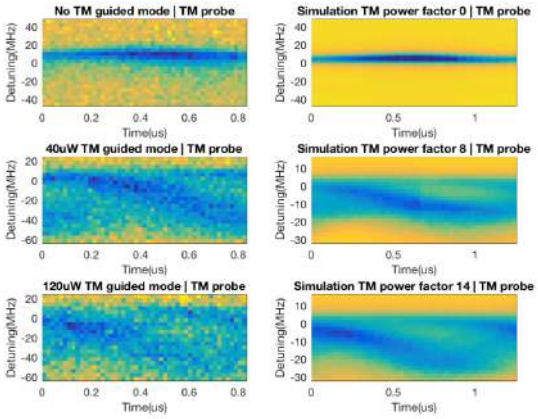


Figure 1: Comparison of data (left column) and simulation (right column) for the atoms delivered to the waveguide using a conveyor belt technique. By varying the power of an off-resonant guided mode beam we observe the separation of different classes of atomic trajectories in time and frequency. Note that the simulation and experiment were conducted at different speeds.

of the device. The direct correspondence between simulation and experiment is apparent in these data; moreover, the data indicate a clear separation of the atomic sample into different classes of atoms experiencing the Stark shifting beam at different arrival times to the structure.

We will present the more detailed approach to the simulations, and how they are utilized to determine atom position near the device. Additionally, we will present recent efforts to achieve high fractional filling of trap sites within the photonic crystal waveguide using the optical lattice delivery system, and discuss future research goals.

References

[1] Yu, S.-P. *et al.* *App. Phys. Lett.* **104**, 111103 (2014).

[2] Douglas, J. S. *et al.* *Nature Photonics* **9**, 326–331 (2015).

[3] Hung, C.-L., González-Tudela, A., Cirac, J. I. & Kimble, H. J. *PNAS* 201603777 (2016).

[4] Asenjo-Garcia, A., Moreno-Cardoner, M., Albrecht, A., Kimble, H. J. & Chang, D. E. *Phys. Rev. X* **7**, 031024 (2017).

Enhancing optical nonlinearities in atomic ensembles to single-photon levels with photonic crystals

T. Yoon[1], J. Flannery[1,3], B. Duong[1,3], B. Semnani[1], P. Anderson[1,3], R. Al Maruf[1,2], Z. Ding[1,3], C. Vickers[1,3], F. Rajabi[1], and M. Bajcsy[1,2]

[1] *Institute for Quantum Computing, University of Waterloo, Waterloo, Ontario, Canada*
[2] *Electrical and Computer Engineering, University of Waterloo, Waterloo, Ontario, Canada*
[3] *Physics and Astronomy Department, University of Waterloo, Waterloo, Ontario, Canada*
e-mail: *mbajcsy@uwaterloo.ca*

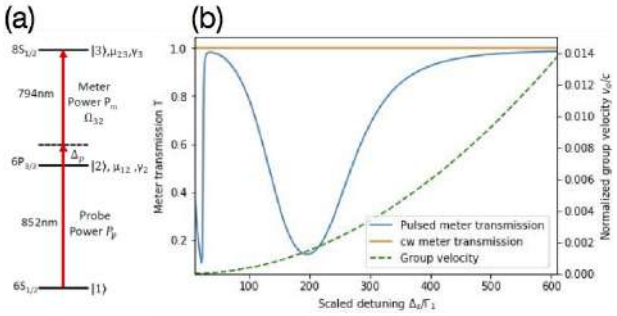


Figure 1: **(a)** The level scheme for two photon absorption in caesium. **(b)** Numerical simulation of the transmission of a 200ns long meter pulse containing a single photon through an ensemble of 10^6 cold atoms confined inside a HCPCF with a 7μm diameter core in the presence of a single-photon probe pulse (blue curve). The probe pulse is also 200ns long and experiences a significant reduction of its group velocity (dashed green curve). When both meter and probe are continuous with power equivalent to 1 photon/s, the transmission of the meter change changes only very slightly (orange curve).

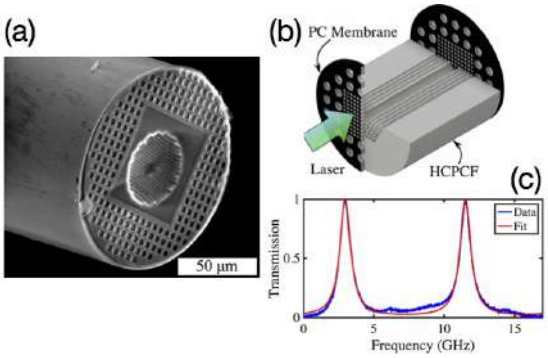


Figure 2: **(a)** A scanning electron microscope image of a photonic crystal membrane attached to the tip of a HCPCF segment with UV glue. The photonic crystal region of the fiber can be seen underneath the center square containing photonic-crystal holes forming the metasurface mirror. **(b)** A HCPCF-integrated Fabry-Pérot cavity. The fiber confines light in the transverse direction, while the pair of photonic crystal (PC) mirrors mounted on the ends of the fiber segment confine light longitudinally. **(c)** A normalized transmission spectrum of a ∼2 cm long fiber-cavity at ∼852nm found by scanning the frequency of a laser coupled into the structure.

We report our progress toward realizing strong optical nonlinearities controlled by single photons. We aim to achieve these nonlinearities in laser-cooled atomic ensembles with the help of two types of photonic-crystal structures: hollow-core photonic-crystal fibers (HCPCF) and planar photonic crystals acting as dielectric metasurface mirrors. Although laser-cooled atomic ensembles confined inside a HCPCF have been explored as a platform for nonlinear optics for the past decade [1, 2], demonstration of single-photon nonlinearity in this system has remained elusive so far.

With our first generation experiment, in which a laser-cooled cloud of caesium atoms is loaded into a short piece of HCPCF and confined with a red-detuned dipole trap, we explore the probe field increase arising from pulse compression due to the reduced group velocity near a single-photon absorptive resonance [3] to achieve simultaneous absorption of two photons in the ladder scheme shown in Fig. 1 (a). Our numerical simulations of pulsed light propagation through the fiber-confined ensemble predict that a significant enhancement of two-photon absorption should be observable with single-photon pulses compared to a HCPCF loaded with room temperature atoms [4].

For our second generation experiment, we have been developing a Fabry-Pérot cavity formed inside the HCPCF when two photonic crystal membranes are attached to the ends of a fiber section (Fig. 2) [5]. These perforated membrane mirrors should allow loading of cold atoms into the hollow core of the fiber and can be designed to be fully transparent for one polarization while highly reflective for the other.

References

[1] M. Bajcsy *et al.*, Phys. Rev. Lett. 102, 203902 (2009)
[2] F. Blatt *et al.*, Phys. Rev. A 94, 043833 (2016)
[3] R. M. Camacho *et al.*, Phys. Rev. A 73, 063812 (2006)
[4] V. Venkatamaran *et al.*, Phys. Rev. Lett. 107, 193902 (2011)
[5] J. Flannery *et al.*, ACS Photonics 5, 337 (2018)

Towards A Quantum Communication Platform Using Rare Earths Chelates

T. Ohana[1], **O.E. Mor**[1], **A. Borne**[1], **A. Shanzer**[2], **and B. Dayan**[1]
[1] *Department of Chemical Physics, Weizmann Institute of Science, 76100 Rehovot, Israel*
[2] *Department of Organic Chemistry, Weizmann Institute of Science, 76100 Rehovot, Israel*
e-mail: *tal.ohana@weizmann.ac.il*

Isolated quantum systems for quantum information were implemented so far mainly with ultra-cold atoms and ions, and with superconducting circuits. In recent years there has been a wide search for alternative solid state systems such as quantum dots and color centres in diamonds. One type of potential candidates is rare-earth ions, due to their partially filled 4f shell. This inner shell is well shielded from the environment, which leads to sharp absorption and emission lines with very long fluorescence lifetimes and long coherence time. To date, most of the experimental efforts have been with rare-earth doped crystals [1]-[2] and recently with doped optical resonators [3]. Though the intra 4f transitions are shielded to some extent, the coupling to crystal phonon bands is significant. Therefore cooling to 4K is mandatory in order to observe naturally-broad lines. Decoherence is also induced by nearby nuclei exhibiting spin through spin-spin coupling. Schemes utilizing lanthanide ions for quantum optical experiments should fulfill two main requirements: preventing parasitic interactions with the environment as well as feasible coupling to optical modes. We propose a bottom-up approach in which we chemically tailor a lanthanide-based complex which couples to the evanescent field of a nanofiber mode (figure 1). This molecule is designed to have less coupling to vibrations in order to demonstrate coherent optical interactions at room temperature. Our preliminary results show significant narrowing of excitation spectra using an ensemble of Yb complexes [4] on the surface of a tapered fiber, and comparable fluorescence lifetime in comparison with a commercial Yb-doped fiber. This molecule will also be used to permanently bind the ion to a surface of a tapered fiber and eventually to the surface of a whispering-gallery-mode (WGM) resonator [5]. Such a system of a single rare earth ion attached to an optical WGM cavity can become a new platform for quantum optics and quantum information processing and possibly a quantum node in future quantum networks.

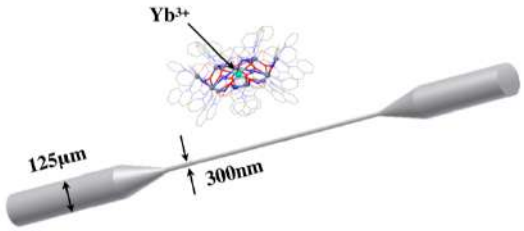


Figure 1: Illustration of an Yb complex deposited on a tapered fiber.

[1] T. Utikal, E. Eichhammer, L. Petersen, A. Renn, S. Gotzinger, V. Sandoghdar, Nat. Comms. **5**, 3627 (2014)

[2] P. Siyushev, K. Xia, R. Reuter, M. Jamali, N. Zhao, N. Yang, C. Duan, N. Kukharchyk, A. D. Wieck, R. Kolesov and J. Wrachtrup, Nat. Comms. **5**, 3895 (2014)

[3] D. Ding, L. M. C. Pereira, J. F. Bauters, M. J. R. Heck, G. Welker, A. Vantomme, J. E. Bowers, M. J. A. de Dood, and D. Bouwmeester, Nat. Photonics **10**, 385 (2016).

[4] E. R. Trivedi, S. V. Eliseeva, J. Jankolovits, M. Olmstead, S. Petoud, and V. L. Pecoraro, Journal of the American Chemical Society, **136**, 1526 (2014)

[5] A. Hatzor, T. Moav, H. Cohen, S. Matlis, J. Libman, A. Vaskevich, A. Shanzer, and I. Rubinstein, Journal of the American Chemical Society, **120**, 13469 (1998)

High-efficiency backward four-wave mixing by quantum interference

Yong-Fan Chen[1,2], **Zi-Yu Liu**[1], **and Chin-Yao Cheng**[1]
[1] *Department of Physics, National Cheng Kung University, Tainan 70101, Taiwan*
[2] *Center for Quantum Technology, Hsinchu 30013, Taiwan*
e-mail: *yfchen@mail.ncku.edu.tw*

Long-distance quantum optical communications usually require e cient wave-mixing processes to convert the wavelengths of single photons. Many quantum applications based on electromagnetically induced transparency (EIT) have been proposed and demonstrated at the photon level, such as quantum memories [1], all-optical transistors [2], and cross-phase modulations [3]. However, EIT-based four-wave mixing (FWM) in a resonant double-Λ configuration has a maximum conversion e ciency (CE) of 25% because of absorptive loss due to spontaneous emission. Here we demonstrate that spontaneous emission can be considerably suppressed by arranging the applied laser beams in a backward configuration. With the backward double-Λ FWM scheme, we observe a CE of 76% in cold rubidium atoms with an optical depth (OD) of 52. The energy level diagram and the experimental arrangements are shown in Fig. 1. Furthermore, we present a theoretical model that includes the phase-mismatch effect in the backward double-Λ FWM system [4]. According to the theoretical model, the present scheme can achieve 96% CE using a medium with a large OD of 200 under ideal conditions. This backward FWM scheme can achieve a near-unity CE, thus providing an easy method of implementing an e cient quantum wavelength converter for narrow-band single photons in all-optical quantum information processing.

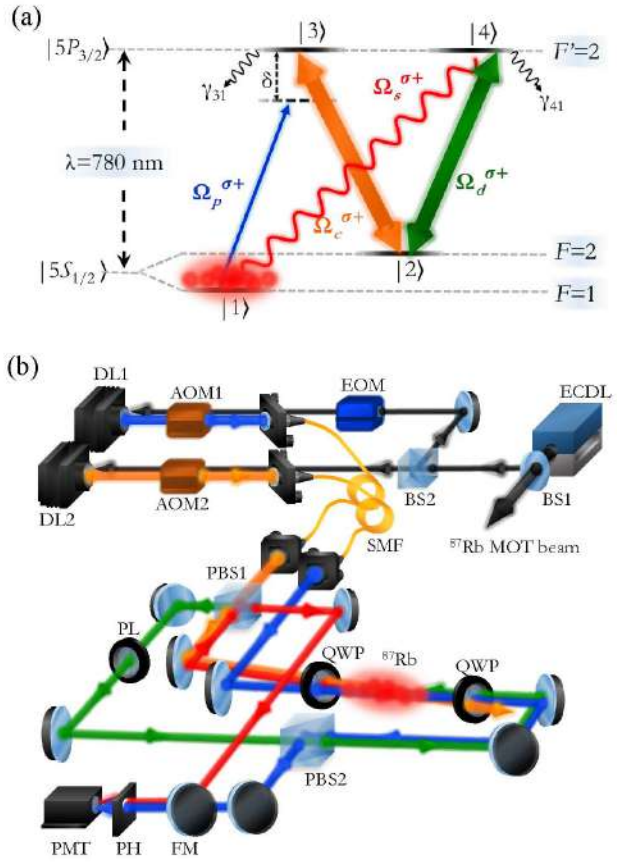


Figure 1: Energy level diagram and experimental arrangements. (a) Energy level of D_2-line transition of ^{87}Rb for EIT-based backward FWM. All fields are on resonance. (b) Schematic of the experimental setup. ECDL, external cavity diode laser; DL, diode laser; EOM, 6.8-GHz electric-optical modulator; AOM, acousto-optic modulator; SMF, single-mode fiber; PL, polarizer; PBS, polarization beam splitter; BS, beam splitter; HWP, half-wave plate; QWP, quarter-wave plate; FM, flipping mirror; PH, pinhole; PMT, photo-multiplier tube. Note that a small angle of approximately 0.4° is set between the probe and coupling beams. The driving beam is exactly counter propagating and coincides with the probe beam. The generated signal field is in the opposite direction of the coupling field, according to phase-match condition.

[1] P. Vernaz-Gris, K. Huang, M. Cao, A. S. Sheremet, and J. Laurat, Nat. Commun. **9**, 363 (2018).

[2] W. Chen, K. M. Beck, R. Bücker, M. Gullans, M. D. Lukin, H. Tanji-Suzuki, and V. Vuletić, Science **341**, 768 (2013).

[3] Z.-Y. Liu, Y.-H. Chen, Y.-C. Chen, H.-Y. Lo, P.-J. Tsai, I. A. Yu, Y.-C. Chen, and Y.-F. Chen, Phys. Rev. Lett. **117**, 203601 (2016).

[4] Z.-Y. Liu, J.-T. Xiao, J.-K. Lin, J.-J. Wu, J.-Y. Juo, C.-Y. Cheng, and Y.-F. Chen, Sci. Rep. **7**, 15796 (2017).

Single-Photon Interferometry with Frequency Comb States

Sun Kyung Lee[1], **Noh Soo Han**[1], **Minhaeng Cho**[1,2], **and Tai Hyun Yoon**[1,3]
[1] *Center for Molecular Spectroscopy and Dynamics, Institute for Basic Science (IBS), Seoul 02841, Korea*
[2] *Department of Chemistry, Korea University, Seoul 02841, Korea*
[3] *Department of Physics, Korea University, Seoul 02841, Korea*
e-mail: *thyoon@korea.ac.kr*

We present a novel frequency comb single-photon interferometry (FCSPI) in a unheralded manner via induced first-order coherence between two independent signal photons by generating indistinguishable idler photon states. By embedding two stimulated parametric down conversion (StPDC) crystals into two arms of the interferometer, we observe that the interference fringe of signal photons with a unit visibility (0.87) where two StPDC crystals are pumped simultaneously by the same pump pulses (adjacent pump pulses), indicating the generation of multi-dimensional (time-bin encoded) single-photon states with multiple frequency comb components. We also show that the FCSPI is capable of quantum measurement with undetected photons of the transmission coefficient of a sample placed on the seed beam path.

A schematic diagram of our FCSPI setup is shown in Fig. 1(a). A frequency comb with $f_{rep} = 250$ MHz at 530 nm (second-harmonic generation (SHG) of 1060 nm) and a ultra-narrow linewidth (1 Hz) cw laser at idler wavelength (1542 nm) are used as two pair of pump beams for two stimulated parametric down conversion (StPDCs) crystals (waveguide PPLN, periodically-poled $LiNbO_3$). Here, the corresponding single-photon emission efficiency is very low so that multi-photon generations by each StPDC crystal can be safely ignored. Then, the first order coherence of the signal field at 807.2 nm is induced via erasing idler path information by generating single-photon-added idler states at 1542 nm with a high-enough coherent-state amplitude $|\alpha|^2 \gg 1$. Therefore, the double pathway configuration from the polarizing BS (PBS) separating the SHG comb into two (upper and lower) paths to the beam-combining BS can be considered as a novel quantum interferometer.

In previous experiments, the path-entangled photon pairs of the signal and idler modes exhibit phase coherence in a two-photon interference, as manifested by coincidence counting rate measurements. Interestingly, however, only when which-path information of the conjugate idler photons is erased, the single-photon coherence of signal field becomes manifest. This can be achieved by making either idler photons paths indistinguishable by perfectly aligning the two idler beams [1] or their photon statistics of the idler fields indistinguishable via injecting a coherent laser at the idler field frequency [2] without heralding idler detection. The latter scheme has been chosen in our

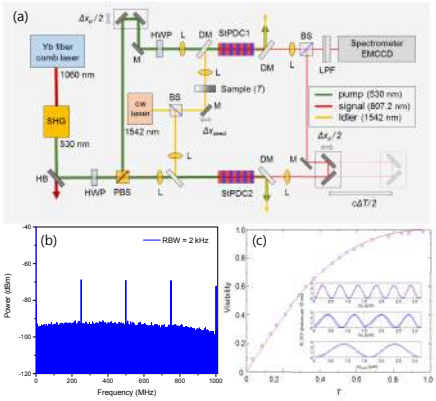


Figure 1: (a) Setup for the proposed FCSPI. (b) Frequency comb structure of signal photons at the average photon number of 5 photons per pulse. (c) Visibility V of FCSPI vs amplitude transmission coefficient T of a sample. (Inset; Interference fringes of FCSPI vs Δx_p, Δx_{seed}, and Δx_s).

experiment. With the FCSPI setup in Fig. 1 (a), we obtain the interference fringes with a unit visibility versus pump beam path length difference, Δx_p, signal beam path length difference, Δx_s, seed beam path length difference, Δx_{seed}, respectively, as in Fig. 1(c). Furthermore, we found that the visibility is still very high as 0.87 when the lower signal beam path is deliberately made to be longer by $c/f_{rep} = 1.2$ m, resulting in the time-bin encoded single-photon states. In this way, we show that the proposed FCSPI is feasible without detecting heralded single photons.

We also show that the visibility V can be modulated by the amplitude transmission coefficient T of the optical sample interacting with one of the injected seed beams (Fig. 1(c)) since the degree of indistinguishability between two idler fields generated by StPDC crystals would depend on the optical samples spatial or spectral characteristics. This is a key non classical feature of our FCSPI, which enable us to implement a novel remote quantum imaging and quantum spectroscopy with undetected photons [4].

[1] A. Heuer *et. al.*, Phys Rev A **92**,033834 (2015).

[2] L. Wang *et. al.*, JOSA B **8**, 978 (1991).

[3] A. Zavatta *et. al.*, Science **306**, 660 (2004).

[4] D. A. Kalashnikov *et. al.*, Nature Photon. **10**, 98 (2016).

Lasing from Cold Ytterbium Atoms

D. Sholokhov, H. Gothe, A. Breunig, M. Steinel, and J. Eschner
Experimentalphysik, Universität des Saarlandes, 66123 Saarbrücken, Germany
e-mail: *dmitriy.sholokhov@physik.uni-saarland.de*

Cold trapped atoms with narrow transitions are interesting systems for implementations of new kinds of lasers such as the super-radiant laser [1]. Several experiments have demonstrated lasing with trapped cold ^{87}Rb [2, 3] or ^{88}Sr [4]. In our work, lasing with ^{174}Yb is demonstrated [5].

A few million ytterbium atoms are magneto-optically trapped, using their $^1S_0 - {}^1P_1$ transition, inside a 5-cm long high-finesse cavity. The atoms are laser-pumped perpendicular to the cavity axis on the $^1S_0 - {}^3P_1$ transition and emit frequency-shifted light into the cavity [5]. For the relevant levels and transitions see Fig. 1.

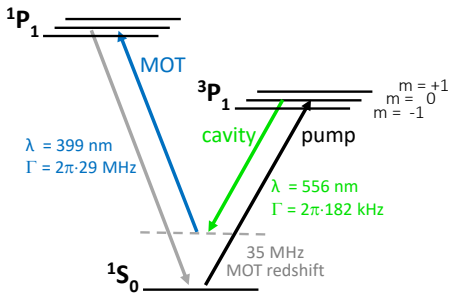


Figure 1: Energy level structure of ^{174}Yb atoms. The arrows indicate the relevant transitions and illustrate our proposed model for the lasing process through a virtual lower level created by the MOT laser.

Single- and multi-mode emission is observed above a threshold pump intensity, see Fig. 2. The emitted photons show a flat g(2) correlation function. These facts indicate a lasing process, partially resembling the one found in cold Sr clouds [4].

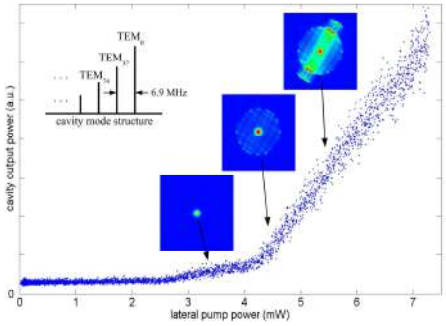


Figure 2: Output power vs. pump power. Higher order modes appear at higher pump powers. The inset shows the cavity mode spectrum.

We also investigated the polarization dependence between pump and cavity output, and concluded about the spatial position of the lasing atoms with respect to the quadrupole B-field of the magneto-optical trap (MOT), see Fig. 3.

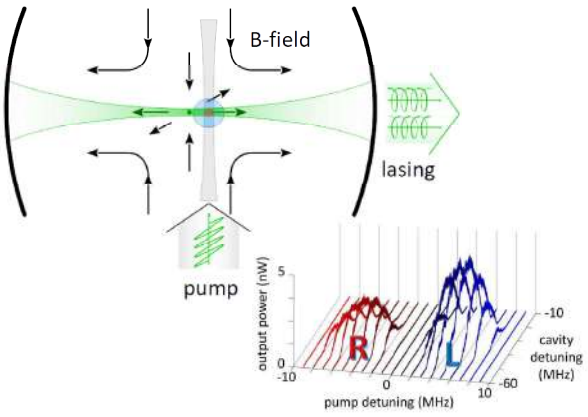


Figure 3: (Top) The polarization of the laser output depends on the pump polarization and the position of the lasing atoms in the MOT B-field. In our case the atoms are displaced from $B = 0$ along the cavity axis and experience an on-axis B-field. Pumped from below with light polarized at 90° to the cavity axis, the atoms can emit right- and left-polarized photons into the cavity. (Bottom) Laser output power at fixed pump power vs. pump and cavity detuning. The two regions of laser action correspond to right- and left-circularly polarized output.

The conditions under which the laser emission occurs, its properties, and our model for the underlying process will be presented in this poster.

[1] J. Bohnet, Z. Chen, J. Weiner, D. Meiser, M. Holland, J. Thompson, Nature 484, 78-81 (2012)

[2] W. Guerin, F. Michaud, R. Kaiser, Phys. Rev. Lett. 101, 093002 (2008)

[3] G. Vrijsen, O. Hosten, J. Lee, S. Bernon, M. Kasevich, Phys. Rev. Lett. 107, 063904 (2011)

[4] M. Norcia, J. Thompson, Phys. Rev. X 6, 011025 (2016)

[5] H. Gothe, D. Sholokhov, A. Breunig, M. Steinel, J. Eschner, arXiv:1711.08707 (2017)

Coherent population trapping (CPT) versus electromagnetically induced transparency (EIT) [1]

Sumanta Khan, Molahalli Panidhara Kumar, Vineet Bharti, and Vasant Natarajan
Department of Physics, Indian Institute of Science, Bangalore-560012, India
e-mail: *sumanta@iisc.ac.in*

We discuss the differences between two well-studied and related phenomena—coherent population trapping (CPT) and electromagnetically induced transparency (EIT). Many differences between the two—such as the effect of power in the beams, detuning of the beams from resonance, and the use of vapor cells filled with buffer gas—are demonstrated experimentally. The experiments are done using magnetic sublevels of the $1 \rightarrow 1$ transition in the D_2 line of ^{87}Rb.

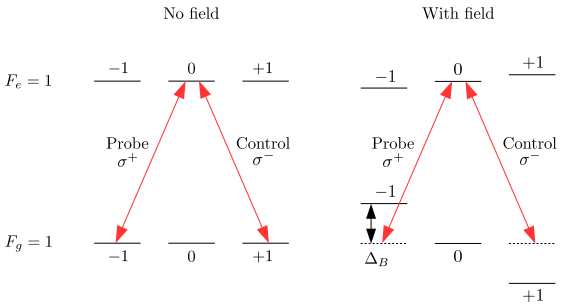


Figure 1: Magnetic sublevels of the $1 \rightarrow 1$ transition used in the experiment. The beams get detuned in the presence of a magnetic field, as shown on the right.

$$R_\delta = \frac{\Gamma}{2}\frac{I/I_s}{1 + I/I_s + 4\delta^2/\Gamma^2} \quad (1)$$

$$R = \frac{\Gamma}{2}\frac{I/I_s}{1 + I/I_s} \quad (2)$$

$$\Gamma = \Gamma_\circ\sqrt{1 + \frac{I}{I_s}} \quad (3)$$

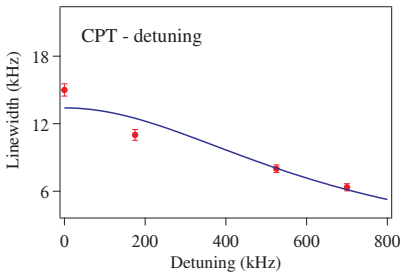


Figure 2: Effect of detuning on CPT resonances. The linewidth decreases because of reduced scattering from the upper level. The solid line is a fit to Eq. (1), which gives the scattering rate in the presence of detuning.

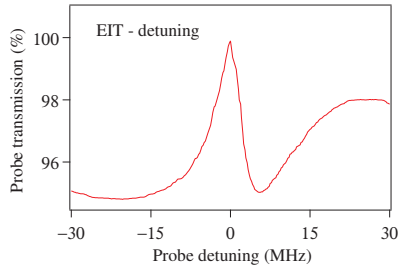


Figure 3: EIT resonance in the presence of detuning, achieved with a magnetic field of 1 G corresponding to a level shift of 0.7 MHz. The lineshape of the resonance is highly asymmetric.

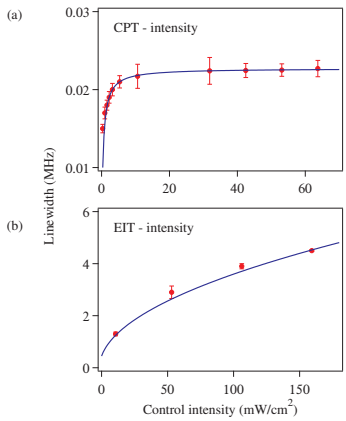


Figure 4: Effect of control intensity on the linewidth of the resonance. (a) For CPT resonances, showing increase in linewidth due to increased decoherence through the upper level. The solid line is a fit to the scattering-rate expression in Eq. (2). (b)For EIT resonances, showing increase in linewidth due to power broadening. The solid line is a fit to the power-broadening expression in Eq. (3).

References

[1] S. Khan, M. P. Kumar, V. Bharti, and V. Natarajan. Coherent population trapping (CPT) versus electromagnetically induced transparency (EIT). *Eur. Phys. J. D*, 71(2):38, 2017. doi:10.1140/epjd/e2017-70676-x. URL `https://doi.org/10.1140/epjd/e2017-70676-x`.

Experimental demonstration of composite stimulated Raman adiabatic passage

A. Bruns[1], **G. T. Genov**[1], **M. Hain**[1], **N. V. Vitanov**[2] **and T. Halfmann**[1]
[1] *Institut für Angewandte Physik, Technische Universität Darmstadt, Hochschulstraße 6, 64289 Darmstadt, Germany*
[2] *Department of Physics, Sofia University, 5 James Bourchier Boulevard, 1164 Sofia, Bulgaria*
e-mail: *alexander.bruns@physik.tu-darmstadt.de*

Quantum information architectures require precise control to prepare, manipulate or preserve quantum states. The main requirements for such control tools are high fidelity and robustness against fluctuations in the experimental parameters.

An important goal for quantum control is robust and high fidelity population inversion. Resonant coherent light-matter interactions such as π-pulses can deliver high e ciency in many quantum systems but suffer substantially from non-optimal conditions which are inevitable in an experiment. A powerful alternative are adiabatic passage techniques. They are based on slow, i.e., adiabatic, variations of the experiments control parameters such that the state of the system does not change in the adiabatic basis. However, the experimental performance of such techniques is limited by inevitable residual diabatic couplings. Stimulated Raman adiabatic passage (STIRAP) is a well established technique with a multitude of applications in physics and chemistry. The original concept allows for e cient population transfer between two states of a three-state system. Although both states are coupled to the same intermediate state by two radiation fields, the intermediate sate remains unpopulated during the interaction. While resonant STIRAP is very sensitive to variations in the initial quantum state, off-resonant STIRAP can be used to invert a quantum system with an arbitrary initial state. This makes off-resonant STIRAP particularly suited for repeated inversion processes. In such repeated sequences, the total inversion e ciency suffers substantially from any ine ciency in the single process.

Composite pulses (CPs), i.e., sequences of pulses with appropriately chosen relative phases, offer a way to boost the robustness of STIRAP. CPs are applicable for accurate and robust qubit rotation, by driving a quantum system on robust pathways through Hilbert space. Most traditional CPs are derived to compensate against a specific kind of of error, e.g., in the pulses area or frequency. Recently, universal composite pulses (UCPs) were proposed and demonstrated [1]. They can compensate against arbitrary systematic pulse errors. A combination of STIRAP with composite pulses (CSTIRAP) was recently proposed by cooperation partners [2].

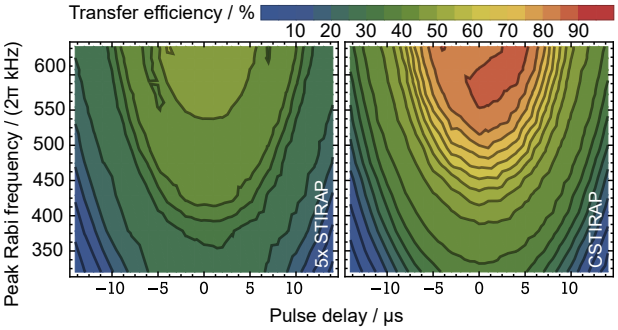


Figure 1: Experimentally measured population transfer efficiency for repeated STIRAP and CSTIRAP at a single photon detuning of 1.75 MHz. Positive delays correspond to the Stokes pulse preceding the pump pulse (i.e., STIRAP configuration).

We present now a proof-of-principle experimental demonstration of CSTIRAP. Specifically, we perform population transfer between the hyperfine ground states of Pr^{3+} ions in a rare-earth doped solid [3]. In the highly detuned regime, we show that CSTIRAP substantially improves both the robustness and the peak transfer e ciency, as compared to repeated STIRAP (see Figure 1). Furthermore, we apply CSTIRAP with universal composite phases and show a systematic improvement compared to the originally proposed CSTIRAP phases. In addition, we compare the experimental findings with numerical simulations.

In the highly detuned regime STIRAP is insensitive to the initial state of the system, which makes it suitable for repeated inversion processes, e.g., for rephasing of atomic coherences in quantum memories. Especially when the spin transition is not directly addressable, e.g., due to forbidden dipole transitions, optical rephasing sequences are necessary. Our results indicate that in these situations CSTIRAP performs significantly more e cient and robust than repeated traditional STIRAP.

[1] G. T. Genov, D. Schraft, T. Halfmann and N.V. Vitanov, Phys. Rev. Lett. **113**, 043001 (2014).

[2] B. T. Torosov and N. V. Vitanov, Phys. Rev. A **87**, 043418 (2013).

[3] J. Klein, F. Beil and T. Halfmann, Phys. Rev. Lett. **99**, 113003 (2007).

Raman Gray Molasses Cooling of Cesium Atoms on the D_2 Line

Ya-Fen Hsiao[1,2], **Yu-Ju Lin**[1], **and Ying-Cheng Chen**[1]

[1] *Institute of Atomic and Molecular Sciences, Academia Sinica, Taipei 10617, Taiwan*

[2] *Molecular Science Technology, Taiwan International Graduate Program, Academia Sinica and National Central University, Taiwan.*

e-mail: *yafenhsiao@gate.sinica.edu.tw*

Sub-Doppler cooling is a powerful technique to increase the phase-space density of most alkali atoms. However, the narrow excited-state structure of the D_2 transition of lithium and potassium makes it difficult to implement the standard red-detuned sub-Doppler cooling. The recent success of blue-detuned, Λ-enhanced sub-Doppler cooling of ^{7}Li[1] has attracted renewed interest in laser cooling based on "dark states", which we referred as Raman grey molasses cooling. Since then, this cooling method has been demonstrated in many other atomic species and isotopes, such as ^{6}Li[2], ^{39}K[3], ^{40}K[4], ^{41}K[5], ^{23}K[6] and ^{87}Rb[7]. In most of the works with Li, K and Na, the Raman grey molasses cooling were implemented with the D_1 transition. Thanks to the large hyperfine splittings in the D_2 transition of ^{87}Rb and ^{133}Cs, it could be easily implemented based on only the trapping and repumping lasers with suitable frequency control. We report the Raman grey molasses cooling of ^{133}Cs to (1.7±0.2) μK with a capture e ciency of >80 % at an initial atom number of 1.94×10^9.

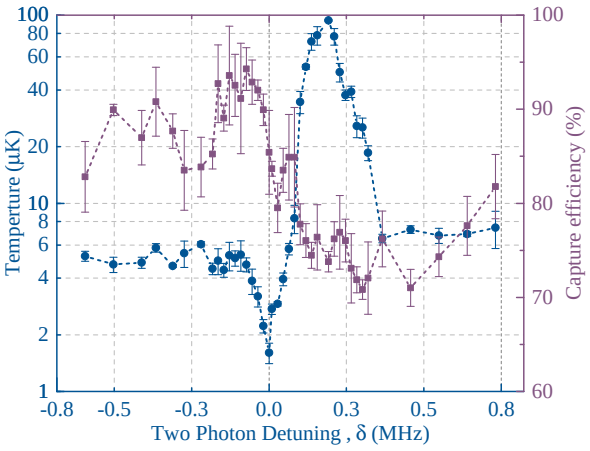


Figure 1: Temperature and capture efficiency as a function of two-photon detuning after 3-ms Raman grey molasses cooling. The one-photon detuning is 6 Γ blue to the $F = 4 \rightarrow F' = 4$ transition and the intensity ratio of repumping to cooling beam is 0.08 with an one-beam intensity of $\sim 0.4\ mW/cm^2$ for the trapping beams.

[1] A. T. Grier, I. Ferrier-Barbut, B. S. Rem, M. Delehaye, L. Khaykovich, F. Chevy and C. Salomon, Phys. Rev. A, **87**, 063411(2013).

[2] A. Burchianti, G. Valtolina, J. A. Seman, E. Pace, M. De Pas, M. Inguscio, M. Zaccanti, and G. Roati. Phys. Rev. A, **90**, 043408(2014)

[3] D. Nath, R. K. Easwaran, G. Rajalakshmi, and C. S. Unnikrishnan. Phys. Rev. A, **88**, 053407(2013).

[4] F. Sievers, N. Kretzschmar, D. R.Fernandes, D. Suchet, M. Rabinovic, Saijun Wu, C.V. Parker, L. Khaykovich, C. Salomon, and F. Chevy. Phys. Rev. A, **91**, 023426(2015).

[5] H.-Z. Chen, X.-C. Yao, Y.-P. Wu, X.-P. Liu, X.-Q. Wang, Y.-X. Wang, Y.-A. Chen, and J.-W. Pan, Phys. Rev. A, **94**, 033408(2016).

[6] G. Colzi, G. Durastante, E. Fava, S.Serafini, G. Lamporesi, and G. Ferrari. Phys. Rev. A, **93**, 023421(2016).

[7] S. Rosi, A. Burchianti, S. Conclave, D. S. Naik, G. Roati, C. Fort, and F. Minardi. Sci. Rep. **8**, 1301(2018).

Ultrabright, narrow-band photon-pair source for atomic quantum memories

Pin-Ju Tsai[1,2], **and Ying-Cheng Chen**[1]

[1] *Institute of Atomic and Molecular Sciences, Academia Sinica, Taipei 10617, Taiwa*

[2] *Department of Physics, National Taiwan University, Taipei 10617, Taiwan*

e-mail: *cditim@hotmail.com*

We demonstrate an ultrabright, narrow-band and frequency-tunable photon-pair source based on cavity-enhanced spontaneous parametric down conversion (SPDC) which is compatible with atomic transition of rubidium D_2-line (780 nm) or cesium D_2-line (852 nm). With the pump beam alternating between a high and a low power phase, the output is switching between the optical parametric oscillator (OPO) and photon pair generation mode. We utilize the OPO output light to lock the cavity length to maintain the double resonances of signal and idler, as well as to lock the signal frequency to cesium atomic transition(see fig.1). With a type-II phase matching and a double-passed pump scheme such that the cluster frequency spacing is larger than the SPDC bandwidth, the photon pair output is in a nearly single-mode operation as confirmed by a scanning Fabry-Perot interferometer with its output detected by a photomultiplier. The achieved generation and detection rates are 7.24×10^5 and 6142 pairs/(s·mW)(see fig.2), respectively. The correlation time of the photon pair is 21.6(2.2) ns, corresponding to a bandwidth of $2\pi \times 6.6(6)$ MHz. The spectral brightness is 1.06×10^5 pairs/(s·mW·MHz). This is a relatively high value under a single-mode operation with the cavity-SPDC scheme. The generated single photons can be readily used in experiments related to atomic quantum memories[1].

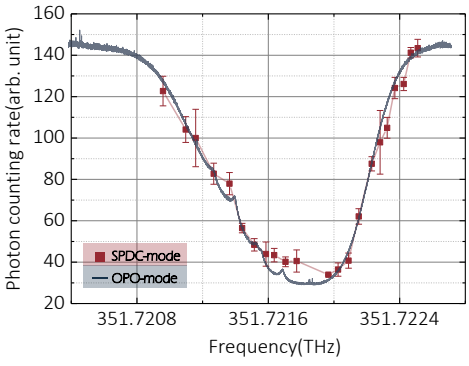


Figure 1: Demonstration of photon-atom interaction. The absorption spectrum in Cesium D_2-line of signal photon under SPDC-mode and OPO-mode.

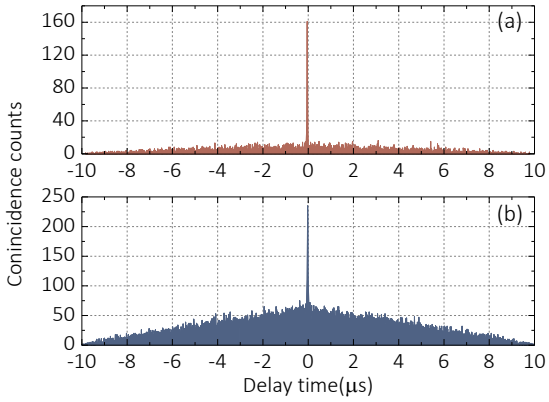


Figure 2: Measurement of the correlation function with different pump power and different detection time. (a) 0.3mW and 250ms; (b) 2.25mW and 50ms.

[1] Pin-Ju Tsai and Ying-Cheng Chen, Quantum Sci. Technol., **3**, 034005(2018)

Random Singlet Phase of Cold Atoms Coupled to One-Dimensional Photonic Crystals

David Z. Li[1], **Marco T. Manzoni**[1] **and Darrick E. Chang**[1,2]
[1] *ICFO-Institut de Ciencies Fotoniques, The Barcelona Institute of Science and Technology, 08860 Castelldefels, Spain*
[2] *ICREA-Institucio Catalana de Recerca i Estudis Avancats, 08015 Barcelona, Spain*
e-mail: *zhaozhe.li@icfo.eu*

Systems consisting of cold atoms trapped near photonic crystal waveguides have recently emerged as an exciting platform for quantum atom-light interfaces. Such a system enables realization of tunable long-range interactions between internal states of atoms (spins), mediated by guided photons. One interesting property of this system is that at low filling fractions, the Hamiltonian can resemble that of a short-ranged disordered system, which exhibits many interesting phenomena. The study of such a Hamiltonian is also relevant because current experiments trapping cold atoms near photonic crystals are not yet able to achieve high fillings. As an example, we show how the system can realize the so-called "random singlet phase", in which all atoms entangle into singlet pairs, but the pairing occurs over a distribution of ranges as opposed to nearest neighbors. Specifically, we use a renormalization group (RG) method and solve the RG flow equation to obtain the distribution of spin entanglement in the random singlet phase, and show how the ground state of such an isolated system can be reached via adiabatic evolution from a non-interacting ground state. We also discuss how experimentally this ground state can be observed.

Exchange of optical vortices using an electromagnetically induced transparency based four-wave mixing setup

H. R. Hamedi, J. Ruseckas, and G. Juzeliūnas
Institute of Theoretical Physics and Astronomy, Vilnius University,
Saulėtekio 3, Vilnius LT-10222, Lithuania
e-mail: *hamid.hamedi@tfai.vu.lt*

We propose a scheme to exchange optical vortices of slow light using the phenomenon of electromagnetically induced transparency (EIT) [1] in a four-level double- Lambda atom-light coupling scheme illuminated by a pair of probe fields as well as two control fields of larger intensity. We study the light-matter interaction for a situation where one control field carries an optical vortex, and another control field has no vortex. We show that the orbital angular momentum (OAM) [2] of the vortex control beam can be transferred to a generated probe field through a four-wave mixing (FWM) process and without switching on and off of the control fields. Such a mechanism of OAM transfer is much simpler than in a double-tripod scheme in which the exchange of vortices is possible only when two control fields carry optical vortices of opposite helicity [3]. The losses appearing during such OAM exchange have been analyzed. It is found that a single photon detuning plays an important role in minimizing the losses. An approximate analytical expression for the optimal one-photon detuning is obtained defining a condition where the losses are minimum while the intensity of generated probe field is maximum [4].

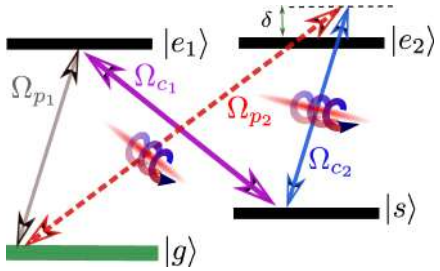


Figure 1: Ecxhange of OAM in double- Lambda atomic scheme

[1] Michael Fleischhauer, Atac Imamoglu, and Jonathan P. Marangos, Rev. Mod. Phys. **77**, 633 (2005).

[2] L. Allen and M. J. Padgett and M. Babiker, Progress in Optics **39**, 291–372 (1999).

[3] J. Ruseckas, V. Kudriašov, Ite A. Yu, and G. Juzeliūnas, Phys. Rev. A **87**, 053840 (2013).

[4] H. R. Hamedi, J. Ruseckas, G. Juzeliūnas, submitted in Phys. Rev. A.

Coupled-cavities quantum electrodynamics with a cavity array in a single optical fiber

Shinya Kato[1,2], **Nikolett Német**[3], **Kohei Senga**[2], **Shota Mizukami**[2], **Xinhe Huang**[2], **Scott Parkins**[3] **and Takao Aoki**[2]

[1] *JST, PRESTO, 4-1-8 Honcho, Kawaguchi, Saitama, 332-0012, Japan*

[2] *Department of Applied Physics, Waseda University, 3-4-1 Okubo, Shinjuku, Tokyo 169-8555, Japan*

[3] *Dodd-Walls Centre for Photonic & Quantum Technologies, Department of Physics, University of Auckland, Private Bag 92019, Auckland 1142, New Zealand*

e-mail: *s.kato6@kurenai.waseda.jp*

A quantum network, in which multiple quantum nodes are connected to each other through quantum channels, is an important physical model to study quantum communication and quantum information processing [1]. In order to realize a quantum network in a scalable and reconfigurable manner, cavity quantum electrodynamical (QED) systems connected through an optical fiber network is a promising experimental platform. As an elementary quantum network, two cavity QED systems with free-space Fabry-Perot optical cavities have been demonstrated, in which quantum information was transferred from one node to the other and entanglement was created between the distant nodes in a probabilistic way [2]. In contrast to directional coupling from one node to the other, coherent coupling between nodes is expected if the loss in the link channel is negligible compare to the coupling rate between the nodes. The coupled-cavities QED, which goes beyond simply connected cavity QED systems with lossy channels, paves the way to study quantum many body physics of photons or polaritons [3, 4].

Here, we experimentally demonstrate such a coupled-cavities QED system with a cavity array imprinted on a single optical fiber, and observe the dressed states of atomic ensembles in the distant nodes, which are more than 1 m apart, with the normal modes of the coupled-cavities. Our cavity array consists of four fiber Bragg grating mirrors in a single optical fiber, which creates three Fabry-Perot cavities in series (Fig. 1). In order to realize interaction between the cavity photon and atomic ensembles, we fabricated nano-fiber regions in the two end cavities where cavity photons can interact with atoms in the vicinity of the fiber surface through the evanescent field [5]. The ensemble of laser cooled cesium atoms are optically trapped using the evanescent fields of red- and blue-detuned trapping lasers which propagate in the optical fiber. In this poster, we will discuss the experimental and theoretical results of the transmission spectroscopy of the coupled-cavities system.

This work was supported by JST CREST Grant Number JPMJCR1771, JSPS KAKENHI Grant Number 16H01055, and JST PRESTO Grant Number JPMJPR1662, Japan. S. P. acknowledges support from the Marsden Fund of the Royal Society of New Zealand (Contract No. UOA1328).

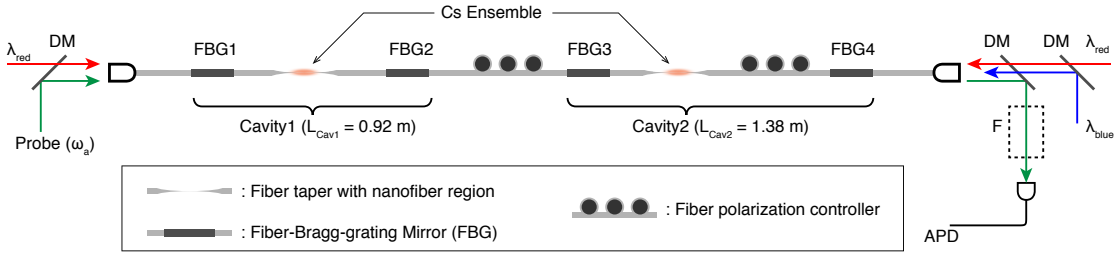


Figure 1: Schematic diagram of the experiment. The optical trapping lasers ($\lambda_{\mathrm{red}}, \lambda_{\mathrm{blue}}$) are superimposed on the probe laser by using dichroic mirrors (DM). The transmission of the probe beam through the coupled-cavities system is detected by an avalanche photo detector (APD) after the filtering system (F) to remove stray light.

[1] H. J. Kimble, Nature **453**, 1023 (2008).

[2] S. Ritter *et al.*, Nature **484**, 195 (2012).

[3] M. J. Hartmann, F. G. S. K. Brandão, and M. B. Plenio, Nature Physics **2**, 849 (2006).

[4] A. D. Greentree *et al.*, Nature Physics **2**, 856 (2006).

[5] S. Kato and T. Aoki, Phys. Rev. Lett. **115**, 093603 (2015).

Stopped light pulses at the single-photon level in a laser-cooled ensemble loaded into a hollow-core fiber

T. Peters[1], **and T. Halfmann**[1]

[1] *Institut für Angewandte Physik, Technische Universität Darmstadt, 64289 Darmstadt, Germany*

e-mail: *thorsten.peters@physik.tu-darmstadt.de*

Strong light-matter interactions at the few-photon level are a key requirement for, e.g., quantum information processing and quantum nonlinear optics [1, 2]. The light-matter coupling coupling strength is proportional to the ratio of the atomic and the mode field cross-sectional areas. Therefore, interactions are maximized by tightly confining both matter and light. One promising method towards tight confinement is based on transferring laser-cooled atoms into a hollow-core photonic crystal fiber (HCPCF) and guiding the atoms in the device by a red-detuned optical dipole trap to avoid collisions of the atoms with the fiber wall (see Fig. 1) [3, 4, 5].

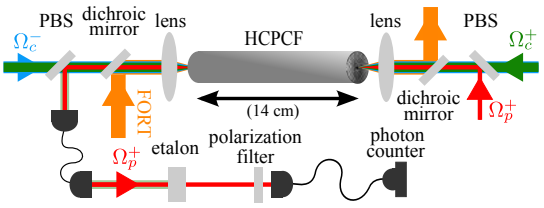


Figure 1: Schematic experimental setup.

In such a system optical depths of up to 1000 have been observed with an optical depth per atom of around 0.004 [5]. Also electromagnetically induced transparency (EIT) has been observed [6, 7, 8], as well as EIT-based slow light [6, 7], light storage and retrieval [7], and stationary light [7] with classical light fields.

We here report on our recent progress on the loading of laser-cooled rubidium atoms from a magneto-optical trap into a hollow-core photonic crystal fiber (core diameter 7 μm) and subsequent EIT-based experiments. A newly built dipole laser trap laser system allows for stable loading of atoms into the hollow-core fiber. We analyze the dipole trapping potential and the atomic ensemble inside the fiber by spectroscopic measurements. Finally, we demonstrate the retrieval (see Fig. 2) of stopped light pulses based on EIT at the single-photon level.

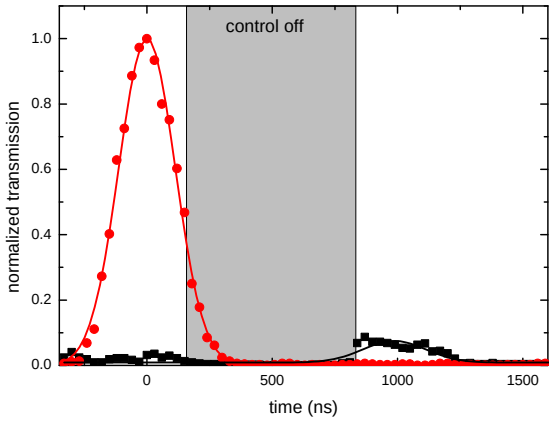


Figure 2: Light storage and retrieval in a HCPCF. Input pulse (red dots) and retrieved probe pulse (black squares) after a storage period of 700 ns.

[1] D. E. Chang, V. Gritsev, G. Morigi, V. Vuletić, M. D. Lukin, and E. A. Demler, Nat. Phys. 4, 884 (2008).

[2] D. E. Chang, V. Vuletić, and M. D. Lukin, Nat. Photonics 8, 685 (2014).

[3] M. Bajcsy, S. Hofferberth, T. Peyronel, V. Balić, Q. Liang, A. S. Zibrov, V. Vuletić, and M. D. Lukin, Phys. Rev. A 83, 063830 (2011).

[4] S. Vorrath, S. A. Mller, P. Windpassinger, K. Bongs, and K. Sengstock, New J. Phys. 12, 123015 (2010).

[5] F. Blatt, T. Halfmann, and T. Peters, Opt. Lett. 39, 446 (2014).

[6] M. Bajcsy, S. Hofferberth, V. Balić, T. Peyronel, M. Hafezi, A. S. Zibrov, V. Vuletić, and M. D. Lukin, Phys. Rev. Lett. 102, 203902 (2009).

[7] F. Blatt, L. S. Simeonov, T. Halfmann, and T. Peters, Phys. Rev. A 94, 043833 (2016).

[8] M. Langbecker, M. Noaman, N. Kjærgaard, F. Benabid, and P. Windpassinger, Phys. Rev. A 96, 041402 (2017).

Collective scattering in nanofiber-trapped atomic ensembles

A. S. Prasad[1], **J. Hinney**[1], **S. Rind**[1], **J. Volz**[1], **P. Schneeweiss**[1], **A. Rauschenbeutel** [1,2]

[1] *Vienna Center for Quantum Science and Technology, TU Wien - Atominstitut, Stadionallee 2, 1020 Vienna, Austria*

[2] *Department of Physics, Humboldt-Universität zu Berlin, 10099 Berlin, Germany*

e-mail: *adarsh.prasad@tuwien.ac.at*

We realize an e cient optical interface between guided light and laser-cooled atoms which are arranged in two linear arrays in a two-color evanescent-field dipole trap created around an optical nanofiber [1]. In this configuration, the probability of a nanofiber-guided photon being absorbed by a single trapped atom can be as high as 10 %.

For a periodic array of atoms, the interference of the light fields scattered by different atoms result in a collective emission. The photons emitted into the non-guided radiative modes are scattered in a cone with a well-defined angle with respect to the fiber axis. We call this cone the Bragg cone as the emission into this cone requires fulfillment of constructive interference condition similar to Bragg condition in solid-state physics. Our simulations show that the collective emission pattern loses its azimuthal symmetry when there are two arrays of trapped atoms. The angle of the collective emission with respect to the fiber axis varies depending on the trapping periodicity and the probe wavelength. We plan to study this collective emission and its dependence on various experimental parameters.

Here we present the experimental setup used for creating large periodic arrays of atoms, outline the theoretical formalism predicting collective scattering, and compare the scattering from the coherent excitation of such large arrays in ideal and realistic scenarios. We show how we plan to observe the Bragg cone by suitably tuning the periodicity of the trapping sites and then imaging the scattered photons with a sensitive camera. Such collective scattering phenomena from the nanofiber trapped atomic ensemble might be interesting, e.g., for realizing novel quantum memories [2].

[1] E. Vetsch et. al., Phys. Rev. Lett. 104, 203603 (2010).

[2] A. Asenjo-Gracia et. al., Phys. Rev. X 7, 031024 (2017).

Atomic frequency comb quantum memory via piecewise adiabatic passage

D. Viscor, J. L. Rubio, J. Mompart, and V. Ahufinger
Departament de Física, Universitat Autònoma de Barcelona, 080193 Bellaterra, Spain
e-mail: *daniel.viscor@uab.cat*

The ability to process flying qubits or strings of flying qubits, and specifically the control of light-matter interfaces capable of storing these qubits and retrieve them on demand for subsequent use, i.e., quantum memories (QM) [1], are key elements for quantum communication. Atomic Frequency Combs (AFC) based QMs [2] have experienced an enormous progress in the last years, achieving spin-wave storage for on-demand retrieval, high-fidelity multiplexing, optimized e ciencies, and telecom wavelength operation.

In this work we propose a method to create an AFC in hot atomic vapors using the piecewise adiabatic passage (PAP) technique [3]. In PAP, the piecewise version of the stimulated Raman adiabatic passage (STIRAP) [4], the pump and dump fields are replaced by trains of pulses with envelopes fulfilling the well-known counter intuitive pulse sequence of STIRAP with a temporal overlap τ (see Fig. 1). Due to the Doppler effect, the trains of pulses used for PAP give rise to a velocity-dependent transfer of the atomic population from the initial state to the target one, thus forming an atomic velocity comb whose periodicity depends not only on the repetition rate of the applied pulses ω, as it is for standard AFCs, but also on the specific atomic transitions considered. In particular, we show that the velocity peaks separation is $v = c\ \omega/\omega_{13}$, with ω_{13} the frequency of the Raman transition $|1\rangle \leftrightarrow |3\rangle$ and c the speed of light. This implies that the predefined retrieval time T_{int} of AFC-QMs is modified by a factor ω_{13}/ω_{34}, where ω_{34} is the frequency of the transition where the photon will be stored. We also derive analytical expressions for other features of the comb such as the tooth width, the finesse, and the number of peaks.

Next, we use the obtained comb to implement a hot-vapor AFC quantum memory. Specifically, we use the $|1\rangle = 6s^2\,{}^1S_0 \leftrightarrow |2\rangle = 6s6p\,{}^1P_1$ and $|2\rangle \leftrightarrow |3\rangle = 6s5d\,{}^1D_2$ transitions of Ba atoms (at 800 °C and density $\varrho = 2.5 \times 10^{20}$ at/m^3) due to the fact that they present a large asymmetry on the Raman transition, they have metastable states, and posses telecom transitions suitable for quantum communication (the photon will be stored with an off-resonant Raman absorption via the state $|2\rangle$ in transition $|2\rangle \leftrightarrow |4\rangle \equiv 6s5d\,{}^3D_2$ not shown in the figure). We perform numerical simulations of a signal photon propagating through the AFC medium (Fig. 2) and study the storage and retrieval e ciencies of the memory as a function of various PAP parameters

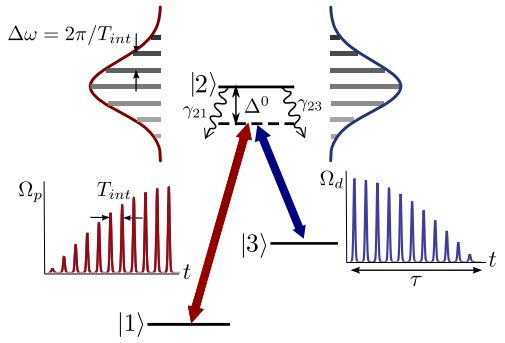


Figure 1: Atomic energy levels with the decay rates γ_{21} and γ_{23}, and the Rabi frequencies of the pump and dump trains of pulses, with pulse temporal spacing T_{int} (see text for additional parameter description).

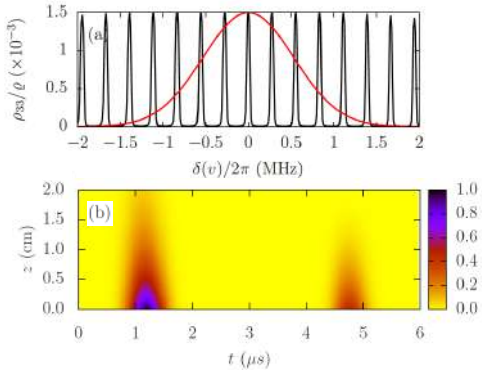


Figure 2: (a) Generated comb as a function of the Raman detuning of the $|3\rangle \leftrightarrow |4\rangle$ transition, compared to the incident signal photon profile. Here we used $T_{int} = 0.7\,\mu$s, $N = 40$, $\Omega_p^0 = \Omega_d^0 = 2\pi \cdot 52$ MHz, and $\Delta^0 = 2\pi \cdot 130$ MHz (see text for definitions). (b) Intensity of the propagating photon as a function of position z and time $t = t' - z/c$.

such as the pump and dump peak Rabi frequencies $\Omega_{p,d}^0$, the number of pulses in the trains N, and the nominal one-photon detuning ^{0}.

[1] A. I. Lvovsky *et al.*, Nat. Photon. **3**, 706 (2009).

[2] H. De Riedmatten *et al.*, Nature **456**, 773 (2008); P. Farrera *et al.*, Optica **3**, 1019 (2016).

[3] E. Shapiro *et al.*, Phys. Rev. Lett. **99**, 033002 (2007).

[4] K. Bergmann *et al.*, Rev. Mod. Phys. **70**, 1003 (1998).

Phase-coherent light scattering from long trapped ion strings

P. Obšil[1], A. Lešundák[2], T. Pham[2], G. Araneda[3], O. Číp[2], R. Filip[1] and L. Slodička[1]

[1] *Department of Optics, Palacký University, 17. listopadu 12, 771 46 Olomouc, Czech Republic*

[2] *Institute of Scientific Instruments of the CAS, Královopolská 147, 612 64 Brno, Czech Republic*

[3] *Institut für Experimentalphysik, Universität Innsbruck, Technikerstraße 25, 6020 Innsbruck, Austria*

e-mail: *slodicka@optics.upol.cz*

Realizing an experimental platform suitable for coherent light scattering from a large ensemble of individual quantum emitters represents a long-standing goal of the experimental quantum optics community [1, 2, 3]. We report on the observation of phase interference of laser light scattered from large strings of trapped $^{40}Ca^{+}$ions [4]. The implemented detection along the symmetry axis of the linear trapping potential allows for scaling up the ion number without considerable effect on their relative fluorescence collection e ciency. The interference phase is tuned by changing the mutual distance between the ions using applied static electric potential and the observed patterns are reproduced very plausibly by a simple theoretical model considering point-like emitters.

The presented experimental scheme allows for the observation of scattered light from the controllable atomic system with a well-defined number of particles. It comprises a linear Paul trap with the tip electrodes which have small apertures used for the collection of light scattered by the ion crystal. For the relatively small solid angles offered by the typical apertures, the light scattered from ion string aligned along the optical axis of the collection optics is detected with approximately the same e ciency for all ions.

The phase interference is observed by scattering the near-resonant laser light propagating with an angle of 45° with respect to ion string axis from the ions. The distance between the ions is determined by the applied tip voltages U which allows for the accurate scan of the relative phase difference between the scattered photons. The Fig. 1 shows the examples of the resulting measured interference patterns for 10, and 20 ions, respectively. The blue curves correspond to the calculation of the observed interference, which assumes equal coherent contributions from all ions with the phase factor calculated according to the numerically estimated mean ion positions. These simplified calculations are in very good agreement with the observed interference pattern, which suggests that the spatial distribution of ions in the crystal corresponds exactly to the ideal positions given solely by the harmonic axial trapping potential and the mutual Coulomb repulsion. In addition, this points to the near-equality of the coherent contribution to the detected signal for all individual ions present in the string.

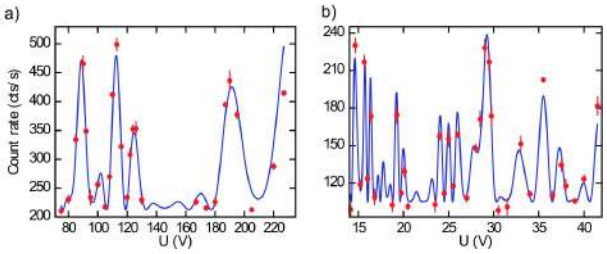


Figure 1: Results of the measurements of phase interference of light scattered from ion crystals containing 10 (a) and 20 (b) ions. The red points correspond to the measured count rates and blue solid lines show the theoretical model based on the numerical calculation of the mean relative ion positions for the given axial voltages U_{tip}, with amplitude and offset fitted to the data. All error bars correspond to statistically evaluated single standard deviation. Note that the mutual ion spacing is not uniform, so that the expected interference patterns are not those of a regular scattering grid.

The presented observations of the coherent scattering from trapped-ion strings containing up to 53 ions correspond to the first unambiguous proof of collective phase-coherent interaction of light with such large samples of individual quantum emitters. These results have the potential to trigger a substantial experimental progress in many research directions which require controllable coherent interaction or enhancement from many quantum emitters and, at the same time, high control over their external and internal degrees of freedom.

References

[1] U. Eichmann, J. C. Bergquist, J. J. Bollinger, J. M. Gilligan, W. M. Itano, D. J. Wineland, and M. G. Raizen, Phys. Rev. Lett. **70**, 16 (1993).

[2] J. Eschner, C. Raab, F. Schmidt-Kaler, and R. Blatt, Nature **413**, 495 (2001).

[3] S. Wolf, J. Wechs, J. von Zanthier, and F. Schmidt-Kaler, Phys. Rev. Lett. **116**, 183002 (2016).

[4] P. Obšil, A. Lešundák, T. Pham, G. Araneda, O. Číp, R. Filip, and L. Slodička, arXiv:1804.01518 (2018).

Quantum gas microscopy of ultracold fermionic atoms in optical lattices allows studying strongly correlated low-temperature phases in the Hubbard model. Through an entropy redistribution technique we have demonstrated long-range antiferromagnetic order extending over our entire sample, a disk spanning ten sites across filled with a two-component spin mixture of ultracold fermionic Li-6 atoms in a square lattice. Besides quantities such as the site-resolved spin correlation function, spin structure factor, and full counting statistics of the staggered magnetization, our microscope also allows to search for particular patterns in the site-projected many-body wavefunction. By hole doping the system away from half-filling we explore regimes of the Hubbard model phase diagram where precise numerical studies become challenging. We study the interplay between hole motion and the antiferromagnetic order: when a hole tunnels in an antiferromagnet, it distorts the surrounding order and may form a spinon-holon string of distorted spin order, which could be an essential aspect of high-temperature superconductivity in cuprates. We discuss our progress in the search for signatures of these string configurations and compare our findings to different theoretical models including the pi-flux model of spin liquid states.

Experimental implementation of a degenerate optical resonator supporting more than 46 Laguerre-Gaussian modes

Zedi Cheng[1,2], **Jinshi Xu**[1,2], **and Chuanfeng Li**[1,2]

[1] *CAS Key Laboratory of Quantum Information, University of Science and Technology of China, Hefei 230026, People's Republic of China*

[2] *Synergetic Innovation Center of Quantum Information and Quantum Physics, University of Science and Technology of China, Hefei 230026, People's Republic of China*

e-mail: *chzhdi@mail.ustc.edu.cn*

Great efforts have been made to investigate photon's orbital angular momentum (OAM) due to its comprehensive applications ranging from micromanipulation to biosciences. Recently, it has been proposed that the unlimited OAM number can be used as synthetic degrees of freedom and can be used for quantum simulation [1, 2, 3]. Here, we demonstrate a vital step in manipulating such kind of unlimited degree of freedom simultaneously. We construct an optical resonator with four spherical mirrors, which is predicted to support lights in different Laguerre-Gaussian modes with well-defined OAMs. The transmitted peaks of more than 46 Laguerre-Gaussian modes are observed to be overlapped within the bandwidth of the resonator. The transmitted beam profiles are further obtained by locking the resonator. Our experimental results establish the critical techniques to manipulate multiple-OAM degrees of freedom, which are useful for quantum simulation. The details are as below.

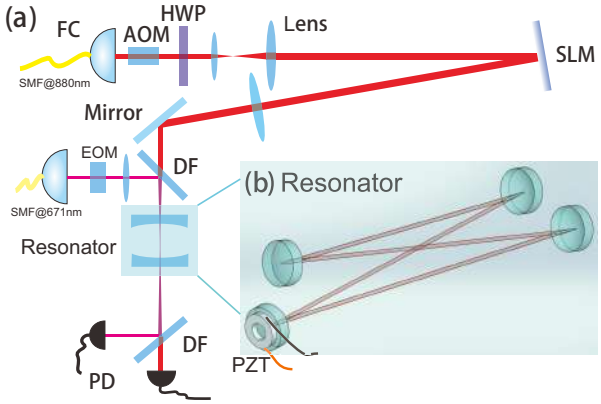


Figure 1: Experimental setup. (a) The layout of the experimental setup. (b) The detailed configuration of the resonator. SMF, single mode fibre; FC, fibre coupler; AOM, acoustic optical modulator; HWP, half-wave-plate; SLM, spatial light modulator; EOM, electro-optic modulator; DF, dichroic filter; PD, photo diode; PZT, piezoelectric transducer.

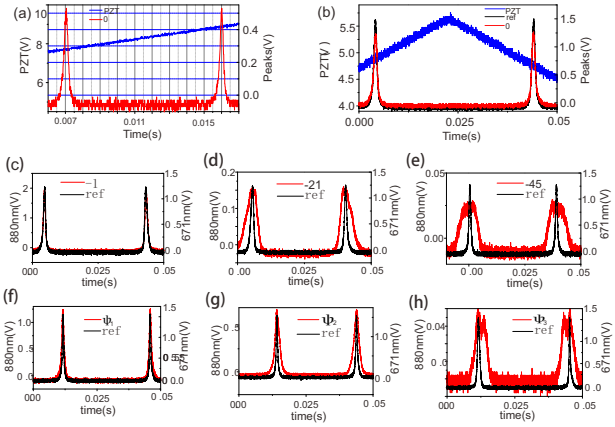


Figure 2: Transmitted peaks with different Laguerre-Gaussian modes. (a) Scanning the length of the resonator over a FSR to estimate the finesse. (b) Transmitted peaks of Gaussian mode with the OAM number $l = 0$. (c)-(e) Transmitted peaks of Laguerre-Gaussian modes with different OAM numbers l. (f)-(h) Transmitted peaks of several super-position states of Laguerre-Gaussian modes. The black signal signed as 'ref' refers to the beam at 671 nm and the red signal refers to the beam at 880 nm in different Laguerre-Gaussian modes. The blue signal, which is left out in (c)-(h), corresponds to the volts added on the PZT.

Finally, our resonator is locked and is shown to support more than 46 OAM modes. Although the output beam profile is imperfect with a large l, interesting quantum simulation still can be implemented in current setup [2].

References

[1] X. W. Luo, X. X. Zhou, C. F. Li, J. S. Xu, G. C. Guo, and Z. W. Zhou. *Nat. Commun.*, **6**, 7704, (2015).

[2] X. W. Luo, X. X. Zhou, J. S. Xu, C. F. Li, G. C. Guo, C. W. Zhang, and Z. W. Zhou. *Nat. Commun.*, **8**, 16097, (2017).

[3] X. F. Zhou, X. W. Luo, S. Wang, G. C. Guo, X. X. Zhou, H Pu, and Z. W. Zhou. *Phys. Rev. Lett.*, **118**, 083603, (2017).

Experimental Quantum Simulation of a Coherence-Enhanced Microscopic Heat Engine in Diamond

J. N. Becker[1], **J. Klatzow**[1], **P. M. Ledingham**[1], **C. Weinzetl**[1], **K. T. Kaczmarek**[1]. **D. J. Saunders**[1], **J. Nunn**[2], **R. Uzdin** [3], **I. A. Walmsley**[1], **and E. Poem**[4]

[1] *Clarendon Laboratory, University of Oxford, Parks Road, Oxford OX1 3PU, United Kingdom*

[2] *Centre for Photonics and Photonic Materials, Department of Physics, University of Bath, Claverton Down, Bath BA2 7AY, United Kingdom*

[3] *Schulich Faculty of Chemistry, Technion Israel Institute of Technology, Haifa 3200000, Israel*

[4] *Department of Physics of Complex Systems, Weizmann Institute of Science, Rehovot 7610001, Israel*

e-mail: *jonas.becker@physics.ox.ac.uk*

A heat engine that extracts work from thermal sources is a fundamental theoretical construct and application of classical thermodynamics. While a classical heat engine does not include coherence amongst its microscopic degrees of freedom, the internal states of a quantum heat engine (QHE) can exist in a coherent superposition of energy levels. A question of interest for such a QHE is whether it can exhibit thermodynamic behavior fundamentally different to that allowed in a classical engine. A microscopic heat engine has recently been implemented using trapped ions [1]. However, so far, these experiments have not shown any non-classical features in the thermodynamic quantities of such an engine. For example, while the e ciency of a QHE is still bound by the Carnot limit, recent theoretical studies have predicted that the presence of coherence can boost the power output of a QHE for actions $<< \hbar$ above the values maximally achievable in any classical engine using the same thermal resources [2]. Moreover, the presence of coherence was predicted to result in the equivalence of different QHE types in the limit of weak driving and short cycle duration.

Here, we have implemented two varieties of quantum heat engines using an ensemble of negative nitrogen-vacancy (NV) centres in diamond. An axial magnetic field was applied to the ensemble to allow us to work beyond the ground state anti-crossing, such that the $|m_s = -1\rangle$ state lies below the $|m_s = 0\rangle$ state. The thermal interaction was implemented using off-resonant optical pumping via the diamond conduction band, introducing a random phase. This allows to controllably emulate thermal Markovian dynamics, equivalent to coupling to hot and cold baths to the ground states, as can be shown analytically. Simultaneously, this process allows for precise spin read-out via optically detected magnetic resonance based on spin dependent NV fluorescence, enabling measurements of small power outputs at extremely low engine driving. The optical pumping results in an population inversion between the $|m_s = 0\rangle$ and $|m_s = -1\rangle$ ground state spins, which enables the extraction of work in the form of stimulated emission of microwave (MW) radiation upon resonant driving.

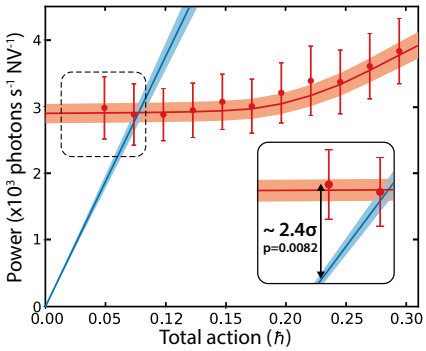


Figure 1: Quantum thermal signatures. Beating the stochastic bound: Measured power output of the two-stroke engine (red dots) vs. coherent stroke length. Solid blue line represents stochastic bound calculated for the work strokes and measured Rabi frequencies used in the experiment, red line is theoretically predicted power.

The thermal interaction and the coupling to the work reservoir can either be interlaced or both be on continuously, which correspondingly implements either a two-stroke engine or a continuous engine. In performing this experiment, we have been able to experimentally demonstrate the coherence-induced power boost, breaking the upper bound for a completely decohered (stochastic) engine using the same resources and stroke scheduling. Such a thermodynamic measurement is known as a Quantum Thermodynamic Signature. This result is displayed in Fig. 1, with the power (red) at the shortest cycle length being $2.4\,\sigma$ above the bound (blue) calculated using measured Rabi frequencies (p value $= 0.0082$). Additionally, we have experimentally demonstrated the equivalence of different engine types in the small action regime, as theoretically predicted. These measurements constitute the first observation of quantum thermodynamic effects in heat machines.

[1] J. Roßnagel et al., Science 352, 325 (2016).

[2] R. Uzdin et al., Phys. Rev. X 5 (2015).

[3] J. Klatzow et al., arXiv 1710.08716 (2017).

Ultrafast many-body electron dynamics in a strongly correlated ultracold Rydberg gas and its application to ordered systems

A. Tanaka[1], **N. Takei**[1,2], **C. Sommer**[1,2], **C. Genes**[3], **G. Pupillo**[4], **S. Takeda**[1,2], **M. Mizoguchi**[1,2], **Y. Zhang**[1,2], **K. Koyasu**[1,2], **H. Chiba**[1,5], **M. Weidemüller**[6] **and K. Ohmori**[1,2]

[1] *Institute for Molecular Science, National Institutes of Natural Sciences, Myodaiji, Okazaki 444-8585, Japan*

[2] *SOKENDAI (The Graduate University for Advanced Studies), Myodaiji, Okazaki 444-8585, Japan*

[3] *Institut für Theoretische Physik, Universität Innsbruck, Technikerstrasse 25, A-6020 Innsbruck, Austria*

[5] *IPCMS (UMR 7504) and ISIS (UMR 7006), University of Strasbourg and CNRS, 67000 Strasbourg, France*

[6] *Faculty of Engineering, Iwate University, 4-3-5 Ueda, Morioka 020-8551, Japan*

[7] *Physikalisches Institut, Universität Heidelberg, Im Neuenheimer Feld 226, 69120 Heidelberg, Germany*

e-mail: *a-tanaka@ims.ac.jp*

Many-body correlations govern a variety of important quantum phenomena such as the emergence of superconductivity and magnetism in condensed matter. Understanding quantum many-body systems is thus one of the central goals of modern sciences. We have demonstrated a new approach towards this goal by generating a strongly correlated ultracold Rydberg gas with a broadband picosecond pulsed-laser excitation of a disordered ensemble of Rb atoms in an optical dipole trap (Fig. 1) [1, 2].

We have applied our ultrafast and ultrahigh-precision coherent control [3–10] to this strongly correlated Rydberg gas, and have successfully observed and controlled its many-body electron dynamics on the attosecond timescale.

In order to uncover more precise many-body dynamics hidden behind when averaging over random atom configurations, we also discuss the application of this approach to an ordered system composed of atoms regularly arranged in an optical lattice [2].

Our approach will offer a versatile platform to observe and manipulate nonequilibrium dynamics of strongly correlated quantum many-body systems on the ultrafast timescale.

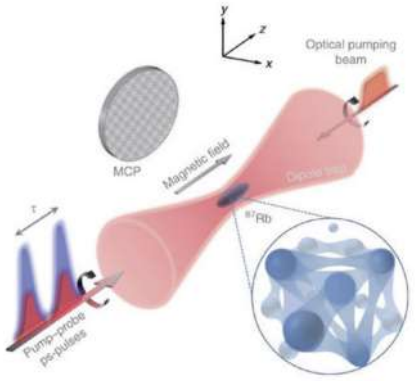


Figure 1: Prototype of ultrafast quantum simulator (Figure is taken from Ref. [1]).

This work has been partly supported by JSPS Grant-in-Aid for Specially Promoted Research, CREST-JST, and Photon Frontier Network Program by MEXT.

[1] N. Takei, C. Sommer, C. Genes, G. Pupillo, H. Goto, K. Koyasu, H. Chiba, M. Weidemller, and K. Ohmori, Nature Commun. **7**, 13449 (2016) (Highlighted by Science **354**, 1388 (2016); IOP PhyscisWorld.com (2016)).

[2] C. Sommer, G. Pupillo, N. Takei, S.Takeda, A. Tanaka, K. Ohmori and C. Genes, Phys. Rev. A **94**, 053607 (2016).

[3] K. Ohmori et. al., Phys. Rev. Lett. **91**, 243003 (2003).

[4] H. Katsuki and K. Ohmori et. al., Science **311**, 1589 (2006).

[5] K. Ohmori et. al., Phys. Rev. Lett. **96**, 093002 (2006).

[6] H. Katsuki and K. Ohmori et. al., Phys. Rev. Lett. **102**, 103602 (2009).

[7] K. Hosaka and K. Ohmori et al., Phys. Rev. Lett. **104**, 180501 (2010) (Highlighted by Nature 465, 138 (2010); Physics 3, 38 (2010)).

[8] H. Goto and K. Ohmori et al., Nature Physics **7**, 383 (2011) (Highlighted by Nature Physics 7, 373 (2011); Nature Photonics 5, 382 (2011)).

[9] H. Katsuki and K. Ohmori et al., Nature Commun. **4**, 2801 (2013).

[10] H. Katsuki and K. Ohmori et al., Phys. Rev. B 92, 094511 (2015).

Atomic quantum simulator of generalized lattice Wilson-Dirac fermions in $(1+1)$ dimensions

Yoshihito Kuno[1], **Ikuo. Ichinose**[2], **and Yoshiro Takahashi**[1]
[1] *Department of Physics, Graduate School of Science, Kyoto University, Kyoto 606-8502, Japan,*
[2] *Department of Applied Physics, Nagoya Institute of Technology, Nagoya, 466-8555 Japan*
e-mail: *ykuno@yagura.scphys.kyoto-u.ac.jp*

The Dirac fermion is important fundamental particle appearing in high-energy and topological insulator physics. In particular, a Dirac fermion in a one-dimensional lattice system exhibits the essential properties of topological physics. However, the system has not been quantum simulated in experiments yet. Herein, we propose a one-dimensional generalized lattice Wilson-Dirac fermion model and study its topological phase structure. We show the experimental setups of an atomic quantum simulator for the model, in which two parallel optical lattices with the same tilt for trapping cold fermion atoms and a laser-assisted hopping schema are used. Interestingly, in the broad regime of the parameter space, we find that the model exhibits nontrivial topological phases characterized by zero-energy edge states and a winding number. Some of the phase diagrams closely resemble those of the Haldane model.

The quantum simulation of Dirac fermions is of fundamental importance because the theory is ubiquitous in theoretical physics. In recent years, topological phases have become one of the most interesting subjects in physics, where Dirac fermions play an important key role.

Experiments on cold atomic gases in an optical lattice have started to construct a "quantum simulator" of 1D topological models. Very recently, the experimental realization of a lattice topological model has been reported in Ref. [4]. As one of the recent remarkable successes in experiments concerning 1D topological models, we note a ladder topological model in a synthetic dimensional optical lattice [3].

Despite such experimental successes, the Dirac fermion model on a lattice called the Wilson-Dirac model is still a toy model in the sense that it has not been realized and not yet quantum simulated in experiments. The 1D Wilson-Dirac model is the simplest and fundamental model that exhibits the essence of a topological insulator [1]. Thus, it is important to propose a quantum simulation for it and investigate its topological properties. Herein, we introduce a 1D generalized Wilson-Dirac model (GWDM) as an important quantum simulator.

Schema for realizing quantum simulators for the standard Dirac-fermion systems, using cold-atomic gases in continuous and lattice systems, have been already proposed [2, 5, 6], and an effective model of two-component cold atoms in a 1D optical superlattice [7]. In our study, the 1D GWDM, which contains nontrivial phases in the hopping terms, is an interesting model by itself because these phases work as free parameters that change the physical properties of the ordinary Wilson-Dirac fermion model. In order to realize the Dirac fermions by cold atomic gases in an optical lattice, the greatest difficulty is the creation of the Dirac-gamma matrices from the nearest-neighbor (NN) hopping amplitudes of cold atoms. To this end, we use two different internal states of a fermionic atom and two parallel "tilted" optical lattices and we explain a general scheme for the generation of Dirac-gamma matrices by using a laser-assisted hopping technique.

[1] S.-Q. Shen, *Topological Insulators* (Springer-Verlag, Berlin, 2012).

[2] V. Galitski and I. B. Spielman, Nature (London) **494**, 49-54 (2013).

[3] M. Mancini, G. Pagano, G. Cappellini, L. Livi, M. Rider, J. Catani, C. Sias, P. Zoller, M. Inguscio, M. Dalmonte, and L. Fallani, Science **349**, 981 (2015).

[4] B. Song, L. Zhang, C. He, T. F. J. Poon, E. Hajiyev, S. Zhang, X.-J. Liu, and G.-B. Jo, Science Advances **4**, eaao4748 (2018)

[5] A. Bermudez, L. Mazza, M. Rizzi, N. Goldman, M. Lewenstein, and M. A. Martin-Delgado, Phys. Rev. Lett. **105**, 190404 (2010).

[6] J. C. Garreau and V. Zehnle, Phys. Rev A **96**, 043627 (2017).

[7] J. I. Cirac, P. Maraner, and J. K. Pachos, Phys. Rev. Lett. **105**, 190403 (2010).

[8] Y. Kuno, I. Ichinose, and Y. Takahashi,, arXiv: 1801.00439 (2018)

Trapping Ultracold Atoms in Sub-Micron-Period Triangular and Square Magnetic Lattices

T. Tran[1], Y. Wang[1], I. Herrera[1], A. Balcytis[2], D. Nissen[3], M. Albrecht[3], S. Whitlock[4], A. Sidorov[1] and P. Hannaford[1]

[1] *Centre for Quantum and Optical Science, Swinburne University of Technology, Melbourne, Australia*
[2] *Centre for Micro-Photonics, Swinburne University of Technology, Melbourne, Australia*
[3] *Institute of Physics, Universität Augsburg, Universitätstrasse 1, 86135 Augsburg, Germany*
[4] *IPCMS and ISIS, Université de Strasbourg and CNRS, 67000 Strasbourg, France*
e-mail: *phannaford@swin.edu.au*

Magnetic lattices consisting of periodic arrays of microtraps created by patterned magnetic films on an atom chip provide a potential complementary tool to optical lattices for simulating condensed matter and many-body phenomena (e.g., [1]). Such lattices have a high degree of design flexibility and may in principle be fabricated with almost arbitrary 2D and ID geometries and lattice spacing, and they may be readily scaled up [2]. However, magnetic lattices are still in their infancy compared with optical lattices due largely to the di culty in fabricating high-quality magnetic microstructures, especially lattices with sub-micron periods needed for quantum tunnelling experiments, and the di culty in trapping atoms in tightly confining traps very close to a surface.

Here, we report the trapping of ultracold ^{87}Rb atoms in multiple sites of 0.7 μm-period triangular and square magnetic lattices on an atom chip. The magnetic lattices are created by a lithographically patterned Co/Pd multi-atomic layer magnetic film plus bias fields [3]. Rubidium atoms in the $|F = 1, m_F = -1\rangle$ state are first trapped and cooled in a Z-wire magnetic trap and then brought very close (300 - 90 nm) to the chip surface by reducing the Z-wire current until the Z-wire trap merges smoothly with the magnetic lattice potential, thereby allowing atoms to be loaded into the tightly confining magnetic lattice traps [4]. The ramping speed of the Z-wire current is adjusted to maximize the number of atoms trapped in the lattice. After the loading stage, the atoms remaining in the Z-wire trap are quickly brought further from the chip surface for imaging (Fig. 1).

The lifetimes of the atoms trapped in the magnetic lattices are currently in the range 0.4 - 2.5 ms, depending on the distance from the chip surface. Model calculations suggest that the trap lifetimes are presently limited mainly by losses due to 1D thermal evaporation following transfer of the atom cloud from the Z-wire trap to the very tight magnetic lattice traps, rather than by fundamental loss processes such as surface interactions, three-body recombination or spin flips due to Johnson magnetic noise. It should be feasible to achieve longer trap lifetimes in a sub-micron-period magnetic lattice by improving the loading procedure.

The trapping of atoms in a 0.7 μm-period magnetic lattice at distances down to about 90 nm from the chip surface represents a significant step towards employing magnetic lattices for quantum tunnelling experiments to simulate condensed matter and many-body phenomena in lattices with non-trivial geometry.

This research is funded by an Australian Research Council Discovery grant No. DP130101160.

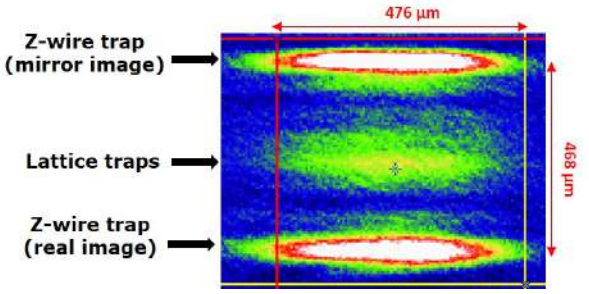


Figure 1: Reflection absorption image of ultracold ^{87}Rb atoms trapped about 90 nm from the chip surface in multiple (unresolved) sites of a 0.7 μm-period triangular magnetic lattice mid-way between the direct and mirror images of the Z-wire trapped atom cloud.

[1] Y. Wang, P. Surendran, S. Jose, T. Tran, I. Herrera, S. Whitlock, R. McLean, A. Sidorov and P. Hannaford, Sci. Bulletin **61**, 1097 (2016).

[2] R. Schmied, D. Leibfried, R. Spreeuw and S. Whitlock, New J. Phys. **12**, 103029 (2010).

[3] I. Herrera, Y. Wang, P. Michaux, D. Nissen, P. Surendran, S. Juodkazis, S. Whitlock, R. McLean, A. Sidorov, M. Albrecht and P. Hannaford, J. Phys. D **48**, 115002 (2015).

[4] Y. Wang, T. Tran, P. Surendran, I. Herrera, A. Balcytis, D. Nissen, M. Albrecht, A. Sidorov and P. Hannaford, Phys. Rev. A **96**, 013630 (2017).

Towards a register of single-atoms in a fiber cavity for multi-particle entanglement

M.Baghdad[1], **F.Ferri**[1], **A.La Rooij**[1], **S.Schwartz**[1], **J.Reichel**[1] **and R.Long**[1]

[1] *Laboratoire Kastler Brossel, ENS-PSL University, CNRS, Sorbonne Universit, College de France, 24 rue Lhomond, 75005 Paris, France*

e-mail: *mohamed.baghdad@lkb.ens.fr*

The study of entanglement and its characterization is a major topic in modern quantum physics, and a key resource enabling the development of future quantum technologies. In this context, we have built a platform combining techniques from optical cavity quantum electro-dynamics and quantum gases microscopes.

More precisely, our goal is to create along the axis of a high finesse fiber-based Fabry Perot micro-cavity a 1D array of single Rb atoms strongly coupled to a cavity mode at 780nm. To maximize the overlap between the atoms and the cavity mode, we use an intracavity far off-resonant lattice trap at twice the coupling wavelength. As shown on Figure 1, the micro-cavity has been placed under a high-resolution microscope, which we plan to use for single-site detection and addressing.

Starting from an optical molasse outside the cavity, we load the 1D lattice trap by transporting a cloud of Rb atoms in a crossed dipole trap: the first laser beam moves thanks to an acousto-optical deflector and the second acts as a guide to target the fiber cavity. As a first signature of atom-cavity coupling, we have recently observed vacuum Rabi splitting from the atoms trapped in the intra-cavity lattice. At the time of the conference, we will present our current efforts towards the creation of a chain of single atoms and single site resolution imaging.

This experimental platform will enable the generation of multi-particle entanglement by collective coupling of all atoms interacting through the cavity mode, while adding the capability to perform local operations on each atom of the register. It will provide an ideal test-bed to investigate nonlocality, multi-particle entanglement as instance in Quantum Zeno Dynamics [1] and in systems exhibiting quantum phase transitions [2].

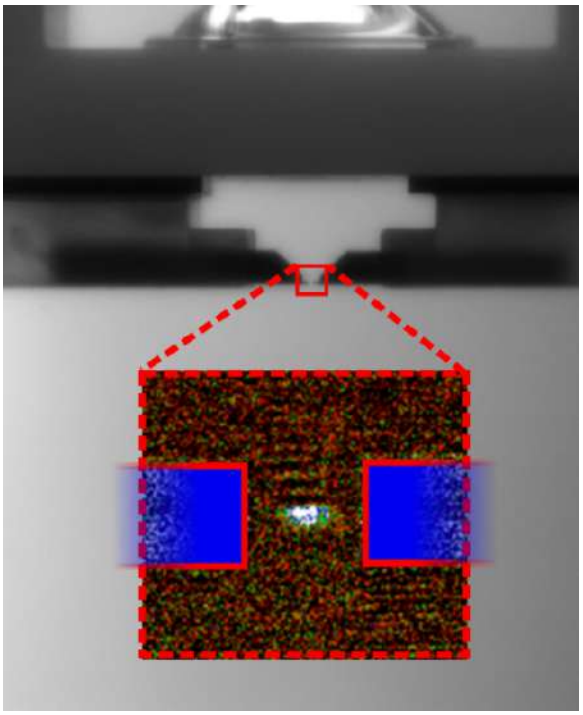


Figure 1: Photo of our all-in-vacuum setup. In the red square, an absorption imaging of a cloud of 2000 atoms trapped in the cavity lattice

References

[1] G. Barontini, L. Hohmann, F. Haas, J. Esteve, et J. Reichel, Deterministic generation of multiparticle entanglement by quantum Zeno dynamics, Science (2015)

[2] F. Dimer, B. Estienne, A. Parkins, et H. Carmichael, Proposed realization of the Dicke-model quantum phase transition in an optical cavity QED system, Physical Review A 75(1), 013804 (2007).

Phase transition kinetics for a Bose Einstein condensate in a periodically driven band system

E Michon[1], **C. Cabrera-Gutiérrez**[1], **A. Fortun**[1], **M. Berger**[1], **M. Arnal**[1], **V. Brunaud**[1], **J. Billy**[1], **C. Petitjean**[2], **P. Schlagheck**[2], **D. Guéry-Odelin**[1]

[1] *Université de Toulouse ; UPS ; Laboratoire Collisions Agrégats Réactivité, IRSAMC ; F-31062 Toulouse, France*

CNRS ; UMR 5589 ; F-31062 Toulouse, France

[2] *Département de Physique, CESAM research unit, University of Liege, 4000 Liège, Belgium*

e-mail: *michon@irsamc.ups-tlse.fr*

The dynamical transition of an atomic Bose-Einstein condensate from a spatially periodic state to a staggered state with antiperiodic symmetry is experimentally studied using a one-dimensional phase modulated optical lattice. We observe the crossover from quantum to thermal fluctuations as the triggering mechanism for the nucleation of staggered states. In good quantitative agreement with numerical simulations based on the Truncated Wigner method, we experimentally investigate how the nucleation time varies with the renormalized tunneling rate, the atomic density, and the driving frequency. The effective inverted energy band in the driven lattice is identified as the key ingredient which explains the emergence of gap solitons as observed in numerics and the possibility to nucleate staggered states from interband excitations as reported experimentally[1].

[1] Michon E. *et al*, New J. Phys. **20** 053035 (2018).

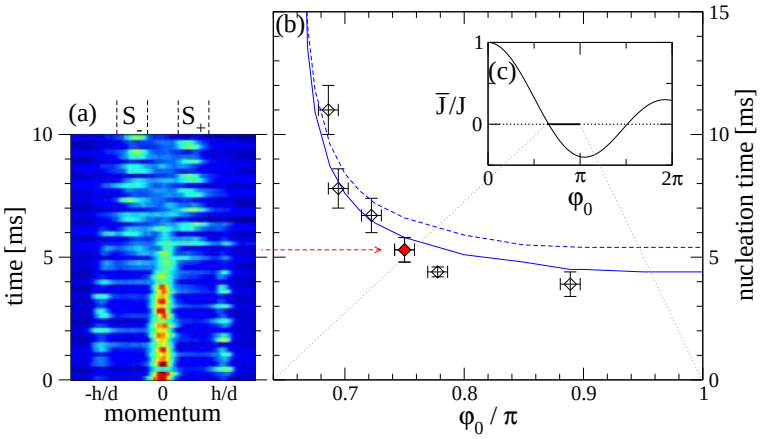


Figure 1: (Color online) (a) Transition to staggered states triggered by a periodically shaken optical lattice (depth $V_0 = 2.6E_L$, driving frequency $\nu = 1.5$ kHz, and shaking amplitude $\varphi_0 = 0.75\pi$) for which the effective time-averaged tunneling rate $\bar{J}$ becomes negative. The absorption images obtained for various evolution times (followed by 25 ms time of free flight in the absence of the lattice) clearly display the passage of a spatially periodic condensate wavefunction to the population of a staggered state lying at the edge of the Brillouin zone. (b) Nucleation time of the formation of staggered states for various values of the shaking amplitude φ_0 for which the effective tunneling matrix element is negative, as shown in the inset (c). The solid (dashed) line shows the numerical results obtained using the TW approach and assuming the presence of 10^5 (5×10^4) atoms within the condensate. A diverging nucleation time is obtained for $\varphi_0 = 0.6588\pi$ at which the first zero of the Bessel function arises in (c).

Evaluation of polariton-number variances in the Jaynes-Cummings-Hubbard model with trapped ions

G. Tomimasu, K. Takayama, M. Tamura, T. Mukaiyama, and K. Toyoda
Graduate School of Engineering Science, Osaka University, 1-3 Machikaneyama, Toyonaka, Osaka, Japan
e-mail: *u323758h@ecs.osaka-u.ac.jp*

A system of trapped ions is a good platform for quantum simulation and quantum computation since they have the advantage of controllability. We have performed quantum simulation of the Jaynes-Cummings-Hubbard (JCH) model using $^{40}Ca^{+}$ in a linear Paul trap [1, 2, 3].

The JCH model has two ground-state phases, namely the superfluid (SF) and Mott-insulator (MI) phases. In this poster we present a result on the investigation of a quantum phase transition from the MI phase to the SF phase with an improved measurement scheme. The Hamiltonian of the system in interest with two sites is written as ($\hbar = 1$)

$$H = \Delta \sum_{j=1,2} |g_j\rangle \langle g_j| + g \sum_{j=1,2} \left(a_j^\dagger \sigma_j^+ + a_j \sigma_j^- \right) + \frac{\kappa}{2} \left(a_1 a_2^\dagger + a_1^\dagger a_2 \right), \quad (1)$$

where Δ is the detuning from the resonance of the blue-sideband (BSB) transition, g is the coupling strength, κ is the phonon hopping rate, and a_j and $a_j^\dagger$ $(j = 1, 2)$ represent, respectively, the annihilation and creation operators of the jth ion. The $\sigma_j^\pm$ are Pauli ladder operators for the jth ion. It should be noted that we used a BSB transition (anti-Jaynes-Cummings coupling) for technical reasons, instead of a red-sideband transition (Jaynes-Cummings coupling) which appeared a natural choice for the JCH model. The two cases are equivalent up to a flip of the internal states.

We observed the phase transition by measuring the variances of the excitation numbers. The internal excitation number for the 1st ion, $\hat{N}_{\mathrm{a},1} = |g_1\rangle \langle g_1|$, can be measured by fluorescence observation. Since a result of BSB Rabi oscillation is a sum of contributions from multiple phonon numbers with different sideband Rabi frequencies, a Fourier analysis on that result gives an expected value for the phonon excitation number $\hat{N}_{\mathrm{p},1} = \hat{a}_1^\dagger \hat{a}_1$. For the exact evaluation of the total excitation number (polariton number) $\hat{N}_{\mathrm{t},1} = \hat{N}_{\mathrm{a},1} + \hat{N}_{\mathrm{p},1}$, the internal and phonon states should be measured simultaneously. A problem is that the heating of the ions during the fluorescence observation makes the phonon state collapse and the correlation are lost. In order to solve the problem, measurements were made in two-steps with a conditional detection scheme as shown in figure 1. First the internal state is measured and then the phonon state is estimated. When the ion does not emit light, the phonon state is measured correctly. On the other hand, when the internal state is $|g\rangle$, the ion is heated and the phonon state collapse. The latter case is rejected in a post-selection process. In the next step the ion is irradiated with a π pulse, which transforms $|g\rangle$ to $|e\rangle$, and a similar sequence is performed. In this way we measure the internal and the phonon states without heating.

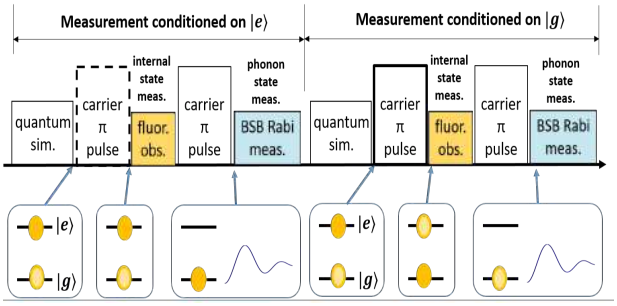


Figure 1: Two-step measurement of the excitation number.

The phase transition experiment were done using rapid adiabatic passage (RAP). First, the state in the system was initialized with $|\Psi\rangle = |g\rangle_1 |g\rangle_2 |0\rangle_1 |0\rangle_2$, and then with RAP the state is transferred to a final state adiabatically. The excitation numbers were evaluated with the above two-step measurement method by truncating the RAP.

The result was that the variance of the total excitation number varied from 0 to finite values. We were able to confirm the phase transition from the MI phase to the SF phase with this result.

References

[1] A. Greentree, C. Tahan, J. Cole, and L. Hollenberg, Nat. Phys. **2**, 856-861 (2006).

[2] P. A. Ivanov, S. S. Ivanov, N. V. Vitanov, A. Mering, M. Fleischhauer, and K. Singer, Phys. Rev. A **80**, 060301(R) (2009).

[3] K. Toyoda, Y. Matsuno, A. Noguchi, S. Haze, and S. Urabe, Phys. Rev. Lett. **111**, 160501 (2013).

Dissipative Bose-Hubbard system with metastable $^3P_2$ state of ytterbium atoms

T. Tomita, S. Nakajima, Y. Takasu, and Y. Takahashi
Department of Physics, Kyoto University, Kyoto, 606-8502, Japan
e-mail: *tomita@scphys.kyoto-u.ac.jp*

Recently, much attention has been paid to novel behaviors of cold atoms with dissipation. For example, the engineering of two-body dissipation with the photo-association technique allows for the investigation of the effect of the dissipaiton on the quantum phase transition [1], in which the delay of the melting of the Mott insulator is observed in a slow ramp-down of the optical lattice. A system of two-electron atoms is also a possible candidate for investigating the effect of dissipation using intrinsic property of strong inelastic collision in the metastable $^3P_2$ state [2] and $^3P_0$ state [3, 4].

Here, we report an experimental study of dynamics of the $^3P_2$ state of bosonic ytterbium atoms ^{174}Yb in an optical lattice. In the optical lattice, the $^3P_2$ state atoms can be regarded as the dissipative Bose-Hubbard system, in which the competition between the tunneling, the on-site interaction and the two-body dissipation provide interesting open quantum many-body physics.

For the full characterization of this system, it is necessary to measure the strength of the on-site interaction between the $^3P_2$ states. We successfully determine the scattering length by establishing a new spectroscopic technique with double excitation process. We firstly excite one $^1S_0$ state atom in the doubly-occupied sites into $^3P_2$ state using adiabatic rapid passage. Then, we apply a second excitation pulse with variable frequency. If the second pulse successfully excites a remaining $^1S_0$ atom in the doubly-occupied sites, we can create two $^3P_2$ state atoms in the same site, resulting in the strong atom loss due to the inelastic collision (Fig. 1). From the spectroscopy, we determine the scattering length as $a_{ee} = +5.8(4)$ nm.

Then we investigate the stability of the singly-occupied Mott insulator of the $^3P_2$ state atoms with the inherent dissipation. Initial state preparation is done by coherent excitation of the singly-occupied Mott insulator of the $^1S_0$ state atoms. We measure the two-body loss rate of $^3P_2$ atoms in the deep 3D optical lattice and observe significant reduction of the loss rate compared to the tunneling rate, which can be understood as the quantum Zeno effect. This dissipation-induced blockade [5] suggests the modification of the Mott insulator–superfluid transition.

After preparing the Mott insulator with $^3P_2$ atoms, we adiabatically ramp down the lattice. The atom momentum distribution obtained by the time-of-flight absorption image is broadened and the interference pattern is unclear compared with the distribution in the $^1S_0$ state (Fig. 2), suggesting the lack of the coherence due to the inherent dissipation. These results are consistent with the previous experiments of dissipative Bose-Hubbard system with engineered on-site two-body dissipation [1].

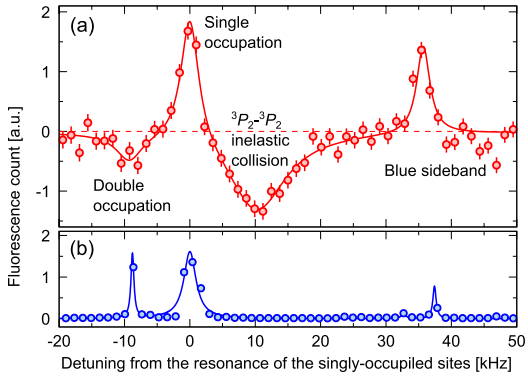


Figure 1: (a) Double-excitation spectroscopy. Here, we use $m_J = -2$ state. The difference from the fluorescence count of the $^3P_2$ state atoms after the first excitation is plotted. (b) Single-excitation spectroscopy for comparison.

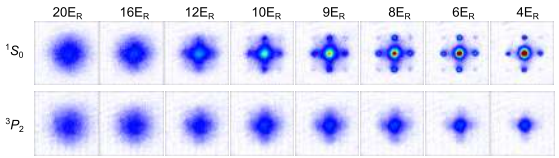


Figure 2: Time-of-flight absorption images of the atoms.

[1] T. Tomita, S. Nakajima, I. Danshita, Y. Takasu, and Y. Takahashi, Science Advances, **3**, e1701513 (2017).

[2] S. Uetake, R. Murakami, J. M. Doyle, and Y. Takahashi, Phys. Rev. A **86**, 032712 (2012).

[3] L. Franchi, L. F. Livi, G. Cappellini, G. Binella, M. Inguscio, J. Catani, and L. Fallani, New J. Phys. **19**, 103037 (2017).

[4] R. Bouganne, M. B. Aguilera, A. Dareau, E. Soave, J. Beugnon, and F. Gerbier, New J. Phys. **19**, 113006 (2017).

[5] N. Syassen, D. M. Bauer, M. Lettner, T. Volz, D. Dietze, J. J. García-Ripoll, J. I. Cirac, G. Rempe, and S. Dürr, Science **320**, 1329–1331 (2008).

Antiferromagnetic spin correlation of SU($\mathcal{N}$) Fermi gas in an optical dimerized lattice

H. Ozawa[1,2], **S. Taie**[2], **Y. Takasu**[2], **and Y. Takahashi**[2]
[1] *RIKEN Center for Emergent Matter of Science, Japan*
[2] *Department of Physics, Graduate School of Science, Kyoto University, Japan*
e-mail: *hideki.ozawa@riken.jp*

In this poster presentation, we report on the observation of the nearest-neighbor antiferromagnetic spin correlations of a Fermi gas with SU($\mathcal{N}$) symmetry trapped in an optical dimerized lattice. By using a dimerized cubic configuration as in Fig. 1, we enhance the exchange coupling within the dimer, which gives rise to an excess of singlets compared with triplets consisting of two different spins [1]. We introduce the Fermi gas of ^{173}Yb into the lattice. This isotope is characterized by SU($\mathcal{N} = 2I + 1$) symmetric repulsive interaction for nuclear spin $I = 5/2$. For this large-spin system, a Pomeranchuk cooling effect is enhanced: large-spin degrees of freedom can effectively cool down the system by absorbing the entropy from motional degrees of freedom. The precise control of the spin degrees of freedom provided by optical pumping technique enables us a straightforward comparison between SU(2) and SU(4) spin systems. By developing a technique for optically inducing a singlet-triplet oscillation (STO) with an effectively produced spin-dependent gradient, the realization of the antiferromagnetic correlation is confirmed. We investigate the spin correlation of the SU(4) and SU(2) systems over a wide range of entropy as in Fig. 2. Our main finding is that the antiferromagnetic spin correlation is enhanced in SU(4) spin system compared with SU(2) as a consequence of the Pomeranchuk cooling effect. In the field of ultracold atoms in optical lattices, this Pomeranchuk cooling method was already demonstrated in the paramagnetic Mott-insulator [2], but no experimental study of this effect on the quantum magnetism was reported, which is clearly demonstrated in this work [3]. This result is an important step towards the realization of novel SU($\mathcal{N} > 2$) quantum magnetism.

[1] D. Greif, T. Uehlinger, G. Jotzu, L. Tarruell, and T. Esslinger, Science **340**, 1307-1310 (2013)

[2] S. Taie, R. Yamazaki, S. Sugawa, and Y. Takahashi, Nature Physics **8**, 825-830 (2012)

[3] H. Ozawa, S. Taie, Y. Takasu, and Y. Takahashi, arXiv:1801.05962 (2018)

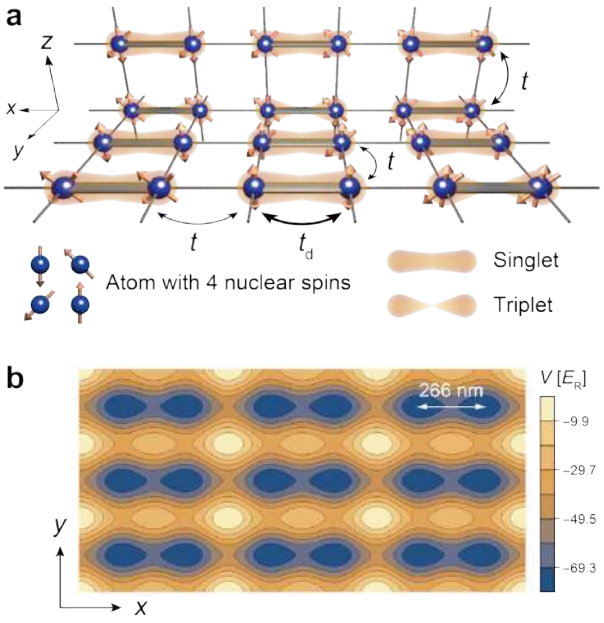


Figure 1: Schematic view of the nearest-neighbor spin correlations. (a) A four-component mixture of fermionic atoms prepared in a dimerized cubic lattice with the strong intra-dimer tunneling t_d and weak inter-dimer tunnelings t. (b) The contour plot of the optical potential landscape in the xy-plane.

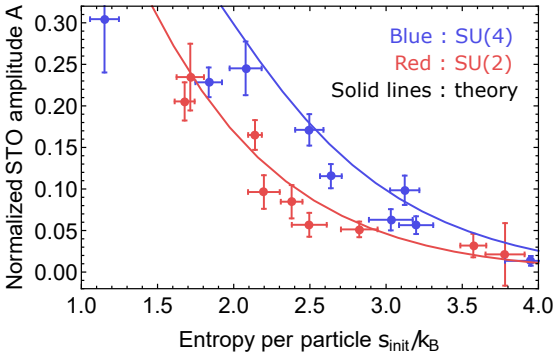


Figure 2: Normalized Singlet-Triplet Oscillation (STO) amplitude of SU(2) and SU(4) Fermi gas in the strongly dimerized cubic lattice. The dependence on the initial entropy in the harmonic trap is shown. The solid line is a theoretical curve that assumes adiabatic loading into the lattice.

Site-resolved imaging of a fermionic Mott insulator using ^{173}Yb

M. Takagi, K. Iguchi, M. Miranda, R. Inoue, and M. Kozuma
Department of physics, Tokyo Institute of Technology, 2-12-1 O-okayama, Meguro-ku, Tokyo 152-8550, Japan
e-mail: *takagi.m.ae@m.titech.ac.jp*

Ultracold atomic gases in an optical lattice have great potential to understand the many-body physics of strongly correlated materials, such as high-temperature superconductivity [1]. Optical lattices filled with a two-spin-component fermi gas of ultracold atoms can be described by the Fermi-Hubbard model, which is deeply concerned with cuprates superconductors. The experiment with ultracold atoms in an optical lattice enables us to obtain the phase diagram of the Fermi-Hubbard model and is expected to reveal the microscopic picture of high-temperature superconductivity. The main difficulty of this research is to realize extremely low temperature which can in principle be obtained by the cooling with a quantum gas microscope, the high-resolution fluorescence imaging device capable of resolving individual atoms in each site of the optical lattice [2].

Ytterbium (Yb) is one of the good candidates for performing the quantum simulation with optical lattice system. Direct probing of the Mott crossover in the SU(N) Fermi-Hubbard model has recently been realized [3]. Here, we report the observation of site-resolved imaging of a fermionic Mott insulator using ^{173}Yb. We employ the photoassociation (PA) technique to remove pairs of atoms in multiply occupied sites and realize parity measurement of the number density [4]. The PA laser is red-detuned by 796 MHz from the $^1S_0 - {}^3P_1$ transition at 556 nm. Pairs of atoms can be removed over 0.44 ± 0.10 ms, where the efficiency of PA process is measured by preliminary experiments. The time of irradiation of PA beam is 5 ms. We successfully obtain site-resolved imaging of a fermionic Mott insulator, as shown in Fig.1. From the atomic-density distribution of the Mott insulator, we measure the temperature $k_BT/U = 0.23 \pm 0.02$, where U denotes on-site interaction energy [5]. Assuming balanced spin population, we calculate the local entropy density and obtain the entropy per particle $S/Nk_B = 2.3 \pm 0.1$.

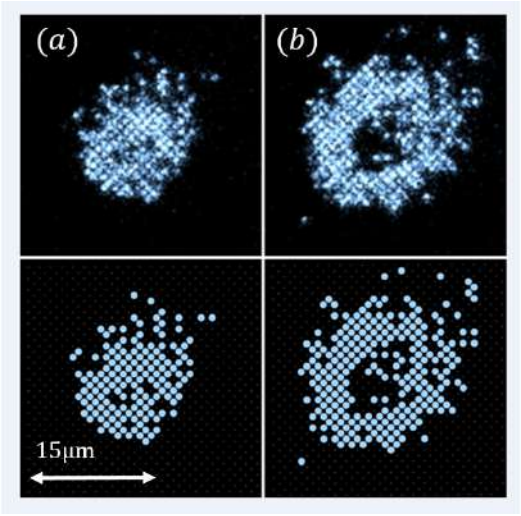


Figure 1: Site-resolved imaging of a fermionic ^{173}Yb Mott shells. Top row shows the raw images. Bottom row shows the reconstructed atomic-density distribution. The estimated global chemical potential μ/U in each image is (a) 0.41 ± 0.03, (b) 0.93 ± 0.04, respectively.

[1] I. Bloch, J. Dalibard, and W. Zwerger, Rev. Mod. Phys. **80**, 885 (2008).

[2] A. Mazurenko, C. S. Chiu, G. Ji, M. F. Parsons, M. Kanász-Nagy, R. Schmidt, F. Grusdt, E. Demler, D. Greif, and M. Greiner, Nature(London) **545**, 462 (2017).

[3] C. Hofrichter, L. Riegger, F. Scazza, M. Höfer, D. R. Fernandes, I. Bloch, and S. Fölling, Phys. Rev. X. **6**, 021030 (2016).

[4] S. Tojo, M. Kitagawa, K. Enomoto, Y. Kato, Y. Takasu, M. Kumakura, and Y. Takahashi, Phys. Rev. Lett. **96**, 153201 (2006).

[5] J. F. Sherson, C.Weitenberg, M. Endres, M. Cheneau, I. Bloch, and S. Kuhr, Nature(London) **467**, 68 (2010).

Preparation of two-dimensional fermionic spin mixtures in a quantum-gas microscope apparatus

B. Peaudecerf[1], **M. Andia**[1], **M. Brown**[1], **E. Haller**[1] **and S. Kuhr**[1]
[1] *Department of Physics, University of Strathclyde, Glasgow G4 0NG, and SUPA, United Kingdom*
e-mail: *bruno.peaudecerf@strath.ac.uk*

Single-atom-resolved detection in optical lattices using quantum-gas microscopes has enabled a new generation of experiments in the field of quantum simulation [1]. In our experiment, we achieve single-site-resolved imaging of individual fermionic potassium 40 atoms in an optical lattice with high fluorescence yield while maintaining a negligible particle loss rate, by laser cooling the atoms to sub-Doppler temperatures while detecting the fluorescence photons emitted during this process. The cooling of fermionic alkaline atoms in optical lattices has proven more challenging than for bosons, and we achieved single-atom-resolved fluorescence imaging of ^{40}K using electromagnetically-induced-transparency (EIT) cooling [2].

A key goal of our quantum-gas microscope experiment is to probe strongly correlated fermionic many-body systems at the single-atom level. To that end we must prepare an atomic sample in a single 2D-lattice plane at the focus of the microscope, containing two spin species that can interact on the lattice sites.

In this contribution I will present the microwave preparation technique we developed, to prepare a equal-weight mixture of two magnetic sub-levels of ^{40}K in a single antinode of an optical lattice in the focal plane of our quantum-gas microscope. The procedure relies on a sequence of adiabatic microwave transfer pulses that are optimised in a trade-off between e ciency and speed. Using these pulses we are able to study the losses that arise when the atoms are placed in the upper hyper-fine manifold ($F = 7/2$), revealing strong atomic interactions. The frequency sensitivity of the pulses also comes as a tool that allows us to perform spectral imaging, and visualize directly on a fluorescence image the magnetic field gradients present in the experiment. I will present the preparation sequence, as well as latest developments from the experiment.

Our fermionic quantum-gas microscope will provide new possibilities to probe strongly correlated fermionic many-body systems at the single-atom level. It will allow the direct observation of spin-spin correlations, or, for example, the study of out-of-equilibrium dynamics and thermalisation of fermionic quantum systems.

[1] S. Kuhr, Natl. Sci. Rev. **3**, 170 (2016).

[2] E. Haller *et al.*, Nature Physics **11**, 738 (2015).

Direct observation of incommensurate magnetism in Hubbard chains

G. Salomon[1], **J. Koepsell**[1], **J. Vijayan**[1], **T. Hilker**[1], **J. Nespolo**[2,3], **L. Pollet**[2], **I. Bloch**[1,2] **and C. Gross**[1]

[1] *Max-Planck-Institut für Quantenoptik, 85748 Garching, Germany*
[2] *Fakultät für Physik, Ludwig-Maximilians-Universität, 80799 München, Germany*
[3] *INO-CNR BEC Center and Dipartimento di Fisica, Universita di Trento, 38123 Povo, Italy*
e-mail: *guillaume.salomon@mpq.mpg.de*

The interplay between magnetism and doping is at the origin of exotic strongly correlated electronic phases and can lead to novel forms of magnetic ordering. One example is the emergence of incommensurate spin-density waves with a wave vector that does not match the reciprocal lattice. In one dimension this effect is a hallmark of Luttinger liquid theory, which also describes the low energy physics of the Hubbard model. Here we use a quantum simulator based on ultracold fermions in an optical lattice to directly observe such incommensurate spin correlations in doped and spin-imbalanced Hubbard chains using fully spin and density resolved quantum gas microscopy [1]. Doping is found to induce a linear change of the spin-density wave vector in excellent agreement with Luttinger theory predictions [3]. For non-zero polarization we observe a decrease of the wave vector with magnetization as expected from the Heisenberg model in a magnetic field. We trace the microscopic origin of these incommensurate correlations to holes, doublons and excess spins which act as delocalized domain walls for the antiferromagnetic order [2]. Finally, when inducing interchain coupling we observe fundamentally different spin correlations around doublons indicating the formation of a magnetic polaron.

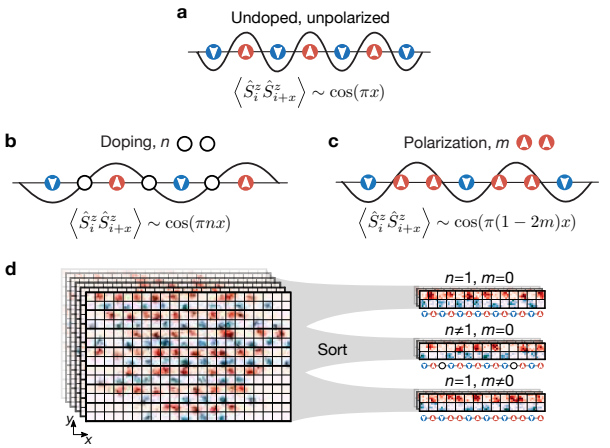


Figure 1: **Probing incommensurate spin correlations in Hubbard chains. a**, Spin correlations in spin-balanced Hubbard chains at half filling ($n = 1$) form at a commensurate wave vector π. **b**, When the system is doped ($n \neq 1$), incommensurate spin correlations at a wave vector πn develop due to delocalized holes and doublons, which act as domain walls stretching the distance between antiferromagnetically correlated spins. **c**, At finite polarization $m \neq 0$, incommensurate spin correlations at a wave vector $\pi(1 - 2m)$ arise due to excess spins. **d**, Left: Single-spin and density-resolved experimental images, each containing 7 independent Hubbard chains along y separated by thick lines where spins $\uparrow$ ($\downarrow$) are represented in red (blue). Right: In post-analysis we group the data by polarization and doping to analyze their individual effect on spin correlations along x.

[1] M. Boll, T. Hilker, G. Salomon *et al.*, Science **353**, 1257-1260 (2016).

[2] T. Hilker *et al.*, Science **357**, 484-487 (2017)

[3] G. Salomon *et al.*, arXiv:1803.08892v1 (2018)

Trapping ions in an optical lattice for quantum simulation

C. Fischer[1], **O. Wipfli**[1], **M. Grau**[1] **and J.P. Home**[1]

[1] *Institute for Quantum Electronics, ETH Zurich, Otto-Stern-Weg 1, 8093 Zurich, Switzerland*

e-mail: *fischchr@phys.ethz.ch*

Quantum systems based on particles in a two-dimensional lattice with long-range interactions produce a number of cases which are hard to simulate on classical computers, limiting our ability to fully understand them. Depending on lattice geometry and the nature of the interaction Hamiltonian, interesting effects come into play, such as frustration, which leads to highly entangled ground states.

I will describe a new experimental setup in which we are trying to realize a trapped-ion quantum simulator comprising a two-dimensional lattice of magnesium ions trapped using a far off-resonant optical standing wave. To this end we have developed a cryogenic vacuum chamber which will house a Paul trap and a co-aligned high-finesse cavity that will be loaded from a MOT. The cavity aims for a power-build up of around 3000, which will pin the ions in one of three dimensions, with confinement in the other performed using static fields. An input optical power of 3 W should allow trapping of two-dimensional arrays of 40 magnesium ions with a 10 µm inter-ion spacing on a triangular lattice.

I will present work on characterizing the performance of the cavity and MOT, as well as Rydberg spectroscopy of the cold magnesium atoms.

Probing many-body dynamics on a Rydberg quantum simulator

A. Keesling[1], **H. Levine**[1], **A. Omran**[1], **H. Bernien**[1], **S. Choi**[1], **R. Samajdar**[1], **H. Pichler**[1,2], **S. Schwartz**[3], **A. S. Zibrov**[1], **M. Endres**[4], **V. Vuletic**[5], **M.Greiner**[1], **M. D. Lukin**[1]

[1] *Department of Physics, Harvard University, Cambridge, MA 02138,USA*

[2] *ITAMP, Harvard-Smithsonian Center for Astrophysics, Cambridge, MA 02138, USA*

[3] *Laboratoire Kastler Brossel, ENS-PSL Research University, CNRS, UPMC-Sorbonne Universits, Collge de France, 24 rue Lhomond, 75005 Paris, France*

[4] *Division of Physics, Mathematics and Astronomy, California Institute of Technology, Pasadena, CA 91125, USA*

[5] *Department of Physics and Research Laboratory of Electronics, Massachusetts Institute of Technology, Cambridge, MA 02139, USA*

e-mail: *keeslingcontreras@g.harvard.edu*

Controllable, coherent many-body quantum systems can provide insights into fundamental properties of quantum matter, enable the realization of exotic quantum phases, and ultimately offer a platform for computation that may surpass classical computing. Here we demonstrate a method for deterministically creating large, reconfigurable arrays of up to 51 individual cold atoms [1]. We engineer strong, coherent interactions among the atoms by coupling them to highly excited Rydberg states. This allows us to realize a programmable Ising-type quantum spin model with a tunable range of interactions.

Within this model, we observe transitions into ordered states that break various discrete symmetries, verify their high-fidelity preparation, and investigate dynamics across the phase transitions, revealing universal scaling properties consistent with the Kibble-Zurek mechanism (Fig. 1). Finally, we study many-body dynamics far from equilibrium, induced by a rapid change in system parameters, producing novel, robust many-body dynamics corresponding to persistent oscillations of the spatial order [2]. These observations enable new approaches for exploring many-body phenomena and open the door for realizations of novel quantum algorithms.

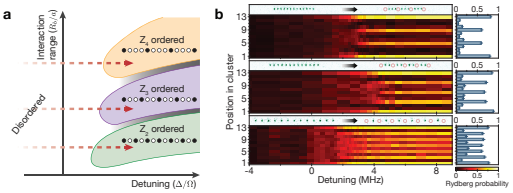


Figure 1: Adiabatic preparation of symmetry breaking states. **a**) Ground state phase diagram of the Rydberg Quantum Simulator. **b**) State evolution going from a disordered initial state to final states breaking distinct spatial symmetries.

[1] M. Endres *et al.*, Science **356**, 1024 (2016).

[2] H. Bernien *et al.*, Nature **551**, 579 (2017).

Strongly-correlated bosons on a dynamical lattice

P. R. Grzybowski[1,2], **D. González-Cuadra**[1], **A. Dauphin**[1] **and M. Lewenstein**[1,3]

[1] *ICFO-Institut de Ciències Fotòniques, The Barcelona Institute of Science and Technology, Av. Carl Friedrich Gauss 3, 08860 Castelldefels (Barcelona), Spain*

[2] *Faculty of Physics, Adam Mickiewicz University, Umultowska 85, 61-614 Poznań, Poland*

[3] *ICREA-Institució Catalana de Recerca i Estudis Avançats, Lluis Companys 23, E-08010 Barcelona, Spain*

e-mail: *przemyslaw.grzybowski@icfo.eu*

We study a one-dimensional system of strongly-correlated bosons on a dynamical lattice by extending the standard Bose-Hubbard Hamiltonian to include extra degrees of freedom on the bonds of the lattice. We show that this minimal model exhibits phenomena similar to those present in usual fermion-phonon models: in particular, we discover a bosonic analog of the Peierls transition.

The Peierls transition is the spontaneous translational symmetry breaking in a one-dimensional electron-phonon system. The basic feature of such systems is that the lattice may exhibit fluctuations or spontaneous order at various wavelenghts. The defining feature of Peierls transitons is that lattice's order wavevector will depend on the electron density i.e., it will be twice the Fermi wavevector. The paradigmatic example of the rich physics of Peierls transitions is the original Su-Schrieffer-Heeger (SSH) model of polyacetylene chains. Here we argue for the importance of including a dynamical lattice in the simulation of analogous physics on optical lattices. While fixed, i.e. externally set by experimenter, superlattices were proposed as realisations of "Peierls phase" we show that our proposal allows for simulations of the following features which are beyond capabilities of simulations with fixed lattices:

- The spontaneous symmetry breaking in Peierls transitons leading to Bond Order Wave (BOW) phases.
- The paradigmatic relation between the order wavevector k_0 in the Peierls phase and the density. This requires spontaneous reorganisation of the lattice periodicity caused by changes in the density.
- The order wavelenght "locking" at values commensurate with the lattice unit resulting in incompressible BOW phases.
- The compressible phases with topological solitons occuring close to the commensurate densities.
- The compressible but gapped long-wavelenght BOW phases.
- Fermion (boson) fractionalisation asociated with solitonic excitations.

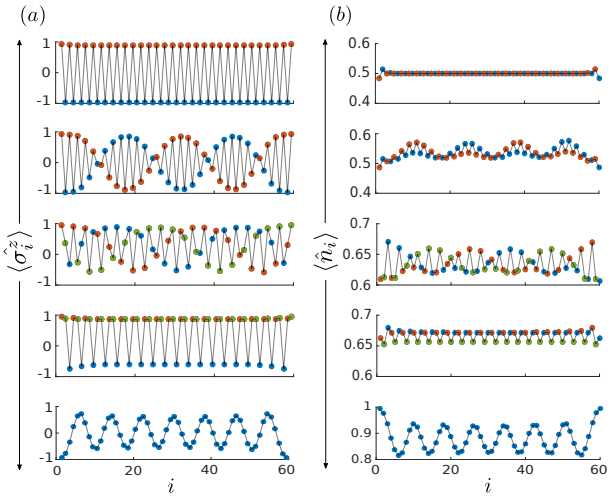


Figure 1: The spatial structure of bond (a) and site (b) expectation values for $\Delta = 0.85$ and different bosonic densities, showing some of the representative orders that can develop. From above to below: $\rho = 1/2$, $\rho = 1/2 + 2/60$, $\rho = 2/3 - 2/60$, $\rho = 2/3$ and $\rho = 0.88$. Different colors represent different sublattice elements, making explicit the long-wavelength modulations on top of the underlying order.

- Dynamically-generated topological defects (analogous to edge states) in the bulk.

We describe DMRG results of those effects for fermions and correlated bosons. We discuss the role of the frequency of lattice dynamics, correlations and system symmetries. In the case of symmetry protected topological phases, we use the quantized Berry phase to characterise them in our many-body system. Finally, we study the possibility of implementing the model using atomic systems.

[1] D. González-Cuadra, P. R. Grzybowski, A. Dauphin, M. Lewenstein, arXiv:1802.05689 (2018)

[2] R. Peierls, *Quantum Theory of Solids*, International series of monographs on physics, Clarendon Press, (1955).

[3] W. P. Su, J. R. Schrieffer and A. J. Heeger, Phys. Rev. Lett., **42**, 1698 (1979).

Synthetic atomic quantum systems with two electron fermions

L. F. Livi[1,2,3], **L. Franchi**[1,2], **G. Cappellini**[1,2,3], **M. Inguscio** [3,1,4], **J. Catani**[3,4,2] **and L. Fallani**[1,2,3,4]

[1] *Dipartimento di Fisica e Astronomia, Università degli Studi di Firenze, Via G. Sansone 1, I-50019 Sesto Fiorentino, Italy*

[2] *INFN Istituto Nazionale di Fisica Nucleare, Sezione di Firenze, Via G. Sansone 1, I-50019 Sesto Fiorentino, Italy*

[3] *INO-CNR Istituto Nazionale di Ottica del CNR, Sezione di Sesto Fiorentino, Via N. Carrara 1, I-50019 Sesto Fiorentino, Italy*

[4] *LENS European Laboratory for Nonlinear Spectroscopy, Via N. Carrara 1, I-50019 Sesto Fiorentino, Italy*

e-mail: *livi@lens.unifi.it*

We report on a series of quantum simulation experiments with ultracold ^{173}Yb atoms aimed at the investigation of some of the fundamental properties of quantum-Hall systems. As a fermionic two-electron atom, ^{173}Yb features an internal nuclear spin degree of freedom in the ground state as well as a long-lived $^3P_0$ metastable level which can be exploited for quantum simulation purposes as a second atomic stable state in addition to the ground level.

In a first experiment [1], exploiting this orbital degree of freedom, we have been able to demonstrate the possibility to implement synthetic spin-orbit coupling (SOC) in optical lattices with single-photon clock transitions between two different electronic states. The implementation of SOC is preliminary to a second experiment in which interpreting the two stable states of ^{173}Yb as a synthetic spatial dimension we have been able to simulate a two leg ladder subjected to an artificial magnetic field, evidencing the onset of chiral currents circulating on the edge of the ladder and characterizing the strength of the chirality as a function of the synthetic field flux up to values not accessible in real solid-state systems.

We also performed a similar experiment mapping the synthetic dimension on the nuclear spin internal degree of freedom of ^{173}Yb atoms [2]. In this case, the coupling provided by two-photon Raman transitions allowed us to realize two and three-leg ladders, enabling the observation of bulk properties. This approach is particularly promising for the realization of synthetic systems with periodic boundary conditions.

References

[1] L. F. Livi *et al.*, Phys. Rev. Lett. **22**, 220401 (2016).

[2] M. Mancini *et al.*, Science **349**, 1510 (2015).

Atomic interactions via diffractive light coupling for magnetic ordering and supersolids

T. Ackemann[1], **I. Krešić**[1,2], **G. Labeyrie**[3], **G. R. M. Robb**[1], **G.-L. Oppo**[1], **P. Griffin**[1], **R. Kaiser**[3]

[1] *SUPA and Department of Physics, University of Strathclyde,Glasgow G4 0NG, Scotland, UK*
[2] *Institute of Physics, Bijenička cesta 46, 10000, Zagreb, Croatia*
[3] *Université Côte d'Azur, CNRS, Institut de Physique de Nice, 06560 Valbonne, France*
e-mail: *thorsten.ackemann@strath.ac.uk*

Recent years have seen huge progress in using well controlled cold atom systems to simulate complex quantum phases. Among others, magnetic ordering [1] and supersolids [2, 3] have been of particular interest. We are analyzing a conceptually simple scheme to achieve light mediated coupling which is based on a laser-cooled or quantum degenerate atomic ensemble irradiated by a detuned laser beam. Most of the light is retro-reflected by a plane feedback mirror at some distance d. A modulation of any atomic state variable will cause a phase modulation of the transmitted wave. Diffraction in the feedback loop leads to conversion of phase-to-amplitude modulation on length scales $\Lambda \approx \sqrt{\lambda d}$. This amplitude modulation can couple back to the atomic degrees of freedom leading to light mediated interactions between atoms. We demonstrate here that any degree of freedom of light on the Poincare sphere can be used to couple atomic degrees of freedom leading to new phases.

Fig. 1 illustrated that a localized perturbation of an atomic state leads – after diffraction in the feedback loop – to an oscillatory profile of the retroreflected light: it will enhance the original perturbation, thus driving the spontaneous instability but it will also drive a perturbation at a finite distance thus leading to the emergence of an ordered lattice.

The amplitude of the light field and optomechanical forces can lead to atomic crystallization as demonstrated for thermal atoms in [4]. If the atomic ensemble is quantum degenerate the result is a supersolid ordering as discussed theoretically in [5]. We will present further analytical and numerical analysis of this case.

The polar angle of light on the Poincare sphere determining the optical helicity or S_3-Stokes parameters can couple to a magnetic dipole moment in an atomic ground state with $J > 0$ via optical pumping nonlinearities. The interpretation of the troughs at half the lattice period in Fig. 2 is then anti-ferromagnetic coupling and of the peaks at the lattice period ferromagnetic coupling. Fig. 2 shows an experimental observation of an anti-ferromagnetic pattern in the ground state of ^{87}Rb using the $F = 2 \rightarrow F' =$ 3-line of the D_2 transition for driving. This ordered state with a magnetization in the z-direction (given by the wavevector of the driving laser beam)

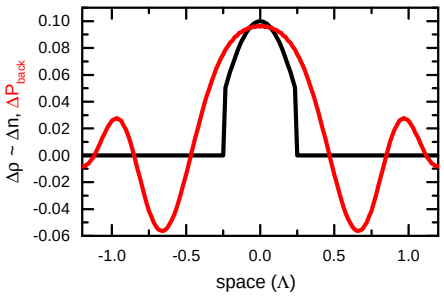


Figure 1: Illustration of effective atomic interaction over the diffractive coupling length Λ. An atomic perturbation (black) creates an optical perturbation (red) coupling back to the atomic states.

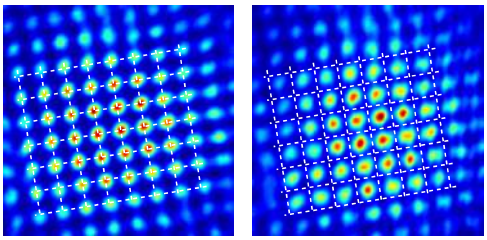


Figure 2: Experimentally observed ordered square patterns in the σ_+ (right) and σ_- (left) light intensity distributions, which are interlaced. Subtraction yields an optical spin pattern indicative of an anti-ferromagnetic state within the Rb ground state.

is destroyed by the coupling to a tranverse magnetic field in close analogy to the quantum phase transition in the transverse Ising model.

The azimuthal angle of light on the Poincare sphere determining the polarization direction or S_1, S_2 Stokes parameters can couple to a $m = 2$ coherence or magnetic quadrupole in an atomic ground state with $J > 1/2$ via a phenomenon related to coherent population trapping. We observed indications for this also on the $F = 2 \rightarrow F' = 3$-line in a strong transverse field.

Similar phenomena are expected for multi-transverse mode resonators providing light-mediated coupling which are also under current investigation.

[1] I. Bloch *et al.* , Nature Phys. **8**, 267 (2012).
[2] J. Léonard *et al.*, Nature **543**, 87 (2017).
[3] J.-R. Li *et al.*, Nature **543**, 91 (2017).
[4] G. Labeyrie *et al.*, Nat. Phot. **8**, 321 (2014).
[5] G. R. M. Robb *et al.*, Phys. Rev. Lett. **114**, 173903 (2015).

Time-Dependent Solution of the Generalized Fano Model

H. Gedeonová, and P. Kolorenč
Charles University, Faculty of Mathematics and Physics, Institute of Theoretical Physics, V Holešovičkách 2, 180 00 Prague, Czech Republic
e-mail: *h.gedeonova@seznam.cz*

In this work, we investigate the time evolution of Fano model, describing a discrete state embedded in a continuum of states with constant coupling, and generalized version of Fano model for an energy dependent coupling. The model is given by the general form of the Hamiltonian

$$H = \left(\begin{array}{c|ccc} E_\varphi & & \mathrm{V} & \\ \hline & \ddots & & 0 \\ V^* & & \mathrm{E} & \\ & 0 & & \ddots \end{array}\right), \qquad (1)$$

given in the basis of the discrete state $|\varphi\rangle$ and the continuum states $|E\rangle$. Here, E_φ is the discrete state energy, E is the energy of the continuum state and V is the discrete state-continuum coupling.

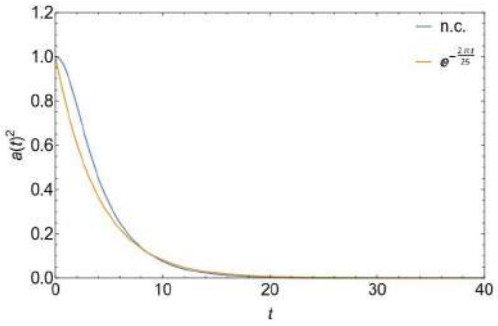


Figure 1: The decay of the discrete state $|\varphi\rangle$ into the continuum of states $|E\rangle$. The blue curve, denoted by n.c., shows numerically calculated probability of the system to be still found in the initial discrete state. Analytically predicted decay is the yellow curve. The parameters of the coupling (2) are $\alpha = 1/5$, $\beta = 1/2$.

In order to solve the the time evolution of the generalized system, the continuum is discretized employing Gauss-Legendre quadrature and the resulting system of differential equations is integrated numerically. As expected [1], the discrete state decays exponentially into the continuum if the coupling depends only weakly on energy, see Fig. 1. However, for a strongly energy-dependent coupling, such as

$$\langle\varphi|H|E\rangle = V = \alpha e^{-\beta E^2}, \qquad (2)$$

the system oscillates between the initial discrete state and the continuum (Fig. 2). In the work, the time

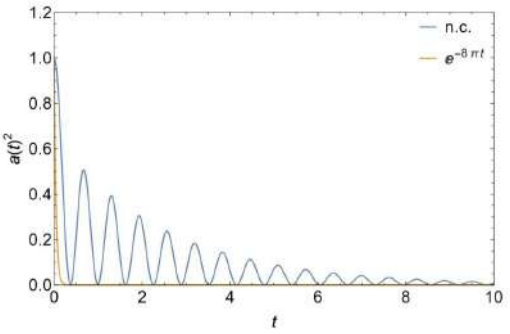


Figure 2: The decay of the discrete state $|\varphi\rangle$ into the continuum of states $|E\rangle$. The blue curve, denoted by n.c., shows numerically calculated probability of the system to be still found in the initial discrete state. Analytically predicted decay is the yellow curve. The parameters of the coupling (2) are $\alpha = 1/5$, $\beta = 1/2$.

evolution is studied for different parameters of the coupling. Transition between oscillatory and non-oscillatory modes is studied in detail and interpretation of the probability oscillation phenomenon is given.

[1] C. Cohen-Tannoudji, J. Dupont-Roc, G. Grynberg, *Atom-Photon Interactions: Basic Processes and Applications*, Wiley, 1998.

Ultracold atoms in a two-dimensional optical quasicrystal

Konrad Viebahn[1], **Matteo Sbroscia**[1], **Edward Carter**[1], **Jr-Chiun Yu**[1], **and Ulrich Schneider**[1]
[1] *Cavendish Laboratory, University of Cambridge, JJ Thomson Avenue, Cambridge CB3 0HE, UK*
e-mail: *kv291@cam.ac.uk*

Quasicrystals are long-range ordered and non-periodic at the same time [1, 2]. This interplay leads to a wealth of intriguing physical phenomena, such as the inheritance of topological properties from higher dimensions, and non-trivial structure on all length-scales. Here, we report on the first experimental realisation of a two-dimensional optical quasicrystal for ultracold atoms. Our eightfold optical lattice (Fig. 1) results in a fractal in momentum space whose self-similarity can be seen by the 'silver mean' scaling $(1+\sqrt{2})$, as shown in Fig. 2. We directly visualise this self-similarity using matter-wave diffraction (Kapitza-Dirac scattering), shown in Fig. 3.

The diffraction dynamics offers an additional signature of quasicrystalline behaviour and it is shown to represent a continuous-time quantum walk on a four-dimensional tight-binding lattice. These measurements pave the way for quantum simulation in higher dimensions. Additionally, our system will enable the observation of phenomena, such as non-power-law scaling near criticality [3], that have so far been unattainable with quasicrystalline systems in condensed matter and photonic contexts.

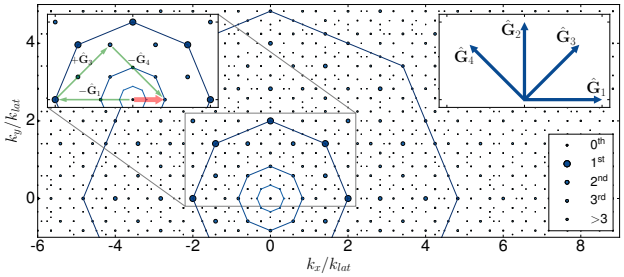


Figure 2: Fractal momentum space structure of the eightfold optical lattice, showing the first 15 possible diffraction orders. The combination of three reciprocal lattice vectors ($\hat{G}_i$, right inset) results in a smaller k-state (red arrow, left inset) that is scaled by the silver mean $1+\sqrt{2}$ with respect to $\hat{G}_i$. The resulting pattern is self-similar, indicated by the octagons.

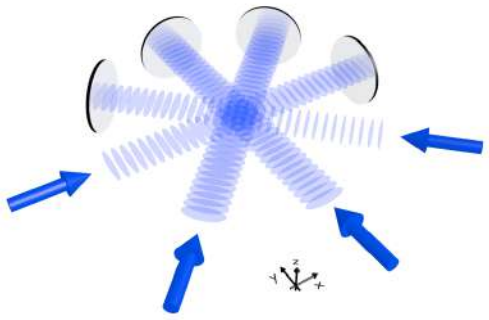


Figure 1: Schematic of the eightfold optical lattice formed by superimposing four independent 1D lattices.

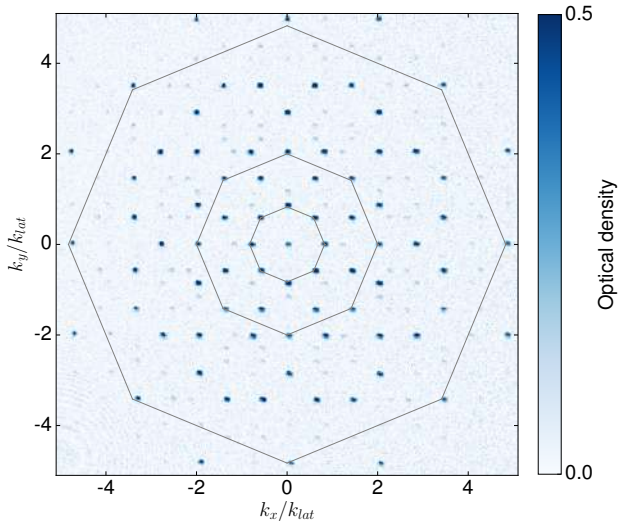


Figure 3: Raw absorption image of ^{39}K atoms at 33ms time-of-flight after exposure to the eightfold optical lattice. The self-similarity of this matter-wave diffraction pattern is highlighted by octagons which are each scaled by $1+\sqrt{2}$.

[1] D. Shechtman, I. Blech, D. Gratias, and J.W. Cahn, Phys. Rev. Lett. **53**, 1951 (1984)

[2] D. Levine and P.J. Steinhardt, Phys. Rev. Lett. **53**, 2477 (1984)

[3] A. Szabó and U. Schneider, arXiv preprint arXiv:1803.09756 (2018)

Simulation of Quantum Chemistry problems using cold atoms

J. Argüello-Luengo[1]

[1] *Max-Planck-Institut fur Quantenoptik, Hans-Kopfermann-Strasse. 1, 85748 Garching, Germany*
e-mail: *javier.arguello@mpq.mpg.de*

Quantum simulation offers the long-standing goal of using a quantum systems to face questions that are hard to understand classically. While full-fledged quantum computers may be built in the distant future, the next generations will be limited in size and by the presence of errors [1]. An alternative way to address quantum many-body problems is analog quantum simulation, where a highly controllable quantum system mimics the interactions of the Hamiltonian one wants to investigate. In fact, analog quantum simulators based on atoms in optical lattices [2] have already performed some simulations of condensed matter physics problems that are out of reach of classical computers [3, 4]. All those problems are based on local or short-range interactions, and are ideally suited for the existing simulators. Problems in quantum chemistry, in contrast, require long-range Coulomb interactions, and thus, it is harder to realize whether analog simulation can help in that field.

Here, we propose an experimental setup to solve quantum chemistry problems using cold atoms trapped in state-dependent optical lattices. In the same way that virtual photons mediate electronic interactions in nature, Coulomb interactions are induced by a spin excitation in a Mott insulator with the same spacing as the fermionic lattice (see Figure 1). We discuss the main sources of systematic deviations rising from the discretization of the Hilbert space and illustrate this method solving the molecular potential for a molecule of Hydrogen. While the setup is discrete and finite, we show that precise results can be obtained for simple real molecules with moderate lattice sizes, and that it can be scaled. Apart from the standard advantages of analog simulation over quantum computing regarding the required degree of control, the present scheme does not rely on a judicious choice of molecular orbitals, but rather directly operates in real space [5].

[1] Preskill, J. (2018). Quantum Computing in the NISQ era and beyond. arXiv:arXiv:1801.00862v2

[2] Lewenstein, M., Sanpera, A., Ahufinger, V., Damski, B., Sen(De), A., Sen, U. (2007). Advances in Physics, 56(2), 243379.

[3] Jordens, R., Strohmaier, N., Gunter, K., Moritz, H., Esslinger, T. (2008). Nature, 455(7210).

[4] Greiner, M., Mandel, O., Esslinger, T., Hnsch, T. W., Bloch, I. (2002). Nature, 415(6867).

[5] Argüello-Luengo J., González-Tudela A., Shi T., Cirac J.I. To be submitted.

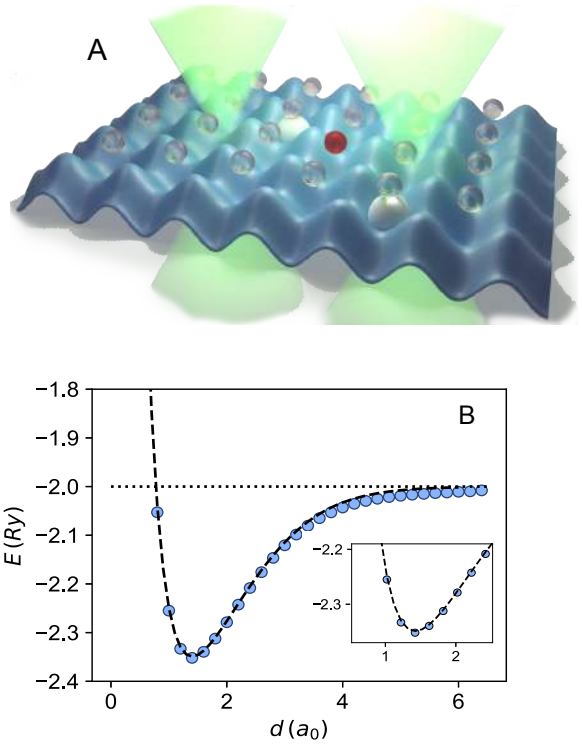


Figure 1: **A** Schematic representation of the analog simulator. The electronic Hamiltonian is mapped to cold atomic fermions hopping in an optical lattice. External lasers induce a light shift, $-V_0/||r||$, that scales inversely with the distance to given points in the lattice representing the position of the nuclei. Electronic repulsion is mediated by a spin excitation moving on a state-dependent lattice with the same spacing as the fermion and on-site scattering when they are placed on the same lattice site. Modifying the position of the external lasers, we can obtain the molecular potential represented in **B**.

Motional quantum state engineering of two heteronuclear atoms with spin-selective optical tweezers

Kunpeng Wang[1,2,3,*], **Xiaodong He**[1,2,†], **Ruijun Guo**[1,2,3], **Cheng Sheng**[1,2,3], **Peng Xu**[1,2], **Min Liu**[1,2], **Jin Wang**[1,2], **and Mingsheng Zhan**[1,2,‡]

[1] *State Key Laboratory of Magnetic Resonance and Atomic and Molecular Physics, Wuhan Institute of Physics and Mathematics, Chinese Academy of Sciences - Wuhan National Laboratory for Optoelectronics, Wuhan 430071, China*

[2] *Center for Cold Atom Physics, Chinese Academy of Sciences, Wuhan 430071, China*

[3] *School of Physical Sciences, University of Chinese Academy of Sciences, Beijing 100049, China*

e-mail: [*] *wangkunpeng@wipm.ac.cn,* [†] *hexd@wipm.ac.cn,* [‡] *mszhan@wipm.ac.cn*

Creation of a low-entropy atomic array is the first essential step for quantum simulation of many-body physics and quantum information processing. Ultracold atoms and molecules are of increasingly interest with excellent controllability and high resolution imaging and detection. The entropy associated with the filling factor of an atomic array can be eliminated with recently demonstrated atom assembly techniques[1][2]. Thermal distribution over motional states often leads to qubit dephasing and quantum gate errors, which plays an important role in quantum computation with atomic qubits, as the depressed entanglement fidelity shown in recent experiments with heteronuclear atoms[3]. The residual entropy associated with atomic thermal motion can be eliminated with ground state cooling techniques.

Here we report motional qautatum state engineering and preparation of a low-entropy system of two heteronuclear atoms in optical micro-traps. We perform three dimensional Raman sideband cooling of two atoms, ^{87}Rb and ^{85}Rb, simultaneously in adjacent optical tweezers. The 3D ground state probability after cooling is estimated via asymmetric sideband spectrum as 0.91(5) for ^{87}Rb, the corresponding $\overline{n}$ for three dimensions are $0.04(3), 0.01(1)$ and $0.04(4)$. Similar results are achieved for ^{85}Rb. We transfer the two atoms into the ground state of a single trap with spin selective transportation. The heating during transfer is as low as 0.01(0.03) vibrational quanta for radial(axial) dimensions.

This system can be used to increase the entanglement fidelity with near frozen atomic motion that suppressing the interaction fluctuation in our previous experiment[3]. The merged two atoms can also be used to associate single molecules [4] [5] and to study controlled collision dynamics and entanglement[6]. This method to prepare motional ground state heteronuclear atoms can be easily extended to other atomic species and can be scaled up to a large defect-free array with atom assembly techniques.

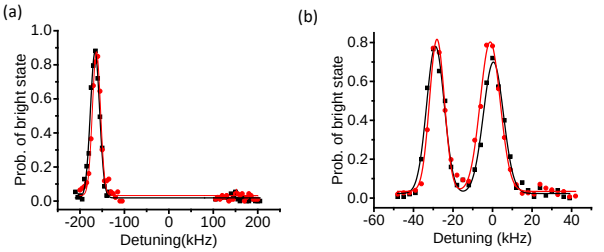


Figure 1: (a) Radial dimensional Raman sideband cooling of ^{87}Rb along two orthogonal axes. (b) Axial dimensional Raman sideband cooling of ^{87}Rb (black squares) and ^{85}Rb (red circles).

[1] M. Endres, H. Bernien, A. Keesling, H. Levine, E. R. Anschuetz, A. Krajenbrink, C. Senko, V. Vuletic, M. Greiner, and M. D. Lukin, Science **354**, 1024 (2016).

[2] D. Barredo, S. de Léséleuc, V. Lienhard, T. Lahaye, and A. Browaeys, Science **354**, 1021 (2016).

[3] Y. Zeng, P. Xu, X. He, Y. Liu, M. Liu, J. Wang, D. J. Papoular, G. V. Shlyapnikov, and M. Zhan, Phys. Rev. Lett. **119**, 160502 (2017).

[4] P. Xu, J. Yang, M. Liu, X. He, Y. Zeng, K. Wang, J. Wang, D. J. Papoular, G. V. Shlyapnikov, and M. Zhan, Nature Communications **6**, 7803 (2015).

[5] L. R. Liu, J. D. Hood, Y. Yu, J. T. Zhang, N. R. Hutzler, T. Rosenband, and K.-K. Ni, Science **360**, 900 (2018).

[6] A. M. Kaufman, B. J. Lester, M. Foss-Feig, M. L. Wall, A. M. Rey, and C. A. Regal, Nature **527**, 208 (2015).

Taking pictures of 'black holes': imaging non-local spin-exchange interactions in an optical cavity

G. Bentsen, E. Davis, L. Homeier, T. Li, and M. Schleier-Smith
Department of Physics, Stanford University, Stanford, CA 94305, USA
e-mail: *gbentsen@stanford.edu*

Nonlocal interactions have recently emerged as a recurring theme in the description of a variety of many-body phenomena. For instance, dynamical processes that rapidly scramble quantum information [1], as well as toy models of black holes such as matrix models and the Sachdev-Ye-Kitaev model [2], rely crucially on couplings between arbitrarily distant degrees of freedom. Strong nonlocal couplings, although di cult to achieve in most experimental setups, are quite naturally realized in cavity QED systems since the cavity mode mediates interactions between atoms regardless of their spatial locations [3]. We demonstrate optically controlled nonlocal spin-exchange interactions between pseudo-spin-1 ^{87}Rb atoms coupled to the mode of a high-finesse optical cavity. In addition, we demonstrate nonlocal spin-mixing dynamics in which atoms prepared in the $m_F = 0$ state are converted into entangled pairs of atoms in $m_F = \pm 1$. We characterize the spin-exchange and spin-mixing interactions by quench dynamics and imaging of spin textures in a millimeter-long atomic cloud as illustrated in Fig. 1. Optical control over the sign of the interactions provides a key tool necessary to implement echo schemes such as those proposed to measure quantum information scrambling [4]. The unique access to spatial information in this setup allows us to watch the spread of quantum information in a nonlocal system, and presents prospects for simulating toy models of black holes for as many as 100 spins in the near future.

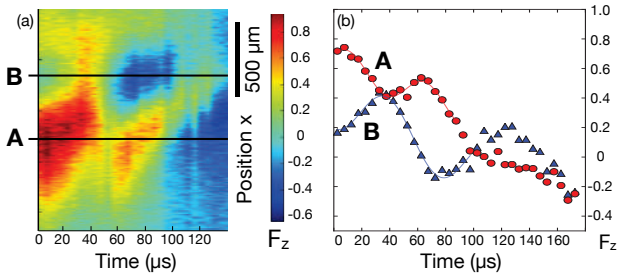


Figure 1: Cavity-mediated spin-exchange interactions. (a) State-sensitive imaging shows spin-exchange dynamics following a quantum quench. Spin excitations hop from filled sites in region A to depleted sites in region B and back. (b) Cuts of the local magnetization versus time in regions A and B.

References

[1] Nima Lashkari, Douglas Stanford, Matthew Hastings, Tobias Osborne, and Patrick Hayden. Towards the fast scrambling conjecture. *Journal of High Energy Physics*, 2013(4):22, Apr 2013.

[2] Alexei Kitaev. "A simple model of quantum holography" talks at KITP. Apr 2015. `http://online.kitp.ucsb.edu/online/entangled15/kitaev/`.

[3] Matthew A. Norcia, Robert J. Lewis-Swan, Julia R. K. Cline, Bihui Zhu, Ana M. Rey, and James K. Thompson. Cavity mediated collective spin exchange interactions in a strontium superradiant laser, Nov 2017. `arXiv:1711.03673`.

[4] Brian Swingle, Gregory Bentsen, Monika Schleier-Smith, and Patrick Hayden. Measuring the scrambling of quantum information. *Phys. Rev. A*, 94:040302, Oct 2016.

Ba-Li: towards a quantum mixture of Barium ions and ultracold Lithium gases

A. Detti[1,2], **L. Duca**[2], **E. Perego**[2,3], **M. Inguscio**[1,4,5] **and C. Sias**[2,5]

[1] *Department of Physics and Astronomy, University of Florence, I-50019 Sesto Fiorentino, Italy*

[2] *INRIM, Istituto Nazionale di Ricerca Metrologica, I-10135 Torino, Italy*

[3] *Politecnico di Torino, Dipartimento di Elettronica e Telecomunicazioni, I-10129 Torino, Italy*

[4] *CNR, Consiglio Nazionale delle Ricerche, I-00185 Roma, Italy*

[5] *LENS, European Laboratory for Nonlinear Spectroscopy, I-50019 Sesto Fiorentino, Italy*

e-mail: *detti@lens.unifi.it*

Hybrid quantum systems represent one of the most promising routes in the progress of experimental quantum physics and in the development of quantum technologies. In a hybrid quantum system two (or more) different quantum systems interact in the same experimental setup. Therefore, these composite systems benefit from both the properties of each single system and from the presence of an interaction term, leading to the emergence of new variables that can be experimentally manipulated.

A promising hybrid quantum system is the one realized by the combination of an ultracold atomic gas and trapped ions [1]. Ultracold atoms and trapped ions are two of the most studied physical systems for the implementation of several quantum technologies, like e.g. quantum simulation, quantum computation, and quantum metrology. When trapped together, atoms and ions interact via an interaction potential that scales asymptotically with R^{-4}, where R is the interparticle distance, due to the electrostatic (attractive) force between the ion's electric monopole and the atom's induced dipole. Interestingly, this potential has a typical range on the order of 100s of nm, i.e. approx. two orders of magnitude longer than the range of atom-atom interactions. Several studies have proposed to use this interaction to realize new quantum simulations [2], study few-body physics [3], and control atom-ion chemical reactions [4, 5].

We are currently developing a new experimental apparatus for the realization of an ultracold atom-ion quantum hybrid system made of a quantum gas of fermionic Lithium and one (or a few) Barium ions. The ions will be trapped using a Paul trap, while the neutral atoms will be first cooled at ultralow temperatures and then transported optically into the ions' trapping region. The choice for the elements ensures that atoms and ions in their electronic ground state will not undergo charge-exchange collisions, i.e. inelastic processes for which an electron is "exchanged" between the two colliding particles. Additionally, the large mass ratio ensures an e cient cooling of the ion in the ultracold gas.

We will present the current state of advancement of the new experimental apparatus - which represents the first ion trapping experiment in Italy - and give an overview of some of the experiments that we plan to realize with this novel atom-ion hybrid system.

We first plan to study atom-ion interactions at the quantum level, i.e. when collisions can be described by one or a few partial waves. In this regime, it will be possible to search for atom-ion Feshbach resonances, which were predicted [6] but never observed so far. By reaching a high level of control over atom-ion interactions we plan to simulate many-body physics with a single impurity probe. In particular, we will investigate out-of-equilibrium phenomena like the Anderson Orthogonality Catastrophe originating in a spin polarized ultracold Fermi gas when the interaction between the fermions and a single localized impurity is suddenly changed [7]. This will be realized e.g. by changing the ion's internal state in the presence of a Feshbach resonance, leading to the creation of a coherent superposition between the ion's internal state and the many-body state evolution. These quantum states of the atom-ion mixture will represent an ideal platform to investigate fundamental quantum mechanics, out-of-equilibrium phenomena and quantum thermodynamics.

References

[1] C. Sias, M. Koehl Chapter 12 in *Quantum gas experiments - exploring many-body states*, edited by P. Törmä and K. Sengstock, Imperial College Press, 2014 arXiv.1401.3188.

[2] U. Bissbort, et al. Phys. Rev. Lett. **111**, 080501 (2013).

[3] R. Côté, V. Kharchenko, and M. D. Lukin Phys. Rev. Lett. **89**, 093001 (2002).

[4] L. Ratschbacher, C. Zipkes, C. Sias, and M. Köhl Nature Phys. **8**, 649 (2012).

[5] F. H. J. Hall, et al. Phys. Rev. Lett. **107**, 243202 (2011).

[6] Z. Idziaszek, T. Calarco, P. S. Julienne, and A. Simoni Phys. Rev. A **79**, 2009, 010702(R).

[7] M. Knap, et al. Phys. Rev. X **2**, 041020 (2012).

A room temperature single-photon source based on strongly interacting Rydberg atoms

T. Pfau[1], **F. Ripka**[1], **F. Christaller**[1], **H. Zhang**[1], **H. Kübler**[1], **and R. Löw**[1]

[1] *5. Physikalisches Institut and Center for Integrated Quantum Science and Technology IQST, Universität Stuttgart, Pfaffenwaldring 57, 70550 Stuttgart, Germany*

e-mail: *t.pfau@physik.uni-stuttgart.de*

Tailored quantum states of light can be created via a transfer of collective quantum states of matter to light modes. Such collective quantum states emerge in interacting many-body systems if thermal fluctuations are overcome by su cient interaction strengths. Therefore, typically ultracold temperatures or strong confinement are required. We show that the exaggerated interactions between giant Rydberg atoms allow for collective quantum states also in a thermal vapor cell above room temperature. The emerging Rydberg blockade allows then only for a single Rydberg excitation. We experimentally implement a four-wave mixing scheme to demonstrate an on-demand single-photon source based on this Rydberg blockade effect as was demonstrated for ultracold atoms [1]. The combination of glass cell technology, identical atoms, and operation around room temperature promises scalability and integrability. This approach has the potential for various applications in quantum information processing and communication.

Prior to this first demonstration coherent dynamics to Rydberg states [2] and su cient Rydberg interaction strengths [3] have been demonstrated in thermal vapors. Additionally, time-resolved probing of collective Rydberg excitation have revealed a lifetime long enough for effective Rydberg interactions [4]. Also coherent Rydberg excitation in microscopic glass cells was studied [5].

Here we report on a significant decrease of photon coincidences for photons at 780 nm when the size of the atomic ensemble is reduced to 1 μm i.e. below the Rydberg blockade radius. The normalized photon pair correlation shows a clear signature for anti-bunched photon statistics and a strong evidence for the observation of a cooperative quantum effect in a thermal atomic ensemble. In other words, we have shown in a proof of principle experiment that strong Rydberg interactions in a hot atomic vapor cell can be used to generate single photons on demand. Advantages of that approach include: (I) no necessity for laser cooling and integrability; (II) effective emission in the forward direction and the potential for storable and potentially identical photons. As next steps, we will increase the repetition rate, optimize the pulse shapes [6] and the relevant parameters like the brightness, determine the indistinguishability of the generated photons, apply optical integration technologies, and combine our source with photon memories based on atomic vapors.

References

[1] Dudin et al., Science **336**, 6083 (2012).

[2] Huber et al., Phys. Rev. Lett. **107**, 243001 (2011)

[3] Baluktsian et al., Phys. Rev. Lett. **110**, 123001 (2013)

[4] Ripka et al., Phys. Rev. A **93**, 053429 (2016)

[5] Kübler et al., Nature Photonics **4**, 112 (2010)

[6] Müller et al. , Phys. Rev. A **87**, 053412 (2013)

Femtosecond multiphoton π-pulse control of Rydberg states in Rubidium atoms

I.J. Afa, J.L. Font, and C. Serrat
Department de Física, Universitat Politècnica de Catalunya, Colom 11, 08222 Terrassa (Barcelona), Spain
e-mail: *iduabo.john.afa@upc.edu*

Highly excited atoms commonly referred to as Rydberg atoms have attracted numerous interests over the past few years due to its numerous exaggerated properties [1]. As shown in some studies, selective excitation and manipulation of Rydberg states play a crucial role in quantum computation, for instance, in the design and implementation of robust, fast quantum gates with recent proposals using neutral atoms and molecules, which allows gate operation times set by the timescale of the laser excitation [2, 3]. We demonstrate an ultrafast femtosecond timescale trichromatic π-pulse illumination scheme for coherent excitation and manipulation of low-lying Rydberg states in rubidium.

In this study, a 4-level cascade configuration of rubidium atoms was chosen and selective population of $nP_{3/2}$ levels with n $\leq$ 12 (level 4) from the ground state $5S_{1/2}$ of Rb through intermediate levels $6P_{3/2}$ (level 2) and $6D_{3/2}$ (level 3) was achieved using 75 fs laser pulses with precisely selected values for coupling the transitions between these energy states [4, 5], as illustrated in Fig. 1. The density matrix equations of the 4-level system beyond the rotating wave approximation are solved to resolve the balance between the principal quantum number, the duration of the laser pulse, the pure dephasing times and the associated ac-Stark effects for the fastest optimal excitation. We also demonstrated the superiority of using the multiphoton π-pulse scheme over a single π-pulse scheme for achieving selective excitation (Fig. 2) [6]. Figure 2 shows the time evolution of the populations for the interaction with 75 fs laser pulses with μ_{34}= 0.5×10^{-29} Cm (n $\sim$ 11), for $T_2 = 1$ ns and $T_2 = 1$ ps. The grey lines (legend on the right) show the case of illumination with a single pulse of area π resonant with the 1-4 transition, considering $\mu_{14} = 0.02 \times 10^{-29}$ Cm and $T_2 = 1$ ns.

The presented mechanism is shown to be robust for selective ultrafast excitation and manipulation of Rydberg states and can readily be extended to different level configurations, with applications in quantum information technology and high precision spectroscopy.

Support from the Spanish Ministry of Economy and Competitiveness through FIS2014-51997-R is acknowledged.

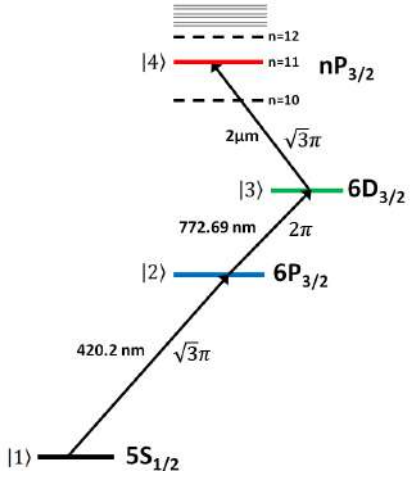


Figure 1: Energy levels configuration of the Rb atom chosen to excite the low-lying Rydberg states $nP_{3/2}$.

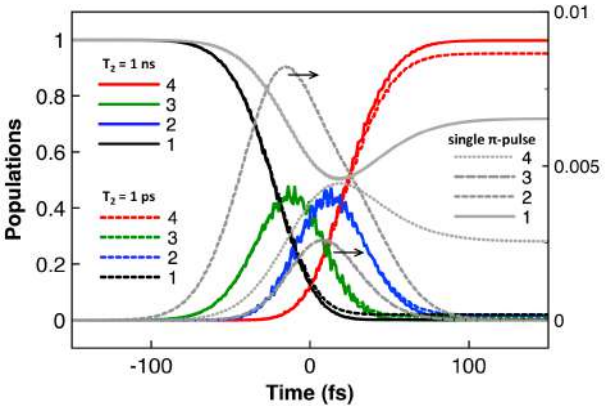


Figure 2: Time evolution of the populations for the interaction with 75 fs laser pulses

[1] M. Saffman and T. G. Walker, Rev. Mod. Phys. **82**, 2313 (2010).

[2] D. Jaksch, J. I. Cirac, and P. Zoller, S. L. Rolston, R. Côté, and M. D. Lukin, Phys. Rev. Lett. **85**, 2208 (2000).

[3] L.-M. Duan, Phys. Rev. Lett. **93**, 100501 (2004).

[4] M. S. Safronova, W. R. Johnson, and A. Derevianko, Phys. Rev. A **60**, 4476 (1999).

[5] M. S. Safronova, Carl J. Williams, and Charles W. Clark, Phys. Rev. A **69**, 022509 (2004).

[6] I.J. Afa, J.L. Font and C. Serrat, Phys. Rev. A **96**, 053843 (2017).

An enhanced optical non-linearity based on Rydberg electromagnetically induced transparency for pulses from 1 to 100s of photons

Josiah Sinclair[1], **Noah Lupu-Gladstein**[1], **Daniela Murcillo**[1], **Qizhong Liang**[1], **Kent Bonsma-Fisher**[1], **Aephraim Steinberg**[1,2]

[1] *Centre for Quantum Information and Quantum Control and Institute for Optical Sciences, Department of Physics, University of Toronto, 60 St. George Street, Toronto, Ontario, Canada M5S 1A7*

[2] *Canadian Institute For Advanced Research, 180 Dundas St. W., Toronto Ontario, CANADA M5G 1Z8*

e-mail: *sinclairjosiah@gmail.com*

Strong interactions between Rydberg atoms provide an exciting platform for quantum nonlinear optics. Rydberg blockade (where a cloud of many atoms is unable to support more than a single excitation due to dipole interactions) combined with electromagnetically induced transparency (EIT) (where on-resonant absorption is suppressed due to the presence of a second coupling field) has been used to demonstrate single photon generation and strong photon-photon interactions. Despite these advances, Rydberg blockade is unsuited for other important applications in quantum nonlinear optics, like quantum non-demolition measurements of photon number, and photon-number squeezing. This is because Rydberg blockade treats all photons after the first photon (which caused the blockade) indistinguishably. Here, we report on an experiment far from the blockade regime where weak Rydberg interactions enable an optical pulse propagating through a cloud of atoms to acquire a phase shift proportional to the number of photons (1-100s) in a second optical pulse. We present observations of the phase shift as a function of photon number and Rydberg principal quantum number. We discuss possible next steps towards harnessing this enhanced Kerr non-linearity for non-demolition measurement and the generation of non-classical states of light.

Figure 1 shows our setup (c), the atomic level scheme (a) and the optical depth (left) and phase (right) (b) experienced by a probe pulse propagating through the magneto-optical trap (MOT) in the presence (black) and absence (gold) of the coupling beam which creates electromagnetically induced transparency for the probe

Figure 2 shows the main result. The phase shift acquired by the probe pulse propagating through the MOT depends linearly on the average number of photons in the signal pulse. This optical nonlinearity arises from Rydberg-Rydberg interactions and increases, as expected, with increasing Rydberg level.

We present a model predicting that the nonlinearity scale like Rydberg level to the power of 11/2 and show that our results are consistent with the model.

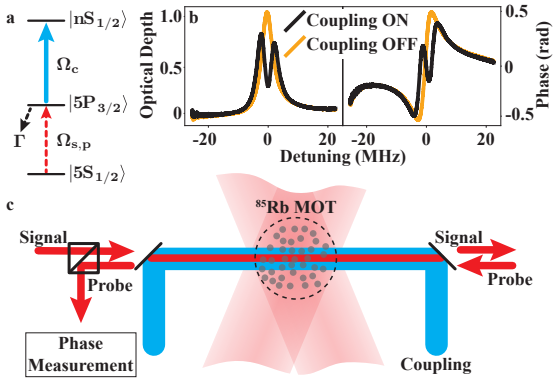


Figure 1: **a**, 780nm and 480nm beams drive EIT in between the $5S_{1/2}, 5P_{3/2}$, and $nS_{1/2}$ states in ^{85}Rb. **b**, absorption (left) and phase (right) measurements as a function of the signal beam detuning shows a typical EIT trace. **c**, Signal, probe and coupling beams address trapped and cooled ^{85}Rb atoms. EIT conditions are met for counter-propagating signal and probe beams with the same coupling beam. The probe is filtered from the signal by polarization and its phase measured by a beat note with an off-resonant frequency component.

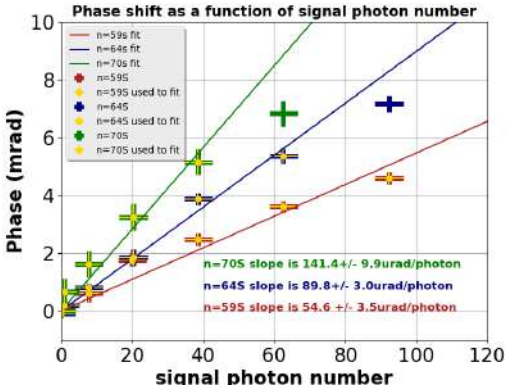


Figure 2: Phase shift acquired by the probe laser as a function of the average number of photons in the signal pulse within a 26ns window for three different Rydberg levels (n=59S, 64S and 70S). Gold points are included in the fit. Error bars are calculated from data and represent the standard error of the mean.

Ionic Impurity in a Bose-Einstein Condensate at Submicrokelvin Temperatures

K. S. Kleinbach, F. Engel, T. Dieterle, R. Löw, T. Pfau, and F. Meinert
5. Physikalisches Institut and Center for Integrated Quantum Science and Technology, Universität Stuttgart, Pfaffenwaldring 57, 70569 Stuttgart, Germany
e-mail: *k.kleinbach@physik.uni-stuttgart.de*

Rydberg atoms immersed in a Bose-Einstein condensate (BEC) interact with the quantum gas via electron-atom and ion-atom interaction. Typically, the electron-atom interaction is the dominant contribution, as the Rydberg electron scatters with the numerous neutral atoms located inside its large orbit. For small separations between the Rydberg core ion and the neighboring atom however, the ion-neutral interaction starts to compete with the electron-neutral interaction and finally dominates for su ciently small separations.

To access the ion-atom interaction, we present a novel experimental approach where the typically dominant electron-atom interaction is suppressed: Giant Rydberg states with a principal quantum number up to $n = 190$ are excited from a dense and tightly trapped micron-sized condensate. Thereby, a regime is entered where the Rydberg orbit exceeds the size of the atomic sample by far and the reduced overlap between the electron probability density and the BEC leads to a strong suppression of the electron-atom interaction. In this case, a detailed line shape analysis of the Rydberg excitation spectrum provides clear evidence for ion-atom interaction.

Exciting the Rydberg state from a condensed sample conceptually maintains the ultralow temperature environment of the parent atomic ensemble, though in our experiment we are mainly limited by the imparted photon-recoil during Rydberg excitation. The interaction of the BEC with the core ion is thus probed at temperatures below a microkelvin, which is about three orders of magnitude lower compared to what has been achieved in more conventional hybrid traps. Moreover, rapid acceleration of the ionic impurity due to detrimental electric stray fields is prevented by the Rydberg electron which provides an effective shielding. Our results may open up ways to enter the quantum regime of ion-atom scattering for the exploration of charged quantum impurities and associated polaron physics.

[1] K. S. Kleinbach, F. Engel, T. Dieterle, R. Löw, T. Pfau, and F. Meinert, Phys. Rev. Lett. **120**, 193401 (2018).

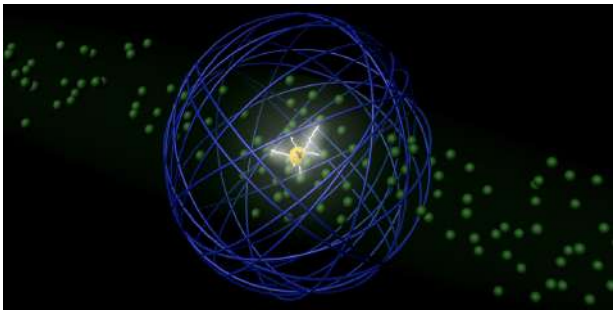


Figure 1: Illustration of the Rydberg core ion interacting with the BEC

Single-shot Non-destructive Detection of Ensembles of Rydberg Atoms with Microwave Cavity Transmission Measurements

S. Garcia[1], **M. Stammeier**[1], **J. Deiglmayr**[2], **F. Merkt**[2], **A. Wallraff**[1]
[1] *Department of Physics, ETH Zürich, CH-8093 Zürich, Switzerland*
[2] *Laboratorium für Physikalische Chemie, ETH Zürich, CH-8093, Zürich, Switzerland*
e-mail: *sgarcia@phys.ethz.ch*

Rydberg atoms are used in an increasing number of experiments, in particular due to their large dipole moment that induces finite range interactions which allows controlled simulations of interacting quantum systems. The usual techniques to detect Rydberg atoms are based on ionization followed by detection of ions or electrons on an avalanche detector, or, in systems of trapped atoms, on detection of presence or absence of atoms. Both methods are very e cient but destructive. Cavity quantum electrodynamics (QED) provides a powerful tool to realize quantum non-demolition measurements of either part of the system, emitter or photon, by observing the effect of the interaction on the other part. Ideal projective measurements allow to detect, to prepare and to manipulate quantum states in a controlled and coherent manner. They are used with atomic or solid-state emitters in the optical or microwave domains. So far, Rydberg atoms in cavity QED systems have mainly been used to measure or create quantum states of light. Using a microwave cavity to detect Rydberg atoms is less explored. It also constitutes a step towards the application of the long coherence time of Rydberg atoms as quantum memories for microwave-based quantum information processing.

Detecting the change in phase $\delta\phi$ of a weak probe tone transmitted through a superconducting 3D microwave cavity [1] allows us to measure the dispersive shift χ induced by an ensemble of helium Rydberg atoms (Fig. 1(a,b)). The system is quantitatively described by the dispersive Tavis-Cummings hamiltonian, as the atom-cavity coupling is dominated by the transition between the 42s and 42p states which has a small detuning from the cavity resonance. Thus, the dispersive shift is given by $\chi = g_1^2 N/$, where the single atom coupling to the cavity g_1 is calculated from the cavity field distribution and the transition dipole moment of the atom. The detuning is measured by intra-cavity spectroscopy and N is the number of Rydberg atoms.

We measured the scaling of the collective dispersive shift with the atom-cavity detuning and the number of Rydberg atoms [2]. The latter provides a non-destructive measurement of the number of Rydberg atoms which we compare to the destructive detection by ionization and collection of electrons on a microchannel plate (see Ref. [2] and Fig. 1(c)). The

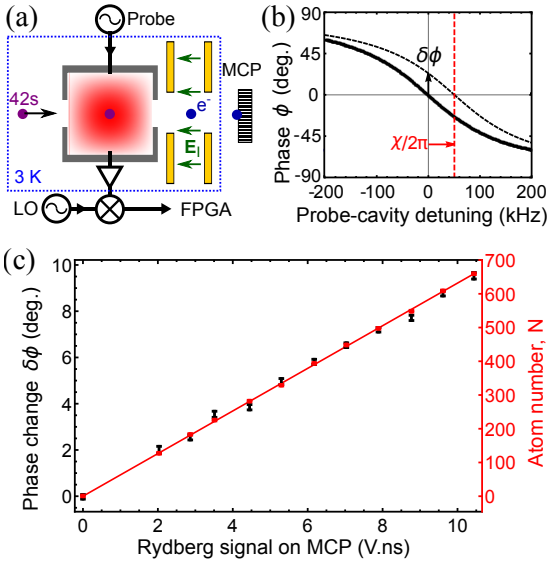


Figure 1: (a) Schematic of the experimental setup combining a non-destructive detection of a Ryberg atom ensemble (helium, 42s state) by transmission measurement of a microwave cavity, and a destructive ionization and detection of resulting electrons by a microchannel plate (MCP). (b) Phase of the bare cavity transmission, measured close to resonance. The dashed curve represents the dispersively shifted phase response. The resulting phase change $\delta\phi$ on resonance is indicated by an arrow. (c) Phase change at cavity center (black) and fitted atom number (red) versus MCP signal while varying the Rydberg atom number. The linear fit (red line) emphasizes the proportionality between the two detections.

technique also offers non-destructive measurements of the internal state of an ensemble of Rydberg atoms by detecting its pseudo-spin polarization. By calibrating the dependence of the response on the probe power, the sensitivity of our atom detector allows to reach a single shot non-destructive detection of ensembles of 300 atoms with an uncertainty on the order of 20%. We discuss possible improvements of this type of non-destructive detector for Rydberg atoms.

[1] M. Stammeier *et al.*, ArXiv, 1712.08631 (2017).

[2] M. Stammeier *et al.*, Phys. Rev. A, **95**, 053855 (2017).

Searching for magnetic micro-defects by magnetic field imaging that employs nitrogen vacancy centers in diamond crystal

A. Berzins[1], **K. Erglis**[2], **J. Smits**[1], **M. Auzins**[1], **R. Ferber**[1], **and A. Cebers**[2]
[1] *Laser Centre, University of Latvia, Zellu Street 25, Riga, Latvia*
[2] *Laboratory of Magnetic Soft Materials, University of Latvia, Zellu Street 25, Riga, Latvia*
e-mail: *andris.berzins@lu.lv*

Nitrogen-vacancy (NV) centers in diamonds have proven to be useful for the imaging of magnetic fields created by various magnetic structures [1], [2], [3]. The reason is that the NV center has a triplet ground state with a zero-field splitting between the $m_s = 0$ and $m_s = \pm 1$ ground-state sublevels of 2.87 GHz. Moreover, in the presence of a local magnetic field the $m_s = \pm 1$ energies components are shifted by 2.8 MHz/G. Due to a non-radiative decay path via a singlet state that preferentially populates the $m_s = 0$ ground-state sublevel, thus the NV center can be polarized optically. The fluorescence from exciting $m_s = 0$ sublevel is more intense than the fluorescence from exciting the $m_s = \pm 1$ sublevels. As a result one can read out the polarization state from the fluorescence intensity.

When a thin layer of NV centers is created close to the surface of a diamond, magnetic field distributions at the position of the NV layer can be imaged. We have constructed a magnetic field microscope and are using it to study magnetic field distributions from magnetic particles, magnetic labyrinths and magnetic thin films made from different materials as well as in search for magnetic defects in macroscopic structures.

As an example of our measurements we present (Fig. 1) results we obtained from mix of 500 nm paramagnetic and 4 μm ferromagnetic particles.

Acknowledgments: A. Berzins gratefully acknowledges support from PostDoc Latvia project 1.1.1.2/VIAA/1/16/024 "Two-way research of thin-films and NV centres in diamond crystal" and LLC "MikroTik" donation, administered by the UoL foundation, for opportunity to improve experimental setup. Other authors acknowledges support by M-ERA-NET project "Metrology at the Nanoscale with Diamonds" (MyND) and Base/Performance Funding Project Nr. AAP2016/B013, ZD2010/AZ27.

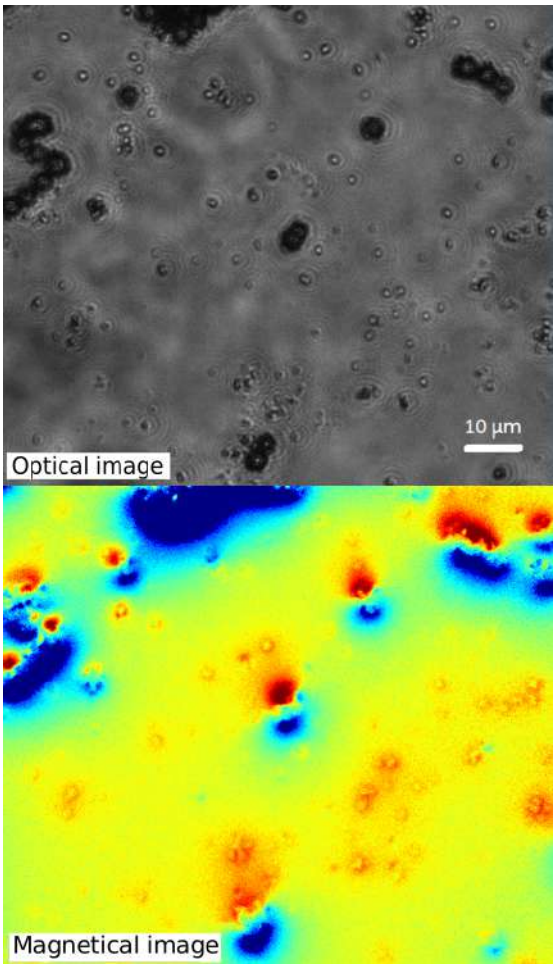


Figure 1: The top panel shows the optical image but the bottom panel shows the magnetic image of the same mix of 500 nm paramagnetic and 4 μm ferromagnetic particles. Paramagnetic particles align their magnetic fields along the external field, but ferromagnetic particles maintain their initial magnetization.

[1] J. Smits *et al.*, Eur. Phys. J. Appl. Phys. **73** 20701 (2016).

[2] L. M. Pham *et al.*, New Journal of Physics **13** 045021 (2011).

[3] D. Le Sage *et al.*, Nature **496** 486 (2013).

Resonant enhancement of optical nonlinearities in a Rydberg gas

C. Hainaut[1], **A. Tebben**[1], **V. Walther**[2], **R. Ferracini Alves**[1], **Y. Zhang**[2], **A. Salzinger**[1], **N. Tchaicharoen**[1], **G. Zürn**[1], **T. Pohl**[2], **and M. Weidemüller**[1,3]

[1] *Physikalisches Institut, Universität Heidelberg, Im Neuenheimer Feld 226, 69120 Heidelberg, Germany*
[2] *Department of Physics and Astronomy, Aarhus University, Ny Munkegade 120, 8000 Aarhus C, Denmark*
[3] *Hefei National Laboratory for Physical Sciences at the Microscale, Shanghai Branch, and CAS Center for Excellence and Synergetic Innovation Center in Quantum Information and Quantum Physics, University of Science and Technology of China, Shanghai 201315, China*
e-mail: *hainaut@physi.uni-heidelberg.de*

The strong light-matter coupling of a Rydberg gas under Electromagnetically Induced Transparency (EIT) conditions enabled the realization of strong effective photon-photon interaction [1] leading to high nonlinearities at the single photon level. These high single photon nonlinearities are keys element for the development of fully deterministic all-optical quantum information processing [2] such as single-photon switches and all optical quantum logic gates. Here we present a new way to enhance the nonlinearities in a Rydberg-EIT medium using Rydberg dressing conditions [3].

We consider a cold atomic cloud on two-photon resonance with a strong coupling beam (Rabi frequency : Ω), addressing a Rydberg state, and a weak probe beam (Rabi frequency : Ω_p) addressing a short lived excited state. Under these conditions, the medium becomes fully transparent to the probe beam as a consequence of destructive quantum interference, revealing the so called EIT phenomenon [4]. Rydberg-Rydberg interaction have the ability to shift out the atoms from two-photon resonance, breaking thus the EIT conditions. As a result, when the population of Rydberg atoms increases in the medium, the transmission decreases accordingly. The Rydberg-Rydberg interaction induces a nonlinear absorption in the medium which follows, for small Ω_p, the expression :

$$-\ln T = \alpha\chi^{(3)}\Omega_p^2, \qquad (1)$$

with T the transmission of the medium, α a constant depending of the system and $\chi^{(3)}$ the imaginary part of the nonlinear electrical susceptibility which is linked to the Rydberg-Rydberg interaction [1].

Solving the Maxwell-Bloch equations including the short lived exited state with a perturbation expansion of the probe field up to the third order allows us to capture and investigate the effect of the resonant dressing on the transmission of the probe beam. The purple curve in fig 1 depicts the transmission for the resonant dressing condition $= \Omega$ as a function of the probe Rabi frequency Ω_p. Realizing a quadratic fit of this curve and using the equation 1 allows us to extract the system nonlinear susceptibility which is $\chi^{(3)}_{\mathrm{rd}} = 1.7 \cdot 10^{-5}$ m^2/V^2. This value has to be compared with the single photon resonant case, represented by the blue curve in fig 1, giving us $\chi^{(3)}_0 = 5.6 \cdot 10^{-6}$ m^2/V^2. For the resonant dressing condition $= \Omega$, the medium's nonlinearity is enhanced.

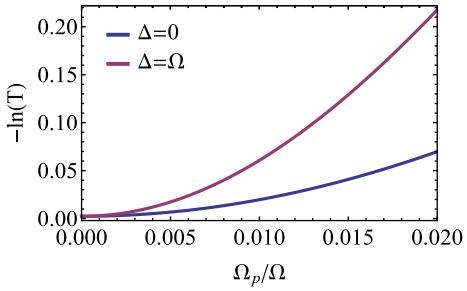


Figure 1: Transmission of the probe beam as a function of the probe Rabi frequency for two different single photon detuning.

In order to spotlight the resonant effect, we also investigate the transmission of the probe beam as a function of $\Omega/$ in figure 2. We observe an enhanced absorption due to an increasing of the nonlinear effects around the resonant dressing condition $\Omega/ = 1$.

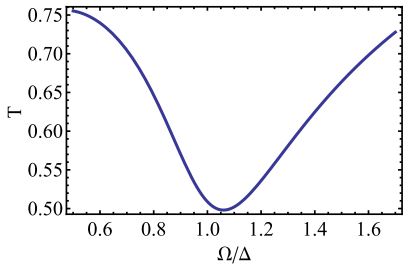


Figure 2: Transmission of the probe beam as a function of Ω/Δ.

[1] C R. Murray *et al.* Advances in Atomic, Molecular, and Optical Physics **65** 321-372 (2016)

[2] J D. Pritchard *et al.* Annual Review of Cold Atoms and Molecules **1** 301-350 (2012)

[3] C. Gaul *et al.* Phys. Rev. Lett. **116** 243001 (2016)

[4] M. Fleischhauer *et al.* Reviews of modern physics 77, 633. (2005)

Rydberg optical Feshbach resonances in cold gases

Rosario González-Férez[1], **Nóra Sándor**[2], **Paul S. Julienne**[3] **and Guido Pupillo**[2]

[1] *Instituto Carlos I de Física Teórica y Computacional and Departamento de Física Atómica, Molecular y Nuclear, Universidad de Granada, 18071 Granada, Spain*

[2] *icFRC, IPCMS (UMR 7504) and ISIS (UMR 7006), University of Strasbourg and CNRS, 67000 Strasbourg, France*

[3] *Joint Quantum Institute, University of Maryland and NIST, College Park, Maryland 20742, USA*

e-mail: *rogonzal@ugr.es*

In this work, we present a new scheme, sketched in Fig. 1, to e ciently tune the scattering length of two colliding ground-state atoms by off-resonantly coupling the scattering-state to an excited Rydberg-molecular state using laser light [1].

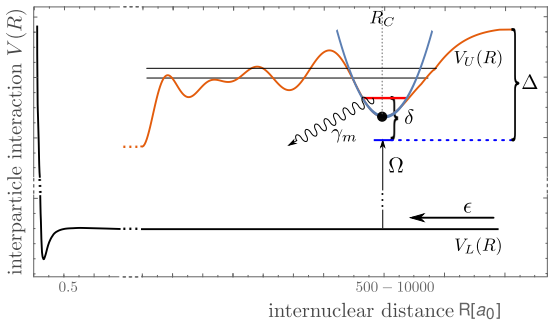


Figure 1: Sketch of a Rydberg optical Feshbach resonance. Figure taken from Ref. [1].

The collision of two ground-state atoms in the light field is treated as an effective three-channel scattering problem. The entrance channel is the two atoms in a s-wave scattering state of the ground-state electronic potential $V_L(R)$ with relative energy ϵ, see Fig. 1. One atom is ^{87}Rb($5S_{1/2}$), whereas the other one could be another alkali metal. The excited channel is a bound state of the adiabatic electronic potential $V_U(R)$ of the Rydberg molecule [2] formed by an excited rubidium, Rb($nS_{1/2}$), and a ground-state atom. The ultralong-range Rydberg molecule is formed due to the low-energy scattering of the Rydberg-electron with the ground-state atom [2]. The spontaneous-decay product represents the third channel. The laser light couples off-resonantly the scattering state and the bound vibrational state with Rabi frequency Ω and red detunings δ and from the molecular resonance and the atomic Rydberg energy, respectively, see Fig. 1. The minima R_b in these ultralong-range potentials is at distances $R_b \sim 10^3 - 10^4 a_0$, much larger than for usual optical Feshbach resonances.

For the s-wave scattering of two colliding ^{87}Rb atoms, we demonstrate that the effective optical length and pole strength of this Rydberg optical Feshbach resonance can be tuned over several orders of magnitude, while incoherent processes and losses are minimized [1]. Useful resonances are those for which the ratio of the real and imaginary parts of the scattering length is much larger than one, while the real part differs significantly from the background scattering length $\alpha_{\rm bg}$. Figure 2 shows that these conditions are fulfilled for a broad range of parameters with Rb atoms.

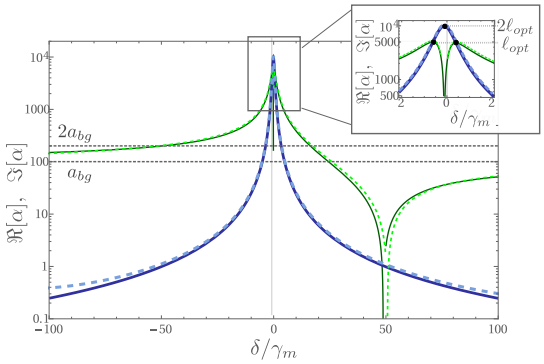


Figure 2: Real (green) and imaginary (blue) parts of the scattering length versus the detuning δ from the lowest-lying molecular states of Rb($27S_{1/2}$)Rb($5S_{1/2}$) and $\Omega/(2\pi) = 0.5$ MHz. The ground-state Rb atoms collide with relative energy $\epsilon = 1\mu K \cdot k_B$. Solid lines: analytical predictions, and dashed lines: coupled channel calculations. This figure is taken from Ref. [1].

The Rydberg molecular states have long lifetimes and are present for atomic species having a negative scattering length for the electron-atom collision [2], thus, the Rydberg optical Feshbach resonances can be applicable to a atoms that do not enjoy magnetic Feshbach resonances.

[1] N. Sándor, R. González-Férez, P. S. Julienne, and G. Pupillo, Phys. Rev. A. **96**, 032719 (2017).

[2] C. H. Greene, A. S. Dickinson, and H. R. Sadeghpour, Phys. Rev. Let. **85**, 2458 (2000).

Electronic Structure of the Rydberg Triatomic Molecule: K(nl)-KRb(νN)

Rosario González-Férez[1], **Seth T. Rittenhouse**[2], **Peter Schmelcher**[3,4] **and H. R. Sadeghpour**[5]

[1] *Instituto Carlos I de Física Teórica y Computacional and Departamento de Física Atómica, Molecular y Nuclear, Universidad de Granada, 18071 Granada, Spain*

[2] *Department of Physics, The Naval Academy, Annapolis, Maryland 21402, USA*

[3] *Zentrum für optische Quantentechnologien, Universität Hamburg*

[4] *The Hamburg Centre for Ultrafast Imaging, Universität Hamburg, Luruper Chaussee 149, 22761 Hamburg, Germany*

[5] *ITAMP, Harvard-Smithsonian Center for Astrophysics 60 Garden St., Cambridge, Massachusetts 02138, USA*

e-mail: *rogonzal@ugr.es*

An exotic type of ultralong-range Rydberg molecules are theoretically predicted to exist if a heteronuclear diatomic molecule, a Λ-doublet or a rotating polar molecule, is immersed into the wave function of a Rydberg atom [1, 2, 3, 4]. The anisotropic scattering of the Rydberg electron from the permanent electric dipole moment of the polar molecule is responsible for the binding mechanism in these Rydberg molecules.

In this work, we explore the electronic structure of ultralong-range triatomic Rydberg molecules formed from a potassium Rydberg atom and the ground-state heteronuclear diatomic molecule KRb. A qualitative sketch of this Rydberg molecule is shown in figure 1. Our focus is on the interaction of K(nl) and K($n > 40$, $l \geq 3$) Rydberg states with ground and rotationally excited KRb diatomic polar molecules.

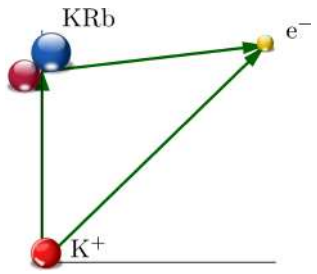


Figure 1: A sketch (not to scale) of the triatomic molecule formed by the Rydberg atom potassium K and a diatomic polar molecule KRb.

We investigate the metamorphosis of the Born-Oppenheimer potential curves, essential for the binding of the molecule, with varying distance of the KRb molecule from the Rydberg core. These electronic states show many consecutive minima with depths of a few GHz or a few MHz depending if they evolve from the Rydberg degenerate manifold or from the Rydberg states with low orbital angular momentum [1, 4]. In both cases, we find vibrational bound states, where these Rydberg molecule could exist.

These molecules could be created by exciting Rydberg atoms, using standard two-photon excitation schemes, in a mixture of ultracold atoms and ultracold molecules, i.e., molecules as K(nS)-KRb or K(nD)-KRb would be created experimentally. Due to the coupling mechanism between the Rydberg atom and the polar molecule, we have found adiabatic electronic states evolving from the Rydberg degenerate manifold with a significant contribution from a low angular momentum Rydberg state. These mixed electronic states are a few GHz deep and have several vibrational bound states, being then good candidates to be created experimentally [5]. The large charge separation between the Rydberg core and the diatomic molecule gives rise to huge permanent dipole moments scaling as n^2. Within these adiabatic electronic states of K-KRb, we have encountered vibrational bound states having permanent dipole moments of a few kilo-Debye. Finally, we also analyze the orientation and alignment of the KRb molecule within the adiabatic potential curves of the triatomic Rydberg molecule.

[1] S.T. Rittenhouse and H.R. Sadeghpour, Phys. Rev. Lett. **104**, 243002 (2010).

[2] S.T. Rittenhouse, M. Mayle, P. Schmelcher and H.R. Sadeghpour, J. Phys. B **44**, 184005 (2011).

[3] M. Mayle, S.T. Rittenhouse, P. Schmelcher and H.R. Sadeghpour, Phys. Rev. A **85**, 052511 (2012).

[4] R. González-Férez, H.R. Sadeghpour and P. Schmelcher, New J. Phys. **17**, 013021 (2015).

[5] R. González-Férez, S. T. Rittenhouse, P. Schmelcher, and H.R. Sadeghpour, preprint (2018).

Coherent Control of Addressable Rydberg Atoms for Hybrid Quantum Information Processing

C. J. Picken, R. Legaie, K. McDonnell, and J. D. Pritchard
Department of Physics and SUPA, University of Strathclyde, Glasgow G4 0NG, United Kingdom
e-mail: *jonathan.pritchard@strath.ac.uk*

Neutral atoms provide an excellent resource for quantum information processing, combining the long atomic coherence times of the hyperfine ground-state with strong dipole-dipole interactions of highly excited Rydberg states for generating deterministic entanglement between qubits separated by < 10 μm [1]. Scalable long-range interactions can be obtained by coupling the atomic array to a superconducting microwave cavity enabling hybrid quantum information processing where the cavity-mediated entanglement allows atoms to be coupled over cm length scales.

We present the first steps towards such an experiment incorporating high fidelity readout using an sCMOS camera [2] and the ability to drive fast, optically addressable rotations of the hyperfine-encoded qubits to the Rydberg state. Using our sub-kHz cavity-stabilised laser system [3] we demonstrate coherent control of single Rydberg atoms, performing Ramsey spectroscopy to determine coherence time and to generate entanglement between a pair of atoms separated by 6 μm. Combining this excitation scheme with our ground-state Raman lasers we show progress towards the implementation of a mesoscopic Rydberg gate based on electromagnetically induced transparency (EIT) offering robust entanglement of multi-atom ensembles [4].

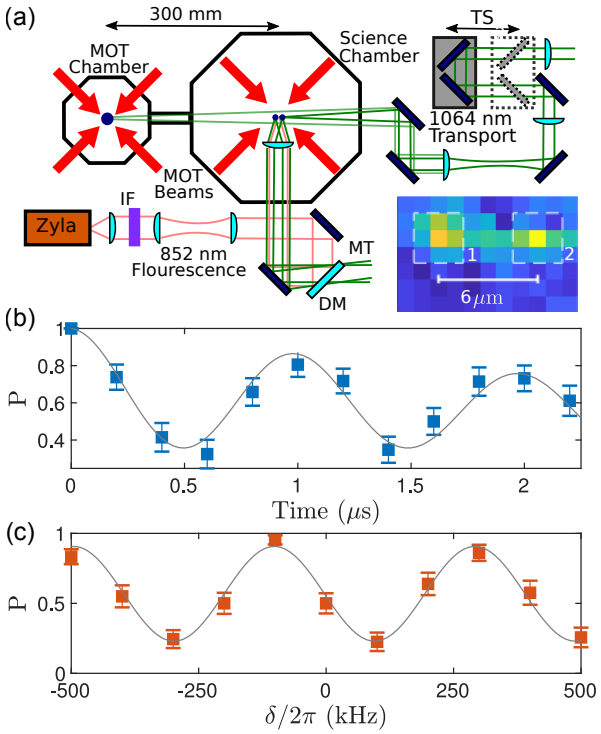


Figure 1: (a) Cs atoms loaded in microscopic tweezer traps separated by 6 μm (b) Single atom Rabi oscillation to $50S_{1/2}$ Rydberg states. (c) Ramsey fringes showing coherent evolution for $T = 2$ μs.

[1] M. Saffman, T. Walker, and K. Mølmer, Rev. Mod. Phys. **82**, 2313 (2010).

[2] C. J. Picken *et al.*, Appl. Phys. Lett. **111**, 164102 (2017).

[3] R. Legaie *et al.*, J. Opt. Soc. Am. B **35**, 892 (2018).

[4] M. Müller *et al.*, Phys. Rev. Lett. **102**, 170502 (2009).

Light-matter interface using cold-atoms coupled to hollow-core fiber

M. Noaman[1], **M. Langbecker**[1], **R. Wirtz**[1], **C. Voss**[1], **P. Islam**[1], **W. Li**[1,2], **S. Banerjee**[1,3] **and P. Windpassinger**[1]

[1]*Institute of Physics, Johannes Gutenberg University, Mainz, Germany*

[2]*School of Instrumentation Science and Opto-electronics engineering, Beihang University, Beijing 100191, P.R. China*

[3]*Indian Institute of Science, Bangalore 560012, India*

e-mail: *monoaman@uni-mainz.de*

Strong light-matter interaction is one of the most important starting points for quantum computation, quantum information or quantum sensing. Among the various existing options like quantum dots, neutral atoms or ions coupled to cavity system, cold-atoms coupled to hollow-core fiber has drawn considerable attraction in the recent times. Combined with the strong and long-range interactions of Rydberg atoms, we present a novel Rydberg atom-fiber system and our progress towards creating photon-photon interaction.

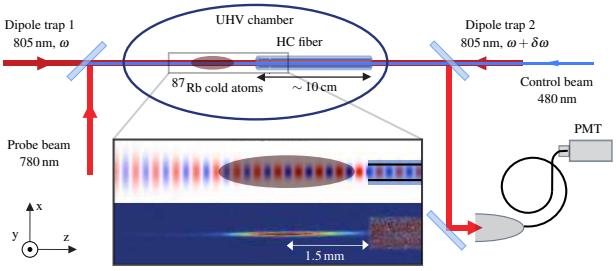


Figure 1: Schematic of the experimental setup taken from [3]. The main part shows a sketch of the vacuum system with the relevant beam paths. The inset shows a sketch of the potential profile of the movable optical lattice (not to scale) and an absorption image of cold atoms close to the fiber tip.

Our experimental setup consists of cold-atoms trapped and transported using an optical lattice where the lattice beams pass through a hollow-core fiber placed inside the vacuum chamber as shown in Figure 1. The high degree of control we have allows us to precisely move the atoms close to or inside the fiber [2]. A probe beam is overlapped with the optical-lattice beams and thus passes through the atoms creating strongly interacting light-matter interface. Due to the confinement provided by the hollow-core fiber, the overlap is not limited to the free-space Rayleigh range and can extend to several centimeters. In such confined geometries, we have successfully been able to excite the cold atoms to Rydberg states via three level electro-magnetically induced transparency (EIT) [1]. Within the parameter space given by our experimental control, the atomic ensemble induces significant lensing which results in highly asymmetric transmission line shapes when detected on single-mode fiber coupled sensor. We also present our model to understand the propagation of a weak probe beam through the confined atomic ensemble as shown in Figure 2. With the strong agreement between the data and the model, we further analyse the line shapes involving Rydberg EIT process [3].

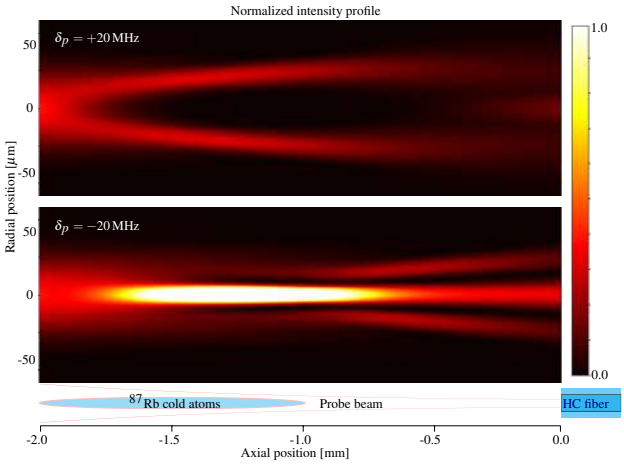


Figure 2: Micro lensing induced intensity profiles taken from [3] for positive and negative detunings of the probe beam. The schematic indicates the position of the atomic cloud and fiber as used in the calculations.

[1] M. Langbecker, M. Noaman, N. Kjærgaard, F. Benabid and P. Windpassinger, Phys. Rev. A **96**, 041402 (2017).

[2] M. Langbecker, R. Wirtz, F. Knoch, M. Noaman, T. Speck and P. Windpassinger, arXiv: 1805.06333 (2018)

[3] M. Noaman, M. Langbecker and P. Windpassinger, arXiv: 1805.11391 (2018)

van der Waals interactions of Rydberg particles near surfaces

J. Block[1] **and S. Scheel**[1]
[1] *Institut für Physik, Universität Rostock, 18059 Rostock, Germany*
e-mail: *johannes.block@uni-rostock.de*

Rydberg systems experience strong van der Waals interactions due to their large transition dipole moments. As these interactions are mediated by photons, they are altered by dielectric surroundings. In order to understand the nature of these changes, we calculate the interaction potentials between Rydberg atoms in front of a perfectly conducting mirror including terms up to electric quadrupole moments[1, 2]. We nd that the presence of the mirror strongly modi es the interactions leading to a signi cant change in the Rydberg blockade [3]. These considerations apply similarly when describing Rydberg excitons in nite thickness crystals. Our results show the importance of the correct description of the dielectric surroundings in the calculations of excitonic interactions.

[1] J.S. Cabral *et al.*, J. Phys. B: At. Mol. Opt. Phys. **44**, 184007 (2011).

[2] J. Stanovevic *et al.*, Phys. Rev. A **78**, 082709 (2008).

[3] J. Block and S. Scheel, Phys. Rev. A **96**, 062509 (2017)

Rydberg-Dressed Magneto-optical Trap

N.C Jackson, R.K, Hanley, A.D. Bounds, P. Huillery and M.P.A. Jones
Joint Quantum Centre Durham-Newcastle, Durham University, Durham, UK
e-mail: *n.c.keegan@durham.ac.uk*

The strong dipolar interactions between Rydberg atoms have been exploited to perform numerous experimental studies of interacting many-body systems. A promising approach to create an interacting many-body quantum gas with tunable interactions is to off-resonantly couple a low-lying atomic state to a Rydberg state [1, 2]. It has been shown that this so-called Rydberg dressing approach could facilitate the formation of interesting states of matter, such as supersolids [3, 4]. Recently, experimental work has demonstrated the tunability of the Rydberg-dressed interaction in optical lattices [6, 5], however the effect of these interactions in a randomly distributed ensemble are yet to be observed.

Our recent work [7] presents a novel Rydberg-dressing scheme using a strontium magneto-optical trap. Here we off-resonantly couple the excited state of a narrow (7 kHz) cooling transition to a high-lying Rydberg state. We show that the Rydberg dressed atoms are trapped, while undergoing active cooling to sub-μK temperatures. Furthermore, the atoms acquire the properties of the Rydberg state, such as enhanced sensitivity to DC electric fields. The experimental results are supported by a quantitative Monte-Carlo model of the MOT.

Currently the achievable density and interaction strengths are limited by the dressing beam profile, which can easily be overcome in future experiments. As such, our work represents a method in which to combine active laser cooling and trapping with the long-range interaction between Rydberg states.

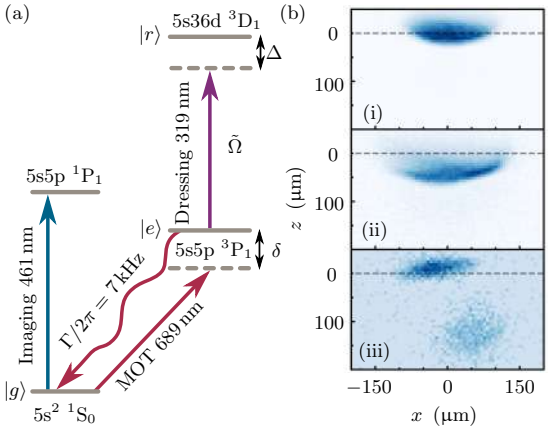


Figure 1: (a) Dressing scheme: A MOT operating on the 689 nm intercombination transition is dressed by off-resonantly coupling state $|e\rangle$ to a Rydberg state $|r\rangle$. The strong 461 nm transition is used for imaging. (b) (i) MOT image in the absence of the coupling laser with a MOT beam detuning of 110 kHz. (ii-iii) MOT image in the presence of the coupling beam with 4 MHz Rabi frequency and MOT beam detuning of −110kHz and +190kHz respectively. The presence of the coupling beam causes an AC Stark shift of the MOT transition. If the MOT beam detuning remains unchanged (ii), the MOT moves to a lower position. By compensating the AC Stark shift (iii), the atoms remain in the coupling beam resulting in a functioning dressed MOT.

[1] L. Santos, G. V. Shlyapnikov, P. Zoller, and M. Lewenstein, Phys. Rev. Lett. **85**, 1791 (2000).

[2] I. Bouchoule and K. Mølmer, Phys. Rev. A **65**, 041803(R) (2002).

[3] N. Henkel, R. Nath, and T. Pohl, Phys. Rev. Lett. **104**, 195302 (2010).

[4] G. Pupillo, A. Micheli, M. Boninsegni, I. Lesanovsky, and P. Zoller, Phys. Rev. Lett. **104**, 223002 (2010).

[5] Y.-Y. Jau, A. M. Hankin, T. Keating, I. H. Deutsch and G. W. Biedermann, Nat. Phys. **12**, 71-74 (2016).

[6] J. Zeiher, R. van Bijnen, P. Schauß, S. Hild, J.-y. Choi, T. Pohl, I. Bloch and C. Gross. Nat. Phys. **12**, 10951099 (2016).

[7] A.D. Bounds, N.C. Jackson, R.K. Hanley, R. Faoro, E.M. Bridge, P. Huillery, and M.P.A. Jones, Phys. Rev. Lett. **120**, 183401 (2018).

[8] L.I.R. Gil, R. Mukherjee, E.M. Bridge, M.P.A. Jones, and T. Pohl, Phys. Rev. Lett. **112**, 103601 (2014).

Rydberg-mediated long-range interactions between stored optical photons

T.Ilieva, N. L. R. Spong, S. W. Ball, H. Busche, P. Huillery, M. P. A. Jones, and C. S. Adams
Joint Quantum Centre (JQC) Durham-Newcastle, Department of Physics, Durham University, South Road, Durham, DH1 3LE, United Kingdom

Rydberg non-linear optics [1] has emerged as a viable approach to induce strong effective photon-photon interactions, e.g. for applications in optical quantum information processing. Using electromagnetically induced transparency and photon storage, the μm-ranged dipolar interactions between collective Rydberg excitations can be mapped onto photons. So far, experiments focussed on observing Rydberg-mediated photon interactions between overlapping modes within a single cold atomic medium [1]. Recently however, we have demonstrated an effective 'contactless' interaction between photons stored in spatially separate atomic ensembles and propagating in non-overlapping modes [2]. During storage, van-der-Waals interactions between the excitations alter the phase relation between the individual atoms contributing to the collective state. As the phase shifts are spatially non-uniform, retrieval of the photons in their original mode is suppressed. By analysing the statistics of the retrieved photons, we observe how the interaction varies while changing the distance between media (Fig. 1), the Rydberg state employed for storage, and the interaction time.

The stored photons can be coherently controlled using an additional microwave field which drives transitions between Rydberg states. The microwave field causes high-fidelity Rabi oscillations and can be used to shape the temporal mode of the retrieval pulse [3]. The degrees of freedom provided by contactless, long-range effective interactions between stored photons combined with microwave control of their state and phase may lead towards a Rydberg-based all-optical quantum gate [4] and applications in quantum simulation.

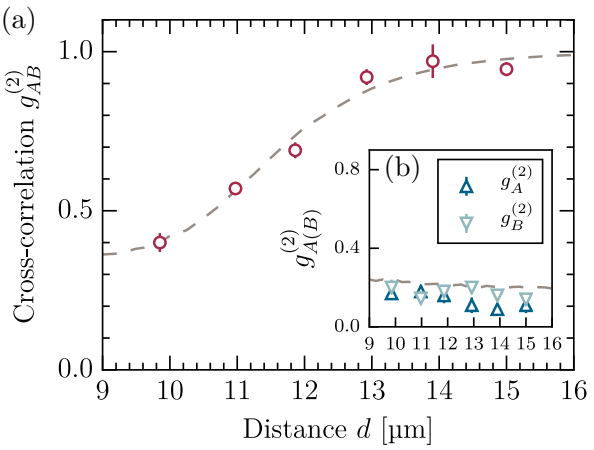


Figure 1: (a) The effect of 'contactless' Rydberg-mediated photon interactions can be observed as an anti-correlation ($g^{(2)}_{AB} < 1$) between channel A and B in the retrieval. (b) Rydberg-mediated interactions also lead to the retrieval of highly non-classical light in the individual channels as indicated by the suppression of the single channel ($g^{(2)}_{A(B)} < 1$).

References

[1] O. Firstenberg, C. S. Adams, and S. Hofferberth, J. Phys. B, **49**, 15 (2016).

[2] H. Busche, P. Huillery, S. W. Ball, T. Ilieva, M. P. A. Jones, and C. S. Adams, Nat. Phys., **13**, 655 (2017).

[3] S. W. Ball *et al.*, in preparation.

[4] D. Paredes-Barato and C. S. Adams, Phys. Rev. Lett., **112**, 040501 (2014).

Rydberg excitation of a Bose-Einstein condensate and Mott insulator with a picosecond laser pulse

M. Mizoguchi[1,2], **A. Tanaka**[1], **N. Takei**[1,2], **Y. Zhang**[1,3], **S. Takeda**[1,2], **K. Koyasu**[1,2], **H. Chiba**[4,1], **T. Kishimoto**[5,1], **G. Pupillo**[6], **D. Jaksch**[7,8], **M. Kiffner**[8,7], **A.W. Glaetzle**[8,7], **J. Schachenmayer**[6], **G. Masella**[6], **M. Weidemüller**[9], **and K. Ohmori**[1,2]

[1] *Institute for Molecular Science, National Institutes of National Sciences, Myodaiji, Okazaki 444-8585, Japan*

[2] *SOKENDAI (The Graduate University for Advanced Studies), Myodaiji, Okazaki 444-8585, Japan*

[3] *Institute of Laser Spectroscopy, Shanxi University, Taiyuan, 030006 Shanxi, China*

[4] *Iwate University, 4-3-5 Ueda, Morioka 020-8551, Japan*

[5] *Department of Engineering Science and Institute for Advanced Science, The University of Electro-Communications, 1-5-1 Chofugaoka, Chofu 182-8585, Japan*

[6] *IPCMS (UMR 7504) and ISIS (UMR 7006), University of Strasbourg and CNRS, 67000 Strasbourg, France*

[7] *Clarendon Laboratory, University of Oxford, Parks Road, Oxford, OX1 3PU, United Kingdom*

[8] *Centre for Quantum Technologies, National University of Singapore, 3 Science Drive 2, 117543, Singapore*

[9] *Physikalisches Institut, Universität Heidelberg, Im Neuenheimer Feld 226, 69120 Heidelberg, Germany*

e-mail: *mizoguchi@ims.ac.jp*

We have generated a strongly correlated ultracold Rydberg gas by broadband picosecond pulsed-laser excitation of a disordered ensemble of ^{87}Rb atoms in an optical dipole trap and established the method to observe and control its ultrafast many-body electron dynamics [1–4]. We are now applying this method to an ordered system and developing an "ultrafast quantum simulator" that simulates many-body electron dynamics within a nanosecond (Figure 1). It would allow us to uncover more precise many-body dynamics hidden behind averaging over a disordered ensemble in the optical dipole trap.

In order to generate an ordered system, first we generate a Bose-Einstein condensate (BEC) and then load it into a 3D optical lattice to create a unit-filling Mott insulator with one atom per each lattice site. In the present poster we will introduce our new experimental systems and present ultrafast electron dynamics after the Rydberg excitation of a BEC and a unit-filling Mott insulator with a broadband picosecond laser pulse.

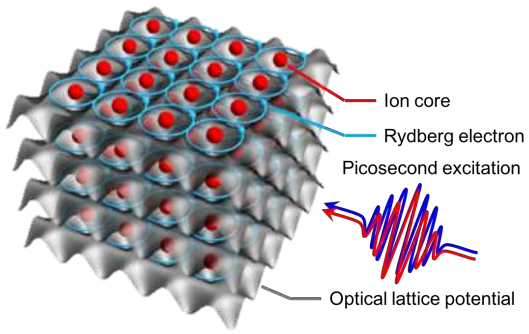


Figure 1: Schematic of ultrafast quantum simulator.

We thank C. Sommer, S. Whitlock, and J. Ye for fruitful discussions. This work has been partly supported by JSPS Grant-in-Aid for Specially Promoted Research, CREST-JST, and Photon Frontier Network program by MEXT. K.O. thanks Alexander von Humboldt foundation, University of Heidelberg, and University of Strasbourg for supporting this international collaboration.

[1] N. Takei, C. Sommer *et al.* Direct observation of ultrafast many-body electron dynamics in an ultracold Rydberg gas. *Nat. Commun.* **7**, 13449 (2016).

[2] C. Sommer *et al.* Time-domain Ramsey interferometry with interacting Rydberg atoms. *Phys. Rev. A* **94**, 053607 (2016).

[3] K. Ohmori. Optically engineered quantum states in ultrafast and ultracold systems. *Found. Phys.* **44**, 813 (2014).

[4] H. Katsuki *et al.* Ultrafast coherent control of condensed matter with attosecond precision. *Acc. Chem. Res.* **51**, 1174 (2018).

Study of light storage with Rydberg-state electromagnetically-induced-transparency in cold rubidium atoms

Bongjune Kim[1], **Ko-Tang Chen**[1], **Chia-Yu Hsu**[1],**Yu-Chih Tseng**[1], **Chin-Yuan Lee**[1], **Shih-Lun Liang**[1], **Yi-Hua Lai**[1], **Yong-Fan Chen**[2,4], **Ying-Cheng Chen**[3,4] **and Ite A. Yu**[1,4]

[1]*Department of Physics, National Tsing Hua University, Hsinchu 30013, Taiwan*

[2]*Department of Physics, National Cheng Kung University, Tainan 70101, Taiwan*

[3]*Institute of Atomic and Molecular Sciences, Academia Sinica, Taipei 10617, Taiwan*

[4]*Center for Quantum Technology, Hsinchu 30013, Taiwan*

e-mail: *upfe11@gmail.com*

Employing strong dipole-dipole interaction between the Rydberg-state atoms can greatly enhance the nonlinear susceptibility of photon-photon interaction via the effect of electromagnetically-induced -transparency (EIT). Further enhancement of interaction strength can be achieved with the interaction time being increased during the light storage. We will present our experimental study of light storage with the Rydberg-EIT transition scheme. The transition from the ground state $|5S_{1/2}, F = 2\rangle$ to the intermediate state $|5P_{3/2}, F = 3\rangle$ is driven by a weak probe field, and that from the intermediate state to the Rydberg state $|30D_{5/2}\rangle$ is driven by a strong coupling field. This work is toward the realization of high conversion e ciency from the input probe pulse to the Rydberg coherence.

Quantum Simulation of Energy Transport with Rydberg atoms

Sayali Shevate[1], **Tobias Wintermantel**[1,2], **Yibo Wang**[1], **S. Wüster**[3] **and S. Whitlock**[1,2]

[1] *IPCMS (UMR 7504) and ISIS (UMR 7006), Universitè de Strasbourg and CNRS, 67000 Strasbourg, France*

[2] *Physikalisches Institut, Universität Heidelberg, Im Neuenheimer Feld 226, 69120 Heidelberg*

[3] *Department of Physics, Indian Institute of Science Education and Research, Bhopal, Madhya Pradesh 462 023, India*

e-mail: *shevate@ipcms.unistra.fr*

Ultracold atoms excited to Rydberg states possessing strong electric dipole moments provide a unique platform for studying quantum dynamics with fully-programmable interactions. This would open a path to simulating key molecular and chemical processes extending far beyond atomic physics. In this poster, we will discuss a novel experimental system (sketched in figure 1) that provides control over the spatial geometry, long range interactions far beyond nearest neighbours and nontrivial system-bath interactions. This will be achieved using individual atoms in microoptical traps which are coherently coupled to two different Rydberg states possessing strong and long range Förster-type interactions. This will be combined with control over the trapping geometries using digital micromirror devices and stroboscopic interaction control and tailored environmental noise using fast acousto-optical defectors for the dressing lasers.

As a specific application, we aim to study how excitations migrate through quantum many-body systems possessing non-trivial correlations and how spatially and temporally correlated noise can enhance the robustness and e ciency of energy transport in synthetic quantum systems. Finding out which underlying properties of the system lead to the most efficient or robust transport, especially in the presence of quantum coherence and correlated noise has immediate relevance to the function of complex molecules (e.g. light harvesting complexes like LH II shown in figure 2). More broadly, the achievement of fully-programmble quantum systems based on Rydberg dressed atomic ensembles could enable breakthroughs in diverse applications of atomic physics, including quantum simulation and quantum computation, quantum matter, quantum networks and quantum chemistry.

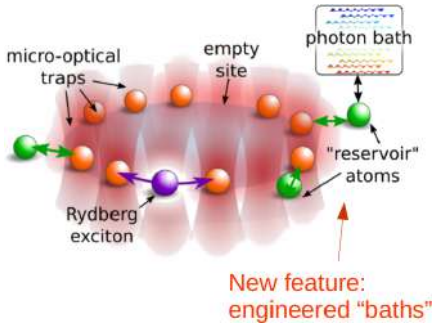


Figure 1: Artificial Atomic Model of LH II

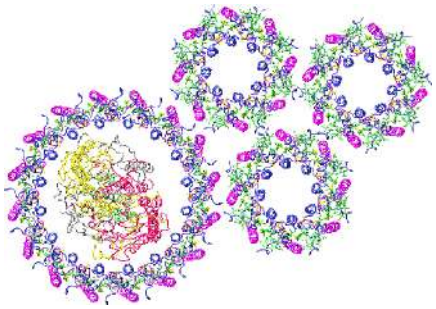


Figure 2: LH II (Light Harvesting Complex in nature)

Stability study of the two-photon detuning using the Rydberg-EIT spectrum of laser-cooled atoms

Ko-Tang Chen[1], **Chia-Yu Hsu**[1], **Yu-Chih Tseng**[1], **Bongjune Kim**[1], **and Ite A. Yu**[1]
[1] *Department of Physics, National Tsing Hua University, Hsinchu 30013, Taiwan*
e-mail: *asd6939937510@gapp.nthu.edu.tw*

Rydberg-state atoms induce strong dipole-dipole interaction and enhance photon-photon interactions as well. Therefore, Rydberg atom is a good candidate in the studies of quantum information science. One can transfer ground-state atoms to Rydberg-state atoms via two-photon electromagnetically-induced-transparency (EIT) transition. The stability of the two-photon detuning between EIT laser fields plays an important role in the Rydberg-EIT transition. We locked the sum frequency of two laser fields by the Pound-Drever-Hall technique, making fluctuation of the two-photon detuning of Rydberg-EIT transition less than 200 kHz. With this small fluctuation, we predict that the decoherence rate of the Rydberg polariton is about $2\pi \times 30$ kHz. This study shows the stability of two-photon resonance condition. This small decoherence rate will improve the transfer efficiency from ground-state atoms to Rydberg-state atoms.

Single shot non destructive photon counting of microwave photons using slow Rydberg atoms

Frédéric Assémat[1], **D. Grosso**[1], **S. Haroche**[1], **J.-M. Raimond**[1], **S. Gleyzes**[1], **and M. Brune**[1]
[1] *Laboratoire Kastler Brossel, Collège de France, CNRS, ENS-PSL Research University, UPMC-Sorbonne Universités, 11, place Marcelin Berthelot, 75231 Paris Cedex 05, France*
e-mail: *frederic.assemat@lkb.ens.fr*

Light detection is usually a destructive process as photons are detected with photosensitive materials that absorb them. However, there exist quantum non-destructive (QND) strategies [1] that permit repeated measurements on the same system yielding identical results. Those non destructive strategies have been for instance experimentally implemented for photon fluxes [2]. Yet, single photon resolution requires an extremely strong light-matter coupling. In the context of cavity quantum electrodynamics, it is possible to achieve QND measurement of the number of photons trapped in a microwave cavity made of two superconducting mirrors by using Rydberg atoms as probes. The presence of n photons induces a light shift of the atomic levels proportional to n, that can be read by Ramsey interferometry. By measuring this light shift for several atoms, information is progressively extracted and the field-state collapses on a given number of photons [3].

We have developed a new experiment where the atoms used for the QND measurement are beforehand prepared from the laser-cooled atomic beam of an atomic fountain. The small velocity of the atom allows us to reach interaction times between the field and the atom up to 100 times longer than before. This long interaction time makes it possible to spectrally resolve the individual light shifts corresponding to different photon numbers. It is thus possible to induce a transition of the atomic state only when the cavity contains exactly n_0 photons. This corresponds to a single shot measurement of n_0 , which can be confirmed by another measurement done immediately afterwards.

This direct measurement allows the preparation of Fock states, opening the way to the creation and manipulation of more general non classical states of the field. More precisely this set up can be used for the observation of interesting dynamics of the field, like quantum Zeno dynamics, where removing a single level from the accessible Hilbert space leads to the deterministic preparation of non-classical states such as Schrödinger cat states [4].

[1] V.B. Braginsky, Y.I. Vorontsov , "Quantum-mechanical limitations in macroscopic experiments and modern experimental technique", Physics-Uspekhi **17**, 644 (1975).

[2] P. Grangier et al. , "Observation of backaction-evading measurement of an optical intensity in a three-level atomic nonlinear system", Physical Review Letters **66**, 14182 (1991).

[3] C. Guerlin et al. , "Progressive field-state collapse and quantum non-demolition photon counting", Nature **448**, 889 (2007).

[4] J-M. Raimond et al. , "Quantum Zeno dynamics of a field in a cavity", Physical Review A **86**, 032120 (2012).

Interacting Rydberg ions

C. Zhang[1], **F. Pokorny**[1], **G. Higgins**[1], **A. Pöschl**[1] **and M. Hennrich**[1]
[1] *Department of Physics, Stockholm University, SE-106 91 Stockholm, Sweden*
e-mail: *chi.zhang@fysik.su.se*

Trapped Rydberg ions are a novel approach for quantum information processing [1]. By combining the high degree of control of trapped ion systems with the long-range dipolar interactions of Rydberg atoms [2], fast entanglement gates may be realised in large ion crystals [1, 3].

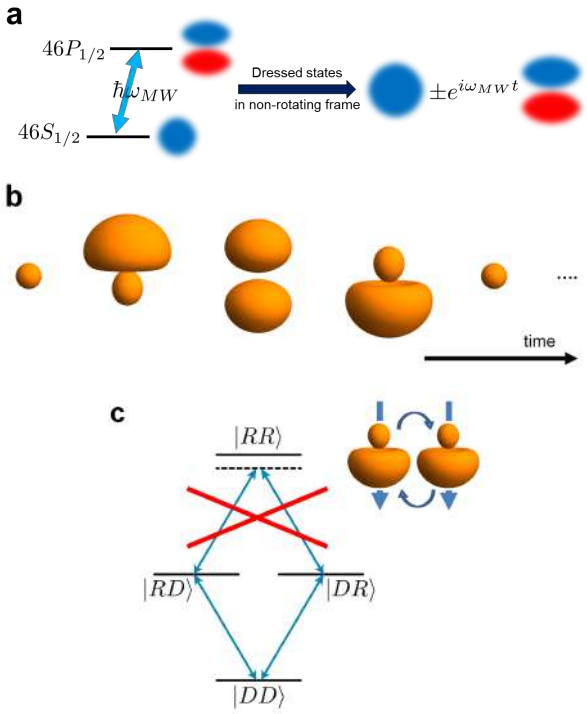


Figure 1: MW induced large oscillating dipole interaction. a. Two Rydberg states, $46S_{1/2}$ and $46P_{1/2}$, are coupled by the MW field, the eigenstates are the MW-dressed states. b. In the dressed states, the probability distribution of the Rydberg electron is oscillating in time, i.e., the electric dipole moment of the ion is oscillating. c. When two dipoles oscillate in phase, the dipole-dipole interaction shifts the energy level of two ions in Rydberg states $|RR\rangle$ so that they cannot be excited from $|DD\rangle$.

Strong interactions between Rydberg ions rely upon using microwave (MW) fields to introduce large rotating dipole moments to the Rydberg ions (Fig. 1). This requires a profound understanding of the properties of the MW-dressed states in the radio-frequency trap. In our experiment [4], we trap $^{88}Sr^{+}$ ions and coherently excite them to Rydberg states using two UV laser fields [5]. We have observed the Autler-Townes splitting in the MW field, and measured the lifetimes and polarizabilities of the MW-dressed states. Additionally, we recently measured strong interactions between two MW-dressed Rydberg ions in a Coulomb crystal. These are very fundamental steps towards a scalable trapped ion quantum computer.

[1] M. Müller, L. Liang, I. Lesanovsky and P. Zoller, New J. Phys. **10**, 093009 (2008).

[2] D. Jaksch, J. I. Cirac, P. Zoller, S. L. Rolston, R. Cote, and M. D. Lukin, Phys. Rev. Lett. **85**, 2208 (2000).

[3] F. Schmidt-Kaler, T. Feldker, D. Kolbe, J. Walz, M. Müller, P. Zoller, W. Li and I. Lesanovsky, New J. Phys. **13**, 075014 (2011).

[4] G. Higgins, W. Li, F. Pokorny, C. Zhang, F. Kress, C. Maier, J. Haag, Q. Bodart, I. Lesanovsky, and M. Hennrich, Phys. Rev. X **7**, 021038 (2017).

[5] G. Higgins, F. Pokorny, C. Zhang, Q. Bodart, and M. Hennrich, Phys. Rev. Lett. **119**, 220501 (2017).

Coherent control of a trapped Rydberg ion

G. Higgins[1], F. Pokorny[1], C. Zhang[1], Q. Bodart[1], F. Kress[2], C. Maier[2], J. Haag[2], W. Li[3], I. Lesanovsky[3] and M. Hennrich[1]

[1] *Department of Physics, Stockholm University, 106 91 Stockholm, Sweden*

[2] *Institut für Experimentalphysik, Universität Innsbruck, 6020 Innsbruck, Austria*

[3] *School of Physics and Astronomy, University of Nottingham, Nottingham, NG7 2RD, United Kingdom*

e-mail: *markus.hennrich@fysik.su.se*

Trapped Rydberg ions are a promising new approach to quantum information processing [1, 2]. This idea combines qubit encoding in the ions' ground states with entanglement operations via the Rydberg interaction. It promises to speed up entanglement operations and make them available in larger ion crystals.

In this presentation, we will report on our experimental results with trapped strontium Rydberg ions. In particular, we have recently mapped the population from ground state to the $42S_{1/2}$ Rydberg state and back using stimulated Raman adiabatic passage (STIRAP) [3] - to our knowledge the first observed coherently manipulated Rydberg excitation of an ion. Moreover, we will present our observation of fundamental trap effects due to the interaction of the Rydberg ion with the electric trapping field [4]. A solid understanding of these effects is essential for future applications in quantum information processing.

In the following step, we excite the ions to even higher Rydberg states and apply microwave radiation to induce large oscillating dipole moments. In this way, ions are able to interact at a distance as required for quantum gates via the Rydberg interaction.

[1] M. Müller, L. Liang, I. Lesanovsky and P. Zoller, New J. Phys. **10**, 093009 (2008).

[2] F. Schmidt-Kaler, T. Feldker, D. Kolbe, J. Walz, M. Müller, P. Zoller, W. Li and I. Lesanovsky, New J. Phys. **13**, 075014 (2011).

[3] G. Higgins, F. Pokorny, C. Zhang, Q. Bodart, and M. Hennrich, Phys. Rev. Lett. **119**, 220501 (2017).

[4] G. Higgins, W. Li, F. Pokorny, C. Zhang, F. Kress, C. Maier, J. Haag, Q. Bodart, I. Lesanovsky, and M. Hennrich, Phys. Rev. X **7**, 021038 (2017).

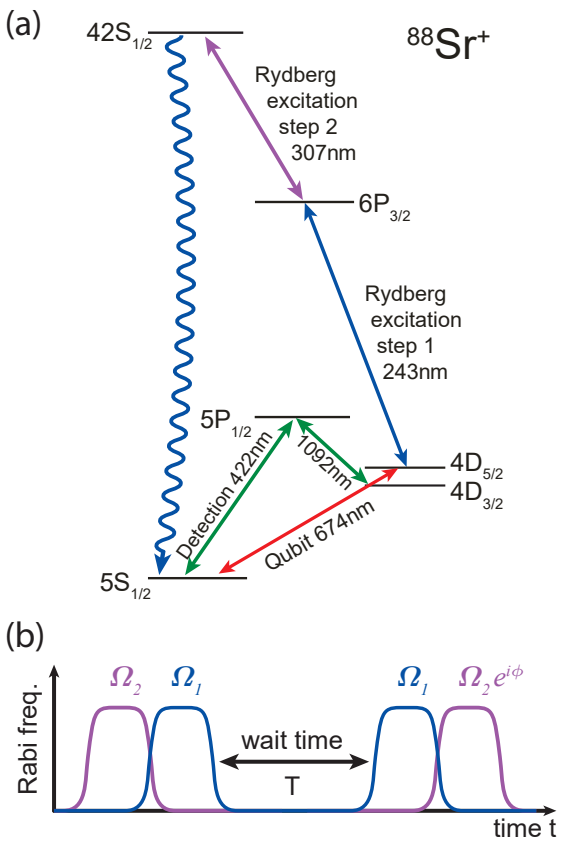


Figure 1: (a) Level scheme for coherent Rydberg excitation of strontium ions. Starting from the initial $4D_{5/2}$ state a two-photon excitation with 243 nm and 307 nm lasers brings the ion to the Rydberg state, from where it can decay predominantly back to the ground state $5S_{1/2}$. Successful Rydberg excitation is detected by the optical pumping to state $5S_{1/2}$. (b) The two Rydberg excitation lasers are applied in a counter-intuitive STIRAP pulse sequence to bring the ion coherently to the Rydberg state and back. By varying the waiting time, we can measure the population that remained in the Rydberg state and is then brought back to the initial state. This characterizes the lifetime of the Rydberg state in the ion trap.

Circular Rydberg Atoms as a Tool for Quantum Simulation

Rodrigo Cortiñas[1], **Thanh-Long Nguyen**[1], **Tigrane Cantat-Moltrecht**[1], **Clément Sayrin**[1], **Serge Haroche**[1], **Jean-Michel Raimond**[1], **Michel Brune**[1]

[1] *Laboratoire Kastler-Brossel, Collège de France, CNRS, ENS-Université PSL, Sorbonne Université, 11 place Marcelin Berthelot, 75005, Paris, France*

e-mail: *rodrigo.cortinas@lkb.ens.fr*

The main objective of quantum simulation is an in-depth understanding of many-body physics, which is important for fundamental issues and for the engineering of new materials. Analytic approaches to many-body systems are limited, and the huge size of their Hilbert space makes numerical simulations on classical computers intractable. A quantum simulator avoids these limitations by transcribing the system of interest into another, with the same dynamics but with its parameters under control and with experimental access to all relevant observables. Quantum simulation of spin systems is being explored with trapped ions, neutral atoms, and superconducting devices. We propose [1] a new paradigm for quantum simulation of spin-1/2 arrays, providing unprecedented flexibility and allowing one to explore domains beyond the reach of other platforms. It is based on laser-trapped circular Rydberg atoms. Their long intrinsic lifetimes, combined with the inhibition of their microwave spontaneous emission (Fig. 1) and their low sensitivity to collisions and photoionization, make trapping lifetimes in the minute range realistic with state-of-the-art techniques.

Ultracold defect-free circular atom chains can be prepared by a variant of the evaporative cooling method. This method also leads to the detection of arbitrary spin observables with single-site resolution. The proposed simulator realizes an XXZ spin-1/2 Hamiltonian, with nearest-neighbor couplings ranging from a few to tens of kilohertz. All the model parameters can be dynamically tuned at will, making a large range of simulations accessible. The system evolution can be followed over times in the range of seconds, long enough to be relevant for ground-state adiabatic preparation and for the study of thermalization, disorder, or Floquet time crystals.

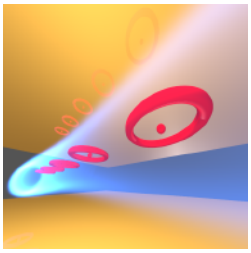


Figure 1: Artist's view of a laser-trapped circular atom chain inside a spontaneous emission-inhibiting capacitor.

[1] Nguyen T-L, *et al*, Phys. Rev. X **8** 011032 (2018).

Towards continuous-wave terahertz laser via optically pumped Rydberg states

Sambit B. Pal[1], **Mark Lam**[1], **Thibault Vogt**[1], **Christian Gross**[1], **and Wenhui Li**[1]
[1] *Centre for Quantum Technologies, National University of Singapore, 117543, Singapore*
e-mail: *cqtsbp@nus.edu.sg*

There have been intensive research activities to develop sources of coherent and high power radiations in the terahertz (THz) band, approximately from 100 GHz to 10 THz. However, compact, narrow-linewidth, and high-power THz sources are still lacking, especially in the range of 5-15 THz [1], despite tremendous advancements in technologies such as quantum cascade lasers [2], optically pumped lasers [3], and difference-frequency generation techniques [4]. The root of this challenge lies in the difficulty of finding suitable media that can e ciently provide strong electric dipole oscillators (be that classical or quantum) in this frequency range.

In this work, we propose a scheme which utilises atomic Rydberg states to generate coherent THz radiation. The energy gaps between adjacent Rydberg states (scaled as $\approx 1/n^3$) are typically in the range of THz frequencies for $n \leq 20$, and these states are strongly coupled to electromagnetic fields due to their large electric dipole moments (scales as $\approx n^2$). The level structure of our scheme is illustrated in Fig. 1, where two specific Rydberg levels shown are $^{10}D_{5/2}$ and $^{11}P_{3/2}$. We use two external cavity diode lasers (ECDL) to pump rubidium atoms, in a vapour cell heated slightly above the ambient room temperature, to the Rydberg state $^{10}D_{5/2}$ via an intermediate $^{5}P_{3/2}$ state. Due to the relatively long lifetime of the $^{10}D_{5/2}$ state and the highly favourable branching ratio for the $^{10}D_{5/2}$ to $^{11}P_{3/2}$ transition, moderately strong pumping creates a population inversion between the $^{10}D_{5/2}$ state and the lower lying $^{11}P_{3/2}$ state. This population inversion together with the large dipole moment leads to strong emission of 3.28 THz radiation. At certain detunings of the two input laser frequencies and large enough Rb-atom densities, the scheme evolves into a four-wave mixing process that simultaneously generates a coherent radiation at 3.28 THz as well as a deep-UV laser light at 311nm.

In addition to the particular energy states illustrated in Fig. 1, we also identify other suitable energy states of Rubidium atoms for generating coherent radiation at multiple discrete frequencies in the range of 3 THz - 13 THz, as shown in Tab. 1.

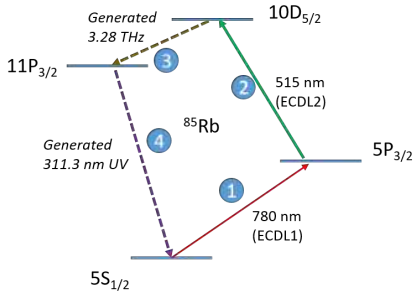


Figure 1: An illustration of the level structure of our coherent THz generation scheme

THz generation transition	Pump laser ECDL2 (nm)	Generated THz Radiation (THz)	Generated UV wavelength via FWM (nm)
$^{10}D_{5/2}$ to $^{11}P_{3/2}$	515.1	3.28	311.3
$^{9}D_{5/2}$ to $^{10}P_{3/2}$	526.1	4.84	315.8
$^{8}D_{5/2}$ to $^{9}P_{3/2}$	543.3	7.55	322.9
$^{7}D_{5/2}$ to $^{9}P_{3/2}$	572.6	12.81	334.9

Table 1: List of terahertz and deep-UV emission lines and respective pump laser wavelengths for Rubidium vapour

[1] S. S. Dhillon, M. S. Vitiello, E. H. Linfield, A. G. Davies, M. C. Hoffmann, J. Booske, C. Paoloni, M. Gensch, P. Weightman, G. P. Williams, *et. al.*, J. Phys. D: Appl. Phys. **50**, 043001 (2017).

[2] G. Liang, T. Liu and Q. J. Wang, IEEE J. Sel. Topics Quantum Electron **23**, 1-18, (2017)

[3] K. Zhong, W. Shi, D. Xu, P. Liu, Y. Wang, J. Mei, C.Yan, S. Fu and J. Yao, Sci. China Technol. Sci. **60**, 1801, (2017)

[4] Yujie J. Ding, J. Opt. Soc. Am. B **31**, 2696, (2014)

Rydberg Excitation of Lattice-trapped Ultra-cold Atoms on a Chip

A. Ramos[1], **J. de Hond**[2], **D. Davtyan**[2], **G. Raithel**[1], **R.J.C. Spreeuw**[2], **H.B. van Linden van den Heuvell**[2] **and N.J. van Druten**[2]

[1] *Physics Department, University of Michigan, Ann Arbor, MI, USA*

[2] *Van der Waals-Zeeman Institute, University of Amsterdam, Amsterdam, The Netherlands*

e-mail: *andramos@umich.edu*

Rydberg atoms are attractive candidates for quantum information because their interactions can be tuned by changing simple experimental parameters such as the principal quantum number [1]. However, when placed near conducting surfaces, Rydberg states can experience unwanted shifts due to their high sensitivity to electric fields [2]. Nonetheless, performing experiments on atom chips is advantageous due to their compactness. As a result, effort has been put into minimizing these undesired effects in atom chip systems (see, e.g. [3, 4] for recent work done at the University of Amsterdam). For the case of our system, (Ref. [3]), only an electric field gradient along the longitudinal direction of the atom-cloud remains.

The capability of doing spatially-selective addressing is needed for quantum information processing. Our goal is to use this electric-field gradient along a lattice-trapped, elongated cold-atom cloud of rubidium ($\sim 1\ \mu$K) to spatially select probing sites. The 860-nm optical lattice has been implemented to improve the confinement and eliminate the expansion along the axial direction, resulting in a linear array of traps. The position-dependent Stark shift on the Rydberg states caused by the existing electric-field gradient will be used to selectively excite Rydberg atoms along this array. In this poster, we discuss the 1D lattice implementation on the atom-chip system and the current experimental status.

References

[1] Saffman, M., Walker, T.G. and Mølmer, K. Quantum information with Rydberg atoms. Rev. of Mod. Phys., 82(3): 2313 (2010).

[2] Gallagher, T.F. Rydberg atoms. Cambridge University Press (2005).

[3] Cisternas, N., de Hond, J., Lochead, G., Spreeuw, R.J.C., van Linden van den Heuvell, H.B. and van Druten, N.J., 2017. Characterizing the local vectorial electric field near an atom chip using Rydberg-state spectroscopy. Phys. Rev. A, 96: 013425 (2017).

[4] Davtyan, D., Machluf, S., Soudijn, M.L., Naber, J.B., van Druten, N.J., van Linden van den Heuvell, H.B. and Spreeuw, R.J.C. Controlling stray electric fields on an atom chip for experiments on Rydberg atoms. Phys. Rev. A 97: 023418 (2018).

Rydberg interactions on an atom chip

Julius de Hond[1], **Rick van Bijnen**[2], **Nataly Cisternas**[1], **R.J.C. Spreeuw**[1], **H.B. van Linden van den Heuvell**[1], **S.J.J.M.F. Kokkelmans**[3], **and N.J. van Druten**[1]

[1] *Van der Waals–Zeeman Instituut, University of Amsterdam, Science Park 904, 1098 XH Amsterdam, The Netherlands*

[2] *Institut für Quantenoptik und Quanteninformation, Österreichische Akademie der Wissenschaften, 6020 Innsbruck, Austria*

[3] *Eindhoven University of Technology, P.O. Box 513, 5600 MB Eindhoven, The Netherlands*

e-mail: *j.j.m.dehond@uva.nl*

Rydberg states are interesting candidates for controlling the interactions between atoms in an ultracold gas. There are many proposals and demonstrations of their usefulness as a tool for quantum information, be it via resonant excitation of Rydberg states, or via off-resonantly mixing in Rydberg character into the ground state (so-called 'dressing'), see e.g. Refs. [1, 2] and references therein.

Atom chips offer appealing opportunities for creating integrated and compact systems, but combining them with Rydberg interactions remains an outstanding challenge. Looking for direct evidence of Rydberg interactions is difficult, because of the electric fields emanating from the surface of a chip, which strongly limit the coherence. This problem can partially be mitigated by using an on-chip wire as an electrode, compensating (a portion of) the stray electric field [3], thereby opening up the path to observing Rydberg–Rydberg interactions when exciting resonantly.

Here we present our first results towards demonstrating and utilizing interactions between Rydberg atoms in the CELSIUS atom chip experiment. We show that it is possible to see clear evidence of the dipole blockade on an atom chip. By varying the duration of the pulse times, the blockade manifested itself as a strong reduction in losses when comparing a single, continuous pulse to a series of shorter pulses with the same total pulse area (see Figure 1).

What's more, for short excitation times we have been able to resolve signs of coherent behavior. This is somewhat remarkable given the spread of electric fields that our system is sampling, and the range of densities that is represented in it. These results were analyzed using calculations that dynamically evolve the Hamiltonian using a reduced basis of superatoms, previously used to study Rydberg crystallization [4].

Presently, the coherence is thought to be limited by a combination of stray electric fields and nearby Rydberg states that are populated by black-body radiation. This mechanism, known since the late 1970s but only recently described in a quantum-information context [5], leads to rapid decoherence via the resonant dipole–dipole interaction between two Rydberg states with different parity. We observe this interaction too when exciting states with higher values of n, where the van der Waals-interaction plays a role as well.

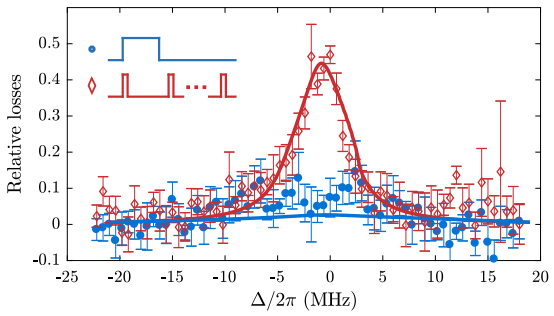


Figure 1: Spectra of the $|28D_{5/2}, m_J = 5/2\rangle$ state of ^{87}Rb obtained using a two-photon excitation scheme (with a 480 nm and a 780 nm wavelength laser) where the frequency of the blue laser was scanned. Two different pulse configurations for the red laser were used (see inset): a continuous pulse of 37.5 μs (solid circles) and a pulse with the same total 'on' time, chopped up in 500 ns segments separated by a 30 μs wait time (open diamonds). The total number of atoms in our chip trap (with axial and radial trap frequencies of $\omega_x/2\pi = 46$ Hz and $\omega_\perp/2\pi = 860$ Hz, respectively) was 21×10^3 at a temperature of $T = 0.7$ μK. A simple theoretical description based on rate equations describes our measurements (solid lines).

[1] M. Saffman, T.G. Walker, and K. Mølmer, *Reviews of Modern Physics* **82**(3), 2313 (2010)

[2] Marcin Płodzień, Graham Lochead, Julius de Hond, N.J. van Druten, and Servaas Kokkelmans, *Physical Review A* **95**(4), 043606 (2017)

[3] N. Cisternas, Julius de Hond, G. Lochead, R.J.C. Spreeuw, H.B. van Linden van den Heuvell, and N.J. van Druten, *Physical Review A* **96**(1), 013425 (2017)

[4] R.M.W. van Bijnen, S. Smit, K.A.H. van Leeuwen, E.J.D. Vredenbregt, and S.J.J.M.F. Kokkelmans, *Journal of Physics B: Atomic, Molecular and Optical Physics* **44**(18), 184008 (2011)

[5] E.A. Goldschmidt, T. Boulier, R.C. Brown, S.B. Koller, J.T. Young, A.V. Gorshkov, S.L. Rolston, and J.V. Porto, *Physical Review Letters* **116**(11), 113001 (2016)

Nonequilibrium many-body spin dynamics in strongly interacting Rydberg systems

Nithiwadee Thaicharoen[1], **Renato Ferracini Alves**[1], **Titus Franz**[1], **Andre Salzinger**[1], **Alexander Müller, Henrik Zahn**[1], **Annika Tebben**[1], **Clément Hainaut**[1], **Gerhard Zürn**[1], **Matthias Weidemüller**[1,2]

[1] *Physikalisches Institut, Universität Heidelberg, Im Neuenheimer Feld 226, 69120 Heidelberg, Germany*
[2] *Shanghai Branch, University of Science and Technology of China, Shanghai 201315, China*
e-mail: *thaicharoen@physi.uni-heidelberg.de*

Non-equilibrium Rydberg-spin systems have complex dynamics due to strong spin-spin interactions [1]. This dynamic can lead to relaxation of the system to either thermal- or nonthermal-fixed points, where effect of disorders, external fields and fluctuations play important roles [2, 3]. In this work, we propose a detection scheme to identify if the initial order of the system persist after relaxation dynamics. This can be performed by measuring diffusion characteristic between two Rydberg spin states separated by a domain wall at various disorder strengths. Utilizing state-selective detection and local down-pumping technique, the global magnetization and its variance will reveal if the system is localized or reaches the thermal equilibrium [4, 5].

[1] A. Piñeiro Orioli et al., Phys. Rev. Lett. **120**, 63601, (2018)

[2] M. Serbyn, et al., Phys. Rev. Lett. **113**, 147204 (2014).

[3] N. Yao, et al., Phys. Rev. Lett. **113**, 243002 (2014).

[4] J. Choi et al., Science **352**, 6293 (2016)

[5] J. Lancaster and A. Mitra, Phys. Rev. E **81**, 061134 (2010)

Microscopic observation of Rydberg macrodimers at the single-atom limit

Jun Rui[1], **Simon Hollerith**[1], **Johannes Zeiher**[1], **Antonio Rubio-Abadal**[1], **Nikola Šibalić**[2], **Thomas Pohl**[2], **Dan M. Stamper-Kurn**[1,3], **Immanuel Bloch**[1,4], **Christian Gross**[1]

[1] *Max-Planck-Institut für Quantenoptik, 85748 Garching, Germany*

[2] *Department of Physics and Astronomy, Aarhus University, DK 8000 Aarhus C, Denmark*

[3] *Department of Physics, University of California Berkeley, Berkeley, CA 94720, U.S.A*

[4] *Fakultät für Physik, Ludwig-Maximilians-Universität München, 80799 München, Germany*

e-mail: *jun.rui@mpq.mpg.de*

Molecules are one of the essential building blocks of complex quantum matter. Microscopic knowledge of their properties, as well as control over their formation, is a prerequisite for the understanding and design of novel exotic quantum states and phases. Typically, the extremely short distances between the constituent atoms in a molecule prevents the direct observation by an optical microscope. On the atomic side, atoms excited to high-lying Rydberg states have received increasing attention in recent years due to their exaggerated properties. Rydberg macrodimers [1, 2] - pure long-range molecules consisting of two Rydberg atoms bound together by their electrostatic interaction - provide a way to leverage the exaggerated atomic properties to the level of molecules.

Here we report on the direct microscopic observation, characterization and control of such Rydberg macrodimers. Starting from a two-dimensional atomic Mott insulator in an optical lattice, the discrete atomic density combined with a narrow-linewidth laser in the ultraviolet spectral range allow for the e cient photo-association of the macrodimers. More than one hundred vibrational levels have been identified, the spacing between which agrees quantitatively with *ab-initio* calculations of Rydberg interaction potentials [3]. Using our single-lattice-site resolved detection [4], we directly image the macrodimers by observing correlated pair-wise atom losses. We demonstrate versatile ways to control the association rate by either spatially tailoring the initial atomic density, choosing even/odd vibrational levels, or tuning the optical polarization. Furthermore, the precise measurement of bound-state energies and relative strengths allows for a detailed benchmark of state-of-the-art Rydberg potential calculations. This work paves the way to realize extreme long-range few-body quantum system, i.e. Rydberg macrotrimmers, and to engineer novel non-local interactions in many-body systems.

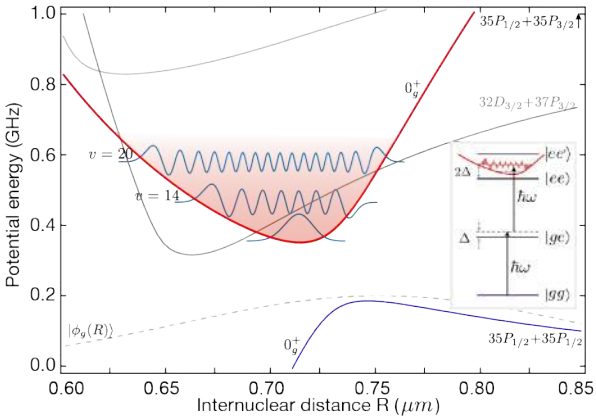


Figure 1: Interaction potentials between Rydberg-atom pairs of $35P_{1/2} + 35P_{1/2}$ and $35P_{1/2} + 35P_{3/2}$. Here only the 0_g^+ molecular potentials are presented.

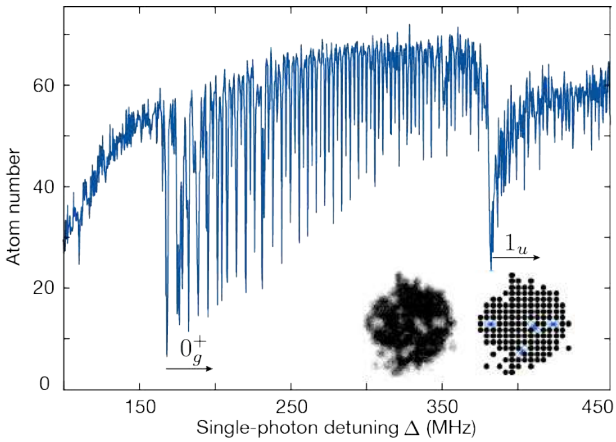


Figure 2: Measured atom-loss spectrum, referred to the transition frequency between the ground state $5S_{1/2}|F = 2, m_F = 0\rangle$ and the Rydberg state $35P_{1/2}$. More than 100 vibrational lines can be identified by comparing to the *ab-initio* potential calculations in the blue detuned side.

[1] C. Boisseau, I. Simbotin and R. Côté, Phys. Rev. Lett. **88**, 133004 (2002).

[2] N. Samboy, J. Stanojevic and R. Côté, Phys. Rev. A **83**, 050501(R) (2011).

[3] S. Weber, C. Tresp, H. Menke, A. Urvoy, O. Firstenberg, H. P. Büchler, S. Hofferberth, J. Phys. B: At. Mol. Opt. Phys. **50**, 133001 (2017)

[4] J. F. Sherson, C. Weitenberg, M. Endres, M. Cheneau, I. Bloch and S. Kuhr, Nature **467**, 68 (2010).

Circular Rydberg states in helium and $\lambda/4$ co-planar microwave waveguide resonators for hybrid cavity QED

A. A. Morgan, V. Zhelyazkova, and S. D. Hogan
University College London, Gower Street, WC1E 6BT, UK
e-mail: *alexandre.morgan.15@ucl.ac.uk*

The long fluorescence lifetimes, wide range of available resonant transition frequencies, and strong coupling to microwave fields that can be achieved with Rydberg states of atoms have seen them widely used in microwave cavity quantum electrodynamics (QED) experiments [1, 2]. Since Rydberg states can also possess large static electric dipole moments (e.g., $\mu_{\rm elec} > 10,000$ D for $n > 50$) atoms in these states can also be efficiently guided, transported, decelerated and trapped using inhomogeneous electric fields [3]. Together, this set of properties make gas-phase Rydberg atoms well suited to hybrid cavity QED experiments in which they are trapped above [4], and coupled to [5] microwave fields in chip-based waveguides and resonators for applications in hybrid quantum optics [6] and quantum information processing [7].

For these applications it is necessary to selectively prepare Rydberg states with long coherence times, Rydberg-Rydberg transition frequencies that are compatible with superconducting resonators ($\leq$ 20 GHz), and low sensitivity to stray electric fields emanating from the surfaces of the resonators. It is also desirable to fabricate co-planar waveguide resonators that allow minimal charge build up and hence time and position-dependent changes in these stray electric fields.

With these requirements in mind, we present the results of experiments in which we have prepared high-n circular Rydberg states in helium, and co-planar superconducting $\lambda/4$ microwave resonators that are well suited to these applications. The circular Rydberg states have been prepared with $n = 70$, and $\ell = |m_\ell| = 69$ using a modified version of the crossed fields method. This involves the initial laser photoexcitation of a ns Rydberg state that is then polarised in a strong electric field before being coherently transferred to an ℓ-mixed Stark state, that evolves adiabatically to the $(n-2)$ circular state in zero electric field. For the circular states prepared, the $\Delta n = +1$ circular-state–to–circular-state transition occurs at 18.78 GHz, with an electric dipole transition moment of 8818 D, and florescence lifetime of 155 ms. The static electric dipole polarisability of these states is $\alpha_{70c} = 4.6 \times 10^{-13}$ C m^2 V^{-1}.

In parallel to this, we have designed and fabricated $\lambda/4$ co-planar NbN waveguide resonators. In this resonator geometry, one end of the resonator is connected to the ground plane. Consequently, charge build-up on the centre-conductor is minimised. This reduces the difficulties that can be encountered with time and position-dependent stray electric fields. [9]

By combining these resonators with transmission-line beam splitters [10] and traps [4], we aim to develop a unique architecture for hybrid quantum optics and information processing in which arrays of trapped Rydberg atoms act as robust quantum memories coupled to each other, and to other qubits, via the superconducting circuits.

[1] D. Meschede, H. Walther, and G. Müller, Phys. Rev. Lett. 54, 551 (1985).

[2] S. Gleyzes, S. Kuhr, C. Guerlin, J. Bernu, S. Deléglise, U. Busk Hoff, M. Brune, M. Raimond and S. Haroche, Nature 446, 297 (2007).

[3] S. D. Hogan, EPJ Techniques and Instrumentation, 3, 1 (2016).

[4] P. Lancuba and S. D. Hogan, J. Phys. B: At. Mol. Opt. Phys. 49, 074006 (2016).

[5] S. D. Hogan, J. A. Agner, F. Merkt, T. Thiele, S. Filipp and A. Wallraff, Phys. Rev. Lett. 108, 063004 (2012).

[6] G. Calajó and P. Rabl, Phys. Rev. A, 95, 043824 (2017).

[7] P Rabl, D DeMille, John M Doyle, Mikhail D Lukin, RJ Schoelkopf, P Zoller, Phys. Rev. Lett., 97, 033003 (2006).

[8] V. Zhelyazkova and S. D. Hogan, Phys. Rev. A, 94, 023415 (2016).

[9] T. Thiele, J. Deiglmayr, M. Stammeier, J. A. Agner, H. Schmutz, F. Merkt, and A. Wallraff, Phys.Rev. A 92, 063425 (2015)

[10] J. Palmer and S. D. Hogan, Phys. Rev. A 95, 053413 (2017).

Generation and detection of Rubidium $20s$ Rydberg atoms with coherent 420 nm and 1050 nm radiation

J. E. Navarro-Navarrete, A. E. Díaz-Calderón, L. M. Hoyos-Campo, S. Hernández-Gómez, J. Flores-Mijangos, F. Ramírez-Martínez and J. Jiménez-Mier

Instituto de Ciencias Nucleares, Universidad Nacional Autónoma de México, Circuito Exterior S/N, Ciudad Universitaria, 04510 Coyoacán, México

e-mail: *ferama@nucleares.unam.mx, jimenez@nucleares.unam.mx*

Direct evidence of the production of $n = 20$ Rydberg atoms with two counter-propagating photons is presented. The experiments were performed in a heated rubidium cell with continuous-wave external cavity diode lasers. A frequency locked 420 nm laser excites the atoms from the ground energy level $5s_{1/2}$ to the $6p_{3/2}$ level, and the Rydberg atoms are produced by excitation with a 1050 nm laser to the $20s_{1/2}$ level.

The 420 nm laser is locked to a hyperfine resonance of the $5s_{1/2} \rightarrow 6p_{3/2}$ transition exploiting a saturated fluorescence spectroscopy fully described in a separate work. Then, light components from the 420 nm and 1050 nm lasers are superimposed in a colinear and counter-propagating configuration within a rubidium spectroscopy cell placed inside a home built oven capable of reaching temperatures of up to 115 °C.

The production of Rydberg atoms is monitored by taking advantage of a high probability of multi-step decays from the excitation path intermediate state $6p_{3/2}$. Once pumped into this state, atoms follow first a two step decay and transit through the lower $5p_j$ $(j = 1/2, 3/2)$ levels. These in turn decay finally back down to the ground state with the emission of either 780 nm or 795 nm fluorescence. As a direct consequence of the Rydberg atom preparation in this scheme, the pumping of the population from the energy level $6p_j$ required for the excitation to the higher energy states brings a proportional decrease in the population of the $5p_j$ levels, and therefore, a drop in the emission of IR fluorescence. This electron shelving effect is due to the longer lifetime of the Rydberg atoms, $\tau \sim 4.6$ μs.

An IR photodiode is placed next to and at the middle of the Rb cell; facing directly and at a right angle with respect to the direction of propagation of the excitation beams; and in the region in which these beams are superimposed and interact with the atomic vapor. A phase sensitive detection system based on modulating the 1050 nm excitation beam with a chopper was also implemented to enhance the signal-to-noise ratio of the detection system.

Finally, a third beam, obtained from the same 420 nm laser and frequency-modulated with an acousto-optical modulator (AOM) in a double pass configuration, was added to the system. This allowed an absolute measurement of the hyperfine energy splitting of the level $20s_{1/2}$, which in addition takes advantage of velocity selection effects in the thermal Rb vapor.

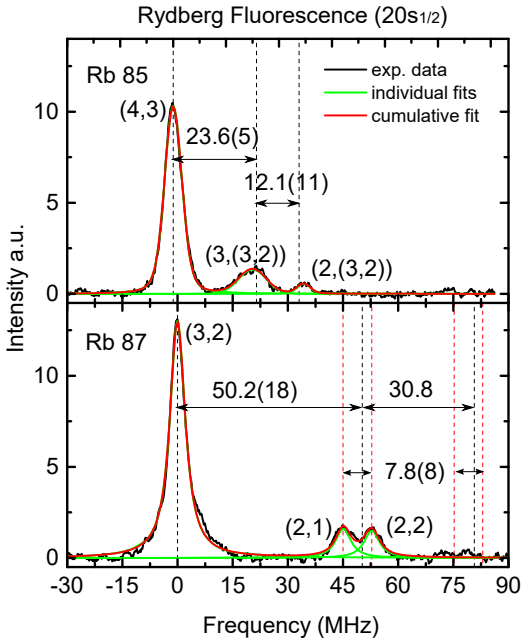


Figure 1: ^{85}Rb and ^{87}Rb fluorescence spectra as a function of 1050 nm laser detuning for the production $20s_{1/2}$ Rydberg atoms. The dominant feature in both spectra corresponds to the $6p_{3/2} \rightarrow 20s_{1/2}$ hyperfine transitions, identified in the graph with the notation $(F, F' = F - 1)$. Taking into consideration velocity selective effects, from these measurements it is only possible to extract hyperfine structure for ^{87}Rb due to the overlapping of the peaks in the other isotope. The vertical lines indicate the expected positions of the resonances as calculated from the values reported in [1].

We thank J. Rangel for his help in the construction of the diode laser. This work was supported by DGAPA-UNAM, México, under projects PAPIIT Nos. IN112516, IN107317, by National Laboratory project 293471. LMHC thanks UNAM-DGAPA for the postdoctoral fellowship and IUPAP for the travel grant. JFM, FRM, and JJM thank the "Programa de Movilidad Académica Internacional, CIC-UNAM".

[1] A. Tauschinsky, *et al.* Phys. Rev. A **87**, 042522 (2013).

Advanced relativistic energy approach and many-body perturbation theory too computing radiation transition energies, probabilities and hyperfine structure constants for heavy ions

E. Ternovsky[2], **V. Ternovsky**[1], **A. Glushkov**[1,2], *andO.Khetselius*[1,2]

[1] *Int. Research Centre for Quantum Optics and Laser Phys., Odessa State Environmental University, 65016 Odessa, Ukraine*

[2] *Departament of Applied Mathematics, Odessa State Environmental University, 65016 Odessa, Ukraine*

e-mail: *ternovskyev@gmail.com*

In this present work we present and advanced version of the relativistic energy approach to computing the radiation transition probabilities (oscillator strengths) in spectra of heavy Rydberg neutral atoms and multicharged ions. The approach is based on S-matrix Gell-Mann and Low formalism and relativistic many-body perturbation theory with optimized model potential zeroth approximation [3-3]. The key feature of the presented basis theory is an implementation of the optimized one-particle representation [2] into the frames of the S-matrix energy formalism. It provides a consistent method to minimization of the gauge-non-invariant contributions to the radiation transition (radiation decay width) probability and thus it makes our approach significantly more advantagable in comparison with standard methods to calculating radiative transition parameters. The important exchange-correlation effects are accounted with using relativistic Kohn-Sham like density functionals. We present the results of computing energies, radiation transition probabilities, oscillator strengths in spectra of the heavy Li-like multicharged ions ($Z > 55$), neutral tantalum and thulium (in particular, transitions to the $4f^{13}_{7/2,5/2}\,6s_{1/2[3/2]}ns, np$ and $4f^{13}_{5/2}6s_{1/2}(2)nsp_{1/2[3/2]}$ states, n=15-40). We have compared the obtained results with the experimental results and other theoretical data, obtained on the basis of the Coulomb approximation with the Coulomb gauge of the photon propagator, the multiconfiguration Hartree-Fock and Dirac-Fock methods. We have checked that the results for oscillator strengths, obtained within our approach in different photon propagator gauges (Coulomb, Babushkin, Landau), are practically equal (difference 0.1-0.3). We also present the results of relativistic calculation of the hyperfine structure parameters for heavy Li-like ions within many-body perturbation theory [1-3] with account of relativistic, correlation, nuclear, QED effects . As illustration in tables 1 and 2 the data of computing the nuclear finite size corrections into energy of some transitions (plus values of the effective radius of nucleus) The detailed analysis of the data and comparison with available theoretical and experimental data is performed.

Table 1. The nuclear finite size correction into energy (cm^1) of some transitions for Li-like ions and values of the effective radius of nucleus ($10^{13}cm$)

Z	$2s_{1/2} - 2p_{1/2}$	$2s_{1/2} - 2p_{3/2}$	R
20	- 15,1	- 15,5	3,26
69	- 20 690,0	- 21 712,0	4,93
79	- 62 315,0	- 66 931,0	5,15
92	- 267 325,0	- 288 312,0	5,42

Table 2. The hyperfine structure constants for some Li-like ions: $A*(cm^{-1}), B*(cm^{-1})$

nlj	Z	20	92
3s1/2	A	26 03	90 03
3p1/2	A	81 04	31 03
3p3/2	A	13 04	22 04
	B	31 05	62 05

[1] E. Ivanova and L. Ivamov, and E. Aglitsky, Phys. Rep. A **166**, 315 (1988).

[2] A. Glushkov, and L. Ivanov, Phys. Lett. A **170**, 33 (1992)

[3] A. Glushkov, et al, Nucl. Phys. A **734**, E21 (2004)

Relativistic theory of excitation and ionization of the heavy Rydberg atoms in a black-body radiation field

O. Khetselius[2], **A. Glushkov**[1,2], **E. Ternovsky**[1,2], **P. Zaichko**[2]

[1] *Int. Research Centre for Quantum Optics and Laser Phys., Odessa State Environmental University, 65016 Odessa, Ukraine*

[2] *Departament of Applied Mathematics, Odessa State Environmental University, 65016 Odessa, Ukraine*

e-mail: *okhetsel@gmail.com*

The accurate radiative transitions probabilities, ionization rates are needed in astrophysics, the ultracold plasma diagnostics etc. We present an advanced relativistic model potential method to computing the spectra, radiation amplitudes for the Na, K, Rb, Cs, Tl Rydberg atoms (RA), the ionization rates of states in the field of blackbody radiation (BBR). The master method is the combined energy approach and relativistic many-body perturbation theory with the zeroth model potential approximation [1,2]. It provides su ciently correct and simultaneously simplified numerical procedure to determination of the corresponding radiative transition and ionization properties. Interaction of the Rydberg atom A(nL) with the BBR induces transitions to the bound states and states of continuum. The energy parameters, radiation amplitudes for RA K, Cs,Tl their ionization rates of states with n = 10-100 in the BBR field (T=300-600K) are presented. It is performed a detailed comparison of some obtained data for lifetimes and BBR-ionization rates with available data of advanced quasiclassical calculations by Beterov et al, Glukhov-Ovsiannikov, model calculation results by Kleppner et al, Theodosiou et al [3-5]. It is established that despite on a good agreement between experimental and theoretical (on the basis of quasiclassical and other) models there is a serious deviation these data from the experiment for a number of Rydberg states n = 25-45, which is provided by no-accounting important exchange-polarization effects, including an effect of essentially non-Coulomb grouping of Rydberg levels, pressure continuum and others. The theory developed takes into account these effects and provides physically reasonable, good agreement with precise experimental data. From physical point of view an influence of the BBR field results in sometimes dramatic reduction of the Rydberg state lifetimes. It is quantitatively determined that the matched maximum of the ionization BBR rate is in the vicinity of n 20-25 (for different states of Na, K, Rb, Cs with large quantum defects) at T=300K and at higher temperatures it shifted towards lower values of n. Fig. 1 shows the experimental and theoretical curves of the total rate of BBR-ionization for the Riderburg (a) nS and (b) nD states of Na (T = 300K): Experiment (circles and squares); Theory: an improved quasiclassical Beterov etal model [5]; our theory (interrupted line).

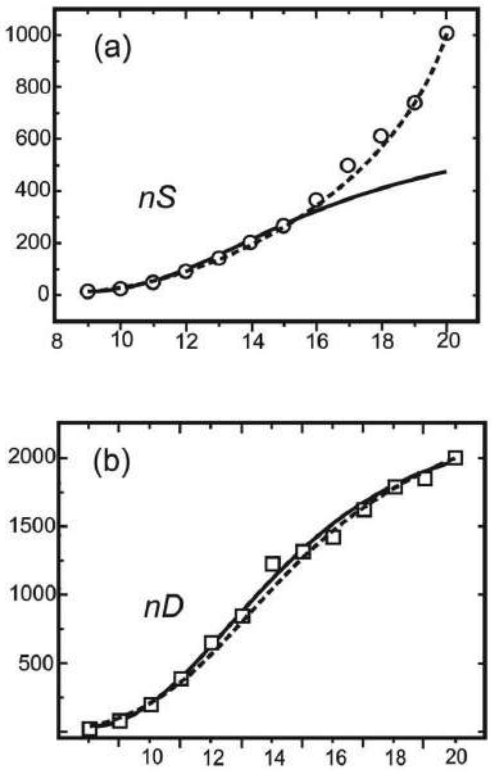


Figure 1: Total velocity of BBR-induced ionization for Riderburg (a) nS states and (b) nD states of sodium atom (T = 300K): Experiment (circles and squares); Theory: an improved quasiclassical Beterov etal model (continuous line) [5]; our theory (interrupted line)

[1] A. Glushkov, Progr. Theor. Chem. Phys. **26**, 231 (2013)

[2] O. Khetselius, A. Glushkov, O. Khetselius, et al, Int.J.Quant.Chem. **111**, 288 (2011)

[3] D. Kleppner, et al, Phys. Rev. A **26**, 1490 (1982)

[4] V. Glukhov, and D. Ovsiannikov, J.Phys. B **42**, 075001 (2009).

[5] I.Beterov, et al, New J. Phys. **11**, 013052 (2009).

Comprehensive calculations of photoabsorption and lifetimes of high-n states of Li

Constantine Theodosiou
School of Science, Manhattan College, Riverdale, NY 10471 USA
e-mail: *constant.theodosiou@manhattan.edu*

We report results of comprehensive calculations of photoabsorption by Li nl states with $n < 5$, covering all the final states in the discrete spectrum and through 100 eV of continuum energy states. The lifetimes of all nl states with $n < 45$ and $l < 5$, including black body radiation effects, are also presented. Good agreement is found with recent experimental results and past high accuracy calculations. The agreement is uniformly good for photoionization cross sections. Some experimental discrete oscillator strength measurements need to be re-evaluated based on our broad-spectrum calculations, which extend from the lowest excited state through the second ionization potential of Li. Our data for lifetimes are fitted to simple analytical expressions to provide easy access to the values for most of the Rydberg states of lithium.

1. Background

The ground-state photoabsorption cross sections of alkali metal atoms are known to have distinct minima, called Cooper minima [1], just above the ionization threshold for Na, K, Rb, and Cs, and below threshold in Li. This is an interesting behavior since the photoabsorption of H, which they closely resemble in terms of their spectra does not exhibit such minima. Their origin lies in the fact that the alkali metal atoms have a finite core that perturbs the otherwise hydrogenic wavefunctions of the outer electrons enough to cause enough "out-of-phase" shift and change in the initial-final state wavefunction overlap that at the appropriate energy the photoabsorption transition matrix element goes through a sign change. Alkali atoms have attracted extensive attention in laser-atom interaction experiments, especially since they are relevant in the development of quantum clocks and Bose-Einstein condensation states. Although now easily accessible by light sources, spectroscopic data and oscillator strengths for the high Rydberg states are not routinely available in the literature. Our work provides a comprehensive set of accurate data for these states.

2. Results

2.1. Photoabsorption cross sections

We have calculated a comprehensive set of photoabsorption cross sections for all alkali metal atoms using self-consistent methods [2] and including relativistic, core-polarization, and spin-orbit effects [3]. Fig. 1 shows as an example the results for Li 2s photoabsorption and their comparison with available experimental and accurate prior theoretical values.

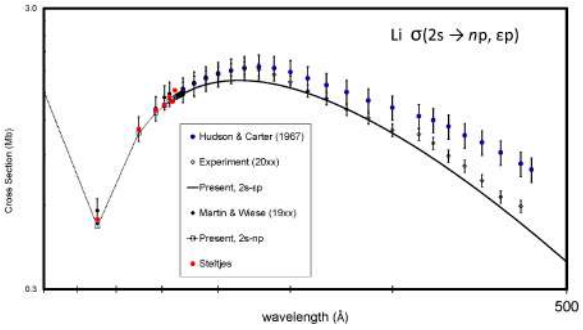


Figure 1: Photoabsorption cross sections of Li (2s) leading to discrete and continuum states.

2.2. Rydberg state lifetimes

A comprehensive set of lifetime values for all alkali metal atom Rydberg states with $n < 45$ and $l < 5$, including the effects of the ambient black-body radiation was also calculated. Our prior work [3] has been augmented with a self-consistent treatment of core-polarization effects on energy levels and wave functions. We fit the data by simple analytical expressions as functions of n and temperature (Fig. 2).

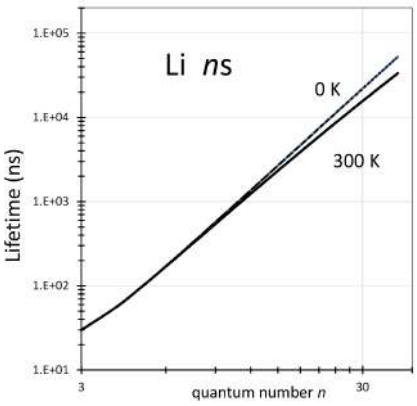


Figure 2: Lifetimes of the ns states in Li for $n < 45$ at 0K and 300K (present theoretical)

[1] U. Fano and J. W. Cooper, Rev. Mod. Phys. 40 (1968) 441

[2] C. E. Theodosiou, Phys. Rev. A 33 (1986) 2164; ibid 4400.

[3] C. E. Theodosiou, Phys. Rev. A 30 (1984) 2881.

High resolution cold atom source of single ions using correlations and Rydberg blockade

A.J.McCulloch, R.W. Speirs, S.H. Wissenberg, B.M. Sparkes, and R.E. Scholten *School of Physics, The University of Melbourne, Victoria 3010, Australia* e-mail: *scholten@unimelb.edu.au*

The cold atom ion source (CAIS), based on photoionisation of laser-cooled atoms, has surpassed conventional liquid metal and gas field ion sources for nanoscale imaging and fabrication [1, 2]. The CAIS offers higher resolution, a broad range of atomic species with associated choice of imaging and etching contrast, and competitively high beam current. Here we investigate the application of cold-atom ion sources to deterministic production of single ions with high spatial and temporal resolution.

In one approach we exploit the correlation between electrons and their associated ions following ionisation of cold atoms [3]. Coincident detection and feedback in combination with Coulomb-driven particle selection allows for high-fidelity heralding of ions at a high repetition rate. Figure 1 is a measured coincidence spectrum of electron and ion detection times for pulsed ionisation. The data show strong correlation with narrow time window of 4.3 ns. We have used detection of the electron to gate the ion beam and enhance the coincidence (Fig. 2).

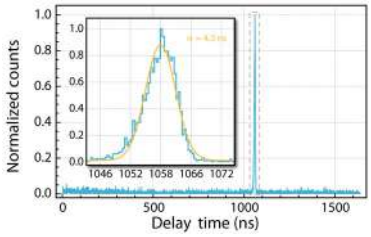


Figure 1: Coincidence spectra of electron and ion detection times with linear vertical scale. Inset shows peak region.

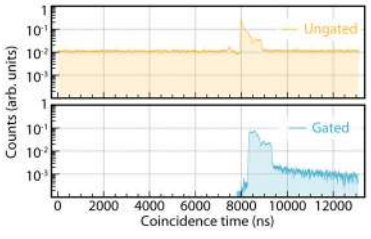


Figure 2: Coincidence spectra, log vertical scale. Lower plot shows enhanced fidelity with feedback: ions gated following electron detection.

Extension of the scheme beyond time-correlated to position/momentum-correlated feedback will provide a general and powerful means to optimize the ion beam brightness for the development of next-generation focused ion beam technologies (Fig. 3). We will show experimental results and the results

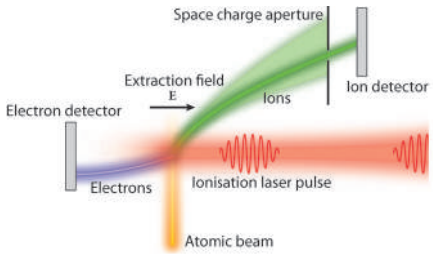


Figure 3: Schematic of a deterministic quasi-single-ion source. Electrons herald ion production, and a space-charge aperture quells multi-ionisation events.

of detailed calculations of a momentum-feedback scheme for a high brightness quasi-single-ion source.

We have also investigated Rydberg blockade for isolating single ions (Fig. 4). We use STIRAP [4] to e ciently ionise atoms and Doppler velocity selection to reduce the ion beam energy spread. Rydberg excitation and field ionisation then produce widely separated ions which are again heralded, and potentially gated, by detection of the correlated electrons.

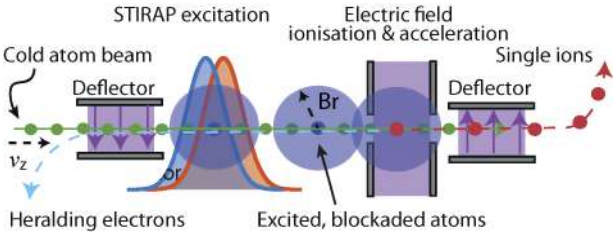


Figure 4: Schematic of a single ion source using Rydberg blockade to widely separat ions.

We are combining these techniques and using a commercial ion beam microscope column to create a powerful tool for characterisation and fabrication of materials at nanometre and potentially atomic scale.

[1] J.J. McClelland, A.V. Steele, B. Knuffman, K.A. Twedt, A. Schwarzkopf and T.M. Wilson, *Appl. Phys. Rev.* **3** 011302 (2016).

[2] A.V. Steele, A. Schwarzkopf, J.J. McClelland and B. Knuffman, *Nano Futures* **1** 015005 (2017).

[3] A.J. McCulloch, R.W. Speirs, S.H. Wissenberg, R.P.M. Tielen, B.M. Sparkes and R.E. Scholten, *Phys. Rev. A* **97** 043423 (2018).

[4] B.M. Sparkes, D. Murphy, R.J. Tayloer, R.W. Speirs, A.J. McCulloch and R.E. Scholten, *Phys. Rev. A* **94** 023404 (2016).

A Photon-Photon Quantum Gate Based on Rydberg Polaritons

Daniel Tiarks, Steffen Schmidt-Eberle, Thomas Stolz, Gerhard Rempe, and Stephan Dürr
Max-Planck-Institut für Quantenoptik, Hans-Kopfermann-Str. 1, 85748 Garching, Germany
e-mail: *stephan.duerr@mpq.mpg.de*

Rydberg polaritons offer a unique way to create strong interactions for photons. We utilize these interactions to demonstrate a photon-photon quantum gate. To achieve this, a photonic control qubit is stored in a quantum memory consisting of a superposition of a ground state and a Rydberg state in an ultracold atomic gas. This qubit interacts with a photonic target qubit in the form of a propagating Rydberg polariton to generate a conditional π phase shift, as in Ref. [1]. Finally, the control photon is retrieved. We measure two controlled-NOT truth tables and the two-photon state after an entangling-gate operation. This work is an important step toward applications in optical quantum information processing.

[1] D. Tiarks et al., Science Advances 2, 1600036 (2016).

Quenched dynamics and spin-charge separation in an interacting topological lattice

L. Barbiero[1], **L. Santos**[2], **and N. Goldman**[1]

[1] *Center for Nonlinear Phenomena and Complex Systems, Université Libre de Bruxelles, CP 231, Campus Plaine, B-1050 Brussels, Belgium*

[2] *Institut für Theoretische Physik, Leibniz Universität Hannover, Appelstr. 2, DE-30167 Hannover, Germany*

e-mail: *Luca.Barbiero@ulb.ac.be*

We analyze the static and dynamical properties of a one-dimensional topological lattice, the fermionic Su-Schrieffer-Heeger model, in the presence of on-site interactions. Based on a study of charge and spin correlation functions, we elucidate the nature of the topological edge modes, which depending on the sign of the interactions, either display particles of opposite spin on opposite edges, or a pair and a holon. This study of correlation functions also highlights the strong entanglement that exists between the opposite edges of the system. This last feature has remarkable consequences upon subjecting the system to a quench, where an instantaneous edge-to-edge signal appears in the correlation functions characterizing the edge modes. Besides, other correlation functions are shown to propagate in the bulk according to the light-cone imposed by the Lieb-Robinson bound. Our study reveals how one-dimensional lattices exhibiting entangled topological edge modes allow for a non-trivial correlation spreading, while providing an accessible platform to detect spin-charge separation using state-of-the-art experimental techniques.

References

[1] L. Barbiero, L. Santos, N. Goldman, arXiv:1803.06957.

Quantum disordered phases arising in some frustrated systems have been in the focus of interest in the last two decades. Characterized by massively degenerated ground states, local indistinguishably and long range entanglement, their study remains often still inconclusive. Here, we propose a method with very low computational cost to analyze quantum spin liquids in frustrated systems. We focus our study in paradigmatic Heisenberg models on the triangular lattice where frustration can be enhanced by anisotropic next or/and second neighbor interactions. A reliable sketch of the corresponding phase diagram is obtained using (i) exact diagonalizaton with random boundary conditions in very small lattices, (ii) post-selecting only those configurations leading to a ground state energy quasi-degenerated with the lowest one and (iii) performing averages over the post-selected states. In all models analyzed here, the phase diagram so obtained reproduces qualitatively the ordered and disordered phases that have been previously reported using 2D-DRMG, quantum Monte Carlo or tensor networks numerical methods.

Topological states in the Kronig–Penney model with arbitrary barriers

I. Reshodko[1], **A. Benseny**[1], **and Th. Busch**[1]

[1] *Okinawa Institute of Science and Technology Graduate University, 9040495, Onna, Okinawa, Japan*

e-mail: *irina.reshodko@oist.jp*

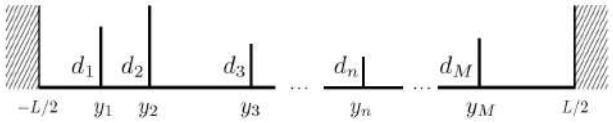


Figure 1: Schematic of the arbitrary KP model. The barriers are located at positions y_1 or y_M and have respective heights of $d_1, \ldots, d_M$. The regions between all scatterers (including the walls) are labelled $n_1 \ldots n_{M+1}$.

The Kronig–Penney model is one of the fundamental models of solid state physics and has since its inception received significant attention. We present a concise expression of an exact analytical solution by means of Bethe ansatz of a Kronig–Penney model with the delta barriers of arbitrary heights positioned at arbitrary points within the box (figure 1). We also demonstrate an application of our solution to a solid-state physics problem in a topologically non-trivial system [1]. We demonstrate appearance of the Hofstadter butterfly-like quasi-momentum spectrum in the Kronig–Penney model with hight-modulated barriers, as well as emergence of a beetle-shaped spectrum in case of shallow lattice. The solution can be readily applied to analytical studies of localization in various distributions of the barrier heights and positions, as well as exact studies of dynamics of Tonks–Girardeau gas or non-interacting fermions.

[1] I. Reshodko, A. Benseny and Th. Busch, in preparation, 2018

Hall conductivity of strongly interacting bosons in optical lattice

K. Patucha[1], **B. Grygiel**[1], **and T. A. Zaleski**[1]

[1] *Institute of Low Temperature and Structure Research, Polish Academy of Sciences, Okolna 2, 50-422 Wroclaw, Poland*

e-mail: *k.patucha@intibs.pl*

In the recent years, techiniques of creating artificial gauge fields in ultracold atomic systems, like Floquet engineering and photon-assisted tunneling [1, 2], have allowed to simulate Harper [3] and Haldane models [4] in optical lattice environment. Until now, topological properties, like Chern number or transverse drift velocity, have been studied experimentally in the limit of non-interacting particles. In parallel, experiments measuring transport properties in optical lattices have been developed [5, 6]. These advances motivates the study of the Hall conductivity of ultracold bosons in optical lattices.

We employ the Bose-Hubbard model in quantum rotor approximation to study the Hall conductivity of ultra-cold bosonic atoms in optical lattice. This approach allows us to describe lattices with non-zero Chern numbers. As examples of such systems we consider square lattice in a synthetic magnetic field as well as the Haldane model. We derive formula for the Hall conductivity, which strongly resembles the famous TKNN formula. We investigate the behavior of conductivity depending on temperature and model parameters. It appears that bosonic systems substantially differ from the fermionic ones, e.g. the presence of non-zero Hall conductivity is not directly related to non-zero value of the Chern number.

[1] A. Eckardt, Rev. Mod. Phys. **89**, 011004 (2017)

[2] J. Dalibard, F. Gerbier, G. Juzeliūnas, and P. Öhberg, Rev. Mod. Phys. **83**, 1523 (2011)

[3] M. Aidelsburger, M. Lohse, C. Schweizer, M. Atala, J. T. Barreiro, S. Nascimbéne, N. R. Cooper, I. Bloch, and N. Goldman, Nat. Phys. **11**, 162 (2015)

[4] G. Jotzu, M. Messer, R. Desbuquois, M. Lebrat, T. Uehlinger, D. Greif, and T. Esslinger, Nature **515**, 237 (2014)

[5] S. Krinner, D. Stadler, D. Husmann, J.-P. Brantut, and T. Esslinger, Nature **517**, 64 (2015)

[6] S. Häusler, S. Nakajima, M. Lebrat, D. Husmann, S. Krinner, T. Esslinger, and J.-P. Brantut, Phys. Rev. Lett. **119**, 030403 (2017)

Anyons from Hard-Core Three-Body Interactions in One-Dimension

N.L. Harshman[1] **and A.C. Knapp**[2]

[1] *Department of Physics, American University, 4400 Massachusetts Ave. NW, Washington, DC 20016-8079, USA*

[2] *Department of Mathematics and Statistics, American University, 4400 Massachusetts Ave. NW, Washington, DC 20016-8050, USA*

e-mail: *harshman@american.edu*

Like hard-core two-body interactions in two spatial dimensions, hard-core three-body interactions introduce defects in configuration space with co-dimension 2 and make the topology of configuration space multiply connected [1]. This opens the possibility for generalized exchange statistics because not all paths connecting initial and final configurations are equivalent [2]. Unlike normal fermionic or bosonic exchange statistics, how the few-body wave function transforms under the exchange of particle depends on how the particles are exchanged. Indistinguishable particles (or quasi-particles) governed by generalized exchange statistics are called anyons and can have exotic dynamical and thermodynamical properties.

This analysis is motivated by proposals to make effective three-body interactions in ultracold atomic gases [3, 4, 5]. Our results suggest that novel kinds of abelian and non-abelian anyons are possible in effectively one-dimensional gases with strong three-body interactions. This possibility does not require the absence of two-body interactions, only that two-body interactions are not also close to the hard-core limit.

For context, the most famous case of generalized exchange statistic are anyons with fractional statistics [6]. These occur when there are singular two-body interactions in two-dimensions among indistinguishable particles and the group realizing exchanges of N indistinguishable particles is given by the braid group B_N. Quasi-particles in the fractional quantum Hall effect are described as abelian braid group anyons and characterized by an exchange phase θ that interpolates between bosons $\theta = 0$ and fermions $\theta = \pi$. There are also one-dimensional models with singular two-body interactions and abelian braid group statistics, like the Calogero-Sutherland-Moser model [7] and the anyon Hubbard model [5]. One- and two-dimensional models with non-abelian braid anyons exist [4, 8] and offer tantalizing properties for quantum computation like topological protection.

We show that hard-core *three-body* interactions with N indistinguishable particles in one dimension lead to a different exchange symmetry group than the braid group, and we call it the *traid* group T_N [1]. Both the braid group B_N and the traid group T_N are generalizations of the symmetric group S_N, which is generated by $(N-1)$ generators σ_i that exchange particles i and $i+1$ and satisfy the following properties:

$$\sigma_i^2 = 1 \text{ for all } i \in N \quad (1)$$

$$\sigma_i\sigma_{i+1}\sigma_i = \sigma_{i+1}\sigma_i\sigma_{i+1} \text{ for all } i \in (N-1) \quad (2)$$

$$\sigma_i\sigma_j = \sigma_j\sigma_i \text{for all } |i-j| \geq 2. \quad (3)$$

The braid group B_N breaks relation (1); therefore $\sigma_i \neq \sigma_i^{-1}$ and 'clockwise' and 'counterclockwise' exchanges are not the same. In contrast, the traid group T_N keeps (1), but breaks relation (2), also called the Yang-Baxter relation and famous from the study of integrable models.

The traid group T_N and its subgroup the pure traid group PT_N (which applies to N distinguishable particles) do not seem to have been studied before. In this poster, we contrast traid anyons, corresponding to irreducible representations of T_N, with braid anyons.

[1] Harshman NL, Knapp AC (2018) *Few-Body Systems* **59**, 79; `arXiv:1803.11000`.

[2] Leinaas JM, Myrheim J (1977) *Nuovo Cim. B* **37**, 1–23.

[3] Cooper NR (2004) *Phys. Rev. Lett.* **92**, 220405; Daley AJ, et al. (2009) *Phys. Rev. Lett.* **102**, 040402; Mahmud KW, Tiesinga E, Johnson PR (2014) *Phys. Rev. A* **90**, 041602; Paul S, Tiesinga E (2015) *Phys. Rev. A* **92**, 023602; Paul S, Johnson PR, Tiesinga E (2016) *Phys. Rev. A* **93**, 043616.

[4] Paredes B, Keilmann T, Cirac JI (2007) *Phys. Rev. A* **75**, 053611.

[5] Keilmann T, Lanzmich S, McCulloch I, Roncaglia M (2011) *Nat. Comm.* **2**, 361.

[6] Wilczek F (1990) *Fractional statistics and anyon superconductivity.* (Singapore: World Scientific); Khare A (1997) *Fractional statistics and quantum theory.* (Singapore: World Scientific).

[7] Polychronakos AP (1989) *Nuc. Phys. B* **324**, 597–622.

[8] Nayak C, et al. (2008) *Rev. Mod. Phys.* **80**, 1083–1159.

Topological characterization of chiral models through their long time dynamics

Maria Maffei[1,2], **Alexandre Dauphin**[1], **Pietro Massignan**[1,3], **Maciej Lewenstein**[1,4]

[1] *Institut de Ciències Fotòniques, The Barcelona Institute of Science and Technology, 08860 Castelldefels, Spain*

[2] *Dipartimento di Fisica, Università di Napoli Federico II, Complesso Universitario di Monte Sant'Angelo, Via Cintia, 80126 Napoli, Italy*

[3] *Departament de Física, Universitat Politècnica de Catalunya, Campus Nord B4-B5, 08034 Barcelona, Spain*

[4] *ICREA – Institució Catalana de Recerca i Estudis Avançats, Pg. Lluis Companys 23, 08010 Barcelona, Spain*

e-mail: *maria.maffei@icfo.eu*

We study chiral symmetric models in one spatial dimension, both static and periodically driven, see Fig.1. We demonstrate that their topological properties may be read out through the long time limit of a bulk observable, the mean chiral displacement [1]. We show that the proposed detection converges rapidly and it can be implemented in a wide class of chiral systems. Furthermore, it can measure arbitrary winding numbers and topological boundaries, and it requires no additional elements, such as external fields, nor filled bands.

We have applied our theoretical findings to two experimental setups, using respectively photons and cold atoms. The first setup is a periodically driven system: a 1D chiral symmetric quantum walk (QW) implemented in the space of the light's Orbital Angular Momentum (OAM) and polarization [2], see Fig.2a. Here we used our method to measure the invariants which fully describe the topology of periodically driven chiral systems, as demonstrated in Ref.[3], and we tested the robustness of the method against a weak temporal disorder.

The second setup is a static 1D chiral symmetric system with controllable disorder implemented via spectroscopic Hamiltonian engineering, based on the laser-driven coupling of discrete momentum states of ultracold atoms [4], see Fig.2b. Here we find evidence for the topological Anderson insulator phase, in which the band structure of an otherwise trivial wire is driven topological by the presence of added disorder.

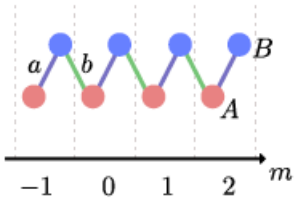


Figure 1: Nearest-neighbor-coupled chiral symmetric wire. The links within the unit cell and those connecting different unit cells have independent tunneling energies.

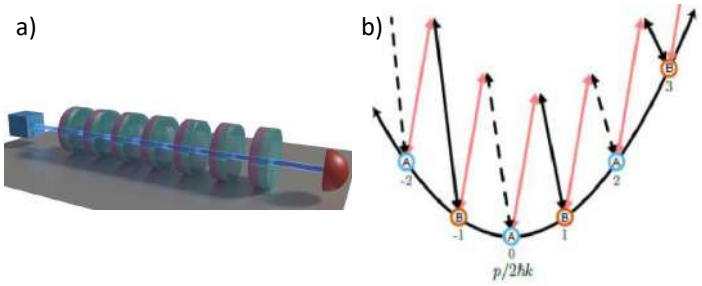


Figure 2: a) Chiral photonic QW. The light beam propagates through a repetition of two plates changing respectively polarization and OAM, [2]. b) Synthetic chiral wire engineered with cold atoms via two-photon Bragg transitions between discrete atomic momentum states, [4].

[1] M. Maffei, A. Dauphin, F. Cardano,M. Lewenstein, and P. Massignan, N.J.P. **20**, 013023 (2017).

[2] F. Cardano, A. D'Errico, A. Dauphin, M. Maffei, B. Piccirillo, C. de Lisio, G. D. Filippis, V. Cataudella, E. Santamato, L. Marrucci, M. Lewenstein, and P. Massignan, Nat. Comm. **8**, 15516 (2017).

[3] J. K. Asboth, H. Obuse, Phys. Rev. B **88**, 121406(R) (2013).

[4] E. J. Meier, F. A. An, A. Dauphin, M. Maffei, P. Massignan, T. L. Hughes, and B. Gadway, arXiv: 1802.02109 (2018).

Majorana Quasi-Particles Protected by Z_2 Angular Momentum Conservation

F. Iemini[1], **L. Mazza**[2], **L. Fallani**[3,4], **P. Zoller**[5,6], **R. Fazio**[1,7] **and M. Dalmonte**[1]

[1] *Abdus Salam International Center for Theoretical Physics, Strada Costiera 11, Trieste, Italy*

[2] *Departement de Physique, Ecole Normale Superieure / PSL Research University, CNRS, 24 rue Lhomond, F-75005 Paris, France*

[3] *Department of Physics and Astronomy, University of Florence, I-50019 Sesto Fiorentino, Italy* [4] *LENS European Laboratory for Nonlinear Spectroscopy, I-50019 Sesto Fiorentino, Italy*

[5] *Institute for Theoretical Physics, University of Innsbruck, A-6020 Innsbruck, Austria*

[6] *Institute for Quantum Optics and Quantum Information of the Austrian Academy of Sciences, A-6020 Innsbruck, Austria*

[7] *NEST, Scuola Normale Superiore and Istituto Nanoscienze-CNR, I-56126 Pisa, Italy*

e-mail: *fernandoiemini@gmail.com*

We show how angular momentum conservation can stabilise a symmetry-protected quasitopological phase of matter supporting Majorana quasiparticles as edge modes in one-dimensional cold atom gases. We investigate a number-conserving four-species Hubbard model in the presence of spin-orbit coupling. The latter reduces the global spin symmetry to an angular momentum parity symmetry, which provides an extremely robust protection mechanism that does not rely on any coupling to additional reservoirs. The emergence of Majorana edge modes is elucidated using field theory techniques, and corroborated by density-matrix-renormalization-group simulations. Our results pave the way toward the observation of Majorana edge modes with alkaline-earth-like fermions in optical lattices, where all basic ingredients for our recipe - spin-orbit coupling and strong inter-orbital interactions - have been experimentally realized over the last two years.

Floquet engineering of optical solenoids and quantized charge pumping along tailored paths in two-dimensional Chern insulators

Botao Wang, F. Nur Ünal, and André Eckardt
Max-Planck-Institut für Physik komplexer Systeme, Nöthnitzer Straße 38, 01187 Dresden, Germany
e-mail: *botao@pks.mpg.de*

The insertion of a local magnetic flux, as the one created by a thin solenoid, plays an important role in *gedanken* experiments of quantum Hall physics. By combining Floquet engineering of artificial magnetic fields with the ability of single-site addressing in quantum-gas microscopes, we propose a scheme for the realization of such local solenoid-type magnetic fields in optical lattices. We show that it can be employed to manipulate and probe elementary excitations of a topological Chern insulator. This includes quantized adiabatic charge pumping along tailored paths inside the bulk, as well as the controlled population of edge modes.

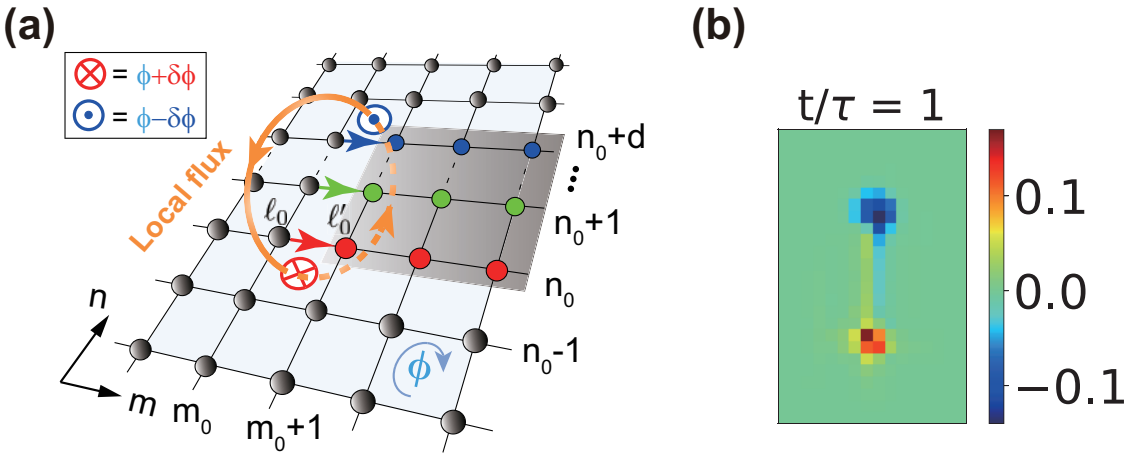


Figure 1: (a) Scheme for realizing solenoid-type local plaquette fluxes in a 2D optical lattice. The bonds labeled by colored arrows acquire an additional Peierls phase $\delta\phi$ as a result of the modification of the driving potentials on the colored rows. (b) Snapshots of the spatial density after ramping $\delta\phi$ from 0 to 2π within time τ. By filling the lowest band with Chern number $C = 1$, a quantum of charge is transported between two plaquettes.

Artificial Gauge Fields with Atom-Chip Based Quantum Simulator

E. Altuntas[1], **Y. Yue**[1], **F. Salces-Carcoba**[1], **A. Putra**[1], **C. Billington**[1] **and I. Spielman**[1]
[1] *Joint Quantum Institute, National Institute of Standards and Technology and University of Maryland, Gaithersburg, Maryland, 20899, USA*
e-mail: *altuntas@umd.edu*

Alkaline hyperfine states coupled with Raman lasers have been employed to realize artificial gauge fields, and subsequently spin-orbit coupling (SOC), which has led to the observation of spin-Hall effect. However, one issue with this method is the light induced heating, which limits the lifetime for moderate Raman coupling strengths in alkali fermions such as ^{40}K and ^{6}Li. Eliminating the source of heating due to spontaneous emission will open new paths to explore artificial gauge fields in alkali fermions and will be a step towards the realization of simulated topological insulators using ultracold atoms. We present a novel atom-chip system that will introduce light-less Raman coupling using radio-frequency (RF) magnetic fields from an atom-chip. We discuss the details of atom-chip design and chip control, and report our progress on realizing light-less Raman coupling with ^{87}Rb.

[1] Y.-J. Lin, R. L. Compton, K. Jimnez-Garca, J. V. Porto and I. B. Spielman, Nature 462, 628-632 (2009).

[2] M. C. Beeler, R. A. Williams, K. Jimnez-Garca, L. J. LeBlanc, A. R. Perry and I. B. Spielman, Nature 498, 201-204 (2013).

Quench dynamics of a synthetic three-leg Hall ladder with ultracold neutral fermions in an optical lattice

Jeong Ho Han[1,2], **Jin Hyoun Kang**[1,2], **and Y. Shin**[1,2]

[1] *Department of Physics and Astronomy and Institute of Applied Physics, Seoul National University, Seoul 08826, Korea*

[2] *Center for Correlated Electron Systems, Institute for Basic Science, Seoul 08826, Korea*

e-mail: *yishin@snu.ac.kr*

The Hofstadter model is a paradigmatic model for the quantum Hall physics of lattice systems, possibly hosting many types of exotic topological phases protected by inherent symmetry. Recent progress on the spin-orbit-coupled cold atom systems using a so-called synthetic dimension frame enables us to explore the physics of these topologically nontrivial states of matter [1]. In this poster, we describe our experimental study on quench dynamics of a synthetic three-leg Hall ladder with ultracold fermionic atoms in an one-dimensional optical lattice. The legs are formed by three hyperfine spin states of the atoms and the complex inter-leg couplings are provided by two-photon Raman transitions between the spin states [2]. We realize the case of the artificial magnetic flux piercing through single plaquette $\phi/\pi = 2/3$, where the magnetic length and the real lattice spacing are commensurate. The presence of artificial gauge fields is demonstrated by measuring semiclassical cyclotron orbit motions. We also investigate some extensions of the scheme such as the system with an additional inter-leg coupling between the synthetic edges and examine its topological properties [3].

[1] A. Celi, P. Massignan, J. Ruseckas, N. Goldman, I. B. Spielman, G. Juzeliūnas, and M. Lewenstein, Phys. Rev. Lett **112**, 043001 (2014).

[2] M. Lee, J. H. Han, J. H. Kang, M.-S. Kim, and Y. Shin, Phys. Rev. A **95**, 043627 (2017).

[3] S. Barbarino, M. Dalmonte, R. Fazio, and G. E. Santoro, Phys. Rev. A **97**, 013634 (2018).

Stability of Floquet topological phases against disorder

O. Shtanko[1] **and R. Movassagh**[2]

[1] *Physics Department, Massachusetts Institute of Technology, Cambridge, MA 02141, US*

[2] *IBM Research, MIT-IBM A.I. Lab, 75 Binney Street, Cambridge, MA 02142, US*

e-mail: *oles@mit.edu*

In the last few years, the dynamics of periodically driven quantum systems has been a subject of vigorous study following the extraordinary success of experiments exploring quantum controlled systems. It has been established that such system can exhibit novel topological behavior even if the initial static system is in a trivial phase [1, 2]. We demonstrate that beyond the high-frequency regime such system can be fragile to disorder present in the system (see Fig. 1). We use effective theory for the phase transition treating disorder corrections a generic random matrix. This method allows us to derive the expression for the spectral gap and show that the critical disorder may many times exceed the spectral gap of the clean system. We show that at high critical disorder when the transition occurs and derive the critical point parameters.

To obtain the result, we use free probability theory [3] to predict the spectral gap of the disordered Floquet Hamiltonian. This method allows estimating the density of states (DOS) of a sum of two Hamiltonian terms with known DOS under a few particular assumptions. This method itself as a powerful tool to obtain the spectrum of various disordered problems in the non-perturbative regime, especially gap problem. Comparison to the exact numerical solution for 1D and 2D systems demonstrate the high precision of the approach and suggest it utilizing in a broader set of problems.

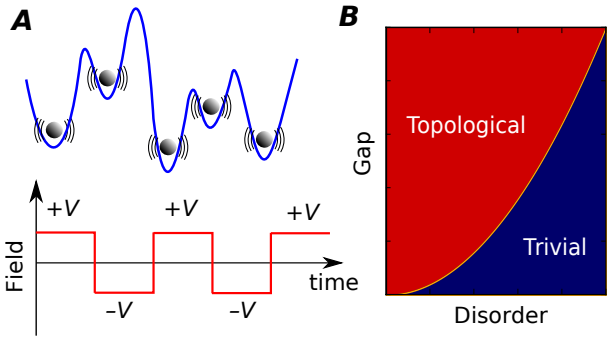


Figure 1: **A.** An isolated disordered quantum system represented by trapped cold atoms. The time periodic field $V(t)$ induces a transition from a trivial to a topological phase. **B.** The phase diagram for the system in the presence of local disorder. An increase of the disorder strength W induces a phase transition at $W_c \sim \Delta_0^{1/2}$, where Δ_0 is the gap of the clean system.

[1] N. H. Lindner, G. Refael, and V. Galitski, Nature Physics **7**, 490 (2011).

[2] Y. Wang, H. Steinberg, P. Jarillo-Herrero, and N. Gedik, Science **342**, 453 (2013).

[3] J. Chen *et al.*, Phys. Rev. Lett., **107**, 097205 (2011).

Evidence for the topological Anderson insulator

Eric J. Meier,[1] **Fangzhao Alex An,**[1] **Alexandre Dauphin,**[2] **Maria Maffei,**[2,3] **Pietro Massignan,**[2,4] **Taylor L. Hughes,**[1] **and Bryce Gadway**[1]

[1] *Department of Physics, University of Illinois at Urbana-Champaign, Urbana, IL 61801-3080, USA*

[2] *ICFO–Institut de Ciencies Fotoniques, The Barcelona Institute of Science and Technology, 08860 Castelldefels (Barcelona), Spain*

[3] *Dipartimento di Fisica, Università di Napoli Federico II, Complesso Universitario di Monte Sant'Angelo, Via Cintia, 80126 Napoli, Italy*

[4] *Departament de Física, Universitat Politècnica de Catalunya, Campus Nord B4-B5, 08034 Barcelona, Spain*

e-mail: *ejmeier2@illinois.edu*

Manipulating the topology or changing the disorder present in a quantum system can have profound effects on its transport properties. These effects have made popular the separate study of disorder and topology. Here we report on the combination of topology and disorder to observe both the robustness of a topological system to disorder and the first evidence for the topological Anderson insulator (TAI) (a system which is only topological when subjected to finite disorder) [1].

To accomplish these measurements we use a unique synthetic lattice technique based on laser-driven coupling of discrete momentum states of ultracold ^{87}Rb [2]. This technique allows us to create one-dimensional chiral symmetric quantum wires with locally tunable disorder.

To sense the topology of our quantum wires we use a dynamical measure called the chiral displacement $\mathcal{C}$. This measure has been shown to converge to the winding number of a system given enough time and disorder averaging [3]. We use the symbol $\langle\bar{\mathcal{C}}\rangle$ to indicate the time- and disorder-averaged chiral displacement.

By measuring the chiral displacement during quench dynamics for many disorder realizations we can therefore measure the topology of our system as a function of the applied disorder. Specifically, we measure two systems.

The first is a BDI class wire which is topological in the zero-low disorder limit. We increase the strength of the disorder in this system (observing a robustness to low disorder strength) until we see the topology change to trivial at a critical disorder value. For more information on this including experimental data see Ref. [4].

The second system we explore is an AIII class wire which is trivial at low disorders. In this system we see a change from a trivial system to a topological system and back again with added disorder. This unintuitive, disorder-reliant topological region we measured here is evidence for a theoretically predicted phase called the topological Anderson insulator [1]. Presented in Fig. 1 are the phase diagram of this system

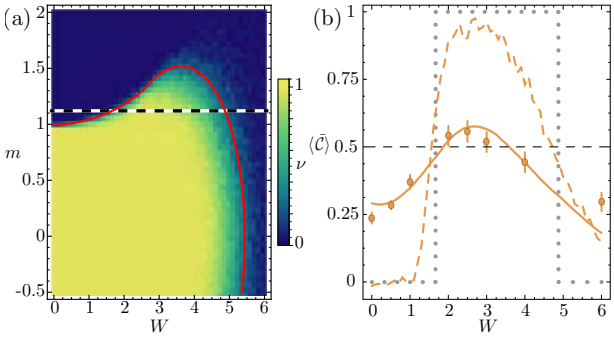


Figure 1: **(a)** Phase diagram of an AIII class topological wire. The color scale represents the computed widing number as a function of disorder strength W and tunneling ratio m. The experimentally explored slice is indicated by the black and white striped line and the solid red curve indicates the computed critical boundary. **(b)** $\langle\bar{\mathcal{C}}\rangle$ as a function of the disorder strength W. The solid orange line indicates the results of a numerical simulation taking into account the size of our system and time-constraints. The dashed orange line represents the results of a numerical simulation allowing for larger lattices and longer timescales. The grey dotted line shows what would be measured in the thermodynamic limit.

as well as the data showing evidence for the topological Anderson insulator. For more details on this experiment see Ref. [4].

[1] J. Li, R.-L. Chu, J. K. Jain, and S.-Q. Shen, Phys. Rev. Lett. 102, 136806 (2009).

[2] E. J. Meier, F. A. An, and B. Gadway, Phys. Rev. A 93 (5), 051602 (2016).

[3] M. Maffei, A. Dauphin, F. Cardano, M. Lewenstein, and P. Massignan, New J. Phys. 20, 013023 (2018).

[4] E. J. Meier, F. A. An, A. Dauphin, M. Maffei, P. Massignan, T. L. Hughes, and B. Gadway, arXiv:1802.02109 (2018).

Probing Topology in Out-of-Equilibrium Cold Atomic Systems

F. Nur Ünal[1], **Babak Seradjeh**[1,2], **and André Eckardt**[1]

[1] *Max-Planck-Institute for the Physics of Complex Systems, Nöthnitzer Straße 38, 01187 Dresden, Germany*

[2] *Department of Physics, Indiana University, Bloomington, Indiana 47405, USA*

e-mail: *unal@pks.mpg.de*

Topologically protected states have recently attracted much attention in a wide community. Particularly, significant developments in experimental realization and probe of mesoscopic physics in the ultracold quantum gases have led to the creation of extremely strong artificial magnetic fields in optical lattices, engineering of topological band structures unaccessible in solid state materials as well as the close inspection of chiral edge modes in narrow strips. Although the initial efforts have been directed to the investigation of topology of simpler settings in the form of measuring the Chern number of a ground state, recently the attention is shifted towards the out-of-equilibrium systems. In a recent paper [1], we have presented the first experimental observation of the Chern number of the Haldane model where we read it with the bare eye in the far-from-equilibrium dynamics of the system. Here, we propose a set of schemes to probe the band topology in different cold atomic settings such as the extension of the band tomography techniques to investigate the anomalous Floquet topological insulators, where the simple classification in terms of the Chern numbers of the bands fails to describe the topological properties of the system fully [2]. Furthermore, by taking advantage of the single-site addressing provided by the quantum gas microscopes, we have proposed a method to dynamically create quasiparticles and quasiholes in quantum Hall insulators as another probe readily accessible to cold atomic systems [3]. We show that this technique can be also employed to induce fractionally charged excitations even in systems as small as four particles on a square lattice [4]. This result is favorable for the prospects of adiabatic preparation of fractional Chern insulators. The creation and dynamical manipulation of fractionally charged excitations in a coherent fashion is highly desirable also for robust quantum information processing.

[1] Matthias Tarnowski, F. Nur Ünal, Nick Fläschner, Benno S. Rem, André Eckardt, Klaus Sengstock and Christof Weitenberg, arXiv: 1709.01046.

[2] F. Nur Ünal, B. Seradjeh and, André Eckardt, under preperation.

[3] Botao Wang, F. Nur Ünal and André Eckardt, Phys. Rev. Lett. XXX (arXiv: 1802.06815).

[4] Mantas Račiūnas, F. Nur Ünal, Egidijus Anisimovas and André Eckardt, arXiv: 1804.02002.

A Continuously Tunable Topological Pump in High-dimensional Cold Atomic Gases

Yan-Bin Yang[1], **L.-M. Duan**[1,2], **and Yong Xu**[1]

[1] *Center for Quantum Information, IIIS, Tsinghua University, Beijing 100084, PR China*

[2] *Department of Physics, University of Michigan, Ann Arbor, Michigan 48109, USA*

e-mail: *yang-yb15@mails.tsinghua.edu.cn*

Over thirty years ago, Thouless introduced the quantized particle transport that can occur in a one-dimensional quantum system under a cyclic adiabatic variation of periodic potentials without a bias voltage. This phenomenon is attributed to the formation of a dynamical Chern insulator on a parameter surface formed by quasimomentum and time. Recently, three-dimensional topological gapless phenomena have sparked tremendous interest in various fields. Here, we demonstrate that dynamical Weyl points and dynamical 4D Weyl nodal rings protected by the first Chern number emerge in a two-dimensional and three-dimensional system, respectively. We find that the topological pump occurs in these systems but the amount of pumped particles is not quantized and can be continuously tuned by controlling experimental parameters over a wide range. Finally, we propose an experimental scheme to realize the dynamical Weyl points and 4D Weyl nodal rings and their corresponding topological pump in cold atomic gases.

[1] Y.-B. Yang, L.-M. Duan and Y. Xu, arXiv:1801.08255 (2018).

Geometry, topology and control of spin-1 atoms

M. Barrios[1], H. M. Bharath[1], M. Boguslawski[1], L. Xin[1] and M. S. Chapman[1]
[1] *School of Physics, Georgia Institute of Technology*
e-mail: *mbarrios@gatech.edu*

Recent explorations into the physical manifestation of geometry and topology of the quantum phase space have been fruitful in revealing techniques for geometric-based, fault-tolerant quantum control, as well as topologically stable states in spatially extended traps of ultracold atoms [2]. Here, we develop a new geometrical representation for spin-1 quantum states and show its applicability to a range of interesting problems. The quantum state of a spin-1/2 system is uniquely represented by a point on the Bloch sphere whose coordinates are given by the expectation values of the spin operators S_x, S_y and S_z. Spin-1 and higher spin quantum states differ in two ways: first, the expectation value of the spin vector, $\vec{S} = (\langle S_x\rangle, \langle S_y\rangle, \langle S_z\rangle)^T$ (here, $\langle\cdot\rangle$ represents the expectation value) is not confined to the surface of the Bloch sphere. It could be present anywhere on or *inside* the Bloch sphere. Second, a quantum state is not uniquely represented by its spin vector. In fact, there can be several different quantum states which share the same spin vector. For spin-1 systems, this ambiguity is resolved by considering the quantum fluctuations of the spin vector, which geometrically is an ellipsoid that surrounds the head of the spin vector (Figure 1(a)).

The ellipsoid represents a rank two tensor $\left(\overleftrightarrow{T}\right)$, whose components are the expectation values of the quadratic spin operators $T_{ij} = \frac{1}{2}\langle\{S_i, S_j\}\rangle - \langle S_i\rangle\langle S_j\rangle$. Together, the pair $\left(\vec{S}, \overleftrightarrow{T}\right)$ uniquely represents a spin-1 quantum state up to an overall phase. Figure 1 (b) shows three examples. In a separate publication, we have used this representation to study non-Abelian geometric phases in ultracold spin-1 atoms [1]. Applying this representation further, we uncover a number of exotic topologically stable states of a ring trap, including those with fractional topological charge. Additionally, we develop a protocol for holonomic, fault-tolerant arbitrary control of a spin-1 state, and discuss applications to spin squeezing experiments.

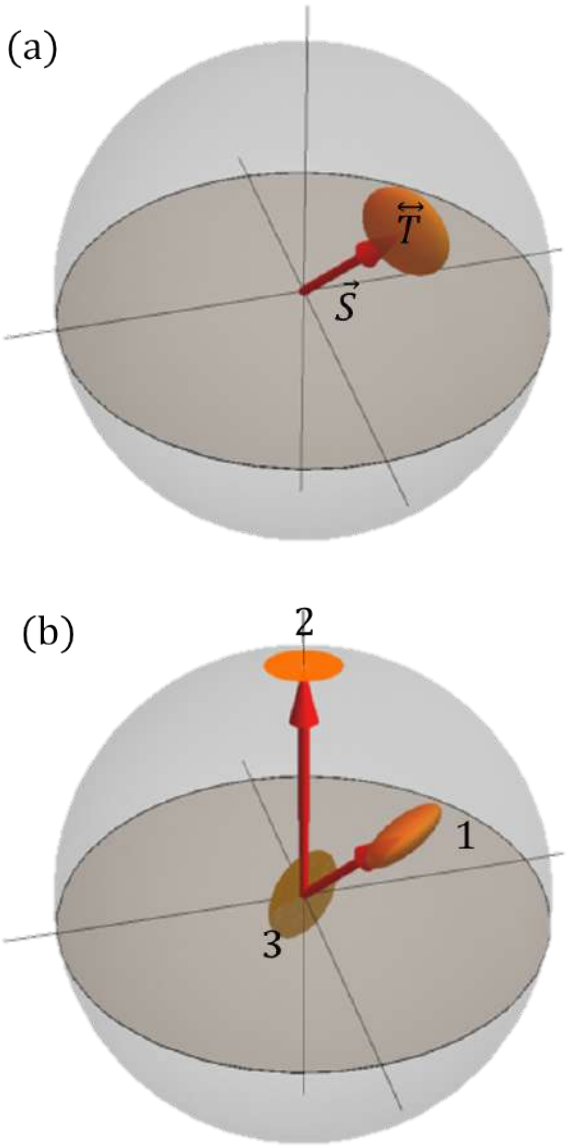


Figure 1: (a) shows that the spin vector $\left(\vec{S}\right)$ and the spin fluctuation tensor $\left(\overleftrightarrow{T}\right)$ can together be represented by a point inside the Bloch sphere surrounded by an ellipsoid. This pair of the vector and the ellipsoid uniquely represent a spin-1 quantum state up to an overall phase. (b) illustrates that the lengths of the ellipsoid's axes are constrained by the length of the spin vector. Explicitly, they are given by $\sqrt{1-|\vec{S}|^2}$ and $\sqrt{\frac{1\pm\sqrt{1-|\vec{S}|^2}}{2}}$. For the three examples labeled 1, 2 & 3, the spin vectors $\vec{S}_{1,2,3}$ satisfy $0 < |\vec{S}_1| < 1, |\vec{S}_2| = 1$ and $|\vec{S}_3| = 0$. The ellipsoid degenerates to a disk for the last two cases.

[1] H. M. Bharath, M. Boguslawski, M. Barrios, Lin Xin and M. S. Chapman, arXiv:1801.00586 (2018).

[2] M. Ueda, *Rep. Prog. Phys.* **77**, 122401 (2014).

Correspondence between a shaken honeycomb lattice and the Haldane model

Michele Modugno[1,2] **and Giulio Pettini**[3]

[1] *Depto. de Física Teórica e Hist. de la Ciencia, Universidad del Pais Vasco UPV/EHU, 48080 Bilbao, Spain*
[2] *IKERBASQUE, Basque Foundation for Science, 48011 Bilbao, Spain*
[3] *Dipartimento di Fisica e Astronomia, Università di Firenze, and INFN, 50019 Sesto Fiorentino, Italy*
e-mail: *michele.modugno@ehu.eus*

We investigate the correspondence between the tight-binding Floquet Hamiltonian of a periodically modulated honeycomb lattice and the Haldane model. We show that – though the two systems share the same topological phase diagram, as reported in a breakthrough experiment with ultracold atoms in a stretched honeycomb lattice [Jotzu *et al.*, Nature **515**, 237 (2014)] – the corresponding Hamiltonians are not equivalent, the one of the shaken lattice presenting a much richer structure [1].

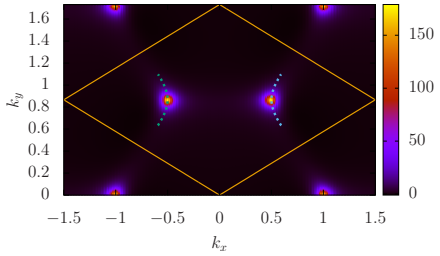


Figure 1: Density plot of the Berry curvature within a rhomboidal Brillouin zone containing the Dirac points. The two dotted lines represents the trajectory along which the Dirac points move.

[1] M. Modugno and G. Pettini, Phys. Rev. A **96**, 053603 (2017).

Transport in optical lattices with flux

A. Hudomal[1], **I. Vasić**[1], **H. Buljan**[2], **W. Hofstetter**[3], **and A. Balaž**[1]
[1] *Scientific Computing Laboratory, Center for the Study of Complex Systems, Institute of Physics Belgrade, University of Belgrade, Serbia*
[2] *Department of Physics, University of Zagreb, Croatia*
[3] *Institut für Theoretische Physik, Johann Wolfgang Goethe-Universität, Frankfurt am Main, Germany*
e-mail: *hudomal@ipb.ac.rs*

Different condensed matter systems, such as electrons in a crystal lattice, can be simulated using ultracold atoms in optical lattices. Unlike electrons, atoms are electrically neutral and therefore do not feel the effects of magnetic field. Artificial gauge potentials have been recently realized in cold-atom experiments with periodically driven optical lattices [1, 2]. In such systems, atoms subjected to a constant external force gain an anomalous velocity in the direction transverse to the direction of the applied force.

Taking into consideration realistic experimental conditions, we perform numerical simulations in order to investigate the dynamics of atomic clouds and relate it to the Chern number of the effective model. We consider incoherent bosons and the full time-dependent Hamiltonian. The effects of weak repulsive interactions between atoms are taken into account using the mean-field approximation.

Our results show that driving, external force and interactions all cause heating and transitions to higher bands, which have significant effects on the dynamics. It turns out that weak interactions can be beneficial, because they make the momentum-space probability density more homogeneous. In the future, we also plan to study the details of the atomic-cloud expansion dynamics, and to simulate the full loading sequence of an initial Bose-Einstein condensate, as it was done in the experiment [2].

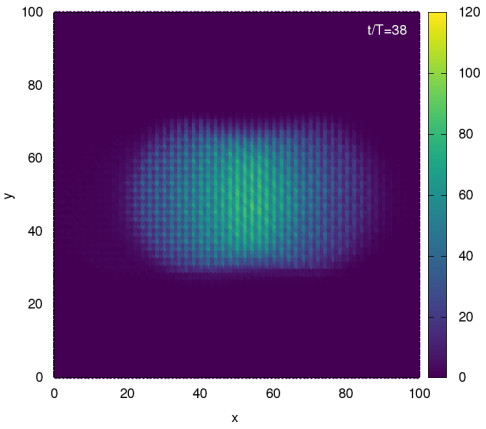


Figure 1: Density profile of an atomic cloud during expansion dynamics after release from a trap in the presence of an artificial gauge field and external force.

[1] G. Jotzu, M. Messer, R. Desbuquois, M. Lebrat, T. Uehlinger, D. Greif, and T. Esslinger, Nature **515**, 237 (2014).

[2] M. Aidelsburger, M. Lohse, C. Schweizer, M. Atala, J. T. Barreiro, S. Nascimbène, N. R. Cooper, I. Bloch, and N. Goldman, Nat. Phys. **11**, 162 (2015).